L. Santiago Medina
Pina C. Sanelli
Jeffrey G. Jarvik   *Editors*

Evidence-Based Neuroimaging Diagnosis and Treatment

Improving the Quality of Neuroimaging in Patient Care

Springer Reference

Evidence-Based Imaging

Series Editors

L. Santiago Medina, C. Craig Blackmore, Kimberly E. Applegate

Aims of the Series

Evidence-Based Imaging: Improving the Quality of Imaging in Patient Care series presents the radiologist and clinician with a user-friendly guide to the evidence-based science and the merit behind the diagnostic imaging performed in medicine. This ideal reference gathers contributions by internationally renowned specialists in the field. The series provides a systematic framework for understanding the best imaging choices for patient care. Chapters highlight key points that support the clinical applications, allowing fast access to pertinent information. Topics include patient selection, imaging, strategies, test performance, cost-effectiveness, and applicability.

By offering a clear understanding of the science behind the evidence, the book fills a void for radiologists, clinicians, physician assistants, nurse practitioners, residents, fellows, students and others with an interest in medical imaging and a desire to implement an evidence-based approach.

L. Santiago Medina • Pina C. Sanelli
Jeffrey G. Jarvik

Editors

Evidence-Based Neuroimaging Diagnosis and Treatment

Improving the Quality of Neuroimaging in Patient Care

With 143 Figures and 123 Tables

Springer Reference

Editors
L. Santiago Medina
Division of Neuroradiology-
Neuroimaging, Department of Radiology
Miami Children's Hospital
Miami, FL, USA
and
Herbert Wertheim College of Medicine
Florida International University
Miami, FL, USA
and
Former Lecturer in Radiology
Harvard Medical School
Boston, MA, USA

Pina C. Sanelli
Department of Radiology
Weill Cornell Medical College/
NewYork-Presbyterian Hospital
New York, NY, USA

Jeffrey G. Jarvik
Department of Radiology
Harborview Medical Center
University of Washington
Seattle, WA, USA

To our patients, who are our best teachers,
and to the researchers, who made this book possible.
To our families, friends, and mentors

To my loving family past, present, and future, Jorge, Susana,
Olga, Camila, and Isabela – LSM

To my loving and supportive husband, George, and our three
children, Isabella, Sophia, and Nicholas, who are truly our pride
and joy – PCS

To my children, Ella, Leah, and Ethan, who make it all
worthwhile, and to my wife, Gail, who makes it all possible – JGJ

Foreword

We are in the midst of a health-care transformation that has accelerated the need for providers to be able to defend the consequences of their decisions. The costs of care in the United States and in many other countries continue to escalate at unsustainable paces. With health care already consuming over 17 % of our GDP, the rate of increase frightens those who appreciate that we are approaching the limits of economic tolerance.

Superimposed on the affordability conundrum is an urgency to deal with health issues associated with an aging population. Congress and governmental agencies are bent on removing costs and imposing barriers to limit expenses. The clear mantra in health care is to do more with less. How to provide quality care and improve the health of our country becomes a formidable challenge in such a demanding environment.

A particular component of this struggle is the focus on imaging. Its success in the past 30-plus years has dramatically improved the lives of millions. When I began my career in 1973, it was common to perform exploratory neurosurgery, myelography, direct carotid puncture angiography, and pneumoencephalography. Today, cross-sectional imaging has obviated such painful and frequently fruitless procedures, while also enabling remarkable increases in diagnostic acumen.

The imaging revolution has also created much consternation, however. I have been on a number of health-care panels where media and government functionaries have railed at "unnecessary" imaging and its associated costs. Of course, it is more difficult to actually define what is "unnecessary." A case in point was my exposure to triage for CT (then a scarce resource) in the 1970s. It was about 10 pm when I was asked by a neurology resident to do an emergency CT on a patient with headache, slight fever, and normal neurologic examination – with only a hunch that there was a significant intracranial problem. He was concerned about a brain abscess, but with a normal exam it was difficult to imagine there was a developing emergency. It seemed to me that the case could wait to the following morning, which it did, with the subsequent scan revealing a large brain abscess pointing to the ventricle. So much for triaging!

Yet today, the concept of triage in the proper use of valuable resources looms larger than ever. And while, arguably, nothing will ever replace the intuition of the gifted physician, there is an unquestionable need to counter the practice of "defensive medicine" – the widespread ordering of tests that serve not to elucidate, but merely to document. Whether the impetus is the

physician's quest for self-protection or the patient's insistence on "proof," the only antidote to unnecessary imaging studies is evidence-based medicine.

A major stumbling block to embracing evidence-based approaches is the common assumption that patient well-being and the exigencies of the "bottom line" are intrinsically at odds. On the contrary, employing the most appropriate diagnostic algorithm is cost effective and patient centered simultaneously. There are innumerable examples of imaging examinations that provide virtually the same information. CT and MR examinations of the brain for this or that generally duplicate findings. There are instances, however, where one study may perhaps be more sensitive, e.g., the superiority of CT for the detection of calcification in a tumor or the detection of acute subarachnoid hemorrhage. Mastery of these nuances enables the neuroradiologist to be a worthy consultant.

Of course, the value of evidence-based medicine hinges above all on the quality of the evidence itself, leading to the fundamental question of how much evidence is truly available. There must be not only reliable, significant data but an accompanying interpretation of that information in the actual clinical context. One must diagnose the potential stroke, for instance, and then request the appropriate imaging study, a prerequisite that – however obvious it sounds – in many cases fails to occur.

Evidence is also a dynamic that changes as discoveries are made and additional knowledge is acquired. The essential need to incorporate the latest knowledge into the guidelines has lagged. In many instances, this is related to studies and results that are underpowered. In other circumstances, it is linked to the reluctance on the part of groups that have a particular interest or bias to participate in well-controlled large clinical trials.

Such disinclination is going to dissipate as payers demand real data. With an underpinning of robust economic incentives, CMS and insurance payers are signaling that they will not accept ad hoc decision making, necessitating institutions and providers to demand proper evidence for particular diagnostic and therapeutic decisions. It is baffling that so little incontrovertible evidence, including data on major and expensive medical conditions, exists today. There are many obvious examples of this issue, but the one that perhaps most dramatically demonstrates the point is the treatment of prostate cancer. First, what is the appropriate therapy for definite prostate cancer: watchful waiting, prostatectomy, radioactive seeds, external radiation, proton beam therapy, high frequency ultrasound, etc.? Even if one decides on surgery, is the costlier robotic surgery that much better than standard surgery? The discussion is further complicated by the PSA test itself, which lacks specificity, leading to the recent recommendation by the US Preventive Services Task Force that widespread PSA testing did not save enough lives to justify the considerable medical consequences of treatment. Even for such a common condition, in other words, there is disturbingly little data available.

An equally crucial yet less recognized and more difficult problem is the inability to effect change in the face of strong evidence. This failure – attributable to inertia and lack of knowledge on the part of both physicians and institutions – is bound to improve, at least in part, with the

implementation of the electronic health record, where evidence-based medicine will be embedded in alerts and accountability for decisions will be demanded.

This book will play a major positive role by informing clinicians about the quality of information they can depend on to enable evidence-based decision making. Neuroclinicians should welcome its publication. Strong outcome measures provide happy ways of doing things. Vigorous outcome measures support the value and utility of imaging. This is essential in the face of the increasing scrutiny by payers: the more available the information is, the easier the justification for the expense of imaging and the role of imagers will be.

Evidence-Based Neuroimaging Diagnosis and Treatment presents its readers with a logical introduction to understanding the foundation of evidence in medicine and then focuses on specific issues related to neuroradiology. It will begin an obligatory confrontation with the data that clinicians must gather in order to facilitate value-based decisions. Readers will gain significant appreciation of the data as it exists today, making the case for particular algorithms as well as the precise role of imaging. This is a major accomplishment and one that will benefit neuroradiologists, neurologists, neurosurgeons, and others with interests in clinical neuroscience.

Hats off to the authors who have presciently identified a need and who, with solid expertise and trenchant analysis, have produced a most worthy and requisite addition to the literature. This book will be the beginning of an ever-increasing torrent of texts and manuscripts focused on value and evidence. The era of evidence-based medicine has arrived – thank goodness!

<div align="right">

Robert I. Grossman M.D.
The Saul J. Farber Dean and CEO
NYU Langone Medical Center

</div>

Preface

All is flux, nothing stays still.
Nothing endures but change.
Heraclitus, 540–480 B.C.

Medical imaging has grown exponentially in the last three decades with the development of many promising and often noninvasive diagnostic studies and therapeutic modalities. In no other area have these changes been more dramatic than in neuroimaging. The corresponding medical literature has also exploded in volume and can be overwhelming to physicians. In addition, the literature varies in scientific rigor and clinical applicability. The purpose of this book is to employ stringent evidence-based medicine criteria to systematically review the evidence defining the appropriate use of medical imaging and to present to the reader a concise summary of the best medical imaging choices for patient care.

The initial book chapters discuss the principles of evidence-based imaging and critical assessment of the literature. This book also includes important chapters on the economic impact, regulatory impact, and medicolegal implications of evidence-based imaging. Given the increased awareness and concern of radiation exposure from medical imaging, a dedicated chapter discussing the current evidence and its implications is presented. The rest of this book covers the most prevalent central nervous system, spine, and neck diseases in developed countries. Most of the chapters have been written by radiologists and imagers in close collaboration with clinical physicians and surgeons to provide a balanced perspective of the different medical topics. In addition, we address in detail both adult and pediatric issues. We cannot answer all questions – medical imaging is a delicate balance of science and art, often without adequate data for guidance – but we can empower the reader with the current evidence supporting medical imaging.

To make this book user friendly and to enable fast access to pertinent information, we have organized all of the chapters in the same format. The chapters are framed around important and provocative clinical questions relevant to the physician's daily practice. A short table of contents at the beginning of each chapter helps three different tiers of users: (1) the busy physician searching for quick guidance, (2) the physician seeking deeper understanding, and (3) the medical-imaging researcher requiring a comprehensive resource. Key points and summarized answers to the important clinical issues are provided at the beginning of the chapters, so the busy

clinician can understand the most important evidence-based imaging data in seconds. Each important question and summary is followed by a detailed discussion of the supporting evidence so that the physician seeking greater depth can have a clear understanding of the science behind the evidence.

In each chapter, the evidence discussed is presented in tables and figures that provide an easy review in the form of summary tables and flowcharts. The imaging case series highlights the strengths and limitations of the different imaging studies with vivid examples. Toward the end of the chapters, the best imaging protocols are described to ensure that the imaging studies are well standardized and done with the highest available quality. The final section of the chapters is Future Research, in which provocative questions are raised for physicians and nonphysicians interested in advancing medical imaging.

Not all research and not all evidence are created equal. Accordingly, throughout this book, we use a four-level classification detailing the strength of the evidence based on the Oxford criteria: level I (strong evidence), level II (moderate evidence), level III (limited evidence), and level IV (insufficient evidence). The strength of the evidence is presented in parenthesis throughout the chapter, and so the reader gets immediate feedback on the weight of the evidence behind each topic.

Finally, we had the privilege of working with a group of outstanding contributors from major medical centers and universities in North America, Europe, Asia, and Australia. We believe that the authors' expertise, breadth of knowledge, and thoroughness in writing the chapters provide a valuable source of information and can guide decision making for physicians and patients. In addition to guiding practice, the evidence summarized in the chapters may have policy-making and public health implications. We hope that this book highlights key points and generates discussion, promoting new ideas for future research. Finally, regardless of the endless hours spent researching the multiple topics in depth, evidence-based imaging remains a work in progress. We value your suggestions and comments on how to improve this book. Please email them to us and the authors so that we can bring you the best of the evidence over the years.

February 2013   L. Santiago Medina, Miami, USA

Pina C. Sanelli, New York, USA

Jeffrey G. Jarvik, Seattle, USA

Biography

L. Santiago Medina Division of Neuroradiology-Neuroimaging, Department of Radiology, Miami Children's Hospital, Miami, FL, USA

Herbert Wertheim College of Medicine, Florida International University, Miami, FL, USA

Former Lecturer in Radiology, Harvard Medical School, Boston, MA, USA

Dr. Santiago Medina is a pediatric radiologist and neuroradiologist at Miami Children's Hospital, Miami, Florida, USA. Currently, he is codirector of the Division of Neuroradiology and cofounder and director of the International Health Outcomes, Policy and Economics Center (HOPE) and clinical professor of radiology at Florida International University (FIU). Dr. Medina is board certified in diagnostic radiology, pediatric radiology, and neuroradiology by the American Board of Radiology. He graduated from the Institute of Health Sciences, CES University, Medellin, Colombia. Dr. Medina completed his radiology residency in the Mallinckrodt Institute of Radiology, Washington University Medical Center, St. Louis, Missouri. He completed both fellowships for pediatric radiology and pediatric neuroradiology at Children's Hospital, Harvard Medical School, Boston, Massachusetts in 1997. Dr. Medina has received numerous prestigious awards including the Scientific Exhibit Cum Laude Award from the Radiological Society of North America (RSNA), the Roentgen Fellow Research Award from the Radiological Society of North America (RSNA) Research and

Education Fund, Outstanding Researcher and Professor from the U.S. Immigration and Naturalization Service, General Electric-Association of University Radiologists Fellow, and the American Society of Neuroradiology (ASNR) Health Services and Outcomes Scholar. He has also a master's degree in public health with concentration in health care management from the Harvard School of Public Health. Dr. Medina has received multiple grants, including grants from the U.S. Department of Defense. He is an expert on evidence-based imaging and research on functional MRI and advanced nueroimaging. Dr. Medina has held various visiting professorships in Children's Hospital Medical Center in Cincinnati, Ohio; Columbia University; Boston University; Malaysia; Hospital for Sick Children, Toronto, Canada; and South Africa. He was the invited/named lecturer of the Dr. Donald Altman Annual Lecture in the Miami Children's Hospital Pediatric Course. Dr. Medina has written more than 50 peer-reviewed scientific manuscripts. He is the author of four books and co-series editor of Springer's *Evidence-Based Imaging*.

Pina C. Sanelli Department of Radiology, Weill Cornell Medical College/ NewYork-Presbyterian Hospital, New York, NY, USA

Pina C. Sanelli, M.D., M.P.H., is an associate professor of radiology and public health at the Weill Cornell Medical College. She also serves as the associate chairman for Practice Quality Improvement and director of the Fellowship Training Program in Neuroradiology at the NewYork-Presbyterian Hospital.

Dr. Sanelli obtained her medical degree from SUNY at Buffalo School of Medicine and Biomedical Sciences. She completed residency training in diagnostic radiology at North Shore University Hospital and fellowship training in neuroradiology at the Massachusetts General Hospital. She is board certified by the American Board of Radiology with Certificate of Added Qualifications in Neuroradiology. Dr. Sanelli obtained a Masters degree in Public Health from Harvard University School of Public Health. She was awarded the GE-AUR Radiology Research Academic Fellowship (GERRAF) and the Scholar's Award from the American Society of Neuroradiology (ASNR).

Her research focused on technology assessment of CT perfusion imaging in aneurysmal subarachnoid hemorrhage and its clinical effectiveness. Dr. Sanelli has also been awarded several private foundation grants for her work and is currently the principal investigator on an NIH-funded prospective clinical trial in the neuro-intensive care unit for outcomes research on CT perfusion imaging in aneurysmal subarachnoid hemorrhage.

Dr. Sanelli is well known in the field of health services and comparative effectiveness research. Her currently funded NIH grant includes performing a cost-effectiveness analysis of CT perfusion imaging in aneurysmal subarachnoid hemorrhage to assess its added value in this population. Dr. Sanelli serves on the executive board for the Radiology Alliance for Health Services Research (RAHSR). She also serves on the research committee and grant reviewer for the American Society of Neuroradiology (ASNR), Radiological Society of North America (RSNA), and the American Roentgen Ray Society (ARRS). She is currently the chairperson of the evidence-based medicine and research committees of the ASNR. She has been an invited speaker and author on the topic of evidence-based imaging. Dr. Sanelli now serves as the health care and socioeconomics editor of the American Journal of Neuroradiology (AJNR).
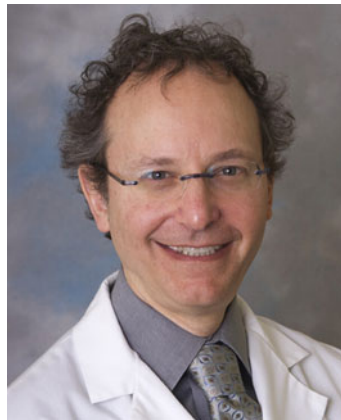
Jeffrey G. Jarvik Department of Radiology, Harborview Medical Center, University of Washington, Seattle, WA, USA

Dr. Jarvik is a professor of radiology and neurological surgery as well as adjunct professor of health services in the School of Public Health and adjunct professor of pharmacy in the School of Pharmacy at the University of Washington. He also serves as director of the Comparative Effectiveness, Cost and Outcomes Research Center (CECORC).

Dr. Jarvik attended the University of California, San Diego, for both undergraduate education and medical schooling. He then did his residency in diagnostic radiology and fellowship in neuroradiology at the Hospital of the University of Pennsylvania. He obtained his M.P.H. from the University of Washington in health services while a Robert Wood Johnson Clinical Scholar. His studies in the RWJ Clinical Scholars Program focused on

the evaluation of diagnostic and therapeutic technologies related to low back pain, with Richard A. Deyo, M.D., M.P.H., as his primary mentor. Dr. Jarvik is a former recipient of the GE-AUR Radiology Research Academic Fellowship (GERRAF), a career development award.

Dr. Jarvik is an internationally recognized expert in MR imaging of the spine as well as in the field of health services and comparative effectiveness research as it relates to radiology. As the director of CECORC, he has led or collaborated on multiple technology assessments using multidisciplinary teams involving a wide variety of medical and surgical specialties as well as nonclinical disciplines of biostatistics, economics, epidemiology, and health services. He has extensive practical experience in the conduct of both observational as well as randomized controlled trials of devices and procedures. He has published studies focused on technology assessment and back pain in numerous prestigious journals including JAMA, The Lancet, and the New England Journal of Medicine.

Dr. Jarvik is the only radiologist to be selected as a principal investigator (PI) for the NIH Collaboratory, an initiative that is part of the NIH Director's fund to foster pragmatic clinical trials. He was also the PI of the Back pain Outcomes using Longitudinal Data (BOLD) project, a $10 million project funded by the Agency for Healthcare Research and Quality that established a large registry to investigate diagnostic and therapeutic interventions in seniors with low back pain.

Contents

Contributors

Nolan Altman Department of Radiology, Miami Children's Hospital, Miami, FL, USA

Yoshimi Anzai Department of Radiology, University of Washington, Seattle, WA, USA

Kimberly E. Applegate Department of Radiology and Imaging Sciences, Emory University School of Medicine, Atlanta, GA, USA

Michal Arkuszewski Department of Neurology, Medical University of Silesia, Central University Hospital, Katowice, Poland

Stephen Ashwal Department of Pediatrics, Loma Linda University School of Medicine, Loma Linda, CA, USA

Amit Balgude Department of Interventional Neuroradiology, Ronald Reagan UCLA Medical Center, Los Angeles, CA, USA

Martha Ballesteros Department of Radiology, Miami Children's Hospital, Miami, FL, USA

Alex M. Barrocas Department of Radiology, Mount Sinai Medical Center, Miami Beach, FL, USA

Byron Bernal Department of Radiology, Miami Children's Hospital, Miami, FL, USA

C. Craig Blackmore Department of Radiology, Virginia Mason Medical Center, Seattle, WA, USA

Nikolai Bogduk Newcastle Bone and Joint Institute, Royal Newcastle Center, University of Newcastle, Newcastle, NSW, Australia

Thomas C. Bryson Department of Radiology, University of Michigan Health System, Ann Arbor, MI, USA

John A. Carrino Russell H. Morgan Department of Radiology and Radiological Science, Johns Hopkins University School of Medicine, Baltimore, MD, USA

Soonmee Cha Department of Radiology and Biomedical Imaging, University of California San Francisco Medical Center, San Francisco, CA, USA

Hui Jie Jenny Chen Department of Neuroradiology, Massachusetts General Hospital, Boston, MA, USA

Daniel Cooke Department of Radiology and Biomedical Imaging, University of California San Francisco, San Francisco, CA, USA

Gary H. Danton Department of Radiology, University of Miami Miller School of Medicine, Miami, FL, USA

Melissa M. Debayle Department of Radiology, Mount Sinai Medical Center, Miami Beach, FL, USA

Colin P. Derdeyn Mallinckrodt Institute of Radiology, Washington University School of Medicine, St. Louis, MO, USA

Manjiri Dighe Department of Radiology, University of Washington Medical Center, Seattle, WA, USA

Brian Eichinger Department of Radiology, University of Texas, Health Science Center at San Antonio, San Antonio, TX, USA

Kathleen R. Fink Department of Radiology, University of Washington, Seattle, WA, USA

Andria L. Ford Department of Neurology, Washington University School of Medicine, St. Louis, MO, USA

Donald P. Frush Department of Radiology, Duke Medical Center, Durham, NC, USA

Matakazu Furukawa Department of Radiology, University of Washington, Seattle, WA, USA

Jan Frank Gerstenmaier Department of Radiology, St. Vincent's University Hospital, Dublin, Ireland

Basavaraj Ghodke Department of Radiology and Neurological Surgery, University of Washington/Harborview Medical Center, Seattle, WA, USA

Y. Pierre Gobin Department of Neurosurgery, Weill Cornell Medical College/NewYork-Presbyterian Hospital, New York, NY, USA

Edward D. Greenberg Department of Neurosurgery, Weill Cornell Medical College/NewYork-Presbyterian Hospital, New York, NY, USA

Brian E. Grottkau Department of Orthopaedic Surgery, Massachusetts General Hospital for Children, Harvard University, Boston, MA, USA

Juan E. Gutierrez Department of Radiology, University of Texas, Health Science Center at San Antonio, San Antonio, TX, USA

Van Halbach Department of Radiology and Biomedical Imaging, University of California San Francisco, San Francisco, CA, USA

Danial K. Hallam Department of Radiology, Harborview Medical Center, University of Washington, Seattle, WA, USA

Gary L. Hedlund Department of Medical Imaging, University of Utah, Primary Children's Medical Center, Salt Lake City, UT, USA

William Hollingworth School of Social and Community Medicine, University of Bristol, Bristol, UK

Barbara A. Holshouser Department of Radiology/MRI, Loma Linda University Medical Center, Loma Linda, CA, USA

Ivan K. Ip Department of Radiology, Harvard Medical School, Center for Evidence-Based Imaging, Brigham and Women Hospital, Brookline, MA, USA

Alan Jackson Wolfson Molecular Imaging Centre, University of Manchester, Withington, Manchester, UK

Diego Jaramillo Department of Radiology, The Children's Hospital of Philadelphia, affiliated with The Perelman School of Medicine at the University of Pennsylvania, Philadelphia, PA, USA

Jeffrey G. Jarvik Department of Radiology, Harborview Medical Center, University of Washington, Seattle, WA, USA

Annette J. Johnson Department of Radiology, Wake Forest School of Medicine, Winston-Salem, NC, USA

Yasha Kadkhodayan Mallinckrodt Institute of Radiology, Washington University School of Medicine, St. Louis, MO, USA

David F. Kallmes Department of Neuroradiology, Mayo Clinic, Rochester, MN, USA

Kejal Kantarci Division of Neuroradiology, Department of Radiology, Mayo Clinic, Rochester, MN, USA

Geetika Khanna Mallinckrodt Institute of Radiology, Washington University, St. Louis, MO, USA

Ramin Khorasani Department of Radiology, Harvard Medical School, Brigham and Women's Hospital, Boston, MA, USA

Aoife Kilcoyne Department of Radiology, St. Vincent's University Hospital, Dublin, Ireland

Jaroslaw Krejza Department of Radiology, University of Pennsylvania Health System, Perelman School of Medicine at the University of Pennsylvania, Philadelphia, PA, USA

College of Medicine, Al–Imam Mohamed bin Saud Islamic University, Riyadh, Saudi Arabia

Jill E. Langer Department of Radiology, University of Pennsylvania Health System, Perelman School of Medicine at the University of Pennsylvania, Philadelphia, PA, USA

David B. Larson Department of Radiology, Cincinnati Children's Hospital Medical Center, Cincinnati, OH, USA

Kim O. Learned Department of Radiology, University of Pennsylvania Health System, Perelman School of Medicine at the University of Pennsylvania, Philadelphia, PA, USA

Jin-Moo Lee Department of Neurology, Washington University School of Medicine, St. Louis, MO, USA

Weili Lin Biomedical Research Imaging Center, University of North Carolina at Chapel Hill, Chapel Hill, NC, USA

Ken F. Linnau Department of Radiology, Harborview Medical Center, University of Washington, Seattle, WA, USA

Laurie A. Loevner Department of Radiology, University of Pennsylvania Health System, Perelman School of Medicine at the University of Pennsylvania, Philadelphia, PA, USA

Michael L. Loftus Department of Radiology, Weill Cornell Medical College/NewYork-Presbyterian Hospital, New York, NY, USA

Kelly M. Malloy Department of Otolaryngology – Head and Neck Surgery, University of Michigan Health System, Ann Arbor, MI, USA

Dermot E. Malone Department of Radiology, St. Vincent's University Hospital, Dublin, Ireland

Amit M. Mathur Department of Pediatrics/Newborn Medicine, Washington University School of Medicine in St. Louis, St. Louis Children's Hospital, St. Louis, MO, USA

Robert C. McKinstry III Departments of Radiology and Pediatrics, Washington University School of Medicine in St. Louis, St. Louis Children's Hospital, St. Louis, MO, USA

L. Santiago Medina Division of Neuroradiology-Neuroimaging, Department of Radiology, Miami Children's Hospital, Miami, FL, USA

Herbert Wertheim College of Medicine, Florida International University, Miami, FL, USA

Former Lecturer in Radiology, Harvard Medical School, Boston, MA, USA

Elias R. Melhem Department of Radiology, University of Pennsylvania, Philadelphia, PA, USA

Toshio Moritani Department of Radiology, University of Iowa Hospitals and Clinics, Iowa City, IA, USA

Suresh K. Mukherji Department of Radiology, University of Michigan Health System, Ann Arbor, MI, USA

Felipe Munera Department of Radiology, University of Miami Miller School of Medicine-Jackson Memorial Hospital/University of Miami Medical System, Miami, FL, USA

Udochukwu E. Oyoyo Department of Biophysics and Bioengineering, Loma Linda University, Loma Linda, CA, USA

Esperanza Pacheco-Jacome Department of Radiology, Miami Children's Hospital, Miami, FL, USA

C. Douglas Phillips Department of Radiology, Weill Cornell Medical College/NewYork-Presbyterian Hospital, New York, NY, USA

Tina Young Poussaint Department of Radiology, Harvard Medical School, Children's Hospital Boston, Boston, MA, USA

Prashant Raghavan Department of Radiology, University of Virginia, Charlottesville, VA, USA

James G. Ravenel Department of Medicine, Medical University of South Caroclina, Charleston, SC, USA

Annemarie Relyea-Chew Department of Radiology, University of Washington, Seattle, WA, USA

Bahman Roudsari Department of Radiology, University of Washington, Seattle, WA, USA

Marla B. K. Sammer Department of Diagnostic Radiology, Children's at Erlanger, Chattanooga, TN, USA

Pina C. Sanelli Department of Radiology, Weill Cornell Medical College/ NewYork-Presbyterian Hospital, New York, NY, USA

Yutaka Sato Department of Radiology, University of Iowa Hospitals and Clinics, Iowa City, IA, USA

Pamela W. Schaefer Department of Neuroradiology, Massachusetts General Hospital, Boston, MA, USA

Leili Shahgholi Department of Neuroradiology, Mayo Clinic, Rochester, MN, USA

Gerard A. Silvestri Department of Medicine, Medical University of South Caroclina, Charleston, SC, USA

Justin B. Smith Department of Radiology, Virginia Mason Medical Center, Seattle, WA, USA

Maciej Swiat Department of Neuroscience, University Hospitals Conventry and Warwickshire, Coventry, UK

Maciej Tomaszewski Department of Radiology, University of Pennsylvania, Philadelphia, PA, USA

Karen A. Tong Department of Neuroscience, Loma Linda University Medical Center, Loma Linda, CA, USA

Elza Vasconcellos Department of Neurology, Miami Children's Hospital, Miami, FL, USA

Daniel N. Vinocur Rady Children's Hospital, San Diego, CA, USA

Department of Radiology, University of California, San Diego, CA, USA

Katie D. Vo Washington University School of Medicine, Mallinckrodt Institute of Radiology, St. Louis, MO, USA

Joanna M. Wardlaw Brain Research Imaging Centre, University of Edinburgh and NHS Lothian, Edinburgh, UK

Jessica R. L. Warsch Medical Student, Department of Medical Education—MD/PhD Program, University of Miami Miller School of Medicine, Miami, FL, USA

Elysa Widjaja Department of Diagnostic Imaging, University of Toronto/ Hospital for Sick Children, Toronto, ON, Canada

William Young Department of Anesthesia and Perioperative Care, University of California San Francisco, San Francisco, CA, USA

Michael E. Zapadka Department of Radiology, Wake Forest School of Medicine, Winston-Salem, NC, USA

Part I

Evidence-Based Imaging: Overview

Evidence-Based Imaging: Principles

L. Santiago Medina, C. Craig Blackmore, and
Kimberly E. Applegate

Contents

L.S. Medina (✉)
Division of Neuroradiology-Neuroimaging, Department of Radiology, Miami Children's Hospital, Miami, FL, USA

Herbert Wertheim College of Medicine, Florida International University, Miami, FL, USA

Former Lecturer in Radiology, Harvard Medical School, Boston, MA, USA
e-mail: smedina@post.harvard.edu; Santiago.medina@mch.com

C.C. Blackmore
Department of Radiology, Virginia Mason Medical Center, Seattle, WA, USA
e-mail: craig.blackmore@vmmc.org

K.E. Applegate
Department of Radiology and Imaging Sciences, Emory University School of Medicine, Atlanta, GA, USA
e-mail: Keapple@emory.edu

Medicine is a science of uncertainty and an art of probability.
Sir William Osler

Discussion of Issues

What Is Evidence-Based Imaging?

The standard medical education in Western medicine has emphasized skills and knowledge learned from experts, particularly those encountered in the course of postgraduate medical education, and through national publications and meetings. This reliance on experts, referred to by Dr. Paul Gerber of Dartmouth Medical School as "eminence-based medicine" [1], is based on the construct that the individual practitioner, particularly a specialist devoting extensive time to a given discipline, can arrive at the best approach to a problem through his or her experience. The practitioner builds up an experience base over years and digests information from national experts who have a greater base of experience due to their focus in a particular area. The evidence-based imaging (EBI) paradigm, in contradistinction, is based on the precept that a single practitioner cannot through experience alone arrive at the best course of action. Assessment of appropriate medical care should instead be derived through an evidence-based process. The role of the practitioner, then, is not simply to accept information from an expert but rather to assimilate and critically assess the research evidence that exists in the literature to guide a clinical decision [2–4].

Fundamental to the adoption of the principles of EBI is the understanding that medical care is not optimal. The life expectancy at birth in the United States for males and females in 2005 was 75 and 80 years, respectively (Table 1.1). This is slightly lower than the life expectancies in other industrialized nations such as the United Kingdom and Australia (Table 1.1). In fact, the World Health Organization ranks the USA 50th in life expectancy and 72nd in overall health. The United States spent at least 15.2 % of the gross domestic product (GDP) in order to achieve this life expectancy. This was significantly more than the United Kingdom and Australia, which spent

about half that (Table 1.1). In addition, the US per capita health expenditure was $6,096, which was twice the expenditure in the United Kingdom or Australia. In short, the United States spends significantly more money and resources than other industrialized countries to achieve a similar or slightly worse outcome in life expectancy. This implies that a significant amount of resources is wasted in the US health-care system. In 2007, the United States spent $2.3 trillion in health care or 16 % of its GDP. By 2016, the US health percent of the GDP is expected to grow to 20 % or $4.2 trillion [5]. Recent estimates prepared by the Commonwealth Fund Commission (USA) on a High Performance Health System indicate that $1.5 trillion could be saved over a 10-year period if a combination of options, including evidence-based medicine and universal health insurance, was adopted [6].

Simultaneous with the increase in health-care costs has been an explosion in available medical information. The National Library of Medicine PubMed search engine now lists over 18 million citations. Practitioners cannot maintain familiarity with even a minute subset of this literature without a method of filtering out publications that lack either relevance or appropriate methodological quality. EBI is a promising method of identifying appropriate information to guide practice and to improve the efficiency and effectiveness of imaging.

Evidence-based imaging is defined as medical decision making based on clinical integration of the best medical imaging research evidence with the physician's expertise and with patient's expectations [2–4]. The best medical imaging research evidence often comes from the basic sciences of medicine. In EBI, however, the basic science knowledge has been translated into patient-centered clinical research, which determines the accuracy and role of diagnostic and therapeutic imaging in patient care [3]. New research may make current diagnostic tests obsolete and provide evidence that new tests are more

Table 1.1 Life expectancy and health-care spending in three developed countries

	Life expectancy at birth (2009)		Percentage of GDP in health care (2008) (%)	Per capita health expenditure (2008)
	Male	Female		
United States	75.7	80.6	16.4	$7,720
United Kingdom	78.3	82.5	8.8	$3,281
Australia	79.3	83.9	8.7	$3,445

Source: Organization for Economic Cooperation and Development: http://stats.oecd.org/Index.aspx?DataSetCode=HEALTH

Reprinted, with revisions, with kind permission of Springer Science+Business Media. Medina LS, Blackmore CC, Applegate KE. Principles of evidence-based imaging. In: Medina LS, Applegate KE, Blackmore CC editors. Evidence-based imaging in pediatrics: optimizing imaging in pediatric patient care. New York: Springer Science+Business Media; 2010.

GDP gross domestic product

accurate, less invasive, safer, and less costly [3]. The physician's expertise entails the ability to use the referring physician's clinical skills and past experience to rapidly identify individuals who will benefit from the diagnostic information of an imaging test [4]. Patient's expectations are important because each individual has values and preferences that should be integrated into the clinical decision making [3]. When these three components of medicine come together, clinicians, imagers and patients form a diagnostic team, which will optimize clinical outcomes and quality of life for our patients.

The Evidence-Based Imaging Process

The EBI process involves a series of steps: (a) formulation of the clinical question, (b) identification of the medical literature, (c) assessment of the literature, (d) types of economic analyses in medicine, (e) summary of the evidence, and (f) application of the evidence to derive an appropriate clinical action. This book is designed to bring the EBI process to the clinician and imager in a user-friendly way. This introductory chapter details each of the steps in the EBI process. Chapter 2, "Assessing the Imaging Literature: Understanding Error and Bias" discusses how to critically assess the literature. The rest of the book makes available to practitioners the EBI approach to important neuroimaging issues. Each chapter addresses common disorders encountered by the neuroradiologist evaluating the brain,

spine, and head and neck. Relevant clinical questions are delineated, and then each chapter discusses the results of the critical analysis of the identified literature. Finally, we provide simple recommendations for the various clinical questions, including the strength of the evidence that supports these recommendations.

(a) Formulating the Clinical Question

The first step in the EBI process is formulation of the clinical question. The entire process of EBI arises from a question that is asked in the context of clinical practice. However, often formulating a question for the EBI approach can be more challenging than one would believe intuitively. To be approachable by the EBI format, a question must be specific to a clinical situation, a patient group, and an outcome or action. For example, it would not be appropriate to simply ask which imaging technique is better – computed tomography (CT) or radiography. The question must be refined to include the particular patient population and the action that the imaging will be used to direct. One can refine the question to include a particular population (which imaging technique is better in pediatric victims of high-energy blunt trauma) and to guide a particular action or decision (to exclude the presence of unstable cervical spine fracture). The full EBI question then becomes, in pediatric victims of high-energy blunt trauma, which imaging modality is preferred, CT or radiography, to exclude the presence of unstable cervical

spine fracture? This book addresses questions that commonly arise when employing an EBI approach for conditions encountered by neuroradiologists. These questions and issues are detailed at the start of each chapter. One popular method used to teach how to develop a good clinical question is called the "PICO" (*P*atient, *I*ntervention, *C*omparison, *O*utcome) format. This method provides structure to formulate the necessary elements for a good clinical question that includes information about the patient, the problem to be solved, the intervention (such as a diagnostic test) and its comparison intervention (perhaps a newer diagnostic test), and the outcome of interest (e.g., what the patient wants, or is concerned about).

(b) Identifying the Medical Literature

The process of EBI requires timely access to the relevant medical literature to answer the question. Fortunately, massive on-line bibliographical references such as PubMed, Embase, Cochrane, and the Web of Science databases are available. In general, titles, indexing terms, abstracts, and often the complete text of much of the world's medical literature are available through these on-line sources. Also, medical librarians are a potential resource to aid identification of the relevant imaging literature. A limitation of today's literature data sources is that often too much information is available and too many potential resources are identified in a literature search. There are currently over 50 radiology journals, and imaging research is also frequently published in journals from other medical subspecialties. We are often confronted with more literature and information than we can process. The greater challenge is to sift through the literature that is identified to select that which is appropriate.

(c) Assessing the Literature

To incorporate evidence into practice, the clinician must be able to understand the published literature and to critically evaluate the strength of the evidence. In this introductory chapter on the process of EBI, we focus on discussing types of research studies.

Chapter 2, "Assessing the Imaging Literature: Understanding Error and Bias" is a detailed discussion of the issues in determining the validity and reliability of the reported results.

1. What Are the Types of Clinical Studies?

An initial assessment of the literature begins with determination of the type of clinical study: descriptive, analytical, or experimental [7]. *Descriptive* studies are the most rudimentary, as they only summarize disease processes as seen by imaging, or discuss how an imaging modality can be used to create images. Descriptive studies include case reports and case series. Although they may provide important information that leads to further investigation, descriptive studies are not usually the basis for EBI.

Analytic or *observational* studies include cohort, case–control, and cross-sectional studies (Table 1.2). Cohort studies are defined by risk factor status, and case–control studies consist of groups defined by disease status [8]. Both case–control and cohort studies may be used to define the association between an intervention, such as an imaging test, and patient outcome [9]. In a cross-sectional (prevalence) study, the researcher makes all of his measurements on a single occasion. The investigator draws a sample from the population (i.e., headache in 15–45-year-old females) and determines distribution of variables within that sample [7]. The structure of a cross-sectional study is similar to that of a cohort study except that all pertinent measurements (i.e., number of head CT and MRI examinations) are made at once, without a follow-up period. Cross-sectional studies can be used as a major source for health and habits of different populations and countries, providing estimates of such parameters as the prevalence of stroke, brain tumors, and congenital anomalies [7, 10].

In *experimental studies* or *clinical trials*, a specific intervention is performed

Table 1.2 Study design

	Prospective follow-up	Randomization of subjects	Controls
Case report or series	No	No	No
Cross-sectional study	No	No	Yes
Case–control study	No	No	Yes
Cohort study	Yes/no	No	Yes
Randomized controlled trial	Yes	Yes	Yes

Reprinted with the kind permission of Springer Science +Business Media from Medina LS, Blackmore CC. Evidence-based imaging: optimizing imaging in patient care. New York: Springer Science+Business Media; 2006

and the effect of the intervention is measured by using a control group (Table 1.2). The control group may be tested with a different diagnostic test and treated with a placebo or an alternative mode of therapy [7, 11]. Clinical trials are epidemiologic designs that can provide data of high quality that resemble the controlled experiments done by basic science investigators [8]. For example, clinical trials may be used to assess new diagnostic tests (e.g., CT perfusion imaging for stroke diagnosis and management) or new interventional procedures (e.g., catheter embolization for cerebral aneurysms).

Studies are also traditionally divided into retrospective and prospective (Table 1.2) [7, 11]. These terms refer more to the way the data are gathered than to the specific type of study design. In *retrospective studies*, the events of interest have occurred before study onset. Retrospective studies are usually done to assess rare disorders, for pilot studies, and when prospective investigations are not possible. If the disease process is considered rare, retrospective studies facilitate the collection of enough subjects to have meaningful data. For a pilot project, retrospective studies facilitate the collection of preliminary data that can be used to

improve the study design in future prospective studies. The major drawback of a retrospective study is incomplete data acquisition and resultant bias [10]. Case–control studies are usually retrospective because the outcome or disease status needs to have occurred in order to form the comparison groups. For example, in a case–control study, subjects in the case group (patients with hemorrhagic stroke) are compared with subjects in a control group (nonhemorrhagic stroke) to determine factors associated with hemorrhage (e.g., hypertension, duration of symptoms, presence of prior neurologic deficit) [10].

In *prospective studies*, the event of interest transpires after study onset. Prospective studies, therefore, are the preferred mode of study design, as they facilitate better control of the design (accounting for potential bias) and the quality of the data acquired [7]. Prospective studies, even large studies, can be performed efficiently and in a timely fashion if done on common diseases at major institutions, as multicenter trials with adequate study populations [12]. The major drawback of a prospective study is the need to make sure that the institution and personnel comply with strict rules concerning consents, protocols, and data acquisition [11]. Persistence and dogged determination are crucial to completing a prospective study. Cohort studies and clinical trials are usually prospective. For example, a cohort study could be performed in children with sickle-cell disease who are poorly compliant with their transfusion therapy in which the risk factor of positive transcranial Doppler studies is correlated with neurocognitive complications, as the patients are followed prospectively over time [10].

The strongest study design is the prospective randomized, blinded clinical trial (Table 1.2) [7]. The randomization process helps to distribute known and

unknown confounding factors, and blinding helps to prevent observer bias from affecting the results [7, 8]. However, there are often circumstances in which it is not ethical or practical to randomize and follow patients prospectively. This is particularly true in rare conditions and in studies to determine causes or predictors of a particular condition [9]. Finally, randomized clinical trials are expensive and may require many years to conduct. Not surprisingly, randomized clinical trials are uncommon in radiology. The evidence that supports much of radiology practice is derived from cohort and other observational studies. More randomized clinical trials are necessary in radiology to provide sound data to use for EBI practice [3]. Also, more "outcomes-based studies" are needed in radiology to generate more relevant EBI data.

2. What Is the Diagnostic Performance of a Test: Sensitivity, Specificity, Positive and Negative Predictive Values, and Receiver Operating Characteristic Curve?

Defining the presence or absence of an outcome (i.e., disease and nondisease) is based on a standard of reference (Table 1.3). While a perfect standard of reference or so-called gold standard can never be obtained, careful attention should be paid to the selection of the standard that should be widely believed to offer the best approximation to the truth [13].

In evaluating diagnostic tests, we rely on the statistical calculations of sensitivity and specificity (see Appendix 1). Sensitivity and specificity of a diagnostic test are based on the two-way (2 × 2) table (Table 1.3). Sensitivity refers to the proportion of subjects with the disease who have a positive test and is referred to as the true positive rate (Fig. 1.1a, b). Sensitivity, therefore, indicates how well a test identifies the subjects with disease [7, 14].

Specificity is defined as the proportion of subjects without the disease who have a negative index test (Fig. 1.1a,b) and is

Table 1.3 Two-way table of diagnostic testing

Test result	Disease (gold standard)	
	Present	Absent
Positive	a (TP)	b (FP)
Negative	c (FN)	d (TN)

Reprinted with the kind permission of Springer Science+Business Media from Medina LS, Blackmore CC. Evidence-based imaging: optimizing imaging in patient care. New York: Springer Science+Business Media; 2006. *FN* false negative, *FP* false positive, *TN* true negative, *TP* true positive

referred to as the true negative rate. Specificity, therefore, indicates how well a test identifies the subjects with no disease [7, 11]. It is important to note that the sensitivity and specificity are characteristics of the test being evaluated and are therefore usually independent of the prevalence (proportion of individuals in a population who have disease at a specific instant) because the sensitivity only deals with the diseased subjects, whereas the specificity only deals with the nondiseased subjects. However, sensitivity and specificity both depend on a threshold point for considering a test positive and hence may change according to which threshold is selected in the study [11, 14, 15] (Fig. 1.1a). Excellent diagnostic tests have high values (close to 1.0) for both sensitivity and specificity. Given exactly the same diagnostic test, and exactly the same subjects confirmed with the same reference test, the sensitivity with a low threshold is greater than the sensitivity with a high threshold. Conversely, the specificity with a low threshold is less than the specificity with a high threshold (Fig. 1.1b) [14, 15].

The positive predictive value is defined as the probability that a patient will have a disease given that the patient's test is positive. In other words, when a group of patients test positive, we want to know how frequently they will have the disease. The formula for the positive predictive value (PPV) is provided in the table in Appendix 1. Similarly, the negative
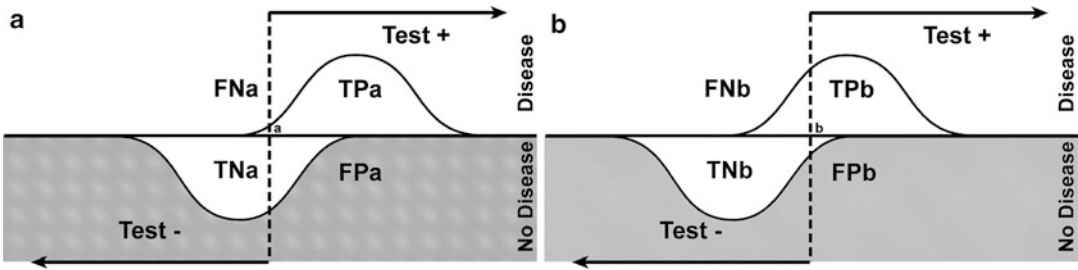
Fig. 1.1 Test with a low (**a**) and high (**b**) threshold. The sensitivity and specificity of a test change according to the threshold selected; hence, these diagnostic performance parameters are threshold dependent. Sensitivity with low threshold (TPa/diseased patients) is greater than sensitivity with a higher threshold (TPb/diseased patients). Specificity with a low threshold (TNa/nondiseased patients) is less than specificity with a high threshold (TNb/nondiseased patients). *FN* false negative, *FP* false positive, *TN* true negative, *TP* true positive (Reprinted with permission of the American Society of Neuroradiology from Medina L. AJNR Am J Neuroradiol 1999; 20:1584–96)

predictive value (NPV) refers to the probability that a group of patients that test negative for a disease or condition will actually not have the disease. It is important to understand that while sensitivity and specificity are relatively independent of disease prevalence, the PPV and NPV are not. Examples 1 and 2 (Appendix 2) provide a demonstration of what happens to the PPV and NPV with a change in disease prevalence. When there is concern about large prevalence effects, the likelihood ratio can be used to estimate the posttest probability of disease. This issue is discussed in the next section.

The effect of threshold on the ability of a test to discriminate between disease and nondisease can be measured by a receiver operating characteristic (ROC) curve [11, 15]. The ROC curve is used to indicate the trade-offs between sensitivity and specificity for a particular diagnostic test and hence describes the discrimination capacity of that test. An ROC graph shows the relationship between sensitivity (*y* axis) and 1 − specificity (*x* axis) plotted for various cutoff points. If the threshold for sensitivity and specificity is varied, an ROC curve can be generated. The diagnostic performance of a test can be estimated by the area under the ROC curve. The steeper the ROC curve, the greater the area and the better the discrimination of the test (Fig. 1.2a–c). A test with perfect discrimination has an area of 1.0, whereas a test with only random discrimination has an area of 0.5 (Fig. 1.2a–c). The area under the ROC curve usually determines the overall diagnostic performance of the test independent of the threshold selected [11, 15]. The ROC curve is threshold independent because it is generated by using varied thresholds of sensitivity and specificity. Therefore, when evaluating a new imaging test, in addition to the sensitivity and specificity, an ROC curve analysis should be done so that the threshold-dependent and threshold-independent diagnostic performance can be fully determined [10].

3. What Are Cost-Effectiveness and Cost–Utility Studies?

Cost-effectiveness analysis (CEA) is a scientific technique used to assess alternative health-care strategies on both cost and effectiveness [16–18]. It can be used to develop clinical and imaging practice guidelines and to set health policy [19]. However, it is not designed to be the final answer to the decision-making process; rather, it provides a detailed analysis of the cost and outcome variables and how they are affected by competing medical and diagnostic choices.
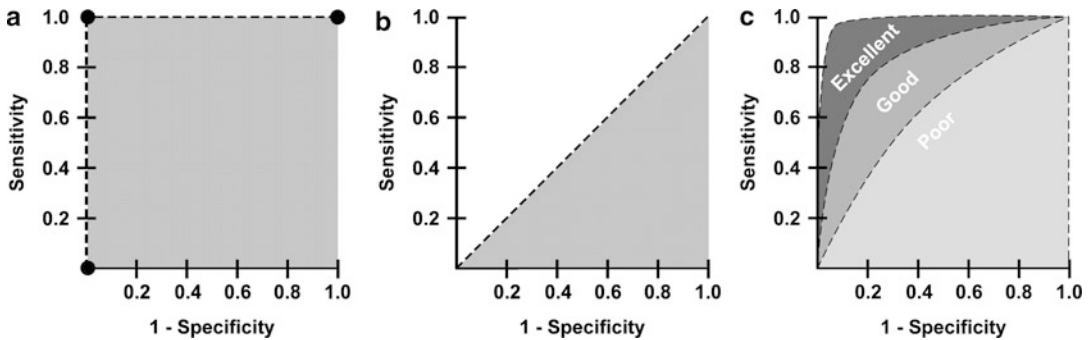
Fig. 1.2 The perfect test (**a**) has an area under the curve (AUC) of 1. The useless test (**b**) has an AUC of 0.5. The typical test (**c**) has an AUC between 0.5 and 1. The greater the AUC (i.e., excellent > good > poor), the better the diagnostic performance (Reprinted with permission of the American Society of Neuroradiology from Medina L. AJNR Am J Neuroradiol. 1999;20: 1584–96)

Health dollars are limited regardless of the country's economic status. Hence, medical decision makers must weigh the benefits of a diagnostic test (or any intervention) in relation to its cost. Health-care resources should be allocated so the maximum health-care benefit for the entire population is achieved [10]. Cost-effectiveness analysis is an important tool to address health cost-outcome issues in a cost-conscious society. Countries such as Australia usually require robust CEA before drugs are approved for national use [10]. Health-care decisions are often made from a "societal perspective," one that looks at a group benefit but which may not result in individual benefit.

Unfortunately, the term *cost-effectiveness* is often misused in the medical literature [20]. To say that a diagnostic test is truly cost-effective, a comprehensive analysis of the entire short- and long-term outcomes and costs needs to be considered. Cost-effectiveness analysis is a technique used to determine which of the available tests or treatments are worth the additional costs [21].

There are established guidelines for conducting robust CEA. The US Public Health Service formed a panel of experts on cost-effectiveness in health and medicine to create detailed standards for cost-effectiveness analysis. The panel's recommendations were published as a book in 1996 [21].

(d) Types of Economic Analyses in Medicine

There are four well-defined types of economic evaluations in medicine: cost-minimization studies, cost–benefit analyses, cost-effectiveness analyses, and cost–utility analyses. They are all commonly lumped under the term *cost-effectiveness analysis*. However, significant differences exist among these different studies.

Cost-minimization analysis is a comparison of the cost of different health-care strategies that are assumed to have identical or similar effectiveness [16]. In medical practice, few diagnostic tests or treatments have identical or similar effectiveness. Therefore, relatively few articles have been published in the literature with this type of study design [22]. For example, a recent study demonstrated that functional magnetic resonance imaging (MRI) and the Wada test have similar effectiveness for language lateralization, but the latter is 3.7 times more costly than the former [23].

Cost–benefit analysis (CBA) uses monetary units such as dollars or euros to compare the costs of a health intervention with its health benefits [16]. It converts all benefits to a cost equivalent and is commonly used in the financial world where the cost and benefits of multiple industries can be changed to only monetary values. One

method of converting health outcomes into dollars is through a contingent valuation or willingness-to-pay approach. Using this technique, subjects are asked how much money they would be willing to spend to obtain, or avoid, a health outcome. For example, a study by Appel et al. [24] found that individuals would be willing to pay $50 for low-osmolar contrast agents to decrease the probability of side effects from intravenous contrast. However, in general, health outcomes and benefits are difficult to transform to monetary units; hence, CBA has had limited acceptance and use in medicine and diagnostic imaging [16, 25].

Cost-effectiveness analysis (CEA) refers to analyses that study both the effectiveness and cost of competing diagnostic or treatment strategies, where effectiveness is an objective measure (e.g., intermediate outcome: number of strokes detected; or long-term outcome: life-years saved). Radiology CEAs often use intermediate outcomes, such as lesion identified, length of stay, and number of avoidable surgeries [16, 18]. However, ideally, long-term outcomes such as life-years saved (LYS) should be used [21]. By using LYS, different health-care fields or interventions can be compared. Given how few exist, there is a need for more "outcome-based studies" in radiology and the imaging sciences.

Cost–utility analysis is similar to CEA except that the effectiveness also accounts for quality of life. Quality of life is measured as utilities that are based on patient preferences [16]. The most commonly used utility measurement is the quality-adjusted life year (QALY). The rationale behind this concept is that the QALY of excellent health is more desirable than the same 1 year with substantial morbidity. The QALY model uses preferences with weight for each health state on a scale from 0 to 1, where 0 is death and 1 is perfect health. The utility score for each health state is multiplied by the length of time the patient spends in that specific health state [16, 26]. For example, assume that a patient

with an untreated Chiari I malformation has a utility of 0.8 and he spends 1 year in this health state. The patient with the Chiari I malformation would have a 0.8 QALY in comparison with his neighbor who has a perfect health and hence a 1 QALY.

Cost–utility analysis incorporates the patient's subjective value of the risk, discomfort, and pain into the effectiveness measurements of the different diagnostic or therapeutic alternatives. Ideally, all medical decisions should reflect the patient's values and priorities [26]. That is the explanation of why cost–utility analysis is the preferred method for evaluation of economic issues in health [19, 21]. For example, in low-risk newborns with intergluteal dimple suspected of having occult spinal dysraphism, ultrasound was the most effective strategy with an incremental cost-effectiveness ratio of $55,100 per QALY. In intermediate-risk newborns with low anorectal malformation, however, MRI was more effective than ultrasound at an incremental cost-effectiveness of $1,000 per QALY [27].

Assessment of Outcomes: The major challenge to cost–utility analysis is the quantification of health or quality of life. One way to quantify health is descriptive analyses. By assessing what patients can and cannot do, how they feel, their mental state, their functional independence, their freedom from pain, and any number of other facets of health and well-being that are referred to as domains, one can summarize their overall health status. Instruments designed to measure these domains are called health status instruments. A large number of health status instruments exist, both general instruments, such as the SF-36 [28], and instruments that are specific to particular disease states, such as the Roland scale for back pain. These various scales enable the quantification of health benefit. For example, Jarvik et al. [29] found no significant difference in the Roland score between patients randomized to MRI versus radiography for low back pain, suggesting that MRI was not worth the additional cost.

Assessment of Cost: All forms of economic analysis require assessment of cost. However, assessment of cost in medical care can be confusing, as the term *cost* is used to refer to many different things. The use of charges for any sort of cost estimation, however, is inappropriate. Charges are arbitrary and have no meaningful use. Reimbursements, derived from Medicare and other fee schedules, are useful as an estimation of the amounts society pays for particular health-care interventions. For an analysis taken from the societal perspective, such reimbursements may be most appropriate. For analyses from the institutional perspective or in situations where there are no meaningful Medicare reimbursements, assessment of actual direct and overhead costs may be appropriate [30].

Direct cost assessment centers on the determination of the resources that are consumed in the process of performing a given imaging study, including *fixed costs* such as equipment and *variable costs* such as labor and supplies. Cost analysis often utilizes activity-based costing and time motion studies to determine the resources consumed for a single intervention in the context of the complex health-care delivery system. Activity-based accounting is a type of accounting that assigns costs to each resource activity based on resource consumption, decreasing the amount of indirect costs with this method. Time and motion studies are time-intensive observational methods used to understand and improve work efficiency in a process. *Overhead*, or *indirect cost*, assessment includes the costs of buildings, overall administration, taxes, and maintenance that cannot be easily assigned to one particular imaging study. Institutional cost accounting systems may be used to determine both the direct costs of an imaging study and the amount of institutional overhead costs that should be apportioned to that particular test. For example, Medina et al. [31] studied the total direct costs of the Wada test ($1,130.01 $\pm$ $138.40) and of functional MR imaging ($301.82 $\pm$ $10.65) that were significantly different ($P < .001$).

The cost of the Wada test was 3.7 times higher than that of functional MR imaging.

(e) Summarizing the Data

The results of the EBI process are a summary of the literature on the topic, both quantitative and qualitative. *Quantitative analysis* involves, at minimum, a descriptive summary of the data and may include formal *meta-analysis*, where there is sufficient reliably acquired data. *Qualitative analysis* requires an understanding of error, bias, and the subtleties of experimental design that can affect the quality of study results. Qualitative assessment of the literature is covered in detail in Chap. 2, "Assessing the Imaging Literature: Understanding Error and Bias"; this section focuses on meta-analysis and the quantitative summary of data.

The goal of the EBI process is to produce a single summary of all of the data on a particular clinically relevant question. However, the underlying investigations on a particular topic may be too dissimilar in methods or study populations to allow for a simple summary. In such cases, the user of the EBI approach may have to rely on the single study that most closely resembles the clinical subjects upon whom the results are to be applied or may be able only to reliably estimate a range of possible values for the data.

Often, there is abundant information available to answer an EBI question. Multiple studies may be identified that provide methodologically sound data. Therefore, some method must be used to combine the results of these studies in a summary statement. *Meta-analysis* is the method of combining results of multiple studies in a statistically valid manner to determine a summary measure of accuracy or effectiveness [32, 33]. For diagnostic studies, the summary estimate is generally a summary sensitivity and specificity, or a summary ROC curve.

The process of performing meta-analysis parallels that of performing primary research.

However, instead of individual subjects, the meta-analysis is based on individual studies of a particular question. The process of selecting the studies for a meta-analysis is as important as unbiased selection of subjects for a primary investigation. Identification of studies for meta-analysis employs the same type of process as that for EBI described above, employing Medline and other literature search engines. Critical information from each of the selected studies is then abstracted usually by more than one investigator. For a meta-analysis of a diagnostic accuracy study, the numbers of true positives, false positives, true negatives, and false negatives would be determined for each of the eligible research publications. The results of a meta-analysis are derived not just by simply pooling the results of the individual studies but instead by considering each individual study as a data point and determining a summary estimate for accuracy based on each of these individual investigations. There are sophisticated statistical methods of combining such results [34].

Like all research, the value of a meta-analysis is directly dependent on the validity of each of the data points. In other words, the quality of the meta-analysis can only be as good as the quality of the research studies that the meta-analysis summarizes. In general, a meta-analysis cannot compensate for selection and other biases in the primary data. If the studies included in a meta-analysis are different in some way, or are subject to some bias, then the results may be too heterogeneous to combine in a single summary measure. Exploration for such heterogeneity is an important component of a meta-analysis.

The ideal for EBI is that all practice be based on the information from one or more well-performed meta-analyses. However, there is often too little data or too much heterogeneity to support a formal meta-analysis. Understanding the hierarchy of next best available evidence, and how to find it, is then critical for readers of the literature.

(f) Applying the Evidence

The final step in the EBI process is to apply the summary results of the medical literature to the EBI question. Sometimes the answer to an EBI question is a simple yes or no, as for this question: Does a normal clinical exam exclude unstable cervical spine fracture in patients with minor trauma? Commonly, the answers to EBI questions are expressed as some measure of accuracy. For example, how good is MRI for detecting acute ischemic infarction ($<6\,$h)? The answer is that MRI has an approximate sensitivity of 91 % and specificity of 95 % [35]. However, to guide practice, EBI must be able to answer questions that go beyond simple accuracy; for example, should MRI then be used for the early detection of acute infarct? To answer this question, it is useful to divide the types of literature studies into a *hierarchical framework* [36] (Table 1.4). At the foundation in this hierarchy is assessment of *technical efficacy*: studies that are designed to determine if a particular proposed imaging method or application has the underlying ability to produce an image that contains useful information. Information for technical efficacy would include signal-to-noise ratios, image resolution, and freedom from artifacts. The second step in this hierarchy is to determine if the image predicts the truth. This is the *accuracy* of an imaging study and is generally studied by comparing the test results to a reference standard and defining the sensitivity and the specificity of the imaging test. The third step is to incorporate the physician into the evaluation of the imaging intervention by evaluating the effect of the use of the particular imaging intervention on physician certainty of a given diagnosis (physician decision making) and on the actual management of the patient (*therapeutic efficacy*). Finally, to be of value to the patient, an imaging procedure must not only affect management but also improve outcome. *Patient outcome efficacy* is the determination of the effect of a given imaging intervention on the length and quality of life of a patient. A final efficacy level

Table 1.4 Imaging effectiveness hierarchy

Technical efficacy: production of an image or information
Measures: signal-to-noise ratio, resolution, absence of artifacts
Accuracy efficacy: ability of test to differentiate between disease and nondisease
Measures: sensitivity, specificity, receiver operator characteristic curves
Diagnostic-thinking efficacy: impact of test on likelihood of diagnosis in a patient
Measures: pre- and posttest probability, diagnostic certainty
Treatment efficacy: potential of test to change therapy for a patient
Measures: treatment plan, operative or medical treatment frequency
Outcome efficacy: effect of use of test on patient health
Measures: mortality, quality-adjusted life years, health status
Societal efficacy: appropriateness of test from perspective of society
Measures: cost-effectiveness analysis, cost–utility analysis

Adapted with permission of Fryback DG, Thornbury JR. Med Decis Making. 1991;11:88–94
Reprinted with the kind permission of Springer Science+Business Media from Medina LS, Blackmore CC, Applegate KE. Evidence-based imaging: improving the quality of imaging in patient care. Revised Edition. New York: Springer Science+Business Media; 2011

is that of society, which examines the question of not simply the health of a single patient but that of the health of society as a whole, encompassing the effect of a given intervention on all patients and including the concepts of *cost* and *cost-effectiveness* [36].

Some additional research studies in imaging, such as clinical prediction rules, do not fit readily into this hierarchy. *Clinical prediction rules* are used to define a population in whom imaging is appropriate or can safely be avoided. Clinical prediction rules can also be used in combination with CEA as a way of deciding between competing imaging strategies [37].

Bayes' Theorem, Predictive Values, and the Likelihood Ratio

Ideally, information would be available to address the effectiveness of a diagnostic test on all levels of the hierarchy. Commonly in imaging, however, the only reliable information that is available is that of diagnostic accuracy. It is incumbent upon the user of the imaging literature to determine if a test with a given sensitivity and specificity is appropriate for use in a given clinical situation. To address this issue, the concept of Bayes' theorem is critical. Bayes' theorem is based on the concept that the value of the diagnostic tests depends not only on the characteristics of the test (sensitivity and specificity) but also on the prevalence (pretest probability) of the

disease in the test population. As the prevalence of a specific disease decreases, it becomes less likely that someone with a positive test will actually have the disease and more likely that the positive test result is a false positive. The relationship between the sensitivity and specificity of the test and the prevalence (pretest probability) can be expressed through the use of Bayes' theorem (see Appendix 2) [11, 14] and the likelihood ratio. The positive likelihood ratio (PLR) estimates the likelihood that a positive test result will raise or lower the pretest probability, resulting in estimation of the posttest probability [where $PLR = sensitivity/(1 - specificity)$]. The negative likelihood ratio (NLR) estimates the likelihood that a negative test result will raise or lower the pretest probability, resulting in estimation of the posttest probability [where $NLR = (1 - sensitivity)/specificity$] [38]. The likelihood ratio (LR) is not a probability but a ratio of probabilities. The positive predictive value (PPV) refers to the probability that a person with a positive test result actually has the disease. The negative predictive value (NPV) is the probability that a person with a negative test result does not have the disease. Since the predictive value is determined once the test results are known (i.e., sensitivity and specificity), it actually represents a posttest probability; hence, the posttest probability is determined by both the prevalence (pretest probability) and the test

information (i.e., sensitivity and specificity). Thus, the predictive values are affected by the prevalence of disease in the study population.

A practical understanding of this concept is shown in examples 1 and 2 in Appendix 2. The example shows an increase in the PPV from 0.67 to 0.98 when the prevalence of carotid artery disease is increased from 0.16 to 0.82. Note that the sensitivity and specificity of 0.83 and 0.92, respectively, remain unchanged. If the test information is kept constant (same sensitivity and specificity), the pretest probability (prevalence) affects the posttest probability (predictive value) results.

The concept of diagnostic performance discussed above can be summarized by incorporating the data from Appendix 2 into a nomogram for interpreting diagnostic test results (Fig. 1.3). For example, two patients present to the emergency department complaining of left-sided weakness. The treating physician wants to determine if they have a stroke from carotid artery disease. The first patient is an 8-year-old boy complaining of chronic left-sided weakness. Because of the patient's young age and chronic history, he was determined clinically to be in a low-risk category for carotid artery disease-induced stroke and hence with a low pretest probability of 0.05 (5 %). Conversely, the second patient is 65 years old and is complaining of acute onset of severe left-sided weakness. Because of the patient's older age and acute history, he was determined clinically to be in a high-risk category for carotid artery disease-induced stroke and hence with a high pretest probability of 0.70 (70 %). The available diagnostic imaging test was unenhanced head CT followed by CT angiography. According to the radiologist's available literature, the sensitivity and specificity of these tests for carotid artery disease and stroke were each 0.90. The positive likelihood ratio (sensitivity/1 − specificity) calculation derived by the radiologist was 0.90/(1 − 0.90) = 9. The posttest probability for the 8-year-old patient is therefore 30 % based on a pretest probability of 0.05 and a likelihood ratio of 9 (Fig. 1.3, dashed line A). Conversely, the posttest probability for the 65-year-old patient is greater than 95 % based on a pretest probability
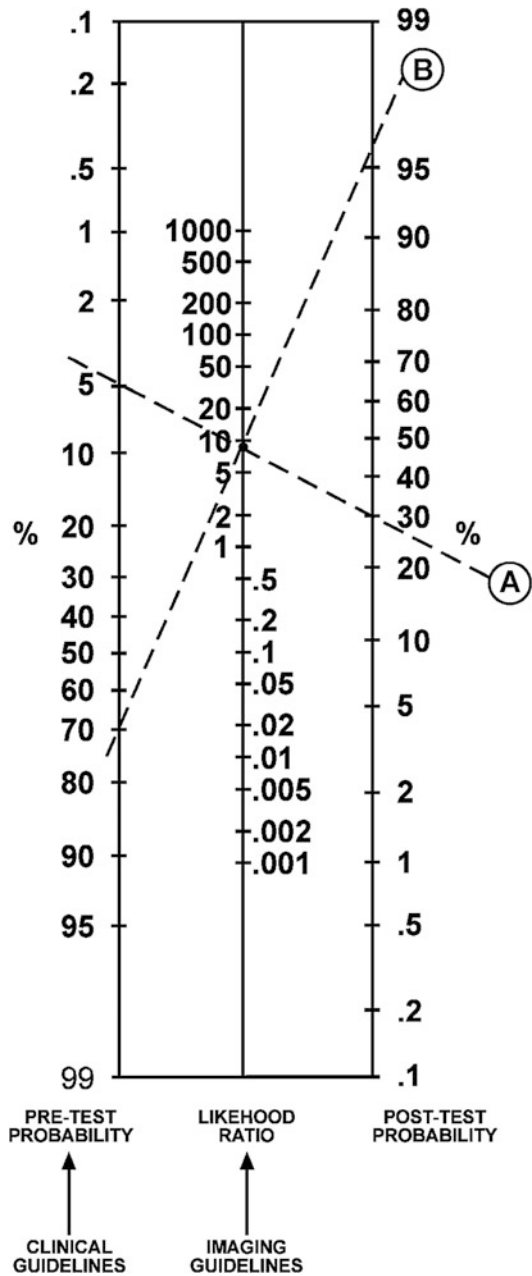
Fig. 1.3 Bayes' theorem nomogram for determining posttest probability of disease using the pretest probability of disease and the likelihood ratio from the imaging test. Clinical and imaging guidelines are aimed at increasing the pretest probability and likelihood ratio, respectively. Worked example is explained in the text (Reprinted with permission from Medina L, Aguirre E, Zurakowski D. Neuroimaging Clin N Am. 2003;13:157–65)

of 0.70 and a positive likelihood ratio of 9 (Fig. 1.3, dashed line B). Clinicians and radiologists can use this scale to understand the probability of disease in different risk groups and for imaging studies with different diagnostic performance.

Jaeschke et al. [38] have proposed a rule of thumb regarding the interpretation of the LR. For PLR, tests with values greater than 10 have a large difference between pretest and posttest probability with conclusive diagnostic impact; values of 5–10 have a moderate difference in test probabilities and moderate diagnostic impact; values of 2–5 have a small difference in test probabilities and sometimes an important diagnostic impact; and values less than 2 have a small difference in test probabilities and seldom have important diagnostic impact. For NLR, tests with values less than 0.1 have a large difference between pretest and posttest probability with conclusive diagnostic impact; values of 0.1 and less than 0.2 have a moderate difference in test probabilities and moderate diagnostic impact; values of 0.2 and less than 0.5 have a small difference in test probabilities and sometimes an important diagnostic impact; and values of 0.5–1 have small difference in test probabilities and seldom have important diagnostic impact.

The role of the clinical guidelines is to increase the pretest probability by adequately distinguishing low risk from high-risk groups. The role of imaging guidelines is to increase the likelihood ratio by recommending the diagnostic test with the highest sensitivity and specificity. Comprehensive use of clinical and imaging guidelines will improve the posttest probability, hence increasing the diagnostic outcome [10].

How to Use This Book

As these examples illustrate, the EBI process can be lengthy [39]. The literature is overwhelming in scope and somewhat frustrating in methodological quality. The process of summarizing data can be challenging to the clinician not skilled in meta-analysis. The time demands on busy practitioners can limit their appropriate use of the EBI approach. This book can mitigate these challenges in the use of EBI and make the EBI accessible to all imagers and users of medical imaging.

This book is organized by major diseases and injuries. In the table of contents within each chapter, you will find a series of EBI issues provided as clinically relevant questions. Readers can quickly find the relevant clinical question and receive guidance as to the appropriate recommendation based on the literature. Where appropriate, these questions are further broken down by age, gender, or other clinically important circumstances. Following the chapter's table of contents is a summary of the key points determined from the critical literature review that forms the basis of EBI. Sections on pathophysiology, epidemiology, and cost are next, followed by the goals of imaging and the search methodology. The chapter is then broken down into the clinical issues. Discussion of each issue begins with a brief summary of the literature, including a quantification of the strength of the evidence, and then continues with detailed examination of the supporting evidence. At the end of the chapter, the reader will find the take-home tables and imaging case studies, which highlight key imaging recommendations and their supporting evidence. Finally, questions are included where further research is necessary to understand the role of imaging for each of the topics discussed.

Take-Home Appendix 1: Equations

Test result	Outcome	
	Present	Absent
Positive	a (TP)	b (FP)
Negative	c (FN)	d (TN)
(a) Sensitivity		$a/(a + c)$
(b) Specificity		$d/(b + d)$
(c) Prevalence		$(a + c)/(a + b + c + d)$
(d) Accuracy		$(a + d)/(a + b + c + d)$
(e) Positive predictive value[a]		$a/(a + b)$
(f) Negative predictive value[a]		$d/(c + d)$

(*continued*)

(g) 95 % confidence interval (CI)	$p \pm 1.96\sqrt{\frac{1-n}{n}}$
	p = proportion
	n = number of subjects
(h) Likelihood ratio	$\dfrac{\text{Senstivit y}}{1 - \text{Senstivit y}} = \dfrac{a(b + d)}{b(a + c)}$

Reprinted with the kind permission of Springer Science+ Business Media from Medina LS, Blackmore CC, Applegate KE. Evidence-based imaging: improving the quality of imaging in patient care. Revised Edition. New York: Springer Science+Business Media; 2011.
[a]Only correct if the prevalence of the outcome is estimated from a random sample or based on an a priori estimate of prevalence in the general population; otherwise, use of Bayes' theorem must be used to calculate positive predictive value (*PPV*) and negative predictive value (*NPV*). *TP* true positive, *FP* false positive, *FN* false negative, *TN* true negative

Take-Home Appendix 2: Summary of Bayes' Theorem

1. Information before test × Information from test = Information after test
2. Pretest probability (prevalence) sensitivity/ 1 − specificity = posttest probability (predictive value)
3. Information from the test also known as the likelihood ratio, described by the equation: sensitivity/1 − specificity
4. Examples 1 and 2 predictive values: The predictive values (posttest probability) change according to the differences in prevalence (pretest probability), although the diagnostic performance of the test (i.e., sensitivity and specificity) is unchanged. The following examples illustrate how the prevalence (pretest probability) can affect the predictive values (posttest probability) having the same information in two different study groups.

Equations for calculating the results in the previous examples are listed in Appendix 1. As the prevalence of carotid artery disease increases from 0.16 (low) to 0.82 (high), the positive predictive value (PPV) of a positive contrast-enhanced CT increases from 0.67 to 0.98, respectively. The sensitivity and specificity remain unchanged at 0.83 and 0.92, respectively. These examples also illustrate that the diagnostic performance of the test (i.e., sensitivity and specificity) does

not depend on the prevalence (pretest probability) of the disease. CTA, CT angiogram.

Example 1: Low prevalence of carotid artery disease

	Disease (carotid artery disease)	No disease (no carotid artery disease)	Total
Test positive (positive CTA)	20	10	30
Test negative (negative CTA)	4	120	124
Total	24	130	154

Example 2: High prevalence of carotid artery disease

	Disease (carotid artery disease)	No disease (no carotid artery disease)	Total
Test positive (positive CTA)	500	10	510
Test negative (negative CTA)	100	120	220
Total	600	130	730

Results: sensitivity = 500/600 = 0.83; specificity = 120/130 = 0.92; prevalence = 600/730 = 0.82; positive predictive value = 0.98; negative predictive value = 0.55
Reprinted with the kind permission of Springer Science+ Business Media from Medina LS, Blackmore CC, Applegate KE. Evidence-based imaging: improving the quality of imaging in patient care. Revised Edition. New York: Springer Science+Business Media, 2011

References

1. Levin A. Ann Intern Med. 1998;128:334–6.
2. Evidence-Based Medicine Working Group. J Am Med Assoc. 1992;268:2420–5.
3. The Evidence-Based Radiology Working Group. Radiology. 2001;220:566–75.
4. Wood BP. Radiology. 1999;213:635–7.
5. Poisal JA, et al. Health Aff. 2007;26:w242–53.
6. Davis K. N Engl J Med. 2008;359:1751–5.
7. Hulley SB, Cummings SR. Designing clinical research. Baltimore: Williams & Wilkins; 1998.
8. Kelsey J, Whittemore A, Evans A, Thompson W. Methods in observational epidemiology. New York: Oxford University Press; 1996.
9. Blackmore C, Cummings P. AJR Am J Roentgenol. 2004;183(5):1203–8.

10. Medina L, Aguirre E, Zurakowski D. Neuroimaging Clin N Am. 2003;13:157–65.
11. Medina L. AJNR Am J Neuroradiol. 1999;20: 1584–96.
12. Sunshine JH, McNeil BJ. Radiology. 1997;205: 549–57.
13. Black WC. AJR Am J Roentgenol. 1990;154:17–22.
14. Sox HC, Blatt MA, Higgins MC, Marton KI. Medical decision making. Boston: Butterworth; 1988.
15. Metz CE. Semin Nucl Med. 1978;8:283–98.
16. Singer M, Applegate K. Radiology. 2001; 219:611–20.
17. Weinstein MC, Fineberg HV. Clinical decision analysis. Philadelphia: WB Saunders; 1980.
18. Carlos R. Acad Radiol. 2004;11:141–8.
19. Detsky AS, Naglie IG. Ann Intern Med. 1990;113:147–54.
20. Doubilet P, Weinstein MC, McNeil BJ. N Engl J Med. 1986;314:253–6.
21. Gold MR, Siegel JE, Russell LB, Weinstein MC. Cost-effectiveness in health and medicine. New York: Oxford University Press; 1996.
22. Hillemann D, Lucas B, Mohiuddin S, Holmberg M. Ann Pharmacother. 1997;31:974–9.
23. Medina L, Aguirre E, Bernal B, Altman N. Radiology. 2004;230:49–54.
24. Appel LJ, Steinberg EP, Powe NR, Anderson GF, Dwyer SA, Faden RR. Med Care. 1990;28:324–37.
25. Evens RG. Cancer. 1991;67:1245–52.
26. Yin D, Forman HP, Langlotz CP. AJR Am J Roentgenol. 1995;165:1323–8.
27. Medina L, Crone K, Kuntz K. Pediatrics. 2001;108:E101.
28. Ware JE, Sherbourne CD. Med Care. 1992;30:473–83.
29. Jarvik J, Hollingworth W, Martin B, et al. J Am Med Assoc. 2003;2810–2818.
30. Blackmore CC, Magid DJ. Radiology. 1997;203:87–91.
31. Medina L, Aguirre E, Byron B, Altman N. Radiology. 2004;230:49–54.
32. Zou K, Fielding J, Ondategui-Parra S. Acad Radiol. 2004;11:127–33.
33. Langlotz C, Sonnad S. Acad Radiol. 1998;5(suppl 2): S269–73.
34. Littenberg B, Moses LE. Med Decis Making. 1993;13:313–21.
35. Fiebach JB, et al. Stroke. 2004;35(2):502–6.
36. Fryback DG, Thornbury JR. Med Decis Making. 1991;11:88–94.
37. Blackmore C. Radiology. 2005;235(2):371–4.
38. Jaeschke R, Guyatt GH, Sackett DL. JAMA. 1994;271:703–7.
39. Malone D. Radiology. 2007;242(1):12–4.

Assessing the Imaging Literature: Understanding Error and Bias

2

C. Craig Blackmore, L. Santiago Medina, James G. Ravenel, Gerard A. Silvestri, and Kimberly E. Applegate

Contents

C.C. Blackmore (✉)
Department of Radiology, Virginia Mason Medical Center, Seattle, WA, USA
e-mail: craig.blackmore@vmmc.org

L.S. Medina
Division of Neuroradiology-Neuroimaging, Department of Radiology, Miami Children's Hospital, Miami, FL, USA

Herbert Wertheim College of Medicine, Florida International University, Miami, FL, USA

Former Lecturer in Radiology, Harvard Medical School, Boston, MA, USA
e-mail: smedina@post.harvard.edu; Santiago.medina@mch.com

J.G. Ravenel • G.A. Silvestri
Department of Medicine, Medical University of South Caroclina, Charleston, SC, USA
e-mail: ravenejg@musc.edu; silvestri@musc.edu

K.E. Applegate
Department of Radiology and Imaging Sciences, Emory University School of Medicine, Atlanta, GA, USA
e-mail: Keapple@emory.edu

The keystone of the evidence-based imaging (EBI) approach is to critically assess the research data that are provided and to determine if the information is appropriate for use in answering the EBI question. Unfortunately, the published studies are often limited by bias, small sample size, and methodological inadequacy. Further, the information provided in published reports may be insufficient to allow estimation of the quality of the research. Two recent initiatives, the CONSORT [1] and the STARD [2], aim to improve the reporting of clinical trials and studies of diagnostic accuracy, respectively. However, these guidelines are only now being implemented and are not well known to readers of the medical literature.

This chapter summarizes the common sources of error and bias in the imaging literature. Using the EBI approach requires an understanding of these issues.

Discussion of Issues

What Are Error and Bias?

Errors in the medical literature can be divided into two main types. *Random error* occurs due to chance variation, causing a sample to be different from the underlying population. Random error is more likely to be problematic when the sample size is small. *Systematic error*, or *bias*, is an incorrect study result due to nonrandom distortion of the data. Systematic error is not affected by sample size but is rather a function of flaws in the study design, data collection, and analysis. A second way to think about random and systematic error is in terms of precision and accuracy [3]. Random error affects the precision of a result (Fig. 2.1). The larger the sample size, the more precision in the results and the more likely that two samples from truly different populations will be differentiated from each other. Using the bull's-eye analogy, the larger the sample size, the less the random error and the larger the chance of hitting the center of the target (Fig. 2.1). Systematic error, on the other hand, is a distortion in the accuracy of an estimate. Regardless of precision, the underlying estimate is flawed by some aspect of the

research procedure. Using the bull's-eye analogy, in systematic error, regardless of the sample size, the bias would not allow the researcher to hit the center of the target (Fig. 2.1).

What Is Random Error?

Random error is divided into two main types: Type I, or alpha error, occurs when an investigator concludes that an effect or a difference is present when in fact there is no true difference. Type II, or beta error, occurs when an investigator concludes that there is no effect or no difference when in fact a true difference exists in the underlying population [3].

Type I Error

Quantification of the likelihood of alpha error is provided by the familiar p value. A p value less than 0.05 indicates that there is a less than 5 % chance that the observed difference in a sample would be seen if there was in fact no true difference in the population. In effect, the difference observed in a sample is due to chance variation rather than a true underlying difference in the population.

There are limitations to the ubiquitous p values seen in imaging research reports [4]. The p values are a function of both sample size and magnitude of effect. In other words, there could be a very large difference between two groups under study, but the p value might not be significant if the sample sizes are small. Conversely, there could be a very small, clinically unimportant difference between two groups of subjects or between two imaging tests, but with a large enough sample size, even this clinically unimportant result would be statistically significant. Because of these limitations, many journals are underemphasizing the use of p values and encouraging research results to be reported by way of confidence intervals (CIs).

Confidence Intervals

Confidence intervals are preferred because they provide much more information than p values. CIs provide information about the precision of

an estimate (how wide are the CIs), the size of an estimate (magnitude of the CIs), and the statistical significance of an estimate (whether the intervals include the null) [5].

If you assume that your sample was randomly selected from some population (that follows a normal distribution), you can be 95 % certain that the CI includes the population mean. More precisely, if you generate many 95 % CIs from many data sets, you can expect that the CI will include the true population mean in 95 % of the cases and not include the true mean value in the other 5 % [4]. Therefore, the 95 % CI is related to statistical significance at the $p = 0.05$ level, which means that the interval itself can be used to determine if an estimated change is statistically significant at the 0.05 level [6]. Whereas the p value is often interpreted as being either statistically significant or not, the CI, by providing a range of values, allows the reader to interpret the implications of the results at either end [6, 7]. In addition, while p values have no units, CIs are presented in the units of the variable of interest, which helps readers to interpret the results. The CIs shift the interpretation from a qualitative judgment about the role of chance to a quantitative estimation of the biologic measure of effect [4, 6, 7].

CIs can be constructed for any desired level of confidence. There is nothing magical about the 95 % that is traditionally used. If greater confidence is needed, then the intervals have to be wider. Consequently, 99 % CIs are wider than 95, and 90 % CIs are narrower than 95 %. Wider CIs are associated with greater confidence but less precision. This is the trade-off [4].

As an example, two hypothetical transcranial Doppler vascular ultrasound studies of the circle of Willis in patients with sickle-cell disease describe mean peak systolic velocities of 200 cm/s associated with 70 % of vascular diameter stenosis and higher risk of stroke. Both articles reported the same standard deviation (SD) of 50 cm/s. However, one study had 50 subjects, while the other one had 500 subjects. At first glance, both studies appear to provide similar information. However, the narrower CIs for the larger study reflect greater precision and indicate the value of the larger sample size. For a smaller sample

$$95\%\mathrm{CI} = 200 \pm 1.96\left(\frac{50}{\sqrt{50}}\right)$$

$$95\%\mathrm{CI} = 200 \pm 14 = 186 - 214$$

For a larger sample

$$95\%\mathrm{CI} = 200 \pm 1.96\left(\frac{50}{\sqrt{500}}\right)$$

$$95\%\mathrm{CI} = 200 \pm 4 = 196 - 204$$

In the smaller series, the 95 % CI was 186–214 cm/s, while in the larger series, the 95 % CI was 196–204 cm/s. Therefore, the larger series has a narrower 95 % CI [4].

Type II Error

The familiar p value alone does not provide information as to the probability of a type II or beta error. A p value greater than 0.05 does not necessarily mean that there is no difference in the underlying population. The size of the sample studied may be too small to detect an important difference even if such a difference does exist. The ability of a study to detect an important difference, if that difference does in fact exist in the underlying population, is called the power of a study. Power analysis can be performed in advance of a research investigation to avoid type II error. To conclude that no difference exists, the study must be powered sufficiently to detect a clinically important difference and have p value or CI indicating no significant effect.

Power Analysis

Power analysis plays an important role in determining what an adequate sample size is, so that meaningful results can be obtained [8]. Power analysis is the probability of observing an effect in a sample of patients if the specified effect size, or greater, is found in the population [3]. Mathematically, power is defined as 1 minus beta $(1 - \beta)$, where β is the probability of having

a type II error. Type II errors are commonly referred to as false negatives in a study population. Type I errors, in contrast, are analogous false positives in a study population [7]. For example, if β is set at 0.10, then the researchers acknowledge that they are willing to accept a 10 % chance of missing a correlation between abnormal computed tomography (CT) angiographic findings in the diagnosis of carotid artery disease. This represents a power of 1 minus 0.10, or 0.90, which represents a 90 % probability of finding a correlation of this magnitude.

Ideally, the power should be 100 % by setting β at 0. In addition, ideally α should also be 0. By accomplishing this, false-negative and false-positive results are eliminated, respectively. However, to do so would require a prohibitively large sample size. Therefore, in practice, power near 100 % is rarely achievable, so, at best, a study should reduce the false negatives (β) and false positives (α) to a minimum [3, 9]. Achieving an acceptable reduction of false negatives and false positives requires a large subject sample size. Optimal power, α and β, settings are based on a balance between scientific rigor and the issues of feasibility and cost. For example, assuming an α error of 0.10, your sample size increases from 96 to 118 subjects per study arm (carotid and noncarotid artery disease arms) if you change your desired power from 85 % to 90 % [10]. Studies with more complete reporting and better study design will often report the power of the study, for example, by stating that the study has 90 % power to detect a difference in sensitivity of 10 % between CT angiography and Doppler ultrasound in carotid artery disease.

What Is Bias?

The risk of an error from bias decreases as the rigor of the study design and analysis increases. Randomized controlled trials (RCTs) are considered the best design for minimizing the risk of bias because patients are randomly allocated. This random allocation allows for unbiased distribution of both known and unknown confounding variables between the study groups. In nonrandomized studies, appropriate study design and statistical analysis can control only for known or measurable bias.

Detection of and correction for bias, or systematic error, in research is a vexing challenge for both researchers and users of the medical literature alike. Maclure and Schneeweiss [11] have identified ten different levels at which biases can distort the relationship between published study results and truth. Unfortunately, bias is common in published reports [12], and reports with identifiable biases often overestimate the accuracy of diagnostic tests [13]. Careful surveillance for each of these individual bias phenomena is critical but may be a challenge. Different study designs are also susceptible to different types of bias, as will be discussed in this section as well. Well-reported studies often include a section on limitations of the work, spelling out the potential sources of bias that the investigator acknowledges from a study as well as the likely direction of the bias and steps that may have been taken to overcome it. However, the final determination of whether a research study is sufficiently distorted by bias to be unusable is left to the discretion of the user of the imaging literature. The imaging practitioner must determine if results of a particular study are true, are relevant to a given clinical question, and are sufficient as a basis to change practice.

A common bias encountered in imaging research is that of *selection bias* [14]. Because a research study cannot include all individuals in the world who have a particular clinical situation, research is conducted on samples. Selection bias can arise if the sample is not a true representation of the relevant underlying clinical population (Fig. 2.2). Numerous subtypes of selection bias have been identified, and it is a challenge to the researcher to avoid all of these biases when performing a study. One particularly severe form of selection bias occurs if the diagnostic test is applied to subjects with a spectrum of disease that differs from the clinically relevant group. The extreme form of this spectrum bias

occurs when the diagnostic test is evaluated on subjects with severe disease and on normal controls. In an evaluation of the effect of bias on study results, Lijmer et al. [13] found the greatest overestimation of test accuracy with this type of spectrum bias.

A second frequently encountered bias in imaging literature is that of *observer bias* [15, 16], also called test-review bias and diagnostic-review bias [17]. Imaging tests are largely subjective. The radiologist interpreting an imaging study forms an impression based on the appearance of the image, not based on an objective number or measurement. This subjective impression can be biased by numerous factors including the radiologist's experience; the context of the interpretation (clinical vs. research setting); the information about the patient's history that is known by the radiologist; incentives that the radiologist may have, both monetary and otherwise, to produce a particular report; and the memory of a recent experience. But because of all these factors, it is critical that the interpreting physician be blinded to the outcome or gold standard when a diagnostic test or an intervention is being assessed. Important distortions in research results have been found when observers are not blinded versus blinded. For example, Schulz et al. [18] showed a 17 % greater outcome improvement in studies with unblinded assessment of outcomes versus those with blinded assessment. To obtain objective scientific assessment of an imaging test, all readers should be blinded to other diagnostic tests and final diagnosis, and all patient-identifying marks on the test should be masked.

Bias can also be introduced by the *reference standard* used to confirm the final diagnosis. First, the interpretation of the reference standard must be made without knowledge of the test results. Reference standards, like the diagnostic tests themselves, may have a subjective component and therefore may be affected by knowledge of the results of the diagnostic test. In addition, it is critical that all subjects undergo the same reference standard. The use of different reference standards (called differential reference standard bias) for subjects with different diagnostic test results may falsely elevate both sensitivity and specificity [13, 16]. Of course, sometimes it is not possible or ethical to perform the same reference standard procedure on all subjects. For example, in a recent meta-analysis of imaging for appendicitis, Terasawa et al. [19] found that all of the identified studies used a different reference standard for subjects with positive imaging (appendectomy and pathologic evaluation) than for those with negative imaging (clinical follow-up). It simply would not be ethical to perform appendectomy on all subjects. Likely, the sensitivity and specificity of imaging for appendicitis were overestimated as a result.

What Are the Inherent Biases in Screening?

Investigations of screening tests are susceptible to an additional set of biases. Screening case–control trials are vulnerable to *screening selection bias*. For example, lung cancer case–control studies have been performed in Japan, where long-running tuberculosis control programs have been in place. This allowed for the analysis of those who were screened to be matched with a database of matched unscreened controls to arrive at a relative risk of dying from lung cancer in screened and unscreened populations. Because screening is a choice in these studies, selection bias plays a prominent role. That is, people who present for elective screening tend to have better health habits [20]. In assessing the exposure history of cases, the inclusion of the test on which the diagnosis is made, regardless of whether it is truly screen or symptom detected, can lead to an odds ratio greater than 1 even in the absence of benefit [21]. Similarly, excluding the test on which the diagnosis is made may underestimate screening effectiveness. The magnitude of bias is further reflected in the disease preclinical phase; the longer the preclinical phase, the greater the magnitude of the bias.

Prospective nonrandomized screening trials perform an intervention on subjects, such as screening for lung cancer, and follow them for

many years. These studies can give information on the stage distribution and survival of a screened population; however, these measures do not allow an accurate comparison to an unscreened group due to lead time, length time, and overdiagnosis bias [22] (Fig. 2.3). *Lead-time bias* results from the earlier detection of the disease, which leads to longer time from diagnosis and an apparent survival advantage, but does not truly impact the date of death. *Length-time bias* relates to the virulence of tumors. More indolent tumors are more likely to be detected by screening, whereas aggressive tumors are more likely to be detected by symptoms. This disproportionally assigns more indolent disease to the intervention group and results in the appearance of a benefit. *Overdiagnosis* is the most extreme form of length-time bias in which a disease is detected and "cured," but it is so indolent that it would have never caused symptoms during life. Thus, survival alone is not an appropriate measure of the effectiveness of screening [23].

For this reason, a RCT with disease-specific mortality as an end point is the preferred methodology. Randomization should even out the selection process in both arms, eliminating the bias of case–control studies and allowing direct comparison of groups that underwent the intervention and those that did not, to see if the intervention lowers deaths due to the target disease. The disadvantage of the RCT is that it takes many years and is expensive to perform. There are two biases that can occur in RCTs and are important to understand: *sticky diagnosis* and *slippery linkage* [24]. Because the target disease is more likely to be detected in a screened population, it is more likely to be listed as a cause of death, even if not the true cause. As such, the diagnosis "sticks" and tends to underestimate the true value of the test. On the other hand, screening may set into motion a series of events in order to diagnose and treat the illness. If these procedures remotely lead to mortality, such as a myocardial infarction during surgery with death several months later, the linkage of the cause of death to the screening may no longer be obvious (slippery linkage). Because the death is not appropriately assigned to the target disease, the value of screening may be overestimated. For this reason, in addition to disease-specific mortality, all-cause mortality should also be evaluated in the context of screening trials [24]. Ultimately, to show the effectiveness of screening, not only more early-stage cancers need to be found in the screened group but also there must be fewer late-stage cancers (stage shift) [22].

Qualitative Literature Summary

The potential for error and bias makes the process of critically assessing a journal article complex and challenging, and no investigation is perfect. Producing an overall summation of the quality of a research report is difficult. However, there are grading schemes that provide a useful estimation of the value of a research report for guiding clinical practice. The method used in this book is derived from that of Kent et al. [25] and is shown in Table 2.1. Use of such a grading scheme is by nature an oversimplification. However, such simple guidelines can provide a useful quick overview of the quality of a research report.

One such tool for the critical assessment of the literature on diagnostic accuracy is called STARD: Standards for Reporting of Diagnostic Accuracy [26]. These consensus-based standards were developed based on previously published checklists to aid authors, reviewers, and editors improve the quality of manuscripts. Readers are encouraged to use the 25-item checklist to assess for themselves the strengths and limitations of these types of publications.

Another tool for the assessment of systematic reviews of diagnostic accuracy studies is called QUADAS: Quality Assessment of Diagnostic Accuracy Statement [27]. This tool is essentially a checklist of items and methods that a systematic review should include for standard reporting of these diagnostic accuracy reviews.

Take-Home Tables and Figures

Table 2.1 and Figs. 2.1, 2.2, and 2.3 serve to highlight key recommendations and supporting evidence.

Table 2.1 Evidence classification for evaluation of a study

Level I: strong evidence

Studies with broad generalizability to most patients suspected of having the disease of concern: a prospective, blinded comparison of a diagnostic test result with a well-defined final diagnosis in an unbiased sample when assessing diagnostic accuracy or blinded randomized control trials or when assessing therapeutic impact or patient outcomes. Well-designed meta-analysis based on level I or II studies

Level II: moderate evidence

Prospective or retrospective studies with narrower spectrum of generalizability, with only a few flaws that are well described so that their impact can be assessed but still requiring a blinded study of diagnostic accuracy on an unbiased sample. This includes well-designed cohort or case–control studies and randomized trials for therapeutic effects or patient outcomes

Level III: limited evidence

Diagnostic accuracy studies with several flaws in research methods, small sample sizes, or incomplete reporting, or nonrandomized comparisons for therapeutic impact or patient outcomes

Level IV: insufficient evidence

Studies with multiple flaws in research methods, case series, descriptive studies, or expert opinions without substantiating data

Reprinted with kind permission of Springer Science+Business Media from Blackmore CC, Medina LS, Ravenel JG, Silvestri GA. Critically assessing the literature: understanding error and bias. In Medina LS, Blackmore DD (eds) Evidence-based imaging: optimizing imaging in patient care. New York: Springer; 2006

High Random Error
Low Sample Size

Low Random Error
High Sample Size
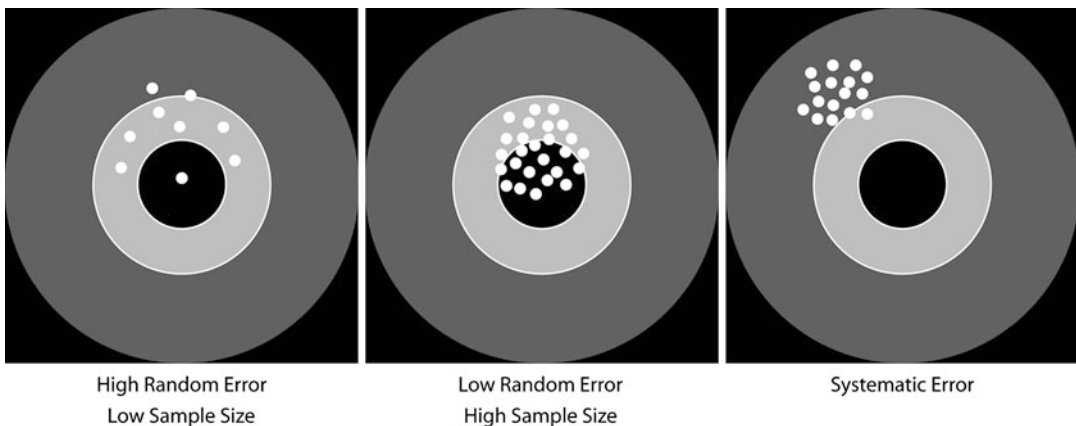
Systematic Error

Fig. 2.1 Random and systematic errors. Using the bull's-eye analogy, the larger the sample size, the less the random error and the larger the chance of hitting the center of the target. In systematic error, regardless of the sample size, the bias would not allow the researcher to hit the center of the target (Reprinted with kind permission of Springer Science+Business Media from Blackmore CC, Medina LS, Ravenel JG, Silvestri GA. Critically assessing the literature: understanding error and bias. In Medina LS, Blackmore DD (eds) Evidence-based imaging: optimizing imaging in patient care. New York: Springer; 2006)
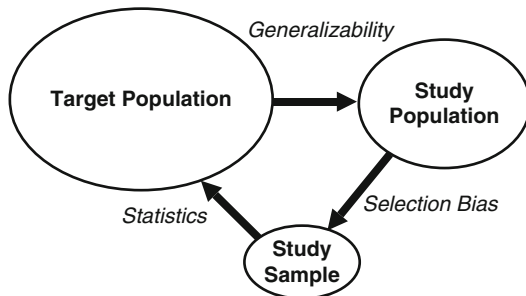
Fig. 2.2 Population and sample. The target population represents the universe of subjects who are at risk for a particular disease or condition. In this example, all subjects with abdominal pain are at risk for appendicitis. The sample population is the group of eligible subjects available to the investigators. These may be at a single center or group of centers. The sample is the group of subjects who are actually studied. Selection bias occurs when the sample is not truly representative of the study population. How closely the study population reflects the target population determines the generalizability of the research. Finally, statistics are used to determine what inference about the target population can be drawn from the sample data (Reprinted with kind permission of Springer Science+Business Media from Blackmore CC, Medina LS, Ravenel JG, Silvestri GA. Critically assessing the literature: understanding error and bias. In Medina LS, Blackmore DD (eds) Evidence-based imaging: optimizing imaging in patient care. New York: Springer; 2006)
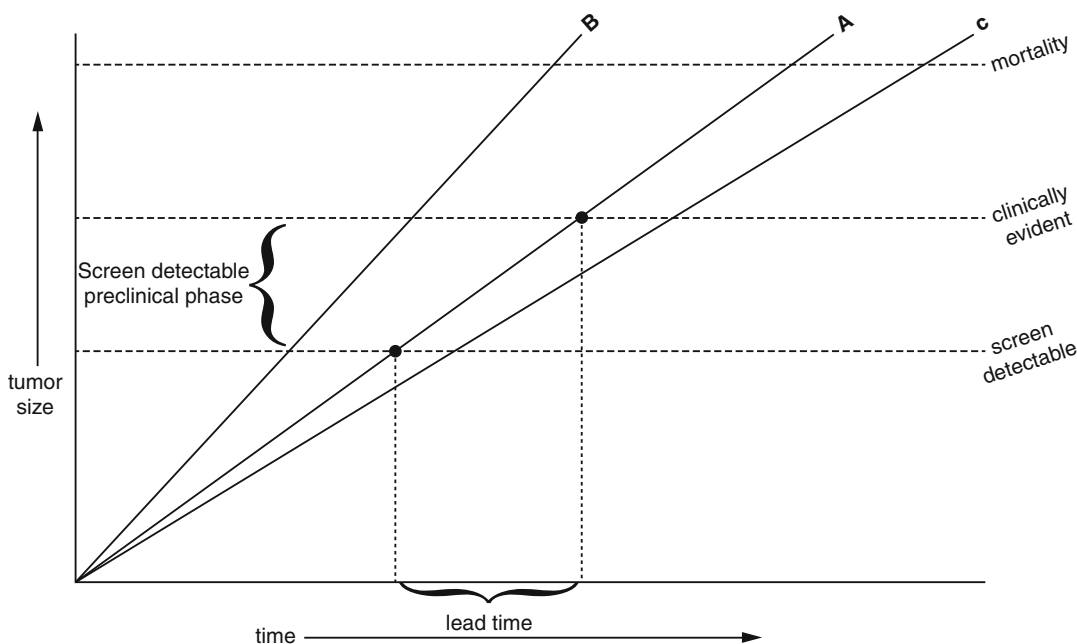
Fig. 2.3 Screening biases. For this figure, cancers are assumed to grow at a continuous rate until they reach a size at which death of the subject occurs. At a small size, the cancers may be evident on screening, but not yet evident clinically. This is the preclinical screen-detectable phase. Screening is potentially helpful if it detects cancer in this phase. After further growth, the cancer will be clinically evident. Even if the growth and outcome of the cancer is unaffected by screening, merely detecting the cancer earlier will increase apparent survival. This is the screening lead time. In addition, slower growing cancers (such as *C*) will exist in the preclinical screen-detectable phase for longer than do faster growing cancers (such as *B*). Therefore, screening is more likely to detect more indolent cancers, a phenomenon known as length bias (Reprinted with kind permission of Springer Science+Business Media from Blackmore CC, Medina LS, Ravenel JG, Silvestri GA. Critically assessing the literature: understanding error and bias. In Medina LS, Blackmore DD (eds) Evidence-based imaging: optimizing imaging in patient care. New York: Springer; 2006)

Conclusion

Critical analysis of a research publication can be a challenging task. The reader must consider the potential for type I and type II random errors, as well as systematic error introduced by biases including selection bias, observer bias, and reference standard bias. Screening includes an additional set of challenges related to lead time, length bias, and overdiagnosis. These challenges may seem daunting, yet without an understanding of them, a medical practitioner cannot learn efficiently from the literature and, in so doing, help their patients with the best evidence we have to offer them.

References

1. Moher D, Schulz K, Altman D. J Am Med Assoc. 2001;285:1987–91.
2. Bossuyt PM, Reitsma J, Bruns D, et al. Acad Radiol. 2003;10:664–9.
3. Hulley SB, Cummings SR. Designing clinical research. Baltimore: Williams and Wilkins; 1998.
4. Medina L, Zurakowski D. Radiology. 2003;226:297–301.
5. Gallagher E. Acad Emerg Med. 1999;6:1084–7.
6. Lang T, Secic M. How to report statistics in medicine. Philadelphia: American College of Physicians; 1997.
7. Gardener M, Altman D. Br Med J. 1986;292:746–50.
8. Medina L, Aguirre E, Zurakowski D. Neuroimaging Clin N Am. 2003;13:157–65.
9. Medina L. AJNR Am J Neuroradiol. 1999;20:1584–96.
10. Donner A. Stat Med. 1984;3:199–214.
11. Maclure M, Schneeweiss S. Epidemiology. 2001;12:114–22.
12. Reid MC, Lachs MS, Feinstein AR. J Am Med Assoc. 1995;274:645–51.
13. Lijmer JG, Mol BW, Heisterkamp S, et al. J Am Med Assoc. 1999;282:1061–6.
14. Blackmore C. Acad Radiol. 2004;11:134–40.
15. Ransohoff DF, Feinstein AR. N Engl J Med. 1978;299:926–30.
16. Black WC. AJR Am J Roentgenol. 1990;154:17–22.
17. Begg CB, McNeil BJ. Radiology. 1988;167:565–9.
18. Schulz K, Chalmers I, Hayes R, Altman D. J Am Med Assoc. 1995;273:408–12.
19. Terasawa T, Blackmore C, Bent S, Kohlwes R. Ann Intern Med. 2004;141:537–46.
20. Marcus P. Lung Cancer. 2003;41:37–9.
21. Hosek R, Flanders W, Sasco A. Am J Epidemiol. 1996;143:193–201.
22. Patz E, Goodman P, Bepler G. N Engl J Med. 2000;343:1627–33.
23. Black WC, Welch HG. AJR Am J Roentgenol. 1997;168:3–11.
24. Black W, Haggstrom D, Welch H. J Natl Cancer Inst. 2002;94:167–73.
25. Kent DL, Haynor DR, Longstreth Jr WT, Larson EB. Ann Intern Med. 1994;120:856–71.
26. Bossuyt PM, Reitsma JB, Bruns DE, Gatsonis CA, Glasziou PP, Irwig LM, Lijmer JG, Moher D, Rennie D, de Vet HC. Radiology. 2003;226(1):24–8.
27. Whiting P, Rutjes A, Reitsma J, Bossuyt P, Kleijnen J. BMC Med Res Methodol. 2003;3:25.

Part II

Evidence-Based Neuroimaging: Special Topics

Workup and Management of Incidental Findings on Imaging

3

Joanna M. Wardlaw and Alan Jackson

Contents

J.M. Wardlaw (✉)
Brain Research Imaging Centre, University of Edinburgh and NHS Lothian, Edinburgh, UK
e-mail: Joanna.Wardlaw@ed.ac.uk

A. Jackson
Wolfson Molecular Imaging Centre, University of Manchester, Withington, Manchester, UK
e-mail: alan.jacks@manchester.ac.uk

Key Points

- Incidental findings are *apparently asymptomatic intracranial abnormalities of potential clinical significance*.
- Incidental findings are common. For every 100 apparently normal asymptomatic subjects scanned, on average about 3 will have an incidental finding, giving a "number needed to scan" (NNS) of 37 (strong evidence).
- Nonneoplastic incidental findings in apparently normal subjects (excluding leukoaraiosis) have a prevalence of 2.0% (95% CI 1.13–3.10) and neoplastic incidental findings have a prevalence of 0.7% (95% CI 0.47–0.98%) (strong evidence).
- Including silent infarcts increases the incidence to above 10% (moderate evidence).
- The frequency of incidental findings increases with age (even after excluding leukoaraiosis) and with the use of more sensitive imaging sequences (sensitive imaging techniques reveal an incidence of 4.3% [CI 3.0–5.8%] versus 1.7% [CI 1.1 to 2.4%] with conventional imaging) (strong evidence).
- Detection of incidental findings is increasing due to overzealous investigation in clinical practice, increasingly easy access to more and more complex neuroimaging, the rise in easy access by the public to commercial imaging health centers (for-profit health screening), and widespread use of neuroimaging in research (moderate evidence).
- Incidental findings vary in their importance, from those that are worth noting in a report but are unlikely to be of any clinical consequence (e.g., small temporal arachnoid cyst) (limited evidence) to those which may be imminently life threatening (8-mm diameter basilar tip aneurysm) (strong evidence).
- Many incidental findings, regardless of whether they are an immediate threat to health, carry implications for insurance (travel, employment, life) as well as ability to obtain a mortgage and other financial risk ramifications (moderate evidence).
- For many incidental findings, there are inadequate data on appropriate management. These require sympathetic management to minimize anxiety in the subject and to minimize their impact on health status (insufficient evidence).

Definition and Pathophysiology

The definition of an incidental finding is an *apparently asymptomatic intracranial abnormality of potential clinical significance*. Common examples include both non-neoplastic lesions such as arachnoid cysts, pineal cysts, cavernous hemangiomas, developmental venous anomalies, aneurysms, inflammatory white matter lesions, and neoplastic lesions such as meningiomas, gliomas, pituitary adenomas, and vestibular schwannoma (Table 3.1) [1].

The pathophysiology varies from lesions that are unlikely ever to be clinically significant to those which are likely to cause symptoms or may already have done so, but that the subject has ignored to those which could be imminently life threatening. Examples of the first group include small temporal arachnoid cysts, of the second group include demyelination or an arteriovenous malformation, and of the third group include large intracranial aneurysms or gliomas. Figures 3.1 and 3.2 show examples of abnormalities discovered in control subjects for research studies.

Epidemiology

Incidental findings are not new [2–4], but awareness has increased in recent years. The likelihood of detection has increased due to a combination of factors which include greater availability of, and referral for, imaging in clinical practice, improved quality of clinical imaging protocols, availability of multiple images through PACS (compared with more limited imaging available on printed films) [5], increased use of imaging in research, and the availability of imaging-based for-profit screening programs.

Some studies have found the prevalence of incidental findings on research brain scans to be as high as 10–28%, ([4, 6, 7]; however, these included all incidental findings, including age-related white matter changes and findings with little or no clinical significance (Table 3.1). Most studies indicate that incidental findings of potential clinical significance are present on neuroimaging in approximately 3% of the apparently normal population [8–11]. In a meta-analysis of 16 studies (published up until May 2008) comprising 19,559 apparently normal asymptomatic subjects, the prevalence of brain neoplasms, silent infarcts, and white matter lesions all increased with age but of nonneoplastic lesions (excluding silent infarcts and white matter lesions) was similar across age groups from 10–29 to 70–89 years [8] (strong evidence). The neoplasms identified were meningiomas (0.29%, 95% CI 0.13–0.51%), pituitary adenomas (0.15%, 95% CI 0.09–0.22%), low-grade gliomas (0.05%, 95% CI 0.02–0.09%), vestibular schwannomas, lipomas and epidermoids (all around 0.03%, 95% CI 0.01–0.07%), and other unspecified neoplastic lesions (0.09%, 95% CI 0.03–0.17). The prevalence of demyelination (definite or possible) was 0.06% (95% CI 0.02–0.15) and 0.03% (95% CI 0.00–0.07%), respectively. Aneurysms (0.35%, 95% CI 0.13–0.67), arachnoid cysts (0.50%, 95% CI 0.21–0.87%), and Chiari malformations (0.24%, 95% CI 0.04–0.58%) were the most frequent non-neoplastic lesions (excluding silent infarcts and leukoaraiosis). Other findings included colloid cysts (0.04%), hydrocephalus (0.10%), extra-axial collections (0.04%), and arteriovenous malformations (0.05%). Two papers published since the systematic review found similar prevalences of neoplastic and non-neoplastic incidental findings. Hartwigsen et al. [10] found incidental findings in 19 of 206 young healthy volunteers (9.2%) undergoing research neuroimaging on a 3-T magnet, of which about half had some clinical implication (pituitary or pineal lesions, cavernomas, or AVMs). Orme et al. [9] reviewed 231 head scans on which they identified 136 incidental findings (42.9%). Of these, five cases (2.2%) were of sufficient significance to required further action.

Silent infarcts occur in 20% of healthy elderly people and increase in prevalence with age [12]. One large study of 1,890 normal elderly subjects described a slightly higher prevalence of 13% in subjects aged 60–64 and 23% in those between 65 and 70 [13]. White matter lesions (WMLs) attributed to cerebral small vessel disease (leukoaraiosis) are not usually present in people under the age of 40–50 years (at least not more than three to five small lesions) but increase in number and extent thereafter. Morris et al. [8] found a prevalence of 2.5% of people aged 30–49, 7% of people aged 50–69, and 17% of people aged 70–89 years. When the amount of WMLs is expressed as a volume of affected tissue, most people aged 45–59 years had less than 5 ml (median 1.8, IQR 1.06–3.17 ml); of those aged 60–74 years, most had less than 7.5 ml (median 3.05, IQR 1.87–5.49 ml); and of those aged 75–97 years, most had less than 15 ml (median 7.74, IQR 2.64–16.49 ml) but some had as much as 50 ml [6].

Microhemorrhage is also described in normal subjects; a recent meta-analysis including 4,641 normal subjects found a prevalence of 5% (95% CI 4–6%) in apparently healthy adults increasing with advancing age [14] (moderate evidence); however, these studies showed significant variation in the scanning sequences employed, and true incidences may be higher with currently available susceptibility imaging sequences [15, 16].

In spinal imaging, there may be incidental findings outside the spinal column or cord, in addition to common findings such as disc degeneration that may not be relevant to the patient's symptoms [5]. Incidental findings on body imaging may be even more frequent than on brain imaging, but a detailed discussion of this is outside the scope of this chapter [11, 17–19].

The prevalence of incidental findings varies with the sensitivity of the investigative process. Thus, studies using higher sensitivity sequences found more clinically significant incidental

findings (4.3%) than did studies using less sensitive MR sequences (1.7%) [8] (strong evidence). Prospective studies using angiographic sequences found higher prevalences of asymptomatic intracranial aneurysms than studies with conventional MRI protocols or comparable postmortem studies (0.35% for conventional MRI, 3.6% for autopsy studies, and 6% for MR angiography studies) [8, 20–22].

Finally, incidental findings are apparently more common in imaging studies performed in research subjects (3.4%) than for inpatients undergoing for-profit screening examinations (2%), or in research controls (1.0%), Chi squared $p < 0.001.8$ (moderate evidence). The reason for this is unknown.

Use of neuroimaging in research is increasing [23]. Incidental findings are not uncommon in research, as one would expect from the above summary, and this raises important ethical and management issues [24–28]. The problem of what to do about incidental findings in research is discussed in a later section.

Overall Cost to Society

No studies have addressed the cost of incidental finding to society which depends on the balance between the benefits of early treatment and the risks associated with the investigation and treatment, plus the impact on the subject's ability to work, drive, obtain insurance, anxiety levels, etc., and the costs incurred by all those steps.

The health-care cost implications will vary in different countries depending on the health-care funding model. In social systems such as the UK National Health Service, there is no financial incentive for the physician to overinvestigate or overtreat the finding. In for-profit health-care systems, there is a possible temptation to perform further investigations and to treat, even when the evidence for intervention may be poor. Examples include the current vogue for stenting of asymptomatic intracranial arterial atheromatous stenosis [29] or for asymptomatic internal carotid stenosis. The danger is that increasing use of imaging to reassure the patient (or the doctor) that there is nothing wrong increases the risk of identifying incidental and irrelevant findings that the patient (and doctor) then worry about. However, there is little evidence that performing investigations is reassuring, even when the results are resoundingly negative [30–33] (moderate evidence).

Many of the consequences and the impact of an incidental finding are outside mainstream medical practice and would be even harder to quantify [34]. These include both direct and indirect factors. The individual's ability to obtain life, health, and travel insurance may be affected with serious consequences. The individual's employment may be put at risk either through increasing time off work due to their anxiety at the discovery or directly because of the loss of insurance or other liability [35, 36]. They may not be able to drive or obtain a mortgage. Their health may suffer through anxiety at knowing they have a "time bomb" through the consequences of overinvestigation or the complications of unnecessary treatment [37, 38].

Goals of Imaging

A physician portrayed by Groucho Marx in *A Day at the Races* was described by his patient (in the film) as "*One of the finest doctors I have known. Why, I didn't know there was anything wrong with me until I met him.*" The overall goal in the management of incidental findings must be to manage them without harm to the subject. Nonmaleficence is a basic guiding principle of all medical care and can be stated as:

> given an existing problem, it may be better not to do something, or even to do nothing, than to risk causing more harm than good.

Some of these findings will have been present since birth or for many years prior to discovery and would be unlikely to cause the subject harm. More harm may be caused to the subject through overzealous reaction to the finding, investigation, and treatment. Referring the anxious only makes them more anxious [39]. Until better evidence is available from more long-term epidemiology

studies and intervention randomized clinical trials, the authors believe that the approach should be cautious [34].

Methodology

We updated a recent systematic review of incidental findings in neuroimaging [8], by searching from end of December 2008 to end of December 2010 in MEDLINE using PubMed (National Library of Medicine, Bethesda, Maryland) for original research publications on incidental findings in the brain or spinal cord on imaging. We also identified studies on potential adverse effects of neuroimaging used in research and commercial applications through two related projects, the first on the wider societal implications of neuroimaging held at the Scottish Universities Insight Institute in 2010 (http://www.scottishinsight.ac.uk/, details of organizations involved provided in report) and the second on the management of incidental findings in research imaging held at the Wellcome Trust, London, in 2010 (http://www.sinapse.ac.uk/media/events/ethics_management. asp; report available at http://www.rcr.ac.uk/docs/radiology/pdf/BFCR(11)8_Ethics.pdf) [40]. The search therefore covered the years 1950 to December of 2010. The search strategy employed different combinations of the following terms: (1) neuroimaging, (2) radiography OR imaging OR computed tomography OR CT OR MR OR MRI OR magnetic resonance imaging, (3) cranial OR brain OR spine OR neuro, (4) brain OR brain diseases OR spine diseases, (5) humans, and (6) ethics. Reviewing the reference lists of relevant papers identified additional articles. This review was limited to human studies and mainly the English language literature. The authors performed an initial review of the titles and abstracts of the identified articles followed by review of the full text in articles that were relevant. Articles identified in the review presented above or in the related projects [8] were handled in a similar way by the investigators of those projects, and as both authors were lead organizers of one or both of those projects, we did not repeat that work.

Discussion of Issues

How to Minimize the Chances of Incidental Findings in Clinical Practice and Why Is this Important?

Summary

The more investigations health-care providers do, the more likely they are to identify incidental findings. Incidental findings have adverse effects: they worry the patient, often unnecessarily [41]; they divert attention away from the original suspected disease of interest, potentially leading to mismanagement of the latter; and they use up additional health-care resources through further investigations and consultations, increasing the cost of health care [34]. These risks are encapsulated in the term "victims of modern imaging technology (VOMIT)" coined by Hayward in 2003 [41].

Consequently, in clinical practice, patients should be referred for neuroimaging only if clinical indications for the presence of the disease of concern, or the need to exclude it, are strong. Evidence-based guidelines help to focus the use of neuroimaging on patients who are, according to the best current evidence, likely to benefit from and not be harmed by the results. Utilization guidelines are provided by radiological societies and by disease-oriented organizations. A comprehensive list of national and international sources for imaging guidelines is available through the NHS National Library of Guidelines (http://www.library.nhs.uk/) and the Agency for Healthcare Research and Quality (http://www.guidelines.gov/). Performing scans only for reassurance increases the risk of incidental findings, encourages the patient to expect investigations the next time they consult [33] (moderate evidence), and there is little evidence that use of investigations in this situation is anxiolytic [32].

Imaging-based for-profit screening is increasingly available [37], and use of imaging in research is common. In both situations, subjects should be warned in advance of the likely risk and the medical and non-medical implications of an

incidental finding [27]. Imaging-based for-profit screening is likely to remain a significant factor because the activities of commercial screening organizations and the widespread media attention given to high-profile scientific publications, such as the paper by Vernooij and colleagues in the New England Journal of Medicine, [6] risk raising concern among the public [42]. People, concerned about their health and personal well-being, may develop the impression that they too should seek reassurance that they do not have a "ticking time bomb" [43].

Supporting Evidence

Until recently, access to investigations was limited so that only patients with good justification for the test were referred; in addition, investigations were less sensitive for the identification of small or subtle incidental findings. This is all changing. Investigations are now widely available, and the barrier to advanced imaging investigation of suspected disease has been lowered [43, 44]. In 1993, the American College of Radiology issued the ACR appropriateness criteria, scientific based guidelines for referring physicians about the appropriate use of diagnostic radiology in given situations [45]. A study, 15 years later, showed that the uptake and application of these guidelines and of other formal guidelines among referring clinicians were very low [46]. Unfortunately there is little firm evidence on how many patients are now referred for neuroimaging investigation solely for reassurance.

Most national colleges and organizations produce guidelines on the use of imaging investigations for clinical purposes based on the best evidence available at the time and regularly update these recommendations. The American College of Radiology (ACR) in the USA and the Royal College of Radiologists (RCR) in the UK produce guidelines on who to refer for imaging, what type, and when (Table 3.2). Readers should refer to their relevant national guidance, as that is most likely to be geared to the resources and practices in their country. Referral to guidelines may also help explain to the patient why investigations should be avoided unless there is very good reason.

The stress of being screened is difficult to quantify and probably depends in part upon the seriousness (in the mind of the screened population) of the disease being sought. Getting a normal test result is not necessarily as anxiolytic as some doctors might assume, although opinion concerning this remains mixed. McDonald et al. [30] assessed patient reassurance after a normal test result in patients undergoing echocardiography for symptoms or an asymptomatic murmur. All those presenting with symptoms remained anxious despite the normal test result and 39/52 people (75%) presenting with an asymptomatic murmur became anxious after detection of the murmur. Over half of these (21/39) remained anxious despite the normal echocardiogram result [30]. Similarly, a study of the effects of investigating cases of possible and probable MS, where diagnosis would not affect management, found that although anxiety seemed to be reduced by testing, overall anxiety levels did not decrease as much as anticipated. Patients also became less optimistic about their future health after testing. Subgroups of patients differed in their response to diagnostic information. Those in whom no definitive diagnosis emerged tend to be more anxious rather than being reassured by the "negative" workup. Individuals with "positive" workups became less anxious and expressed favorable feelings about the diagnostic workup even though they often faced a chronic disease [47]. In contrast, Sox et al. [48] measured clinical outcomes of 176 patients thought clinically to have nonspecific chest pain who were randomly allocated either to have a routine electrocardiogram and serum creatine phosphokinase tests (test group) or to have all diagnostic tests withheld (no-test group). Fewer patients in the tests group (20%) reported short-term disability than patients in the no-test group (46%) ($p = 0.001$). The use of diagnostic tests was an independent predictor of recovery. Patients in the test group felt that care was "better than usual" more often (57%) than patients in the no-test group (31%) ($p = 0.001$).

Some commercial screening organizations provide results of investigations in an unhelpful way to the individual, for example, which suggest

that there may be an abnormality of concern when in fact there is not, which the screened individual then has to take to their family doctor for advice and treatment [38].

What Is the Expectation of Research Studies in Identifying and Reporting Incidental Findings?

Summary

Use of imaging in research is a common source of incidental findings and the subject of much debate about how best to manage them.

Guidance on how to manage incidental findings detected during research imaging is less well developed. Advice from national and international ethics and regulatory research bodies is limited and variable [27] and likely to change with evolving attempts to minimize the administration burden involved in research [49]. A large group of imaging experts, professional, grant funding, ethics, and regulatory bodies recently formulated guidance on best practice for the UK [40]. However, the evidence on which to base much practice related to incidental findings in research is lacking.

Points for consideration requiring further evaluation methods include the following. Full radiological review of all research examinations, preferably by a specialist neuroradiologist, is attractive but carries significant cost implications. Neuroradiology and radiology resource is finite and limited so that full review of all research scans is impractical in most institutions. Indeed, many imaging-based research studies are conducted in nonclinical centers with principal investigators who are not necessarily clinically qualified. Despite this, some legal authorities have stated that the reactive model, where incidental findings noted by investigators are referred for further assessment, ignores the duties owed to the subject of research and may invite litigation [50]. In addition, studies in the US showed that the institutional review board at 22% of research centers required involvement of a neuroradiologist in neuroimaging studies [51]. A further issue of importance is that many research scans,

such as those used for functional MRI, would be considered entirely inadequate for diagnostic use [27]. Current opinion varies considerably [27, 52], and review of current practice reveals a wide range of methods for dealing with incidental findings in research studies. Management models range from no radiology reporting at all through "reactive radiology" where suspicious findings noticed by investigators are referred to a radiologist for an opinion, "proactive radiology" where all research images are reported, and "very proactive radiology," where images additional to those required for the research may be acquired routinely to improve detection or characterization of any incidental findings [27].

Whatever model is employed, it is important to understand that many volunteers will expect expert examination of research images to be routine. In one study which sought research volunteers opinion, the majority of volunteers expected that their images would be examined and medical anomalies would be disclosed to them, *regardless of the written information they were given during the consent process or whether the research took place in a medical on nonmedical environment* [53]. There is currently no consensus on the appropriate model to employ, and clear legal and ethical guidance is either conflicting or incomplete [27].

Supporting Evidence

Researchers have a clear and legally binding duty of care to their research subjects that includes dealing with problems arising from incidental findings [40, 54]. It has been stated that systems which rely on the identification of significant incidental findings by inadequately qualified personnel ignore the duties owed to the subject by the investigator [40, 55] and may invite litigation [50]. A review of legal precedent in the USA found only two cases related to incidental findings [56]. In the first, a control group participant in a neuroimaging study was found to have a severe AVM; the patient was referred for treatment which was unsuccessful and led to a lawsuit aimed at the treating clinicians rather than the researchers who identified the original

abnormality. In the second case, failure to identify an incidental finding on a liver scan led to delayed treatment and the successful prosecution of the radiologist. The authors conclude that these legal holdings do not dictate that a researcher who fails to detect or report a potentially dangerous incidental finding on a research scan can be held to the same standard of care as radiologists or other physicians who read clinical scans for specific patients in a clinical setting. However, they do suggest that individuals whose condition worsens, or their survivors, may seek to impose liability on the person who first reviewed the scan if earlier treatment would have yielded a better clinical outcome. Other legal opinions have concluded that the relationship between the investigator and subject does not carry the same degree of fiduciary responsibility as that between clinician and his patient [55, 57], although the legal position remains relatively untested in case law [58].

Current guidance for researchers, ethics committees, and institutional review boards on how to manage incidental findings is rare or difficult to find with little or no consensus. National and supranational ethics and human rights guidance is given in various research documents but is also hard to find [27, 40].

Having a radiologist review images is likely to provide the most accurate interpretation. In general, nonradiological researchers are not used to identifying lesions that are outside their immediate sphere of knowledge (or even within it) and in addition are prone to mistaking artifacts or completely insignificant findings (e.g., falx calcification) for clinically significant abnormalities. Thus, they may cause undue alarm to research subjects. Despite this there is evidence of widespread use of variations of the "reactive radiology" approach that have been widely supported [52, 59] and implemented. Some workers have suggested that reporting of incidental findings is unnecessary or inappropriate [60, 61], whereas others believe that all research scans on healthy controls should undergo expert review [50]. Cramer and colleagues [52] described a system for the management of incidental findings in neuroimaging studies where investigators who

suspected an abnormality would refer the images on a web-based system for specialist review. Over a 5-year period, 27 scans were submitted to review from an estimated 5,000. Interestingly, the abnormalities identified by the investigators showed only limited agreement with the specialist review. The authors argue that this is a cost-effective ($50 per scan reviewed) system for the management of suspected incidental findings. However, the referral rate of half a percent observed in this study must raise significant anxieties that the referral process overlooked other and potentially significant incidental findings. Interestingly, the authors state, "some investigators at our institution used this facility more than others," raising the possibility that there is wide variation in the ability of nonradiological investigators to identify potentially important incidental findings.

There is clear evidence that most research subjects expect that their images will be looked at by a competent trained individual [62]. Furthermore, this belief is not affected by information given in the consent process. However, most imaging research is not done by radiologists or even near to a radiology department and not looked at by a radiologist, so there are genuine practical difficulties and costs in obtaining review of the images. In fact, one survey showed that the most senior person who examined any images obtained during neuroimaging research examinations was usually a junior postdoctoral assistant [51]. It is somewhat unlikely that someone who has only recently completed a PhD in a focused scientific aspect of neuroimaging (e.g., fMRI or tractography) will be adequately trained to recognize or accurately interpret and manage incidental findings.

Thus, while publications from many countries suggest that many agree that research imaging should be reported by radiologists [24, 28, 53, 63–65] (strong evidence), it is less clear as to how this should be achieved in practice [66]. Although it seems unlikely that any would disagree that abnormal scans should be reviewed by specialist radiologist, there is a clear problem in developing systems that will allow sufficiently sensitive and appropriately specific identification

of those examinations that need specialist review. Having a protocol in place for recognition, review and management of incidental findings is important, and this must include clear guidelines on construction of consent, the consent process and methods, and policies for disclosure [40, 59].

These issues were discussed at a UK national (with international participants) meeting on management of incidental abnormalities found on research scans held on 1st June 2010 [40] and further information, including videos and transcripts, can be accessed at http://www.sinapse.ac.uk/media/events/ethics_management.asp and the report at http://www.rcr.ac.uk/docs/radiology/pdf/BFCR(11)8_Ethics.pdf.

How to Manage Incidental Findings

Summary

Discovery of an incidental finding whose management experience is outside the expertise of the investigator should be referred for an expert opinion. It is worthwhile doing this at an early stage since it may preempt the need for further investigation and resolve anxiety. The situation should be discussed with the patient as early as possible, and subsequent investigations should be expedited.

With a few exceptions (intracranial aneurysms [67], internal carotid stenosis [68]), the management of many incidental findings is not guided by good evidence, often because the natural history of the condition is not adequately understood. In some cases, there is guidance available in literature about the management of individual conditions, which may commonly be found as incidental findings. However, the majority of these studies do not deal with the management of potentially asymptomatic incidental findings but rather with the management of the same disease when it has been discovered due to clinical presentation.

The potential negative impact on the individual subject with an incidental finding whose potential importance is unclear, or incorrectly assessed, must also be considered [24, 60]. For example, Royal et al.[60] illustrate an example of a normal subject with an abnormality of unknown significance, thought most likely to be a normal variant, which led to the participant being advised to undergo a course of periodic additional MRI exams with significant associated expense and anxiety.

Supporting Evidence

In the majority of cases, there are no randomized clinical trials describing the natural history or optimal management of asymptomatic incidental findings so that the majority must be managed on an individual basis. Table 3.3 gives a brief description of the clinical management appropriate to common asymptomatic incidental findings, together with appropriate references where possible. However, the majority of these are retrospective case reviews of symptomatic cases and may not be directly applicable in the case of an incidental finding.

There is often considerable debate in the literature concerning the optimal treatment of apparently asymptomatic disorders. One interesting example is in the management of minimally or apparently asymptomatic arachnoid cyst. Typically, surgeons have been reluctant to decompress arachnoid cyst in the absence of significant or dramatic symptoms. However, in recent years there have been a number of studies suggesting that cyst decompression improved the function of adjacent brain tissue, supporting the view that patients with clinically silent cysts may profit from decompression [69–71]. Partly in response to this, some neurosurgeons have adopted a far more aggressive approach with apparently substantial clinical benefits and a low risk of complications [72] (limited evidence).

Special Case: Applicability to Children
Summary

The majority of neuroimaging research is performed in adults, although this may change with the rising interest in use of neuroimaging to study behavioral responses and educational abilities that might predict future antisocial behavior, learning difficulties, or job-related skills [73]. Although there are relatively few studies specific to the detection of incidental findings in children, it has been shown that there

is a higher prevalence of incidental findings relating to otitis, mastoid items, and sinusitis in the pediatric population (approximately 20–25%). Furthermore, investigation of the subjects shows that many are suffering from clinically significant but unsuspected pathology so that identification of signal abnormalities within the ear and mastoid cavity should stimulate referral for ENT review [74, 75]. Other pathologies appear to have similar incidence to adults so that similar concerns apply. However, the range of intracerebral incidental findings in children is less well documented than in adults, and management strategies for many pathologies differ significantly. Under these circumstances, it would seem reasonable to propose a more active form of review for studies in pediatric populations.

Supporting Evidence

There is very little information about incidental neuroradiological findings specifically in children. One small retrospective study ($n = 225$) found that the prevalence of those requiring clinical referral was low (around 7%) and only one required urgent referral [76] (moderate evidence). Other studies have identified a higher prevalence in the pediatric population. In a Japanese cohort study of 110 children, incidental findings were seen in 36.4%; however, 26.4% were due to sinusitis and/or otitis media [61]. The prevalence of incidental findings when these are excluded was 10.9%, but only one patient required urgent referral for assessment. A similar study of 666 children with a mean age of 9.8 years found incidental findings in 25.7%; 17% represented normal variants and only one patient required referral for further assessment [77]. A study of 953 children aged 5–14 years suffering from sickle-cell disease found a 6.6% prevalence of incidental findings, but again only three patients required urgent referral and over half were considered normal variants which did not require further assessment [78]. The high prevalence of middle ear and mastoid abnormalities in children, usually represented as high signal on T2-weighted images, has also been studied by two groups [74, 75], both of whom found

significant prevalence of MR abnormalities (12% and 27%). Both found that in a significant proportion of these groups MR findings were paralleled by previously unidentified clinical symptoms, and both concluded that incidental findings of this kind should prompt a referral for clinical assessment. Incidental findings in the pediatric age group are likely to be little different from the prevalence of non-neoplastic findings in young adults, that is, 2.0% [8]. A major difference to adults is that most neoplasms that present in childhood need to be treated, so there is likely to be less uncertainty about whether or not to treat and when than with, for example, meningiomas in adults. Here the issue is that there are three parties affected by the finding – doctor, patient, and their parents, with substantially more anxiolytic potential.

Special Case: What Benefits Arise from Detection of Incidental Findings?
Summary

There is little evidence about the potential benefits from detention of incidental findings on brain imaging. Although early detection of abnormalities such as cerebral aneurysms or neoplastic lesions would appear to be desirable, the incidence of these is small, and definitive evidence-based guidance concerning optimal management of asymptomatic lesions is commonly unavailable. Even the benefits of identifying unruptured cerebral aneurysms are uncertain, and the benefit of treatment continues to be contentious. A large study published in 1998 showed that the annual rate of rupture of unruptured aneurysms was lower than had previously been believed [79]. Following this, the Stroke Council of the American Heart Association issued guidelines in 2000, [80] which concluded that screening for cerebral aneurysms was not warranted even in subjects where a family member had died from aneurysmal subarachnoid hemorrhage. When unruptured cerebral aneurysms are identified incidentally, current practice suggests that those less than 5 mm should be managed conservatively, those greater than 5 mm in patients below 60 years of age should be considered for surgery,

and only those greater than 10 mm in diameter should be treated under any circumstances [80].

Supporting Evidence

In their large meta-analysis, Morris et al. [8] examined only the prevalence of incidental findings but reviewing the subsequent impact was beyond the remit of the study. Other studies also provide only limited information concerning the benefits or harm derived from the identification of incidental findings. Orme et al. [9] found abnormalities in 136 of 231 scans but referred only five of these for further investigation, of whom one had a sphenoid sinus aspergillus infection and the other a cerebral ependymoma. Vernooij and colleagues [6] described a particularly high incidence of brain abnormalities in a sample of 2,000 normal individuals over the age of 45. The most common abnormalities were asymptomatic infarction (7.2%), cerebral aneurysm (1.8%), meningioma (1.6%), and arachnoid cyst (1.1%). It is interesting therefore to note that of almost 250 patients with reported abnormalities surgery was performed in only two [6]. These were a single patient with a subdural hematoma and one of 35 patients with cerebral aneurysms. Although other details concerning treatment and further management are not given, the authors do state that all aneurysms except for three were less than 7 mm in diameter.

Special Case: Should Image Based For-Profit Health Screening Be Avoided

Summary

Over the past 10 years, an increasing number of companies have begun to offer for-profit clinical screening services using either whole-body CT or increasingly MRI. These services have been particularly popular in the USA and are increasingly available in Europe. They have been highly contentious largely due to the paucity of evidence showing benefit but also due to the risks of over-investigation that we have described above. In particular, whole-body CT has been heavily criticized for its radiation dose which has led to increasing availability of whole-body MRI. There has also been extensive criticism of the increasing social inequality arising from the availability of improved health care to those who can afford to pay for screening.

Supporting Evidence

The arguments concerning the potential benefit/hazards of screening, which have been discussed extensively above, apply equally to commercial screening procedures. Many correspondents [37, 81] and national organizations, including the FDA and the US National Institutes of Health, have been cautious or even critical of these services [82, 83]. Particular criticism has been directed at the use of screening investigations in the brain. Several authors have examined the potential benefits and hazards of an incidental finding of cerebral aneurysm, cerebral tumor, or common incidental findings such as Chiari malformations [37, 81]. Each has reached the conclusion that the benefits, if any, are outweighed by the potential risks of investigation and treatment. In a commentary in the Mayo Clinic Proceedings, Komotar, and colleagues state [81]:

> In New York City, brain MRI screening can be performed for less than $200, regardless of age or medical history, so that brain lesions can be detected at an earlier stage. Although this program appears to have great benefits, closer analysis shows that brain MRI scans should not be recommended for screening healthy populations because of unequal accessibility, disproportionate allocation of health care resources, screening bias, low prevalence, poor predictive value, and limited need and effectiveness of intervention. Further, early detection programs often have negative consequences, and benefit that justifies possible sequelae has not been demonstrated.

There has been little published concerning the incidence of incidental findings in attendees of commercial screening services. The available data suggest that the reported incidence is lower than in research cases with a prevalence of 2% compared to 3.4% in research subjects (weak evidence). The reason for this is extremely unclear. Dr Barnett Kramer, director of the US National Institutes of Health Office of Disease Prevention, said:

for every 100 healthy people who undergo a scan, somewhere between 30 and 18 of them will be told that there is something that needs a workup and it will turn out to be nothing.

This represents a major apparent dichotomy between the reported incidence of incidental findings and the apparent detection rate of abnormalities which may represent a trend to overinvestigate insignificant incidental findings in patients attending screening programs. Interestingly, popularity for these services appears to have waned in the USA with closure of some companies [84].

Take-Home Tables

Tables 3.1 through 3.3 highlight prevalence of incidental findings, guidelines on use of imaging investigations from radiological societies and disease-oriented organizations, and options for management of common incidental findings, respectively.

Imaging Case Studies

Case 1: Asymptomatic 64-year-old scanned as a control subject in a study of vascular depression (Fig. 3.1a, b)

Case 2: A 56-year-old woman scanned as a control subject in a study of cerebral vascular disease (Fig. 3.2a, b)

Table 3.1 Prevalence of incidental findings

Incidental finding	Prevalence (%)
Arachnoid cyst	0.5
Aneurysm	0.35
Meningioma	0.29
Cavernous malformation	0.16
Hydrocephalus	0.1
White matter lesions suggestive of an inflammatory disorder	0.06
Low-grade glioma	0.05
Arteriovenous malformation	0.05
Common developmental variants, rarely of medical importance	Precise unknown

Adapted with permission from Morris Z, Whiteley WN, Longstreth WT, Jr et al. Incidental findings on brain magnetic resonance imaging: systematic review and meta-analysis. Br Med J. 2009;339:b3016

Table 3.2 Guidelines on use of imaging investigations from radiological societies and disease-oriented organizations

Radiological Societies	
American College of Radiologists http://www.acr.org/secondarymainmenucategories/quality_safety/guidelines.aspx	
Royal College of Radiologists http://www.rcr.ac.uk/content.aspx?PageID=995	
Canadian Association of Radiologists http://www.car.ca/en/standards-guidelines/guidelines.aspx	
British Society of Paediatric Radiologists http://www.bspr.org.uk/guidelines.htm	
National Organizations	
Scottish Intercollegiate Guidelines Network (SIGN) http://www.sign.ac.uk/guidelines/published/index.html	
National Institute for Clinical Excellence http://guidance.nice.org.uk/	
UK National Guideline on Management of Incidental Findings in Research Imaging http://www.rcr.ac.uk/docs/radiology/pdf/BFCR(11)8_Ethics.pdf [40]	
Disease-Oriented Organizations	
European Stroke Organization http://www.eso-stroke.org/recommendations.php?cid=9&sid=1	
American Heart Association (cardiac disease and stroke) http://www.americanheart.org/presenter.jhtml?identifier=2158	
European Federation of Neurological Societies http://www.efns.org/Guideline-Archive-by-topic.389.0.html	

Table 3.3 Summary of the management options for common incidental findings

Incidental finding	Commonest potential complications	Treatment of asymptomatic findings
Arachnoid cyst	Pressure on adjacent brain structures	Neurosurgical decompression is not indicated for asymptomatic cysts (no RCTs [72])
Aneurysm	Hemorrhage (risk influenced by aneurysm site and size)	Endovascular coiling or neurosurgical clipping is available, but there is uncertainty about their use because of the lack of published RCTs comparing treatment with conservative management for asymptomatic aneurysms
Meningioma	Pressure on adjacent brain structures	Neurosurgical excision and radiotherapy tend to be used when meningiomas cause symptoms (no RCTs [85])
Cavernous malformation	Hemorrhage and epileptic seizure(s)	Neurosurgical excision and stereotactic radiosurgery are available, but there are no case series or RCTs supporting their use for asymptomatic cavernous malformations [86]
Hydrocephalus	Headache and drowsiness	Intervention is often not indicated for people without symptoms [87]
White matter lesions suggestive of an inflammatory disorder	Later development of multiple sclerosis	Immunological treatments are not indicated. Cautious medical review and advice may be needed [88]
Low-grade glioma	Pressure on adjacent brain structures and epileptic seizure(s)	Neurosurgical excision may be used, but who to treat and when are uncertain (no RCTs). Occasionally more malignant primary brain tumors like glioblastomas have been reported as first presenting during scanning for other purposes
Arteriovenous malformation	Hemorrhage and epileptic seizure(s)	Endovascular embolization, neurosurgical excision, and stereotactic radiosurgery are available. There is an ongoing RCT comparing treatment with conservative management for unruptured AVMs
Common developmental variants, rarely of medical importance[a]		May alarm nonexpert

RCT randomized controlled trial

[a]Additional common developmental or normal variants that are of little health relevance but may alarm the untrained observer include mega cisterna magna, callosal lipoma, asymmetrical ventricles, and enlarged perivascular spaces. Other anomalies that may sometimes be of health relevance and that are not listed above include Arnold Chiari malformations, cerebellar atrophy, and pineal cysts
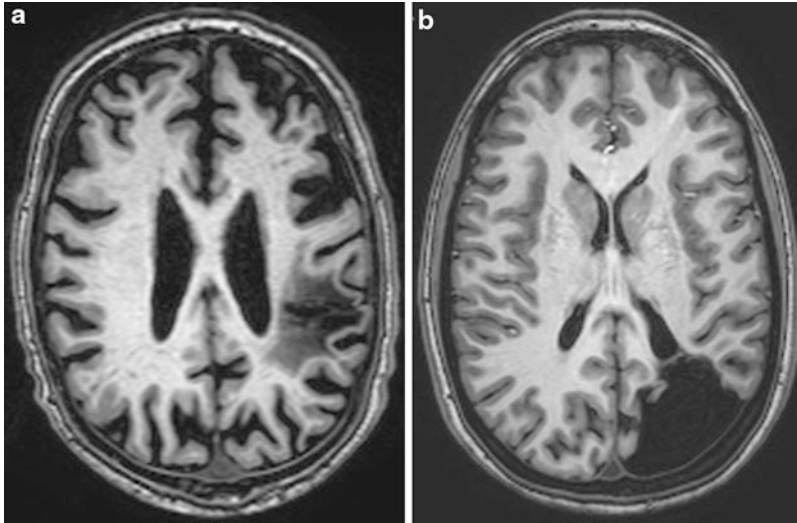
Fig. 3.1 (**a**) An asymptomatic 64-year-old scanned as a control subject in a study of vascular depression. The scan reveals a large long-standing left-sided cerebral infarction. (**b**) A 24-year-old normal volunteer for a functional MR study. Scan shows a large left-sided posterior abnormality believed to represent a long-standing ischemic insult. The patient was referred for clinical assessment and no significant neurological deficit could be demonstrated
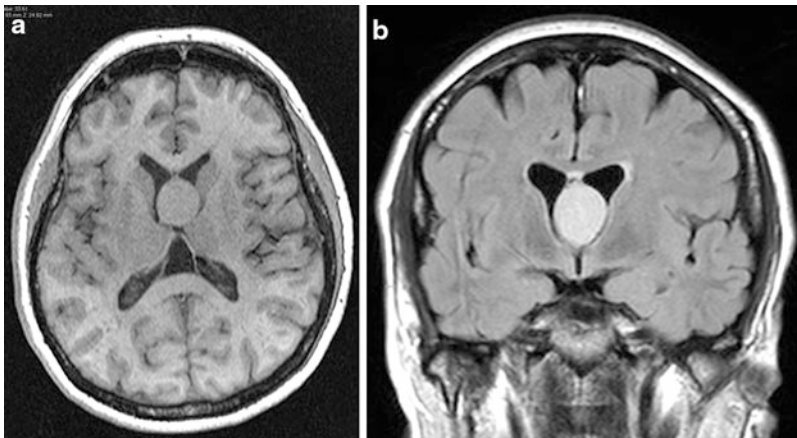
Fig. 3.2 Images from a 56-year-old woman scanned as a control subject in a study of cerebral vascular disease. The scans show a large intraventricular tumor thought most likely to be a colloid cyst. The patient was referred for a neurosurgical opinion, and although she was entirely asymptomatic, the lesion was treated by surgical excision, largely due to the patient's underlying anxiety concerning the diagnosis

Future Research

It should be clear from the forgoing that there are many unanswered questions concerning the incidence and management of incidental findings in clinical practice, health services or commercial screening, and research. The incidence of many incidental findings varies with age, as some conditions are simply more common at some ages than others, but as yet there are too few age-specific studies that published this data.

Population-based imaging studies, health-care providers, and other organizations should endeavor to record and publish information on their incidental finding rates, the medical consequences, and any personal consequences for the patients or volunteers.

For many incidental findings, there is a lack of evidence from well-conducted population studies on the natural history or the finding, the likelihood of progressing to symptoms, or any life-threatening consequences. More information on, for example, vascular malformations such as cavernomas, aneurysms, and developmental lesions should continue to be collected. Centralized health-care statistics could play a key role in facilitating this, where such exist. Consideration should be given to establishing incidental findings registries, making use of internet and image banking expertise that is now emerging. Without better information on natural history, it will be difficult to provide good advice and appropriate medical management.

As a result of the lack of the above, and for many other reasons, there is also a lack of information on the best medical management in relation to specific treatment or the need for regular monitoring if it is decided that no treatment is necessary at the time of detection. This is not a problem that is unique to incidental findings but also affects other conditions like prostate cancer where it is still unclear whether early detection of marginally raised prostate-specific antigen by screening and then treatment is beneficial for the majority or not.

The impact of the additional workload generated by injudicious requests for imaging by clinicians, or use by for-profit screening companies, or in research, on private or publicly funded health-care services has not been quantified but is likely to be considerable. It is also likely to further overload already overloaded health-care providers, detracting from the evidence-based care that they are funded to provide to symptomatic patients, particularly in publicly funded health-care systems. Imaging requests should always be kept to a minimum to help avoid spurious findings and, in the case of CT scanning, to reduce radiation doses. Cost estimates of the likely impact of incidental findings would help health-care providers to manage their use of imaging investigations better.

There is little information on volunteers and patients attitudes toward, or awareness of, incidental findings. It is probably fair to assume that most people would rather not have an incidental finding as it is likely to raise anxieties even if it turns out to be of no medical consequence. Nonetheless, how best to manage these from the patient or volunteer's point of view is currently largely based on speculation and a few case reports. Further studies are needed to determine the best ways of managing incidental findings to minimize anxiety to patients or volunteers as this would help develop policies for imaging research and clinical practice.

The true full extent of the wider implications of incidental findings, such as employment, insurance (health, travel, life, etc.), and mortgages for house purchase, is not well known and probably varies. However, with the increasing use of imaging, it will be important for insurance companies and employers to develop thoughtful, equitable, and sensible approaches to otherwise healthy individuals.

References

1. Di Costanzo A, Tedeschi G, Di Salle F, et al. J Neurol Neurosurg Psychiatry. 1993;56:207–8.
2. Illes J. Nat Clin Pract Neurol. 2006;2:60–1.
3. Grossman RI, Bernat JL. Neurology. 2004;62:849–50.
4. Katzman GL, Dagher AP, Patronas NJ. J Am Med Assoc. 1999;282:36–9.
5. Kamath S, Jain N, Goyal N, et al. Clin Radiol. 2009;64:353–61.
6. Vernooij MW, Ikram MA, Tanghe HL, et al. N Engl J Med. 2007;357:1821–8.
7. Soultati A, Alexopoulou A, Dourakis SP, et al. Eur J Intern Med. 2010;21:123–6.
8. Morris Z, Whiteley WN, Longstreth Jr WT, et al. Br Med J. 2009;339:b3016.
9. Orme NM, Fletcher JG, Siddiki HA, et al. Arch Intern Med. 2010;170:1525–32.
10. Hartwigsen G, Siebner HR, Deuschl G, et al. J Comput Assist Tomogr. 2010;34:596–600.
11. Lumbreras B, Donat L, Hernandez-Aguado I. Br J Radiol. 2010;83:276–89.
12. Vermeer SE, Longstreth Jr WT, Koudstaal PJ. Lancet Neurol. 2007;6:611–19.

13. Bryan RN, Cai J, Burke G, et al. AJNR Am J Neuroradiol. 1999;20:1273–80.
14. Cordonnier C, Al-Shahi Salman R, Wardlaw J. Brain. 2007;130:1988–2003.
15. Goos JD, van der Flier WM, Knol DL, et al. Stroke. 2011;42:1894–900.
16. Vernooij MW, Ikram MA, Wielopolski PA, et al. Radiology. 2008;248:272–7.
17. Furtado CD, Aguirre DA, Sirlin CB, et al. Radiology. 2005;237:385–94.
18. MacHaalany J, Yam Y, Ruddy TD, et al. J Am Coll Cardiol. 2009;54:1533–41.
19. Morin SHX, Cobbold JFL, Lim AKP, et al. Eur J Radiol. 2009;72:529–33.
20. Rinkel GJ, Djibuti M, Algra A, et al. Stroke. 1998;29:251–6.
21. International Study of Unruptured Intracranial Aneurysms Investigators. Lancet. 2003;362:103–10.
22. Wardlaw JM, White PM. Brain. 2000;123:205–21.
23. Illes J, Kirschen MP, Gabrieli JD. Nat Neurosci. 2003;6:205.
24. Wolf SM, Lawrenz FP, Nelson CA, et al. J Law Med Ethics. 2008;36:219–48.
25. Illes J, Kirschen MP, Edwards E, et al. Science. 2006;311:783–4.
26. Hoggard N, Darwent G, Capener D, et al. J Med Ethics. 2009;35:194–9.
27. Booth TC, Jackson A, Wardlaw JM, et al. Br J Radiol. 2010;83:456–65.
28. Heinemann T, Hoppe C. Klin Neuroradiol. 2009;19:108–10.
29. Qureshi AI, Feldmann E, Gomez CR, et al. J Neuroimaging. 2009;19(Suppl 1):1S–10.
30. McDonald IG, Daly J, Jelinek VM, et al. Br Med J. 1996;313:329–32.
31. Howard L, Wessely S, Leese M, et al. J Neurol Neurosurg Psychiatry. 2005;76:1558–64.
32. Spence D. Br Med J. 2011;342:d1039.
33. Marshall T. Reducing unnecessary consultation – a case of NNNT? http://www.medicine.ox.ac.uk/bandolier/band44/b44-4.html (1997)
34. Stone HJ. N Engl J Med. 2006;26:2748–9.
35. Thomson B. Lancet. 1998;352:1216–18.
36. Raeburn S. Community Genet. 2002;5:102–9.
37. Al-Shahi Salman R, Whiteley W, Warlow C. J Med Screen. 2007;14:2–4.
38. Warlow C. Br Med J. 2009;338:1274.
39. Spence D. Br Med J. 2011;342:d1197.
40. The Royal College of Radiologists. Management of incidental findings detected during research imaging. London: Royal College of Radiologists; 2011.
41. Hayward R. Br Med J. 2003;326:1273.
42. Illes J. Lancet Neurol. 2008;7:23–4.
43. Hendee WR, Becker GJ, Borgstede JP, et al. Radiology. 2010;257:240–5.
44. Lehnert BE, Bree RL. J Am Coll Radiol. 2010;7:192–7.
45. American College of Radiology. ACR appropriateness criteria: background and development. www.acr.org/SecondaryMainMenuCategories/quality_safety/app_criteria/Background-andDevelopment.aspx (2012)
46. Bautista AB, Burgos A, Nickel BJ, et al. AJR Am J Roentgenol. 2009;192:1581–5.
47. Mushlin AI, Mooney C, Grow V, et al. Arch Neurol. 1994;51:67–72.
48. Sox HC, Margulies I, Sox CH. Ann Intern Med. 1981;95:680–5.
49. Emanuel EJ, Menikoff J. N Engl J Med. 2011;365(12):1145–50.
50. Milstein AC. J Law Med Ethics. 2008;36:356–60.
51. Illes J, Kirschen MP, Karetsky K, et al. J Magn Reson Imaging. 2004;20:743–7.
52. Cramer SC, Wu J, Hanson JA, et al. Neuroimage. 2011;55:1020–3.
53. Mamourian A. AJNR Am J Neuroradiol. 2004;25:520–2.
54. Wolf SM, Paradise J, Caga-anan C. J Law Med Ethics. 2008;36:361–83.
55. UK Biobank Ethics and Governance Council. Involving publics in biobank research and governance. London: UK Biobank Ethics and Governance Council; 2009.
56. Tovino SA. Account Res. 2008;15:242–61.
57. Morreim EH. J Law Med Ethics. 2005;33:586–98.
58. Morreim EH. J Law Med Ethics. 2004;32:474–84.
59. Booth TC, Waldman AD, Wardlaw JM, et al. Br J Radiol. 2012;85(1009):11–21.
60. Royal JM, Peterson BS. J Law Med Ethics. 2008;36:305–14.
61. Seki A, Uchiyama H, Fukushi T, et al. J Epidemiol. 2010;20:S498–504.
62. Kirschen MP, Jaworska A, Illes J. J Magn Reson Imaging. 2006;23:205–9.
63. Burger I, Kass N. J Am Coll Radiol. 2006;3:932–9.
64. Kleinschmidt A. Curr Opin Neurol. 2007;20:387–9.
65. Brown DA, Hasso AN. AJNR Am J Neuroradiol. 2009;29:1425–7.
66. Illes J, Kirschen MP, Edwards E, et al. Neurology. 2008;70:384–90.
67. Molyneux AJ, Kerr RS, Yu LM, et al. Lancet. 2005;366:809–17.
68. Halliday A, Mansfield A, Marro J, et al. Lancet. 2004;363:1491–502.
69. De Volder AG, Michel C, Thauvoy C, et al. B J Neurol Neurosurg Psychiatr. 1994;57:296–300.
70. Lang W, Lang M, Kornhuber A, et al. Eur Arch Psychiatry Neurol Sci. 1985;235:38–41.
71. Raeder MB, Helland CA, Hugdahl K, et al. Neurology. 2005;64:160–2.
72. Helland CA, Wester KA. J Neurol Neurosurg Psychiatry. 2007;78:1129–35.
73. Illes J, Raffin TA. Cerebrum. 2005;7:33–46.
74. Balci A, Sangun O, Okuyucu S, et al. Int J Pediatr Otorhinolaryngol. 2008;72:1849–54.
75. Blomgren K, Robinson S, Lonnqvist T, et al. Int J Pediatr Otorhinolaryngol. 2003;67:757–60.
76. Kim BS, Illes J, Kaplan RT, et al. AJNR Am J Neuroradiol. 2002;23:1674–7.

77. Gupta SN, Belay B. J Neurol Sci. 2008;264:34–7.
78. Jordan LC, McKinstry III RC, Kraut MA, et al. Pediatrics. 2010;126:53–61.
79. The International Study of Unruptured Intracranial Aneurysms Investigators. N Engl J Med. 1998;339:1725–33.
80. Bederson JB, Awad IA, Wiebers DO, et al. Stroke. 2000;31:2742–50.
81. Komotar RJ, Starke RM, Connolly ES. Mayo Clin Proc. 2008;83:563–5.
82. Health Canada. Whole body screening using MRI or CT technology. http://www.hc-sc.gc.ca/hl-vs/alt_formats/pacrb-dgapcr/pdf/iyh-vsv/med/mri-irm-eng.pdf (2003)
83. Royal Australian and New Zealand College of Radiologists. The use of diagnostic imaging for screening purposes and non-referred investigations: RANZCR statement of principles. Sydney: RNAZCR; 2005.
84. Gottlieb S. Br Med J. 2005;330:272.
85. Rubin G, Herscovici Z, Laviv Y, et al. Isr Med Assoc J. 2011;13:157–60.
86. Brunon J, Nuti C. Neurochirurgie. 2007;53:122–30.
87. Guillaume DJ. Neurosurg Clin N Am. 2010;21:653–72.
88. Sellner J, Schirmer L, Hemmer B, et al. J Neurol. 2010;257:1602–11.

Decision Support in Diagnostic Radiology

4

Ivan K. Ip and Ramin Khorasani

Contents

———————————————

I.K. Ip (✉)
Department of Radiology, Harvard Medical School, Center for Evidence-Based Imaging, Brigham and Women Hospital, Brookline, MA, USA
e-mail: iip@partners.org

R. Khorasani
Department of Radiology, Harvard Medical School, Brigham and Women's Hospital, Boston, MA, USA
e-mail: rkhorasani@partners.org

Key Points

- To improve quality of care and reduce waste in healthcare, broad system change is sorely needed. Health information technology (HIT) solutions will be core components and enablers of this change.
- Knowledge-enabled HIT tools that deliver point-of-care, context-specific, decision support (DS) can encourage evidence-based practice, improving quality and reducing waste (limited to moderate evidence).
- The meaningful use of a computerized physician order entry (CPOE) system with clinical DS can help guide appropriate use of imaging studies. Despite growing evidence of its benefits, CPOE adoption has been slow, with only 9.6 % of US hospitals having CPOE completely available as of 2002 (limited evidence).
- An imaging CPOE system with embedded DS can be integrated into an organization's healthcare information technology infrastructure and be broadly accepted in clinical practice (moderate evidence).
- There is substantial opportunity for CPOE to contribute to imaging services, including gains in quality of care as well as patient safety and reduction in waste. CPOE with embedded DS can help reduce inappropriate testing, thereby decreasing unnecessary radiation exposure and costs. Real-time capture of relevant clinical information at the time of order entry can help improve the quality of radiologist's interpretation. As demonstrated in a case study, the implementation of an integrated computerized DS into CPOE is associated with a decrease in overall use and increase in yield of computed tomography (CT) angiograms in the evaluation of pulmonary embolism (moderate evidence).

Definition

Computerized physician order entry (CPOE) is a process of order entry where physicians and other providers communicate instructions for the care of patients electronically over a computer network. A physician may indicate diagnostic tests, such as imaging studies, they want to order by choosing from a predetermined set of menus. Information regarding patient's symptoms, past medical history, and probable diagnoses are collected through a series of check boxes and free text fields. One important feature of CPOE is patient-centered decision support (DS). DS is an iterative interaction of a user with a computer using brief, automated, actionable, context-specific, real-time feedback to optimize user decisions and actions. DS is designed to educate, encourage, and enforce the use of evidence in day-to-day practice. It educates physicians through technology with the most updated, evidence-based guidelines. It encourages new approaches to improve quality of healthcare delivery. Lastly, it also can enforce appropriate ordering patterns through accountability.

Trends and Use

Over the past four decades, advances in diagnostic imaging have revolutionized the practice of medicine. These advances have enhanced physicians' understanding of diseases, improved diagnostic accuracy, and contributed tremendously to patient care [1]. Along with these benefits, imaging studies also lead to harm, such as increased cancer risk from radiation exposure and contrast-associated adverse effects, and carry substantial financial costs [2]. In the report, Crossing the Quality Chasm, the Institute of Medicine identified waste as an unwanted but ever-present feature of our healthcare delivery system [3]. Heterogeneity and variability in clinical practice

patterns contribute to this waste. Unwarranted practice variation has resulted in underuse, misuse, and overuse of care, thus compromising overall quality of healthcare delivery [4]. Some estimates suggest that 30–40 % of all imaging studies performed in the United States may be unnecessary [5].

Overall Cost to Society

The financial cost of medical imaging has grown rapidly over the past decade. In 2008, imaging services expenditures totaled $11.7 billion among Medicare beneficiaries [6]. Between 1998 and 2001, utilization of high-cost imaging studies, including magnetic resonance (MR), computed tomography (CT), and ultrasonography (US), increased by 8.3–16.6 % annually per Medicare enrollee [7]. Similar trends were observed in private insurance groups and individual institutions [8, 9]. Medical imaging is now estimated to account for 5–10 % of healthcare expenditures [10].

The use of a computerized physician order entry (CPOE) system has been proposed as a means to improve quality and efficiency and to reduce health disparities [11–15]. To stimulate its adoption, the federal government has allocated $19 billion through the Health Information Technology for Economic and Clinical Health Act [16]. Yet, it is estimated that the creation of a national health information network may cost as much as $156 billion in capital investment and $48 billion in annual operating costs [17].

Goals of CPOE

Using decision support (DS), HIT solutions are not only capable of automating workflow processes to improve efficiency but also of delivering knowledge at the point of care to inform clinical decision making [18].

Methodology

A MEDLINE search was performed using PubMed research publications discussing the use of computerized decision support on imaging utilization, quality, and clinical outcomes. The search covered the years January 2000 to June 2011. Additional articles were identified by reviewing the reference lists of all relevant papers.

Discussion of Issues

Why Is Decision Support Important in Radiology?

Summary
Significant variations in diagnostic radiology practices exist, resulting in underuse, overuse, and misuse of technology (limited to moderate evidence). System-wide HIT solutions are needed to cross the quality chasm.

Supporting Evidence
Patients, healthcare providers, healthcare delivery systems, and payers would agree that safety, quality, and efficiency are the key features of an optimal healthcare system. Yet in Crossing the Quality Chasm [3], waste was identified by the Institute of Medicine as an unwanted but ever-present feature of our current healthcare delivery system. It is also clear that even when scientific evidence exists, the practice of medicine lags behind the knowledge base by several years [3, 19]. Lomas et al. [19] found that the adoption of published guidelines into routine practice may take an average of 5 years. Furthermore, the adoption of evidence into practice is often heterogeneous [20, 21]. Unwarranted practice variation has resulted in underuse of effective care, misuse of preference-sensitive care, and overuse of supply-sensitive care, compromising the overall healthcare quality [4].

Variations in diagnostic radiology practices are well documented. A study using Medicare claims from 1999 through 2006 found substantial differences in radiology ordering patterns across US regions, which were considered unlikely related to patient characteristics [22]. Arnold et al., using the Pediatric Health Information System database, found that diagnostic imaging utilization and costs vary widely across 40 US children's hospitals despite case-mix adjustment [23]. This practice variation has resulted in suboptimal quality and waste.

Over the past 20 years, the utilization of imaging studies has increased significantly, with associated financial burdens. In one university-affiliated quaternary care emergency department (ED), the intensity of abdominal imaging examinations per 1,000 ED visits increased by 2.7-fold in relative value units (RVUs) between 1990 and 2009 [24]. The prevalence of CT or MRI use during US ED visits for injury-related conditions increased from 6 % in 1998 to 15 % in 2007, without an equal increase in the prevalence of life-threatening conditions [25]. Not only does this increase in imaging utilization result in higher cost of healthcare, it also poses potentially unnecessary radiation exposure risk to patients. It is estimated that as many 29,000 cancers could be related to CT scans alone in the United States annually [26].

Although the overall use of imaging has increased, many pockets of underuse persist. Technology underuse is defined as the portion of eligible patients who could benefit from a procedure but who do not receive it. Screening mammography is an example of underuse in radiology. Studies identified that the use of screening mammography over extended periods of time is rare [27]. The average number of mammograms received during a 10-year period was 5.06, 51 % of what the American Cancer Society recommended. In the overall population, only 6 % of women received annual mammography as recommended over a decade.

Potential driving forces for radiology practice variation may include "defensive medicine," knowledge gap about evidence and appropriateness, information gap regarding availability of prior images, poor understanding of the risks of recurrent radiation exposure, and accountability gap in the current healthcare financial model. As suggested by the Institute of Medicine's report, inefficient and suboptimal quality of care will not be resolved by working harder; system-wide changes will be necessary to cross the quality chasm. These changes include HIT solutions that can (1) automate workflow processes to improve efficiency and productivity, (2) deliver knowledge at the point of care to inform clinical decision making, and (3) improve patient safety and quality of care [18]. Electronic health records (EHRs) and CPOE have been proposed as a means to improve quality and efficiency and to reduce some of the aforementioned gaps [11–15].

Why the Urgency?

Summary

Financial issues, physicians' resistance, and concern about HIT system interoperability are some barriers to the widespread adoption of healthcare information technology (insufficient evidence).

Supporting Evidence

The widespread adoption of EHR and CPOE has become important cornerstones of national healthcare policy [28]. Their use in clinical practice has been associated with improvements in medication safety, efficiency, physician ordering patterns, and cost reduction [12–15, 29]. To catalyze the national adoption of EHR, Congress passed the Health Information Technology for Economic and Clinical Health (HITECH) Act as part of the American Recovery and Reinvestment Act (ARRA) of 2009. The ARRA authorized the Centers for Medicare and Medicaid Services to provide financial incentives for providers who successfully implement "meaningful use" of technology, including CPOE [30].

Initial experience shows promising CPOE impact on some physician imaging ordering practices [31]. Despite growing evidence of its benefits, CPOE adoption has been slow, with only 9.6 % of US hospitals having CPOE completely available [32]. Financial barriers, physicians'

resistance, and concern about interoperability have been cited as potential obstacles to adoption [33]. The meaningful use of healthcare IT can improve patient safety, efficiency, and quality of care. For example, with DS, the percentage of low-utility imaging studies may decrease by as much as 57 % [34].

What Types of Radiology Decision Support Systems Are Available?

Summary
Types of radiology decision support systems include imaging appropriateness, patient safety, and reporting quality (insufficient evidence).

Supporting Evidence
In its broadest definition, DS can help enhance user actions and decisions across every component of the imaging care delivery process, including ordering, scheduling, planning, performance, interpretation, results communication, and follow-up imaging results, to ensure optimal quality of care. Several arbitrary categories of decision support below illustrate potential capabilities of DS.

Appropriateness Decision Support
Appropriateness DS provides evidence about the appropriateness of a test to a requesting physician at the time of ordering with advice to either cancel the inappropriate examination or follow an alternate, more appropriate recommendation. Unlike radiology benefits management programs in which companies utilize ancillary personnel to manually review orders, CPOE can be integrated into an EHR to deliver appropriateness DS in real time [35–38]. Figure 4.1a–c illustrates an example of this type of DS when ordering an abdominal radiograph for a patient with suspected appendicitis. DS triggers a low-utility message with recommendations for a higher yield examination.

Various sources of evidence for this type of DS exist. The strength of evidence [39] presented in DS is likely to have a substantial impact on its adoption into clinical practice. The optimal evidence is peer-reviewed literature, particularly research using decision analytic, decision rule, or cost-effective analysis [40–50]. Practice guidelines, such as the American College of Radiology (ACR) Appropriateness Criteria [51] may potentially be useful [52, 53]; however, critics have argued that these criteria are not evidence based, but rather, they are based on consensus of expert panels [54]. Local best practices, if established, could also serve as a source of content that reflects the organization's own practice pattern.

Patient Safety Decision Support
Patient safety DS can help address key safety concerns in radiology. DS can incorporate real-time access to a healthcare organization's clinical data repository in order to deliver advice based on patient allergy information, renal function, or other relevant data. Examples of safety DS may include messages to premedicate a patient with a prior mild to moderate reaction to intravenous contrast. Alternatively, radiation safety, particularly for pregnant patients and children, as well as repeat imaging, has also elicited increasing interest. Figure 4.2a–d shows a patient safety DS example for the use of MRI intravenous contrast in a patient at risk for nephrogenic systemic fibrosis (NSF).

Reporting Quality Decision Support
Reporting quality DS can be delivered to radiologists at the time of interpretation to improve the quality of the report. There are many such examples, some of which are described below to illustrate the opportunities for performance improvement.

One potential use of DS is to help radiologists make evidence-based follow-up recommendations. It has been reported that substantial variation exists in radiologists' follow-up recommendations when reporting cystic pancreatic lesions, which may contribute to suboptimal care [55, 56]. DS derived from the American College of Radiology recommendations for follow-up of incidental findings [57] may help guide the reporting of these incidental findings. DS can also deliver automatic reminders regarding relevant Physician Quality Reporting System

(PQRS) measures established by the Centers for Medicare & Medicaid Services (CMS). One radiology-specific metric is Measure 10, "Stroke and Stroke Rehabilitation: Computed Tomography (CT) or Magnetic Resonance Imaging (MRI) Reports." The reporting component of Measure 10 assesses documentation of presence or absence of hemorrhage, mass, and acute infarction. DS with the ability to remind users when a component of reporting is missing may enhance rates of adherence to the measure and help improve report quality and enhance reimbursement. Evidence-based guidelines are a critical first step in establishing best practice. DS embedded in structured reporting solutions or enabled by natural language processing tools can help ensure optimal format and content of radiology reports [58].

What Are the General Features of Effective Radiology Decision Support?

Summary

A system's speed, usability, need for duplicate data entry, integration into workflow, and actionability are important technical features in the success of DS implementation (insufficient evidence).

Supporting Evidence

A number of features associated with effective decision support tools have been described [59]. From a radiology perspective, they include the following:

- *Speed*. The time it takes to access DS is critical to users [60, 61]. Speed is characterized as (1) "screen refresh rate," or the time elapsed in moving from one screen to next, and (2) the number of "mouse clicks" needed to perform a function. The effectiveness of DS delivery and adoption of the technology will be seriously challenged if issues of speed are not sufficiently addressed [62–64].
- *Usability*. Simple, intuitive design is critical to maintaining credibility with users [59]. Online help tools and tutorials can be useful.

The need to minimize scrolling and mouse clicks is essential in clinical areas. Extensive predeployment testing in an environment that mimics its intended function serves great importance to improve usability.

- *Eliminate duplicate data entry*. Integration of various applications and databases are often necessary and can be done using standards-based technology such as that supported by the Integrating the HealthCare Enterprise (IHE) initiative [65]. The need to log in individually to different applications or repeatedly enter clinical information will reduce the adoption of these technologies. As it is unlikely that a single vendor is capable of delivering all the functionality necessary to automate a complex healthcare delivery organization, integration is key to success, which may require significant resource allocation.
- *DS must be embedded in workflow*. Simply making information available electronically has little effect on clinical practice [66]. Practitioners are likely to ignore DS unless it is concise, context specific, and relevant to their current decision, delivered at the point of care.
- *DS must be actionable*. Messages such as "the opinion on this topic is varied" are useless. Such DS is likely to result in user fatigue [67]. Effective DS must be easily translatable to specific actions. When actionable DS is presented, physicians can either accept or override DS, unless the test will pose a patient safety risk.
- *DS must be evidence based, referenced, and up to date*. Evidence-based DS helps build credibility in the application. It is important to provide users with references to online abstracts, as well as the methodology used to maintain the knowledge base. There should also be opportunities for users to send feedback to those who manage the applications and its content.
- *Monitor use, feedback, and modify as necessary*. Constant monitoring and modifications as needed are critical to ensure DS has the desired effects. It often is important to identify predetermined metrics and potential downstream effects of the DS. For example, it may

be useful to monitor the proportion of radiology orders entered electronically by physicians if the DS is designed to target physician users.

- *Nonphysician use*. Care should be taken to assess the needs of nonphysician users when designing DS. If a practice has administrative staff that enters radiology orders as proxy for physicians, the language of DS should be targeted to suit the knowledge base of those staff.
- *Bundle DS with other tools designed to impact physician behavior*. Education alone is often not enough to change physician behaviors [68]. Use of complimentary tools may have synergistic effects in helping change physician behavior. Peer-to-peer review, in which a physician who ignored DS when ordering a test is required to discuss the case with a peer before being allowed to proceed, is an example. Quarterly reports publishing individual providers' rates of guideline adherence and financial incentive are other examples.
- *Managing change*. The most well-designed DS delivery software will fail without attention to organizational processes and corporate culture [69]. A culture emphasizing quality and safety and a clearly stated vision from the highest levels of the organization are essential elements in the success of HIT.

What Is the Current State of Decision Support in Imaging?

Summary
There is substantial opportunity for CPOE to contribute to imaging services, including gains in quality of care as well as patient safety and reduction in waste (moderate evidence).

Supporting Evidence
The balance of this chapter focuses on the use and impact of appropriateness decision support in imaging. In 2001, Khorasani highlighted efficiency gains, improved test selection, and test appropriateness along with cost savings as potential benefits of CPOE in radiology [10]. While there is still much to accomplish, significant progress has been made. A recent systematic review of the impact of CPOE on medical imaging services identified 14 relevant articles in the past 10 years. In the majority of studies, findings suggest that significant imaging efficiency gains can be achieved, particularly in promoting adherence to existing guidelines. A time-series study was conducted in the medical emergency departments of two French teaching hospitals. During the intervention periods, DS was displayed, with focus on chest radiographs, abdominal plain radiographs, and brain CT. The proportion of orders that did not adhere to guidelines decreased from 33.2 % to 26.9 % ($p < 0.0001$) when DS was activated [70]. Peer management through a resource utilization committee using CPOE reduced provider variability in test-ordering behaviors [71]. In addition, a retrospective study concluded that CPOE and a simple change in the business logic resulted in a substantial decrease in the ordering of low-yield imaging exams [72]. Blackmore et al. implemented evidence-based DS for selected high-volume imaging procedures that include lumbar MRI, brain MRI, and sinus CT; the use of DS was associated with large decreases in the utilization of these targeted studies [73].

Preliminary data regarding the impact of the imaging CPOE on quality has been encouraging. However, it is important to emphasize that the success of DS relies heavily on institutionalizing change in the organizational culture [74]. Peer-to-peer review of orders and distribution of practice pattern variation reports comparing physicians with similar specialties and case mix [75] are also important complements in addressing the unwarranted variation in use of healthcare resources. A time-series study examined the imaging utilization of a commercial patient population compared to Medicare beneficiaries from 2003 to 2007 at an institution who had implemented CPOE with embedded decision support. In addition to CPOE with DS, the intervention for the commercial population included targeted peer-to-peer review for examinations in which testing appropriateness remained ambiguous, as well as the distribution of a quarterly practice pattern variation report to physicians

responsible for the care of the commercial population being studied. While the number of advanced imaging tests per Medicare beneficiary increased by 24.2 %, from 0.33 studies per beneficiary in 2003 to 0.41 in 2007 [76], high-cost imaging utilization in the commercial population decreased by 9.3 % (Fig. 4.3).

Case Study 1: Implementation and Adoption of CPOE with Embedded Decision Support

At Brigham and Women's Hospital, an imaging CPOE was implemented in 1998. After a period of design, prototype development, pilot testing, user feedback, and integration planning, radiology CPOE was gradually phased into clinical practice in 2000.

The CPOE system is a Web-enabled tool (Percipio™, Medicalis Corp., San Francisco, CA). Without any financial incentives to encourage use, CPOE adoption rose steadily during the implementation, from 0.5 % in 2000 to 94.6 % in 2010 ($p < 0.005$). During the same time span, CPOE meaningful use (defined as the proportion of imaging studies performed with orders electronically created or electronically signed by an authorized provider) also increased significantly ($p < 0.005$). Figure 4.4 illustrates the adoption of CPOE over time. Based on this experience, an imaging CPOE system with embedded DS can be broadly accepted and used in clinical practice.

Case Study 2: Utilization of CT for Evaluation of Pulmonary Embolism

Data from multiple clinical trials, including the Prospective Investigation of Pulmonary Embolism Diagnosis II (PIOPEP II) trial, have previously validated a diagnostic algorithm in patients suspicious for PE that emphasizes the use of a clinical decision rule, known as the Wells criteria, along with D-dimer testing and CTs. Using this simple clinical model and D-dimer testing, it was found that further testing with CTs can be avoided in low-risk patients, thereby preventing unnecessary exposure to intravenous contrast and radiation [77, 78]. Yet, in recent years, the use of CTs in the emergency room has

increased significantly, reportedly fivefold at one large academic institution between 2001 and 2006 [79]. Therefore, at Brigham and Women's Hospital, a DS intervention was implemented on CT performed in the ED for PE [80].

The appropriateness DS tool required ordering clinicians to input both a D-dimer level ("elevated," "normal," and "not done") and the clinical suspicion of pulmonary embolus ("high," "intermediate," and "low"). Depending on the inputted data, a DS message was automatically displayed in patients with a medium or low level of suspicion and in whom a D-dimer was not performed: "Measuring a D-dimer value in patients with a low/intermediate clinical suspicion of pulmonary embolism is an appropriate first step in the workup of acute PE and will exclude the need for CT in some patients." In addition, in patients who had a normal D-dimer and medium or low suspicion, another DS message informed the ordering physician of its low yield: "Based on current evidence as well as our experience, diagnosing an acute pulmonary embolism by CT pulmonary angiography in low or intermediate risk patients with a normal D-dimer is extremely unlikely." At each stage, clinicians could either cancel the imaging order or ignore the advice.

The simple implementation of the DS tool into CPOE at the time of order entry resulted in a significant decrease in utilization and improvement in the yield of CTs. The quarterly use of CT rose 82.1 % before implementation of DS, from 14.5 to 26.4 CTs/1,000 patients ($p < 0.0001$). After implementation of DS, quarterly use decreased by 20.1 %, from 26.4 CTs/1,000 patients to 21.1 CTs/1,000 patients ($p = 0.04$). Of all the CTs performed during this 6-year period, 686 (10.0 %) were positive for PE, and the yield by quarter increased from 5.8 % to 9.8 % subsequent to the implementation of DS ($p = 0.03$) [80].

Take-Home Figures

Figures 4.1a–c and 4.2a–d show examples of decision support systems. Figures 4.3 and 4.4 demonstrate trends in imaging utilization.

Fig. 4.1 Screenshots of the computerized physician order entry (CPOE) system of exam selection (**a**), indication menu (**b**), and decision support (**c**) (Percipio™, Courtesy of Medicalis Corporation, San Francisco, CA)

a

BWH **Ordering Physician:** Ip, Ivan K., M.D.   **Site:** TEST PRACTICE   ⌄   Logoff

Welcome to Percipio - PHSAPP1-ORM1

MRI Head with Perfusion (Tumor) Indications   **Order Placement**

Patient Name: **OETEST, BRIDGET**		FH MRN **00001007**	
Birth Date: May 1, 1941	Age: 70 years	Gender: Female	Phone Number:
Ordering Provider: **Ip, Ivan K, MD**		Payor: BWH - Self Pay	
Exam: **MRI Head with Perfusion (Tumor)**		Order ID: 17671468	Room: N/A
Created By: N/A		Ordering Site: TEST PRACTICE	

Decision Support

MRI is contraindicated and will not be performed for patients with Cardiac Pacemakers, Implanted Cardiac Defibrillator (ICD), Cardiac Electrodes, Pacing Wires, Internal Electrodes, Cochlear, Otologic or other Ear Implants. Patients with surgical staples should not be imaged until 7 days post-op unless approved by a radiologist.

If patient has a Brain Aneurysm Clip, please see More Info.

All patients must complete an MR Screening Form prior to their study. Please provide this form and instruct patient to complete and bring to scheduled exam.
- Click for English Spanish BWH MR Screening Form
- Click here for DFCI MR Screening Form

This information is presented to assist you in providing care to your patients. It is your responsibility to exercise your independent medical knowledge and judgment in providing what you consider to be in the best interest of the patient.

More Info

Feedback

Submit   Reset Order

b

Decision Support

Nephrogenic Systemic Fibrosis (NSF) is a rare disease that has been described in patients with **renal insufficiency** receiving intravenous MRI contrast material (gadolinium). In rare cases NSF has resulted in lung or heart failure and patient death.

Patients with the following conditions may be at increased risk for severe renal insufficiency (eGFR <30) and therefore at increased risk for NSF.

- Personal or family history of kidney failure
- Diabetes Mellitus treated with oral hypoglycemic and/or insulin
- Multiple Myeloma or other paraproteinemia syndromes or diseases
- Lupus or other collagen vascular diseases

Other conditions that have been associated with NSF include:

- Current dialysis treatment
- Acute renal failure
- Hepatorenal syndrome
- Awaiting or 6 weeks status post liver transplantation
- End stage liver disease

More Info

Feedback

1) Do any of the above conditions apply?
○ Yes ○ No

2) Is the patient currently taking Cox-1 or Cox-2 inhibitors nonsteroidal anti-inflammatory drugs (e.g. naproxen, celecoxib, ibuprofen)?
○ Yes ○ No

This information is presented to assist you in providing care to your patients. It is your responsibility to exercise your independent medical knowledge and judgment in providing what you consider to be in the best interest of the patient.

Submit

Fig. 4.2 (continued)

c

Decision Support

To reduce the risk of NSF in patients taking Cox-1 and Cox-2 inhibitors with these pre-existing conditions and treatments, obtain an eGFR within 24 hours prior to the scheduled appointment.

If Cox-1 and Cox-2 inhibitors can be discontinued 24 hours prior to MRI then an eGFR within 3 weeks prior to the scheduled appointment is needed. Patient may resume medications immediately after the exam.

Please see **More Info** button for information regarding Nephrogenic Systemic Fibrosis (NSF).

This information is presented to assist you in providing care to your patients. It is your responsibility to exercise your independent medical knowledge and judgment in providing what you consider to be in the best interest of the patient.

More Info

Feedback

Continue   Reset Order

d

Decision Support

As gadolinium may be administered, a recent **(within 3 weeks of appointment) Serum Creatinine and estimated glomerular filtration rate (eGFR)** will be required. If not available, the appointment will be rescheduled.

Please see "**More Info**" button for information regarding Nephrogenic Systemic Fibrosis (NSF).

This information is presented to assist you in providing care to your patients. It is your responsibility to exercise your independent medical knowledge and judgment in providing what you consider to be in the best interest of the patient.

More Info

Feedback

Continue   Reset Order

Fig. 4.2 Example of patient safety decision support. General safety decision support: educating users on MRI safety (**a**), safety decision support for MRI contrast use and nephrogenic systemic fibrosis (**b–d**) (Percipio™, Courtesy of Medicalis Corporation, San Francisco, CA)
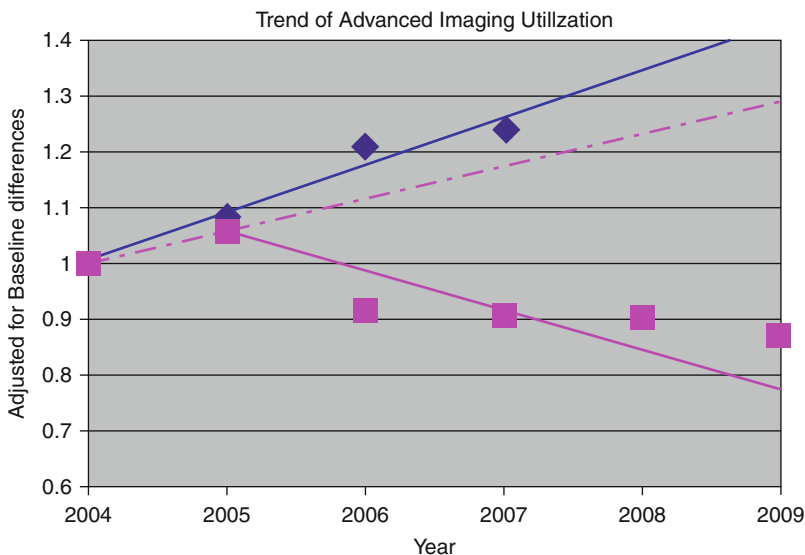
Fig. 4.3 Comparison of adjusted imaging utilization trends between Medicare (*blue*) and a commercial patient panel (*pink*). *Solid pink line* represents linear component of the piecewise regression with a break point in 2005. *Dashed pink line* shows utilization at preimplementation growth rate

Adoption and Meaningful Use of CPOE in Radiology 2000–2010
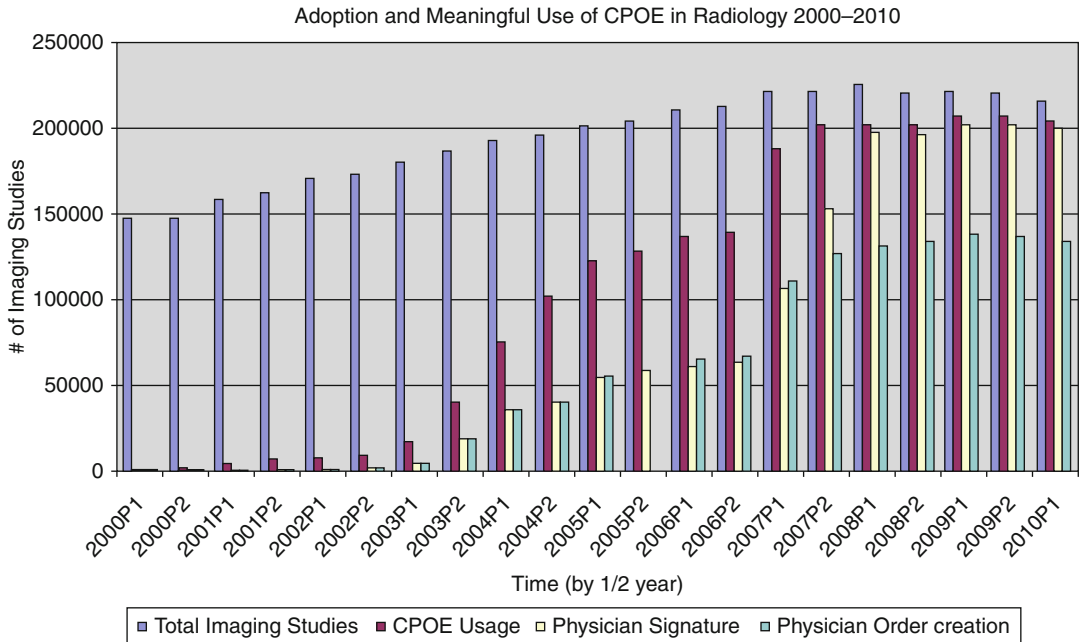
Fig. 4.4 Trends of imaging utilization, adoption of computerized physician order entry (CPOE) system, physician meaningful use by electronic order creation, and physician meaningful use by electronic order signature from 2000 to 2010

Conclusion and Future Research

In conclusion, significant gaps exist in efficiency, clinical decision making, patient safety, and quality of care for diagnostic radiology. Broad system changes are necessary and information systems will be core features of this needed change.

Knowledge-enabled IT tools are needed to deliver real-time, context-specific, decision support to optimize the process of healthcare delivery. There is substantial opportunity for CPOE to contribute to imaging services, including gains in quality of care as well as patient safety and reduction in waste. CPOE with embedded DS can help reduce unnecessary testing, thereby decreasing unnecessary radiation exposure and costs. Preliminary impact of the imaging CPOE on quality has been encouraging.

With incentives such as those in the HITECH legislation, widespread adoption of EHR and CPOE is likely. As they become increasingly important cornerstones of national healthcare policy, more research will be needed regarding the drivers of adoption, meaningful use, and their clinical impact. Furthermore, radiologists, radiology as a specialty, and industry partners must lead in developing the necessary base of evidence and knowledge that is needed to be delivered at the point of care.

References

1. Holmes GW. J Am Med Assoc. 1947;135(6):327–30.
2. Iglehart JK. N Engl J Med. 2006;354(26):2822–8.
3. Institute of Medicine CoHCiA. Crossing the quality chasm: a new health system for the 21st century. Washington, DC: National Academy Press; 2001.
4. Wennberg JE. Health Aff (Millwood) 2004; Suppl Web Exclusives:VAR140-VAR144.
5. Pare G, Lepanto L, Aubry D, et al. Int J Technol Assess Health Care. 2005;21:471–9.
6. A data book: healthcare spending and the Medicare program. Medicare Payment Advisory Commission Web site. Available at: http://www.medpac.gov/documents/Jun10DataBookEntireReport.pdf. Published June 2010. Accessed 15 Jan 2011.
7. Bhargavan M, Sunshine JH. Radiology. 2005; 234(3):824–32.

8. Matin A, Bates DW, Sussman A, Ros P, Hanson R, Khorasani R. Am J Roentgenol. 2006;186:7–11.

9. Mitchell J. Med Care. 2008;46(5):460–6.

10. Khorasani R. Radiographics. 2001;21:1015–18.

11. Gandhi RK, Weingart SN, Borus J, et al. N Engl J Med. 2003;348(16):1556–64.

12. Kaushal R, Jha AK, Franz C, et al. J Am Med Inform Assoc. 2006;13(3):261–6.

13. Dexter PR, Perkins S, Overhage M, Maharry K, Kohler RB, McDonald CJ. N Engl J Med. 2001;345:965–70.

14. Hwang JI, Park HA, Bakken S. Int J Med Inform. 2002;65:213–23.

15. Alkasab TK, Alkasab JR, Abujudeh HH. J Am Coll Radiol. 2009;6(3):194–200.

16. Centers for Medicare & Medicaid Services. EHR incentive programs: overview. Accessed at www.cms.gov/ehrincentiveprograms/. Accessed 23 Aug 2011.

17. Kaushal R, Blumenthal D, Poon EG, Jha AK, Franz C, Middleton B, Glaser J, Kuperman G, Christino M, Fernandopulle R, Newhouse JP, Bates DW, Cost of National Health Information Network Working Group. Ann Intern Med. 2005;143:165–73.

18. Davenport TH, Glaser J. Harv Bus Rev. 2002;80(7):107–11. 126.

19. Lomas J, Sisk JE, Stocking B. Milbank Q. 1993;71(3):405–10.

20. Cabana MD, Rand CS, Powe NR, Wu AW, Wilson MH, Abboud PA, et al. J Am Med Assoc. 1999;282(15):1458–65.

21. Bradford WD, Chen J, Krumholz HM. Pharmacoeconomics. 1999;15(3):257–68.

22. Song YS, Skinner J, Bynum J, Sutherland J, Wennberg JE, Fisher ES. N Engl J Med. 2010;363:45–53.

23. Arnold RW, Graham DA, Melvin PR, Taylor GA. Pediatr Radiol. 2011;41(7):867–74.

24. Raja AS, Mortele KJ, Hanson R, Sodickson AD, Zane R, Khorasani R. Int J Emerg Med. 2011;4:19.

25. Korley FK, Rham JC, Kirsch TD. J Am Med Assoc. 2010;304(13):1465–71.

26. Gonzalez B, Mahesh M, Kim KP, Bhargavan M, Lewis R, Mettler F, Land C. Arch Intern Med. 2009;169(22):2071–7.

27. Blanchard K, Colbert JA, Puri D, Weissman J, Moy B, Kopans DB, et al. Cancer. 2004;101(3):495–507.

28. Blumenthal D, Tavenner M. N Engl J Med. 2010;363(6):501–4.

29. Metzger J, Welebob E, Bates DW, Lipsitz S, Classen DC. Health Aff. 2010;29(4):655–63.

30. Department of Health and Human Services. Health information technology: initial set of standards, implementation specifications, and certification criteria for electronic health record technology. Final rule. Fed Regist 2010; 75(144):44589–44654.

31. Rosenthal DI, Weilburg JB, Schultz T, et al. J Am Coll Radiol. 2006;3(10):799–806.

32. Ash JS, Gorman PN, Seshardi V, Hersh WR. J Am Med Inform Assoc. 2004;11(2):95–9.

33. Jha AK, DesRoches CM, Campbell EG, Donelan K, Rao SR, Ferris TG, Shields A, Rosenbaum S, Blumenthal D. N Eng J Med. 2009;360(16):1628–38.

34. Sistrom CL, Dang PA, Weilburg JB, Dreyer KJ, Rosenthal DI, Thrall JH. Radiology. 2009;251(1):147–55.

35. Mekhjian HS, Kumar RR, Kuehn L, Bentley TD, Teater P, Thomas A, et al. J Am Med Inform Assoc. 2002;9(5):529–39.

36. Cordero L, Kuehn L, Kumar RR, Mekhjian HS. J Perinatol. 2004;24(2):88–93.

37. Bates DW, Kuperman G, Rittenberg E, Teich J, Fiskio J, Ma'luf N, et al. Am J Med. 1999;196:144–59.

38. Bates DW, Cohen M, Leape LL, Overhage JM, Shabot MM, Sheridan T. J Am Med Inform Assoc. 2001;8(4):299–308.

39. Guyatt G, Gutterman D, Bauman MH, Addrizzo D, Hylek EM, Phillips B, Raskob G, Lewis SZ, Schunemann H. Chest. 2006;129:174–81.

40. Stiell IG, Lesiuk H, Wells GA, McKnight RD, Brison R, Clement C, et al. Ann Emerg Med. 2001;38(2):160–9.

41. Stiell IG, Greenberg GH, McKnight RD, Nair RC, McDowell I, Reardon M, et al. J Am Med Assoc. 1993;269(9):1127–32.

42. Stiell IG, Greenberg GH, Wells GA, McDowell I, Cwinn AA, Smith NA, et al. J Am Med Assoc. 1996;275(8):611–15.

43. Carlos RC, Scheiman JM, Hussain HK, Song JH, Francis IR, Fendrick AM. Acad Radiol. 2003;10(6):620–30.

44. Carlos RC, Axelrod DA, Ellis JH, Abrahamse PH, Fendrick AM. AJR Am J Roentgenol. 2003;181(6):1653–61.

45. Blackmore CC, Ramsey SD, Mann FA, Deyo RA. Radiology. 1999;212(1):117–25.

46. Visser K, Kuntz KM, Donaldson MC, Gazelle GS, Hunink MG. J Vasc Interv Radiol. 2003;14(1):53–62.

47. Stewart TR, Mumpower JL. J Policy Anal Manage. 2004;23(4):908–20.

48. Buskens E, Nederkoorn PJ, Buijs-Van Der Woude T, Mali WP, Kappelle LJ, Eikelboom BC, et al. Radiology. 2004;233(1):101–12.

49. Talwalkar JA, Angulo P, Johnson CD, Petersen BT, Lindor KD. Hepatology. 2004;40(1):39–45.

50. Wardlaw JM, Keir SL, Seymour J, Lewis S, Sandercock PA, Dennis MS, et al. Health Technol Assess. 2004;8(1):iii. ix–iii, 180.

51. ACR. American College of Radiology ACR Appropriateness Criteria 2000. Radiology. 2000;215(Suppl):1–1511.

52. Kahn Jr CE, Pingree MJ, Longworth NJ. Acad Radiol. 1998;5(3):188–97.

53. Sistrom CL, Honeyman JC. J Digit Imaging. 2002;15(4):216–25.

54. Blackmore CC, Medina LS. J Am Coll Radiol. 2006;3:505–9.

55. Ip IK, Mortele KJ, Prevedello LM, Khorasani R. Radiology. 2011;259(1):136–41.
56. Macari M, Megibow AJ. Radiology. 2011;259:20–3.
57. Berland LL, Silverman SG, Gore RM, Mayo-Smith WW, Megibow AJ, Yee J, Brink JA, Baker ME, Federle MP, Foley WD, Francis IR, Herts BR, Israel GM, Krinsky G, Platt JF, Shuman WP, Taylor AJ. J Am Coll Radiol. 2010;7(10):754–73.
58. Schwartz LH, Panicek DM, Berk AR, Li Y, Hricak H. Radiology. 2011;260(1):174–81.
59. Bates DW, Kuperman GJ, Wang S, Gandhi T, Kittler A, Volk L, et al. J Am Med Inform Assoc. 2003;10(6):523–30.
60. Lee F, Teich JM, Spurr CD, Bates DW. J Am Med Inform Assoc. 1996;3(1):42–55.
61. McDonald CJ. N Engl J Med. 1976;295(24):1351–5.
62. Sinha U, El Saden S, Duckwiler G, Thompson L, Ardekani S, Kangarloo H. A customizable MR brain imaging atlas of structure and function for decision support. AMIA Annu Symp Proc 2003;2003:604–608.
63. Siegel E, Reiner B. J Digit Imaging. 2001; 14(2 Suppl 1):125–7.
64. Siegel E, Channin D, Perry J, Carr C, Reiner B. J Digit Imaging. 2002;15(1):2–4.
65. Integrating the Healthcare Enterprise (IHE). web site. 11-22-2004. 11-22-2004.
66. Maviglia SM, Zielstorff RD, Paterno M, Teich JM, Bates DW, Kuperman GJ. J Am Med Inform Assoc. 2003;10(2):154–65.
67. Abookire SA, Teich JM, Sandige H, Paterno MD, Martin MT, Kuperman GJ, et al. Proc AMIA Symp 2000;2–6.
68. Stiell IG, Clement CM, Grimshaw JM, Brison RJ, Row BH, Lee JS, Shah A, Brehaut J, Holroyd BR, Schull MJ, McKnight RD, Eisenhauer MA, Dreyer J, Letovsky E, Rutledge T, Macphall I, Ross S, Perry JJ, Ip U, Lesiuk H, Bennett C, Wells GA. Can Med Assoc J. 2010;182(14):1527–32.
69. Kotter JP, Schlesinger LA. Harv Bus Rev. 1979;57(2): 106–14.
70. Carton M, Auvert B, Guerini H, Boulard JC, Heautot JF, Landre MF, Beauchet A, Sznajderi M, Brun-Ney D, Chagnon S. Clin Radiol. 2002;57(2):123–8.
71. Neilson EG, Johnson KB, Rosenbloom ST, Dupont WD, Talbert D, Giuse DA, Kaiser A, Miller RA. Ann Intern Med. 2004;141(3):196–204.
72. Vartanians VM, Sistrom CL, Weilburg JB, Rosenthal DI, Thrall JH. Radiology. 2010;255(3):842–9.
73. Blackmore CC, Mecklenburg RS, Kaplan GS. J Am Coll Radiol. 2011;8:19–25.
74. Kotter JP. Harv Bus Rev. 2007;1:96–103.
75. Prevedello LM, Raja AS, Zane RD, Sodickson A, Lipsitz S, Schneider L, Hanson R, Mukundan S, Khorasani R. Am J Med 2012; 1555–7162.
76. The United States Government Accountability Office. Medicare imaging payments. GAO-08-1102R. http://www.gao.gov/htext/d081102r.html. Accessed on 9 Oct 2009.
77. Stein PD, Fowler SE, Goodman LR, et al. N Engl J Med. 2006;354:2317–27.
78. Wells PS, Anderson DR, Rodger M, et al. Ann Intern Med. 2001;135:98–107.
79. Lee J, Kirschner J, Pawa S, Wiener DE, Newman DH, Shah K. Ann Emerg Med. 2010;56(6):591–6.
80. Raja AS, Ip IK, Prevedello L, Sodickson A, Farkas C, Zane R, Hanson R, Goldhaber S, Gill R, Khorasani R. Radiology. 2012;262(2):468–74.

Radiation Exposure from Medical Imaging

5

Michael L. Loftus, Pina C. Sanelli, Donald P. Frush
and Kimberly E. Applegate

Contents

M.L. Loftus (✉) • P.C. Sanelli
Department of Radiology, Weill Cornell Medical College/NewYork-Presbyterian Hospital, New York, NY, USA
e-mail: mikelyonloftus@gmail.com; pcs9001@med.cornell.edu

D.P. Frush
Department of Radiology, Duke Medical Center, Durham, NC, USA
e-mail: Donald.frush@duke.e

K.E. Applegate
Department of Radiology and Imaging Sciences, Emory University School of Medicine, Atlanta, GA, USA
e-mail: Keapple@emory.edu

Key Points

- Medical radiation currently accounts for an increasing percentage (approximately 50%) of the total radiation exposure for the US population (30 years ago about 15%) (Moderate Evidence).
- Children are 2–5 times more sensitive to radiation exposure than adults (moderate evidence).
- There are no data that prove a direct link between low-level radiation from diagnostic imaging and the development of cancer in adults. The best data regarding the long-term effects of low-level radiation exposure (100–150 mSv) come from the longitudinal survivor study (LSS) of atomic bomb survivors (Moderate Evidence).
- Most major medical and scientific organizations accept the linear, no-threshold model as the preferred model for low-level radiation and cancer risk estimation; however, direct evidence linking medical use of low-level radiation with cancer induction is lacking, with the exception of a recent study which found an increased incidence of leukemia and brain tumor in pediatric patients who underwent CT with a cumulative dose >50 mGy (Limited Evidence).
- The estimated lifetime risk of developing cancer from a single, noncontrast head CT at age 40 is approximately 1:8,100 for women and 1:11,080 for men (Limited Evidence). The estimated lifetime risk for a child with a similar exposure is expected to be somewhat higher given the increased radiosensitivity of children and the longer lifetime over which to develop cancer, and for children exposed to higher cumulative doses (>50 mGy for leukemia and >60 mGy for brain cancer), their risk of cancer may increase up to threefold (Limited Evidence).
- While newer CT techniques in neuroradiology (such as CT angiography and CT perfusion) are associated with higher radiation doses, they are often performed in situations in which the potential clinical benefit outweighs the risk (Insufficient Evidence).

Definition and Pathophysiology

Medical radiation is used for both diagnostic and therapeutic purposes. The X-ray is an invisible beam of light that passes through the body and is altered by different tissues to create images. Imaging tests that use ionizing radiation include radiographs, fluoroscopy, nuclear imaging, and computerized tomography (CT) scans. Diagnostic imaging uses low-level radiation, defined as an effective dose (ED) <100–150 milli Sieverts (mSv).

Radiation Terminology

Measurements are presented in standard international units (SI = *Systeme Internationale*) [1] (Table 5.1). Incident X-ray radiation *intensity* can be characterized by exposure in coulombs/kilogram (ionizations in coulombs per mass), or the preferred air kerma in Gray (Gy) (kinetic energy transferred per unit mass). The *absorption* of this radiation intensity is then, simply, the *absorbed dose*, also measured in Gy. The energy transfer will depend on factors including the physical properties of the material as well as depth in the body, including skin and other organ doses. The biological *impact* to tissue is represented by the *equivalent dose* in Sieverts (Sv), represented as the product of the absorbed dose and a weighting factor (value depends on the type of radiation that causes ionization in tissue with the factor being 1.0 for diagnostic medical imaging). Finally, the *effective dose equivalent* (alternatively, effective dose) in Sv is the sum of products of dose equivalents multiplied by weighting factors depending on the radiosensitivity of the organs exposed. Effective doses represent a whole body equivalent (as if the whole body was exposed) for exposures that may be regional. Because absorbed dose and effective dose represent energy deposition and

ionization in tissues, these terms are typically used in discussions of radiation risk estimations in humans. Effective dose is a more often discussed, but less accurate measure of assigning risk estimations as absorbed organ dose is impractical in clinical practice.

Radiation Mechanisms of Effect

Ionizing radiation particles include X-rays (photons). These high-energy photons interact with tissue depositing energy at the nuclear level causing ionizations. Ionizations then damage DNA either directly or secondarily through generation of free radicals, especially hydroxyl-free radicals. Single-stranded DNA damage is usually repaired but double-stranded damage is more difficult to repair completely. Biological effects may be immediate causing *cell death* (such as radiation necrosis), which may lead to organism death, or consist of *cell damage* leading to other effects such as birth defects or cancer. Cell damage could be due to direct DNA damage, but may also be due to other effects such as genomic instability (with additional DNA aberrations in cell progeny) and cellular regulatory mechanisms. For diagnostic imaging levels of radiation dose, the most pertinent bioeffect is carcinogenesis. The development of radiation-induced cancer is a multistep process and genetic factors may also play a role in determining susceptibility [2] (Table 5.2).

Types of Biological Effects

There are two types of biological effects: stochastic and deterministic. Deterministic effects have a threshold below which the effect is not seen (Table 5.3). These effects include cataracts, skin burns, and epilation (hair loss). These types of effects were traditionally almost all seen when interventional procedures were performed with doses well above the low-level radiation seen in diagnostic imaging. However, recently epilation in a band-like distribution has been reported with

diagnostic CT perfusion (CTP) studies, and a series of articles in the lay press have brought the issue of radiation risk from diagnostic imaging to the forefront [3]. Stochastic effects on the other hand do not have a threshold. The risk of a particular effect increases with increasing radiation dose; however, the severity of the effect is independent of dose. Radiation carcinogenesis and radiation-induced genetic damage are stochastic phenomena. While other biological effects of low-level radiation have been assessed [4, 5], the overwhelming majority of investigations regarding low-level radiation are focused on cancer risk. For the purposes of this chapter, the stochastic effects of radiation exposure, specifically carcinogenesis, will be the primary focus.

Radiation Doses in Medical Imaging

Radiation doses for the imaging modalities of radiography, fluoroscopy/angiography, and computed tomography vary depending on the type of dose measurement, age of the patient, examination, and techniques used. A detailed discussion of dose ranges for these various modalities is beyond the scope of this chapter; however, readers are referred to the UNSCEAR report [6] for a comprehensive review of dose ranges for many of these modalities.

Fluoroscopy including angiography procedures are better described in terms of dose rates, since the dose from these procedures will depend on imaging time, as well as the number of radiographs (CR, DR, or conventional screen film) [7]. For the purposes of clinical practice, it can be helpful to describe these common fluoroscopic (and other diagnostic imaging) procedures in terms of dose equivalents compared with naturally occurring background radiation (Table 5.4) or compared to more commonly encountered sources, such as airplane travel or living at high altitude (Table 5.5). It is worth mentioning, since CT is a relatively large component of total radiation dose from medical imaging, that there are methods for estimating patient dose based on the

CT dose index (CTDI) in mGy and the dose length product (DLP) in mGy.cm (the product of CTDI and the length of the scan). It is important to realize that this dose represents only the determination from acrylic phantoms and has nothing to do with the individual patient on the scanner. However, conversion factors to change the dose length product into an effective dose estimate are available and have been well reviewed [8–10].

Epidemiology and Medical Utilization of Ionizing Radiation

Everyone is exposed to small amounts of radiation from soil, rocks, building materials, air, water, and cosmic radiation. This naturally occurring background radiation dose is about 3.0 mSv annually in the USA, although this partly depends on geography. When medical radiation is added to this background, the average dose for the US population is about 6.2 mSv [11]. The largest contributors to medical radiation dose are CT scanning (up to one-half of medical exposure) followed by nuclear medicine (about one-quarter of medical exposure). Medical imaging is predominantly used in developed as opposed to developing nations.

Medical imaging is an extremely important diagnostic tool. In a recent survey, leaders in internal medicine ranked CT and MR imaging as the most important medical innovations in the twentieth century [12]. With continued technologic advances and new potential applications, the benefits to patients and society will continue to increase and become more diverse over time. However, there are inherent risks with modalities that depend on ionizing radiation for image formation. In the context of this chapter, radiography, fluoroscopy/angiography, and computed tomography are most relevant. One risk that has been debated and publicized most vigorously is the potential for cancer development. While there are clearly established relationships between cancer development and radiation exposure from studies of atomic bomb survivors who were exposed to medium and high levels of radiation

(>100–150 mSv), the risks in the lower range are debated. In general, the model accepted by most medical and scientific organizations is that this risk follows a linear no-threshold model. There are no data from medical exposures in the low-level range that directly link diagnostic imaging with cancer development. Our understanding of this potential link comes from the atomic bomb data, with some additional contribution from epidemiologic studies from doses of radiation used for both diagnostic and therapeutic purposes, as well as some unfortunate nuclear accidents. This adds support for subscribing to the ALARA principle (as low as reasonably achievable) meaning that we should strive to use the lowest radiation dose possible while maintaining image quality and diagnostic performance to answer the clinical question. However, a reasonable balance must be sought with the concurrent desire for imaging exams and procedures to also be as diagnostic as reasonably achievable. There is little benefit to reducing the level of radiation for a particular exam to such a degree as to make the images nondiagnostic. Widespread application of these principles may help alleviate the concerns of physicians and other healthcare providers as well as patients and families regarding cancer induction from medical imaging that may bias their selection of the most appropriate imaging study.

Increased Dose from Medical Imaging

CT scans contribute the highest dose from medical radiation in developed nations. Worldwide, there are an estimated 260,000,000 CT examinations performed annually. The USA accounts for an estimated 25% of all CT exams worldwide, representing 70,000,000 CT exams each year [6]. Up to 75% of radiation exposure from medical imaging is now attributed to CT scans [13]. The rising numbers of CT scanners in use and the improved speed and throughput on the scanners themselves have led to markedly increased patient access to CT scans in the USA. While this availability has certainly had a positive impact on patient care, with indicated studies performed

without any undue delay, the sheer increase in the number of exams also represents an increase in the number of scans which are performed for questionable clinical indications. In addition to the radiation exposure associated with these exams, there are the related false-positive studies and subsequent interventions that may accompany these findings. Careful clinical evaluation and appropriate imaging utilization are a key part of managing the overall CT dose to the population. The American College of Radiology (ACR) publishes "appropriateness criteria" for each imaging modality for the most commonly encountered clinical scenarios (Table 5.6). These criteria can be used as a starting point for clinical decision making when it comes to imaging.

While increased frequency of use is partly responsible for increasing radiation exposure to the population, technical advances have also resulted in some increase in radiation exposure. For example, newer CT techniques such as CT angiography (CTA) and CT perfusion (CTP) have improved the diagnostic utility of CT in evaluating cerebrovascular diseases. However, these newer procedures also may further increase radiation exposure to patients because of the scanning parameters used, such as thinner slice acquisition or slice increased number of images compared to a standard head CT. Another contributing factor is the general lack of guidelines for utilization of these new imaging techniques in specific populations, perhaps leading to overutilization of these specialized imaging tools in clinical practice [14].

dose from imaging can vary and may be relatively high. This is particularly important since imaging use has grown. This increased use has not occurred without scrutiny; Brenner and Hall outlined the growing use of CT with respect to potential cancer development late in 2007 [16], and a number of more recent articles in the lay press have focused on the increased use of CT.

This chapter will discuss radiation risks associated with medical imaging by primarily addressing what is known about low-level radiation – less than 100–150 mSv [17] – resulting from diagnostic imaging rather than oncologic radiation treatment. In targeted radiotherapy for oncologic purposes, radiation bioeffects are clearly present and risks more definitively established due to doses that may be orders of magnitude greater. While cumulative doses from diagnostic imaging may exceed the "low-level" threshold, especially with repeated scans, most material focuses on low-level doses from a single exposure.

The topic of radiation and biological impact is extensive and discussion will be focused primarily on diagnostic imaging in neuroradiology. Information will be provided from a perspective of diagnostic radiology rather than radiation biology, health or radiation physics, or epidemiology. More extensive information on radiation and the potential effects can be found in other comprehensive sources [18]. Finally, discussion will not include strategies for further dose management with radioprotectants [19, 20].

Assessing Risk Versus Benefit When Using Medical Imaging

Medical imaging is often now the first-line intervention in the diagnosis of injury and illness in both children and adults. The information obtained from imaging alone can be life altering or lifesaving [15]. However, the decision to obtain imaging examinations needs to balance this potential benefit with both established and potential risks, including exposure to ionizing radiation. As will be discussed later, the radiation

Cost to Society

The American healthcare system costs more than $2.3 trillion annually, more money per capita than any other developed nation. The cost of medical imaging is estimated at $100 billion per year and is the fastest growing segment of the healthcare system, growing at approximately 10–15% annually.

Medical imaging and particularly CT utilization occurs primarily in the USA and developed nations. Compared to the USA, other developed

nations have much lower use and spending on healthcare in general and imaging in particular, yet have similar life expectancy. There is a growing debate among both physicians and government about the number of either unindicated or questionably indicated studies performed in the USA that utilize ionizing (CT, radiography, fluoroscopy, nuclear medicine) and nonionizing (MRI, sonography) imaging techniques. The benefit from true-negative imaging tests and the harm from false-positive imaging tests have not been fully addressed. Furthermore, there is the potential cost to society associated with radiation-induced sequelae such as cataract formation or cancer induction. However, these costs are difficult to directly measure and have yet to be well studied.

Goals of Imaging

The goal of diagnostic imaging is to diagnose or exclude medical conditions that are necessary for the healthcare of the patient. Imaging, like any test, should ideally improve patient health outcomes and reduce the intensity and use of resources, including cost of care. Diagnostic imaging guides clinicians in the management of patients. Imaging tests have both risks and benefits that must be carefully considered for each patient individually.

Methodology

Information for this chapter was obtained primarily through a MEDLINE search using PubMed (National Library of Medicine, Bethesda, Maryland http://www.ncbi.nlm.nih.gov/sites/entrez) from 1968 to March 2011. Keywords were *ALARA* (*As Low As Reasonably Achievable*), *radiation*, *radiation risk*, *CT*, *diagnostic imaging*, *neuroradiology*, and the resultant related fields from this original database. The authors performed a critical review of the title and abstracts of the indexed articles followed by a review of the full text of articles that were relevant.

Discussion of Issues

Is There a Cancer Risk from Low-Level Radiation Found in Medical Imaging?

Summary

There is strong research evidence for cellular and organism damage from high levels of ionizing radiation (strong evidence). At lower levels of radiation (<100–150 mSv), the linear no-threshold model suggests an increased cancer risk. Although most major medical and scientific organizations accept the linear, no-threshold model as the preferred model for low-level radiation and cancer risk estimation, consistent direct evidence linking medical use of low-level radiation with cancer induction is lacking in adults. Pediatric radiation exposure from medical imaging will be discussed separately below (insufficient evidence).

Supportive Evidence

Assumptions in Estimating Radiation Risks One of the difficulties in determining if there is a significant risk of cancer development or mortality from low-level radiation exposure is that the radiation-induced cancer often follows a lengthy (decades) latency period, and studies to evaluate the marginal increased risk from medical imaging would require a very large population study over a long period of time. For example, solid tumors may take more than three decades to develop. To confirm a statistically significant effect may require a long-term study of an exposed population of several million individuals with doses near the 10 mSv range [21]. According to Kleinerman [22], a large population size is usually required to evaluate the risk of cancer induction because cancer from low-level radiation is a very low probability compared with the overall incidence of cancer (about 40%). In addition, the lower the radiation dose, the larger the population size required in order to detect a radiation effect.

The data that are currently discussed arise largely from other sources, predominantly the atomic bomb longitudinal survivor study (LSS). Brenner et al. summarize the atomic bomb LSS

data stating that the epidemiologic study with the highest statistical power for evaluating low-dose risk is the LSS cohort of atomic bombs survivors. In this cohort, there was evidence of an increase in cancer risks for protracted doses >100 mSv and acute doses above approximately 50 mSv [21, 23]. However, the exposure to this population differs from medical imaging exposure in that the atomic bomb radiation consisted of radiation types other than gamma radiation (X-ray equivalent), the radiation exposure occurred in a single acute dose compared to protracted exposure (such as with multiple CT examinations), and the exposure occurred to the whole body compared to regional exposure as is commonly seen with medical imaging. Prasad also argues that health risks of doses <100 mGy (absorbed dose) in humans depend not only on dose but a host of other factors (including dose rate, DNA repair mechanisms, and others), making accurate estimation by mathematical models challenging [24].

In general, medium- and high-level radiation dose effects are linear although reports suggest that there may be some nonlinearity at higher effects [25]. Radiation from diagnostic imaging tends to involve doses that are low level (<100–150 mSv), and because of potentially small effects, the data have been less conclusive. There are several possible extrapolation models for cancer risk with low-level radiation. The linear, no-threshold model is in general the most widely accepted model, being supported by scientific committees, major imaging organizations, and other scientific bodies including the Committee to Assess Health Risks from Exposure to Low Levels of Ionizing Radiation, Biological Effects of Ionizing Radiation of the National Academy of Sciences (BEIR VII), National Council on Radiation Protection and Measurements (NCRP), International Commission on Radiological Protection (ICRP), Radiological Society of North America (RSNA), and the Society for Pediatric Radiology (SPR).

Cancer Risk and Radiation Following Diagnostic Medical Imaging Berrington de Gomez and Darby estimated cancer risk from diagnostic imaging and concluded that the attributable risk in developed countries varied from 0.6% to as high as 3.2% [26], similar to projections reported by Brenner [27]. However, the projections in this study also based conclusions on the LSS Hiroshima data and may not reflect contemporary imaging techniques. In addition, there is no provision for the benefit achieved by diagnostic imaging. Ron et al. discuss the development of leukemia, thyroid, and breast cancer from diagnostic X-rays [28], and these data are generally in agreement with those of atomic bomb survivors. Other reviews of fluoroscopic and angiographic procedures have shown mixed results in terms of cancer risk in both the pediatric and adult populations [27, 29–32].

However, radiation dose from CT represents the largest contribution from medical imaging to populations in the developed world and will be the primary focus of this chapter. CT examinations provide a relatively high dose per examination compared with some other techniques used in diagnostic medical imaging; however, the risk of radiation-induced cancer from CT should be put into context against the statistical risk of developing cancer in the entire population. The average risk of fatal cancer developing over a person's lifetime is approximately 22%. So, for every 1,000 individuals, 220 will develop fatal cancer in their lifetime regardless of radiation exposure from medical imaging. The estimated increased risk of cancer over a person's lifetime from a single CT scan is controversial but has been estimated to be a fraction of this risk. For example, the estimated risk from a single CT of the head will be discussed below, but is estimated to be on the order of 1 in 8,100 women or 1 in 11,080 men. It is also important to remember that these estimates are population-based rather than estimates for an individual patient.

In response to concerns about radiation overexposure with these studies, the US Food and Drug Administration (FDA) issued an initial warning in October 2009 and subsequent updates in December 2009 and November 2010 recommending a review of radiation dosing protocols for all CT perfusion exams to ensure that patient doses are correctly planned. Additionally, the FDA recommended multiple steps to insure

that exams are performed appropriately by adequately trained technologists with radiologist oversight. The Medical Imaging and Technology Alliance (MITA) along with the American Association of Physicists in Medicine (AAPM) have worked with other regulatory and industry organizations to create a set of recommended notification values for CT scans – otherwise called the "Dose Check" standard [33]. These values are CTDIvol or DLP doses above which the CT technologist receives a message in a pop-up window that a specific scan will exceed a prescribed dose limit.

What Is the Estimated Risk from a Single CT Scan of the Head?

Summary

The effective dose from a single CT of the head is as much as 100 times higher than a plain X-ray but still low (2–3 mSv). The ACR appropriateness criteria define "low" as 1–10 mSv in an adult [34–36]. The estimated lifetime risk of developing cancer from a single head CT at age 40 is approximately 1:8,100 for women and 1:11,080 for men (limited evidence). In the setting of trauma or other acute clinical situations that require rapid information about a potentially life-threatening condition, a CT of the head is readily available and rapidly performed providing valuable diagnostic information. Therefore, there is generally little concern in these settings regarding radiation exposure as the clinical benefit clearly outweighs the potential risk from radiation.

Furthermore, the risks of the clinical concern that prompted the performance of the CT are immediate, whereas the potential risks associated with radiation from the CT are unlikely to occur until years in the future. Some have proposed that the absolute risks of cancer quoted by the literature be "discounted" due to the inherent ambiguity of a future event using the same calculations that other industries use to value future events. For example, a 1 in 100 chance of an immediate adverse event as a result of a diagnostic exam performed today intuitively has a much different impact on a patient's decision making than a 1 in 100 chance of that same adverse event in 30–40 years. While these concepts should not be used to oversimplify the risks associated with ionizing radiation, they can potentially be a relevant part of the risk-benefit discussion between a patient and the ordering physician.

As mentioned above, the expected lifetime risk of radiation-induced cancer is higher in the pediatric population due to their increase radiation susceptibility and significantly longer potential latency period. According to Brenner et al., of the over 600,000 patients under the age of 15 who undergo CT examinations of the head or abdomen, an estimated 500 (0.08%) will ultimately die from radiation-induced cancer [27]. However, it is also pointed out that this absolute risk is only 0.35% increase over the natural background rate of cancer mortality for patients who have had no additional radiation from medical imaging. These risks were estimated from higher CT doses than current pediatric head CT techniques employed today. Pearce et al. [37] studied pediatric patients who received CT scans prior to age 22 and found that doses above 50 mGy or 60 mGy could triple a patients risk for leukemia or brain cancer respectively in the patient's lifetime. However, the absolute risk remained small, with one excess case of either leukemia or brain tumor per 10,000 head CTs performed.

Supportive Evidence

According to the Biological Effects of Ionizing Radiation (BEIR) VII Phase 2 report, epidemiologic data support an increased risk of cancer in individuals who received exposures between 10 and 100 mSv among the survivors of the Hiroshima and Nagasaki atomic bombs [38]. Exposures from diagnostic and therapeutic medical procedures can certainly (and often do) reach this level. For example, single and multiphase CT exams of the abdomen often deliver an effective dose >10 mSv, and CT angiography of the lungs, heart, and brain can all deliver effective doses well above 20 mSv [36, 39, 40].

Radiation exposure to the brain tends to result in a somewhat lower effective dose because of the brain's relative lower radiosensitivity as well as the smaller area imaged. For example,

a noncontrast CT of the head is typically on the order of 2–3 mSv, while a standard noncontrast CT of the abdomen and pelvis is closer to 10 mSv [39]. Smith-Bindman et al. utilized data from the BEIR VII (2006) report to estimate the lifetime attributable risk (LAR) of cancer based on the average effective dose for a given diagnostic imaging study and concluded that the estimated risk for a 40-year-old man who receives a standard noncontrast CT of the head is approximately 1 in 11,080. In other words, on average, 11,080 head CT exams would need to be performed before a cancer would be caused.

However, modern techniques go well beyond a standard noncontrast CT of the head, and newer techniques such as CT angiography and CT perfusion studies provide potentially lifesaving information, but at the cost of higher radiation doses. Some publications suggest that the average exposure from a single stroke workup is in the range of 10 mSv [41] while others suggest that most literature actually underestimates the actual doses and accurate doses for a stroke workup including a CTA and CTP exam are closer to 18 mSv. In the later case, the estimated LAR of cancer induction following a CT workup of suspected stroke was as high as 1 in 660 female patients and 1 in 1,120 male patients [34]. However, as will be discussed below, the patient population generally being imaged for suspected stroke is an older morbid population, with the risks of delayed diagnosis potentially resulting in catastrophic sequelae. The benefits of imaging due to potentially life-altering information provided in this acute setting outweigh the potential risks from imaging studies.

Understanding Benefit Versus Risk of Imaging Tests in Well-Indicated Studies Compared to Studies with Very Low Probability of Disease

Summary
It is critical to weigh both the benefits and the risks when using any test, including medical imaging with ionizing radiation. The benefit to a patient should outweigh its risks. In addition to

considering the lifetime cancer risk, the overall risk from an imaging test must also include the potential risks of other agents, such as contrast media, as well as associated risks with a false-positive and false-negative test result that may lead to unnecessary intervention and anxiety as well as the consequences of not detecting a disease. However, there is insufficient evidence in the literature estimating these risks for different patient populations.

In general terms, patients with a high risk of a particular disease, such as head injury from a high-speed motor vehicle accident, are considered at relatively low risk for the potential effects of radiation exposure from CT imaging because of its benefit for an accurate and rapid diagnosis. However, in patients with a low risk for disease, such as head injury from a low-impact trauma, there is often little benefit in using CT when considering the risk of false-positive results and radiation exposure that may outweigh any true benefit. In clinical practice, this benefit-risk analysis is ultimately performed on an individual basis by the physicians providing care for the patient.

Supportive Evidence
Health benefit or lifesaving use of CT has been shown in several populations, including but not limited to acute motor vehicle trauma, head trauma, suspected stroke, acute infection, and acute abdominal pain. Traditionally, the appropriate use of imaging has not been well researched or well funded by research agencies. However, this is beginning to change as medical and public awareness about radiation safety grows and governmental reimbursement for imaging begins to be tied to appropriateness criteria.

An Example: The Use of Head CT in Children with Headache
Medina and colleagues investigated the clinical role and cost of head CT and MR in children with headache utilizing a decision-analytic Markov model [42]. They compared three diagnostic strategies: (a) magnetic resonance imaging (MRI), (b) computed tomography followed by MRI for positive results (CT-MRI), and (c) no neuroimaging with close clinical follow-up in the

evaluation of children suspected of having a brain tumor. The children were grouped into low, medium, and high risk for brain tumor prior to imaging based on a combination of physical exam findings and clinical history. With a high pretest probability of brain tumor (4% risk), MR imaging of the head was the recommended and cost-effective imaging strategy. When there was an intermediate pretest probability of brain tumor (0.4%), imaging was very expensive (CT then MR if CT was positive).

When children had chronic headache, the pretest probability of tumor was low (0.01%), and neither CT nor MR was recommended. Even with high sensitivity and specificity of CT (95%, 95%), the posttest probability of tumor was only 16%. In the short term, this means children are being submitted to a false-positive rate (low positive predictive value). MR imaging would have the same results but avoid ionizing radiation exposure to the child. On the other hand, there is a small risk from sedation or anesthesia in young children undergoing MR that would not be needed with CT. If, however, the study is well indicated, CT has more benefit than risk in the high-risk group of children with headache. CT may reduce short-term morbidity and mortality.

Kuppermann et al. utilized age-specific prediction rules to estimate the risk of death from traumatic brain injury, performance of neurosurgery, intubation for greater than 24 h, or hospital admission of two or more nights and potentially obviate the need for routine CT. Their "prediction rule" for children younger than 2 years was normal mental status, no scalp hematoma (except frontal), nonsevere injury mechanism, no loss of consciousness, no palpable skull fracture, and acting normally according to parents. This set of criteria had a negative predictive value for clinically important traumatic brain injury of 100% (CI 99.7–100.0%) in patients less than 2 years old. For children over 2 years and less than 18 years, their criteria included normal mental status, no loss of consciousness, no vomiting, nonsevere injury mechanism, no signs of basilar skull fracture, and no headache. These criteria

had a negative predictive value for clinically important traumatic brain injury of 99.95% (CI 99.81–99.99% Pearce et. al, studied pediatric patients who received CT scans prior to age 22 and found that doses above 50 mGy or 60 mGy could triple a patients risk for leukemia or brain cancer respectively in the patient's lifetime. However, the absolute risk remained small, with one excess case of either leukemia or brain tumor per 10,000 head CTs performed.%). The authors concluded that these prediction rules could identify children at very low risk for clinically significant traumatic brain injury and thus allow clinicians to avoid exposing these children to the radiation dose associated with a head CT [43].

How Should I Communicate Radiation Risk from Imaging to Patients?

Summary

There are growing numbers of web sites and published literature that provide both appropriate language and data to discuss the benefits and risk of medical imaging to consumers. There are survey data that suggest that patients and families both want to know and can understand these issues [44].

Supportive Evidence

The Internet has revolutionized access to scientific and medical information for consumers. There are growing numbers of both scientific and medical web sites that target consumers and include the Image Gently Campaign (www. imagegently.org) for children, the National Cancer Institute (www.cancer.gov/cancertopics/ causes/radiation-risks-pediatric-CT), the Health Physics Society (http://hps.org), and the collaborative sites of the American College of Radiology and the Radiological Society of North America (www.radiologyinfo.org) and the Image Wisely Campaign (www.imagewisely.org).

The Image Gently Campaign is an educational and awareness campaign created by the Alliance for Radiation Safety in Pediatric Imaging that was formed in July 2007 for radiation protection

in medical imaging in children. It is a coalition of healthcare organizations dedicated to providing safe, high quality pediatric imaging nationwide. There are four founding members – Society for Pediatric Radiology, American Association of Physicists in Medicine, American College of Radiology, and the American Society of Radiologic Technologists – including over 55 national and international societies in this coalition representing over 750,000 healthcare professionals in radiology, pediatrics, medical physics, and radiation safety. The site provides information for all stakeholders in medicine including relative radiation doses to children for common imaging examinations. Another element of this campaign is "Step Lightly," which is an educational program focusing on radiation safety in pediatric interventional radiology. For adults, the "Image Wisely" campaign is a collaboration between the American College of Radiology, the Radiological Society of North America, the American Association of Physicists in Medicine, and the American Society of Radiologic Technologists, which formed the Joint Task Force on Adult Radiation Protection to address concerns about the rapidly rising public exposure to radiation from medical imaging.

Information about radiation and the role of all stakeholders to improve radiation safety in medicine is summarized in a Blue Ribbon Panel article [45]. ACR guidelines also now include dose estimates for imaging tests and reference levels for acceptable doses in all appropriateness criteria.

However, patients are still often unaware of both the radiation dose delivered by CT and the potential risks associated with that radiation. Lee and colleagues surveyed patients in the emergency department about their understanding of the radiation dose from a CT versus a standard chest radiograph and found that patients were significantly more likely than expected to underestimate the CT dose; 28% of patients actually believed that a CT scan delivered less radiation than a chest radiograph [46]. However, there is also evidence that patients can be educated about ionizing radiation and the associated risks and more often than not are still willing to agree to the exam [44]. Patient education opportunities offer the ordering physician or radiologist a chance to dispel some of the potential misinformation regarding ionizing radiation in medical imaging.

The risk of radiation-induced cancer from CT should also be put into context against the statistical risk of developing cancer in the entire population. As mentioned above, the average risk of fatal cancer developing over a person's lifetime is approximately 22%. So, the development of cancer is not uncommon. The estimated increased risk of cancer over a person's lifetime from a single CT scan remains controversial, but is still estimated to be low, and should be weighed against the potential for clinical benefit. With this information, the physician-patient team can make an educated decision about the appropriateness of a proposed imaging exam.

Special Situation: Radiation Exposure from CT Perfusion

Summary
Advanced multislice CT techniques such as dynamic computed tomography perfusion (CTP) can provide vital information in the setting of acute stroke or aneurysmal subarachnoid hemorrhage; however, the current lack of standardized technique or utilization guidelines has led to the potential for radiation overexposure.

Supportive Evidence
In the setting of acute stroke, the information provided by modern imaging techniques can be assist in decision making regarding the use of thrombolytic therapy. CTP generates parametric maps of the cerebral hemodynamics by gathering information about the flow of contrast media through the cerebral vasculature and tissue beds [47]. These findings are more sensitive and more accurate than standard unenhanced CT [48, 49]. Similarly, in the setting of aneurysmal subarachnoid hemorrhage, imaging is a critical part of

immediate and accurate diagnosis. CTA and CTP may improve the diagnostic accuracy of vasospasm detection, leading to improved risk-benefit analysis when debating potential therapies [50–52]. These exams are generally reserved for a highly "at-risk" population, where the clinical question is both crucial and time sensitive.

However, there is considerable debate about the safety of CTP given several well-publicized incidents of radiation overexposure. A comprehensive stroke CT protocol can deliver radiation exposure up to six times that of a standard noncontrast CT of the head when CTA and CTP are included, even when performed according to FDA recommendations [53]. A July 2010 New York Times report outlined several cases from across the country where patients had been exposed to levels of radiation far above what would be considered standard practice, resulting in hair loss and skin erythema in multiple instances [54–56]. Doses reported for CTP studies in the literature vary widely across institutions, with Smith-Bindman et al. recording a range from 4 to 56 mSv across four San Francisco Bay Area institutions. Hypothesized reasons for this wide variation are a relative unfamiliarity by technologists who may overrely on automated scanner settings (which have been demonstrated to paradoxically increase radiation dose rather than decrease it in certain situations), inappropriate protocols (which may increase the dose by trying to improve image quality beyond the level clinically necessary in the setting of stroke or aneurysmal subarachnoid hemorrhage), and an overall lack of active monitoring of patient dose. Furthermore, patients may receive several such scans over the course of a single hospitalization, leading to high cumulative doses in certain clinical settings [14].

Public concerns about the potential for radiation overexposure with this CT technique led to a safety investigation by the US Food and Drug Administration (FDA) in October 2009 and updated recommendations in December 2009 and November 2010 which suggested that all CTP scan protocols should be reviewed to ensure correct doses are planned and also recommended documentation that technologists are trained for the specific imaging protocols being utilized.

The American Association of Physicists in Medicine (AAPM) has recently published a set of open access brain CTP protocols that are vendor specific to provide basic requirements of the exam and reconstruction parameters. This information is timely, given the increase in clinical use of CTP, the lack of standardized protocols, and ongoing concerns about its high radiation doses and risks to patients [57].

Lowering CT Dose in CT Perfusion

There is a need for increased knowledge and awareness among radiologists and technologists regarding radiation doses and potential mechanisms for reducing patient exposure. Protocol selection should be carefully monitored to prevent accidental overexposure, and monitoring of actual doses received by patients should be regularly performed. Dose reduction techniques that may prove beneficial in further reducing radiation dose from CT include iterative reconstruction algorithms that can supplement or potentially replace filtered back projection (although iterative reconstruction holds great promise for radiation dose reduction, the technique is not yet routinely applied to CTP datasets) and protocols utilizing lower kVp and mAs. The effective dose associated with a CTP exam can potentially be approximately equal to that of an unenhanced head CT (2–3 mSv), when these techniques are performed [58–60].

In addition, structured imaging guidelines for the appropriate utilization of CTP in a given disease can further reduce cumulative radiation exposure over the course of a hospitalization by encouraging imaging at clinically optimal time-points and discouraging unnecessary or suboptimal imaging periods [14].

Take-Home Tables

Tables 5.1 through 5.7 serve to highlight key recommendations and supporting evidence.

Table 5.1 Radiation dose units

Absorbed dose – Gray (Gy) – rad (rad) is prior unit
1 Gy = 100 rad
1 cGy = 1 rad
1 mGy = 100 mrad
Equivalent dose – Sievert (Sv) – rem (rem) is prior unit,
Sv = Gy × quality factor (=1)
1 Sv = 100 rem
10 mSv = 1 rem
1 mSv = 100 mrem

Reprinted with permission from Frush, DP ST. Biological effects of diagnostic radiation on children. In: Slovis TL, editor. Caffey's pediatric diagnostic imaging. Philadelphia: Elsevier; 2007. p. 29–41

Table 5.2 Inherited human syndromes associated with sensitivity to X-rays

Ataxia–telangiectasia
Basal cell nevoid syndrome
Cockayne's syndrome
Down syndrome
Fanconi's anemia
Gardner's syndrome
Nijmegan breakage syndrome
Usher's syndrome

Reprinted and adapted from Frush, DP ST. Biological effects of diagnostic radiation on children. In: Slovis TL, editor. Caffey's pediatric diagnostic imaging. Philadelphia: Elsevier: 2007. p. 29–41; and from Hall EJ. Radiobiology for the radiologist. Philadelphia: Lippincott Williams & Wilkins; 2000. p. 45, with permission

Table 5.3 Deterministic effects: relatively high radiation doses needed compared to what is used in diagnostic imaging

Tissue injury	Approximate threshold
(a) Skin	
Transient erythema	2 Gy (200 rad)
(b) Eyes	
Cataracts (acute)	>2.0 Gy (>200 rad)

Reprinted and adapted from Frush, DP ST. Biological effects of diagnostic radiation on children. In: Slovis TL, editor. Caffey's pediatric diagnostic imaging. Philadelphia: Elsevier; 2007. p. 29–41; and from Hall EJ. Radiobiology for the radiologist. Philadelphia: Lippincott Williams & Wilkins; 2000. p. 45, with permission

Table 5.4 Effective radiation doses relative to background radiation

Procedure	Estimated effective radiation dose	Comparable to background radiation
Computed tomography (CT) of the abdomen and pelvis	10 mSv	3 years
Computed tomography (CT) of the head	2 mSv	8 months
Computed tomography (CT) of the spine	6 mSv	2 years
Myelography	4 mSv	16 months

Data from www.radiologyinfo.org (RSNA) and www.acr.org (ACR Appropriateness Criteria®)

Table 5.5 Relative radiation doses for adults

Source	Estimated effective dose (mSv)
Natural background radiation	3 mSv per year
Airline passenger (cross-country)	0.03 mSv
Chest X-ray (single view)	0.01 mSv
Head CT	2 mSv
Chest CT	Up to 7 mSv
Abdominal CT	15 mSv

Based on USA data and data from www.imagewisely.org

Table 5.6 Appropriateness of common radiologic exams and associated radiation risk

Indication	Modality	ACR appropriateness criteria	Radiation risks
Suspected stroke (new neurological deficit)			
	Head CT	8 (usually appropriate)	"Low"
	CTA	8 (usually appropriate)	"Low"
Head trauma (minor injury without focal neurological deficit)			
	Head CT	7 (usually appropriate)	"Low"
Head trauma (minor injury with focal deficit)			
	Head CT	9 (usually appropriate)	"Low"
Cervical trauma (does not meet NEXUS criteria)			
	Cervical spine CT	1 (usually NOT appropriate)	"Low"
Cervical trauma (meets NEXUS criteria)			
	Cervical spine CT	9 (usually appropriate)	"Low"
Suspected child abuse (no focal symptoms)			
	Skeletal survey	9 (usually appropriate)	"Low"
	Head CT	7 (usually appropriate)	"Low"
Suspected child abuse (suspected head trauma)			
	Head CT	9 (usually indicated)	"Low"
		(ACR literature defines "low" as 1–10 mSv)	

Data from ACR Appropriateness Criteria®; www.acr.org
Rating scale: 1, 2, 3 usually not appropriate; 4, 5, 6 may be appropriate; 7, 8, 9 usually appropriate

Table 5.7 Atomic bomb (longitudinal survivor study) data showing excess solid cancers linked to radiation exposure doses (dose in Sv)

Observed and expected solid cancer deaths 1950–1997 by dose group

Dose	People	1950–1997			1991–1997		
		Deaths	Expected background	Fitted excess	Deaths	Expected background	Fitted excess
<0.005	37,458	3,833	3,844	0	742	718	0
0.005–0.1	31,650	3,277	3,221	44	581	596	12
0.1–0.2	5,732	668	622	39	137	109	10
0.2–0.5	6,332	763	678	97	133	118	24
0.5–1	3,299	438	335	109	75	62	28
1–2	1,613	274	157	103	68	31	27
2+	488	82	38	48	20	8	13
Total	86,572	9,335	8,895	440	1,756	1,642	114

Reprinted with permission from Preston DL et al. Radiat Res. 2003;32:700–706
Atomic bomb (longitudinal survivor study) data 1950–1997

Future Research

- Increase multicenter outcomes research on the health benefits/risks of imaging for common conditions (trauma, abdominal pain, infection, and cancer)
- Increase understanding of the trend in utilization of imaging, in particular those with relatively high ionizing radiation doses (e.g., CT, PET) and potential nonionizing radiation alternative imaging (e.g., sonography, MRI)
- Increase development of dose reduction strategies for ultra low-dose CT examinations, particularly CT angiography and perfusion techniques
- Development of cumulative radiation dose records for patients

References

1. Huda W. Radiol Soc North Am. 2006;167–182.
2. Frush DP, Slovis T. Biological effects of diagnostic radiation on children. In: Slovis TL, editor. Caffey's pediatric diagnostic imaging. Philadelphia: Elsevier; 2007. p. 29–41.
3. Imanishi Y, Fukui A, Niimi H, Itoh D, Nozaki K, Nakaji S, et al. Eur Radiol [Internet]. 2005; 15(1):41–6. Available from: http://www.ncbi.nlm.nih.gov/pubmed/15351903
4. Hall P, Adami H-O, Trichopoulos D, Pedersen NL, Lagiou P, Ekbom A, et al. Br Med J [Internet]. 2004;328(7430):19. Available from: http://www.ncbi.nlm.nih.gov/pubmed/14703539
5. Berrington A, Darby SC, Weiss HA, Doll R. Br J Radiol [Internet]. 2001;74(882):507–19. Available from: http://www.ncbi.nlm.nih.gov/pubmed/11459730
6. Clarke R, Radiological N, Board P. UNSCEAR 2000 report. 2000;5–9
7. Gaca AM, Jaffe TA, Delaney S, Yoshizumi T, Toncheva G, Nguyen G, et al. Pediatr Radiol [Internet]. 2008;38(3):285–91. Available from: http://www.ncbi.nlm.nih.gov/pubmed/18183380
8. Thomas KE, Wang B. Pediatr Radiol [Internet]. 2008;38(6):645–56. Available from: http://www.springerlink.com/index/10.1007/s00247-008-0794-0
9. Huda W, Vance A. AJR Am J Roentgenol [Internet]. 2007 [cited 2010 Jul 7];188(2):540–6. Available from: http://www.ncbi.nlm.nih.gov/pubmed/17242266
10. Deak PD, Smal Y, Kalender WA. Radiology [Internet]. 2010;257(1):158–66. Available from: http://www.ncbi.nlm.nih.gov/pubmed/20851940
11. Mettler FA, Thomadsen BR, Bhargavan M, Gilley DB, Gray JE, Lipoti JA, et al. Health Phys [Internet]. 2008;95(5):502–7. Available from: http://www.ncbi.nlm.nih.gov/pubmed/18849682
12. Fuchs VR, Sox HC. Health Aff [Internet]. 2001;20(5):30–42. Available from: http://content.healthaffairs.org/cgi/doi/10.1377/hlthaff.20.5.30
13. Wiest PW, Locken JA, Heintz PH, Mettler FA. Semin Ultrasound Ct and Mr [Internet]. 2002;23(5): 402–10. Available from: http://www.ncbi.nlm.nih.gov/pubmed/12509110
14. Loftus ML, Minkowitz S, Tsiouris A J, Min RJ, Sanelli PC. AJR Am J Roentgenol [Internet]. 2010 [cited 2011 Apr 22];195(1):176–80. Available from: http://www.ncbi.nlm.nih.gov/pubmed/20566813
15. Vargas HA, Akin O, Zheng J, Moskowitz C, Soslow R, Abu-Rustum N, et al. Radiology. 2011; 258(3):785–92.
16. Brenner DJ, Hall EJ. Computed tomography – an increasing source of radiation exposure. New Engl J Med. 2007;357(22):2277–84.
17. Brenner DJ, Doll R, Goodhead DT, Hall EJ, Land CE, Little JB, et al. Proc Natl Acad Sci USA [Internet]. 2003;100(24):13761–6. Available from: http://www.pubmedcentral.nih.gov/articlerender.fcgi?artid=283495&tool=pmcentrez&rendertype=abstract
18. Protection R. Leukemia [Internet]. 2005;(93):93–6. Available from: http://scholar.google.com/scholar?hl=en&btnG=Search&q=intitle:BEIR+VII:+HEALTH+RISKS+FROM+EXPOSURE+TO+LOW+LEVELS+OF+IONIZING+RADIATION#5
19. Weiss JF, Landauer MR. Ann NY Acad Sci [Internet]. 2000;899:44–60. Available from: http://www.ncbi.nlm.nih.gov/pubmed/10863528
20. Grdina DJ, Murley JS, Kataoka Y. Oncology [Internet]. 2002;63(Suppl 2):2–10. Available from: http://www.karger.com/doi/10.1159/000067146
21. Prasad KN, Cole WC, Hasse GM. Exp Biol Med [Internet]. 2004;229(5):378. Available from: http://www.ebmonline.org/cgi/content/abstract/229/5/378
22. Kleinerman RA. Pediatr Radiol [Internet]. 2006;36(Suppl 2):121–5. Available from: http://www.pubmedcentral.nih.gov/articlerender.fcgi?artid=2663653&tool=pmcentrez&rendertype=abstract
23. Preston DL, Ron E, Tokuoka S, Funamoto S, Nishi N, Soda M, et al. Radiat Res [Internet]. 2007;168(1): 1–64. Available from: http://www.ncbi.nlm.nih.gov/pubmed/17722996
24. Prasad KN, Cole WC, Haase GM. Br J Radiol [Internet]. 2004;77(914):97–9. Available from: http://www.ncbi.nlm.nih.gov/pubmed/15010379
25. Linet MS, Kim KP, Rajaraman P. Pediatr Radiol [Internet]. 2009;39(Suppl 1):S4-26. Available from: http://www.pubmedcentral.nih.gov/articlerender.fcgi?artid=2814780&tool=pmcentrez&rendertype=abstract

26. Berrington De González A, Darby S. Lancet [Internet]. 2004;363(9406):345–51. Available from: http://www.ncbi.nlm.nih.gov/pubmed/15070562

27. Brenner D, Elliston C, Hall E, Berdon W. AJR Am J Roentgenol [Internet]. 2001;176(2):289–96. Available from: http://www.ncbi.nlm.nih.gov/pubmed/11159059

28. Ron E. Pediatr Radiol [Internet]. 2002 [cited 2011 Mar 26];32(4):232–7; discussion 242–4. Available from: http://www.ncbi.nlm.nih.gov/pubmed/11956701

29. Modan B, Keinan L, Blumstein T, Sadetzki S. Int J Epidemiol [Internet]. 2000;29(3):424–8. Available from: http://www.ncbi.nlm.nih.gov/pubmed/10869313

30. Spengler RF, Cook DH, Clarke EA, Olley PM, Newman AM. Pediatrics. 1983;71(2):235–9.

31. McLaughlin JR, Kreiger N, Sloan MP, Benson LN, Hilditch S, Clarke EA. Int J Epidemiol. 1993;22(4): 584–91.

32. Donnelly LF, Emery KH, Brody AS, Laor T, Gylys-Morin VM, Anton CG, et al. AJR Am J Roentgenol. 2001;176(2):303–6.

33. American Association of Physicists in Medicine (AAPM). Dose check standards [Internet]. Available from: http://www.aapm.org/pubs/CTProtocols/documents/NotificationLevelsStatement_2011-04-27.pdf

34. Smith-Bindman R, Lipson J, Marcus R, Kim K-P, Mahesh M, Gould R, et al. Arch Intern Med [Internet]. 2009;169(22):2078–86. Available from: http://www.ncbi.nlm.nih.gov/pubmed/20008690

35. Mettler FA. Effective doses in radiology and diagnostic nuclear medicine. 2008;248(1):254–63.

36. Wall BF, Hart D. Br J Radiol [Internet]. 1997;70(833):437–9. Available from: http://www.ncbi.nlm.nih.gov/pubmed/9227222

37. Pearce MS, Salotti JA, Little MP, McHugh K, Lee C, Kim KP, Howe NL, et al. Radiation exposure from CT scans in childhood and subsequent risk of leukaemia and brain tumours: a retrospective cohort study. The Lancet. 2012;6736(12)

38. Higson D. J Radiol Protect: Official J Soc Radiol Protect. 2005;25(3):324–5.

39. Pantos I, Thalassinou S, Argentos S, Kelekis N, Panayiotakis G, Efstathopoulos E. Br J Radiol [Internet]. 2011;1–11. Available from: http://www.ncbi.nlm.nih.gov/pubmed/21266399

40. Eisenberg MJ, Afilalo J, Lawler PR, Abrahamowicz M, Richard H, Pilote L. Can Med Assoc J [Internet]. Can Med Assoc J. 2011;183(4):430–63. Available from: http://www.cmaj.ca/cgi/content/abstract/cmaj.100463v1

41. Cohnen M, Wittsack H-J, Assadi S, Muskalla K, Ringelstein A, Poll LW, et al. AJNR Am J Neuroradiol [Internet]. 2006;27(8):1741–5. Available from: http://www.ncbi.nlm.nih.gov/pubmed/16971627

42. Medina LS, Kuntz KM, Pomeroy S. Pediatrics [Internet]. 2001;108(2):255–63. Available from: http://pediatrics.aappublications.org/cgi/doi/10.1542/peds.108.2.255

43. Kuppermann N, Holmes JF, Dayan PS, Hoyle JD, Atabaki SM, Holubkov R, et al. Lancet [Internet]. 2009;374(9696):1160–70. Available from: http://linkinghub.elsevier.com/retrieve/pii/S0140673609615580

44. Larson DB, Rader SB, Forman HP, Fenton LZ. AJR Am J Roentgenol [Internet]. 2007;189(2):271–75. Available from: http://www.ncbi.nlm.nih.gov/pubmed/17646450

45. Amis ES, Butler PF, Applegate KE, Birnbaum SB, Brateman LF, Hevezi JM, et al. J Am Coll Radiol JACR [Internet]. 2007;4(5):272–84. Available from: http://www.ncbi.nlm.nih.gov/pubmed/17467608

46. Lee CI, Haims AH, Monico EP, Brink JA, Forman HP. Radiology [Internet]. 2004;231(2): 393–98. Available from: http://radiology.rsna.org/content/231/2/393.full

47. Zussman B, Flanders A, Rosenwasser R, Jabbour P. Blood. 2010;5(2):1–4.

48. Wintermark M, Flanders AE, Velthuis B, Meuli R, Van Leeuwen M, Goldsher D, et al. Stroke: A J Cereb Circ [Internet]. 2006;37(4):979–85. Available from: http://www.ncbi.nlm.nih.gov/pubmed/16514093

49. Schaefer PW, Roccatagliata L, Ledezma C, Hoh B, Schwamm LH, Koroshetz W, et al. AJNR Am J Neuroradiol [Internet]. 2006;27(1):20–5. Available from: http://www.ncbi.nlm.nih.gov/pubmed/16418350

50. Binaghi S, Colleoni ML, Maeder P, Uské a, Regli L, Dehdashtia R, et al. AJNR. Am J Neuroradiol [Internet]. 2007;28(4):750–8. Available from: http://www.ncbi.nlm.nih.gov/pubmed/17416833

51. Chaudhary SR, Ko N, Dillon WP, Yu MB, Liu S, Criqui GI, et al. Cerebrovasc Dis Basel Switzerland [Internet]. 2008;25(1–2):144–50. Available from: http://www.ncbi.nlm.nih.gov/pubmed/18073468

52. Wintermark M, Ko NU, Smith WS, Liu S, Higashida RT, Dillon WP. AJNR Am J Neuroradiol [Internet]. 2006;27(1):26–34. Available from: http://www.ncbi.nlm.nih.gov/pubmed/16418351

53. Mnyusiwalla A, Aviv RI, Symons SP. Neuroradiology [Internet]. 2009;51(10):635–40. Available from: http://www.ncbi.nlm.nih.gov/pubmed/19506845

54. Boom TR, Scans AS, Face P, Health S. Health San Francisco [Internet]. 2010;1–9. Available from: http://www.nytimes.com/2010/08/01/health/01radiation.html?_r=2&partner=rss&emc=rss

55. Smith a B, Dillon WP, Gould R, Wintermark M. AJNR. Am J Neuroradiol [Internet]. 2007 [cited 2010 Jul 11];28(9):1628–32. Available from: http://www.ncbi.nlm.nih.gov/pubmed/17893208

56. Wintermark M, Lev MH. AJNR. Am J Neuroradiol. 2010;31(1):2–3. Available from: http://www.ncbi.nlm.nih.gov/pubmed/19892810

57. American Association of Physicists in Medicine (AAPM). Brain CTP Protocols [Internet]. Available from: http://www.aapm.org/pubs/CTProtocols/documents/AdultBrainPerfusionCT_2011-01-11.pdf

58. Hara AK, Paden RG, Silva AC, Kujak JL, Lawder HJ, Pavlicek W. AJNR. Am J Neuroradiol [Internet]. 2009;193(3):764–71. Available from: http://www.ncbi.nlm.nih.gov/pubmed/19696291

59. Konstas AA, Goldmakher GV, Lee T-Y, Lev MH. AJNR. Am J Neuroradiol [Internet]. 2009;30(4): 662–8. Available from: http://www.ncbi.nlm.nih.gov/pubmed/19270105

60. Konstas AA, Goldmakher GV, Lee T-Y, Lev MH. AJNR. Am J Neuroradiol [Internet]. 2009;30(5): 885–92. Available from: http://www.ncbi.nlm.nih.gov/pubmed/19299489

Intravenous Contrast in CT and MR Imaging: Risks

6

Aoife Kilcoyne, Jan Frank Gerstenmaier, and Dermot E. Malone

Contents

A. Kilcoyne (✉) • J.F. Gerstenmaier • D.E. Malone
Department of Radiology, St. Vincent's University Hospital, Dublin, Ireland
e-mail: aoifekilcoyne@gmail.com; gerstenmaierj@fastmail.us; dmalone@ucd.ie

Key Points

- Serum creatinine as an absolute measure is an unreliable indicator of kidney function. GFR is considered to be a more appropriate index of kidney function and can be estimated from the serum creatinine [1] (strong evidence).
- Patients with impaired renal function should be identified in advance of contrast administration by assessment of risk factors, measurement of serum creatinine, and calculation of eGFR (strong evidence).
- Prehydration and administration of *N*-acetylcysteine and sodium bicarbonate are beneficial in optimizing renal function in patients with impaired renal function (strong evidence).
- Gadolinium-based contrast agents have variable risk profiles in patients with renal impairment. High-risk agents – Optimark (gadoversetamide), Magnevist (gadopentetate dimeglumine), and Omniscan (gadodiamide) – are unsafe in patients with impaired renal function. Their use in this patient group should be avoided [2] (strong evidence).
- Life-threatening anaphylactic reactions due to iodinated contrast media are rare. Anaphylaxis related to gadolinium-based compounds is even more uncommon. In unselected patients, the usefulness of premedication is doubtful. There is no convincing evidence supporting the use of premedication in patients with a history of allergic reactions [3] (strong evidence).

Definition and Pathophysiology

Contrast-induced nephropathy is defined as a serum creatinine level increase of at least 0.5 mg/dL within 3 days of contrast medium administration without an alternative cause [4]. The exact mechanism of contrast-induced nephropathy is uncertain, but certain patient groups are at a higher risk. Many potential mechanisms have been proposed. A vasoconstrictive effect leading to hypoxic or ischemic tubular cell injury and a direct tubulotoxicity mediated by the generation of reactive oxygen species are currently considered to be implicated [5]. The free radical mechanism of direct tubular toxicity has led several investigators to focus on the use of *N*-acetylcysteine (NAC) for the prevention of CIN, as NAC has been previously shown to have antioxidant properties (15).

Nephrogenic systemic fibrosis (NSF) is a fibrosing disorder that has occurred exclusively among patients with renal impairment. The first case of NSF was observed in 1997, and the disease was initially reported in 2000 in a case series of 14 patients undergoing hemodialysis who had developed characteristic skin lesions on their trunk and extremities [6]. The mechanism of NSF induction by gadolinium has not yet been fully elucidated; however, transmetalation with dissociation of free gadolinium from its chelate has been suggested to be involved [7].

Gadolinium is a member of the lanthanide series of transition metals. It has strong hydrogen proton spin–lattice relaxation effects that can be exploited to provide enhanced contrast between healthy and diseased tissue [8].

Gadolinium in the free ionic form (Gd3+) is highly toxic. To prevent deleterious effects of Gd3+, it needs to be sequestered by nontoxic substances. This is achieved by binding Gd3+ to another agent. The newly created complex is the chelate complex. Two categories of gadolinium chelate exist: (a) macrocyclic molecules where Gd3+ is caged in the preorganized cavity of a ligand and (b) linear molecules [9].

Metals such as iron are capable of inducing the dissociation of gadolinium from its chelate (transmetalation). Some patients with renal insufficiency may have a heightened susceptibility to iron mobilization which may contribute to gadolinium toxicity and nephrogenic systemic fibrosis [7].

Epidemiology

In Europe and the United States, contrast-induced nephropathy accounts for more than 10 % of all cases of hospital-acquired acute renal failure [10].

Particular attention should be paid to patients over 70 years old, patients who are dehydrated or with cardiac failure, diabetics, patients on nephrotoxins, or those with gout. These patients are more likely to have impaired renal function.

Solomon and Barrett [11] reviewed the available literature to examine the prognosis and clinical course of patients having an acute decline in the glomerular filtration rate following contrast exposure. Most of the data in the series was from cohorts having percutaneous coronary intervention. A number of short- and long-term outcomes were studied, including kidney function, need for dialysis, major adverse cardiovascular events, and death during the index hospitalization, as well as death rates by 1 or 5 years postcontrast. Dialysis for CIN was required in 0.15–12 % of cases. There was some variability regarding whether the patients involved required short-term dialysis alone or proceeded to long-term dialysis. Gruberg et al. [12] reported that almost 13 % of patients dialyzed remained dialysis dependant in the long term, whereas McCullough et al. reported that 50 % did so in their earlier cohort [13]. Whether patients recover to become dialysis independent may depend on the severity of the acute insult, as well as how close to end-stage renal disease they are at the time of exposure to contrast. Patients having coronary intervention may also be particularly likely to have multiple mechanisms of kidney injury, including hemodynamic instability and atheroembolism.

The studies analyzed in the report also consistently found an association of acute increase in serum creatinine after contrast with higher death rates both during the index hospitalization and in the longer term. The reason for this was unclear. A proposed possibility is that acute renal injury initiates or aggravates pathologies (including vascular) such that later death ensues even though kidney function improves. If this is true, then interventions that reduce the risk of CIN may also improve longer-term prognosis.

Nephrogenic systemic fibrosis appears to affect males and females in approximately equal numbers. It affects middle-aged adults most commonly [14]. It has been identified in patients from a wider variety of ethnic backgrounds and from North America, Europe, and Asia [15].

NSF has a chronic and unremitting course in most patients. In a review of the published literature, 28 % of the patients had no improvement, 20 % had modest improvement, and 28 % of patients died [16]. More severe and rapid progression of the skin disease is associated with a poor prognosis and death.

A fulminant form of NSF, with development of flexion contractures and loss of mobility, has been described in 5 % of patients [14]. Such patients may become wheelchair bound within weeks. It is possible that some of these patients had received repeated administrations of gadolinium.

Improvement in or remission of NSF has been described, primarily in patients who recovered renal function [14, 16]. In such patients, the improvement in renal function seems to slow or stop disease progression and, in many patients, results in gradual reversal of the disease. In the review by Mendosa, less than 40 % of patients underwent complete remission following the cessation of dialysis.

Overall Cost to Society

The cost to society of contrast reactions does not appear, from our review of the literature, to have been studied extensively. This is likely because it is a side effect, not a primary disease process. There are no cost-effectiveness or feasibility studies that evaluate protocols for aggressive identification of high-risk patients undergoing contrast radiography and utilization of standardized hydration protocols to reduce radiocontrast-induced nephropathy. Two studies suggest most patients with normal renal function can be easily identified by simple questionnaire, resulting in significant cost savings from a reduction in the number of routine serum creatinine levels obtained prior to imaging [17, 18]. The cost-effectiveness of using pharmacologic pretreatment with N-acetylcysteine has not been studied.

Goals of Imaging

To achieve diagnostic quality imaging while optimizing imaging protocols such that renal function is not adversely affected and the patient safety and well-being is maintained.

Methodology

The PICO methodology was used to design a focused clinical question for CT and for MR [19, 20]. A MEDLINE search was performed using PubMed (National Library of Medicine, Bethesda, Maryland) for original research publications discussing iodinated contrast media and gadolinium-based contrast media used in CT and MR in the last 10 years (from January 1, 2001 to March 30, 2011). An additional search of these topics was also performed using PubMed limited to guidelines in English in the last 5 years.

An initial review of the titles and abstracts of the identified publications was performed by the first and second author. Inclusion criteria were primary research studies, systematic reviews, and meta-analyses addressing contrast-induced nephropathy, contrast-induced anaphylaxis, and nephrogenic systemic fibrosis. Exclusion criteria included articles for which no abstract was available and letters and publications not in English. Any disagreements between the authors were resolved by discussion or by consulting with the senior author. This was followed by review of the full text in relevant publications.

The AGREE instrument [21] was used to appraise the relevant guidelines. All other data was ranked as Level 1–4 using the system recommended by the editors of this textbook. This process found the most reliable guidelines were those recently produced by the European Society of Urogenital Radiology (Version 7.0, 2011) [4]. Other strong guidelines used were those from the American College of Radiology [22] and The Canadian Association of Radiologists [23]. A search of the primary literature following the release of these guidelines did not yield additional useful information.

Discussion of Issues

Issues relating to CT and MR are dealt with separately in this section. They are each discussed under the following subheadings: method of administration, mechanism of reaction, subdivision of reactions, risk factors for reactions, prevention of reactions, and management of reactions. Prior to this discussion, the benefit of sodium bicarbonate versus *N*-acetylcysteine versus hydration in the prevention of contrast-induced nephropathy is addressed.

What Is the Role of Hydration Versus Sodium Bicarbonate Versus *N*-Acetylcysteine in the Prevention of Contrast-Induced Nephropathy?

Regarding prevention of contrast-induced nephropathy, the evidence basis for preprocedure hydration versus sodium bicarbonate versus *N*-acetylcysteine has been the subject of much controversy.

A review of the primary and secondary literature regarding the benefit of preprocedural *N*-acetylcysteine with hydration revealed multiple large-scale meta-analyses in favor of NAC. Many of these were affected by significant clinical heterogeneity; however, the most recent large-scale study was homogenous and found a statistically significant benefit in using NAC [24]. While much of this data pertained to patients undergoing coronary angiography who are high risk from a cardiovascular and a renal point of view, NAC was demonstrated to be beneficial. This inexpensive drug with a low side effect profile should be used for high-risk patients undergoing CT, at a recommended dose of 1,200 mg twice daily for 2 days beginning the day before contrast administration.

There have been a number of large-scale studies reviewing the benefit of periprocedural sodium bicarbonate. Similarly, early meta-analyses were limited by heterogeneity. However, a large meta-analysis analyzing 17 trials including 2,633 subjects found that sodium

bicarbonate-based hydration was found to be superior to normal saline in prevention of contrast-induced nephropathy [25].

Another large-scale meta-analysis analyzed 12 trials with 1,854 participants [26]. Sodium bicarbonate significantly decreased the risk of contrast-induced nephropathy, without a significant difference in need for renal replacement therapy, in hospital mortality, or in congestive cardiac failure compared with controls. Similar results were seen for the risk of contrast-induced nephropathy when sodium bicarbonate was compared with normal saline alone but not when sodium bicarbonate/*N*-acetylcysteine combination was compared with *N*-acetylcysteine/normal saline combination.

Regarding hydration, review of the secondary literature recommended that intravenous hydration is superior to oral hydration. Oral hydration with water alone should not be used. Hydration with isotonic saline solution is superior to one-half normal saline (UpToDate®) [27].

CT: Iodinated Contrast Media

What Is the Method of Administration?
Intravenous

What Is the Mechanism of Reaction?
General frequency of adverse events related to administration of contrast media has decreased considerably, with changes in usage from high-osmolality contrast media to low-osmolality contrast media. Most side effects are mild and non-life threatening. Almost all life-threatening reactions occur immediately or within the first 20 min after contrast media injection. The precise pathologic mechanism is unclear, and in general, accurate prediction of a contrast reaction is not possible.

How Are Reactions Subdivided?
Contrast reactions can be classified into nonrenal, renal, and miscellaneous types.

Nonrenal
Nonrenal reactions can be further subclassified depending on their acuity. Acute nonrenal

reactions are regarded as those occurring within 1 h of contrast media injection. These can be mild (nausea, vomiting, urticaria, itching), moderate (severe vomiting, marked urticaria, bronchospasm, facial/laryngeal edema, vasovagal attack), or severe (hypotensive shock, respiratory arrest, cardiac arrest, convulsions). Late reactions are those that occur between 1 h and 1 week after contrast media injections. These include nausea, vomiting, headache, musculoskeletal pain, fever, and skin reactions or drug eruptions. Thyrotoxicosis is a reaction that is considered to occur very late, i.e., 1 week or more after contrast media administration.

Renal
The two principal renal reactions after contrast media administration are contrast medium-induced nephropathy and lactic acidosis in patients taking metformin.

Miscellaneous
A range of miscellaneous reactions are recognized. These relate to pulmonary effects (bronchospasm, increased pulmonary vascular resistance, and pulmonary edema); extravasation of contrast into tissues; and effects of iodinated contrast media on blood and endothelium, such as thrombosis and increased risk of thromboembolic events. Further, contrast media have the potential to interact with other drugs and clinical tests.

What Are the Risk Factors for the Reactions?
Nonrenal
Certain risk factors for nonrenal reactions can again be categorized according to the chronicity of the reaction. In acute reactions, a previous history of a moderate or severe acute contrast reaction is a strong risk factor. High-osmolality ionic contrast media also increase the risk of an acute reaction, but these agents are rarely, if ever, used intravenously nowadays. Further, a history of asthma and allergy requiring medical treatment are considered risk factors to acute reactions. Any severity of previous contrast reaction is considered a risk factor for late reactions. Current treatment with interleukin-2 is also

a recognized risk factor for late reactions. Very late reactions, i.e., thyrotoxicosis, are more likely in patients with untreated Graves' disease and patients with multinodular goiter and thyroid autonomy.

Renal

The principal risk factors for renal complications are an eGFR of less than 60 mL/min/1.73 m^2; dehydration; congestive heart failure; gout; age over 70; concurrent administration of nephrotoxic drugs, e.g., NSAIDs; treatment with aminoglycosides; or ACE inhibitors. In addition, high-osmolality contrast agents and large doses of contrast medium increase the risk.

Miscellaneous

Contrast Medium Extravasation

Several factors increase the risk of contrast extravasation: use of a power injector, less optimal injection sites, large volume of contrast medium, high-osmolar contrast media, patient inability to communicate, fragile/damaged veins, arterial insufficiency, compromised lymphatic and/or venous drainage, and obesity.

Pulmonary Effects

The three main risk factors for patients to suffer pulmonary reactions from contrast administration are asthma, pulmonary hypertension, and incipient cardiac failure.

Effects on Blood and Endothelium

The use of high-osmolar contrast media is the only recognized significant risk factor for reactions relating to blood and endothelium.

How Are Contrast Reactions Best Prevented?

Nonrenal Acute

Several preventative measures are recommended to avoid nonrenal reactions: Where possible, a nonionic contrast medium should be used. The patient should be kept in the Radiology Department for 30 min after contrast medium injection. Drugs and equipment for resuscitation should be readily available. Further, an alternative test not requiring iodinated contrast should be considered. If this is not an option, the use of a different iodinated agent should be sought. Premedication can be considered. Clinical evidence of the effectiveness of premedication is limited. If used, a suitable premedication is prednisolone 30 mg (or methylprednisolone 32 mg) orally 12 and 2 h before contrast medium is given in some centers.

Nonrenal Late

For late reactions, prophylaxis is generally not recommended, but patients who have had a previous serious late adverse reaction can be given steroid prophylaxis.

Nonrenal Very Late

Iodinated contrast media should not be given to patients with manifest hyperthyroidism. Prophylaxis is generally not necessary. However, in selected high-risk patients, prophylactic treatment may be given by an endocrinologist. This is more relevant in areas of dietary iodine deficiency. Patients at risk should be closely monitored by an endocrinologist after iodinated contrast medium injection. Intravenous cholangiographic contrast media should not be given to patients at risk.

Renal: At the Time of Referral

Elective Examination

What Is the Best Method to Calculate the eGFR? The most common methods utilized to estimate the GFR in adults are the serum creatinine concentration, the creatinine clearance, and estimation equations based on the serum creatinine concentration: the Cockcroft-Gault equation and Modification of Diet in Renal Disease. However, the estimation equations have not been validated and may be less accurate in some populations. These include children, certain ethnic groups, pregnant women, and those with unusual muscle mass, body habitus, and weight (e.g., morbid obesity or malnourished). Some, therefore, recommend measuring the creatinine clearance to estimate the GFR in these patients with stable renal function (UpToDate).

How Is eGFR Used to Stratify the Risk of Nephrotoxicity in Iodinated Contrast? For elective examinations, firstly, patients with an eGFR of less than 60 mL/min/1.73 m^2 (or raised serum creatinine) should be identified, and their eGFR (or serum creatinine) measured within 7 days of contrast medium administration. Other patients at risk are diabetic patients taking metformin, patients who will receive intra-arterial contrast medium, and patients who have a history suggesting the possibility of reduced GFR. This includes renal disease, renal surgery, proteinuria, diabetes mellitus, hypertension, gout, and recent nephrotoxic drugs.

Secondly, diabetic patients taking metformin should be identified. Depending on their eGFR/serum creatinine level, metformin will have to be stopped either before or at the time of contrast medium administration.

Emergency Examination

Patients with a known eGFR of less than 60 mL/min/1.73 m^2 (or raised serum creatinine) should be identified where possible. Diabetic patients taking metformin should be identified and eGFR (or serum creatinine) measured if the procedure can be deferred until the result is available without harm to the patient. In extreme emergency, if eGFR (or serum creatinine measurement) cannot be obtained, follow the protocol for patients with eGFR less than 60 mL/min/1.73 m^2 (or raised serum creatinine) as closely as clinical circumstances permit.

Renal: Prior to the Examination
Elective Examination

For patients with eGFR less than 60 mL/min/1.73 m^2 and those at increased risk of nephrotoxicity, an alternative imaging method not using iodinated contrast media should be considered. Nephrotoxic drugs, mannitol, and loop diuretics should be stopped at least 24 h before contrast medium administration. Hydration, e.g., 1 mL/kg body weight per hour of normal saline for at least 6 h before and after the procedure should be commenced.

Regarding diabetic patients, taking metformin, if eGFR >60 mL/min/1.73 m^2, the patient can continue to take metformin. If eGFR 30-60 mL/min/1.73 m^2 (or serum creatinine is raised), metformin should be stopped 48 h before contrast medium administration. These patients should remain off metformin for 48 h after contrast medium. Metformin should only be restarted if serum creatinine is unchanged 48 h after contrast medium. In cases of eGFR <30, metformin is not approved in most countries, and iodinated contrast medium should be avoided if possible.

Emergency Examination

For patients at increased risk of nephrotoxicity, consider an alternative imaging method not using iodinated contrast media. Intravenous hydration should be started as early as possible before contrast medium administration.

In diabetic patients taking metformin with an eGFR >60 mL/min/1.73 m^2, proceed as for elective patients. In case of eGFR 30–60 mL/min/1.73 m^2 or serum creatinine raised or unknown, the risks and benefit of contrast medium administration should be weighed against each other and an alternative imaging method considered. If contrast medium is deemed essential, take the following precautions: Stop metformin; hydrate the patient, e.g., at least 1 mL per hour per kg b.w. of IV normal saline up to 6 h after contrast medium administration; monitor renal function (eGFR/serum creatinine), serum lactic acid, and pH of blood; and look for symptoms and biochemical markers of lactic acidosis: vomiting, somnolence, nausea, epigastric pain, anorexia, hyperpnea, lethargy, diarrhea and thirst, and blood pH < 7.25 with plasma lactate >5 mmol/L.

Renal: At the Time of the Examination
How Can Patients Be Optimized in Order to Prevent Contrast-Induced Nephropathy?

For patient at increased risk, low/iso-osmolar contrast media and the lowest dose of contrast medium consistent with a diagnostic result should be used.

For patients with no increased risk of contrast-induced nephropathy, the lowest dose of contrast medium consistent with a diagnostic result should be used.

Miscellaneous

Contrast Medium Extravasation

Meticulous IV technique is necessary using an appropriate sized plastic cannula placed in a suitable vein to handle the flow rate used during the injection. A test injection with normal saline should be performed. The use of nonionic contrast medium is preferred.

Pulmonary Effects

Low- or iso-osmolar contrast media should be used, and large doses of contrast media avoided.

Blood and Endothelium

Meticulous angiographic technique using low- or iso-osmolar contrast media is necessary.

What Is the Management of Contrast Reactions?

Nonrenal

Acute

Transient Nausea and Vomiting Supportive treatment is needed only. For severe, protracted cases, consider appropriate antiemetic drugs.

Urticaria Scattered, transient urticaria requires supportive treatment, including observation.

Scattered, protracted cases warrant appropriate H1-antihistamine intramuscularly or intravenously. Drowsiness and/or hypotension may occur. For profound cases, consider adrenaline 1:1,000, 0.1–0.3 mL (0.1–0.3 mg) intramuscularly in adults (50 % of adult dose to children between 6 and 12 years old; 25 % of adult dose to children below 6 years old). Repeat as needed.

Bronchospasm The treatment of bronchospasm comprises of oxygen by mask (6–10 L/min) a beta-2-agonist metered dose inhaler (2–3 deep inhalations) and adrenaline. In case of normal blood pressure, intramuscular adrenaline should be administered: 1:1,000, 0.1–0.3 mL (0.1–0.3 mg). A smaller dose should be used in patients with coronary artery disease or in elderly patients. Pediatric patients require a dose of 0.01 mg/kg up to 0.3 mg maximally. In case of decreased blood pressure, intramuscular

adrenaline – 1:1,000, 0.5 mL (0.5 mg) – should be administered. Pediatric patients, 6–12 years, require a dose of 0.3 mL (0.3 mg) intramuscularly. Children less than 6 years require 0.15 mL (0.15 mg) intramuscularly.

Laryngeal Edema Give oxygen by mask (6–10 L/min) and intramuscular adrenaline (1:1,000), 0.5 mL (0.5 mg) for adults. Repeat as needed. In pediatric patients, 6–12 years, 0.3 mL (0.3 mg) intramuscularly should be administered. Pediatric patients less than 6 years require 0.15 mL (0.15 mg) intramuscularly.

Isolated Hypotension In cases of isolated hypotension, elevate the patient's legs and administer oxygen by mask (6–10 L/min). Administer intravenous fluid rapidly, normal saline or lactated Ringer's solution. If the patient is unresponsive, adrenaline 1:1,000, 0.5 mL (0.5 mg) intramuscularly, should be administered. Repeat as needed. In pediatric patients 6–12 years, 0.3 mL (0.3 mg) intramuscularly should be administered. Pediatric patients less than 6 years should receive 0.15 mL (0.15 mg) intramuscularly.

Vagal Reaction (Hypotension and Bradycardia) Elevate patient's legs. Administer oxygen by mask (6–10 L/min). Administer atropine 0.6–1.0 mg intravenously; repeat if necessary after 3–5 min, to 3 mg total (0.04 mg/kg) in adults. Regarding pediatric patients, 0.02 mg/kg intravenously (max. 0.6 mg per dose) should be given; repeat if necessary to 2 mg total. Intravenous fluids should be given rapidly, normal saline or lactated Ringer's solution.

Generalized Anaphylactoid Reaction Call for the resuscitation team. Suction the airway as needed. Elevate the patient's legs if hypotensive. Administer oxygen by mask (6–10 L/min). Intramuscular adrenaline should be given (1:1,000), 0.5 mL (0.5 mg) in adults. Repeat as needed. In pediatric patients 6–12 years old, give 0.3 mL (0.3 mg) intramuscularly. Children less than 6 years old should receive 0.15 mL (0.15 mg) intramuscularly.

Late

Treat symptomatically and in a similar manner to the management of other drug-induced skin reactions.

Very Late

Patients at risk should be closely monitored by an endocrinologist after contrast medium injection.

Renal
After the Examination

For patients with eGFR less than 60 mL/min/1.73 m^2 (or raised serum creatinine), continue hydration for at least 6 h. For diabetic patients taking metformin with eGFR less than 60 mL/min/1.73 m^2, measure eGFR (or serum creatinine) at 48 h after contrast medium administration. If there has been no deterioration, metformin can be restarted. Metformin is not approved in most countries for patients with abnormal renal function.

Miscellaneous
Contrast Medium Extravasation

Conservative management is adequate in most cases. This includes limb elevation, application of ice packs, and careful monitoring. If compartment syndrome is suspected, seek the advice of a surgeon.

Pulmonary Effects These are treated symptomatically.

MRI: Gadolinium-Based Contrast Media

What Is the Method of Administration?
Intravenous

What Is the Mechanism of Reaction?
This is discussed in the section on "Pathophysiology."

What Are the Types of Reactions?
Acute

The risk of an acute reaction to a gadolinium contrast agent is significantly lower than the risk

with an iodinated contrast agent. Similar reactions can occur as with iodinated contrast.

Late

Reactions are not documented.

Very Late Reactions: Nephrogenic Systemic Fibrosis
Clinical Features

Onset: From the day of exposure for up to 2–3 months, sometimes up to years after exposure. Initially this presents with pain, pruritus, swelling, and erythema. It usually starts in the legs. Later, thickened skin and subcutaneous tissues with "woody" texture and brawny plaques arise. Fibrosis of internal organs, e.g., muscle, diaphragm, heart, liver, and lungs, follows. The results are contractures, cachexia, and death in some patients.

Risk Factors for Reactions
Acute

Risk factors for acute reactions include a patient history of previous acute reaction to a gadolinium contrast agent and asthma as well as allergy requiring medical treatment. The risk of reaction is not related to the osmolality of the contrast agent. The low doses used make the osmolar load very small.

Late

Reactions to gadolinium are not documented.

Very Late

Patients are divided into high, intermediate, and low risk based on patient-specific risk factors and the type of gadolinium used.

Higher Risk
- Patients with CKD4 and 5 (GFR <30 mL/min), patients on dialysis, and patients with reduced renal function who have had or are awaiting liver transplantation.
- Gadodiamide (Omniscan). Ligand: nonionic linear chelate (DTPA-BMA). Incidence of NSF: 3–7 % in at-risk subjects.
- Gadopentetate dimeglumine (Magnevist). Ligand: ionic linear chelate (DTPA). Incidence of NSF: 0.1–1 % in at-risk subjects.

- Gadoversetamide (Optimark). Ligand: non-ionic linear chelate (DTPA-BMEA). Incidence of NSF: Unknown.
- In September 2010, the FDA issued a news release describing Omniscan, Magnevist, and Optimark as inappropriate for use among patients with acute kidney injury or chronic severe kidney disease [2].

Intermediate Risk
- Gadobenate dimeglumine (Multihance). Ligand: ionic linear chelate (BOPTA). Incidence of NSF: No unconfounded cases have been reported. Special feature: Similar diagnostic results can be achieved with lower doses because of its 2–3 % protein binding.
- Gadofosveset trisodium (Vasovist). Ligand: ionic linear chelate (DTPA-DPCP). Incidence of NSF: No unconfounded cases reported but experience is limited.
Special feature: It is a blood pool agent with affinity to albumin. Diagnostic results can be achieved with 50 % lower doses than extracellular Gd-CM. Biological half-life is 12 times longer than for extracellular agents (18 h compared to 1.5 h, respectively).
- Gadoxetate disodium (Primovist). Ligand: ionic linear chelate (EOB-DTPA). Incidence of NSF: No unconfounded cases have been reported, but experience is limited. Special feature: organ-specific gadolinium contrast agent with 10 % protein binding and 50 % excretion by hepatocytes. Diagnostic results can be achieved with lower doses than extracellular Gd-CM.

Lower Risk
- Patients with CKD3 (GFR 30–59 mL/min); children under 1 year, because of their immature renal function.
- Gadobutrol (Gadovist). Ligand: nonionic cyclic chelate (BT-DO3A). Incidence of NSF: No unconfounded cases have been reported.
- Gadoterate meglumine (Dotarem). Ligand: ionic cyclic chelate (DOTA). Incidence of NSF: No unconfounded cases have been reported.

- Gadoteridol (Prohance). Ligand: nonionic cyclic chelate (HP-DO3A). Incidence of NSF: No unconfounded cases have been reported.
- Note: If two different Gd-CM had been injected, it is impossible to determine with certainty which agent triggered the development of NSF and the situation is described as "confounded."

Not at risk are patients with normal renal function.

What Are Recommended Preventative Measurements?
Acute
- Keep the patient in the Radiology Department for 30 min after contrast medium injection. Have drugs and equipment for resuscitation readily available.
- Consider an alternative test not requiring gadolinium. Use a different gadolinium agent for previous reactors to contrast medium.
- Consider the use of premedication. There is no clinical evidence regarding the effectiveness of premedication. If used, a suitable premedication regime is prednisolone 30 mg (or methylprednisolone 32 mg) orally given 12 and 2 h before contrast medium.

Late
These are not documented.

Very Late
Risk stratifies according to the particular contrast agent used.

How Is eGFR Used to Stratify the Risk of Nephrotoxicity in MRI Contrast?
High Risk
High-risk agents are contraindicated in:
- Patients with CKD4 and 5 (GFR < 30 mL/min), including those on dialysis
- Patients with reduced renal function who have had or are awaiting liver transplantation
  High-risk agents should be used with caution in:

- Patients with CKD3 (GFR 30–60 mL/min)
- Children less than 1 year old
- Serum creatinine (eGFR) measurement before administration: mandatory

Intermediate Risk
- Serum creatinine (eGFR) measurement before administration: not mandatory

Low Risk
- Serum creatinine (eGFR) measurement before administration: not mandatory

The European Medicines Agency in 2009 [28] recommended that for high-risk gadolinium-containing contrast agents:
- They should not be used in:
- Patients with severe kidney problems.
- Patients around the time of liver transplantation.
- Newborn babies less than 4 weeks of age.
- Dose should be restricted to the minimum recommended dose in patients with moderate kidney problems and infants up to 1 year of age.
- There should be a period of at least 7 days between scans.
- Breast-feeding should be discontinued for at least 24 h after the patient has received a high-risk agent.
- All patients should be screened for kidney problems using laboratory tests before receiving these agents.

Management of Reactions

As for iodinated contrast media.

Take-Home Tables and Figures

CT

See Tables 6.1 and 6.2 for renal insufficiency questions and general screening questionnaire, respectively.

See Fig. 6.1 for an algorithm for prevention of contrast-induced nephropathy.

Table 6.1 Choyke renal insufficiency questions

1. Have you ever been told that you have renal problems?
2. Have you ever been told that you have protein in your urine?
3. Do you have high blood pressure?
4. Do you have diabetes?
5. Do you have gout?
6. Have you ever had kidney surgery?

Reprinted with permission from Choyke et al. [18]

Table 6.2 General screening questionnaire to be completed by referring clinician

For iodine-based contrast media administration
History of moderate or severe reaction to an iodinated contrast medium?
History of allergy requiring treatment?
History of asthma?
Hyperthyroidism?
Heart failure?
Diabetes mellitus?
History of renal disease?
Previous renal surgery?
History of proteinuria?
Hypertension?
Gout?
Most recent serum creatinine?
Is the patient currently taking any of the following drugs:
Metformin for diabetes/IL2/beta blockers/aminoglycosides/NSAIDS?

Modified with permission from Ref. [4]

Table 6.3 General screening questionnaire to be completed by referring clinician

For MRI contrast media administration
History of moderate or severe reaction to an MRI contrast medium?
History of allergy requiring treatment?
History of asthma?
Does the patient have end-stage renal failure or is the patient on dialysis?
Recent serum creatinine?

Modified with permission from Ref. [4]

Suggested questionnaire to be completed by referring clinician (ESUR Guidelines) [3]
Assess patient's risk factors:

- eGFR < 60ml/min/1.73m^2
- Dehydration
- Congestive Cardiac Failure
- Gout

- Over 70 years old
- Concurrent administration of nephrotoxins
- High osmolality contrast agents
- Larger doses of contrast medium

Is the patient at increased for contrast induced nephropathy?

No

Yes

Is an appropriate alternative test available?

No

Yes

Perform original test

Perform original test
Implement prophylaxis

Perform alternative test
No additional prophylactic measures required

Fig. 6.1 Algorithm for prevention of contrast-induced nephropathy

Suggested questionnaire to be completed by referring clinician (ESUR Guidelines) [3]

With reference to renal status:

Normal

Abnormal

Send blood sample for biochemistry (creatinine; eGFR)

Normal

Abnormal

Proceed with test

Discuss with referring clinician

Fig. 6.2 Algorithm for prevention of nephrogenic systemic fibrosis

MR

See Table 6.3 for general screening questionnaire.

See Fig. 6.2 for an algorithm for prevention of nephrogenic systemic fibrosis.

In All Patients

- Use the smallest amount of contrast medium necessary for a diagnostic result.
- Always use an agent that leaves the smallest amount of gadolinium in the body.
- Never deny a patient a clinically well-indicated enhanced MRI examination.

Suggested Imaging Protocols

Regarding iodinated contrast media:
- Avoid iodinated contrast media wherever possible.
- Avoid nephrotoxic drugs 48 h before contrast media.
- Avoid high-osmolar contrast media. Use iso-osmolar or low-osmolar contrast media.
- Minimize contrast volume and avoid repeat contrast injection within 72 h.
- Consider *N*-acetylcysteine and/or sodium bicarbonate.
- Follow up GFR assessment 48 h postcontrast media injection in patients with GFR 0–60 mL/min.

Regarding gadolinium-based contrast agents, the FDA recommends that health-care professionals:
- Estimate kidney function through laboratory testing for patients at risk for chronically reduced kidney function.
- Avoid use of gadolinium-based contrast agents in patients suspected to have impaired drug elimination unless the imaging is essential and not available without contrast.
- Monitor for signs and symptoms of NSF if a gadolinium-based contrast agent is administered to a patient with acute kidney injury or chronic, severe kidney disease.
- Administer a gadolinium-based contrast agent once during an imaging session.

Future Research

- Large-scale robust studies are necessary to evaluate the role of *N*-acetylcysteine and sodium bicarbonate specifically in a population undergoing CT.
- The precise pathologic mechanism of idiosyncratic "allergic" reaction to iodinated contrast media is poorly understood. Further research in this area would be of significant benefit.
- Nephrogenic systemic fibrosis is a relatively new disease entity which is not entirely understood.

References

1. National Kidney Foundation. Am J Kidney Dis. 2002;39(2 Suppl 1):S1–266.
2. FDA. New warnings required on use of gadolinium-based contrast agents. U.S. Food and Drug Administration; 2010. http://www.fda.gov/NewsEvents/Newsroom/PressAnnouncements/ucm225286.htm. Accessed 29 March 2011.
3. Tramer MR, von Elm E, Loubeyre P, Hauser C. Br Med J. 2006;333(7570):675.
4. ESUR guidelines for the administration of contrast media. European Society of Urogenital Radiology; 2011. http://www.esur.org/Contrast-media.51.0.html. Accessed 28 March 2011.
5. Murphy SW, Barrett BJ, Parfrey PS. J Am Soc Nephrol. 2000;11(1):177–82.
6. Cowper SE, Robin HS, Steinberg SM, Su LD, Gupta S, LeBoit PE. Lancet. 2000;356(9234):1000–1.
7. Swaminathan S, Horn TD, Pellowski D, Abul-Ezz S, Bornhorst JA, Viswamitra S, Shah SV. N Engl J Med. 2007;357(7):720–2.
8. Weinmann HJ, Brasch RC, Press WR, Wesbey GE. AJR Am J Roentgenol. 1984;142(3):619–24.
9. Port M, Idee JM, Medina C, Robic C, Sabatou M, Corot C. Biometals. 2008;21(4):469–90.
10. Briguori C, Tavano D, Colombo A. Prog Cardiovasc Dis. 2003;45(6):493–503.
11. Solomon R., Barrett B. Kidney Int Suppl. 2006;100: S46–50.
12. Gruberg L, Mintz GS, Mehran R, Gangas G, Lansky AJ, Kent KM, Pichard AD, Satler LF, Leon MB. J Am Coll Cardiol. 2000;36(5):1542–8.
13. McCullough PA, Wolyn R, Rocher LL, Levin RN, O'Neill WW. Am J Med. 1997;103(5):368–75.
14. Cowper SE. Curr Opin Rheumatol. 2003;15(6):785–90.
15. Bucala R. J Am Coll Radiol. 2008;5(1):36–9.
16. Mendoza FA, Artlett CM, Sandorfi N, Latinis K, Piera-Velazquez S, Jimenez SA. Semin Arthritis Rheum. 2006;35(4):238–49.

17. Tippins RB, Torres WE, Baumgartner BR, Baumgarten DA. Radiology. 2000;216(2):481–4.

18. Choyke PL, Cady J, DePollar SL, Austin H. Determination of serum creatinine prior to iodinated contrast media: is it necessary in all patients? Tech Urol. 1998;4(2):65–9.

19. Haynes RB. Evid Based Nurs. 2005;8(1):4–6.

20. Staunton M. Radiology. 2007;242(1):23–31.

21. AGREE. Agree instrument. Agree Collaboration; 2001. http://www.agreecollaboration.org/instrument/. Accessed 29 March 2011.

22. ACR. ACR manual on contrast media version 7. ACR Committee on Drugs and Contrast Media; 2010. http://www.acr.org/SecondaryMainMenuCategories/quality_safety/contrast_manual/FullManual.aspx. Accessed 31 March 2011.

23. Benko A, Fraser-Hill M, Magner P, Capusten B, Barrett B, Myers A, Owen RJ. Can Assoc Radiol J. 2007;58(2):79–87.

24. Trivedi H, Daram S, Szabo A, Bartorelli AL, Marenzi G. Am J Med. 2009;122(9):874–9, 815.

25. Meier P, Ko DT, Tamura A, Tamhane U, Gurm HS. BMC Med. 2009;7:23.

26. Navaneethan SD, Singh S, Appasamy S, Wing RE, Sehgal AR. Am J Kidney Dis. 2009;53(4):617–27.

27. UpToDate® Section: hydration, mannitol and diuretics. Summary. http://www.uptodate.com/contents/prevention-of-contrast-induced-nephropathy?source=search_result&selectedTitle=1%7E44. Accessed 10 June 2011.

28. EMA. Recommendations to minimise risk of nephrogenic systemic fibrosis with gadolinium-containing contrast agents. European Medicines Agency; 2009. http://www.ema.europa.eu/ema/index.jsp?curl=pages/medicines/human/public_health_alerts/2010/09/human_pha_detail_000013.jsp&murl=menus/medicines/medicines.jsp&mid=WC0b01ac058001d126. Accessed 29 March 2011.

Evidence-Based Medicine on Radiology: Economic and Regulatory Impact

7

David B. Larson and William Hollingworth

Contents

D.B. Larson (✉)
Department of Radiology, Cincinnati Children's Hospital Medical Center, Cincinnati, OH, USA
e-mail: david.larson@cchmc.org

W. Hollingworth
School of Social and Community Medicine, University of Bristol, Bristol, UK
e-mail: William.hollingworth@bristol.ac.uk

Key Points

- US health-care expenditures have nearly continuously increased over the past 40 years not only in real dollars but also in almost every other measurable term.
- If current rates of increase were to continue, long-term growth in medical spending would eventually consume all growth in per capita income, and, in 30 years, more than one-third of the US gross domestic product (GDP) would be devoted to health-care costs http://www.whitehouse.gov/assets/documents/CEA_Health_Care_Report.pdf.
- According to some analyses, much of the stagnation of standard of living of the working-class can be explained by the continued rise in medical costs, without which American working families would continue to enjoy a rising standard of living.
- Most other industrialized countries routinely use cost-effectiveness analysis (CEA) to improve the value of medical care, decreasing both inappropriate underutilization and overutilization.
- Example of overutilization: self-referral. From 2001 to 2006, the volume of CT imaging performed at in-office facilities owned by radiologists rose by 85 %. The volume of imaging performed at in-office facilities in which non-radiologist referring clinicians had a financial stake rose by 263 %.
- Some physician groups have had success both lowering costs and improving quality. Whatever their organizational structure, so-called accountable care organizations tend to have certain elements in common: physicians and hospitals tend to have a close working relationship, most of them use electronic medical record systems to track and improve care, and they generally encourage a culture of restrained spending and collaboration with competitors for the benefit of patients.
- The two main thrusts of policy makers' efforts are (1) to pay for appropriate care that, based on the evidence, is most likely to improve health outcomes and (2) to encourage providers to work more closely together to make sure that evidence-based care is provided consistently and efficiently. Ideas that are taking root include decreasing reimbursement, using third parties to help decrease inappropriate imaging, and changing the reimbursement incentive structure.
- The recently enacted US health-care reform statute has two main priorities: to expand coverage and control costs. While the coverage provisions of the act have received the majority of the attention in the press, the second priority of the statute, that of cost control, probably has more potential to affect radiologists and other physicians.
- The challenge has been issued to the medical community, including radiology, to move evidence-based imaging from a theory or a collection of anecdotes to one that can be effectively implemented on a broad scale.

Introduction

Over the last few decades, medical care has grown from a relatively small sector of the world-wide economy to one of the most dominant sectors, with no end in sight to its unsustainable growth. Much of this can be attributed to an explosion in technology, which is now far beyond what an individual practitioner can master. However, a large percentage of costs are often attributed to inefficiencies of the system; health care still behaves much like a cottage industry, built upon loosely networked individual practitioners whose practices are both highly variable and opaque, resulting in inconsistent, fragmented care. Growth in health-care costs and dissatisfaction with service and outcomes have pushed the debate into the public sphere like never before. Subsequently, the issue of health-care reform has become a subject of bitter partisan politics. At the same time, worldwide recession and mounting public debts have prompted austerity measures, limiting the resources available for the provision and improvement of medical care. There has never been a greater need to build systems that efficiently incorporate evidence-based care into care processes.

Discussion of Issues

What Political and Economic Forces Influence the US Health-Care System?

Summary
Internationally, the US health-care system is a clear outlier in the low proportionate contribution of government to health-care expenditures. Therefore, the US system is widely perceived to be a "free-market" system. However, two major factors substantially limit the efficiency of the US health-care market: employer-based health insurance and the sizeable role of government payers.

On one hand, many US voters strongly oppose government involvement in the regulation and administration of medical care. On the other hand, many of the same voters adamantly support current government-sponsored programs.

This has led to political division and, in the absence of consensus, has resulted in a system in which no single payer or set of cohesive market rules control health-care expenditures [1].

Supporting Evidence
The US health-care system is based on a disparate mix of private and government payers. The health-care system is widely perceived to be a "free-market" system. However, two major factors substantially limit the efficiency of the US health-care market. First, the majority of individuals with private health insurance (150 million out of a population of 311 million Americans) obtain it through an employer [2]. Thus, at least two intermediaries – the employer and the insurance company – are placed between the customer (the patient) and the supplier (the provider). This profoundly alters the normal interaction between supply and demand that is expected in a free market. Second, US government sources contribute 48 % of all health expenditure payments in the United States (Fig. 7.1) [3]. The governments of other high-income countries cover, on average, 72 % of their citizens' total health-care expenditures; in the United Kingdom, New Zealand, and most of the Nordic countries,

the contribution exceeds 80 % [4], funded through tax or mandatory social insurance as well as contributions from citizens and employers. Thus, the perception that the United States is the only major industrialized country without a government-sponsored universal health-care system is misleading. Only the governments of two other major industrialized countries, Norway and Denmark, pay more for their citizens' health care on a per capita basis [5].

The disconnect between the perception of a market-based US health-care system versus the reality of a government- and insurance-financed system has created predictable problems. On one hand, many voters strongly oppose government involvement in the regulation and administration of medical care. On the other hand, many of the same voters adamantly support current government-sponsored programs. President Barack Obama articulated the conflict by quoting a constituent, who reportedly told him, "I don't want government-run health care, I don't want socialized medicine, and don't touch my Medicare" [6]. Compounded by the disproportionate influence of special-interest groups, politicians find themselves facing incompatible demands to ensure widespread access to advanced medical care while at the same time limiting government intervention and expenditures. This has led to political division and, in the absence of consensus, has resulted in a system in which no single payer or set of cohesive market rules control health-care expenditures [1].

What Is the Impetus Driving US Health-Care Reform Now?

Summary
US health-care expenditures have nearly continuously increased over the past 40 years not only in real dollars but also in almost every other measurable term. Especially since 1985, growth in US health-care costs has substantially exceeded that of any other comparable nation.

If current rates of increase were to continue, long-term growth in medical spending would eventually consume all growth in per capita

income [7], and, in 30 years, more than one-third of the US GDP would be devoted to health-care costs [8] http://www.whitehouse.gov/assets/documents/CEA_Health_Care_Report.pdf.

Supporting Evidence

Sustained market-style demand without the usual market-style constraints has led to continued increases in spending. US health-care expenditures as a percentage of GDP are nearly double those of any other major developed country, and the per capita expenditures are more than double. At the same time, US health outcomes are not significantly better, and, in many cases are worse, than those of other major developed countries [9].

US health-care expenditures have nearly continuously increased over the past 40 years not only in real dollars but also in almost every other measurable term. Figure 7.2 demonstrates US national health expenditures from 1965 to 2018 (2008–2018 projected). National health expenditures increased 57-fold from $42 billion in 1965 to $2.4 trillion in 2008 and are projected to reach $4.4 trillion in 2018. This represents an average yearly increase of 9.6 % from 1965 to 2008, which is 4.9 % greater than the rate of inflation [10]. Adjusted for population growth, the annual increase is 3.9 % [11]. This indicates that the portion of economic output spent on health care for the average person in the United States is five times that of the amount spent for a person in 1965.

All countries struggle to contain health-care costs to some extent, and real increases in health-care expenditure are the norm as societies get wealthier. But, the US system appears to be particularly vulnerable to unsustainable cost increases. Since 1985, the annual increases seen in the United States have been more than double those seen in other high-income countries [12]. The large influence that other countries can exert through government budgeting (as in the United Kingdom) or government negotiation with a small number of nonprofit social insurers (as in France) undoubtedly factors into their relatively stable health-care costs.

Spending in the United States is expected to continue to escalate in the coming years. If current rates of increase were to continue, long-term

growth in medical spending would eventually consume all growth in per capita income [7], and, in 30 years, more than one-third of the US GDP would be devoted to health-care costs [8] http://www.whitehouse.gov/assets/documents/CEA_Health_Care_Report.pdf. Economists, business executives, and government officials are urgently reporting that this constitutes a major threat to the United States' economic well-being and ability to compete in a global marketplace [13].

How Are Rising Costs of Health Care Affecting Governments and Individuals?

Summary

According to some analyses, much of the stagnation of standard of living of the working-class can be explained by the continued rise in medical costs, without which American working families would continue to enjoy a rising standard of living [14].

In its summary of the 2009 annual report, the Medicare trustees projected that, unless changes to the revenue or payment system or both are made, the Hospital Insurance (HI) trust fund, which has already begun to contract, will be exhausted by 2017 while spending commitments will continue to increase.

Supporting Evidence

Escalating costs are increasingly impacting individual American families. The total annual medical cost for the average family of four is approximately $16,771, of which the employee pays $6,824 and the employer pays $9,947 [15]. For a family with a median income of approximately $52,233, health insurance premiums and out-of-pocket costs make up approximately 13 % of household take-home salary. However, when benefits paid by the employer are taken into consideration, health costs for the median worker account for approximately 25 % of total compensation ($17,000 of $66,570) [14].

Adjusting for inflation, after-medical-cost compensation of households in the median income level and below has essentially remained flat for the last 30 years, and is projected to

decrease in coming years. According to some analyses, much of this stagnation of standard of living of the working-class can be explained by the continued rise in medical costs, without which American working families would continue to enjoy a rising standard of living [14].

Costs that are burdensome for healthy families with medical insurance can be financially devastating for those with a family member who becomes ill. Medical costs for hospitalized individuals quickly reach the hundreds of thousands of dollars, and those without insurance can expect to be charged, on average, two to three times that of a person with insurance [16]. Families of those without insurance or with insufficient insurance are commonly held liable for most, if not all, of this amount. In 2007, 62 % of all bankruptcies were linked to medical expenses. Nearly 80 % of persons involved in such bankruptcies had health insurance [17]. Furthermore, each year approximately 1.5 million US families lose their homes to foreclosure due to medical crises [18].

In addition to the increasing financial burden on individual families, rising health-care costs are also increasingly straining government budgets. Medicare, the US federal government's insurance program for the elderly, is financed from two trust funds: the Hospital Insurance (HI) fund, which pays for hospital services and related inpatient care, and the Supplemental Medical Insurance (SMI) fund, which pays for physician and outpatient services (part B) and prescription drugs (part D). In its summary of the 2009 annual reports, the Medicare trustees projected that, unless changes to the revenue or payment system or both are made, the Hospital Insurance (HI) trust fund, which has already begun to contract, will be exhausted by 2017 while spending commitments will continue to increase. The Supplemental Medical Insurance (SMI) fund is more difficult to project, since the projections incorporate two unlikely assumptions. First, current law calls for continued physician reimbursement rate cuts of more than 20 %; Congress has overridden adjustments to the sustainable growth rate for the past 7 years and will likely do so again. Second, premium increases for most enrollees are disallowed under the current law, and the deficit is compensated by unusually large premium increases for the unprotected minority of enrollees; the resulting disparity would likely be very unpopular. Therefore, while the trustees do not directly project the Supplemental Medical Insurance (SMI) fund status, it is likely to follow a similar course as the Hospital Insurance (HI) fund, with depletion by around 2017 [19].

Increasing health-care expenditures have been the main driving force behind the 2009 legislative efforts to overhaul health care. In a White House speech in March 2009, President Obama remarked, "the greatest threat to America's fiscal health is not Social Security, though that's a significant challenge; it's not the investments that we've made to rescue our economy during this crisis. By a wide margin, the biggest threat to our nation's balance sheet is the skyrocketing cost of health care. It's not even close" [20]. In his address to a joint session of Congress in September 2009, he stated, "If we do nothing to slow these skyrocketing costs, we will eventually be spending more on Medicare and Medicaid than every other government program combined. Put simply, our health-care problem is our deficit problem. Nothing else even comes close" [13]. While rising health-care costs have been a source of concern by policy makers for many years, the recently passed health-care reform law indicates that we have finally reached the point that such concerns outweigh the considerable political resistance to changing the system. Though much of what is contained in the law is rejected by Republicans, President Obama's sentiment that health-care expenditures are too high and must be addressed is generally accepted by both parties.

While policy shifts in the United States have been driven by cost concerns, improving access to care has been a more important motive for change in countries with heavily publically funded systems. In Sweden, often cited as the archetypical system of socialized medicine, about one-quarter of primary care facilities are now privately operated [21]. In the United Kingdom, lengthy and seemingly intractable waiting times for elective surgical procedures at

public hospitals eventually led to the government opening up the market and purchasing care from privately run treatment centers [22]. In both cases, the dominant role of the government in funding care has not been seriously questioned, but the monopoly of public hospitals and clinics in providing that care has been removed in an attempt to increase capacity, stimulate competition, and provide care more efficiently.

Do Increased Health Expenditures Lead to Better Care?

Summary

Wide regional variation in US health-care expenditures cannot be adequately explained by illness severity, cost of living, quality of care, or improved health outcomes.

Because of this apparent overutilization, many experts believe that the opportunity exists to simultaneously improve quality and decrease costs.

Most other industrialized countries routinely use cost-effectiveness analysis (CEA) to improve the value of medical care, decreasing both inappropriate underutilization and overutilization.

Supporting Evidence

While rising health-care costs are the major driver for the recent health-care reform initiative in the United States, an additional major cause of concern for payers and policy makers is that much of the health-care spending is not contributing to improved health outcomes. Awareness of this possibility was first raised by Dr. John Wennberg and his group at Dartmouth Medical Center. Beginning in the 1970s, Wennberg and his colleagues demonstrated that Medicare spending varied considerably by region [23]. This finding naturally led to questions of appropriateness of care and medical spending, which has been summed up by Princeton health economist Uwe Reinhardt, who asks, "How can it be that 'the best medical care in the world' costs twice as much as the best medical care in the world?" [24]. Further research has shown that this variation cannot be adequately explained by illness severity, cost of living, quality of care, or

improved health outcomes. Fisher found that, at the regional level, increased spending on health care is actually associated with *worse* health outcomes [25]. Because of this apparent overutilization, many experts believe that the opportunity exists to simultaneously improve quality and decrease costs. Peter Orszag, then the director of the Congressional Budget Office, stated in 2008 that "researchers have estimated that nearly 30 % of Medicare's costs could be saved without negatively affecting health outcomes if spending in high- and medium-cost areas could be reduced to the level in low-cost areas – and those estimates could probably be extrapolated to the health-care system as a whole" [26]. In other words, the US health-care system does not necessarily need to look to foreign countries for examples of how to decrease costs, but can look at regions within its own borders.

The causes for the wide variation in health-care expenditures have been elusive. The factor that seems to best explain variation in health-care utilization is capacity [25]. The most reliable way to predict the per capita health-care expenditures in a region is to measure the per capita availability of hospital beds, specialists, and capital equipment. Given high health-care expenditures, it is perhaps not surprising that the United States has twice as many MRI and CT scanners per head of population as other high-income countries, being outdone in imaging capacity only by Japan The other predictor, which is more difficult to measure, is the local "culture." In other words, in terms of recommending more office visits, ordering more tests, and directing longer hospital admissions, physicians tend to behave similarly to other physicians in his or her region [27]. These are likely highly correlated with one another and neither is especially surprising to many authors, given the current reimbursement environment that financially rewards increased utilization, punishes decreased utilization, and virtually ignores quality and appropriateness of care [25].

Not only does the system reward more care rather than better care, it is further flawed in that physicians and physician groups are rewarded for working alone and in competition rather than as members of cooperative teams. It is not

surprising that the result is an expensive, fragmented health-care system. In an article in *The New Yorker* magazine in June 2009, Atul Gawande [28] likens the provision of health care to the building of a house in which the electrician, plumber, and carpenter are paid for each outlet, faucet, and cabinet they install, without a subcontractor to oversee the project. You would not be surprised, he contends, if the final product resulted in a home containing "a thousand outlets, faucets, and cabinets, at three times the cost you expected, and the whole thing fell apart a couple of years later." This lack of coordination remains a major problem, he argues, no matter how competent the providers are or who pays for their work. Contrast this with the UK system where patient access to most specialist and hospital care is regulated by the general practitioner, a subcontractor in the analogy above, who has no financial incentive to refer for unneeded specialist care.

From the perspective of the federal government and other US payers, misaligned provider incentives result in inappropriate overutilization of care much more often than inappropriate underutilization. However, some screening procedures and other public health initiatives are inappropriately underutilized, even though they have proven to be cost-effective. For example, mammographic screening has a very competitive cost-effectiveness ratio (CER) of $10,000 to $25,000 per quality-adjusted life-years; interventions with a CER of less than $100,000 are generally considered to be worthwhile. However, utilization rates of mammography are only 50–70 %, well below the 80 % plus rates that have been achieved in Finland, the Netherlands, and Spain ([1, 29]). Osteoporosis screening has similar CER but even lower implementation of 35 % [1].

Most other industrialized countries routinely use cost-effectiveness analysis (CEA) in an attempt to improve the value of medical care, decreasing both inappropriate underutilization and overutilization [1] (see Chap. 1, "Evidence-Based Imaging: Principles"). However, the Center for Medicare and Medicaid Services (CMS) has deliberately avoided CEA, largely due to political considerations [30]. The current CMS remits to pay for all care that meets the ill-defined criteria of being "reasonable and necessary" is in sharp contrast to the UK National Institute of Health and Clinical Excellence (NICE) established in 1999 explicitly to "appraise the clinical benefits and the costs of. . . interventions" [31]. As we will discuss later in this chapter, this US avoidance of CEA may change with recently enacted health-care reform legislation.

How Does Supplier-Driven Demand Influence Imaging Utilization?

Summary

From 2001 to 2006, the volume of CT imaging performed at in-office facilities owned by radiologists rose by 85 %. The volume of imaging performed at in-office facilities in which non-radiologist referring clinicians had a financial stake rose by 263 % [32].

Supporting Evidence

One of the most obvious examples of so-called supplier-driven demand, where the sales of goods or services are highly influenced by the seller, occurs when physicians refer patients for imaging in which the same physician stands to gain financially from the imaging study. Radiologists refer to this as "self-referral." It has been a recognized conflict of interest for many years, and legislation has been enacted to prevent this from occurring (known as Stark laws). However, imaging performed in the physician's own office is exempted from the restriction. Imaging volume in these offices has increased substantially in the past few years. For example, from 2001 to 2006, while the volume of CT imaging performed at in-office facilities owned by radiologists rose by 85 %, it rose by 263 % in facilities owned by non-radiologists [32]. Another study showed that physicians who referred patients to themselves or those of the same specialty were up to twice as likely to refer a patient for imaging as those who referred patients to radiologists [33]. The June 2009 Medicare Payment Advisory Commission (MedPAC) report to Congress found that self-referring physicians ordered between 5 %

and 104 % more imaging than nonself-referring physicians [34].

Not surprisingly, self-referral is a controversial issue. The issue of self-referral has been a focus of discussion by the ACR leaders on Capitol Hill for years, but no significant changes have occurred in regulations. Self-referral has typically been viewed by lawmakers as a turf battle between radiologists and other imaging providers. The Patient Protection and Accountability Act only indirectly addresses self-referral, with a provision that requires physicians to inform patients that they may obtain imaging services from other providers and to supply patients with a list of such providers [35].

While it is unclear whether self-referral will be more regulated in the near future, judging from the number of times the subject has been highlighted in recent policy reports and major news articles, it at least has gained increasing attention by lawmakers. An entire report from the Government Accountability Office in June 2008 was dedicated to the subject, which urged CMS to consider further expansion of imaging management practices or utilization of intermediary companies to restrict overutilization [36]. Private insurers have already realized the role of self-referral in increased utilization and, through radiology benefit management (RBM) companies, are beginning to limit self-referral, which may obviate the need for further legislative action.

Self-referral for imaging in the United States is an egregious example of supplier-driven demand, but it is far from unique to the US system of care; in fact much of the empirical data on this phenomenon comes from Europe and beyond [37]. In particular, it is likely to be a problem wherever reimbursement methods, such as fee for service, designed to incentivize clinicians to provide more care known to be effective also inadvertently stimulate care of little or no benefit to the patient.

What Can Be Learned from "High-Value" Systems?

Summary

Whatever their organizational structure, so-called accountable care organizations tend to have certain elements in common: physicians and hospitals tend to have a close working relationship, most of them use electronic medical record systems to track and improve care, and they generally encourage a culture of restrained spending and collaboration with competitors for the benefit of patients.

Supporting Evidence

Historically, research on variation in care has highlighted examples of overuse of health-care services, like self-referred imaging. However, by documenting variation, researchers at Dartmouth and elsewhere recently have begun to highlight regions that consistently demonstrate improved health outcomes at lower costs than the national average. Increasing attention has been paid to these regions to discover how they are able to achieve such remarkable results. The theme that commonly resurfaces is that they are dominated by groups of clinicians who work together in a cooperative way to study and systematically improve care from the perspective of the patient. Elliott Fisher has termed these types of organizations "accountable care organizations" (ACOs) [38]. They may be highly organized into an integrated delivery system, like the Mayo Clinic in Rochester, or they may be a community of unaffiliated care providers like that in Grand Junction, Colorado [39].

Whatever their organizational structure, these groups of providers tend to have certain elements in common: physicians and hospitals tend to have a close working relationship, most of them use electronic medical record systems to track and improve care, and they generally encourage a culture of restrained spending and collaboration with competitors for the benefit of patients. They also are dominated by nonprofit health systems [40].

Under the fee-for-service system, organizations that achieve improved outcomes at lower costs often do so at their own financial peril. For example, large investments that improve coordination of care, like implementation of a multi-hundred-million-dollar electronic medical record system, have been borne by the hospital or health system. When physicians choose to avoid unnecessary imaging and

procedures, they forgo the potential income. And when hospitals work together to discharge patients sooner, arranging better post-discharge care, resulting in decreased readmission rates, all of the savings are retained by the payer, and lost to the care provider [28]. Hence, the fee-for-service payment structure incentivizes behavior that is not necessarily optimal for the patient.

Cost-Control Strategies: Rationing Versus Reducing Inappropriate Care

Summary

The two main thrusts of policy makers' efforts are (1) to pay for appropriate care that, based on the evidence, is most likely to improve health outcomes and (2) to encourage providers to work more closely together to make sure that evidence-based care is provided consistently and efficiently. Ideas that are taking root include decreasing reimbursement, using third parties to help decrease inappropriate imaging, and changing the reimbursement incentive structure.

Supporting Evidence

Spiraling health-care costs in the face of budget constraints have finally pushed lawmakers to tackle this issue legislatively. While this is not the first attempt at health-care cost control, it differs in significant ways from prior attempts. Policy makers have realized that simply limiting access to health care or attempting to pay providers less for the same service is not politically palatable, does nothing to address inefficiencies in the system, and is not sustainable. While across-the-board reimbursement cuts are likely to be used in some cases, policy makers are beginning to realize the perversity of the financial incentives inherent in the current reimbursement structure and are seeking payment systems that reward appropriate care and discourage inappropriate care [26].

In general, the two main thrusts of their efforts are (1) to pay for appropriate care that, based on the evidence, is most likely to improve health outcomes and (2) to encourage providers to work more closely together to make sure that evidence-based care is provided consistently

and efficiently. While there are many ideas circulating regarding how to accomplish these objectives as they relate to imaging, ideas that are taking root include decreasing or refining reimbursement, using third parties to help decrease inappropriate imaging, and changing the reimbursement incentive structure.

(a) Reimbursement Cuts and Refinements

In its annual report to Congress in March 2009, MedPAC specifically examined reimbursement rates for diagnostic imaging. While recognizing the rapid technological progress in diagnostic imaging which enables physicians to more rapidly and precisely diagnose and treat illness, the Commission expressed concern that "the rapid volume growth of costly imaging services over the past several years may signal that they are mispriced" [36].

CMS reimburses providers separately for performing imaging studies (technical component) and interpreting the studies (professional component). The technical component is generally larger than the professional component, often much larger; for example, for MRI of the brain, the technical component accounts for 88 %, and the professional component accounts for 12 % of the total reimbursement. Under a fee-for-service arrangement, a practice is reimbursed according to the volume of imaging performed. Therefore, once a practice has invested in a scanner, it has a strong incentive to perform as many scans as possible to recoup the investment and then to make a profit. MedPAC argues that the technical component for expensive services such as MRI and CT scans likely are too high, encouraging practices that would otherwise have insufficient volume to justify purchasing a scanner to make the investment and overutilize it. The Commission believes that, if the reimbursement were lowered, fewer scanners would be purchased, decreasing the pressure for overutilization.

CMS sets reimbursement rates based on the estimation that equipment is utilized 25 h per week. MedPAC states in its report that this estimate was not based on empirical data and is not accurate [36]. In 2006, MedPAC sponsored a survey that found that CT scanners are in

operation an average of 42 h per week (median 40 h) and MRI scanners 52 h per week (median 46 h). In order to discourage the purchase of excessive equipment, MedPAC recommended that the equipment-use factor be changed. This was incorporated into the Patient Protection and Accountable Care Act [35], which changed the utilization factor from one based on 25 h per week to one based on 37.5 h per week [35]. This had the effect of decreasing the technical component by 33 % when the provision took effect on January 1, 2011.

The act also decreases continuous body part reimbursement. Currently, when an imaging study is performed on two continuous body parts, the technical component of the examinations is discounted by 25 %. Under the new law, this discount will be increased to 50 % [35]. This continues a trend of recent reimbursement cuts and limitations, including those imposed under the Deficit Reduction Act of 2005, recent imaging-based RVU adjustments, and Medicare conversion factor changes [41]. This process reflects the rather crude nature of price setting in CMS and, in fact, the wider world. A survey of reimbursement levels for MRI of the brain across four countries revealed 400 % variation [42].

These sweeping cuts do not address the fundamental problem that the current payment level for any diagnostic imaging procedure is based loosely on the cost of providing the procedure, not its value to patients. If we wish to use reimbursement to promote evidence-based imaging, a value-based pricing system might be preferable. To date, the value-based pricing debate has mainly focused on the pharmaceutical industry. One form of value-based pricing implemented in the United Kingdom is flexible pricing. [43] Under flexible pricing, the price of the drug may depend on the indication it is being used for, for example, a higher price for indications where the effect size is larger or more clearly demonstrated. The concept of value-based pricing has been explored in diagnostic imaging [44]. However, a key barrier to implementation is the lack of evidence on the value of, for instance, the use of FDG-PET in a patient with possible Alzheimer's disease *vis à vis* any other indication.

(b) Intermediaries (Radiology Benefit Management Organizations)

Responding to escalating costs, many payers have contracted with third-party radiology benefit management (RBM) organizations that assist in decreasing inappropriate utilization on a case-by-case basis. The RBM model is derived from the pharmacy benefit management (PBM) programs that emerged in the 1990s to control the growth of spending on prescription medications. RBM programs attempt to limit overutilization of imaging in a variety of ways. For more expensive imaging procedures, most RBMs utilize prior authorization to approve or deny payment on the basis of predetermined criteria. RBM organizations also may grant privileges to physicians and sites based on training and equipment, especially for in-office imaging. Many RBMs establish their own network of imaging providers, independently negotiating discounts with and processing medical claims from physicians and physician groups and then passing on those discounts and claims to the payer. RBM organizations also evaluate the practice patterns of ordering clinicians compared to a standard or benchmark and provide feedback and incentives to change ordering behavior [34].

RBM organizations have been effective in controlling imaging utilization and associated costs [45, 46], making the model an extremely attractive option for payers and regulators. To the extent that they are able to do this using evidence-based guidelines makes them even more attractive. The model gives payers an option to decrease spending by decreasing inappropriate utilization rather than cutting reimbursement rates [36].

The American College of Radiology (ACR) has responded to the growth of such organizations by issuing a set of best practices guidelines for the organizations [47]. The report calls for judicious use of preauthorization (including an after-hours approval process), simplification of administrative processes, and transparency of decision-making and reporting procedures. The ACR does not, however, endorse the RBM model; rather, it believes that cost and quality

goals can be reached through alternative processes, including order entry decision support and referring physician education, without the added administrative complexity of third-party RBM organizations. There is some trial evidence to support this stance, suggesting that educational reminder messages can reduce requests for radiological tests by as much as 20 %, at least in the short term [48].

Despite the position of the ACR, payers are increasingly embracing the RBM model. In 2007, at least five major firms provided RBM service in the United States, covering an estimated 88 million persons [46]. In a 2008 report, the Government Accountability Office (GAO) recommended that CMS either adopt practices used by RBMs, including privileging and prior authorization, or simply contract with RBM companies directly [36]. This was not included in the health-care reform act, but, as we will see, this could very quickly become a reality without the approval of Congress.

The RBM model is likely to have a mixed effect on individual radiologists. On one hand, RBM organizations constitute an extra layer of administration between the ordering physician and the radiologist. On the other hand, if using an RBM leads to more consistent use of evidence-based ordering practices, then this loss of individual control may be worth the potential to decrease costs in a way that is not detrimental to health outcomes. At the same time, RBM organizations provide an infrastructure for limiting inappropriate imaging by prospectively applying evidence in individual cases. RBM organizations also are able to objectively argue against costly self-referral practices – an argument that is often perceived as turf protection when delivered by radiologists.

Radiology benefit management organizations are likely to increase in prevalence, at least in the short run. Radiologists have essentially three options for dealing with RBM growth: do nothing with the hope that market forces will naturally encourage RBM organizations to behave in patients' best interest (which is not inconceivable), attempt to replicate the functions of RBM organizations (preventing their penetration into local markets) through processes such as computerized physician order entry and physician feedback, and either form partnerships with RBM organizations that are more receptive to radiologists' input or become involved with the selection of an RBM organization before the decision is made for them. Active opposition to the RBM model without a viable alternative is not likely to be successful at this point, given the track record of decreasing costs and the level of market penetration already achieved by RBM organizations.

(c) Change in Reimbursement Structure (Accountable Care Organizations)

The idea of the accountable care organization (ACO) was first proposed in 2006 [38] and was included in expanded form in MedPAC's annual report to congress in 2009 [34]. The overall objective is to find a way to provide financial incentives for greater cooperation between physician groups and hospitals by rewarding them for minimizing cost increases and maintaining quality. As proposed by MedPAC, each ACO would be centered around an individual hospital or local hospital network. Primary care physicians and specialists would be assigned to the same ACO as the hospital caring for most of their patients. The size of the organization might range from a single hospital with local physicians to a large hospital network and affiliated physician groups. The relationships could also vary, from unaffiliated physician groups and hospitals to staff-model integrated delivery systems. Regardless of the affiliation, the ACO would need to meet two criteria: have a minimum number of patients – in order to distinguish improvement from random variation, MedPAC recommends a minimum of 5,000 patients – and have a formal organizational structure that would allow it to make decisions regarding capacity. Once the ACO is recognized, each member would accept joint responsibility for the quality and cost of care received by the ACO's panel of patients.

The underlying philosophy of the accountable care organization is that organizations should share in the savings when they make appropriate utilization decisions that save costs

and preserve quality of care. MedPAC proposed that 80 % of those savings be given to the organizations and 20 % retained by Medicare. A fixed dollar amount of spending growth targets would be established for all organizations. A bonus would be allotted to physicians and hospitals in those ACOs with lower-than-average spending increases [34]. The MedPAC report provides an example of a low-use, average-use, and high-use ACO with baseline spending per capita of $7,000, $10,000, and $12,000, respectively. Each would be given an allowance for growth of $500. Therefore, in order to meet the spending targets, they would need to spend less than $7,500, $10,500, and $12,500 per beneficiary, respectively. This is a percent increase of 7.1 %, 5.0 %, and 4.2 %, respectively. As shown in the example, while the opportunity to meet the spending target is equal from the perspective of dollar growth, the low-use ACO enjoys an advantage from the perspective of percentage growth.

The ACO model attempts to balance the incentives of capitation and fee-for-service plans. A major criticism of the capitation plans common in the 1990s was that they created incentives for providers and hospitals to underutilize services, since spending for care financially penalized the provider, regardless of necessity. On the other hand, the currently predominant fee-for-service model incentivizes overutilization, with reimbursement dependent on the volume of services provided. The ACO model combines elements of both capitation and fee-for-service, with additional rewards for provision of evidence-based care.

In addition to spending targets, accountable care organizations would also need to meet quality targets. Initially, these would be based on process measures, with more limited outcomes measures. Eventually, outcomes measures would be incorporated, which might include mortality rates, avoidable hospital admissions, readmissions, and patient satisfaction. A weighted quality score would likely be established, and the ACO would need to meet the target to be eligible for the bonus. Quality measures would likely include assessments of how well their organizations adhere to evidence-based guidelines. Rather than micromanage utilization behavior, the objective of the ACO structure is to provide incentives for the practice of evidence-based medicine at the level at which clinicians make decisions – at the local, regional, or health system level – and let the clinicians and hospitals work together to determine how to make it happen. The desired result is that when clinicians and hospitals work together to provide the best care for the lowest cost, the care will naturally become more evidence based.

The Patient Protection and Affordable Care Act provides for the establishment of ACO pilot projects by organizations that meet certain criteria. If they meet cost and quality criteria, they will share in the Medicare savings averaged over a 3-year period [35].

How Is the Recently Passed US Health-Care Reform Initiative Expected to Influence Cost and Quality?

Summary

The US health-care reform statute has two main priorities: to expand coverage and control costs. While the coverage provisions of the act have received the majority of the attention in the press, the second priority of the statute, that of cost control, probably has more potential to affect radiologists and other physicians.

The Patient Protection and Affordable Care Act provides for the establishment of a large number of demonstration projects and initiatives that will be carried out over the next few years.

The question of whether the provisions contained in the Patient Protection and Affordable Care Act will go forward likely depend to a great extent on the current administration's ability to execute its provisions.

Supporting Evidence

Concepts of simultaneous cost control have played a prominent role in the Patient Protection and Affordable Care Act signed into law on March 30, 2010. It was passed by a narrow majority in the US Congress after more than a year of

bitter partisan politics, having been nearly defeated on several occasions. It represents a considerable political risk on the part of the President and Democratic lawmakers; it is now in their interest to make it work.

The statute has two main priorities: to expand coverage and control costs. The Democrats felt that it was important to expand coverage first, since without that protection, cost-control mechanisms would likely exclude large elements of the population. The statute expands coverage through a variety of mechanisms, including health insurance exchanges, penalties for nonparticipants, assistance for low-income individuals, increases in insurance oversight, and expansion of Medicaid [35]. While the coverage provisions of the act have received the majority of the attention in the press, the second priority of the statute, that of cost control, probably has more potential to affect radiologists and other physicians.

(a) Learning What Works

The cost-control provisions reflect the desire to move beyond across-the-board reimbursement cuts and to change the incentive structure to one that rewards quality rather than quantity. However, there are few examples of practical ways to accomplish this. Therefore, the Act provides for the establishment of a large number of demonstration projects and initiatives that will be carried out over the next few years. Examples are listed in Table 7.1.

Most of these projects and initiatives will involve a limited number of health-care networks, providers, and patients at first. However, evidence gathered from these projects will guide implementation of changes that will affect a broader cross-section of the US population. Therefore, while the effects of cost-control initiatives are not likely to be felt immediately, after a few years of study, we may witness waves of sweeping changes driven by research that is currently getting underway.

(b) Coming Changes

A comprehensive discussion of the projects and initiatives included in the PPACA is beyond the scope of this chapter. Several of these provisions have already been discussed. One more deserves special attention: the Independent Payment Advisory Board (IPAB).

The IPAB provision was a relatively low-profile element of PPACA that has high-potential impact on the future of the US health-care system. In 1997, Congress established the Medicare Payment Advisory Commission and tasked them with advising Congress on issues affecting Medicare, primarily dealing with access, cost, and quality [35]. MedPAC has provided many recommendations to Congress since that time. However, once they are put before Congress, they are subjected to political processes that make it difficult to enact the unpopular changes that are often put forth. Having witnessed this for over a decade, authors of the health-care reform act saw the need for a body that not only was independent of congress, but whose recommendations could be insulated from the political process.

The IPAB will be made up of 15 members, nominated by the President and confirmed by Congress to 6-year terms. Beginning in 2014, any year in which the Medicare per capita financial growth rates exceed targeted rates (which is likely to occur most years), the board will be required to recommend Medicare spending reductions. These recommendations will automatically become law unless Congress passes an alternative. Furthermore, the President can veto Congress' alternative. While the board has some limitations – it may not recommend provisions that ration care, raise taxes or beneficiary premiums, or change Medicare benefits, eligibility, or cost-sharing standards – it may have significant authority to quickly enact politically charged changes needed to control costs.

(c) Political Outlook

The Patient Protection and Affordable Care Act is widely considered to be one of the most sweeping, but politically divisive, US legislative initiative in decades. Legal challenges to several provisions in the law are already wending their way through the US legal system, with mixed results to date. Most of the beneficial provisions take effect relatively soon, while implementation of many of the controversial decisions has been intentionally delayed. The authors of the statute hope that this will help garner political support for

the act before legal or legislative challenges can overturn it [49]. It is widely believed that the law will be reviewed by the Supreme Court, which will decide its fate. While the Supreme Court may not overturn the entire statute, if it rules unconstitutional the mandate that individuals purchase insurance, then it will likely render much of the law ineffectual, as mandatory participation is a key element in preventing individuals from waiting until they are sick to purchase insurance [50].

Given the current political makeup of Congress and the White House, it is unlikely that the bill will be overturned legislatively during the Obama Administration. Even if opponents of the bill were able to overturn the statute, the task of controlling escalating health-care costs that dominate the US budget deficit would not go away. Whether cost control will evolve along the lines of the Accountable Care Act as described above or by limiting access to care or through other means will likely depend to a great extent on the current administration's ability to execute its provisions as well as the political makeup of future congresses and presidential administrations.

What Are the Challenges and Opportunities for Evidence-Based Imaging?

Summary

The common element of nearly all of the concepts discussed in this chapter is a desire to encourage and enable the use of evidence-based medical care and to discourage use of care that is not evidence-based. Policy makers have learned that it is not sustainable to enforce blunt cuts in reimbursement and services, and have placed their faith in what they have been told by quality and evidence-based practiced advocates – that we can both decrease costs and improve health-care quality at the same time.

The challenge has been issued to the medical community, including radiology, to move evidence-based imaging from a theory or a collection of anecdotes to one that can be effectively implemented on a broad scale.

Supporting Evidence

While it may not be obvious now, these developments provide a significant opportunity for the advancement of evidence-based medicine. The common element of nearly all of the concepts discussed in this chapter is a desire to encourage and enable the use of evidence-based medical care and to discourage use of care that is not evidence based. Policy makers have learned that it is not sustainable to enforce blunt cuts in reimbursement and services, and have placed their faith in what they have been told by quality and evidence-based practiced advocates – that we can both decrease costs and improve health-care quality at the same time. The next few years will provide an opportunity for organizations to demonstrate whether that can be achieved. The challenge has been issued to the medical community, including radiology, to move evidence-based imaging from a theory or a collection of anecdotes to one that can be effectively implemented on a broad scale. This will require research to determine how to do this effectively. In other words, wide adoption of evidence-based imaging (EBI) will require evidence-based EBI implementation.

Relative to other specialties, radiology finds itself in a favorable position. The American College of Radiology (ACR) has taken a role in terms of evidence-based image utilization with the ACR Appropriateness Criteria®. These guidelines, and international equivalents [51], were developed to assist referring physicians and other providers in making the most appropriate imaging or treatment decision. While they have their shortcomings, they constitute a relatively objective and comprehensive set of criteria that can serve as the basis for local implementation of image utilization [52, 53]. For example, Appropriateness Criteria® are established through committee consensus through the modified Delphi process – a valuable technique for group decision making [52]. However, consensus methodology renders the distillation of evidence susceptible to political influences. Nevertheless, although the appropriateness criteria are not formed through accepted EBI methods, a critical review of the evidence forms the basis

for many of the panel recommendations. The evidence tables and narrative literature reviews prepared by the panel leaders thus constitute a valuable starting point for EBI [54]. Furthermore, what the appropriateness criteria lack in depth they make up for in breadth, covering over 170 topics [54]. The appropriateness criteria have been incorporated into at least some RBM algorithms and into the computerized physician order entry system of at least one large academic medical center, with resultant decreased growth in utilization of imaging [55].

An alternative method for guideline generation is that used by the NICE in the United Kingdom through the recently established diagnostics assessment program (DAP). NICE commissions an independent academic group to prepare a review of the clinical and cost-effectiveness of selected diagnostic technologies. The evidence assessment is based on a systematic review of the literature including data supplied by the manufacturers. The final guidelines reflect the stakeholder input only at the discretion of the guideline developers [52]. With few exceptions, imaging strategies recommended by most radiology textbooks do not incorporate accepted EBI methodology. The purpose of this text is to provide systematic reviews of clinical issues in imaging, presenting concise summaries of the best imaging choices for patient care, along with evaluations of the strength of the evidence [54].

Government and private payers are likely to continue to encourage incorporation of such criteria, guidelines, and protocols into local health-care information systems. Under such a financial incentive structure, those providing and interpreting imaging services are likely to be in a better financial position if they follow evidence-based guidelines. One could argue that radiologists are at an advantage in that, since they only rarely refer patients for imaging, radiologists themselves are rarely the direct cause of overutilization.

As these initiatives move forward, radiologists have an opportunity to take a strong position locally and (inter)nationally in promoting the use of evidence-based imaging. On a national level, the simultaneous efforts of radiology researchers in investigating the effects of self-referral on image utilization with the development of evidence-based appropriateness criteria place radiologists in a favorable light as an interested but relatively objective party. By continuing to develop the evidence base and continually refining imaging criteria, radiology can continue to be a recognized leader in this regard.

A similar opportunity exists at the local level. Financial incentive structures are likely to move increasingly toward rewarding radiologists who actively cooperate with other physicians to implement evidence-based guidelines and ordering systems in local health networks. Radiology groups who are active in promoting such guidelines and implementing such systems within their own hospitals are likely to be prepared for such an evolution. However, they may find it difficult spending the time and effort on such activities that do not provide direct reimbursement in the short run. Even simple efforts such as standardization of imaging protocols and increased coordination with ordering clinicians are likely to be well received as financial incentives increasingly move toward rewarding a more teams- and evidence-based practice of medicine.

Take-Home Tables and Figures

Figure 7.1: Government sources pay for 48 % of all national health expenditures in the United States, for a total of $1.2B in 2010. Only the governments of two other major industrialized countries, Norway and Denmark, pay more for their citizens' health care on a per capita basis. Thus, the perception that the United States without a government-sponsored universal healthcare system is misleading.

Figure 7.2: US health-care expenditures have nearly continuously increased over the past 40 year not only in real dollars but also in almost every other measurable term. The portion of economic output spent on health care for the average person in the United States is five times that of the amount spent per person in 1965.

2010 US National Health Expenditures ($B)
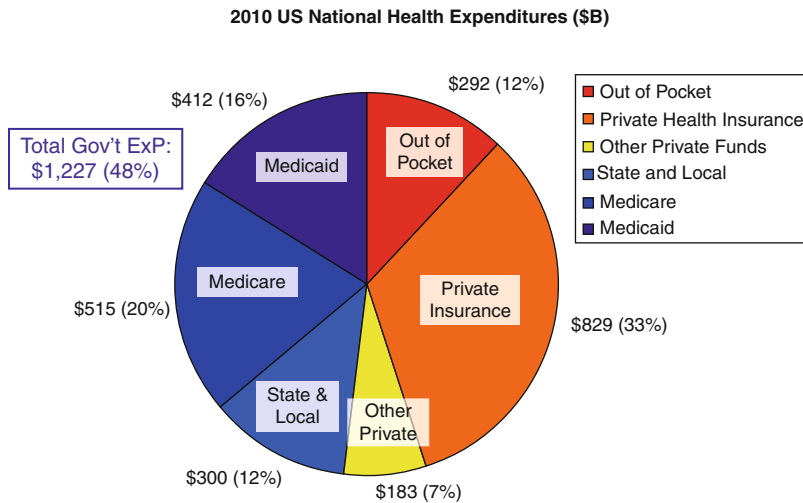
Fig. 7.1 Source of payment of US health expenditures, 2010 (Source: Created from data at http://www.cms.gov/NationalHealthExpendData/downloads/proj2009.pdf. Reprinted with permission from Larson DB. The

economic and regulatory impact of evidence-based medicine on radiology. In Medina LA, Blackmore CC, Applegate KE, editors. Evidence-based imaging: improving the quality of imaging in patient care. New York: Springer; 2011
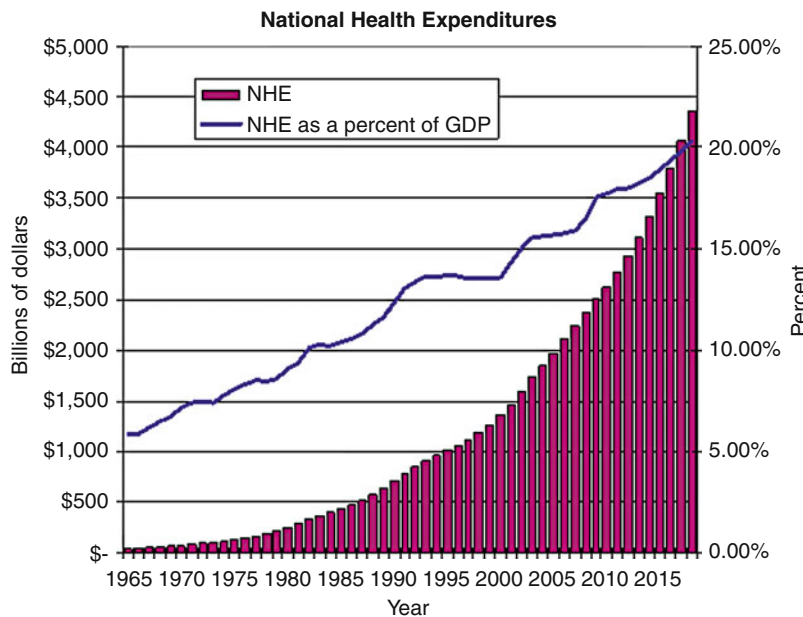
Fig. 7.2 US national health expenditures, in dollars and as a percent of GDP. Data for 2008 and greater are projections (Source: Created from data from Centers for Medicare and Medicaid Services, US Department of Health and Human Services, National Health Expenditure Projects: forecast summary 2008–2018. Baltimore: Centers for Medicare and Medicaid Services; 2008. http://www.cms.hhs.gov/NationaHealthExpendData/downloads/proj2008.pdf; and Center for Medicare and Medicaid Services, National

Health Expenditure Data. "NHE Historical and Projections, 1965–2018 (ZIP, 32 KB)." https://www.cms.gov/National-HealthExpendData/03_NationalHealthAccountsProjected.asp; (Reprinted with permission from Larson DB. The economic and regulatory impact of evidence-based medicine on radiology. In Medina LA, Blackmore CC, Applegate KE, editors. Evidence-based imaging: improving the quality of imaging in patient care. New York: Springer; 2011

Table 7.1 Examples of demonstration projects and initiatives included in the Patient Protection and Affordable Care Act

Establishment of an independent payment advisory board
Extension of the physician quality reporting initiative (PQRI) through 2014
Establishment of a national strategy to improve health-care delivery, patient outcomes, and population health
Interagency working group on health-care quality convened by the president
Establishment of a center for Medicare and Medicaid innovation
Accountable care organizations (ACOs) demonstration projects
Bundled payments demonstration projects
Medical home demonstration projects
Medicare value-based purchasing program for hospitals
Preventable Medicare readmissions adjustment
Reimbursement adjustments for imaging services and power-driven wheelchairs
Medicare advantage (MA) quality bonus payments
Medicare hospital productivity adjustment
Establishment of a health delivery system research center
Use of medication management services
Establishment of a patient-centered outcomes research institute
Uniform standards for financial and administrative health-care transactions

Reprinted with permission from Larson DB. The economic and regulatory impact of evidence-based medicine on radiology. In Medina LA, Blackmore CC, Applegate KE, editors. Evidence-based imaging: improving the quality of imaging in patient care. New York: Springer; 2011

References

1. Neumann PJ, Rosen AB, Weinstein MC. N Engl J Med. 2005;353(14):1516–22.
2. Kaiser Commission on Medicaid and the Uninsured. The Henry Kaiser Family Foundation website. http://www.kff.org/uninsured/upload//7451-06.pdf. Published December 2010. Accessed 15 March 2011.
3. National Health Expenditure Projections 2009–2019. Centers for Medicare and Medicaid Services website. http://www.cms.gov/NationalHealthExpendData/downloads/proj2009.pdf. Published 2009. Accessed 15 March 2011.
4. OECD Health Data Updates: Data, Sources and Methods, and Software Updates. OECD website. http://www.oecd.org/document/44/0,3746,en_2649_34631_2085228_1_1_1_1,00.html. Published 21 October 2010. Accessed 15 March 2011.
5. World Health Statistics. World Health Organization website. http://www.who.int/whosis/whostat/2009/en/; 2009. Published 2010. Accessed 15 March 2011.
6. Remarks by the President in AARP Tele-Townhall on Health Care Reform. White House.gov website. http://www.whitehouse.gov/the_press_office/Remarks-by-the-President-in-AARP-Tele-Town-Hall-on-Health-Care-Reform/. Published 28 July 2009. Accessed 15 March 2011.
7. Chernew ME, Hirth RA, Cutler DM. Health Aff. 2009;28(5):1253–5.
8. Executive Office of the President of the United States. The economic case for health care reform. http://www.whitehouse.gov/assets/documents/CEA_Health_Care_Report.pdf. Accessed 30 Sept 2009.
9. Davis K, Schoen C, Guterman S, Shih T, Schoenbaum C, Weinbaum I. Slowing the growth of U.S. health care expenditures: what are the options? The Commonwealth Fund website. http://www.commonwealthfund.org/usr_doc/Davis_slowinggrowthUShltcareexpenditureswhatareoptions_989.pdf. Published January 2007. Accessed 15 March 2011.
10. Bureau of Labor Statistics. Databases, Tables & Calculators by Subject. United States Department of Labor Bureau of Labor Statistics website. http://www.bls.gov/data/inflation_calculator.htm. Accessed 30 Sept 2009.
11. US Census Bureau. Population Estimates Program. United States Census Bureau website. http://www.census.gov/popest/archives/1990s/popclockest.txt. Internet release date 11 April 2000. Revised 28 June 2000. Accessed September 30, 2009.
12. White C. Health Aff. 2007;26(1):154–61.
13. Office of the Press Secretary. Remarks by the President to a joint session of Congress on health care. The White House website. http://www.whitehouse.gov/the-press-office/remarks-president-a-joint-session-congress-health-care. Released 9 Sept 2009. Accessed 15 March 2011.
14. Polsky D, Grande D. N Engl J Med. 2009;361(5):437–9.
15. Milliman Inc. Milliman Medical Index. http://publications.milliman.com/periodicals/mmi/pdfs/milliman-medical-index-2009.pdf. Published May 2009. Accessed 15 March 2011.
16. Anderson GF. Health Aff. 2007;26(3):780–9.
17. Himmelstein DU, Thorne D, Warren E, Woolhandler S. Am J Med. 2009;122(8):741–6.
18. Robertson CT, Egelhof R, Hoke M. Health Matrix J Law-Med. 2008;18(1):65–104.
19. Social Security Administration Actuarial Publications. Status of the Social Security and Medicare Programs. Social Security Online. http://www.ssa.gov/OACT/TRSUM/index.html. Accessed 30 Sept 2009.
20. Administration of Barack H. Obama. Remarks at the White House Forum on Health Reform. GPO Access website. http://www.gpoaccess.gov/presdocs/2009/DCPD200900130.pdf. Accessed 11 Nov 2009.
21. Mason C. Can Med Assoc J. 2008;179(2):129–31.
22. Timmins N. Br Med J. 2005;331(10):1193–5.

23. The Dartmouth Institute for Health Policy and Clinical Practice. Q&A with Dr. Jack Wennberg. http://www.dartmouthatlas.org/press/Wennberg_interviews_DartMed.pdf. Accessed 30 Sept 2009.
24. Kolata G. Sharp regional incongruity found in medical costs and treatments. The New York Times website. http://www.nytimes.com/1996/01/30/science/sharp-regional-incongruity-found-in-medical-costs-and-treatments.html. 30 Jan 1996. Accessed 15 March 2011.
25. Fisher ES. J Am Coll Radiol. 2007;4(12):879–85.
26. Orszag P. Opportunities to increase efficiency in health care. Congressional Budget Office. http://finance.senate.gov/healthsummit2008/Statements/Peter%20Orszag.pdf. Accessed 30 Sept 2009.
27. Sirovich B, Gallagher PM, Wennberg DE, Fisher ES. Health Aff. 2008;27(3):813–23.
28. Gawande A. The cost conundrum. The New Yorker. 2009. p. 11.
29. Applied Research Program, Division of Cancer Control and Population Sciences. Participation rates and target populations for breast cancer screening programs in 27 ICSN countries, 2007–2008. International Cancer Screening Network website. http://appliedresearch.cancer.gov/icsn/breast/participation.rates.html. Updated 24 Feb 2011. Accessed 15 March 2011.
30. Neumann PJ, Tunis SR. N Engl J Med. 2010;362(5):377–9.
31. House of Commons Health Committee. National Institute for Health and Clinical Excellence First Report of Session 2007–2008, Vol 1. UK Parliament website. http://www.publications.parliament.uk/pa/cm200708/cmselect/cmhealth/27/27.pdf. Published 10 Jan 2008. Accessed 15 March 2011.
32. Levin DC, Rao VM, Parker L, Frangos AJ, Sunshine JH. J Am Coll Radiol. 2008;5(12):1206–9.
33. Gazelle GS, Halpern EF, Ryan HS, Tramontano AC. Radiology. 2007;245(2):517–22.
34. Hackbarth G. Report to congress: improving incentives in the Medicare Program. Medicare Payment Advisory Commission (MedPAC) website. http://www.medpac.gov/documents/Jun09_EntireReport.pdf. Published June 2009. Accessed 15 March 2011.
35. 111th Congress of the United States of America. Bill Text 111th Congress H.R. 3590 ENR Patient Protection and Affordable Care Act. Library of Congress. http://thomas.loc.gov/cgi-bin/query/D?c111:7:./temp/~c111dZ9QKY. Published 23 March 2010. Accessed 15 March 2011.
36. U.S. Government Accountability Office. Medicare Part B imaging services: rapid spending growth and shift to physician offices indicate need for CMS to consider additional management practices. U.S. Government Accountability Office website. http://www.gao.gov/new.items/d08452.pdf. Accessed 11 Nov 2009.
37. Léonard C, et al. Health Policy. 2009;91:121–34.
38. Fisher ES, Staiger DO, Bynum JP, Gottlieb DJ. Health Aff. 2007;26(1):w44–57.
39. Nichols L, Weinberg M, Barnes J. Grand junction, Colorado: a health community that works. New America Foundation website. http://www.newamerica.net/files/GrandJunctionCOHealthCommunityWorks.pdf. Published August 2009. Accessed 30 Sept 2009.
40. Galewitz P. Local hospitals and doctors join forces to improve health care, restrain costs. Kaiser Health News website. http://www.kaiserhealthnews.org/Stories/2009/July/22/Hospital.aspx. Published 22 July 2009. Accessed 15 March 2011.
41. Hackbarth G. Report to the congress: Medicare payment policy. Medicare Payment Advisory Commission (MedPAC) website. http://www.medpac.gov/documents/Mar09_March%20report%20testimony_WM%20FINAL.pß. Published 17 March 2009. Accessed 15 March 2011.
42. Blankart R, Schreyogg J, Busse R. Technol Health Care. 2008;16(3):171–82.
43. Towse A. Br J Clin Pharmacol. 2010;70(3):360–6.
44. Garrison LP, et al. Acad Radiol. 2011;18(90):1109–14.
45. Senate Committee on Finance. America's Healthy Future Act of 2009 [chairman's mark]. United States Senate Committee on Finance website. http://finance.senate.gov/sitepages/leg/LEG%202009/091609%20Americas_Healthy_Future_Act.pdf. Published 19 Oct 2009. Accessed 15 March 2009.
46. Mitchell JM, Lagalia RR. Med Care Res Rev. 2009;66(3):339–51.
47. American College of Radiology and Radiology Business Management Association. Best practices guidelines on radiology benefits management programs. American College of Radiology website. http://www.acr.org/SecondaryMainMenuCategories/GR_Econ/WhatsNew/ACRRBMABestPracticesonRBMPs.aspx. Published 24 Jan 2009. Accessed 15 March 2011.
48. Eccles M, Steen N, Grimshaw J, et al. Lancet. 2001;357(9266):1406–9.
49. Farrington B. White House, experts: health care suit will fail. The San Diego Union-Tribune website. Associated Press. http://www.signonsandiego.com/news/2010/mar/23/white-house-experts-health-care-suit-will-fail/. Retrieved 07 April 2010. Published 23 March 2010. Accessed 15 March 2011.
50. Cooper M. Health law is dealt a blow by a court on mandate. The New York Times website. http://www.nytimes.com/2011/08/13/us/13health.html?scp=1&sq=health%20law%20is%20dealt%20blow%20by%20a%20court%20on%20mandate&st=cse. Published 12 Aug 2011.
51. Royal College of Radiologists. Referral guidelines: making the best use of clinical radiological services (MBUR). 6th ed. London: Royal College of Radiologists; 2007.
52. Blackmore CC, Medina LS. J Am Coll Radiol. 2006;3(7):505–9.
53. Bettmann MA. J Am Coll Radiol. 2006;3(7):510–12.
54. Medina LS, Blackmore CC. Radiology. 2007;244(2):331–6.
55. Sistrom CL, Dang PA, Weilburg JB, Dreyer KJ, Rosenthal DI, Thrall JH. Radiology. 2009;251(1):147–55.

Evidence-Based Neuroimaging in Medical-Legal Cases and its Developing Role

8

Annemarie Relyea-Chew

Contents

A. Relyea-Chew
Department of Radiology, University of Washington, Seattle, WA, USA
e-mail: archew@u.washington.edu

Key Points

- Most medical malpractice cases do not proceed to trial, but are withdrawn, go into arbitration, or are settled.
- To date, there are limited reported legal opinions regarding EBM or use of clinical or imaging guidelines in neuroimaging.
- Relative to general radiologists, neuroradiologists and interventional neuroradiologists may be at enhanced risk of litigation arising from use of medical devices or products.
- Proof related to evidence-based diagnostic imaging has been admissible in US courts in malpractice, products liability, and denial of benefits claims.

Overall Cost to Society

Claims in the USA from state and federal courts under theories of medical malpractice, products liability, the Emergency Medical Treatment and Active Labor Act (EMTALA) [1], Federal Tort Claims Act (FTCA) [2], and the Employee Retirement Insurance Security Act (ERISA) [3] are substantial. A recent study estimates the annual medical liability system costs the USA $55.6 billion in 2008 dollars, of which approximately 80 % ($45.59 billion) is attributable to defensive medicine [4].

Methodology

Searches were conducted on Medline, PubMed, LexisNexis Academic, Westlaw, and HeinOnline (10/20/2011). Terms included are evidence-based medicine (EBM), evidence-based radiology, neuroradiology, neuroimaging, interventional neuroradiology, clinical guidelines, best practices, practice parameters, and PPACA.

Background and Discussion of Issues

- Does evidence-based medicine (EBM) differ from evidence in law?
- How is EBM introduced as evidence in a legal proceeding?
- Does deviation from EBM principles or clinical practice guidelines constitute breach of the applicable standard of care?
- In what areas of law is evidence-based diagnostic imaging likely to become the subject of litigation?

Adoption of the principles of evidence-based medicine into health-care practice and policy in the USA has been uneven [5]. Although separate constructs, evidence in science and law are routinely conflated, resulting in vigorous debate in and out of the courtroom [6]. Evidence in law is a distinct discipline whose function is to ensure only trustworthy and relevant facts are admitted as proof in a case or controversy. Sources for rules of evidence include federal and state statutory, legislative, case, and common law, and may take the form of tangible, oral, or recorded testimony [7]. Scientific and medical evidence are usually subject to *in limine*, or evidentiary hearings, which precede acceptance by the court as evidence in a case. This includes hearings for expert witness testimony in medical malpractice cases and the introduction of scientific and medical evidence, including practices using evidence-based medicine (EBM) [8].

Evidentiary rules regarding the admissibility of EBM in federal and state courts vary by jurisdiction. Litigants most frequently attempt to introduce clinical practice guidelines (CPGs), or an analogue, as direct and indirect evidence of the standard of care. Clinical practice guidelines can be, but are not necessarily, within the penumbra of EBM and can vary widely in quality and

timeliness [9]. CPGs are often used synonymously in medical and legal literature as "algorithms," "clinical pathways," "best practices," and "practice parameters" [10]. Clinical practice guidelines rely increasingly on EBM methodology to produce more robust, empirical evidence in support of recommendations. Nevertheless, evidence-based CPGs promulgated by third-party payers to control costs of health care do not necessarily improve patient outcomes, can be rife with conflict of interest, and some practices claiming to be EBM lack scientific rigor [11].

The federal government and agencies such as the Institute of Medicine (IOM) and Health and Human Services (HHS) are currently at the forefront of advancing CPGs that are developed using EBM methodology [12]. Current federal support of evidence-based practice and guidelines, such as the National Guideline Clearinghouse, has resulted in a systematic collection of guidelines [13]. The IOM has released two consensus reports: Clinical Practice Guidelines We Can Trust [14] and Finding What Works in Health Care: Standards for Systematic Reviews [15]. The American College of Radiology (ACR) issues and routinely updates its Practice Guidelines, Technical Standards, and Appropriateness Criteria [16].

The appropriation and distribution of 1.1 billion dollars in federal funding under Title VIII of American Recovery and Reinvestment Act (ARRA) to conduct comparative effectiveness research (CER) underscores a commitment to EBM [17]. The 2010 Patient Protection and Accountable Care Act (PPACA) provided funding for the creation of the Patient-Centered Outcomes Research Institute (PCORI). The PCORI is currently in the process of defining its mission; by statute, it is required to disseminate research findings related to clinical effectiveness and appropriateness rapidly. The statute also states that the research findings from the institute shall, "... not be construed as mandates for practice guidelines, coverage recommendations, payment or policy recommendations" [18]. There is, however, pending federal legislation in the House of Representatives entitled "Empowering Patients First Act," which creates an affirmative defense and limitation of damages, to a claim of medical malpractice if a health-care provider is in compliance with best practices guidelines [19].

It is likely that evidence-based practice guidelines promulgated by the federal government and viewed as codified standards of medical care will be controversial. In an earlier effort to contain health care and insurance costs, several jurisdictions – Maine [20] Minnesota [21], Vermont [22], Kentucky [23], Florida [24] – passed prescriptive legislation to limit the use of CPGs in litigation. Most are now repealed, and these statutes are problematic, raising constitutional issues implicating the right to a jury trial, due process, and equal protection. The American Bar Association (ABA) sets its position in 2011, issuing a formal resolution that (1) it supports development and use of EBM or medical practice guidelines or standards and recognizes that such guidelines are not necessarily the applicable standard of care, and (2) it opposes federal or state legislation that creates an evidentiary presumption that a health-care provider is either presumptively negligent or not negligent, or responsible, for an adverse outcome solely on the basis that the health-care provider either practiced, or failed to practice, in conformity with EBM, clinical or medical practice guidelines or standards [25].

EBM as a Legal Standard of Care

Summary
The standard of care to which a physician practicing in the specialty of neuroimaging is held varies by jurisdiction. Whether an evidence-based CPG constitutes evidence of, or is the legal standard of care to which a physician may be held, is a developing area of law.

Supporting Evidence

Standards of care are practices or services considered medically necessary that a health-care provider is required to render under same or similar circumstances [26]. The legal standard of care to which a physician is held is defined in each of the 50 states and the District of Columbia by statute or case law. Approximately 40 % of states adhere to the locality rule, i.e., that is the standard of care practiced by physicians in the same community, or a variation such as the "same or similar locality," or within the entire state [27]. For example, in defining the elements necessary to prove medical malpractice, the state of Washington defines breach of the accepted standard of care to be the failure, ". . . to exercise that degree of care, skill, and learning expected of a reasonably prudent health care provider at that time in the profession or class to which he or she belongs, in the state of Washington, acting in the same or similar circumstances" [28]. A majority of states and entities under federal jurisdiction have some form of national standard. Whether an evidence-based CPG (or analogue) constitutes evidence of, or is the legal standard of care to which a physician may be held, is an open debate [29]. Compliance with a CPG does not necessarily assure the best medical care; deviating from a CPG does not always indicate poor care [30].

Litigants routinely attempt to offer guidelines, or a functional equivalent, as substantive evidence of the standard of care [31], indirect evidence of standard of care [32], for impeachment of witnesses or rebuttal [33], and as learned treatises [34]. Regardless, introduction of scientific or medical evidence is subject to pretrial review by the court (judge) functioning as gatekeeper in pretrial hearings to review proffered evidence using expert witness testimony in state and federal jurisdictions [35]. In federal court, pretrial evidentiary *Daubert* hearings are conducted to establish (1) whether the scientific/medical evidence or testimony is reliable (defined as scientific validity) and also (2) whether the evidence or testimony is relevant [36]. As an alternative, a CPG or analogue might be admissible as a government standard/public record under Federal Rules of Evidence (Fed. R. Evid.) 803

(8) or, under Fed. R. Evid. 201, the court may simply take judicial notice and no testimony. This presupposes that particular guidelines or the practice of EBM become recognized as beyond factual dispute, thereby requiring no expert testimony for admissibility [37].

Neuroimaging and EBM

Summary

There is little legal precedent in the area of evidence-based diagnostic imaging. Those practicing neuroimaging may be likely to be codefendants in lawsuits with neurosurgeons or neurologists, or in liability cases associated with medical devices and products.

Supporting Evidence

Evidence employing or related to evidence-based diagnostic imaging has been admissible as proof in US courts primarily in three situations: (1) the tort of medical malpractice, (2) products liability [38], and (3) entitlement to benefits claims [39].

Medical Malpractice

To date, there are limited reported cases specifically against radiologists that involve EBM or use of clinical or imaging guidelines in neuroimaging. Facts and results of medical-legal cases in the USA are reported in official published opinions if there is an appeal from a lower court or tribunal ruling. Most medical malpractice cases do not go to trial, but are withdrawn, go into arbitration, or are settled in some fashion [40]. Selected cases of interest, although officially not reported, are published in proprietary practitioners' publications that lack public access. These cases do not have precedential value, but are highly instructive and guide practice [41]. Neuroimaging evidence in medical malpractice cases most often involves physicians in the neurosciences against whom lawsuits are brought as a result of an alleged diagnostic or therapeutic mishap [42]. Diagnostic radiologists are often swept into the fray as codefendants, consultants, or expert witnesses in cases against surgeons and neurologists.

In *Jerden v. Klamath* [43], an Oregon neurosurgeon performed an unnecessary craniotomy based on his interpretation of the plaintiff's magnetic resonance imaging (MRI) and magnetic resonance angiogram (MRA). The defendant neurosurgeon failed to read and consider the interpretation by the defendant hospital radiologist that had stated, "Scattered white matter lesions bilaterally suggesting changes of demyelinating disease." The plaintiff did, in fact, have multiple sclerosis, not a brain tumor. Although multiple medical experts for the defendant and plaintiff testified at trial regarding the proper interpretation of the MRI and MRA reports, none was a radiologist [44].

The standard of care for treatment of subarachnoid hemorrhage (SAH) and cerebral vasospasm (VSP) was explored in *Haines vs. Gifford*, a 2001 California case not officially reported but instructive [45]. During the period at which the plaintiff, Ms. Haines, was at high risk for VSP after SAH surgery by a defendant neurosurgeon, she was left unmonitored, underwent VSP, and suffered permanent neurological damage. The plaintiff sued the community hospital where treatment had occurred, the staff radiologist, and staff neurosurgeons. Claims included failure to meet the then standard of care in (1) misdiagnoses of the patient's computed tomography (CT) scans, (2) not monitoring the patient when she was at high risk for VSP, and (3) failing to transfer the plaintiff to another facility that employed interventional radiologists and neurosurgeons qualified to diagnose and treat SAH with advanced procedures such as coiling and angioplasty.

Liability and Medical Products

Relative to general radiology, the subspecialties of neuroradiology and interventional neuroradiology may to be at enhanced risk of litigation arising from use of medical devices and products. Increasing numbers of individual and class action lawsuits are being filed on behalf of patients injured by defective or misapplied medical devices such as stents, or pharmaceuticals such as gadolinium.

Stents

Mrs. Waldt, the 52-year-old plaintiff in *Waldt vs. UMMSC*, was diagnosed with an aneurysm in the middle cerebral artery (MCA) [46]. Three treatment options were presented to her: monitor the status of the aneurysm, undergo surgical clipping, or endovascular coiling. After lengthy consultation with the defendant neuroradiologist, the plaintiff elected the coiling procedure. The plaintiff also agreed to the defendant's use of a Neuroform stent, a device used in Europe but pending approval by the US Food and Drug Administration (FDA). During the procedure, a coil became ensnared in the mesh stent, and the neuroradiologist spent over two hours attempting to remove it. The MCA perforated and the plaintiff suffered a stroke resulting in severe impairment. Although Mrs. Waldt brought a lawsuit alleging negligence and lack of informed consent against the neuroradiologist and his employer, she did not prevail at trial or at the Maryland Court of Appeals [47].

Gadolinium

In 2006, it was reported that patients with severe renal disease can develop nephrogenic systemic fibrosis (NSF) after undergoing gadolinium-enhanced MRI exams [48]. The precise etiology is unknown. The well-publicized issues around NSF, its relationship to gadolinium-based contrast agents, and the FDA's requirement of "black box warnings" appear to have effected a reduction in new cases of NSF and appropriate changes in radiology practice [49]. Litigation by advocates of patients who developed NSF has resulted in hundreds of claims filed in state and federal courts against gadolinium-based contrast agent (GBCA) manufacturers. In excess of 500 cases were consolidated as multi-district litigation (MDL) in the Northern District of Ohio, Eastern Division, for the pretrial discovery and gatekeeper phases. In May 2010, the US District Court judge issued a ruling permitting expert witnesses for the class action plaintiffs and defendants to testify for, and against, the "free gadolinium theory" of NSF causation [50]. This has prompted settlements with plaintiffs by GBCA manufacturers.

Off-Label Use

Although the FDA has not approved the GBCAs for MRA, gadolinium-based contrasts have also been used for fistulography, arthrography, and in patients where iodinated contrast is contraindicated [51]. Off-label use of pharmaceuticals poses risks for patients and providers. The 2009 US Supreme Court case, *Wyeth vs. Levine*, holds that FDA labeling regulations do not preempt state labeling regulations. Therefore, plaintiffs may seek recourse for injury in state courts for "failure to warn" in off-label and improper application of pharmaceuticals [52]. A subsequent US Supreme Court case, *Pliva, Inc., et al. vs. Mensing*, however, limits *Wyeth vs. Levine* to nongeneric pharmaceuticals approved by the FDA [53].

CT Perfusion Scans

The issue of overutilization and exposure to unnecessarily high radiation doses in patients undergoing computed tomography is well documented [54]. In 2009, the FDA issued an alert regarding instances of excessive radiation delivered to patients undergoing CT perfusion studies for diagnosis and treatment of stroke [55]. After investigation, the FDA found there are at least six hospitals involving almost 385 patients exposed to excessive radiation during CT perfusion studies. Recommendations made by the FDA in its investigation suggest that the scanners in issue functioned properly. However, information and training for imaging professionals by manufacturers, particularly about automatic exposure controls (AEC) settings, was stressed [56]. Class action lawsuits were filed by injured patients and are pending in California and Alabama.

Denial of Benefits

Centers for Medicare & Medicaid Services (CMS) and other insurers often deny patients desiring to undergo experimental or controversial medical therapies or diagnostic testing; this has led to costly litigation [57]. More problematic are denials of insurance coverage for procedures that are widely disseminated and may enhance the quality of health care yet lack supporting scientific evidence. Recent EBM-based studies and health technology assessment (HTA) programs have encouraged some states and CMS to limit or deny coverage for imaging procedures where evidence does not support efficacy or effectiveness. This includes computed tomography colonography (CTC) or virtual colonoscopy (VC) for colorectal cancer screening [58], upright or positional MRI, and discography, kyphoplasty, and sacroplasty [59]. The Washington State Health Care Authority, and its Health Technology Assessment Program, has been a national leader in this area [60]. Nevertheless, decisions by CMS to not reimburse certain procedures, such as CTC, have propelled advocates, industry, and physician groups to support federal legislation to mandate group, individual, and federal employees' health benefits plans to provide coverage [61]. It is likely that politicization of similar insurance coverage decisions for other procedures, medical treatment or therapy, will not diminish.

Future Research

- Future research should review the ongoing development of EBM-based diagnostic neuroimaging practice guidelines promulgated by federal agencies such as HHS and PCORI.
- Whether and to what degree EBM-based guidelines affect the legal standard of care, or become the standard of care overtime, will be of interest to researchers.

References

1. 42 U.S.C. § 1395dd.
2. 28 U.S.C. § 346(b), 2671, et seq.
3. 29 U.S.C. § 1001, et seq.
4. Mello MM, Chandra A, Gawande AA, Studdert DM. Health Aff. 2010;29:1569–77.
5. Gray BH, Gusmano MK, Collins SR. Health Aff. 2003;25:W3-283–307. The authors write: "Health services research, an AHSR lobbyist once said, was as difficult to sell as a dead fish wrapped in newspaper".
6. Rosoff AJ. J Health Polit Policy Law. 2001;26:327–68.
7. Garner BA, Black HC. Black's law dictionary. 8th ed. St. Paul: West Publication; 2004.

8. Strong JW, Dix GE, Imwinkelried EJ, et al. McCormick on evidence. 6th ed. St. Paul: West Publication; 2007. p. 302–37.

9. Shekelle PG, Ortiz E, Rhodes S, et al. J Am Med Assoc. 2001;286:1461–7.

10. Berlin L. AJR Am J Roentgenol. 2003;181:945–50.

11. Steinberg EP, Luce BR. Health Aff. 2005;24:80–92.

12. The National Guideline Clearinghouse™, a federal website of AHRQ. http://www.guideline.gov/. Accessed 25 Oct 2011.

13. Agency for Healthcare Research and Quality. http://www.guideline.gov/index.aspx. Accessed 25 Oct 2011.

14. http://www.iom.edu/Reports/2011/Clinical-Practice-Guidelines-We-Can-Trust.aspx. Accessed 25 Oct 2011.

15. http://www.iom.edu/Reports/2011/Finding-What-Works-in-Health-Care-Standards-for-Systematic-Reviews.aspx. Accessed 24 Oct 2011.

16. Amis Jr ES. AJR Am J Roentgenol. 2000;174:307–10.

17. http://www.hhs.gov/recovery/programs/cer/execsummary.html. Federal Coordinating Counsel for Comparative Effectiveness Research, Report to the President, HHS (June 2009). http://www.hhs.gov/recovery/programs/cer/cerannualrpt.pdf. Accessed 29 Oct 2011.

18. Public Law 111–148, Subtitle D, Sec. 6301(a) (D): Patient-Centered Outcomes Research: Release of Research Findings (8)(A)(iv). http://www.gao.gov/about/hcac/pcor_sec_6301.pdf. Accessed 15 Nov 2011.

19. H.R. 3000 (112th Congress): Empowering Patients First Act, § 508 Limitation on Recovery in a Health Care Lawsuit Based on Compliance with Best Practice Guidelines. http://thomas.loc.gov/cgi-bin/query/F?c112:1:./temp/~c1126jyO6Z:e223704. Accessed 27 Oct 2011.

20. Maine's Medical Malpractice Liability Demonstration Project (1992), renewed in 1997, and repealed in 2002. Me Rev Stat Ann Tit 24 §§ 2971–2979.

21. Minnesota Health Care Cost Containment Law: Minn Stat § 62J 34 (1993); repealed in1995 in Minn Stat 234 art. 5 § 24.

22. Vermont Health Care Reform Law: Vt Acts 160 § 46 (1991); Leichter HM. Health care reform in Vermont: a model. Health Aff. Summer 1993, p. 71–82.

23. Kentucky Rev Stat Ann §§ 216B § 145; 1995; repealed Ky Acts ch. 371; 1996.

24. Florida Health Insurance Reform Act, Fla Stat Ann § 408.02; 1993.

25. American Bar Association Resolution; 2011. http://www.americanbar.org/content/dam/aba/migrated/2011_build/house_of_delegates/113_2011_my.authcheckdam.pdf. Accessed 22 Oct 2011.

26. Mulrow CD, Lohr KN. J Health Polit Policy Law. 2001;26:249–66.

27. Lewis MH, Gohagan JK, Merenstein DJ. JAMA. 2007;297:2633–7.

28. Wash. Rev. Code § 7.70.040. Necessary elements of proof that injury resulted from failure to follow accepted standard of care.

29. Rosoff AJ. J Health Polit Policy Law. 2001;26:327–68.

30. Mulrow CD, Lohr KN. J Health Polit Policy Law. 2001;26:249–66.

31. Taylor v. Boudreaux MD., et al. 25 So.3rd 216 (La. App. 2009).

32. Brenner RJ, Ulissey MJ, Wilt RM. AJR Am J Roentgenol. 2006;186:48–51.

33. Mello MM. Of Swords and shields: the role of clinical practice guidelines in medical malpractice litigation, 149 U. Pa. L. Rev. 645 (2001).

34. Helling v. Carey, 519 P.2d 981 (Wash. 1974).

35. Thomas, et ux. v. Alford MD, Sweetwater Medical Asso, and Robert Malone, MD. 230S.W.3rd 853 (Tex. App. 2007).

36. Fed. R. Evid.702 incorporates Daubert v. Merrell Dow Pharms., Inc., 509 U.S. 597; 1993, General Electric Co. v. Joiner, 522 U.S. 136; 1997, Kumho Tire Co. v. Carmichael, 526 U.S. 137; 1999

37. Daubert v. Merrell Dow Pharmaceuticals, Inc., 509 U.S. 597; 1993.

38. In re Fosamax Prods. Liab. Litig., 2009 U.S. Dist. LEXIS 70246 (S.D.N.Y., Aug 4, 2009); In re Viagra Prods. Liab. Litig., 572F. Supp. 2nd 1071; 2 April 2008.

39. Holifield vs. Unum Life Insur. Co., et al., 2009 U.S. Dist. LEXIS 72208 (C. D. Cal Aug 4, 2009); Reimann v. Anthem Insur. Co., Inc., 45 Employee Benefits Cas. (BNA) 1420; 31 Oct 2008.

40. Golann D. Health Aff. 2011;30:1343–50.

41. Levitt v. Ross, Cal. App., 2nd Dist, 2nd Div; 2010. Unpublished.

42. Jena AB, Seabury S, Lakdawalla D, et al. N Engl J Med. 2011;365:629–36.

43. Jerden v. Klamath Neurosurgery Clinic; et al. 2004 U.S. Dist. LEXIS 9048 (Ore. Dist. 2004).

44. Jerden v. Amstutz, 430F.3d 1231; 2005.

45. Haines vs. Gifford, 7 Trials Digest 11th 15; 2007. Cal. St.B.J. Unpublished.

46. Waldt vs. UMMSC, 181 Md. App. 217; 2008.

47. UMMSC vs. Waldt, 411 Md. 207; 2009.

48. Marckmann P, Skov L, Rossen K, et al. J Am Soc Nephrol. 2006;17:2359–62.

49. Altun E, Martin DR, Wertman R, et al. Radiology. 2009;253:689–96.

50. In re: Gadolinium-based contrast agents products liability litigation. N.D. Ohio (May 4, 2010): Memorandum and Order; Case No. 1:08 GD 50000, MDL No. 1909.

51. Kay J. Cleve Clin J Med. 2008;75:112–17.

52. Wyeth v. Levine, 555 U.S. 555; 2009.

53. Pliva vs. Mensing, 564 U.S.; 2011.

54. Brenner DJ, Hall EJ. N Engl J Med. 2007;357:2277–84. FDA White Paper: Initiative to reduce unnecessary radiation exposure from medical imaging. http://www.fda.gov/Radiation-EmittingProducts/RadiationSafety/RadiationDoseReduction/ucm199994.htm. Accessed 29 Oct 2011.

55. Safety investigation of CT brain perfusion scans: initial notification. http://www.fda.gov/MedicalDevices/Safety/AlertsandNotices/ucm193293.htm. Accessed 28 Oct 2011.

56. Safety investigation of CT brain perfusion scans: update 11-09-2010. http://www.fda.gov/medicaldevices/safety/alertsandnotices/ucm185898.htm. Accessed 28 Oct 2011.

57. Jacobson PD, Rettig RA, Aubry WM. J Health Polit Policy Law. 2007;32:5.

58. Centers for Medicare & Medicaid Services. Decision for screening computed tomography colonography (CTC) for colorectal cancer. https://www.cms.hhs.gov/mcd/viewdecisionmemo.asp?id=220. Accessed 28 Oct 2011.

59. Blackmore CC, Budenholzer B. J Am Coll Radiol. 2009;6:366–71.

60. Washington State Health Care Authority: Health Technology Assessment Program. www.hta.hca.wa.gov. Accessed 28 Oct 2011.

61. The Colorectal Cancer Prevention, Early Detection and Treatment Act, Sen, 494, 112th Congress. http://thomas.loc.gov/cgi-bin/query/z?c112:s494. Related bill: H.R. 912. Accessed 28 Oct 2011.

Part III

Brain: Evidence-Based Neuroimaging

Multiple Sclerosis and Acute Disseminated Encephalomyelitis: Evidence-Based Neuroimaging

9

Michael E. Zapadka and Annette J. Johnson

Contents

M.E. Zapadka (✉) • A.J. Johnson
Department of Radiology, Wake Forest School of Medicine, Winston-Salem, NC, USA
e-mail: mzapadka@wakehealth.edu; anjohnso@wakehealth.edu

Key Points

- There is limited evidence that MRI improves diagnostic accuracy for MS, with several recent reviews providing differing conclusions (limited evidence). However, MRI-based measures have been formally incorporated into widely accepted clinical diagnostic criteria for MS for nearly a decade. Experts perceive that use of MRI in these patients serves multiple clinical purposes beyond diagnosis, including the exclusion of other pathologies (limited evidence).
- There is insufficient evidence to suggest that MRI findings can distinguish MS from ADEM (insufficient evidence).
- Regarding prognostic utility of MRI in MS, observational studies have yielded inconsistent results with regard to correlations between MRI-based measures and cognitive performance or disability in MS patients (limited evidence). However, use of MRI-based measures in recent clinical trials suggest that some imaging-based measures (especially the number of new T2 lesions and number of enhancing lesions) may correlate with both relapse rate and risk of disability progression (moderate to strong evidence).
- There is insufficient evidence to suggest that advanced MRI techniques improve the diagnostic accuracy of MRI for MS (insufficient evidence).
- Studies involving advanced MRI techniques in MS patients have largely contributed to a better understanding of the pathophysiology of the disease. There is early evidence that advanced techniques could be prognostically useful: based on one recent RCT of a new treatment, rate of cerebral atrophy (a semiautomated volumetric MRI-based measure) may correlate with relapse rate (moderate to strong evidence).

Definition and Pathophysiology

Among the demyelinating diseases (characterized by destruction of normal myelin with relative preservation of the axon) affecting the CNS,

multiple sclerosis is the most common [1, 2]. While the etiology of multiple sclerosis remains uncertain, the current most widely held view is that MS is an autoimmune process resulting from the interplay of environmental factors in those with a genetic predisposition [3]. The mechanism of injury includes inflammation, focal demyelination, and variable degrees of axonal destruction [4, 5]. At pathologic evaluation, the microscopic appearance will vary based on the activity of disease, with active lesions demonstrating perivascular and parenchymal inflammation with associated macrophage and lymphocyte infiltration, and inactive lesions demonstrating hypocellularity, astrogliosis, and loss of oligodendrocytes [1]. Remyelination may occur with early MS lesions ("shadow plaques"), though histologically, the myelin density in these areas is diminished with sparse or absent remyelination seen in chronic MS plaques [6]. MS lesions are distributed throughout the CNS with a predilection for involvement of the periventricular white matter, corpus callosum, optic nerves, spinal cord, brain stem, and cerebellum [5]. MS exhibits a wide diversity of neurologic signs and symptoms, with the clinical presentation largely based on location of the demyelinating lesion[s].

The clinical presentation of MS is quite heterogeneous, but common clinical manifestations include deficits in sensory or motor pathways, brain stem, and cerebellar structures, as well as autonomic function. Individuals that initially present with an acute focal neurologic disturbance referred to as a clinically isolated syndrome (CIS) are at risk for developing MS [7]. In adult patients with optic neuritis, the 10-year risk of developing MS is 38 % but increases to 56 % when one or more lesions typical for MS are present on MRI. The disease course varies from a single acute monophasic attack to the more common relapsing-remitting or progressive phases [8]. Relapses reflect worsening of neurologic function secondary to a new inflammatory lesion or reactivation of an existing lesion, with a relapse defined by symptom duration of at least 24 h [7]. Progression is defined as continual worsening of clinical signs and symptoms over a minimum of 6–12 months [9]. For standardization of nomenclature, the

various clinical courses have been defined in 1996 by Lublin et al. [10]:

1. Relapsing-remitting MS (RRMS) – relapses with full recovery or with sequelae and residual deficit upon recovery; periods between disease relapses characterized by a lack of disease progression.
2. Secondary progressive MS (SPMS) – initial relapsing-remitting disease course is followed by progression with or without occasional relapses, minor remissions, and plateaus.
3. Primary progressive MS (PPMS) – disease progression from onset with occasional plateaus and temporary minor improvements allowed.
4. Progressive-relapsing MS (PRMS) – progressive disease from onset, with clear acute relapses, with or without full recovery; periods between relapses characterized by continuing progression.

Treatment is aimed at preventing neurologic disability. Acute relapses are typically treated with intravenous or oral corticosteroids with several disease-modifying agents currently approved by the Food and Drug Administration for use in reducing the number of attacks in relapsing-remitting MS including immunomodulating injectable and more recently emerging oral therapies [11–13].

Acute disseminated encephalomyelitis (ADEM) is an immune-mediated disorder of the CNS resulting in perivascular inflammation and demyelination [14]. ADEM usually presents in individuals within weeks following a viral illness, after vaccination, or in some cases may occur spontaneously [2]. Pathologic evaluation demonstrates inflammatory infiltrates consisting of lymphocytes and macrophages along a perivenular distribution, with preservation of the axon [15]. ADEM typically involves white matter of the cerebrum and spinal cord as well as cerebral cortex and deep gray structures. In contrast to multiple sclerosis, ADEM is typically a monophasic, self-limited disease lasting 2–4 weeks, although relapses have been reported [16]. ADEM is more frequently seen in children but can occur at any age. Prodromal symptoms of fever, headache, malaise, and myalgias commonly occur prior to the onset of neurologic signs. Like MS, neurologic signs and symptoms are manifested based on location of the demyelinating lesion, with severity ranging from irritability to depressed consciousness and coma. Neurologic abnormalities include unilateral or bilateral long tracts signs, hemiparesis, ataxia, optic neuritis, cranial nerve palsies, and seizures. Despite the lack of placebo-controlled, double-blinded studies evaluating efficacy of treatment options, steroids are the primary treatment for ADEM with patients typically receiving an intravenous course of therapy for 3–5 days followed by a taper of oral steroids. Treatment options also include IV acyclovir in combination with steroids, IV immunoglobulin with or without steroids, or plasmapheresis in those who fail initial treatment courses [14].

Epidemiology

Multiple sclerosis is the most common nontraumatic neurologic disorder resulting in disability in young and middle-aged people in the developed world, affecting approximately 350,000 people in the United States and 1–2 million people worldwide [7, 11, 12, 17, 18]. Risk factors for developing MS include both genetic and environmental factors. Genetic factors include those that are familial, with first-degree relatives at 10–25 times increased risk of developing MS over the general population; ethnic, with whites having the greatest prevalence and near absence of the disease in Chinese; and sex related, with the disease being more common in women [19]. Environmental risk factors include history of positive Epstein-Barr virus serology, smoking history and geography, with a general trend of increasing latitude conferring increased risk of developing MS [19]. MS has the greatest incidence in Europe, North America, southern Australia, and New Zealand (prevalence rate of 30 or more per 100,000), with the country of origin persisting as a risk factor despite later migration to a region with a lower prevalence [3, 17, 19]. The reported protective effect of vitamin D in the prevention of MS may help explain the link between latitude and development of MS [limited evidence] [20].

Of the various clinical courses of MS, the relapsing-remitting type is the most common, representing approximately 85 % of cases, while progressive forms comprise the remaining 15 % [21]. Females are affected more frequently than males (ranging from 2:1 to 3:1) with a peak age of onset at 30 years [3, 9, 11, 22, 23]. Onset after the age of 55 is rare, with greatest proportion of cases presenting between 20 and 40 years of age. Females tend to have a younger age at disease onset, and the female preponderance over males declines with increasing age at initial diagnosis. Predominantly small, retrospective studies reporting the incidence of MS in the pediatric population estimate that 2.7–5 % of all MS patients have disease onset before the age of 16, while onset before the age of 10 is rare (0.2–0.7 %) [24, 25]. Over time, most cases of relapsing-remitting MS will convert to secondary progressive form, with a median of 19 years disease duration [9, 26]. Time between the first and second neurologic attacks has a mean of 6 years and median of 2 years [21]. The primary risk factor for conversion from the relapsing-remitting to secondary progressive forms is age at the time of disease onset, with more advanced age correlating with a shorter time to progression [27]. Females and those with a longer interval between the first and second neurologic attacks are more likely to experience a later evolution of the progressive phase [26]. Accumulative disability varies between individuals, with overall life expectancy only marginally reduced [21, 28].

ADEM is relatively uncommon with incidence in children less than 15 years of age reported to be 0.64/100,000 persons per year in a Japanese study between 1998 and 2003 [29]. Similar results were obtained in a San Diego County-based population with an incidence of 0.4/100,000 persons per year among individuals <20 years of age, with increased incidence in children aged 0–4 (0.6/100,000) and in children aged 5–9 (0.8/100,000) [30]. In contrast to MS, a slight male preponderance has been described with the mean age at presentation ranging between 5 and 8 years of age [31–34]. Seasonal variation has been reported with increased incidence in winter and spring months [31]. Long-term outcome is excellent with full recovery reported in 57–94 % [16, 35, 36].

Overall Cost to Society

The economic burden to society secondary to multiple sclerosis is substantial and based largely on loss of work capacity in younger individuals who are in the early phases of their careers [37]. The estimated annual combined direct and indirect costs of multiple sclerosis in the United States are $6.8 billion and in the United Kingdom, £1.2 billion [38, 39]. Physical disability impacts the ability to conduct activities of daily living and often necessitates skilled assistance. The need for hospitalization with disease exacerbations and the development and increased utilization of disease-modifying agents are directly related to increased costs of MS in the health-care system. The costs related to MS increase with disease progression. A cross-sectional cost-of-care study in patients with mild, moderate, and severe MS (grouped according to the Expanded Disability Status Score) revealed total 3-month cost estimates ranging from $1,928 to $5,678 in France, $2,772 to $5,701 in Germany, and $5,125 to $14,622 in the United Kingdom, with increased cost associated with greater disability [39]. In the United States, annual expenditures were reported as $7,677 per privately insured enrollee with MS versus $2,394 for all privately insured enrollees [40]. Asche et al. estimated the total mean 12-month all-cause costs were $18,829 for MS patients versus $4,038 for healthy comparisons, including higher rates of hospitalization, radiology services, ER, outpatient visits, and mean cost of $8,839 for use of an MS injectable drug [41].

Goals of Neuroimaging

- MRI is a sensitive paraclinical study (defined as a test that can identify a nonclinically evident lesion in the CNS) for detecting white

matter lesions that in the appropriate clinical context provides supporting evidence for predicting or confirming the diagnosis of multiple sclerosis (limited to moderate evidence). MRI is also useful to diagnose alternative pathology that could mimic a demyelinating disease (limited evidence).

- MRI can potentially help to differentiate ADEM from the first presentation of MS based not only on the initial distribution of lesions but also on follow-up imaging (insufficient evidence).
- MRI is used as a surrogate marker for evaluating disease progression (moderate to strong evidence), predicting cognitive and physical disability (limited evidence), and as an outcome measure in clinical trials.
- Advanced MR imaging techniques, likely the focus of future research, have contributed to our knowledge of the pathophysiology of MS and may correlate with disease relapse (moderate to strong evidence).

Methodology

A comprehensive MEDLINE search was performed using PubMed (National Library of Medicine, Bethesda, Maryland) for original research publications relating to the accuracy of test used to diagnose multiple sclerosis and acute disseminated encephalomyelitis performed between 1966 and December 2010. The search strategy employed different combinations of the following terms: *multiple sclerosis, acute disseminated encephalomyelitis, demyelinating disease, clinical criteria, imaging criteria, MRI, gadolinium enhancement, fMRI, DTI, spectroscopy, perfusion, CSF, oligoclonal bands, and evoked potentials*. Review of the reference lists of relevant papers identified additional articles. This review was limited to human studies and the English language literature. The authors performed initial reviews of the titles and abstracts of the identified articles followed by review of the full text in articles that were relevant.

Discussion of Issues

How Accurate Are the Diagnostic Criteria for Multiple Sclerosis?

Summary

There have been numerous studies investigating the diagnostic utility of MRI (conventional imaging techniques) in MS, most of which have provided limited strength of evidence that MRI improves diagnostic accuracy for this disease (limited evidence). Three reviews (two from expert groups and one systematic) of the available literature in 2003–2004 presented various conclusions (limited to moderate evidence) about the diagnostic accuracy of MRI or partly MRI-based diagnostic criteria, but all acknowledged that the clinical utility of MRI scanning in these patients involves more complex issues than basic measures of sensitivity and specificity (e.g., excluding other diseases, possibly facilitating earlier diagnosis, providing patient reassurance, providing a baseline for monitoring disease progression). MRI-based measures have been formally incorporated into the most widely accepted clinical diagnostic criteria for MS (Table 9.1); therefore, it seems unlikely that future strong or moderate evidence studies of the diagnostic accuracy of MRI will be performed in the future.

Supporting Evidence

No single clinical or diagnostic test is sufficient to establish the diagnosis of multiple sclerosis. Evaluation requires both detailed clinical history and neurologic examination with objective evidence of demyelinating lesions involving the CNS. Because it is not feasible to have histologic confirmation to definitively diagnose patients suspected of having MS, various diagnostic models have evolved over the past several decades. While the criteria have changed over time, certain features among the various iterations have remained constant including (1) the diagnosis of multiple sclerosis can be based solely on clinical evidence of demyelinating lesions involving the CNS and (2) the diagnosis

requires that there is no better alternative explanation of the patient's signs and symptoms [4]. A hallmark of clinically definite MS is that lesions are disseminated in time and space. While this characteristic feature can be ascertained by clinical history and evaluation, patients presenting initially with a clinically isolated syndrome (CIS) have some delay until the second neurologic attack. In one of the longest follow-up studies of patients with optic neuritis, the estimated 15-year risk of developing MS was 40 % (95 % CI 31–52 %) with 60 % of patients diagnosed with MS within 3 years from onset of optic neuritis [42]. A definitive diagnosis of MS is desirable after this first neurologic episode since the institution of early therapy with disease modifying treatment can delay the onset of future attacks [moderate to strong evidence] [43–46].

Criteria established by Poser et al. in 1983 were the reference standard for diagnosing MS for nearly 20 years and were applied not only to clinical practice but also to experimental trials as inclusion criteria (e.g., by which other tests were evaluated). The criteria included categories of (1) clinically definite MS, (2) laboratory-supported definite MS (dependent on CSF analysis for oligoclonal bands/increased IgG), (3) probable MS (supported by clinical or laboratory evidence), and (4) possible MS [47]. Because MRI was relatively new at this time, Poser classified it as a supporting paraclinical study, but no specific imaging criteria were described. Inconsistencies exist among even neurologists in differentiating clinical symptoms caused by one or more separate lesions in the CNS, potentially misclassifying patients with clinically definite MS [48]. While clinical diagnosis of MS remains the gold standard for diagnosis, inherent inconsistencies in clinical evaluation support the use of paraclinical studies to aid in the diagnosis of MS [48, 49].

Multiple studies have suggested that MRI is a valuable paraclinical test to demonstrate anatomic evidence of discrete lesions separated in space at the time of initial clinical presentation (Table 9.2). Paty et al. reported a high sensitivity of MRI in detecting T2 signal abnormalities in patients with clinically definite MS, although a study by Lee et al. demonstrated a relatively low specificity when followed prospectively (57 %) [49, 50]. Fazekas et al. applied retrospective criteria to review patients with an established diagnosis of MS in order to improve specificity (100 %); however, specificity decreased when applied to subsequent prospective studies [51, 52]. Tas et al. demonstrated that contrast enhancement of white matter lesions improves specificity (80 %) in diagnosing multiple sclerosis [52]. Furthermore, because enhancement of an MS lesion may be visible for 2–8 weeks, MRI can establish dissemination in time even at the initial clinical presentation by virtue of identifying both new (enhancing) and old (non-enhancing) lesions on a single study [52, 53].

McDonald et al. updated the Poser criteria in 2001 to include MRI specific imaging-based criteria [43, 54, 55]. The MRI criteria adopted by McDonald were established largely based on data from Barkhof et al. and Tintore et al., which showed improved specificity of MRI, particularly with inclusion of enhancement criteria [52, 54–56]. Dalton et al. validated the use of the McDonald criteria in clinical settings with reasonably good sensitivity (83 %), specificity (83 %), positive predictive value (75 %), and negative predictive value (89 %) for predicting development of clinically definite MS at 1 year with an overall accuracy of 83 % at 3 years [57].

While MRI is a major component in the current diagnostic algorithm for MS, several reviews have been recently published on the utility of MRI in diagnosing suspected MS. In 2003, Frohman et al. presented a review and recommendations undertaken by the Therapeutics and Technology Assessment Subcommittee of the American Academy of Neurology, based upon their review of the literature to date [58]. Based upon this group's review of the literature (in which they found serious concerns about the validity of some study results), they concluded that there was strong evidence that, in patients with CIS, the presence of three or more T2 WM lesions is a sensitive predictor (>80 %) of the development of MS within the next 7–10 years. Other imaging-based features that they

concluded were predictive included two or more enhancing lesions at baseline and new T2 lesions or enhancing lesions three or more months after the CIS episode. Miller et al. in 2004 presented the review and recommendations of the European Magnetic Resonance in MS Group, which they based on the available literature at that time, in which they focus especially on limitations of the McDonald 2001 criteria [59]. They conclude that longer term follow-up studies suggest that the presence of T2 lesions in CIS does not guarantee the development of MS but that MRI can provide a more accurate prediction of the likelihood of MS. Following these two reviews, a systematic review by Whiting et al. concluded that MRI is a relatively poor test for either ruling in or ruling out MS and the disease remains predominantly a clinical diagnosis, suggesting that previous studies have not focused on the more relevant question of what added value MRI has in diagnosing MS compared with history and clinical examination alone [60]. Nevertheless, in 2005, the McDonald criteria were revised specifically to provide clarification of MRI criteria in order to show dissemination in time and for spinal cord lesions [61] (Tables 9.1, 9.3). Though these revised criteria have not been prospectively validated formally, a recent expert panel included a consensus statement that MRI has an important role in the diagnosis of MS and a recommendation for adopting protocols and reporting based on the revised McDonald criteria [62].

Despite the widespread acceptance of the McDonald criteria to diagnose adult MS, its validity in children with possible MS has been called into question. In a retrospective cohort study by Hahn et al., a significant number of children with MS did not meet established McDonald criteria for diagnosis, with dissemination in space criteria only met in 53 % of children at the time of their first neurologic attack and in 67 % of children at the time of their clinical MS defining attack [63]. Potential explanations for reduced sensitivity of the McDonald criteria in children include inherent age-related differences in disease pathology with shorter time for accrual of clinically silent white matter lesions,

age-related differences in lesion distribution, or differing reparative mechanisms in children limiting overall lesion burden [64]. While evidence evaluating the McDonald criteria in children with MS is limited, a subsequent consensus report by the International Pediatric MS Study Group in 2007 used the McDonald MRI criteria to define a diagnosis of pediatric MS [65]. In 2009, a retrospective cohort study by Callen et al. proposed pediatric modifications to the McDonald criteria including at least two of the following: (1) total of five or more T2 lesions, (2) two or more periventricular lesions, and (3) one or more brain stem lesions [64]. These criteria yielded improved sensitivity compared to McDonald criteria (85 % vs. 76 %, respectively) and similar specificity (98 % vs. 100 %) but have not been prospectively validated [64].

CSF analysis is another paraclinical test used in the diagnosis of MS. Typical abnormalities include the presence of oligoclonal bands and increased IgG synthesis in the CSF. CSF analysis is also important for excluding other infectious or inflammatory disorders that could mimic MS, or to confirm MS when clinical evaluation and MRI are inconclusive (limited evidence). Jin et al. showed that detection of oligoclonal bands is a prognostic marker (hazard ratio = 5.39, 95 % CI 1.56–18.61) for the development of clinically definite MS in patients initially presenting with optic neuritis (moderate evidence) [66]. However, CSF analysis may be normal in 30 % of patients early in MS [11]. Tintore et al. demonstrated greater specificity (70 %, CI 0.61–0.79 vs. 43 %, CI 0.34–0.52) and accuracy (69 %, CI 0.6–0.78 vs. 52 %, CI 0.43–0.61) for Barkhof's MRI criteria when compared to oligoclonal bands for predicting conversion to clinically definite MS in patients initially presenting with an isolated syndrome (moderate evidence) [67]. Both oligoclonal bands and MRI had similar negative predictive values, 88 % and 87 %, respectively. However, the greatest specificity (77 %, CI 0.69–0.85) and accuracy (73 %, CI 0.65–0.81) were achieved when both MRI criteria and oligoclonal bands were used together, which more closely mirrors common clinical practice.

Evoked potentials are another paraclinical study traditionally used in the diagnosis of MS, with the most common being visual (VEP), brain stem auditory (BAEP), and sensory (SEP). Alterations in conduction pathways due to demyelination cause slowing of electrical activity. The VEP is the most valuable measure and can detect subclinical evidence of optic nerve involvement, particularly at the onset of a clinically isolated optic neuritis [4]. Various studies have demonstrated sensitivity of VEP ranging from 26 % (odds ratio 0.6, CI 0.2–1.6) to 72 % (odds ratio 0.9, CI 0.3–2.2) with specificities of 25 % (odds ratio 0.9, CI 0.3–2.2) to 77 % (odds ratio 2.9, CI 0.8–10.8) [43]. However, data from evidence-based reviews do not substantiate the inclusion of evoked potentials in MS diagnostic criteria (moderate evidence) [43, 68].

Can Clinical and MRI Studies Differentiate ADEM from the First Initial Onset of MS?

Summary
There is insufficient evidence to suggest that MRI findings can distinguish ADEM from MS (insufficient evidence).

Supporting Evidence
Unlike for the diagnosis of MS, there are no established clinical criteria used as a reference standard in the diagnosis of acute disseminated encephalomyelitis. The diagnosis of ADEM is generally presumptive based on excluding disease mimickers by means of clinical history, neurologic evaluation, neuroimaging findings, and CSF analysis, with the differential diagnosis primarily including an acute viral encephalitis or MS [14, 30]. Characteristically, ADEM is a monophasic demyelinating process with clinical findings usually occurring within weeks (mean latency 2 weeks) following an infection or vaccination, or symptoms may occur spontaneously [33, 69]. A clinical relapse in patients with ADEM which is thought to be related to the initial demyelinating event is termed multiphasic disseminated encephalomyelitis (MDEM); however, if the demyelinating events are separated in time and space, a diagnosis of MS is made. In the absence of a clearly definable preceding cause typical for ADEM, differentiation between the onset of MS and ADEM becomes a clinical conundrum with significant implications for long-term prognosis and for instituting immunomodulating therapy [34].

Certain clinical features may help differentiate ADEM from MS. Patients with ADEM commonly present with encephalopathy including headache, vomiting, drowsiness, and meningismus, which are uncommon in MS [33, 69]. Seizures may be seen in 13–35 % of patients with ADEM, whereas seizures are rare in MS [69]. Alteration in consciousness is more common in ADEM (45–75 %) versus MS (13–15 %) [69]. Patients with ADEM are more often polysymptomatic (reported as high as 91 %) versus a more typical monosymptomatic presentation of MS (62 %) [35].

There is significant overlap between the MR imaging findings of ADEM and MS. The most common imaging findings of ADEM are areas of abnormal high T2 signal in the supratentorial white matter, basal ganglia, brain stem, cerebellum, and spinal cord. A longitudinal observational study of 48 children presenting with one or more episodes of demyelination by Dale et al. demonstrated a greater propensity for periventricular distribution with MS compared to ADEM, whereas ADEM had a greater propensity for involvement of the thalamus and basal ganglia (Table 9.4) [35]. A retrospective review by Murthy et al. demonstrated lesion distribution similar to Dale's findings in 18 patients with ADEM [33].

In a cohort study, Mikaeloff et al. defined a brain MRI suggestive of ADEM when lesions were indistinct and also involved the thalamus and/or basal ganglia, while an MRI suggestive of MS showed multiple well-delineated lesions with periventricular and/or subcortical involvement [70]. In this study, MRI criteria suggestive of MS accurately diagnosed 57 % of patients diagnosed with clinically definite MS, while only 11 % of patients with MRI criteria

suggestive of ADEM were ultimately reclassified as having clinically definite MS [70]. A different cohort study by Mikaeloff et al. used MRI findings to predict the likelihood of a second neurologic attack following an initial demyelinating episode, revealing that lesions oriented perpendicular to the long axis of the corpus callosum and/or the presence of well-defined lesions were very specific criteria (100 %), but not as sensitive (21 %) as Barkhof's MS criteria in predicting a second neurologic attack [71]. A retrospective review by Callen et al. reviewed MRI exams at the time of initial presentation in 28 children subsequently diagnosed with MS and 20 children diagnosed with ADEM [72]. Based on Callen's analysis, diagnostic criteria predicting progression to clinically definite MS included any two of the following: (1) two or more periventricular lesions, (2) presence of T1 black holes, and (3) absence of diffuse and bilateral lesion distribution, resulting in 81 % sensitivity, 95 % specificity, 95 % positive predictive value, and 79 % negative predictive value.

Two retrospective observational studies have suggested that lesion size is a poor discriminator between MS versus ADEM with both small (less than 1.0 cm) and large (greater than 2.0 cm) lesions identified in both entities [69, 72]. Overall lesion number also does not differentiate ADEM versus MS, although in ADEM, lesions are often more asymmetric [72]. Both MS and ADEM lesions show contrast enhancement [73]. Case reports have suggested that restricted diffusion in lesions of patients with ADEM was associated with poor clinical outcome based on the presence of cytotoxic edema; however, subsequent reports have not substantiated these findings [74, 75]. Spinal cord lesions in ADEM have been reported as usually larger than in MS, associated with cord swelling, and more commonly present in the thoracic cord, while MS lesions are more common in the cervical cord [69]. Follow-up imaging is helpful to establish complete (37 %) or at least partial (53 %) resolution of initial MRI abnormalities in ADEM, whereas in MS, new lesions can often be expected [35].

According to the longitudinal study by Dale et al., CSF analysis in ADEM typically shows evidence of inflammation with increased protein (60 %) and lymphocytosis (64 %), while intrathecal oligoclonal bands were entirely absent in 47 % of ADEM patients studied [35]. In contrast, CSF analysis in patients with MS showed that 82 % had evidence of intrathecal oligoclonal bands at some point during their course, though in their study, there was not a statistically significant difference in the detection of CSF oligoclonal bands in ADEM versus MS [35]. A summary of significant differentiating features of ADEM versus MS based on this study can be found in Table 9.5.

Do Conventional MRI Sequences Correlate with or Predict Disease Progression and Acquired Disability in Multiple Sclerosis?

Summary

Multiple observational studies have yielded inconsistent results with regard to the correlation between MRI-based measures and cognitive performance or EDSS scores (limited evidence). However, some of the MRI-based measures have been used in recent clinical trials of new treatments for MS, with results suggesting that these imaging-based measures – particularly the number of new T2 lesions and number of enhancing lesions – may correlate with both relapse rates and risk of disability progression (moderate to strong evidence).

Supporting Evidence

The majority of patients presenting initially with a clinically isolated syndrome (CIS) suggestive of multiple sclerosis will go on to develop clinically definite MS. Studies that have supported the use of the McDonald criteria and subsequent revision to predict the development of MS at the time of first clinical onset have been based on the presence of T2-weighted signal abnormalities and T1-weighted enhancing lesions [61]. MRI is an established paraclinical study to diagnose MS and is supported by long-term longitudinal studies revealing that up to 88 % of patients with a CIS and abnormal T2 lesions on MRI at the

time of presentation may develop MS [76, 77]. MRI is also used to predict the natural history of patients with MS and as a measure of clinical disability; however, the association between degree of MRI abnormalities and development of disability is relatively weak [45, 46, 78, 79].

Conventional T2-weighted MRI is highly sensitive for detecting demyelinating lesions disseminated in the CNS at the time of a CIS and also reveals clinically silent lesions between relapses [80]. However, T2 lesions lack specificity, and similar appearing lesions may be caused by inflammation, gliosis, edema, or axonal loss due to other pathologic entities [78, 81]. Despite the lack of specificity, the number and volume of T2 lesions have been used as a surrogate marker for clinical disability. Brex et al. demonstrated that the volume of T2 lesions acquired in the first 5 years following a CIS shows only moderate correlation with long-term disability at 14 years ($r = 0.45$) as measured by the expanded disability status score (EDSS), concluding that the T2 lesion volume alone may not be an adequate marker for instituting therapy with disease-modifying agents [77, 82]. Filippi et al. found a weak correlation between EDSS and the number of new ($r = 0.13$) and enlarging ($r = 0.18$) T2 lesions [83]. Tintore et al. demonstrated a moderate correlation between EDSS at year 5 and the number of T2 lesions at baseline as well as the number of Barkhof criteria fulfilled ($r = 0.40$ and $r = 0.46$, respectively) [84]. Because the EDSS is weighted more heavily toward motor dysfunction, Riahi et al. not unexpectedly demonstrated a slightly greater correlation between EDSS and T2 lesions specifically involving the corticospinal tracts ($r = 0.67$) versus overall T2 volume load ($r = 0.60$) [85]. Minneboo et al. evaluated the significance of T2 lesion location in order to predict EDSS score progression and found that 2 or more infratentorial lesions were the best predictor for disability (hazard ratio, 6.3) [86]. A 20-year follow-up study again demonstrated only moderate correlation between T2 lesion volume at all time points and disability by EDSS (r range $= 0.48$ to 0.67) [87]. Unlike the moderate correlation demonstrated by the preceding authors, the Optic

Neuritis Study Group found no correlation between baseline MRI and disability at 10 years of follow-up in patients with a CIS presenting with optic neuritis [88]. Foong et al. also found no correlation between T2 lesion load and physical disability based on the EDSS, but lesion load did correlate with various neuropsychological and cognitive scores [89].

Gadolinium enhancement reflects blood–brain barrier breakdown and serves as a marker for the active, inflammatory phase of MS lesions. Enhancing lesions can precede new T2 lesions by hours or days [90]. Most enhancing lesions persist for 2–6 weeks, but are rare beyond 6 months [91, 92]. He et al. demonstrated that enhancing lesions are most commonly small with a nodular pattern of enhancement (68 %), while 23 % show ring-like enhancement, and 9 % showed neither of these patterns (arc-like) [91]. The presence of a single enhancing lesion on baseline MRI has been positively correlated with subsequent relapse in the following 6 months; however, most newly enhancing MRI lesions are clinically silent [92, 93]. A small study by Molyneux et al. found no correlation between the presence of newly enhancing lesions and changes in EDSS [94]. A meta-analysis by Kappos et al. in 1999 also concluded that while enhancing lesions on MRI predict subsequent relapses, enhancement is not a strong predictor for developing disability [95].

A number of T2 hyperintense MS lesions (5–20 %) will appear hypointense to normal-appearing gray matter on T1-weighted sequences [96]. In the acute phase, the T1 hypointensity may reflect elements of edema related to inflammation and demyelination, with subsequent normalization of isointense T1 signal as the inflammation resolves and as remyelination may ensue. Chronic T1 "black holes" are thought to reflect more severe injury with greater loss of axonal density than T1 lesions that are not hypointense [97]. Chronic black holes are defined by their persistence for at least 6 months, but in the absence of serial examinations for comparison, a T1 black hole is assumed by the lack of associated contrast enhancement [96, 98]. Various studies have evaluated progressive

whole-brain or central cerebral atrophy associated with an increased volume of T1 black holes, which may contribute to worsening cognitive and physical decline [99]. Paolillo et al. found a significant correlation between T1 hypointense lesion load and supratentorial brain volume ($r = 0.48$), but not with T2 hyperintense lesion load [100]. Bermel et al. found that brain parenchymal fraction was lower in patients with MS and correlated inversely with T1 hypointense lesion volume, but not T2 lesion volume [101]. Conversely, Rudick et al. found no correlation with measurable progressive whole-brain atrophy and clinical manifestations [102].

Despite the sometimes inconsistent findings on these multiple observational studies (predominantly providing limited strength of evidence), multiple investigators have utilized MRI parameters in prospective clinical trials of various medications used in the treatment of MS. Trials involving interferon beta-1b and interferon beta-1a have generally failed to show the expected correlation of MRI measures and treatment effects [103–106]; however, trials of newer treatments have shown more promising results. Using imaging data from an RCT evaluating the efficacy of treatment with glatiramer acetate (GA), Filippi et al. found that the relapse rate was 33 % lower in GA-treated patients compared with placebo patients [107]. MRI findings correlated with clinical findings in this study, with a significant decrease in the number of new T2 lesions, the number of new enhancing lesions, and the percentage of new T2 lesions that evolved into T1 black holes in GA-treated patients compared with placebo patients [107, 108]. Large RCTs involving oral fingolimod as a treatment for MS have provided evidence that MRI parameters correlate with clinical endpoints of disease activity in clinical trial settings. Kappos et al. found that the annualized relapse rate was 0.77 in the placebo group, as compared with 0.35 in the lower dose fingolimod-treated group and 0.36 in the higher dose fingolimod group, and also found a corresponding decrease in the median number of enhancing lesions on MRI in the fingolimod groups compared with the placebo group [109]. In testing the efficacy of fingolimod

compared with interferon beta-1a, Cohen et al. in a large RCT found that fingolimod treatment was associated with lower relapse rates, fewer new T2 lesions, and fewer enhancing lesions compared with interferon beta-1a treatment [110]. In a 2-year double-blind RCT, Kappos et al. found that relapse rate, risk of disability progression, number of new T2 lesions, and number of enhancing lesions were all decreased in the fingolimod group compared with the placebo group [111].

Do Advanced Imaging Techniques Offer Clinical Utility over Conventional MRI in Evaluating MS Patients?

Summary

There is insufficient evidence to suggest that advanced MRI techniques improve the accuracy of MRI in diagnosing MS (insufficient evidence). Table 9.6 summarizes areas of research in which advanced MRI techniques may yet prove to be useful. Studies involving advanced techniques have to date largely contributed to a better understanding of the pathophysiology of the disease and have provided direction for future research; Table 9.6 summarizes areas in which early research has suggested potential usefulness beyond pathophysiology. Few of these techniques have been used in recent clinical trials, but one RCT has shown that rate of cerebral atrophy (by semiautomated volumetric MRI-based measurement) correlates with relapse rate (moderate to strong evidence). There is insufficient evidence of the effectiveness of these techniques in improving the clinical care of MS patients (insufficient evidence).

Supporting Evidence

There has been much interest in the use of advanced MRI techniques in the setting of MS, including especially magnetization transfer (MT), diffusion-weighted (DWI) or diffusion tensor imaging (DTI), volumetric measurements, MR spectroscopy (MRS), and perfusion imaging. However, there have not been studies that have evaluated the effect of these techniques on the

accuracy of MRI in diagnosing MS. Rather, most studies have attempted to use advanced MRI techniques to better understand the pathophysiology of the disease, to predict prognosis, or to monitor response to therapy.

Magnetization transfer (MT) imaging is a technique based on the magnetization interaction between bulk water protons and macromolecular protons so that diseased tissues with altered protein-water interactions become more conspicuous with MT technique [112]. Most studies utilizing MT imaging have contributed to an improved understanding of the pathophysiology of MS. Some studies have been more clinically focused, however, with most providing limited evidence given study design issues. In a 5-year study, Pike et al. found that a decline in MT ratio was present not only within T2 lesions in MS patients but also in areas in normal-appearing white matter (NAWM) that later became focal lesions, with the MT ratio abnormalities being detectable up to 18 months before the lesions appeared on T2-weighted images [113]. Cercignani et al. found that MT ratio metrics were lower in NAWM in MS patients compared with NAWM in healthy controls, finding similar MT ratio metric differences in normal-appearing gray matter (NAGM) in MS patients compared with healthy controls. Summers et al. found that MT ratio in NAWM in MS patients predicts cognitive decline over 5 years in relapsing-remitting multiple sclerosis (RRMS) [114]. However, different studies have shown inconsistent results with regard to correlations between MT ratio metrics and disease-related disability [115–118].

Diffusion and DTI techniques have been widely used in research involving MS patients, with Ge et al. providing an inclusive review of interesting findings as of 2005 [119]. Most have been small studies (limited evidence) that have sought to contribute to an improved understanding of the pathophysiology of MS. Multiple investigators have found that plaque-like T2 lesions in MS patients have increased mean diffusivity (MD) compared with NAWM in patients and healthy controls [120–126]. Multiple studies have suggested that NAWM in MS patients shows increased MD and decreased fractional anisotropy (FA) compared with NAWM in healthy controls [124, 125, 127–133]. In two very small observational studies (limited evidence), investigators found some evidence that either diffusivity or ADC changes preceded development of gadolinium-enhancing focal lesions [129, 134]. Multiple studies have shown differences in diffusion-based measures by disease phenotype [123, 135–139]. One of the larger of these focused on GM involvement, finding that GM diffusivity was not different between controls and patients with RRMS, but finding that diffusivity was different between RRMS and SPMS, and between SPMS and PPMS [136]. Recent studies have found correlations between diffusion-based measures and contemporaneous measures of cognitive performance or disability [140, 141]. A prospective observational study of RRMS patients being treated with GA found that there were decreases in MD and entropy in patients at 2 years compared with baseline measures [142].

Although not based on advanced acquisition techniques, *volumetric measurements* have been investigated as a newer post-processing method (i.e., automated or semiautomated) that might be useful in MS patients, given the common clinical finding of global atrophy in these patients. Multiple investigators have found correlations between atrophy measures by MRI and disease disability or disease progression in MS patients [143, 144], with several finding that measures of GM atrophy correlate better than measures of WM volume or lesion load [145–148], and some finding that T1 hypointense lesion volume correlates with clinical disability [149, 150]. A few longitudinal studies have found that various volumetric measures may actually predict future disease progression, but these methods have not been tested prospectively (limited to moderate evidence). Summers et al. found that global atrophy rate over the first year from baseline as well as T1 lesion volume at baseline could predict cognitive decline over 5 years in RRMS patients [114]. Horakova et al. found that percent

brain volume change as early as 6 months could predict clinical progression versus stability in RRMS over 5 years and that GM volume loss in the first 24 months predicted disability progression over 5 years [151]. Lukas et al. suggested that the rate of ventricular enlargement could predict disease progression after medium term follow-up in early MS [99]. In the 2-year double-blind RCT by Kappos et al., the rate of atrophy was found to be lower in those treated with fingolimod compared with the placebo group; the fingolimod-treated group also showed decreased relapse rates and risk of disability progression [111].

MR spectroscopy (MRS) has also been fairly widely used in research settings involving MS patients. Various investigators have sought to find a relationship between decreased NAA or NAA/Cr ratio and T2 lesions or NAWM or disability measures; results have been inconsistent across studies [133, 152–158]. Saindane et al. found that metabolite profiles of high-grade gliomas and tumefactive MS lesions were similar overall, with central NAA/Cr ratio being somewhat lower in high-grade gliomas [159].

MR perfusion imaging techniques have been tried in recent years in MS research. Law et al. found decreased perfusion and prolonged MTT in lesions and NAWM in MS patients compared with controls and found that enhancing lesions showed highly variable CBV [160]. Subsequent studies have found variable-decreased CBF and/or CBV in NAWM, lesions, and GM of patients compared with controls, suggesting that perfusion abnormalities may exist in a continuum beginning in WM and spreading to GM with disease progression [161, 162]. However, these techniques have not been tested prospectively (limited evidence).

Take-Home Tables

Table 9.1 summarizes the combined MRI and clinical criteria established for the 2005 "McDonald Revisions," which is currently the most widely used diagnostic paradigm for MS.

Table 9.2 summarizes the sensitivity and specificity of conventional MRI criteria used in diagnosing clinically definite multiple sclerosis. Table 9.3 summarizes the criteria required by MRI to establish dissemination in time of MS lesions, according to the 2005 "McDonald Revisions." Table 9.4 summarizes the common distribution of lesions in ADEM/MDEM versus MS as reported by Dale et al. Table 9.5 summarizes differentiating features between ADEM/MDEM and MS clinical presentations based on data by Dale et al. Table 9.6 summarizes the potential areas of clinical usefulness of advanced MRI techniques.

Imaging Case Studies

Case 1: Typical MRI Findings of Multiple Sclerosis (Fig. 9.1a–e)

History: A 34-year-old female diagnosed with multiple sclerosis 4 years earlier now presenting with worsening gait. Patient has had multiple hospitalizations and treatment with IV steroids, currently managed with monthly natalizumab.

Case 2: Enhancing MS Lesions with Resolution at Follow-Up (Fig. 9.2a–d)

History: A 48-year-old female with 10-year history of relapsing-remitting MS currently managed on interferon beta-1a.

Case 3: Acute Disseminated Encephalomyelitis (Fig. 9.3a–c)

History: A 4-year-old male presented to the Emergency Department with seizure and history of recent fever and leukocytosis.

Case 4: Tumefactive Multiple Sclerosis (Fig. 9.4a–e)

History: A 38-year-old female with 9-year history of relapsing-remitting MS, now with rapidly worsening left hemiparesis and hemianesthesia. Patient was treated with intravenous steroids and plasmapheresis during hospitalization. Due to aggressive nature of patient's MS, she was started on injectable mitoxantrone for therapy.

Table 9.1 2005 McDonald criteria for diagnosing multiple sclerosis

MR imaging criteria	Clinical presentation	Additional data for diagnosis
1. Requires three of the following: (a) At least 1 gadolinium-enhancing lesion or 9 T2 hyperintense lesions if there is no gadolinium-enhancing lesion (b) At least 1 infratentorial lesion (c) At least 1 juxtacortical lesion (d) At least 3 periventricular lesions Note: A spinal cord lesion can be considered equivalent to a brain infratentorial lesion: An enhancing spinal cord lesion is considered to be equivalent to an enhancing brain lesion, and individual spinal cord lesions can contribute together with individual brain lesions to reach the required number of T2 lesions	1. Two or more attacks; objective evidence of ≥2 lesions 2. Two or more attacks; objective evidence of 1 lesion 3. One attack; objective clinical evidence of ≥2 lesions 4. One attack; objective clinical evidence of 1 lesion (monosymptomatic presentation; CIS) 5. Insidious neurologic progression suggestive of MS	1. None 2. Dissemination in space, demonstrated by: (a) MRI *or* (b) ≥2 MRI-detected lesions consistent with MS plus positive CSF *or* (c) Await further clinical attack implicating different site 3. Dissemination in time, demonstrated by: (a) MRI *or* (b) Second clinical attack 4. Dissemination in space, demonstrated by: (a) MRI *or* (b) ≥2 MRI-detected lesions consistent with MS plus positive CSF *and* (c) Dissemination in time, demonstrated by MRI *or* (d) Second clinical attack 5. One year of disease progression (retrospectively or prospectively determined) *and* two of the following: (a) Positive brain MRI (9 T2 lesions or ≥4 T2 lesions with positive VEP) (b) Positive spinal cord MRI (2 focal T2 lesions) (c) Positive CSF

Reprinted with permission from [61]

Table 9.2 Sensitivity and specificity of conventional MR imaging in diagnosing clinically definite multiple sclerosis

Author	No. of patients	Sensitivity (%)	Specificity (%)	Comments	Quality of study
Paty et al. [49]	200	94	57	Prospective, lesions classified as hyperintense on T2WI and at least 3 mm in size; strongly suggestive of MS defined by total # of 4 white matter lesions or 3 lesions, one of which is periventricular	Limited evidence
Fazekas et al. [51]	91	88	100	Retrospective review; defined by 3 lesions with at least two of following criteria: (1) infratentorial lesion, (2) periventricular lesion, or (3) a lesion >6 mm	Limited evidence
Tas et al. [52]	57	59	80	Prospective at 1st presentation; criteria defined as at least 1 enhancing and 1 non-enhancing lesion	Moderate evidence
Barkhof et al. [55]	74	82	78	Criteria defined by three of the four following findings: (1) 1 gadolinium-enhancing lesion or 9 T2 hyperintense lesions, if there is no gadolinium-enhancing lesion, (2) at least 1 infratentorial lesion, (3) at least 1 juxtacortical lesion, and (4) at least 3 periventricular lesions	Limited evidence

Table 9.3 Establishing dissemination in time

2005 MRI criteria requires the following
1. Detection of gadolinium enhancement at least 3 months after the onset of the initial clinical event, if not at the site corresponding to the initial event
2. Detection of a *new* T2 lesion if it appears at any time compared with a reference scan done at least 30 days after the onset of the initial clinical event

Reprinted with permission from [61]

Table 9.5 Differentiating features between ADEM/MDEM and MS clinical presentations

Finding	ADEM/MDEM (%)	MS (%)
Prodromal illness	74	38
Polysymptomatic presentation	91	38
Encephalopathy	69	15
Seizure	17	0
Serum pleocytosis	64	22
Periventricular WM lesions on MRI	44	92

Data from [35]

Table 9.4 Distribution of lesions in ADEM/MDEM versus MS

	ADEM/MDEM (%)	MS (%)
Periventricular WM	44	92
Deep and subcortical WM	91	92
Brainstem	50	56
Thalamus	41	25
Basal ganglia	28	8
Spinal cord	28	25

Data from [35]

Table 9.6 Potential clinical usefulness of advanced MRI techniques

MRI Technique	Potential clinical usefulness	Strength of evidence
MT	Predicting cognitive decline	Limited
DWI/DTI	Distinguishing phenotypes, correlating with cognitive decline/disability	Limited
Volumetrics	Predicting disease progression/cognitive decline, correlating with treatment response	Limited to moderate
MRS	Correlating with disability	Limited
Perfusion	Correlating with or predicting disease progression	Limited
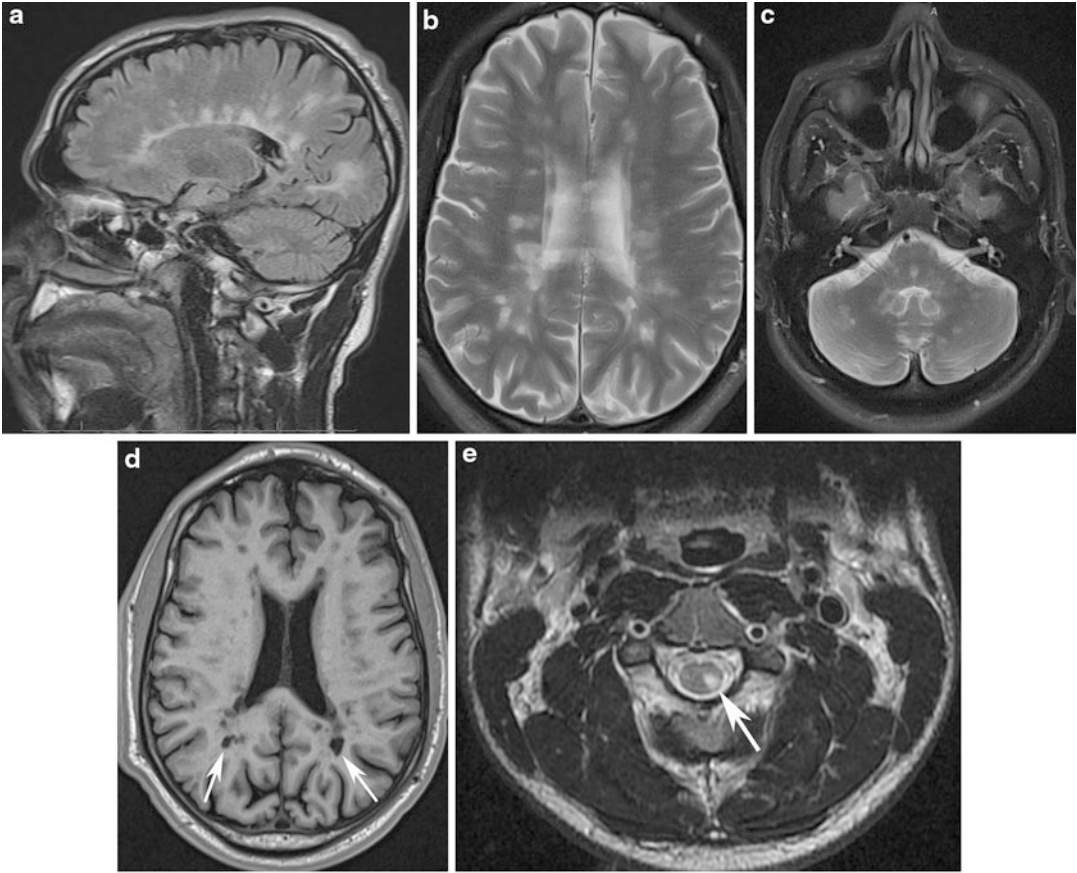
Fig. 9.1 (**a–e**) Paramidline sagittal FLAIR (**a**) shows numerous abnormal hyperintense lesions in the pericallosal white matter, many of which have an ovoid configuration radiating away from the ventricular margin. Axial T2 sequences demonstrate numerous round and ovoid hyperintense lesions in the supratentorial (**b**) and infratentorial (**c**) white matter with involvement of the corpus callosum, pons, and cerebellar white matter. Axial T1 FLAIR (**d**) shows multiple "T1 black holes" (*arrows*). Axial T2 of the cervical spine (**e**) reveals a hyperintense lesion in the left dorsolateral aspect of the cord (*arrow*)
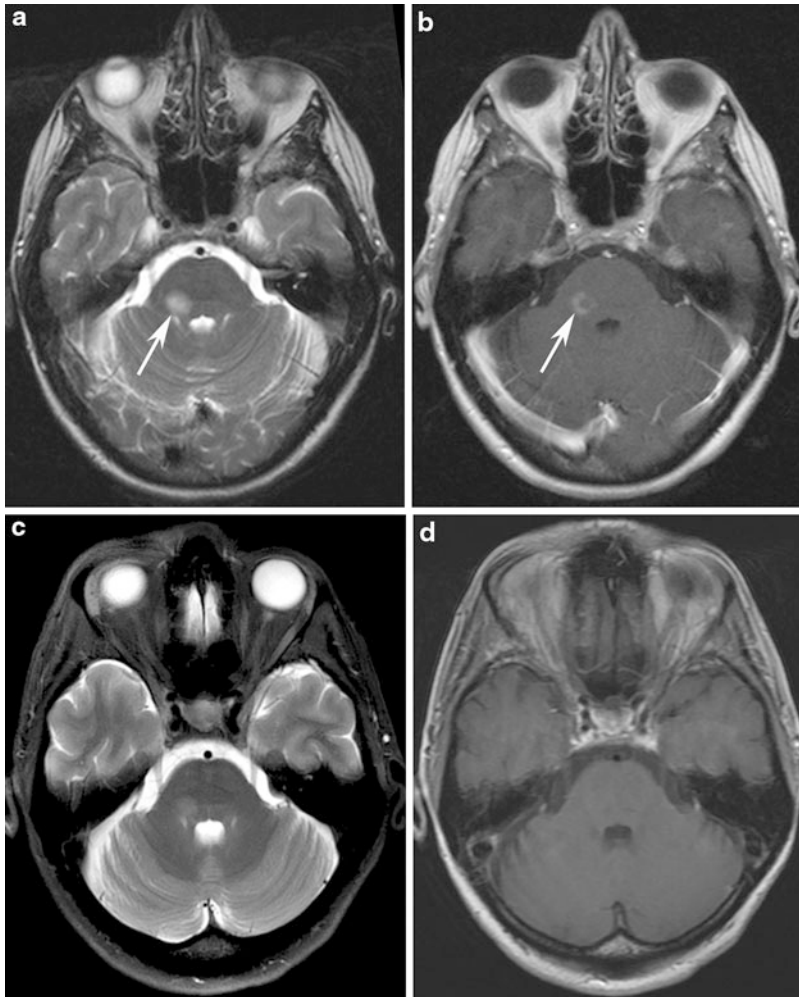
Fig. 9.2 (**a–d**) Axial T2 at the level of the brainstem (**a**) demonstrates globular hyperintense signal in the posterior right pons (*arrow*). Accompanying postcontrast T1 (**b**) shows corresponding incomplete ring enhancement (*arrow*). Follow-up MRI 4 weeks later shows residual, but improved T2 hyperintensity (**c**) and complete resolution of enhancement (**d**)
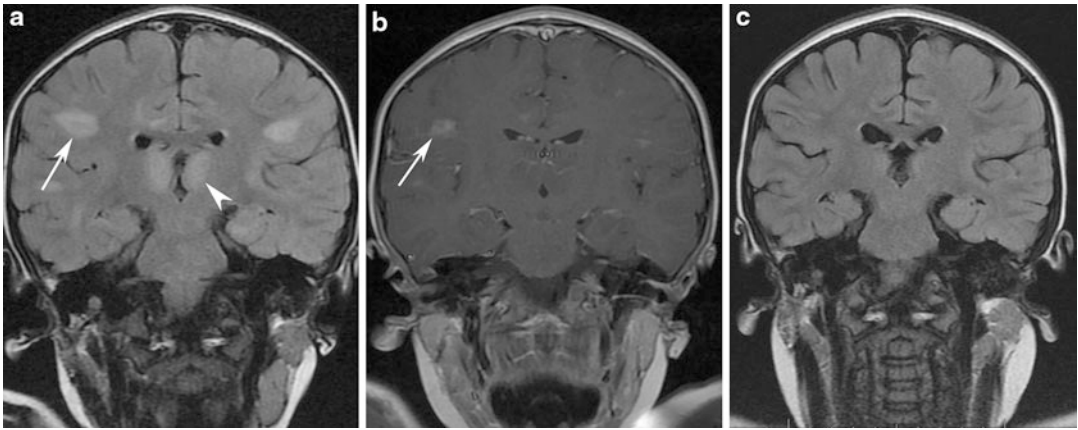
Fig. 9.3 (**a–c**) Coronal FLAIR (**a**) demonstrates multiple hyperintense lesions within the subcortical white matter (*arrow*) and involving the thalamus bilaterally (*arrowhead*). Postcontrast coronal T1 (**b**) shows enhancement of some of these lesions, with the largest irregular focus of enhancement in the right parietal white matter (*arrow*). Coronal FLAIR (**c**) obtained 5 weeks later after course of intravenous and oral steroids shows resolution of previous regions of hyperintense signal abnormality with no residual neurologic sequelae
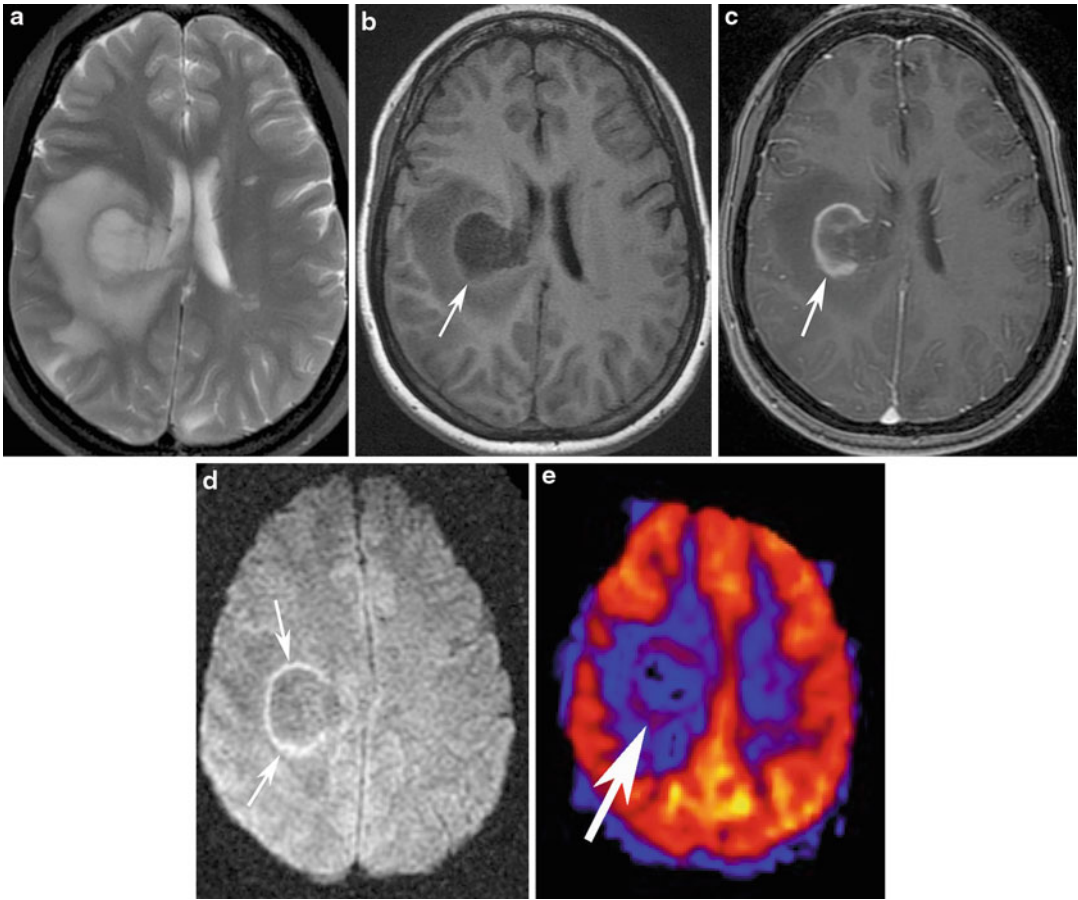
Fig. 9.4 (**a–e**) Axial T2 (**a**) demonstrates large mass-like hyperintense lesion in the posterior right frontal white matter abutting the ventricular margin. Axial T1 FLAIR (**b**) at the same level shows marked central hypointensity (*arrow*). Postcontrast T1 (**c**) shows incomplete ring enhancement (*arrow*) with open portion of ring facing the ventricle. Diffusion-weighted sequence (**d**) shows restricted diffusion along the leading edge of demyelination (*arrows*). Pulsed arterial spin-labeled MR perfusion (**e**) also reveals increased blood flow corresponding to the leading edge of demyelination (*arrow*)

Suggested Imaging Protocols

The following MRI brain and spinal cord protocols are recommended (some are modified from published guidelines by an international consensus group sponsored by the Consortium of Multiple Sclerosis Centers (CMSC) in 2001) [163] (insufficient to limited evidence):

Brain

- Axial sections should follow the subcallosal line (joins the undersurface of the rostrum and splenium of the corpus callosum).
- Axial FSE PD/T2 and axial FLAIR – both are recommended when acquiring a diagnostic scan for CIS and also for MS follow-up.

- Axial gadolinium-enhanced T1 is recommended for a diagnostic scan for CIS.
- Axial pregadolinium T1 is optional, but nonetheless considered useful for comparison with non-contrasted images.
- Sagittal FLAIR is recommended for diagnostic scan for CIS, but optional for MS follow-up.
- The CMSC gave no specific guidelines for acquiring diffusion-weighted imaging, but a subsequent review by Lovblad et al. included DWI as an optional sequence and helpful to differentiate other diagnoses [155].

Spine

- Pre- and postgadolinium-enhanced sagittal T1 sequences are recommended.
- Precontrast sagittal FSE PD/T2 sequence is recommended.
- Precontrast axial FSE PD/T2 is recommended (through suspicious lesions).
- Postcontrast axial T1 is recommended (through suspicious lesions).
- 3D T1 is optional.

General Imaging Principles

- Standard dose of 0.1 mmol/kg is injected over 30 s, and image acquisition should begin a minimum of 5 min after start of injection.
- In MS, MRI of the brain and spinal cord should be performed on at least a 1 T magnet, if possible.

Future Research

- Though desirable from an evidence-based perspective, Level 1 or Level 2 studies of the diagnostic accuracy of MRI (conventional) are not likely to be performed in the future – since MRI-based measures have been formally incorporated into clinical diagnostic criteria for MS since 2001.

- There is a paucity of literature on the effect of advanced MRI techniques on the diagnostic accuracy of MRI in MS.
- Though some advanced techniques have been used in recent clinical trials, there is a need for more prospective evidence that these advanced MRI measures correlate with or predict clinical outcomes such as relapse or progression of disability.

References

1. Ellison D, Love S, Chimelli L, Harding B, Lowe J, Vinters H. Neuropathology: a reference text of CNS pathology. 2nd ed. Mosby: Elsevier; 2004.
2. Atlas S. Magnetic resonance Imaging of the brain and spine. 4th ed. Philadelphia: Lippincott Williams & Wilkins; 2009.
3. Kurtzke JF. Phys Med Rehabil Clin N Am. 2005;16:327–49.
4. Lublin FD. Neurol Clin. 2005;23:1–15.
5. Lucchinetti C, Parisi J, Bruck W. Neurol Clin. 2005;23:77–105.
6. Lassmann H, Bruck W, Lucchinetti CF. Brain Pathol. 2007;17:210–8.
7. Simon JH. Magn Reson Imaging Clin N Am. 2006;14:203–24. vi.
8. Kantarci OH, Weinshenker BG. Neurol Clin. 2005;23:17–38. v.
9. Confavreux C, Vukusic S. Neuroimaging Clin N Am. 2008;18:589–622.
10. Lublin F, Reingold SC. Neurology. 1996;46:907–11.
11. Courtney AM, Treadaway K, Remington G, Frohman E. Med Clin North Am. 2009;93:451–76.
12. Inglese M. Multiple sclerosis: new insights and trends. AJNR Am J Neuroradiol. 2006;27:954–57.
13. Fox EJ. Am J. Manag Care. 2010;16:S219–S26.
14. Noorbakhsh F, Johnson RT, Emery D, Power C. Neurol Clin. 2008;26:759–80. ix.
15. Stadelmann C, Bruck W. Neurol Sci. 2004;25:s319–s22.
16. Hynson JL, Kornberg JA, Coleman LT, Shield L, Harvey AS, Kean MJ. Neurology. 2001;56:1308–12.
17. Koch-Henriksen N, Soelberg Sørensen P. The changing demographic pattern of multiple sclerosis epidemiology. Lancet Neurol. 2010;9:520–32.
18. Anderson DW, Ellenberg JH, Leventhal CM, Reingold SC, Rodriguez M, Silberberg DH. Ann Neurol. 1992;31:333–6.
19. Ramagopalan S, Dobson R, Meier U, Giovannoni G. Lancet Neurol. 2010;9:727–39.
20. Ascherio A, Munger KL, Simon KC. Lancet Neurol. 2010;9:599–612.
21. Confavreux C, Vukusic S, Adeleine P. Brain. 2003;126:770–82.

22. Wallin MT, Page WF, Kurtzke JF. Ann Neurol. 2004;55:65–71.
23. Ascherio A, Munger K. Semin Neurol. 2008;28: 17–28.
24. Ness JM, Chabas D, Sadovnick AD, Pohl D, Banwell B, Weinstock-Guttman B. Neurology. 2007;68:S37–45.
25. Ruggieri M, Iannetti P, Polizzi A, Pavone L, Grimaldi* LME. Neurol Sci. 2004;25:s326–s35.
26. Vukusic S, Confavreux C. J Neurol Sci. 2003;206:135–7.
27. Eriksson M, Anderson O, Runmarker B. Mult Scler. 2003;9:260–74.
28. Koch-Henriksen N, Bronnum-Hansen H, Stenager E. J Neurol Neurosurg Psychiatry. 1998;65:56–9.
29. Torisu H, Kira R, Ishizaki Y, Sanefuji M, Yamaguchi Y, Yasumoto S, Murakami Y, Shimono M, Nagamitsu S, Masuzaki M, Amamoto M, Kondo R, Uozumi T, Aibe M, Gondo K, Hanai T, Hirose S, Matsuishi T, Shirahata A, Mitsudome A, Hara T. Brain Dev. 2010;32:454–62.
30. Leake JAD, Albani S, Kao AS, et al. Acute disseminated encephalomyelitis in childhood: epidemiologic, clinical and laboratory features. Pediatr Infect Dis J. 2004;23:756–64.
31. Tenembaum S, Chitnis T, Ness J, Hahn JS. Neurology. 2007;68(Suppl 2):S23–S36.
32. Tenembaum S, Chamoles N, Fejerman N. Neurology. 2002;59:1224–31.
33. Murthy SN, Faden HS, Cohen ME, Bakshi R. Pediatrics. 2002;110:21–8.
34. Wender M. J Neuroimmunol. 2011;231(1–2):92–9.
35. Dale RC, de Sousa C, Chong WK, Cox TCS, Harding B, Neville BGR. Brain. 2000;123:2407–22.
36. Pavone P, Pettoello-Mantovano M, Le Pira A, et al. Neuropediatrics. 2010;41:246–55.
37. Rotstein Z, Hazan R, Barak Y, Achiron A. Autoimmun Rev. 2006;5:511–6.
38. Whetten-Goldstein K, Sloan FA, Goldstein LB, Kulas ED. Mult Scler. 1998;4(5):419–25.
39. Murphy N, Confavreux C, Haas J, Konig N, et al. Pharmacoeconomics. 1998;5:607–22.
40. Pope GC, Urato CJ, Kulas ED, Kronick R, Gilmer T. Neurology. 2002;58:37–43.
41. Asche CV, Singer ME, Jhaveri M, Chung H, Miller A. J Manag Care Pharm. 2010;16:703–12.
42. Miller D, Barkhof F, Montalban X, Thompson A, Filippi M. Lancet Neurol. 2005;4:281–8.
43. Schaffler N, Kopke S, Winkler L, et al. Acta Neurol Scand. 2011;124(3):151–64.
44. Goodin DS, Bates D. Mult Scler. 2009;15:1175–82.
45. Jacobs LD, Beck RW, Simon JH, Kinkel R, Brownwscheidle CM, Murray TJ, Simonian NA, Slasor PJ, Sandrock AW. N Eng J Med. 2000;343:898–904.
46. Comi G, Filippi M, Barkhof F, et al. Lancet. 2001;357:1576–82.
47. Poser CM, Paty DW, Scheinberg L, McDonal WI, Davis FA, Ebers GC, Johnson KP, Sibley WA, Silberberg DH, Tourtellotte WW. Ann Neurol. 1983;13:227–31.
48. Uitdehaag B, Kappos L, Bauer L, Freedman MS, Miller D, Sandbrink R, Polman CH. A proposal for standardization. Mult Scler. 2005;11: 227–31.
49. Paty DW, Oger JJF, Kastrukoff LF, Hashimoto SA, Hooge JP, Eisen AA. Neurology. 1988;38:180–5.
50. Lee KH, Hashimoto S, Hooge JP, Kastrukoff LF, Oger JJ, Li DK. Neurology. 1991;41:657–60.
51. Fazekas F, Offenbacher H, Fuchs S, Schmidt R, Niederkorn K, Horne S. Neurology. 1988;38: 1822–5.
52. Tas MW, Barkhof F, van Walerveen MA, Polman CH, Hommes OR, Valk J. AJNR Am J Neuroradiol. 1995;16:259–64.
53. Simon JH. Phys Med Rehabil Clin N Am. 2005;16:383–409. viii.
54. Tintore M, Rovira A, Martinez MJ, et al. AJNR Am J Neuroradiol. 2000;21:702–6.
55. Barkhof F, Filippi M, Miller DH, Scheltens P, Campi A, Polman CH, Comi G, Ader HJ, Losseff N, Valk J. Brain. 1997;120:2059–69.
56. McDonald WI, Compston A, Edan G, et al. Ann Neurol. 2001;50:121–7.
57. Dalton CM, Brex PA, Miszkiel KA, et al. Ann Neurol. 2002;52:47–53.
58. Frohman EM, Goodin DS, Calabresi PA, et al. Neurology. 2003;61:602–11.
59. Miller DH, Filippi M, Fazekas F, et al. Ann Neurol. 2004;56:273–8.
60. Whiting P, Harbord R, Main C, et al. Br Med J. 2006;332:875–84.
61. Polman CH, et al. Ann Neurol. 2005;58:840–6.
62. Lovblad KO, Anzalone N, Dorfler A, et al. AJNR Am J Neuroradiol. 2010;31(6):983–9.
63. Hahn C, Shroff MM, Blaser SI, Banwell BL. Neurology. 2004;62:806–8.
64. Callen DJ, Shroff MM, Branson HM, et al. Neurology. 2009;72:961–7.
65. Krupp LB, Banwell BL, Tenembaum S, International Pediatric MS Study Group. Neurology. 2007;68: S7–S12.
66. Jin YP, de Pedro-Cuesta J, Huang YH, Soderstrom M. Mult Scler. 2003;9:135–41.
67. Tintore M, Rovira A, Brieva L, et al. Mult Scler. 2001;7:359–63.
68. Gronseth GS, Ashman EJ. Neurology. 2000;54: 1720–5.
69. Dale RC, Branson JA. Arch Dis Child. 2005;90: 636–9.
70. Mikaeloff Y, Suissa S, Vallee L, et al. J Pediatr. 2004;144:246–52.
71. Mikaeloff Y, Adamsbaum C, Husson B, Vallee L, Ponsot G, Confavreux C, Tardieu M, Suissa S. Brain. 2004;127:1942–7.
72. Callen DJ, Shroff MM, Branson HM, et al. Neurology. 2009;72:968–73.

73. Honkaniemi J, Dastidar P, Kahara V, Haapasalo H. AJNR Am J Neuroradiol. 2001;22:1117–24.

74. Axer H, Ragoschke-Schumm A, Bottcher J, Fitzek C, Witte OW, Isenmann S. J Neurol Neurosurg Psychiatry. 2005;76:996–8.

75. Donmez FY, Aslan H, Coskun M. Acta Radiol. 2009;50:334–9.

76. O'Riordan JI, Thompson AJ, Kingsley DPE, MacManus DG, Kendell BE, Rudge P, McDonald WI, Miller DH. Brain. 1998;121:495–503.

77. Brex PA, Ciccarelli O, O'Riordan JI, Sailer M, Thompson AJ, Miller DHA. N Eng J Med. 2002;346:158–64.

78. Barkhof F. Curr Opin Neurol. 2002;15:239–45.

79. Rovira A, Leon A. Eur J Radiol. 2008;67:409–14.

80. Barkhof F. Mult Scler. 1999;5:283–6.

81. Bruck W, Bitsch A, Kolenda H, Bruck Y, Stiefel M, Lassmann H. Ann Neurol. 1997;42:783–93.

82. Kurtzke JF. Neurology. 1983;33:1444–52.

83. Filippi M, Paty DW, Kappos L, Barkhof F, Compston DAS, Thompson AJ, Zhao GJ, Wiles CM, McDonald WI, Miller DH. Neurology. 1995;45:255–60.

84. Tintore M, Rovira A, Rio J, Nos C, Grive E, Tellez N, Pelaya R, Comabella M, Sastre-Garriga J, Montalban X. Neurology. 2006;67:968–72.

85. Riahi F, Zijdenbos A, Narayanan S, Arnold D, Francis G, Antel J, Evans AC. Brain. 1998;121: 1305–12.

86. Minneboo A, Barkhof F, Polman CH, Uitdehaag B, Knol DL, Castelijns JA. Arch Neurol. 2004;61:217–21.

87. Fisniku LK, Brex PA, Altmann DR, et al. Brain. 2008;131:808–17.

88. Group ONS. Arch Neurol. 2004;61:1386–9.

89. Foong J, Rozewicz L, Quaghebeur G, Davie CA, Kartsounis LD, Thompson AJ, Miller DH, Ron MA. Brain. 1997;120:15–26.

90. Miller DH, Rudge P, Johnson G, Kendall BE, Macmanus DG, Moseley IF, Barnes D, McDonald WI. Brain. 1988;111:927–39.

91. He J, Grossman RI, Ge Y, Mannon LJ. AJNR Am J Neuroradiol. 2001;22:664–9.

92. Barkhof F, Scheltens P, Frequin S, Nauta J, Tas MW, Valk J, Hommes OR. AJR Am J Roentgenol. 1992;159:1041–7.

93. Koudriavtseva T, Thompson AJ, Fiorelli M, Gasperini C, Bastianello S, Bozzao A, Paolilo A, Pisani A, Galgani S, Pozzilli C. J Neurol Neurosurg Psychiatry. 1997;62:285–7.

94. Molyneux PD, Filippi M, Barkhof F, Gasperini C, Yousry TA, Truyen L, Lai HM, Rocca MA, Moseley IF, Miller DH. Ann Neurol. 1998;43:332–9.

95. Kappos L, Moeri D, Radue EW, et al. Lancet. 1999;353:964–9.

96. Simon JH. Radiol Clin North Am. 2006;44:79–100. viii.

97. van Walderveen MAA, Kamphorst W, Scheltens P, van Waesberghe JHTM, Ravid R, Valk J, Polman CH, Barkhof F. Neurology. 1998;50:1282–8.

98. Sahraian MA, Eshaghi A. Clin Neurol Neurosurg. 2010;112:609–15.

99. Lukas C, Minneboo A, de Groot V, et al. J Neurol Neurosurg Psychiatry. 2010;81:1351–6.

100. Paolillo A, Pozzilli C, Gasperini C, Giugni E, Mainero C, Giuliani S, Tomassini V, Millefiorini E, Bastianello S. J Neurol Sci. 2000;174:85–91.

101. Bermel R, Sharma J, Tjoa CW, Puli SR, Bakshi R. J Neurol Sci. 2003;208:57–65.

102. Rudick RA, Fisher E, Lee JC, Simon J, Jacobs L. Neurology. 1999;53:1698–704.

103. Li DK, Paty DW. Ann Neurol. 1999;46:197–206.

104. Inglese M, van Waesberghe JH, Rovaris M, et al. Neurology. 2003;60:853–60.

105. Wiendl H, Hohlfeld R. Neurology. 2009;72(11): 1008–15.

106. Ford CC. J Neurol. 2006;253:VI/37–VI/44.

107. Comi G, Filippi M, Wolinsky JS. Ann Neurol. 2001;49:290–7.

108. Filippi M, Rovaris M, Rocca MA, Sormani MP, Wolinsky JS, Comi G. Neurology. 2001;57:731–3.

109. Kappos L, Antel J, Comi G, et al. N Engl J Med. United States: 2006 Massachusetts Medical Society. 2006;355(11):1124–40.

110. Cohen JA, Barkhof F, Comi G, et al. N Engl J Med. United States: 2010 Massachusetts Medical Society. 2010;362(5):402–15.

111. Kappos L, Radue EW, O'Connor P, et al. N Engl J Med. United States: 2010 Massachusetts Medical Society. 2010;362(5):387–401.

112. Elster AE, Burdette JH. Questions & answers in magnetic resonance imaging. 2nd ed. Philadelphia: Mosby; 2001. p. 244–5.

113. Pike GB, De Stefano N, Narayanan S, et al. Radiology. 2000;215:824–30.

114. Summers M, Fisniku L, Anderson V, Miller D, Cipolotti L, Ron M. Mult Scler. 2008;14(2):197–204.

115. Dehmeshki J, Chard DT, Leary SM, et al. J Neurol. 2003;250:67–74.

116. Ramio-Torrenta L, Sastre-Garriga J, Ingle GT, et al. J Neurol Neurosurg Psychiatry. 2006;77(1):40–5.

117. Rovaris M, Judica E, Sastre-Garriga J, et al. Mult Scler. 2008;6(2):455–64.

118. Fisniku LK, Altmann DR, Cercignani M, et al. Mult Scler. 2009;15(6):668–77.

119. Ge Y, Law M, Grossman RI. Ann NY Acad Sci. 2005;1064:202–19.

120. Larsson HB, Thomsen C, Frederiksen J, Stubgaard M, Henriksen O. Magn Reson Imaging. 1992;10:7–12.

121. Christiansen P, Gideon P, Thomsen C, Stubgaard M, Henriksen O, Larsson HB. Acta Neurol Scand. 1993;87:195–9.

122. Horsfield MA, Lai M, Webb SL, et al. Apparent diffusion coefficients in benign and secondary progressive multiple sclerosis by nuclear magnetic resonance. Magn Reson Med. 1996;36: 393–400.

123. Droogan AG, Clark CA, Werring DJ, Barker GJ, McDonald WI, Miller DH. Magn Reson Imaging. 1999;17(5):653–61.
124. Filippi M, Iannucci G, Cercignani M, Assunta Rocca M, Pratesi A, Comi G. Arch Neurol. 2000;57(7):1017–21.
125. Cercignani M, Iannucci G, Rocca MA, Comi G, Horsfield MA, Filippi M. Neurology. 2000;54: 1139–44.
126. Roychowdhury S, Maldjian JA, Grossman RI. AJNR Am J Neuroradiol. 2000;21:869–74.
127. Bammer R, Augustin M, Strasser-Fuchs S, et al. Magn Reson Med. 2000;44(4):583–91.
128. Filippi M, Cercignani M, Inglese M, Horsfield MA, Comi G. Neurology. 2001;56:304–11.
129. Rocca MA, Cercignani M, Iannucci G, Comi G, Filippi M. Neurology. 2000;55:882–4.
130. Cercignani M, Bozzali M, Iannucci G, Comi G, Filippi M. J Neurol Neurosurg Psychiatry. 2001;70:311–7.
131. Guo AC, Jewells VL, Provenzale JM. AJNR Am J Neuroradiol. 2001;22:1893–900.
132. Guo AC, MacFall JR, Provenzale JM. Radiology. 2002;222:729–36.
133. Ranjeva JP, Pelletier J, Confort-Gouny S, et al. Mult Scler. 2003;9:554–65.
134. Werring DJ, Brassat D, Droogan AG, et al. Brain. 2000;123(Pt 8):1667–76.
135. Filippi M. Neurol Sci. 2001;22:195–200.
136. Bozzali M, Cercignani M, Sormani MP, Comi G, Filippi M. AJNR Am J Neuroradiol. 2002;23:985–8.
137. Rocca MA, Iannucci G, Rovaris M, Comi G, Filippi M. J Neurol. 2003;250:456–60.
138. Rovaris M, Bozzali M, Iannucci G, et al. Arch Neurol. 2002;59(9):1406–12.
139. Nusbaum AO. AJNR Am J Neuroradiol. 2002;23: 899–900.
140. Benedict RH, Bruce J, Dwyer MG, et al. Mult Scler. 2007;13:722–30.
141. Tavazzi E, Dwyer MG, Weinstock-Guttman B, et al. Neuroimage. 2007;36(3):746–54.
142. Zivadinov R, Hussein S, Stosic M, et al. Glatiramer acetate recovers microscopic tissue damage in patients with multiple sclerosis. A case–control diffusion imaging study. Pathophysiology. 2011;18(1): 61–8.
143. Minneboo A, Jasperse B, Barkhof F, et al. J Neurol Neurosurg Psychiatry. 2008;79:917–23.
144. Horakova D, Cox JL, Havrdova E, et al. J Neurol Neurosurg Psychiatry. 2008;79(4):407–14.
145. Tedeschi G, Dinacci D, Comerci M, et al. Mult Scler. 2009;15(2):204–11.
146. Fisniku LK, Chard DT, Jackson JS, et al. Ann Neurol. 2008;64:247–54.
147. Fisher E, Lee JC, Nakamura K, Rudick RA. Ann Neurol. 2008;64:255–65.
148. Rudick RA, Lee JC, Nakamura K, Fisher E. J Neurol Sci. 2009;282(1–2):106–11.
149. Sailer M, Losseff NA, Wang L, Gawne-Cain ML, Thompson AJ, Miller DH. Eur J Neurol. 2001;8(1):37–42.
150. Minneboo A, Uitdehaag BM, Jongen P, et al. Mult Scler. 2009;15(5):632–7.
151. Horakova D, Dwyer MG, Havrdova E, et al. J Neurol Sci. 2009;282(1–2):112–9.
152. Davie CA, Silver NC, Barker GJ, et al. J Neurol Neurosurg Psychiatry. 1999;67:710–5.
153. Falini A, Calabrese G, Filippi M, et al. AJNR Am J Neuroradiol. 1998;19:223–9.
154. Bonneville F, Moriarty DM, Li BS, Babb JS, Grossman RI, Gonen O. AJNR Am J Neuroradiol. 2002;23:371–5.
155. Filippi M, Bozzali M, Rovaris M, et al. Brain. 2003;126:433–7.
156. Oh J, Henry RG, Genain C, Nelson SJ, Pelletier D. J Neurol Neurosurg Psychiatry. 2004;75:1281–6.
157. Brass SD, Narayanan S, Antel JP, Lapierre Y, Collins L, Arnold DL. Can J Neurol Sci. 2004;31:225–8.
158. Benedetti B, Rovaris M, Rocca MA, et al. Mult Scler. 2009;15:789–94.
159. Saindane AM, Cha S, Law M, Xue X, Knopp EA, Zagzag D. AJNR Am J Neuroradiol. 2002;23: 1378–86.
160. Law M, Saindane AM, Ge Y, et al. Radiology. 2004;231(3):645–52.
161. Adhya S, Johnson G, Herbert J, et al. Neuroimage.. 2006;33:1029–35.
162. Varga AW, Johnson G, Babb JS, Herbert J, Grossman RI, Inglese M. J Neurol Sci. 2009;282(1–2):28–33.
163. Simon JH, Li D, Traboulsee A, et al. Am J Neuroradiol. 2006;27:455–61.

Acute Ischemic Stroke: Evidence-Based Neuroimaging

10

Andria L. Ford, Jin-Moo Lee, Weili Lin, and Katie D. Vo

Contents

A.L. Ford (✉) • J.-M. Lee
Department of Neurology, Washington University School of Medicine, St. Louis, MO, USA
e-mail: forda@neuro.wustl.edu; leejm@wustl.edu

W. Lin
Biomedical Research Imaging Center, University of North Carolina at Chapel Hill, Chapel Hill, NC, USA
e-mail: weili_lin@med.unc.edu

K.D. Vo
Washington University School of Medicine, Mallinckrodt Institute of Radiology, St. Louis, MO, USA
e-mail: vok@wustl.edu

Key Points

- Noncontrast head CT should be performed in all patients who are candidates for thrombolytic therapy to exclude intracerebral hemorrhage (ICH) [Strong Evidence]. Magnetic resonance imaging (MRI) is likely equivalent to CT in the detection of intracranial hemorrhage for patients <6 h from onset [Strong Evidence].
- Magnetic resonance (MR) (diffusion-weighted imaging) is superior to CT for detection of cerebral ischemia within the first 24 h of symptom onset [Strong Evidence]; however, identification of ischemia may confirm a clinical diagnosis without influencing immediate clinical decision-making or outcomes.
- Advanced imaging such as MR perfusion, CT perfusion, xenon CT, and positron emission tomography (PET) hold promise to improve patient selection and individualize the therapeutic window [Limited Evidence], but the data does not currently support routine use in the management of acute ischemic stroke patients.
- Randomized placebo-controlled trials selecting patients with diffusion-perfusion mismatch for thrombolytic treatment have shown no benefit over placebo up to 9 h from stroke symptom onset [Strong Evidence].

Definition and Pathophysiology

This chapter focuses on the imaging of acute ischemic stroke patients within the first few hours of stroke onset when issues relating to the decision to administer thrombolytics are of paramount importance. Stroke is a clinical term that describes an acute neurological deficit due to a sudden disruption of blood supply to the brain. Stroke is caused by either an occlusion of an artery (ischemic stroke or cerebral ischemia/infarction) or rupture of an artery leading to bleeding into or around the brain (hemorrhagic stroke or intracranial hemorrhage). The vast majority of strokes are ischemic (87 %) while 10 % are intracerebral hemorrhages and 3 % are subarachnoid hemorrhages [1]. Ischemic stroke can be divided into several subtypes based on etiology: small vessel (40 %), large-vessel atherothrombotic (20 %), cardioembolic (20 %), and unknown etiology (20 %) [2]. Risk factors for stroke include age, male gender, race (African American), previous history of stroke, diabetes, hypertension, heart disease, atrial fibrillation, smoking, and alcohol use. Treatment of ischemic stroke can be divided into acute therapies, consisting of thrombolysis with tissue plasminogen activator (tPA) and management of secondary complications (edema, herniation, hemorrhage), and preventative therapies aimed at reducing the risk of recurrent stroke.

Epidemiology

It is estimated that approximately 795,000 new or recurrent strokes occur annually of which nearly 700,000 are ischemic. A new stroke occurs every 40 s in the United States [1, 3]. Fifteen to thirty percent of stroke survivors are permanently disabled or require institutional care making it the leading cause of severe long-term disability and the leading diagnosis from hospital to long-term care [4–6]. Stroke is the third leading cause of mortality after heart disease and cancer, accounting for 134,000 deaths per year in the United States [3]. In 1995, the Food and Drug Administration approved tPA for the treatment of acute ischemic stroke after tPA was shown to reduce neurological disability at 3 months compared to placebo [7]. Despite having strong evidence for the benefit of acute treatment, it is estimated that only 1.8–3 % of ischemic stroke patients receive tPA [8, 9]. The reasons for the low rates of tPA treatment are largely due to patients arriving outside of the approved tPA window. Additionally, many hospitals are not equipped with the infrastructure required to evaluate tPA candidates in an expedited manner. A recent study confirmed that the majority of US hospitals did not administer tPA to acute stroke patients over a 2-year period [10].

Overall Cost to Society

The estimated direct and indirect costs of stroke totaled 74 billion dollars in 2010 with 66 % of the cost related directly to medical expenditures [3]. Acute inpatient hospital cost accounts for 70 % of the first-year costs post stroke. Diagnostic tests during the initial hospitalization contribute nearly 20 % to total hospital costs [11]. These diagnostic tests include MR and/or CT (91 % of patients), echocardiogram (81 %), noninvasive carotid artery evaluation (48 %), angiography (20 %), and electroencephalography (6 %). Additional diagnostic testing with CT or MR angiography and perfusion are increasingly being obtained for special situations (i.e., to select patients for endovascular therapy when patients do not show a clinical response to intravenous tPA), but also on a routine basis at some institutions. Although clinical benefit has not yet been proven for these diagnostic tests, several studies have modeled the cost-benefit ratio in the acute ischemic stroke population [12–14].

Goals of Imaging

The primary goal of neuroimaging in patients presenting with acute neurological deficits and suspected ischemic stroke is to exclude hemorrhagic stroke. Secondary goals may include confirmation of ischemic stroke and exclusion of other diagnoses that may mimic stroke. Finally, emerging goals of acute stroke imaging are to determine if brain tissue is viable and thereby amenable to therapies beyond the currently approved tPA treatment window and to determine the localization of vascular occlusion when an interventional treatment would be considered.

Methodology

A comprehensive MEDLINE search (United States National Library of Medicine database) for original articles published between January 1966 and March 2011 using the OVID and PubMed search engines was performed using combinations of the following keywords: ischemic stroke, hemorrhage, diagnostic imaging, CT, MR, PET, angiography, gadolinium, circle of Willis, carotid artery, brain, technology assessment, evidence-based medicine, and cost. The search was limited to English-language articles and human studies. The abstracts were reviewed and selected based on well-designed methodology, clinical trials, outcomes, and diagnostic accuracy. Additional relevant articles were selected from the references of reviewed articles and published guidelines.

Discussion of Issues

What Is the Imaging Modality of Choice for the Exclusion of Intracranial Hemorrhage in Acute Ischemic Stroke?

Summary
Computed tomography is widely accepted as the gold standard for imaging intracerebral hemorrhage; however, it has not been rigorously examined in prospective studies, and thus the precise sensitivity and specificity are unknown [Limited Evidence]. However, in the evaluation of thrombolytic candidates, CT is the modality of choice for exclusion of intracerebral hemorrhage based on randomized controlled trials [Strong Evidence] [7, 15]. By many measures, MR is likely as sensitive as CT in the detection of intracerebral hemorrhage and is more sensitive during the chronic phase. Recent studies indicate that the accuracy of MR in detecting intraparenchymal hemorrhage is likely equivalent to CT even in the hyperacute setting (within 6 h of ictus) [Moderate Evidence] [16, 17].

Supporting Evidence
(a) Computed Tomography It is essential that an imaging study reliably distinguish intracerebral hemorrhage (ICH) from ischemic stroke because of the divergent management of these two conditions (see flowchart, Fig. 10.1). This is especially critical for patients who present within

4.5 h of symptom onset under consideration for thrombolytic therapy. Noncontrast CT is currently the modality of choice for detection of acute ICH. Although MRI has been increasingly found to be as sensitive as CT for detection of acute ICH, CT has advantages over MRI, including widespread availability, shorter scanning time, lower cost, and fewer patient contraindications than MRI. Acute hemorrhage appears hyperdense on CT for several days due to the high protein concentration of hemoglobin and retraction of clot, but becomes progressively isodense and then hypodense over a period of weeks to months. Rarely acute hemorrhage can be isodense in severely anemic patients with a hematocrit less than 20 % or 10 g/dl [18]. Although it has been accepted that CT identifies ICH with high sensitivity, surprisingly few studies have been conducted to support this [19, 20]. In 1974, Paxton and Ambrose [21] diagnosed 66 patients with ICH using the first-generation CT scanner; the study was observational, lacking autopsy confirmation. Subsequently, in an autopsy series of 79 patients, CT did not detect 4 out of 17 patients with ICH – all were brainstem hemorrhages [Limited Evidence] [22]. There is little doubt that the sensitivity of third-generation CT scanners for the detection of ICH is superior to that of the first-generation scanners; however, it is of interest that the precise sensitivity and specificity of this well-accepted modality are unknown.

Four studies evaluating third-generation CT scanners in patients with nontraumatic subarachnoid hemorrhage identified by CT or cerebrospinal fluid (CSF) have been reported [23–26]. The overall sensitivity of CT was 91–92 %, but was dependent on the time interval between symptom onset and scan time. Sensitivity was 100 % (80/80) for patients imaged within 12 h, 93 % (134/144) within 24 h, and 84 % (31/37) after 24 h [Limited Evidence] [25, 26]. These numbers were confirmed by two other studies that demonstrated a sensitivity of 98 % (117/119) for scans obtained within 12 h, 95 % (1,313/1,378) within 24 h, 91 % (1,247/1,378) between 24 and 48 h, and 74 % after 48 h (1,017/1,378) [Moderate Evidence] [23, 24].

These studies relied on a diagnosis made by CT, or by blood detected in CSF in the absence of CT findings. No studies with autopsy confirmation have been reported.

Therefore, although CT is commonly regarded as the modality of choice for imaging ICH, the precise sensitivity and specificity are unknown and depends on time after onset, hemoglobin concentration, and size and location of the hemorrhage.

(b) Magnetic Resonance Imaging Like CT, the appearance and identification of ICH on magnetic resonance imaging (MRI) depend on the age of the patient and location (intraparenchymal or subarachnoid) of the hemorrhage. In addition, the strength of the magnetic field and type of MR sequence influence its sensitivity [27]. As the hematoma ages, oxyhemoglobin breaks down sequentially into several paramagnetic products: first deoxyhemoglobin, then methemoglobin, and finally hemosiderin. Iron exposed to surrounding water molecules in the form of deoxyhemoglobin creates signal loss on susceptibility-weighted and T2-weighted (T2W) sequences [28, 29]. Thus, the earliest detection of hemorrhage depends on the conversion of oxyhemoglobin to deoxyhemoglobin which was believed to occur after the first 12–24 h [27, 30]. However, this early assumption has been questioned with reports of ICH detected by MRI within 6 h and as early as 23 min from symptom onset [31, 32]. More recently, studies have assessed MRI (diffusion-, T2-, and T2*-weighted images) for the evaluation of ICH within 6 h of onset. One study evaluated 62 ICH patients and 62 controls, with three experienced readers (two stroke neurologists and one neuroradiologist) utilizing CT as the reference standard. The readers, blinded to clinical and CT results, identified all acute hemorrhages on MRI yielding 100 % sensitivity and specificity compared to CT [Moderate Evidence] [16]. A study comparing CT and MRI for detection of both ischemic and hemorrhagic stroke found a lower sensitivity of 84 % using MRI (of 25 acute hemorrhages on CT, 21 were identified on MRI) [Moderate Evidence] [17]. The four patients not identified by MRI

included two cases in which "acute" ICH was classified as "chronic," one case with hemorrhagic conversion of ischemic stroke by DWI, and one case in which acute ICH was missed. This study was methodologically limited because sensitivity and specificity were measured based on the clinical discharge diagnosis. Compared to discharge diagnosis, MRI had 81 % sensitivity and 100 % specificity, while CT had 89 % sensitivity and 100 % specificity. Three cases of ICH identified on MRI but not on CT included a subdural hematoma, a hemorrhagic metastasis, and a temporal lobe hematoma. Other studies have also noted that cases of acute hemorrhagic transformation of an ischemic stroke could be seen on MRI (GRE) but not on CT [33]. Therefore, it appears that rare cases of early ICH may be missed on either MRI or CT. Studies with tissue confirmation, allowing for measurement of the exact accuracy of both modalities, are lacking.

Recently, susceptibility-weighted imaging (SWI) has allowed for greater sensitivity to detect very small hemorrhages, both acute and chronic, compared to CT- and MRI-obtained GRE [Limited Evidence] [34]. When faced with decisions regarding thrombolysis in acute ischemic stroke patients, the heightened sensitivity of MRI SWI to microbleeds that are not otherwise detected on CT could lead to consideration of an increased risk of hemorrhagic transformation with thrombolysis in these patients (Fig. 10.2) [35]. However, thus far, several studies suggest that neither the presence nor the number of cerebral microbleeds is associated with a significant increased risk of hemorrhagic transformation in tPA-treated or untreated patients [Moderate Evidence] [36–38].

What Are the Imaging Modalities of Choice for the Identification of Brain Ischemia?

Summary

Based on strong evidence, MRI (diffusion-weighted imaging) is superior to CT for identifying ischemic stroke within the first 12 h of symptom onset. However, despite its superiority, MRI may not always affect clinical decision-making and has not been shown to improve clinical outcomes. Moreover, MRI may be less readily available and often requires additional time for patient screening and scanning relative to CT. Time-sensitive factors are of critical importance since time to thrombolytic treatment is one of the strongest predictors of clinical outcome after ischemic stroke [39].

Supporting Evidence

(a) Computed Tomography CT images are commonly normal during the acute phase of ischemia and therefore the diagnosis of ischemic stroke is based on clinical history and physical examination. At times, patients may present with stroke-like symptoms due to non-stroke etiologies including seizure, postictal state, migraine with prolonged aura, brain tumor, toxic-metabolic conditions, peripheral vertigo, subdural hematoma, herpes encephalitis, demyelinating disease, or conversion disorder [40]. Based purely on history and physical examination alone without confirmation by CT, stroke mimics may account for 13–19 % of cases initially diagnosed with stroke [40, 41]. Sensitivity of diagnosis improves when noncontrast CT is used, but 5 % of cases are still misdiagnosed as stroke [42].

Increased scrutiny of hyperacute CT scans, especially following the early thrombolytic trials, suggests that some patients with large areas of ischemia may demonstrate subtle early signs of ischemia, even when imaged less than 3 h after symptom onset. These early CT signs include parenchymal hypodensity, loss of the insular ribbon [43], obscuration of the lentiform nucleus [44], loss of gray and white matter differentiation, visualization of hyperdense clot in the region of the proximal middle cerebral artery (MCA) known as the "dense MCA sign," subtle effacement of the cortical sulci, and local mass effect (Fig. 10.3a , b). Early changes are found in 31 % of CTs performed within 3 h of ischemic stroke [Moderate Evidence] [45], precluding its reliability as a positive sign of ischemia. When performed within 5 h of MCA stroke onset (demonstrated angiographically), early CT signs were found in 81 % of patients [Moderate Evidence] [46].

Early CT signs, however, are often subtle and difficult to detect even among experienced readers [Moderate Evidence] [47–49].

Early CT signs of infarction, especially involving more than one-third of the MCA distribution, have been reported to be associated with severe stroke, increased risk of hemorrhagic transformation [49–52], and poor outcome [53]. Because of these associations, several trials involving thrombolytic therapy including European Cooperative Acute Stroke Study-2 (ECASS-2) excluded patients with early CT signs in an attempt to avoid treatment of patients at increased risk for hemorrhagic transformation [54]. Recently, ECASS-3, which excluded these patients, demonstrated efficacy of intravenous tPA administration within 3–4.5 h after stroke onset [15]. The Alberta Stroke Program Early CT Scores (ASPECTS), a 10-point scoring system, was developed as a tool for detection of early ischemic changes on head CT that would be more reliable and prognostic than simple visual inspection of the MCA territory. A normal ASPECT score is 10 with 1 point subtracted for each abnormal brain region (of 10, 7 cortical and 3 subcortical) within the affected hemisphere [55]. Both methods (visual inspection and ASPECTS) require training to ascertain subtle ischemic changes, although ASPECTS has not clearly demonstrated superior reliability compared to visual inspection [56]. While studies have demonstrated that ASPECTS predicts hemorrhagic transformation after thrombolytics and functional outcome, data comparing ASPECTS with simple visual inspection are lacking [55, 57]. In contrast to ECASS-3, the National Institute of Neurological Disorders and Stroke tPA trial [7] did not exclude patients with early CT signs, and, therefore, early CT signs should not be used to exclude patients who are otherwise eligible for thrombolytic treatment within 3 h of stroke onset [Strong Evidence] [7].

(b) Magnetic Resonance Imaging Unlike CT, MR diffusion-weighted imaging (DWI) is capable of detecting very early physiologic changes during cerebral ischemia, demonstrating changes within minutes of ischemia in rodent stroke models [58–60]. Moreover, the sequence detects lesions as small as 4 mm in diameter [61]. The signal alteration observed in DWI after acute ischemia is believed to be due to influx of intracellular water, thereby restricting water motion and resulting in a bright signal on DWI [62, 63]. As duration of ischemia increases, a DWI lesion becomes progressively brighter, leading to the added contribution of hyperintense T2W signal known as "T2 shine through" [64]. To differentiate between true restricted diffusion and "T2 shine through," a bright DWI lesion should also show hypointense signal on the corresponding apparent diffusion coefficient (ADC) map, which is a more quantitative and direct measure of restricted diffusion.

The relatively high sensitivity and specificity of DWI for the detection of ischemia make it an ideal sequence for positive identification of hyperacute stroke. Two studies evaluating DWI within 6 h of stroke onset reported 88–100 % sensitivity and 95–100 % specificity, using final clinical diagnosis as the reference standard [Moderate Evidence] [65, 66]. In another study, 50 patients were randomized to DWI or CT within 6 h of stroke onset, and subsequently received the other imaging modality with a mean delay of 30 min. Sensitivity and specificity of ischemia detection among blinded expert readers were significantly better with DWI (91 % and 95 %, respectively) compared to CT (61 % and 65 %) [Moderate Evidence] [67]. A recent large prospective study including 190 ischemic stroke patients assessed the accuracy of DWI compared to CT as a function of time from symptom onset [17]. As time from symptom onset increased, the sensitivity of DWI for final diagnosis of ischemic stroke increased: 73 %, 81 %, and 92 % for <3 h, 3–12 h, and >12 h, respectively, whereas CT had only 12 %, 20 %, and 16 % sensitivity at these three respective time intervals [Strong Evidence].

Although DWI is the optimal test for imaging acute ischemia, the highest level data suggests that the sensitivity for detection within 6 h of onset is 81–91 %; therefore, the absence of a DWI lesion does not rule out ischemia. As described above, the sensitivity of DWI increases as time from stroke onset increases in the first 24 h. False negatives have been reported in small

subcortical and vertebrobasilar infarctions and in patients with low National Institutes of Health Stroke Scale (NIHSS) scores [Moderate Evidence] [17, 66, 68–70]. Furthermore, within the first 6 h of stroke onset, DWI demonstrates delayed signal evolution after changes in perfusion [71]. Therefore, the location and size of ischemia, time from onset, and perfusion status are among several factors contributing to the DWI lesion. Restricted diffusion has been reported with other nervous system pathologies such as brain abscesses [72], herpes encephalitis [73, 74], Creutzfeldt-Jakob disease [75], highly cellular tumors such as lymphoma or meningioma [76], epidermoid cysts [77], seizures [78], and hypoglycemia [79] [Limited Evidence]. However, the clinical history and appearance of these lesions on the remaining standard MR sequences should allow for diagnosis of these different pathologies. Diagnosis of ischemic stroke with DWI should be interpreted in conjunction with conventional MR sequences and within the proper clinical context.

Acute DWI lesion volume (<24 h from symptom onset) correlates with final infarct volume, the initial stroke severity as measured by the NIHSS, and long-term clinical outcome as measured by disability scales such as Barthel Index and modified Rankin Scale [80–82]. In anterior circulation strokes, especially strokes involving the cortex, acute DWI lesion volume appears to correlate well with baseline clinical stroke severity, final lesion volume, and clinical outcome [Moderate Evidence] [81–83]. In contrast, small, subcortical, and posterior-circulation strokes demonstrate poor correlation between DWI volume and initial stroke severity [Limited Evidence] [80, 83]. This is likely related to the discordance between small infarct size and increased severity of neurological deficits seen with some brainstem strokes and subcortical strokes affecting motor pathways and centers of wakefulness.

Regarding CT vs. MRI for first-line imaging in patients with suspected acute ischemic stroke, several critical factors have not been adequately studied. These factors include practicality (including scanner, technician, and radiologist/neurologist access round-the-clock, patient eligibility and

tolerability, and scan duration), cost-effectiveness, and effect on clinical decision-making and patient outcomes. A large study assessing CT vs. MRI for diagnosis of acute ischemic stroke excluded 11 % of patients due to issues such as patient intolerability and claustrophobia in the MR scanner, MR contraindications such as pacemaker placement, and medical instability [17]. One study compared the cost-effectiveness of immediate vs. delayed CT for all patients compared with a subset of acute stroke patients and found that an immediate CT in all patients was more cost-effective than delayed CT in a subset of patients [84]. However, similar studies have not yet been performed for MRI and are greatly needed.

What Imaging Modalities May Identify the Presence of Viable Tissue: The Ischemic Penumbra?

Summary

Determination of tissue viability using advanced imaging has tremendous potential to individualize therapy and extend the therapeutic time window for some acute ischemic stroke patients. Several imaging modalities, including MRI, CT, and PET, have been examined in this role. Operational hurdles have limited the use of some of these modalities in the acute stroke setting (e.g., PET), while others such as MRI have been studied in large clinical trials. Thus far, randomized controlled trials have not demonstrated a benefit of thrombolytic treatment in patients who are selected using MR-based criteria such as diffusion-perfusion mismatch [Strong Evidence]; however, studies are ongoing. Positive clinical trials will be required prior to the use of penumbral imaging techniques in routine clinical decision-making.

Supporting Evidence

(a) Magnetic Resonance Imaging The primary investigation into imaging viable tissue using MRI has relied upon information gained from DWI and perfusion-weighted imaging (PWI) techniques. In acute ischemia, PWI is most commonly performed by repeated and rapid

acquisition of images after injection of contrast agent using a 2D gradient echo or spin-echo echo-planar imaging (EPI) sequence termed "dynamic susceptibility contrast" (DSC) [85, 86]. Signal changes induced by the first passage of contrast in the brain can be used to obtain estimates of a variety of hemodynamic parameters, including cerebral blood flow (CBF) and cerebral blood volume (CBV), as well as several time-based perfusion parameters including mean transit time (MTT), time to peak (TTP), and Tmax (Table 11.2) [86–89]. Another MRI method developed to measure cerebral perfusion is arterial spin labeling (ASL) which measures blood flow by labeling specific feeding vessel territories rather than the DSC method which utilizes the combination of all vasculature supply to the brain. ASL has a major advantage over DSC as it does not require intravenous contrast; however, it is currently limited by low signal-to-noise ratio especially in brain regions that are severely ischemic [90].

After acute arterial occlusion, brain tissue dies over a period of minutes to hours following arterial occlusion. Initially, a "core" of tissue dies within minutes, but it is theorized that surrounding brain tissue, while dysfunctional, remains viable and comprises the "ischemic penumbra." If blood flow is not restored in a timely manner, the penumbral tissue "at risk" will die, resulting in growth of the ischemic core [91]. The temporal profile of signal changes seen on DWI and PWI follows a pattern that is strikingly similar to the theoretical construct of the penumbra described above. In MR images obtained within hours of stroke onset, the DWI lesion is often smaller than the area of PWI lesion, and smaller than the final infarct (defined by T2W images obtained weeks later). If the arterial occlusion persists, the DWI lesion grows until it matches the initial perfusion defect, which is often similar in size and location to the final infarct (chronic T2W lesion) (Fig. 10.4a–d) [Limited Evidence] [92, 93]. The area of normal DWI signal but abnormal PWI signal is known as the diffusion-perfusion mismatch and has been postulated to represent the ischemic penumbra. The presence of mismatch tissue varies greatly depending on the definitions of DWI and PWI thresholds used, ranging from 49 %

to 88 % of ischemic stroke patients (up to 12 h after stroke onset) [94–96]. Growth of the DWI lesion over time has been documented in a randomized trial testing the efficacy of the neuroprotective agent, citicoline [Moderate Evidence] [81]. Growth of the DWI lesion volume (obtained at <24 h) into the final T2W scan (obtained at 12 weeks) was 180 % in the placebo group compared to only 34 % in the citicoline-treated group suggesting a treatment effect. However, efficacy of the agent was not demonstrated using clinical outcome measures [97]. One small prospective study enrolled acute ischemic stroke patients with mismatch who were treated with intra-arterial thrombolysis. Patients with successful recanalization salvaged larger areas of mismatched tissue compared to patients who did not successfully recanalize [Limited Evidence] [98].

The promise of diffusion-perfusion mismatch is to provide a measure of salvageable ischemic brain tissue, and thereby individualize therapeutic time windows for acute treatments. Since lesion growth into the final infarct may not occur until hours to days later in some individuals [Limited Evidence] [92, 93], tissue could potentially be salvaged beyond the tPA window. One assumption underlying the mismatch hypothesis is that the acute DWI lesion represents irreversibly injured tissue or the ischemic core. However, it has been known for some time that DWI lesions are reversible after transient ischemia in animal stroke models [99, 100], and reversible lesions in humans have been reported following TIA [101] or after reperfusion [Limited Evidence] [102]. These data suggest that at least some brain tissue within the DWI lesion may represent reversibly injured tissue. While one study found that the majority of DWI lesions measured between 3 and 6 h are eventually incorporated into the final infarct, other studies have found that lesions prior to 3 h may reverse after reperfusion and may not proceed to infarction [Limited Evidence] [71, 103]. The second assumption underlying the mismatch hypothesis is that the acute PWI lesion encompasses all tissue "at risk" for infarction if not reperfused. Several studies found that PWI lesions included regions of benign oligemia (tissue with low CBF, but neurological function remains intact

and is not at risk for infarction) and therefore overestimated the amount of tissue at risk [104]. Two large trials testing the mismatch hypothesis, DEFUSE and EPITHET (see next paragraph), utilized a liberal PWI threshold (Tmax >2 s) to define the region of tissue at risk, resulting in a high proportion of patients with mismatch [94, 96]. When the DEFUSE study was reanalyzed using a more conservative threshold (Tmax >4–6 s), the PWI volumes more closely approximated the final infarct volume and clinical outcome [105]. Given the profound differences that result from varying the PWI parameter (CBF, MTT, Tmax, etc.) and threshold, several groups have attempted to identify the optimal map for outlining the extent of tissue at risk, however a consensus has not been reached [106–110].

Several clinical trials have been performed to validate diffusion-perfusion mismatch or used mismatch to empirically select patients for treatment beyond the current tPA window. One important study, DEFUSE, aimed to validate diffusion-perfusion mismatch by comparing clinical outcome in mismatched compared to matched patients, all of whom were treated with tPA [96]. Seventy-four acute ischemic stroke patients presenting within 3–6 h of stroke onset were treated with tPA. All patients were serially imaged with MRI prior to tPA treatment (to assess for the presence of diffusion-perfusion mismatch) and 3–6 h after tPA treatment (to assess for tissue reperfusion). After excluding patients with unsuccessful PWI scans or patients with a "small lesion profile," 45 patients were analyzed, of whom 34 had mismatch and 11 did not. In the 34 patients with mismatch, those with reperfusion had a significantly better clinical outcome than patients without reperfusion. However, due to the small number of patients without mismatch, the converse, that matched patients did not improve with reperfusion, could not be proven. Furthermore, patients with mismatch did not have a greater chance of good clinical outcome (38 %) compared to patients without mismatch (54 %). Although DEFUSE is commonly cited as validation for use of diffusion-perfusion mismatch, there was no evidence showing that mismatch patients improved

more with reperfusion-promoting therapy (tPA) than non-mismatch patients. The small size of the matched group and the lack of a placebo arm make study conclusions difficult [Moderate Evidence].

Subsequent randomized controlled trials have utilized diffusion-perfusion mismatch to select patients for therapy beyond the currently approved tPA window. In EPITHET [94], stroke patients arriving after 3 h from symptom onset were serially imaged (1) prior to administration of tPA vs. placebo, (2) at 3–5 days, and (3) at 90 days after treatment. The EPITHET hypothesis was that tPA treatment would result in less infarct growth (as measured from the baseline DWI to the day 90 T2W scan) compared to placebo in the subset of mismatch patients. Of 91 enrolled patients with usable imaging data, 44 were given tPA (of whom 37 had mismatch) and 47 were given placebo (of whom 43 had mismatch); 88 % of the 91 patients had mismatch. The primary endpoint showed no significant difference in infarct growth between the tPA and placebo groups. Three additional studies, DIAS [111], DEDAS [54], and DIAS-2 [112], examined the efficacy of a novel thrombolytic, desmoteplase, compared to placebo in patients with mismatch between 3 and 9 h after stroke onset. While the initial phase-2 studies, DIAS and DEDAS, demonstrated safety and early signs of efficacy for desmoteplase, the phase-3 study, DIAS-2, was a negative trial with unexpectedly high mortality and no overall clinical benefit of desmoteplase [Strong Evidence]. DIAS-2 differed from the initial phase-2 studies in that it allowed patients to be selected for study entry based on both MR- and CT-perfusion-defined mismatch. This change in imaging inclusion criteria could be one explanation, of several, for the divergent results. Because the active agent, desmoteplase, had not been studied in other acute stroke trials <3 h from onset, it is unclear if desmoteplase lacked efficacy or if the imaging screen failed.

Additional MR techniques such as proton MR spectroscopy (MRS) and T2* blood oxygen level–dependent (BOLD) MR have been explored

for the identification of salvageable tissue [113, 114]. MRS measures the presence of lactate and N-acetylaspartate (NAA) following ischemia. Lactate is elevated within minutes of ischemia in animal models, remaining elevated for days to weeks [115]. While the lactate signal can normalize with immediate reperfusion [116]. NAA, found exclusively in neurons, decreases gradually over a period of hours after stroke onset [117, 118]. It has been suggested that increased lactate with a normal or mild reduction in NAA during acute ischemia may represent the ischemic penumbra [113]. One study correlated DWI to both NAA and lactate in ischemic stroke patients up to 24 h after onset [119]. While lactate correlated with DWI and PWI, NAA did not, suggesting that DWI and PWI measures may better predict early neuronal loss than NAA [Limited Evidence].

Cerebral metabolic rate of oxygen consumption ($CMRO_2$) has been measured in a small study of seven acute stroke patients using MRI, based on the T2* BOLD signal, and a threshold value has been proposed to define irreversibly injured brain tissue [Insufficient Evidence] [120]. Though preliminary, these results appear to be in agreement with data obtained using positron emission tomography (PET, see below) [121]. Measurement of $CMRO_2$ has theoretical advantages over other measures (e.g., CBF, CBV), as the threshold value for irreversible injury is likely to be time independent [122].

(b) Computed Tomography CT is capable of providing hemodynamic measurements, accomplished with either intravenous injection of nonionic contrast or inhalation of xenon gas. Like MR, perfusion parameters are obtained by tracking a contrast bolus or inhaled xenon gas in blood vessels and brain parenchyma with sequential CT imaging. Using a 320-row detector, the study can image the entire brain (~14 cm) compared to limited coverage (~3.5 cm) using old technology with a 64-row detector. For a protocol including CT perfusion and CT angiography, the effective radiation dose is increased to 10.6 milliSievert (mSv) for the 320-row detector compared to 7.5 mSv for the 64-row detector, with higher radiation dose to the lens, given the broader cranial coverage [123].

Xenon, an inert gas with an atomic number similar to iodine, can attenuate x-rays similar to intravenous contrast. However, unlike CT contrast, the gas is freely diffusible and can cross the blood-brain barrier. Sequential imaging permits the tracking of progressive accumulation and washout of the gas in brain tissue, and quantitative CBF and CBV maps can be calculated [124]. CBF values from xenon CT have been highly accurate compared with radioactive microsphere and iodoantipyrine techniques under different physiologic conditions and a wide CBF range in baboons (correlation coefficient r = 0.67–0.92) [125, 126]. Low CBF (<15 ml/100 g/min) correlated with early CT signs of infarction, proximal M1 occlusion, severe edema, and life threatening herniation. Very low CBF values (<7 ml/100 g/min) predicted irreversibly injured tissue [Limited Evidence] [127, 128]. Limitations of xenon CT include the need for a high xenon concentration in order to ensure a sufficient signal-to-noise ratio. The high dose may cause respiratory depression and cerebral vasodilation, and thus confound CBF measurements [129].

In addition to inhaled xenon, bolus nonionic contrast is used to generate a CT perfusion map. Rapid repeated serial images are acquired during the first pass of intravenous contrast to generate relative CBF, CBV, and time-based perfusion maps such as MTT and TTP. Despite the disappointing results of the MR diffusion-perfusion mismatch studies, perfusion CT has largely been validated against MRI. In a prospective multicenter study, acute ischemic stroke patients were imaged <12 h from stroke onset with CT and MRI. The perfusion CT parameter most accurately reflecting the ischemic core (as compared to DWI) was absolute CBV <2 ml/100 g, while the parameter most accurately reflecting the penumbra was a relative MTT >145 % of the contralateral hemisphere [Moderate Evidence] [130]. However, in more recent and larger studies, relative CBF was found to be more predictive of the ischemic core and final infarct volume than absolute CBV [Moderate Evidence] [131–133].

Perfusion CT has the advantage of increased efficiency and wider availability than MRI; however, major limitations of perfusion CT include ionizing radiation and a lower signal-to-noise ratio compared to MRI. Reduced anatomic coverage has recently limited the utility of perfusion CT, however, modern multi-detector scanners allow full brain coverage [133]. Unlike MRI, there have been no clinical trials of perfusion CT alone empirically selecting patients for delayed thrombolysis. Only in DIAS-2, perfusion CT was allowed along with MR perfusion for inclusion criteria to select patients with mismatch [112].

(c) Positron Emission Tomography Positron emission tomography (PET) has provided fundamental information on the pathophysiology of human cerebral ischemia, although its widespread clinical utility is limited, given the methodological hurdles of this modality. Quantitative perfusion and metabolic measurements can be obtained, namely, CBF, CBV, oxygen extraction fraction (OEF), and the cerebral metabolic rate of oxygen consumption ($CMRO_2$) using multiple tracers and serial arterial blood samplings. Based on these parameters, three distinct pathophysiologic states of ischemic stroke have been identified: oligemia, ischemia (increased OEF with preserved $CMRO_2$ – thought to represent the penumbra), and irreversible injury (low $CMRO_2$ – thought to represent the ischemic core) [134–136]. A decline in $CMRO_2$ below 1.4 mg/100 g/min heralds the transition from reversible to irreversible injury [121]. In three serial observational studies of acute ischemic stroke, elevation of OEF in the setting of low CBF has been suggested to be the marker of tissue viability in ischemic tissue and has been identified up to 48 h from stroke onset [Moderate Evidence] [137–140]. However, confirmation of tissue viability in regions of elevated OEF would require large randomized controlled trials demonstrating that reperfusion to regions of high OEF prevents progression to infarction. Such studies are difficult since PET is limited to major medical centers and requires considerable expertise and time and intra-arterial line placement, which precludes PET's use when administering thrombolytics.

One study assessed relative CBF using PET after thrombolysis in 12 ischemic stroke patients within 3 h of symptoms onset [141]. In all patients, early reperfusion of severely ischemic tissue (<12 ml/100 g/min in gray matter) predicted better clinical outcome and limited infarction.

What Is the Role of Noninvasive Intracranial Vascular Imaging?

Summary

With the development of different delivery approaches for thrombolysis in acute ischemic stroke, there is increasing demand for noninvasive vascular imaging modalities. Digital subtraction angiography (DSA) is typically the reference standard for diagnosing intracranial vascular pathology; however, the method requires arterial puncture and contrast to delineate the vasculature as well as carries a small risk of peri-procedural stroke. While data are available comparing MRA and CTA to DSA in subacute and chronic stroke patients, evidence supporting the use of such approaches in acute stroke management is lacking. Prospective studies examining the accuracy of acute noninvasive vascular imaging and if it alters clinical outcome after stroke are needed. The ongoing interventional management of stroke phase-3 (IMS-3) study will determine if intravenous plus intra-arterial tPA is superior to intravenous tPA alone for acute ischemic stroke within 3 h from symptom onset [142]. If the trial demonstrates benefit of interventional therapy, future acute stroke management may include vascular imaging in patients who meet the IMS-3 inclusion/exclusion criteria.

Supporting Evidence

(a) CT Angiogram One advantage of CT angiogram (CTA) is that it can be performed immediately following the prerequisite noncontrast CT for all stroke patients. The entire examination can be completed within a few minutes using 100 cc of nonionic intravenous contrast. A meta-analysis of eight high-quality studies and 864 patients compared carotid stenosis as measured by CTA to

DSA. For 70–99 % ICA stenosis, the overall sensitivity and specificity were 85 % and 93 %, respectively. For detection of ICA occlusion, the sensitivity and specificity were 97 % and 99 %, respectively [Strong Evidence] [143]. Similar high-level data for CTA use in intracranial stenosis is limited. In several small case series, the sensitivity and specificity of CTA for trunk occlusions of the circle of Willis were 83–100 % and 99–100 %, respectively, compared to DSA [Limited Evidence] [144–150]. One study with two blinded raters comparing CTA to DSA measured 475 short segments of intracranial arteries in 41 patients [151]. For detection of ≥50 % stenosis, CTA had 97.1 % sensitivity and 99.5 % specificity [Moderate Evidence]. A similar study of 672 intracranial vessel segments in 28 patients found 98 % sensitivity and 98 % specificity for stenosis and 100 % sensitivity and 100 % specificity for occlusion, using DSA as the reference standard [152]. This study also compared time-of-flight MRA to CTA and found CTA to have significantly higher sensitivity and positive predictive value than MRA [Moderate Evidence].

(b) MR Angiogram MR angiography (MRA) is capable of imaging the intracranial vasculature without contrast using a technique called "time-of-flight" or with contrast called "contrast-enhanced" MRA. For proximal ICA lesions, the sensitivity and specificity of contrast-enhanced MRA are high when compared to DSA. In a meta-analysis of 41 studies in 2,541 patients looking at ICA lesions of 70–99 % stenosis on DSA, contrast-enhanced MRA was found to be the most sensitive (94 %) and specific (95 %) of four modalities: enhanced MRA, non-enhanced MRA, Doppler ultrasound, and CTA [Strong Evidence] [153]. In another study of proximal ICA pathology, DSA and MRA were compared to surgical and histological findings of specimens removed during endarterectomy. Agreement for MRA was 89 % and for DSA was 93 % as compared with the measured stenosis from histological specimens, while plaque morphology was in agreement in 91 % of cases for MRA and 94 % of cases for DSA [Moderate Evidence] [154].

For extracranial proximal vertebral artery stenosis, contrast-enhanced MRA and CTA were performed in 46 prospective patients undergoing DSA. Contrast-enhanced MRA had the highest accuracy for detecting ≥50 % stenosis with higher sensitivity (83–89 %) than CTA (58–68 %) but similar specificity (87–89 % for MRA and 91–93 % for CTA) [Moderate Evidence] [155]. While MRA appears to be a useful tool for measuring stenosis in large vessels, its sensitivity decreases for smaller caliber intracranial vessels. Although contrast-enhanced MRA of the extracranial arteries appears to be better at defining the degree of stenosis than the time-of-flight MRA technique [156, 157], assessment of the intracranial vessels with contrast is limited due to venous contamination. In the study of intracranial disease discussed above comparing CTA and MRA to DSA in 28 patients (in 672 vessel segments), time-of-flight MRA had a sensitivity of 70 % and 81 % and specificity of 99 % and 98 % for intracranial stenosis and intracranial occlusion, respectively [Moderate Evidence] [152]. The Stroke Outcomes and Neuroimaging of Intracranial Atherosclerosis (SONIA) trial was a prospective, multicenter study comparing the diagnostic accuracy of transcranial Doppler (TCD) and MRA to DSA [158]. The SONIA study found that both TCD and MRA have high negative predictive values (86 % and 91 %, respectively) but low positive predictive values (36 % and 59 %, respectively) [Strong Evidence]. Sensitivity and specificity could not be obtained since not every patient had DSA [158].

Special Situation: Acute Neuroimaging in Pediatric Stroke

Summary

The recognition of pediatric acute stroke is often delayed by parents and caregivers due to a lack of awareness and education regarding this condition. Moreover, a subset of children and neonates may have a less clear and more gradual onset of stroke symptoms. Therefore, studies evaluating the pediatric acute stroke population are few, limiting our

knowledge regarding the utility of neuroimaging for early therapeutic decision-making.

Supporting Evidence

Compared to stroke in the adult population, pediatric stroke is a relatively uncommon disorder with typically very different pathophysiology. The overall incidence of ischemic stroke is 2–13 per 100,000 children with the highest rate occurring in the perinatal period (26.4 per 100,000 infants less than 30 days old) [159, 160]. The reported incidence of ischemic stroke has increased over the past decades, due to better population-based studies (the Canadian Pediatric Stroke Registry), more sensitive imaging techniques (fetal MR, DWI), and an increased survival of immature neonates due to improved treatment modalities (extracorporeal membrane oxygenation). The etiologies of ischemic stroke in children are due to non-atherosclerotic causes such as transient cerebral arteriopathy, post-infectious vasculopathy, cervical artery dissection, Moyamoya disease, congenital heart disease, sickle cell anemia, and coagulation disorders, and are idiopathic in 20–25 % of cases [159, 161, 162].

There are no randomized clinical trials for the treatment of acute ischemic stroke in the pediatric population; however, the Thrombolysis in Pediatric Stroke (TIPS) study, an international multicenter study, will assess the safety and feasibility of intravenous tPA at 0–3 h and intra-arterial tPA at 3–6 h after stroke onset in children age 2–17 [163]. In contrast to the adult NINDS tPA trial which required only a noncontrast head CT prior to tPA administration, TIPS will require imaging confirmation of ischemic stroke using MRI DWI as well as confirmation of arterial occlusion in the same territory as the visualized stroke using MRA or CTA. Additional requirement of advanced imaging in a pediatric acute stroke evaluation is not without challenges. In children <8 years old, sedation and anesthesia are often required to minimize motion artifact [162]. Administration of anesthesia requires a specialized team to be available at all hours. If required, both imaging and administration of anesthesia will lead to delay in stroke treatment. Extrapolating from adult data, MRI is likely much more sensitive than CT for acute ischemic stroke. In one study of 74 children with acute ischemic stroke, only 12 could be detected with CT alone and the remainder required MRI confirmation [Moderate Evidence] [164]. Although data on vascular imaging are sparse in the pediatric population, vascular imaging with MRA, CTA, or DSA is often recommended to identify the site of arterial occlusion or other vasculopathy. Advantages of MRA over CT are the lack of radiation and that time-of-flight MRA does not require contrast. The advantages of CT include its wider availability and the speed of image acquisition which may limit the need for sedation. Despite its invasive nature, DSA is considered the reference standard and may be preferable when a definitive etiology has not been identified.

Diagnostic imaging is particularly important in perinatal stroke due to subtle clinical findings on presentation. While approximately 60 % of infants develop symptoms within a few days of stroke onset, the remaining 40 % have delayed presentations beyond 1 month [165]. For suspected perinatal stroke, initial neuroimaging is commonly cranial ultrasound. However, a prospective study of 47 neonates revealed that cranial ultrasound had low sensitivity (68 %) in the first few days after symptom onset when compared to MRI [Limited Evidence] [166]. Brain CT is often deferred due to its low sensitivity and radiation exposure. Increasingly, DWI is considered the most accurate marker of ischemia in perinatal stroke, although data validating DWI with final stroke volume or clinical diagnosis are lacking [165–167]. Beyond its diagnostic use, MRI in perinatal stroke has been found to correlate with measures of long-term clinical outcome. A prospective study in 100 children with perinatal stroke found that stroke location, specifically corticospinal tract involvement, was predictive of hemiplegia at 2 years of age [Moderate Evidence] [168].

The lack of proven treatment for acute pediatric stroke limits the utility of acute neuroimaging for early therapeutic decision-making. However, in children with sickle cell anemia, there are two important randomized controlled trials for stroke prevention (STOP I and STOP II) [169, 170]. These trials demonstrated

a highly significant reduction of recurrent strokes with regular blood transfusions for patients with peak mean blood flow velocities greater than 200 cm per second measured by transcranial Doppler ultrasonography [Strong Evidence]. Imaging in sickle cell anemia will be covered in greater depth in a separate chapter.

Take Home Figure and Tables

Figure 10.1 is an imaging flowchart for acute stroke imaging.

Tables 10.1 and 10.2 highlight data and evidence.

Imaging Case Studies

Case 1

Cerebral microbleeds (Fig. 10.2)

Table 10.1 Diagnostic performance of different imaging modalities in patients presenting with acute neurological deficits

	Sensitivity	Specificity	References	Evidence
Acute intraparenchymal hemorrhage (<6 h)				
CT	100 %[a]	100 %[a]		[a]
MRI	100 %	100 %	[16]	Strong
Acute ischemic infarction (<3 h)				
CT	12 %	100 %	[17]	Strong
MRI	73 %	92 %	[17]	Strong
Acute ischemic infarction (<6 h)				
CT	61 %	65 %	[16]	Moderate
MRI	91 %	95 %	[16]	Moderate
Acute ischemic infarction (<12 h)				
CT	20 %	96 %	[17]	Strong
MRI	81 %	99 %	[17]	Strong

[a]Although the exact sensitivity or specificity of CT for detecting intraparenchymal hemorrhage is unknown [Limited Evidence], it serves as the reference standard for detection in comparison to other modalities

Reprinted with permission of Springer Science+Business Media from Vo KD, Lin W, Lee J-W. Neuroimaging in Acute Ischemic Stroke. In Medina LS, Blackmore CC (eds): Evidence-Based Imaging: Optimizing Imaging in Patient Care. New York: Springer Science+Business Media, 2006

** Hyper-acute MRI can be performed instead of CT at hospitals with immediate availability of MRI. Scan duration should be minimized to essential sequences (DWI for detection of ischemia and T2*/GRE/SWI for detection of ICH and should not exceed more than a few minutes such that tPA treatment is not delayed (since time from onset to tPA treatment is closely related to clinical outcome). Of importance, DWI is not 100% sensitive and may be normal in some cases of acute ischemic stroke and should not preclude IV tPA in patients who are suspected to have an ischemic stroke clinically.

Fig. 10.1 Acute stroke imaging flowchart

Table 10.2 Acute ischemic stroke perfusion-weighted imaging parameters

Parameter	Units	Description
Cerebral blood flow (CBF)	ml/100 g tissue/min	Volume of blood flowing through brain tissue over time CBF is decreased in the ischemic core and penumbra
Cerebral blood volume (CBV)	ml/100 g tissue	Volume of blood within a given amount of brain tissue CBV is decreased in the ischemic core and is normal in the penumbra
Mean transit time (MTT)	Seconds	Time for contrast to traverse a volume of brain tissue MTT is increased in the ischemic core and penumbra
Time to peak (TTP)	Seconds	Time-point of maximum signal intensity loss after the passage of the contrast agent in brain tissue TTP is increased in the ischemic core and penumbra
Time to maximum (Tmax)	Seconds	Time to maximum of the tissue residue function obtained by deconvolution; Tmax may be affected by temporal dispersion due to large artery stenosis or occlusion Tmax is increased in the ischemic core and penumbra

Data from Ostergaard [89]
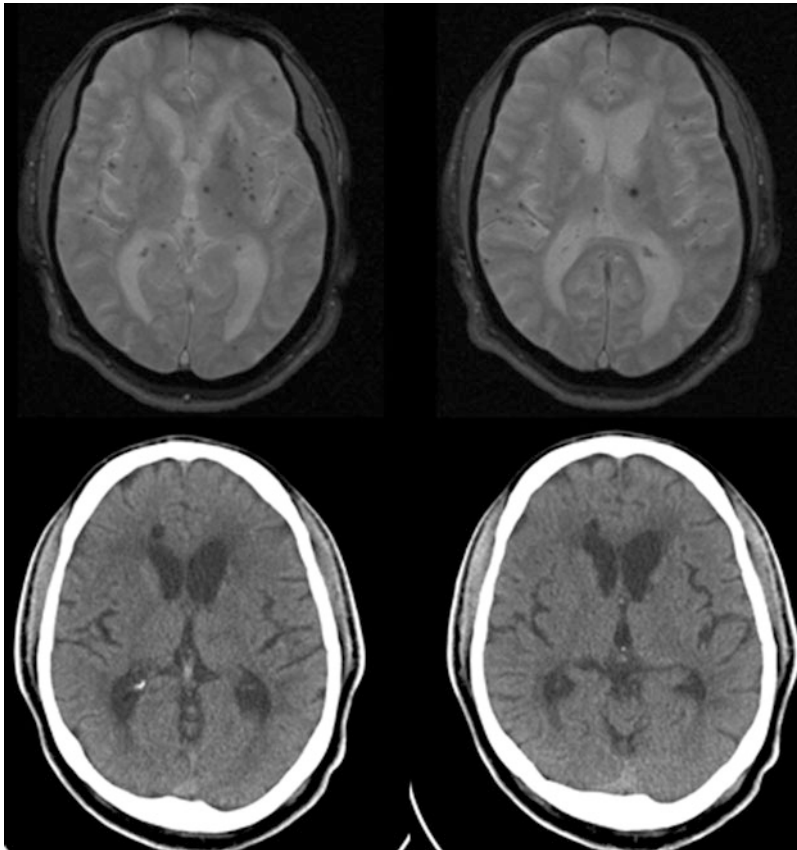
Fig. 10.2 Microhemorrhages. *Top row*: Two sequential images of T2* MR sequence show innumerable small low signal lesions scattered throughout both cerebral hemispheres compatible with microhemorrhages. *Bottom row*: Noncontrast axial CT at the same anatomic levels does not show the microhemorrhages (Reprinted with permission of Springer Science+Business Media from Vo KD, Lin W, Lee J-W. Neuroimaging in Acute Ischemic Stroke. In Medina LS, Blackmore CC (eds): Evidence-Based Imaging: Optimizing Imaging in Patient Care. New York: Springer Science+Business Media, 2006)
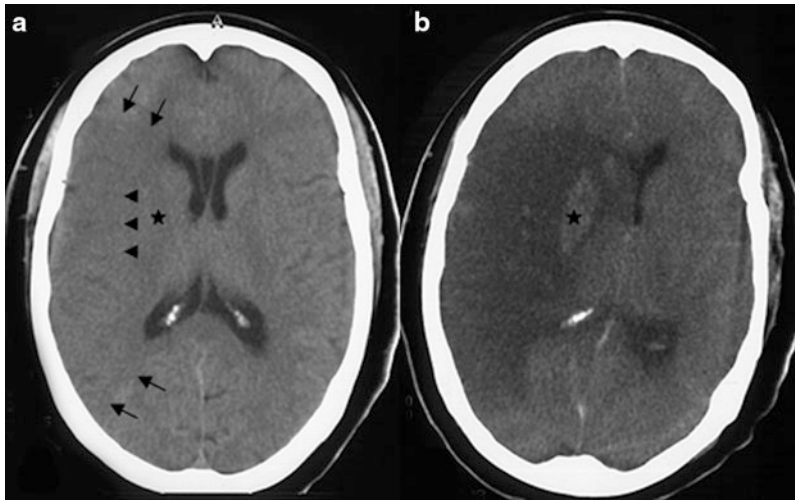
Fig. 10.3 (**a**, **b**) Early CT Signs of infarction. (**a**) Noncontrast axial CT performed at 2 h after stroke onset shows a large low attenuated area involving the entire right middle cerebral artery distribution (bounded by *arrows*) with associated effacement of the sulci and sylvian fissure. There is obscuration in the right lentiform nucleus (*star*) and loss of the insular ribbon (*arrow head*). (**b**) Follow-up noncontrast axial image 4 days later confirms the infarction in the same vascular distribution.

There is hemorrhagic conversion (*star*) in the basal ganglia with mass effect and subfalcine herniation (Reprinted with permission of Springer Science+Business Media from Vo KD, Lin W, Lee J-W. Neuroimaging in Acute Ischemic Stroke. In Medina LS, Blackmore CC (eds): Evidence-Based Imaging: Optimizing Imaging in Patient Care. New York: Springer Science+Business Media, 2006)
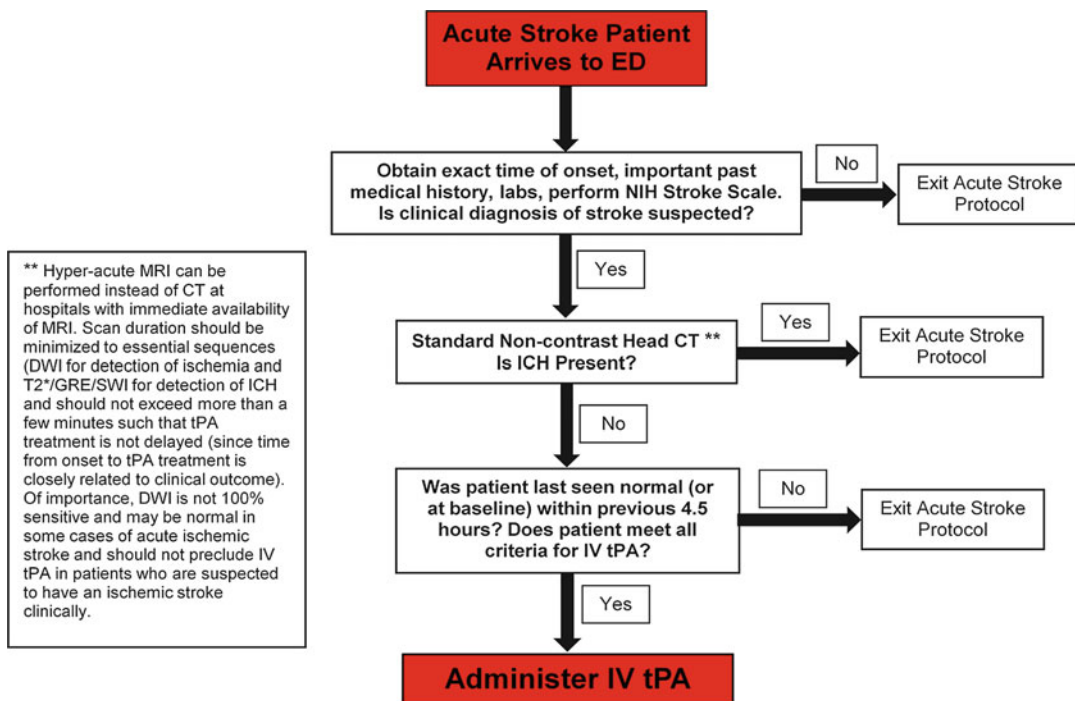
Case 2

Signs of infarction (Fig. 10.3a, b)

Case 3

Evolution of left middle cerebral artery distribution infarction (Fig. 10.4a–d)

Acute Imaging Protocols

Head CT – Indicated for all patients presenting with acute focal deficits
Noncontrast examination
Sequential or spiral CT with 5 mm slice thickness from the skull base to the vertex
Head MR – Indicated if stroke is in doubt
Axial DWI (EPI) with ADC map, GRE or EPI T2*, FLAIR, T1W
Optional sequences [insufficient evidence for routine clinical practice]:

MRA of the circle of Willis (3D TOF technique) or contrast-enhanced
PWI (EPI FLASH, 14 slices per measurement for 50 measurements, with 10 s injection delay, injection rate of 5 cc/s with single bolus of gadolinium, followed by a 20 cc normal saline flush)
Axial T1W post contrast

Future Research

- Use of neuroimaging to select patients for acute therapies:
  - Imaging the ischemic penumbra to extend the empirically determined therapeutic windows for certain individuals.
  - Predict individuals at high risk for hemorrhagic conversion.
  - As more therapies are made available, neuroimaging has the potential to help determine which modality might be most efficacious (e.g., imaging large-vessel
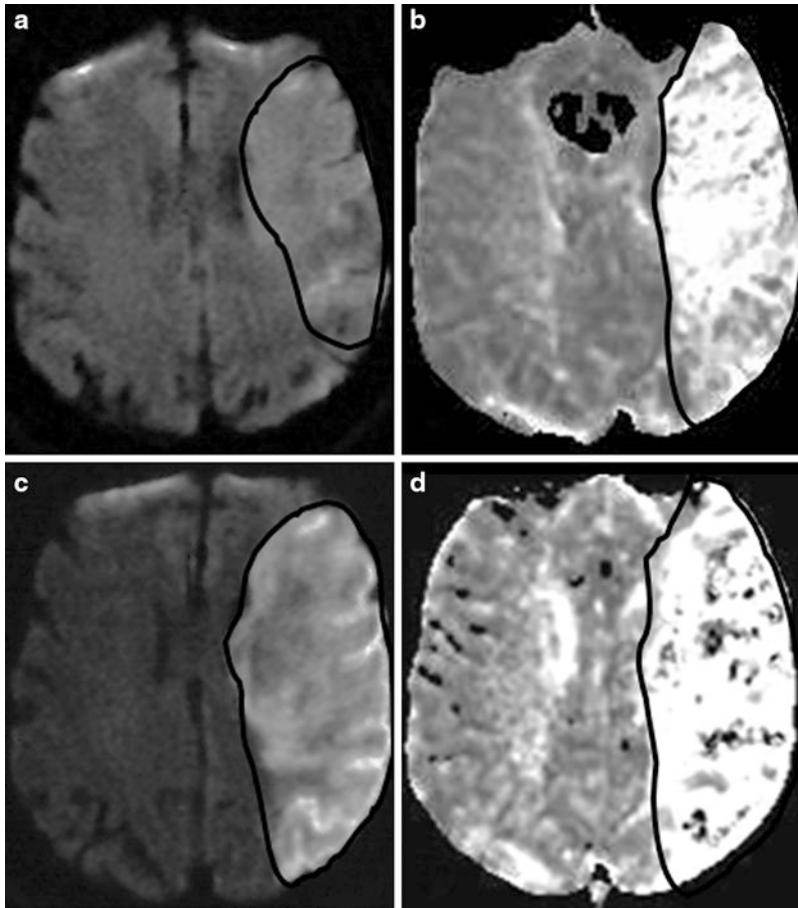
Fig. 10.4 (**a–d**) Evolution of the right middle cerebral distribution infarction on MRI. MRI at 3 h after stroke onset shows an area of restricted diffusion on DWI (**a**) with a larger area of perfusion defect on PWI (**b**). The area of normal DWI but abnormal PWI represents an area of diffusion-perfusion mismatch. Follow-up MRI at 3 days post ictus shows interval enlargement of the lesion on DWI (**c**) to the same size as the initial perfusion deficit (**b**). There is now a matched diffusion-perfusion (**c, d**) (Reprinted with permission of Springer Science+Business Media from Vo KD, Lin W, Lee J-W. Neuroimaging in Acute Ischemic Stroke. In Medina LS, Blackmore CC (eds): Evidence-Based Imaging: Optimizing Imaging in Patient Care. New York: Springer Science+Business Media, 2006)

occlusions for use of intra-arterial thrombolysis or clot retrieval).
- Use of neuroimaging to predict outcome:
  - Useful for prognostic purposes, or for discharge planning
  - Useful as a surrogate measure of outcome in clinical trials

References

1. American Heart Association. Heart disease and stroke statistics update at-a-glance. Dallas, TX: AHA; 2010.
2. Bogousslavsky J, Van Melle G, Regli F. Stroke. 1988;19(9):1083–92.
3. Roger VL, et al. Circulation. 123(4):e18–e209.
4. American Heart Association. Heart disease and stroke statistics update. Dallas, TX: AHA; 2004.
5. Report, M.A.M.W., Centers for Disease Control and Prevention/National Center for Health Statistics. 2001;50(7).
6. Sacco RL, et al. Am J Epidemiol. 1998;147(3):259–68.
7. NINDS. N Engl J Med. 1995;333(24):1581–7.
8. Qureshi AI, et al. Neurosurgery. 2005;57(4):647–54; discussion 647–54.
9. Kleindorfer D, et al. Stroke. 2008;39(3):924–8.
10. Kleindorfer D, et al. Stroke. 2009;40(11):3580–4.
11. Diringer MN, et al. Stroke. 1999;30(4):724–8.

12. Young KC, Benesch CG, Jahromi BS. Neurology. 2010;75(19):1678–85.
13. Earnshaw SR, et al. Stroke. 2009;40(5):1710–20.
14. Jackson D, et al. AJNR Am J Neuroradiol. 2010; 31(9):1669–74.
15. Hacke W, et al. N Engl J Med. 2008;359(13): 1317–29.
16. Fiebach JB, et al. Stroke. 2004;35(2):502–6.
17. Chalela JA, et al. Lancet. 2007;369(9558):293–8.
18. New PF, Aronow S. Radiology. 1976;121(3 Pt. 1): 635–40.
19. Culebras A, et al. Stroke. 1997;28(7):1480–97.
20. Beauchamp Jr NJ, et al. Radiology. 1999;212(2): 307–24.
21. Paxton R, Ambrose J. Br J Radiol. 1974;47(561): 530–65.
22. Jacobs L, Kinkel WR, Heffner Jr RR. Neurology. 1976;26(12):1111–8.
23. Adams Jr HP, et al. Neurology. 1983;33(8):981–8.
24. van der Wee N, et al. J Neurol Neurosurg Psychiatry. 1995;58(3):357–9.
25. Sames TA, et al. Acad Emerg Med. 1996;3(1): 16–20.
26. Sidman R, Connolly E, Lemke T. Acad Emerg Med. 1996;3(9):827–31.
27. Bradley Jr WG. Radiology. 1993;189(1):15–26.
28. Gomori JM, et al. Radiology. 1985;157(1):87–93.
29. Edelman RR, et al. AJNR Am J Neuroradiol. 1986; 7(5):751–6.
30. Thulborn K, Atlas S. Intracranial hemorrhage. New York: Raven; 1991.
31. Schellinger PD, et al. Stroke. 1999;30(4):765–8.
32. Patel MR, Edelman RR, Warach S. Stroke. 1996; 27(12):2321–4.
33. Kidwell CS, et al. JAMA. 2004;292(15):1823–30.
34. Wycliffe ND, et al. Magn Reson Imaging. 2004;20(3):372–7.
35. Nandigam RN, et al. AJNR Am J Neuroradiol. 2009;30(2):338–43.
36. Fiehler J, et al. Stroke. 2007;38(10):2738–44.
37. Lee SH, et al. J Neurol Neurosurg Psychiatry. 2008; 79(8):913–6.
38. Kakuda W, et al. Neurology. 2005;65(8):1175–8.
39. Lees KR, et al. Lancet. 375(9727):1695–703.
40. Libman RB, et al. Arch Neurol. 1995;52(11): 1119–22.
41. Norris JW, Hachinski VC. Lancet. 1982;1(8267): 328–31.
42. Kothari RU, et al. Stroke. 1995;26(12):2238–41.
43. Truwit CL, et al. Radiology. 1990;176(3):801–6.
44. Tomura N, et al. Radiology. 1988;168(2):463–7.
45. Patel SC, et al. JAMA. 2001;286(22):2830–8.
46. von Kummer R, et al. AJNR Am J Neuroradiol. 1994;15(1):9–15; discussion 16–8.
47. Schriger DL, et al. JAMA. 1998;279(16):1293–7.
48. Grotta JC, et al. Stroke. 1999;30(8):1528–33.
49. Hacke W, et al. JAMA. 1995;274(13):1017–25.
50. Toni D, et al. Neurology. 1996;46(2):341–5.
51. Larrue V, et al. Stroke. 1997;28(5):957–60.
52. Larrue V, et al. Stroke, Radiology. 1997;205(2): 327–33.
53. von Kummer R, et al. Acute stroke: usefulness of early CT findings before thrombolytic therapy, Radiology. 1997;205(2):327–33.
54. Furlan A, et al. JAMA. 1999;282(21):2003–11.
55. Barber PA, et al. Lancet. 2000;355(9216):1670–4.
56. Puetz V, et al. Int J Stroke. 2009;4(5):354–64.
57. Dzialowski I, et al. Stroke. 2006;37(4):973–8.
58. Kucharczyk J, et al. Diffusion/perfusion MR imaging of acute cerebral ischemia. Magn Reson Med. 1991;19(2):311–5.
59. Reith W, et al. Neurology. 1995;45(1):172–7.
60. Mintorovitch J, et al. Magn Reson Med. 1991;18(1): 39–50.
61. Warach S, et al. Ann Neurol. 1995;37(2):231–41.
62. Moseley ME, et al. Magn Reson Med. 1990;14(2): 330–46.
63. Hoehn-Berlage M, et al. J Cereb Blood Flow Metab. 1995;15(6):1002–11.
64. Warach S, Boska M, Stroke KM. 1997;28(3):481–2.
65. Gonzalez RG, et al. Radiology. 1999;210(1): 155–62.
66. Lovblad KO, et al. AJNR Am J Neuroradiol. 1998;19(6):1061–6.
67. Fiebach JB, et al. Stroke. 2002;33(9):2206–10.
68. Marks MP, et al. Radiology. 1996;199(2):403–8.
69. Kidwell CS, et al. Stroke. 1999;30(6):1174–80.
70. Ay H, et al. Neurology. 1999;52(9):1784–92.
71. An H, et al. Stroke. 2011;42(5):1276–81.
72. Ebisu T, et al. Magn Reson Imaging. 1996;14(9): 1113–6.
73. Ohta K, et al. J Neurol. 1999;246(8):736–8.
74. Sener RN. Comput Med Imaging Graph. 2001;25(5):391–7.
75. Bahn MM, et al. Arch Neurol. 1997;54(11):1411–5.
76. Gauvain KM, et al. AJR Am J Roentgenol. 2001;177(2):449–54.
77. Chen S, et al. AJNR Am J Neuroradiol. 2001;22(6): 1089–96.
78. Chu K, et al. Arch Neurol. 2001;58(6):993–8.
79. Hasegawa Y, et al. Stroke. 1996;27(9):1648–55; discussion 1655–6.
80. Linfante I, et al. Arch Neurol. 2001;58(4):621–8.
81. Warach S, et al. Ann Neurol. 2000;48(5):713–22.
82. Tong DC, et al. Neurology. 1998;50(4):864–70.
83. Lovblad KO, et al. Ann Neurol. 1997;42(2):164–70.
84. Wardlaw JM, et al. Stroke. 2004;35(11):2477–83.
85. Villringer A, et al. Magn Reson Med. 1988;6(2): 164–74.
86. Rosen BR, et al. Magn Reson Med. 1991;19(2): 285–92.
87. Rosen BR, et al. Magn Reson Med. 1990;14(2): 249–65.
88. Ostergaard L, et al. Magn Reson Med. 1996;36(5): 726–36.
89. Ostergaard L. Cerebral perfusion imaging by bolus tracking. Top Magn Reson Imaging. 2004;15(1):3–9.

90. van Laar PJ, van der Grond J, Hendrikse J. Radiology. 2008;246(2):354–64.
91. Astrup J, Siesjo BK, Symon L. Stroke. 1981; 12(6):723–5.
92. Baird AE, et al. Ann Neurol. 1997;41(5):581–9.
93. Beaulieu C, et al. Ann Neurol. 1999;46(4):568–78.
94. Davis SM, et al. Lancet Neurol. 2008;7(4):299–309.
95. Perkins CJ, et al. Stroke. 2001;32(12):2774–81.
96. Albers GW, et al. Ann Neurol. 2006;60(5):508–17.
97. Clark WM, et al. Neurology. 2001;57(9):1595–602.
98. Uno M, et al. Neurosurgery. 2002;50(1):28–34; discussion 34–5.
99. Minematsu K, et al. Stroke. 1992;23(9):1304–10; discussion 1310–1.
100. Hasegawa Y, et al. Neurology. 1994;44(8):1484–90.
101. Kidwell CS, et al. Ann Neurol. 2000;47(4):462–9.
102. Fiehler J, et al. Stroke. 2002;33(1):79–86.
103. Chemmanam T, et al. Neurology. 75(12):1040–7.
104. Takasawa M, et al. Stroke. 2008;39(3):870–7.
105. Olivot JM, et al. Stroke. 2009;40(2):469–75.
106. Kane I, et al. Stroke. 2007;38(12):3158–64.
107. Olivot JM, et al. Neurology. 2009;72(13):1140–5.
108. Butcher KS, et al. Stroke. 2005;36(6):1153–9.
109. Sobesky J, et al. Stroke. 2004;35(12):2843–7.
110. Christensen S, et al. Stroke. 2009;40(6):2055–61.
111. Hacke W, et al. Stroke. 2005;36(1):66–73.
112. Hacke W, et al. Lancet Neurol. 2009;8(2):141–50.
113. Barker PB, et al. Radiology. 1994;192(3):723–32.
114. Grohn OH, Kauppinen RA. NMR Biomed. 2001; 14(7–8):432–40.
115. Decanniere C, et al. Magn Reson Med. 1995; 34(3):343–52.
116. Bizzi A, et al. Magn Reson Imaging. 1996;14(6): 581–92.
117. Sager TN, Laursen H, Hansen AJ. J Cereb Blood Flow Metab. 1995;15(4):639–46.
118. Munoz Maniega S, et al. Neurology. 2008; 71(24):1993–9.
119. Cvoro V, et al. Stroke. 2009;40(3):767–72.
120. Lee JM, et al. Ann Neurol. 2003;53(2):227–32.
121. Powers WJ, et al. J Cereb Blood Flow Metab. 1985;5(4):600–8.
122. Baron JC. Cerebrovasc Dis. 1999;9(4):193–201.
123. Diekmann S, et al. AJNR Am J Neuroradiol. 2010;31(6):1003–9.
124. Gur D, et al. Science. 1982;215(4537):1267–8.
125. Wolfson Jr SK, et al. Stroke. 1990;21(5):751–7.
126. DeWitt DS, et al. Stroke. 1989;20(12):1716–23.
127. Firlik AD, et al. Stroke. 1997;28(11):2208–13.
128. Firlik AD, et al. J Neurosurg. 1998;89(2):243–9.
129. Plougmann J, et al. J Neurosurg. 1994;81(6):822–8.
130. Wintermark M, et al. Stroke. 2006;37(4):979–85.
131. Mayer TE, et al. AJNR Am J Neuroradiol. 2000; 21(8):1441–9.
132. Bivard A, et al. Cerebrovasc Dis. 2011;31(3): 238–45.
133. Campbell B, et al. Predicting infarct core using CT perfusion: comparison of CT perfusion parameters to concurrent diffusion MRI. In: International stroke conference; 2011: Los Angeles.
134. Baron JC, et al. J Cereb Blood Flow Metab. 1989;9(6):723–42.
135. Baron JC, et al. Stroke. 1981;12(4):454–9.
136. Powers RH, et al. Cancer Res. 1992;52(7): 1699–703.
137. Wise RJ, et al. Brain. 1983;106(Pt 1):197–222.
138. Heiss WD, et al. J Cereb Blood Flow Metab. 1992;12(2):193–203.
139. Furlan M, et al. Ann Neurol. 1996;40(2):216–26.
140. Markus R, et al. Brain. 2004;127(Pt 6):1427–36.
141. Heiss WD, et al. J Cereb Blood Flow Metab. 1998;18(12):1298–307.
142. Khatri P, et al. Int J Stroke. 2008;3(2):130–7.
143. Koelemay MJ, et al. Stroke. 2004;35(10):2306–12.
144. Hirai T, et al. AJNR Am J Neuroradiol. 2002; 23(1):93–101.
145. Katz DA, et al. Radiology. 1995;195(2):445–9.
146. Knauth M, et al. AJNR Am J Neuroradiol. 1997; 18(6):1001–10.
147. Shrier DA, et al. AJNR Am J Neuroradiol. 1997; 18(6):1011–20.
148. Wildermuth S, et al. Stroke. 1998;29(5):935–8.
149. Verro P, et al. Stroke. 2002;33(1):276–8.
150. Graf J, et al. J Neurol. 2000;247(10):760–6.
151. Nguyen-Huynh MN, et al. Stroke. 2008;39(4): 1184–8.
152. Bash S, et al. AJNR Am J Neuroradiol. 2005; 26(5):1012–21.
153. Wardlaw JM, et al. Lancet. 2006;367(9521): 1503–12.
154. Liberopoulos K, et al. Int Angiol. 1996;15(2): 131–7.
155. Khan S, et al. Stroke. 2009;40(11):3499–503.
156. Cloft HJ, et al. Magn Reson Imaging. 1996;14(6): 593–600.
157. Willig DS, et al. Radiology. 1998;208(2):447–51.
158. Feldmann E, et al. Neurology. 2007;68(24): 2099–106.
159. Lynch JK, et al. Pediatrics. 2002;109(1):116–23.
160. Agrawal N, et al. Stroke. 2009;40(11):3415–21.
161. Kirkham FJ, et al. J Child Neurol. 2000;15(5): 299–307.
162. Jordan LC, Hillis AE. Nat Rev Neurol. 2011; 7(4):199–208.
163. Amlie-Lefond C, et al. Neuroepidemiology. 2009; 32(4):279–86.
164. Srinivasan J, et al. Pediatrics. 2009;124(2):e227–34.
165. Chabrier S, et al. Thromb Res. 2011;127(1):13–22.
166. Cowan F, et al. Arch Dis Child Fetal Neonatal Ed. 2005;90(3):F252–6.
167. Dudink J, et al. AJNR Am J Neuroradiol. 2009; 30(5):998–1004.
168. Husson B, et al. Pediatrics. 2010;126(4):912–8.
169. Adams RJ, Brambilla D. N Engl J Med. 2005; 353(26):2769–78.
170. Adams RJ, et al. N Engl J Med. 1998;339(1):5–11.

Sickle-Cell Disease and Stroke: Evidence-Based Neuroimaging

11

Jaroslaw Krejza, Michal Arkuszewski, Maciej Swiat, Maciej Tomaszewski, and Elias R. Melhem

Contents

J. Krejza (✉)

Department of Radiology, University of Pennsylvania Health System, Perelman School of Medicine at the University of Pennsylvania, Philadelphia, PA, USA

College of Medicine, Al–Imam Mohamed bin Saud Islamic University, Riyadh, Saudi Arabia
e-mail: jaroslaw.krejza@uphs.upenn.edu

M. Arkuszewski
Department of Neurology, Medical University of Silesia, Central University Hospital, Katowice, Poland
e-mail: Michal.arkuszewski@gmail.com

M. Swiat
Department of Neuroscience, University Hospitals Conventry and Warwickshire, Coventry, UK

M. Tomaszewski • E.R. Melhem
Department of Radiology, University of Pennsylvania, Philadelphia, PA, USA
e-mail: Elias.Melhem@uphs.upenn.edu

Key Points

- Implementation of the Stroke Prevention Trial in Sickle Cell Anemia (STOP) primary prevention strategy using transcranial Doppler screening results in lower rates of stroke admissions (limited evidence).
- Presence of silent infarcts on MR scans in asymptomatic children with SCD is associated with higher risk for future stroke (limited evidence).
- In asymptomatic children with SCD and hemoglobin (Hb) SS in whom intracranial arterial velocities are over 200 cm/s on transcranial Doppler examination, the risk of first stroke can be substantially reduced by chronic transfusions (strong evidence).
- Children with SCD and acute stroke require immediate non-contrast CT to exclude intracranial hemorrhage (moderate–strong evidence).
- Children with symptoms of stroke and a negative CT for hemorrhage require urgent MRI/DWI/MRA to assess the degree and extent of brain structural abnormalities and PET/SPECT or MRS to determine the degree of ischemia (moderate evidence).
- Presence of intracranial arterial stenosis and new lesions on MR imaging in patients with stroke history are associated with high risk for recurrent stroke (limited evidence).
- In children with SCD, there are no specific neuroimaging findings to indicate when blood transfusions can be safely halted (strong evidence).
- There are no data that evaluate the cost-effectiveness of different neuroimaging modalities in the evaluation of symptomatic and asymptomatic patients with SCD and suspected stroke (limited evidence).

Definition, Pathophysiology, and Clinical Presentation

SCD is the family of recessively inherited disorders of hemoglobin (Hb) [1], which have developed in response to strong evolutionary selection by malaria [2, 3]. Sickle-cell anemia (SCA), the most severe form of SCD, refers specifically to homozygosity for the HbS (βS), a variant of the HbB gene (which encodes β-globin), whereas people who inherit only one sickle gene are sickle-cell carriers [4, 5]. HbS homozygotes suffer from SCD, but heterozygotes have a tenfold reduced risk of severe malaria [6, 7]. SCD also includes other variants of the HbB gene, namely, HbC and HbE [8–11] and regulatory defects of HbA and HbB, which cause α and ß thalassemia (Sß + or Sß0) [12–14]. The evolutionary pressure has risen to high frequencies of HbS allele in malaria-exposed populations despite the fatal consequences for homozygotes (HbSS) [2]. Different populations have developed independent evolutionary responses to malaria at both the global and the local levels [15]. The most striking example is the Hb gene, in which three different coding single nucleotide points confer protection against malaria: Glu6Val (HbS), Glu6Lys (HbC), and Glu26Lys (HbE) [3]. The HbS allele is common in Africa but rare in Southeast Asia, whereas the opposite is true for the HbE allele [3, 15]. At the local level, not only frequency of the HbC and HbS allele varies [8], but the frequency of their haplotypes also varies; for instance, the HbS allele is found in four distinct haplotypes in West Africa region [16–18].

Pathophysiology

Sickle deoxyhemoglobin tends to polymerize to gel-like consistency while the red blood cell (RBC) becomes more rigid and deformed to a less pliable sickle shape [19–21]. This increases blood viscosity and mechanical stress on RBCs during their passage through microcirculation, resulting in hemolytic anemia [22, 23] and chronic inflammation with elevated levels of biologic mediators and ongoing activation of the coagulation system, even when they are in "steady state" [23–25]. As a result, the viscosity of the oxygenated sickle blood is about 1.5-fold that of normal at equal shear rates, but blood viscosity increases tenfold in the deoxygenation state [26].

Cerebral blood flow (CBF) and systemic circulation in SCD adapt to the altered rheologic conditions [27] especially by recruiting vasodilatation to reduce resistance to flow and increase flow velocity, which decreases apparent viscosity [28, 29]. CBF and cerebral blood volume (CBV) in children with SCD are higher than in controls by a factor of 1.5 and vary inversely with the degree of anemia [30]. Faster transit time lowers oxygen extraction and increases venous hemoglobin oxygen saturation, which probably are protective [29]. Chronic vasodilatation and tissue hyperemia lead to increase in blood flow velocity in major cerebral arteries, with subsequent higher wall shear stress and reactive intimal hyperplasia and stenosis that increases the risk of ischemic stroke [31]. Under physiologic conditions, the upper limit of cerebral dilatation corresponds to a tissue perfusion rate of approximately 200 ml/100 g/min, and this limit is clearly approached in young anemic patients [31]. Also, oxygen affinity to hemoglobin is reduced to facilitate oxygen delivery during shorter transit time through microvasculature [32]. If velocity at the level of microvasculature drops due to, for instance, a proximal large artery narrowing, oxygen extraction increases and proportionally more sticky deoxyhemoglobin arrives to venules. This increases risk of vaso-occlusions, infarctions, hemolysis, and inflammation [21, 33, 34]. The damaged RBCs release free radicals and free hemoglobin into the plasma, which strongly bind to nitric oxide, causing functional nitric oxide deficiency and contributing to further development of vasculopathy and stroke [21].

Clinical Symptoms

There is a wide range of values for all RBC indices in chronic SCA [35]. The reduction in volume of RBC restricts the oxygen-carrying capacity of Hb, leading to chronic oxyhemoglobin desaturation [36]. Children with HbSS are more vulnerable to frequent episodes of pain, chest crisis, stroke [37–40], and delayed growth [41] than those with HbSC or HbSβ0 thalassemia, who usually have less severe neurological complications in later life [21].

Stroke – typically defined as a cerebral vascular accident (CVA) of sudden onset with focal neurological deficit persisting after 24 h, developed either spontaneously or in the context of an acute illness such as infection – is a major cause of morbidity in SCD [42]. There is a high risk of CVA recurrence – particularly for patients presenting spontaneously – that is reduced but not eliminated by regular blood transfusion [42, 43].

Both ischemic and hemorrhagic strokes as well as common subclinical strokes called "silent infarcts" may be encountered [37, 44, 45]. The typical areas of infarction are the frontal and parietal lobes, particularly in boundary zones of territories supplied by the internal carotid and middle and anterior cerebral arteries; the posterior circulation is affected less frequently [44]. There is a broad spectrum of acute presentations with CVA and other neurological complications in patients with SCD [46–49]. Patients with SCD also can have transient ischemic attacks (TIAs), with symptoms and signs resolving within 24 h [46–48], although many of these individuals are found to have had recent cerebral infarction or atrophy on imaging [37]. The insidious onset of "soft neurological signs," such as difficulty in tapping quickly, is an indicator of associated cerebral infarction [50, 51]. Melek et al. observed that in over 95 % of SCD patients with silent infarcts, at least one soft sign was present [50]. In addition, seizures (20–48 %) [52, 53], decreased levels of consciousness [54], and headache (6.9 %) [55, 56] are also indicators of stroke and CVA in children with SCD. Altered mental status – with or without reduced level of consciousness, headache, seizures, visual loss, or focal signs – can occur in numerous contexts, including infection, shunted hydrocephalus [57], acute chest syndrome (ACS) [58, 59], and aplastic anemia (secondary to parvovirus [60], after surgery [55], transfusion [61], or immunosuppression [62, 63]), and apparently spontaneously [64]. In one large series of 538 patients with ACS, 3 % of children had neurological symptoms at presentation, and such symptoms developed in a further 7–10 % in association with ACS [58]. These patients are classified clinically as having had a CVA [37], although there is a wide

differential of focal and generalized vascular and nonvascular pathologies – often distinguished using acute magnetic resonance techniques [64] – with important management implications [52, 57, 61, 65–68]. Sixty-seven percent of those who have had an initial stroke and are not transfused will develop another stroke, most likely within 36 months [69]. With each episode, the child is usually left with greater neurological deficits, including some degree of mental retardation [70].

Epidemiology

SCD is one of the most prevalent genetic disorders and primarily affects people originating from sub-Saharan Africa, the Middle East, the Mediterranean, the Indian subcontinent, the Caribbean, and South America and descendants of these people in other parts of the world who emigrated from the above-mentioned regions [71–81]. The incidence of SCA in the African American population is 0.2–0.3 %; that of SS trait is 9–11 %, and that of SC disease is 3 % [76, 82–85]. The sickle gene is present in about 20 % of the indigenous black population in Africa [78, 86, 87]. Approximately 72,000 African Americans in the USA have SCD [88]. About 1 in 12 African Americans and about 1 in 100 Hispanic Americans are carriers of the disease [89]. This prevalence has remained constant primarily because the trait provides partial protection against malarial infection from *Plasmodium falciparum* [78, 90, 91]. The malaria parasite has a complex life cycle and spends part of it in red blood cells. In a carrier, the presence of plasmodium causes the RBC with defective Hb to rupture prematurely, making the plasmodium unable to reproduce. Furthermore, the deoxygenation that leads to polymerization of Hb affects the ability of the parasite to digest Hb in the first place. The parasites by themselves lower the pH and cause the cells to sickle faster. Therefore, in areas where malaria is a problem, chances of survival actually increase if individuals are carriers of the sickle-cell trait (selection for the heterozygote). Such protection has become irrelevant in the USA, where malaria is no longer endemic.

Epidemiology of Stroke

The overall prevalence of stroke in all forms of SCD is 4 % and 5 % in those with SCA. First stroke occurs in all age groups, except for children under 1 year of age. The annual incidence of first stroke is approximately 0.6 per 100 patient-years or 600/100,000/year in SCA children. However, the highest incidence occurs in the first decade of life, with rates of 1.02 per 100 patients-years in 2–5-year-old SCA patients and 0.8 in those 6–9 years old [37]. The cumulative risk of first stroke in SCA patients is 11 % by age of 20, 15 % by age 30, and 24 % by age 45 [37]. The combined incidence of hemorrhagic and ischemic strokes in a general sample of American children 14 years of age was reported as 3.3 per 100,000 yearly or 0.0033 per 100 patient-years [92]. The types of stroke differ between adults and children with SCD. In the Cooperative Study of Sickle Cell Disease (CSSCD) report, 9.6 % of first strokes in SCD patients under age 20 were hemorrhagic, while 52 % of all strokes in those over 20 years were hemorrhagic. In the CSSCD, stroke occurred less frequently in the other common genotypes of SCD. Age-adjusted prevalence rates of stroke at study entry were 2.43 % for Sβ0 thalassemia (SCD-Sβ0), 1.29 % for SCD-Sβ+, and 0.84 % for SCD-SC. Twenty-one percent of SCD-SC patients who had a stroke were less than 10 years old compared to those with SCD-SS (31 % under age 10).

Risk of Stroke

Clinically apparent stroke represents the most significant and recurrent threat to the SCD patient population. When compared with their peers, children with SCD have a 220-fold increase in stroke risk and a 410-fold increase in cerebral infarction specifically [37]. Seventeen to thirty-five percent of SCD children without a compatible history of a cerebrovascular event have "silent" infarctions detectable with MRI [45, 68, 93, 94]. Children with silent infarcts are at higher risk for further ischemia than are SCD children with a normal MRI [45, 68, 93]. In CSSCD

study, the overall incidence of first stroke was 0.46 per 100 patient-years, and the age-adjusted incidence of first CVA was 0.61 % per 100 patient-years [37]. The incidence and prevalence of CVA is given in Table 11.1.

Epidemiology of Recurrent Stroke

Stroke in SCD has a high tendency to recur. In untransfused patients, there is a 67 % recurrence rate, with 70 % of the recurrent strokes occurring within the first 3 years following the initial stroke [69]. The high risk of CVA recurrence can be reduced but not eliminated by chronic blood transfusion [42, 43]. Estimated risk of stroke in children with SCD receiving blood transfusion therapy for at least 5 years after initial stroke is 2.2 per 100 patient-years [42]. There is no sufficient evidence to state that hydroxyurea therapy reduces the risk of stroke [95, 96]; however, data from nonrandomized clinical series suggest that hydroxyurea may be an alternative to transfusion for primary stroke prevention (insufficient evidence) [97]. Ongoing studies are investigating the role of hydroxycarbamide in the prevention of cerebrovascular disease [98]. In the Stroke with Transfusions Changing to Hydroxyurea (SWiTCH) study, the efficacy of regular blood transfusions and iron chelation was compared with hydroxyurea and phlebotomy in children with SCD and stroke [99]. The study was stopped because of the higher number of strokes in the hydroxyurea group [99]. Once a stroke has occurred, the risk of recurrence is more than 60 %, although this risk is substantially reduced by starting a transfusion program (insufficient evidence) [100]. Further research on the use of transfusion in preventing secondary stroke as well as on defining the risk factors for recurrent stroke is required, to avoid unnecessary blood transfusions. Some children have progressive vasculopathy, with a moyamoya-like syndrome and further strokes despite transfusion; neurosurgical revascularization might be helpful in these circumstances (insufficient evidence) [101]. Chance of stroke recurrence in SCD patients is given in Table 11.2.

Epidemiology of Silent Infarcts Diagnosed by MRI

Children with silent infarcts are at higher risk for further ischemia than are SCD children with a normal MRI [68, 90, 92]. About 17– 35 % of SCD children without a compatible history of a CVA have "silent" infarctions [68, 93, 102], and up to 25 % have silent infarction by adolescence, typically between the ACA and MCA or between MCA and PCA territories [68, 103, 104]. There is evidence of white matter damage in these border zones, even in those with normal T2-weighted MRI [105] and neurological symptoms [50, 51]. These patients, however, might have had subtle transient ischemic attacks, headaches, or seizures [104]. Cognitive difficulties [106, 107], which commonly affect attention [106] and executive function [108], are common in SCD, sometimes from infancy on [108]; they can be progressive [109] and are associated with brain abnormalities on MRI [105, 106, 109, 110].

Overall Cost to Society

In 2005, there were an estimated 28,426 black children with SCD in the USA. Adjusting by 10 % to account for nonblack children with SCD yielded an estimated number of 31,269 children [111]. SCD-attributable medical expenditures in children were conservatively and approximately estimated at $335 million in 2005 [111]. Children with SCD incurred medical annual expenditures that were $9,369 and $13,469 higher than those of children without SCD enrolled in Medicaid and private insurance, respectively. In other words, expenditures for children with SCD were 6 and 11 times those of children without SCD enrolled in Medicaid and private insurance, respectively [112]. Total health-care costs generally rise with age, from $892 to $2,562 per patient-month in the 0–9- and 50–64-year age groups, respectively, on average $1,389 [112]. At $1,341 per patient-month or about $16,000 annually, the estimated cost of medical care for the 70,000 individuals with SCD in the USA exceeds $1.1 billion [113].

Overall, 51.8 % of care is directly related to SCD, the majority of which (80.5 %) is associated with inpatient hospitalizations [112]. Patients with SCD also incur substantial health-care costs that may not be directly attributable to the disease itself. Non-SCD-related costs were substantially higher than those reported for the general US population [114]. Non-SCD-related costs were estimated at $786 per patient-month, $9,428 on an annualized basis, compared to reported average total medical expenses of $3,601 for 2003 ($3,917 in 2005 dollars) [112, 115]. On an annualized basis, the total care cost of health care for patients with SCD ranged from $10,704 (±24,696) for individuals aged 0–9 years to $34,266 (±52,224) for those aged 30–39 years [112]. For an average patient with SCD reaching age 45, total undiscounted health-care costs were estimated to reach $953,640. At a 3 % discount rate, the present value of lifetime costs is $460,151. Median lifetime costs were estimated at $392,940 (undiscounted) and $186,406 (discounted). These results suggest a discounted (3 % discount rate) lifetime cost of care averaging $460,151 per patient with SCD [112]. Interventions designed to prevent SCD complications and avoid hospitalizations may reduce the significant economic burden of the disease [111, 112]. This estimated cost does not include direct and indirect non-health-related costs, time lost from school and workplace for both the patient and the patient's family, reduced productivity of the patient, lost earnings of unpaid caregivers, transportation expenses, and income lost from premature death. Taken together, the full burden of SCD is quite higher than the figures reported above [116].

Cost of Screening

The average annual rate of TCD screening reported on data from California is 11.4 per 100 person-years after 1999, and 24.5 (10.2–58.8, 95 % CI) in year 2004 [117]. Thus, based on the 2004 estimate, the average TCD exams cost $18.08 million (31,269 children times 24.5/100 × $236), giving an average reimbursement of

$236 per TCD exam per year [118], while the estimated financial impact of recommended chronic transfusion therapy for SCD is substantial, with charges approaching $400,000 per patient decade for patients who require deferoxamine chelation [119, 120]. However, the time on transfusions necessary to decrease the stroke risk for patients with SCD remains unclear.

Cost-Effectiveness Analysis

To date, no data exist concerning the cost-effectiveness of assessing the risk of first stroke, of neuroimaging in acute stroke, or of predicting stroke outcomes in children with SCD.

Goals of Imaging

The goal of neuroimaging such as computed tomography (CT), magnetic resonance (MR), positron emission tomography (PET), single-photon emission CT (SPECT), and TCD in acute stroke is to document whether the stroke is ischemic or hemorrhagic, to assess the extent of parenchymal abnormalities, and to determine presence of cerebrovascular changes. However, initiation of neuroprotective therapy, including exchange transfusion therapy to minimize secondary brain damage and neutralize "ischemic cascade," should not be delayed for the arrangement for imaging studies. CT without contrast is the primary imaging modality for the assessment of acute stroke because of its 24/7 availability, ease of accessibility, and ability to exclude hemorrhagic causes (moderate evidence) [121]. However, CT use has been consecrated more by availability than by randomized studies comparing its effectiveness with MRI. Either CT or MRI should be used for the definition of stroke type and treatment of stroke [121]. MRI can detect acute and chronic ICH (moderate evidence) [121]. Although the detection of SAH is possible with MRI, currently CT scan is the diagnostic procedure of choice (moderate evidence).

MRI and MRA are recommended for better assessment of the extent of infarction and demonstration of cerebrovascular abnormalities (limited evidence) [121]. MRA can detect large vascular abnormalities and is as effective as cerebral angiography in detecting large vascular abnormalities (limited evidence) [122, 123]. MR spectroscopy and diffusion-weighted imaging with MRA increase the sensitivity of MRI for detecting ischemia and infarction (limited evidence) [124]. In cases where MRI is not immediately available in early stages, non-contrast CT is usually the first modality requested. In the acute phase of cerebral infarction, parenchymal abnormalities due to arterial ischemic stroke and venous thrombosis are easily missed and may be subtle on CT. Early or small lesion(s) in the posterior fossa can also be easily missed. CT angiography (CTA) is a noninvasive method for evaluation of intracranial and extracranial circulation. CTA performed in early stages of cerebral ischemia may provide crucial information regarding cerebral circulation (limited evidence) [125, 126]. Disadvantages of CTA include radiation exposure, use of intravenous contrast, and the difficulty in timing the contrast bolus in small children.

The gold standard for the definite assessment of cerebral vasculature is cerebral angiography (DSA); it should be considered in children when pathology of small distal artery is suspected, with moyamoya disease and with an unexplained infarct or hemorrhage that is not elucidated by MRI or MRA evaluation [127].

In the case of hemorrhagic stroke, the goal is to identify with DSA an arteriovenous malformation or aneurysm(s) amenable to surgery or catheter intervention.

The ultimate goals are to preserve brain function and to prevent the progression of preclinical ischemia to permanent neuronal loss with disability. The first step is to identify young children at high risk of stroke before development of focal neurological deficits. The preferred imaging is dependent upon the neuroradiologist and the institution. Typically, large-vessel velocity measurements with TCD are confirmed by MRI and MRA (Fig. 11.1). This should be followed by preventive therapy in those with evidence of parenchymal and/or cerebrovascular changes. In patients with neurological symptoms and negative MRI/MRA findings, PET or SPECT can detect brain perfusion deficits, and such an early detection may be clinically useful in the subsequent follow-up of these patients, since it is known that cerebral perfusion deficit can lead to silent infarct and/or overt stroke (limited evidence) [30, 128, 129].

Methodology

We conducted a systematic review of the literature using a database search of MEDLINE (PubMed, National Library of Medicine, Bethesda, MD) and of Web of Science® (Institute of Scientific Information, Philadelphia, PA) to identify studies dealing with sickle-cell disease and stroke and relevant to neuroimaging. The search spanned January 1990 to June 2011 and used the following key terms: (1) sickle-cell disease and (2) stroke and one of the following: "exp cerebral ischemia," "cerebral infarction," "cerebrovascular disorders," or "cerebrovascular accidents," "epidemiology," "cost," "ultrasound," "TCD or transcranial Doppler sonography," "TCCS or transcranial color-coded sonography," "TCCD or transcranial color-coded duplex sonography," "MRI or magnetic resonance imaging," "MRA or magnetic resonance angiography," "angiography," "DSA or digital contrast angiography," "CT or computed tomography," "PET or positron emission tomography," and "SPECT or single-photon emission computerized tomography." There was one randomized controlled trial, no meta-analyses, and no cost analysis of neuroimaging diagnostic options. We expanded our retrieval to also include clinical trials, cohort studies, multicenter studies, comparative studies, case-control studies, and case reports having more than five subjects for the key question of the age-specific natural history of ischemic stroke. Reviews, letters, hospital bulletins, and single case reports were excluded.

Discussion of Issues

What Is the Role of Neuroimaging in Acute Stroke in Children with Sickle-Cell Disease?

Summary
CT without contrast is the best tool to exclude hemorrhagic stroke in children as well as in adults. There is need for a research study, however, to determine whether anatomical MR can replace CT [130, 131]. Patients without hemorrhagic stroke should then undergo MRI with DWI and MRA to detect an infarct(s) and to determine location and extent of ischemic lesions and presence of large vessel occlusion/narrowing as soon as possible, preferably on an emergency basis (moderate evidence). Vascular imaging of the neck vasculature with CT or MR angiography to exclude arterial dissection [132] and venous thrombosis should be undertaken within 48 h of presentation with arterial ischemic stroke. MRI and MR angiography is preferable to CT and CTA due to noninvasive nature and absence of ionizing radiation (moderate evidence). MR venogram must be specifically requested if cerebral venous thrombosis is suspected [133]. Imaging of the aortic arch to the intracranial vasculature should be performed in all children with arterial ischemic stroke (moderate evidence). Transcranial Doppler (TCD) is not useful in acute stroke (limited evidence) [134–136].

Symptomatic children with negative CT and MR studies should be followed subacutely by PET or SPECT to identify loss of cerebral neuronal metabolic function (limited evidence).

Supporting Evidence
CT Non-contrast CT provides sufficient information to make decisions about emergency management in hyperacute stroke, that is, <6 h after onset of symptoms (moderate evidence) [137–140]. Unenhanced CT has 57 % sensitivity and 100 % specificity for acute stroke detection [141]. The sensitivity can be improved up to 80 % by using variable window width and center level settings or a 10-point topographic scoring system [141–143]. The utility of CTA in acute adult stroke relies on demonstrating occlusion or significant arterial narrowings within intracranial vessels and on evaluating the carotid and vertebral arteries in the neck. The sensitivity of CTA was determined to be 88.5–98 % in these aspects [144, 145]. The utility of CTA in SCD children with stroke has not been determined.

MRI MRI with diffusion-weighted imaging (DWI) provides additional useful information on the presence of ischemic stroke (moderate evidence) and visualization of silent cerebral infarcts (moderate evidence) [146–149]. DWI determines ischemic regions that later progress to infarction, and the volume of acute infarct correlates well with clinical outcome. Based on adult data, DWI has high sensitivity and specificity, 88–100 % and 86–100 %, respectively, using perfusion evaluation as a reference standard [150–154]. DWI is superior to conventional MR imaging and CT for detecting ischemic stroke during the first 24 h after presentation (moderate evidence) [131, 155–158]. The pattern of ischemic changes in the brain can be indicative but not specific for a particular stroke etiology (insufficient evidence) [159, 160].

MRA Like CT angiography, MR angiography (MRA) is useful for detecting intravascular occlusion due to a thrombus and for evaluating the carotid bifurcation in patients with acute stroke. Kandeel and colleagues reported that MRA is 85 % accurate with a sensitivity of 81 % and a specificity of 94 % when compared to DSA [159]. In a study of 22 SCD patients, an MRA abnormality in a long segment (6 mm) with reduced distal flow correlated with subclinical infarction, while short focal areas of abnormal MRA, most commonly in branching regions, showed no associated MRI infarction [161].

More recent data from adults showed that MRA has 70–86 % sensitivity in detecting intracranial stenosis on DSA, while the sensitivity of CTA is 98 % [144, 145, 162]. MRA does not need a contrast agent, while CTA requires intravenous

contrast, whose toxicity can exacerbate symptoms in acute stroke [163]. MR spectroscopy can distinguish an ischemic lesion from other non-ischemic changes, but the utility of MRS in acute stroke is limited in children with SCD.

Angiography Digital subtraction angiography (DSA) is not part of the standard acute stroke imaging in children with SCD [164]. DSA is accurate in detecting intracranial vascular abnormalities (AVM, aneurysm, dissection, occlusion) and quantifying arterial narrowing (moderate evidence), but it is invasive and carries a 1.3 % risk of neurologic complications [165–168]. MR is not as accurate as DSA in evaluating the vasculature (limited evidence); however, CT angiography is an accurate tool for the diagnosis of ruptured intracranial aneurysms and can be integrated as a primary examination tool into the imaging and treatment algorithm for patients with subarachnoid hemorrhage at presentation; the chance of missing a ruptured aneurysm with CT angiography is no more than 2 % (moderate evidence) [159, 169–174]. DSA, however, is performed when endovascular therapy is anticipated.

Nuclear Medicine (PET, SPECT) PET and SPECT can be used to detect the functional activity of the cerebral tissues by measuring glucose metabolism 2-deoxy-2 [^{18}F] fluoro-D-glucose (FDG) and microvascular perfusion ([^{15}O]H$_2$O) if CT and MR are negative in patients with clinical stroke (limited evidence) [129, 175]. PET studies [30, 175, 176] that have been performed in patients with SCD have shown a variety of abnormalities including hypometabolism in frontal areas of the brain and areas of low perfusion that appear normal on MRI. The study of Powars et al. [129] suggested that few patients with SCD have normal PET studies and areas of hypometabolism in brain regions with normal MR appearance are not uncommon (not sufficient evidence). The authors suggest that PET could be used to select patients for treatment, since four patients showed improvement in metabolism and perfusion with transfusion treatment. The most powerful predictor of ischemia in other

applications of PET is an increased oxygen extraction fraction, but this application as well as metabolism measurements remains to be established in children with SCD.

What Is the Role of Neuroimaging in Children with Sickle-Cell Disease at Risk of Their First Stroke?

Summary

TCD is currently used in primary stroke prevention to identify children at high risk of first stroke (strong evidence). Patients with velocities over 200 cm/s in the terminal internal carotid artery (ICA) and middle cerebral artery (MCA) are at 10 % risk of first stroke a year [177]. TCD screening is recommended in children starting at 2 years of age and should be continued annually if TCD is normal and every 4 months if TCD shows velocities over 170 cm/s but less than 200 cm/s [178, 179]. Asymptomatic children with velocities over 200 cm/s should be retested within 2–4 weeks to confirm abnormal velocities before implementing preventive transfusions. The stroke risk may vary among children with SCD who have abnormal TCD results because high velocity can be consistent with arterial narrowing as well as hyperemic high blood flow [180]. The risk of ischemic stroke is higher in children with silent infarctions on MRI. Silent infarct was found to be the strongest independent predictor of stroke (hazard ratio = 7.2) in one study, whereas the adjusted relative risk of incident stroke was found to be increased with multiple (more than one) silent infarcts (hazard ratio 1.9 [1.2–2.8]) in another study (moderate evidence) [45, 181]. Presence of cerebrovascular disease on MRA may be associated with increased risk of stroke; however, there is insufficient supporting evidence.

Supporting Evidence

TCD is currently the most common screening method to identify children at high risk of both first and recurrent stroke (strong evidence) [177, 178, 182]. TCD is a noninvasive, well-tolerated, relatively low-cost procedure in which the

velocity of blood flow can be measured in intracranial arteries using an ultrasound probe placed over the temporal bone [183, 184]. In a comparison with DSA, TCD showed a sensitivity of 90 % and specificity of 100 % for the diagnosis of 50 % or greater stenosis (limited evidence) [165, 171]. The interclass correlation coefficient for interoperator variability for TCD velocity measurement was reported to vary from 0.67 to 0.9 depending on the level of the operator's experience and on the measured velocity [185]. The STOP trial showed associations between stroke risk and TCD velocities in the MCA or terminal ICA (Table 11.3).

The NHLBI recommends TCD screening every 6 months in all children with SCD between the ages of 2 and 16 and consideration of chronic transfusions in those with two abnormal TCDs [186]. The timing of repeated TCDs is not clearly defined. If TCD is normal, annual testing is proposed, but if TCD is marginal, then testing every 4 months is recommended. Children with abnormal TCD results should be retested within 2–4 weeks (limited evidence) [119, 178, 187, 188].

Fullerton et al. [189] evaluated administrative data comparing the rates of hospital admissions for the first stroke in children with SCD between the early 1990s (before STOP) and from 1998 to 2000 (after STOP). These authors found a sharp reduction in first stroke admissions (limited evidence). A recent retrospective analysis confirmed previous findings [190]. An ongoing clinical trial testing presence of silent infarcts on MRI (SILENT Cerebral Infarct Multi-Center Clinical Trial) [191] as a screening criterion for stroke prevention may show better outcomes in the future.

Color imaging TCD has become widely employed because it allows for more accurate than conventional TCD for identification of intracranial arteries, placement of a sample volume in an artery, and correction of velocity measurements for the error related to the angle of insonation. Imaging TCD is better than conventional TCD in other applications [192–194]; however, there are no data to support that imaging TCD is better that TCD in risk assessment in children with SCD (insufficient evidence).

There are several articles suggesting that imaging TCD flow velocity measurements obtained without correction for the angle of insonation may be better for identifying children at high risk of stroke than conventional TCD (limited evidence) [136, 182, 195–199]. Recently, reference TCD values for the ratios of flow velocity in the intracranial and extracranial arteries and interhemispheric differences in blood flow parameters for children with SCA have been proposed [200, 201].

Elevation of cerebral blood flow velocities in TCD may precede abnormal findings in MRA [202, 203]. MRA is more costly, and children under 3 years old may require general anesthesia; however, MRA can confirm the presence and extent of cerebrovascular disease in those with elevated TCD velocities (limited evidence) [159, 161, 204].

Kogutt and colleagues [205] reported 85 % accuracy of MRA compared to conventional angiography in depicting arterial stenosis. Seibert and colleagues [206] have shown that MRA can identify SCD patients at greatest risk of stroke. MRA results in cases where a stenosis was suspected on TCD were in excellent agreement with arteriography [171]. Three-dimensional time-of-flight MRA has been shown to correlate well with the results of angiography [159, 207, 208]. Positive MRA with a positive TCD in an asymptomatic patient in long-term follow-up suggests a trend for developing clinical stroke [206]. In STOP trial [202], a larger proportion of patients in the standard care arm than in the transfusion arm had vessel abnormalities on MRA, in particular severe stenosis. Thus, there is insufficient evidence to determine value of MRA in predicting stroke.

Risk of Symptomatic Stroke in Children with Silent Infarct on MRI

Data from the CSSCD showed that silent infarction seen on MRI was associated with an increased risk of symptomatic stroke (1.03 per 100 patient-years) and progression of silent infarction (7.06 per 100 patient-years) (moderate evidence) [45, 68, 104]. The Silent Cerebral Infarct Multi-Center Clinical Trial will

randomize an estimated 204 children with silent infarction on MRI to chronic blood transfusions or observation. This trial is currently enrolling patients and will report results after 2012 [209].

What Is the Role of Neuroimaging in the Prevention of Recurrent Ischemic Stroke in Children with Sickle-Cell Disease?

Summary

Recurrent stroke is observed in children with SCD despite a proper regimen of transfusion therapy. Arterial stenosis is the main risk factor for recurrent stroke. Elevated cerebral artery velocities (>200 cm/s) on TCD and new lesions on MRI or MRA indicate a higher risk of recurrent stroke. SCD children should be monitored after first stroke episode with TCD and MRI/MRA, although no randomized or controlled data are available to optimize frequency of follow-up.

Supporting Evidence

Two studies found a high risk of stroke recurrence in children who had arterial abnormalities on DSA (limited evidence) [210, 211]. Moyamoya syndrome is characterized by chronic progressive narrowing of proximal segments of intracranial arteries, with the characteristic distal collateral network on angiography. It is a risk factor for stroke recurrence even in those children undergoing regular transfusion (limited evidence) [212, 213].

Serial MRI scans in these individuals with preexisting cerebral damage might show new lesions as well as extension of existing abnormality [214]. Some studies indicate that this risk seems to be reduced after extracranial–intracranial (EC–IC) bypass or indirect revascularization [215, 216] (limited evidence). Further studies of these procedures are needed, as some researchers have not found progression [217], and the cerebrovascular disease can stabilize as demonstrated on both MRA [218] and TCD (limited evidence) [119].

Are There Imaging Criteria Indicating that Blood Transfusions Can Be Safely Halted?

Summary

Limited data on the discontinuation of blood transfusion suggest that halting transfusions increases the risk of stroke. A decision analysis model suggests following up SCD children during transfusion therapy with annual TCD until age 10 and continuing transfusions until age 18 in children with high risk of stroke. The main risk of prolonged blood transfusions is iron overload, which can result in organ failure and death.

Supporting Evidence

The STOP II trial followed the children in STOP I and showed that discontinuation of transfusions led to recurrence of TCD abnormalities and development of new stroke events (moderate evidence) [209, 219]. However, only the baseline TCD results were used to determine stroke risk against follow-up observations. Transfusion therapy converts approximately 60 % of patients to normal TCD results [219, 220] (moderate evidence). Similar findings were observed on MRA examinations [119] (limited evidence). The STOP II trial concluded that transfusions should not be stopped once TCD results were normal (moderate evidence) [219].

However, 20 % of children who discontinued transfusion therapy did not develop abnormal TCD or stroke. Mazumdar et al. created a decision analysis model to compare various stroke prevention strategies for a hypothetical cohort of 2-year-old children [221]. This model compared the following strategies: (1) annual transcranial Doppler ultrasonography screening until age 16 with children at high risk of stroke receiving monthly transfusion for life, (2) annual transcranial Doppler ultrasonography until age 16 with transfusions until age 18, (3) biannual transcranial Doppler ultrasonography until age 16 with transfusions until age 18, (4) annual transcranial Doppler ultrasonography until age 10 with transfusions until age 18, (5) 1-time screening at age 2 with transfusions until age 18, and (6) no intervention.

The optimal stroke-prevention strategy was annual transcranial Doppler ultrasonography screening until age 10 with transfusions for children at high risk until age 18. Better adherence to chelation therapy would improve life expectancy in all intervention strategies, with fewer deaths from iron overload in comparison to other more intensive strategies [221–223] (limited evidence).

What Is the Role of Neuroimaging in Hemorrhagic Stroke in Children with SCD?

Summary

CT without contrast is still the first line examination in diagnosing hemorrhagic stroke. In acute intraparenchymal hemorrhage (ICH), the accuracy of MRI seems to be similar to the accuracy of CT, especially when gradient echo sequences are used [130, 131]. In patients with subarachnoid hemorrhage (SAH), CT is superior [224]. TCD seems to be ineffective in predicting hemorrhagic stroke [178]. The role of TCD in pediatric SAH is unclear, though in adults it is used to detect and monitor vasospasm. In cases with ICH, DSA is advisable in order to rule out lesions that should be treated with surgery (moderate evidence). In cases with SAH, DSA is used to detect ruptured cerebral aneurysms. Hydration and reduction of HbS to less than 30 % prior to DSA comprise the usual method of preparation, and there have been few reports of stroke complications since this practice was initiated.

It is not known if transfusion prevents recurrent hemorrhage. Children with any form of intracranial bleeding, except from trauma, need evaluation for a surgically correctable aneurysm even if the bleeding appears to be primarily intracerebral. If there is no aneurysm, then transfusion for at least a year is often recommended, but it is not clear if this helps. Recurrent hemorrhage is less common than recurrent ischemic stroke, partly because more first events are fatal.

Supporting Evidence

About 9.6 % of first strokes in SCD-SS patients less than 20 years old were hemorrhagic compared to 52 % of first strokes in those patients over 20 years old [37], in whom there is nearly a 250-fold increase in the risk of hemorrhagic stroke compared with children [48]. In the CSSCD study, almost all fatal cases (24 %) were due to hemorrhagic stroke. In the first published series, the mortality rate associated with hemorrhagic stroke was over 50 % [225], similar to the rate (40 %) reported by Strouse et al. [61]. The typical clinical presentation of hemorrhagic stroke in SCD includes focal neurological deficits, severe headache, nuchal rigidity, and coma.

The risk of hemorrhagic stroke increases with decreasing steady-state Hb concentration (RR 1.61 per 1 g/dL decrease) and increasing leukocyte count (1.94 per 5×10^9/L increase) (limited evidence) [37]. Associations with hypertension, recent blood transfusions, treatment with corticosteroids, previous ischemic stroke, moyamoya, cerebral aneurysms, or acute chest syndrome (ACS) were also reported (insufficient evidence) [61, 66, 212, 226–229].

In the emergency setting, non-contrast CT is adequate and the most cost effective strategy in diagnosing acute hemorrhagic stroke (moderate evidence) [230]. In acute ICH, the accuracy of MRI is similar to the accuracy of CT, especially with use of gradient echo sequences [130, 131] (strong evidence). MRI is better than CT in evaluations of chronic hemorrhage [130, 131] (strong evidence). MRI, however, is not feasible in up to 20 % of acute stroke patients due to contraindications to MRI, impaired consciousness, hemodynamic compromise, vomiting, agitation, and lack of cooperation [231]. To obtain successful MRI results, patients often need general anesthesia.

CT should be used if SAH is suspected [224] (insufficient evidence). DSA is used to identify the source of bleeding [230, 232] (limited evidence), but most children require general anesthesia and the method itself carries a risk of stroke [168, 233]. CTA and MRA are less accurate then DSA in depicting intracranial vascular anatomy, especially in visualization of tertiary branches and small cerebral arteries [230]. The advantage of DSA is the potential to initiate therapy such as

endovascular coiling of aneurysms and embolization of AVMs. TCD is not effective in predicting hemorrhagic stroke [178]; however, TCD can be used to detect and monitor intracranial vasospasm in patients after SAH [234] (limited evidence).

Take-Home Tables and Figures

Tables 11.1 through 11.3 highlight data and evidence.

Figure 11.1 shows a decision tree about the role of neuroimaging in the primary prevention against stroke and management of children with SCD with neurological symptoms.

Imaging Case Studies

Figure 11.2a, b shows a CT angiography with reconstruction of bony structures of the skull and an image from the transcranial color-coded duplex sonographic study.

Suggested Imaging Protocol

This is shown in Fig. 11.1.

Table 11.1 Incidence (%) of first stroke and prevalence of CVA in the population of children with sickle-cell disease

	Hb SS	Hb SC	Hb Sβ⁺	Hb Sβ⁰	Total
Overall incidence	0.61	0.17	0.11	0.10	0.46
Age-adjusted incidence	0.61	0.15	0.09	0.08	
Overall prevalence	4.07	0.80	1.48	1.56	3.75
Age-adjusted prevalence	4.01	0.84	1.29	2.43	

Data from [235]
Reprinted with kind permission of Springer Science + Business Media from Krejza J, Swiat M, Tomaszewski M, Melhem ER. In: Medina LS, Applegate KE, Blackmore CC, editors. Evidence-based imaging in pediatrics: optimizing imaging in pediatric patient care. New York: Springer; 2010

Future Research

- Is TCD useful for assessing the risk of stroke among children with hemoglobin SC and β thalassemia?
- Is advanced MR imaging helpful in better selecting SCD patients for chronic transfusions?
- Is advanced MR imaging useful in secondary stroke prediction?
- Is neuroimaging useful for identifying children in whom chronic transfusions can be safely stopped?
- Is there a role for PET-CT to better identify of ischemia in children with SCD?
- Neuroimaging as a surrogate outcome for other alternatives to blood transfusions which may have fewer side effects.

Table 11.2 Risk of recurrent stroke in SCD patients in accordance to initial event

Initial event	Events per 100 patient-years
Symptomatic stroke [37]	
Before age 20	6.4
After age 20	1.6
Silent infarct [68]	0.54

Data from [235, 236]
Reprinted with kind permission of Springer Science + Business Media from Krejza J, Swiat M, Tomaszewski M, Melhem ER. In: Medina LS, Applegate KE, Blackmore CC, editors. Evidence-based imaging in pediatrics: optimizing imaging in pediatric patient care. New York: Springer; 2010

Table 11.3 Risk of stroke in SCD patients in accordance with initial TCD velocities

TCD velocity	Stroke risk (%)
≥200 cm/s	40
>170 cm/s	7
<170 cm/s	2

Data from [237]
Reprinted with kind permission of Springer Science + Business Media from Krejza J, Swiat M, Tomaszewski M, Melhem ER. In: Medina LS, Applegate KE, Blackmore CC, editors. Evidence-based imaging in pediatrics: optimizing imaging in pediatric patient care. New York: Springer; 2010
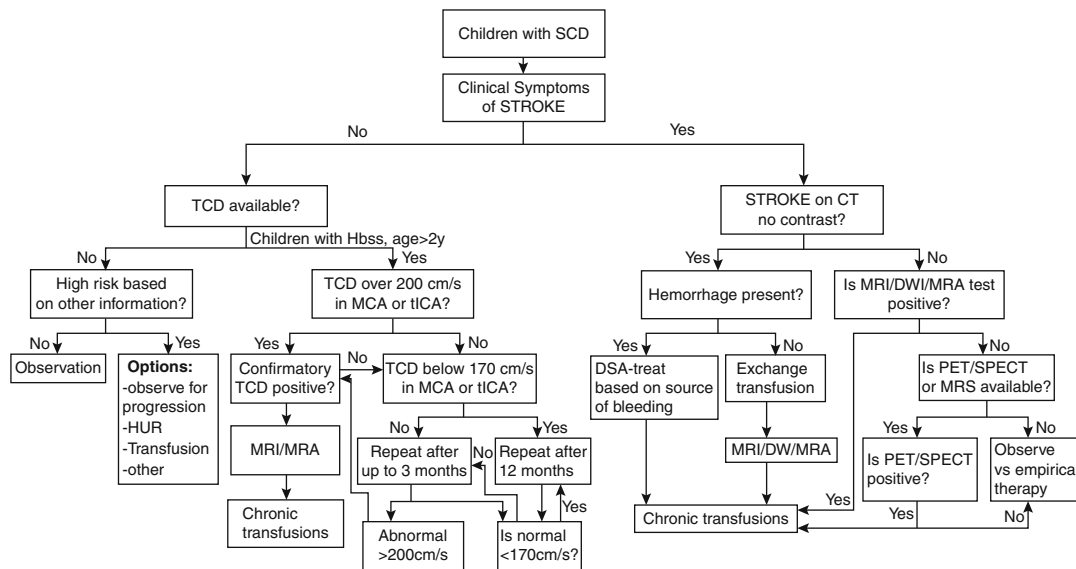
Fig. 11.1 The flow chart proposes a neuroimaging algorithm for children with sickle-cell disease at high risk of stroke (*left part*) and with suspicion of stroke (*right part*) (Reprinted with kind permission of Springer Science+ Business Media from Krejza J, Swiat M, Tomaszewski M, Melhem ER. In: Medina LS, Applegate KE, Blackmore CC, editors. Evidence-based imaging in pediatrics: optimizing imaging in pediatric patient care. New York: Springer; 2010)
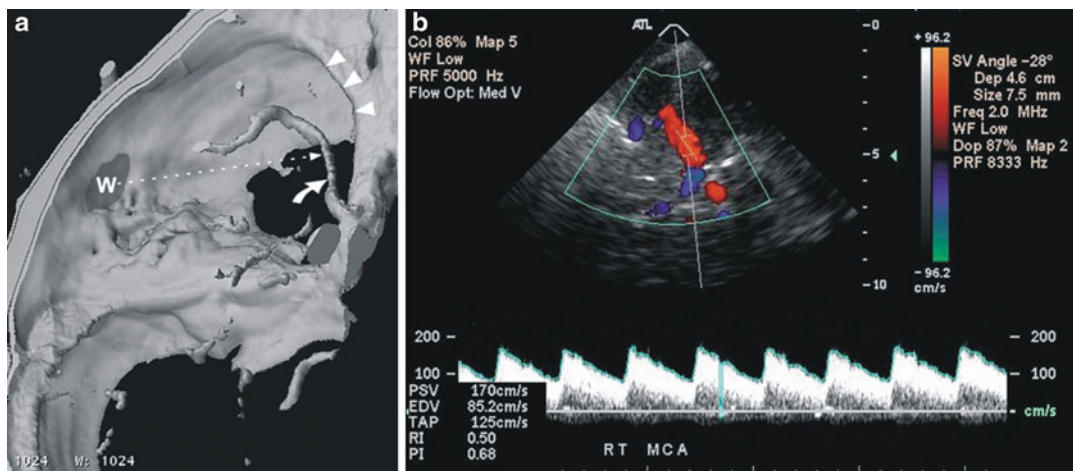
Fig. 11.2 CT angiography with reconstruction of bony structures of the skull (**a**) and an image from the transcranial color-coded duplex sonographic (TCCS) study (**b**). On (**a**), (*W*) denotes the site of a temporal acoustic window in the squamosal temporal bone, *long dotted line* defines the direction of the ultrasound beam, short curved *arrow* indicates the middle cerebral artery, and arrowheads indicate the edge of the lesser wing of sphenoid bone. On (**b**), the middle cerebral artery is shown in *red color*, anterior cerebral artery in *blue color*. The sample volume is placed on the *red color* of the middle cerebral artery, and the angle of insonation (28°) is adjusted to the course of the artery. *Below* the image of arteries, a Doppler velocity waveform from the middle cerebral artery is displayed as well as velocity measurements, which were obtained by automatic tracing of the outline of the waveform. In conventional TCD, only the velocity waveform is obtained; placement of the sample volume in a specific site of the artery therefore is not accurate, and correction for the angle of insonation is not possible

References

1. National Institutes of Health. Genes and disease: anemia, sickle cell. National Center for Biotechnology Information; 1998. Available from: http://www.ncbi.nlm.nih.gov/books/NBK22238/

2. Flint J, Harding RM, Boyce AJ, Clegg JB. Baillieres Clin Haematol. 1998;11:1–51.

3. Tishkoff SA, Williams SM. Nat Rev Genet. 2002;3:611–21.

4. Feng Z, Smith DL, McKenzie FE, Levin SA. Math Biosci. 2004;189:1–19.

5. Hedrick P. J Evol Biol. 2004;17:221–4.

6. Hill AV, Allsopp CE, Kwiatkowski D, Anstey NM, Twumasi P, Rowe PA, Bennett S, Brewster D, McMichael AJ, Greenwood BM. Nature. 1991;352: 595–600.

7. Ackerman H, Usen S, Jallow M, Sisay-Joof F, Pinder M, Kwiatkowski DP. Ann Hum Genet. 2005;69:559–65.

8. Agarwal A, Guindo A, Cissoko Y, Taylor JG, Coulibaly D, Kone A, Kayentao K, Djimde A, Plowe CV, Doumbo O, Wellems TE, Diallo D. Blood. 2000;96:2358–63.

9. Modiano D, Luoni G, Sirima BS, Simpore J, Verra F, Konate A, Rastrelli E, Olivieri A, Calissano C, Paganotti GM, D'Urbano L, Sanou I, Sawadogo A, Modiano G, Coluzzi M. Nature. 2001;414:305–8.

10. Chotivanich K, Udomsangpetch R, Pattanapanyasat K, Chierakul W, Simpson J, Looareesuwan S, White N. Blood. 2002;100:1172–6.

11. Ohashi J, Naka I, Patarapotikul J, Hananantachai H, Brittenham G, Looareesuwan S, Clark AG, Tokunaga K. Am J Hum Genet. 2004;74:1198–208.

12. Flint J, Hill AV, Bowden DK, Oppenheimer SJ, Sill PR, Serjeantson SW, Bana-Koiri J, Bhatia K, Alpers MP, Boyce AJ, et al. Nature. 1986;321:744–50.

13. Williams TN, Maitland K, Bennett S, Ganczakowski M, Peto TE, Newbold CI, Bowden DK, Weatherall DJ, Clegg JB. Nature. 1996;383:522–5.

14. Allen SJ, O'Donnell A, Alexander ND, Alpers MP, Peto TE, Clegg JB, Weatherall DJ. Proc Natl Acad Sci USA. 1997;94:14736–41.

15. Kwiatkowski DP. Am J Hum Genet. 2005;77: 171–92.

16. Chebloune Y, Pagnier J, Trabuchet G, Faure C, Verdier G, Labie D, Nigon V. Proc Natl Acad Sci USA. 1988;85:4431–5.

17. Nagel RL, Ranney HM. Semin Hematol. 1990;27: 342–59.

18. Lapoumeroulie C, Dunda O, Ducrocq R, Trabuchet G, Mony-Lobe M, Bodo JM, Carnevale P, Labie D, Elion J, Krishnamoorthy R. Hum Genet. 1992;89:333–7.

19. Pavlakis SG, Kingsley PB, Bialer MG. J Child Neurol. 2000;15:308–15.

20. Prohovnik I, Pavlakis SG, Piomelli S, Bello J, Mohr JP, Hilal S, De Vivo DC. Neurology. 1989;39:344–8.

21. Stuart MJ, Nagel RL. Lancet. 2004;364:1343–60.

22. Lipowsky HH, Cram LE, Justice W, Eppihimer MJ. Microvasc Res. 1993;46:43–64.

23. Lipowsky HH. Microcirculation. 2005;12:5–15.

24. Mulivor AW, Lipowsky HH. Am J Physiol Heart Circ Physiol. 2004;286:H1672–80.

25. Hebbel RP, Osarogiagbon R, Kaul D. Microcirculation. 2004;11:129–51.

26. Kaul DK, Fabry ME, Nagel RL. Blood Rev. 1996;10:29–44.

27. Chien S, Usami S, Bertles JF. J Clin Invest. 1970;49:623–34.

28. Lorthois S, Cassot F, Lauwers F. Neuroimage. 2011;54:2840–53.

29. Boas DA, Jones SR, Devor A, Huppert TJ, Dale AM. Neuroimage. 2008;40:1116–29.

30. Herold S, Brozovic M, Gibbs J, Lammertsma AA, Leenders KL, Carr D, Fleming JS, Jones T. Stroke. 1986;17:692–8.

31. Prohovnik I, Hurlet-Jensen A, Adams R, De Vivo D, Pavlakis SG. J Cereb Blood Flow Metab. 2009;29: 803–10.

32. Johnson CS. Hematol Oncol Clin North Am. 2005;19:827–37.

33. Garcia JH, Anderson ML. Crit Rev Neurobiol. 1989;4:303–24.

34. Di Roio C, Jourdan C, Terrier A, Artru F. Ann Fr Anesth Reanim. 1997;16:967–9.

35. Serjeant GR. Br J Haematol. 2001;112:3–18.

36. Stuart MJ, Setty BN. Pediatr Pathol Mol Med. 2001;20:27–46.

37. Ohene-Frempong K, Weiner SJ, Sleeper LA, Miller ST, Embury S, Moohr JW, Wethers DL, Pegelow CH, Gill FM. Blood. 1998;91:288–94.

38. Embury SH. Microcirculation. 2004;11:101–13.

39. Miller S, Sleeper L, Pegelow C, Enos L, Wang W, Weiner S, Wethers D, Smith J, Kinney T. N Engl J Med. 2000;342:83–9.

40. Wethers DL. Am Fam Physician. 2000;62:1309–14.

41. Stevens MC, Maude GH, Beckford M, Grandison Y, Mason K, Taylor B, Serjeant BE, Higgs DR, Teal H, Weatherall DJ, et al. Blood. 1986;67:411–4.

42. Scothorn D, Price C, Schwartz D, Terrill C, Buchanan G, Shurney W, Sarniak I, Fallon R, Chu J, Pegelow C, Wang W, Casella J, Resar L, Berman B, Adamkiewicz T, Hsu L, Ohene-Frempong K, Smith-Whitley K, Mahoney D, Scott J, Woods G, Watanabe M, Debaun M. J Pediatr. 2002;140:348–54.

43. Hulbert M, Scothorn D, Panepinto J, Scott J, Buchanan G, Sarnaik S, Fallon R, Chu J, Wang W, Casella J, Resar L, Berman B, Adamkiewicz T, Hsu L, Smith-Whitley K, Mahoney D, Woods G, Watanabe M, DeBaun M. J Pediatr. 2006;149:710–2.

44. Merkel KH, Ginsberg PL, Parker Jr JC, Post MJ. Stroke. 1978;9:45–52.

45. Miller S, Macklin E, Pegelow C, Kinney T, Sleeper L, Bello J, DeWitt L, Gallagher D, Guarini L, Moser F, Ohene-Frempong K, Sanchez N, Vichinsky E,

Wang W, Wethers D, Younkin D, Zimmerman R, DeBaun M. J Pediatr. 2001;139:385–90.

46. Ganesan V, Prengler M, McShane MA, Wade AM, Kirkham FJ. Ann Neurol. 2003;53:167–73.
47. Kirkham FJ, Prengler M, Hewes DK, Ganesan V. J Child Neurol. 2000;15:299–307.
48. Earley C, Kittner S, Feeser B, Gardner J, Epstein A, Wozniak M, Wityk R, Stern B, Price T, Macko R, Johnson C, Sloan M, Buchholz D. Neurology. 1998;51:169–76.
49. Ballas SK, Lieff S, Benjamin LJ, Dampier CD, Heeney MM, Hoppe C, Johnson CS, Rogers ZR, Smith-Whitley K, Wang WC, Telen MJ. Am J Hematol. 2010;85:6–13.
50. Melek I, Akgul F, Duman T, Yalcin F, Gali E. Tohoku J Exp Med. 2006;209:135–40.
51. Mercuri E, Faundez JC, Roberts I, Flora S, Bouza H, Cowan F, Pennock J, Bydder G, Dubowitz L. Eur J Pediatr. 1995;154:150–6.
52. Prengler M, Pavlakis SG, Boyd S, Connelly A, Calamante F, Chong WK, Saunders D, Cox T, Bynevelt M, Lane R, Laverty A, Kirkham FJ. Ann Neurol. 2005;58:290–302.
53. Fullerton HJ. Stroke Rounds. 2004:2.
54. Huttenlocher PR, Moohr JW, Johns L, Brown FD. Pediatrics. 1984;73:615–21.
55. Kirkham FJ, Calamante F, Bynevelt M, Gadian DG, Evans JP, Cox TC, Connelly A. Ann Neurol. 2001;49:477–85.
56. Hines PC, McKnight TP, Seto W, Kwiatkowski JL. J Pediatr. 2011;159(3):472–8.
57. Kirkham F, Hewes D, Prengler M, Wade A, Lane R, Evans J. Lancet. 2001;357:1656–9.
58. Vichinsky E, Neumayr L, Earles A, Williams R, Lennette E, Dean D, Nickerson B, Orringer E, McKie V, Bellevue R, Daeschner C, Manci E, National Acute Chest Syndrome Study Group. N Engl J Med. 2000;342:1855–65.
59. Lee KH, McKie VC, Sekul EA, Adams RJ, Nichols FT. J Pediatr Hematol Oncol. 2002;24:585–8.
60. Wierenga K, Serjeant B, Serjeant G. J Pediatr. 2001;139:438–42.
61. Strouse J, Hulbert M, DeBaun M, Jordan L, Casella J. Pediatrics. 2006;118:1916–24.
62. Coley S, Porter D, Calamante F, Chong W, Connelly A. AJNR Am J Neuroradiol. 1999;20:1507–10.
63. Horton D, Ferriero D, Mentzer W. Pediatr Neurol. 1995;12:77–80.
64. Gadian D, Calamante F, Kirkham F, Bynevelt M, Johnson C, Porter D, Chong W, Prengler M, Connelly A. J Child Neurol. 2000;15:279–83.
65. Sebire G, Tabarki B, Saunders DE, Leroy I, Liesner R, Saint-Martin C, Husson B, Williams AN, Wade A, Kirkham FJ. Brain. 2005;128:477–89.
66. Powars D, Adams R, Nichols F, Milner P, Charache S, Sarnaik S. J Assoc Acad Minor Phys. 1990;1: 79–82.
67. Balkaran B, Char G, Morris J, Thomas P, Serjeant B, Serjeant G. J Pediatr. 1992;120:360–6.

68. Pegelow C, Macklin E, Moser F, Wang W, Bello J, Miller S, Vichinsky E, DeBaun M, Guarini L, Zimmerman R, Younkin D, Gallagher D, Kinney T. Blood. 2002;99:3014–8.
69. Jeffries BF, Lipper MH, Kishore PR. Surg Neurol. 1980;14:291–5.
70. Ashley-Koch A, Murphy CC, Khoury MJ, Boyle CA. Genet Med. 2001;3:181–6.
71. Aluoch J, Jacobs P. S Afr Med J. 1996;86:982–3.
72. Al-Riyami A, Ebrahim G. J Trop Pediatr. 2003;49(Suppl 1):i1–20.
73. De D. Br J Nurs. 2005;14:447–50.
74. Balgir R. J Assoc Physicians India. 1996;44:25–8.
75. Fattoum S. Tunis Med. 2006;84:687–96.
76. Hamdallah M, Bhatia AP. Lancet. 1995;346:707–8.
77. Kamble M, Chatruvedi P. Indian Pediatr. 2000;37: 391–6.
78. Williams T, Mwangi T, Wambua S, Alexander N, Kortok M, Snow R, Marsh K. J Infect Dis. 2005;192:178–86.
79. Al-Qurashi MM, El-Mouzan MI, Al-Herbish AS, Al-Salloum AA, Al-Omar AA. Saudi Med J. 2008;29: 1480–3.
80. Al-Awamy BH. Saudi Med J. 2000;21:8–17.
81. El-Hazmi M, Warsy A. East Mediterr Health J. 1999;5:1147–53.
82. Petrakis N, Wiesenfeld S, Sams B, Collen M, Cutler J, Siegelaub A. N Engl J Med. 1970;282:767–70.
83. Scott R. N Engl J Med. 1970;282:164–5.
84. Boyle EJ, Thompson C, Tyroler H. Arch Environ Health. 1968;17:891–8.
85. Nietert P, Silverstein M, Abboud M. Pharmacoeconomics. 2002;20:357–66.
86. Hicks E, Miller G, Horton R. Am J Public Health. 1978;68:1135–7.
87. Ashley-Koch A, Yang Q, Olney R. Am J Epidemiol. 2000;151:839–45.
88. Brousseau DC, Panepinto JA, Nimmer M, Hoffmann RG. Am J Hematol. 2010;85:77–8.
89. Learning About Sickle Cell Disease. National Human Genome Research Institute. 2010. Updated 7 July 2010. Available from: www.genome.gov/10001219
90. Rodriguez-Ojea Menendez A, Garcia de la Osa M. Rev Cubana Med Trop. 1992;44:62–5.
91. Das L. Ind J Malariol. 2000;37:34–8.
92. de Veber G, Roach ES, Riela AR, Wiznitzer M. Semin Pediatr Neurol. 2007;7:309–17.
93. Steen R, Emudianughe T, Hankins G, Wynn L, Wang W, Xiong X, Helton K. Radiology. 2003;228:216–25.
94. Kwiatkowski JL, Zimmerman RA, Pollock AN, Seto W, Smith-Whitley K, Shults J, Blackwood-Chirchir A, Ohene-Frempong K. Br J Haematol. 2009;146: 300–5.
95. Charache S, Terrin M, Moore R, Dover G, Barton F, Eckert S, McMahon R, Bonds D. N Engl J Med. 1995;332:1317–22.
96. Hankins JS, Ware RE, Rogers ZR, Wynn LW, Lane PA, Scott JP, Wang WC. Blood. 2005;106: 2269–75.

97. Gulbis B, Haberman D, Dufour D, Christophe C, Vermylen C, Kagambega F, Corazza F, Devalck C, Dresse M, Hunninck K, Klein A, Le P, Loop M, Maes P, Philippet P, Sariban E, Van Geet C, Ferster A. Blood. 2005;105:2685–90.

98. Zimmerman SA, Schultz WH, Burgett S, Mortier NA, Ware RE. Blood. 2007;110:1043–7.

99. Stroke With Transfusions Changing to Hydroxyurea (SWiTCH). ClinicalTrials.gov. 2005. Updated 25 June 2010. Available from: http://www.clinicaltrials.gov/ct/show/NCT00122980

100. Verduzco LA, Nathan DG. Blood. 2009;114:5117–25.

101. Smith ER, McClain CD, Heeney M, Scott RM. Neurosurg Focus. 2009;26:E10.

102. Moser F, Miller S, Bello J, Pegelow C, Zimmerman R, Wang W, Ohene-Frempong K, Schwartz A, Vichinsky E, Gallagher D, Kinney T. AJNR Am J Neuroradiol. 1996;17:965–72.

103. Bernaudin F, Verlhac S, Freard F, Roudot-Thoraval F, Benkerrou M, Thuret I, Mardini R, Vannier JP, Ploix E, Romero M, Casse-Perrot C, Helly M, Gillard E, Sebag G, Kchouk H, Pracros JP, Finck B, Dacher JN, Ickowicz V, Raybaud C, Poncet M, Lesprit E, Reinert PH, Brugieres P. J Child Neurol. 2000;15:333–43.

104. Kinney T, Sleeper L, Wang W, Zimmerman R, Pegelow C, Ohene-Frempong K, Wethers D, Bello J, Vichinsky E, Moser F, Gallagher D, DeBaun M, Platt O, Miller S. Pediatrics. 1999;103:640–5.

105. Baldeweg T, Hogan A, Saunders D, Telfer P, Gadian D, Vargha-Khadem F, Kirkham F. Ann Neurol. 2006;59:662–72.

106. DeBaun M, Schatz J, Siegel M, Koby M, Craft S, Resar L, Chu J, Launius G, Dadash-Zadeh M, Lee R, Noetzel M. Neurology. 1998;50:1678–82.

107. Watkins K, Hewes D, Connelly A, Kendall B, Kingsley D, Evans J, Gadian D, Vargha-Khadem F, Kirkham F. Dev Med Child Neurol. 1998;40:536–43.

108. Hogan A, Kirkham F, Prengler M, Telfer P, Lane R, Vargha-Khadem F, Haan M. Br J Haematol. 2006;132:99–107.

109. Wang W, Enos L, Gallagher D, Thompson R, Guarini L, Vichinsky E, Wright E, Zimmerman R, Armstrong F. J Pediatr. 2001;139:391–7.

110. Schatz J, Buzan R. J Int Neuropsychol Soc. 2006;12:24–33.

111. Amendah DD, Mvundura M, Kavanagh PL, Sprinz PG, Grosse SD. Am J Prev Med. 2010;38:S550–6.

112. Kauf TL, Coates TD, Huazhi L, Mody-Patel N, Hartzema AG. Am J Hematol. 2009;84:323–7.

113. Centers for Disease Control and Prevention. Sickle cell disease. Updated 21 Jan 2010. Available from: http://www.cdc.gov/NCBDDD/sicklecell/data.html

114. Shankar SM, Arbogast PG, Mitchel E, Cooper WO, Wang WC, Griffin MR. Am J Hematol. 2005;80:262–70.

115. Health, United States. National center for health statistics. Washington, DC: U.S. Government Printing Office; 2006. p. 2006.

116. Ballas SK, Barton FB, Waclawiw MA, Swerdlow P, Eckman JR, Pegelow CH, Koshy M, Barton BA, Bonds DR. Health Qual Life Outcomes. 2006;4:59.

117. Armstrong-Wells J, Grimes B, Sidney S, Kronish D, Shiboski SC, Adams RJ, Fullerton HJ. Neurology. 2009;72:1316–21.

118. McCarville MB, Goodin GS, Fortner G, Li CS, Smeltzer MP, Adams R, Wang W. Pediatr Blood Cancer. 2008;50:818–21.

119. Bernaudin F, Verlhac S, Coic L, Lesprit E, Brugieres P, Reinert P. Pediatr Radiol. 2005;35:242–8.

120. Wayne A, Schoenike S, Pegelow C. Blood. 2000;96:2369–72.

121. Masdeu JC, Irimia P, Asenbaum S, Bogousslavsky J, Brainin M, Chabriat H, Herholz K, Markus HS, Martinez-Vila E, Niederkorn K, Schellinger PD, Seitz RJ. Eur J Neurol. 2006;13:1271–83.

122. Husson B, Rodesch G, Lasjaunias P, Tardieu M, Sebire G. Stroke. 2002;33:1280–5.

123. Nowak-Gottl U, Gunther G, Kurnik K, Strater R, Kirkham F. Semin Thromb Hemost. 2003;29:405–14.

124. Venkataraman A, Kingsley PB, Kalina P, Pavlakis SG, Buckwald S, Spinazzola R, Harper RG. CNS Spectr. 2004;9:436–44.

125. Atkinson Jr DS. Semin Ultrasound CT MR. 2006;27:207–18.

126. Lopez-Vicente M, Ortega-Gutierrez S, Amlie-Lefond C, Torbey MT. J Stroke Cerebrovasc Dis. 2010;19:175–83.

127. Ganesan V, Savvy L, Chong WK, Kirkham FJ. Pediatr Neurol. 1999;20:38–42.

128. Al-Kandari FA, Owunwanne A, Syed GM, Ar Marouf R, Elgazzar AH, Shiekh M, Rizui AM, Al-Ajmi JA, Mohammed AM. Ann Nucl Med. 2007;21:439–45.

129. Powars D, Conti P, Wong W, Groncy P, Hyman C, Smith E, Ewing N, Keenan R, Zee C, Harold Y, Hiti A, Teng E, Chan L. Blood. 1999;93:71–9.

130. Kidwell C, Chalela J, Saver J, Starkman S, Hill M, Demchuk A, Butman J, Patronas N, Alger J, Latour L, Luby M, Baird A, Leary M, Tremwel M, Ovbiagele B, Fredieu A, Suzuki S, Villablanca J, Davis S, Dunn B, Todd J, Ezzeddine M, Haymore J, Lynch J, Davis L, Warach S. J Am Med Assoc. 2004;292:1823–30.

131. Fiebach J, Schellinger P, Gass A, Kucinski T, Siebler M, Villringer A, Olkers P, Hirsch J, Heiland S, Wilde P, Jansen O, Rother J, Hacke W, Sartor K. Stroke. 2004;35:502–6.

132. Mokri B, Sundt Jr TM, Houser OW, Piepgras DG. Ann Neurol. 1986;19:126–38.

133. de Bruijn SF, Stam J. Stroke. 1999;30:484–8.

134. Adams R, Nichols F, McKie V, McKie K, Milner P, Gammal T. Neurology. 1988;38:1012–7.

135. Brambilla D, Miller S, Adams R. Pediatr Blood Cancer. 2007;49:318–22.

136. Seibert J, Miller S, Kirby R, Becton D, James C, Glasier C, Wilson A, Kinder D, Berry D. Radiology. 1993;189:457–66.

137. Switzer J, Hess D, Nichols F, Adams R. Lancet Neurol. 2006;5:501–12.
138. Kirkham F. Nat Clin Pract Neurol. 2007;3:264–78.
139. Paediatric Stroke Working Group. Stroke in childhood: clinical guidelines for diagnosis, management and rehabilitation. Clinical Effectiveness and Evaluation Unit, Royal College of Physicians. 2004.Updated November 2004. Available from: http://www.rcplondon.ac.uk/pubs/books/childstroke/childstroke_guidelines.pdf
140. Winrow N, Melhem E. Neuroimaging Clin N Am. 2003;13:185–96.
141. Lev MH, Farkas J, Gemmete JJ, Hossain ST, Hunter GJ, Koroshetz WJ, Gonzalez RG. Radiology. 1999;213:150–5.
142. Lin K, Rapalino O, Law M, Babb JS, Siller KA, Pramanik BK. AJNR Am J Neuroradiol. 2008;29:931–6.
143. Kosior RK, Lauzon ML, Steffenhagen N, Kosior JC, Demchuk A, Frayne R. Stroke. 2010;41:455–60.
144. Katz DA, Marks MP, Napel SA, Bracci PM, Roberts SL. Radiology. 1995;195:445–9.
145. Bash S, Villablanca JP, Jahan R, Duckwiler G, Tillis M, Kidwell C, Saver J, Sayre J. AJNR Am J Neuroradiol. 2005;26:1012–21.
146. Beyer J, Platt A, Kinney T, Treadwell M. J Soc Pediatr Nurs. 1999;4:61–73.
147. DeBaun M, Glauser T, Siegel M, Borders J, Lee B. J Pediatr Hematol Oncol. 1995;17:29–33.
148. Pavlakis S, Bello J, Prohovnik I, Sutton M, Ince C, Mohr J, Piomelli S, Hilal S, De Vivo D. Ann Neurol. 1988;23:125–30.
149. Dowling MM, Quinn CT, Rogers ZR, Buchanan GR. Pediatr Blood Cancer. 2010;54:461–4.
150. Marks MP, de Crespigny A, Lentz D, Enzmann DR, Albers GW, Moseley ME. Radiology. 1996;199:403–8.
151. Gonzalez RG, Schaefer PW, Buonanno FS, Schwamm LH, Budzik RF, Rordorf G, Wang B, Sorensen AG, Koroshetz WJ. Radiology. 1999;210:155–62.
152. Lovblad KO, Laubach HJ, Baird AE, Curtin F, Schlaug G, Edelman RR, Warach S. AJNR Am J Neuroradiol. 1998;19:1061–6.
153. Eastwood JD, Lev MH, Wintermark M, Fitzek C, Barboriak DP, Delong DM, Lee TY, Azhari T, Herzau M, Chilukuri VR, Provenzale JM. AJNR Am J Neuroradiol. 2003;24:1869–75.
154. Schramm P, Schellinger PD, Klotz E, Kallenberg K, Fiebach JB, Kulkens S, Heiland S, Knauth M, Sartor K. Stroke. 2004;35:1652–8.
155. Mullins M, Schaefer P, Sorensen A, Halpern E, Ay H, He J, Koroshetz W, Gonzalez R. Radiology. 2002;224:353–60.
156. Lansberg M, Albers G, Beaulieu C, Marks M. Neurology. 2000;54:1557–61.
157. Lansberg M, Norbash A, Marks M, Tong D, Moseley M, Albers G. Arch Neurol. 2000;57:1311–6.
158. Paonessa A, Limbucci N, Tozzi E, Splendiani A, Gallucci M. Eur J Radiol. 2010;74:77–85.
159. Kandeel A, Zimmerman R, Ohene-Frempong K. Neuroradiology. 1996;38:409–16.
160. Rovira A, Grive E, Alvarez-Sabin J. Eur Radiol. 2005;15:416–26.
161. Gillams A, McMahon L, Weinberg G, Carter A. Pediatr Radiol. 1998;28:283–7.
162. Korogi Y, Takahashi M, Nakagawa T, Mabuchi N, Watabe T, Shiokawa Y, Shiga H, O'Uchi T, Miki H, Horikawa Y, Fujiwara S, Furuse M. AJNR Am J Neuroradiol. 1997;18:135–43.
163. Kielpinska K, Walecki J, Giedrojc J, Turowska A, Kordecki K. Acad Radiol. 2002;9:283–9.
164. Srinivasan A, Goyal M, Al Azri F, Lum C. Radiographics. 2006;26(Suppl 1):S75–95.
165. Adams R, Nichols F, Figueroa R, McKie V, Lott T. Stroke. 1992;23:1073–7.
166. Dawkins A, Evans A, Wattam J, Romanowski C, Connolly D, Hodgson T, Coley S. Neuroradiology. 2007;49:753–9.
167. Rao K, Lee M. Radiology. 1983;147:600–1.
168. Willinsky RA, Taylor SM, TerBrugge K, Farb RI, Tomlinson G, Montanera W. Radiology. 2003;227:522–8.
169. Coley S, Wild J, Wilkinson I, Griffiths P. Neuroradiology. 2003;45:843–50.
170. Qureshi N, Lubin B, Walters M. Expert Opin Biol Ther. 2006;6:1087–98.
171. Verlhac S, Bernaudin F, Tortrat D, Brugieres P, Mage K, Gaston A, Reinert P. Pediatr Radiol. 1995;25(Suppl 1):S14–9.
172. Chooi W, Woodhouse N, Coley S, Griffiths P. AJNR Am J Neuroradiol. 2004;25:1251–5.
173. Alkan O, Kizilkilic E, Kizilkilic O, Yildirim T, Karaca S, Yeral M, Kasar M, Ozdogu H. Eur J Radiol. 2010;76:151–6.
174. Westerlaan HE, van Dijk MJ, Jansen-van der Weide MC, de Groot JC, Groen RJ, Mooij JJ, Oudkerk M. Radiology. 2011;258:134–45.
175. Reed W, Jagust W, Al-Mateen M, Vichinsky E. Am J Hematol. 1999;60:268–72.
176. Rodgers GP, Clark CM, Larson SM, Rapoport SI, Nienhuis AW, Schechter AN. Arch Neurol. 1988;45:78–82.
177. Adams R, McKie V, Hsu L, Files B, Vichinsky E, Pegelow C, Abboud M, Gallagher D, Kutlar A, Nichols F, Bonds D, Brambilla D. N Engl J Med. 1998;339:5–11.
178. Adams R, Brambilla D, Granger S, Gallagher D, Vichinsky E, Abboud M, Pegelow C, Woods G, Rohde E, Nichols F, Jones A, Luden J, Bowman L, Hagner S, Morales K, Roach E. Blood. 2004;103:3689–94.
179. Goldstein LB, Bushnell CD, Adams RJ, Appel LJ, Braun LT, Chaturvedi S, Creager MA, Culebras A, Eckel RH, Hart RG, Hinchey JA, Howard VJ, Jauch EC, Levine SR, Meschia JF, Moore WS, Nixon JV, Pearson TA. Stroke. 2011;42:517–84.
180. Ausavarungnirun P, Sabio H, Kim J, Tegeler C. J Neuroimag. 2006;16:311–7.

181. Bernick C, Kuller L, Dulberg C, Longstreth Jr WT, Manolio T, Beauchamp N, Price T. Neurology. 2001;57:1222–9.

182. Adams R, Pavlakis S, Roach E. Ann Neurol. 2003;54:559–63.

183. Krejza J, Rudzinski W, Pawlak M, Tomaszewski M, Ichord R, Kwiatkowski J, Gor D, Melhem E. AJNR Am J Neuroradiol. 2007;28:1613–8.

184. Adams R. J Pediatr Hematol Oncol. 1996;18:331–4.

185. Shen Q, Stuart J, Venkatesh B, Wallace J, Lipman J. J Clin Monit Comput. 1999;15:179–84.

186. National Heart, Lung, and Blood Institute. Clinical alert: periodic transfusions lower stroke risk in children with sickle cell anemia. Updated 9 Oct 1997. Available from: http://www.nlm.nih.gov/databases/alerts/sickle97.html.

187. Lee M, Piomelli S, Granger S, Miller S, Harkness S, Brambilla D, Adams R. Blood. 2006;108:847–52.

188. Bulas D. Pediatr Radiol. 2005;35:235–41.

189. Fullerton H, Adams R, Zhao S, Johnston S. Blood. 2004;104:336–9.

190. Enninful-Eghan H, Moore RH, Ichord R, Smith-Whitley K, Kwiatkowski JL. Transcranial Doppler ultrasonography and prophylactic transfusion program is effective in preventing overt stroke in children with sickle cell disease. J Pediatr. 2010;157(3):479–84.

191. Silent Cerebral Infarct Multi-Center Clinical Trial. ClinicalTrials.gov. 2003.Updated 6 May 2010. Available from: http://www.clinicaltrials.gov/ct/show/NCT00072761

192. Krejza J, Kochanowicz J, Mariak Z, Lewko J, Melhem E. Radiology. 2005;236:621–9.

193. Krejza J, Mariak Z, Lewko J. AJR Am J Roentgenol. 2003;181:245–52.

194. Swiat M, Weigele J, Hurst RW, Kasner SE, Pawlak M, Arkuszewski M, Al-Okaili RN, Swierca M, Ustymowicz A, Opala G, Melhem ER, Krejza J. Crit Care Med. 2009;37:963–8.

195. Jones A, Seibert J, Nichols F, Kinder D, Cox K, Luden J, Carl E, Brambilla D, Saccente S, Adams R. Pediatr Radiol. 2001;31:461–9.

196. Malouf AJ, Hamrick-Turner J, Doherty M, Dhillon G, Iyer R, Smith M. Radiology. 2001;219:359–65.

197. McCarville M, Li C, Xiong X, Wang W. AJR Am J Roentgenol. 2004;183:1117–22.

198. Riebel T, Kebelmann-Betzing C, Götze R, Overberg U. Eur Radiol. 2003;13:563–70.

199. Lowe L, Bulas D. Pediatr Radiol. 2005;35:54–65.

200. Pawlak MA, Krejza J, Rudzinski W, Kwiatkowski JL, Ichord R, Jawad AF, Tomaszewski M, Melhem ER. Radiology. 2009;251:525–34.

201. Krejza J, Chen R, Romanowicz G, Kwiatkowski JL, Ichord R, Arkuszewski M, Zimmerman R, Ohene-Frempong K, Desiderio L, Melhem ER. Stroke. 2011;42:81–6.

202. Abboud M, Cure J, Granger S, Gallagher D, Hsu L, Wang W, Woods G, Berman B, Brambilla D, Pegelow C, Lewin J, Zimmermann R, Adams R. Blood. 2004;103:2822–6.

203. Wang W, Gallagher D, Pegelow C, Wright E, Vichinsky E, Abboud M, Moser F, Adams R. J Pediatr Hematol Oncol. 2000;22:335–9.

204. Wiznitzer M, Ruggieri P, Masaryk T, Ross J, Modic M, Berman B. J Pediatr. 1990;117:551–5.

205. Kogutt MS, Goldwag SS, Gupta KL, Kaneko K, Humbert JR. Pediatr Radiol. 1994;24:204–6.

206. Seibert JJ, Glasier CM, Kirby RS, Allison JW, James CA, Becton DL, Kinder DL, Cox KS, Flick EL, Lairry F, Jackson JF, Graves RA. Pediatr Radiol. 1998;28:138–42.

207. Smith AS, Haacke EM, Lin W, Berman B, Wiznitzer M. AJNR Am J Neuroradiol. 1994;15:1557–64.

208. Gaa J, Weidauer S, Requardt M, Kiefer B, Lanfermann H, Zanella FE. Acta Radiol. 2004;45:327–32.

209. Kirkham F, Lerner N, Noetzel M, DeBaun M, Datta A, Rees D, Adams R. Pediatr Neurol. 2006;34:450–8.

210. Russell M, Goldberg H, Hodson A, Kim H, Halus J, Reivich M, Schwartz E. Blood. 1984;63:162–9.

211. Wilimas J, Goff J, Anderson HJ, Langston J, Thompson E. J Pediatr. 1980;96:205–8.

212. Dobson S, Holden K, Nietert P, Cure J, Laver J, Disco D, Abboud M. Blood. 2002;99:3144–50.

213. Ganesan V, Prengler M, Wade A, Kirkham F. Circulation. 2006;114:2170–7.

214. Woodard P, Helton K, Khan R, Hale G, Phipps S, Wang W, Handgretinger R, Cunningham J. Br J Haematol. 2005;129:550–2.

215. Kirkham F, DeBaun M. Curr Treat Options Neurol. 2004;6:357–75.

216. Fryer R, Anderson R, Chiriboga C, Feldstein N. Pediatr Neurol. 2003;29:124–30.

217. Walters M, Storb R, Patience M, Leisenring W, Taylor T, Sanders J, Buchanan G, Rogers Z, Dinndorf P, Davies S, Roberts I, Dickerhoff R, Yeager A, Hsu L, Kurtzberg J, Ohene-Frempong K, Bunin N, Bernaudin F, Wong W, Scott J, Margolis D, Vichinsky E, Wall D, Wayne A, Pegelow C, Redding-Lallinger R, Wiley J, Klemperer M, Mentzer W, Smith F, Sullivan K. Blood. 2000;95:1918–24.

218. Steen R, Helton K, Horwitz E, Benaim E, Thompson S, Bowman L, Krance R, Wang W, Cunningham J. Ann Neurol. 2001;49:222–9.

219. Adams R, Brambilla D. N Engl J Med. 2005;353:2769–78.

220. Minniti C, Gidvani V, Bulas D, Brown W, Vezina G, Driscoll M. J Pediatr Hematol Oncol. 2004;26:626–30.

221. Mazumdar M, Heeney M, Sox C, Lieu T. Pediatrics. 2007;120:e1107–16.

222. Inati A. Recent advances in improving the management of sickle cell disease. Blood Rev. 2009;23(Suppl 1):S9–13.

223. Cappellini MD, Porter J, El-Beshlawy A, Li CK, Seymour JF, Elalfy M, Gattermann N, Giraudier S, Lee JW, Chan LL, Lin KH, Rose C, Taher A, Thein SL, Viprakasit V, Habr D, Domokos G, Roubert B, Kattamis A. Haematologica. 2010;95:557–66.

224. Adams Jr HP, del Zoppo G, Alberts MJ, Bhatt DL, Brass L, Furlan A, Grubb RL, Higashida RT, Jauch EC, Kidwell C, Lyden PD, Morgenstern LB, Qureshi AI, Rosenwasser RH, Scott PA, Wijdicks EF. Stroke. 2007;38:1655–711.

225. Powars D, Wilson B, Imbus C, Pegelow C, Allen J. Am J Med. 1978;65:461–71.

226. Diggs LW, Brookoff D. South Med J. 1993;86: 377–9.

227. Royal JE, Seeler RA. Lancet. 1978;2:1207.

228. Stockman J, Nigro M, Mishkin M, Oski F. N Engl J Med. 1972;287:846–9.

229. Henderson J, Noetzel M, McKinstry R, White D, Armstrong M, DeBaun M. Blood. 2003;101:415–9.

230. Wardlaw JM, White PM. Brain. 2000;123(Pt 2): 205–21.

231. Singer OC, Sitzer M, du Mesnil de Rochemont R, Neumann-Haefelin T. Neurology. 2004;62:1848–9.

232. Chappell ET, Moure FC, Good MC. Neurosurgery. 2003;52:624–31.

233. Burger IM, Murphy KJ, Jordan LC, Tamargo RJ, Gailloud P. Stroke. 2006;37:2535–9.

234. Lysakowski C, Walder B, Costanza MC, Tramer MR. Stroke. 2001;32:2292–8.

235. Ohene-Frempong K, Weiner SJ, Sleeper LA, Miller ST, Embury S, Moohr JW, Wethers DL, Pegelow CH, Gill FM. Cerebrovascular accidents in sickle cell disease: rates and risk factors. Blood. 1998;91:288–294.

236. Balkaran B, Char G, Morris J, Thomas P, Serjeant B, Serjeant G. Stroke in a cohort of patients with homozygous sickle cell disease. J Pediatr. 1992;120: 360–366.

237. Adams R, McKie V, Hsu L, Files B, Vichinsky E, Pegelow C, Abboud M, Gallagher D, Kutlar A, Nichols F, Bonds D, Brambilla D. Prevention of a first stroke by transfusions in children with sickle cell anemia and abnormal results on transcranial Doppler ultrasonography. N Engl J Med. 1998;339: 5–11.

Acute Ischemic Stroke Patient: Evidence-Based Endovascular Treatment

12

Danial K. Hallam and Ken F. Linnau

Contents

D.K. Hallam (✉) • K.F. Linnau
Department of Radiology, Harborview Medical Center, University of Washington, Seattle, WA, USA
e-mail: dhallam@uw.edu; klinnau@uw.edu

Key Points

- IV thrombolysis is the standard of care for treatment of acute anterior ischemic infarct within 3 h of symptom onset. The treatment window may reasonably be extended to 4.5 h (strong evidence).
- Intra-arterial thrombolysis may be used at a qualified stroke center to treat patients with major stoke due to MCA occlusion <6 h who cannot receive IV alteplase (strong evidence).
- Larger more proximal clots (ICA, M1 MCA) exhibit lower recanalization rates with IV thrombolytic treatment. Such patients tend to have worse prognosis (limited evidence).
- FDA has approved two devices (Merci and Penumbra) for intracranial clot removal in appropriately selected patients. Although considered appropriate for emergency stroke treatment, the effect on outcomes has not been established (moderate evidence).
- Other mechanical treatments such as stenting and angioplasty, occasionally employed at experienced centers, have not been studied systematically (insufficient evidence).

Definition and Pathophysiology

Large artery thromboembolic occlusion, cardioembolism, and lacunes account for the majority of ischemic strokes. Compromise of blood flow and energy supply to the brain actuates several mechanisms contributing to cell death including inflammation, apoptosis, excitotoxicity and ionic imbalance, oxidative stress, and peri-infarct depolarization [1].

Although permanent brain damage begins in minutes following sufficient perfusion decline, the final extent of brain injury reflects the end result of a complex, dynamic interplay involving the initiating occlusion, its severity, potential recanalization along with the presence and extent of collaterals, as well as other hemodynamic factors. Extensive research and clinical experience has validated the concept of an ischemic penumbra – potentially salvageable tissue adjacent to an infarcted core region. Accordingly, great effort is now being directed at therapies targeting rapid restoration of perfusion to the ischemic penumbra.

Epidemiology

Stroke rates declined in the 1980s likely due to widespread blood pressure control. Most data indicate rate stabilization since. Significant racial disparities exist. Among African Americans, incidence of first ever hospitalized or autopsied stroke was 288 per 100,000. Among whites, the incidence was 179 per 100, 000 [2].

Stroke in young adults represents an important subgroup reflecting a combination of etiologies seen mainly in older patients with young adult causes. The Helsinki Young Stroke Registry disclosed an annual occurrence of 10.8/100,000 in ages 15–49 years which increased exponentially with age [3]. Although overall strokes in males exceeded those in females (1.7:1), females predominated in the <30 group. Males increased above this age with a sharp increase around 44 years. Cardioembolism was the case in 20 % and arterial dissection in 15 %. Common risk factors included dyslipidemia, smoking, and hypertension. The proportion of stroke ascribed to large vessel atherosclerosis and small-vessel disease rose at age 35.

Pediatric stroke (age 1 month to 18 years) is less common with incidence reported from 2.5 to 13 per 100,000 [4–6]. Increased incidence is reported in male and African American children.

Overall Cost to Society

Stroke now represents the third most common cause of death and single most common cause of disability in the North America. Greater than 750,000 strokes occur yearly resulting in 200,000 deaths and 250,000 new disability cases. The NIH estimates annual cost in the USA to exceed $50 billion with 60 % of the cost related to health care and remaining 40 % due to lost productivity.

Half or more children who suffer stroke are left with epilepsy or significant neurologic deficit [7, 8]. Loss of decades of productive life, long-term care, and multiple treatments yield profound societal burdens.

Goal of Imaging

The goal of endovascular intervention is straightforward: minimize the neurologic consequence of ischemic stroke while managing treatment risk.

Options

In the appropriate time window, the first option for treatment of acute ischemic stroke is IV alteplase. Options for endovascular treatment begin with intra-arterial administration of alteplase in the <6-h time window for the anterior circulation. Combined treatment with IA thrombolytic therapy following IV thrombolytic therapy is another option. Several mechanical devices have been specifically developed for this indication and two have received FDA approval: Merci Retriever (Concentric Medical) and the Penumbra aspiration system (Penumbra). A variety of other devices are employed off label including stents and balloon angioplasty. Mechanical thrombectomy may be performed following IV thrombolytic treatment in the setting of persistent amenable vessel occlusion. Treatment choice depends on time after symptom onset and numerous patient factors.

Methodology

A MEDLINE search was performed using PubMed (National Library of Medicine, Bethesda, Maryland) for original research publications discussing acute intervention in ischemic stroke. The search covered the years January 1995 to July 2011. The review was limited to human studies and the English language literature. As the germane literature on the subject is very extensive, the initial search was further limited to major stroke journals. Additional articles were identified by reviewing the reference lists of relevant papers. Emphasis was placed on higher quality evidence which rightly determines current treatment. The authors performed an initial review of the titles and abstracts of the identified articles followed by review of the full text in articles that were relevant.

Discussion of Issues

What Is the Role of Intravenous Thrombolysis in the Acute Ischemic Stroke Patient?

Summary
The NINDS stroke study proved efficacy for use of IV alteplase within 3 h of stroke onset in patients with MCA stroke and no hemorrhage on CT [9]. A number of studies followed which failed to prove efficacy of IV alteplase in the 3- to 6-h time window. More recently, a meta-analysis was undertaken evaluating data from negative trials only in the 3- to 4.5-h time window as well as the ECASS 3 trial. The meta-analysis showed efficacy of treatment with IV alteplase from 3 to 4.5 h after MCA stroke onset in patients with no hemorrhage and no signs of significant early infarct by CT [10] (strong evidence).

Supporting Evidence
Strong evidence supporting use of IV alteplase in treatment of acute anterior circulation stroke became available in 1995 with the publication of the National Institute of Neurological Disorders and Stroke rtPA Study Group (NINDS) stroke study [9]. Treatment was limited to 3 h after stroke onset and was the first study to prove efficacy. Treatment consisted of 0.9 mg/kg tPA (10 % as bolus and remainder over an hour). Imaging evaluation consisted only of a non-contrast head CT. Patients were excluded for signs of hemorrhage but not for signs of early major infarct. At 3 months, patients treated with alteplase were at least 30 % more likely to have minimal or no disability on the assessment scales when compared to those treated with placebo.

The benefit occurred despite higher rate of intracerebral hemorrhage in alteplase-treated patients compared to control (6.4 % vs. 0.6 %). Mortality was similar in the two groups both at 90 days (17 % vs. 20 %) and at 1 year (24 % vs. 28 %). A subsequent subgroup analysis focused on patients with CT signs of early MCA infarct exceeding >1/3 MCA distribution [11]. Although such patients exhibited a higher symptomatic hemorrhage, they did not exhibit higher adverse outcome. Treatment with IV alteplase within 3 h of stroke onset was endorsed early on by the Special Writing Group of the Stroke Council, American Heart Association [12]. The NINDS stroke study profoundly altered the ischemic stroke treatment paradigm from one of observation to one of acute intervention.

In the first of two large European trials, ECASS 1, patients were treated up to 6 h of ictus and larger dose of tPA was utilized (1.1 mg/kg vs. 0.9 mg/kg) [13]. No benefit was noted in the treated group. A higher hemorrhage rate with tPA was again seen (20 % vs. 7 %). In this study, 52 patients who were randomized for treatment exhibited evidence of early large infarct on CT – this subset did poorly. Post hoc analysis of subset treated within 3 h showed benefit, confirming the NINDS study results [14]. A second European trial, ECASS 2, drew on experience from the first with several modifications [15]. First, the dose of tPA was decreased to 0.9 mg/kg. Second, greater effort was directed at excluding a subset of patients with evidence for large MCA infarct on initial CT. Specifically, those patients with evidence for infarct greater than 1/3 MCA distribution were excluded. A 6-h time window was employed and again the results were negative. Increased rate of intracerebral hemorrhage (ICH) with treatment (8.1 % vs. 0.8 %) was again observed. A second North American trial (ATLANTIS) investigated efficacy of treatment with IV tPA (0.9 mg/kg) between 3 and 5 h of stroke onset [16]. The results showed no benefit of treatment on all outcome measures. Symptomatic ICH was greater with treatment (11.4 % vs. 4.7 %). Of special concern, in this cohort, 90-day mortality was borderline higher in patients treated with alteplase (11.0 %) compared to placebo (6.9 %, *P*_0.09).

Subsequent pooled analysis of the above IV tPA trial data was performed in an effort to validate the importance of rapid treatment [17]. The results of the analysis of treatment in 2,775 patients clearly showed earlier treatment to yield better outcomes. More specifically, odds ratios of improved outcome were 2.81 for treatment 0–90 min (95 % CI 1.8–4.5), 1.55 for treatment 91–180 min (CI 1.1.2.2), and 1.40 for 181–270 min (CI 1.1–1.9). The results indicated a longer time window of treatment did not increase rates of symptomatic hemorrhage or death. As such, the pooled analysis supports treatment benefit up to 4.5 h. Following the encouraging results of the pooled analysis, the ECASS investigators undertook a randomized, placebo controlled trial to address specifically the efficacy of treatment in the 3- to 4.5-h time window [18] (ECASS 3). Eight hundred and twenty-one patients were randomly enrolled with mean time to treatment of 3 h 59 min. Patients treated with alteplase exhibited improved outcome with odds ratio 1.34 (95 % CI 1.02–1.76), findings consistent with the above described pooled analysis. Given the borderline statistical significance, concerns were rightly raised regarding result reliability. Consistent with all other IV alteplase trials, the rate of symptomatic hemorrhage was higher in the treated group but the rate observed was no higher than that reported previously among patients treated within 3 h. Despite the increased hemorrhage, there was no increase in mortality at 90 days. Indeed, a nonsignificant reduction in 90-day mortality was derived.

Recognizing the results of the negative ATLANTIS study and the marginally positive ECASS 3 study to be somewhat in conflict, Lansberg et al. undertook a meta-analysis of data from all major IV alteplase studies in which patients were treated during the 3- to 4.5-h time window [10]. The study included data from ECASS 1, ECASS 2, and ECASS 3 along with ATLANTIS resulting in a sample size of 1622. Benefit for alteplase treatment was shown with odds ratio of 1.31 (95 % CI 1.1–1.56). The results carried a somewhat higher confidence interval for OR estimate and P = 0.002.

Of special note, 90-day mortality showed no consistent association with treatment in the 3- to 4.5-h time window. The meta-analysis supports IV alteplase in acute anterior circulation ischemic infarction up to 4.5 h (strong evidence).

With the above data, the practice of extending the IV alteplase window to 4.5 h has disseminated. Multiple registries have been established to verify the safety of the extended time window treatment. Published results support safety and efficacy comparable to that in patients treated within 3 h from onset [19–21].

What Is the Role of Intra-arterial Thrombolysis in the Ischemic Stroke Patient?

Summary
The PROACT II studied provided level one evidence supporting on primary outcome measure of IA prourokinase administered within 6 h in patients with M1 or M2 occlusion [22] (strong evidence).

Supporting Evidence
For a thrombolytic agent to succeed, an effective dose must be delivered to the site of thrombus. Such delivery is compromised by diminished flow often accompanying acute stroke – perhaps accounting in part for limited success of IV trials. IA therapy offers several hypothetical advantages over IV treatment. First, IA delivery guarantees maximal dose of therapeutic agent at the thrombus. Depending on delay related to angiography initiation, the time to delivery of therapeutic dose may be less. Also, IA therapy provides for direct clot monitoring thereby allowing optimal dose titration in order to maximize benefit while minimizing risk. In addition to drug delivery, IA provides opportunity for other maneuvers such as mechanical clot disruption.

Multiple noncontrolled case studies have been published proving the feasibility of IA thrombolysis while hinting at potential efficacy [23–29]. Therapeutic agents utilized included both pro-UK and tPA. In general, the reports claimed fairly high complete or partial recanalization rates with

IA therapy, likely besting those seen with IV treatments. Variable clinical outcomes were reported.

A series of randomized controlled studies were undertaken in the late 1990s to evaluate the utility of IA administration of pro-UK in patients with MCA stroke under the moniker PROACT (Prolyse in Acute Cerebral Thromboembolism). The first PROACT study was a phase II trial aimed at establishing safety and efficacy in recanalization [30]. The study confirmed the efficacy of IA drug administration in promoting vessel recanalization compared to placebo. Hemorrhage rates twice that seen with placebo were observed (15.4 % vs. 7.1 %).

Based on these results, the PROACT II trial was then implemented to determine the clinical efficacy and safety of intra-arterial (IA) recombinant prourokinase (r-pro-UK) in patients with acute stroke [22]. Only patients with MCA infarct <6 h from onset and no evidence of hemorrhage or early signs of major infarct on CT were included. Additional exclusion criteria included age >85 years, mild stroke (NIHSS < 4), and rapidly improving symptoms. Angiographic inclusion criteria were either complete occlusion (TIMI 0) or contrast penetration with minimal perfusion (TIMI 1) of either M1 or an M2 division of the MCA. Angiographic exclusion criteria were arterial dissection, arterial stenosis precluding safe passage of microcatheter, non-atherosclerotic arteriopathy, no visible occlusion, or occlusion of artery other than M1/M2 MCA. Following angiography, 180 patients met criteria. These patients were randomized in a 2:1 ratio to receive 9 mg of IA r-pro-UK plus heparin ($n = 121$) or heparin only ($n = 59$). Heparin was administered as 2,000 U bolus followed by infusion of 500 μm per hour for 4 h beginning at time of angiography. An infusion microcatheter ($<3.0 °F$) with single end hole was place into the proximal one third of the MCA thrombus using steerable microguidewire. If intra-thrombus positioning was not possible, the catheter was to be place as close as possible to the proximal surface of the clot. Mechanical disruption of the clot was not permitted.

The results indicated benefit for the treated group. Specifically, 40 % of pro-UK patients

compared to 25 % of control patients had little or no neurological disability at 90 days ($P = .04$), the primary outcome measure (Rankin 0–2). Mortality was 25 % for the pro-UK group and 27 % for the control group. The improved outcome in the treated group was noted despite increased frequency of early symptomatic hemorrhage (within 24 h, 10 % in treated vs. 2 % of controls). The recanalization rate was 66 % for the r-pro-UK group and 18 % for the control group ($P < .001$). The results represent a 15 % absolute and a 58 % relative benefit for IA thrombolysis. It is worth noting, however, that the benefit did not encompass strokes of all severities. Specifically, treated and control patients with lesser strokes (NIHSS $\leq$ 10) did equally well. Patients with more severe strokes (NIHSS $>$ 10) were twice as likely as controls to achieve the desired outcome measure. The PROACT II study provides level one evidence supporting efficacy of treatment of MCA ischemic infarct, <6 h after onset in appropriately selected patients.

Several features of the trial merit comment. In some regard, study inclusion criteria and treatment restrictions created a near worst possible circumstance scenario. Significant occlusions were part of the inclusion criteria, and the providers were constrained by the prohibition of mechanical maneuvers. The time to treatment was a lengthy median 5.3 h. Although difficult to standardize and thus systematically study, mechanical clot disruption appears to help as an adjuvant treatment. A preponderance of data and understanding points to earlier treatment as more effective in IV therapy [31] – a result likely to generalize to IA therapy. With these considerations in mind, many investigators suspect the demonstrated PROACT II benefit represents a lower limit for treatment efficacy.

Prourokinase has not been approved by the FDA for clinical use in ischemic stroke. Wide clinical consensus and extensive case study data have allowed for the extrapolation of the PROACT II results with prourokinase to both alteplase and urokinase. For urokinase, the extrapolation is fairly straightforward as the drug is chemically quite similar. For alteplase, the extrapolation derives from the extensive IV data.

Case–control analysis using registry data from Japan's Multicenter Stroke Investigator's Collaboration (J-MUSIC) provides data supportive of IA therapy [32]. A favorable outcome defined as modified Rankin Scale 0–2 was more often observed in the urokinase treatment group (51 %) than the control group (34 %; $P = 0.01$). As such, the results support those of the PROACT II study (moderate evidence).

The MELT trial evaluated the safety and clinical efficacy of IA urokinase infusion in patients with acute stroke treated within 6 h of symptom onset, providing further strong evidence for IA thrombolysis [33]. Only patients displaying angiographic occlusions of the M1 or M2 MCA segments were randomized. Unlike PROACT II, thrombus disruption was permitted but only with a microwire. No other mechanical techniques were allowed. IA infusion of UK (120,000 U for 5 min) was performed and repeated until the total dose of 600,000 U was reached, 2 h had passed after starting infusion, or complete recanalization was achieved. The trial was terminated early by the steering committee after the approval of IV alteplase in Japan. At the time, a total of 114 patients (57 patients in each group) had undergone randomization. The primary end point (90-day mRS score, 0–2) was more frequent in the UK group than in the control group (49.1 % vs. 38.6 %; OR, 1.54; 95 % CI, 0.73–3.23), but this difference did not reach significance ($P = .345$). However, two preplanned secondary end points reached statistical significance. The rate of excellent functional outcome (90-day mRS score $\leq$ 1) was significantly more frequent in the UK group compared with the control group (42.1 % vs. 22.8 %; $P = .045$; OR, 2.46; 95 % CI, 1.09–5.54). In addition, there were significantly more patients with NIHSS scores of 0–1 at 90 days in the urokinase group than in the control group (35.1 % vs. 14.0 %, $P = .017$). Partial or complete recanalization was achieved in 42 of 57 of the IA-treated patients (73.7 %). There was no significant difference in the 90-day mortality (5.3 % vs. 3.5 %, $P = 1.00$) or ICH rate within 24 h of treatment (9 % vs. 2 %, $P = .206$).

A few comments regarding the relative merits of IA vs. IV therapy are warranted. IV therapy

can be initiated more rapidly but may not achieve therapeutic dose of thrombolytic agent at site of occlusion as quickly. IA therapy allows for titration of dose to clot lysis and can be used in settings for which systemic thrombolytics are contraindicated. IA therapy is more costly and carries with it the inherent risk of angiography including super-selective catheterization. IV treatment is proven effective at up to 3 h, and there is now justification for lengthening the treatment window to 4.5 h. In general, IV therapy is generally regarded to be less effective in recanalizing large occlusive clots [34], such as those of the terminal ICA or M1 MCA, an observation supported by experimental data [35] and thrombolytic trials [36, 37]. The presence of a dense MCA sign on CT indicating complete occlusion bodes poorly for patients treated with IV tPA [38, 39]. Recanalization rates for larger more proximal thromboemboli are low when IV tPA is utilized. IV tPA yields recanalization rates of 30 % for proximal MCA occlusion and 10 % for ICA occlusion [40] – significantly lower than the rates reported in multiple IA studies. A carefully crafted meta-analysis has been performed which confirmed a very strong correlation between early recanalization and outcome in acute ischemic stroke [41]. The authors derived a four- to fivefold increase in odds of good functional outcome and a four- to fivefold reduction in mortality. Improved recanalization rates with IA therapy should be balanced against the negative consequence of additional time to treatment [42]. Based on a subgroup analysis of the NINDS stroke study, despite low rates of recanalization with proximal occlusions, IV tPA improves outcome in large strokes [43]. Presumably, much of the benefit of IV treatment derives from recanalization of smaller more distal branches.

IA therapy has been specifically applied in the post-op setting when IV treatment was considered too risky. A retrospective case series provides level two data supporting safety of IA thrombolysis in post-op major surgery with the exception of intracranial surgery [44]. Thirty-six patients were identified who suffered ischemic stroke soon after surgery (1 h to 120, mean time

after surgery 29). Minor surgical site bleeding occurred in 25 %. Major surgical bleeds included two post-craniotomy ICHs and one hemopericardium post-bypass – all were fatal. The mortality rate for the study was similar to that reported for prior IA thrombolysis trials (limited evidence).

Little good data exists directly comparing the benefits of IV and IA thrombolytic therapy. A randomized study of 27 patients was performed comparing IV urokinase with IA urokinase in the first 6 h of MCA infarction [45]. Early study termination due to high mortality rate (26 %) dictated the small sample size. There were four deaths in the IV group and three in the IA group. IA-treated patients showed more improvement although the trend proved insignificant by outcome measures (insufficient evidence).

Noting the guarded prognosis in patients with dense MCA sign [38], an observational study was undertaken to evaluate the relative efficacy of IV vs. IA thrombolytic treatment in the dense MCA stroke subset [46]. Cohorts from two different hospitals were analyzed. In one hospital, IV alteplase was given for patients <3 h from symptom onset according to now standard protocol. In the other hospital, treatment consisted of IA urokinase 500,000–1,250,000 IU over 60–90 min. The two groups were well matched in age (mean 61), and percentage of patients with hypertension and atrial fibrillation. Potentially confounding differences included higher percentage with diabetes in IV-treated group (18 % vs. 13 %) and higher percentage of men in IV-treated group (67 % vs. 51 %). Clinical outcome measures were mortality and modified Rankin Scale at 3 months, dichotomized as in PROACT II as favorable (0–2) and unfavorable (3–6). Seventeen (15 %) of the 112 patients included in the review were dead at 3 months, most due to their initial stroke. Lower mortality was observed in the IA-treated group, a result which held up on univariate but not multivariate analysis. In the 95 survivors, clinical outcome preferred the IA treatment group. Favorable outcome was achieved in the IA-treated group 53 % of the time compared to 23 % of the time in the IV-treated group ($P = 0.022$). The results are especially noteworthy

upon consideration of the longer time from symptom onset to treatment in the IA-treated group (244 + 63 min) compared to the IV-treated group (156 = 21 min; $P = 0.0001$) (limited evidence).

Recognizing the trade-offs between IV and IA thrombolytic therapy, combined therapy consisting of IV treatment followed by IA treatment has been suggested and studied [47]. The IMS II trial compared combined IV/IA thrombolytic treatment to historical controls of IV thrombolytic alone and placebo from the NINDS stroke study [48]. Eighty-one patients who could be treated with IV alteplase within 3 h from symptom onset were enrolled. IV treatment consisted of two-third the usual alteplase dose administered as 15 % bolus over 1 min followed by remainder over 30 min. Once IV treatment had been initiated, the patient was transferred to the angiography suite. If an IA treatment amenable clot was identified, IA treatment was performed in which either a standard microcatheter or MicroLysUS infusion (US emitting) catheter was placed in the clot and the remaining one third alteplase dose administered. If no IA amenable clot was identified at angiography, the remaining one third alteplase dose was completed IV. Of 81 patients enrolled, 55 underwent combined treatment with remaining receiving IV treatment alone. The combined IV/IA treatment patients exhibited a better outcome than NINDS alteplase-treated subjects by Barthel Index but not by other outcome measures. The combined treatment patients had significantly better outcome at 3 months than NINDS placebo patients on all outcome measures ($OR > 2$). Three-month mortality for IMS combined treatment patients (16 %) trended lower than NINDS placebo (24 %) and alteplase-treated subjects (21 %). The difference was not statistically significant.

A prospective registry (RECANALISE study) compared recanalization rates, 24-h improvement, and 3-month functional outcome between patients in two-time intervals who underwent different thrombolytic protocols [49]. In the first time period, patients within 3 h of symptom onset were treated with IV alteplase according to standard protocol. In the second time interval, patients were treated with a combined technique

similar to IMS II. Early neurological recovery (defined as NIHSS 0 or 1 or a 4-point improvement in same) occurred in 60 % of combined treatment patients compared with 39 % of IV treatment patients ($P = 0.07$). A marginal difference in 3-month functional outcome was noted with favorable (mRS 0–2) occurring in 57 % of combined treatment compared with 44 % of IV treatment patients ($p = 0.35$). Ninety mortality and symptomatic intracranial hemorrhage rates were not appreciably different. The most pronounced difference observed was in the recanalization rate: 87 % of combined treatment patients vs. 52 % of IV treatment patients ($P = 0.0002$) (moderate evidence).

What Is the Role of Mechanical Endovascular Intervention in the Acute Ischemic Stroke Patient?

Summary

Mechanical clot removal has not been evaluated in a randomized controlled fashion. Two devices specifically designed for acute stroke have been evaluated in a non-randomized fashion, the Merci Retriever (Concentric Medical) and the Penumbra aspiration system (Penumbra) [50–52]. The studies were prospective multicenter single arm design trials. A historical control from PROACT II was often used. Of note, the studies allowed patients to be treated up to 8 h following ictus. Safety was demonstrated along with high rates of a surrogate outcome measure, recanalization. Efficacy data is lacking (limited evidence).

Supporting Evidence

Much recent interest centers on the development of devices that provide mechanical clot removal. Such techniques offer several potential advantages, including faster flow restoration and access to patients for whom thrombolytic agents are contraindicated. The devices may be categorized as performing thrombectomy or clot disruption and aspiration. Several reviews are available [53, 54]. Two systems have achieved wide recognition, FDA approval, and are now used commonly throughout the USA: the Merci Retriever

(Concentric Medical) and the Penumbra aspiration system (Penumbra).

The Merci Retriever consists of a nitinol-coiled wire that is used to engage and drag the target clot into a guide catheter for removal. The technique involves placing a fairly large balloon guide catheter in a proximal vessel (ideally the ICA or vertebral artery). Through the guide catheter, a specific microcatheter is advanced over a microwire into and through the target clot. With the microwire removed, the retriever is then advanced through the microcatheter and deployed distal to the clot. The retriever is then pulled back and into the clot. With the clot so engaged, the balloon of the guide catheter is inflated and aggressive aspiration performed proximally in an attempt to achieve flow reversal and avoid distal embolization of clot fragments. The retriever along with the clot is then pulled into the guide catheter and removed.

The Merci system has gone through several generations of devices aimed at improving the efficacy of clot removal. The first generation (X5, X6) consisted of a conical helix. In the second generation (L4, L5, L6), the nitinol wire was altered to a simple helix to which a series of filaments were attached. The filaments were attached to increase the surface area of the device engaging the clot. The simple helix was designed to increase vessel wall apposition. A third generation (V series) retains the use of filaments, incorporates a variable pitch to the helix, and uses a subtle taper in the distal end. A series of studies have evaluated the Merci Retriever and have shown improved flow restoration with the above modifications [51, 52, 55]. The evidentiary merit of the studies will be discussed below. The Merci device was approved by the FDA in 2004 specifically for the indication of intracranial clot retrieval.

In the Penumbra aspiration system, the clot is fragmented and then aspirated through a catheter designed for intracranial use (reperfusion catheter) [50, 56]. Through the reperfusion catheter, a device labeled a separator is advanced to and fro through the clot yielding clot disruption and preventing blockage of the catheter. The catheter is connected to an aspiration system.

The separator consists of a wire to which an appropriately sized nearly conical polymer has been affixed. As with the Merci system, multiple device sizes are available depending on the site of occlusion. The Penumbra system was approved in 2008 by the FDA.

Multiple studies have validated the safety of the Merci and Penumbra systems along with clear evidence of improved flow restoration. The studies were prospective multicenter single arm design trials. There was no randomization and if there was a control group, it was a historical control (PROACT II). In the latest of the Merci trials, Multi MERCI [51], mechanical thrombectomy was utilized in large vessel stroke, both anterior and posterior circulation, within 8 h of onset. Patients with persistent large vessel occlusion after IV alteplase were included. They observed successful recanalization in 57.3 % (75 of 131) and a higher rate of 69.5 % (91 of 131) after adjunctive therapy consisting of intra-arterial alteplase. The study also showed improved efficacy in recanalization with the new generation devices. Significant complications were defined as those procedural complications resulting in NIHSS decline of ≥ 4 or death or groin complication necessitating surgery and/or blood transfusion. Such clinically significant complications were observed in nine patients (5.5 %). Symptomatic ICH occurred in 16 patients (9.8 %). There was one L5 device fracture which occurred on withdrawal. The device was successfully retrieved with a snare and there was no untoward consequence for the patient.

In the Penumbra Pivotal trial, patients with treatable large vessel stroke in <8 h from onset were enrolled [50]. They observed high recanalization rates (TIMI 2 or 3) of 81.6 %; 12.8 % of patients (18 of 125) endured procedural complications (12.8 %) with 2.4 % (3 patients) considered serious. Sixteen (12.8 %) patients experienced procedural events including vasospasm, reocclusion of target vessel, dissection, perforation, ICH, subarachnoid hemorrhage, anemia, embolization of previously uninvolved vessel, and stroke in new distribution. Of these, three (2.4 %) were judged serious and resulted in significant negative impact on the patient.

Taken together, the three Merci studies and the single Penumbra study provide moderate evidence for mechanical thrombectomy as a reasonable option in experienced centers. However, evidence to support improved patient outcome is lacking (limited evidence). Importantly, in these early device trials, the time window for treatment has been expanded to 8 h, further increasing the number of patients who may be so treated.

Angioplasty and stenting have been used in many centers in both extra- and intracranial stroke. The literature is mostly limited to anecdotal reports and case series. Stenting has been reported in symptomatic carotid artery dissection [57]. Patients who suffer carotid artery occlusion with MCA embolism represent a unique challenge as the cervical carotid must be recanalized followed by removal of the MCA clot. Encouraging results were reported in one series in which the carotid was treated with angioplasty/stenting followed by mechanical thrombectomy with or without thrombolysis of the MCA [58]. In another series, the authors described a cohort of ICA occlusion patients falling into two categories [59]. The first group consisted of truly acute patients <6 h onset. The second group exhibited subacute presentation with fluctuating symptoms. Carotid artery stenting yielded a high overall recanalization rate (92 %; 23 of 25) and the clinical outcomes were promising. Intracranial revascularization using angioplasty with or without stenting has been described [60, 61]. A large series of 350 patients who underwent intra-arterial thrombolysis has been reported [62]. The authors employed an array of adjunctive measures including clot fragmentation, aspiration, balloon angioplasty, and stent placement. Higher recanalization rates were achieved when such measures were employed.

A newer product has been evaluated in human studies as a novel embolectomy device for large vessel occlusion. The Solitaire FR revascularization device (EV3) consists of a stent which may be deployed for treatment and then fully retrieved. The device is first deployed so that the distal portion is a few millimeters beyond the clot. After 1–2 min of deployment, a guide catheter balloon is inflated in the neck and continuously aspirated in order to reverse flow in the proximal artery as the deployed device is withdrawn. A single center pilot study has been published in which patients with M1 occlusion, ICA/MCA tandem occlusion, or ICA terminus occlusion were treated [63]. In 20 patients, they observed high recanalization rates (90 %) and no significant procedural complications. Enrollment in the "Solitaire FR with the Intention for Thrombectomy (SWIFT) Study" which compares the Solitaire device with Merci Retrieval System has been completed. Outcome data collection and analysis is ongoing. A similar stent retriever device, Trevo (Concentric Medical), has been developed and is currently for sale in Europe and Canada.

Special Case: Posterior Circulation Ischemic Stroke
Summary
Given the difficulty encountered in enrolling subjects for acute ischemic stroke treatment, all large trials have focused on MCA distribution stroke. The current practice is to treat posterior circulation strokes by analogy with their MCA counterparts. Also, recognizing the dismal prognosis associated with untreated basilar occlusion, treatment for longer time window of up to 24–48 h is common. No randomized trials have been performed proving efficacy (insufficient evidence).

Supporting Evidence
Regarding posterior circulation infarction, although there are plenty of anecdotal reports [64], and a few case series [65], there is only one randomized trial. A small multicenter randomized study was performed in which 16 patients with angiographic evidence of basilar or vertebral artery occlusion were enrolled. The patients were randomized to either IA urokinase treatment within 24 h or anticoagulation alone within 24 h of stroke onset [66]. Heparinization was performed in all patients followed by transition to warfarin. Fifty percent mortality rate was noted

both in the treatment and control groups. Of the survivors, four of eight treatment arm patients exhibited a good outcome compared to one of eight patients in the control arm. Of note, the strokes randomized to the treatment group were overall worse. Withdrawal of the UK from the Australian market combined with difficult recruitment resulted in early discontinuation of the study. Given the small sample size, the data at best amounts to level three evidence in support of IA thrombolytics vs. anticoagulation in this setting.

A recent meta-analysis compared relative efficacy of IV and IA thrombolytic treatment in patients afflicted with basilar artery occlusion [67]. The literature search returned data from 344 patients in 10 studies of IA treatment and from 76 patients in 3 studies of IV treatment. Analysis of the data suggested equivalence in the two treatments. Rates of death or dependency were 77.6 % in the IV-treated patients and 75.6 % in the IA-treated patients. Mortality was 55 % following IA treatment and 50 % following IV treatment. The rate of good outcome (inconsistently defined) was comparable as well (24 % with IA and 22 % with IV). Also, hemorrhagic complications were similar (11 % after IV treatment; 8 % after IA treatment). Only recanalization rate was determined to be statistically significant. A rate of 65 % was observed after IA treatment compared to 53 % after IV treatment ($P = 0.05$). The results of the meta-analysis have been criticized on multiples grounds [68]. In many of the IV-treated cases, only MRA used to establish the diagnosis of basilar artery occlusion. MRA is insensitive to slower flow so the findings may simply have represented tight stenosis in some cases. In the IA-treated patients, complete occlusion was always confirmed angiographically.

A prospective registry study (Basilar Artery International Cooperation Study, BASICS) enrolled patients from 2002 to 2007 in an effort to provide some understanding of the relative efficacy of currently employed treatments for basilar artery occlusion [69]. Data from 592 patients who received either antithrombotic therapy alone, IV thrombolysis, or IA thrombolysis

were analyzed. Initial stroke severity was dichotomized as either severe (coma, locked-in, or tetraplegia) or mild-moderate deficit (not severe). Outcome was assessed at one month with mRS 4–5 defined as poor. None of the treatment strategies showed significant superiority. Most patients (68 %) exhibited a poor outcome.

Special Case: Ischemic Stroke in Children

Data on IV thrombolysis and IA intervention in children is very limited. A recent literature review elucidates the considerations [70]. The largest series of treatment in childhood stroke presented data on 46 patients [71]. However, critical elements could not be adequately assessed including stroke severity at presentation, imaging findings, time to treatment, thrombolytic dose, pre- and post-angiographic findings, and outcome. Once the authors of the literature review excluded all studies lacking sufficient data, they were left with adequate data on only 17 patients. Although the data suggest reasonable safety profile, the results are no doubt confounded by publication bias. The data to support endovascular treatment of stroke in children is insufficient (insufficient evidence).

Take Home Table

Table 12.1 is an evidence summary table.

Imaging Case Studies

Case 1: A 67-year-old man 4 h after acute onset aphasia/right hemiparesis (Fig. 12.1)

Case 2: A 56-year-old woman with basilar occlusion diagnosed 12 h after symptom onset (Fig. 12.2)

Case 3: A 64-year-old male with acute hemiparesis and aphasia (Fig. 12.3)

Case 4: A 55-year-old man progressed to basilar occlusion over 18 h (Fig. 12.4)

Table 12.1 Summary of the evidence

IV thrombolysis	Safe and efficacious up to 4.5 h in anterior circulation	Strong evidence
IA thrombolysis	Option for treatment in MCA stroke up to 6 h in patients not candidates for IV treatment. Requires experienced center	Strong evidence
Mechanical intervention: Merci/Penumbra	Reasonable option <8 h, however outcomes date lacking	Moderate evidence
		Insufficient evidence
Endovascular treatment in posterior circulation stroke	Case series and anecdotal data with some conflicting results	Limited evidence
Endovascular treatment in children	Case series and anecdotal data	Insufficient evidence
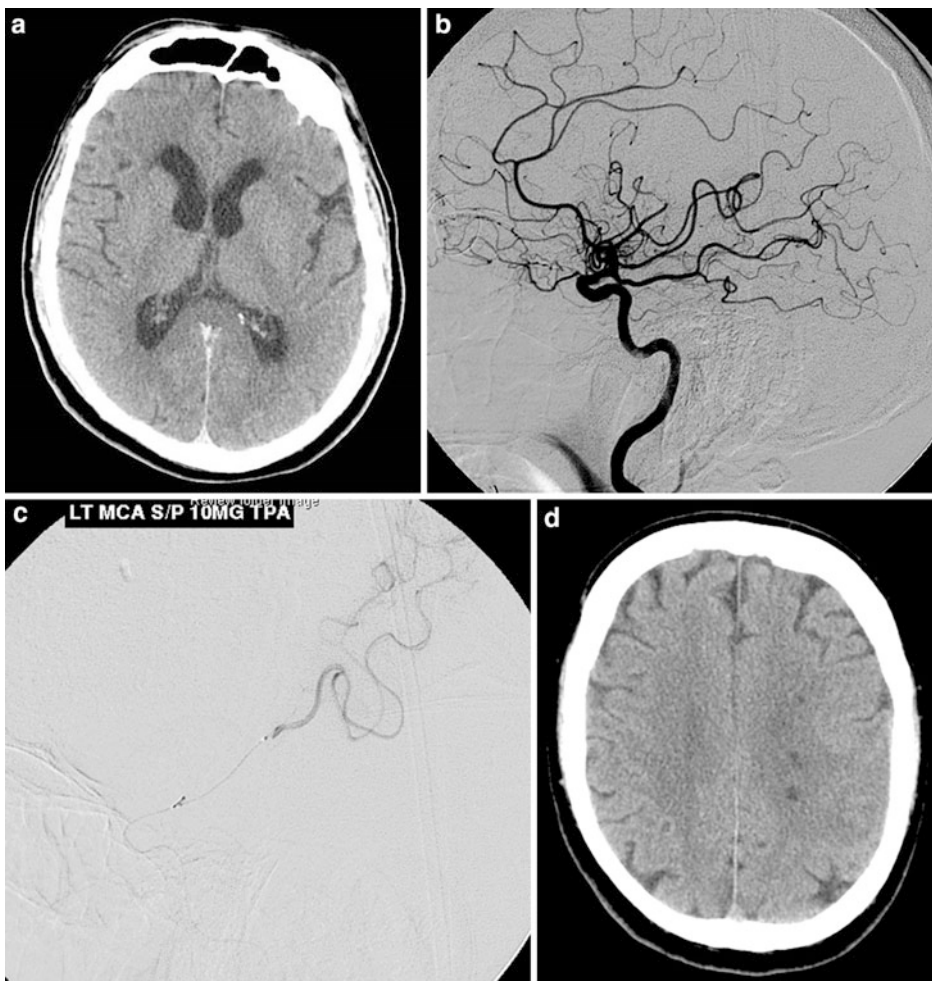
Fig. 12.1 (**a–d**) A 67-year-old man 4 h after acute onset aphasia/right hemiparesis. (**a**) Non-contrast head CT shows dense M2 branch. (**b**) Lateral view from left ICA angiogram shows occlusion at M2 branch point. (**c**) Lateral view from microcatheter injection at occlusion site following IA administration of 10 mg tPA. One of the two branches has been recanalized. (**d**) CT next day shows infarct limited to anterior parietal region. Patient regained full language and nearly normal strength
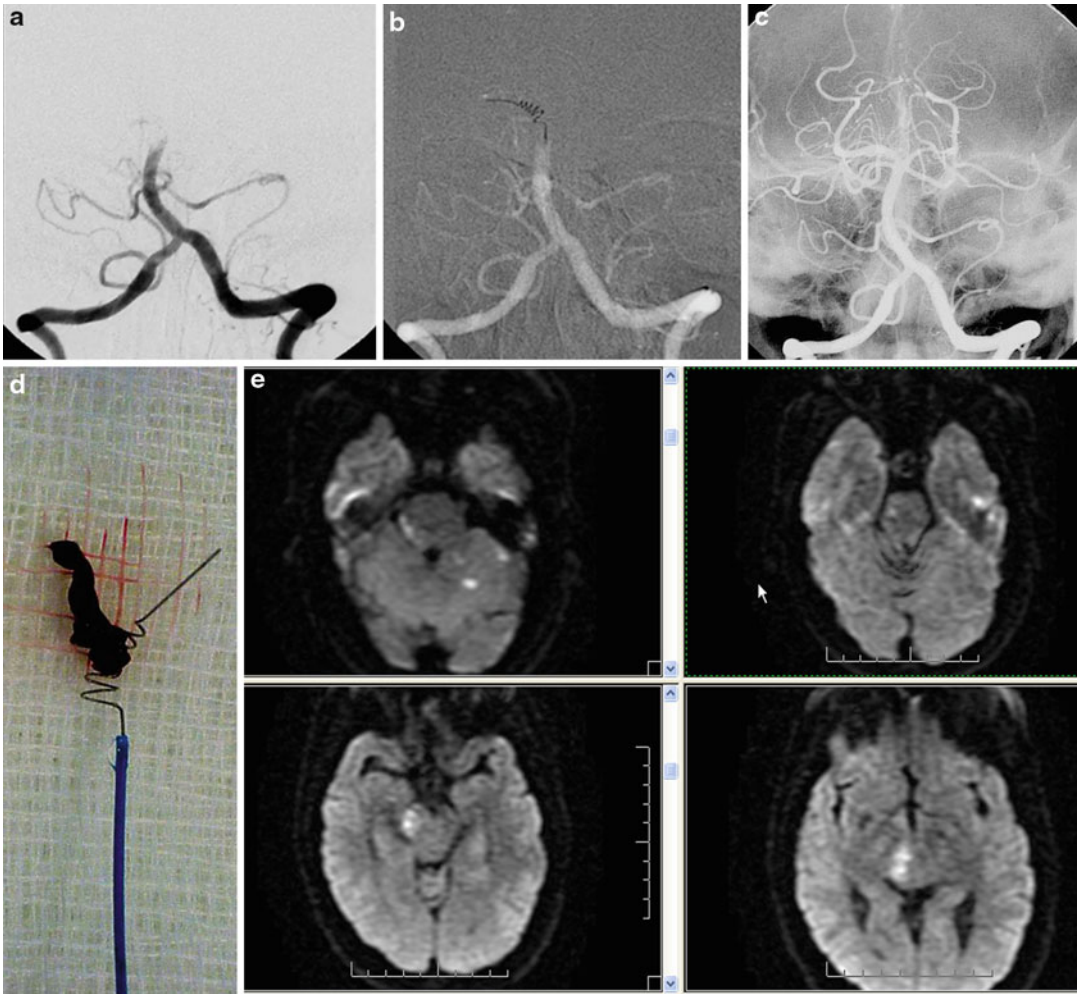
Fig. 12.2 (**a–e**) A 56-year-old woman with basilar occlusion diagnosed 12 h after symptom onset. (**a**) Left vertebral angiogram proves occlusion suspected on CT. (**b**) Merci retrieval device deployed in P1 segment right PCA as clot is being engaged prior to withdrawal. (**c**) Recanalization basilar achieved after 6 passes with retrieval device. (**d**) Clot after retriever, still on Merci device. (**e**) Several images from posttreatment diffusion MRI show limited infarction
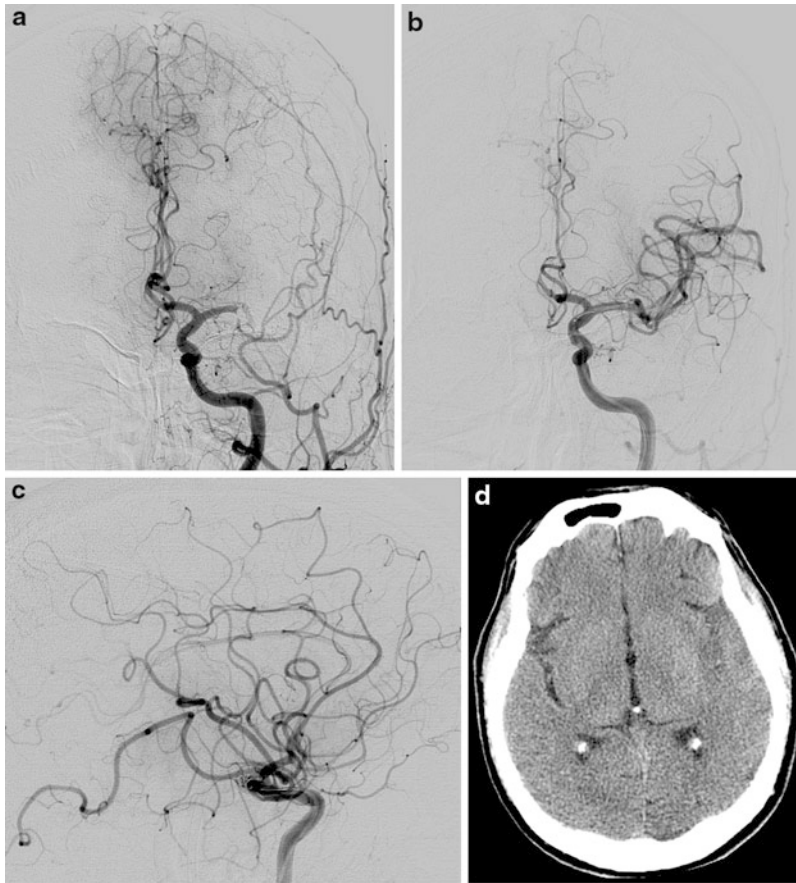
Fig. 12.3 (**a–d**) A 64-year-old male with acute hemiparesis and aphasia. Received IV tPA at 2 h following symptom onset. Transferred for intervention. (**a**) M1 MCA occlusion persists at 4 h despite IV tPA. (**b**) Following initial pass with Penumbra device, M1 has been recanalized but significant flow compromise in M2 parietal branch persists. (**c**) Lateral view shows occlusion of parietal MCA M2 trunk. (**d**) After Penumbra device employed to recanalize the M2, patient was left with only an insular ribbon infarct
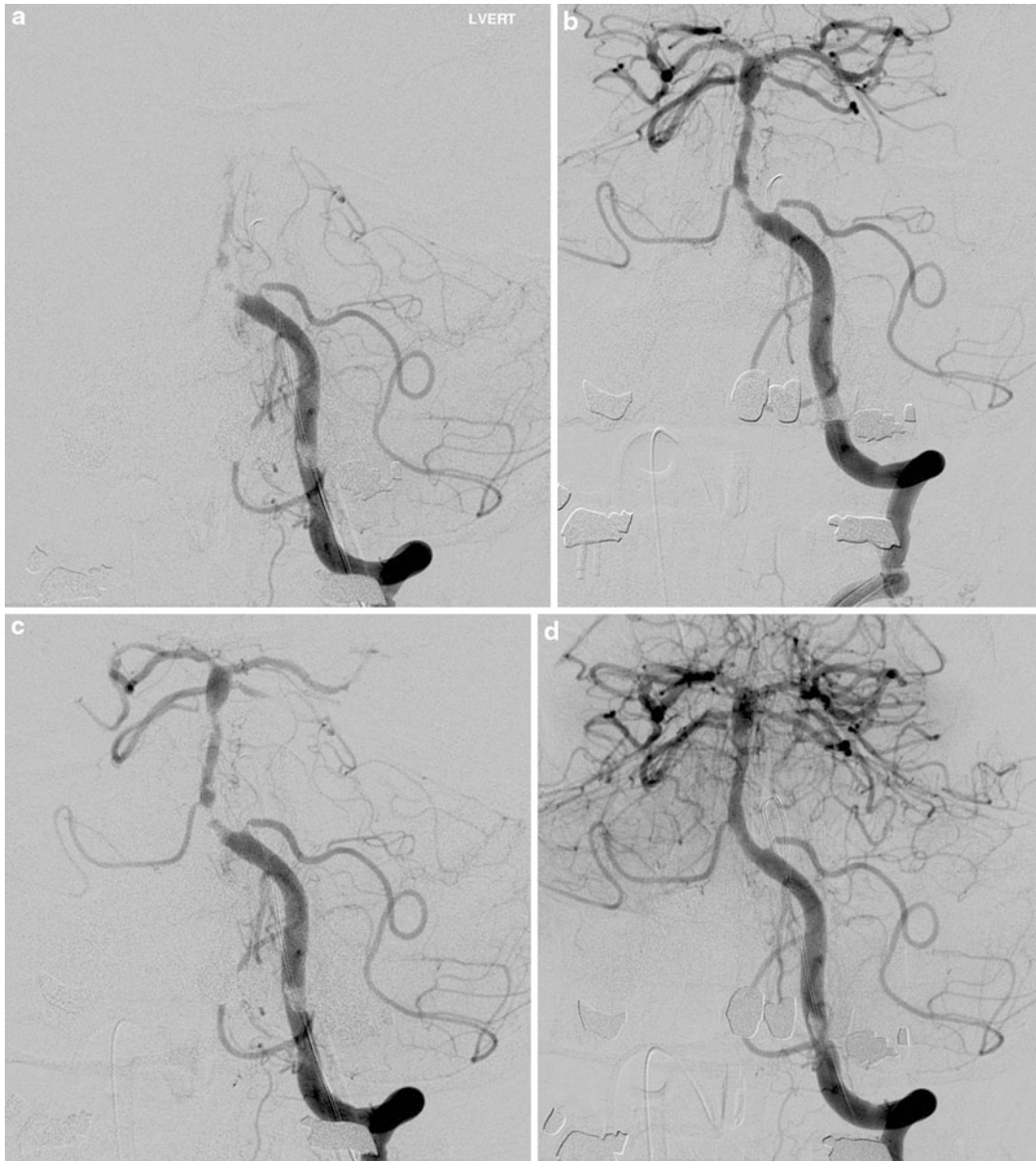
Fig. 12.4 (**a–d**) A 55-year-old man progressed to basilar occlusion over 18 h, locked-in. (**a**) Basilar occlusion beginning at vertebrobasilar junction. (**b**) Following initial pass with Penumbra 041 reperfusion catheter, recanalization achieved but stenosis, most notable in proximal basilar, persists. (**c**) Delayed angiographic run following several minutes discloses progressive narrowing of stenosis, judged to progress to occlusion without further intervention. (**d**) Stenosis treated with balloon angioplasty followed by deployment of Wingspan stent. Left vertebral angiogram shows full and stable reconstitution of flow. Patient experienced excellent outcome with minimal residual deficit

Suggested Protocol for Acute Ischemic Stroke Treatment

- Patient arrival in ER with acute neurologic deficit
- Immediate neurology consult
- CT scanner cleared
- STAT blood draw
- Short history and physical exam – critical elements are as follows:
    - Time of onset
    - Quantify deficit – NIHSS
- Electrocardiogram
- STAT to CT:
    - Non-con head CT to start – decision to proceed with CTA made in scanner
    - Alert pharmacy if tPA may be needed
- CT scan reviewed immediately by qualified physician
- If acute ICH (subarachnoid or parenchymal), then not ischemic stroke intervention candidate, consult neurosurgery
- If no acute ICH:
- And symptom onset less than 4 h, then IV tPA candidate
    - Review inclusion/exclusion criteria
    - Call pharmacy
    - Obtain consent
- If symptom onset between 4 and 7 h and CTA shows vessel occlusion amenable to IA access, then IA treatment candidate
- Notify:
    - NeuroIR
    - Angiography lab
- Review inclusion/exclusion criteria
- Obtain consent
- Transfer to angiography lab

Future Research

As the preceding discussion demonstrates, strong direct evidence proving efficacy of mechanical embolectomy in acute stroke intervention is lacking. A series of obstacles threaten to deter efforts to directly study efficacy. First, at dedicated stroke centers in the USA, mechanical intervention is commonly used and to many experts effective in the appropriately selected patient. Hence, it is difficult to withhold from a patient meeting criteria. Beyond this, the cost of such studies would be very high and given the variety of the disease process requires large patient enrollment. Acquiring truly informed consent from family in dire circumstances represents a major challenge and is often elusive. Finally, noting the ongoing development of new and seemingly more effective devices, any thorough study would be outdated by its completion.

The best support for mechanical thrombectomy derives from the consistently observed high rate of recanalization. As previously discussed, recanalization serves as a reasonable surrogate for treatment success. Future studies will likely focus on comparing different mechanical intervention devices based on recanalization efficacy and safety in a manner similar to the ongoing SWIFT study.

References

1. Barone FC, Feuerstein GZ. J Cereb Blood Flow Metab. 1999;19(8):819–34.
2. Broderick J, et al. Stroke. 1998;29(2):415–21.
3. Putaala J, et al. Stroke. 2009;40(4):1195–203.
4. Broderick J, et al. J Child Neurol. 1993;8(3):250–5.
5. Giroud M, et al. J Clin Epidemiol. 1995;48(11):1343–8.
6. Lynch JK, et al. Pediatrics. 2002;109(1):116–23.
7. de Veber GA, et al. J Child Neurol. 2000;15(5):316–24.
8. Pavlovic J, et al. Neuropediatrics. 2006;37(01):13,19.
9. The National Institute of Neurological Disorders and Stroke rt-PA Stroke Study Group. N Engl J Med. 1995;333(24):1581–8.
10. Lansberg MG, Bluhmki E, Thijs VN. Stroke. 2009;40(7). doi:2438.
11. Patel SC, et al. J Am Med Assoc. 2001;286(22):2830–8.
12. Adams HP, et al. Circulation. 1996;94(5):1167–74.
13. Hacke W, Kaste M, Hacke W, Kaste M, et al. J Am Med Assoc. 1995;274(13):1017–25.
14. Steiner T, Bluhmki E, Kaste M, Toni D, Trouillas P, von Kummer R, Hacke W. Cerebrovasc Dis. 1998;8(4):198–203.
15. Hacke W, et al. Lancet. 1998;352(9136):1245–51.
16. Clark WM, et al. J Am Med Assoc. 1999;282(21):2019–26.
17. Hacke W, ATLANTIS Trials Investigators; ECASS Trials Investigators; NINDS rt-PA Study Group Investigators, et al. Lancet. 2004;363(9411):768–74.
18. Hacke W, et al. N Engl J Med. 2008;359(13):1317–29.

19. Wahlgren N, et al. Lancet. 2008;372(9646):1303–9.
20. Topakian R, et al. Eur J Neurol. 2011;18(2):306–11.
21. Ahmed N, et al. Lancet Neurol. 2010;9(9):866–74.
22. Furlan A, et al. J Am Med Assoc. 1999; 282(21):003–2011.
23. del Zoppo G, et al. Stroke. 1988;19(3):307–13.
24. Barnwell SL, et al. AJNR Am J Neuroradiol. 1994;15(10):1817–22.
25. Barr JD, et al. J Vasc Interv Radiol. 1994;5(5):705–13.
26. Becker K, et al. AJNR Am J Neuroradiol. 1996;17(2):255–62.
27. Brandt T, et al. Stroke. 1996;27(5):875–81.
28. Hacke W, et al. Stroke. 1988;19(10):1216–22.
29. Jansen O, et al. AJNR Am J Neuroradiol. 1995;16(10):1977–86.
30. del Zoppo GJ, et al. Stroke. 1998;29(1):4–11.
31. Marler JR, et al. Neurology. 2000;55(11):1649–55.
32. Inoue T, Kimura K, Minematsu K, Yamaguchi T, Inoue T, Kimura K, Minematsu K, Yamaguchi T. Cerebrovasc Dis. 2005;19:225–8.
33. Ogawa A, et al. Stroke. 2007;38(10):2633–9.
34. Demchuk AM TD, Hill MD, Kasner SE, Hanson S, Grond M, Levine SR, The Multicentre tPA Stroke Survey Group. Neurology. 2001;57(3):474–80.
35. Zivin JA, Fisher M, et al. Science. 1985;230(4731):1289–92.
36. del Zoppo GJ, Poeck K. Ann Neurol. 1992; 32(1):78–86.
37. Sekoranja L, et al. Stroke. 2006;37(7):1805–9.
38. Tomsick T, et al. AJNR Am J Neuroradiol. 1996;17(1):79–85.
39. Agarwal P, Kumar S, Hariharan S, Eshkar N, Verro P, Cohen B, Sen S. Cerebrovasc Dis. 2004;17(2–3):182–90.
40. Wolpert SM, et al. AJNR Am J Neuroradiol. 1993;14(1):3–13.
41. Rha J-H, Saver JL. Stroke. 2007;38(3):967–73.
42. Qureshi AI. Lancet. 2004;363(9411):804–13.
43. The NINDS t-PA Stroke Study Group. Generalized efficacy of t-PA for acute stroke. Subgroup analysis of the NINDS t-PA Stroke Trial. Stroke. 1997;28(11): 2119–25.
44. Chalela JA, et al. Stroke. 2001;32(6):1365–9.
45. Ducrocq X, Bracard S, Taillandier L, Anxionnat R, Lacour JC, Guillemin F, Debouverie M, Bollaert PE. J Neuroradiol. 2005;32(1):26–32.
46. Mattle HP, et al. Stroke. 2008;39(2):379–83.
47. Investigators, T.I.S. Stroke. 2004;35(4):904–11.
48. Investigators, T.I.I.T. Stroke. 2007;38(7):2127–35.
49. Mazighi M, et al. Lancet Neurol. 2009;8(9):802–9.
50. Investigators, T.P.P.S.T. The Penumbra Pivotal Stroke Trial. Stroke. 2009;40(8):2761–8.
51. Smith WS, et al. Stroke. 2008;39(4):1205–12.
52. Smith WS, et al. Stroke. 2005;36(7):1432–8.
53. Nogueira RG, et al. AJNR Am J Neuroradiol. 2009;30(5):859–75.
54. Nesbit GM, Luh G, Tien R, Barnwell SL. J Vasc Interv Radiol. 2004;15(1):S103–10.
55. Smith WS, Smith WS, Multi MERCI Investigators. AJNR Am J Neuroradiol. 2006;27(6):1177–82.
56. Bose A, et al. AJNR Am J Neuroradiol. 2008;29(7):1409–13.
57. Cohen JE, et al. Stroke. 2003;34(12):e254–7.
58. Nedeltchev K, et al. Radiology. 2005;237(3):1029–37.
59. Jovin TG, et al. Stroke. 2005;36(11):2426–30.
60. Gupta R, et al. Urgent endovascular revascularization for symptomatic intracranial atherosclerotic stenosis. Neurology. 2003;61(12):1729–35.
61. du Mesnil de Rochemont R, et al. Neuroradiology. 2004;46(7):583–6.
62. Brekenfeld C, Remonda L, et al. Neurol Res. 2005;27:29–35.
63. Castaño C, et al. Stroke. 2010;41(8):1836–40.
64. Kirton A, et al. Pediatrics. 2003;112(3):e248–51.
65. Lin DDM, et al. AJNR Am J Neuroradiol. 2003;24(9):1827–33.
66. Macleod MR DS, et al. Cerebrovasc Dis. 2005;20:12–7.
67. Lindsberg PJ, Lindsberg PJ, Mattle HP, Mattle HP. Stroke. 2006;37(3):922–8.
68. Schulte-Altedorneburg G, et al. Stroke. 2007;38(1):9.
69. Schonewille WJ, et al. Lancet Neurol. 2009;8(8):724–30.
70. Arnold M, et al. Stroke. 2009;40(3):801–7.
71. Janjua N, et al. Stroke. 2007;38(6):1850–4.

Brain Arteriovenous Malformations: Evidence-Based Diagnosis and Treatment

13

Daniel Cooke, Basavaraj Ghodke, Van Halbach, and William Young

Contents

D. Cooke (✉) • V. Halbach
Department of Radiology and Biomedical Imaging, University of California San Francisco, San Francisco, CA, USA
e-mail: Daniel.cooke@ucsf.edu

B. Ghodke
Department of Radiology and Neurological Surgery, University of Washington/Harborview Medical Center, Seattle, WA, USA
e-mail: bghodke@u.washington.edu

W. Young
Department of Anesthesia and Perioperative Care, University of California San Francisco, San Francisco, CA, USA
e-mail: youngW@anesthesia.ucsf.edu

Key Points

- Brain AVMs (BAVMs) are relatively rare, although the morbidity and mortality of intracranial hemorrhage associated with their rupture, the relatively young age at which many present, and the existence of effective treatments make their diagnosis and management vital to neuroradiologists.
- BAVMs have a 2–4 % average annual risk of intracranial hemorrhage (ICH), but this rate ranges from under 1 % to as high as 34 %, depending on the clinical presentation and associated imaging features [1, 2] (moderate evidence).
- Non-contrast CT and CT angiography are excellent screening methods in the initial diagnosis of a BAVM (moderate evidence).
- MR and contrast-enhanced MR angiography are excellent methods for treatment planning as well as for following BAVMs conservatively or following treatment (limited evidence).
- Catheter-based digital subtraction angiography should be performed on all newly diagnosed BAVMs providing fine angioarchitectural detail essential in prognosis and treatment planning.
- Spetzler-Martin grade I and II lesions in non-eloquent areas should be considered for microsurgical resection, while small (<30 mm) lesions involving eloquent regions should be considered for radiosurgical treatment (limited evidence).
- BAVMs require multidisciplinary evaluation for optimal management; this is especially important for Spetzler-Martin grade III lesions which often require some combination of embolization, microsurgery, and/or radiosurgical treatment (limited evidence).
- Spetzler-Martin grades IV and V lesions are complex and need case by case consideration not amenable to generalized treatment recommendations (insufficient evidence).
- Palliative embolization should be reserved to treat those patients with progressive neurological deficits and/or angiographic features associated with presumed increased risk of hemorrhage (aneurysms, venous stenosis, or high-flow AV fistulas) (insufficient evidence).
- When weighing natural history risks to treatment risks, it is important to consider that treatment risks are reported usually as disabling deficits and death, whereas natural history risk is generally considered to be the spontaneous hemorrhage rate. The sequelae of ICH in the AVM population is generally more mild than other forms of adult spontaneous ICH syndromes (roughly half, or about 40 % death or dependence) [3]. Therefore, these factors should be considered when weighing the risks and benefits of treatment (limited evidence).

Definition and Pathophysiology

An arteriovenous malformation (AVM) is a complex arteriovenous anastomosis with a discernible nidus, though lacking a true capillary bed. AVMs within the central nervous system pose a significant risk of morbidity and mortality. BAVMs have been traditionally thought to arise in utero. Although a small fraction of patients have AVMs present at birth, there is an emerging view that lesions may arise postnatally. There are no data available regarding possible inciting events that lead to a BAVM when acquired [4–7] or causes of incomplete penetrance when familial. The vast majority (>95 %) are not familial.

Epidemiology

BAVMs affect the sexes equally and present in relative equal frequency in young (less than 40 years) and old (greater than 40 years) adults peaking in the fourth or fifth decade [8, 9]. They manifest in various ways, including seizure (13–69 %), headache (7–48 %), or other progressive neurological deficits (5–15 %), although most commonly (30–82 %) as intracerebral hemorrhage (ICH) [1, 5, 9–16]. They are relatively rare with an estimated prevalence of 10–18 per

100,000 people and an incidence of approximately 1.0–1.5 per 100,000 people per year [5, 8, 9, 11, 12, 14, 15, 17, 18]. They represent approximately 1 % of stroke, although they are the most common etiology of nontraumatic ICH in young adults and pediatric stroke [5, 11]. The annual incidence of BAVM-related ICH varies widely depending on multiple factors including prior ICH, BAVM size, the presence of associated aneurysms, deep venous flow, obstructed venous outflow, and evidence of higher intranidal resistance [5, 12, 15, 16, 19–26]; the range of the annual rate extends from below 1 % to as high as 34 % (moderate evidence, Table 13.4). Care must be taken in not applying the average rate to a given patient in estimating the risks and benefits of treatment.

Overall Cost to Society

Epidemiology

Miller et al. prospectively studied the societal cost of brain vascular malformations over a 3-year interval as part of the Scottish Intracranial Vascular Malformation Study [27]. They found an average 3-year healthcare cost/adult of £15,784 ($32,041 in 2010 US dollars) and an average 3-year productivity loss of £17,111($34,734 in 2010 US dollars) [27]. Stratification of variables revealed higher costs for those patients <65 years of age, those presenting with hemorrhage, and those undergoing any method of intervention. Sub-selection of treatment modalities demonstrated combined methods (embolization and radiosurgery > embolization and microsurgery) were more costly than any individual method (radiosurgery > microsurgery > embolization). However, this population-based study in Scotland probably greatly underestimates costs in the USA.

Imaging

Jordan et al. retrospectively reviewed 882 patients over a 2.5-year period who had

a non-focal neurological exam and underwent CT [28]. Of these, 31.8 % had an abnormal finding on CT, although only 1 % demonstrated a result that required change in management. The authors noted an incremental cost per clinically significant case of $50,078 ($54,165 in 2010 US dollars). Jordan et al. retrospectively reviewed 328 patients over a 3-year period who had a non-focal neurological exam and underwent MR [29]. Of these, 50 % had an abnormal finding on MR, although only 1.5 % demonstrated a result that required change in management. The authors noted an incremental cost per clinically significant case of $34,535 ($46,199 in 2010 US dollars). There is no supportive literature describing the economic burden related to the differential use of cross-sectional imaging (MR or CT) or digital substation angiography in the management of brain AVMs.

Treatment

There is no level I or II level data describing cost analysis between treatment modalities, although there are two retrospective studies examining the topic. Berman et al. retrospectively studied the cost of microsurgery with or without preoperative embolization noting a combination therapy cost of $78,400 ($104,880 in 2010 US dollars) and $49,300 ($65,951 in 2010 US dollars), although without significant differences in length of hospital stay [30]. Their report also revealed incremental increase in cost with higher Spetzler-Martin scores [30]. Patients ranged in preoperative risk category from Spetzler-Martin grades II through V, with an average increase of $20,100 in total cost per Spetzler-Martin grade (95 % CI, $13,500–$28,100). After surgical resection of an AVM, new neurologic deficits were associated with large differences in cost: $68,500 ± $6,100 and 15 ± 2 days in hospital for patients who were neurologically worse after surgery versus $44,700 ± $3,900 and ± 1 day for patients who were unchanged.

Jordan et al. also retrospectively studied the cost of microsurgery with or without preoperative embolization examining both direct and indirect

costs, noting combination therapy cost of $71,366 ($110,917 in 2010 US dollars) and surgery alone of $78,506 ($122,014 in 2010 US dollars) [31]. It should, however, be noted that surgical control data ranged from 1961 to 1988 and healthcare-related costs were based on institutional estimates as opposed to billing information generated by each case [31]. There is no supportive literature describing the economic burden related to the differential use of embolic agents in the management of brain AVMs.

Goals of Imaging

Given that the majority of BAVMs present with hemorrhage, non-contrast CT and CTA in combination offer a high degree of sensitivity and specificity in identifying lesions (moderate evidence). MR and MRA are also helpful during the initial workup particularly in defining temporal flow features with more recent contrast-enhanced techniques (limited evidence). Catheter angiography remains the gold standard, and all patients should undergo DSA prior to treatment. Assessment of the AVM size, location, and pattern of venous drainage is paramount in evaluating potential operative risk.

Methodology

A Medline pubmed.gov search using the terms "brain," "arteriovenous malformation or AVM," and "prospective or retrospective" was performed. The three searches were combined with "and" between each individual search with results limited to "human" and "English" subcategories; 737 citations were found meeting the aforementioned criteria ranging from 1965 to February 2011. The abstracts were reviewed and 127 articles are selected given their applicability to the following aspects of brain AVMs: diagnostic imaging, economic burden, natural history, treatment, and pediatrics.

Discussion of Issues

Who Should Undergo Imaging for Workup of a Potential BAVM?

Summary
BAVMs manifest in various ways, including seizure (13–69 %), headache (7–48 %), or other progressive neurological deficits (5–15 %), although most commonly (30–82 %) as intracerebral hemorrhage (ICH) [1, 5, 9–16]. In the setting of a new onset headache (within the last 12 months) without seizure, progressive, or new focal neurological deficit, an initial non-contrast head CT is recommended (limited evidence). Based on the findings of the initial exam, a combination of cross-sectional imaging, be it CT or MR, angiography is recommended.

Supporting Evidence
There is no strong evidence (level 1) to support cross-sectional imaging in the setting of new headache without focal neurological findings or seizures in the nontraumatic setting. Given the scarcity of BAVMs, there is little data describing the rate of detection of BAVMs in setting of headache within outpatient and emergency department (ED) settings. In light of such limitations, data describing the use of cross-sectional imaging (most often CT) in the settings of new headache (within the last 12 months) will have to suffice (please see Chap. 24, "Headache Disorders: Evidence-Based Neuroimaging"). Outpatient and emergency use of CT in the setting of trauma or for seizure or other focal neurological deficit is supported [32–34]. These clinical scenarios, however, make up the minority of indications for imaging, the most common being nontraumatic headache. Over 10 million patients per year are seen by ED and primary care (PC) physicians for headache [32]. As part of ED visits, headache is the second leading indication for CT (7.5 % of all visits), and CT is performed in more than 35 % of patients presenting with a chief complaint of headache [35]. The majority (∼90 %) of these will have a primary etiology, namely, migraine, tension, or cluster types, with the remaining 10 % composed

of secondary causes, one of which is BAVM. Prospective and retrospective series have documented rates of intracranial pathology, as detected by CT, altering management in 10–33 % of patients presenting with new onset headache [36–38]. Again, of these disease states, BAVMs will be a rare cause. Please see Chap. 24, "Headache Disorders: Evidence-Based Neuroimaging" section "adults."

Applicability to Children

BAVMs in the pediatric population may have comparable presentations to the adult population, although in the neonatal setting, large arteriovenous shunts may lead to cardiac failure. Even more so than in adults, hemorrhage is the primary presentation of an AVM [12]. Fullerton et al. in a retrospective analysis of more than 1200 patients, did however, find a reduced risk of subsequent hemorrhage following initial hemorrhagic ictus relative to an adult population [39]. The higher incidence of hemorrhagic presentation in children may be in part secondary to reduced rates of imaging for other more ill-defined clinical complaints. For example, in the setting of new onset headache without focal neurological deficit, Lateef et al. retrospectively studied 364 patients aged 2–5 years of age. Following history and physical examination, only 16 patients underwent CT [40]. Ninety-four percent (15 of 16) demonstrated no abnormality, the single abnormal being a brainstem glioma. In children, history and physical exam should dictate the need for cross-sectional imaging as central nervous system space-occupying lesions tend to manifest in the physical examination [41]. See Chap. 24, "Headache Disorders: Evidence-Based Neuroimaging" section "Children."

Which Imaging Modality(s) Should Be Used?

Summary

The role of diagnostic imaging in the evaluation of BAVMs is different depending whether the clinical situation requires primary diagnosis or follow-up of a treated lesion. Given the

potentially devastating effects of ICH, much attention has been given to delineating those clinical and imaging features portending initial or recurrent hemorrhage. As described above, given that the majority of BAVMs present with hemorrhage, non-contrast CT and CTA in combination offer a high degree of sensitivity (greater than 90 %) and specificity in identifying lesions (limited evidence, Table 13.1). MR and MRA (Figs. 13.1bc, 13.4d, 13.5a–d) are also helpful during the initial workup particularly in defining temporal flow features with more recent contrast-enhanced techniques. Catheter angiography remains the gold standard, and all patients should undergo DSA prior to treatment (moderate evidence). For those patients with known untreated or partially treated BAVMs, MR and MRA are recommended with supplementation by DSA following complete obliteration or excision (limited evidence, Table 13.2). The lack of ionizing radiation, minimization of metallic artifact, and the temporal and excellent spatial resolution MR provides make it the primary tool for follow-up evaluation of BAVMs.

Supporting Evidence

Non-contrast CT has good (>90 %) sensitivity for acute (<48 h.) subarachnoid hemorrhage [42, 43] and, although limited in detecting vascular malformations, can demonstrate features, including enlarged or calcified vessels (Fig. 13.1a) along the margin of the hemorrhage or regions of increased density corresponding to the vascular nidus, suggestive of an underlying vascular anomaly [44] (limited evidence). The location of intraparenchymal hemorrhage (Figs. 13.2a and 13.3a) can also be helpful in differentiating a primary from secondary etiology where the deep cerebral and brainstem regions are more often related to primary hypertensive etiologies. Delgado Almandoz et al. [44] studied 623 patients presenting with intraparenchymal hemorrhage and used features on non-contrast CT to separate studies into low (29.4 %), indeterminate (67.6 %), and high probability (3 %, Fig. 13.1a) for underlying vascular anomaly. They found the positive predictive (84.2 %) and negative predictive (97.8 %) values for the low and high probability populations

in identifying the presence or absence of a vascular anomaly. It should be noted, however, that the majority of vascular anomalies found came from patients with indeterminate non-contrast CT findings (moderate evidence).

The presence of any vascular anomaly, as defined by catheter DSA or operative inspection, in the setting of CT-diagnosed intraparenchymal hemorrhages varies widely (14.8–52.5 %) depending largely on the cohort demographics [44]. As described above, the overwhelming majority of patients will have non-contrast CT features indeterminate for a vascular anomaly, AVM or otherwise, and should undergo cross-sectional angiography. CTA has excellent spatial resolution and is minimally invasive, fast, and readily available [45–47]. There are various reports (Table 13.1) describing the accuracy of CTA (Fig. 13.3bc) relative catheter-based DSA with high degrees of sensitivity (83.6–100 %) and of specificity (77.2–100 %) for the detection of an underlying vascular anomaly in the setting of IPH [44, 48, 49] (moderate evidence). CTA is, however, limited in that it involves ionizing radiation and is degraded by metallic streak artifacts, often encountered in patients following treatment.

Historically, once a BAVM is identified, DSA is recommended to further characterize the lesion (please see discussion of reporting standards for details). DSA, and more recently three-dimensional rotational angiography (Fig. 13.7a), is the diagnostic gold standard as it has the highest degree of spatial and temporal resolution of all diagnostic imaging modalities [12, 25, 46, 50, 51] (moderate evidence).

Applicability to Children

There is little data describing the relative utility of imaging in the diagnosis of brain AVMs within the pediatric population. Brunelle et al. described the use of CT and catheter angiography to define BAVMs with moderate specificity (77 %) [52]. Since this publication, MR and CT angiographic techniques have been developed as well as improvements to digital subtraction angiography. More recently, Koelfen et al. reviewed 67 MR exams of children with neurological

disorders, five of whom had vascular malformations [53]. The nidus and major arterial feeders were demonstrated, although definition was more difficult for larger, more complex, and hemorrhagic lesions. Despite a dearth of literature on the topic, the data describing contemporary adult imaging may be largely applicable to the pediatric population. Usage, however, should be different between adult and pediatric groups to minimize ionizing radiation, though long-term, posttreatment follow-up angiography may be useful in children as there are reports of AVM recurrence (insufficient evidence). For infants, transcranial US can also be used for larger AVMs, particularly those involving the vein of Galen [54–56].

Which Imaging Findings Should Be Reported?

Summary

Assessment of the AVM size, location, and pattern of venous drainage is paramount in evaluating potential operative risk (strong evidence).

Supporting Evidence

The Spetzler-Martin classification system (Table 13.3) enumerates these features on a five-point scale and has proved an accurate predictor of surgical risk assessment with those with lower scores (I–II) having significantly less chance (less than 3 %) of posttreatment permanent neurological deficit than those with higher scores (approximately 20 %) [5, 22, 57]. The relative prevalence of each Spetzler-Martin grade is unknown, although a multisite tertiary care center review of 1289 patients found that 55 % of patients had a lesion 30–60 mm, 55 % had deep venous drainage, and 71 % involved eloquent anatomy [11]. These figures would suggest that the majority of BAVMs are grade III or higher, although the referral bias to these centers of excellence certainly misrepresents the volume of grade I and II lesions treated in the community at large.

The largest dimension by MR and DSA in millimeters should be used for Spetzler-Martin grading, although assessment in three orthogonal

dimensions and volume estimated using the ABC/2 formula is also recommended [25]. Eloquence should be determined using physiological imaging or neuropsychological testing, although by anatomic criteria, the Joint Writing Group on AVM report standards lists the sensorimotor (Figs. 13.1, 13.2, 13.3, 13.8), visual, and language cortices (Fig. 13.6), basal ganglia, thalamus (Fig. 13.5), hypothalamus, brain stem, cerebellar peduncle (Fig. 13.4), internal capsule, and deep cerebellar nuclei (Fig. 13.7) as being eloquent regions [22, 25]. Spetzler and Martin dichotomize venous drainage into superficial or deep patterns (Fig. 13.3f). When evaluating BAVMs, however, the specific drainage patterns, including number of veins, presence of subependymal venous involvement, and number of veins reaching a sinus, should be reported to better assess management risk [12, 25]. Features such as venous ectasia (Fig.13.1c), venous reflux or occlusion, flow-related or nidal arterial aneurysms (Fig. 13.7a), angiopathy, angiogenesis, or pial-pial collaterals (Fig. 13.1f) are not part of standard reporting, although recommended given their potential prognostic significance [1, 12, 16, 25]. Associated aneurysms occur in 3–58 % of patients and may be remote or intranidal in location, with the latter type being associated with a higher annual rate of ICH [5], as entities with their own inherent rupture risk (insufficient evidence). Given their flow-related nature, following treatment, remote aneurysms may involute without directed therapy [58] (insufficient evidence).

Recently, a supplementary scoring system to the Spetzler-Martin scale was proposed [59]. This supplementary score considers unruptured (Fig. 13.3c) presentation as a risk factor for poorer outcome after resection, along with age, and diffuseness of the AVM border. Not segregating surgical outcomes stratified by rupture status has been problematic in the literature [60].

Applicability to Children

The angiographic architectural findings pertinent in the adult setting are similar to those in the pediatric setting.

Which Treatment Modality(s) Should Be Employed?

Summary

The most recent statement from a writing group of the American Stroke Association [12] supported a collaborative approach to BAVM treatment with the method(s) based on the patient's age, clinical presentation, angiographic features, and of course the Spetzler-Martin classification. For those lesions less than 30 mm located in non-eloquent cortex, microsurgical resection with or without adjuvant embolization is recommended, while those similarly sized lesions situated in eloquent locations or with complex arterial anatomy should undergo radiosurgical treatment (Fig. 13.4) (moderate evidence, Table 13.4). Larger, more complex lesions (Spetzler-Martin grade IV and V) likely necessitate a combination of treatments (Figs. 13.1, 13.5) and require a case-specific approach. In many instances, such lesions should be managed conservatively unless deleterious clinical symptoms require treatment (limited evidence, Table 13.4). High treatment risk patients and low natural history risk patients should be considered for conservative medical management; given the progress that continues to be made in vascular biology of the disease and treatment modalities, the risks and benefits may change appreciably in the next decade with the introduction of new therapies.

Supporting Evidence

To date, there is no level I evidence (strong) comparing interventional modalities relative to one another or against observational management. A major decision point in the BAVM treatment algorithm is if the patient has or has not had a hemorrhage. The literature, retrospective in nature, supports intervention for those with a hemorrhagic history given the higher frequency of repeated events, especially within the first year after ictus. The nonhemorrhagic population, however, has proved more controversial. There are a few series examining outcomes between patients undergoing intervention (surgical, radiosurgical, and/or embolization) relative

medical treatment in the nonhemorrhagic cohort [15, 61–63]. These series do, however, note better clinical outcomes in the conservatively managed group relative to those undergoing intervention in the short follow-up interval [15, 61–63] (moderate evidence). To help further address this controversy, the ongoing NINDS-funded prospective randomized trial, *A Randomized Trial of Unruptured Brain Arteriovenous Malformations* (ARUBA), began recruiting in 2007 (NCT00389181). Patients with BAVMs that have not bled and are thought suitable for therapeutic intervention are eligible and randomized to best medical therapy (conservative management) or the standard interventional treatment prescription as decided upon by the local treatment team [64]. The study will provide follow-up for a minimum of 5 years. Through February 2011, ARUBA has enrolled 144 of the targeted 400 patients.

Following complete clinical and imaging evaluation, treatment recommendations are based on the expected hemorrhagic risk of the lesion and availability of treatment regimens. Lifetime hemorrhagic risk can be roughly estimated using the equation [12, 17]

$$\text{Lifetime risk}(\%) = 105 - \text{age (years)}$$

Weighing these risks guides conservative observational management against microsurgery, trans-arterial embolization, and radiosurgery whether as solitary or combined methods. Depending on the clinical presentation, estimates of 20-year cumulative risk of hemorrhage range 43–56 % [65]. Operative risk has been assessed using a number of different grading schemes, although the Spetzler-Martin classification system is most commonly employed. The relative simplicity and reproducibility in both retrospective and prospective studies to assess operative risk make the grading system widely implemented. Unfortunately, there is a lack of level I (strong evidence) data describing their behavior. To date, there are no prospective randomized controlled trials looking at the efficacies of these treatments relative to each other or to nonintervention. Retrospective analysis of

multiple large cohorts suggests an overall treatment-related complication rate of 14–20 % with 6–8 % manifesting a permanent neurological deficit and 0.5–1.5 % resulting in death [5] (limited evidence).

The primary goal of BAVM intervention is to obliterate the vascular nidus and remove the risk of spontaneous ICH. This can be accomplished a number of ways, although surgical excision remains the primary method for the majority of lesions. For Spetzler-Martin grade I and II BAVMs, surgical excision is recommended with literature demonstrating good to excellent outcomes in 92–100 % of patients [12] (moderate evidence). Grade III lesions (Figs. 13.3, 13.7, 13.8) should also be treated surgically with 88.2 % demonstrating excellent long-term outcome, although given the greater heterogeneity of this group, multidisciplinary evaluation should be done prior to elective removal [5, 12, 22, 57] (limited evidence). Grades IV and V (Figs. 13.1, 13.5) more often necessitate multiple forms of treatment working in combination to minimize hemorrhagic risk and to reduce morbidity related to open surgery. These lesions carry higher rates of periprocedural morbidity (31 % IV; 50 % V) as well as permanent neurological deficits (30 % IV; 17 % V) [12, 22] (limited evidence).

The role for trans-arterial embolization of BAVMs has greatly expanded over the past twenty years with the method now routinely employed. Embolization is used as the definitive treatment modality (Fig. 13.9) for a minority of cases (9–49 %) with the overwhelming majority being performed as neo-adjunctive intervention for both microsurgical and radiosurgical treatment (Figs. 13.8, 13.9) [5, 12, 66] (insufficient evidence). In the setting where embolization is curative, lesions are more often less than 30 mm and have fewer arterial feeders (Fig. 13.9) [66]. Endovascular therapy is also used in a palliative manner for those patients with lesions not amenable to other forms of treatment with progressive neurological deficits or refractory seizures. In these instances, the goal of intervention is to minimize hemorrhagic risk (embolization to minimize venous hypertension or treat associated aneurysms) or to reduce the nidal volume to a size more

amenable to open or radiosurgical techniques [12, 66] (insufficient evidence). There is literature supporting embolization for partial occlusion of BAVMs, although there is also evidence of a higher rate of hemorrhage in those undergoing such incomplete treatment [66]. Embolization is a safe technique with an overall complication rate of 9–14 % and permanent neurological deficits reported in 2–10 % of cases and mortality rates less than 4 % [5, 12, 66, 67] (limited evidence).

As with microsurgical resection, the purpose of radiosurgery is obliteration of the vascular nidus. Focused external beam radiation of the BAVM nidus induces endothelial injury and eventual thrombosis [65]. The technique is more successful for those lesions smaller than 30 mm in greatest dimension or less than 10 cm^3 and more often employed for lesions with eloquent locale [5, 12] (limited evidence). The risks of radiosurgery, although certainly less in the immediate post-procedural period relative to embolization or microsurgery, accrue over the 2–3-year interval expected for a nidus to involute. There is the potential for radiation-related edema and necrosis (5–7 %) as well as the risk for hemorrhage, although there is controversy regarding the incidence of bleeding [5, 12, 65]. Overall radiosurgery is effective in 80–88 % of patients at 2 years post initial treatment [12] (limited evidence).

Applicability to Children
As with the adult population, there are multiple series describing embolization, microsurgical, and radiosurgical treatment options in singular and combined use, although no level I or II level (strong or moderate evidence) data exists. The largest of the series reported morbidity and mortality rates of 18 % and 11 % for surgery and 28 % and 16 % for embolization, respectively [68, 69]. Yen et al. reported the largest (186 patients) radiosurgical series noting a hemorrhage rate of 5.4 % within 2 years after treatment and 0.8 % between 2 and 5 years and only six patients manifesting neurological deficits associated with radiation-induced injury [70].

Which Embolic Material(s) Should Be Used in Endovascular Treatment?

Summary
BAVM embolization is routinely performed primarily as a neo-adjunct treatment to microsurgery or radiosurgery with evidence demonstrating the efficacy of particles, n-butyl cyanoacrylate (n-BCA) (Fig. 13.8cd), and now Onyx relative to one another in regard to angiographic nidal embolization (moderate evidence). Despite these prospective trials, there are no societal guidelines regarding which material(s) to use in the treatment of BAVM, be it neo-adjunctive, palliative, or curative in nature. Choice of embolic agent(s) remains operator specific with single or multiple materials used depending on the clinical scenario and angio-architecture.

Supporting Evidence
The aim of any intervention is to reduce the AVM nidus and occlude those vessels more difficult to access with open surgical methods. Paramount to successful nidal obliteration is peri-nidal access of its primary feeding arteries. Neurointerventional surgeons use over-the-wire catheters and softer flow-directed catheters to access individual arterial feeders for delivery of a number of different types of embolic materials. Historically, absolute alcohol (Fig. 13.9) and particle-type materials were used, such as polyvinyl alcohol (PVA), coils (Fig. 13.8cd), and detachable balloons, and are still used in specific situations (aneurysms, high-flow fistulas, protection of an en passage artery), although they have largely been replaced by liquid embolic materials in part given the ability to deliver them via smaller catheters affording more immediate peri-nidal access [5, 12, 62, 66, 67, 71–73].

n-BCA and ethylene vinyl alcohol copolymer (Onyx) have both proved effective in embolization. n-BCA rapidly polymerizes and can flow quickly [66, 67, 71] (limited evidence). Early polymerization can lead to inadequate nidal penetration, while delayed polymerization can cause nontarget venous embolization and resultant

increase in nidal pressures. Brief periods of pharmacologically induced cardiac pause with adenosine have been used help control delivery of n-BCA [37, 74]. Onyx, a more recent addition to the interventional armamentarium, is nonadherent to the endothelium, flows much slower, and provides a greater degree of control during embolization affording for greater penetration into the nidus [66, 67]. Its slower flow, however, comes at the price of longer fluoroscopic times and increased radiation exposure. Recently, a prospective trial comparing Onyx to n-BCA demonstrated no significant difference between the two materials in regard to degree of nidal embolization or technical risk [75] (moderate evidence). Both agents have demonstrated lower rates of recanalization relative to particle-type embolic materials [67, 71] (moderate evidence).

Applicability to Children

Unlike the adult population, there is no level II data discussing the utility of embolic agents relative to one another, although the data likely extrapolates to the pediatric population. However, given the longer life expectancy of children, well-conducted prospective studies are lacking in regard to the long-term effectiveness of embolic agents in this population.

Take-Home Tables

Tables 13.1 through 13.4 highlight data and evidence.

Imaging Case Studies

Case 1 Vascular calcifications and prominent flow voids (Fig. 13.1a–f).
Cases 2 and 3: Left frontal subcortical and basal ganglia hemorrhage (Figs. 13.2a–d, 13.3a–f).
Case 4: Third intraventricular hemorrhage and prominent vessels along the tectum (Fig. 13.4a–f)

Case 5: Multiple left pulvinar flow voids, an enlarged falcine sinus, and enlarged left PCA (Fig. 13.5a–g).
Case 6: Diffuse left temporal AVM nidus (Fig. 13.6a–f).
Case 7: Compact right cerebellar hemispheric AVM supplied by ipsilateral anterior-inferior and superior cerebellar arteries (Fig. 13.7a–c).
Case 8: Compact insular AVM nidus supplied by lenticulostriate and insular MCA branches (Fig. 13.8a–d).
Case 9: Compact left choroidal AVM nidus supplied by an enlarged posterior-lateral choroidal artery (Fig. 13.9a–d).

Suggested Imaging Protocols

Figures 13.10 and 13.11 show diagnostic imaging workup of nontraumatic isolated intraparenchymal hemorrhage and nontraumatic intraventricular and/or subarachnoid hemorrhage with or without intraparenchymal hemorrhage, respectively.

MRA

Due to the heterogeneity of vendors and associated imaging techniques, a standard MR protocol for brain AVMs is not available. Despite this variability, however, the authors found the imaging protocols by Petkova et al. and Hadizedah et al. helpful for contrast-enhanced MR angiography at 1.5 and 3.0 T, respectively [97–100] :

- Petkova et al. 1.5 T 3D dynamic TR-CE-MRA TRICKS ASSET Protocol: TR\TE\flip angle 3.7\1.4\25°, field of view 30 cm, acquisition matrix 320 × 192 mm, fourfold ASSET reduction factor (2 × 2), Nex 0.5, 20 overlapping partitions with partition thickness 6 mm, spatial resolution at acquisition $0.93 \times 1.56 \times 6$ mm^3 and, after interpolation, $0.58 \times 0.58 \times 3$ mm^3. Image acquisition initiated 15 s after a bolus injection of 10 ml of gadoterate meglumine administered at a rate of 1.4 ml/s followed

Table 13.1 Performance characteristics of CT and MR in evaluation of intracranial vascular pathology

Author(s)	Patients (n)	Modality	Reference standard	Pathology	Sensitivity % (95 % CI)	Specificity % (95 % CI)	PPV % (95 % CI)	NPV % (95 % CI)
White et al. (2000)[a,b] [76]	677	CTA	DSA	Cerebral aneurysm	92 [89–95]	94 [88–99]	98 [96–99]	80 [73–86]
Chappell[a] et al. (2003)[c] [77]	1197	CTA	DSA	Cerebral aneurysm	93	77	NA	NA
van Gelder et al. (2003)[a,c] [78]	616	CTA	DSA	Cerebral aneurysm	84	99	NA	NA
Wintermark et al. (2003)[b] [79]	50	CTA	DSA	Cerebral aneurysm	99 [98–100]	95 [94–96]	99	95
Dammert et al. (2004)[c] [80]	50	CTA	DSA	Cerebral aneurysm	90	83	97	56
Karamessini et al. (2004)[c] [81]	82	CTA	Surgery	Cerebral aneurysm	89 [78–96]	100	100	93 [63–84–97]
Kouskouras et al. (2004)[c] [82]	35	CTA	Surgery	Cerebral aneurysm	97	50	92	75
Hiratsuka et al. (2008)[b] [83]	38	CTA	DSA	Cerebral aneurysm	95	96	NA	NA
McKinney et al. (2008)[b] [84]	36	CTA	DSA	Cerebral aneurysm	96	90	96	90
Romijn et al. (2008)[c] [85]	88	CTA	DSA, surgery	Cerebral aneurysm	99 [93–100]	90 [69–98]	98 [92–100]	95 [74–100]
Chen et al. (2009)[c] [86]	152	CTA	DSA, surgery	Cerebral aneurysm	98 [92–100]	100 [95–100]	100 [96–100]	97[90–100]
Li et al. (2009)[c] [87]	96	CTA	DSA, surgery	Cerebral aneurysm	99	100	100	92
White et al. (2000)[a,b] [76]	926	MRA	DSA	Cerebral aneurysm	87 [84–90]	92 [88–94]	93 [90–95]	84 [80–88]
Hiratsuka et al. (2008)[b] [83]	38	MRA	DSA	Cerebral aneurysm	96	92	NA	NA
Kokkinis et al. (2008)[b] [88]	198	CTA	DSA, surgery	Cerebral aneurysm or BAVM	98	NA	100	94
Khandelwal et al. (2006)[b] [89]	50	CTV	MRV	Cerebral venous or sinus thrombosis	75–100[d]	82–100[d]	75–100[d]	90–100[d]
Linn et al. (2007)[b] [49]	19	CTV	MRV	Cerebral venous or sinus thrombosis	100	100	100	100
Kitajima et al. (2005)[b] [90]	21	CE-MR[e]	DSA	Retrograde venous drainage in DAVF	51–100[d]	82–100[d]	NA	NA
Yeung et al. (2009)[b] [91]	55	CTA	DSA	Vascular etiology of spontaneous ICH	89	92	91	91
Delgado Almandoz et al. (2009)[b] [44]	623	CTA	DSA, surgery	Vascular etiology of spontaneous IPH	96 [88–99.0]	99 [94–100]	97 [90–100]	99 [93–99]
Romero et al. (2009)[b] [92]	43	CTA	DSA, surgery	Vascular etiology of spontaneous IPH	96 [79–99]	100 [74–99]	100	94
Yoon et al. (2009)[b] [93]	78	CTA	DSA	Vascular etiology of spontaneous IPH	96	100	100	98

[a]Meta-analysis
[b]Per patient analysis
[c]Per aneurysm analysis
[d]Range describing various deep and superficial venous anatomy
[e]Contrast-enhanced MR using a 3D magnetization-prepared rapid gradient-echo (MP-RAGE) technique

Table 13.2 Agreement between MR angiography and DSA in evaluation of brain AVMs

Author	Patients (n)	Technique	Reference standard	AVM size	Venous drainage (%)	Arterial supply	Spetzler-Martin
Unlu et al. (2006) [94]	20	CE 3D FISP[a] MRA	DSA	NA	88.2	85.9 %	NA
Warren et al. (2007) [95]	40	CE 3D SLINKY[b] MRA	DSA	97.6 %	97.6	80.7 %	95.1 %
Heidenreich et al. (2007) [96]	10	3D TOF MRA	DSA	NA[f]	73, 60[g]	65 %	NA
Hadizadeh et al. (2007) [97]	18	CE 4D SENSE[c], CENTRA[d], keyhole MRA	DSA	100 %	100	NA[h]	100 %
Saleh et al. (2008) [98]	10	CE GRAPPA[e] (4X) MRA	DSA	100 %	100	100 %	100 %

[a]Fast imaging with steady precession (FISP)
[b]Sliding-slab interleaved k_y (SLINKY)
[c]Sensitivity encoding (SENSE)
[d]Randomly segmented central k-space ordering
[e]Generalized autocalibrating partially parallel acquisition (GRAPPA)
[f]MRA tended to overestimate the size of smaller AVMs and underestimate the size of larger AVMs
[g]Venous drainage: superficial, deep
[h]Selective DSA demonstrated additional small feeding arteries in 3 of 18 patients retrospectively seen on 4D MRA

Table 13.3 Spetzler-Martin AVM classification system

Characteristic	Points
SIZE	
<3 cm	1
3–6 cm	2
>6 cm	3
Location	
Eloquent	1
Non-eloquent	0
Venous drainage	
Deep	1
Superficial	0

by a 20-ml saline flush. Scan time 21 s including 5 s for the mask data obtained before the arrival of contrast with complete k-space coverage, followed by 16 phases of 0.9 s each, spaced by 50 ms. After imaging, maximum intensity projections (MIP) and mask subtraction are obtained automatically within 15 min. In this implementation of TRICKS, k-space is divided in 4 regions: A, B, C, and D, in the phase-encoding dimension.

• Hadizedah et al. 3.0 T 4D CENTRA, keyhole, and parallel imaging MRA Protocol: Eight-channel sensitivity encoding–capable head coil. A biphasic injection protocol using an automatic power injection: First, 10 ml of gadopentetate dimeglumine injected at a flow rate of 3 ml/s, followed by 10 ml gadopentetate dimeglumine at a flow rate of 1.5 ml/s and by a saline flush of 25 ml. Four-dimensional contrast-enhanced MR angiographic acquisition was initiated 10 s after the injection of contrast medium was started. To generate the T1-weighted 3D gradient-echo sequence: Repetition time msec/echo time msec, 2.2/0.9; flip angle, 15°; rectangular field of view, 100 %; slab thickness, 154 mm; image matrix, 224×178 over a 256-mm field of view; and 140 thin partitions of 1.1 mm, with voxel size of $1.1 \times 1.4 \times 1.1$ mm. Transverse T2-weighted fast spin-echo sequence (3277/80; section thickness, 5 mm; number of sections, 24).

CTA: Standard Protocol for 16- or 64-Slice Computed Tomography

Depending on the protocol, images may be prospectively processed as 1.25 mm axial sections from base of C1 to the skull vertex with the

Table 13.4 Summary of the evidence

Author	Year	Evidence	Patients	Info	PMID
Kukuk et al.	2010	II	16	DI	20065859 [136]
Patrux et al.	1994	II	54	DI	8041438 [137]
Jagadeesan et al.	2011	III	60	DI	21088245 [138]
Hartwigsen et al.	2010	III	206	DI	20657230 [139]
Iancu-Gontard et al.	2007	III	50	DI	17353328 [140]
Nagaraja et al.	2006	III	40	DI	16944119 [141]
Unlu et al.	2006	III	20	DI	16965882 [94]
Hans et al.	2005	III	12	DI	16317599 [142]
Vates et al.	2002	III	30	DI	12188939 [143]
Stapf et al.	2002	III	207	DI	11810010 [14]
Cloft et al.	1999	III		DI	9933266 [144]
Smith et al.	1998	III	15	DI	3258719 [145]
Meder et al.	1997	III	102	DI	9296188 [146]
Koelfen et al.	1995	III	13	DI	7748357 [53]
Lee et al.	1995	III	30	DI	7491188 [147]
Yan et al.	2010	IV	1	DI	20574100 [148]
Loy et al.	2009	IV		DI	19408991 [149]
Norris et al.	1999	IV	31	DI	10193612 [150]
Abe et al.	1995	IV	14	DI	7566388 [151]
Brunelle et al.	1983	IV	30	DI	6622689 [52]
Al-Shahi et al.	2009	III	229	EB	19359648 [27]
Berman et al.	1999	III	126	EB	10588135 [30]
Al-Shahi et al.	2003	II	181	NH	12702837 [9]
Al-Shahi et al.	2003	II		NH	12702840 [152]
Halim et al.	2002	II	336	NH	11872886 [153]
Gabriel et al.	2010	III	401	NH	19926839 [18]
Choi et al.	2009	III	735	NH	19729171 [154]
van Beijnum et al.	2009	III	90	NH	19042932 [3]
Cordonnier et al.	2008	III	141	NH	17488785 [155]
Hernesniemi et al.	2008	III	238	NH	19005371 [156]
Laakso et al.	2008	III	623	NH	18797354 [157]
Kim et al.	2007	III	1,464	NH	17673729 [26]
Choi et al.	2006	III	241	NH	16614321 [2]
Stapf et al.	2006	III	622	NH	16682666 [1]
Fullerton et al.	2005	III	1,219	NH	16141419 [39]
Halim et al.	2004	III	790	NH	15166396 [158]
Kim et al.	2004	III	314	NH	15157291 [58]
Stapf et al.	2003	III	284	NH	12690217 [15]
Stapf et al.	2003	III	542	NH	14576378 [159]
ApSimon et al.	2002	III	240	NH	12468772 [160]
Stefani et al.	2002	III	390	NH	11988594 [161]
Hofmeister et al.	2000	III	1,289	NH	10835449 [11]
Mast et al.	1997	III	281	NH	10213548 [23]
Kader et al.	1994	III	449	NH	7914356 [162]
Ondra et al.	1990	III	166	NH	2384776 [163]
Crawford et al.	1986	III	217	NH	3958721 [164]
Fults et al.	1984	III	131	NH	6504280 [165]

(*continued*)

Table 13.4 (continued)

Author	Year	Evidence	Patients	Info	PMID
Gerosa et al.	1981	III	56	NH	7297176 [166]
Mohr et al.	2010	I	400	TX	20634478 [64]
Wedderburn et al.	2008	II	114	TX	18243054 [61]
n-BCA Trial	2002	II	104	TX	12006271 [167]
Loh et al.	2010	II	170	TX	20433277 [75]
Hartmann et al.	2000	II	144	TX	11022064 [24]
Lawton et al.	2010	III	300	TX	20190666 [59]
van Beijnum et al.	2008	III	229	TX	18787195 [168]
Lv et al.	2010	III	141	TX	20642886 [169]
Jayaraman et al.	2008	III	192	TX	17974613 [170]
Haw et al.	2006	III	306	TX	16509496 [171]
Hartmann et al.	2002	III	233	TX	12105359 [172]
Yuki et al.	2010	III	74	TX	19835467 [173]
Andreou et al.	2008	III	25	TX	19035724 [174]
Natarajan et al.	2008	III	28	TX	18824988 [175]
Yakes et al.	1997	III	17	TX	9179886 [175]
Yu et al.	2004	III	27	TX	15313697 [176]
Debrun et al.	1997	III	54	TX	8971833 [177]
Wong et al.	1997	III	21	TX	9395814 [178]
Fournier et al.	1991	III	49	TX	2072159 [179]
Wallace et al.	1995	III	65	TX	8559287 [180]
Panagiotopoulos et al.	2009	III	82	TX	18842759 [181]
Katsaridis et al.	2008	III	101	TX	18408923 [182]
Mounayer et al.	2007	III	94	TX	17353327 [183]
Weber et al.	2007	III	47	TX	17762736 [184]
Thiex et al.	2010	III	15	TX	19749215 [185]
Sorimachi et al.	1999	III	36	TX	10472993 [186]
Perrini et al.	2004	III	14	TX	15254797 [187]
Song et al.	2000	III	70	TX	10839255 [188]
Pierot et al.	2009	III	50	TX	19223075 [189]
Mounayer et al.	2007	III	94	TX	17353327 [183]
Frenzel et al.	2008	III	12	TX	18212521 [190]
Meisel et al.	2002	III	326	TX	12376769 [191]
Rodesch et al.	1995	III	26	TX	7621485 [55]
Kondziolka et al.	1992	III	132	TX	1562906 [192]
Javalkar et al.	2009	III	15	TX	19934562 [193]
Maruyama et al.	2008	III	211	TX	19123891 [194]
Vachhrajani et al.	2008	III	973	TX	19123881 [195]
Karlsson et al.	2007	III	133	TX	17937217 [196]
Maruyama et al.	2007	III	500	TX	17327789 [197]
Inoue et al.	2006	III	114	TX	18503332 [198]
Andrade-Souza et al.	2005	III	45	TX	15617586 [199]
Schlienger et al.	2000	III	169	TX	10725623 [200]
Young et al.	1997	III	130	TX	9164684 [200]
Pica et al.	1996	III	41	TX	8844887 [201]

Table 13.4 (continued)

Author	Year	Evidence	Patients	Info	PMID
Yamamoto et al.	1996	III	40	TX	8727815 [202]
Young et al.	1995	III	66	TX	7502730 [203]
Lunsford et al.	1991	III	227	TX	1885968 [204]
Coffey et al.	1990	III	161	TX	2080380 [205]
Kiran et al.	2009	III	308	TX	19415175 [206]
Sirin et al.	2006	III	28	TX	16385325 [207]
Karlsson et al.	2005	III	28	TX	15987539 [208]
Miyawaki et al.	1999	III	73	TX	10421543 [209]
Mathis et al.	1995	III	24	TX	7726076 [210]
Dawson et al.	1990	III	7	TX	2120988 [211]
Uno et al.	2004	III	112	TX	14977057 [212]
Huh et al.	2000	III	348	TX	10942665 [213]
Deruty et al.	1996	III	67	TX	8686534 [214]
Kelly et al.	2008	III	76	TX	18518720 [215]
Yen et al.	2010	III	186	TX	21039165 [70]
Nicolato et al.	2005	III	63	TX	15654635 [216]
Baumann et al.	1996	III	27	TX	8873161 [217]
Buis et al.	2008	III	22	TX	18283398 [218]
Wara et al.	1995	III	33	TX	8584819 [219]
Sasaki et al.	1998	III	101	TX	9452237 [220]
Han et al.	2003	III	73	TX	12546345 [221]
Davidson et al.	2010	III	640	TX	20173544 [222]
Hamilton et al.	1994	III	120	TX	8121564 [223]
Post et al.	2008	III	7	TX	18401826 [224]
Nagata et al.	2006	III	33	TX	16801046 [225]
Morgan et al.	2004	III	237	TX	15046648 [226]
Lawton et al.	2003	III	174	TX	12657169 [227]
Russel et al.	2002	III	44	TX	12383355 [228]
Hartmann et al.	2005	III	119	TX	16224095 [62]
Jafar et al.	1993	III	33	TX	8416244 [229]
Richling et al.	1991	IV	21	TX	1803885 [230]
Dehdashti et al.	2010	IV	135	TX	20059323 [231]
Zuccaro et al.	2010	IV	5	TX	20658296 [232]
Weprin et al.	1996	IV	1	TX	8916155 [233]
Lanino et al.	1997	IV	13	TX	9068697 [234]
Chang et al.	1998	IV	36	TX	10235006 [235]
Koelfen et al.	1995	III	13	DI	7748357 [53]
Brunelle et al.	1983	IV	30	DI	6622689 [52]
Fullerton et al.	2005	III	1219	NH	16141419 [39]
Gerosa et al.	1981	III	56	NH	7297176 [166]
Thiex et al.	2010	III	15	TX	19749215 [185]
Rodesch et al.	1995	III	26	TX	7621485 [55]
Kondziolka et al.	1992	III	132	TX	1562906 [192]
Lasjaunias et al.	1995	III	179	TX	7758015 [69]
Humphreys et al.	1996	III	160	TX	9348147 [68]

(*continued*)

Table 13.4 (continued)

Author	Year	Evidence	Patients	Info	PMID
Yen et al.	2010	III	186	TX	21039165 [70]
Nicolato et al.	2005	III	63	TX	15654635 [216]
Baumann et al.	1996	III	27	TX	8873161 [217]
Buis et al.	2008	III	22	TX	18283398 [218]
Wara et al.	1995	III	33	TX	8584819 [219]
Zuccaro et al.	2010	IV	5	TX	20658296 [232]
Weprin et al.	1996	IV	1	TX	8916155 [233]

PMID PubMed identifier, *DI* diagnostic imaging, *EB* economic burden, *NH* natural history, *TX* treatment, *RS* radiosurgery
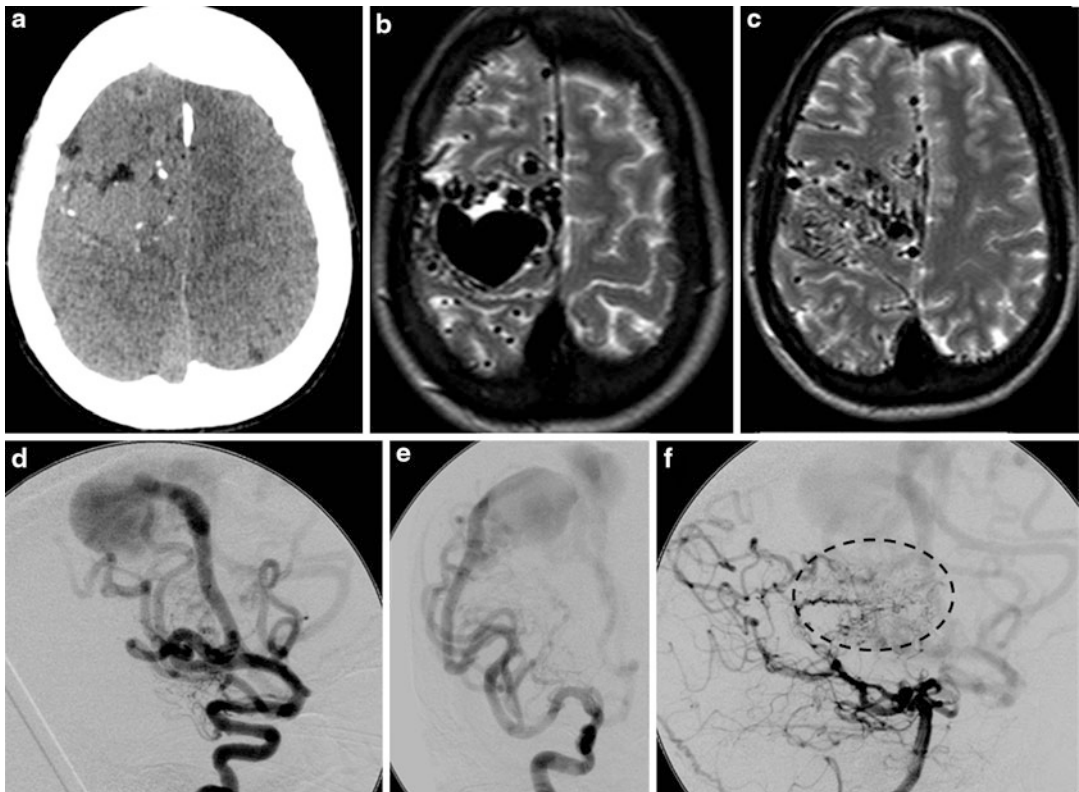

Fig.13.1 (**a–f**) Non-contrast CT (**A**) and T2-weighted MR (**b**, **c**) demonstrating vascular calcifications and prominent flow voids, respectively, associated with a venous varix. Anterior-posterior (AP) and lateral right internal carotid artery (**e**, **d**) DSA demonstrating a high-flow middle cerebral artery (MCA) arteriovenous shunt with associated venous varix. There is an adjacent diffuse AVM nidus within the insula. Lateral left vertebral artery (**f**) DSA demonstrating proliferative angiopathy (*dotted circle*) arising from medial and lateral posterior choroidal and posterior splenial arteries
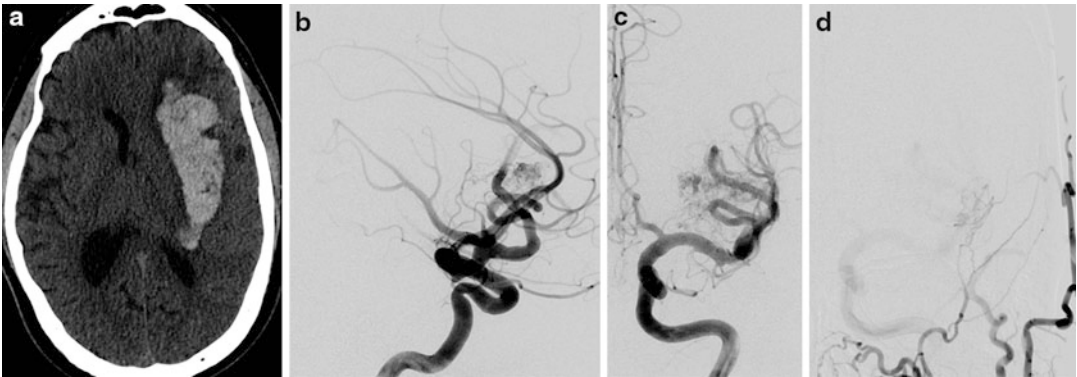
Fig. 13.2 (**a–d**) Non-contrast CT (**a**) demonstrating a left frontal subcortical and basal ganglia hemorrhage. Lateral and AP *left* internal carotid artery (**b**, **c**) DSA demonstrating a compact AVM nidus supplied by lenticulostriate and insular MCA branches. AP left external carotid artery (**d**) DSA demonstrating AVM supply by the middle meningeal artery
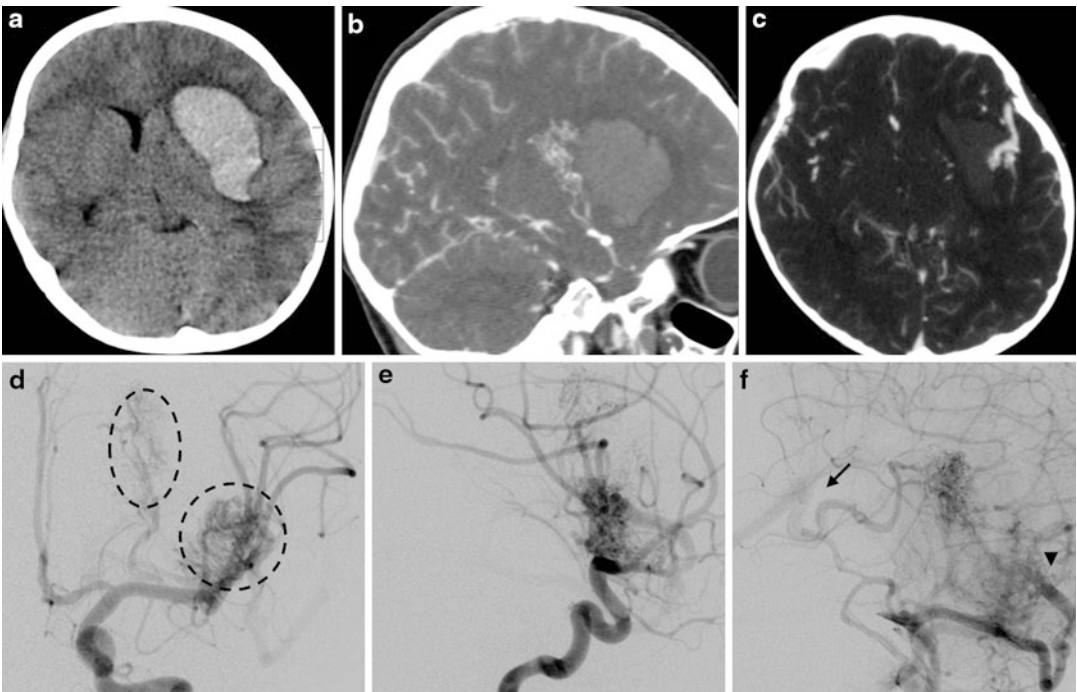

Fig. 13.3 (**a–f**) Non-contrast CT (**a**) demonstrating a left frontal subcortical and basal ganglia hemorrhage. Lateral and axial CTA (**b**, **c**) demonstrating an AVM nidus split by the hemorrhage. AP and lateral arterial phase left internal carotid artery DSA (**d**, **e**) better demonstrating the split AVM nidus (*dotted circles*) as supplied by lenticulostriate and insular MCA branches. Lateral venous phase left internal carotid artery (**f**) DSA demonstrating both superficial (*arrowhead*, superficial middle cerebral vein to the sphenoparietal sinus) and deep (*arrow*, basal vein of Rosenthal to vein of Galen to straight sinus) venous drainage
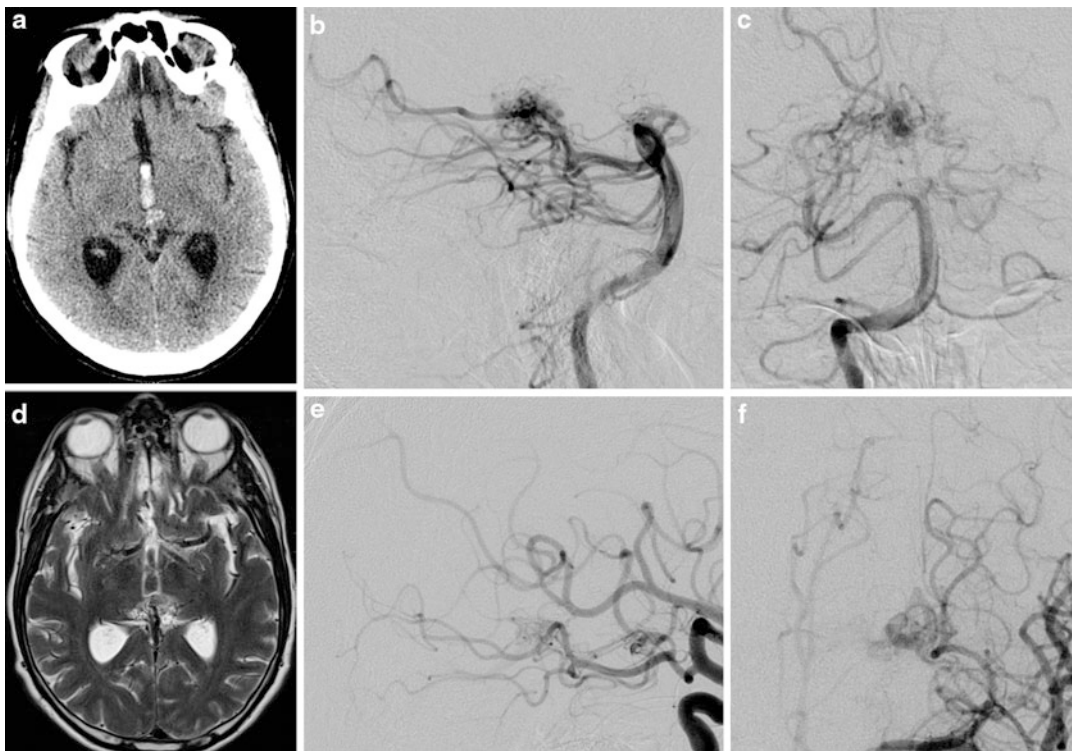
Fig. 13.4 (**a–f**) Non-contrast CT (**a**) and T2-weighted MR (**d**) demonstrating third intraventricular hemorrhage and prominent vessels along the tectum. Lateral and AP right vertebral (**b**, **c**) and *left* internal carotid (**e**, **f**) artery DSA demonstrating a compact tectal AVM nidus supplied by enlarged P1 posterior cerebral artery (PCA) segment long and short circumflex mesencephalic arterial branches. Note that the *left* P1 segment is hypoplastic (**c**) with the dominant PCA supply arising from the posterior communicating artery (**f**)

following acquisition parameters: field of view (220 mm), pitch (0.5), automated mA (120-max), and noise index (15.4), peak kV (120–140); 150 ml contrast agent and 30 ml normal saline are delivered using a power injector at 4–5 ml/s into 20 gauge access (or larger) catheter in an antecubital vein. An automatic contrast bolus triggering method or a 25 s delay from initial injection to image acquisition should be employed. Axial, sagittal, and coronal maximum intensity projections should be reformatted from source data.

Catheter DSA (Biplane Fluoroscopy)

Prior to the procedure, cross-sectional imaging should be reviewed to better tailor the angiographic exam. Using a 4-French sheath via the femoral artery, a 4-French vertebral catheter and glide wire are used to access the great vessels. For preliminary evaluation, a 6-vessel study should be performed with standard angiographic views and power injections. Images should be collected at a minimum 2–3 frames/s with higher frame rates (8/s) for high-flow fistulas. Rate of injection and volume of contrast will vary on the BAVM size and degree of associated shunting, though the following are general guidelines: ICA (rate, 6–8 ml/s; volume, 8–10 ml), ECA (rate, 3 ml/s; volume, 6–8 ml), and vertebral artery (rate, 5 ml/s; volume, 10–12 ml). Angiographic runs should be extended through the physiological venous phase to complete vascular anatomy. For all major arterial distributions contributing to the vascular nidus, as well as associated aneurysms, 3D rotational angiography should be performed.
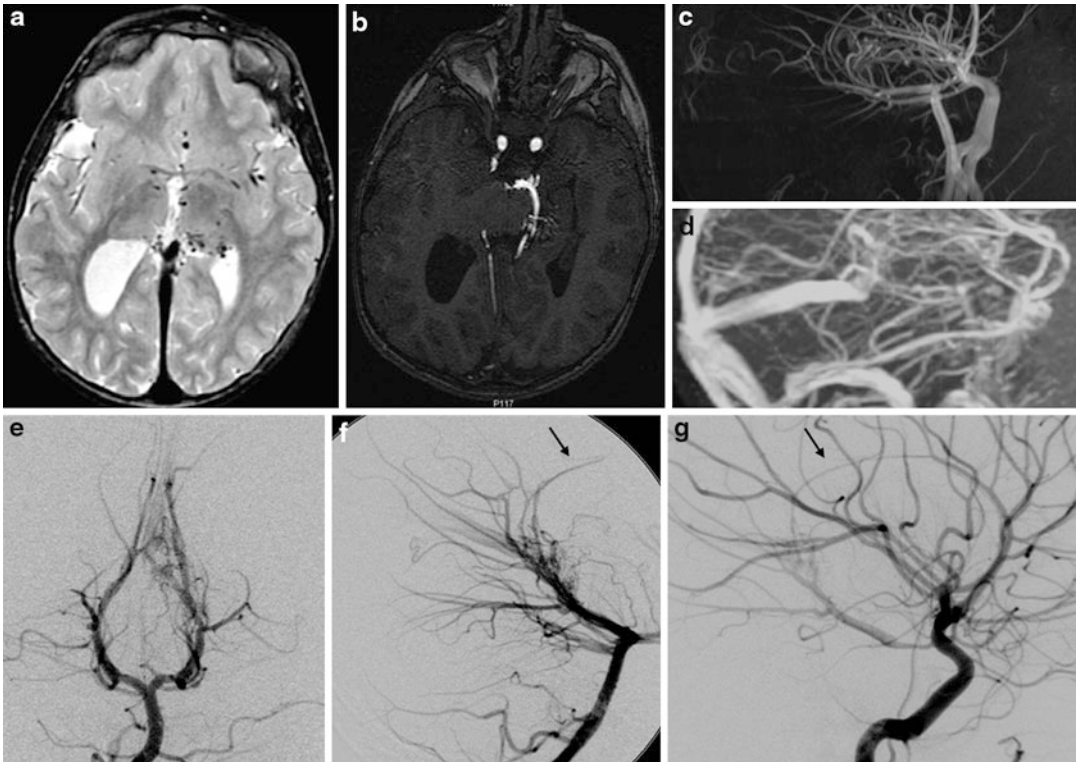
Fig. 13.5 (**a–g**) T2 (**a**) and MRA (**b**) images demonstrating multiple left pulvinar flow voids (**a**), an enlarged falcine sinus (**a**), and enlarged left PCA (**b**). Maximum intensity pixel (MIP) MRA (**c**) and MRV (**d**) images demonstrating a diffuse, left peri-thalamic AVM nidus with venous outflow to the persistent falcine sinus. AP and lateral left vertebral (**e**, **f**) and lateral internal carotid (**g**) artery DSA demonstrating AVM supply by anterior (**f**) and posterior (**e**, **f**) thalamo-perforating arteries. There is additional supply from the left posterior choroidal arteries. Note the presence of the supply from the left pericallosal artery via a limbic arch (*arrow*, **g**)

Future Research

- *ICH Risk Scoring*. Multicenter studies of natural history hemorrhage risk are needed. In order to devise a comprehensive predictive model of hemorrhagic risk, a large *discovery* cohort is needed that has ample outcome events (ICH) to allow consideration of a large number of covariants (risk factors). Then, several *validation* cohorts are needed to test the model. This will require a sea change in the level of cooperation and collaboration among teams that care for and do research on this disease. There is sufficient patient material available worldwide to devise a natural history risk scoring that can improve clinical management.

- *Genetics*. An important subgroup of these kinds of large studies is the development of a sufficiently large number of cases for whom DNA is collected along with clinical information. Genetic studies – even in the sporadic, non-inherited form of the disease – are very likely to give important clues to the biology of the disease, even if the information is regarding modifier genes that determine biological or clinical aspects of the phenotype [101–110]. But as important, it is likely that genetic variation, such as identification of single nucleotide polymorphisms associated with adverse outcomes, can be used as a means of risk stratification.

- *Surrogate Markers for Studies of BAVM*. A major challenge to developing medical therapy for BAVM is that it is a rare disease
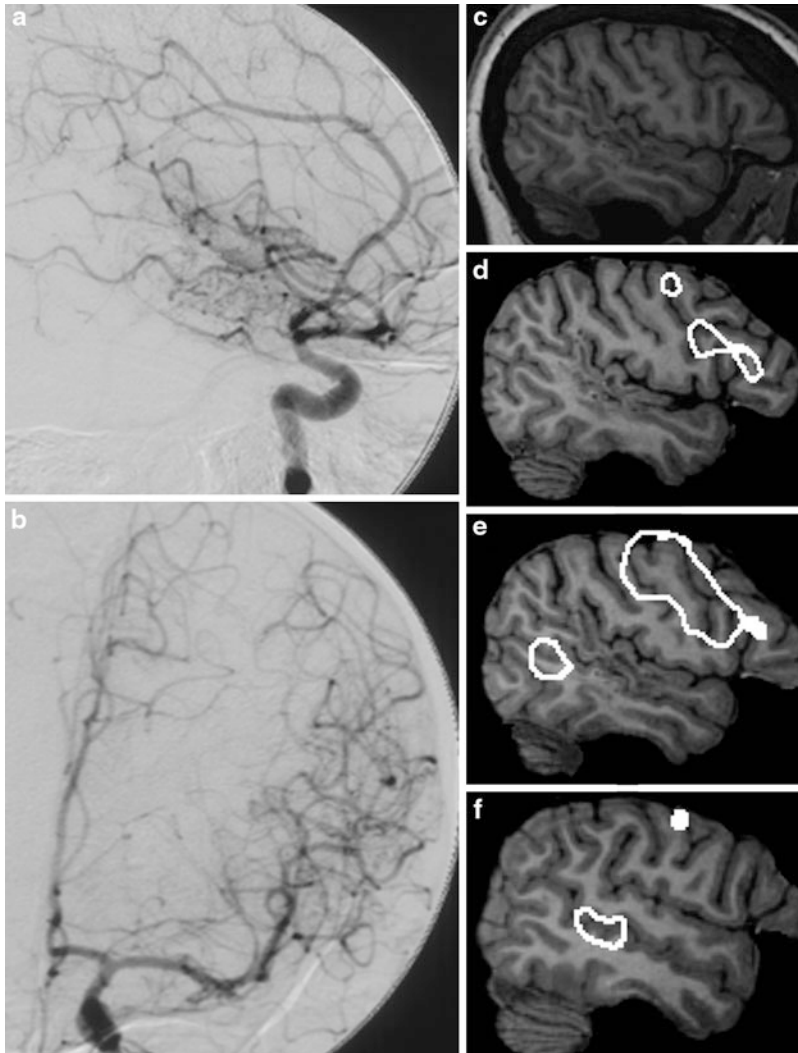
Fig. 13.6 Lateral and AP left internal carotid artery (**a**, **b**) DSA demonstrating a diffuse, left temporal AVM nidus. Parasagittal T1 MR (**c**) and functional blood oxygen level-dependent (BOLD) map (**d**, **e**, **f**) images demonstrating prominent flow voids within the left superior temporal gyrus (**c**, **d**, **e**), activation within Broca's area during verb generation (**d**), activation within Broca's and Wernicke's areas during rhyming (**e**), and activation within Herschel's gyrus during passive listening (**f**)

(new detection rate 1/100,000 per year) coupled with the most morbid sequelae being a relatively low frequency rate of ICH (2–4 % per year). Design of trials with sufficient power to detect even modest effect sizes will require a considerable outlay of resources, and surrogate markers could greatly facilitate progress by providing evidence that a drug will have a sufficient biological effect to make a larger scale efficacy trial more attractive.

- Therefore, there is a pressing need to develop surrogate markers for testing clinical efficacy of potential pharmacological or gene therapeutic agents. The BAVM lesion is a fragile, rupture-prone locus [111, 112] that displays inflammation as part of their lesional phenotype [113]. Further, pro-inflammatory genotypes are associated with a more aggressive, hemorrhagic phenotype in longitudinal clinical studies [105, 106, 114, 115], consistent
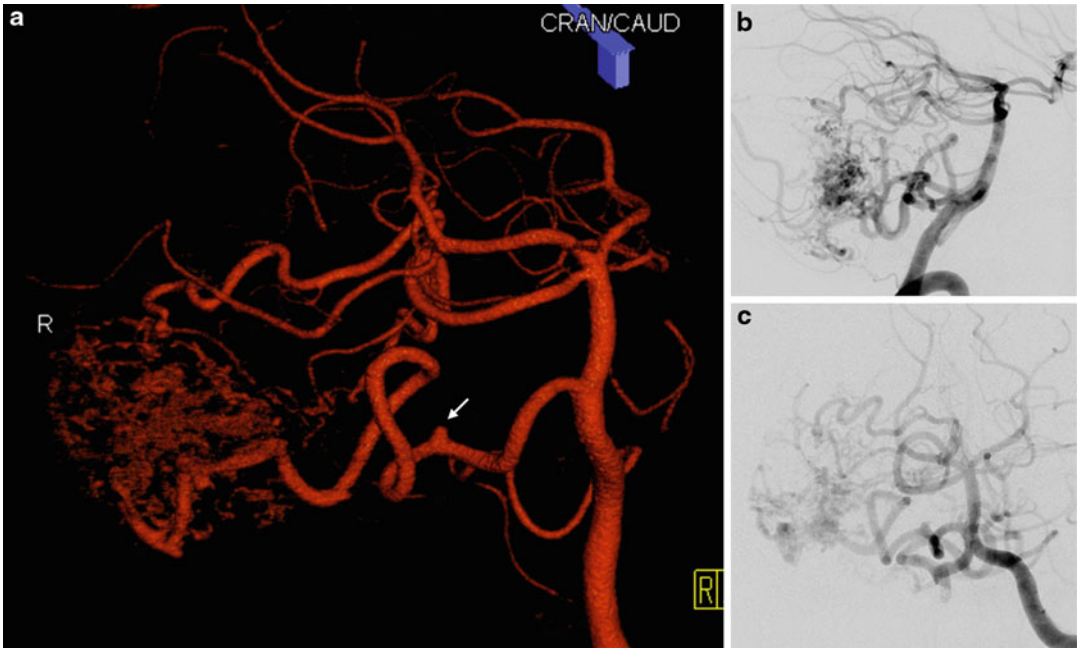
Fig. 13.7 (**a–c**) 3D rotational (**a**) and conventional lateral and AP (**b**, **c**) *left* vertebral artery DSA demonstrating a compact, right cerebellar hemispheric AVM supplied by ipsilateral anterior-inferior and superior cerebellar arteries. Note the peri-nidal aneurysm (*arrow*) along the anterior-inferior cerebellar artery, best seen on the 3DRA

with accumulating evidence that inflammatory pathways contribute to disease progression of vascular malformations throughout the circulation [116].

- A relatively new method is available for assessing macrophage infiltration into the lesional tissue [117–119]. Ferumoxytol is an iron oxide monocrystalline nanoparticle coated with a semisynthetic modified carbohydrate with low molecular weight and formulated with mannitol. The general term for such agents is USPIO. The FDA approved ferumoxytol (Feraheme™) in 2009 to treat iron deficiency anemia and adult chronic kidney disease patients [120]. The recommended therapeutic dose is similar to the dose used for imaging.

- If a link can be established between brain imaging of macrophage infiltration and the risk of future hemorrhage, therapeutic trials might be aimed first at evaluating this surrogate marker. Despite the case to be made for the notion that enhanced vascular remodeling

is the mechanism for rupture of BAVM, more work is needed to definitely demonstrate this concept.

- Plasma biomarkers are another option. Tissue angiogenic factors and inflammatory cytokines have been used to monitor disease course and treatment response in several settings, both in the CNS [121–125] and a wide range of vascular or angiogenic disorders outside of it [126–130]. Most importantly, various plasma signals are elevated in hereditary hemorrhagic telangiectasia (HHT), notably vascular endothelial growth factor (VEGF). Interestingly, there are only two studies of plasma VEGF in BAVMs, and they had discordant findings; one found elevated levels [131]; the other lower levels, which normalized after treatment [132]. Plasma matrix metalloproteinase (MMP)-9 has been demonstrated to be elevated in BAVM patients [133, 134]. In one study, levels were elevated compared to controls at baseline, increased immediately after resection, and
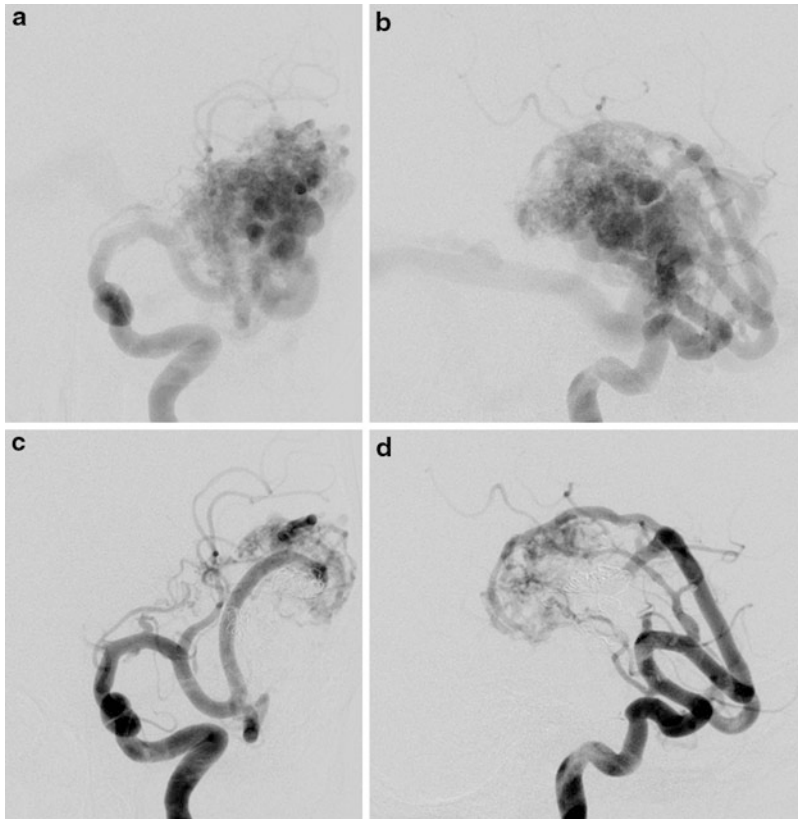
Fig. 13.8 (**a–d**) AP and lateral *left* internal carotid artery (**a**, **b**) DSA demonstrating a compact, insular AVM nidus supplied by lenticulostriate and insular MCA branches. AP and lateral left internal carotid artery (**c**, **d**) following staged coil and n-BCA embolization of multiple posterior MCA division branches. The more anterior MCA branch supply was not treated given it more suitable to microsurgical access

decreased to pretreatment levels over follow-up. If circulating levels of pro-angiogenic and pro-inflammatory signal are shown to be increased, and respond to treatment, the mechanisms responsible for their elevation will also be important.

- *Development of Medical Therapy*. A safe and effective pharmacological means of providing protection against BAVM-related neurological morbidity – especially ICH – would be a significant improvement in patient care. Roughly 20 % of AVM patients are not offered any treatment. Further, there is controversy over whether unruptured AVMs should be treated. However, there is no available specific medical therapy. Radiosurgical treatment accounts for roughly 30 % of all primary treatment prescriptions for the management of the disease, but there is a long period between irradiation and nidus obliteration, termed the "latency period"; BAVM obliteration does not occur until 2–4 years after radiosurgery, and only about 70–80 % achieve eradication.

- *Development of Small Animal Models*. Although progress is being made [135], there is no ideal animal model of BAVMs, at least in terms of the specific human disease that includes a nidus, arteriovenous shunting, and a syndrome of recurrent spontaneous ICH. Therefore, a major component of therapy development for preclinical testing of medical therapies is in need of further development.
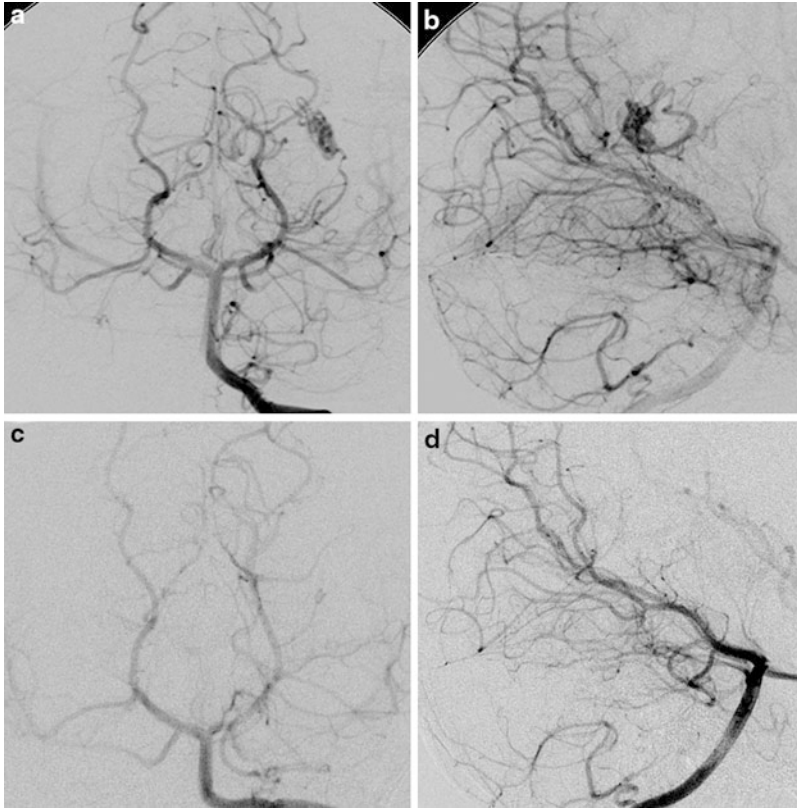
Fig. 13.9 (**a–d**) AP and lateral *left* vertebral artery (**a**, **b**) DSA demonstrating a compact, *left* choroidal AVM nidus supplied by an enlarged posterior-lateral choroidal artery. AP and lateral left vertebral artery (**c**, **d**) DSA following alcohol embolization of the left posterior-lateral choroidal artery demonstrating no residual filling of the AVM nidus
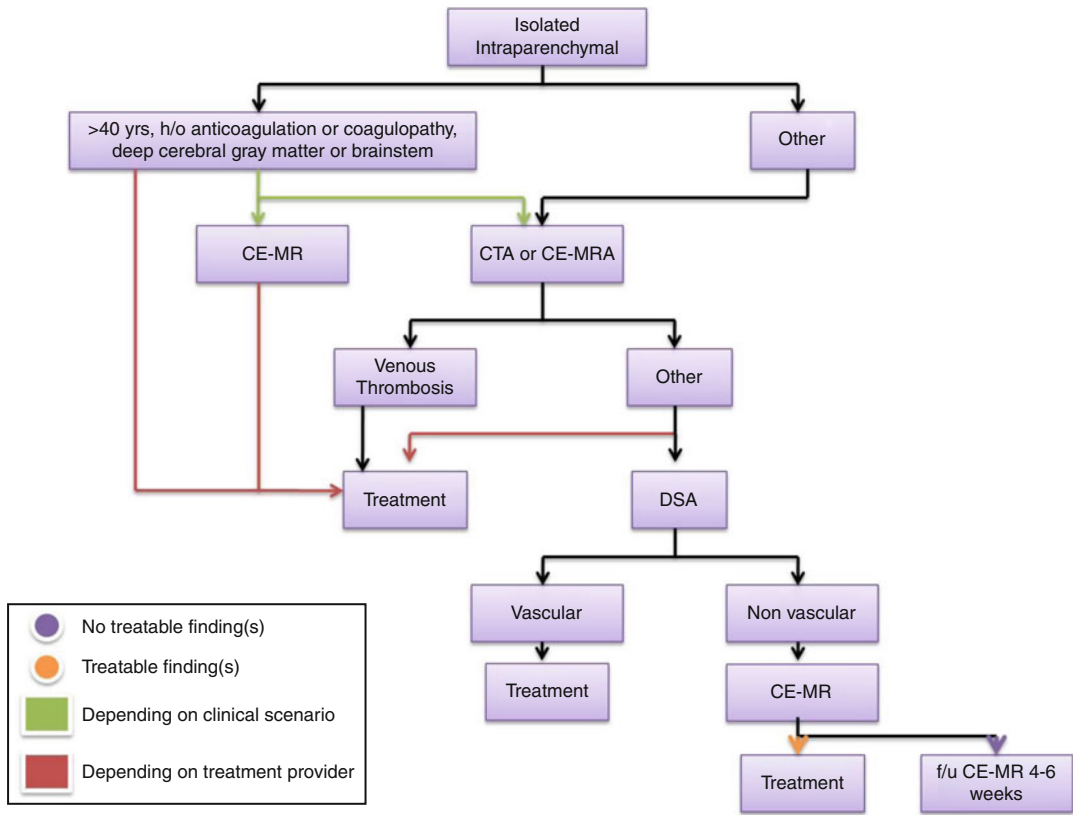
Fig. 13.10 Diagnostic imaging workup of nontraumatic isolated intraparenchymal hemorrhage
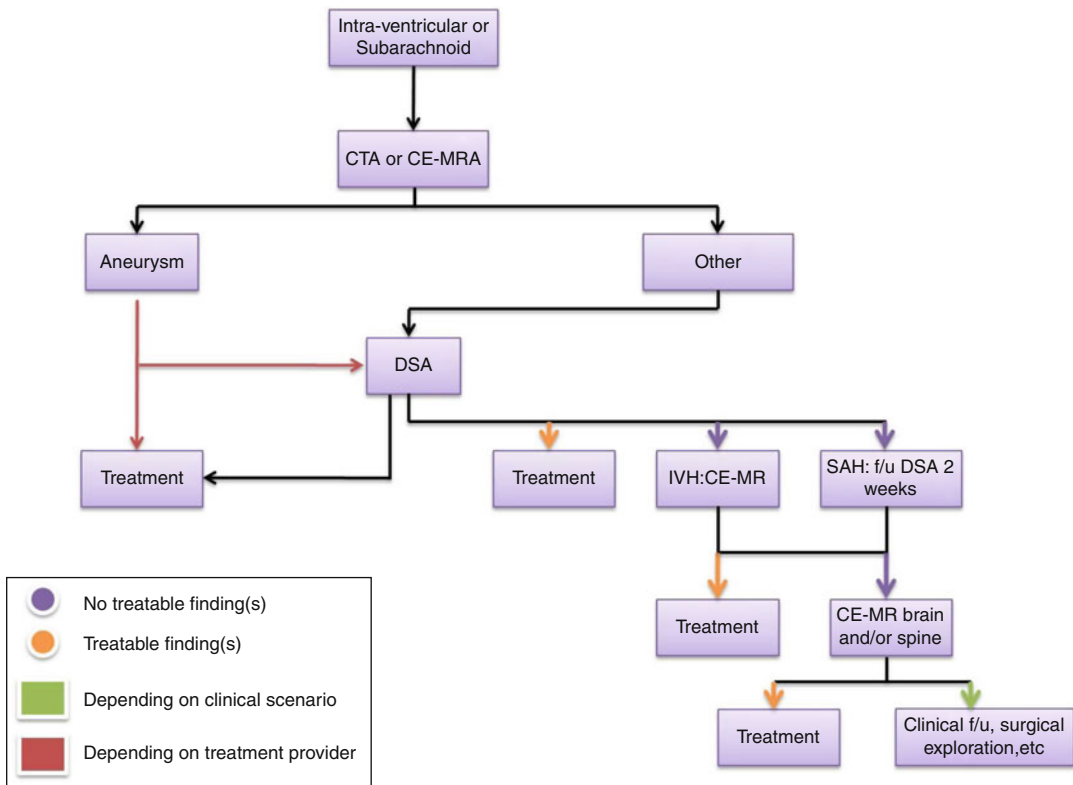
Fig. 13.11 Diagnostic imaging workup of nontraumatic intraventricular and/or subarachnoid hemorrhage with or without intraparenchymal hemorrhage

References

1. Stapf C, Mast H, Sciacca R, et al. Neurology. 2006;66(9):1350–5.
2. Choi JH, Mast H, Sciacca RR, et al. Stroke. 2006;37(5):1243–7.
3. van Beijnum J, Lovelock CE, Cordonnier C, et al. Brain. 2009;132(Pt 2):537–43.
4. Moftakhar P, Hauptman J, Malkasian D, Martin N. Neurosurg Focus. 2009;26(5):E10.
5. Arteriovenous Malformations Study Group. N Engl J Med. 1999;340(23):1812–8.
6. Kim H, Su H, Weinsheimer S, Pawlikowska L, Young W. Acta Neurochir. 2011;111:83–92.
7. Kim H, Pawlikowska L, Young W. Stroke: pathophysiology, diagnosis, and management. 5th ed. Philadelphia: Churchill Livingstone/Elsevier; 2011.
8. Al-Shahi R, Fang J, Lewis S, Warlow C. J Neurol Neurosurg Psychiatry. 2002;73(5):547–51.
9. Al-Shahi R, Bhattacharya J, Currie D, et al. Stroke. 2003;34(5):1163–9.
10. Hartmann A, Mast H, Mohr J, et al. Stroke. 1998;29(5):931–4.
11. Hofmeister C, Stapf C, Hartmann A, et al. Stroke. 2000;31(6):1307–10.
12. Ogilvy C, Stieg P, Awad I, et al. Stroke. 2001;32(6):1458–71.
13. Hoh B, Chapman P, Loeffler J, Carter B, Ogilvy C. Neurosurgery. 2002;51(2):303–9; discussion 309–311.
14. Stapf C, Labovitz D, Sciacca R, Mast H, Mohr J, Sacco R. Cerebrovasc Dis. 2002;13(1):43–6.
15. Stapf C, Mast H, Sciacca R, et al. Stroke. 2003;34(5): e29–33.
16. da Costa L, Wallace M, Ter Brugge K, O'Kelly C, Willinsky R, Tymianski M. Stroke. 2009;40(1):100–5.
17. Kondziolka D, McLaughlin M, Kestle J. Neurosurgery. 1995;37(5):851–5.
18. Gabriel RA, Kim H, Sidney S, et al. Stroke. 2010;41(1):21–6.
19. Fiehler J, Stapf C. Neuroradiology. 2008;50(6):465–7.
20. Choi J, Mast H, Hartmann A, et al. Clinical and morphological determinants of focal neurological deficits in patients with unruptured brain arteriovenous malformation. J Neurol Sci. Dec 15 2009; 287(1–2):126–30.

21. Moftakhar P, Hauptman J, Malkasian D, Martin N. Neurosurg Focus. 2009;26(5):E11.
22. Spetzler R, Martin N. J Neurosurg. 1986; 65(4):476–83.
23. Mast H, Young W, Koennecke H, et al. Lancet. 1997;350(9084):1065–8.
24. Hartmann A, Stapf C, Hofmeister C, et al. Stroke. 2000;31(10):2361–4.
25. Joint Writing Group of the Technology Assessment Committee American Society of Interventional and Therapeutic Neuroradiology; Joint Section on Cerebrovascular Neurosurgery a Section of the American Association of Neurological Surgeons and Congress of Neurological Surgeons; Section of Stroke and the Section of Interventional Neurology of the American Academy of Neurology. Stroke. 2001;32(6):1430–42.
26. Kim H, Sidney S, McCulloch CE, et al. Stroke. 2007;38(9):2430–7.
27. Miller CE, Quayyum Z, McNamee P, Al-Shahi Salman R, Committee SS. Stroke. 2009;40(6):1973–9.
28. Jordan YJ, Lightfoote JB, Jordan JE. J Natl Med Assoc. 2009;101(4):331–5.
29. Jordan JE, Ramirez GF, Bradley WG, Chen DY, Lightfoote JB, Song A. J Natl Med Assoc. 2000;92(12):573–8.
30. Berman MF, Hartmann A, Mast H, et al. AJNR Am J Neuroradiol. 1999;20(10):2004–8.
31. Jordan JE, Marks MP, Lane B, Steinberg GK. AJNR Am J Neuroradiol. 1996;17(2):247–54.
32. Field AG, Wang E. Emerg Med Clin North Am. 1999;17(1):127–52, ix.
33. Edlow JA, Panagos PD, Godwin SA, Thomas TL, Decker WW. J Emerg Nurs. 2009;35(3):e43–71.
34. Consortium UH. Evidence-based guidelines in the primary care setting: neuroimaging in patients with nonacute headache. Minneapolis: American Academy of Neurology 2000.
35. Larson DB, Johnson LW, Schnell BM, Salisbury SR, Forman HP. Radiology. 2011;258(1):164–73.
36. Lledo A, Calandre L, Martinez-Menendez B, Perez-Sempere A, Portera-Sanchez A. Headache. 1994;34(3):172–4.
37. Pile-Spellman J, Young WL, Joshi S, et al. Neurosurgery. 1999;44(4):881–6; discussion 886–887.
38. Duarte J, Sempere AP, Delgado JA, Naranjo G, Sevillano MD, Clavería LE. Acta Neurol Scand. 1996;94(1):67–70.
39. Fullerton HJ, Achrol AS, Johnston SC, et al. Stroke. 2005;36(10):2099–104.
40. Lateef TM, Grewal M, McClintock W, Chamberlain J, Kaulas H, Nelson KB. Pediatrics. 2009;124(1):e12–7.
41. The epidemiology of headache among children with brain tumor. J Neurooncol. 1991;10(1):31–46.
42. Byyny RL, Mower WR, Shum N, Gabayan GZ, Fang S, Baraff LJ. Ann Emerg Med. 2008;51(6):697–703.
43. McCormack RF, Hutson A. Acad Emerg Med. 2010;17(4):444–51.
44. Delgado Almandoz J, Schaefer P, Forero N, Falla J, Gonzalez R, Romero JD. AJNR Am J Neuroradiol. 2009;30(6):1213–21.
45. Tanabe S, Uede T, Nonaka T, Ohtaki M, Hashi K. J Clin Neurosci. 1998;5(Suppl):33–8.
46. Prestigiacomo C, Niimi Y, Setton A, Berenstein A. AJNR Am J Neuroradiol. 2003;24(7):1429–35.
47. Sanelli P, Mifsud M, Stieg P. AJR Am J Roentgenol. 2004;183(4):1123–6.
48. Goddard A, Tan G, Becker J. Clin Radiol. 2005;60(12):1221–36.
49. Linn J, Ertl-Wagner B, Seelos K, et al. AJNR Am J Neuroradiol. 2007;28(5):946–52.
50. Kakizawa Y, Nagashima H, Oya F, et al. J Neurosurg. 2002;96(4):770–4.
51. Gailloud P, Oishi S, Carpenter J, Murphy K. AJNR Am J Neuroradiol. 2004;25(4):571–3.
52. Brunelle FO, Harwood-Nash DC, Fitz CR, Chuang SH. Radiology. 1983;149(2):455–61.
53. Koelfen W, Wentz U, Freund M, Schultze C. Magnetic resonance angiography in 140 neuropediatric patients. Pediatric Neurology. 1995 Jan;12(1):31–38.
54. Lasjaunias P, ter Brugge K, Berenstein A. Surgical neuroangiography: clinical and interventional aspects in children. Vol 3. 2 edn. Leipzig: Springer; 2006.
55. Rodesch G, Malherbe V, Alvarez H, Zerah M, Devictor D, Lasjaunias P. Childs Nerv Syst. 1995;11(4):231–41.
56. Niazi TN, Klimo P, Anderson RC, Raffel C. Neurosurg Clin N Am. 2010;21(3):443–56.
57. Heros R, Korosue K, Diebold P. Neurosurgery. 1990;26(4):570–7; discussion 577–578.
58. Kim EJ, Halim AX, Dowd CF, et al. Neurosurgery. 2004;54(6):1349–57; discussion 1357–1348.
59. Lawton MT, Kim H, McCulloch CE, Mikhak B, Young WL. Neurosurgery. 2010;66(4):702–13; discussion 713.
60. Lawton MT, Du R, Tran MN, et al. Neurosurgery. 2005;56(3):485–93; discussion 485–493.
61. Wedderburn CJ, van Beijnum J, Bhattacharya JJ, et al. Lancet Neurol. 2008;7(3):223–30.
62. Hartmann A, Mast H, Mohr J, et al. Stroke. 2005;36(11):2431–5.
63. Stapf C, Mohr JP, Choi JH, Hartmann A, Mast H. Curr Opin Neurol. 2006;19(1):63–8.
64. Mohr JP, Moskowitz AJ, Stapf C, et al. Stroke. 2010;41(8):e537–40.
65. Achrol A, Guzman R, Varga M, Adler J, Steinberg G, Chang S. Neurosurg Focus. 2009;26(5):E9.
66. Fiorella D, Albuquerque F, Woo H, McDougall C, Rasmussen P. Neurosurgery. 2006;59(5 Suppl 3): S163–77; discussion S3-13.
67. Natarajan S, Ghodke B, Britz G, Born D, Sekhar L. Neurosurgery. 2008;62(6):1213–25; discussion 1225–1216.
68. Humphreys RP, Hoffman HJ, Drake JM, Rutka JT. Pediatr Neurosurg. 1996;25(6):277–85.

69. Lasjaunias P, Hui F, Zerah M, et al. Childs Nerv Syst. 1995;11(2):66–79; discussion 79.

70. Yen CP, Monteith SJ, Nguyen JH, Rainey J, Schlesinger DJ, Sheehan JP. J Neurosurg Pediatr. 2010;6(5):426–34.

71. n-BCA Trial Investigators. AJNR Am J Neuroradiol. 2002;23(5):748–755.

72. Lee B-B. Management of arteriovenous malformations: A multidisciplinary approach. In: Do Y, Yakes W, Kim D, Mattassi R, Hyon W, eds. Vol 39. J Vasc Surg 2004:590–600.

73. Al-Shahi R, Warlow C. Database Syst Rev. 2006; 2006(1):CD003436.

74. Hashimoto T, Young WL, Aagaard BD, Joshi S, Ostapkovich ND, Pile-Spellman J. Anesthesiology. 2000;93(4):998–1001.

75. Loh Y, Duckwiler GR, Investigators OT. J Neurosurg. 2010;113(4):733–41.

76. White P, Wardlaw J, Easton V. Radiology. 2000;217(2):361–70.

77. Chappell E, Moure F, Good M. Neurosurgery. 2003;52(3):624–31; discussion 630–621.

78. van Gelder J. Neurosurgery. 2003;53(3):597–605; discussion 605–596.

79. Wintermark M, Uske A, Chalaron M, et al. J Neurosurg. 2003;98(4):828–36.

80. Dammert S, Krings T, Moller-Hartmann W, et al. Neuroradiology. 2004;46(6):427–34.

81. Karamessini M, Kagadis G, Petsas T, et al. Eur J Radiol. 2004;49(3):212–23.

82. Kouskouras C, Charitanti A, Giavroglou C, et al. Oct 2004;46(10):842–850

83. Hiratsuka Y, Miki H, Kiriyama I, et al. Magn Reson Med Sci. 2008;7(4):169–78.

84. McKinney A, Palmer C, Truwit C, Karagulle A, Teksam M. AJNR Am J Neuroradiol. 2008;29(3):594–602.

85. Romijn M, Gratama van Andel H, van Walderveen M, et al. AJNR Am J Neuroradiol. 2008;29(1):134–9.

86. Chen W, Wang J, Xing W, et al. Surg Neurol. 2009;71(1):32–42.

87. Li Q, Lv F, Li Y, Luo T, Li K, Xie P. Radiology. 2009;252(3):808–15.

88. Kokkinis C, Vlychou M, Zavras G, Hadjigeorgiou G, Papadimitriou A, Fezoulidis I. Br J Neurosurg. 2008;22(1):71–8.

89. Khandelwal N, Agarwal A, Kochhar R, et al. AJR Am J Roentgenol. 2006;187(6):1637–43.

90. Kitajima M, Hirai T, Korogi Y, et al. AJNR Am J Neuroradiol. 2005;26(6):1532–1538.

91. Yeung R, Ahmad T, Aviv R, de Tilly L, Fox A, Symons S. Can J Neurol Sci. 2009;36(2):176–80.

92. Romero J, Artunduaga M, Forero N, et al. Emerg Radiol. 2009;16(3):195–201.

93. Yoon D, Chang S, Choi C, Kim W, Lee J. AJNR Am J Neuroradiol. 2009;30(5):962–7.

94. Unlu E, Temizoz O, Albayram S, et al. Eur J Radiol. 2006;60(3):367–78.

95. Warren D, Hoggard N, Walton L, et al. Neurosurgery. 2007;61(1 Suppl):187–96; discussion 196–187.

96. Heidenreich J, Schilling A, Unterharnscheidt F, et al. Acta Radiol. 2007;48(6):678–86.

97. Hadizadeh D, von Falkenhausen M, Gieseke J, et al. Radiology. 2008;246(1):205–13.

98. Saleh R, Lohan D, Villablanca J, Duckwiler G, Kee S, Finn J. AJNR Am J Neuroradiol. 2008;29(5):1024–31.

99. Petkova M, Gauvrit J, Trystram D, et al. J Magn Reson Imaging. 2009;29(1):7–12.

100. Saleh R, Singhal A, Lohan D, Duckwiler G, Finn P, Ruehm S. Top Magn Reson Imaging. 2008;19(5): 251–7.

101. Pawlikowska L, Tran MN, Achrol AS, et al. Oct 2004;35(10):2294–2300

102. Pawlikowska L, Tran MN, Achrol AS, et al. Stroke. 2005;36(10):2278–80; a journal of cerebral circulation.

103. Achrol AS, Pawlikowska L, McCulloch CE, et al. Stroke. 2006;37(1):231–4; a journal of cerebral circulation.

104. Chen Y, Pawlikowska L, Yao JS, et al. Ann Neurol. 2006;59(1):72–80.

105. Pawlikowska L, Poon KY, Achrol AS, et al. Neurosurgery. 2006;58(5):838–43; discussion 838–843.

106. Achrol AS, Kim H, Pawlikowska L, et al. Neurosurgery. 2007;61(4):731–9; discussion 740.

107. Kim H, Hysi PG, Pawlikowska L, et al. Cerebrovasc Dis. 2009;27(2):176–82.

108. Weinsheimer S, Kim H, Pawlikowska L, et al. Circ Cardiovasc Genet. 2009;2(5):476–82.

109. Su H, Kim H, Pawlikowska L, et al. Am J Pathol. 2010;176(2):1018–27.

110. Mikhak B, Weinsheimer S, Pawlikowska L, et al. Cerebrovasc Dis. 2011;31(4):338–45.

111. Kim H, Su H, Weinsheimer S, Pawlikowska L, Young WL. Acta Neurochir Suppl. 2011;111: 83–92.

112. Kim H, Pawlikowska L, Young WL. Genetics and vascular biology of brain vascular malformations (Chapter 12). In: Mohr JP, Wolf PA, Grotta JC, Moskowitz MA, Mayberg M, von Kummer R, editors. Stroke: pathophysiology, diagnosis, and management. 5th ed. Philadelphia: Churchill Livingstone/Elsevier; 2011. p. 169–86.

113. Chen Y, Fan Y, Poon KY, et al. Front Biosci. 2006;11:3121–8.

114. Achrol AS, Kim H, Pawlikowska L, et al. Stroke. 2007;38(2):597–8; a journal of cerebral circulation.

115. Hysi PG, Kim H, Pawlikowska L, et al. Stroke. 2007;38(2):456; a journal of cerebral circulation.

116. Frosen J, Piippo A, Paetau A, et al. Stroke. 2004;35(10):2287–93; a journal of cerebral circulation.

117. Weinstein JS, Varallyay CG, Dosa E, et al. J Cereb Blood Flow Metab. 2010;30(1):15–35.

118. Dosa E, Guillaume DJ, Haluska M, et al. Neuro Oncol. 2011;13(2):251–60.

119. Dosa E, Tuladhar S, Muldoon LL, Hamilton BE, Rooney WD, Neuwelt EA. Stroke. 2011;42(6): 1581–8; a journal of cerebral circulation.

120. Ferumoxytol (feraheme) – a new parenteral iron formulation. The Medical letter on drugs and therapeutics. 2010;52(1334):23.

121. Testai FD, Aiyagari V, Hillmann M, Amin-Hanjani S, Dawson G, Gorelick P. Neurocrit Care. 5-May 18 2011.

122. Jayaraman T, Berenstein V, Li Z, et al. Neurosurgery. 2005;57(3):558–64; discussion 558–564.

123. Fontanella M, Rainero I, Gallone S, et al. Neurosurgery. 2007;60(4):668–72; discussion 672–663.

124. Wang Y, Zhong M, Tan XX, et al. Neurosci Bull. 2007;23(3):151–5.

125. Scheufler KM, Drevs J, van Velthoven V, et al. J Cereb Blood Flow Metab. 2003;23(1):99–110.

126. Ricciuto DR, Dos Santos CC, Hawkes M, et al. Crit Care Med. 2011;39(4):702–10.

127. Han SY, Jun JK, Lee CH, Park JS, Syn HC. Hypertens Pregnancy. 9-Sep 23 2010.

128. Ong T, McClintock DE, Kallet RH, Ware LB, Matthay MA, Liu KD. Crit Care Med. 2010;38(9):1845–51.

129. Kopczynska E, Makarewicz R, Biedka M, Kaczmarczyk A, Kardymowicz H, Tyrakowski T. Eur J Gynaecol Oncol. 2009;30(6):646–9.

130. Bolin M, Wiberg-Itzel E, Wikstrom AK, et al. Am J Hypertens. 2009;22(8):891–5.

131. Sandalcioglu IE, Wende D, Eggert A, et al. Cerebrovasc Dis. 2006;21(3):154–8.

132. Kim GH, Hahn DK, Kellner CP, et al. Stroke. 2008;39(8):2274–9; a journal of cerebral circulation.

133. Gaetani P, Rodriguez y Baena R, Tartara F, et al. Neurol Res. 1999;21(4):385–90.

134. Starke RM, Komotar RJ, Hwang BY, et al. Neurosurgery. 2010;66(2):343–8; discussion 348.

135. Walker EJ, Su H, Shen F, et al. Ann Neurol. 2011;69(6):954–62.

136. Kukuk GM, Hadizadeh DR, Boström A, et al. Invest Radiol. 2010;45(3):126–32.

137. Patrux B, Laissy JP, Jouini S, Kawiecki W, Coty P, Thiébot J. Neuroradiology. 1994;36(3):193–7.

138. Jagadeesan BD, Delgado Almandoz JE, Moran CJ, Benzinger TL. Stroke. 2011;42(1):87–92.

139. Hartwigsen G, Siebner HR, Deuschl G, Jansen O, Ulmer S. J Comput Assist Tomogr. 2010;34(4):596–600.

140. Iancu-Gontard D, Weill A, Guilbert F, Nguyen T, Raymond J, Roy D. AJNR Am J Neuroradiol. 2007;28(3):524–7.

141. Nagaraja S, Lee KJ, Coley SC, et al. Neuroradiology. 2006;48(11):821–9.

142. Hans FJ, Reinges MH, Reipke P, Reinacher P, Krings T. Zentralbl Neurochir. 2005;66(4):170–9.

143. Vates GE, Lawton MT, Wilson CB, et al. Neurosurgery. 2002;51(3):614–23; discussion 623–617.

144. Cloft HJ, Joseph GJ, Dion JE. Stroke. 1999;30(2):317–20.

145. Smith HJ, Strother CM, Kikuchi Y, et al. AJR Am J Roentgenol. 1988;150(5):1143–53.

146. Meder JF, Oppenheim C, Blustajn J, et al. AJNR Am J Neuroradiol. 1997;18(8):1473–83.

147. Lee BC, Park TS, Kaufman BA. Pediatr Radiol. 1995;25(6):409–19.

148. Yan L, Wang S, Zhuo Y, et al. Radiology. 2010;256(1):270–9.

149. Loy DN, Rich KM, Simpson J, Dorward I, Santanam L, Derdeyn CP. Neurosurg Focus. 2009;26(5):E13.

150. Norris JS, Valiante TA, Wallace MC, et al. J Neurosurg. 1999;90(4):673–9.

151. Abe T, Matsumoto K, Horichi Y, Hayashi T, Ikeda H, Iwata T. Neurol Med Chir (Tokyo). 1995;35(8): 580–3.

152. Al-Shahi R, Bhattacharya JJ, Currie DG, et al. Stroke. 2003;34(5):1156–62.

153. Halim AX, Singh V, Johnston SC, et al. Stroke. 2002;33(3):675–9.

154. Choi JH, Mast H, Hartmann A, et al. J Neurol Sci. 2009;287(1–2):126–30.

155. Cordonnier C, Al-Shahi Salman R, Bhattacharya JJ, et al. J Neurol Neurosurg Psychiatry. 2008;79(1):47–51.

156. Hernesniemi JA, Dashti R, Juvela S, Väärt K, Niemelä M, Laakso A. Neurosurgery. 2008;63(5):823–9; discussion 829–831.

157. Laakso A, Dashti R, Seppänen J, et al. Neurosurgery. 2008;63(2):244–53; discussion 253–245.

158. Halim AX, Johnston SC, Singh V, et al. Stroke. 2004;35(7):1697–702.

159. Stapf C, Khaw AV, Sciacca RR, et al. Stroke. 2003;34(11):2664–9.

160. ApSimon HT, Reef H, Phadke RV, Popovic EA. Stroke. 2002;33(12):2794–800.

161. Stefani MA, Porter PJ, terBrugge KG, Montanera W, Willinsky RA, Wallace MC. Stroke. 2002;33(5):1220–4.

162. Kader A, Young WL, Pile-Spellman J, et al. Neurosurgery. 1994;34(5):801–7; discussion 807–808.

163. Ondra SL, Troupp H, George ED, Schwab K. J Neurosurg. 1990;73(3):387–91.

164. Crawford PM, West CR, Chadwick DW, Shaw MD. J Neurol Neurosurg Psychiatry. 1986;49(1):1–10.

165. Fults D, Kelly DL. Neurosurgery. 1984;15(5):658–62.

166. Gerosa MA, Cappellotto P, Licata C, Iraci G, Pardatscher K, Fiore DL. Childs Brain. 1981;8(5):356–71.

167. Investigators n-BT. AJNR Am J Neuroradiol. 2002;23(5):748–755.

168. van Beijnum J, Bhattacharya JJ, Counsell CE, et al. Stroke. 2008;39(12):3216–21.

169. Lv X, Wu Z, Jiang C, et al. Interv Neuroradiol. 2010;16(2):127–32.

170. Jayaraman MV, Marcellus ML, Hamilton S, et al. AJNR Am J Neuroradiol. 2008;29(2):242–6.

171. Haw CS, terBrugge K, Willinsky R, Tomlinson G. J Neurosurg. 2006;104(2):226–32.

172. Hartmann A, Pile-Spellman J, Stapf C, et al. Stroke. 2002;33(7):1816–20.

173. Yuki I, Kim RH, Duckwiler G, et al. Clinical article. J Neurosurg. 2010;113(4):715–22.

174. Andreou A, Ioannidis I, Lalloo S, Nickolaos N, Byrne JV. J Neurosurg. 2008;62(6):1213–25; discussion 1225–1216.

175. Yakes WF, Krauth L, Ecklund J, et al. Neurosurgery. 1997;40(6):1145–52; discussion 1152–1144.

176. Yu SC, Chan MS, Lam JM, Tam PH, Poon WS. AJNR Am J Neuroradiol. 2004;25(7):1139–43.

177. Debrun GM, Aletich V, Ausman JI, Charbel F, Dujovny M. Neurosurgery. 1997;40(1):112–20; discussion 120–111.

178. Wong SH, Tan J, Yeo TT, Ong PL, Hui F. Ann Acad Med Singapore. 1997;26(4):475–80.

179. Fournier D, TerBrugge KG, Willinsky R, Lasjaunias P, Montanera W. J Neurosurg. 1991;75(2):228–33.

180. Wallace RC, Flom RA, Khayata MH, et al. Neurosurgery. 1995;37(4):606–15; discussion 615–608.

181. Panagiotopoulos V, Gizewski E, Asgari S, Regel J, Forsting M, Wanke I. AJNR Am J Neuroradiol. 2009;30(1):99–106.

182. Katsaridis V, Papagiannaki C, Aimar E. Neuroradiology. 2008;50(7):589–97.

183. Mounayer C, Hammami N, Piotin M, et al. AJNR Am J Neuroradiol. 2007;28(3):518–23.

184. Weber W, Kis B, Siekmann R, Jans P, Laumer R, Kühne D. Neurosurgery. 2007;61(2):244–52; discussion 252–244.

185. Thiex R, Williams A, Smith E, Scott RM, Orbach DB. AJNR Am J Neuroradiol. 2010;31(1):112–20.

186. Sorimachi T, Koike T, Takeuchi S, et al. AJNR Am J Neuroradiol. 1999;20(7):1323–8.

187. Perrini P, Scollato A, Cellerini M, et al. Acta Neurochir (Wien). 2004;146(8):755–66.

188. Song JK, Eskridge JM, Chung EC, et al. J Neurosurg. 2000;92(6):955–60.

189. Pierot L, Januel AC, Herbreteau D, et al. J Neuroradiol. 2009;36(3):147–52.

190. Frenzel T, Lee CZ, Kim H, et al. Cerebrovasc Dis. 2008;25(1–2):157–63.

191. Meisel HJ, Mansmann U, Alvarez H, Rodesch G, Brock M, Lasjaunias P. Acta Neurochir (Wien). 2002;144(9):879–87; discussion 888.

192. Kondziolka D, Humphreys RP, Hoffman HJ, Hendrick EB, Drake JM. Can J Neurol Sci. 1992;19(1):40–5.

193. Javalkar V, Pillai P, Vannemreddy P, Caldito G, Ampil F, Nanda A. Neurol India. 2009;57(5):617–21.

194. Maruyama K, Koga T, Shin M, Igaki H, Tago M, Saito N. J Neurosurg. 2008;109(Suppl):73–6.

195. Vachhrajani S, Fawaz C, Mathieu D, et al. J Neurosurg. 2008;109(Suppl):2–7.

196. Karlsson B, Jokura H, Yamamoto M, Söderman M, Lax I. J Neurosurg. 2007;107(4):740–4.

197. Maruyama K, Shin M, Tago M, Kishimoto J, Morita A, Kawahara N. Neurosurgery. 2007;60(3):453–8; discussion 458–459.

198. Inoue HK. J Neurosurg. 2006;105(Suppl):64–8.

199. Andrade-Souza YM, Zadeh G, Scora D, Tsao MN, Schwartz ML. Neurosurgery. 2005;56(1):56–63; discussion 63–54. Int J Radiat Oncol Biol Phys. 2000;46(5):1135–42.

200. Young C, Summerfield R, Schwartz M, O'Brien P, Ramani R. Can J Neurol Sci. 1997;24(2):99–105.

201. Pica A, Ayzac L, Sentenac I, et al. Radiother Oncol. 1996;40(1):51–4.

202. Yamamoto M, Jimbo M, Hara M, Saito I, Mori K. Neurosurgery. 1996;38(5):906–14.

203. Young CS, Schwartz ML, O'Brien P, Ramaseshan R. Acta Neurochir Suppl. 1995;63:57–9.

204. Lunsford LD, Kondziolka D, Flickinger JC, et al. J Neurosurg. 1991;75(4):512–24.

205. Coffey RJ, Lunsford LD, Bissonette D, Flickinger JC. Stereotact Funct Neurosurg. 1990;54–55:535–40.

206. Kiran NA, Kale SS, Kasliwal MK, et al. Acta Neurochir (Wien). 2009;151(12):1575–82.

207. Sirin S, Kondziolka D, Niranjan A, Flickinger JC, Maitz AH, Lunsford LD. Neurosurgery. 2006;58(1):17–27; discussion 17–27.

208. Karlsson B, Lindqvist M, Blomgren H, et al. Neurosurgery. 2005;57(1):42–9; discussion 42–49.

209. Miyawaki L, Dowd C, Wara W, et al. Int J Radiat Oncol Biol Phys. 1999;44(5):1089–106.

210. Mathis JA, Barr JD, Horton JA, et al. AJNR Am J Neuroradiol. 1995;16(2):299–306.

211. Dawson RC, Tarr RW, Hecht ST, et al. AJNR Am J Neuroradiol. 1990;11(5):857–64.

212. Uno M, Satoh K, Matsubara S, Satomi J, Nakajima N, Nagahiro S. Neurol Res. 2004;26(1):50–4.

213. Huh SK, Lee KC, Lee KS, Kim DI, Park YG, Chung SS. J Clin Neurosci. 2000;7(5):429–33.

214. Deruty R, Pelissou-Guyotat I, Amat D, et al. Acta Neurochir (Wien). 1996;138(2):119–31.

215. Kelly ME, Guzman R, Sinclair J, et al. J Neurosurg. 2008;108(6):1152–61.

216. Nicolato A, Foroni R, Seghedoni A, et al. Childs Nerv Syst. 2005;21(4):301–7; discussion 308.

217. Baumann GS, Wara WM, Larson DA, et al. Pediatr Neurosurg. 1996;24(4):193–201.

218. Buis DR, Dirven CM, Lagerwaard FJ, et al. J Neurol. 2008;255(4):551–60.

219. Wara W, Bauman G, Gutin P, et al. Stereotact Funct Neurosurg. 1995;64(Suppl 1):118–25.

220. Sasaki T, Kurita H, Saito I, et al. J Neurosurg. 1998;88(2):285–92.

221. Han PP, Ponce FA, Spetzler RF. J Neurosurg. 2003;98(1):3–7.

222. Davidson AS, Morgan MK. Neurosurgery. 2010;66(3):498–504; discussion 504–495.

223. Hamilton MG, Spetzler RF. Neurosurgery. 1994;34(1):2–6; discussion 6–7.

224. Post N, Russell SM, Huang P, Jafar J. Minim Invasive Neurosurg. 2008;51(2):114–8.

225. Nagata S, Matsukado K, Natori Y, Sasaki T, Fukui M. Br J Neurosurg. 2006;20(3):146–9.

226. Morgan MK, Rochford AM, Tsahtsarlis A, Little N, Faulder KC. Neurosurgery. 2004;54(4):832–7; discussion 837–839.
227. Lawton MT, Project UBAMS. Neurosurgery. 2003;52(4):740–8; discussion 748–749.
228. Russell SM, Woo HH, Joseffer SS, Jafar JJ. Neurosurgery. 2002;51(5):1108–16; discussion 1116–1108.
229. Jafar JJ, Davis AJ, Berenstein A, Choi IS, Kupersmith MJ. J Neurosurg. 1993;78(1):60–9.
230. Richling B, Bavinzski G. Acta Neurochir Suppl (Wien). 1991;53:50–9.
231. Dehdashti AR, Thines L, Willinsky RA, et al. Clinical article. J Neurosurg. 2010;113(4):742–8.
232. Zuccaro G, Argañaraz R, Villasante F, Ceciliano A. Childs Nerv Syst. 2010;26(10):1381–94.
233. Weprin BE, Hall WA, Cho KH, Sperduto PW, Gerbi BJ, Moertel C. Pediatr Neurol. 1996;15(3):193–9.
234. Lanzino G, Fergus AH, Jensen ME, Kongable GL, Kassell NF. Surg Neurol. 1997;47(3):258–63. discussion 263–264.
235. Chang SD, Steinberg GK, Levy RP, et al. Neurol Med Chir (Tokyo). 1998;38(Suppl):200–7.

Intracranial Aneurysms and Vasospasm: Evidence-Based Diagnosis and Treatment

14

Edward D. Greenberg, Kathleen R. Fink, and Y. Pierre Gobin

Contents

E.D. Greenberg (✉) • Y.P. Gobin
Department of Neurosurgery, Weill Cornell Medical College/NewYork-Presbyterian Hospital, New York, NY, USA
e-mail: edward.greenberg.98@alumni.brown.edu; yvg2001@med.cornell.edu

K.R. Fink
Department of Radiology, University of Washington, Seattle, WA, USA
e-mail: ktozer@u.washington.edu

Key Points

- DSA remains the most accurate method of intracranial aneurysm diagnosis, although recent technological advances in CTA have led to almost equivalent diagnostic performance (strong evidence).
- If a patient has a classic clinical presentation and CT pattern of perimesencephalic hemorrhage, DSA may not be indicated if the initial CT angiogram is negative for aneurysm (limited evidence).
- Regarding ruptured cerebral aneurysms that can be treated by both endovascular and surgical techniques, endovascular coiling results in lower morbidity at 1 year and lower mortality at 5 years after treatment, despite a slightly higher re-hemorrhage rate (strong evidence).
- Regarding unruptured cerebral aneurysms, there is insufficient evidence to recommend a standard method of management. Such aneurysms should be managed on a case-by-case basis with the estimated risks of treatment carefully weighed against the risk of rupture (insufficient evidence).
- Compared to DSA, TCD is an accurate method for diagnosis of MCA vasospasm with a diagnostic performance of approximately 80 %. CTA is more accurate than TCD, with a diagnostic performance of 98 % (moderate evidence).
- There is insufficient evidence regarding the diagnostic accuracy of MRA, MRP, and CTP for vasospasm diagnosis, although preliminary studies have shown some promising results (insufficient evidence).
- Nimodipine and magnesium are beneficial for preventing delayed cerebral ischemia when used prophylactically in aneurysmal subarachnoid hemorrhage (A-SAH) patients, although there are conflicting reports about the benefits of treatment with hydroxymethyl-glutaryl coenzyme A reductase inhibitors (statins) (strong evidence).
- There is insufficient evidence that "Triple H" therapy improves patient outcomes, although there is limited evidence that the hypertension component of the "Triple H" treatment increases cerebral blood flow (CBF) (insufficient evidence).
- Papaverine infusion and balloon angioplasty are effective treatments for vasospasm and have been shown to result in clinical improvement, although there are no prospective randomized clinical trials to show an effect on patient outcomes (moderate evidence).
- Intra-arterial infusion of vasodilatory medications, such as verapamil and other calcium channel blockers, appears to be effective for the treatment of vasospasm, although their utility is not established in randomized controlled studies (insufficient evidence).

Definition and Pathophysiology

An aneurysm is an abnormal dilatation of an artery that can be saccular or fusiform in shape. Although the pathophysiology of cerebral aneurysm formation is incompletely understood, aneurysm formation is thought to be the result of a complex cascade involving hemodynamic stress, abnormal vascular remodeling, and inflammation [1, 2]. Risk factors for aneurysms include a personal or family history of aneurysms and/or subarachnoid hemorrhage (SAH), autosomal dominant polycystic kidney disease, type IV Ehlers-Danlos syndrome, Marfan syndrome, fibromuscular dysplasia, alpha-1-antitrypsin deficiency, the presence of an arteriovenous malformation, abdominal aortic aneurysms, atherosclerosis, and sickle cell disease. Risk factors for subarachnoid hemorrhage include family history, cigarette smoking, hypertension, alcohol consumption (>2 drinks per day), non-white ethnicity, cocaine use, and/or the use of sympathomimetic drugs [3, 4].

Patients with A-SAH who survive the initial hemorrhage should be treated by endovascular coiling or surgical clipping of the ruptured aneurysm in order to prevent re-bleeding. In the post-hemorrhage period, A-SAH patients are prone to developing both cerebral vasospasm and delayed cerebral ischemia (DCI), the pathophysiology of

which is also not completely understood. The term "cerebral vasospasm" is commonly used to refer to both the clinical findings of delayed onset of neurologic deficits and the narrowing of cerebral vessels documented by imaging studies. However, such a definition does not account for the fact that many patients do not necessarily exhibit both clinical and imaging findings of vasospasm. Recently, an expert opinion recommended that the term vasospasm be reserved for the presence of anatomic arterial narrowing documented on imaging studies [5]. In addition, DCI has been shown to be best defined as the delayed onset of neurological deterioration or the presence of cerebral infarction documented on imaging studies, which is not explained by other causes. Others suggest the diagnosis of DCI be reserved for cases of delayed neurological deterioration or infarction when the cause was felt to be attributable to vasospasm [6].

Epidemiology

The overall prevalence of cerebral aneurysms in the general population is estimated at 2.3 %. Prevalence tends to increase with age, and aneurysms are associated with the risk factors delineated above [7]. A-SAH accounts for 5 % of all strokes in the United States and affects as many as 30,000 Americans each year. The annual incidence of A-SAH varies by country, from 2.0 per 100,000 population in China to 22.5 per 100,000 in Finland [3]. A-SAH has a poor prognosis, with mortality rates as high as 45 % from the initial hemorrhage and significant morbidity among survivors [3]. In patients with A-SAH, cerebral vasospasm, defined as arterial narrowing on DSA, is seen in up to 70 % of patients, although DCI affects approximately 20–30 % of the A-SAH population [6, 8, 9].

Overall Cost to Society

There are few studies that analyze the cost to society of cerebral aneurysms and A-SAH. A German study calculated the total first-year

costs of treating and caring for a patient with A-SAH at EUR 38,300 (approximately 54,000 USD) [10]. This amount includes both direct and indirect costs (productivity losses). A British cost of illness analysis estimates health-care costs from aneurysmal SAH to be 23,294 lb sterling 2005 (approximately 41,000 2010 USD), with additional informal care costs of 5800 (approximately 10,300 USD) per patient, and loss of future earnings of 38,600 per patient (men and women, approximately 68,300 USD) [11]. An analysis of cost data from the International Subarachnoid Aneurysm Trial (ISAT) reported that mean total health-care costs for A-SAH patients at 24 months after the initial hemorrhage were approximately pound sterling 28,175 (approximately 45,000 USD) in patients with delayed ischemic neurological deficit and pound sterling 18,805 (approximately 30,000 USD) in patients without delayed ischemic neurological deficit [12]. A recent study on the cost of vasospasm in A-SAH patients concluded that the total inpatient cost was 27 % higher for patients with symptomatic vasospasm ($143,201) compared to those without symptomatic vasospasm ($113,092) [13].

One potentially important variable in the cost of SAH treatment is how critically ill the patient is on arrival. An analysis of poor WFNS grade SAH patients (grades 4 and 5) in the UK in 2001 reported the acute-care cost (including aneurysm evaluation and treatment if performed as well as intensive care costs) for this cohort was approximately 23,000 2010 USD and the cost per life saved was approximately 77,000 USD. Of this cohort, 15 % of patients achieved a favorable outcome, but only 53 % of the patients included in this study underwent treatment of their aneurysm. The rest were managed supportively and all died [14].

Another potentially important variable in the cost of treating SAH is how experienced the health-care providers are in providing care for these critically ill patients. A cost-utility analysis of patients receiving SAH treatment at low-volume (<20 admissions per year) versus high-volume (≥20 admissions per year) hospitals found that while costs associated with treatment

were higher at high-volume centers, the gain in QALYs achieved in patients treated at high-volume centers was cost-effective ($10, 548/ QALY) [15].

Goals of Imaging

In the setting of a suspected cerebral aneurysm, the first goal of imaging is to diagnose or to confidently exclude the presence of an aneurysm. If an aneurysm is present, the goals of imaging are the precise determination of the aneurysm location, orientation, and size, including neck and dome measurements. It is of critical importance to define the relationship of the aneurysm to the parent vessel and to accurately depict any arterial branches that may arise from the aneurysm. In cases where no aneurysm is detected, other vascular causes of the patient's symptoms must also be excluded, such as arteriovenous malformations, dural arteriovenous fistulae, vasculitis, dissections, or venous obstruction, among others. For A-SAH patients who are suspected of having cerebral vasospasm, the goal of imaging is to accurately, confidently, and quickly diagnose or exclude vasospasm so that proper treatment may be administered without delay.

Methodology

Several MEDLINE searches were performed using PubMed (National Library of Medicine, Bethesda, Maryland) for original research publications discussing (1) the diagnostic performance of CTA compared to DSA for aneurysm diagnosis, (2) the use of CTA in cerebral aneurysm treatment planning, (3) the treatment of ruptured and unruptured cerebral aneurysms, (4) the diagnostic accuracy of noninvasive imaging modalities for vasospasm diagnosis, and (5) the effectiveness of vasospasm treatments. The search covered the dates up to March 2011 and was limited to human studies and the English language literature. The search strategy employed different combinations of the following terms: (1) digital

subtraction angiography, (2) CT angiography, (3) MR angiography, (4) cerebral aneurysm, (5) vasospasm, (6) treatment, and (7) accuracy. Additional articles were identified by reviewing the reference lists of the relevant papers. The author performed an initial review of the titles and abstracts of the identified articles followed by review of the full text in articles that were relevant.

Discussion of Issues

Intracranial Aneurysms

Intracranial Aneurysm Diagnosis and Treatment Planning
Summary
DSA continues to remain the most accurate imaging tool in the workup of a suspected intracranial aneurysm, although CTA has nearly equivalent diagnostic performance according to the most recent data. The benefit of the additional information obtained by DSA must be weighed against its risks and costs, as compared with CTA. MRA has the advantages of lack of exposure to ionizing radiation and iodinated contrast material, but its reported diagnostic accuracy is lower than CTA or DSA. CTA or DSA may serve as primary tools in the diagnostic workup of patients suspected of harboring cerebral aneurysms, but it is important for radiologists and clinicians to fully understand the strengths and weaknesses inherent in each modality in order to realize their full potential. In SAH patients with a classic perimesencephalic hemorrhage pattern, there is some initial evidence that DSA may not be indicated if the initial CT angiogram is negative for aneurysm.

Supporting Evidence
Aneurysm Diagnosis DSA and CTA are regarded as the two most accurate methods for cerebral aneurysm diagnosis. Four meta-analyses have been published which compared the accuracy of CTA and DSA in the detection of intracranial aneurysms, and all four have shown that DSA is superior to CTA. A meta-analysis performed by White et al. in 2000 demonstrated

a per-patient sensitivity of 92 % and a per-patient specificity of 94 % of CTA for the detection of both ruptured and unruptured aneurysms compared with cerebral angiography in patients with SAH or symptoms suggesting an aneurysm. CTA had a greater sensitivity of 96 % for detection of aneurysms larger than 3 mm compared to detection of aneurysms 3 mm or smaller (61 % sensitivity) [16]. A meta-analysis by van Gelder et al. in 2003 further studied the accuracy of CT angiography, with the majority of studies performed between 1993 and 1998. Similarly, the articles comprising this meta-analysis used single-detector CT scanners. The per-aneurysm sensitivity of CT angiography in patients with SAH or symptoms suggesting an aneurysm ranged from 53 % for 2-mm aneurysms to 95 % for 7-mm aneurysms compared with DSA or surgery as the reference standards. The overall specificity of CTA was 99 % [17]. A meta-analysis by Chappell et al. in 2003 showed CTA to have a per-patient sensitivity of 93 % and a specificity of 88 % compared to DSA in depicting aneurysms in patients presenting with SAH or symptoms suggesting a cerebral aneurysm [18]. Again, all the studies in this meta-analysis used single-detector row CT scanners. The most recent meta-analysis assessing the diagnostic performance of CTA represents an advance as most of the studies included in the analysis (30 out of 50) used 4 detector scanners and the remainder of the studies utilized 16 or 64 detector CT scanners. This meta-analysis demonstrated a per-patient sensitivity of 98 % and a specificity of 100 % of CTA for the diagnosis of cerebral aneurysms in patients presenting with acute SAH [19]. The reference standard in this study was DSA, surgery, endovascular treatment, or autopsy, a more robust reference standard than DSA alone. Seventy-one patients out of 4,097 total patients had ruptured aneurysms that were not diagnosed by CTA. The majority of these patients harbored small aneurysms of the internal carotid and posterior communicating arteries located near the central skull base, adjacent to bony structures that may interfere with accurate CTA interpretation.

When considering the results of these meta-analyses, it is important to acknowledge their limitations. The studies comprising the meta-analyses were performed on patients with a high prevalence of cerebral aneurysms, a factor that may result in artificially high estimations of sensitivity and specificity. Furthermore, there is the very real potential for publication bias in all four of these meta-analyses, given that smaller studies, and studies with less favorable results, are less likely to be published compared to larger studies which show positive results. Additionally, authors who are publishing studies comparing CTA and DSA likely have significant experience with these modalities, which may not reflect the reality at all sites where these modalities are utilized.

Newer DSA and CTA techniques have the potential to further improve the diagnostic accuracy of both modalities, although there is not yet enough evidence to determine their impact. 3-D rotational angiography has been shown to improve the diagnostic accuracy of DSA in small series of patients [20–22]. Bone subtraction techniques for CTA such as "matched mask bone elimination" and "dual energy methods" have been designed to improve the accuracy of aneurysm detection adjacent to bony structures. Although there have been some relatively small studies which have shown promising results, currently, there is insufficient data to determine the utility of such techniques [23, 24].

MR angiography is a third modality that can be used to diagnose cerebral aneurysms with high diagnostic accuracy. Given the lack of exposure to ionizing radiation and iodinated contrast material, MRA has definite advantages over both DSA and CTA. There is only one systematic review comparing MRA to DSA for cerebral aneurysm diagnosis. That study compiled the results of 38 studies and reported a per-patient sensitivity of 87 % and specificity of 92 % for cerebral aneurysm diagnosis [16]. A prospective, blinded study published after that systematic review compared MRA to DSA for cerebral aneurysm detection and reported a per-patient sensitivity of 74 % and specificity of 94 %, with lower sensitivity and specificity when calculations were made on a per-aneurysm basis as well as for small aneurysms (<5 mm) [25].

MRA has also been used to screen asymptomatic patients for incidental aneurysms. A cost-effectiveness analysis based on a Markov (mathematical) model found screening for asymptomatic aneurysms with MRA to be cost-effective if the annual rate of aneurysm rupture was 2 % but not if the rupture rate was 0.5 % [26]. Sensitivity analysis found the incidence of asymptomatic aneurysm had some impact on the cost-effectiveness ratios, but this was overwhelmed by other factors. A 2010 cost-effectiveness analysis examined this further, modeling screening patients with two first-degree relatives with aneurysm using MRA [27]. This model found screening to be effective and suggested an optimal screening strategy of obtaining MRA every 7 years from ages 20–80.

Treatment Planning As detailed above, there is strong evidence supporting the superior diagnostic performance of DSA compared to CTA for detecting cerebral aneurysms. However, the high diagnostic accuracy of CTA, coupled with its non-invasiveness, has led many to question whether it could potentially serve as a first-line diagnostic modality for A-SAH patients. When considering the use of CTA as a first-line diagnostic modality, it is important to balance the added information obtained from a DSA examination against the risks and costs associated with DSA. Such added information includes detection of additional, unruptured cerebral aneurysms in addition to the culprit aneurysm, as well as better delineation of vessels emanating from the parent vessel or from the aneurysm itself [28]. The most recent meta-analysis on the diagnostic performance of CTA by Westerlaan et al. calculated the sensitivity and specificity of CTA on a per-patient basis, as opposed to a per-aneurysm basis. The authors acknowledge this limitation and state that there is probably value in detecting as many incidental aneurysms as possible, both for treatment planning in the acute setting as well as for follow-up.

Despite the advantages of DSA, several studies have shown that many patients can be triaged for treatment based solely on CTA results, although this remains a subject of controversy, and no strong evidence exists to support a single approach. A few relatively small studies showed that 64- and 16-detector row CTA are useful in the triage of most patients for interventional or surgical treatment of ruptured intracranial aneurysms but that there is a considerable amount of variability and subjectivity among the physicians making these determinations [29–31]. One study showed that in 133/224 patients with acute symptoms of a cerebral aneurysm, CTA was successfully used as a first-line test in treatment planning, with neurosurgical ($n = 55$) or endovascular treatment ($n = 78$) following the CTA examination alone [32]. However, there is no long-term follow-up on these patients, and therefore, the implications of using CTA as a sole first-line method of triage for A-SAH patients are unknown.

In SAH patients with a classic perimesencephalic hemorrhage pattern of hemorrhage, there is some initial evidence that DSA may not be indicated if the initial CTA is negative for an aneurysm. In a retrospective study of 93 patients with a perimesencephalic pattern of hemorrhage, all had negative findings on CTA which were confirmed on DSA [31]. The same study showed that in patients with an aneurysmal pattern of SAH and a negative CTA, DSA is able to diagnose aneurysms and other causes of SAH, such as vasculitis, arterial dissection, or dural arteriovenous malformations not seen on CTA [31]. In SAH patients with an aneurysmal pattern of hemorrhage and no aneurysm seen on the initial CTA and/or DSA, repeat delayed DSA is currently recommended, although there is insufficient evidence to fully support this practice [33–35].

Treatment of Intracranial Aneurysms: Coiling Versus Clipping
Summary

Surgical clipping and endovascular coiling are both viable options for treatment of ruptured and/or unruptured cerebral aneurysms. For ruptured aneurysms that can be treated by endovascular or surgical techniques, endovascular coiling results in lower morbidity at 1-year follow-up and lower mortality at 5-year follow-up, despite a slightly higher re-hemorrhage rate. There is insufficient evidence to recommend a standard method of management for unruptured cerebral

aneurysms. Such aneurysms should be managed on a case-by-case basis with the estimated risks of treatment weighed against the estimated risk of rupture.

Supporting Evidence

In the case of ruptured cerebral aneurysms, the options for treatment include surgical clipping or endovascular coiling, and there is an abundance of strong evidence that both treatments improve patient outcomes by reducing the risk of aneurysm re-bleeding. Several reports have shown favorable results for endovascular coiling [9, 36, 37], although the only large, prospective, randomized trial comparing surgery and endovascular techniques is the International Subarachnoid Aneurysm Trial (ISAT) [38, 39]. In that study, 2143 patients with ruptured intracranial aneurysms were enrolled between 1994 and 2002 at 43 neurosurgical centers and randomly assigned to clipping or coiling. The 1-year rate of death and dependency was significantly lower in the endovascular group compared to the surgical group (23.5 % vs. 30.9 %) [38]. Long-term follow-up (6–14 years) of the ISAT study patients showed that there was a significantly increased risk of re-bleeding from a coiled aneurysm compared with a clipped aneurysm but that the overall risk of death at 5 years was still significantly lower in the coiled group than in the clipped group [39].

There is much controversy in the interpretation of the results of the ISAT trial [40, 41]. Some common criticisms include the fact that 78 % of the eligible participants were excluded from randomization because of their clinical status or their aneurysm angioanatomy, which did not allow for both endovascular coiling and surgical clipping. The increased time to treatment in the surgical group (1.7 days) compared to endovascular group (1.1 day) has also been raised as a potential bias against clipping, as some patients in the surgical group re-bled in the pretreatment period, which contributed to increased morbidity and mortality in that group. Concerns have also been raised regarding the skill of both the surgeons and neurointerventionalists who participated in the ISAT trial and

the accuracy of the postal questionnaire to adequately assess clinical status. Since the majority of the ISAT patients were treated in the United Kingdom, questions have been raised regarding the generalizability of the results. Given the increased re-bleeding rate in the coiling group, concerns have also been raised that the benefits of coiling may eventually be diminished over the very long term.

Regarding the treatment of unruptured aneurysms, there have been no randomized comparisons of coiling and clipping, although a large, statewide, retrospective study in California from 1990 to 1998 reported that endovascular treatment was associated with better patient outcomes than surgery. In the context of that study, adverse outcomes were defined as in-hospital death or discharge to a nursing home, and such adverse outcomes were more frequently seen among the 1,699 patients treated with surgery (25 %) compared to the 370 patients treated by endovascular techniques (10 %) [42]. Regardless of treatment method, when considering the treatment of an unruptured cerebral aneurysm, the estimated risk of bleeding must be weighed against the risk of treatment on a case-by-case basis. However, the annual risk of bleeding from an unruptured aneurysm is a controversial topic. Many series and meta-analyses have reported a rate of rupture of between 0.05 % and 2 % per year [43], with more than half of such patients suffering major morbidity or death following rupture [44, 45].

The International Study of Unruptured Intracranial Aneurysms (ISUIA) is the largest and highest-quality study of the natural history of unruptured intracranial aneurysms, involving multiple centers and a total of 4,060 patients throughout the United States, Canada, and Europe [45]. That study showed that aneurysm size and location were reliable predictors of aneurysm rupture, with larger aneurysms and posterior circulation aneurysms associated with increased rates of rupture. Of the patients managed conservatively in this study, 3 % had SAH over the 5-year follow-up. Aneurysms in the anterior circulation measuring less than 7 mm in patients without a personal history of SAH had an extremely low annual rate of rupture

(approximately 0.1 % per year). Aneurysms of similar size and location in patients with a personal history of SAH had a higher rate of rupture (approximately 0.3 % per year). Rupture rates did not differ significantly between patients with and without a personal history of SAH for aneurysms greater than 7 mm in size for any location.

The reported very low rate of rupture of anterior circulation aneurysms <7 mm (0.1 % per year) is a result which has caused much controversy as many claim that such a low value does not seem to be supported by actual practice. Such critics hypothesize that the selection and intervention biases of the ISUIA study may have led to artificially low estimates of rupture rates. Patients in the study who were managed conservatively were evaluated and counseled by neurosurgeons, and a determination was ultimately made that those patients could be managed conservatively, since they were considered to be at low risk for aneurysm rupture. Furthermore, these patients may have been able to modify their risk factors for rupture, thereby decreasing the rupture rate and leading to a falsely low rate of rupture. Such biases raise the possibility that the reported probability of aneurysm rupture in the ISUIA study may indeed be artificially low and not generalizable to all patients.

Given that there is no randomized controlled study comparing conservative management of unruptured aneurysms to interventional or surgical treatments, there is insufficient evidence to recommend a standardized course of action in a given patient. Management decisions for patients with unruptured aneurysms need to be made on a case-by-case basis, with the following considerations taken into account: size and location of the aneurysm, any specific risk factors for rupture, the patient's life expectancy, and the estimated risks associated with treatment [46].

Applicability to Children

The incidence of cerebral aneurysms and subarachnoid hemorrhage in the pediatric age group is extremely low, accounting for 1–2 % of all aneurysm cases with approximately 700 cases described in the literature [47]. Pediatric aneurysms are most commonly located at the internal carotid artery bifurcation (26 %), anterior communicating artery (19 %), middle cerebral artery bifurcation (17 %), and posterior circulation (17 %) [47]. SAH is the most common presentation of pediatric aneurysms, but mortality after SAH is lower than in adults, ranging from 10 % to 20 % [48]. Most children with intracranial aneurysms can be successfully treated with low morbidity and mortality using either surgical or endovascular techniques [49].

Cost-Effectiveness Analysis

Most of the available data shows that coiling is associated with lower total costs and shorter hospital stays when compared with clipping. The largest study performed in the United States to date on this topic is from the University of Florida, where researchers conducted a national analysis using data from the Nationwide Inpatient Sample (NIS) from the Healthcare Cost and Utilization Project for all cases of clipping or coiling of both unruptured and ruptured aneurysms between 2002 and 2006 [50]. A total of 19,034 hospitalizations were included, with approximately half representing ruptured aneurysms and the other half unruptured. For both groups, clipping compared to coiling was associated with a significantly longer hospital stay and significantly higher total hospital charges [50]. An Australian study showed a similar result, with clipping associated with higher total costs compared to coiling [51]. However, a study from the UK examined costs associated with the ISAT patients and showed no significant difference in costs between either treatment modality at 12 and 24 months [52].

Vasospasm

What Are the Respective Diagnostic Performances of TCD, CTA, CTP, MRA, and MRP Compared to DSA for Vasospasm Diagnosis?
Summary
Noninvasive methods of vasospasm diagnosis include clinical examination, TCD, CTA, CTP, MRA, and MRP. Although there is no perfect

method of vasospasm diagnosis, DSA is widely regarded as the current gold standard. At best, there is moderately strong evidence regarding the diagnostic accuracy of the noninvasive modalities mentioned above. According to a meta-analysis of CTA and CTP, the sensitivities and specificities are approximately 80 % and 93 % for CTA and 74 % and 93 % for CTP, respectively [53]. TCD sensitivity and specificity for detection of MCA vasospasm are approximately 67 % and 99 % [54]. There is insufficient data regarding the diagnostic performance of MRA or MRP for vasospasm diagnosis. Regarding vasospasm treatment, there is strong evidence supporting the use of nimodipine in A-SAH patients, although its effects are thought to be related to neuroprotection and not the prevention of angiographic vasospasm. There is preliminary evidence that induced hypertension is effective in increasing CBF, although this is insufficient. There is moderate evidence that papaverine infusion results in short-lived clinical improvement in approximately 40 % of patients treated for vasospasm [55]. However, there is still insufficient evidence regarding the utility of other vasodilatory medications such as verapamil, which are being used more frequently given their lower incidence of adverse reactions compared to papaverine. Balloon angioplasty has been shown to result in clinical improvement in approximately 60 % of patients, although no prospective randomized clinical trials have been performed to show that it ultimately improves patient outcomes [55].

Supporting Evidence

Several diagnostic modalities are commonly utilized in clinical practice for the diagnosis of vasospasm in A-SAH patients. To date, DSA is the most widely accepted gold standard for vasospasm, and other diagnostic modalities such as TCD, CTA, CTP, MRA, and MRP have been compared to it in order to determine their relative diagnostic performances. Regarding the evidence behind CTA and CTP, there is a single meta-analysis published comparing CTA and CTP to DSA for the diagnosis of vasospasm in A-SAH patients [53]. This meta-analysis was limited by the number of relevant studies available for

statistical analysis, incomplete data reporting in many of the studies, the high variability in methodology between studies, and the overall high level of heterogeneity of the data. Despite these limitations, this meta-analysis provides the best current estimate of the diagnostic accuracy of CTA and CTP, although the results should be considered preliminary. The estimated pooled sensitivity and specificity of CTA were 79.6 % (95 % CI, 74.9–83.8 %) and 93.1 % (95 % CI, 91.7–94.3 %), respectively, and the estimated pooled sensitivity and specificity of CTP were 74.1 % (95 % CI, 58.7–86.2 %) and 93.0 % (95 % CI, 79.6–98.7 %), respectively [53]. The area under the summary receiver operating characteristic (SROC) curve was 98 ± 2.0 % for CTA and 97 ± 3.0 % for CTP [53].

Regarding TCD, a meta-analysis comparing TCD with DSA showed that for the middle cerebral artery (5 trials, 317 tests) and using a velocity threshold of 120 cm/s, the sensitivity was 67 % (95 % CI, 48–87 %), and the specificity was 99 % (95 % CI, 98–100 %). For the anterior cerebral artery (3 trials, 171 tests), sensitivity was 42 % (95 % CI, 11–72 %), and specificity was 76 % (95 %, CI 53–100 %). Data for the meta-analysis was only available from 7 trials, and the authors indicate that most of these data were of low methodological quality [54]. Since that meta-analysis, a number of studies have been performed to further assess the diagnostic performance of TCD compared to DSA for vasospasm diagnosis. A prospective study on TCD diagnosis of MCA vasospasm using DSA as the gold standard demonstrated that the diagnostic accuracy of TCD for moderate-to-severe MCA vasospasm using peak systolic velocity and Lindegaard index was 0.93 and 0.95, respectively. For the diagnosis of mild MCA vasospasm, diagnostic accuracy based on these two parameters was 0.90 and 0.91, respectively [56]. A second prospective study compared TCD and transcranial color sonography (TCCS) using DSA as the reference standard for the diagnosis of MCA vasospasm. The authors of that study reported that the TCD and TCCS accuracy ranged from 76 % to 82 % [57]. A retrospective study of TCCS accuracy compared to DSA concluded that the overall

diagnostic accuracy of TCCS for the diagnosis of MCA vasospasms was 0.8, with ROC analysis indicating that the optimal tradeoff between sensitivity and specificity in diagnosing vasospasm was at a threshold peak systolic velocity of 182 cm/s [58]. Another retrospective study evaluating the accuracy of TCD compared to DSA in predicting angiographic vasospasm demonstrated that in patients with TCD findings positive for vasospasm, the diagnostic odds ratio of detecting vasospasm on angiography was 27 for the ACA territory and 17 for the MCA territory [59].

MRA and MRP have also been studied for their potential role in vasospasm diagnosis. In a small series of 21 patients, Blasel et al. evaluated the accuracy of time-of-flight MR angiography (TOF-MRA) for the diagnosis of vasospasm in A-SAH patients. They report that 44.2 % of maximum intensity projection (MIP) images overestimated the vascular narrowing seen on DSA and therefore conclude that TOF-MRA may not be an appropriate test for vasospasm diagnosis [60]. Another study comparing MRA and DSA for vasospasm diagnosis reported MRA to have a 92 % sensitivity and a 97 % specificity for vasospasm diagnosis, but those results are based upon a definition of vasospasm as >25 % vessel narrowing, thus combining moderate and severe vasospasm patients into a single group [61]. Regarding MRP imaging and vasospasm diagnosis, there are a limited number of small studies in the literature, most of which involve few patients and are retrospective analyses. One prospective study correlating DSA findings with MRP time-to-peak (TTP) values reported significant delays in cerebral circulation time as measured by MRP in patients with vasospasm seen on DSA [62]. A second prospective study in which MRP and DSA were performed about 5 days after onset of SAH reported decreased rCBF and rCBV in patients with SAH and vasospasm, with the decrease in rCBF proportional to the degree of vasospasm [63]. MRP has been shown to be useful for determining the hemodynamic effects of balloon angioplasty in the treatment of vasospasm. A prospective study of 10 patients by

Beck et al. reported improvement in MRP parameters after balloon angioplasty treatment for vasospasm [64].

Efficacious Vasospasm Treatments

All A-SAH patients should undergo prophylactic measures to prevent vasospasm and delayed cerebral ischemia. There is strong evidence supporting the use of nimodipine in A-SAH patients, although its effects are thought to be related to neuroprotection and not to the prevention of angiographic vasospasm. Nimodipine antagonizes voltage-gated calcium channels and reduces the entry of calcium into smooth muscle cells and neurons. Several randomized trials have shown that nimodipine has a statistically significant positive effect on outcome in patients with A-SAH [65–71]. A Cochrane database systematic review of calcium antagonists in the setting of A-SAH concluded that calcium antagonists reduce the risk of poor outcome and secondary ischemia after A-SAH and are therefore indicated in these patients [72].

The use of hydroxymethylglutaryl coenzyme A reductase inhibitors (statins) has been shown in some studies to prevent vasospasm in A-SAH patients [73–75]. The randomized controlled studies currently available show that statins do indeed reduce the incidence of delayed cerebral ischemia in A-SAH patients, with a trend toward lower mortality also reported [76]. However, when observational studies are included in the analysis, statins have no statistically significant effect on the incidence of delayed cerebral ischemia in this patient population [76].

Magnesium administration has been shown to have some benefit for preventing vasospasm in A-SAH patients. The largest randomized controlled trial to date showed a 34 % reduction in the risk of delayed ischemic injury in patients receiving magnesium, and a smaller randomized controlled study reported a 29 % decreased risk [77, 78]. A meta-analysis demonstrated that although administration of magnesium reduced the likelihood of a poor

outcome after SAH (death, vegetative state, or dependency), patient mortality was not improved [79].

A systematic review analyzing the potential benefit of prophylactic "Triple H" (hypertension, hypervolemia, and hemodilution) or "hyperdynamic" therapy in A-SAH patients reported an overall paucity of data as well as significant limitations in the design of the available studies which precluded an accurate assessment of the potential benefit of this treatment [80].

A multicenter, randomized clinical trial performed to evaluate the utility of prophylactic balloon angioplasty on cerebral vasospasm and outcome in patients with Fisher grade III SAH showed that balloon angioplasty does not result in improvement in outcome of Fisher grade III A-SAH patients [81].

Patients with vasospasm are typically treated with "Triple H" therapy, intra-arterial infusion of vasodilators, and/or balloon angioplasty. Regarding "Triple H" therapy, there are no randomized clinical trials on the effect of such therapy on patient outcome. A Cochrane systematic review found no sound evidence for the use of volume expansion (hypervolemia) in patients with A-SAH [82]. Likewise, there is no data to support hemodilution in the setting of A-SAH. A systematic review on the effect of "Triple H" therapy on CBF in A-SAH patients concluded that there is no good evidence that such therapy results in an increase in CBF, although induced hypertension is considered the most promising component of "Triple H" therapy [83]. The conclusions of this study are only preliminary given the small sample sizes (4–51 patients per study), the heterogeneity of the interventions and the study populations, and the fact that only 1 of 11 studies was a randomized trial. Despite the lack of strong evidence regarding "Triple H" therapy, one prospective study demonstrated a significantly decreased rate of delayed cerebral ischemia as well as improved patient outcomes for those patients treated after the adoption of hypervolemic hemodilution strategies when compared with A-SAH

patients treated prior to the incorporation of such strategies [84].

Selective intra-arterial infusion of vasodilatory medications is also used in the treatment of vasospasm. Papaverine hydrochloride, a derivative of opium, is known to cause arterial dilatation, probably by a phosphodiesterase inhibitory mechanism. The reported success rates of intra-arterial papaverine infusion range widely in the literature. However, a systematic review performed by Hoh et al. in 2005 found that there was overall clinical improvement in 43 % of patients (148/346) [55]. Important limitations of papaverine infusion include its short-lived effect as well as its tendency to increase intracranial pressure. Given these limitations, other intra-arterial vasodilating agents have come into favor more recently, such as verapamil and other calcium channel blockers [85–87]. Although these agents appear to be safer than papaverine, their utility is not established.

An initial study of balloon angioplasty in 33 A-SAH patients with vasospasm reported successful treatment of angiographic vasospasm and improved clinical symptoms [88]. Subsequent retrospective studies supported these initial findings, showing improvement rates in clinical symptoms from 31 % to 92 % [89]. However, no prospective randomized clinical trial has been performed regarding balloon angioplasty to show that it ultimately improves patient outcomes. A systematic review performed by Hoh et al. in 2005 analyzed the benefit of balloon angioplasty and infusion of intra-arterial vasodilators. The authors reported overall clinical improvement in 62 % of patients (328/530) after balloon angioplasty [55]. There is some evidence that clinical improvement may be related to the timing of the angioplasty procedure, with significantly better results reported with angioplasty done within 24 h and within 2 h of the neurological change [90, 91]. However, a study by Eskridge et al. showed that patients treated within 12 h from the onset of symptoms did not differ significantly from patients treated within 18 h [92].

Take-Home Tables

Tables 14.1 and 14.2 highlight aneurysm detection and vasospasm diagnosis, respectively.

Imaging Case Studies

Case 1: 65-Year-Old Female with No Past Medical History Presented with "the Most Painful Headache of My Life" (Fig. 14.1a–g)

Case 2: 59-Year-Old Female Presented with "the Most Painful Headache of My Life" (Fig. 14.2a–e)

Case 3: 51-Year-Old Female with a Family History of Aneurysms and Subarachnoid Hemorrhage Presented with Frequent Headaches (Fig. 14.3a–c)

Case 4: 52-Year-Old Woman with Right-Hand Clumsiness (Fig. 14.4a–d)

Case 5: Patient Developed Increased Lethargy 14 Days Post Hemorrhage (Fig. 14.5a–c)

Case 6: 48-Year-Old Male Presented to the ED with Headache in the Setting of Cocaine Use (Fig. 14.6a–d)

Suggested Imaging Protocol: Nontraumatic SAH

The following imaging protocol (Fig. 14.7) was adapted from Agid et al. [31]. An important caveat of this imaging protocol is that patients treated solely on the basis of CTA findings may rarely harbor additional aneurysms, or other vascular lesions, not detected by that modality, and the impact of this is not certain.

Table 14.1 Aneurysm detection

Modality	Sensitivity	Specificity	AUC (ROC)	Limitations	Costs
DSA	NA	NA	NA	Invasive procedure, contrast, and radiation	$$$$
CTA, per patient. Westerlaan et al.	98.0 %	100 %	1.00	Contrast and radiation	$$
MRA, per patient. White et al.	87.0 %	92.0 %	0.89	No significant risks	$$$

Table 14.2 Vasospasm diagnosis

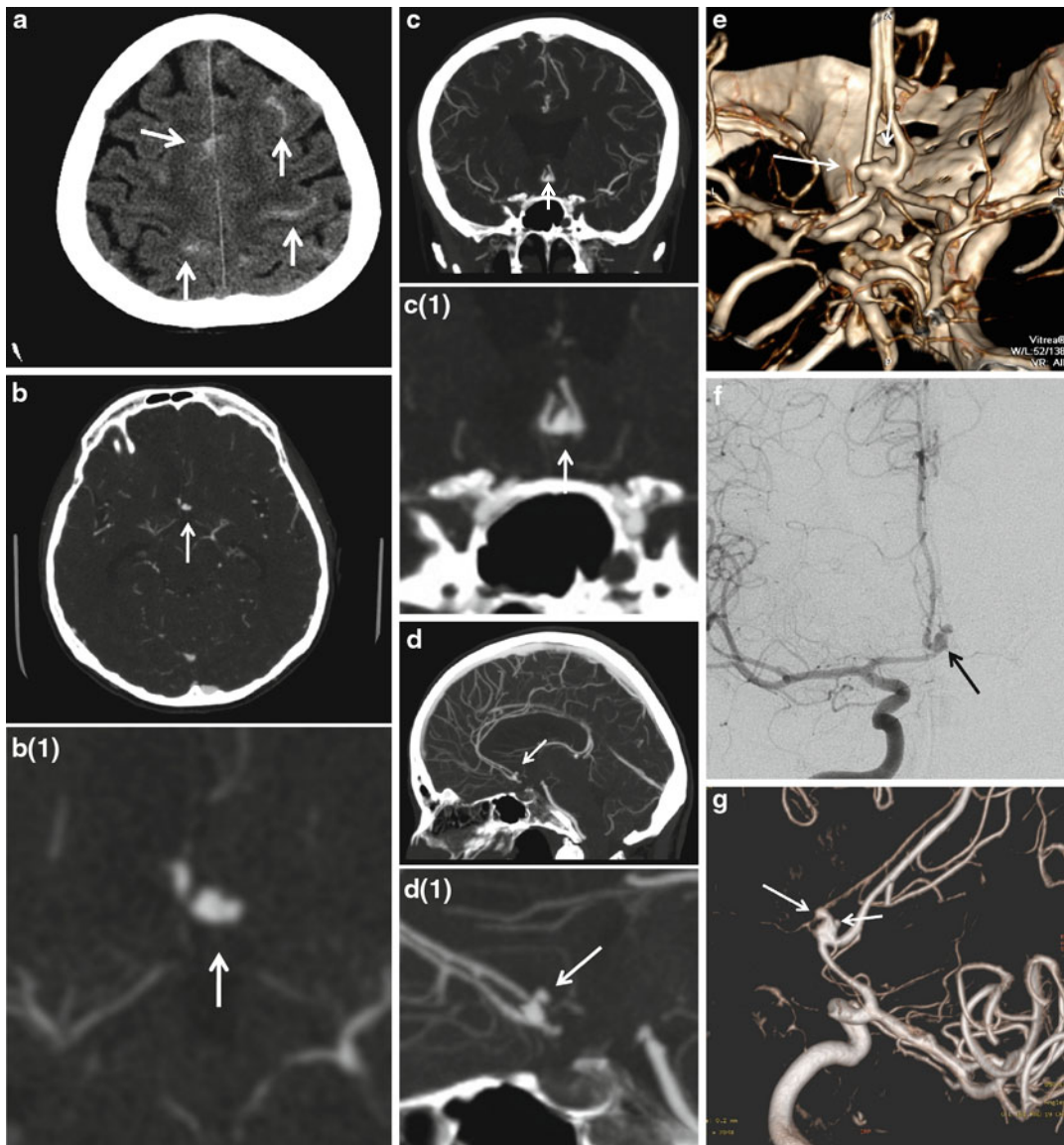| TCD (MCA vasospasm, 120 cm/s velocity threshold)	67.0 %	99.0 %	NA	Operator dependence and lack of adequate sonographic windows to evaluate all vessels	$
CTA	79.6 %	93.1 %	0.98	Contrast and radiation	$$
CTP	74.1 %	93.0 %	0.97	Contrast and radiation	$$
MRA (42 patients, Grandin et al.)	92.0 %	97.0 %	NA	No significant risks	$$$
MRP	NA	NA	NA	Contrast material reaction and NSF	$$$

Fig. 14.1 (**a–g**) A 65-year-old female with no past medical history presented with "the most painful headache of my life." (**a**) Non-contrast-enhanced CT(NECT) of the head shows SAH (*white arrows*). (**b**) Subsequent CTA shows a multilobulated aneurysm of the anterior communicating artery. Axial source images demonstrate the aneurysm (*white arrow*), which extended over several slices above and below the displayed image. The magnification (**b**(1)) view shows the aneurysm to better advantage (*white arrow*). (**c**) Coronal maximum intensity projection (MIP) reformats show both **a**2 segments of the anterior cerebral arteries arise from the aneurysm (*white arrow*); **c**(1) is the magnification. (**d**) Sagittal maximum intensity projection (MIP) reformats reveal the superiorly and posteriorly oriented daughter sac (*white arrow*); **d**(1) is the magnification. (**e**) 3-D surface-rendered reformatted image again shows the orientation of the aneurysm and its relationship to the parent vessel, and clearly shows the two lobulations, or daughter sacs (*white arrows*). Both **a**2 segments of the anterior cerebral arteries arise from the aneurysm. (**f**) Right ICA injection from DSA confirms the CTA findings (*black arrow*). (**g**) 3-D rotational angiography was performed via a right internal carotid artery injection. The reconstructed images nicely illustrate the lobular contour of the aneurysm, as well as the *right* **a**2 segment arising from the aneurysm (the *left* **a**2 segment is not seen on this injection)
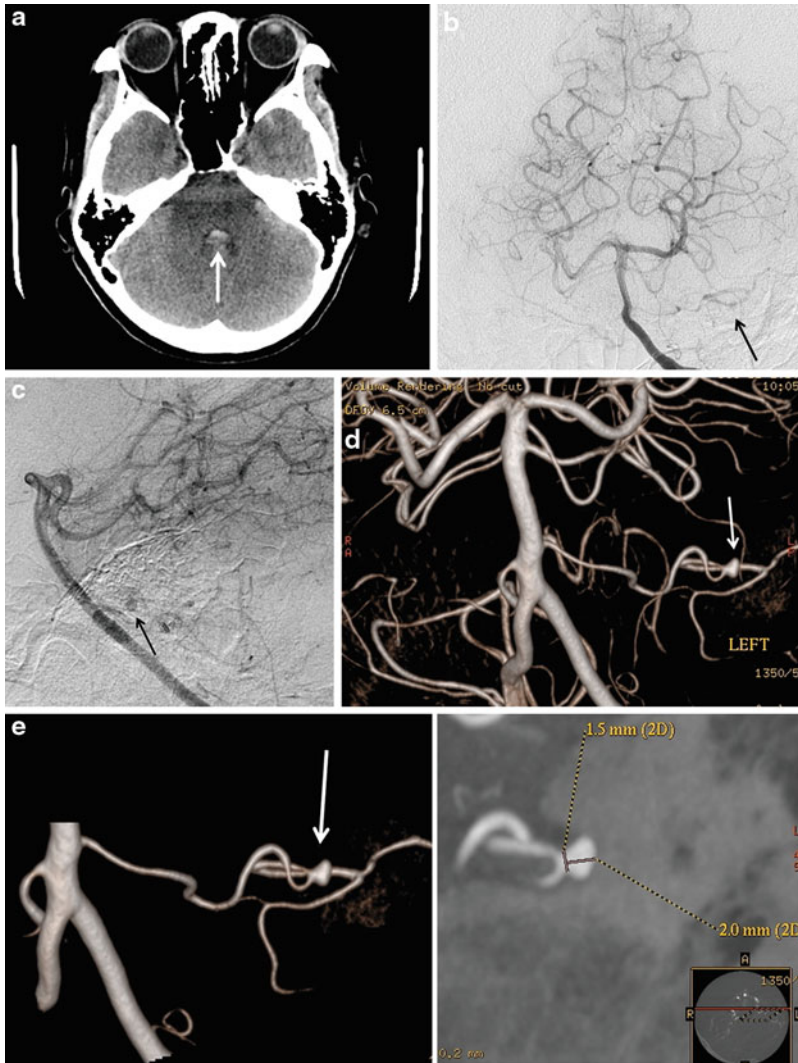
Fig. 14.2 (**a**–**e**) A 59-year-old female presented with "the most painful headache of my life." (**a**) NECT shows fourth ventricular hemorrhage (*white arrow*). No aneurysm was detected by CTA. (**b**, **c**) Left vertebral injection of DSA showed questionable prominence of vessels in the region of the distal left anterior inferior cerebellar artery (AICA) (*black arrows*). (**d**, **e**) Surface-rendered reformats from 3-D rotational clearly demonstrate an aneurysm of the left AICA measuring 2.0 × 1.5 mm (*white arrows*). The patient underwent endovascular embolization of the aneurysm and parent artery with NBCA glue, with excellent result
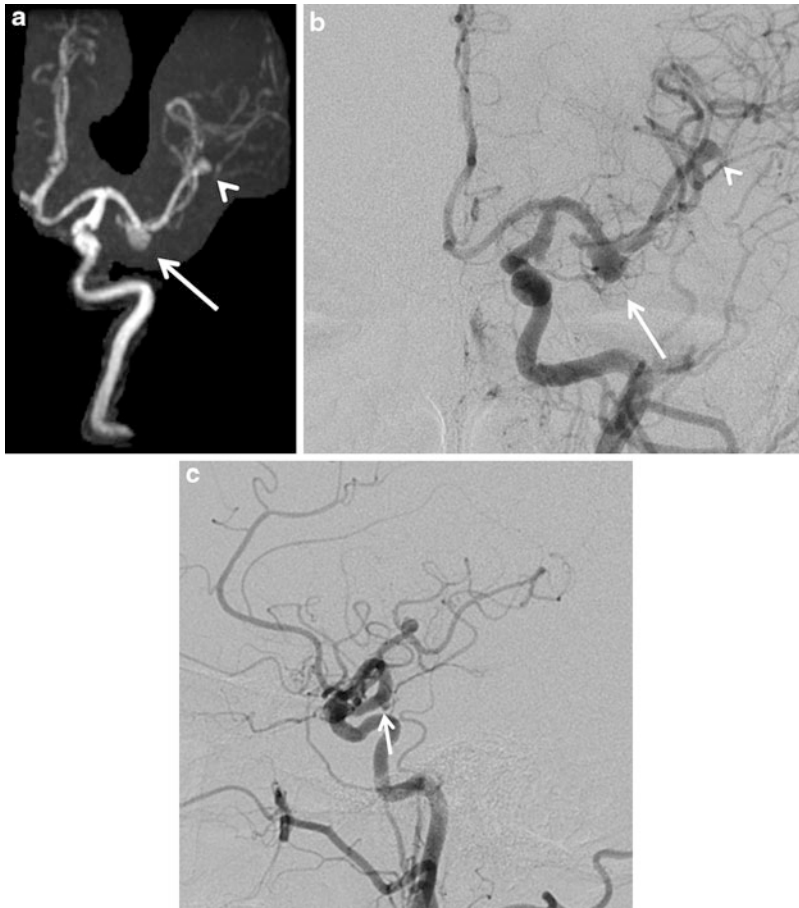
Fig. 14.3 (**a–c**) A 51-year-old female with a family history of aneurysms and subarachnoid hemorrhage presented with frequent headaches. (**a**) 3-D TOF MRA detected two left MCA aneurysms, one at the bifurcation directed inferiorly (*white arrow*) and a second more distal aneurysm directed superolaterally (*white arrowhead*). In addition, a possible anterior choroidal aneurysm or infundibulum was noted. (**b**, **c**) Frontal and lateral projections from a left common carotid injection redemonstrate the two MCA aneurysms (*white arrow and white arrowhead*, respectively). However, on the lateral projection of this DSA, there is clearly an infundibulum of the left anterior choroidal artery, not an aneurysm (*white arrow*)
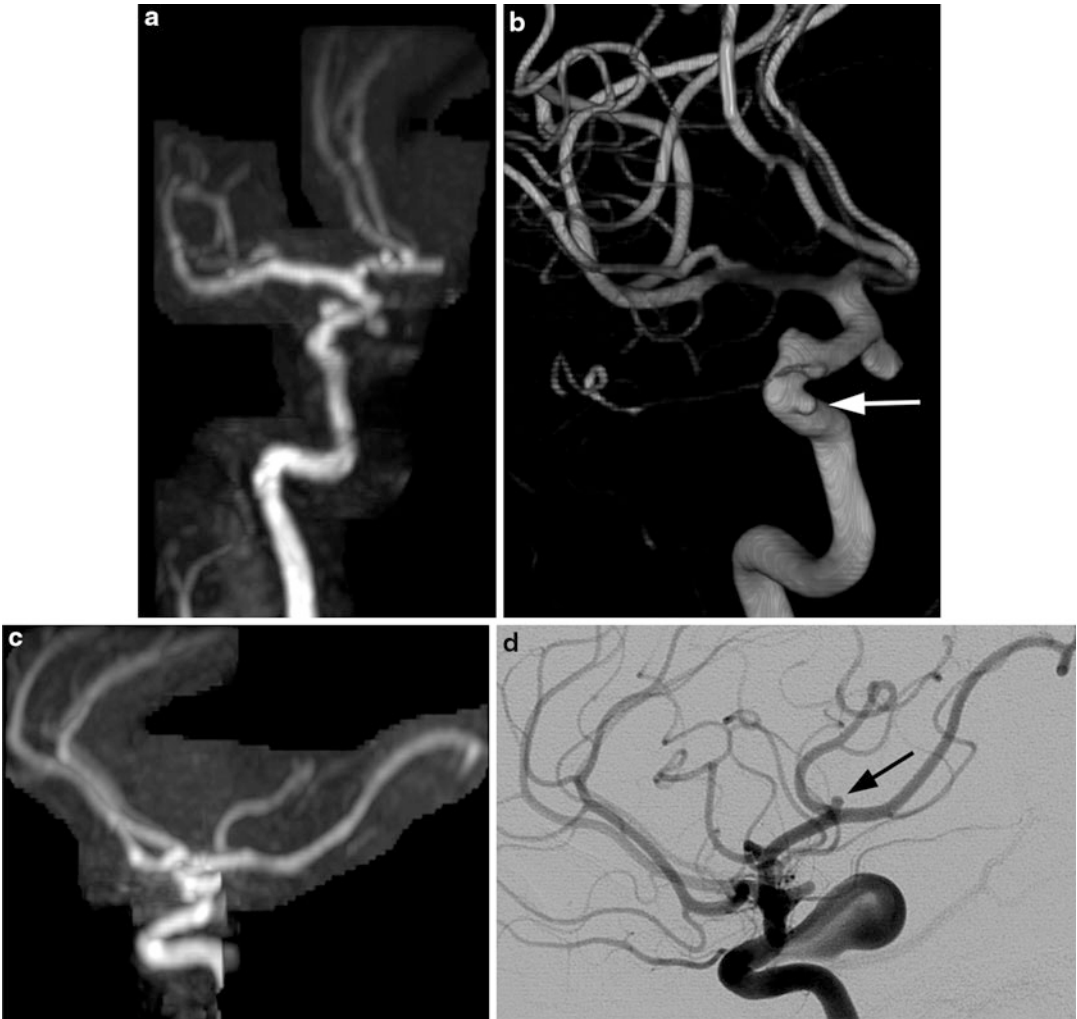
Fig. 14.4 (**a**–**d**) 52-year-old woman with right-hand clumsiness. MRA was obtained as part of evaluation for stroke, and multiple aneurysms were found. (**a**) 3-D volume-rendered reformat of the right ICA shows a posterior communicating artery and supraclinoid carotid artery aneurysm. (**b**) Subsequent DSA demonstrates an additional cavernous ICA aneurysm, occult by MRA (*white arrow*). (**c**, **d**) DSA also demonstrates an occult left MCA bifurcation aneurysm (*black arrow* in **d**)
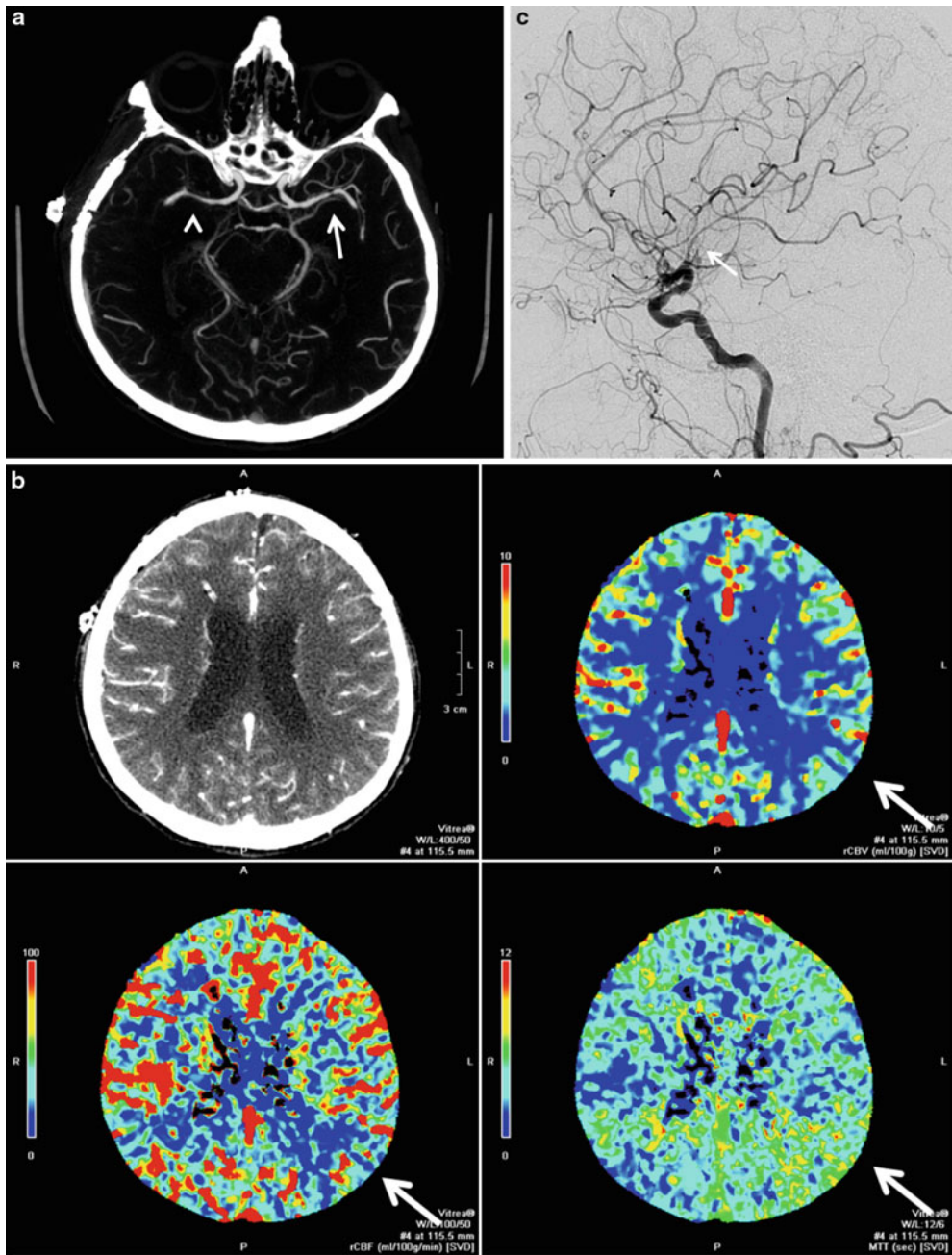
Fig. 14.5 (a–c) On day 14 post hemorrhage, the patient whose initial imaging is depicted in Fig. 14.1 developed increased lethargy. CTA and CT perfusion (CTP) performed to evaluate for vasospasm. (a) CTA demonstrates severe focal narrowing of the left distal M1 segment of the MCA, consistent with vasospasm (*white arrow*). There is also moderate narrowing of the right M1 (*white arrowhead*). (b) CTP demonstrates elevated mean transit time (MTT) in the left parietal lobe (*bottom right*) with corresponding decreased cerebral blood flow (CBF, *bottom left*) and preserved cerebral blood volume (CBV, *top right*) (*white arrows*). These findings suggest cerebral hypoperfusion secondary to vasospasm. (c) On the basis of these clinical and imaging findings, the patient was taken DSA. A lateral projection of a left common carotid injection confirms the presence of vasospasm, with multiple areas of arterial narrowing involving left MCA (*white arrow*)
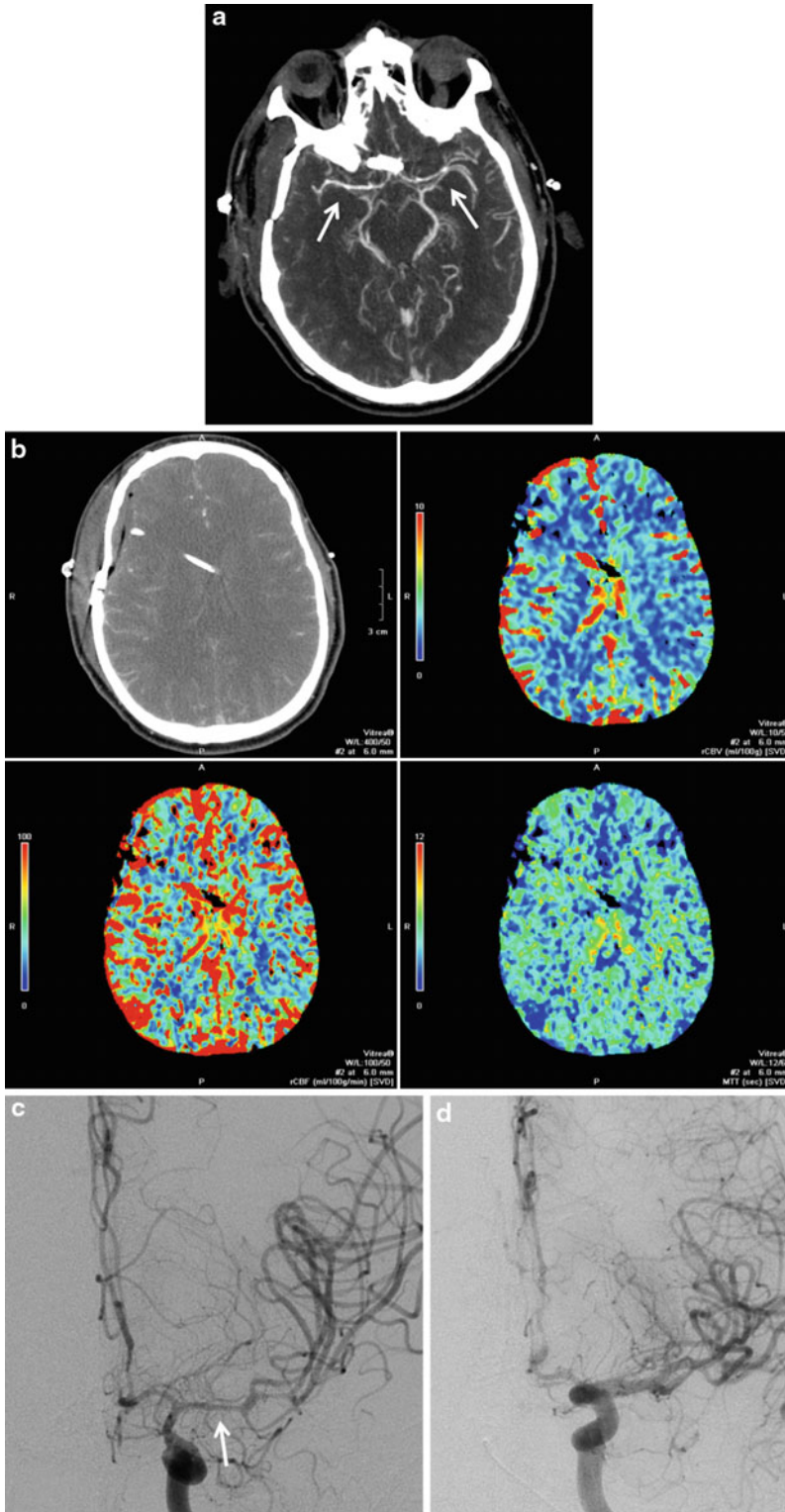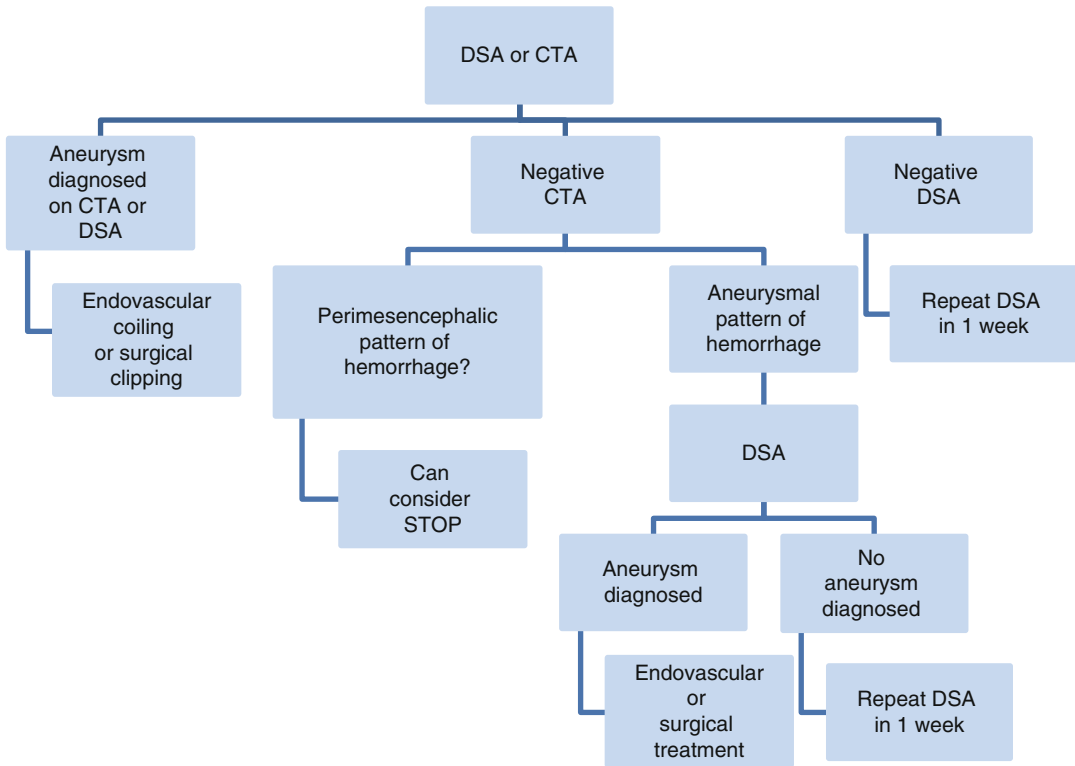
Fig. 14.6 (continued)

Fig. 14.7 Suggested imaging protocol for nontraumatic SAH

Fig. 14.6 (**a**–**d**) A 48-year-old male presented to the ED with headache in the setting of cocaine use. Diagnostic workup revealed a ruptured right MCA aneurysm which was surgically clipped. Ten days after hemorrhage, the patient presented with nonspecific personality changes. CTA and CTP was performed. (**a**) Axial MIP image from CTA shows moderate to severe bilateral MCA narrowing consistent with vasospasm (*white arrows*). (**b**) CTP demonstrates symmetric perfusion, with no definite focal perfusion deficit noted. (**c**) Based on the clinical and CTA findings, the patient underwent DSA. PA projection of left internal carotid artery injections demonstrates moderate to severe vasospasm of the proximal left MCA, with involvement of the **a**1 and **a**2 segments of the left ACA as well (*white arrows*). (**d**) The patient was treated with a combination of intra-arterial verapamil and balloon angioplasty of the left MCA. Posttreatment PA projection demonstrates marked improvement in caliber of the M1 and M2 segments, in the regions where angioplasty was performed (*white arrow*)

Future Research

- Improving the diagnostic performance of CTA and MRA, with the goal of acquiring diagnostic information similar to DSA without having to perform an invasive procedure
- Assessing the risk of aneurysm rupture as well as predictors of aneurysm rupture in order to better stratify patients for treatment
- Assessing long-term outcomes for patients who have undergone surgical or interventional treatment for an intracranial aneurysm(s)
- Assessing the diagnostic performance of perfusion studies (CTP and MRP) for vasospasm diagnosis
- Understanding the underlying pathophysiology of cerebral vasospasm in an attempt to improve diagnostic and treatment approaches
- Performing randomized trials of the various medical and interventional treatments for vasospasm

References

1. Krings T, Piske RL, Lasjaunias PL. Neuroradiology. 2005;47:931–7.
2. Hashimoto T, Meng H, Young WL. Neurol Res. 2006;28:372–80.
3. Bederson JB, Connolly Jr ES, Batjer HH, et al. Stroke. 2009;40:994–1025.
4. Feigin VL, Rinkel GJ, Lawes CM, et al. Stroke. 2005;36:2773–80.
5. Vergouwen MD, Vermeulen M, van Gijn J, et al. Stroke. 2010;41:2391–5.
6. Frontera JA, Fernandez A, Schmidt JM, et al. Stroke. 2009;40:1963–8.
7. Rinkel GJ, Djibuti M, Algra A, van Gijn J. Stroke. 1998;29:251–6.
8. Fisher CM, Roberson GH, Ojemann RG. Neurosurgery. 1977;1:245–8.
9. Murayama Y, Nien YL, Duckwiler G, et al. J Neurosurg. 2003;98:959–66.
10. Dodel R, Winter Y, Ringel F, et al. Stroke. 2010;41:2918–23.
11. Rivero-Arias O, Gray A, Wolstenholme J. Cost Eff Resour Alloc. 2010;8:6.
12. Rivero-Arias O, Wolstenholme J, Gray A, et al. J Neurol. 2009;256:364–73.
13. Chou CH, Reed SD, Allsbrook JS, Steele JL, Schulman KA, Alexander MJ. Neurosurgery. 2010;67:345, 51; discussion 351–2.
14. Wilby MJ, Sharp M, Whitfield PC, Hutchinson PJ, Menon DK, Kirkpatrick PJ. Stroke. 2003;34:2508–11.
15. Bardach NS, Olson SJ, Elkins JS, Smith WS, Lawton MT, Johnston SC. Circulation. 2004;109:2207–12.
16. White PM, Wardlaw JM, Easton V. A systematic review. Radiology. 2000;217:361–70.
17. van Gelder JM. Neurosurgery. 2003;53:597, 605; discussion 605–6.
18. Chappell ET, Moure FC, Good MC. Neurosurgery. 2003;52:624, 31; discussion 630–1.
19. Westerlaan HE, van Dijk MJ, Jansen-van der Weide MC, et al. Radiology. 2011;258:134–45.
20. van Rooij WJ, Sprengers ME, de Gast AN, Peluso JP, Sluzewski M. AJNR Am J Neuroradiol. 2008;29:976–9.
21. van Rooij WJ, Peluso JP, Sluzewski M, Beute GN. AJNR Am J Neuroradiol. 2008;29:962–6.
22. Ishihara H, Kato S, Akimura T, Suehiro E, Oku T, Suzuki M. J Clin Neurosci. 2007;14:252–5.
23. Zhang LJ, Wu SY, Poon CS, et al. J Comput Assist Tomogr. 2010;34:816–24.
24. Zhang LJ, Wu SY, Niu JB, et al. AJR Am J Roentgenol. 2010;194:23–30.
25. White PM, Teasdale EM, Wardlaw JM, Easton V. Radiology. 2001;219:739–49.
26. Yoshimoto Y, Wakai S. Stroke. 1999;30:1621–7.
27. Bor AS, Koffijberg H, Wermer MJ, Rinkel GJ. Neurology. 2010;74:1671–9.
28. Taschner CA, Thines L, Lernout M, Lejeune JP, Leclerc X. J Neuroradiol. 2007;34:243–9.
29. van der Jagt M, Flach HZ, Tanghe HL, et al. Cerebrovasc Dis. 2008;26:482–8.
30. Miley JT, Taylor RA, Janardhan V, Tummala R, Lanzino G, Qureshi AI. Neurocrit Care. 2008;9:300–6.
31. Agid R, Lee SK, Willinsky RA, Farb RI, ter Brugge KG. Neuroradiology. 2006;48:787–94.
32. Westerlaan HE, Gravendeel J, Fiore D, et al. Neuroradiology. 2007;49:997–1007.
33. Topcuoglu MA, Ogilvy CS, Carter BS, Buonanno FS, Koroshetz WJ, Singhal AB. J Neurosurg. 2003;98:1235–40.
34. Urbach H, Zentner J, Solymosi L. The need for repeat angiography in subarachnoid haemorrhage. Neuroradiology. 1998;40:6–10.
35. du Mesnil de Rochemont R, Heindel W, Wesselmann C, et al. Radiology. 1997;202:798–800.
36. Casasco AE, Aymard A, Gobin YP, et al. J Neurosurg. 1993;79:3–10.
37. Gobin YP, Vinuela F, Gurian JH, et al. J Neurosurg. 1996;84:55–62.
38. Molyneux AJ, Kerr RS, Yu LM, et al. Lancet. 2005;366:809–17.
39. Molyneux AJ, Kerr RS, Birks J, et al. Lancet Neurol. 2009;8:427–33.
40. Raper DM, Allan R. Neurosurgery. 2010;66:1166, 9; discussion 1169.
41. Bakker NA, Metzemaekers JD, Groen RJ, Mooij JJ, Van Dijk JM. Neurosurgery. 2010;66:961–2.

42. Johnston SC, Zhao S, Dudley RA, Berman MF, Gress DR. Stroke. 2001;32:597–605.
43. Weir B, Disney L, Karrison T. Sizes of ruptured and unruptured aneurysms in relation to their sites and the ages of patients. J Neurosurg. 2002;96:64–70.
44. Raymond J, Meder JF, Molyneux AJ, et al. J Neuroradiol. 2006;33:211–19.
45. Wiebers DO, Whisnant JP, Huston 3rd J, et al. Lancet. 2003;362:103–10.
46. Bederson JB, Awad IA, Wiebers DO, et al. Stroke. 2000;31:2742–50.
47. Huang J, McGirt MJ, Gailloud P, Tamargo RJ. Surg Neurol. 2005;63:424, 32; discussion 432–3.
48. Lasjaunias P, Wuppalapati S, Alvarez H, Rodesch G, Ozanne A. Childs Nerv Syst. 2005;21:437–50.
49. Hetts SW, Narvid J, Sanai N, et al. AJNR Am J Neuroradiol. 2009;30:1315–24.
50. Hoh BL, Chi YY, Lawson MF, Mocco J, Barker 2nd FG. Stroke. 2010;41:337–42.
51. Bairstow P, Dodgson A, Linto J, Khangure M. Australas Radiol. 2002;46:249–51.
52. Wolstenholme J, Rivero-Arias O, Gray A, et al. Stroke. 2008;39:111–19.
53. Greenberg ED, Gold R, Reichman M, et al. AJNR Am J Neuroradiol. 2010;31(10):1853–60.
54. Lysakowski C, Walder B, Costanza MC, Tramer MR. Stroke. 2001;32:2292–8.
55. Hoh BL, Ogilvy CS. Neurosurg Clin N Am. 2005;16:501, 16, vi.
56. Krejza J, Kochanowicz J, Mariak Z, Lewko J, Melhem ER. Radiology. 2005;236:621–9.
57. Swiat M, Weigele J, Hurst RW, et al. Crit Care Med. 2009;37:963–8.
58. Mariak Z, Krejza J, Swiercz M, Kordecki K, Lewko J. J Neurosurg. 2002;96:323–30.
59. Kincaid MS, Souter MJ, Treggiari MM, Yanez ND, Moore A, Lam AM. J Neurosurg. 2009;110:67–72.
60. Hattingen E, Blasel S, Dumesnil R, Vatter H, Zanella FE, Weidauer S. Neurosurg Rev. 2010;33:431–9.
61. Grandin CB, Cosnard G, Hammer F, Duprez TP, Stroobandt G, Mathurin P. AJNR Am J Neuroradiol. 2000;21:1611–17.
62. Weidauer S, Lanfermann H, Raabe A, Zanella F, Seifert V, Beck J. Stroke. 2007;38:1831–6.
63. Hattingen E, Blasel S, Dettmann E, et al. Neuroradiology. 2008;50:929–38.
64. Beck J, Raabe A, Lanfermann H, et al. J Neurosurg. 2006;105:220–7.
65. Allen GS, Ahn HS, Preziosi TJ, et al. N Engl J Med. 1983;308:619–24.
66. Barker 2nd FG, Ogilvy CS. J Neurosurg. 1996;84:405–14.
67. Mee E, Dorrance D, Lowe D, Neil-Dwyer G. Neurosurgery. 1988;22:484–91.
68. Ohman J, Heiskanen O. J Neurosurg. 1988;69:683–6.
69. Petruk KC, West M, Mohr G, et al. J Neurosurg. 1988;68:505–17.
70. Philippon J, Grob R, Dagreou F, Guggiari M, Rivierez M, Viars P. Acta Neurochir (Wien). 1986;82:110–14.
71. Pickard JD, Murray GD, Illingworth R, et al. BMJ. 1989;298:636–42.
72. Dorhout Mees SM, Rinkel GJ, Feigin VL, et al. Cochrane Database Syst Rev. 2007;3:CD000277.
73. Lynch JR, Wang H, McGirt MJ, et al. Stroke. 2005;36:2024–6.
74. Tseng MY, Czosnyka M, Richards H, Pickard JD, Kirkpatrick PJ. Stroke. 2005;36:1627–32.
75. Tseng MY, Hutchinson PJ, Czosnyka M, Richards H, Pickard JD, Kirkpatrick PJ. Stroke. 2007;38:1545–50.
76. Kramer AH, Fletcher JJ. Neurocrit Care. 2010;12:285–96.
77. van den Bergh WM, Algra A, van Kooten F, et al. Stroke. 2005;36:1011–15.
78. Westermaier T, Stetter C, Vince GH, et al. Crit Care Med. 2010;38:1284–90.
79. Zhao XD, Zhou YT, Zhang X, Zhuang Z, Shi JX. J Clin Neurosci. 2009;16:1394–7.
80. Treggiari MM, Walder B, Suter PM, Romand JA. J Neurosurg. 2003;98:978–84.
81. Zwienenberg-Lee M, Hartman J, Rudisill N, et al. Stroke. 2008;39:1759–65.
82. Rinkel GJ, Feigin VL, Algra A, van Gijn J. Cochrane Database Syst Rev. 2004;4:CD000483.
83. Dankbaar JW, Slooter AJ, Rinkel GJ, Schaaf IC. Crit Care. 2010;14:R23.
84. Vermeij FH, Hasan D, Bijvoet HW, Avezaat CJ. Stroke. 1998;29:924–30.
85. Feng L, Fitzsimmons BF, Young WL, et al. AJNR Am J Neuroradiol. 2002;23:1284–90.
86. Badjatia N, Topcuoglu MA, Pryor JC, et al. AJNR Am J Neuroradiol. 2004;25:819–26.
87. Biondi A, Ricciardi GK, Puybasset L, et al. IAJNR Am J Neuroradiol. 2004;25:1067–76.
88. Zubkov YN, Nikiforov BM, Shustin VA. Acta Neurochir (Wien). 1984;70:65–79.
89. Haque R, Kellner CP, Komotar RJ, et al. Neurol Res. 2009;31:638–43.
90. Bejjani GK, Bank WO, Olan WJ, Sekhar LN. Neurosurgery. 1998;42:979, 86; discussion 986–7.
91. Rosenwasser RH, Armonda RA, Thomas JE, Benitez RP, Gannon PM, Harrop J. Neurosurgery. 1999;44:975, 9; discussion 979–80.
92. Eskridge JM, McAuliffe W, Song JK, et al. Neurosurgery. 1998;42:510, 6; discussion 516–7.

Seizure Disorders: Evidence-Based Neuroimaging

15

Elysa Widjaja, Byron Bernal, and Nolan Altman

Contents

E. Widjaja (✉)
Department of Diagnostic Imaging, University of Toronto/Hospital for Sick Children, Toronto, ON, Canada
e-mail: elysa.widjaja@sickkids.ca

B. Bernal • N. Altman
Department of Radiology, Miami Children's Hospital, Miami, FL, USA
e-mail: Byron.bernal@mch.com; Nolan.altman@mch.com

Key Points

- The main goal of neuroimaging in acute seizures is to rule out focal lesions that could threaten the patient's life, such as neoplasm or other intracranial space-occupying lesion.
- CT scan is the best imaging study in the evaluation of patients with acute nonfebrile symptomatic seizures because it detects important abnormalities such as acute intracranial hemorrhage, which may require immediate medical or surgical treatment (limited evidence).
- Neuroimaging is not recommended for simple febrile seizure (limited evidence).
- The most important role of neuroimaging in epilepsy is to identify the structural substrate of the epileptogenic focus.
- MRI is the neuroimaging study of choice in the workup of first unprovoked seizures (moderate evidence).
- Focal neurological deficit is an important predictor of an abnormality in the neuroimaging examination (moderate evidence).
- MR evaluation should be performed in non-acute symptomatic seizure patients with confusion and postictal deficits (moderate evidence).
- MR should be performed in children with unexpected cognitive or motor delays or children under 1 year of age, with symptomatic seizures (moderate evidence).
- Patients with focal seizures or abnormal EEG should be imaged (moderate evidence).
- MRI is the imaging modality of choice in focal epilepsy, including temporal lobe epilepsy (moderate evidence).
- Ictal SPECT is the best neuroimaging examination to localize seizure activity (moderate evidence).

Definitions and Pathophysiology

A seizure is a symptom; epilepsy is a disease. Seizures occur as the result of an electrical discharge in the brain. Epilepsy is a disease characterized by more than one seizure. The International League Against Epilepsy [1] has proposed a classification of the epileptic syndromes, epilepsies, and related seizure disorders. Generalized and focal seizures are defined as seizures occurring in and rapidly involving bilaterally distributed networks (generalized) and within networks limited to one hemisphere, either discretely localized or more widely distributed (focal). Genetic, structural-metabolic, and unknown represent modified concepts to replace idiopathic, symptomatic, and cryptogenic categories in the prior classification. The causes of epilepsies are organized by electro-clinical syndromes, nonsyndromic epilepsies with structural-metabolic causes, and epilepsies of unknown cause.

The numerous categories produced from the classification of epilepsies can be confusing not only for the general physician but also for specialists. Some of the terminology from previous classification of seizures [2], such as idiopathic, symptomatic, and cryptogenic seizures, is still in use in clinical practice. Seizures have been categorized based on clinical findings: *symptomatic and non-symptomatic seizures*. The term "symptomatic" indicates that the seizure is a symptom with an underlying cause. This may be systemic (e.g., hyponatremia, hypocalcemia) or localized (e.g., tumor, focal cortical dysplasia, abscess). Depending upon how long the underlying cause predates the seizure, seizures are divided into "acute symptomatic" and "remote" symptomatic seizures. *Acute symptomatic seizures* occur as the result of a proximate precipitant such as fever, electrolyte imbalance, drug intoxication, alcohol withdrawal, brain trauma, central nervous system (CNS) infection, or aggressive neoplasm. In *remote symptomatic seizures*, the lesion is preexistent and the seizure is the main or only symptom; the lesions include focal cortical dysplasia, ganglioglioma, hippocampal sclerosis, scar, or gliosis. Non-symptomatic seizures include cryptogenic and idiopathic seizures. In *cryptogenic seizures* (or epilepsy), no cause can be found, even though one is clinically suspected by focal electroencephalography (EEG) or lateralized neurological examination. The term "unprovoked seizures" is used for seizures in patients without

history or abnormal *neurological* examination. They may turn out to be cryptogenic, idiopathic, or remote symptomatic after the appropriate workup. In the revised classification [1], seizures are categorized into generalized, focal, and unknown. Generalized seizures are subgrouped into tonic-clonic, absence, myoclonic, clonic, tonic, and atonic. Descriptions of focal seizures are based on the degree of impairment during seizure, such as dyscognitive or focal motor, and with or without impairment of consciousness or awareness.

Epidemiology

The prevalence of epilepsy in industrialized countries is between 5 and 10 cases per 1,000 persons [3]; hence, epilepsy affects between 1.5 and 3.0 million in the USA. Higher prevalence of epilepsy has been reported in developing countries [4], with some few exceptions. The incidence of epilepsy is age dependent. It peaks at the extremes of life, ranging between 100 and 140 per 100,000 in neonates and infants, and about 140 cases per 100,000 persons in the elderly. The incidence is lowest in early adulthood (25 per 100,000), followed by an increase during late adulthood [5]. Fifty percent of cases occur under the age of one year or over 60 years of age [3]. A different age-specific distribution is seen in developing countries with a second peak in early adulthood [6, 7].

Specific Epidemiological Data

Febrile seizures affect children between 6 months and 6 years of age. The cumulative incidence of febrile seizures is 2 % in children [8]. The two most important predictors for first episode of febrile seizures are age less than 1 year and family history of febrile seizures [9]. The overall incidence of febrile seizures recurrence is 35 % [10]. The recurrence of seizures after a focal febrile seizure lasting more than 15 min (complex febrile seizure) is two- to fourfold compared to an initial simple febrile seizure [11].

Acute afebrile symptomatic seizures affect 31 of 100,000 people per year and accounts for 40 % of all new-onset afebrile seizures. The incidence is highest in the neonatal period (100 per 100,000 inhabitants), with a second peak in patients older than 75 years (123 per 100,000).

The probability for recurrent seizures after an initial *unprovoked seizure* is 36 % by one year of age and increases yearly up to 56 % by 5 years [12]. The presence of neurodevelopmental abnormalities increases the probability of future unprovoked seizures [13]. The recurrence of all types of seizures ranges between 24 % and 67 % [14]. Of all patients with recurrent seizures, up to 20 % may have intractable epilepsy [15].

Overall Cost to Society

Murray et al. [16] analyzed the cost of neuroimaging in the US health system in 1994 for adult refractory epilepsy. CT was used in 60 % of new and in 5 % of existing cases of epilepsy, whereas MRI was requested in 90 % of new and 12 % of existing cases [16]. Cost was determined by multiplying the CT or MR incidence rate of usage, times the incidence of new-onset seizures, times the cost of the exam. The cost for an MRI of the brain in the United States is between $1,200 and $2,000 [17]. Therefore, the CT and MR workup expenses of new-onset seizures in the United States are between 28,000 and 84,000 dollars, per 100,000 inhabitants per year.

A French cohort study on medical costs of epilepsy in 1,942 patients [18] reported that neuroimaging studies accounted for 8 % of the total health-care costs for these patients.

Bronen et al. [19] have reported the economic impact of replacing CT with MR imaging for refractory epilepsy, based on the "assumption" that the higher sensitivity of MR in lesion detection would result in reducing the costs of intraoperative electrocorticography otherwise needed to localize the site of the epileptogenic focus. They found that in 29 of 117 patients, the replacement of CT by MRI eliminated the need for surgical placement of intracranial electrodes with potential savings of $1,450,000.

Goals of Imaging

The main goal of neuroimaging in seizures and epilepsy is to rule out focal lesions that could threaten the patient's life. Neuroimaging also allows the identification of the structural substrate of the epileptogenic focus. Neuroimaging may increase or decrease the pretest probability of having a particular etiology or confirm a clinical diagnosis.

Methodology

For each of the procedures ("proc"), MRI, CT, SPECT, PET, magnetoencephalography (MEG), fMRI, and diffusion tensor imaging (DTI) optic radiations, a systematic review of the literature was performed utilizing PubMed (National Library of Medicine, Bethesda, MD) with the following criteria:

1. ((Epilepsy [Title] OR seizure [Title]) AND (neuroimaging [Title] OR neuroimage [Title])) Field: Title, Limits: Publication Date from January of 1982 to September of 2011, only with abstracts in English, and in humans
2. ((Epilepsy [Title] OR Seizure [Title]) AND ("*proc*" [Title])). Field: Title, Limits: Publication Date from January of 1982 to September of 2011, only with abstracts in English, and in humans
3. Same keywords replacing [Title] by [Text Word]
4. ((EBM [Title] OR Evidence [Title]) AND (("seizures" [MeSH Terms] OR seizures [Text Word]) OR ("epilepsy" [MeSH Terms] OR epilepsy [Text Word]))) Field: Title, Limits: Publication Date from January of 1982 to September of 2011, only with abstracts in English, and in humans.

Titles and abstracts were reviewed to determine appropriateness of content. Articles were excluded if they had less than 20 patients, lacked pathological verification, had no standard of reference, or had no significant influence on clinical decision making. MRI articles less than 1.5 T were also excluded. The specificity, sensitivity, likelihood ratios, probability, predictors, and techniques were summarized for each procedure.

Seizures were divided into two main categories: new-onset seizures and established epilepsy, with particular emphasis on partial types. Adult and childhood epilepsy were addressed as well as febrile and temporal lobe epilepsy due to their clinical and radiological importance.

Each of the selected articles was reviewed, abstracted, and classified by two reviewers.

Of a total of 864 abstracts, 152 articles met inclusion criteria and the full text was reviewed in detail.

Discussion of Issues

Do Patients with Febrile Seizures Need Neuroimaging?

Summary
Neuroimaging is not recommended for a simple febrile seizure (limited evidence).

Supporting Evidence
No articles meeting the strong or moderate evidence criteria were found. Offringa et al. [20] reported an evidence-based study for the management of febrile seizures and the role of neuroimaging in regard to detection of meningitis (limited evidence). The overall prevalence of meningitis detected by CT/MRI scans was 1.2 % of 2,100 cases of seizures associated with fever. This manuscript, as well as the study by the American Academy of Pediatricians [21] (limited evidence), suggests that CT or MRI is not recommended for a simple febrile seizure.

What Neuroimaging Examination Do Patients with Acute Nonfebrile Symptomatic Seizures Need?

For clarity, acute nonfebrile symptomatic seizures occur in nonfebrile patients having neurological findings pointing to an underlying abnormality. It excludes meningitis, encephalitis, abscess, and empyema.

Summary

CT scan is the best imaging study in the evaluation of patients with acute symptomatology as it is sensitive for finding abnormalities such as acute intracranial hemorrhage, which may require immediate medical or surgical treatment. CT is also fast and readily available (limited evidence).

Supporting Evidence

No articles meeting the criteria for strong or moderate evidence were found. Several level III (limited evidence) studies were found as discussed. Eisner and colleagues [22] reported a study with 163 patients, who presented to the emergency room with first seizure (Table 15.1). All patients older than 6 years of age who had recent head trauma, focal neurologic deficit, or focal seizure activity underwent head CT. Of 19 patients, 5 (25 %) had CT abnormalities including one subdural hematoma, resulting in a change of medical care. Earnest and colleagues [23] found CT abnormalities in 6.2 % of 259 patients with alcohol withdrawal seizures. In 3.9 %, medical management was changed because of the CT result. Reinus and colleagues [24] retrospectively evaluated the medical records of 115 consecutive patients who had seizures after acute trauma and underwent a non-contrast cranial CT. An abnormal neurologic examination predicted 95 % (19 of 20) positive CT scans, P < .00004.

Henneman et al. [25] conducted a retrospective study on 333 patients with new-onset seizures, not associated with acute head trauma, hypoglycemia from diabetic therapy, or alcohol or recreational drugs. Of the 325 patients studied with CT scans, 134 (41 %) had clinically significant results.

Bradford and Kyriakedes [26] have reported an evidence-based review (limited evidence) of diagnostic tests in this population. The authors report a diagnostic yield of 87 % for CT. Predictors of abnormal CT scan in patients with new onset of seizures were head trauma, abnormal neurological findings, focal or multiple seizures (within a 24-h period), previous CNS disorders, and history of malignancy. The article concludes that there is supportive data to perform CT scanning in the evaluation of all first-time acute seizures of unknown etiology.

What Is the Role of Neuroimaging in Patients with First Unprovoked Seizures?

Summary

MRI is the neuroimaging study of choice in the workup of first unprovoked seizures (moderate evidence). Neuroimaging is positive in 3–38 % of cases. The probability is higher in patients with partial seizures and focal neurological deficit (Fig. 15.2a, b). Neuroimaging is advised in children less than 1 year of age and in those with significant unexplained cognitive or motor impairment, or prolonged postictal deficit. Significant neuroimaging findings impacting medical care were found in up to 50 % of adults and in 12 % of children.

Supporting Evidence

No level I (strong evidence) studies were available (Table 15.2). One level II paper (moderate evidence) was found describing a cohort study in which neuroimaging studies were performed in 218 of 411 children [27]. CT was performed in 159 and MR in 59 cases. The cohort was followed for a mean of 10 years, and none of the patients had evidence of neoplasm (accepted as the reference standard). Twenty-one percent of the 218 exams were abnormal. The most frequent diagnoses were encephalomalacia (16 cases) and cerebral dysgenesis (11 cases). Six children had gray matter migration disorders, which were only seen on MRI. In this study, a higher number of MRIs (34 %) than CT studies (22 %) were abnormal. In 4 cases (1.8 %), the results altered both the diagnosis and the acute management of the patient. Children in this study who had a neurological deficit (56 % vs. 12 %, P < 0.001), or abnormal EEG and partial seizures (P < 0.05) were more likely to have abnormal imaging.

A level III (limited evidence) study of 300 adults and children with an unexplained first seizure was reported by King et al. [28]. Ninety-two percent of these patients had neuroimaging. A total of 263 patients had MRI and 14 had only CT. Epileptogenic lesions were found in 38 patients (13 %). Of these, 17 had neoplasm, which changed medical care. MRI detected

abnormalities in 17 % of 154 patients with partial epilepsy. CT was performed in 28 of the 38 cases with lesions on MRI being concordant with MRI in only 12 cases. CT missed a cavernous angioma and eight tumors. In 49 patients that had generalized epilepsy as supported by generalized epileptiform abnormalities on EEG, all 49 had no lesions on MRI.

In pediatric studies, neuroimaging diagnostic performance was similar to the adult literature, according to an evidence-based study by Hirtz et al. [29] (limited evidence). However, the overall effect of neuroimaging on medical management was less in children than adults [29].

The role of CT in evaluating children with new-onset unprovoked seizure was analyzed in a retrospective study by Maytal et al. [30] (limited evidence). Of 66 patients, 21.2 % had abnormal CT results. The seizure etiology was clinically determined to be cryptogenic in 33 patients. Two of these children (6 %) had abnormal nonspecific CT findings that did not require intervention. No abnormal CT results were seen in 13 cases with complex febrile seizures.

In a level III (limited evidence) study of 408 adults, CT scanning revealed tumors in 3 % of patients. These patients were more likely to have recurrent seizures [31]. Other studies have shown a higher percentage of positive imaging results in this population. A total of 119 adult patients with new-onset seizure underwent CT of the brain. Focal structural brain lesions were found in 40 patients (34 %; 95 % confidence interval, 25–42 %). In 50 % of the patients, the imaging findings prompt an important change in therapeutic management. The major predictor for finding a focal lesion on CT was the presence of a focal neurological deficit (sensitivity of 50 %, specificity of 89 %) [32]. Another study evaluated 50 patients referred for CT from a group of 107 children with first unprovoked seizure. A total of 19 children had brain abnormalities on CT. Of these, six patients had significant changes in medical workup or treatment [33].

The Quality Standards Subcommittee of the American Academy of Neurology, the Child Neurology Society, and the American Epilepsy Society have published a special report on practice guidelines in the evaluation of first nonfebrile seizures in children (unprovoked seizure) based on EBM [29] (limited evidence). The selection criteria included some small sample studies, which lack stringent evidence-based medicine criteria. This review article included studies in adults and children. Analysis of the results found that a range of 0–7 % of children had lesions on CT, which changed management of epilepsy (i.e., tumors, hydrocephalus, arachnoid or porencephalic cysts, and cysticercosis). Focal lesions on CT were more common in adults (18–34 %).

Overall MRI found more lesions than CT but did not always change medical management (i.e., atrophy, mesial temporal sclerosis, and brain dysgenesis). This report concluded that there is insufficient evidence to support the recommendation for routine neuroimaging after the first unprovoked seizure. Neuroimaging, however, may be indicated in cases of focal seizures associated with positive neurological clinical findings. If a neuroimaging study is required, MR is the preferred modality. Emergency imaging with CT or MR should be performed in cases of long-lasting postictal focal deficit, or in those patients who remain confused several hours after the seizure. Nonurgent imaging studies with MRI should be considered in children less than 1 year of age, significant and unexplained cognitive or motor impairment, a partial seizure, EEG findings not consistent with benign partial epilepsy of childhood, and primary generalized epilepsy.

What Is the Most Appropriate Study in the Workup of Patients with Temporal Lobe Epilepsy of Remote Origin?

Summary

MRI is the imaging modality of choice in temporal lobe epilepsy (moderate evidence). The seizure focus may be lateralized by MRI volumetric techniques. MRI sensitivity reaches 97 % for hippocampal sclerosis using fluid-attenuated inversion recovery (FLAIR) imaging. Loss of digitations of the hippocampal head has a sensitivity of 92 % for

hippocampal sclerosis. Quantitative measurement of hippocampal size has a higher sensitivity than qualitative inspection with 76 % versus 71 %, respectively.

Supporting Evidence

No level I (strong evidence) studies available (Table 15.3). There is one prospective cohort level II study (moderate evidence) of neuroimaging in temporal lobe epilepsy of childhood [34]. Sixty-three children with new-onset temporal lobe epilepsy were included. MRI was performed in 58 (92 %) and CT in 48 (76 %). MRI was abnormal in 23 children (36.5 %) and included unilateral hippocampal sclerosis in 12, bilateral hippocampal sclerosis in one, temporal lobe tumor in eight, arachnoid cyst in one, and cortical dysplasia in one. CT was positive in 23 % of cases, which included all tumors, but failed to detect cases of hippocampal sclerosis. CT demonstrated calcifications in the posterior area of the hippocampus in one case that was not detected on MR. This lesion was shown to be a small hamartoma pathologically. The authors proposed three groups to classify partial seizures based on the relationship between neuroimaging findings, prior history, and age. Group I: developmental temporal lobe epilepsy (10 patients). Seizures begin in mid- to late childhood (mean age 8.2 years), and neurobehavioral problems are infrequent. This epilepsy is associated with tumors and malformations that are usually long-standing and nonprogressive cortical lesions such as gangliogliomas, dysembryoplastic neuroepithelial tumors, and pilocytic xanthochromic astrocytomas. Group II: temporal lobe epilepsy with hippocampal sclerosis (18 patients), including children with significant prior clinical history of neurologic insult, including complicated febrile seizures, hypoxic-ischemic encephalopathy, and meningitis. Group III: cryptogenic temporal lobe epilepsy (34 patients) in whom no etiology could be determined. A level III study (limited evidence) by Kramer et al. [35] studied the predictive value of abnormal neurological findings on the neuroimaging of 143 children with partial seizures. Fifty patients had neuroimaging abnormalities and 36 had abnormal clinical findings. The neurological

examination findings of hemiparesis, mental retardation, and neurocutaneous stigmata were risk factor in predicting abnormal neuroimaging findings. However, the abnormalities detected on neurological examination, or the type of seizure, were not predictive parameters in determining tumor resectability as shown by neuroimaging.

A recent level III study (limited evidence) by Berg and coworkers [36] reported the neuroimaging findings of a group of 613 children with newly diagnosed temporal lobe epilepsy. A total of 359 patients had partial seizures. Of this group, 312 (86.3 %) underwent imaging; 283 had MRI alone or with CT. Relevant abnormalities were found in 43 (13.8 % of those imaged). The strongest predictor of abnormal imaging was an abnormal motor examination (odds ratio: 18.9; 95 % confidence interval, 9.9–36.3 %; P < .0001).

The MR findings in 186 of 274 consecutive patients who underwent temporal lobectomy for intractable epilepsy were retrospectively reviewed (moderate evidence) (Table 15.4) [37]. This was a blinded study with pathology as the reference standard. MR imaging detected 121 hippocampal/amygdala abnormalities (sensitivity and specificity of 93 % and 83 %, respectively) and 60 other abnormalities in the remainder of the temporal lobe (sensitivity and specificity of 97 % and 97 %, respectively). Increased signal of the hippocampus on T2-weighted images had a sensitivity of 93 % and specificity of 74 % in predicting mesial temporal sclerosis (Fig. 15.3). Forty-two temporal tumors were detected with a sensitivity and specificity of 83 % and 97 %, respectively.

The sensitivity of CT and MRI in temporal lobe pathology was recently reported by Sinclair et al. [38] (limited evidence). Forty-two pediatric patients were studied. All patients underwent temporal lobectomy for intractable epilepsy, hence, providing histopathology as the reference standard. MRI revealed abnormalities in 27 cases (64 %) while CT scan in 12 of 39 cases (31 %). MRI was clearly more sensitive than CT in the detection of pathology.

The MRI sensitivity to demonstrate the epileptogenic zone determined by EEG (a weak standard reference) was investigated in a level

III study (limited evidence). The weakness of the reference standard is in part compensated by the number of cases. Pooled data of 809 patients, of whom 370 had temporal lobe abnormalities, were analyzed [39]. The sensitivity of MRI was 55 % for temporal epileptogenic zones and 43 % for extratemporal regions as determined by EEG.

Moore et al. [40] address the incidence of hippocampal sclerosis in normal subjects in a level III article (limited evidence). They studied 207 patients referred for hearing loss with high-resolution MRI and found two cases of unsuspected hippocampal sclerosis. Retrospective chart review revealed that both patients had seizures. One of them had seizure onset 18 months prior to the MRI study that was believed to be associated with hemorrhage from an arteriovenous malformation ipsilateral to the hippocampal sclerosis.

The most important neuroimaging findings in hippocampal sclerosis are small size (atrophy) and intense T2 signal of the hippocampus (Table 15.5). These signs have been quantified in a level III retrospective study (limited evidence) of 41 MRI of patients who underwent temporal lobectomy [41]. The authors compared measurements of the left and right hippocampal formations and found them to have 76 % sensitivity and 100 % specificity for correct seizure lateralization.

Watson et al. [42] performed a comparison among different types of epilepsy with volumetric measurement of the hippocampus in 110 patients with chronic epilepsy, of which 81 had partial seizures (limited evidence). Seventeen patients had pathologically proven hippocampal sclerosis. All 17 patients with hippocampal sclerosis had reduced absolute hippocampal volumes, greater than two standard deviations (SD) below the mean of the control group. The degree of reduced hippocampal size correlates well with the severity of the hippocampal sclerosis. Hippocampal volumes were within normal range in all patients with generalized epilepsy, and in extratemporal, and extra-hippocampal temporal lesions.

Oppenheim et al. [43] proposed that the loss of digitations of the hippocampal head on MRI be considered a major criterion of hippocampal sclerosis along with signal abnormality and reduced volume. In a level III case series study (limited evidence) of 193 patients with intractable epilepsy evaluated retrospectively for atrophy, 63 patients were diagnosed as having mesial temporal sclerosis based on T2 signal changes and loss of digitations of the hippocampal head. Twenty-four of these patients underwent surgery and hippocampal sclerosis was confirmed in all of them. A control group of 60 patients with frontal seizures and normal MRI was also studied. The digitations of the hippocampal head were evaluated in the two groups. Digitations were not visible in 51 and poorly visible in 8 of the 63 patients with mesial temporal sclerosis. Of 24 hippocampi in which hippocampal sclerosis was confirmed histologically, 22 had no MRI-visible digitations. In the control group, digitations were sharply visible in 55 and poorly visible in five. The sensitivity and specificity of complete loss of hippocampal head digitations in hippocampal sclerosis was 92 % and 100 %, respectively.

Jack et al. [44] in a level II study (moderate evidence) compared the accuracy of a fluid-attenuated inversion recovery (FLAIR) sequence with that of conventional dual spin echo (SE) sequence in the identification of increased signal of hippocampal sclerosis. The study was blinded and controlled with a reference standard criterion of the histopathologic examination. A total of 36 patients were included. The sensitivity was 97 % for FLAIR versus 91 % for SE in the diagnosis of hippocampal sclerosis.

MRI findings as predictors of outcome of temporal lobectomy were studied in a cohort (moderate evidence) study of 135 patients [45]. Sixty months after surgery, 69 % of patients with neuroimaging lesions, 50 % with hippocampal sclerosis, and 21 % with normal MRIs had no postoperative seizures. Outcome was worse in those with normal MRI examinations.

Does 3 T Improve the Yield of Lesion Detection Compared to 1.5 T in Patients with Intractable Epilepsy?

Summary

In patients with no abnormality or a questionable lesion identified on 1.5 T MRI, 3 T can

potentially identify a lesion, in particular focal cortical dysplasia, not visualized on 1.5 T (Fig. 15.4a, b) (limited evidence).

Supporting Evidence

There are no level I or II (strong or moderate evidence) studies available. Zijlmans and colleagues [46] examined the yield of 3 T imaging in 37 patients who have had 1.5 T MRI that was ambiguous (limited evidence). The authors found 3 T could identify focal cortical dysplasia better than 1.5 T, while 1.5 T scan was better at demonstrating gliosis and mesial temporal sclerosis. Overall, 3 T identified 29 lesions while 1.5 T detected 17 lesions. Another study by Knake et al. [47] evaluated 40 patients with focal epilepsy using 3 T phased array surface coil and compared the findings with 1.5 T (limited evidence). Three Tesla phased array MRI yielded additional diagnostic information in 48 % compared to 1.5 T, and in 37.5 % of cases, the additional information changed clinical management. In 23 patients with normal 1.5 T MRI, 3 T phased array MRI identified a new lesion in 65 % of cases; in 15 patients with known lesions, 3 T phased array MRI better defined the lesion in 33 %. In both of these studies, there was no histological confirmation of the findings.

When Should Functional Imaging Be Performed in Seizure Patients and Which Is the Study of Choice?

Summary

Functional neuroimaging can provide additional data in seizure patients (Table 15.6). The sensitivity of SPECT for localizing epileptogenic focus increases from interictal (44 %) to ictal examinations (97 %) (moderate evidence). The sensitivity is lower in cases of extratemporal partial epilepsy in which only the ictal examination is reliable (sensitivity of 92 %). Subtraction techniques of the interictal from the ictal study may be helpful; however, the ictal study remains the preferred examination. PET is more sensitive than interictal SPECT in localizing temporal and extratemporal epilepsy but less sensitive

than ictal SPECT for the localization of epileptogenic foci. Magnetic source imaging (MSI) can provide information on the extent of electrode coverage for invasive intracranial EEG monitoring (moderate evidence). Functional MRI (fMRI) can help to lateralize language in the workup of patients for epilepsy surgery (limited evidence). fMRI has sensitivity greater than 91 % for language lateralization, when the intracarotid Amytal test (Wada test) is used as the reference standard (Table 15.7). fMRI influences the seizure team's diagnostic and therapeutic decision making (moderate evidence). Diffusion tensor tractography can identify Meyer's loop and the position relative to temporal pole. Therefore, tractography can be used to assess the risk of visual field defect prior to temporal lobe resection (limited evidence).

Supporting Evidence

Single Photon Emission Computed Tomography (SPECT)

There is only one randomized control study of the utility of ictal SPECT in patients with mesial temporal lobe epilepsy [48]. One hundred and twenty-four patients were randomly assigned to ictal SPECT, and 116 were assigned to non-SPECT group. Despite the 35 % higher cost and the increased hospital stay by one day in the SPECT group, the proportion of patients who were seizure free after surgery was similar in the SPECT (59 %) group compared with the non-SPECT group (54 %).

In the level II meta-analysis study (moderate evidence) reported by Spencer [39], ictal SPECT was performed in 108 patients. Eighty epileptogenic foci were localized by SPECT in the temporal lobe. In temporal lobe epilepsy, the diagnostic sensitivity for ictal or postictal SPECT is 90 % and the specificity of 73 %. In extratemporal lobe epilepsy, ictal SPECT sensitivity decreases to 81 % and specificity increases to 93 % when using EEG criteria as the standard of reference. False localization was found in 5 % of cases. Interictal SPECT sensitivity and specificity were found to be significantly lower, at 66 % and 68 % for temporal lobe, respectively,

and at 60 % and 93 % for extratemporal regions, respectively, when compared to EEG. False localization was found in 10–25 %. Devous and colleagues [49] presented a second meta-analysis of SPECT brain imaging in partial epilepsy, both temporal and extratemporal epilepsy (moderate evidence). The pooled data was gathered from 624 interictal, 101 postictal, and 136 ictal cases. The vast majority of patients were adults. The reference standard was EEG and/or surgical outcome (162 cases). The results from this study showed that the sensitivity of technetium-99 m-labeled HMPAO SPECT in localizing a temporal lobe epileptic focus increased from 44 % in interictal studies to 75 % in postictal studies and reached 97 % in ictal studies. False positives when compared to surgical outcome were 4.4 % for interictal and 0 % for postictal and ictal studies.

Newton and colleagues [50] evaluated 177 patients with partial epilepsy and showed similar results (limited evidence). In 119 patients with known unilateral temporal lobe epilepsy, correct localization by ictal SPECT was demonstrated in 97 % of cases. Postictal SPECT was correct in 71 % of cases and interictal SPECT in 48 % of cases. In extratemporal epilepsy, the yield of ictal SPECT studies was 92 % and postictal SPECT was 46 %. The interictal SPECT was of little value in extratemporal epilepsy. A multicenter study (limited evidence) evaluated ictal and interictal SPECT in 74 patients with temporal lobe epilepsy and found the sensitivity was 84 % for ictal SPECT and 55 % for interictal SPECT [51].

Matsuda and colleagues [52] evaluated 123 patients with temporal and extratemporal lobe epilepsy using SPECT compared to surgery (limited evidence). Compared to the surgical site, the concordance rate was 0.65 for SISCOM and 0.72 for side-by-side visual comparison in temporal lobe epilepsy; the concordance rate was 0.49 for SISCOM and 0.45 for side-by-side visual comparison in extratemporal lobe epilepsy. Lewis et al. [53] have reported a small case series (limited evidence) of 38 patients with seizures not associated with hippocampal sclerosis using subtraction techniques of interictal SPECT from ictal SPECT. In 58 % of the studies, the subtraction images "contributed additional information" but were confusing in 9 %.

Seo et al. [54] reported a small case series of 27 pediatric patients with normal MRI undergoing ictal SPECT and PET study (limited evidence). Eighteen out of 27 cases (67 %) showed focal localizing features on ictal SPECT, and 21 of 27 cases (78 %) showed abnormal findings on PET.

FDG-PET

In a level III study (limited evidence) of 312 patients pooled by Spencer [39], PET was compared to EEG for localization. A total of 205 patients had reduced temporal lobe metabolism of which 98 % were concordant with EEG findings. Thirty-two patients had hypometabolism in an extratemporal location, which was concordant with EEG in 56 % of cases. In 75 patients, the abnormalities were not localized by PET; 36 of these patients had temporal lobe EEG abnormalities. The diagnostic sensitivity for FDG-PET was 84 % (specificity of 86 %) for temporal and 33 % (specificity of 95 %) for extratemporal epilepsy, respectively.

A meta-analysis has been done on PET in adults with temporal lobe epilepsy from published English literature from 1992 to 2006 [55] (limited evidence). The authors included only those articles that reported surgical outcome and excluded extratemporal lobe epilepsy, tumors, and children. Forty-six out of 83 studies were included, and 153 TLE patients were analyzed. Ipsilateral PET hypometabolism showed a predictive value of 86 % for good outcome. The predictive value was 80 % in patients with normal MRI and 72 % in patients with non-localized ictal scalp EEG.

A prospective observational study (moderate evidence) examined FDG-PET in 51 patients age ranging from 1 to 60 years with temporal and extratemporal epilepsy who underwent intracranial EEG and subsequent surgical resection [56].

The sensitivity, specificity, and positive and negative predictive values of PET with respect to seizure freedom following surgery were 59 %, 79 %, 83 %, and 54 %, respectively.

A retrospective study (limited evidence) by Lee and colleagues [57] evaluated 21 pediatric patients who had TLE with ictal SPECT and interictal PET. PET correctly localized the epileptogenic zone in 20 of 21 patients (95 %) and SPECT in 12 of 15 patients (80 %). Another study by Kim et al. [58] assessed PET and SPECT in 42 children with temporal lobectomy (23 cases) and extratemporal lobe resection (19 cases) (limited evidence). PET localized lesions correctly in 73 % of temporal lesions and 63 % of extratemporal lesions. SISCOM localized in 67 % of temporal and 85 % of extratemporal cases. Another study examined 20 children who had FDG-PET and subsequently undergone epilepsy surgery and were seizure free [59] (limited evidence). Visual analysis and statistical parametric mapping were compared. The sensitivity, specificity, positive predictive value, and negative predictive value of visual analysis of FDG-PET were 62 %, 89 %, 82 %, and 73 % and for SPM (with p < 0.001) were 71 %, 86 %, 79 %, and 75 %, respectively. SPM was more likely to identify medially located epileptic cortical areas that were missed by visual assessment.

There was one study that evaluated the cost-effectiveness of additional imaging with PET and ictal SPECT in patients with intractable epilepsy undergoing epilepsy surgery. O'Brien et al. [60] reported the PET and ictal SPECT localized seizures in 75 % and 60 % of cases, respectively. PET was found to be more cost-effective than ictal SPECT for Engel class I/II surgical outcomes in patients with non-localizing or non-concordant video electroencephalography or MRI, and sensitivity analysis did not alter the findings.

Magnetoencephalography (MEG) and Magnetic Source Imaging (MSI)

MEG measures the extracranial magnetic fields perpendicular to the direction of intracellular electrical currents in cortical neurons and is one of the noninvasive tools to localize the epileptogenic zone. When MEG is combined with structural imaging, this is referred to as magnetic source imaging (MSI). A systematic review was conducted on MEG and its use in the presurgical evaluation of localization-related epilepsy [61] (limited evidence). The authors reviewed data in English language from 1987 to 2006 and included studies that had ≥4 patients undergoing epilepsy surgery, compared MEG focus to the resected or operated area, and those that reported seizure outcomes and had postsurgical follow-up of ≥6 months. Seventeen of the 192 articles were analyzed and of these, five reported patients with only temporal lobe epilepsy, three reported only extratemporal lobe epilepsy, eight reported both temporal and extratemporal lobe epilepsy, and one article did not specify the type of epilepsy. The sensitivity of MEG was 0.84 ± 0.12 (range: 0.20–1.00), specificity was 0.52 ± 0.24 (range: 0.06–1.0), positive likelihood ratio was 1.07 ± 0.20 (range: 0.67–2.0), and negative likelihood ratio was 1.12 ± 0.72 (range: 0.40–2.13).

Since then, a prospective, blinded, crossover-controlled, observational case series has been reported [62] (moderate evidence). Sixty-nine sequential patients with neocortical partial epilepsy were studied and demonstrated that MSI provided additional information in 33 % of cases, led to different intracranial EEG coverage in 23 %, added intracranial EEG electrodes in 13 %, and changed the surgical decision in another 20 % of cases.

A prospective observational study (moderate evidence) examined MSI in 62 patients with temporal and extratemporal epilepsy who underwent intracranial EEG and subsequent surgical resection [56]. The authors have found that MSI has sensitivity of 55 %, specificity of 75 %, positive predictive value of 78 %, and negative predictive value of 51 % when compared to the reference standard of Engel class I surgical outcome. The study also evaluated the test performance of MEG, PET, and SPECT in a smaller subset of

patients (n = 27) who have all three investigations done. Among the three investigations, ictal SPECT has the highest sensitivity (62 %), specificity (86 %), and positive (80 %) and negative (71 %) predictive values; PET has sensitivity of 54 %, specificity of 86 %, and positive and negative predictive values of 78 % and 67 %, respectively; MSI has sensitivity of 31 %, specificity of 79 %, positive predictive value of 57 %, and negative predictive value of 55 %. Subsequently, the same group of investigators also evaluated the contribution of MSI on intracranial electrode placement [63] in 160 patients who had insufficient seizure localization from seizure semiology, EEG, and MRI (moderate evidence). Of the 77 patients who proceeded to invasive intracranial EEG monitoring, MSI indicated additional electrode coverage in 23 %, and in 39 % of patients, seizure-onset intracranial EEG patterns involved the additional electrodes indicated by MSI. Another finding was that highly localized MSI was significantly associated with seizure-free outcome for the entire surgical population.

The American Clinical MEG Society [64] issued the statement that on the basis of the current published evidence, the ACMEGS supports the routine use of MEG/MSI in presurgical epilepsy evaluation, as it can improve noninvasive evaluation and can enhance the yield of invasive studies by directing the placement of grids, strips, and depth electrodes. In particular, the ACMEGS supports the routine use of MEG/MSI when traditional EEG methods and MRI provide insufficient localizing information. The information obtained from MEG may in turn reduce overall costs and improve the accuracy of epilepsy evaluations, thus making surgery a more appealing treatment option.

Functional MRI (fMRI)

fMRI is increasingly used to replace the more invasive and expensive Wada intracarotid amobarbital examination in the lateralization and location of language in patients who are

candidates for epilepsy surgery. Most fMRI papers are based on small samples.

One study described procedures and results of language dominance lateralization in 100 patients with partial epilepsy performing a covert word generation task (limited evidence) [65]. The reference standard was bilateral Wada intracarotid amobarbital test (IAT) performed in all cases. The results impacted clinical decision making. There was 91 % concordance between both tests. Divergent results between the tasks included two cases in which the IAT showed absence of lateralization. Discordance was much higher in cases of left-sided extratemporal epilepsy (25 %). Another case series study described the findings of language lateralization in a group of 30 patients with temporal lobe epilepsy (limited evidence) [66]. They used IAT in 21 cases as the reference standard. Eighteen cases had temporal resection and further follow-up. There were no divergent results (i.e., methods pointing to the opposite side). One case showed bilateral fMRI activation and lateralized IAT. Two cases had bilateral IAT and left lateralized fMRI.

A prospective study (moderate evidence) investigated the role of fMRI in the diagnostic evaluation and surgical treatment of patients with seizure disorders [67]. In 35 (58.3 %) of the 60 patients, fMRI results altered patient and family counseling. In 38 (63.3 %) of the 60 patients, fMRI avoided further studies including Wada test. In 31 (51.6 %) and 25 (41.7 %) of the 60 patients, fMRI altered intraoperative mapping plans and surgical approach plans, respectively. In 5 (8.3 %) patients, a two-stage surgery with extra-operative direct electrical stimulation mapping was averted and resection could be accomplished in a one-stage surgery. In 4 (6.7 %) patients, the extent of surgical resection was altered because eloquent areas were identified close to the seizure focus. The authors concluded that fMRI influences the seizure team's diagnostic and therapeutic decision making [67].

A Bayesian analysis study has been performed to assess the role of fMRI in determining how this

test modifies pretest to posttest probabilities of language dominance in the epilepsy population [68]. The study pooled data from studies published between 1995 and 2002 on language fMRI compared with Wada tests or electrocortical stimulation as the standard of reference. Two hundred and forty cases having both examinations were pooled. From the literature review and utilizing the Wada test as the reference study, the authors found that the sensitivity of fMRI in language lateralization was 92.5 % (95 % CI: 89.1 %, 95.9 %) and the likelihood ratio was 12.3 [(sensitivity)/(1-specificity); 95 % CI: 8.2, 23.4)]. When compared to the reference standard of electrocortical stimulation, sensitivity was 90.3 % (95 % CI: 80 %–100 %) and the likelihood ratio was 9.3 (95 % CI: 4, ∞). From the Bayesian analysis the authors concluded that epilepsy patients with right-hand dominance or ambidexterity, the posttest probability (of truly language lateralization in the left hemisphere) was greater than 95 %. In the left-handed epilepsy patients, there was high posttest probability (80–97 %) of a correlation between fMRI hemisphere activation and definite left-handed language dominance [68].

The costs of fMRI and IAT (Wada test) were compared for the workup of language lateralization in patients who were candidates for epilepsy surgery [69]. Two age-matched groups were studied prospectively. Twenty-one patients had fMRI and 18 IAT. Total direct costs of the Wada test ($1130.01 +/− $138.40) and of functional MR imaging ($301.82 +/−$10.65) were significantly different (P < 0.001). The cost of the Wada test was 3.7 times higher than that of functional MR imaging.

Diffusion Tensor Imaging Tractography of the Optic Radiations

No large prospective studies have been done to address the role of diffusion tensor imaging tractography of the optic radiations in patients undergoing temporal lobe resection for epilepsy. Several case series have been reported abnormality in diffusion tensor tractography of the optic radiations in patients who developed visual field defects following temporal lobe resection [70–72] (insufficient evidence). These studies suggest that tractography of the optic radiations may be useful to visualize Meyer's loop so as to assess the risk of visual field defect prior to temporal lobe resection. Yogarajah and colleagues [73] demonstrated the variability in the distance from the tip of Meyer's loop to the temporal pole and that both the distance from the tip of Meyer's loop to the temporal pole and the size of resection were significant predictors of postoperative visual field defects in patients undergoing temporal lobe resection (limited evidence).

Take-Home Tables and Figures

Figure 15.1 provides a decision-making algorithm for seizure disorders.

Tables 15.1 through 15.7 highlight important data and evidence.

Imaging Case Studies

Figures 15.2 through 15.4 presented below highlight advantages and limitations of the different neuroimaging modalities.

Future Research

- To define better the different seizure risk groups so neuroimaging can be tailored appropriately
- To determine the advantages, limitations, indications, and pitfalls of new imaging studies such as diffusion tensor imaging
- To determine the impact that imaging has in the outcome of patients with seizure disorders
- To perform formal cost-effectiveness analysis of the role of imaging in patients with seizure disorders
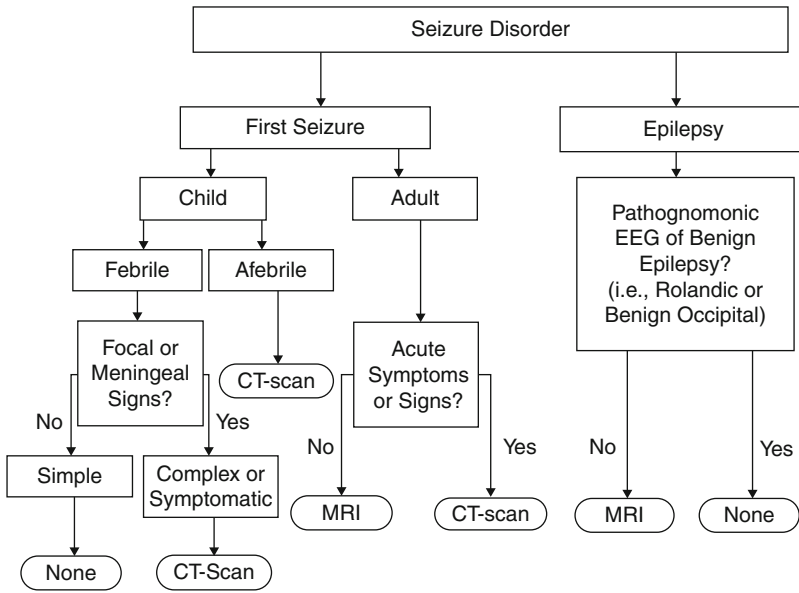
Fig. 15.1 Decision-making algorithm for seizure disorders (Reprinted with kind permission of Springer Science+Business Media from Bernal B, Altman N. Neuroimaging of seizures. In Medina LS, Blackmore CC, editors. Evidence-based imaging: optimizing imaging in patient care. New York: Springer; 2006.)

Table 15.1 Neuroimaging in acute symptomatic seizures (CT/MRI)

Author	Number of patients	CT/MR	% of positives	Comments
Eisner et al. [22]	163	19	25	Positive results in 3 % of the total of patients
Earnest et al. [23]	259	259	6.2	Only patients with seizures after alcohol withdrawal were included; 3.9 % of patients resulted in significant treatment changes
Reinus et al. [24]	115	?	36	Post-acute head trauma (60 patients had previous seizure disorder)
Henneman et al. [25]	333	325	41	Seizures no associated with head trauma

Reprinted with kind permission of Springer Science+Business Media from Bernal B, Altman N. Neuroimaging of seizures. In Medina LS, Blackmore CC, editors. Evidence-based imaging: optimizing imaging in patient care. New York: Springer; 2006

Table 15.2 Neuroimaging in first unprovoked seizure

Author	Patients	CT/MRI	% of positives	Comments
Shinnar et al. [27]	218	186/59	34/22	1.8 % significant findings
King et al. [28]	300	263/14	17/8	
Hirtz et al. [29]	(EBM review)		18–34	In children: significant findings in less than 7 %
Maytal et al. [30]	66	66/20	21	None with significant findings
Hopkins et al. [31]	408	408/0	?	3 % tumors
Schoenenberger et al. [32], Shinnar et al. [27]	119218	119/0186/59	3434/22	17 % with significant findings 1.8 % significant findings
Garvey et al. [33]	50	50/0	17	12 % with significant findings

Reprinted with kind permission of Springer Science+Business Media from Bernal B, Altman N. Neuroimaging of seizures. In Medina LS, Blackmore CC, editors. Evidence-based imaging: optimizing imaging in patient care. New York: Springer; 2006

Table 15.3 Neuroimaging in temporal lobe epilepsy (TLE) and other partial seizures

Author	Patients	CT/MRI	% of positives	Comments
Harvey et al. [34]	63	48/58	23/36.5	Study done with two magnets: 0.3 T and 1.5 T. Etiologies: 13 HS, 8 tumors, 1 cortical dysplasia, 1 arachnoidal cyst, 1 hamartoma
Kramer et al. [35]	143	117/42	(35)	Study in children and adolescents. Eight diffuse atrophies, 8 porencephalic cysts, 6 tumors, 6 neurocutaneous syndromes, 6 dysgeneses. Neither an abnormality in the neurological exam nor the type of seizure were predictors for finding a tumor
Berg et al. [36]	359	(312)	(13.8)	All pediatric patients. In three normal CT cases, the MRI was abnormal. The strongest predictor of abnormal imaging was abnormal motor examination
Lee et al. [37]	274	0/186	97	Patients with intractable TLE. Sixty-five percent had HS; 32 had abnormalities in the rest of the temporal lobe. Forty-two tumors in pediatric patients
Sinclair et al. [38]	42	39/42	31/64	Patients with intractable partial epilepsy. Postoperative findings: 13 tumors, 8 HS, 5 dual pathologies, 4 cortical dysplasias, 4 tuberous scleroses, 1 porencephalic cyst
Spencer et al. [39]	809	?	43–55	A total of 370 patients with temporal lobe abnormalities. The lowest % for extratemporal lobe epilepsy

Reprinted with kind permission of Springer Science+Business Media from Bernal B, Altman N. Neuroimaging of seizures. In Medina LS, Blackmore CC, editors. Evidence-based imaging: optimizing imaging in patient care. New York: Springer; 2006
Table Note: In parenthesis, the reported data is not divided due to lack of further information

Table 15.4 MRI sensitivity and specificity in temporal lobe epilepsy

Item	Sensitivity (%)	Specificity (%)	Reference
Hippocampal lesion	93	83	Lee et al. [37]
Non-hippocampal temporal lobe lesion	97	97	Lee et al. [37]
Global sensitivity for tumor detection	83	97	Lee et al. [37]
High T2 signal for hippocampal sclerosis	93	74	Lee et al. [37]
High FLAIR signal for hippocampal sclerosis	97	?	Jack et al. [44]

Reprinted with kind permission of Springer Science+Business Media from Bernal B, Altman N. Neuroimaging of seizures. In Medina LS, Blackmore CC, editors. Evidence-based imaging: optimizing imaging in patient care. New York: Springer; 2006

Table 15.5 MRI sensitivity and specificity for hippocampal sclerosis

Author	Patients	Sensitivity	Specificity	Comments
Spencer et al. [39]	153	71	?	Review
Moore et al. [40]	207*	100	100	* = Study conducted in "normal volunteers"
				Two had HS, who had prior history of seizures in detailed chart review
Jack et al. [41]	41	76	100	Quantitative volumetric measurement of the hippocampus
Oppenheim et al. [43]	63	92	100	Based on loss of digitations in hippocampal head
Jack et al. [44]	36	97	?	FLAIR sequence was compared to SE (91 % sensitivity)

Reprinted with kind permission of Springer Science+Business Media from Bernal B, Altman N. Neuroimaging of seizures. In Medina LS, Blackmore CC, editors. Evidence-based imaging: optimizing imaging in patient care. New York: Springer; 2006

Table 15.6 Functional neuroimaging in epileptic focus detection

Author	Proc.	Pte/ proc.	Ictal sen/spec	Postictal sen/spec	Interictal sen/spec	Comments
Spencer et al. [39]	SPECT	108	90/73[a] 81/93[b]	90/73[a]	66/68[a] 60/93[b]	Compared to EEG. False localization was found in 10–25 %
	PET	312	–	–	84/86[a] 33/95[b]	
Seo et al. [54]	SPECT	27	67/[a,b]			Pediatric patients only
						Neocortical epilepsy
	PET	27			78/[a,b]	
Lee et al. [57]	SPECT	21	80/[a]			Pediatric patients only
	PET	21			95/[a]	
Kim et al. [58]	SPECT	42				SISCOM: 67/[a], 85/[b]
	PET				73/[a] 63/[b]	
Velasco et al. [48]	SPECT	240	59/[a]			
Devous et al. [49]	SPECT	624	97/[a]	75/[a]	44/[a]	Compared to EEG and/or surgical outcome
Newton et al. [50]	SPECT	177	97/[a] 92/[a]	71/[a] 46/[b]	48/[a] –	
Matsuda et al. [52]	SPECT	123				Side-by-side visual assessment: 72/[a], 45/[b]; SISCOM: 65/[a], 49/[b]
Willmann et al. [55]	PET	153			86/[a]	Meta-analysis
Knowlton et al. [56]	PET	51			59/79[a,b]	
Kumar et al. [59]	PET	20			Visual analysis: 62/89[a,b]; SPM: 71/86[a,b]	Pediatric patients only
Lau et al. [61]	MEG	244			84/52[a,b]	Meta-analysis
Sutherling et al. [62]	MEG	69				MEG provided additional information in 33 %, changed surgical decision in 20 %
Knowlton et al. [56]	MEG	62			55/75[a,b]	
Knowlton et al. [63]	MEG	77				MEG indicated additional electrode coverage in 23 %

Reprinted with kind permission of Springer Science+Business Media from Bernal B, Altman N. Neuroimaging of seizures. In Medina LS, Blackmore CC, editors. Evidence-based imaging: optimizing imaging in patient care. New York: Springer; 2006

[a]In temporal lobe epilepsy

[b]In extratemporal lobe epilepsy

Table 15.7 Functional MRI in language lateralization for epilepsy surgery

Author	Paradigm	Patients	Reference standard	Sensitivity %	Comments
Woermann et al. [65]	Word generation	100	Bilateral IAT	91	Cases with localization-related epilepsy. Discordant categorization between fMR and IAT includes absence of IAT lateralization in two cases
Gaillard et al. [66]	Reading and naming	30	Bilateral intracarotid amobarbital test (IAT)	93	All cases temporal lobe epilepsy. No disagreement with reference standard

Reprinted with kind permission of Springer Science+Business Media from Bernal B, Altman N. Neuroimaging of seizures. In Medina LS, Blackmore CC, editors. Evidence-based imaging: optimizing imaging in patient care. New York: Springer; 2006
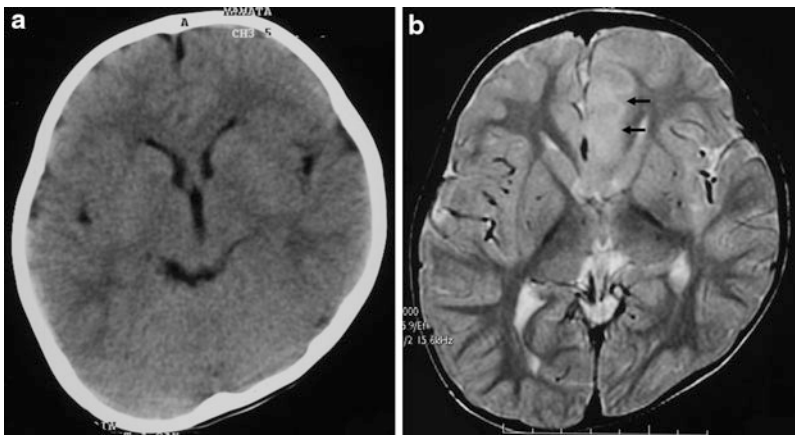

Fig. 15.2 (**a**, **b**) CT versus MRI sensitivity in non-acute symptomatic seizure. This figure illustrates the higher sensitivity of MRI in the detection of cortical dysplasia. The transverse CT (**a**) is compared to the MR (**b**) in a child with intractable epilepsy and postural plagiocephaly. The region of cortical dysplasia in the left parasagittal frontal lobe is clearly seen only on the MRI exam by the loss of gray–white matter interface and the increased T2-weighted signal intensity (Reprinted with kind permission of Springer Science+Business Media from Bernal B, Altman N. Neuroimaging of seizures. In Medina LS, Blackmore CC, editors. Evidence-based imaging: optimizing imaging in patient care. New York: Springer; 2006)
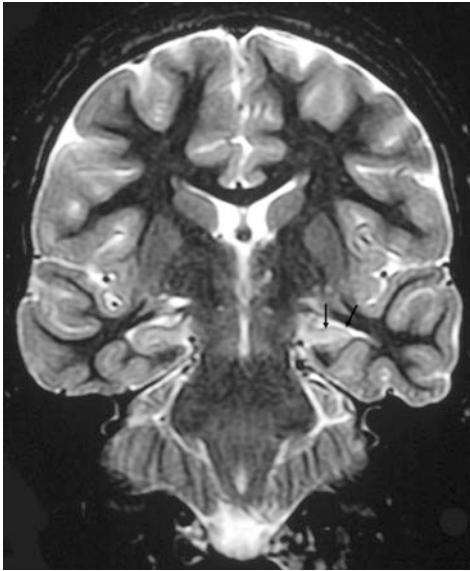
Fig. 15.3 T2-inversion recovery MRI. The image corresponds to a patient with intractable epilepsy and EEG findings of left temporal origin. Coronal image at the level of the temporal lobes demonstrates left hippocampal sclerosis characterized by reduction in size, and increased signal intensity (*arrows*), compared to the normal right hippocampus (Reprinted with kind permission of Springer Science+Business Media from Bernal B, Altman N. Neuroimaging of seizures. In Medina LS, Blackmore CC, editors. Evidence-based imaging: optimizing imaging in patient care. New York: Springer; 2006)
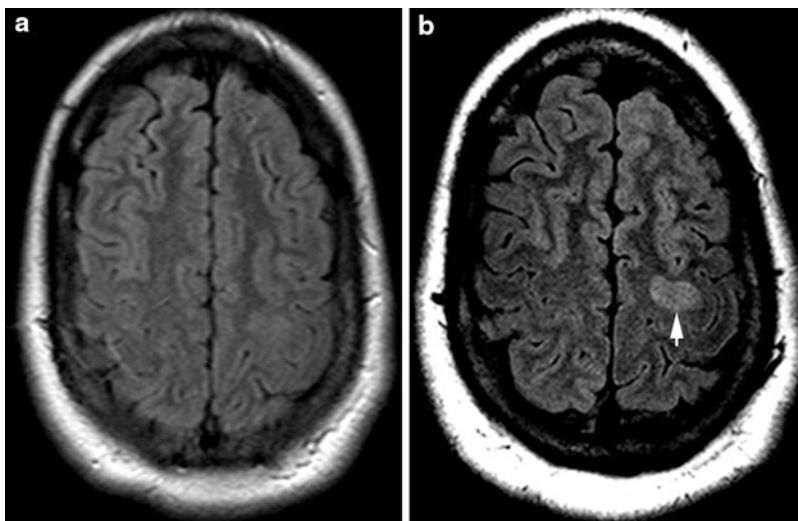

Fig. 15.4 (**a**, **b**). (**a**) Fluid-attenuated inversion recovery (FLAIR) at 1.5 T does not demonstrate a lesion in a patient with rolandic epilepsy. (**b**) FLAIR at 3 T shows high signal in the cortex anterior to the left precentral gyrus (*arrow*), in keeping with focal cortical dysplasia

References

1. Berg AT, Berkovic SF, Brodie MJ, et al. Epilepsia. 2010;51:676–85.
2. Commission on Classification and Terminology of the International League Against Epilepsy. Epilepsia. 1989;30:389–99.
3. Bell GS, Sander JW. Seizure. 2001;10:306–14; quiz 315–6.
4. Senanayake N, Roman GC. Bull World Health Organ. 1993;71:247–58.
5. Hauser WA, Annegers JF, Kurland LT. Epilepsia. 1993;34:453–68.
6. Lavados J, Germain L, Morales A, Campero M, Lavados P. Acta Neurol Scand. 1992;85:249–56.
7. Rwiza HT, Kilonzo GP, Haule J, et al. Epilepsia. 1992;33:1051–6.
8. Hauser WA, Annegers JF, Rocca WA. Mayo Clin Proc. 1996;71:576–86.
9. Berg AT, Shinnar S, Hauser WA, Leventhal JM. J Pediatr. 1990;116:329–37.
10. Knudsen FU. Arch Dis Child. 1985;60:1045–9.
11. Offringa M, Bossuyt PM, Lubsen J, et al. J Pediatr. 1994;124:574–84.
12. Annegers JF, Shirts SB, Hauser WA, Kurland LT. Epilepsia. 1986;27:43–50.
13. Berg AT, Shinnar S. Neurology. 1996;47:562–8.
14. Berg AT, Shinnar S. Neurology. 1991;41:965–72.
15. Shorvon SD. Epilepsia. 1996;37(Suppl 2):S1–3.
16. Murray MI, Halpern MT, Leppik IE. Epilepsy Res. 1996;23:139–48.
17. Ho SS, Kuzniecky RI. J Neuroimaging. 1997;7:236–41.
18. De Zelicourt M, Buteau L, Fagnani F, Jallon P. Seizure. 2000;9:88–95.
19. Bronen RA, Fulbright RK, Spencer SS, Spencer DD, Kim JH, Lange RC. Magn Reson Imaging. 1997;15:857–62.
20. Offringa M, Moyer VA. West J Med. 2001;175:254–9.
21. American Academy of Pediatrics. Provisional Committee on Quality Improvement, Subcommittee on Febrile Seizures. Pediatrics. 1996;97:769–72; discussion 773–5.
22. Eisner RF, Turnbull TL, Howes DS, Gold IW. Ann Emerg Med. 1986;15:33–9.
23. Earnest MP, Feldman H, Marx JA, Harris JA, Biletch M, Sullivan LP. Neurology. 1988;38:1561–5.
24. Reinus WR, Wippold 2nd FJ, Erickson KK. Ann Emerg Med. 1993;22:1298–303.
25. Henneman PL, DeRoos F, Lewis RJ. Ann Emerg Med. 1994;24:1108–14.
26. Bradford JC, Kyriakedes CG. Emerg Med Clin North Am. 1999;17:203–20, ix–x.
27. Shinnar S, O'Dell C, Mitnick R, Berg AT, Moshe SL. Epilepsy Res. 2001;43:261–9.
28. King MA, Newton MR, Jackson GD, et al. Lancet. 1998;352:1007–11.
29. Hirtz D, Ashwal S, Berg A, et al. Neurology. 2000;55:616–23.
30. Maytal J, Krauss JM, Novak G, Nagelberg J, Patel M. Epilepsia. 2000;41:950–4.
31. Hopkins A, Garman A, Clarke C. Lancet. 1988;1:721–6.
32. Schoenenberger RA, Heim SM. BMJ. 1994;309:986–9.
33. Garvey MA, Gaillard WD, Rusin JA, et al. J Pediatr. 1998;133:664–9.
34. Harvey AS, Berkovic SF, Wrennall JA, Hopkins IJ. Neurology. 1997;49:960–8.
35. Kramer U, Nevo Y, Reider-Groswasser I, et al. Neuroimaging of children with partial seizures. Seizure. 1998;7:115–18.
36. Berg AT, Testa FM, Levy SR, Shinnar S. Pediatrics. 2000;106:527–32.
37. Lee DH, Gao FQ, Rogers JM, et al. AJNR Am J Neuroradiol. 1998;19:19–27.
38. Sinclair DB, Wheatley M, Aronyk K, et al. Pediatr Neurosurg. 2001;35:239–46.
39. Spencer SS. Epilepsia. 1994;35(Suppl 6):S72–89.
40. Moore KR, Swallow CE, Tsuruda JS. AJNR Am J Neuroradiol. 1999;20:1609–12.
41. Jack Jr CR, Sharbrough FW, Twomey CK, et al. Radiology. 1990;175:423–9.
42. Watson C, Cendes F, Fuerst D, et al. Arch Neurol. 1997;54:67–73.
43. Oppenheim C, Dormont D, Biondi A, et al. AJNR J Neuroradiol. 1998;19:457–63.
44. Jack Jr CR, Rydberg CH, Krecke KN, et al. Radiology. 1996;199:367–73.
45. Berkovic SF, McIntosh AM, Kalnins RM, et al. Neurology. 1995;45:1358–63.
46. Zijlmans M, de Kort GA, Witkamp TD, et al. J Magn Reson Imaging. 2009;30:256–62.
47. Knake S, Triantafyllou C, Wald LL, et al. Neurology. 2005;65:1026–31.
48. Velasco TR, Wichert-Ana L, Mathern GW, et al. Neurosurg. 2011;68:431–6; discussion 436.
49. Devous Sr MD, Thisted RA, Morgan GF, Leroy RF, Rowe CC. J Nucl Med. 1998;39:285–93.
50. Newton MR, Berkovic SF, Austin MC, Rowe CC, McKay WJ, Bladin PF. J Neurol Neurosurg Psychiatry. 1995;59:26–30.
51. Zaknun JJ, Bal C, Maes A, et al. Eur J Nucl Med Mol Imaging. 2008;35:107–15.
52. Matsuda H, Matsuda K, Nakamura F, et al. Ann Nucl Med. 2009;23:283–91.
53. Lewis PJ, Siegel A, Siegel AM, et al. J Nucl Med. 2000;41:1619–26.
54. Seo JH, Noh BH, Lee JS, et al. Seizure. 2009;18:625–9.
55. Willmann O, Wennberg R, May T, Woermann FG, Pohlmann-Eden B. Seizure. 2007;16:509–20.
56. Knowlton RC, Elgavish RA, Bartolucci A, et al. Ann Neurol. 2008;64:35–41.
57. Lee JJ, Kang WJ, Lee DS, et al. Seizure. 2005;14:213–20.

58. Kim JT, Bai SJ, Choi KO, et al. Seizure. 2009;18:504–10.
59. Kumar A, Juhasz C, Asano E, Sood S, Muzik O, Chugani HT. J Nucl Med. 2010;51:1901–7.
60. O'Brien TJ, Miles K, Ware R, Cook MJ, Binns DS, Hicks RJ. J Nucl Med. 2008;49:931–7.
61. Lau M, Yam D, Burneo JG. Epilepsy Res. 2008;79:97–104.
62. Sutherling WW, Mamelak AN, Thyerlei D, et al. Neurology. 2008;71:990–6.
63. Knowlton RC, Razdan SN, Limdi N, et al. Ann Neurol. 2009;65:716–23.
64. Bagic A, Funke ME, Ebersole J. J Clin Neurophysiol. 2009;26:290–3.
65. Woermann FG, Jokeit H, Luerding R, et al. Neurology. 2003;61:699–701.
66. Gaillard WD, Balsamo L, Xu B, et al. Neurology. 2002;59:256–65.
67. Medina LS, Bernal B, Dunoyer C, et al. Radiology. 2005;236:247–53.
68. Medina LS, Bernal B, Ruiz J. Radiology. 2007;242:94–100.
69. Medina LS, Aguirre E, Bernal B, Altman NR. Radiology. 2004;230:49–54.
70. Powell HW, Parker GJ, Alexander DC, et al. Neurology. 2005;65:596–9.
71. Nilsson D, Starck G, Ljungberg M, et al. Epilepsy Res. 2007;77:11–16.
72. Winston GP, Yogarajah M, Symms MR, McEvoy AW, Micallef C, Duncan JS. Epilepsia. 2011;52:1430–8.
73. Yogarajah M, Focke NK, Bonelli S, et al. Brain. 2009;132:1656–68.

Dementia and Alzheimer Disease: Evidence-Based Neuroimaging

16

Juan E. Gutierrez, Brian Eichinger, and Kejal Kantarci

Contents

J.E. Gutierrez (✉) • B. Eichinger
Department of Radiology, University of Texas, Health Science Center at San Antonio, San Antonio, TX, USA
e-mail: gutierrezje@uthscsa.edu; eichinger@uthscsa.edu

K. Kantarci
Division of Neuroradiology, Department of Radiology, Mayo Clinic, Rochester, MN, USA
e-mail: kantarci.kejal@mayo.edu

Key Points

- By differentiating potentially treatable causes, structural imaging with either CT or MRI influences patient management during the initial evaluation of dementia (strong evidence).
- No evidence exists on the choice of either CT or MRI for the initial evaluation of dementia (insufficient evidence).
- Diagnostic accuracy of PET and SPECT to distinguish patients with AD from normal is not higher than clinical evaluation (moderate evidence).
- Hippocampal atrophy on MR-based volumetry and regional decrease in cerebral perfusion on SPECT correlates with the pathologic stage in AD (moderate evidence).
- PET, SPECT, and dynamic susceptibility contrast-enhanced MRI are not cost-effective for the diagnostic workup of AD with the assumed minimal effectiveness of the drug donepezil hydrochloride (moderate evidence).
- Use of PET in early dementia can increase the accuracy of clinical diagnosis without adding to the overall costs of the evaluation (moderate evidence).
- Longitudinal decrease in MR-based hippocampal volumes, NAA levels on ^{1}H MRS, glucose metabolism on PET, and cerebral blood flow on SPECT are associated with the rate of cognitive decline in patients with AD (moderate evidence).
- The validity of imaging techniques as surrogate markers for therapeutic efficacy in AD has not been tested in a positive disease-modifying drug trial (insufficient evidence).

Definition and Pathophysiology

AD is a progressive neurodegenerative dementia. The pathological hallmarks of AD are accumulation of neurofibrillary tangles and senile plaques. The neurofibrillary pathology, which is associated with cognitive dysfunction, neuron, and synapse loss, involves the limbic cortex early in the disease course and extends to the neocortex as the disease progresses. In addition to the histopathological changes, there is a gradual loss of cholinergic innervation in AD, which has been the basis for cholinesterase inhibitor therapy.

Epidemiology

AD is the most common cause of dementing illnesses. Prevalence of AD increases with age, and the disease is becoming a significant health problem as the aging population grows [1, 2]. In 2010, the prevalence of AD in Americans age 65 or older was over five million. The prevalence is projected to increase to 13.5 million by 2050 [3].

Overall Cost to Society

The cost to US society has been estimated at 172 billion dollars per year in 2010, and it is projected to increase to over 1.08 trillion dollars by 2050 [3].

Goals of Imaging

The goals of imaging are to: (1) exclude a potentially reversible cause of dementia in subjects with possible Alzheimer's disease, (2) identify subjects at risk for Alzheimer's disease, (3) quantify stage of disease to enable tracking of treatment response, and (4) identify subjects who may respond to therapy. Although no currently available treatments have been proven to stabilize or reverse the neurodegenerative process, phase III clinical trials of disease-modifying agents (anti-amyloid-β antibodies) in the mild to moderate stages of dementia are underway to assess for cognitive benefit [4–7]. Imaging markers that can accurately discriminate individuals at risk and are sensitive to disease onset and progression are needed for trials involving disease-modifying therapies.

Methodology

A literature search was conducted using MEDLINE. The search included articles published from January 1966 to February 2004. The main search term was Alzheimer or Alzheimer's disease. Other terms combined with the main topic were: clinical diagnosis, clinical criteria, neuroimaging, MRI, MR spectroscopy, PET, SPECT, and cost-effectiveness. The MEDLINE search yielded 3,284 articles. Animal studies, non-English articles, and articles published before 1980 were excluded, and only articles relevant to our search questions were included for review. An update was performed in October 2011 to include articles published between March 2004 and September 2011. The MEDLINE search returned 2,496 articles using similar search criteria.

Discussion of Issues

How Accurate Are the Clinical Criteria for the Diagnosis of AD?

Summary
There is strong evidence that DSM-IIIR and NINCDS-ADRDA criteria are reliable for the diagnosis of dementia and AD (strong evidence). There are, however, limitations to the data supporting clinical criteria for the diagnosis of AD. Diagnostic accuracy of clinical criteria may vary with the extent of the disease and the skills of the clinician. Clinical criteria for AD need to be validated by clinicians with different levels of expertise and at different clinical settings if such criteria will have widespread use to identify patients for therapeutic interventions (insufficient evidence).

Supporting Evidence
Clinical diagnosis of AD in a living person is labeled either possible or probable AD. Definite diagnosis of AD requires tissue examination, through biopsy or autopsy of the brain. Histopathologic hallmarks of the disease are neurofibrillary

tangles and senile plaques, which show marked heterogeneity in the pathologic progression of AD, and are also encountered to a lesser extent in elderly individuals with normal cognition [8–12]. Thus, the boundary between the histopathologic changes in elderly individuals considered to be cognitively normal and patients with AD is quantitative, not qualitative. The most recent recommendations for diagnosis of AD by the work group sponsored by the National Institute on Aging and the Alzheimer's Association define AD as "the clinical signs and symptoms of cognitive and behavioral changes that are typical for patients who have substantial AD neuropathologic change." The workgroup also provides recommendations on diagnosis of mild cognitive impairment (MCI) due to AD, the "symptomatic predemential phase" of AD. These diagnoses are intended to be made on the basis of clinical judgment alone [13–15].

Diagnostic accuracy of clinical criteria is assessed by using pathologic diagnosis as a standard. A shortcoming of this approach is that clinical and pathologic findings do not correlate perfectly. For example, some clinically demented patients do not meet the pathologic criteria for AD or any other dementing illness. Similarly, some patients who are clinically normal have extensive pathological changes of AD. However, from a practical standpoint, by taking pathologic diagnosis as a gold standard, it is possible to assess the diagnostic accuracy of clinical or neuroimaging criteria for the diagnosis of AD. The two commonly used clinical criteria that were subject to assessment for the diagnosis of dementia and AD are the Diagnostic and Statistical Manual, 3rd edition (DSM-IIIR) [16], and the National Institute of Neurologic, Communicative Disorders and Stroke–AD and Related Disorders Association (NINCDS-ADRDA) criteria [17].

When both DSM-IIIR and NINCDS-ADRDA criteria are applied to the diagnosis, clinical-pathological correlation ranges from 75 % to 90 % in studies involving a broad spectrum of patients [18–20] (strong evidence). The disagreement between clinical and pathologic diagnosis in 10–25 % of the cases provides the

motivation to develop neuroimaging markers that can accurately identify the effects of AD pathology even in the presymptomatic phase.

Sensitivity of DSM-IIIR and NINCDS-ADRDA criteria for the diagnosis of AD ranges from 76 % to 98 % and specificity from 61 % to 84 % [21–25] providing strong evidence that the accuracy of the two commonly used clinical criteria for identifying pathologically diagnosed AD is good but show marked variability across academic centers. When community-based and clinic-based patients were evaluated by the same physicians, both sensitivity and specificity of the clinical diagnosis were lower for the community than for the clinic-based cohorts (92 % and 79 % for community vs. 98 % and 84 % for clinic) [21] (strong evidence).

Inter-rater agreement on the diagnosis of dementia and AD with DSM-IIIR criteria and NINCDS-ADRDA criteria has been good (kappa = 0.54–0.81 for DSM-IIIR [26, 27] and kappa = 0.51–0.72 for NINCDS-ADRDA criteria [22, 28]) in population-based studies (strong evidence).

Does Neuroimaging Increase Accuracy of the Diagnosis of AD in the Clinical Setting?

Structural Neuroimaging
Summary
The traditional use of structural neuroimaging to differentiate potentially reversible or modifiable causes of dementia such as brain tumors, subdural hematoma, normal pressure hydrocephalus, and vascular dementia from AD is widely accepted [29]. There is strong evidence that structural imaging influences patient management during the initial evaluation of dementia. There is moderate evidence that the diagnostic precision of structural neuroimaging is higher with volume measurements than visual evaluation especially in mildly demented cases, but the figures are still comparable to clinical evaluation.

Supporting Evidence
Besides the potential causes of dementia mentioned above, structural neuroimaging can also identify anatomic changes that occur due to the pathologic involvement in AD [30]. Neurofibrillary pathology which correlates with neuron loss and cognitive decline in patients with AD follows a hierarchical topologic progression course in the brain [10, 31–33]. It initially involves the anteromedial temporal lobe and limbic cortex; as the disease progresses, it spreads over to neocortex and lastly involves the primary sensory cortices [31]. The macroscopic result of this pathologic involvement is atrophy, which is related to the decrease in neuron density [34]. For this reason, the search for anatomic imaging markers of AD has targeted the anteromedial temporal lobe, particularly the hippocampus and entorhinal cortex, which are involved earliest and most severely with the neurofibrillary pathology and atrophy in AD.

One study with a pathologically confirmed cohort [35] revealed that structural neuroimaging can help to identify vascular dementia or vascular component of AD (mixed dementia) by increasing the sensitivity of the clinical evaluation from 6 % to 59 %, and management of the vascular component may in turn slow down cognitive decline (strong evidence).

Visual evaluation or measurements of the anteromedial temporal lobe width with CT detected 80–95 % of the pathologically confirmed AD cases [25, 36]. However, the accuracy declined to 57 % when only mild AD cases with low pretest probability were quota studied, and the clinical diagnosis with NINCDS-ADRDA criteria was more accurate than CT measurements for identifying AD patients at pathologically early stages of the disease (strong evidence) [36].

A reliable and reproducible method for quantifying medial temporal lobe atrophy is MR-based volume measurements of the hippocampus and the entorhinal cortex [30, 37, 38]. Antemortem hippocampal atrophy was not found to be specific for AD in a pathologically

confirmed cohort; however, hippocampal volumes on MRI correlated well with the pathologic stage of the disease (r = –0.63, p = 0.001) [39]. Structural neuroimaging changed clinical diagnosis in 19–28 % of the cases, and changed patient management in 15 % [40] (strong evidence).

Visual evaluation of the anteromedial temporal lobe for atrophy on MRI to differentiate patients with AD from normal had a sensitivity of 82–91 % and a specificity of 82–98 % in clinically confirmed cohorts [40–43]. Although visual evaluation of the temporal lobe accurately distinguishes AD patients in experienced hands, evidence is lacking on the precision of visual evaluation at different clinical settings. Diagnostic accuracy of this technique for distinguishing AD patients from normal has been 79–94 % in clinically confirmed cohorts [44, 45], being comparable in mildly and moderately demented cases [46]. Routine use of volumetry techniques for the diagnosis of AD may be time-consuming and cumbersome in a clinical setting. However, the intimate correlation between pathologic involvement and hippocampal volumes is encouraging for the use of hippocampal volumetry as an imaging marker for disease progression (moderate evidence). By differentiating potentially treatable causes, structural imaging with either CT or MRI influences patient management during the initial evaluation of dementia (strong evidence). Evidence is lacking for the choice of either CT or MRI. CT may be appropriate when a brain tumor or subdural hematoma is suspected; MRI may be the modality of choice for vascular dementia because of its superior sensitivity to vascular changes. The decision should be based on clinical impression at this time (insufficient evidence).

Functional Neuroimaging
Summary
SPECT and PET are the two widely investigated functional neuroimaging techniques in AD. Measurements of regional glucose metabolism with PET and regional perfusion measurements with SPECT indicate a metabolic decline and a decrease in blood flow in the temporal and parietal lobes of patients with AD relative to normal elderly. There is moderate evidence that diagnostic accuracy of either SPECT or PET is not higher than the clinical criteria in AD. Nonetheless, both functional imaging techniques appear promising for differentiating other dementia syndromes (frontotemporal dementia and dementia with Lewy bodies) from AD due to differences in regional functional involvement.

Supporting Evidence
With visual evaluation of SPECT images for temporoparietal hypoperfusion, the sensitivity for distinguishing AD patients from normal differed from 42 % to 79 % at a specificity of 86–90 %, being lower in patients with mild than severe AD in both clinically and pathologically confirmed cases [47–49], and not superior to the clinical diagnosis based on NINCDS-ADRDA criteria [50] (strong evidence). The regional decrease in cerebral perfusion on SPECT correlated with the neurofibrillary pathology staging of AD [51] (strong evidence). SPECT increased the accuracy of clinical evaluation for identifying AD pathology; however, cases with other types of dementia were not included [52] (moderate evidence).

Sensitivity and specificity of the temporoparietal metabolic decline on PET for differentiating pathologically confirmed AD from normal was 63 % and 82 %, respectively, similar to the sensitivity (63 %) but lower than the specificity (100 %) of clinical diagnosis in the same cohort [53] (strong evidence). On the other hand, occipital hypometabolism on PET distinguished pathologically confirmed patients with dementia with Lewy bodies from AD with a comparable specificity (80 %) and higher sensitivity (90 %) than clinical evaluation (strong evidence) [54, 55].

Visual evaluation of SPECT images for temporoparietal hypoperfusion distinguished clinically confirmed AD patients from those with frontotemporal dementia by correctly

classifying 74 % of AD patients with decreased blood flow in the parietal lobes and 81 % of frontotemporal dementia patients with decreased blood flow in the frontal lobes [56] (moderate evidence).

Visual interpretation of PET images for temporoparietal glucose metabolism was reliable [kappa = 0.42–0.61 (Hoffman 1996) and ICC 0.86–0.96 (Mosconi 2005)] [57, 58], and PET was more useful than SPECT for differentiating clinically confirmed patients with AD from normal elderly [59]. With automated data analysis methods, PET could distinguish clinically confirmed AD cases from normal with sensitivity of 93–99 % at 93–98 % specificity [60, 61] (moderate evidence).

Other MR Techniques
Summary
Due to the ease of integrating an extra pulse sequence into the standard structural MRI exam, and advantage of obtaining metabolic or functional information different from that of the anatomic MRI, other MR techniques have also been investigated for the diagnosis of AD. Utility of these MR techniques remains to be confirmed with the standard of histopathology (moderate evidence).

Supporting Evidence
One of the most extensively studied MR techniques for the diagnosis of AD is ^{1}H MR spectroscopy (^{1}H MRS), which provides biochemical information from hydrogen proton-containing metabolites in the brain (Fig. 16.1). Decrease in the ratio of the neuronal metabolite N-acetylaspartate (NAA) to the metabolite myoinositol (MI) distinguished AD patients from normal with a sensitivity of 82–83 % and specificity of 80–85 % in a pathologically confirmed cohort [62]. Decrease in NAA levels on ^{1}H MR spectroscopy of the frontal lobe also distinguished clinically diagnosed patients with frontotemporal dementia from patients with AD with an accuracy of 84 % [63] (moderate evidence). Another functional imaging

technique: dynamic susceptibility MRI has been proposed as an alternative to SPECT for quantitation of temporoparietal hypoperfusion in AD, and the sensitivity and specificity of this technique has been comparable to SPECT [64] (moderate evidence).

Diagnostic accuracy of other quantitative MRI techniques: diffusion-weighted MR imaging (DWI) and magnetization transfer MR imaging to distinguish AD patients from normal elderly in clinically confirmed cohorts were lower than clinical evaluation [65, 66], and evidence is lacking on the diagnostic accuracy of either functional MRI or phosphorous (^{31}P)-MRS in AD (insufficient evidence).

Can Neuroimaging Identify Individuals at Elevated Risk and Predict Future Development of AD?

Prodromal AD or Mild Impairment Syndromes
Summary
There is moderate evidence that quantitative MR techniques and PET are sensitive to the structural and functional changes in patients with amnestic mild cognitive impairment (MCI). MR-based evaluation of the hippocampal volumes is associated with the rate of future development of AD in individuals with MCI based on clinically confirmed cases, and PET can predict subsequent clinical behavior in cognitively normal elderly.

Supporting Evidence
Risk groups for AD are composed of individuals identified either through clinical examination, or family history and genetic testing, who have a greater probability of developing AD than members of the general population, and in whom the relevant exposures are absent. The rationale for identifying imaging criteria for those at elevated risk comes from recent advances on disease-modifying therapies. Individuals with elevated probability of

developing AD are the primary targets of these treatments trials aimed to prevent or delay the neurodegenerative process. Thus, biomarkers that can accurately distinguish individuals at risk and predict if and when they will develop AD are required in order to utilize these interventions before the neurodegenerative disease advances and irreversible damage occurs.

Aging is a risk factor for AD, and elderly individuals who develop AD pass through a transitional phase of a decline in memory function before meeting the clinical criteria for AD [67]. This early symptomatic or prodromal phase has several clinical definitions, some of which are as follows: MCI, age-associated memory impairment, clinical dementia rating score of 0.5, cognitive impairment, or minimally impaired. While the clinical criteria for each syndrome show similarities, they are subtly different. Longitudinal studies show that individuals with MCI, specifically amnestic MCI, are at a higher risk of developing AD than normal elderly [68]. Patients with MCI possess the earliest features of AD pathology with neuron loss and atrophy in the anteromedial temporal lobe, specifically the entorhinal cortex, which is involved in memory processing [69]. There is strong evidence that there is an association between pathologic involvement and cognitive impairment in the evolution of AD [8, 10, 11]. Hence, patients with MCI reside between normal aging and AD, both in the pathological and in the cognitive continuum (Fig. 16.2) (strong evidence).

In concordance with the pathologic evolution of AD, MR-based volumetry identified smaller hippocampal and entorhinal cortex volumes in patients with MCI than normal elderly [37, 70] (Fig. 16.3a–d). Among several regions in the temporal lobe, reduced hippocampal volumes on MRI and hippocampal glucose metabolism on PET were the best discriminators of patients with MCI from normal elderly [71]. Hippocampal volumes were also comparable to entorhinal cortex volumes for distinguishing patients with MCI [37, 71], elderly individuals with mild memory problems, and very mild AD

[72, 73] from normal (moderate evidence). Other quantitative MRI techniques like DWI and magnetization transfer MRI measurements have also revealed that the diffusivity of water is increased and magnetization transfer ratios are decreased in the hippocampi of patients with MCI relative to normals, both of which indicate an increase in free water presumably due to hippocampal neuronal damage [65, 74, 75] (moderate evidence).

Because all patients with MCI do not develop AD at a similar rate, markers that can predict the rate of development of AD have important implications for assessing the effectiveness of therapies aimed at preventing or delaying development of AD in patients with MCI. Premorbid hippocampal and parahippocampal volumes [76], visual ranking of hippocampal atrophy [77, 78], and measurements of entorhinal cortex volume [73] were associated with future development of AD in patients with mild memory difficulties and MCI. PET [79–81] and SPECT [82–84] have also been shown to predict subsequent development of MCI and AD in clinically determined normal elderly individuals, people with memory impairment, MCI, and questionable AD (moderate evidence).

Two ^{1}H MRS studies revealed that MI/creatine (Cr) levels are higher in both MCI and AD patients than normal elderly. Furthermore, NAA/Cr levels were lower in AD but not in MCI patients than normal elderly in the posterior cingulate gyri of clinically confirmed cases [85, 86] (Fig. 16.4). Similar findings were encountered from neocortical regions in mild AD patients [87], which suggest that MI/Cr levels increase before a significant decrease in the neuronal metabolite NAA/Cr (moderate evidence).

The finding of an early increase in MI/Cr in MCI is encouraging because NAA/Cr is a marker for neuronal integrity. Thus, increase in MI/Cr levels in patients with MCI may predict future development of AD before substantial neuronal damage occurs. This hypothesis remains to be tested with longitudinal studies on these individuals (insufficient evidence).

No study has yet investigated the pathologic correlates of neuroimaging findings in patients with MCI (insufficient evidence).

Asymptomatic ApoE ∈4 Carriers
Summary
The most recognized susceptibility gene in sporadic AD is ApoE ∈4 allele, which has been shown to influence age of onset [88] and amyloid plaque burden [89] in AD. Posterior cingulate gyrus hypometabolism, and the rate of decline in glucose metabolism on PET, is associated with ApoE genotype in people with normal cognition (moderate evidence).

Supporting Evidence
While some studies showed that ApoE genotype does not have any influence on hippocampal volumes [90, 91], others found an association between ApoE genotype and medial temporal lobe atrophy [92, 93]. The dissociation between hippocampal volumes and ApoE genotype may increase the accuracy of both markers for predicting development of AD in the elderly, when combined in prediction models. Posterior cingulate gyrus hypometabolism, and the rate of decline in glucose metabolism on PET on the other hand, is associated with ApoE genotype in people with normal cognition [94–96] (moderate evidence).

Evidence is lacking on the predictive value of PET for development of AD in carriers versus noncarriers of the ApoE ∈4 allele, which requires further investigation with longitudinal studies. No studies were identified on the neuroimaging correlates of ApoE genotype in pathologically confirmed cohorts (insufficient evidence).

Is Neuroimaging Cost-effective for Clinical Evaluation of AD?

Summary
Current treatment options for AD may reduce the social and economic costs of the disease by slowing the rate of cognitive decline, improving the quality of life, and delaying nursing home placement. Neuroimaging may contribute to identification of individuals with early AD who may benefit from such therapies. Use of PET in early dementia can increase the accuracy of clinical diagnosis without adding to the overall costs of the evaluation (moderate evidence). However, the cost-effectiveness analysis revealed that addition of SPECT, dynamic susceptibility contrast-enhanced MRI, and PET to the diagnostic workup of AD was not cost-effective considering the currently available treatment options (moderate evidence).

Supporting Evidence
One study indicated that PET increases the diagnostic accuracy for early AD, reducing the rate of false-negative and false-positive diagnosis, avoiding unnecessary treatment costs and late interventions, without increasing the costs of evaluation and management of AD [97]. On the other hand, the cost-effectiveness analysis of SPECT, dynamic susceptibility contrast-enhanced MRI [98], and PET [99, 100] for the diagnosis of AD revealed that addition of functional neuroimaging to the diagnostic workup of AD in an Alzheimer disease clinic is not cost-effective with the assumed effectiveness of the drug donepezil hydrochloride (moderate evidence).

Cost-effectiveness of a diagnostic modality is directly related to the effectiveness of the therapy for the condition being diagnosed. Thus, cost-effectiveness studies on the diagnostic procedures in AD should be viewed in the context of minimal effectiveness of currently available treatment options. Outcome of cost-effectiveness analyses of diagnostic modalities in AD could change dramatically when more effective therapies become available. No study investigated the cost-effectiveness of neuroimaging in clinical decision making in pathologically confirmed cohorts (insufficient evidence).

Can Neuroimaging Be a Surrogate for Disease Progression and Therapeutic Efficacy in AD?

Summary

Recent advances in treatments aimed at inhibiting the pathologic process of AD created a need for biologic markers that can accurately measure the effectiveness of therapeutic interventions. Neuropsychologic measures of memory and cognitive function can monitor the symptomatic progression in patients with AD. Yet, monitoring biological progression is only possible with markers closely related to the neurodegenerative pathology. The usefulness of neuroimaging as a surrogate for therapeutic efficacy in AD remains to be tested in trials with large cohorts and positive therapeutic outcomes. Currently, there is insufficient evidence that neuroimaging can be a surrogate for therapeutic efficacy in AD (insufficient evidence).

Supporting Evidence

MR-based hippocampal volumetry and regional perfusion on SPECT correlate with the stage of pathologic involvement in AD [39, 51] (strong evidence). Serial measurements of whole brain volumes using the boundary shift integral method on MRI [101–103] and MR-based hippocampal volumetry [104, 105] revealed that rate of atrophy is associated with cognitive decline in patients with AD overtime. Serial MR measures of rate of atrophy in AD may be a valuable surrogate in drug trials. Serial brain to ventricular volume ratio measurements on MRI indicate that to detect a 20 % excess rate of atrophy with 90 % power in AD in 6 months, 135 subjects would be required in each arm of a randomized placebo-controlled trial, and for 30 % excess rate of atrophy, 61 subjects would be required [106] (moderate evidence).

MR-based volume measurements of the whole brain and the hippocampus are valid macroscopic measures of ongoing atrophy in AD. Functional imaging techniques on the other hand, provide markers related to the neurodegenerative pathology at microscopic level. Longitudinal decrease of the neuronal metabolite NAA on ^{1}H MRS [107, 108], regional glucose metabolism on PET [109], and cerebral blood flow on SPECT [110, 111] are associated with the cognitive decline in AD (moderate evidence).

Although it is possible to monitor AD pathology once it is established, irreversible damage characterized by neuron and synapse loss in the anteromedial temporal lobe starts earlier [8–12]. The effectiveness of disease-modifying treatments is expected to be greatest on those patients who are at the very early stages of pathologic involvement but have not yet met the current clinical criteria for AD. For these treatment trials, the most crucial stage for monitoring pathologic progression is the prodromal phase, such as MCI [68]. Rate of hippocampal volume loss measured with serial MRI exams in patients with MCI and normal elderly individuals correlates with cognitive decline, as these individuals progress in the cognitive continuum from normal to MCI and to AD [112] (moderate evidence). Similarly, the decrease in whole brain volumes [113] and cerebral metabolism on PET [114] are associated with cognitive decline in patients under genetic risk of developing AD, although outcome of these risk groups are not known at this time (moderate evidence).

Clinical rating scales and neuropsychological tests are regarded as the gold standard for assessing disease progression and therapeutic efficacy in AD. However, imaging markers may be more accurate in measuring pathologic progression. Estimated sample sizes required to power an effective therapeutic trial (25–50 % reduction in rate of deterioration over 1 year) in MCI indicate that the required sample sizes are substantially smaller for MRI volumetry than commonly used cognitive tests or clinical rating scales at the early stages of disease progression [115]. These data support the use of MRI along with clinical and psychometric measures as surrogate markers of disease progression in AD therapeutic trials (moderate evidence).

Take-Home Tables and Figures

serve to highlight key recommendations and supporting evidence.

Imaging Case Studies

Case 1: T1-weighted three-dimensional spoiled gradient echo images at the level of hippocampal heads showing subjects with MCI and AD as well as normal subjects (Fig. 16.3a–d).
Case 2: [1]H MR spectra obtained from the posterior cingulate volume of interest (VOI) with an echo time of 30 ms in normal subjects and subjects with MCI and AD (Fig. 16.4).

Suggested Imaging Protocols

CT Imaging

- *CT without contrast.* Axial 5–10 mm images should be used to assess for cerebral hemorrhage, mass effect, normal pressure hydrocephalus, or calcifications.
- *CT with contrast.* Axial 5–10 mm enhanced images should be used in patients with suspected neoplasm, infection, or other focal intracranial lesion. If indicated, CT angiography can be performed as part of the enhanced CT.

Table 16.1 Sensitivity and specificity of neuroimaging techniques in distinguishing Alzheimer's disease from normal elderly

Source	N-controls	N-AD	Neuroimaging modality	Sensitivity	Specificity
Jack et al. [46]	126	94	MRI (hippocampal volumes)	CDR 0.5: 78 %	80 %
				CDR 1: 84 %	
				CDR 2: 87 %	
O'Brien et al. [40]	40	77	MRI (visual evaluation)	83 %	80 %
Laasko et al [45]	42	55	MRI (hippocampal volumes)	82–90 %	86–98 %
Wahlund et al. [41]	66	41	MRI (visual evaluation + MMSE scores)	95 %	96 %
Xu et al. [37]	30	30	MRI (hippocampal volumes)	83 %	80 %
Burton et al. [42][a]	35	11	MRI (visual evaluation)	91 %	94 %
Duara et al. [43]	208	53	MRI (visual evaluation	85 %	82 %
Herholtz et al. [60]	110	395	PET (automated analysis)	93 %	93 %
Silverman et al. [116][a]	97	18	PET (visual evaluation)	94 %	73 %
Mosconi et al. [61]	110	199	PET (automated analysis)	99 %	98 %
Claus et al. [47]	60	48	SPECT (visual evaluation)	42–79 %[b]	90 %
Kantarci et al. [62][a]	34	20	^{1}H MRS (myoinositol/N-acetylaspartate)	82–83 %	80–85 %
Kantarci et al. [117]	61	22	^{1}H MRS (N-acetylaspartate/myoinositol)	82 %	80 %

Reprinted with kind permission of Springer Science+Business Media from Kantarci K, Jack Jr CR. Neuroimaging in Alzheimer disease. In: Medina LS, Blackmore CC, editors. Evidence-based imaging: optimizing imaging in patient care. New York: Springer; 2006

CDR clinical dementia rating scale, *MMSE* mini-mental status examination, *MRI* magnetic resonance imaging, *MRS* magnetic resonance spectroscopy, *PET* positron emission tomography, *SPECT* single photon emission computed tomography

[a]The diagnoses were pathologically confirmed
[b]Mild to severe AD

Table 16.2 Suggested diagnostic evaluation for suspected dementia or MCI

1.	Detailed clinical evaluation
2.	Structural imaging with CT or MRI
3.	PET and SPECT if the diagnosis is still uncertain

Reprinted with kind permission of Springer Science+ Business Media from Kantarci K, Jack Jr CR. Neuroimaging in Alzheimer disease. In: Medina LS, Blackmore CC, editors. Evidence-based imaging: optimizing imaging in patient care. New York: Springer; 2006

MR Imaging

- A scout image is acquired to ensure symmetric positioning of the brain within the field of view.
- Sagittal T1-weighted spin-echo sequence (TR/TE = 500/20) for standard diagnostic purposes and measuring intracranial volume where applicable.
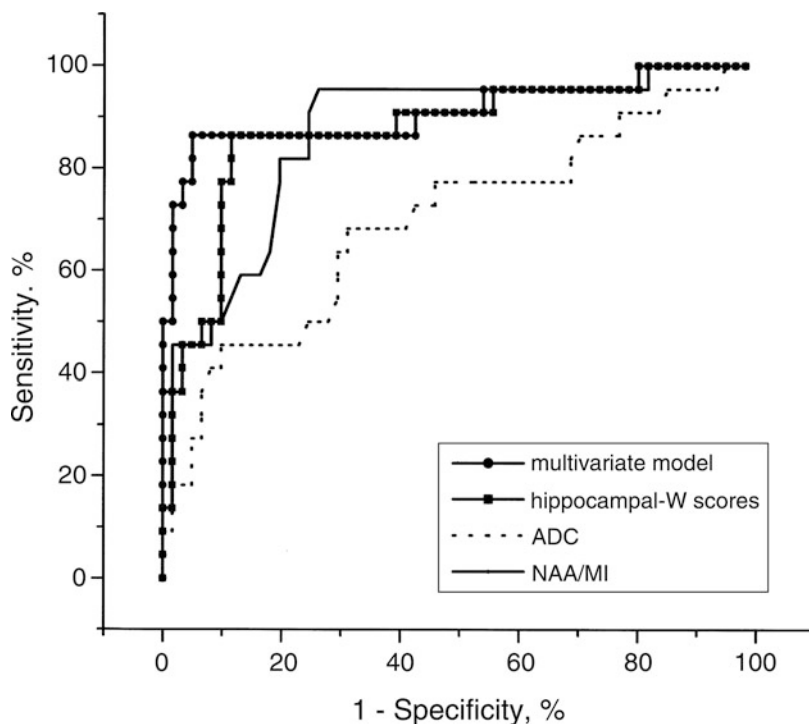

Fig. 16.1 Receiver operating characteristic (ROC) plots of MR measurements in distinguishing patients with a clinical diagnosis of AD from cognitively normal elderly. MRI-based hippocampal volumetry (W scores), hippocampal apparent diffusion coefficients (*ADC*) on diffusion-weighted MRI, *N*-acetylaspartate/myoinositol (*NAA/mI*) on ^{1}H MR spectroscopy, and the multivariate model derived from these three MR measurements were plotted. While the multivariate model is slightly more accurate in distinguishing AD from normal, there is no significant difference between the hippocampal W scores and NAA/mI in distinguishing the two groups. The hippocampal ADC on the other hand is less accurate than hippocampal W scores and NAA/mI [117] (From Kantarci K, Xu YC, Shiung MM, et al. Comparative diagnostic utility of different MR modalities in mild cognitive impairment and Alzheimer's disease. Dementia Geriatric Cognitive Disord. 2002;14(4):198–207; with permission)
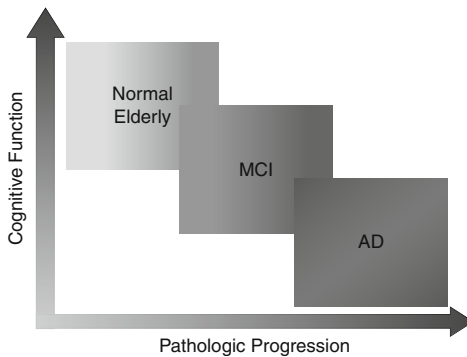
Fig. 16.2 In the cognitive continuum, people with mild cognitive impairment (*MCI*) reside at a transitional clinical state between cognitively normal elderly and people with Alzheimer's disease (*AD*). People with MCI are also at an intermediate stage between asymptomatic elderly individuals with early pathological involvement of AD and people with established AD (Reprinted with kind permission of Springer Science+Business Media from Kantarci K, Jack Jr CR. Neuroimaging in Alzheimer disease. In: Medina LS, Blackmore CC, editors. Evidence-based imaging: optimizing imaging in patient care. New York: Springer; 2006)

- Coronal three-dimensional volumetric acquisition with 124 partitions and 1.6 mm slice thickness (TR/TE/flip angle = 23/6/25).
- Axial double spin-echo (TR/TE = 2200/ 30 and 80) or axial fast-FLAIR (fluid attenuation inversion recovery) sequences (TR/TE/TI = 16000/140/2600) for standard diagnostic purposes and assessment of cerebrovascular disease.
- In patients with suspected neoplasm, infection, or focal intracranial lesions, gadolinium-enhanced T1-weighted conventional spin-echo (TR/TE = 500/20) images should be acquired in at least two planes.

FDG-PET and SPECT Imaging

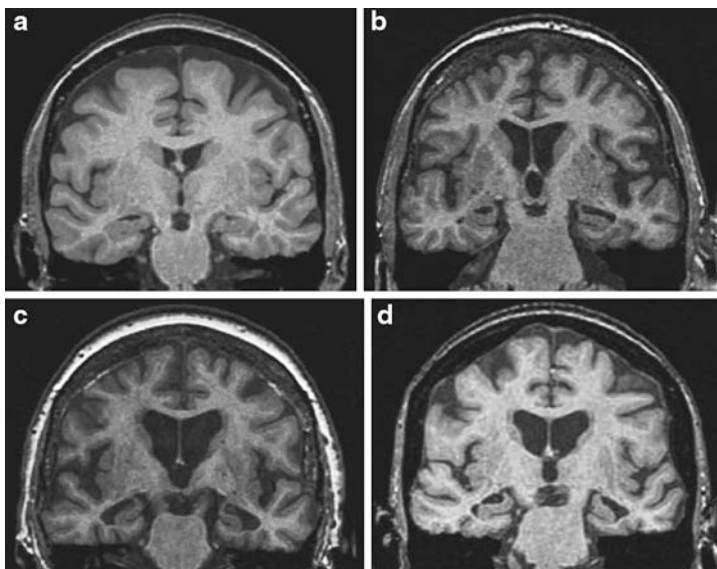- Standard brain FDG-PET and SPECT protocols can be used.

Fig. 16.3 T1-weighted three-dimensional spoiled gradient echo images at the level of hippocampal heads. (**a**) A 76-year-old cognitively normal subject. (**b**) A 77-year-old patient with mild cognitive impairment (*MCI*). (**c**) A 75-year-old patient with Alzheimer's disease (*AD*). (**d**) A 95-year-old cognitively normal subject. Patients with AD, MCI, and the 95-year-old cognitively normal subject have brain atrophy, which is marked in the hippocampi and the temporal lobes in the MCI and AD subject, compared to the younger normal subject. Atrophy is more severe in the AD subject than in the MCI subject. In this case, the age-adjusted regional and global volume measurements would be useful in differentiating atrophy due to normal aging from atrophy due to AD pathology (Reprinted with kind permission of Springer Science +Business Media from Kantarci K, Jack Jr CR. Neuroimaging in Alzheimer disease. In: Medina LS, Blackmore CC, editors. Evidence-based imaging: optimizing imaging in patient care. New York: Springer; 2006)
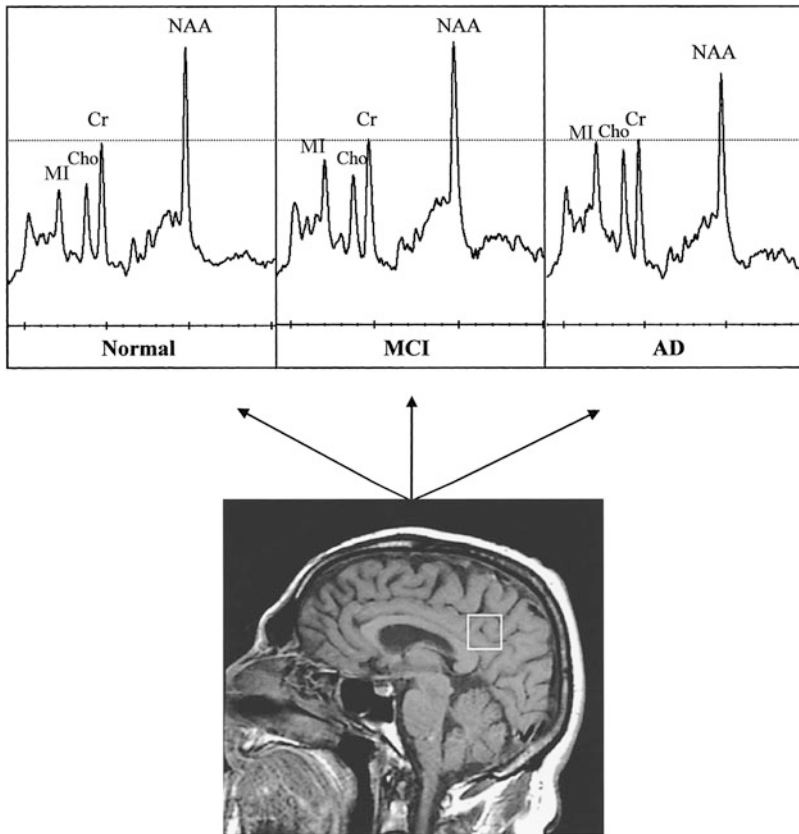
Fig.16.4 Examples of ¹H MR spectra obtained from the posterior cingulate volume of interest (VOI) with an echo time of 30 ms in an 81-year-old cognitively normal subject, a 77-year-old patient with mild cognitive impairment (*MCI*), and a 79-year-old patient with Alzheimer's disease (*AD*). The volume of interest is placed on a midsagittal T1-weighted localizing image, which includes right and left posterior cingulate gyri and inferior precunei. The ¹H MR spectra are scaled to the creatine (*Cr*) peak (*dashed line*). Cr peak is found to be stable in AD and is commonly used as an internal reference for quantitation of other metabolite peaks. Myoinositol (*MI*)/Cr ratio is higher in the patient with MCI than the normal subject. Choline (*Cho*)/Cr and MI/Cr ratio is higher, N-acetylaspartate (*NAA*)/Cr ratio is lower in the patient with AD than both the patient with MCI and the normal subject (Reprinted with kind permission of Springer Science+Business Media from Kantarci K, Jack Jr CR. Neuroimaging in Alzheimer disease. In: Medina LS, Blackmore CC, editors. Evidence-based imaging: optimizing imaging in patient care. New York: Springer; 2006)

- The intravenously injection of the radio-pharmaceutical should take place in a controlled environment with minimal sensory input (dimly lit room with minimal ambient noise).
- The dose of radiopharmaceuticals (FDG for PET, ⁹⁹ᵐTc ECD (bicisate) or ⁹⁹ᵐTc HMPAO (exametazime) for SPECT) may differ between scanners.

Future Research Areas

- Validation of the clinical criteria for AD by clinicians with different levels of expertise and at different clinical settings
- Determining the choice of either CT or MRI for the initial evaluation of dementia in large-scale clinical trials

- Validating the usefulness of PET, SPECT, MR techniques for the diagnosis of AD with autopsy confirmation in large-scale clinical trials
- Determining the cost-effectiveness of neuroimaging techniques as effective treatments become available for AD
- Determining the usefulness of neuroimaging as a surrogate for therapeutic efficacy in trials with positive therapeutic outcomes

References

1. Kokmen E, Beard CM, O'Brien PC, et al. Neurology. 1993;43:1887–92.
2. Beard CM, Kokmen E, O'Brien PC, et al. Neurology. 1995;45:75–9.
3. Alzheimer's Association. Changing the trajectory of Alzheimer's disease: a national imperative. http://www.alz.org/alzheimers_disease_trajectory.asp; 2011. Accessed 18 Oct 2011.
4. Knapp MJ, Knopman DS, Solomon PR, et al. J Am Med Assoc. 1994;271(13):985–91.
5. Rogers SL, Farlow MR, Doody RS, et al. Neurology. 1998;50(1):136–45.
6. Kercher GA, Boxer AL. Expert Opin Biol Ther. 2010;10(7):1121–30.
7. Panza F, Frisardi V, Imbimbo BP, Seripa D, Solfrizzi V, Pilotto A. Expert Opin Biol Ther. 2011;11(6):679–86. Epub 2011 Apr 19.
8. Price JL, Morris JC. Ann Neurol. 1999;45:358–68.
9. Schmitt FA, Davis DG, Wekstein DR, Smith CD, et al. Neurology. 2000;55:370–6.
10. Grober E, Dickson D, Sliwinski MJ, et al. Neubiol Aging. 1999;20(6):573–9.
11. Delacourte A, David JP, Sergeant N, et al. Neurology. 1999;52:1158–65.
12. Morris JC, Storandt M, McKeel Jr DW, et al. Neurology. 1996;46:707–19.
13. Albert MS, DeKosky ST, Dickson D, Dubois B, Feldman HH, Fox NC, Gamst A, Holtzman DM, Jagust WJ, Petersen RC, Snyder PJ, Carrillo MC, Thies B, Phelps CH. Alzheimers Dement. 2011;7(3):270–9.
14. McKhann GM, Knopman DS, Chertkow H, Hyman BT, Jack Jr CR, Kawas CH, Klunk WE, Koroshetz WJ, Manly JJ, Mayeux R, Mohs RC, Morris JC, Rossor MN, Scheltens P, Carrillo MC, Thies B, Weintraub S, Phelps CH. Alzheimers Dement. 2011;7(3):263–9.
15. Montine TJ, Hyman BT, et al. National Institute on Aging-Alzheimer's Association guidelines for the neuropathologic assessment of Alzhimer's disease. Draft 8 July 2011. http://www.alz.org/documents_custom/neuropathologic.pdf. Accessed 18 Oct 2011.
16. American Psychiatric Association. DSM-III-R. Diagnostic and statistical manual of mental disorders. 3rd ed. Washington, DC: American Psychiatric Association; 1987.
17. McKhann GM, Drachman D, Folstein M, et al. Neurology. 1984;34:939–44.
18. Lim A, Tsuang D, Kukull W, et al. J Am Geriatr Soc. 1999;47(5):564–9.
19. Victoroff J, Mack WJ, Lyness SA, et al. Am J Psychiatry. 1995;152(10):1476–84.
20. Galasko D, Hansen LA, Katzman R. Arch Neurol. 1994;51(9):888–95.
21. Massoud F, Devi G, Stern Y, et al. Arch Neurol. 1999;56(11):1368–73.
22. Blacker D, Albert MS, Bassett SS, et al. The National Institute of mental health genetics initiative. Arch Neurol. 1994;51(12):1198–204.
23. Kukull WA, Larson EB, Reifler BV, et al. Neurology. 1990;40(9):1364–9.
24. Massoud F, Devi G, Moroney JT. J Am Gastric Soc. 2000;48:1204–10.
25. Jobst KA, Barnetson LP, Shepstone BJ. Int Psychogeriatr. 1998;10(3):271–302.
26. Fratiglioni L, Grut M, Forsell Y, et al. Clinical diagnosis of Alzheimer's disease and other dementias in a population survey. Agreement and causes of disagreement in applying diagnostic and statistical manual of mental disorders, revised third edition, criteria. Arch Neurol. 1992;49(9):927–32.
27. Graham JE, Rockwood K, Beattie BL, et al. Neuroepidemiology. 1996;15(5):246–56.
28. Baldereschi M, Amato MP, Nencini P, et al. Neurology. 1994;44(2):239–42.
29. Knopman DS, DeKosky ST, Cummings JL, et al. Neurology. 2001;56:1143–53.
30. Jack Jr CR, Petersen RC, O'Brien PC, et al. Neurology. 1992;42:183–8.
31. Braak H, Braak E. Acta Neuropathol (Berl). 1991;82:239–59.
32. Gomez-Isla T, Hollister R, West H, et al. Ann Neurol. 1997;41:17–24.
33. Arriagata PV, Growdon JH, Hedley-Whyte ET, et al. Neurology. 1992;42:631–9.
34. Bobinski M, de Leon MJ, Wegiel J, et al. Neuroscience. 2000;95(3):721–5.
35. Chui H, Qian Z. Evaluation of dementia. Neurology. 1997;49(4):925–35.
36. Nagy Z, Hindley NJ, Braak H. Dement Geriatr Cogn Disord. 1999;10(2):109–14.
37. Xu Y, Jack Jr CR, O'Brien PC, et al. Neurology. 2000;54:1760–7.
38. Frisoni GB, Fox NC, Jack Jr CR, Scheltens P, Thompson PM. Nat Rev Neurol. 2010;6(2):67–77.
39. Jack Jr CR, Dickson DW, Parisi JE, et al. Neurology. 2002;58:750–7.
40. O'Brien JT, Desmond P, Ames D, Schweitzer I, Chiu E, Tress B, et al. Psychol Med. 1997;27(6):1267–75.
41. Wahlund LO, Julin P, Johansson SE, et al. J Neurol Neurosurg Psychiatr. 2000;69(5):630–5.
42. Burton EJ, et al. Brain. 2009;132:195–203.

43. Duara R, Loewenstein DA, Potter E, Appel J, Greig MT, Urs R, Shen Q, Raj A, Small B, Barker W, Schofield E, Wu Y, Potter H. Neurology. 2008;71(24):1986–92.
44. Juottonen K, Laasko MP, Insausti R, et al. Neurobiol Aging. 1998;19(1):15–22.
45. Laakso MP, Soininen H, Partanen K, et al. Neurobiol Aging. 1998;19(1):23–31.
46. Jack CR, Petersen RC, Xu Y, et al. Neurology. 1997;49:786–94.
47. Claus JJ, van Harskamp F, Breteler MM. Neurology. 1994;44(3 Pt 1):454–61.
48. Van Gool WA, Walstra GJ, Teunisse S, et al. J Neurol. 1995;242(2):401–5.
49. Bonte FJ, Weiner MF, Bigio EH, et al. Radiology. 1997;202(3):793–7.
50. Mattman A, Feldman H, Forster B, et al. Can J Neurol Sci. 1997;24(1):22–8.
51. Bradley KM, O'Sullivan VT, Soper ND, et al. Brain. 2002;125(8):1772–81.
52. Jagust W, Thisted R, Devous MD, et al. Neurology. 2001;56:950–6.
53. Hoffman JM, Welsh-Bohmer KA, Hanson MW, et al. J Nucl Med. 2000;41(11):1920–8.
54. Minoshima S, Foster NL, Sima AA, et al. Ann Neurol. 2001;50(3):358–65.
55. McKeith IG, Ballard CG, Perry RH, et al. Neurology. 2000;54:1050–8.
56. Pickut BA, Saerens J, Marien P, et al. J Nucl Med. 1997;38(6):929–34.
57. Hoffman JM, Hanson MW, Welsh KA, et al. Invest Radiol. 1996;31(6):316–22.
58. Mosconi L, De Santi S, Li Y, et al. Eur J Nucl Med. 2006;33:210–21.
59. Messa C, Perani D, Lucignani G, et al. J Nucl Med. 1994;35(2):210–6.
60. Herholz K, Salmon E, Perani D, et al. Neuroimage. 2002;17:302–16.
61. Mosconi L, Tsui WH, Herholz K, Pupi A, Drzezga A, Lucignani G, Reiman EM, Holthoff V, Kalbe E, Sorbi S, Diehl-Schmid J, Perneczky R, Clerici F, Caselli R, Beuthien-Baumann B, Kurz A, Minoshima S, de Leon MJ. J Nucl Med. 2008;49(3):390–8. Epub 2008 Feb 20.
62. Kantarci K, Knopman DS, Dickson DW, Parisi JE, Whitwell JL, Weigand SD, Josephs KA, Boeve BF, Petersen RC, Jack Jr CR. Radiology. 2008;248(1):210–20.
63. Ernst T, Chang L, Melchor R, et al. Radiology. 1997;203:829–36.
64. Harris GJ, Lewis RF, Satlin A, et al. AJNR Am J Neuroradiol. 1998;19(9):1727–32.
65. Kantarci K, Jack CR, Xu YC, et al. Radiology. 2001;219:101–7.
66. Hanyu H, Asano T, Iwamoto T, et al. AJNR Am J Neuroradiol. 2000;21:1235–42.
67. Petersen RC, Smith GE, Ivnik RJ, et al. Neurology. 1994;44:867–72.
68. Petersen RC, Smith GE, Waring SC, et al. Arch Neurol. 1999;56:303–8.
69. Kordower JH, Chu Y, Stebbins GT, et al. Ann Neurol. 2001;49:202–13.
70. Du AT, Schuff N, Amend D, et al. J Neurol Neurosurg Psychiatry. 2001;71(4):431–2.
71. De Santi S, de Leon MJ, Rusinek H, et al. Neurobiol Aging. 2001;22(4):529–39.
72. Dickerson BC, Goncharova I, Sullivan MP, et al. Neurobiol Aging. 2001;22(5):747–54.
73. Killany RJ, Gomez-Isla T, Moss M, et al. Ann Neurol. 2000;47:430–9.
74. Kabani NJ, Sled JG, Shuper A, et al. Magn Reson Med. 2002;47:143–8.
75. Kantarci K, Petersen RC, Boeve BF, Knopman DS, Weigand SD, O'Brien PC, Shiung MM, Smith GE, Ivnik RJ, Tangalos EG, Jack Jr CR. Neurology. 2005;64(5):902–4.
76. Jack CR, Petersen RC, Xu Y, et al. Neurology. 1999;52:1397–403.
77. Visser PJ, Scheltens P, Verhey FR, et al. J Neurol. 1999;246(6):477–85.
78. de Leon MJ, Golomb J, George AE, et al. AJNR Am J Neuroradiol. 1993;14:897–906.
79. de Leon MJ, Convit A, Wolf AT, et al. Proc Natl Acad Sci USA. 2001;286:2120–7.
80. Chetelat G, Desgranges B, de la Sayette V, Viader F, Eustache F, Baron JC. Neurology. 2003;60:1374–7.
81. Drzezga A, Lautenschlager N, Siebner H, et al. Eur J Nucl Med Mol Imaging. 2003;30(8):1104–13.
82. Huang C, Wahlund LO, Svensson L, Winblad B, Julin P. BMC Neurol. 2002;2(1):9.
83. Tanaka M, Fukuyama H, Yamauchi H, et al. J Neuroimaging. 2002;12(2):112–8.
84. Johnson KA, Jones K, Holman BL, et al. Neurology. 1998;50:1563–71.
85. Kantarci K, Jack CR, Xu YC, et al. Neurology. 2000;55(2):210–7.
86. Catani M, Cherubini A, Howard R. Neuroreport. 2001;12(11):2315–7.
87. Huang W, Alexander GE, Chang L, et al. Neurology. 2001;57:626–32.
88. Tsai MS, Tangalos E, Petersen R, et al. Am J Hum Genet. 1994;54:643–9.
89. Gomez-Isla T, West HL, Rebeck GW, et al. Ann Neurol. 1996;39:62–70.
90. Jack CR, Petersen RC, Xu Y, et al. Ann Neurol. 1998;43:303–10.
91. Barber R, Gholkar A, Scheltens P, et al. Arch Neurol. 1999;56(8):961–5.
92. Geroldi C, Pihlajamaki M, Laasko MP, et al. Neurology. 1999;53:1825–32.
93. Lehtovirta M, Soininen H, Laasko MP, et al. J Neurol Neurosurg Psychiatry. 1996;60:644–9.
94. Small GW, Mazziotta JC, Collins MT, et al. J Am Med Assoc. 1995;273:942–7.
95. Reiman EM, Caselli RJ, Yun LS, et al. N Engl J Med. 1996;334:752–8.

96. Small GW, Ercoli LM, Silverman DH, et al. Proc Natl Acad Sci USA. 2000;97(11):6037–42.
97. Silverman DH, Gambhir SS, Huang HW. J Nucl Med. 2002;43(2):253–66.
98. McMahon PM, Araki SS, Neumann PJ, et al. Radiology. 2000;217:58–68.
99. McMahon PM, Araki SS, Sandberg EA, Neumann PJ, Gazelle GS. Radiology. 2003;228:515–22.
100. Kulasingam SL, Samsa GP, Zarin DA, et al. Value Health. 2003;6(5):542–50.
101. Freeborough PA, Fox NC. IEE Trans Med Imaging. 1997;15:623–9.
102. Fox NC, Cousens S, Scahill R, et al. Arch Neurol. 2000;57(3):339–44.
103. Fox NC, Warrington EK, Rossor MN. Lancet. 1999;353:2125.
104. Jack CR, Petersen RC, Xu Y, et al. Neurology. 1998;51:993–9.
105. Laasko MP, Lehtovirta M, Partanen K, et al. Biol Psychiatry. 2000;47(6):557–61.
106. Bradley KM, Bydder GM, Budge MM, et al. Br J Radiol. 2002;75(894):506–13.
107. Adalsteinsson E, Sullivan EV, Kleinhans N, et al. Lancet. 2000;355:1696–7.
108. Jessen F, Block W, Träber F, et al. Neurology. 2001;57(5):930–2.
109. Smith GS, de Leon MJ, George AE, et al. Arch Neurol. 1992;49:1142–50.
110. Brown DR, Hunter R, Wyper DJ, et al. J Psychiatr Res. 1996;30(2):109–26.
111. Shih WJ, Ashford WJ, Coupal JJ, et al. Clin Nucl Med. 1999;24(10):773–7.
112. Jack CR, Petersen RC, XU Y, et al. Neurology. 2000;55:484–9.
113. Fox NC, Crum WF, Scahill RI, et al. Lancet. 2001;358:201–5.
114. Reiman EM, Caselli RJ, Chen K, et al. Proc Natl Acad Sci USA. 2001;98:3334–9.
115. Jack CR, Shiung MM, Gunter JL, et al. Neurology. 2004;62:591–600.
116. Silverman DHS, Small GW, Chang CY, et al. J Am Med Assoc. 2001;286(17):2120–7.
117. Kantarci K, Xu YC, Shiung MM, et al. Dement Geriatr Cogn Disord. 2002;14(4):198–207.

Children with Attention-Deficit-Hyperactivity Disorder (ADHD): Evidence-Based Neuroimaging

17

Gary L. Hedlund

Contents

G.L. Hedlund

Department of Medical Imaging, University of Utah, Primary Children's Medical Center, Salt Lake City, UT, USA
e-mail: gary.hedlund@imail.org

Key Points

- ADHD is considered by many as the most common childhood neurobehavioral disorder (moderate evidence).
- ADHD is a disorder of executive function. Elements of inattention, hyperactivity, and impulsivity are seen to varying degrees. Impaired behavioral inhibition may be the cornerstone of ADHD (moderate evidence).
- ADHD is a clinical diagnosis lacking a specific confirmatory laboratory or cognitive test (moderate evidence).
- There is no indication for imaging in ADHD unless associated comorbidities, relevant history, or clinical examination warrants (moderate evidence).
- There is not currently a known benefit of imaging patients with ADHD (insufficient evidence).

Definition and Pathophysiology

ADHD is a clinically diagnosed neurobehavioral disorder where the affected individual experiences abnormalities of executive function. Impaired behavioral inhibition is a key element in ADHD, and some authors feel that inattention and hyperactivity follow. There is variability in the presence and magnitude of attention-deficit hyperactivity and impulsivity domains among affected children [1–3]. There is no pathognomonic diagnostic laboratory, imaging, or cognitive test to confirm the diagnosis [3]. It is generally accepted that a child presenting with symptoms of ADHD should initially undergo hearing and vision screening to address treatable problems mimicking ADHD [1–3] (moderate evidence).

There is ample evidence that abnormal dopamine transmission in the frontal lobes and within the fronto-striatal neuronal circuitry plays an important role in the pathogenesis of ADHD [4]. This is supported by the clinical knowledge of the efficacy of medications that modulate catecholamine transmission in the dopaminergic pathways [4]. The role of the dopaminergic pathway in ADHD has lead many investigators to pursue molecular genetic studies, focusing upon genes that play a role in dopamine transport and reception [5, 6]. Some molecular genetic studies have shown an association between ADHD and oppositional defiant disorder (ODD) [6]. At least three dopamine receptor genes have been linked to ADHD [7–9]. Other potential causes of ADHD are under active investigation, including the environmental impact of television watching upon attention [10].

Neurologic and/or psychiatric conditions such as epilepsy, depression, and sleep disorders may present with the clinical symptoms of ADHD. Thoughtful clinical diagnosis is important to detect comorbidities such as hypothyroidism, phenylketonuria, and lead exposure that may mimic or coexist with ADHD in order to tailor the most effective therapies [11–13].

The neurobiology and structural characterization of the brain in ADHD centers in large part on the prefrontal cortex which is a critical structure relating to attention [4]. MRI cerebral volumetric studies, MR assessment of gray matter volume, cortical convolutional mapping, corpus callosum, basal ganglia, and cerebellar volume assessment have received much attention [4, 14–16]. Structural and functional imaging findings will be addressed under the section "Goals of Imaging."

Epidemiology

The clinical diagnostic criteria for ADHD are based upon criteria in the fourth Edition of *Diagnostic and Statistical Manual of Mental Disorders* (DSM-IV). When inclusion of the three classifications of ADHD occurs, the number of affected individuals increases [17]. The prevalence of ADHD using DSM-IV criteria is roughly 5–12 % [18, 19] (moderate evidence).

Overall Cost to Society

It has been estimated that the symptoms of ADHD appear in roughly 5 % of children as early as preschool. Early detection and

intervention can mitigate the impact that ADHD may have on the child's development and subsequent health and function as an adolescent and adult. Over the course of an individual's life with ADHD, the social and societal costs may be large [20]. Individuals with ADHD have difficulties with personal relationships, academic performance, delinquency, and occupational underachievement [21]. Approximately 50 % of adults who were diagnosed with ADHD in childhood will suffer from persistent disabilities in adulthood. Pelham et al., using an ADHD prevalence rate of 5 %, established a conservative estimate of the annual societal costs of illness in the United States of affected children and adolescents at $42.5 billion [22] (moderate evidence).

Goals of Imaging

In patients with ADHD as with other neurobehavioral disorders, such as autism or oppositional defiant disorder (ODD), there is no clinical indication for brain imaging unless there are localizing neurological abnormalities or coexistent conditions or comorbidities that warrant imaging [19, 23].

Some indications for imaging in children diagnosed with ADHD include associations with head trauma, known perinatal injury, epilepsy, or the presence of a phakomatosis such as neurofibromatosis type I [24–28] (moderate evidence).

Methodology

A Medline search was performed using PubMed (National Library of Medicine) from 1985 to 2010 (Bethesda, Maryland). A query for original research of publications discussing the performance and effectiveness of imaging strategies in pediatric patients with ADHD was done. The review was limited to human studies and the English language literature. References were identified with the terms "attention-deficit hyperactivity disorder (ADHD)," "attention deficit disorder (ADD)," "brain," "neuroimaging,"

"MRI," "functional MRI," and "diffusion tensor imaging."

The author performed a critical review of the title and abstracts of the indexed articles followed by a review of the full text of articles that were relevant.

Discussion of Issues

Imaging Strategies for the Child with Attention-Deficit Hyperactivity Disorder (ADHD): Which Patients Should Undergo Imaging? What Imaging, If Any, Is Appropriate?

Magnetic Resonance Imaging (MRI)
Summary
In stable children with ADHD, there is no clinical indication for brain imaging. The coexistence of ADHD with conditions such as epilepsy, trauma, neurofibromatosis type I, or a history of very low brain weight (prematurity) may warrant MRI evaluation [24–28] (moderate evidence).

Supporting Evidence
MRI has provided insights into structural anatomy of children, adolescents, and adults with ADHD [4, 29]. The neuroanatomic basis of ADHD is postulated by some researchers to involve those neural circuits responsible for attention and executive function [4, 16, 29]. This has led to the active investigation of whole brain volume, as well as regional, and focal cerebral and cerebellar volume changes in ADHD [4, 14, 16, 30–33]. Several studies have shown a total cerebral reduction in volume, especially involving the right hemisphere [4, 16, 34]. Disturbance in the action-oriented networks (prefrontal lobes and orbito-frontal subdivisions) demonstrate diminished volume [33–35]. McAlonan et al. have shown significant regional volume deficits in ADHD patients predominantly involving the right hemispheric frontal-pallidal-parietal gray matter [16]. The prefrontal cortex plays a crucial role in attention function. Li et al. demonstrated reductions of prefrontal cortex volume and reduced cortical convolutional

complexity in patients with ADHD [36]. Wolosin et al. showed a reduction of cortical volume and reduced cortical folding in patients with ADHD [30]. More circumscribed sites of volume loss include the dorsolateral prefrontal cortex, motor and pre-motor cortices, and the posterior cingulate region [14, 16, 32, 34]. Boys with the clinical diagnosis of ADHD show a reduction in basal ganglia volumes, particularly the caudate head and putamen [37–39]. This gender difference may reflect a fundamentally different neuropathophysiologic process in boys and girls. Soliva et al. reported significant right caudate volume loss in patients with ADHD [39]. Another target of volume loss in the patient with ADHD is the corpus callosum. Reduction in splenium volume in patients with ADHD may in part correlate with known deficits in response control [40, 41]. Total cerebellar volume loss and vermian volume loss (particularly superior vermis) have also been reported in patients with ADHD [14, 16, 42, 43]. The summed sample size for these ADHD patients is greater than one hundred.

In 2007, a meta-analysis by Valera et al. showed significant cerebral volume deficits in ADHD patients compared to controls. They found the largest volume differences within the posterior inferior vermis of the cerebellum, followed by the splenium of the corpus callosum, reduction in total cerebral volume, and finally diminished volume of the right caudate nucleus [44] (moderate evidence).

Diffusion tension imaging (DTI) has been found to be a useful MRI adjunct yielding insights into the microstructural cerebral anatomy in several disorders including ADHD [45]. Microstructural integrity in ADHD has been shown to be disturbed in several regions including the right anterior cingulate bundle (reduced white matter fractional anisotropy) and bilateral fronto-occipital fasciculi [45–47].

Functional Magnetic Resonance Imaging (fMRI)

Summary

The use of fMRI in the study of ADHD represents a rapidly evolving field of research, although complex in nature, common themes of activation have been reported [45]. Functional magnetic resonance imaging (fMRI) is well suited to study pediatric and adult patients with ADHD who exhibit both resting state and task-related network connectivity disturbances [4, 48–51] (moderate evidence).

Supporting Evidence

Numerous studies have demonstrated both task and resting state dysfunction in pediatric and adult patients with ADHD. Burston and Cubillo elucidated the maturational delay in the ventral fronto-striatal circuitry in children with ADHD [49, 50]. Interference suppression in ADHD has been found to be associated with reduced frontal-striatal-temporal-parietal network connections, whereas response in inhibition performance relies upon frontal-striatal and right superior cingulum networks [51]. Schneider et al. further defined impairment of the frontal-striatal and parietal cerebral networks in adults with ADHD [52]. Rodriguez et al. further elucidated brain attention and impulse control disorders in individuals with ADHD by using fMRI to investigate the subtypes of ADHD (ADHD-inattentive type, ADHD-hyperactive/ADHD-impulsive type, and ADHD-combined type) [53]. Functional abnormalities of the prefrontal cortex and basal ganglia have shown that developmental changes in ADHD symptoms and signs are associated with functional changes in the ventral lateral prefrontal cortex [54]. Heightened distractibility has been indexed by increased reaction time in patients with ADHD. Fassbender et al. have demonstrated that increased distractibility in at least some patients with ADHD may be due to an inability to suppress activity in the default attention network in response to increasing difficulty of a task [55].

Functional MRI has also provided insights among children with ADHD and children with pure conduct disorders. Children with ADHD demonstrate a process-related disassociation of prefrontal dysfunction. Reward-related dysfunction in the orbito-frontal cortex was seen in children with conduct disorders [56]. Depue et al. not only showed reductions in the inhibitory control and reduced activity of the right lateral prefrontal cortex in ADHD but also demonstrated

that the right lateral prefrontal cortex exerts control over memory and motor processes [57].

Alterations in baseline brain activity can be studied in the resting state (in nonsedated, as well as sedated patients). [58] Zang et al. have shown resting state abnormalities in children diagnosed with ADHD in the prefrontal-striatal circuit, cerebellum, and brain stem [58].

The effects of psychostimulants can be measured with functional MRI [59]. The well-known dysfunction of the frontal-striatal and frontal-cerebellar circuitries can be modified by stimulant medication [59]. Children diagnosed with ADHD treated with methylphenidate showed increased activation of the right frontal cortex during interference suppression [60]. Peterson et al. studied the effects of psychostimulants on brain activation of children and adolescents with ADHD performing the Stroop color and word test. They believe that psychostimulants prescribed to youths with ADHD showed improved suppression of the default mode activity in the ventral anterior cingulate and posterior cingulate cortices [61].

Positron Emission Tomography (PET) Summary

Positron emission tomography (PET) elucidates glucose metabolism and cerebral blood flow in normal and pathologic states. PET provides a powerful tool for the noninvasive cerebral spatial distribution assessment of radiolabeled compounds and to indirectly assess blood flow, metabolism, and neurotransmitter function [4, 62]. Data on the use of PET in ADHD is limited. Early PET studies of glucose metabolism in women with ADHD demonstrated reductions of global glucose metabolism of 8.1 % lower than controls. Other studies have shown reduced glucose utilization in the fronto-striatal regions of patients with ADHD (moderate evidence).

Supporting Evidence

Positron emission tomography has an advantage over structural imaging tools in the ability to noninvasively assess perturbations of brain chemistry [62]. In ADHD, the catecholamine-rich cortical and subcortical networks of the frontal lobes demonstrate [4, 62] deregulation of catecholamine and dopaminergic neurotransmitters. Some believe that excess dopamine in the brain may lead to hyperactive behavior [62].

Early PET studies of glucose metabolism in women with ADHD demonstrated reductions of global glucose metabolism of 8.1 % lower than controls [62]. Ernst et al. in 2003 showed reduced glucose utilization in the fronto-striatal regions of patients with ADHD [63].

Recent PET investigations of patients with ADHD have illuminated the role of dopaminergic neurotransmission in ADHD [62]. Dopamine transporter (DAT) plays a key role in presynaptic reuptake of dopamine. PET investigation of DAT activity and the therapeutic response to antihyperactivity medications is providing greater insights into the biochemistry of ADHD [4, 62]. Although PET has an advantage in being able to longitudinally follow antihyperactivity therapy in ADHD patients, PET lacks spatial resolution compared to modalities such as fMRI [4, 62, 63] (moderate evidence).

Take-Home Table

Table 17.1 shows the options for imaging the child with ADHD and relative strengths, weaknesses, and costs.

Imaging Case Studies

Case 1: 11-year-old boy with combined form of ADHD (Fig. 17.1).

Future Research

- To better define the role that structural imaging such as MRI, DTI, and functional imaging (fMRI) may play in the diagnosis, monitoring, and assessment of targeted therapies for ADHD patients
- To determine the cost effectiveness of imaging strategies in assessing novel therapies in patients suffering from ADHD

Table 17.1 Imaging options for ADHD

Imaging studies	Sedation required	Anatomic detail	Functional assessment	Radiation	Costs
MRI	+++	+++	-	No	$$$
DTI[a]	++	+++	+	No	No
fMRI[b]	− or ++	+	+++	No	$$$
PET	++	+	+++	Yes	$$$

Relative costs established by reviewing technical and professional fees at Primary Children's Medical Center, Salt Lake City, Utah

[a]DTI is performed in the same setting as MRI

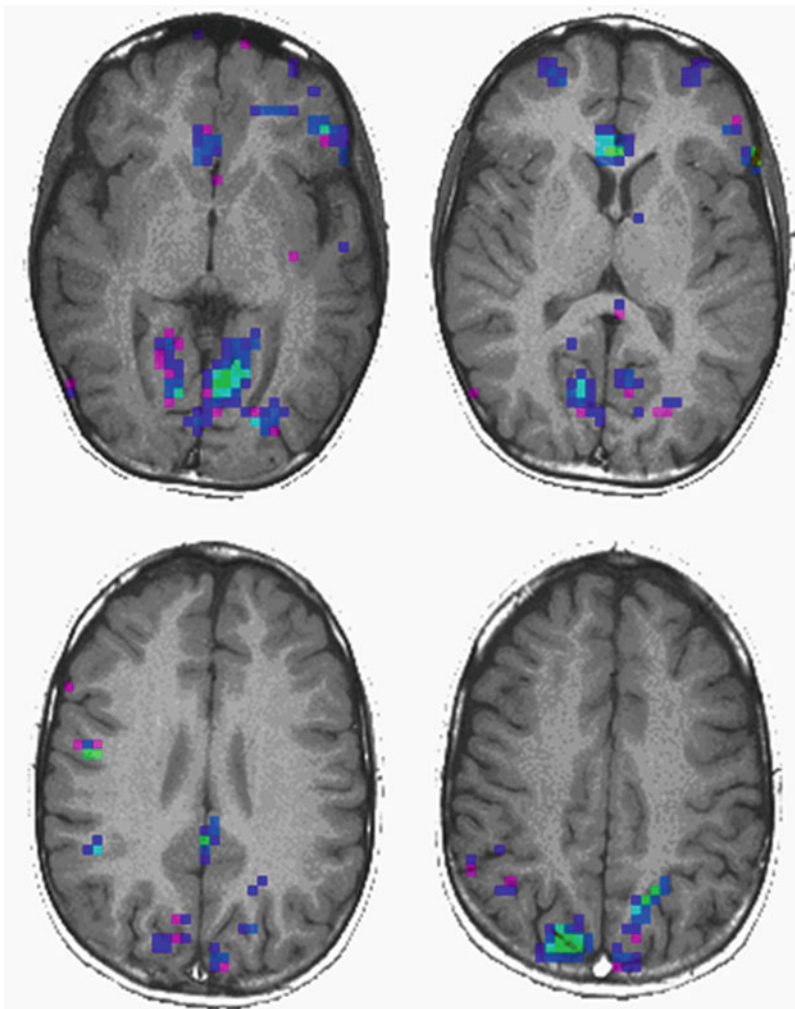[b]In mildly affected patients, sedation may not be required

Fig. 17.1 Color Stroop-fMRI in an 11-year-old boy with combined form of ADHD. Paradigm design: visually presented words. Control block: congruent color test, e.g., *red*. Activation block: incongruent color test, e.g., *blue*. Activation map overlaid on a T1-weighted MRI, color coded for intensity from *light green* (max) to *dark blue* (min). Main areas of activation are seen in the anterior cingulate gyrus and visual and posterior parietal lobes. Weak and scanty activation is obtained in the frontal lobes. No activation was obtained in the basal ganglia as expected in normal subjects. Images are in radiological orientation (Courtesy of Miami Children's Hospital, Radiology Department)

References

1. Cormier E. J Pediatr Nurs. 2008;23:345.
2. Katragadda S, Schubiner H. Prim Care Clin Office Pract. 2007;34:317–41.
3. Wilens TE, Spencer TJ. Postgrad Med. 2010;122:97.
4. Kobel M, Bechtel N, Specht K, et al. Psychiatr Res: Neuroimaging. 2010;183:230–6.
5. Cheon KA, Ryu YH, Kim YK, et al. Eur J Nucl Med Mol Imaging. 2003;30:306–11.
6. Kent L. Curr Psychiatry Rep. 2004;6:143.
7. Payton A, Holmes J, Barrett JH, et al. Am J Med Genet. 2001;105:464.
8. Faraone SV, Doyle AE, Mick E, et al. Am J Psychiatry. 2001;58:1052.
9. Palmer CG, Bailey NJ, Ramey C, et al. Psychiatr Genet. 1999;9:157.
10. Christakis DA, Zimmerman FJ, DiGiuseppe DL, et al. Pediatrics. 2004;113:708.
11. Rovet JF. Child Neuropsychol. 2002;8:150.
12. Suresh PA, Sebastian S, George A, et al. Pediatr Neurol. 1999;20:192.
13. Antshel KM, Waisbren SE. Neuropsychology. 2003;17:458.
14. Castellanos FX, Lee PP, Sharp W, et al. J Am Med Assoc. 2002;288:1740.
15. Brieber S, Neufang S, Bruning N, et al. J Child Psychol Psychiatry. 2007;48:1251–8.
16. McAlonan GM, Cheung V, Cheung C, et al. Psychiatry Res. 2007;154:171–80.
17. American Academy of Child, Adolescent Psychiatry. J Am Acad Child Adolesc Psychiatry. 1997;36:855–1218.
18. Baumgaertel A, Wolraich ML, Dietrich M. J Am Acad Child Adolesc Psychiatry. 1995;34:629.
19. Giedd JN, Blumenthal J, Molloy E, et al. Ann N Y Acad Sci. 2001;931:35–49.
20. Bernfort L, Nordfeldt S, Persson J. Acta Paediatr. 2008;97:239–45.
21. Scott S, Knapp M, Henderson J, et al. Br Med J. 2001;323:1–5.
22. Pelham WE, Foster M, Robb JA. J Pediatr Psychol. 2007;32:711–27.
23. Brown TE. Attention-deficit disorders and co-morbidities in children, adolescents, and adulthood. Washington, DC: American Psychiatric Press; 2000.
24. Gerring J, Brady K, Chen A, et al. Brain Inj. 2000;14:205.
25. Wassenberg R, Max JE, Lindgren SD, et al. Brain Inj. 2004;18:751.
26. Foulder-Hughes LA, Cooke RW. Dev Med Child Neurol. 2003;45:97.
27. Toft PB. Pediatr Neurol. 1999;21:602.
28. Rosser TL, Packer RJ. Curr Neurol Neurosci Rep. 2003;3:129.
29. Garrett A, Penniman L, Epstein J, et al. J Am Acad Child Adolesc Psychiatry. 2008;47:11.
30. Wolosin SM, Richardson ME, Hennessey JG, et al. Hum Brain Mapp. 2009;30:175–84.
31. Wang J, Jiang T, Cao Q, et al. AJNR Am J Neuroradiol. 2007;28:543–7.
32. Overmeyer S, Bullmore ET, Suckling J, et al. Psychol Med. 2001;31:1425–35.
33. Van't Ent D, Lehn H, Derks EM, et al. Neuroimage. 2007;35:1004–20.
34. Mostofsky SH, Cooper KL, Kates WR, et al. Biol Psychiatry. 2002;52:785.
35. Seidman LJ, Valera EM, Makris N. Biol Psychiatry. 2005;57:1263–72.
36. Li X, Jiang J, Zhu W, et al. Brain Dev. 2007;29:649–55.
37. Tremols V, Bielsa A, Soliva JC, et al. Psychiatry Res. 2008;163:270–9.
38. Qiu A, Crocetti D, Adler M, et al. Am J Psychiatry. 2009;166:74–82.
39. Soliva JC, Fauquet J, Bielsa A, et al. Psychiatr Res: Neuroimaging. 2010;182(3):238–43.
40. Cao Q, Sun L, Gong G, et al. Brain Res. 2010;1310:172–80.
41. McNally MA, Crocetti D, Mahone EM, et al. J Child Neurol. 2010;25:453–62.
42. Roth RM, Saykin AJ. Psychiatr Clin North Am. 2004;27:83–6.
43. Bledsoe J, Semrud-Clikeman M, Pliszka SR. Biol Psychiatry. 2009;65:620–4.
44. Valera EM, Faraone SV, Murray KE, et al. Biol Psychiatry. 2007;61:1361–9.
45. Xavier Castellanos F, Hyde Z. Diffusion tensor imaging provides new clues in adults with ADHD. Comment Eur J Neurosci. 2010; 31:910–11.
46. Davenport ND, Karatekin C, Tonya W, et al. Psychiatr Res: Neuroimaging. 2010;181:193–8.
47. Silk TJ, Vance A, Rinehart N, et al. Hum Brain Mapp. 2009;30:2757–65.
48. Paloyelis Y, Mehta MA, Kuntsi J, et al. Expert Rev Neurother. 2007; 1337–56.
49. Durston S, Tottenham NT, Thomas KM, et al. Biol Psychiatry. 2003;53:871–8.
50. Cubillo A, Halari R, Ecker C, et al. J Psychiatr Res. 2010;44:629–39.
51. Vaidya CJ, Gunge SA, Dudukovich NM, et al. Am J Psychiatry. 2005;162:1605–13.
52. Schneider MF, Krick CM, Retz W, et al. Psychiatry Res. 2010;183:75–84.
53. Rodriguez PD, Baylis GC. Behav Neurol. 2007;18:115–30.
54. Schulz KP, Newcorn JH, Fan J, et al. J Am Acad Child Adolesc Psychiatry. 2005;44:47–54.
55. Fassbender C, Zhang H, Buzy WM, et al. Brain Res. 2009;1273:11–1128.
56. Rubia K, Smith AB, Halari R, et al. Am J Psychiatry. 2009;166:83–94.
57. Depue BE, Burgess GC, Willcutt EG, et al. Neuropsychologia. 2010;48:3909–17.
58. Zang YE, He Y, Zhu CZ, et al. Brain Dev. 2007;29:83–91.

59. Epstein JN, Casey BJ, Toney ST, et al. J Child Psychol Psychiatry. 2007;48:899–913.
60. Lee YS, Hand DH, Lee JH, et al. Psychiatr Investig. 2010;7:49–54.
61. Peterson BS, Potenza MN, Wang Z, et al. Am J Psychiatry. 2009;166:1286–94.
62. Zimmer L. Neuropharmacology. 2009;57:601–7.
63. Ernst M, Grant SJ, London ED, et al. Am J Psychiatry. 2003;160:33–40.

Children with Autism: Evidence-Based Neuroimaging

18

Gary L. Hedlund

Contents

G.L. Hedlund
Department of Medical Imaging, University of Utah, Primary Children's Medical Center, Salt Lake City, UT, USA
e-mail: gary.hedlund@imail.org

Key Points

- The neurodevelopmental disorder of autism affects social interactions, communication skills, and patterns of activity (moderate evidence).
- For the patient with autism, there is no indication for imaging unless there is a localizing neurological abnormality and/or attendant clinical concerns existing that warrant imaging (moderate evidence).
- Inadequate data exists regarding the future clinical benefit and cost effectiveness of structural and/or functional imaging in patients with ASD (insufficient evidence).
- fMRI and PET are starting to elucidate the spectrum of functional and metabolic abnormalities of the brain (mild to moderate evidence), but more and large studies are still required before it can be used as outcome measure (surrogate outcome) in future therapeutic trials.

Definition and Pathophysiology

Autism represents a neurodevelopmental disorder generally characterized by how an individual relates to and communicates with others. It is defined by criteria in several behavioral domains (social interaction, communication skills, and patterns of activity) [1–3]. The terms autism, autistic, and autistic spectrum disorder (ASD) are often used interchangeably [1–5]. ASD encompasses three categories of disorders (autism, Asperger, and pervasive developmental disorders not otherwise specified) all sharing common symptoms [4, 5]. Autistic disorder is used in a more restrictive fashion and is defined by the American Psychiatric Association *Diagnostic and Statistical Manual of Mental Disorders*, 4th Edition (DSM-IV and DSM-IV-TR) criteria (American Psychiatric Association 1994, 2000) [6] (Table 18.1).

Autism is a heterogeneous disorder when it comes to etiology [4, 5]. Theories of causation are many including genetic, vascular, maternal trauma, association with comorbidities such as tuberous sclerosis complex (TSC), and maternal use of drugs (ergotamine, misoprostol, and thalidomide) [4, 5, 7]. Postmortem studies by Kemper and Bauman showed an increase in brain size and weight among autistic subjects. They also reported curtailment in forebrain neuron development (smaller and more densely packed neurons, decrease in Purkinge cells, and age-related changes in cell size, particularly cells within the diagonal band of Broca, the cerebellar nuclei, and inferior olivary structures [8]. Other authors have detected an increase in white matter volume particularly within the radiate zones (arcuate fibers of the frontal lobes) [9–12]. The frontal lobes have been shown to demonstrate disproportionate increase in white matter volume [13, 14]. Pickett et al. reported neuropathologic features of the cerebral cortex in autistic subjects focusing upon cerebral mini-column anatomy consisting of radially oriented pyramidal cells and their aligned myelinated axons [15]. Brains of autistic subjects showed significant narrowing of mini-column cortical width [15].

Genome-wide linkage screens have refuted a monogenetic mode of autism inheritance [13, 14]. That being said, autism in monozygotic twins is roughly 12 times more common than in the general population and four times more common among dizygotic twins [13, 14]. Autism is also known to occur in the presence of other medical conditions including tuberous sclerosis complex (TSC), other chromosomal anomalies (fragile X syndrome), and mitochondrial disorders, inborn errors of metabolism, such as phenoketonuria (PKU), and the velocardiofacial and Möbius syndromes. Roughly 8 % of autistic patients have a specific associated clinically defined abnormality [13, 14].

There is some agreement that in autism there is little or no evidence of acute cellular change and that a monotropic event early in brain development (during or just after closure of the neural plate) leads to the subsequent cascade of secondary neuropathologic changes [2, 3, 15]. Thus, in the consideration of the neuropathology of autism differentiating the fundamental core pathology from secondary changes remains a challenge. Most authors agree that the neuropathology of

autism is widespread and that the fronto-temporal cortex is preferentially affected [2, 3, 15].

Epidemiology

Autism prevalence ranges from 5 to 10 cases of classic autism per 10,000 live births to 60–65 cases per 10,000 live births when including the entire spectrum of autism disorder (ASD) [13–15]. The Centers for Disease Control & Prevention (CDC) estimate the prevalence of autism to be 1:110 [16] (moderate evidence).

Overall Cost to Society

The daunting challenge of estimating cost associated with autism spectrum disorder (ASD) begins with the recognition that autism holds a lifetime of personal, social, and economic consequences. Estimating costs associated with ASD includes a consideration of the estimation of autism prevalence, age at diagnosis, magnitude of autism disability, scope of services needed including health-related, hospitalization, special education, and special housing needs. Additionally, considerations of the impact economically on the health and well-being of the affected individual and their family, social integration costs, and the impact upon the quality of life for the affected individual and family are to be considered and are challenging to estimate. Two recent studies, one from the United Kingdom and the second from the United States, investigated the costs associated with autism spectrum disorder. In a study by Knapp et al., the economic cost of autism in the United Kingdom was evaluated in a comprehensive study, which incorporated the economic consequences of health and social care, services including special education, housing outside of the family home, cost of leisure services, and estimates of opportunity costs of lost productivity of the affected individual and family members. When costs were adjusted to 2005–2006 price levels, the lifetime costs associated with autism including disability in the affected individual within the United Kingdom

was 3.1 million Great Britain pounds or 5.1 million dollars. Less than 6 % of this total was associated with health-care costs including hospital and social care components. Imaging services, and particularly brain imaging, such as MRI, functional MRI, or PET imaging, were not mentioned in the study [17].

In a more recent study in the United States by Ganz et al., health care, child care, adult care, home and care modification costs, special education needs, and estimated productivity loss for the individual affected and family members put the estimated lifetime cost at 3.2 million dollars per affected individual. Again, diagnostic imaging costs were not specifically mentioned in this study [18] (moderate evidence).

Goals of Imaging

The overall goal of imaging children with autism in a clinical setting is to address attendant clinical concerns over a lateralizing sign(s) on the neurologic examination or to address clinically suspected comorbidities that may be associated with autism. Known associations include tuberous sclerosis complex (TSC), fragile X syndrome, cerebral palsy, bilateral deafness, and inborn errors of metabolism such as phenoketonuria (PKU) [13, 14, 19] (moderate evidence).

Methodology

A Medline search was performed using PubMed (National Library of Medicine) from 1985 to 2010 (Bethesda, Maryland), for original research of publications discussing the performance and effectiveness of imaging strategies in pediatric patients with autism. The review was limited to human studies and the English language literature. References were identified with the terms "autism," "autism spectrum disorders (ASD)," "Asperger's syndrome," "brain," "neuroimaging," "MRI," "functional MRI," "diffusion tensor

imaging," and "positron emission tomography (PET)." The author performed a critical review of the title and abstracts of the indexed articles followed by a review of the full text of articles that were relevant.

Discussion of Issues

Brain Imaging Strategies for the Child with Autistic Spectrum Disorder: Who Should Undergo Medical Imaging? What Imaging Is Appropriate? What Are the Evolving Imaging Considerations?

Magnetic Resonance Imaging (MRI)
Summary

In autistic patients with lateralizing neurological signs and/or other associated comorbidities (epilepsy, TSC, PKU, etc.), MRI is the imaging study of choice when imaging is determined to be indicated based upon the presence of comorbidities (moderate evidence).

Supporting Evidence

Magnetic resonance imaging (MRI) provides a detailed look into the brain and yields valuable insights into the neuroanatomy and in some cases, neurobiology of autism [13]. MRI adjuncts such as diffusion tensor imaging (DTI) and functional MRI (fMRI) contribute to a broader understanding of the pathophysiologic mechanisms of autism [13, 14, 19].

As early as 1943, reports were made of macrocephaly in children with autism [13, 14, 19]. Piven et al. in 1992 highlighted larger mid sagittal brain areas in autistic children [20]. Subsequent studies have shown that the increase of brain volume in autistic children was not generalized but favored the frontal lobes [10, 11, 19]. Other studies have shown the increased autistic brain volume to represent a post natal brain overgrowth [13, 21–23]. Recent quantitative structural imaging studies reveal reduction of gray matter in the fronto-striatal and parietal networks and ventral and superior temporal gyri [19, 21, 22]. Boys with autism have been shown to have larger right inferior frontal language

cortex, a reversal from normal individuals with larger left language regions [19, 21–24]. The cerebellum has also been extensively studied in autism with early reports of vermal hypoplasia involving lobules VI and VII (reflecting a reduction of Purkinge cells) [13, 19, 25, 26]. The meta-analysis by Stanfield confirmed a reduction in size of vermian lobules VI and VII in autistic patients [27]. Amygdala volumes have been found to be enlarged in younger autistic patients [28]. The cingulate gyrus which represents the cortical portion of the limbic system shows significantly decreased volume and decreased metabolic activity in autistic subjects compared to controls [19, 29]. The corpus callosum in autistic subjects has been shown to be reduced in size. This finding may affect interhemispheric connection and impact cognitive function [30, 31]. The basal ganglia have a wide range of functions including voluntary motor control, procedural learning and activity in routine behaviors, eye movement, and cognitive and emotional functions. In autistic patients, the caudate nucleus of the basal ganglia has been shown to be enlarged [13, 19]. The caudate nucleus plays a role in inhibitory behavior. There is a reported correlation between ritualistic and repetitive behaviors and increased caudate volume [19, 27].

In the same imaging setting that structural MRI is performed, diffusion tensor imaging (DTI) can be performed with a small investment of additional time. DTI characterizes the microstructure of white matter tracts and provides useful information in many conditions, including autism spectrum disorders (ASD) [19, 32]. In ASD, there is an early overgrowth of the frontal lobe. DTI characterizes the axonal structure and integrity and fiber angle orientation of the axonal connections that constitute the white matter. A study by Barnea-Goraly et al. reported decreased anisotropy within the anterior cingulum and temporal lobe white matter, which also is known to connect to the amygdala. This indicates a disruption in connectivity in regions that are involved in social functionality [33]. Thakkar et al. elucidated the relationships between diminished fractional anisotropy within the anterior cingulate white matter and the relationships with functional impairment [34].

Autistic patients use alternate white matter connections for cognitive tasks related to linguistic function [35]. Fletcher et al. and Kumar et al. demonstrated impairment of white matter tract integrity within the arcuate fasciculus, and this may be causal to the foundational language problems in autism [36]. Currently, DTI techniques are readily available on all major magnetic resonance imaging scanning platforms but have not been fully integrated into active clinical practice. Much interest is held in DTI and its potential to yield insights into the morphometrics of connectivity within the brain [19, 32] (mild to moderate evidence).

Functional Magnetic Resonance Imaging (fMRI)
Summary
Functional-magnetic resonance imaging (fMRI) has contributed significantly to the understanding of neural connectivity or dysfunction in ASD [37]. Currently, fMRI provides a robust research tool for advancing our understanding of ASD. In the current guidelines for the clinical diagnostic evaluation of suspected ASD in children, adolescents, and adults, there is no recommendation for routine fMRI (mild to moderate evidence).

Supporting Evidence
Early and current fMRI research of ASD has focused on the identification of the neural substrates for perceiving and integrating social information [37]. The utilization of fMRI in the population of patients with ASD has focused on face perception, cognition, and attention [38, 39].

It is well known that patients with ASD exhibit alterations in the neural circuitry of face perception [40]. This impairment in face processing, which includes identity and recognition, has been studied by numerous authors. Schultz et al. demonstrated hypoactivation of the fusiform face area (FFA) in ASD patients [41]. Kleinhans and Schultz have shown altered functional connectivity between the amygdala and the FFA regions [42, 43]. Wang et al. showed reduced functional MR imaging activity while ASD subjects were viewing faces

[44]. Difficulty perceiving and understanding information conveyed through the eyes and facial expressions may be the primary factor in the impaired social development of patients with autism [42–44].

Disturbance in neural functional connectivity affecting cognitive tasks among ASD subjects in part may be explained on the basis of localized areas of hyperconnectivity in the brain [19]. Hyperconnectivity may lead to increased neural noise and impair the development of long-range cognitive and neural connections [19].

Fundamental to neural connectivity disorder in ASD is the patient's lack of realization that others have thoughts different from their own, what is considered to be theory of the mind. ASD patients showed decreased functional MRI activity between the right temporal parietal junction and the left medial frontal gyrus [45]. Recently, Anderson et al. have shown disturbed cortical interconnectivity in autistic males involving sensorimotor cortices, anterior insula, fusiform gyrus, superior temporal gyrus, and the superior parietal lobule [46]. These researchers have also shown increased bilaterality of receptive language among autistic patients compared to controls [47] (mild to moderate evidence).

Functional MRI has the capacity to further elucidate the neural mechanism of autism and holds promise in assessing and monitoring therapies targeted to disturbances of face perception, cognition, and attention. A challenge lies in the fact that the heterogeneity of symptom expression across individuals with ASD is broad. Functional MRI has the ability to differentiate various ASD subgroups. Practically speaking, the milder forms of ASD may be able to undergo fMRI without sedation, but more severely affected children will require sedation, with variable results. Thus, fMRI will become increasingly important as a tool for the identification of etiologic mechanisms involved with ASD and for exploring opportunities for interventions and response to treatment.

Positron Emission Tomography (PET)
Summary
Positron emission tomography (PET) has elucidated glucose metabolism and cerebral

blood flow in the autistic brain. More recently PET imaging has investigated perturbations of neurotransmitters, particularly serotonin, dopamine, and GABA-aminobutyric acid in autism patients [19] (mild to moderate evidence).

Supporting Evidence

Positron emission tomography (PET) has contributed understanding to the measurement and imaging of biochemical and molecular processes within the brain of normal individuals and a multitude of disorders including autism. Glucose metabolism and cerebral blood flow studies show a variety of global and focal alterations among patients with ASD. Frontal, medial prefrontal, temporal, and anterior cingulate cortical regions, as well as basal ganglia structures and regions of the cerebellum have drawn particular interest [29, 48, 49]. PET imaging of resting cerebral blood flow and glucose utilization has shown decrease of flow and diminished utilization of glucose within the temporal lobes in autistic patient [50]. In a resting state, Chugani et al. demonstrated bitemporal glucose hypometabolism particularly in the superior temporal gyrus and hippocampal regions [51]. During verbal learning tasks, Haznedar et al. demonstrated diminished glucose metabolism bilaterally within the caudate, putamen, and thalami [52].

In recent years, there has been attention focused on neurotransmitter function in autism. Schain, Friedman, and Chugani demonstrated that autistic children showed a period of high brain serotonin synthesis [53]. Other authors have elucidated altered serotonin, dopamine, and GABA-aminobutyric acid function in autism. Serotonin and GABA-aminobutyric (GABA) acid was shown by Ernst et al. to be diminished as were dopaminergic activities within the anterior medial prefrontal cortex and occipital cortex in patients with ASD [54].

Take-Home Tables

Table 18.1 highlights the clinical spectrum of autism. Table 18.2 reviews the relative comparison of imaging studies that have been studied in autistic patients and relative cost comparisons.

Table 18.1 Spectrum of autism

I.	Classic autism
	Involves severe qualitative defects in the behavioral domains of social interaction (language, communication and play); deficits manifested as stereotypes, preservation and narrow range of interests and activities
II.	Asperger's syndrome
	Disorder in non-retarded often clumsy children without speech delay who have deficient sociability and narrow interests
III.	Disintegrative disorder – also known as Heller's syndrome
	Previously normal children who undergo a massive developmental regression between 2 and 10 years resulting in severe acquired autism
IV.	Rett's disorder
	Limited to girls with acquired microcephaly, infantile regression, lack of hand use, stereotypic hand movements, and severe retardation
V.	Pervasive developmental disorder not otherwise specified

Adapted from DSM-IV (American Psychiatric Association. Diagnostical and statistical manual of mental disorders. 4th ed. Washington, DC: American Psychiatric Association; 1994)

Table 18.2 Imaging options for autism

Imaging studies	Sedation required	Anatomic detail	Functional assessment	Radiation	Costs
MRI	+++	+++	−	No	$$$
DTI[a]	++	+++	+	No	No
fMRI[b]	− or ++	+	+++	No	$$$
PET	++	+	+++	Yes	$$$

Relative costs established by reviewing technical and professional fees at Primary Children's Medical Center, Salt Lake City, Utah as of January 2011
[a]DTI is performed in the same setting as MRI
[b]Most of the fMRI in autism is done without sedation in relative functional patients
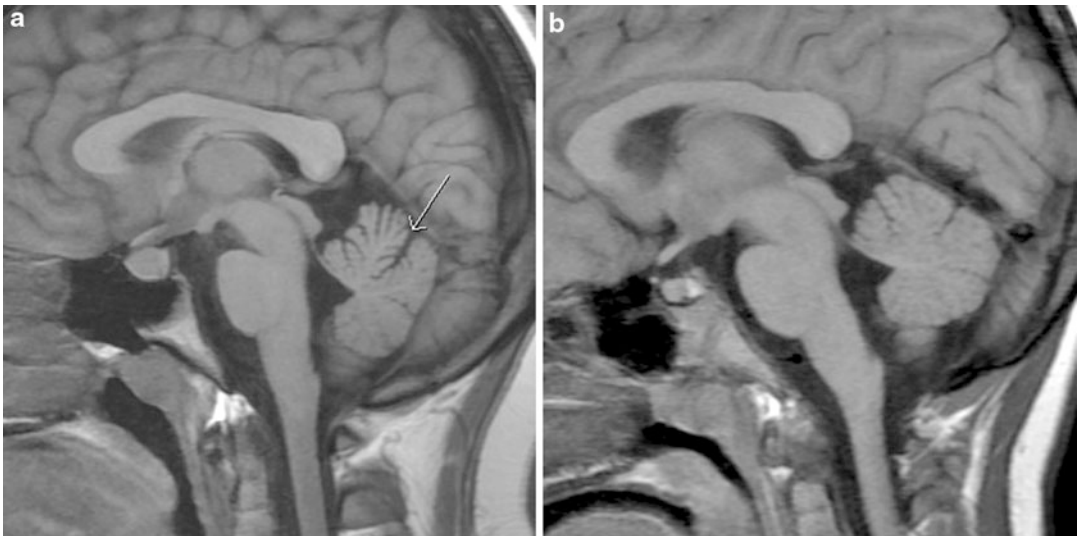
Fig. 18.1 (**a**) Sagittal T_1–weighted MR image of a child with autism shows diminished volume of the anterior vermis and upper portion of the posterior superior vermis (*arrow*). (**b**) Sagittal T_1-weighted MR image of a normal age matched control

Imaging Case Studies

Case 1: MR image of child with autism versus MR image of normal control match (Fig. 18.1a, b)

Case 2: Functional connectivity MRI showing template brain with areas shaded for significantly weaker interhemispheric connectivity in autistic subjects (Fig. 18.2)

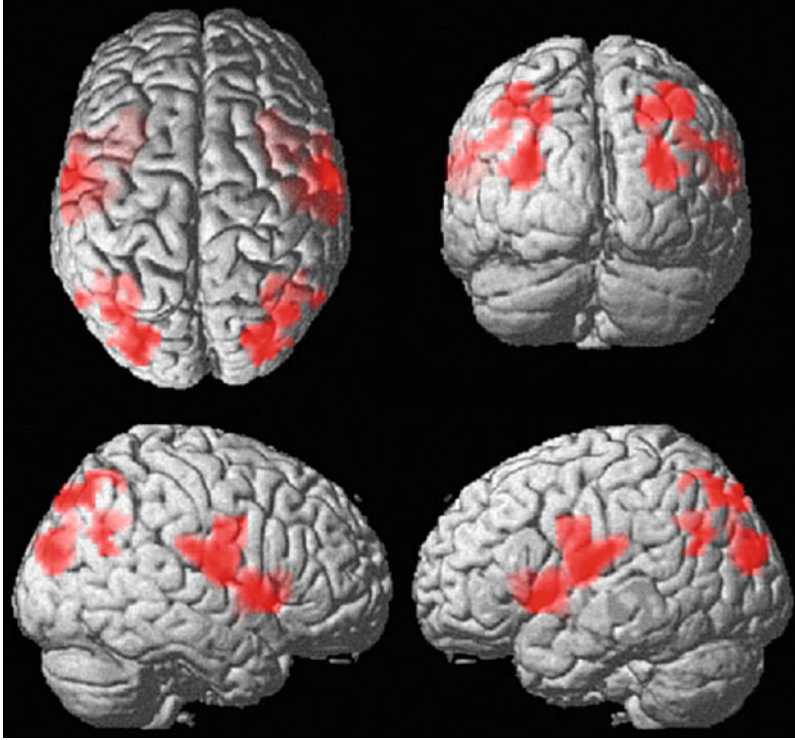**Fig. 18.2** Rendered images of a template brain are shown with areas shaded where autism subjects showed significantly weaker interhemispheric connectivity by functional connectivity MRI than age- and IQ-matched control subjects (Courtesy of Jeffrey S. Anderson, M.D., Ph.D.)

Future Research

- To further define the role of functional imaging (fMRI) in the diagnosis, characterization, and follow-up of autistic patients
- To determine the clinical feasibility of using diagnostic imaging (DTI, fMRI, PET) to monitor response to targeted autism therapies

References

1. American Academy of Pediatrics, Council on Children with Disabilities, Section of Developmental Behavioral Pediatrics; Bright Futures Steering Committee; Medical Home Initiatives for Children with Special Needs Project Advisory Committee. Pediatrics. 2006;118:405–20.
2. Casanova MF. Brain Pathol. 2007;17:422–33.
3. Palmen SJMC, van Engeland H, Hot PR, et al. Brain. 2004;127:2572–83.
4. Dover CJ, Le Couteur A. Arch Dis Child. 2007;92:540–5.
5. Miles JH, Takahashi TN, Bagby S, et al. Am J Med Genet. 2003;135:171–80.
6. American Psychiatric A. Diagnostic and statistical manual of mental disorders. 4th ed. Washington, DC: American Psychiatric Association; 2000. Text Revision.
7. Amaral D, Schumann C, Nordahl C. Trends Neurosci. 2008;31:137–45.
8. Bauman ML, Kemper TL. In: Bauman ML, Kemper GL, editors. Neuroanatomic observations of the brain in autism, in the neurobiology of Autism. Baltimore MD: Johns Hopkins University Press; 1994.
9. Aylward EH, Minshew NJ, Field K, et al. Neurology. 2002;59:175–83.
10. Courchesne E, Press GA, Yeung-Courchesne R. AJR Am J Roentgenol. 1993;160:387–93.
11. Courchesne E, Karns CM, Davis HR, et al. Neurology. 2001;57:245–54.
12. Fidler DJ, Bailey JN, Smalley SL. Dev Med Child Neurol. 2000;42:737–40.
13. Lainhart JE. Semin Med Genet. 2006;142:33–9.
14. Acosta MT, Pearl PL. Semin Pediatr Neurol. 2004;11:205–13.

15. Pickett J, London E. J Neuropathol Exp Neurol. 2005;64:925–35.
16. CDC releases new data on autism spectrum disorders (ASDs) from multiple communities in the United States. http://www.cdc.gov/od/oc/media/pressrel/2007/1070208.htm, 18 Feb 2007.
17. Knapp M, Romeo R, Beecham J. Sage Publications and the National Autistic Society 2009;13:317–336.
18. Cimera RE, Cown RJ. Sage Publications and the National Autistic Society 2009;13:285–302.
19. Verhoeven JS, De Cock P, Lagae L, et al. Neuroradiol. 2010;52:3–14.
20. Piven J, Nehme E, Simon J, et al. Biol Psychiatry. 1992;31:491–504.
21. Giedd JN, Rapoport JL. Neuron. 2010;67(5):728–34.
22. Hrdlicka M. Neuroendocrinol Lett. 2008;29:281–6.
23. Williams D. Neuroimaging Clin N Am. 2007;17:495–6.
24. Ecker C, Marquand A, Mourão-Miranda J, et al. J Neurosci. 2010;30:10612–23.
25. Courchesne E, Yeung-Courchesne R, Press GA, et al. N Engl J Med. 1988;318:1349–54.
26. Hardan AY, Minshew NJ, Harenski E, et al. J Am Acad Child Adolesc Psychiatry. 2001;40:666–72.
27. Stanfield AC, McIntosh AM, Spencer MD, et al. Eur Psychiatry. 2008;23:289–99.
28. Aylward EH, Minshew NJ, Goldstein G, et al. Neurology. 1999;53:2145–50.
29. Dziobek I, Bahnemann M, Convit A, et al. Arch Gen Psychiatry. 2010;67:397–405.
30. Egaas B, Courchesne E, Saitoh O. Arch Neurol. 1995;52:794–801.
31. Hardan AY, Minshew NJ, Keshavan MS. Neurology. 2000;55:1033–6.
32. Alexander AL, Lee JE, Lazar M, et al. Neuroimage. 2007;34:71–3.
33. Barnea-Goraly N, Menon V, Eckert M, et al. Cerebral Cortex. 2005;15:1848–54.
34. Thakkar KN, Polli FE, Joseph RM, et al. Response monitoring, repetitive behaviour and anterior cingulate abnormalities in ASD. Brain. 2008;2:2464–2478.
35. Sahyoun CP, Belliveau JW, et al. Brain Cogn. 2010;73:180–8.
36. Fletcher TP, Whitaker RT, Tao R, et al. Neuroimage. 2010;51:1117–25.
37. Minshew NJ, Keller TA. Curr Opin Neurol. 2010;23:124–30.
38. Cherkassky VI, Dana RK, Keller TA, et al. Neuroreport. 2006;17:1687–90.
39. Bőlte S, Hubl D, Dierks T, et al. J Neural Transm. 2008;115:545–52.
40. Critchley HD, Daly EM, Bullmore ET, et al. Brain. 2000;123:2203–12.
41. Schultz RT, In J. Dev Neurosci. 2005;23:125–41.
42. Kleinhans NM, Richards T, Sterling L, et al. Brain. 2008;131:1000–12.
43. Schultz RT, Gauthier I, Klin A, et al. Arch Gen Psychiatry. 2000;57:331–40.
44. Wang AT, Dapretto M, Hariri AR, et al. J Am Acad Child Adolesc Psychiatry. 2004;28:137–51.
45. Mason RA, William DL, Kana RK, et al. Neuropsychologia. 2008;46:269–80.
46. Anderson JS, Druzgal TJ, Froehlich A, et al. Cerebral Cortex Advance Access. 2011;21:1134–46.
47. Anderson JS, Lange N, Froehlich A, et al. AJNR Am J Neuroradiol. 2010;31:131–9.
48. Rumsey J, Duara R, Grady C, et al. Arch Gen Psychiatry. 1985;42:448–55.
49. Herold S, Frackowiak R, Le Couteur A, et al. Psychol Med. 1988;18:823–31.
50. Horwitz B, Rumsey J, Grady C, et al. Arch Neurol. 1988;45:749–55.
51. Chugani DC, Sukel K. Bringing the brain of the child with autism back on track. Cerebrum (an online journal of the Dana Foundation); August 2006.
52. Haznedar MM, Buchsbaum MS, Hazlett EA, et al. Am J Psychiatry. 2006;163:1252–63.
53. Schain RJ, Freedman DX. J Pediatr. 1961;59:315–20.
54. Ernst M, Zamatkin AJ, Matochik JA, et al. Lancet. 1997;350:638.

Full-Term Neonates with Hypoxic-Ischemic Encephalopathy: Evidence-Based Neuroimaging

19

Amit M. Mathur and Robert C. McKinstry III

Contents

A.M. Mathur (✉)
Department of Pediatrics/Newborn Medicine, Washington University School of Medicine in St. Louis, St. Louis Children's Hospital, St. Louis, MO, USA
e-mail: mathur_a@kids.wustl.edu

R.C. McKinstry III
Departments of Radiology and Pediatrics, Washington University School of Medicine in St. Louis, St. Louis Children's Hospital, St. Louis, MO, USA
e-mail: mckinstryb@mir.wustl.edu

Key Points

- Clinical neurological evaluation of the neonate with depression and/or encephalopathy is nonspecific. The neonatal course may suggest hypoxic-ischemic insult, but the clinical examination cannot fully evaluate the extent or severity of the brain injury (moderate evidence).
- The role of ultrasound (US) and computed tomography (CT) in the evaluation of hypoxic-ischemic brain injury at term is limited. Ultrasound could be used to evaluate neonates in the neonatal ICU if the patient is too sick to travel to the MR scanner. CT can be used to assess for traumatic brain injury if there is a history of complicated delivery. CT also plays a role in the acute management of suspected acute intracranial hemorrhage. However, CT and US fall short of MR imaging in the evaluation of the parenchymal changes of hypoxic-ischemic injury (moderate evidence).
- Conventional MR imaging with T1-weighted, T2-weighted, and T2*-weighted imaging is more sensitive than US and at least as sensitive as CT for HIE (moderate evidence).
- Diffusion-weighted imaging (DWI) is complementary to conventional MR imaging, improving sensitivity to ischemic injuries during the first week after the ischemic insult (moderate to strong evidence).
- MR spectroscopy (MRS) may detect injuries in the first week after the insult that are otherwise occult. Elevated lactate and decreased NAA predict a poor clinical outcome (moderate to strong evidence).
- FLAIR and contrast-enhanced imaging sequences do not improve sensitivity of the MR exam beyond the other conventional sequences, DWI and MRS (moderate evidence).
- MR imaging holds promise for evaluating prognosis, triaging patients for neuroprotective therapies, and serving as early predication of therapeutic efficacy (limited to moderate evidence).

Definition and Pathophysiology

Hypoxic-ischemic brain injury in term neonates is often preceded by a significant obstetric history (uterine rupture, abruption, cord prolapse, etc.), evidence of impaired placental gas exchange (metabolic acidosis on the cord gas), poor adaptation at birth needing resuscitation (low Apgar scores), presence or development of encephalopathy, and evidence of other end organ injury (e.g., liver or kidney) [1].

Standard of care for this condition has been restricted to maintaining the respiratory/metabolic milieu, keeping the infant normothermic, and treating seizures when they arise. A review of recent multicenter trials has shown improved survival in moderate and severe encephalopathy with both head cooling and body cooling [2].

Recent evidence from clinical and experimental models has demonstrated a biphasic pattern of injury following reversal of the hypoxic-ischemic process [3–5]. It has been recognized that the physiologic consequences of hypoxia-ischemia evolve over hours to days. The hypoxic-ischemic cascade results in two phases of energy failure that culminate in brain injury. The "primary" energy failure occurs at the time of the hypoxic-ischemic insult itself, resulting in depletion of high-energy metabolites (ATP and phosphocreatine), progressive depolarization of cells, severe cytotoxic edema, tissue acidosis, and extracellular accumulation of excitatory amino acids due to a failure of reuptake by astroglial cells and also excessive release due to depolarization [6]. Loss of ionic homeostasis results in an influx of calcium into cells, triggering a number of destructive pathways by activating lipases, proteases, and endonucleases [7]. Once the cerebral blood flow and oxygenation are reestablished, the initial metabolic impairments resolve over 30–60 min. This is followed by a latent phase after which there may be complete recovery or development of a secondary phase. Whether injury reversal occurs depends on several factors including the severity of the primary injury, body temperature, substrate availability, preconditioning, and simultaneous disease processes [1].

The "secondary" phase of energy failure starts about 6–15 h later and extends over several hours to days. This phase is clinically associated with seizures and a worsening neurological examination. There is secondary cytotoxic edema, excitotoxic amino acid accumulation, mitochondrial failure, altered growth factors and protein synthesis, and apoptotic cell death [8–10].

In term infants with moderate to severe encephalopathy, MR spectroscopy results are consistent with this model of biphasic injury. MR spectroscopy demonstrates normal oxidative metabolism shortly after birth followed by a secondary phase of energy failure. The severity of this secondary phase correlates with neurodevelopmental outcome in these infants [2].

Epidemiology

Neonatal encephalopathy secondary to hypoxic-ischemic injury (HIE) affects 1.6 per 1,000 live term-born infants (American College of Obstetricians and Gynecologists 2003) [11]. Perinatal HIE is but one subset of neonatal encephalopathy; other subsets include those resulting from prenatal stroke, infection, cerebral malformation, genetic disorders, and many other conditions. Although there are longitudinal studies that have shown a decrease in the incidence of perinatal HIE in the past few decades, this has not been consistent across different countries. In the United States, the incidence of perinatal HIE in the state of California declined from 14.8 per 1,000 live births in 1991 to 1.3 per 1,000 live births in 2000 [12]. A similar decline was seen in a British hospital from 7.7 per 1,000 live births in the 1970s to 1.9 per 1,000 in the mid-1990s [13, 14]. However, a Swedish report showed a slight increase in the incidence of birth asphyxia and neonatal encephalopathy between 1985 and 1991 [15]. This difference could reflect a trend in moving away from using the diagnosis of "birth asphyxia" to currently used terminology of "perinatal hypoxic-ischemic encephalopathy" or "neonatal encephalopathy." Perinatal HIE carries an appreciable burden of illness and has a mortality of 15–20 % in the newborn period.

In addition, 25 % of survivors have permanent neurological deficits such as cerebral palsy or mental retardation [16].

Overall Cost to Society

The long-term consequence of neonatal HIE is most commonly cerebral palsy, a nonprogressive disorder of the developing brain principally affecting the motor system. Cerebral palsy affects 2–3 per 1,000 newborns, with a conservative estimate of its impact on society being about $5 billion per year [17]. Cerebral palsy can be associated with epilepsy and abnormalities of speech, vision, and intellect. The impact of diseases affecting the newborn is much greater than diseases that affect the elderly because of the burden of disease when one considers mortality, years of life lost, and years of productive life lost. Lifetime costs for all patients with cerebral palsy are estimated to total $11.5 billion [17].

Goals of Imaging

When a neonate is encephalopathic and hypoxic-ischemic injury is suspected, the goals of the MR imaging study are the following:

- Establish whether the brain development has progressed normally for gestational age. Malformations of cortical development or other significant congenital brain malformations could present with a similar clinical picture.
- Establish timing of injury to assess whether there is evidence for in utero brain injury that preceded events during labor and delivery. Subacute and/or chronic brain injury detected on conventional MR imaging in the first few days of life is likely the result of an unfavorable maternal–fetal milieu rather than HIE related to events during the birthing process.
- Differentiate between the various patterns of HIE in the newborn, and establish the extent and severity of the brain injury. With this information, the NICU team can begin to analyze the potential etiologies (e.g., hypercoagulable state associated with

sinus venous thrombosis) and take appropriate measures to minimize further injury.

- Help to establish prognosis for the family and caregivers. Armed with the prognostic information, an appropriate care plan can be developed and early intervention can be initiated to maximize the child's neurological and cognitive potential.

Methodology

The authors queried the MEDLINE database using PubMed (National Library of Medicine, Bethesda, MD) through a combination of the web-based interface (http://www.ncbi.nlm.nih. gov/sites/entrez) and searches performed using Endnote (Thomson Reuters, New York). Initial imaging queries were generated using terms including *magnetic resonance imaging* and *MRI*, limiting the searches with *English, Human*, and *Newborn: birth–1 month*. Terms *hypoxia, ischemia, hypoxic-ischemic, hypoxia-ischemia, HIE*, and *encephalopathy* were added to evaluate the role of MR imaging in the evaluation of the encephalopathic neonate. Specific modifiers included *outcome, prediction*, and *hypothermia*. The role of individual MR sequences was evaluated with the terms *diffusion, perfusion, spectroscopy, FLAIR, T2*, susceptibility, hemorrhage, functional MRI*, and *fMRI*. To expand the search, each query generated by the PubMed web interface was expanded by following links to related articles, which were then examined for relevance. No limits were placed on the date range of the PubMed search. Therefore, the queries spanned dates from 1950 to June 2008.

Discussion of Issues

What Are the Clinical Features of Neonatal HIE?

Summary
Clinical neurological evaluation of the neonate with depression and/or encephalopathy is nonspecific. The neonatal course may suggest a hypoxic-ischemic insult, but the clinical examination may not fully reveal the extent or severity of the brain injury (moderate evidence).

Supporting Evidence
The neurological syndrome that accompanies significant neonatal HIE is essential to the diagnosis. The three cardinal features that point to the perinatal origin of HIE include evidence of fetal distress (abnormal fetal heart rate tracing, meconium-stained amniotic fluid), depression at birth, and an overt neonatal neurological syndrome in the first several hours to days of life. The severity of neonatal encephalopathy is assessed using criteria described by Sarnat and Sarnat and modified by Finer [18] (Table 19.1).

The diagnosis of neonatal HIE is based on a detailed history of pregnancy, labor, and resuscitation including fetal acid–base status, neurological examination, metabolic parameters such as hypoglycemia, hyponatremia, hypocalcemia, hypoxemia, lactate level, and acidosis. Non-HIE causes of neonatal encephalopathy such as meningitis or metabolic disorders should be considered [1].

In addition to the history and physical examination, supplementary evaluations including electroencephalography (EEG) and neuroimaging are very important [19].

MR imaging is the most accurate imaging modality in the evaluation of neonatal encephalopathy to assess the timing, extent, and severity of injury [19–21]. Although the advantage with MRI of superlative anatomical detail is tempered by the need to study the infant within a magnet, away from the neonatal intensive care unit (NICU), the information obtained on MRI is superior to other neuroimaging modalities [19].

What Is the Optimal Time and What Are the Ideal MRI Sequences to Image Neonatal HIE?

Summary
Diffusion-weighted imaging (DWI) is complementary to conventional MR imaging, improving

sensitivity to ischemic injuries during the first week after the ischemic insult (moderate to strong evidence).

MR spectroscopy (MRS) may detect injuries in the first week after the insult that are otherwise occult. Elevated lactate and decreased NAA predict a poor clinical outcome (moderate to strong evidence).

FLAIR and contrast-enhanced imaging sequences do not improve sensitivity of the MR exam beyond the other conventional sequences, DWI and MRS (moderate evidence).

See Table 19.2 for a summary of MR imaging evaluation of evolving hypoxic-ischemic injury.

Supporting Evidence

Ideally, neonates with perinatal HIE should have two MR scans. The first scan is optimally performed within 24–48 h of life. Proton spectroscopy is the most sensitive MR technique at this time to identify brain injury, showing elevation of lactate and, in severe cases, a reduction in *n*-acetyl aspartate (NAA) in the cerebral cortex more so than the deep nuclear gray matter [22, 23]. MRS detected abnormalities in the deep nuclear gray matter in all six patients on whom it was performed versus conventional T1 and T2 images, which only showed mild edema in 3/7 patients [24]. Diffusion-weighted imaging (DWI) can give false-negative results in up to 30 % of infants if performed in the first few hours of delivery [25] and will underestimate the extent of injury if performed in the first 24 h of life. Sensitivity is increased by analyzing apparent diffusion coefficient (ADC) values [26], which can be abnormal even when DWI does not show abnormalities. An early scan may help guide clinicians in deciding the timing, severity, and extent of injury. Early changes on conventional T1 and T2 images with negative diffusion are likely to indicate an onset of injury remote from birth. This information, along with data from electroencephalographic studies and the clinical course of the infant, is vital for both parents of these infants and neonatologists in deciding the plan of care.

The second scan should be undertaken at 7–10 days of life. At this time, diffusion imaging,

T2-weighted spin echo images with long repetition times, and inversion recovery/spoiled gradient echo T1-weighted sequences are preferred for detecting brain injury [27]. Affected cortex appears hyperintense on T2-weighted images. T1-weighted images show areas of low signal intensity in the involved cortex. The most obvious finding is the loss of gray–white matter distinction. Injury over the high convexities of the cortex is best visualized in coronal and sagittal planes. An exception is in perirolandic injury where T1-weighted images may show hyperintense signal in the cortex (Fig. 19.1c). The pattern of diffusion abnormalities changes over time. Initial diffusion abnormalities in the deep nuclear gray matter may pseudonormalize by the end of the first week, and new diffusion restriction may become apparent in the corpus callosum (Fig. 19.1a–c) or the posterior limb of the internal capsule (PLIC). This may represent Wallerian degeneration or injury in the "secondary phase" of the cascade of brain injury [28–31]. Some studies have shown that even though ADC values in affected areas may pseudonormalize by the end of the first week [25, 32], FA values remain abnormal [33].

If only one MR scan can be obtained, a scan at 3–4 days of life can help establish timing, extent, and severity of the injury. Specifically, the DWI and ADC will show the maximum deflection from normal neonatal values, the lactate peak of the MR spectrum will remain elevated, and the conventional MR sequences will be abnormal. A single scan at the end of the first week will delineate the injury but will make timing difficult or impossible.

T1- and T2-weighted imaging is a standard part of every MR protocol as they are designed to image the intrinsic relaxation properties of brain water. MR imaging is recommended, when evaluated against cranial sonography and computed tomography, for detection of brain injury in the term newborn [34].

T2*-weighted images are designed to detect small fluctuations in the local magnetic field due to susceptibility effects associated with hemorrhage and/or calcification. Presently, three T2*-weighted options are available: gradient

echo (GRE) imaging, echo planar imaging (EPI), and susceptibility-weighted imaging (SWI). EPI has the benefit of extremely fast scan times, followed by GRE and SWI. In terms of sensitivity to small amounts of cerebral hemorrhage, there is a moderate evidence (level 2) study that SWI is the superior technique [35, 36]. However, SWI is time consuming and may not be suitable for evaluation of an unsedated newborn. A moderate evidence (Level 2) study has shown that GRE is more sensitive in the posterior fossa, while both GRE and EPI performed well for detection of supratentorial hemorrhage [37].

The value of FLAIR T2-weighted and contrast-enhanced sequences in the newborn period is a matter of some debate in the literature. There is no strong evidence (level 1) that directly addresses the value of FLAIR. Recent evidence from moderate evidence (Level 2) study directly addressed the relative value of T1, T2, FLAIR, DWI, and contrast-enhanced images in the evaluation of HIE [38]. These investigators found that adding FLAIR and contrast-enhanced images to T1, T2, and DWI did not improve detection of HIE. An earlier limited evidence (level 3) study concluded similarly that FLAIR did not improve detection of HIE, largely due to hypomyelination of the newborn brain [39].

Diffusion MR imaging has received the most attention for the detection HIE in the term neonate [22, 25, 26, 40–52] because of its established utility in adult stroke. Diffusion imaging complements T1-weighted and T2-weighted imaging for detection of the acute injury (Fig. 19.2a, b), the timing of the insult [25, 48], and the associated secondary injury pattern [29–31]. Some studies have shown that DWI and ADC during the first week of life are less sensitive than conventional imaging [42, 47], with reported sensitivity as low as 47 %. Others report high sensitivity (100 %) with low specificity (20 %) [41]. However, ADC changes dramatically over the first 2 weeks following an injury [25, 32, 46, 53], with maximum restriction occurring at day 3–4 of life [25] and pseudonormalization of the ADC at the end of the first week [25, 33]. Therefore, sensitivity and specificity will be highly dependent on the timing of the exam relative to the injury. At this point, the imaging "gold standard" for HIE remains the conventional MR sequences obtained at 7–10 days of life.

Why Should Infants with Neonatal Encephalopathy Be Imaged?

Summary
The clinical neurological examination in term neonates with HIE can be subjective and nonspecific. Early diagnosis of brain injury is important for both neuroprotective interventions and prognosis. Neuroimaging plays an essential role in the assessment of brain injury in these patients by helping establish the timing and likely cause of injury and the expected neurological outcome (strong evidence).

While sonography (US), computerized tomography (CT), and magnetic resonance imaging (MRI) have all been used in imaging infants with HIE, MRI has emerged as the imaging modality of choice because of lack of ionizing radiation exposure, high interobserver reliability, and high predictive value of neurodevelopmental outcome (moderate to limited evidence).

Unsedated MRI examination is possible in neonates. In addition to conventional T1- and T2-weighted MR images, MR spectroscopy and diffusion-weighted imaging (with apparent diffusion coefficient maps for quantitative analysis) are needed to establish timing and extent of brain injury (strong evidence).

Supporting Evidence
The central nervous system (CNS) of the neonate may be injured by a number of different mechanisms including hemorrhage, hypoxia-ischemia, hypoglycemia, inborn errors of metabolism, hyperbilirubinemia, and neonatal infections. Neurological assessment of the affected neonate includes assessment for encephalopathy, cranial nerve function, motor function (tone, posture, movement, power, and reflexes), primitive reflexes, and sensory examination. However, because of the immaturity of the CNS in the neonate, this clinical assessment is imprecise. Although it may alert the examiner to the presence or absence of injury, the precise cause of injury and the severity, extent, and location of

injury are difficult to establish on clinical grounds alone. Neuroimaging plays a critical role in the assessment of brain injury in these patients [20, 21].

The role of ultrasound (US) and computed tomography in the evaluation of hypoxic-ischemic brain injury at term is limited. Although sonography was shown to be useful in evaluating neonatal HIE with good accuracy (91 %) and sensitivity (100 %) and but poor specificity (33 %) when compared prospectively to MRI in a single series [54], its use has not been routinely recommended in evaluation of neonatal HIE because it is operator dependent and has poor interobserver reliability [34, 55] (moderate evidence).

CT can be used to assess for traumatic brain injury (fracture or hemorrhage) if there is a history of complicated delivery. However, in a head-to-head study [56], MRI had better interobserver agreement and demonstrated findings of HIE as well as CT. Further, MRI eliminates the use of ionizing radiation, a putative cause of malignancy (moderate evidence).

MRI examination is considered an established tool in the evaluation of term neonates with encephalopathy [57]. It is the most sensitive and specific technique for examining infants with HIE [58] and is a good predictor of neurodevelopmental outcome [34, 59].

Recent advances in MR imaging of neonates have included the availability of MR-compatible incubator and ventilator systems that can provide a stable environment for the often critically ill and unstable neonate [60]. Neonates can be safely and successfully imaged without sedation using standard monitoring with an MR-compatible pulse oximeter and a cardiorespiratory monitor [61]. In addition, custom-built coils have dramatically improved signal-to-noise ratios (SNR). MR diffusion imaging including diffusion tensor imaging (DTI), diffusion-weighted imaging (DWI), and fractional anisotropy (FA) provide valuable insights about timing of injury [62–64], while MR spectroscopy (MRS) helps evaluate the metabolic state in the injured brain [34, 65–67]. Emerging MR techniques include neonatal perfusion imaging, which noninvasively measures cerebral blood flow, and functional MR imaging, which evaluates brain function and connectivity.

Diffusion-weighted imaging (DWI) is complementary to conventional MR imaging, improving sensitivity to ischemic injuries during the first week after the ischemic insult [62–64].

Does the Pattern of Brain Injury on MR Help Predict Outcome in Neonatal HIE?

Summary

While it is accepted that the risk of an abnormal neurodevelopmental outcome increases with the severity of the injury, the pattern of injury on MRI also conveys important prognostic information. In particular, the basal ganglia–thalamus and watershed patterns of injury are associated with impairments in different developmental domains. The basal ganglia–thalamus predominant pattern or abnormal signal intensity in the posterior limb of the internal capsule on MRI is associated with severely impaired motor and cognitive outcomes. Given the frequent occurrence of cerebral watershed injury with the basal ganglia–thalamus predominant pattern, cognitive deficits may result from damage to areas outside the deep gray nuclei themselves. By contrast, newborns with the watershed pattern have predominantly cognitive impairments that often occur without functional motor deficits (moderate evidence).

Supporting Evidence

Selective neuronal necrosis is the most common form of injury following perinatal HIE and is prevalent in almost all cases [16]. The distribution of the lesion depends on the severity and duration of the hypoxia-ischemia.

In *severe and prolonged insults*, *diffuse neuronal injury* is seen in the cerebral cortex, hippocampus, deep nuclear gray matter, brainstem, cerebellum, and spinal cord [16, 68]. This lesion carries a high mortality (35 %) [68], and survivors (65 %) are likely to have quadriparesis, severe seizure disorder (10–30 %) [19], choreoathetosis, microcephaly, and mental retardation [68].

There is often abnormal signal intensity and restricted diffusion in the posterior limb of the internal capsule (PLIC). Abnormalities in the

PLIC are excellent predictors of abnormal outcome in term infants with HIE [59, 69]. The internal capsule is an area of great importance in the evaluation of the brain of the newborn infant. It myelinates around term age and is therefore a marker of maturation that is readily identifiable on MRI scans. Absent or abnormal myelination within the posterior portion of the internal capsule is found in many metabolic disorders; it is also a strong predictor of normal and abnormal motor outcome in HIE [28]. The absence of normal signal in the PLIC was shown to predict an abnormal outcome with a sensitivity of 0.90, a specificity of 1.0, a positive predictive value of 1.0, and a negative predictive value of 0.87. The test correctly predicted motor outcome in 93 % of infants with moderate HIE [59] in more detail correlation of these predictors with outcome.

Prolonged partial insults cause a cerebral cortical-deep nuclear neuronal injury. The affected area includes the parasagittal and perirolandic cortex, hippocampus, basal ganglia, and thalamus. Brainstem involvement may also occur. This pattern is seen in 35–65 % of cases of HIE [70]. These lesions are associated with predominantly motor deficits with tone and posture abnormalities. Choreoathetoid movements may become apparent between 1 and 4 years of life in these infants [19]. Intellectual function is relatively preserved in infants with later onset disease [71]. Infants with involvement of the thalamus have associated cognitive delay [72].

Severe and abrupt insults such as those following placental abruption, cord prolapse, or uterine rupture result in a pattern of injury that involves predominantly *deep nuclear gray matter and brainstem*. All surviving infants are likely to develop motor disability in the form of cerebral palsy. Cognitive impairment depends on associated cortical injury that may overlap in 50 % of these cases [68, 73]. Twenty to thirty percent of infants in this group may require gastrostomy feeding tubes [74].

Parasagittal cerebral injury is another pattern that is predominantly an ischemic lesion in term infants. The lesions are usually bilateral and involve the cerebral cortex and subcortical white matter in the "watershed areas" between major cerebral arteries [16]. This lesion is seen in the setting of *acute hypotension* and is seen in about 45 % of surviving infants with HIE [75]. It results in spastic quadriparesis along with specific cognitive deficits such as disproportionate disturbance in the development of language or of visual–spatial abilities or both [76].

Does Cooling Alter the Pattern of Brain Injury?

Summary
Therapeutic hypothermia (whole body or head) is an accepted treatment modality in infants with HIE. It is unclear as to what impact hypothermia has on MR images in these infants (limited evidence).

Supporting Evidence
Two studies have looked at MR changes in infants who underwent therapeutic hypothermia for perinatal HIE. Rutherford et al. looked at MR imaging in 14 infants with HIE who underwent head cooling, 20 infants with body cooling, and 52 noncooled infants with similar severity of HIE [77]. They found that both modes of hypothermia were associated with a decrease in basal ganglia and thalamic lesions, which are predictive of abnormal outcome.

Inder et al. analyzed a group of 26 infants with HIE. Infants were randomized to either body cooling or normothermia [78]. The hypothermia group had less cortical gray matter signal abnormality on MR imaging. They postulated that there might be differing regional benefits from systemic cooling. Although the studies are difficult to interpret because the initial distribution of injury is not known, there does appear to be a decrease in the amount of injury.

Take-Home Tables

Table 19.1 presents grading of neonatal encephalopathy. Table 19.2 discusses MR imaging of evolving hypoxic-ischemic injury.

Table 19.1 Grading of neonatal encephalopathy

Encephalopathy grade	Clinical features
Mild or stage 1	Hyperalertness, decreased sleep
	Uninhibited reflexes, excessive reaction to stimuli, weak suck but normal tone
	Sympathetic overactivity – eyes wide open, decreased blinking, mydriasis
	Duration less than 24 h
Moderate or stage 2	Lethargy or obtundation (i.e., delayed and incomplete response sensory stimuli), mild hypotonia
	Cortical thumbs, suppressed primitive reflexes
	Seizures, hypotonia, lethargy
	Parasympathetic activation with miosis (even on dim light), heart rate less than 120 beats per minute, increased peristalsis, and copious secretions
Severe or stage 3	Stupor response only to strong stimuli with withdrawal or decerebrate posturing only
	Rarely coma, severe hypotonia (i.e., flaccidity)
	Suppression of deep tendon and primitive (i.e., Moro, tonic neck, oculocephalic, suck) reflexes
	Suppression of brainstemreflexes (corneal or gag)
	Clinical seizures less frequentthan Stage 2

Modified with permission from Sarnat HB, Sarnat MS. Arch Neurol. 1976;33(10):696–705. Copyright © 1976, American Medical Association. All rights reserved
Reprinted with permission from Mathur AM, McKinstry RC. Imaging of hypoxic-ischemic encephalopathy in the full term neonate. In: Medina LS, Applegate KE, Blackmore CC, editors. Evidence-based imaging in pediatrics. New York: Springer; 2010

Table 19.2 MR imaging evaluation of evolving hypoxic-ischemic injury

MR sequence	Day 1	Days 3–4	Day 7	Year 2
T1	−	+	+	±
T2	−	−	+	+
FLAIR	−	−	−	+
DWI/ADC	±	+	−	−
MRS	+	+	±	−

Plus signs indicate that the test is a specific indicator at the time point. Minus signs indicate that the test is insensitive at the specified time point. If inconsistent results have been reported, the plus/minus designation is shown
Reprinted with permission from Mathur AM, McKinstry RC. Imaging of hypoxic-ischemic encephalopathy in the full term neonate. In: Medina LS, Applegate KE, Blackmore CC, editors. Evidence-based imaging in pediatrics. New York: Springer; 2010

Fig. 19.1 (**a**) Neonate with encephalopathy and seizures. T1-weighted images on day 1 of life (*left*) are unremarkable. By day 10, the T1-weighted images demonstrate the classic pattern of deep nuclear gray matter injury (*arrows*). This illustrates that T1-weighted and T2-weighted (not shown) imaging alone are not sensitive to the earliest changes of HIE. (**b**) DWI on day 1 (*left*) shows reduced diffusion in the posterior limb of the internal capsule bilaterally and the adjacent ventrolateral thalami. By day 10 (*right*), those regions have pseudonormalized on DWI, and there is early Wallerian degeneration of the splenium of the corpus callosum (*arrow*). (**c**) DWI (*left*) on DOL 1 shows reduced diffusion in the distribution of the corticospinal tracts bilaterally (*arrows*). The T1-weighted images on day 10 show

hyperintensity of the cortex bordering the central sulcus. At 1 month, the child was doing well with no further seizures or obvious deficits, which reinforce that MR imaging must be correlated with long-term outcome to assess its true utility. This case illustrates the variable sensitivity of MR by pulse sequence and time after the injury. In addition, the Wallerian degeneration of the splenium of the corpus callosum without overt parieto-occipital injury suggests that not all of the primary injury is evident (Reprinted with permission from Mathur AM, McKinstry RC. Imaging of hypoxic-ischemic encephalopathy in the full term neonate. In: Medina LS, Applegate KE, Blackmore CC, editors. Evidence-based imaging in pediatrics. New York: Springer; 2010)
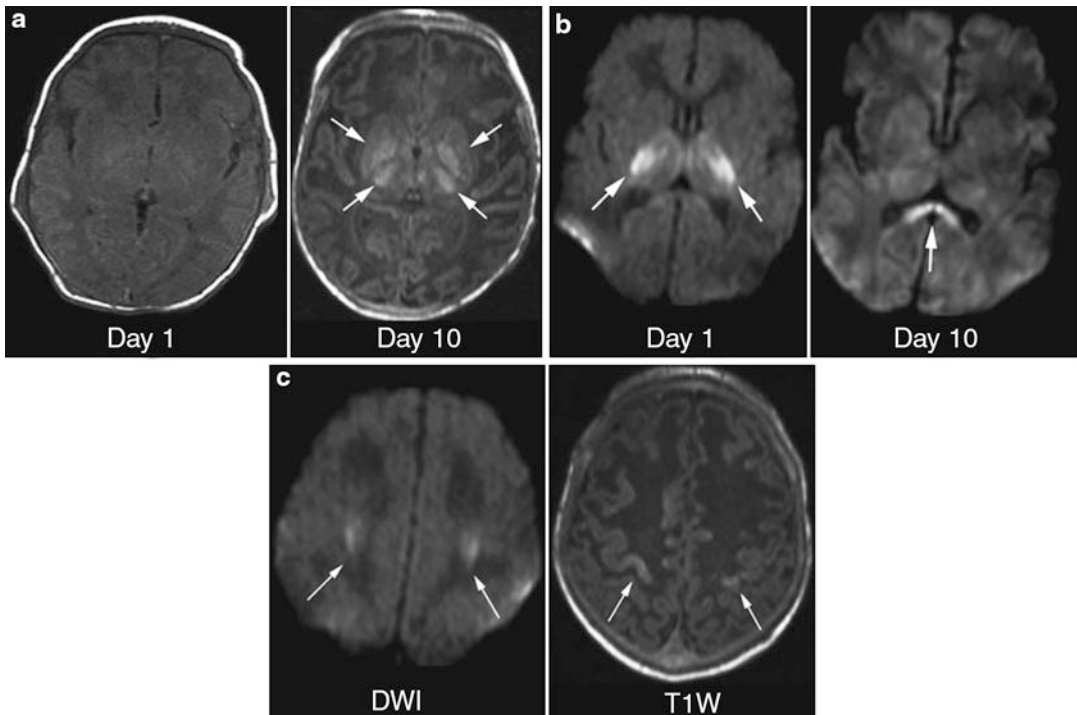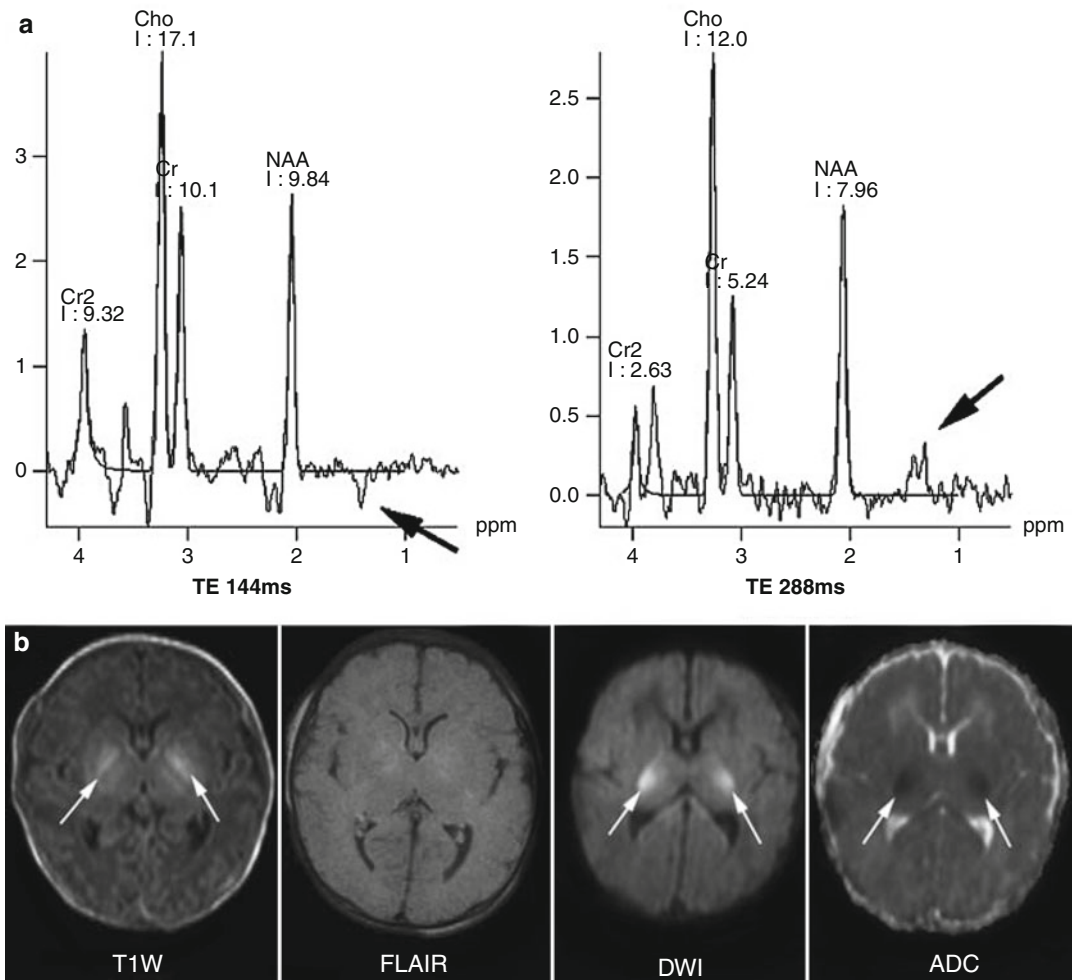
Fig. 19.2 (**a**) Neonate with encephalopathy on day of life 2. Single voxel PRESS proton MR spectroscopy from the left deep nuclear gray matter region with TE 144 ms (*left*) and TE 288 ms (*right*) shows the characteristic inversion of the lactate doublet at 1.33 ppm. The degree of elevation of the lactate peak is inversely correlated with clinical outcome. (**b**) T1-weighted images (far left) show subtle abnormality in the deep nuclear gray matter region (*arrows*). FLAIR fails to show the abnormality. DWI and ADC show restricted diffusion in the thalami bilaterally. Despite a neonatal ICU course marked by seizures and abnormal MR imaging and spectroscopy, the neurodevelopment outcome (Bayley Scales of Infant Development) assessed at 1 year of age is within normal limits. Again, the neonatal imaging predicts a poor outcome, yet the clinical assessment is normal 1 year later. If MR is to serve as a predictor of outcome, long-term clinical follow-up studies will be needed to establish the positive and negative predictive values of MR imaging in the newborn period (Reprinted with permission from Mathur AM, McKinstry RC. Imaging of hypoxic-ischemic encephalopathy in the full term neonate. In: Medina LS, Applegate KE, Blackmore CC, editors. Evidence-based imaging in pediatrics. New York: Springer; 2010)

Imaging Case Studies

Case 1

Figure 19.1a–c presents images of a neonate with encephalopathy and seizures.

Case 2

Figure 19.2a, b presents images of a neonate with encephalopathy on DOL 2.

Suggested Imaging Protocols

A comprehensive evaluation of neonatal encephalopathy must address the issues discussed above. Has the brain developed normally? Are there signs of subacute/chronic injury? Are there signs of recent brain injury? If brain injury is present, what are the extent and severity of the injury? Are there signs of complication such as hemorrhage or hydrocephalus? Based on the literature cited herein, the suggested MR protocol for evaluation of the term neonate with suspected HIE is:

1. T1-weighted images
2. T2-weighted images
3. T2*-weighted images
4. Diffusion-weighted images with computation of the apparent diffusion coefficient (ADC)
5. Proton MR spectroscopy

Future Research

The gaps in our current knowledge point to future research opportunities for MR imaging in neonatal HIE. One shortcoming is that MR imaging on the first day of life does not consistently characterize the severity and extent of HIE that eventually manifests on follow-up MR imaging [25]. Advanced MR spectroscopy methods [79] hold promise for predicting severity on the first day of life, but routine MRI and MRS currently underestimate the injury. If MR imaging is to serve as an objective measure for triage of encephalopathic neonates with suspected HIE for novel interventions, then more work needs to be focused on improving sensitivity on day 1 of life. Potential avenues for research include arterial spin label (ASL) perfusion [80] and functional connectivity MRI [81], which have not yet been reported in the evaluation of HIE.

While structural MR imaging with diffusion and MR spectroscopy on days 3–4 of life have shown prognostic value, it remains unproven that early detection of severity and extent of HIE improves patient outcomes. Clinicians and families may initiate rehabilitation programs with the intent of maximizing the child's neurodevelopmental potential. However, the MRI adds cost to the initial evaluation of the neonate, with the presumption that the overall cost to society will be reduced if early intervention yields better outcomes. This still needs to be proven.

Another open question is whether MRI can serve as a surrogate for clinical outcomes in trials of novel therapeutic intervention. MRI could afford significant cost savings in prospective therapeutic trials if interim analyses and short-term outcomes could be based on objective imaging endpoints rather than on neurodevelopmental assessments that may take months or years to reach significance. MR imaging is commonly used to assess endpoints in adult multiple sclerosis trials, and MRI endpoints are central to the design of an ongoing pediatric therapeutic trial [82]. An open question remains whether cooling alters the time course of diffusion restriction in HIE. If so, what is the optimal timing of the MR scan if one wants to detect HIE changes in the brain of a neonate who is being cooled?

To date, most studies of HIE attempt to correlate clinical outcome with severity of the injury pattern on MRI. However, there are examples of rule breakers that come through our clinical practice on a regular basis. Why do neonates with a deep nuclear gray matter injury or periventricular white matter injury have seizures? Presumably, the MRI is not detecting the full spectrum of brain injury in this population. How do we avoid the problem of satisfaction of search? What strategies should we pursue to

detect brain injury that does not fit one of the classic imaging patterns? Many questions remain unanswered at this point.

References

1. Shankaran S, Laptook AR. Clin Obstet Gynecol. 2007;50(3):624–635.
2. Jacobs S, Hunt R, Tarnow-Mordi W, Inder T, Davis P. Cochrane Database Syst Rev. 2007;4:CD003311.
3. Lorek A, Takei Y, Cady EB, et al. Pediatr Res. 1994;36(6):699–706.
4. Penrice J, Cady EB, Lorek A, et al. Pediatr Res. 1996;40(1):6–14.
5. Gluckman PD, Williams CE. Dev Med Child Neurol. 1992;34(11):1010–1014.
6. Gunn AJ, Thoresen M. NeuroRx. 2006;3(2):154–169.
7. Siesjo BK. Magnesium. 1989;8(5–6):223–237.
8. Fellman V, Raivio KO. Pediatr Res. 1997;41(5):599–606.
9. Liu XH, Kwon D, Schielke GP, Yang GY, Silverstein FS, et al. J Cereb Blood Flow Metab. 1999;19(10):1099–1108.
10. Tan WK, Williams CE, During MJ, et al. Pediatr Res. 1996;39(5):791–797.
11. Gynecologists ACoOa. Neonatal encephalopathy and cerebral palsy: defining the pathogenesis and pathophysiology. Washington, DC: American College of Obstetricians and Gynecologists; 2003.
12. Wu YW, Backstrand KH, Zhao S, Fullerton HJ, Johnston SC. Pediatrics. 2004;114(6):1584–1590.
13. Hull J, Dodd KL. Br J Obstet Gynaecol. 1992;99(5):386–391.
14. Smith J, Wells L, Dodd K. BJOG. 2000;107(4):461–466.
15. Thornberg E, Thiringer K, Odeback A, Milsom I. Acta Paediatr. 1995;84(8):927–932.
16. Volpe JJ. Ment Retard Dev Disabil Res Rev. 2001;7(1):56–64.
17. Derrick M, Drobyshevsky A, Ji X, Tan S. Stroke. 2007;38(2 Suppl):731–735.
18. Sarnat HB, Sarnat MS. Arch Neurol. 1976;33(10):696–705.
19. Volpe JJ. Neurology of the newborn. 5th ed. Philadelphia: Saunders; 2008. p. 414–427.
20. Barkovich AJ, Hajnal BL, Vigneron D, et al. AJNR Am J Neuroradiol. 1998;19(1):143–149.
21. Kaufman SA, Miller SP, Ferriero DM, Glidden DH, Barkovich AJ, et al. Pediatr Neurol. 2003;28(5):342–346.
22. Barkovich AJ, Westmark KD, Bedi HS, Partridge JC, Ferriero DM, et al. AJNR Am J Neuroradiol. 2001;22(9):1786–1794.
23. Hanrahan JD, Cox IJ, Azzopardi D, et al. Dev Med Child Neurol. 1999;41(2):76–82.
24. Coskun A, Lequin M, Segal M, Vigneron DB, Ferriero DM, et al. AJNR Am J Neuroradiol. 2001;22(2):400–405.
25. McKinstry RC, Miller JH, Snyder AZ, et al. Neurology. 2002;59(6):824–833.
26. Jissendi Tchofo P, Christophe C, David P, Metens T, Soto Ares G, et al. J Neuroradiol. 2005;32(1):10–19.
27. Barkovich AJ. Pediatric neuroimaging. 4th ed. Philadelphia: Lippincott Williams & Wilkins; 2005. p. 226.
28. Cowan FM, de Vries LS. Semin Fetal Neonatal Med. 2005;10(5):461–474.
29. Groenendaal F, Benders MJ, de Vries LS. Semin Perinatol. 2006;30(3):146–150.
30. Mazumdar A, Mukherjee P, Miller JH, Malde H, McKinstry RC. AJNR Am J Neuroradiol. 2003;24(6):1057–1066.
31. Neil JJ, Inder TE. J Child Neurol. 2006;21(2):115–118.
32. Winter JD, Lee DS, Hung RM, et al. Pediatr Neurol. 2007;37(4):255–262.
33. Ward P, Counsell S, Allsop J, et al. Pediatrics. 2006;117(4):e619–e630.
34. Ment LR, Bada HS, Barnes P, et al. Neurology. 2002;58(12):1726–1738.
35. Akter M, Hirai T, Hiai Y, et al. Acad Radiol. 2007;14(9):1011–1019.
36. de Souza JM, Domingues RC, Cruz Jr LC, Domingues FS, Iasbeck T, et al. AJNR Am J Neuroradiol. 2008;29(1):154–158.
37. Liang L, Korogi Y, Sugahara T, et al. AJNR Am J Neuroradiol. 1999;20(8):1527–1534.
38. Liauw L, van der Grond J, van den Berg-Huysmans AA, Palm-Meinders IH, van Buchem MA, et al. Radiology. 2008;247(1):204–212.
39. Sie LT, Barkhof F, Lafeber HN, Valk J, van der Knaap MS. Eur Radiol. 2000;10(10):1594–1601.
40. Cowan FM, Pennock JM, Hanrahan JD, Manji KP, Edwards AD. Neuropediatrics. 1994;25(4):172–175.
41. Dag Y, Firat AK, Karakas HM, Alkan A, Yakinci C, et al. Diagn Interv Radiol. 2006;12(3):109–114.
42. Forbes KP, Pipe JG, Bird R. AJNR Am J Neuroradiol. 2000;21(8):1490–1496.
43. Johnson AJ, Lee BC, Lin W. AJR Am J Roentgenol. 1999;172(1):219–226.
44. Khong PL, Tse C, Wong IY, et al. J Child Neurol. 2004;19(11):872–881.
45. Krishnamoorthy KS, Soman TB, Takeoka M, Schaefer PW. J Child Neurol. 2000;15(9):592–602.
46. Malik GK, Trivedi R, Gupta RK, et al. Neuropediatrics. 2006;37(6):337–343.
47. Rutherford M, Counsell S, Allsop J, et al. Pediatrics. 2004;114(4):1004–1014.
48. Soul JS, Robertson RL, Tzika AA, du Plessis AJ, Volpe JJ. Pediatrics. 2001;108(5):1211–1214.
49. Takeoka M, Soman TB, Yoshii A, et al. Pediatr Neurol. 2002;26(4):274–281.
50. Thornton JS, Ordidge RJ, Penrice J, et al. Magn Reson Med. 1998;39(6):920–927.
51. Wolf RL, Zimmerman RA, Clancy R, Haselgrove JH. Radiology. 2001;218(3):825–833.
52. Zarifi MK, Astrakas LG, Poussaint TY, Plessis Ad A, Zurakowski D, et al. Radiology. 2002;225(3):859–870.

53. van Pul C, Buijs J, Janssen MJ, Roos GF, Vlaardin-gerbroek MT, et al. AJNR Am J Neuroradiol. 2005;26(3):469–481.

54. Daneman A, Epelman M, Blaser S, Jarrin JR. Pediatr Radiol. 2006;36(7):636–646.

55. Blankenberg FG, Loh NN, Bracci P, et al. AJNR Am J Neuroradiol. 2000;21(1):213–218.

56. Robertson RL, Robson CD, Zurakowski D, Antiles S, Strauss K, et al. Pediatr Radiol. 2003;33(7):442–449.

57. Jyoti R, O'Neil R, Hurrion E. Pediatr Radiol. 2006;36(1):38–42.

58. Barkovich AJ. AJNR Am J Neuroradiol. 1997;18(10):1816–1820.

59. Rutherford MA, Pennock JM, Counsell SJ, et al. Pediatrics. 1998;102(2 Pt 1):323–328.

60. Bluml S, Friedlich P, Erberich S, Wood JC, Seri I, et al. Radiology. 2004;231(2):594–601.

61. Mathur AM, Neil JJ, McKinstry RC, Inder TE. Pediatr Radiol. 2008;38(3):260–264.

62. Conturo TE, McKinstry RC, Akbudak E, Robinson BH. Magn Reson Med. 1996;35(3):399–412.

63. Le Bihan D, Mangin JF, Poupon C, et al. J Magn Reson Imaging. 2001;13(4):534–546.

64. Neil JJ, Shiran SI, McKinstry RC, et al. Radiology. 1998;209(1):57–66.

65. Cappellini M, Rapisardi G, Cioni ML, Fonda C. Radiol Med (Torino). 2002;104(4):332–340.

66. da Silva LF, Hoefel Filho JR, Anes M, Nunes ML. Pediatr Neurol. 2006;34(5):360–366.

67. Kadri M, Shu S, Holshouser B, et al. J Perinatol. 2003;23(3):181–185.

68. Roland EH, Poskitt K, Rodriguez E, Lupton BA, Hill A. Ann Neurol. 1998;44(2):161–166.

69. Hunt RW, Neil JJ, Coleman LT, Kean MJ, Inder TE. Pediatrics. 2004;114(4):999–1003.

70. Kuenzle C, Baenziger O, Martin E, et al. Neuropediatrics. 1994;25(4):191–200.

71. Saint Hilaire MH, Burke RE, Bressman SB, Brin MF, Fahn S. Neurology. 1991;41(2 Pt 1): 216–222.

72. Barnett A, Mercuri E, Rutherford M, et al. Neuropediatrics. 2002;33(5):242–248.

73. Rutherford MA, Ward P, Malamatentiou C. Semin Fetal Neonatal Med. 2005;10(5):445–460.

74. Pasternak JF, Gorey MT. Pediatr Neurol. 1998;18(5):391–398.

75. Miller SP, Ramaswamy V, Michelson D, et al. J Pediatr. 2005;146(4):453–460.

76. Gonzalez FF, Miller SP. Arch Dis Child Fetal Neonatal Ed. 2006;91(6):F454–F459.

77. Rutherford MA, Azzopardi D, Whitelaw A, et al. Pediatrics. 2005;116(4):1001–1006.

78. Inder TE, Hunt RW, Morley CJ, et al. J Pediatr. 2004;145(6):835–837.

79. Wang ZJ, Vigneron DB, Miller SP, et al. AJNR Am J Neuroradiol. 2008;29(4):798–801.

80. Wang J, Licht DJ. Neuroimaging Clin N Am. 2006;16(1):149–167. ix.

81. Fair DA, Cohen AL, Dosenbach NU, et al. Proc Natl Acad Sci USA. 2008;105(10):4028–4032.

82. Vendt BA, McKinstry RC, Ball WS, et al. J Digit Imaging. 2009;22(3):326–343.

Intraventricular Hemorrhage Spectrum in Premature Neonates: Evidence-Based Neuroimaging

Amit M. Mathur and Robert C. McKinstry III

Contents

A.M. Mathur (✉)
Department of Pediatrics/Newborn Medicine, Washington University School of Medicine in St. Louis,
St. Louis Children's Hospital, St. Louis, MO, USA
e-mail: mathur_a@kids.wustl.edu

R.C. McKinstry III
Departments of Radiology and Pediatrics, Washington University School of Medicine in St. Louis,
St. Louis Children's Hospital, St. Louis, MO, USA
e-mail: mckinstryb@mir.wustl.edu

Key Points

- Despite the decreasing incidence in premature infants, the burden of IVH remains high due to improved survival of extremely premature infants. The clinical presentation of IVH is extremely variable, and the majority of infants with IVH may be "clinically silent" (moderate evidence).
- Head ultrasound (HUS) via the anterior and mastoid fontanelle is the mainstay of radiological screening for the detection of IVH and CH in the first 1–2 weeks of life (moderate evidence).
- Serial HUS scans are ideal for follow-up to detect posthemorrhagic ventricular dilatation (PHVD) in infants with IVH. The timing of these follow-up scans should be within 4–7 days after the detection of severe (grades 3–4) IVH and twice a week thereafter until the ventricular size stabilizes. For grades 1–2 IVH, follow-up scans should be performed once a week for 3–4 weeks or until the ventricular size stabilizes (limited evidence).
- White matter injury and cerebellar injury following IVH is best detected with MR imaging at term-equivalent age (moderate evidence).
- Both HUS and MR imaging at term-equivalent age accurately identify infants with IVH who are at high risk for neurodevelopmental delay (moderate evidence).

Definition and Pathophysiology

Intraventricular hemorrhage (IVH), herein encompassing germinal matrix-intraventricular and intraparenchymal hemorrhage, is a characteristic lesion of the preterm neonate. The severity of hemorrhage [1] ranges from germinal matrix hemorrhage (grade 1), where the bleeding is restricted to the subependymal zone of the ventricles, through intraventricular hemorrhage (grade 2 when the blood occupies < 50% of the ventricle) or (grade 3 when blood occupies >50 % of the ventricle and distends it). The most severe form of the IVH grading system is intraparenchymal hemorrhage or periventricular hemorrhagic infarction (PHI or grade 4), which may not have significant hemorrhage into the ventricles.

The etiology and pathophysiology of IVH is multifactorial and includes hemodynamic (cerebral perfusion and blood pressure), intravascular (structural issues with the capillary network in the germinal matrix), and extravascular factors (deficient vascular tissue support and fibrinolytic activity). The germinal matrix (GM) is the site of origin of grades 1–3 IVH. This region is the primary site for neuronal and glial precursors during gestation and is highly cellular, richly vascularized, and gelatinous. The fragile capillary bed in the GM is composed of relatively large, irregular endothelial lined vessels that mature into a venous structure near term. The arterial supply to the GM is via branches from the anterior and middle cerebral arteries and the anterior choroidal artery. These terminal branches constitute an arterial end zone at the GM and may be vulnerable to ischemia/reperfusion injury. The venous drainage from the anterior periventricular white matter, choroid plexus, striatum, and thalamus drains via the terminal vein which courses along the GM draining into the vein of Galen. PHI (grade 4) occurs as a result of a venous hemorrhagic infarction in this drainage system and is distinct in this manner from the other grades of hemorrhage.

In terms of cerebellar hemorrhage (CH), the common focal unilateral hemispheric lesions may originate in the external granular layer, a germinal matrix, whereas the less common vermian hemorrhages may originate in the residual germinal matrix of the ventricular zone in the roof of the fourth ventricle. Etiology is likely multifactorial, as with supratentorial germinal matrix–intraventricular hemorrhage [2].

The ill preterm infant has a pressure-passive state of cerebral circulation with marked fluctuations in cerebral blood flow occurring with fluctuations in blood pressure. Clinical variables such as asynchronous ventilation, hypercarbia, patent ductus arteriosus, hypovolemia, and agitation episodes are associated with fluctuations in cerebral blood flow velocity that may result in

ischemia–reperfusion injury in the arterial end zones. Cerebral venous pressure increases with respiratory interventions such as tracheal suctioning, higher inflation pressures on ventilation, and pneumothorax [3, 4]. These events may also be associated with hypo-/hypertension episodes compromising cerebral perfusion pressure. Intrapartum events, likely resulting in increased cerebral venous pressure, have also been implicated in the pathophysiology of IVH. Vaginal delivery and length of labor are associated with increased rates of IVH in premature infants [5]. Intravascular factors such as platelet and coagulation disturbances have been implicated in the causation of IVH, but results from studies have been inconclusive [6, 7] and studies using prophylactic fresh frozen plasma or antithrombin III [8] have not shown benefit (limited evidence).

Epidemiology

The incidence of IVH in the premature population has declined over the past two decades and currently has an overall rate of 20–25 % [9, 10]. However, with the increasing incidence of premature births [11] and the improved survival of extremely premature infants over this period, IVH remains a significant contributor to morbidity in this population. The severity of grade of hemorrhage varies inversely with gestational age at birth, and the incidence of severe IVH in infants between 500 and 749 g is about 45 % [12]. CH is being increasingly recognized as an additional complication, especially in infants <750 g at birth with an incidence of 17 %, while it occurs in about 2 % of infants >750 g [13]. IVH, especially grades III and IV, is a major contributor to adverse neurodevelopmental outcome in premature infants with 50–75 % of infants developing cerebral palsy and major cognitive handicaps that persist into later childhood [14]. While information on neurodevelopmental outcomes with lower grades of IVH (grades I and II) is limited, some evidence suggests that there may be a slight increase in risk of cognitive and motor delay. However, whether this delay is attributable to hemorrhage alone or to the associated white matter injury remains unclear [15, 16]. In addition, while lower grades of IVH are not associated with increased mortality, grades III and IV hemorrhage are associated with higher mortality rates than gestational age matched subjects without grades III–IV IVH [17].

Overall Cost to Society

IVH and its associated complications of PHVD and periventricular white matter injury are major contributors to adverse cognitive (mental retardation) and motor delay (cerebral palsy) in premature infants [2]. Based on data from the U.S. Census Bureau, the NICHD Neonatal Network, and the Centers for Disease Control, there are over 3,600 new cases of mental retardation attributable to IVH in the United States each year, and the lifetime care costs for these children exceed 3.6 billion dollars [14, 18].

Goals of Imaging

The goals of imaging in neonatal IVH are twofold: (1) Diagnosis of IVH neuroimaging is recommended for high-risk infants to diagnose IVH and (2) detection of complications of IVH, such as posthemorrhagic ventricular dilatation (PHVD) and white matter injury (WMI) [19].

Methodology

The authors searched the literature (January 1975 to March 2011) for both primary literature (scientific articles) and secondary literature (evidence-based reviews) on the topics of GM–IVH–IPH in premature infants. The National Library of Medicine (NLM) database, MEDLINE, was searched using the PubMed search engine for primary evidence. Articles were retrieved using the following medical subject heading (MeSH) terms that applied to the clinical question: (1) GM, IVH, IPH; (2) cerebellar hemorrhage; (3) pathogenesis; (4) head

ultrasound; (5) MRI or magnetic resonance imaging; (6) white matter injury; (7) posthemorrhagic ventricular dilatation; and (8) neurodevelopmental outcome. The following limits were applied to restrict the focus of our search: human neonates and English language. The title and abstracts of the retrieved papers were reviewed to find relevant literature. The bibliographies of these articles were also reviewed to identify any other relevant papers.

Discussion of Issues

What Are the Clinical Patterns of Presentation of IVH in Preterm Neonates?

Summary

The clinical presentation of IVH in premature neonates is variable and is often clinically silent. Serial clinical examinations, especially a change in mental state and activity and an unexplained drop in hemoglobin levels, may offer clues to the onset of IVH (limited evidence).

Supporting Evidence

There are four basic clinical patterns of presentation of IVH:

(a) *Clinically silent* – This is the most common presentation of IVH (25–50 % of cases) and is often diagnosed on a screening head ultrasound [20]. Cerebellar hemorrhages often present silently as well [21]. A valuable sign is an unexplained drop in hematocrit or failure of a rise in hematocrit following a packed cell transfusion. In addition, other subtle clinical features including tight fontanelle, decreased spontaneous activity and tone, abnormal eye signs, and seizures predict IVH in 54 % of patients [20] (limited evidence).

(b) *Mild and fluctuating encephalopathy* – This presentation is less common and can evolve over hours to days. Detection of these signs requires careful serial clinical examination and includes an alteration in the level of consciousness or mental state, a reduction in the quantity and quality of spontaneous activity and responsiveness, hypotonia, or changes in eye position and movement [2] (limited evidence).

(c) *Catastrophic* – This sudden onset of severe encephalopathy with deep stupor or coma, seizures, respiratory and hemodynamic instability, decerebrate posturing, bulging anterior fontanelle, and severe hypotonia is less commonly seen with IVH but nevertheless is associated with the more severe spectrum of IVH [22] (moderate evidence).

(d) *Agitation episodes* – This presentation has been recently associated with the onset of CH, and sudden onset of increased agitation should prompt screening with a head ultrasound [23] (limited evidence).

What Imaging Is Most Appropriate for the Diagnosis of IVH and Who Should Be Screened?

Summary

Head ultrasound (HUS) screening is the imaging method of choice when evaluating premature infants for IVH (moderate evidence). This screening is recommended for all infants born <30 weeks gestation or any premature infant with an unstable clinical course and should be performed on or before 4 days of life and then again between 7 and 10 days of life to detect the majority of infants with "clinically silent" hemorrhages (moderate evidence). In addition to the anterior fontanelle, a mastoid fontanelle view is also recommended to detect cerebellar hemorrhage (see section on "What Is the Best Imaging Modality for Cerebellar Hemorrhage?") (moderate evidence).

Supporting Evidence

In view of the high incidence of IVH in the premature population and the clinically silent presentation in the majority of cases, it is prudent to have a screening tool for diagnosis in all premature infants admitted to a neonatal intensive care unit [24]. Availability of high-resolution imaging, portability, cost-effectiveness, and lack of ionizing radiation make portable ultrasonography the

imaging modality of choice in this situation [2] (moderate evidence). Computerized tomography (CT) scanning demonstrates the site and extent of IVH very effectively. However, the exposure to ionizing radiation and usual lack of portability (a few portable CT models are currently available) reduce the utility of this technique in neonates [25]. Magnetic resonance (MR) imaging, while providing better resolution imaging, has the disadvantage of cost and lack of portability that precludes its use as a screening tool for IVH in the first few days of life in premature infants [2, 26]. The ability to perform MRI scans in this population has been greatly enhanced by the availability of MRI compatible immobilizers, ventilators, and monitoring equipment. In addition, an MRI compatible incubator is also commercially available for use in smaller infants. When these measures are taken, high-quality MRI scans can be obtained safely without sedation in this population [27–32] (limited evidence).

Issues with Head Ultrasounds

The inter-rater reliability of HUS interpretation in premature neonates has been found to be very good for grades III–IV IVH (kappa = 0.84) but was poor for lower grades of IVH. Similarly, local interpretation of grades III–IV IVH was highly accurate as compared to a "gold standard" central reader interpretation (sensitivity, 87–90 %; specificity, 92–93 %), but sensitivity was fair–poor for grades I–II IVH (48–68 %) [33, 34] (moderate evidence).

The poor interobserver reliability and accuracy for grades I and II IVH and for any white matter injuries suggest that HUS is less useful for defining these types of brain injuries. It is not surprising that there is difficulty with the identification and classification of mild IVH. Small subependymal hemorrhages may be missed if the key images through the caudo-thalamic grooves are not obtained. Small amounts of intraventricular blood may not be visible on HUS, especially if the hemorrhage is along the choroid plexus [35].

Who Should Be Screened?

Twelve to fifty one percent of infants with BW of <1,500 g and/or GA of ≤33 weeks have cranial US abnormalities [36–39]. However, major abnormalities such as grades III and IV IVH, cystic PVL, and ventriculomegaly, which might alter treatment or provide prognostic information, are considerably more common (20–25 %) in infants with GA of ≤30 weeks [19].

Stable infants born ≥25 weeks gestation may not need further screening for IVH if they have had two normal HUS scans performed a week apart (limited evidence).

Unstable or infants born ≤25 weeks gestation are at higher risk for late IVH, ventriculomegaly, and WMI and should have a follow-up scan at term-equivalent age even if the first two scans were normal [40] (moderate evidence).

In a 10-year study of 1,220 premature infants born between 30 and 34 weeks gestation, Bhat et al. found that only 38 % of infants underwent head ultrasounds. Of the scanned infants, they reported an IVH incidence of 3.3–6.3 % of which 1.5 % infants had severe IVH. Thus, screening HUS should be considered for all preterm infants who have had clinical instability in the neonatal period [24] (moderate evidence).

When Should Infants Be Screened?

Grading of IVH is based on HUS findings [1], and serial imaging has provided clues about the timing of IVH. The likelihood of early onset of IVH varies inversely with birth weight with 62 % of IVH in infants between 500 and 700 g occurring within 18 h of life [41]. About 90 % of all IVH has an onset in the first 4 days of life, and 20–40 % of these lesions progress over the course of the subsequent 4–5 days [42, 43]. Thus, two scans in the first 7–10 days would be able to detect the majority of IVH [2]. However, a practice parameter on neuroimaging of the neonate – Report of the Quality Standards Subcommittee of the American Academy of Neurology and the Practice Committee of the Child Neurology – concluded that "A routine screening head ultrasound (HUS) should be performed on all infants <30 weeks' gestation once between 7 and 14 days of age and should be optimally repeated between 36 and 40 weeks' postmenstrual age" [19]. This recommendation is intended to detect all severe forms of IVH

and periventricular leukomalacia (PVL) and ventriculomegaly both common lesions in premature infants. This consensus statement was created by reviewing evidence from literature searches using MEDLINE and EMBASE for 1990–2000. Of the >1,320 citations produced by the search using key words, 90 met their inclusion criteria. Each article was reviewed and the strength of the evidence ranked by two independent reviewers. Recommendations were derived based on the strength of the evidence [19] (moderate evidence).

What Is the Best Imaging Modality for Cerebellar Hemorrhage?

Summary

Early detection of larger (>3 mm) CH is accomplished by HUS screening that incorporates the mastoid fontanelle, the thinnest region of the temporal bone at the junction of the squamosal, lambdoidal, and occipital sutures. MR imaging detects a larger proportion of cerebellar hemorrhages that are smaller (1–3 mm) and missed on HUS (limited evidence).

Supporting Evidence

Head ultrasound through the anterior fontanelle (AF) is the screening method of choice for the detection of IVH. However, visualization of infratentorial structures located farther away from the transducer is poor due to the echogenic tentorium and vermis [13]. Imaging through the mastoid fontanelle (MF) provides a better view of the posterior fossa [21, 44, 45]. Recent studies have indicated that MR imaging improves the detection of CH especially small punctate hemorrhagic lesions in the hemispheres and vermis that are 1–3 mm in size [46]. When compared to CH detected on MRI, HUS with the MF view had a positive predictive value of 100 % and a negative predictive value of 89 % and a sensitivity of 45 % and specificity of 100 % [47]. However, the CH detected only on MR imaging is associated with a better neurological outcome than that visible on HUS [46] (limited evidence).

What Imaging Is Appropriate for Evaluating Complications Associated with IVH?

Summary

Of the two major complications/associations of IVH, posthemorrhagic ventricular dilatation (PHVD) is best detected by serial HUS scans performed starting within 4–7 days following detection of a severe IVH (grades 3–4) and then twice a week for 4 weeks or until the ventricular size stabilizes. Standard ventricular measures including the ventricular index, anterior horn width, and thalamo-occipital distance can aid in the serial evaluation of ventricular dilatation. WMI can be imaged with either HUS or MR imaging at term-equivalent age although the latter is more sensitive at detecting mild/moderate injury. MR imaging without sedation has been shown to be safe, feasible, and successful at this age in premature infants (moderate evidence).

Supporting Evidence

Complications of IVH stem from (a) obstruction of CSF flow (acute) and/or decreased absorption of CSF due to obliterative arachnoiditis (subacute) resulting in posthemorrhagic ventricular dilatation (PHVD), (b) preceding or concomitant white matter injury (especially in periventricular hemorrhagic infarction or grade 4 IVH) from inflammatory and free radical mediated injury, and (c) destruction of the germinal matrix and glial precursors [2].

PHVD

About 30–50 % of infants with IVH will develop PHVD [48], and of these 25–50 % develop progressive PHVD [49] that is associated with a threefold increase in cognitive and psychomotor delay [50]. Serial assessment of ventricular size by HUS is critical since the classic clinical signs of hydrocephalus, i.e., full fontanelle, rapid head growth, and sutural separation, may not appear for days to weeks after dilatation of the ventricles [51, 52]. PHVD usually evolves over a course of 1–4 weeks and occurs earlier for the more severe grades of hemorrhage. Thus, the acute variety of PHVD may occur within

a week of severe IVH while the subacute type of PHVD may start 2–3 weeks later [53].

Reference ranges for ventricular size (anterior horn width and thalamo-occipital distance) are established across gestational ages [54], and normative ventricular indices have been described on HUS in premature neonates [55]. These measures are important in defining the timing of surgical intervention in PHVD. In a retrospective review of 73 infants with PHVD requiring intervention over a 5-year period in a Dutch group of neonatal units, deVries et al. demonstrated that earlier intervention in PHVD with CSF drainage (lumbar punctures and ventricular drainage devices) prior to the ventricular indices exceeding the 97th centile + 4 mm size resulted in improved neurodevelopmental outcomes and decreased need for ventriculoperitoneal shunt [56].

White Matter Injury

IVH is associated with a five- to ninefold increased risk of WMI regardless of size, laterality, or extent of lesions. Compared with infants with neither IVH nor ventriculomegaly, infants with both were at 18- to 29-fold greater risk of WMI [57]. Detection of white matter injury (WMI) in the premature neonate is best accomplished with an MRI performed at term-equivalent age. MR imaging can be accomplished without sedation in the majority of infants making it feasible in this population [27]. The availability of immobilizing devices suitable for neonates, MR compatible incubator with an integrated head coil, vital signs monitoring system, and intravenous pumps has improved the success rate of these scans without sedation [27]. Infants are fed and wrapped in a blanket and the immobilizer with leads for monitoring vital signs. Most infants sleep through the scan and the success rate approaches 90 % once the team gets familiar with the procedure. However, MR imaging needs to be accompanied by specialized neuroradiology services and a clinical neonatologist or pediatric neurologist who can explain the findings and their clinical impact on the infant. There is growing evidence that moderate to severe WMI detected at term-equivalent age in premature infant is associated with poor neurodevelopmental outcomes across all domains of development [58]. In addition, adverse outcomes are associated with major destructive lesions in the WM, diffuse excessive high signal intensity (DEHSI) within the white matter on T2 imaging, cerebellar hemorrhage, and ventricular dilation after intraventricular hemorrhage, but not with punctate white matter lesions, hemorrhage, or ventricular dilation without IVH [59, 60]. Evidence for the utility of HUS in detecting WMI at term-equivalent age varies by institution and individual expertise. While HUS was shown to be capable of detecting most severe forms of white matter injury, it was poorly predictive of mild/moderate injury [61]. However, in experienced hands not only did HUS identify all severe WMI identified on MR imaging, but infants with a normal HUS at term-equivalent age had either mild/no injury on MRI performed on the same day [62]. The addition of imaging via the mastoid fontanelle while improving the detection of CH does not improve the overall ability of HUS to diagnose it.

What Is the Impact of Imaging in This Population?

Summary

The variable and often subtle clinical syndrome that heralds the onset of IVH in premature infants and the significant association with complications and outcome makes screening imaging the key diagnostic approach to identify infants with IVH. In addition, these infants are at significant risk of PHVD and WMI neither of which is easily detected clinically. Follow-up imaging is thus warranted to detect these complications that may require intervention or close monitoring (strong evidence).

Supporting Evidence

The clinical presentation of the IVH spectrum in premature neonates is clinically variable. While the catastrophic presentation with obvious neurological signs provides a high index of suspicion in some infants, even careful, serial neurological

examination may miss IVH in 25–50 % of infants [2, 20]. Portable HUS scan remains the imaging modality of choice for screening high-risk premature neonates <30 weeks gestation for IVH [19]. The grade and extent of the IVH can be detected early, and the information obtained helps the treating neonatologist in assessing prognosis and risk for complications.

The development of PHVD secondary to severe grades of IVH evolves over 1–3 weeks. Due to the anatomical nature of the preterm brain with paucity of cerebral myelin, relative water excess in the white matter, and the relatively large subarachnoid space, clinical signs of increased intracranial pressure do not appear for weeks after ventricular dilatation is present [2]. This delay in clinical diagnosis may be detrimental to cerebral perfusion and neurophysiologic function as demonstrated by Doppler studies of cerebral blood flow velocity and visual evoked potentials [63, 64]. Serial HUS screening offers the best modality for detecting PHVD, and normative values for ventricular indices are available to assist in determining timing of intervention in progressive cases [54].

WMI in premature infants with IVH is best accomplished using MR imaging at term-equivalent age (see evidence from the section "What Imaging Is Appropriate for Evaluating Complications Associated with IVH?").

What Is the Long-Term Neurodevelopmental Impact of IVH?

Summary

All premature infants with IVH are at a significantly higher risk of developmental delay and need periodic follow-up neurodevelopmental testing for early detection of delay for timely intervention with appropriate therapy services. While the risk of adverse outcome is higher with more severe grades of IVH, even lower grades of IVH are associated with adverse outcomes albeit less often (moderate evidence).

Supporting Evidence

The risk of neurodevelopmental delay in survivors following severe IVH remains high [14, 48]. 50–75 % of infants with grades 3–4 IVH develop disabling cerebral palsy while 45–86 % of preterm infants with grades 3–4 IVH have been reported to have major cognitive delay with 75 % of them requiring special education intervention in school [19]. These more severe grades of IVH are significantly associated with mental retardation at 2–9 years with odds ratio values ranging from 9.97 to 19.0 [65]. In addition, extremely low-birth-weight infants with severe IVH that requires shunt insertion are at greatest risk for adverse neurodevelopmental and growth outcomes at 18–22 months compared with children with and without severe intraventricular hemorrhage and with no shunt [66].

Not only are infants with severe IVH at risk for neurodevelopmental delay, but even infants with low-grade IVH need careful follow-up. In a review of 362 extremely low-birth-weight infants with either normal (258/362) or grades I–II IVH (104/362), Patra et al. found that the neurodevelopmental outcomes of infants with IVH was significantly worse when compared with a cohort of similar infants with normal HUS scans across domains. Using the Bayley Scale of Infant and Toddler Development II, they reported a significantly lower mean mental developmental index (MDI) score than infants with normal HUS (74 ± 16 vs. 79 ± 14, $P = .006$). They had higher rates of MDI $\ll 70$ (45 % vs. 25 %; OR, 2.00; 95 % CI, 1.20 to 3.30; $P = .008$), major neurologic abnormality (13 % vs. 5 %; OR, 2.60; 95 % CI, 1.06 to 6.36; $P = .036$), and neurodevelopmental impairment (47 % vs. 28 %; OR, 1.83; 95 % CI, 1.11 to 3.03; $P = .018$) at 20 months chronological age, even when adjusting for confounding factors [15].

CH has been associated with significantly increased risk for subsequent neurodevelopmental disabilities when compared with preterm infants without hemorrhage. In addition to motor abnormalities, there is particular prominence of dysfunction in non-motor

domains, specifically the high prevalence of significant deficits in cognition, communication (both receptive and expressive), and social–behavioral function. In addition, while motor outcomes were worse in infants with associated IVH, the cognitive, language, and social sequelae were no worse in infants with combined CH and IVH than in infants with isolated CH [67].

Imaging Options

Table 20.1 shows the utility of imaging modalities for the detection of IVH and complications.

Imaging Case Studies

Case 1 A 24-week gestation infant imaged with severe respiratory distress and hypotension imaged on DOL#5 (Fig. 20.1) with grade 4 hemorrhage

Case 2 A Former 26-week gestation infant imaged on DOL# 15 with PHVD (Fig. 20.2)

Case 3 A former 24-week gestation infant imaged on DOL#10 with a right side cerebellar hemorrhage (Fig. 20.3)

Case 4 A former 27-week gestation infant imaged at term-equivalent age demonstrating bilateral cerebellar hemorrhages (Fig. 20.4)

Case 5 A former 28-week twin female infant with a history of grade 4 IVH on the right imaged at term-equivalent age (Fig. 20.5)

Case 6 A former 29-week gestation infant imaged at term-equivalent age who developed

necrotizing enterocolitis and gram-negative sepsis on DOL#17 (Fig. 20.6)

Suggested Imaging Protocol

A typical HUS is performed using a 10v4 transducer (vector transducer with a frequency range from 10 MHz down to 4 MHz) using five focal zones to improve spatial resolution. Via the anterior fontanelle, at least six oblique coronal sections (anterior to posterior) and seven parasagittal sections (one midline, three on the right, and three on the left) are obtained. Using the mastoid fontanelle as an acoustic window, one section is obtained in coronal and sagittal orientation. Modern equipment and PACS workstations allow for routine cine sweep clips to be stored and played back in real time to minimize the operator dependence of the final image interpretation.

MRI of the newborn brain can be performed at 1.5 T, but 3.0 T is preferable given the higher signal to noise ratio (SNR) afforded by the higher field strength. There are a number of options for RF coil selection. In practice, smaller coils and multichannel coils yield higher SNR than larger, single channel coils. The ideal coil is a multichannel (typically 8–12 channels), specifically designed for newborns. However, many centers have to use a multichannel extremity coil or head coil if a multichannel, neonatal head coil is not available. The imaging protocol should include a 3D T1-weighted scan with isotropic voxels no larger than 1 mm^3 (e.g., MPRAGE). The inversion time (IR), flip angle, repetition time (TR), and echo time (TE) will be vendor dependent but should be set to optimize contrast in the

Table 20.1 Utility of imaging modalities for the detection of IVH and complications

Imaging	IVH	CH	PHVD	WMI	Costs
HUS	Suitable – FC	Limited	Suitable – FC	Limited	$
MRI	Suitable	Suitable – FC	Suitable	Suitable – FC	$$$
CT	Suitable – NR	Suitable – NR	Suitable – NR	Limited – NR	$$

FC, first choice modality after considering sensitivity, specificity, and cost; NR, not recommended weighing risks against alternative imaging modalities

Fig. 20.1 A 24-week gestation infant imaged with severe respiratory distress and hypotension imaged on DOL#5. A HUS coronal view demonstrating bilateral grade 4 hemorrhages (intraparenchymal hemorrhage) that appear in a fan-shaped distribution anterolateral to the ventricle

Fig. 20.2 A former 26-week gestation infant imaged on DOL# 15. A coronal HUS view demonstrating PHVD. Note the resolving germinal matrix (grade 1) hemorrhage on the right. Scalar measures of the anterior horn width on the right and ventricular index on the left are also demonstrated
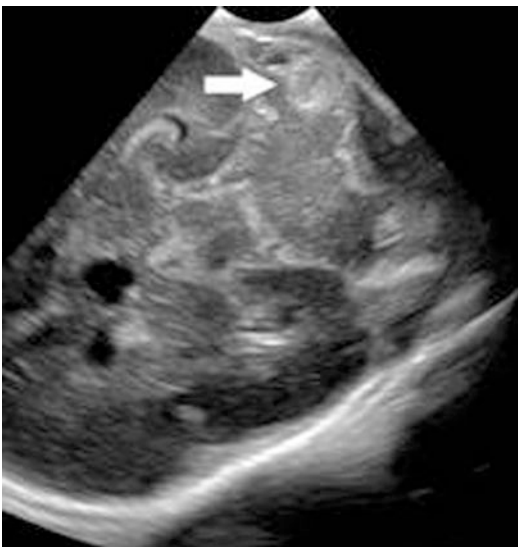

Fig. 20.3 A former 24-week gestation infant imaged on DOL#10. A right side cerebellar hemorrhage (*arrow*) shown on a HUS through the mastoid fontanelle. This infant also had a germinal matrix hemorrhage. Due to the high risk of associated complications, a follow-up MR imaging at term equivalent would detect the extent of WMI and cerebellar injury

Fig. 20.4 A former 27-week gestation infant imaged at term-equivalent age. A T2-weighted MR scan demonstrating bilateral cerebellar hemorrhages (*arrows*). Note the mild ventriculomegaly (likely due to decreased white matter volume), the wide interhemispheric fissure, and asymmetric appearance of the basal ganglia. All these findings are concerning for a significant increase in neurodevelopmental disability
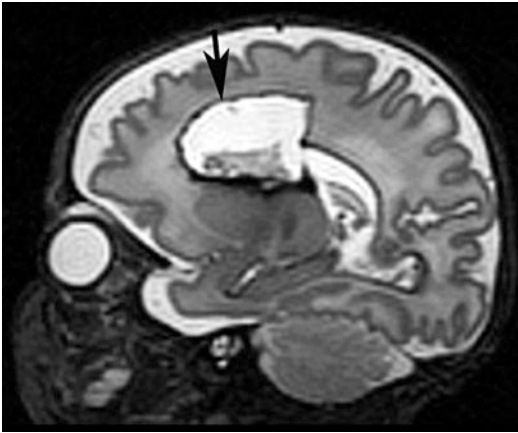
Fig. 20.5 A former 28-week twin female infant with a history of grade 4 IVH on the right imaged at term-equivalent age. A T2-weighted sagittal view demonstrating the porencephalic cyst (*arrow*) that has developed in the area of the prior IPH. This infant demonstrated a mild hemiparesis on the left with normal mental development on follow-up testing at 2 years of age

Fig. 20.6 A former 29-week gestation infant imaged at term-equivalent age. This infant developed necrotizing enterocolitis and gram-negative sepsis on DOL#17. A T2-weighted coronal MR image demonstrating the diffuse excessive high signal intensity (DEHSI) in the white matter (*arrows*), ventriculomegaly, increased interhemispheric fissure, and extra-axial space reflecting loss of white matter volume

newborn brain. Ideally, a high resolution or 3D T2-weighted scan (e.g., SPACE) with isotropic 1-mm^3 resolution to match the 3D T1-weighted scan would be obtained. Sagittal imaging orientation with coronal and transaxial reformations provides the most efficient scanning in terms of scan time. A gradient echo T2*-weighted scan improves sensitivity to many forms of hemorrhage. When possible, susceptibility-weighted imaging (SWI) at 3.0 T yields imagines with higher sensitivity and superior spatial resolution than 2D gradient echo imaging. Diffusion-weighted imaging and MR spectroscopy are typically performed as part of a newborn protocol but add little to the evaluation of IVH, PHVD, and CH; however, they may strengthen the diagnosis of WMI at term-equivalent age. Gadolinium-based contrast agent is typically not administered to newborns with IVH and associated complications unless a concurrent infection is suspected. MR venography may be performed if the pattern of hemorrhage suggests an etiology other than GMH or PHI.
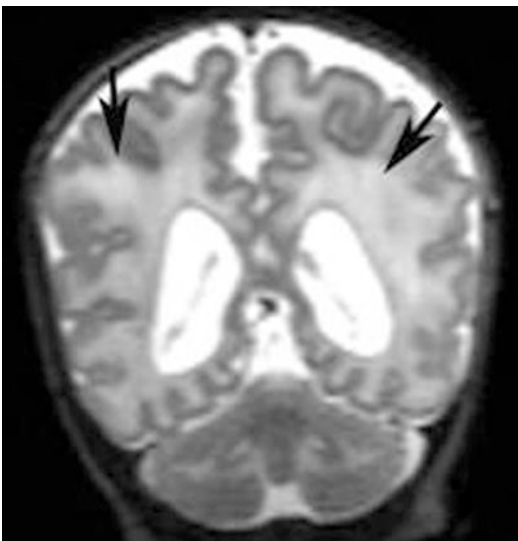
Future Research

- Advances in MR imaging resolution, sequences, and analysis continue to reveal insights into the biological spectrum of brain injury and abnormal development in the premature infant. Resting state functional connectivity MR imaging (fcMRI) is being investigated to ascertain connectivity in the premature neonatal brain. Diffusion tensor imaging combined with conventional T1- and T2-weighted imaging provides quantitative and qualitative evaluation of the white matter. Diffusion tractography is being studied to look at white matter development in premature infants. Automated volumetric and surface segmentation techniques are being evaluated to detect global and regional differences in brain development and injury.
- Diffuse optical imaging (DOI) based on the blood oxygen level–dependant (BOLD) signal is a portable qualitative imaging modality that is being evaluated in premature infants as a marker of connectivity.

References

1. Papile LA, et al. J Pediatr. 1978;92(4):529–34.
2. Volpe JJ, editor. Neurology of the newborn. 5th ed. Philadelphia: Saunders Elsevier; 2008. p. 1094.
3. Skinner JR, et al. Arch Dis Child. 1992;67(4 Spec No):374–7.
4. Cowan F, Thoresen M. Acta Paediatr Scand. 1987;76(2):239–47.
5. Leviton A, et al. J Child Neurol. 1991;6(1):35–40.
6. Amato M, Fauchere JC, Hermann Jr U. Neuropediatrics. 1988;19(3):154–7.
7. Lupton BA, et al. Am J Dis Child. 1988;142(11):1222–4.
8. Fulia F, et al. Biol Neonate. 2003;83(1):1–5.
9. Larroque B, et al. J Pediatr. 2003;143(4):477–83.
10. Horbar JD, et al. Pediatrics. 2002;110(1 Pt 1):143–51.
11. Martin JA, et al. Pediatrics. 2008;121(4):788–801.
12. Wilson-Costello D, et al. Pediatrics. 2005;115 (4):997–1003.
13. Limperopoulos C, et al. Pediatrics. 2005;116(3):717–24.
14. McCrea HJ, Ment LR. Clin Perinatol. 2008;35(4):777–92. vii.
15. Patra K, et al. J Pediatr. 2006;149(2):169–73.
16. Inder TE. J Pediatr. 2006;149(2):152–4.
17. Whitelaw A. Semin Neonatol. 2001;6(2):135–46.
18. Centers for Disease Control and Prevention. Economic costs associated with mental retardation, cerebral palsy, hearing loss, and vision impairment – United States, 2003. MMWR Morb Mortal Wkly Rep. 2004;53(3):57–9.
19. Ment LR, et al. Neurology. 2002;58(12):1726–38.
20. Lazzara A, et al. Pediatrics. 1980;65(1):30–4.
21. Merrill JD, et al. Pediatrics. 1998;102(6):E62.
22. Hellstrom-Westas L, Rosen I, Svenningsen NW. Neuropediatrics. 1991;22(1):27–32.
23. Ecury-Goossen GM, et al. Eur J Pediatr. 2010;169(10):1249–53.
24. Bhat V, et al. J Matern Fetal Neonatal Med. 2012;25(2):116–9.
25. El-Dib M, et al. Am J Perinatol. 2010;27(10):803–18.
26. Counsell SJ, et al. Arch Dis Child Fetal Neonatal Ed. 2003;88(4):F269–74.
27. Mathur AM, et al. Pediatr Radiol. 2008;38(3):260–4.
28. Bluml S, et al. Radiology. 2004;231(2):594–601.
29. Erberich SG, et al. Neuroimage. 2003;20(2):683–92.
30. Groenendaal F, et al. J Med Eng Technol. 2002;26(2):71–4.
31. Rona Z, et al. Eur J Paediatr Neurol. 2010; 14(5):410–7.
32. Whitby EH, et al. Pediatrics. 2004;113(2):e150–2.
33. Hintz SR, et al. J Pediatr. 2007;150(6):592–6–596 e1-5.
34. Harris DL, et al. Arch Dis Child Fetal Neonatal Ed. 2005;90(6):F494–9.
35. Vaucher YE, Pretorius DH. J Pediatr. 2007;150(6):575–7.
36. Harding D, Kuschel C, Evans N. J Paediatr Child Health. 1998;34(1):57–9.
37. Perlman JM, Rollins N. Arch Pediatr Adolesc Med. 2000;154(8):822–6.
38. Batton DG, et al. J Pediatr. 1994;125(4):623–5.
39. Boal DK, et al. Pediatr Radiol. 1995;25(6):425–8.
40. Nwafor-Anene VN, DeCristofaro JD, Baumgart S. J Perinatol. 2003;23(2):104–10.
41. Perlman JM, Volpe JJ. Am J Dis Child. 1986;140(11):1122–4.
42. Dolfin T, et al. Am J Perinatol. 1984;1(2):107–13.
43. Ment LR, et al. J Pediatr. 1984;104(3):419–25.
44. Buckley KM, et al. AJR Am J Roentgenol. 1997;168(4):1021–5.
45. Enriquez G, et al. Pediatr Radiol. 2006;36(6):532–40.
46. Tam EW, et al. J Pediatr. 2011;158(2):245–50.
47. Steggerda SJ, et al. Radiology. 2009;252(1):190–9.
48. Brouwer A, et al. J Pediatr. 2008;152(5):648–54.
49. Murphy BP, et al. Arch Dis Child Fetal Neonatal Ed. 2002;87(1):F37–41.
50. O'Shea TM, et al. Pediatrics. 2008;122(3):e662–9.
51. Korobkin R. Pediatrics. 1975;56(1):74–7.
52. Volpe JJ, Pasternak JF, Allan WC. J Dis Child. 1977;131(11):1212–5.
53. Hill A, Shackelford GD, Volpe JJ. Pediatrics. 1984;73(1):19–21.
54. Davies MW, et al. Arch Dis Child Fetal Neonatal Ed. 2000;82(3):F218–23.
55. Levene MI. Arch Dis Child. 1981;56(12):900–4.
56. de Vries LS, et al. Acta Paediatr. 2002;91(2):212–7.
57. Kuban K, et al. The developmental epidemiology network. J Pediatr.. 1999;134(5):539–46.
58. Woodward LJ, et al. N Engl J Med. 2006; 355(7):685–94.
59. Dyet LE, et al. Pediatrics. 2006;118(2):536–48.
60. Maalouf EF, et al. J Pediatr. 1999;135(3):351–7.
61. Leijser LM, et al. Neuroradiology. 2010;52(5):397–406.
62. Horsch S, et al. Arch Dis Child Fetal Neonatal Ed. 2010;95(5):F310–4.
63. Lui K, et al. Childs Nerv Syst. 1990;6(5):250–3.
64. McSherry JW, Walters CL, Horbar JD. Electroencephalogr Clin Neurophysiol. 1982;53(3):331–3.
65. Vohr BR, et al. Pediatrics. 2003;111(4 Pt 1):e340–6.
66. Adams-Chapman I, et al. Pediatrics. 2008;121(5): e1167–77.
67. Limperopoulos C, et al. Pediatrics. 2007; 120(3):584–93.

Children with Suspected Craniosynostosis: Evidence-Based Neuroimaging

21

Daniel N. Vinocur and L. Santiago Medina

Contents

D.N. Vinocur (✉)
Rady Children's Hospital, San Diego, CA, USA

Department of Radiology, University of California, San Diego, CA, USA
e-mail: vinocur@gmail.com

L.S. Medina
Division of Neuroradiology-Neuroimaging, Department of Radiology, Miami Children's Hospital, Miami, FL, USA

Herbert Wertheim College of Medicine, Florida International University, Miami, FL, USA

Former Lecturer in Radiology, Harvard Medical School, Boston, MA, USA
e-mail: smedina@post.harvard.edu; Santiago.medina@mch.com

Key Points

- Plain skull radiography demonstrates moderate to high sensitivity and specificity in craniosynostosis.
- Numerous publications support three-dimensional CT as the imaging modality with the best diagnostic performance, with reported sensitivities of 96–100 %. CT also detects associated intracranial pathology.
- Higher diagnostic performance is obtained with plain films and CT if the studies are of good quality and interpreted by an experienced reviewer.
- Cranial sonography shows preliminary promise as a diagnostic test for craniosynostosis. The evidence is based on small cohort studies; hence, larger series are needed before it is routinely used in clinical practice.
- Imaging strategies for children with suspected craniosynostosis should be based on their risk group. In healthy children with head deformity including posterior plagiocephaly, skull radiography is recommended. Syndromes such as Apert, Crouzon, and Pfeiffer nearly always have associated craniosynostosis and, hence, require 3D CT imaging for surgical planning.
- Imaging is not necessary for diagnosis or preoperative planning in isolated craniosynostosis with unequivocal clinical findings. However, in countries with significant societal expectations and medicolegal issues, imaging may still be employed. Recently renewed interest in pediatric imaging radiation dose reduction may change customary practices and, when indicated, limits the role of imaging to low-dose protocols.
- Intracranial anomalies can be seen in patients with craniosynostosis, but the exact incidence is not precisely known.
- Small retrospective US and MRI studies demonstrate the feasibility of prenatal diagnosis of craniosynostosis. However, large prospective studies are still required to understand the prenatal role of imaging in craniosynostosis and its effect on postnatal outcome.

Definition and Pathophysiology

Craniosynostosis is the premature fusion of the skull sutures. The resulting asymmetric calvarial growth causes characteristic cranial deformities. The clinical outcome varies between minor cosmetic deformity and dental malocclusion to severe head growth restriction with mental retardation and cranial palsies [1, 2].

Craniosynostosis cases can be classified in nonsyndromic (isolated) and syndromic. The exact etiology of this disorder has not been fully elucidated. However, it is generally believed that craniosynostosis results from abnormalities in the equilibrium between proliferation and differentiation of the osteoprogenitor cells of the cranial sutures from perturbations in signaling, tissue interactions, or a combination of these elements [2]. Furthermore, it is now known that the majority of craniosynostosis syndromes are caused by mutations in genes encoding fibroblast growth factor receptor (FGFR)-1, FGFR-2, and FGFR-3 and transcription factors TWIST and MSX2 [2–6]. Finally, an increasing number of mutations have been attributed to isolated, nonsyndromic craniosynostosis [7].

Epidemiology

The overall prevalence of craniosynostosis in the general population ranges from 34 to 48 per 100,000 live births [8, 9].

Higher incidence has been reported in the state of Colorado, USA [10], but the reason for this difference is unclear. In the general population, syndromic cases of craniosynostosis are less common than nonsyndromic cases [11–14]. Isolated sagittal and isolated coronal craniosynostoses are the most frequent types, accounting for 56 % and 22 % of the cases, respectively [9]. Interestingly, Selber et al. reported an increase in the relative frequency of metopic craniosynostosis over the last 24 years from approximately 3.7–27.3 % of cases [15]. In children with syndromic craniosynostotic disorders such

as Crouzon, Apert, and Pfeiffer syndromes, craniosynostosis is almost universally present [11–14]. Phenotypically unusual combined craniosynostosis is reported to occur in approximately 7.5 % of the cases (as reported by a large tertiary care center) [6].

Deformational plagiocephaly (also known as positional or postural molding plagiocephaly) is defined as the asymmetric flattening of the head due to repeated pressure. Since 1992, there has been an exponential increase in the number of infants seen with deformational posterior plagiocephaly [16, 17]. The estimated prevalence of deformational plagiocephaly reaches approximately 20 % during the first 4 months of life [7]. The most likely explanation is the 1992 American Academy of Pediatrics recommendation that infants sleep in the supine position to decrease the risk of sudden infant death syndrome (SIDS) and the increased awareness among pediatricians and other primary care providers for detection of plagiocephaly [18–22]. This specific entity usually presents some time after birth, progresses until 6 months of age, and remains stable thereafter [17]. The skull deformity is generally considered to be only of cosmetic significance, and in the vast majority of the cases, it will respond to conservative measures, such as changing sleeping position or corrective helmets [4, 18, 23, 24].

Overall Cost to Society

We are not aware of studies documenting national costs of diagnosis or treatment of craniosynostosis or deformational plagiocephaly before or after the 1992 recommendations from the American Academy of Pediatrics. We did find a comprehensive publication by Judith Weiss and colleagues regarding the hospital use and associated costs of craniofacial malformations in the state of Massachusetts [25]. In their detailed analysis, they included cost figures for craniosynostosis in the state of Massachusetts for children up to 2 years of age. For the 1998–2002 period, a total of 139 new cases of

craniosynostosis were recorded. These patients required a total of 1,386 hospital days, with a mean of 10 hospital days per patient. Adjusted cost figures for 2003 dollars estimate a total cost of $2,911,690, with a mean cost of $20,947 per patient.

The cost of imaging studies and cost-effectiveness analysis are discussed in detail below.

Goals of Imaging

The overall goal of neuroimaging for infants with suspected craniosynostosis is early detection and characterization of this entity to enable appropriate treatment. Delayed diagnosis and treatment may lead to (1) cosmetic calvarial deformity which may be difficult to correct or may require more extensive cranioplasty and (2) potentially irreversible neurological impairment [22]. Specific imaging goals include detailed characterization of the number of sutures affected, extent of suture involvement, and complexity of 3D calvarial deformity. Secondary goals include uncovering underlying brain anomalies associated with syndromic craniosynostotic disorders. More recently, there has been growing interest in the prenatal diagnosis of this disorder.

Methodology

Scientific article search was performed using the MEDLINE/PubMed electronic database (National Library of Medicine, Bethesda, MD) and Ovid (Wolters Kluwer, New York, New York) for original research publications discussing the diagnostic performance and effectiveness of imaging strategies in craniosynostosis. The search for neuroimaging-related publications covered the period 1980 to January 2011. The search strategy employed different combinations of the following terms: (1) craniosynostosis, (2) sensitivity, (3) specificity, and (4) diagnosis. This review was limited to human studies and the English-language literature. The authors performed an initial

review of the titles and abstracts of the identified articles followed by a full-text detailed review of the relevant articles.

Discussion of Issues

What Is the Role of Imaging in the Diagnosis of Craniosynostosis?

Summary

Plain skull radiography demonstrates moderate to high sensitivity and specificity in craniosynostosis (limited to moderate evidence).

Numerous publications show 3D CT as the test with the best diagnostic performance, with reported sensitivities of 96–100 % (limited to moderate evidence). Additionally, CT allows the detection of associated intracranial pathology. Higher diagnostic performance is obtained when radiographs and CTs are of good quality and interpreted by experienced radiologists (limited to moderate evidence). An imaging diagnostic algorithm is summarized in Fig. 21.1.

The diagnostic algorithm is based on the clinical differentiation between syndromic and isolated craniosynostosis. In isolated (nonsyndromic) cases, we advocate starting with plain radiographs. If the radiographs are negative, clinical follow-up would be indicated. In equivocal cases, or when the radiographs are positive, further characterization with 3D CT is recommended. Syndromic cases are best evaluated directly with 3D CT, with surgical consultation indicated in positive cases. Less-experienced radiologists may prefer using 3D CT rather than plain radiographs because of its higher sensitivity for detecting craniosynostosis and less difficulty in identifying and characterizing the sutures.

Head sonography shows preliminary promise as a diagnostic test for craniosynostosis, with estimated sensitivities and specificities in the 94–100 % range. The evidence is based on small cohort studies; hence, larger series are needed before routine use in medical practice (limited evidence). Bone scintigraphy has fallen out of use, mainly due to its low accuracy estimated at 66 %. In addition, interpretation of images is complex and requires great expertise (limited evidence).

Supporting Evidence

Skull Radiographs Plain radiographs are classically considered the first-line imaging modality in craniosynostosis [26, 27]. The standard series includes an anteroposterior view, Towne projection, and both lateral views. The low cost per study, low radiation, and universal availability have made it an attractive diagnostic choice [28]. However, large prospective studies addressing the diagnostic accuracy of this imaging modality are lacking. In a retrospective study by Cerovac and colleagues, the overall diagnostic accuracy of plain radiography was estimated at 91 % [27] (limited evidence). Vannier and colleagues [29] reported wide ranges of diagnostic accuracies depending on the suture evaluated, ranging from 56 % for the metopic suture to 88 % for the sagittal suture. Overall sensitivity and specificity were reported between 57–80 % and 54–100 %, respectively (limited to moderate evidence). Pilgram et al. showed that poor-quality radiographic studies had a significant decrease in sensitivity and specificity estimated at 60 % and 78 %, respectively [30] (Table 21.1) (limited to moderate evidence). In an older study of 36 patients from 1985 [22], plain radiography was reported to have an accuracy rate of 89 % when compared to surgical inspection and pathologic examination (limited evidence).

Computed Tomography (CT) The introduction of computed tomography revolutionized the imaging of craniosynostosis. This modality not only depicts the osseous pathology exquisitely but also allows for the detection of associated intracranial abnormalities, including hydrocephalus and brain developmental anomalies, such as agenesis of the corpus callosum [31]. In addition, CT can identify alternative causes for asymmetric cranial morphology, such as brain hemiatrophy and chronic subdural collections [26].

Numerous studies have been published in the literature demonstrating the high diagnostic performance of CT (Table 21.1). Agrawal et al. [32] reported an overall sensitivity of 100 % for CT diagnosis of craniosynostosis when correlated with intraoperative findings and surgical specimens (limited evidence). A blinded study performed on a relatively small cohort (25 infants) reported the sensitivity of CT with 3D surface-rendered reconstructions in the range of 96–100 %, when correlated with surgical findings (limited evidence) [33]. An older study from 1985 using thicker axial slices and no 3D reconstructions [22] reported an overall accuracy for CT diagnosis of 94 %. In this study, pathologic and surgical findings were used as gold standard.

The quality of the CT images and the reviewer's experience play an important role in the achieved diagnostic performance. Vannier et al. demonstrated sensitivity and specificity of 96 % and 100 %, respectively, for experienced CT reviewers (limited to moderate evidence) [33] versus a specificity of 43–83 % and 100 % sensitivity for less-experienced reviewers (limited to moderate evidence) (Table 21.1) [33]. Pilgram et al. demonstrated that poor-quality CT studies also had a significant decrease in sensitivity and specificity estimated at 73 % and 78 %, respectively (limited to moderate evidence) [30].

The use and risks of sedation or general anesthesia to perform CT examinations in children have been considered by several authors [27, 28]. The overall risk of death from sedation is very low and has been estimated at 1 in one million [34, 35]. Furthermore, with the advent of spiral and multidetector CT, imaging time has been reduced drastically; hence, most children no longer need sedation for routine head CT.

Imaging post-processing also has an impact on the diagnostic performance of CT. Vannier et al. [29] compared and concluded that 3D shaded surface rendering of the skull was superior to the combined information from 2D CT and plain radiography (limited to moderate evidence). In a technical note, Medina [36] reported from a small group of ten patients the advantages of 3D maximum intensity projections (MIP) in the comprehensive assessment of craniosynostosis (limited evidence).

Ultrasound (US) Lately growing interest has been placed on ultrasonographic examination for craniosynostosis given its lack of ionizing radiation and need for sedation. However, sonography is operator dependent, requires specially trained technologists, and is not feasible in infants older than 13 months [37]. Technically, the examination consists of scanning the sutures with high-frequency transducers (typically 7.5 MHz and above) utilizing gel as a coupling medium.

In 2006, Jan Regelsberger and colleagues from Hamburg, Germany, published a small series of 26 patients in which the diagnosis of craniosynostosis was established by ultrasound and confirmed later with CT. The study reported US sensitivity of 100 % relative to CT (limited evidence) [37]. More recently, Natalia Simanovsky and colleagues from Hadassah Hebrew University in Jerusalem, Israel, published a small retrospective study of 24 patients in whom the initial examination for suspected craniosynostosis had been performed with US. They correlated the sonographic results with a combination of clinical follow-up, CT examinations, and intraoperative findings. From their data, the calculated sensitivity and specificity were 100 % and 94 %, respectively [38] (limited evidence).

Plagiocephaly is a common problem, with an estimated prevalence of approximately 20 % during the first year of life [7]. There was a sharp increase in posterior plagiocephaly over a 25-year period [17], after the widespread adoption of the 1992 AAP positioning recommendations to decrease the incidence of SIDS [39]. A few articles addressed the use of ultrasound for this specific clinical concern (i.e., unilateral occipital craniosynostosis vs. deformational molding) [37, 40]. Sze and colleagues [40] published a prospective study of 41 subjects (including controls) to understand

the role of US in characterizing posterior plagiocephaly (limited to moderate evidence). Their study correlated ultrasonographic findings with CT results. The overall sensitivity for US diagnosis was 100 %, and the specificity was 89 % (limited to moderate evidence).

Scintigraphy Older literature emphasized the role of Tc99m-based osseous scintigraphy for the diagnosis of craniosynostosis. The literature estimates the overall accuracy of scintigraphy to be approximately 66 % [22], which renders it essentially valueless for current practice. In addition, interpretation of this modality requires expert knowledge regarding the different normal phases of activity along calvarial bone maturation [41].

Other Diagnostic Studies Additional imaging techniques for the evaluation of skull deformity have been recently published in the literature. Fruhwald and colleagues from Vienna, Austria, compared the accuracy of stereolithographic models to CT examinations in patients with craniofacial malformations [42]. Stereolithographic models are laser-carved corporeal 3D structures. The spatial information obtained from CT scans is used to laser cure liquid resin and manufacture skull models. They concluded that this innovative method provides an accurate reproduction of the skull for preoperative planning in complex procedures. The diagnostic accuracy of this technique in the evaluation of suspected craniosynostosis has not been addressed.

Finally, Schaaf et al. from Glessen, Germany, published a cohort of 100 patients with non-synostotic cranial deformities studied with three-dimensional photogrammetric images. [43]. Three-dimensional photogrammetry is the practice of determining the geometric properties of objects with 3D photographic images. In craniomaxillofacial surgery, standardized 3D images are taken, and quantification of angles, surfaces, and volumes is performed. The authors concluded that this technique is a reliable tool for treatment planning and follow-up of skull deformities in infancy. Its diagnostic value in craniosynostosis has not been evaluated.

What Is the Cost and Cost-Effectiveness of Imaging in Children with Suspected Craniosynostosis?

Summary

Selection of children with suspected craniosynostosis based on their risk group and use of the most appropriate evaluation strategy could maximize clinical and economic outcomes for these patients. In healthy children with head deformity including posterior plagiocephaly, the skull radiographic strategy had a reasonable cost per quality-adjusted life year (QALY) gained. Three-dimensional CT was more effective but had a high cost per QALY gained. In children with syndromic craniofacial disorders (high risk), 3D CT was the most effective strategy and had a reasonable cost per QALY gained. Figure 21.1 summarizes the best imaging approach in suspected craniosynostosis.

Supporting Evidence

The cost (not charge) of skull radiographs is $38–76, and CT is $191–261 (Table 21.2) [28]. Sedation, if needed, adds $121 to the cost of CT examinations (Table 21.2). Medina et al. [28] published a formal cost-effectiveness analysis (CEA) on diagnostic strategies in children with suspected craniosynostosis (moderate to strong evidence). Three risk groups were analyzed on the basis of the prevalence (pretest probability) of disease: low risk (completely healthy children; prevalence, 34/100,000), intermediate (healthy children with head deformity; prevalence, 1/115), and high risk (children with syndromic craniofacial disorders [i.e., Crouzon syndrome or Apert syndrome]; prevalence, 9–10/10). In the low-risk group, the radiographic and 3D CT strategies resulted in a cost per quality-adjusted life year (QALY) gained of more than $560,000. In the intermediate-risk group, the radiographic strategy resulted in a cost per QALY gained of $54,600. Three-dimensional CT was more effective than the two other strategies but at a higher cost – hence, with a cost per QALY gained of $374,200. In the high-risk group, 3D CT was the most effective strategy

with a cost per QALY gained of $33,800. Less-experienced radiologists and poor-quality studies increased the evaluation cost per QALY gained for all of the risk groups because of decreased effectiveness.

The authors concluded that radiologic screening of completely healthy children (low risk) for craniosynostosis is not warranted because of the high cost per QALY gained of the radiographic and 3D CT strategies. In healthy children with head deformity (intermediate risk), the radiographic strategy had a reasonable cost per QALY gained. Three-dimensional CT was more effective but had a high cost per QALY gained. In children with syndromic craniofacial disorders (high risk), 3D CT was the most effective strategy and had a reasonable cost per QALY gained. Therefore, selection of children with suspected craniosynostosis based on their risk group and use of the most appropriate evaluation strategy could maximize clinical outcome and cost-effectiveness for these patients.

Is Imaging Required When the Clinical Diagnosis Has Clearly Been Made?

Summary
Isolated craniosynostosis with unequivocal clinical findings probably does not warrant preoperative imaging for diagnostic correlation and preoperative planning (moderate evidence), though imaging may be important for medicolegal considerations. Recently renewed interest in pediatric imaging radiation dose reduction may change customary practices and avoid unnecessary imaging.

Supporting Evidence
In the last few years, there has been renewed concern for the long-term consequences of radiation exposure [44]. The medical literature as well as the lay press has echoed this concern with numerous publications [45]. Furthermore, the Alliance for Radiation Safety in Pediatric Imaging had launched the "image gently

campaign" with the ultimate goal of minimizing unnecessary radiation exposure in pediatric patients [46]. Numerous articles have been published regarding CT dose reduction in the evaluation of craniosynostosis [45, 47, 48].

Agrawal et al. [32] studied the usefulness of preoperative imaging of clinically diagnosed isolated sagittal craniosynostosis. In their retrospective study of 114 cases, they correlated clinical diagnosis and presurgical imaging (plain radiography and CT) with surgical and pathologic findings and found a correlation of 100 % for clinical diagnosis (moderate evidence). Both imaging studies also had a 100 % correlation with surgical pathology results. In this preliminary work, they concluded that clinically typical isolated sagittal craniosynostosis does not warrant imaging.

Similarly, Cerovac and colleagues from the Great Ormond Street Hospital for Children in the UK [27] published a retrospective series of 109 clinically diagnosed cases of isolated craniosynostosis and correlated them with presurgical imaging (CT and radiography) and surgical findings. They also demonstrated 100 % confirmation of the clinical and CT diagnoses (moderate evidence). Furthermore, they reported no additional treatment benefit from CT in screening for intracranial abnormalities or change in surgical planning.

More recently, Fearon et al. published a prospective multicenter study of 67 patients, in whom the diagnosis of craniosynostosis was solely based on physical examination by a craniofacial surgeon. These patients subsequently underwent CT examinations. The imaging findings were correlated with the physical examination diagnosis. The overall accuracy of physical examination was estimated at 98 %, with the authors reporting only one false-positive case (a deformational plagiocephaly case misdiagnosed as lambdoid synostosis by physical exam) [49] (moderate evidence).

Da Silva Freitas et al. published a retrospective cohort of 89 patients with craniosynostosis, comparing clinical findings with CT examinations [50]. They found 93 % diagnostic

agreement between the clinical findings and CT results. Out of the six patients with clinical-imaging disagreement, two demonstrated additional sutural involvement not detected by clinical exam, and the rest revealed incidental intracranial findings. Of note, the authors indicated that the additional diagnostic information afforded by CT would have probably had no significant clinical consequences (limited to moderate evidence).

Finally, Jeevan and colleagues introduced the concept of preoperative CT venography for mapping venous drainage abnormalities in patients with complex craniosynostosis. They presented a small cohort of 11 patients with known syndromic craniosynostosis. In 9 of the 11 patients (81 %), significant trans-osseous venous drainage was present; and in four of them, the trans-osseous route was the main pathway of cerebral venous drainage. Furthermore, in at least one patient, the information discovered by the CTV prevented an otherwise planned craniofacial surgery [51] (limited evidence).

How Often and What Intracranial Abnormalities Are Seen in Craniosynostosis?

Summary

There are a few studies addressing this question, and those published have been small and without well-defined cohorts. Therefore, intracranial anomalies can be seen in some patients with craniosynostosis, but the exact incidence is not well known.

Supporting Evidence

The exact incidence of associated intracranial anomalies in craniosynostosis is not well known. In a study from 1982, Goldstein and Kidd [52] reported on a heterogeneous group of patients with a variety of syndromic and isolated craniosynostoses (limited evidence). In this group, 5 out of 13 patients (38 %) demonstrated an associated intracranial abnormality, most commonly hydrocephalus. However, only one of the five patients with an intracranial abnormality led to change in therapy (insertion of a shunt for hydrocephalus).

On the other hand, Hayward et al. [53] published a selective study of 30 patients with severe craniosynostosis and complex clinical syndromes who had MR imaging. The authors found a variety of associated pathologies with the following prevalence: hindbrain herniation (19/30), syringomyelia (1/30), hydrocephalus (12/30), and nonspecified anomalies of cerebral white matter (4/30).

Thompson et al. reported in 1995 a retrospective cohort of 74 cases of isolated craniosynostosis in which direct subdural pressure was measured (moderate evidence). The authors found an incidence of 17 % of definite intracranial hypertension and 38 % of borderline hypertension [54]. Leikola et al. from Finland reported a 5.6 % prevalence of Chiari I malformation in children with nonsyndromic single-suture craniosynostosis [55]. In a cohort of 89 patients, published by Yale University [50], the following intracranial findings were reported: prominence of the subarachnoid space with a calculated prevalence of 3.7 %, cerebral atrophy (2.2 %), subarachnoid tumor (1.1 %), and deformational dysplasia of the mesencephalon (1.1 %). In addition, 5.6 % of cases demonstrated fluid in the middle ear and mastoid antra.

The association of intracranial anomalies with syndromic craniosynostosis has been well established. Greene and colleagues from Children's Hospital Boston reported an incidence of 77 % of elevated intracranial pressure in patients with phenotypically unusual combined craniosynostosis [6]. Crouzon syndrome is associated with chronic tonsillar herniation (Chiari I malformation) in approximately 70 % of cases and syringomyelia in 20 % of cases. Other associations include hydrocephalus and absence of the corpus callosum [56].

Apert syndrome has been associated with megalencephaly and stable ventriculomegaly. Interestingly, progressive hydrocephalus appears to be relatively uncommon (20 %) [57]. Additional associations include agenesis of the corpus callosum/septum pellucidum, encephalocele [58], limbic and gyral malformations, and

heterotopic gray matter among others [31, 57]. Structural inner ear anomalies in Apert syndrome are reported to occur in 100 % of the individuals when examined with CT [59].

Finally, Pfeiffer syndrome demonstrates considerable heterogeneity, with subgroups of patients with mild phenotypes without mental retardation [60] to more severe phenotypes associated with hydrocephalus and Arnold-Chiari II malformation [56].

What Is the Role of Imaging in the Prenatal Diagnosis of Craniosynostosis?

Summary
Small retrospective US and MRI studies in the prenatal diagnosis of craniosynostosis have been published (limited evidence). However, large prospective studies are still required to understand the prenatal role of imaging in craniosynostosis and their effect on parental counseling, surgical planning, and postnatal outcome.

Supporting Evidence
Recently, there has been increasing interest in the antenatal diagnosis of craniosynostosis. Early detection could potentially allow for different interventions, including elective termination of the pregnancy in severe syndromic craniosynostosis, elective cesarean section, early postnatal surgery, and perhaps fetal surgery [61].

Ultrasound (US)
In the largest series found in the literature, Delahaye and colleagues [5] performed a retrospective study in 40 fetuses with high risk of craniosynostosis. The inclusion criteria were (1) patient with a family history of craniosynostosis and (2) those with an abnormal screening obstetrical ultrasound. Abnormal screening ultrasounds were based on altered head measurements and indices. Reported specificity and sensitivity was 100 % and 97 %, respectively, for this retrospective study (limited evidence).

Miller and colleagues used screening ultrasound (nontargeted) in the second and third trimester to compile a heterogeneous retrospective cohort of 21 fetuses with craniosynostosis. In this study, the authors correlated postnatal diagnosis with indirect signs of craniosynostosis on screening ultrasound examinations (cranial geometry and indices). Their study demonstrated poor correlation between parameters of a non-dedicated prenatal ultrasound in the proper identification of craniosynostosis (limited evidence). Using cranial geometry and indices, only 15 of the 26 (estimated sensitivity 58 %) cases were diagnostic of postnatally documented craniosynostosis (limited evidence) [61].

MRI
Fjortoft and colleagues reviewed the imaging in a small group of 15 fetuses that demonstrated abnormal screening US during the second and third trimesters and were subsequently studied with fetal MRI imaging with the specific suspicion of craniosynostosis. In this cohort, MRI demonstrated 100 % sensitivity and specificity when correlated to follow-up postnatal medical records (limited evidence) [62]. To date, no prospective MR imaging studies are found.

Take-Home Figures and Tables

Figure 21.1 is an algorithm with a suggested diagnostic approach for suspected craniosynostosis.

Tables 21.1 and 21.2 discuss the performance of imaging tests for suspected craniosynostosis and the costs of imaging tests, respectively.

Imaging Case Studies

Case 1: Isolated sagittal craniosynostosis (Fig. 21.2)
Case 2: Non-synostotic occipital plagiocephaly (Positional molding or deformational plagiocephaly) (Fig. 21.3)
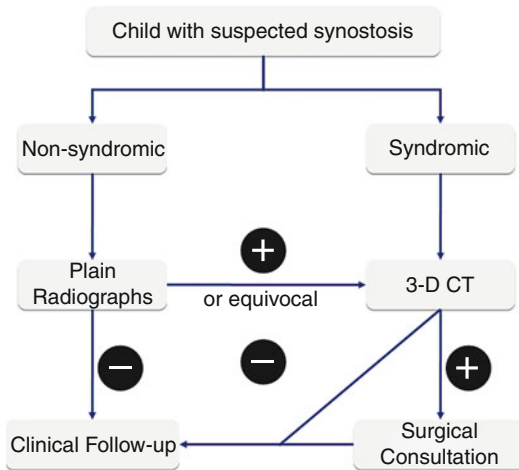Case 3: Apert syndrome (Fig. 21.4)

Fig. 21.1 Suggested diagnostic approach for suspected craniosynostosis (Reprinted with permission from Vinocur DN, Medina LS. Imaging in the evaluation of children with suspected craniosynostosis. In: Medina LS, Applegate KE, Blackmore CC, editors. Evidence-based imaging in pediatrics. New York: Springer; 2010)

Table 21.1 Performance of imaging tests for suspected craniosynostosis

Diagnostic test	Sensitivity (%)	Reference
Radiographs (good quality)		
Sensitivity (%)	80	[13]
Specificity (%)	95	[13]
Radiographs (poor quality)		
Sensitivity (%)	60	[12]
Specificity (%)	78	[12]
CT [a,b] (experienced reviewer)		
Sensitivity (%)	96.4	[14]
Specificity (%)	100	[14]
CT [a,b] (less-experienced reviewer)		
Sensitivity (%)	96.4	[14]
Specificity (%)	100	[14]
CT (poor quality)		
Sensitivity (%)	73	[12]
Specificity (%)	78	[12]

Modified with permission from Medina et al. AJR Am J Roentgenol. 2002; 179:215–21. Reprinted with permission from Vinocur DN, Medina LS. Imaging in the evaluation of children with suspected craniosynostosis. In: Medina LS, Applegate KE, Blackmore CC, editors. Evidence-based imaging in pediatrics. New York: Springer; 2010
[a]CT with three-dimensional reconstructions
[b]Good quality

Table 21.2 Costs of imaging tests for suspected craniosynostosis

Variable	Direct cost ($)	Total cost[a] ($)	Medicaid[b] ($)
Skull radiography	44	76	38
CT with three dimensions	80	191	261
Sedation	70	121	0[c]
CT plus sedation	150	312	261

Modified with permission from Medina et al. AJR Am J Roentgenol. 2002; 179:215–21. Reprinted with permission from Vinocur DN, Medina LS. Imaging in the evaluation of children with suspected craniosynostosis. In: Medina LS, Applegate KE, Blackmore CC, editors. Evidence-based imaging in pediatrics. New York: Springer; 2010)
[a]Medical center cost estimates include direct (fixed and variable) and indirect (overhead) costs
[b]Medicaid reimbursement (Ohio). This cost was used for the case-based study
[c]Sedation by nonanesthesiologist is not reimbursed by Medicaid

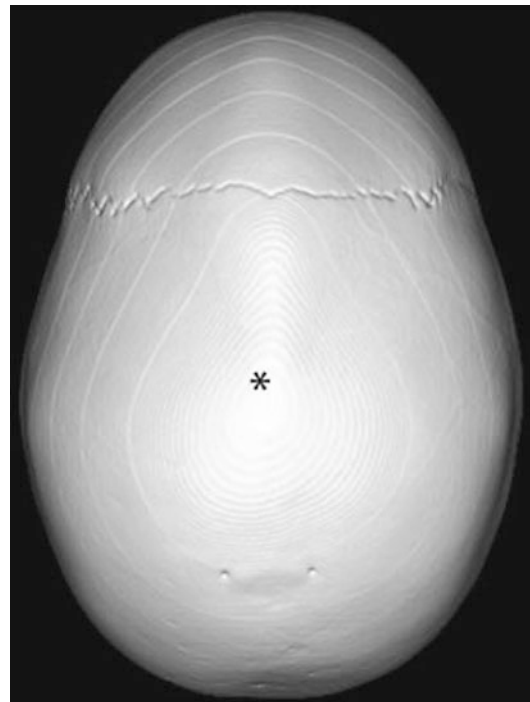**Fig. 21.2** Case 1. Another case of isolated sagittal craniosynostosis. Superior view from a 3D CT reconstruction demonstrating fusion of the sagittal suture (*star*) with associated dolichocephaly (Reprinted with permission from Vinocur DN, Medina LS. Imaging in the evaluation of children with suspected craniosynostosis. In: Medina LS, Applegate KE, Blackmore CC, editors. Evidence-based imaging in pediatrics. New York: Springer; 2010)
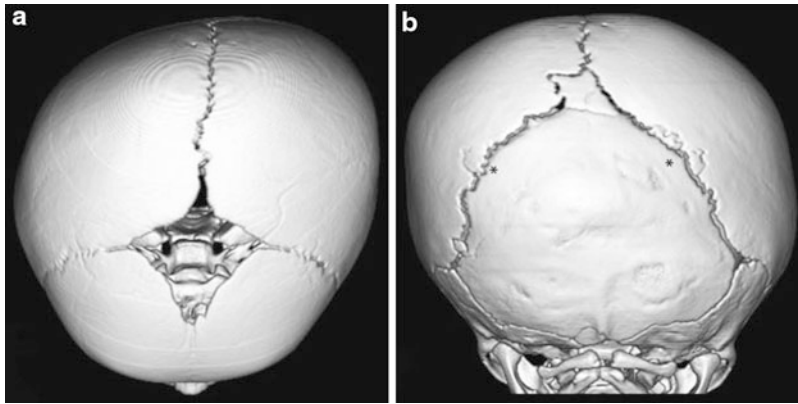
Fig. 21.3 Case 2. Non-synostotic occipital plagiocephaly (positional molding or deformational plagiocephaly). (**a**) Superior projection from a 3D CT reconstruction demonstrating the skull deformity. (**b**) Posterior projection from a 3D CT reconstruction demonstrating patent lambdoid sutures (*stars*) (Reprinted with permission from Vinocur DN, Medina LS. Imaging in the evaluation of children with suspected craniosynostosis. In: Medina LS, Applegate KE, Blackmore CC, editors. Evidence-based imaging in pediatrics. New York: Springer; 2010)
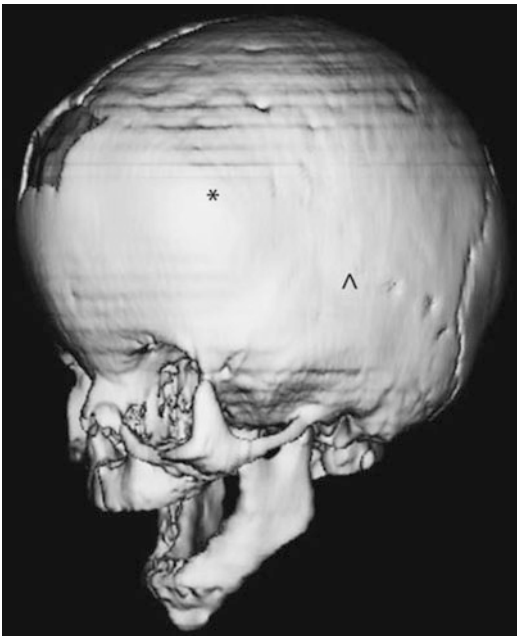
Fig. 21.4 Case 3. Apert syndrome. Anterior oblique projection from a 3D CT reconstruction demonstrating coronal (*star*) and squamosal (^) sutures synostosis. Also note the facial hypoplasia (Reprinted with permission from Vinocur DN, Medina LS. Imaging in the evaluation of children with suspected craniosynostosis. In: Medina LS, Applegate KE, Blackmore CC, editors. Evidence-based imaging in pediatrics. New York: Springer; 2010)

Suggested Imaging Protocol

Plain Radiographs

Excellent quality plain films including anteroposterior, Towne, and both lateral radiographs.

CT

Spiral or MDCT with surface rendering and maximum intensity projections. Suggested parameters:
- 120 kVp
- (40–200) mA age and weight corrected
- Thickness 2.5 mm
- Parenchymal reconstruction: 5 mm with soft tissue algorithm

3D images: source 0.625-mm high-resolution bone reconstruction using 3D volume rendering and high-definition maximum intensity projection.

Future Research

- Large studies are needed to evaluate the role of ultrasound in the diagnosis of craniosynostosis, particularly in the differentiation

between this entity and the more common deformational plagiocephaly.

- Further research is required to establish the role of MRI and US in the prenatal diagnosis of craniosynostosis.
- Better-defined cohorts should be studied to determine the incidence of intracranial abnormalities based on the type of craniosynostotic disorder.

References

1. Fernbach SK. Pediatr Radiol. 1998;28(9):722–8.
2. Slater BJ, Lenton KA, Kwan MD, Gupta DM, Wan DC, Longaker MT. Plast Reconstr Surg. 2008;121(4):170e–8.
3. Blaumeiser B, Loquet P, Wuyts W, Nothen MM. Prenat Diagn. 2004;24(8):644–6.
4. van Vlimmeren LA, Helders PJ, van Adrichem LN, Engelbert RH. Eur J Pediatr. 2004;163(4–5):185–91.
5. Delahaye S, Bernard JP, Renier D, Ville Y. Ultrasound Obstet Gynecol. 2003;21(4):347–53.
6. Greene AK, Mulliken JB, Proctor MR, Meara JG, Rogers GF. Plast Reconstr Surg. 2008;122(3):853–62.
7. Cunningham ML, Heike CL. Curr Opin Pediatr. 2007;19(6):645–51.
8. Lajeunie E, Le Merrer M, Bonaiti-Pellie C, Marchac D, Renier D. Am J Med Genet. 1995;55(4):500–4.
9. Cohen Jr MM. Epidemiology of craniosynostosis. In: Cohen Jr MM, editor. Diagnosis, evaluation and management. 2nd ed. New York: Oxford University Press; 2000. p. 112–18.
10. Alderman BW, Fernbach SK, Greene C, Mangione EJ, Ferguson SW. Arch Pediatr Adolesc Med. 1997;151(2):159–64.
11. Cohen Jr MM. Biological background. In: Cohen Jr MM, editor. Craniosynostosis: diagnosis, evaluation, and management. 2nd ed. New York: Oxford University Press; 2000. p. 3–50.
12. Cohen Jr MM. Sutural pathology. In: Cohen Jr MM, editor. Craniosynostosis: diagnosis evaluation, and management. 2nd ed. New York: Oxford University Press; 2000. p. 51–68.
13. Cohen Jr MM. Anatomic, genetic, nosologic, diagnostic, and psychosocial considerations. In: Cohen Jr MM, editor. Craniosynostosis: diagnosis, evaluation, and management. 2nd ed. New York: Oxford University Press; 2000. p. 119–46.
14. Blank CE. Ann Hum Genet. 1960;24:151–64.
15. Selber J, Reid RR, Chike-Obi CJ, et al. Plast Reconstr Surg. 2008;122(2):527–33.
16. Mulliken JB, Vander Woude DL, Hansen M, Labrie RA, Scott RM. Plast Reconstr Surg. 1999;103(2):371–80.
17. Jones BM, Hayward R, Evans R, Britto J. Br Med J. 1997;315(7110):693–4.
18. Argenta LC, David LR, Wilson JA, Bell WO. J Craniofac Surg. 1996;7(1):5–11.
19. Kane AA, Mitchell LE, Craven KP, Marsh JL. Pediatrics. 1996;97(6 Pt 1):877–85.
20. Turk AE, McCarthy JG, Thorne CH, Wisoff JH. J Craniofac Surg. 1996;7(1):12–18.
21. Willinger M, Hoffman HJ, Hartford RB. Pediatrics. 1994;93(5):814–19.
22. Gellad FE, Haney PJ, Sun JC, Robinson WL, Rao KC, Johnston GS. Pediatr Radiol. 1985;15(5):285–90.
23. Lipira AB, Gordon S, Darvann TA, et al. Pediatrics. 2010;126(4):e936–45.
24. Rogers GF, Miller J, Mulliken JB. Plast Reconstr Surg. 2008;121(3):941–7.
25. Weiss J, Kotelchuck M, Grosse SD, et al. Birth Defects Res A Clin Mol Teratol. 2009;85(11):925–34.
26. Abrahams JJ, Eklund JA. Clin Plast Surg. 1995;22(3):373–405.
27. Cerovac S, Neil-Dwyer JG, Rich P, Jones BM, Hayward RD. Br J Neurosurg. 2002;16(4):348–54.
28. Medina LS, Richardson RR, Crone K. AJR Am J Roentgenol. 2002;179(1):215–21.
29. Vannier MW, Hildebolt CF, Marsh JL, et al. Radiology. 1989;173(3):669–73.
30. Pilgram TK, Vannier MW, Hildebolt CF, et al. Radiology. 1989;173(3):675–9.
31. de Leon GA, de Leon G, Grover WD, Zaeri N, Alburger PD. Arch Neurol. 1987;44(9):979–82.
32. Agrawal D, Steinbok P, Cochrane DD. Childs Nerv Syst. 2006;22(4):375–8.
33. Vannier MW, Pilgram TK, Marsh JL, et al. AJNR Am J Neuroradiol. 1994;15(10):1861–9.
34. Cote CJ. Pediatr Clin North Am. 1994;41(1):31–58.
35. Holzman RS. Pediatr Clin North Am. 1994;41(1):239–56.
36. Medina LS. AJNR Am J Neuroradiol. 2000;21(10):1951–4.
37. Regelsberger J, Delling G, Helmke K, et al. J Craniofac Surg. 2006;17(4):623–5. discussion 626–8.
38. Simanovsky N, Hiller N, Koplewitz B, Rozovsky K. Eur Radiol. 2009;19(3):687–92.
39. American Academy of Pediatrics (AAP). Task force on infant positioning and SIDS: positioning and SIDS. Pediatrics. 1992;89(6 Pt 1):1120–6.
40. Sze RW, Parisi MT, Sidhu M, et al. Pediatr Radiol. 2003;33(9):630–6.
41. Fernbach SK, Feinstein KA. Neurosurg Clin N Am. 1991;2(3):569–85.
42. Fruhwald J, Schicho KA, Figl M, Benesch T, Watzinger F, Kainberger F. J Craniofac Surg. 2008;19(1):22–6.
43. Schaaf H, Pons-Kuehnemann J, Malik CY, et al. Neuropediatrics. 2010;41(1):24–9.
44. Slovis TL. Pediatrics. 2003;112(4):971–2.
45. Domeshek LF, Mukundan Jr S, Yoshizumi T, Marcus JR. Plast Reconstr Surg. 2009;123(4):1313–20.
46. Goske MJ, Applegate KE, Bell C, et al. Semin Ultrasound CT MR. 2010;31(1):57–63.

47. Chan CY, Wong YC, Chau LF, Yu SK, Lau PC. Pediatr Radiol. 1999;29(10):770–5.
48. Craven CM, Naik KS, Blanshard KS, Batchelor AG, Spencer JA. Br J Radiol. 1995;68(811):724–30.
49. Fearon JA, Singh DJ, Beals SP, Yu JC. Plast Reconstr Surg. 2007;120(5):1327–31.
50. da Silva Freitas R, de Freitas Azzolini T, Shin JH, Persing JA. J Craniofac Surg. 2010;21(2):411–13.
51. Jeevan DS, Anlsow P, Jayamohan J. Childs Nerv Syst. 2008;24(12):1413–20.
52. Goldstein SJ, Kidd RC. Comput Radiol. 1982;6(6):331–6.
53. Hayward R, Harkness W, Kendall B, Jones B. Scand J Plast Reconstr Surg Hand Surg. 1992;26(3):293–9.
54. Thompson DN, Malcolm GP, Jones BM, Harkness WJ, Hayward RD. Pediatr Neurosurg. 1995;22(5): 235–40.
55. Leikola J, Koljonen V, Valanne L, Hukki J. Childs Nerv Syst. 2010;26(6):771–4.
56. Lachman R. Taybi and Lachman's radiology of syndromes, metabolic disorders and skeletal dysplasias. 5th ed. St. Louis: Mosby; 2006.
57. Cohen Jr MM, Kreiborg S. Am J Med Genet. 1990;35(1):36–45.
58. Gershoni-Baruch R, Nachlieli T, Guilburd JN. Childs Nerv Syst. 1991;7(4):231–2.
59. Zhou G, Schwartz LT, Gopen Q. Otol Neurotol. 2009;30(2):184–9.
60. Teebi AS, Kennedy S, Chun K, Ray PN. Am J Med Genet. 2002;107(1):43–7.
61. Miller C, Losken HW, Towbin R, et al. Cleft Palate Craniofac J. 2002;39(1):73–80.
62. Fjortoft MI, Sevely A, Boetto S, Kessler S, Sarramon MF, Rolland M. Neuroradiology. 2007;49(6):515–21.

Traumatic Brain Injury: Evidence-Based Neuroimaging

22

Karen A. Tong, Udochukwu E. Oyoyo, Barbara A. Holshouser, Stephen Ashwal, and L. Santiago Medina

Contents

K.A. Tong (✉)
Department of Neuroscience, Loma Linda University Medical Center, Loma Linda, CA, USA
e-mail: ktong@llu.edu

U.E. Oyoyo
Department of Biophysics and Bioengineering, Loma Linda University, Loma Linda, CA, USA
e-mail: uoyoyo@llu.edu

B.A. Holshouser
Department of Radiology/MRI, Loma Linda University Medical Center, Loma Linda, CA, USA
e-mail: bholshouser@llu.edu

S. Ashwal
Department of Pediatrics, Loma Linda University School of Medicine, Loma Linda, CA, USA
e-mail: sashwal@llu.edu

L.S. Medina
Division of Neuroradiology-Neuroimaging, Department of Radiology, Miami Children's Hospital, Miami, FL, USA

Herbert Wertheim College of Medicine, Florida International University, Miami, FL, USA

Former Lecturer in Radiology, Harvard Medical School, Boston, MA, USA
e-mail: smedina@post.harvard.edu; Santiago.medina@mch.com

Key Points

- Head injury is not a homogeneous phenomenon and has a complex clinical course. There are different mechanisms, varying severity, diversity of injuries, secondary injuries, and effects of age or underlying disease.
- Classifications of injury and outcomes are inconsistent. Differences in diagnostic procedures and practice patterns prevent direct comparison of population-based studies.
- There are a variety of imaging methods that measure different aspects of injury (Table 22.1), but there is no one all-encompassing imaging method.
- CT is the mainstay of imaging in the acute period. The majority of evidence relates to the use of CT for detecting injuries that may require immediate treatment or surgery. Speed, availability, ease of exam, and lesser expense of CT studies remain important factors for using this modality in the acute setting. Sensitivity of detection also increases with repeat scans in the acute period (strong evidence).
- The sensitivity and specificity of MRI for brain injury is generally superior to CT, although most studies have been retrospective and few direct comparisons have been performed in the recent decade. CT is clearly superior to MRI for the detection of fractures. MRI outperforms CT in detection of most other lesions (limited to moderate evidence), particularly diffuse axonal injury (DAI). MRI allows more detailed analysis of injuries, including metabolic and physiologic measures, but further evidence-based research is needed.
- Accurate prognostic information is important for determining management, but there are different needs for different populations. In severe TBI, information is important for acute patient management, long-term rehabilitation, and family counseling. In mild or moderate TBI, patients with subtle impairments may benefit from counseling and education.
- Prediction rules such as the CHALICE prediction rule (Table 22.2) and the CATCH decision rule (Table 22.3) have the potential to improve and standardize the care of pediatric patients with head injuries (moderate evidence). In addition, minimizing the use of CT in children with very low risk of clinically important TBI may reduce the risk of radiation-induced malignancies.
- Calvarial plain radiographs have a poor sensitivity for identifying pediatric patients with intracranial pathology (moderate to strong evidence) and, hence, are not recommended unless for highly selected patients with suspected nonaccidental trauma.
- It is safe to discharge children with TBI, to home, after a negative CT study (moderate to strong evidence).

Definition and Pathophysiology

Head trauma is difficult to study because it is a heterogeneous entity that encompasses many different types of injuries that may occur together (Table 22.4). Definitions of age groups, injuries, and outcomes are also variable. Classification of injury severity is usually defined by the Glasgow Coma Scale (GCS) score, a scale ranging from 3 to 15, which is often grouped into mild, moderate, or severe categories. There is inconsistency in timing of measurement, with some investigators using "initial or field GCS" while others use "post-resuscitation GCS." Grouping of GCS scores also varies. There is no universal definition of mild or minor head injury [1], as some use GCS scores of 13–15 [2], while others use 14–15 [2], and others use only 15 [2, 3]. Variable definitions result in inconsistencies in imaging recommendations [1]. Moderate TBI is generally defined by GCS of 9–12. Severe TBI is defined by GCS of 3–8.

Classification and measures of outcome are even more variable. The most commonly used outcome measure is the Glasgow Outcome Scale (GOS) [4]. It is an overall measure based on degree of independence and ability to participate in

normal activities, with five categories: (5) good recovery, (4) moderate disability, (3) severe disability, (2) vegetative state (VS), and (1) death. The GOS is often dichotomized, although grouping is variable. A subsequent modification, the extended GOS [5], has eight categories: (8) good recovery, (7) good recovery with minor physical or mental deficits, (6) moderate disability, able to return to work with some adjustments or (5) works at lower level of performance, (4) severe disability, dependent on others for some activities, (3) completely dependent on others, (2) VS, and (1) death. Less common outcome scales include the Differential Outcome Scale (DOS) [6], the Rappaport Disability Rating Scale (DRS) [7], the Disability Score (DS) [8], the Functional Independence Measure (FIM) instrument [9], the Supervision Rating Scale [10], and the Functional Status Examination [11, 12].

Timing of outcome measurement also varies. Some investigators measure outcomes at discharge, 3, 6, or 12 months (or more) after injury. This may be problematic because outcomes often improve with time. However, there is moderate to strong evidence that 6 months is an appropriate time point to measure outcomes for clinical trials [13]. Neuropsychological assessment is the most sensitive measure of outcome, although this is difficult to perform in severely injured patients, resulting in selection bias. There is a wide variety of psychometric scales for various components of cognitive function such as intellect, orientation, attention, language, speech, information processing, motor reaction time, memory, learning, visuoconstructive ability, verbal fluency, mental flexibility, executive control, and personality.

Epidemiology

The prevalence of TBI is difficult to determine, because many less severely injured patients are not hospitalized and cases with multiple injuries may not be included. In addition, the number of people with TBI who are not seen in an emergency department or who receive no care is unknown. It is estimated that 1.7 million people per year sustain a TBI [14]. About 1.365 million (nearly 80 %) are treated and released from an emergency department. Most of these injuries are concussions or other forms of mild TBI [15]. However, approximately 52,000 people with TBI die, and about 275,000 are hospitalized. In addition, TBI contributes to a third (30.5 %) of all injury-related deaths in the USA. Children aged 0–4 years, adolescents aged 15–19 years, and adults aged 65 years and older are most likely to sustain a TBI; in all age groups, TBI rates are higher for males than females. Almost half a million (473,947) ED visits per year for TBI are by children aged 0–14 years. Falls are a leading cause of TBI (35.2 %), particularly for children aged 0–4 years and adults aged 75 years and older. Motor vehicle accidents account for 17.3 % of TBI but is the leading cause of TBI-related death, particularly in adults aged 20–24 years [16].

Overall Cost to Society

Over the last 30 years, there has been a progressive and significant reduction in severe TBI mortality, from 50 % to less than 25 % [16], probably from multiple factors including improvements in medical care, use of evidence-based guidelines, and injury-prevention efforts. An estimated 5.3 million US residents live with permanent TBI-related disabilities [17]. Direct costs are estimated at $48.3 billion/year [18]. In 2000, total direct and indirect costs of TBI were estimated at $60 billion/year [19]. There are little data on costs of TBI related solely to imaging. There has been one small study (limited evidence) that determined that 60 % of patients were found to have additional lesions on MRI, but because none of these additional findings changed management, MRI resulted in a nonvalue-added benefit incremental increase of $1,891 per patient and a $3,152 incremental increase in charges to detect each patient with a lesion not identified on CT [20].

Goals of Imaging

- To detect the presence of injuries that may require immediate surgical or procedural intervention
- To detect the presence of injuries that may benefit from early medical therapy
- To determine the prognosis of patients to tailor rehabilitative therapy or help with family counseling

Methodology

A search of the Medline/PubMed electronic database (National Library of Medicine, Bethesda, MD) was performed using keywords including (1) head injury, head trauma, brain injury, brain trauma, and traumatic brain injury, or TBI, and (2) CT, computed tomography, computerized tomography, MR, magnetic resonance, spectroscopy, diffusion, diffusion tensor, functional magnetic, functional MR*, T2*, FLAIR, and GRE, gradient echo. A systematic literature review was performed through March 2010. Limits included English language, abstracts, and human subjects. A search of the National Guideline Clearinghouse at www.guideline.gov was also performed using keywords including (1) head injury, head trauma, and brain injury and (2) parameter and guideline.

Discussion of Issues

Which Patients with Head Injury Should Undergo Imaging in the Acute Setting?

Summary
The need for acute imaging is generally based on the severity of injury. It is agreed that severe TBI (based on GCS score) indicates the need for urgent CT imaging to determine the presence of lesions that may require surgical intervention

(strong evidence). There is greater variability concerning recommendations for imaging of patients with mild or moderate TBI, or in pediatric TBI patients, although there are several recent guidelines (strong evidence) summarized in take-home Tables 22.2, 22.3, and 22.5.

Supporting Evidence
There are several clinical prediction rules (strong evidence) for evaluating mild/minor head injury in adults, based on prospective studies. The Canadian Head CT Rule [21] was developed from prospective analysis of 3,121 patients with GCS scores of 13–15. CT scan was recommended if a patient had any of the following: GCS score <15 after 2 h, suspected open or depressed skull fracture, any sign of basal skull fracture, episode(s) of vomiting, age greater than 65 (associated with high risk for neurosurgical intervention), amnesia for the period occurring 30 min or more before impact, or if injury was due to a dangerous mechanism, such as being struck by or ejected from a motor vehicle (associated with a medium risk for brain injury on CT). Another guideline by Haydel and colleagues was developed after prospective analysis of 520 patients in the first phase and 909 patients in the second phase. After recursive partitioning of variables in the first phase, seven variables were tested in the second phase, including headache, vomiting, age over 60 years, drug or alcohol intoxication, short-term memory deficits, physical evidence of trauma above the clavicles, and seizures. All patients with positive CT scans had at least one variable, resulting in 100 % sensitivity [22]. An older guideline by Madden and colleagues prospectively analyzed 51 clinical variables in 540 patients in the first phase and ten remaining variables in 273 patients in the second phase. The resulting sensitivity and negative predictive value were 96 % and 94 %, respectively [23].

A guideline, "Practice management guidelines for the management of mild traumatic brain injury" developed by the Eastern Association for the Surgery of Trauma (EAST) Practice Management Guidelines Work Group (2001) [2], was based on

level II evidence from several studies (three retrospective and one uncontrolled prospective). They reported that 3–17 % of patients with mild injuries had significant CT findings, although they noted that there was no uniform agreement as to what constitutes a "positive" CT scan in different studies. They also reported that a patient with a normal head CT had 0–3 % probability for neurological deterioration. Therefore, if a patient had a GCS of 15 and no neurologic/cognitive abnormalities, it was recommended that the patient be discharged. CT was recommended for all patients with transient neurological deficits.

One guideline for severe TBI, "Management and Prognosis of Severe Traumatic Brain Injury," was jointly developed by the Brain Trauma Foundation (BTF), American Association of Neurological Surgeons (AANS) Joint Section on Neurotrauma and Critical Care, and was also approved by the American Society of Neuroradiology, the American Academy of Neurology, the American College of Surgeons, the American College of Emergency Physicians, the Society for Critical Care Medicine, and the American Academy of Physical Medicine and Rehabilitation [24, 25]. An extensive review of previous CT literature supported the need for CT in the acute period. CT was reported to be abnormal in 90 % of patients with severe head injury. CT is included as a necessary step in the algorithm of initial management. A more recent 3rd edition of *Guidelines for the Management of Severe Traumatic Brain Injury* (2007) does include the same CT information as the 2000 edition.

What Is the Sensitivity and Specificity of Imaging for Injury Requiring Immediate Treatment/Surgery?

Summary

CT is the mainstay of imaging in the acute period. The majority of evidence relates to the use of CT for detecting injuries that may require immediate treatment or surgery. Speed, availability, and lesser expense of CT studies remain important factors for using this modality in the acute setting. Sensitivity of detection also increases with repeat scans in the acute period (strong evidence).

Supporting Evidence

The incidence of injury-related abnormalities on CT is related to the severity of injury. After minor head injury, the incidence is approximately 6 % [26] and increases up to 15 % in the elderly population [27]; those with GCS 13 or 14 have higher frequency of abnormalities than those with GCS 15 [28]. The incidence of CT abnormalities in moderate head injury (with GCS of 9–13) has been reported to be 61 % [29]. The sensitivity of CT for detecting abnormalities after severe TBI (GCS below 9) varies from 68 % to 94 %, while normal scans range from approximately 7 % to 12 % [30]. Several studies have shown that timing of CT studies also affects the sensitivity. Oertel and colleagues (strong evidence) prospectively studied 142 patients with moderate or severe injury, who had undergone more than one CT scan within the first 24 h, and found that the initial CT scan did not detect the full extent of hemorrhagic injuries in almost 50 % of patients, particularly if scanned within the first 2 h [31]. Likelihood of progressive hemorrhagic injury that potentially required surgical intervention was greatest for parenchymal hemorrhagic contusions (51 %), followed by epidural hematoma (EDH) (22 %), subarachnoid hemorrhage (SAH) (17 %), and subdural hemorrhage (SDH) (11 %). Servedei and colleagues (strong evidence) prospectively studied 897 patients with more than one CT scan and found that 16 % of patients with diffuse brain injury demonstrated significant evolution of injury. This was more frequent in those with midline shift, often evolving to mass lesions [31]. Similar results have been seen in retrospective studies [32]. Therefore, it may be useful to perform repeat CT scans in the acute period, particularly after moderate and severe injury, although the timing has not been clearly determined.

What Is the Overall Sensitivity and Specificity of Imaging in the Diagnosis and Prognosis of Patients with Head Trauma?

Summary

The overall sensitivity and specificity of MRI for brain injury is generally superior to CT, although most studies have been retrospective and very few head-to-head comparisons have been performed in the recent decade. CT is clearly superior to MRI for the detection of fractures. MRI outperforms CT in detection of most other lesions (limited to moderate evidence), particularly DAI. Because different sequences vary in ability to detect certain lesions, it is often difficult to compare results. MRI allows more detailed analysis of injuries, including metabolic and physiologic measures, but further evidence-based research is needed.

There are fewer pediatric studies regarding the use of imaging and outcome predictions.

Supporting Evidence

Early research on CT predictors was performed with older technology that was less sensitive to the presence of injuries. Some studies analyzed the first scans while others analyzed the worst scans. Many studies used a crude categorization system, with limited information regarding the degree of abnormalities. Others have attempted to assess outcome prediction using more detailed classification schemes. Accordingly, there has been variability in the reported predictors and success at prediction.

MRI has higher sensitivity than CT, though most comparison studies were performed in the late 1980s and early 1990s (with older-generation or lower-field scanners). Orrison and colleagues (moderate evidence) retrospectively studied 107 patients with MRI and CT within 48 h and showed MRI had an overall sensitivity of 97 % compared to 63 % for CT, even when a low-field MRI scanner was used, with better sensitivity for contusion, shearing injury, and subdural and EDH [33]. Ogawa and colleagues (moderate evidence)

detected more lesions with conventional MRI than CT with the exception of subdural and SAHs, in a prospective study of 155 patients, although they were studied at variable time points [34]. Other studies (moderate evidence) showed better detection of nonhemorrhagic contusions and shearing injuries [35] and of brain stem lesions [36], using MRI.

Some lesions, such as DAI, are clearly better detected with MRI and have been reported in up to 30 % of patients with mild head injury with normal CT [37] (limited evidence). However, sensitivity depends on the sequence, field strength, and type of lesion. *Gradient echo* (*GRE*) sequences are best for detecting hemorrhagic DAI, although the proportion of hemorrhagic versus nonhemorrhagic DAI is not truly known. An early report (limited evidence) suggested that less than 20 % of DAI lesions were visibly hemorrhagic [38], but this is likely to be erroneously low, due to poor sensitivity of the imaging methods available at that time. Scheid and colleagues (moderate evidence) prospectively studied 66 patients using high-field (3.0 T) MRI and found that T2*-weighted GRE sequences detected significantly more lesions than conventional T1- or T2-weighted sequences [39]. Tong and colleagues studied a new susceptibility-weighted imaging (SWI) sequence (at 1.5 T) that is a modified GRE sequence and have shown significantly better detection of small hemorrhagic shearing lesions compared to conventional GRE [40] (limited evidence).

The *fluid attenuated inversion recovery* (*FLAIR*) sequence is useful for detecting SAH, SDH, contusions, nonhemorrhagic DAI, and perisulcal lesions, but there are few studies comparing the sensitivity of FLAIR to other sequences. One study (limited to moderate evidence) found that FLAIR sequences were significantly more sensitive than spin echo (SE) sequences ($p < 0.01$) in detection of all lesions studied within 1–36 days (0.5 T), particularly in those who had DAI-type lesions [41].

Diffusion-weighted imaging (*DWI*) has also recently been shown to improve the detection of nonhemorrhagic shearing lesions, although there

are only a few small studies describing sensitivity. A small study (insufficient evidence) of patients scanned within 48 h found that DWI identified an additional 16 % of shearing lesions that were not seen on conventional MRI. The majority of DWI-positive lesions (65 %) had decreased diffusion [42]. Another descriptive study (limited evidence) characterized several different types and patterns of DWI lesions, although there was no comparison with other MRI sequences or analysis of diffusion changes over time [43]. A recent study (limited evidence) found a strong correlation between apparent diffusion coefficient (ADC) histograms and GCS score [44]. There are even less data on the sensitivity of *diffusion tensor imaging* (*DTI*). A few small studies (insufficient or limited evidence) have shown decreased anisotropy in brain parenchyma of TBI patients [45–47].

There are various studies demonstrating the use of specific imaging findings or patterns for outcome prediction. These are discussed in the sections that follow.

Imaging Classification Schemes

Several classification schemes have now been used to predict clinical outcomes. The earliest and most widely studied scheme, often named the "Marshall CT classification," is based on CT findings in the Trauma Coma Databank (TCDB), developed by Marshall and colleagues [48]; it is based on the status of cisterns, midline shift, and mass lesions. Six categories include (a) diffuse injury I (normal): no visible intracranial pathology; (b) diffuse injury II (small lesions): cisterns are present, midline shift <5 mm, and no lesions greater than 25 cm^3; (c) diffuse injury III (swelling): cisterns are compressed, midline shift <5 mm, and no lesions greater than 25 cm^3; (d) diffuse injury IV (shift): midline shift of >5 mm, no lesions greater than 25 cm^3; (e) any surgically evacuated lesion; and (f) any nonevacuated mass lesion greater than 25 cm^3. The TCDB classification was developed in severely injured patients (GCS < 8) and initially compared to discharge outcomes although it has more recently been validated using 3- and 6-month GOS [49]. It is reasonably good at predicting mortality, but it may not be as applicable to

mild/moderately injured patients and has been criticized as poorly predictive of functional recovery [50]. The TCDB classification has been variously modified, often to include the type, number [32, 51], or location of lesions [52]. In the BTF/AANS guideline [25], an extensive review of the previous CT literature (strong evidence) showed that the TCDB CT classification scheme strongly correlated with outcome.

Maas and colleagues subsequently developed a more discriminative six-point CT score, deemed the "Rotterdam Classification Scheme," in which certain individual CT characteristics of the Marshall CT classification were emphasized, and other findings were added. The scoring was based on four main features: (a) status of basal cisterns (normal, compressed, or absent), (b) degree of midline shift (normal, shift less than 5 mm, or greater than 5 mm), (c) presence of traumatic subarachnoid or intraventricular hemorrhage, and (d) presence of different types of mass lesions (epidural vs. SDH). This prognostic scoring system was tested in a large study population of moderate and severely injured patients involved in the International and North American Tirilazad trials. They showed that this combination of individual CT indicators had a better prediction and discrimination of long-term outcome than the Marshall CT classification system alone (strong evidence) [53].

Normal Scans

Extensive review (strong evidence) shows that normal CT scans in severe TBI patients are predictive of favorable outcome (61–78.5 % positive predictive value) [30]. In a more recent study (moderate evidence), normal CT scans in moderate/severe TBI patients were associated with better neuropsychological performance at 6 months [54].

Brain Swelling

Brain swelling is a subjective finding and more difficult to evaluate as an outcome predictor. Partly compressed ventricles and cisterns are not as reliably measured as obliterated ventricle and cisterns [55]. Marshall and colleagues (strong evidence) studied the TCDB classification in 746 patients and reported that brain swelling on

CT (categorized by diffuse injury III) was predictive of mortality and that survivors showed a trend of worse GOS associated with increasing grade of diffuse injury [48]. Compressed basal cisterns have been associated with a threefold risk of raised ICP and two- to threefold increase in mortality [25]. However, brain swelling on CT does not appear to correlate with neuropsychological outcomes [56] (moderate evidence).

Midline Shift

Midline shift is felt to be less important than other CT parameters for predicting mortality or GOS [25]. However, some investigators have shown that midline shift may be predictive of worse outcomes based on rehabilitation measures such as greater need for assistance with ambulation, activities of daily living (ADLs), and supervision at rehabilitation discharge [57].

Hemorrhage

The presence of hemorrhage has different prognostic significance depending on extent and location of blood. Traumatic SAH is a significant independent prognostic indicator [25, 58] (strong evidence), associated with a twofold increase in mortality and a 70 % positive predictive value for unfavorable outcome [25]. Mortality is higher and outcome is worse with acute subdural hematoma compared to extradural hematoma [25]. Hematoma volume correlates with outcome and has a 78–79 % positive predictive value for an unfavorable outcome [25]. Another study (moderate evidence) found that patients with combined SDH + ICH on CT had poor outcome even after surgery compared to EDH or ICH alone [59]. A small study (limited evidence) also found that IVH in all four ventricles was significantly associated with poor outcome [60].

Number, Size, and Depth of Lesions

Some investigators have attempted to evaluate the predictive ability of number, size, depth, or location of lesions. Van der Naalt and colleagues (moderate evidence) studied 67 patients with mild/moderate TBI and found that the outcome (1-year extended GOS or DOS) was related to number, size, and depth of lesions on CT [6].

Kido and colleagues (moderate evidence) found GOS was correlated with the size of intracranial lesions (independent of compartment or brain region) on CT [61]. A small MRI study (limited evidence) suggested that size, depth, and multiplicity of lesions correlated with neurobehavioral outcomes [62].

Location of lesions is partly related to mechanism of injury and is associated with different outcomes. The most available evidence is related to brain stem injuries. Firsching and colleagues (moderate evidence) studied 102 patients in coma with MRI in the first 8 days and found that mortality was 100 % with lesions in the bilateral pons [52]. Kampfl and colleagues (moderate evidence) studied 80 patients and also showed that lesion location could predict recovery from post-traumatic VS by 12 months, whereas clinical variables such as initial GCS, age, and pupillary abnormalities were poor predictors. Logistic regression showed that corpus callosum and dorsolateral brain stem injuries were predictive of nonrecovery. This information is helpful in that almost half of the patients with initial VS may recover within 1 year [63]. The association between extent or location of injuries and neuropsychological recovery has been, up to now, less studied, with only a few studies (limited evidence) that suggest that location of injury may be associated with specific neuropsychological impairments [62, 64].

Diffuse Axonal Injury

It has been repeatedly demonstrated that CT and MR findings are poor predictors of functional outcome of TBI patients, probably because DAI is frequently not detected [7]. Because *CT* clearly underestimates DAI, this can lead to inaccurate prediction of outcome. CT studies, many of which were performed with older-generation CT scanners, predominantly report that DAI is associated with mortality (limited evidence) [65] or poor outcome (moderate evidence) [66, 67]. However, it has been shown that patients with mild or moderate injuries can also have DAI [37] that is better detected with newer-generation CT scanners or MRI, and therefore better

outcomes than previously realized. Severe DAI can transform young productive individuals into dependent patients requiring institutionalized care; milder DAI can result in neuropsychiatric problems, cognitive deficits including memory loss, concentration difficulties, decreased attention span, intellectual decline, headaches, and seizures [68]. The improved ability to detect DAI on CT even in milder injuries has also allowed comparison with neuropsychological outcome. Wallesch and colleagues (moderate evidence) studied 60 patients with mild or moderate injuries, who underwent neuropsychological assessment 18–45 weeks later. Patients with DAI identified on CT had relatively transient deficits of psychomotor speed, verbal short-term memory, and frontal lobe cognitive functions, whereas patients with frontal contusions had persistent behavior alterations [69].

MRI studies also suggest an association between TBI severity and depth of axonal injury as well as outcomes. However, most MRI studies evaluating prognosis after DAI have consisted of small sample sizes. Small studies (limited to moderate evidence) have demonstrated that patients in VS are more likely to have DAI lesions in the corpus callosum and dorsolateral brain stem [70], compared to patients with mild TBI who were more likely to have lesions in the subcortical white matter without involvement of the corpus callosum or brain stem [66]. The presence of hemorrhage in DAI lesions may also affect prognosis, although results depend on the MRI sequence. One study of patients in VS (moderate evidence) found more nonhemorrhagic DAI lesions than hemorrhagic lesions, although only T1- and T2-weighted sequences were used [70]. In contrast, another study (limited evidence) showed that hemorrhage in DAI lesions (detected by GRE) was associated with poor outcomes (6-month GOS) and that isolated nonhemorrhagic DAI lesions were not associated with poor outcome [71]. There is also disagreement over whether the degree of hemorrhage correlates with outcomes, although this may be partly due to differences in outcome measures. One study (moderate evidence) found that the number of lesions (hypointense or hyperintense) detected by

T2*-weighted GRE images correlated with duration of coma and 3-month GOS [72]. However, another study (moderate evidence) (MRI sequence not specified) found no correlation between hemorrhagic lesion volume and neuropsychological outcome measures obtained more than 6 months after injury [73]. A more recent prospective study (moderate evidence) of 66 patients imaged with T2*-weighted GRE at 3.0 T found no correlation between the total amount of microhemorrhages and patient outcomes measured by GOS. However, these patients were imaged in the chronic phase [39].

Combinations of Imaging Abnormalities and Progressive Brain Injury

Some studies have shown that combinations of imaging abnormalities are predictive of outcome, although not necessarily in agreement. Fearnside and colleagues (strong evidence) prospectively studied 315 patients and found three CT findings to be highly predictive of mortality – cerebral edema, intraventricular blood, and midline shift. Three other CT findings were highly predictive of poor outcome in survivors – SAH, intracerebral hematoma, or intracerebral contusion [74]. In contrast, Lanoo and colleagues (moderate evidence) retrospectively reviewed 115 patients and found that subarachnoid, intracerebral, and SDH were predictive of mortality but not significantly related to morbidity [75]. Wardlaw and colleagues (moderate evidence) retrospectively reviewed 414 patients and developed a simple rating system of "overall appearance" of CT findings. They reported that "massive" injuries and SAH could predict poor prognosis (1-year GOS) [50].

Measures of Atrophy

Quantification of the atrophy of various brain structures/regions (such as corpus callosum, hippocampus, and ventricles) has also been studied with respect to predicting outcome, but is time-consuming, and often requires experienced raters and specialized software. Blatter and colleagues (moderate evidence) studied 123 patients with moderate to severe TBI compared to 198 healthy volunteers using MRI

volumetric analysis of total brain volume, total ventricular volume, and subarachnoid CSF volume. TBI patients, particularly if studied later, had the greatest decrease in brain volume, suggesting that progressive brain atrophy in TBI patients occurs at a rate greater than with normal aging [76]. However, because atrophy takes time to develop, it cannot be used acutely as an early predictor of outcome. Blatter and colleagues also showed that correlations with cognitive outcomes did not become significant until after 70 days [76]. One study of late CT scans (moderate evidence) of Vietnam War veterans with penetrating or closed head injuries found that total brain volume loss and enlargement of the third ventricle were significantly related to cognitive abnormalities and return to work [77]. Another study (moderate evidence) showed that frontotemporal atrophy on late MRI was predictive of 1-year outcome (measured by extended GOS or DOS) [6]. In an MRI study (moderate evidence) of late MRI findings and neuropsychological outcome, hippocampal atrophy was correlated with verbal memory function, whereas temporal horn enlargement was correlated with intellectual outcome [78].

Combinations of Clinical and Imaging Findings

Numerous studies have attempted to analyze combinations of clinical and imaging findings to determine the best approach to predicting outcome. The diversity of TBI makes this a difficult although worthy task. There is agreement that there is no one single variable that can predict outcome after TBI. In fact, there is often disagreement between studies regarding the predictive value of certain clinical variables, including GCS. Ideally, a combined clinical and imaging approach to outcome prediction would likely be most accurate. Ratanalert and colleagues (moderate evidence) studied 300 patients and reported that logistic regression showed that age, status of basal cisterns on initial CT, GCS at 24 h, and electrolyte derangement strongly correlated with a 6-month GOS score [79]. Ono and colleagues (moderate evidence) retrospectively studied 272 patients who were first divided

into CT categories according to the TCDB classification and found that within certain groups, additional variables such as age and GCS score were helpful predictors of outcome [51]. Schaan and colleagues (moderate evidence) studied the utility of creating a single score based on a weighted scale of clinical variables and CT findings including pupillary reaction, hemiparesis, brain stem signs, contusion, SDH, EDH, and cerebral edema. In their retrospective study of 554 patients, they divided the range of scores into three severity groups and found that there were significant differences in mortality and GOS scores between groups, suggesting that this approach had predictive value [80].

What Are Considerations for Imaging of Children with Head Trauma?

Summary

Pediatric TBI patients are known to have different biophysical features, risks, mechanisms, and outcomes after injury. There are also differences between infants and older children, although this remains controversial. Categorization of pediatric age groups is variable, and measures of injury or outcomes are inconsistent. The GCS and GOS have been used for pediatric studies, sometimes with modifications [81–83], or with variable dichotomization [81, 84]. For infants and toddlers, some investigators have used a Children's Coma Scale (CCS) [85]. There are several pediatric adaptations of the GOS, such as the King's Outcome Scale for Childhood Head Injury (KOSCHI) [86], the Pediatric Cerebral Performance Category Score (PCPCS), or the Pediatric Overall Performance Category Score (POPCS) [87].

A highly sensitive clinical decision rule, the CHALICE rule (Table 22.2), has been derived for the identification of children over 2½ years of age, who should undergo CT imaging after head trauma of any severity (moderate evidence). The authors of the decision rule also showed that calvarial plain radiographs have a poor sensitivity for identifying pediatric patients with intracranial pathology (moderate to strong evidence) and hence are not recommended unless for highly

selected patients with suspected nonaccidental trauma [88]. A recommended decision tree for children with acute head injury is shown in Fig. 22.1. Two other prediction rules have been developed for children with mild head injury (moderate to strong evidence) [89, 90]. These rules have the potential to improve and standardize the care of pediatric patients with head injuries.

Supporting Evidence

The CHALICE (Children's Head injury ALgorithm for the prediction of Important Clinical Events) study, conducted by Dunning and colleagues, was a large prospective multicenter diagnostic cohort study of 22,772 children over the age of 2.5 years, with head injury of any severity in the UK [88] (moderate evidence). All children who had a clinically significant head injury (death = 15, need for neurosurgical intervention = 137, or abnormality on a CT study = 281) were identified. Multivariate recursive partitioning on 40 clinical variables was performed in order to create a highly sensitive rule for predicting significant intracranial pathology. Abnormalities on CT included intracranial hematomas of any size, cerebral contusion, diffuse cerebral edema, and depressed skull fractures. Simple or nondepressed skull fractures alone were not considered to be significant predictors of intracranial injury [88]. The CHALICE rule was derived (Table 22.2) with a sensitivity of 98 % (95 % confidence interval (CI) 96–100 %) and a specificity of 87 % (95 % CI 86–87 %) for the prediction of clinically significant head injury and requires a CT imaging rate of 14 %. Prospective validation of this rule with new cohorts is ongoing.

Two recent studies have been performed to develop rules for use of CT in children with mild head injury. The larger of the two studies was performed by Kuppermann and colleagues [89], who conducted a large multicenter prospective study in North America, in which 42,412 pediatric patients (younger than 18 years old) with GCS scores of 14–15 were divided into those younger than 2 years of age and those

2 years or older. Given increasing awareness of radiation-induced malignancy, the investigators sought to identify children at very low risk of clinically important TBI, for whom CT might be unnecessary. They developed prediction rules for clinically important TBI – defined as death from TBI, neurosurgery, intubation >24 h, or hospital admission ≥2 nights. In the validation population of children under 2 years of age, there was a negative predictive value for clinically important TBI of 100 % (95 % CI 99.7–100 %) and sensitivity of 100 % (95 % CI of 86.3–100 %) if there was normal mental status, no scalp hematoma (except frontal), no loss of consciousness or LOC of less than 5 s, non-severe injury mechanism, no palpable skull fracture, and acting normally according to the parents. In the validation population of children 2 years or older, there was a negative predictive value of 99.95 % (95 % CI of 99.81–99.99 %) and sensitivity of 96.8 % (95 % CI of 89.0–99.6 %) if there was normal mental status, no LOC, no vomiting, non-severe injury mechanism, no signs of basilar skull fracture, and no severe headache. Neurosurgery events were not missed in either age group.

A more recent prospective multicenter cohort study was performed in Canada, which resulted in the development of the CATCH (Canadian Assessment of Tomography for Childhood Head injury) rule (Table 22.3) [90]. The investigators enrolled 3,866 pediatric patients (aged 0–16 years) with GCS of 13–15 and performed recursive partitioning to find the best combination of predictor variables that were highly sensitive (with maximal specificity) for detecting neurological injury and presence of brain injury on CT. Four high-risk factors were identified as being 100.0 % sensitive (95 % CI of 86.2–100.0 %) for predicting the need for neurological intervention and would result in 30.2 % of patients undergoing CT; these risk factors included failure to reach GCS score of 15 within 2 h, suspicion of open skull fracture, and worsening headache and irritability. Three medium-risk factors were identified as being 98.1 % sensitive (95 % CI of 94.6–99.4 %) for predicting brain injury by CT and would result in

50.2 % of patients undergoing CT: these risk factors included large boggy hematoma of the scalp, signs of basal skull fracture, and dangerous mechanism of injury.

Oman and colleagues studied the test performance of the eight-variable NEXUS II decision instrument to detect the presence of clinically import intracranial injury (ICI) in 1,666 pediatric patients with blunt head trauma and who had CT. The decision instrument utilized seven variables and correctly identified 136/138 cases (98.6 % sensitivity) and classified 230 as low risk (99.1 % NPV, 230/232; 15.1 % specificity, 230/1,528). Findings showed that significant ICI is extremely unlikely in any child who does not exhibit at least one of the following high-risk criteria: (1) evidence of significant skull fracture (diastatic, depressed, open, or basilar), (2) altered level of consciousness, (3) neurological deficit, (4) persistent vomiting, (5) presence of scalp hematoma, (6) abnormal behavior, and (7) coagulopathy (moderate to strong evidence) [91].

Palchak and colleagues derived a rule on 2,043 pediatric patients under 18 years who had head trauma and positive findings on history or clinical examination such as loss of consciousness, memory loss, headache, or emesis [92]. Of the nine predictive variables studied, abnormal mental status, clinical findings of calvarial fracture, history of emesis, scalp hematoma in children 2 years of age or less, and cephalalgia were identified in 96 of 98 patients with a positive intracranial lesion on CT (98 % sensitivity, 95 % CI 93–100 %) (moderate evidence). Since then, they have tested the decision rule against clinician judgment and found that application of the rule to the study population would have required 24.7 % (289/1,168) fewer CT scans. The decision rule had 98.9 % sensitivity (88/89) versus 94.4 % (84/89) for clinician judgment. Specificity of the rule was 26.7 % (288/1,079) versus 30.5 % (329/1,079) for judgment. The decision rule classified children as being at very low risk of ICI if none of the following findings were present: abnormal mental status, clinical signs of skull fracture, a history of

vomiting, scalp hematoma (in children <2 years), and headache (strong evidence) [93].

Greenes and Shutzman [94] performed a prospective study on 608 patients under 2 years of age in a single hospital setting (moderate evidence). Their study demonstrated that pediatric patients with suspected nonaccidental trauma, lethargy, or a major scalp hematoma had an increased risk of significant intracranial injury. This study found that loss of consciousness, seizures, or emesis alone was not an adequate predictor of intracranial injury, and, furthermore, the absence of clinical symptoms or signs did not fully exclude the possibility of having positive intracranial pathology [94]. They allocated patients into four risk groups, with CT imaging recommended in the highest risk group of children who vomited more than three times or had loss of consciousness, lethargy, a high-risk mechanism, or considerable bruising [94]. This study and the CHALICE study showed that it was safe to discharge children with a negative CT study [88, 94].

Haydel and Shembekar [95] evaluated the adult New Orleans criteria [22] in children under age 5 years. They studied 175 children with GCS of 15 at a single institution. They concluded that the 14 positive CT scans could be identified with this adult predictive rule [95]. The Canadian CT rule for children was proposed by the UK National Institute of Clinical Excellence before the CHALICE study was published [88]. The CHALICE group assessed the diagnostic performance of this rule in children [96] to detect intracranial injury and found a sensitivity of 94 % (95 % CI 91–97 %), specificity of 89 % (95 % CI 89–90 %), and a CT ordering rate of 12 % [88].

Boran and colleagues [97] studied 421 children with GCS of 15 and without any focal neurological deficit (moderate evidence). Intracranial lesion was noted in 37 cases (8.8 %). The clinical parameters associated with an increased incidence of intracranial pathology were post-traumatic seizures and loss of consciousness. However, when patients with these predictive parameters were subtracted, intracranial lesions were still identified in 4.1 % of

the cases, and 1.8 % required neurosurgical operation. Boran and colleagues also found a low sensitivity of plain radiographs of 43.2 % and specificity of 93 % [97]. The CHALICE study [88] and other studies [98] support the recommendation of not performing skull radiographs except for highly selected patients who may have had a nonaccidental injury. Calvarial plain radiographs have a poor sensitivity for identifying pediatric patients with intracranial pathology (moderate to strong evidence) [88].

The literature on repeat CT scans in pediatric patients seems to differ from adult studies, in that the yield of new clinically significant lesions is low in routine repeat studies (moderate evidence). In addition, because of the long-term effects of CT radiation exposure, the decision to order a CT scan also should be weighed against the risk of long-term radiation exposure. Hollingworth and colleagues studied the prevalence of worsening brain injury on repeat CT, predictors of worsening CT findings, and the frequency of neurosurgical intervention after the repeat CT, in 521 pediatric patients with moderate or severe TBI. For severe TBI, the multivariate-adjusted OR for worsening or new second CT findings was 2.4. Children with moderate or severe TBI, especially if they had ICI, were more likely to have deteriorating CT (43 %, 107/248), and 10 % (11/107) required surgery. Of those with stable CT (57 %, 141/248), only 3 % (4/141) required surgery. In most surgical patients, repeat CT was preceded by rapid decline in neurological status or elevated ICP [99]. Figg and colleagues performed a retrospective study in severely injured children and demonstrated that most second scans showed no change (53 %). Some showed improvement (34 %), and even less showed worsening (13 %). Only five (4.3 %) patients had a surgical intervention based on the results of the second CT scan, but all five scans were ordered based on a clinical indicator (increased intracranial pressure or worsening neurological status) and not on routine follow-up [100] (moderate evidence). Similar findings were reported by Tabori and colleagues (limited evidence) [101]. Therefore, repeat CT scans may be considered when there is evidence of neurological deterioration or increasing intracranial pressure. Routine repeat CT scans are not recommended.

There is less literature on imaging and prediction of outcome from head injury in pediatric subjects, compared to adults. Importantly, within the pediatric population, age may be a confounding variable or effect modifier for outcomes. Levin and colleagues (moderate evidence) studied 103 children at one of the original four centers participating in the TCDB and found heterogeneity in 6-month outcomes based on age. Worst outcomes were found in the 0–4-year-old patients, and best outcomes were found in the 5–10-year-old patients, while adolescents had intermediate outcomes. They suggested that studies involving severe TBI in children should analyze age-defined subgroups rather than pooling a wide range of pediatric ages [102].

Many studies have consisted of relatively small sample sizes and used varying outcome, possibly accounting for conflicting reports regarding outcomes related to TBI in children. There have been several studies evaluating CT in predicting outcome in children with variable results. Suresh and colleagues (moderate evidence) studied 340 children and compared CT findings to discharge GOS outcomes. They found that poor outcome (death) occurred in 16 % of their patients. In addition, progressively worse outcomes were found with fractures, EDH, contusion, diffuse head injury, and acute SDH [84]. Hirsch and colleagues (moderate evidence) studied 248 children after severe TBI and compared initial CT findings to the level of consciousness (measured by a modified GCS score) at 1 year after injury. They found that children with normal CT, or isolated SDH or EDH, were least impaired, while children with diffuse edema had the most impairment. Those with parenchymal hemorrhage, ventricular hemorrhage, or focal edema had intermediate outcomes [103]. A study of 82 children (moderate evidence) found that unfavorable prognosis (using a three-category Lidcombe impairment scale) was more likely to occur after shearing injury or intracerebral/subdural hematomas, whereas a better outcome was more likely

in patients with EDH [104]. Another study of 74 children (moderate evidence) found that the presence of traumatic SAH on CT was an independent predictor of poorer discharge outcome ($p < 0.001$) but did not find that DAI or diffuse swelling was associated with outcome. After stepwise logistic regression analysis, CT findings did not have prognostic significance compared to other variables such as GCS and the oculocephalic reflex [82]. Another study (moderate evidence) compared 59 children and 59 adults and found that a CT finding of absent ventricles/cisterns was associated with a slightly lower frequency of poor outcome (6-month GOS) in children, suggesting that diffuse swelling may be more benign in children than adults unless there was a severe primary injury or a secondary hypotensive insult [55].

Bonnier and colleagues studied 50 children with severe TBI before 4 years of age (moderate evidence) [105]. TBI severity (initial GCS or coma duration) was significantly associated with subcortical lesions. A greater deterioration in intellectual quotient over time was noted in patients with subcortical lesions. Sigmund and colleagues studied 40 children with TBI using CT and MRI (moderate evidence) [106]. T2-weighted, FLAIR, and susceptibility-weighted MRI findings showed no significant difference in lesion volume between normal and mild outcome groups but did indicate significant differences between normal and poor and between mild and poor outcome groups. CT revealed no significant differences in lesion volume between any groups. The findings suggest that these MRI sequence findings provide a more accurate assessment of injury severity and detection of outcome-influencing lesions than does CT in pediatric DAI patients (moderate evidence).

There have been some studies specifically evaluating MRI for outcome prediction in children with TBI. Prasad and colleagues (moderate evidence) prospectively studied 60 children with acute CT and MRI. Hierarchical multiple regression indicated that the number of lesions, as well as certain clinical variables such as GCS (modified for children) and duration of coma, was predictive of outcomes up to 1 year

(modified GOS) [81]. Several investigators have studied the correlation between depth of lesion and outcomes, with varying results. Levin and colleagues (moderate evidence) studied 169 children prospectively as well as 82 patients retrospectively with MRI at variable time points and showed a correlation between depth of brain lesions and functional outcome [107]. Grados and colleagues (moderate evidence) studied 106 children with an SPGR (T1-weighted) MRI sequence obtained 3 months after TBI and classified lesions into a depth-of-lesion model. They found that depth and number of lesions predicted outcome, although correlation was better with discharge outcomes than 1-year outcomes [108]. Blackman and colleagues (moderate evidence) studied 92 children in the rehabilitation setting (using variable imaging modalities) and used a depth-of-lesion classification (based on the Grados model) to study neuropsychological outcomes. They found that this classification had limited usefulness. Although patients with deeper lesions tended to have longer stays in rehabilitation, they were able to "catch up" after sufficient time had elapsed [109].

In a study of acute hemorrhagic DAI lesions (moderate evidence) on MRI, Tong and colleagues studied 40 children and found that the degree and location of hemorrhagic lesions correlated with GCS, duration of coma, and outcomes at 6–12 months after injury [110]. Children with normal outcomes or mild disability ($n = 30$) at 6–12 months had, on average, fewer hemorrhagic lesions ($p = 0.003$) and lower volume ($p = 0.003$) of lesions than those who were moderately or severely disabled or in a vegetative state. In a subgroup of these patients, Babikian and colleagues studied 18 children and adolescents 1–4 years after injury using SWI (limited evidence). Negative correlations between lesion number and volume with neuropsychologic functioning were shown [111].

Some have also studied volumetric changes after TBI in children. Levin and colleagues (moderate evidence) showed that in children, as in adults, corpus callosum area (measured on subacute MR) correlated with functional outcome. They found that the size of the corpus callosum

decreased after severe TBI in contrast to mild/moderately injured children who showed growth of the corpus callosum on follow-up studies [112]. Wilde and colleagues studied 16 children with DAI and 16 individually matched uninjured children (limited evidence) [113], using morphologic measurements on MRI. Analysis demonstrated significant volume loss in the hippocampus, amygdala, and globus pallidus in the TBI group. They also found that a significant group difference was found in cerebellar white matter volume with children in the TBI group (limited evidence) [114].

What Is the Role of Advanced Imaging (Functional MRI, MR Spectroscopy, Diffusion Imaging, SPECT, and PET) in TBI?

Summary

There is moderate evidence that MR spectroscopic changes can help predict outcome after TBI. SPECT hypoperfusion abnormalities may be an indicator of a worse outcome in children (moderate evidence). Brain PET metabolic abnormalities may also predict outcome (limited to moderate evidence). Data about functional MRI (fMRI), MR perfusion, and DTI are limited. Large studies are required with these advanced imaging modalities to determine the role and outcome after TBI.

Supporting Evidence

Table 22.1 describes briefly the current imaging methods of TBI including principle, advantages/limitations, and use.

DWI has also recently been shown to improve the detection of nonhemorrhagic shearing lesions, although there are only a few small studies describing sensitivity. A small study (insufficient evidence) of patients scanned within 48 h found that DWI identified an additional 16 % of shearing lesions that were not seen on conventional MRI. The majority of DWI-positive lesions (65 %) had decreased diffusion [42]. Another descriptive study (limited evidence) characterized several different types and patterns of DWI lesions,

although there was no comparison with other MRI sequences or analysis of diffusion changes over time [43]. Schaefer and colleagues studied 26 patients (age range 4–72 years) with closed head injury (limited evidence) [115]. This study demonstrated strongest correlation between signal-intensity abnormality volume on DWI and modified Rankin score ($r = 0.772$, $p < 0.001$). Total lesion number also correlated well with the modified Rankin score [115].

A few investigators have studied the role of *DTI*. Wozniak and colleagues studied 14 children with TBI and 14 controls aged 10–18 years who had DTI studies and neurocognitive evaluations at 6–12 months [116]. The TBI group had lower fractional anisotropy (FA) in three white matter regions: inferior frontal, superior frontal, and supracallosal (limited evidence). Supracallosal FA correlated with motor speed and behavior ratings. Parent-reported executive deficits were inversely correlated with FA. Levin and colleagues studied the use of DTI in 32 children with moderate to severe TBI, compared to 36 children with orthopedic injury (OI). They found that fractional anisotropy and ADC values differentiated the groups and that both cognitive and functional outcome measures were related to the DTI findings. Dissociations were present wherein the relation of fractional anisotropy to cognitive performance differed between the TBI and OI groups. A DTI composite measure of white matter integrity was related to global outcome in the children with TBI (moderate evidence) [117].

Magnetic resonance spectroscopy (*MRS*) can detect subtle cellular abnormalities that may more accurately estimate the extent of brain injury, particularly DAI, compared to conventional MRI. Investigators have compared MRS findings from noncontused brain with various measures of clinical neurological outcome such as GOS or DRS scores and found a general trend of reduced NAA corresponding to poor outcome (limited evidence) [118–121]. However, results are difficult to compare since varied anatomical areas were studied, and results were often acquired over a wide range of times after injury. It is uncertain whether the timing of MRS measurement affects outcome prediction. Subacute

MRS studies have suggested that decreased NAA correlates with poor outcomes. There have been few acute MRS studies evaluating outcome prediction. In a prospective MRS study [122] of 42 severely injured adults (limited to moderate evidence), Shutter and colleagues measured quantitative metabolite changes as soon as possible (mean of 7 days) after injury, in normal appearing GM and WM. In contrast to other studies, they found no correlation between NAA-derived metabolites and outcomes at 6–12 months, possibly because their MRS studies were performed earlier than others. However, glutamine/glutamate (Glx) and Cho were significantly elevated in occipital GM and parietal WM in patients with poor 6–12-month outcomes, and these two variables predicted outcome at 6–12 months with 89 % accuracy. A combination of Glx and Cho ratios with the motor component of the GCS score provided the highest predictive accuracy (97 %). It may be that elevated Glx and Cho are more sensitive indicators of injury and predictors of poor outcome when spectroscopy is obtained early after injury. This may be a reflection of early excitotoxic injury (i.e., elevated Glx) and of injury associated with membrane disruption secondary to DAI (i.e., increased Cho). An example of spectra from parietal and occipital GM in a TBI patient with poor outcome is shown in case study 2.

There have been few published results comparing data from multivoxel MR spectroscopy (MRSI) to clinical outcomes. Holshouser and colleagues studied MRSI (limited to moderate evidence) in 42 patients with severe TBI, obtained through the corpus callosum and surrounding GM and WM. MRSI showed significant decreases in NAA/Cre and increases in Cho/Cre ratios in areas of visibly injured and normal-appearing brain. Averaged ratios from all regions were able to differentiate between patients with mild, moderate, and severe/vegetative neurological outcomes as measured with the GOS at 6 months compared to control values. The results suggest that decreased NAA-derived ratios and increased Cho/Cre ratios, detected by MRSI, are associated with worse outcomes [123].

There are a few MRS studies in children. Makaroff and colleagues studied 11 children with TBI (limited evidence) [124]. Four children demonstrated elevated lactate and diminished NAA within several regions, indicating global ischemic injury. All four children had seizures, abnormal neurological examination, and required admission to the PICU. In four other children, lactate was detected at least in one region, indicating a focal ischemic injury. Two children had seizures and two had abnormal neurological examination. The remaining three children had no evidence of elevated lactate. Clinically, no seizures were demonstrated and no PICU admission was required. Holshouser and colleagues performed MRS in 40 children with TBI 1–16 days after injury (moderate evidence) [125]. Neurological outcome was evaluated at 6–12 months after TBI. A logistic regression model demonstrated a significant decrease in the NAA/creatine and increase in the choline/creatine ratios in normal-appearing ($p < 0.05$) and visibly injured brain ($p < 0.001$). In normal-appearing brain, NAA/creatine decreased more in patients with poor outcomes (1.32 ± -0.54) than in those with good outcomes (1.61 ± -0.50). Babikian and colleagues studied 20 children and adolescents and demonstrated a moderate to strong correlation between decreased NAA and worse cognitive scores (limited evidence) [126]. Ashwal and colleagues in 38 children with TBI demonstrated that the occipital glutamate/glutamine in the short-echo MRS was significantly increased in TBI when compared with controls (limited evidence) [127]. No difference was seen in this ratio between children with good versus poor outcome. They also demonstrated that occipital gray matter myoinositol was increased in these children with TBI (4.30 ± 0.73) compared with controls (3.53 ± 0.48; $p = 0.003$). In addition, those with poor outcomes 6–12 months after injury had higher myoinositol levels (4.78 ± 0.68) than those with good outcomes (4.15 ± 0.69; $p = 0.05$) (moderate evidence) [128] indicating that myoinositol elevation after pediatric TBI is associated with a poor neurological outcome. The reasons for the increased myoinositol may be due to astrogliosis or a disturbance in osmotic function.

In this same group of children, Ashwal and colleagues (moderate evidence) also demonstrated significant decreases in NAA-derived ratios and elevation of Cho/Cre measured in occipital GM within 13 days of neurological insult. These metabolite changes correlated with poor neurological outcome at 6–12 months after injury ($n = 52$) [129]. In a subgroup of these patients ($n = 24$), neuropsychological evaluations were performed at 3–5 years after neurological insult. It was found that these metabolite changes strongly correlated with below-average functioning in multiple areas including full-scale IQ, memory, sensorimotor, and attention/executive functioning [130].

Single photon emission computed tomography can measure regional cerebral blood flow (CBF) and assess localized perfusion deficits that may correlate with cognitive deficits even in the absence of structural abnormalities. However, SPECT has low spatial and temporal resolution and does not permit imaging of transient cognitive events and interpretation is often highly subjective. In addition, results of studies vary, possibly related to the severity of injury or timing of studies. SPECT studies generally show patchy perfusion deficits, often in areas with no visible injury on CT. One of the largest studies, although retrospective, was performed by Abdel-Dayem and colleagues (moderate evidence) who reviewed SPECT findings in 228 subjects with mild or moderate TBI. They found focal areas of hypoperfusion in 77 % of patients. However, there was no comparison to CT or MRI [131]. Stamatakis and colleagues (moderate evidence) studied 61 patients with SPECT and MRI, within 2–18 days after injury, and found that SPECT detected more extensive abnormality than MRI in acute and follow-up studies [132]. A small study (limited evidence) of patients with persistent post-concussion syndrome after mild TBI found that SPECT showed abnormalities in 53 % of patients, whereas MRI and CT only showed abnormalities in 9 % and 5 %, respectively [133]. A more recent study by Gowda and colleagues [134] studied 28 children and 64 adults with SPECT using technetium Tc99m ethyl cysteinate dimer within 72 h of the traumatic brain injury. The most common abnormality was hypoperfusion of the temporal lobe in children and the frontal lobe in adults (moderate evidence). A significantly higher number of perfusion abnormalities were seen in patients with post-traumatic amnesia ($p = 0.03$), loss of consciousness ($p = 0.02$), and post-concussion syndrome ($p = 0.01$) than in patients without these symptoms. CT findings were abnormal in 31 (34 %) versus SPECT in 58 (63 %). Difference between the SPECT and CT detection rate was statistically significant ($p < 0.05$). The largest study with patient outcomes was performed by Jacobs and colleagues (moderate to strong evidence) who prospectively studied 136 patients with mild injury, within 4 weeks of injury. SPECT had a high sensitivity and negative predictive value. A normal scan reliably excluded clinical sequelae of mild injury [135]. A small study (limited evidence) of patients with severe TBI and diffuse brain injury showed that total CBF values initially increased above normal in the first 1–3 days and then decreased below normal in the subacute period of 14–42 days. The early CBF increase has been postulated to reflect vasodilatation due to high tissue CO_2 and lactic acidosis. They found that the initial elevation and subsequent drop in blood flow was more marked in the poor-outcome group [136]. However, another small study (limited evidence) of patients with a spectrum of injury, studied within 3 weeks of brain injury, found that focal zones of hyperemia in normal-appearing brain were associated with slightly better outcomes than patients without hyperemia [93]. SPECT findings have also been compared with neuropsychological outcomes, although studies have consisted of small sample sizes, and have found varying results [133, 137].

Positron emission tomography can measure regional glucose and oxygen utilization, CBF at rest, and CBF changes related to performances of different tasks. Spatial and temporal resolution is also limited, although better than SPECT.

However, PET is not widely available. A few PET studies have reported various areas of decreased glucose utilization, even without visible injury. Bergsneider and colleagues (limited to moderate evidence) prospectively studied 56 patients with mild to severe TBI, evaluated with ^{18}F fluorodeoxyglucose (FDG)-PET within 2–39 days of injury, 14 of which had subsequent follow-up studies. They describe in this and previous reports that TBI patients demonstrate a triphasic pattern of glucose metabolism changes that consist of early hyperglycolysis, followed by metabolic depression, and subsequent metabolic recovery (after several weeks). These patients recovered metabolically, with similar patterns of changes in glucose metabolism suggesting that FDG-PET cannot estimate degree of functional recovery [138]. Wu and colleagues [139] performed a study evaluating the gray matter and white matter with PET. Fourteen TBI patients and 19 normal volunteers were studied with a quantitative FDG-PET, a quantitative H_2 ^{15}O-PET, and MRI acutely following TBI. The gray to white matter ratios for both FDG uptake rate and changes of glucose metabolic rate were significantly decreased in TBI patients ($p < 0.001$). The changes of glucose metabolic rate decreased significantly in gray matter ($p < 0.001$) but not in white matter ($p > 0.1$). The glucose to white matter ratios of changes in glucose metabolic rate correlated with the initial Glasgow Coma Scale (GCS) score of TBI patients, with $r = 0.64$. The patients with higher changes of glucose metabolic rate (>1.54) showed good recovery a year after TBI. A more recent study by Lupi and colleagues evaluated PET in 58 consecutive patients (age range 14–69 years) with brain injury (44 with TBI) and demonstrated relative hypermetabolic cerebellar vermis as a common finding in an injured brain regardless of the nature of the trauma [140].

There are few small studies evaluating sensitivity of *xenon CT* and even fewer describing the sensitivity of fMRI or MR perfusion. Newsome and colleagues studied eight children with moderate to severe TBI and eight matched, uninjured control children with fMRI using an N-back task to test effects of TBI on working memory performance and brain activation (limited evidence) [141]. Two patterns in TBI patients were seen. Patients whose criterion performance was reached at lower memory loads than control children demonstrated less extensive frontal and extrafrontal brain activation than controls. Patients who performed the same, highest (3-back) memory load as controls demonstrated more frontal and extrafrontal activation than controls. This is a small series and further longitudinal studies are needed.

MR perfusion can also provide a measure of tissue perfusion similar to results found using PET or SPECT methods of CBF determination. However, there have been little data in the literature regarding its use in predicting outcome after TBI. To date, there is one small study (insufficient evidence) that showed that patients who had reduced regional cerebral blood volume in areas of contusions had poorer outcome. A subset of these patients that had reduced regional cerebral blood volume in normal-appearing white matter had significantly poorer outcomes [142]. *fMRI* can provide noninvasive, serial mapping of brain activation, such as with memory tasks. This form of imaging can potentially assess the neurophysiological basis of cognitive impairment, with better spatial and temporal resolution than SPECT or PET. However, it is susceptible to motion artifact and requires extremely cooperative subjects and therefore is more successful in mildly injured than moderate or severely injured patients. There have only been a few small studies (insufficient evidence) attempting to correlate fMRI with outcomes [143, 144].

Take-Home Tables and Figure

Table 22.1 lists current imaging methods for TBI. Table 22.2 shows suggested guidelines for acute neuroimaging in children with severe TBI. Table 22.3 shows suggested guidelines for acute neuroimaging in children with mild TBI. Table 22.4 shows a list of possible types of head injuries, excluding penetrating or

Table 22.1 Current imaging methods of traumatic brain injury (TBI)

Modality	Principle and advantages/limitations	Use in TBI	Potential correlation with outcome
CT	Based on X-rays, measures tissue density; rapid, inexpensive, and widespread	Detects hemorrhage and "surgical lesions"	Short-term outcome – mortality versus survival
Xenon CT perfusion	Inhalation of stable xenon gas which acts as a freely diffusible tracer; requires additional equipment and software that is available only in a few centers	Detects disturbances in CBF due to injury, edema, or infarction	Long-term outcome – global or neuropsychological
MRI	Uses RF pulses in magnetic field to distinguish tissues, employs many different techniques; currently has highest spatial resolution; complex and expensive	Detection of various injuries and sensitivity varies with different techniques	Long-term outcome – global or neuropsychological
MRI – FLAIR	Suppresses CSF signal	Detection of edematous lesions, particularly near ventricles and cortex, as well as extra-axial blood	Long-term outcome – global or neuropsychological
MRI – T2* GRE	Accentuates blooming effect, such as blood products	Detection of small parenchymal hemorrhages	Long-term outcome – global or neuropsychological
MRI – DWI	Distinguishes water mobility in tissue	Detection of recent tissue infarction or traumatic cell death	Long-term outcome – global or neuropsychological
MRI – DTI	Based on DWI, maps degree, and direction of major fiber bundles; requires special software	Detects impaired connectivity of white matter tracts, even in normal-appearing tissue	Long-term outcome – global or neuropsychological
MRI – MT	Suppression of "background" brain tissue containing protein-bound H_2O, enhances contrast between water and lipid-containing tissue	May detect microscopic neuronal dysfunction, even in normal-appearing tissue	Long-term outcome – global or neuropsychological
MRI – MRS	Analyzes chemical composition of brain tissue; requires special software	Metabolite patterns indicate neuronal dysfunction or axonal injury, even in normal-appearing tissue	Long-term outcome – global or neuropsychological
MR volumetry	Measures volumes of various brain structures or regions, time-consuming, requires special software	Detects atrophy of injured tissue and can quantitate progression over time	Long-term outcome – global or neuropsychological
fMRI	Measures small changes in blood flow related to brain activation; requires cooperative patients	Detects impairment or redistribution of areas of brain activation	Long-term outcome – neuropsychological
MR perfusion (global, non-fMRI)	Measures tissue perfusion using contrast or noncontrast methods; better temporal resolution than PET, SPECT; not as well studied	Detects disturbances in CBF due to injury, edema, or infarction	Long-term outcome – global or neuropsychological
SPECT	Photon emitting radioisotopes used to measure CBF	Detects disturbances in CBF due to injury, edema, or infarction	Long-term outcome – global or neuropsychological

(*continued*)

Table 22.1 (continued)

Modality	Principle and advantages/limitations	Use in TBI	Potential correlation with outcome
PET	Positron emitting radioisotopes act as freely diffusible tracers, used to measure CBF, metabolic rate (glucose metabolism or oxygen consumption), or response to cognitive tasks; available only in a few centers	Detects disturbances in CBF due to injury, edema, or infarction	Long-term outcome – global or neuropsychological

Reprinted with kind permission of Springer Science+Business Media from Tong KA, Oyoyo U, Holshouser BA, Ashwal S. Neuroimaging for traumatic brain injury. In: Medina LS, Blackmore CC, editors. Evidence-based imaging: optimizing imaging in patient care. New York: Springer; 2006

CT computed tomography, *MRI* magnetic resonance imaging, *FLAIR* fluid attenuated inversion recovery, *GRE* gradient recalled echo, *DWI* diffusion-weighted imaging, *DTI* diffusion tensor imaging, *MT* magnetization transfer, *MRS* magnetic resonance spectroscopy, *fMRI* functional magnetic resonance imaging, *SPECT* single photon emission computed tomography, *PET* positron emission tomography, and *CBF* cerebral blood flow

Table 22.2 The children's head injury algorithm for the prediction of important clinical events (CHALICE) rule

A computed tomography scan is required if *any* of the following criteria are present
History
Witnessed loss of consciousness of >5 min duration
History of amnesia (either antegrade or retrograde) of >5 min duration
Abnormal drowsiness (defined as drowsiness in excess of that expected by the examining doctor)
≥3 vomits after head injury (a vomit is defined as a single discrete episode of vomiting)
Suspicion of nonaccidental injury (NAI, defined as any suspicion of NAI by the examining doctor)
Seizure after head injury in a patient who has no history of epilepsy
Examination
Glasgow Coma Score (GCS) <14, or GCS <15 if <1 year old
Suspicion of penetrating or depressed skull injury or tense fontanelle
Signs of a basal skull fracture (defined as evidence of blood or cerebrospinal fluid from ear or nose, panda eyes, Battle's sign, hemotympanum, facial crepitus, or serious facial injury)
Positive focal neurology (defined as an focal neurology, including motor, sensory, coordination, or reflex abnormality)
Presence of bruise, swelling, or laceration >5 cm if <1 year old
Mechanism
High-speed road traffic accident either as pedestrian, cyclist, or occupant (defined as accident with speed >40 m/h)
Fall of >3 m in height
High-speed injury from a projectile or an object
If none of the above variables are present, the patient is at low risk of intracranial pathology

Reprinted with permission by BJ Publishing Group LTD from Dunning J, Daly JP, Lomas JP et al. Arch Dis Child. 2006;91:885–891

Table 22.3 Canadian assessment of tomography for childhood head injury: the CATCH rule

CT of the head is required for children with minor head injury[a] if any one of the following findings are present
High risk (need for neurological intervention)
1. Glasgow Coma Scale score <15 at 2 h after injury
2. Suspected open or depressed skull fracture
3. History of worsening headache
4. Irritability on examination
Medium risk (brain injury on CT scan)
1. Any sign of basal skull fracture (e.g., hemotympanum, "raccoon" eyes, otorrhea or rhinorrhea of the cerebrospinal fluid, Battle's sign)
2. Large, boggy hematoma of the scalp
3. Dangerous mechanism of injury (e.g., motor vehicle crash, fall from elevation ≥3 ft or 5 stairs, fall from bicycle with no helmet)

Reprinted with permission from Osmond MH, Klassen TP, Wells GA et al. Can Med Assoc J. 2010;182(4):341–348

CT computed tomography

[a]Minor head injury is defined as injury within the past 24 h associated with witnessed loss of consciousness, definite amnesia, witnessed disorientation, persistent vomiting (more than one episode), or persistent irritability (in a child under 2 years of age) in a patient with a Glasgow Coma Scale score of 13–15

Table 22.4 Types of head injury (excluding penetrating/missile injuries and nonaccidental trauma)

Primary injuries
Peripheral, non-intracranial
Scalp or soft tissue injury
Facial or calvarial fractures
Extra-axial
Extradural or epidural hemorrhage
Subdural hemorrhage
Traumatic subdural effusion or "hygroma"
Subarachnoid hemorrhage
Intraventricular hemorrhage
Parenchymal
Contusion
(a) Hemorrhagic
(b) Nonhemorrhagic
(c) Both
Shearing injury or "diffuse axonal injury"
(a) Hemorrhagic
(b) Nonhemorrhagic
(c) Both
Vascular
Arterial dissection/laceration/occlusion
Dural venous sinus laceration/occlusion
Carotid-cavernous fistula
Secondary injuries
Cerebral edema
Focal infarction
Diffuse hypoxic-ischemic injury
Hydrocephalus
Infection

Reprinted with kind permission of Springer Science+Business Media from Tong KA, Oyoyo U, Holshouser BA, Ashwal S. Neuroimaging for traumatic brain injury. In: Medina LS, Blackmore CC, editors. Evidence-based imaging: optimizing imaging in patient care. New York: Springer; 2006

missile injuries, or nonaccidental trauma. Table 22.5 shows suggested guidelines for acute CT imaging in adult patients with mild TBI, modified from the Canadian Head CT Rule [21], EAST guidelines [2], and the Neurotraumatology Committee of the World Federation of Neurosurgical Societies [32].

Figure 22.1 is an algorithm for children with acute head injury.

Imaging Case Studies

Cases presented below highlight advantages and limitations of the different neuroimaging modalities.

Case 1: Example of MR Imaging for TBI

This case study illustrates imaging findings of DAI in a 10-year-old male struck by a car (Fig. 22.2a–e).

Case 2: Example of MR Spectroscopy

This case study illustrates metabolite changes in single-voxel short echo time proton spectra (TE = 20 ms) from a 28-year-old male admitted to hospital with severe TBI (GCS of 4) following a motor vehicle accident, compared to a normal 27-year-old control subject (Fig. 22.3a–d).

Table 22.5 Suggested guidelines for acute neuroimaging in adult patients with mild TBI (GCS 13–15)

If GCS 13–15, CT recommended if have any one of the following
High risk
GCS remains <15 at 2 h after injury
Suspected open or depressed skull fracture
Any clinical sign of basal skull fracture
Two or more episodes of vomiting
Aged 65 years or older
Medium risk
Possible loss of consciousness
Amnesia for period before impact, of at least 30 min time span
Dangerous mechanism (pedestrian vs. motor vehicle, ejected from motor vehicle, or fall from greater than 3 ft or 5 stairs)
Any transient neurological deficit
Headache and vomiting
If GCS of 15, patient can be discharged home without CT scan if
Low risk
GCS remains 15
No loss of consciousness or amnesia
No neurologic/cognitive abnormalities
No headache, vomiting

Sources: Data from the Canadian Head CT Rule (21), EAST guidelines (2), and the Neurotraumatology Committee of the World Federation of Neurosurgical Societies (32) Reprinted with kind permission of Springer Science+ Business Media from Tong KA, Oyoyo U, Holshouser BA, Ashwal S. Neuroimaging for traumatic brain injury. In: Medina LS, Blackmore CC, editors. Evidence-based imaging: optimizing imaging in patient care. New York: Springer; 2006

CT computed tomography, *TBI* traumatic brain injury, *GCS* Glasgow Coma Scale
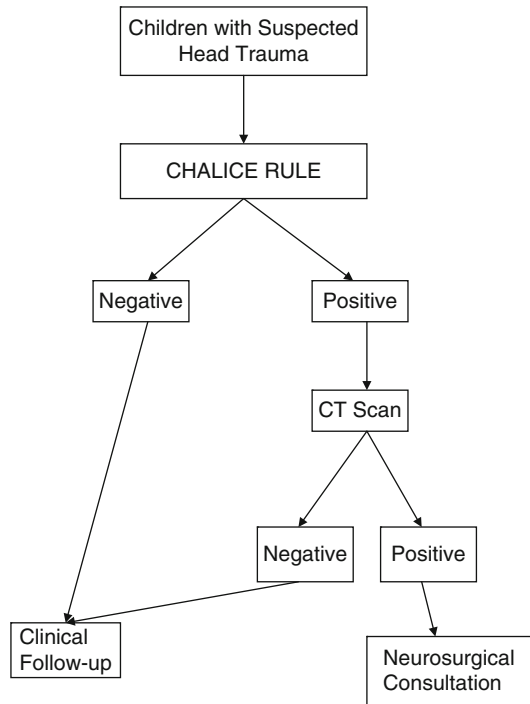

Fig. 22.1 Recommended decision tree for children with acute head injury (Reprinted with kind permission of Springer Science+Business Media from Tong KA, Oyoyo UE, Holshouser BA, Ashwal S, Medina SA. Evidence-based neuroimaging for traumatic brain injury in children. In: Medina LS, Applegate KE, Blackmore CC, editors. Evidence-based imaging in pediatrics: optimizing imaging in pediatric patient care. New York: Springer; 2010)

Suggested Protocols for Acute TBI Imaging

- CT: axial 5-mm images in standard and bone algorithms; viewed with brain, intermediate, and bone windows
- MR: T1-weighted, T2-weighted, FLAIR, T2*-weighted GRE or SWI, DWI

Future Research

- Clinical trials have been disappointing in TBI research, perhaps due to different mechanisms of injury included in trials but also probably due to nonuniformity in classification of injuries and outcomes. There is a need for a consistent, widely accepted classification of information to facilitate comparisons of different groups of patients and institutions. The vast amount of clinical and imaging data can yield elaborate approaches, but this must be balanced with practicality in clinical
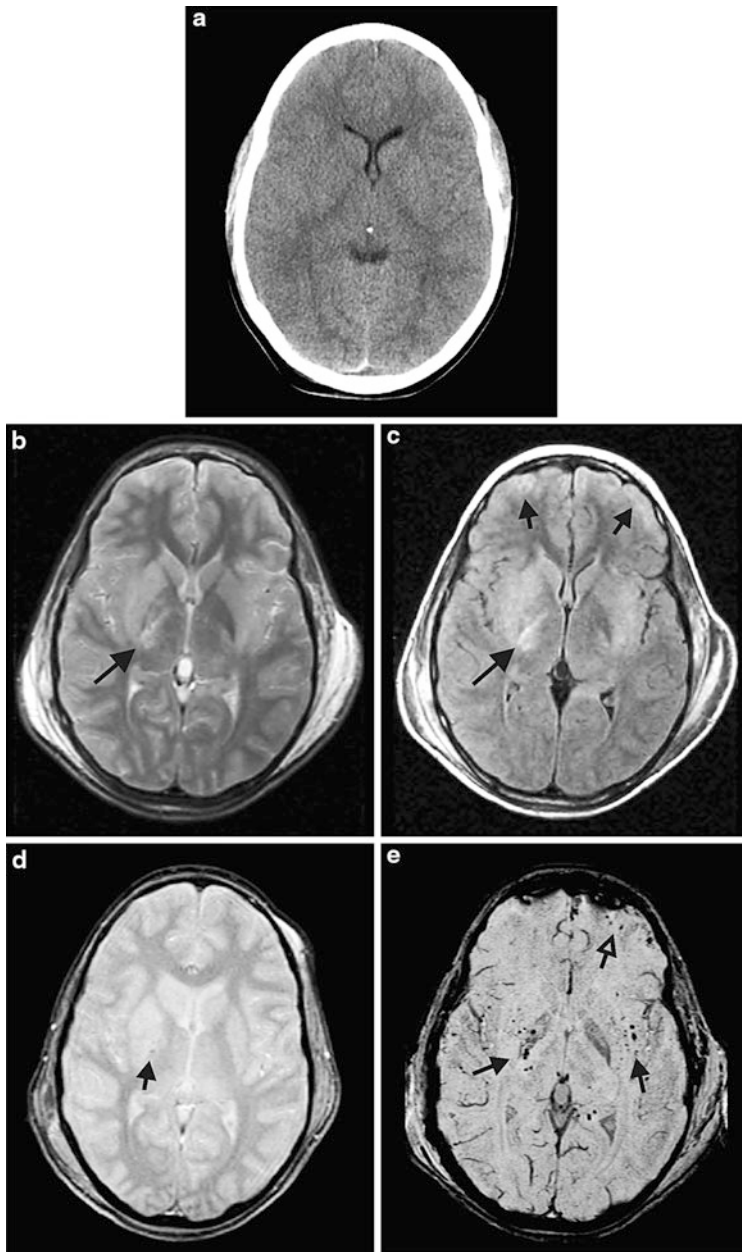
Fig. 22.2 (**a**–**e**) Magnetic resonance imaging findings of diffuse axonal injury (DAI) in a 10-year-old boy who was struck by a car. He had an initial GCS score of 3, was in a coma for 11 days, and had an elevated ICP. (**a**) His admission CT scan was normal. (**b**) An MRI was obtained 2 days after injury. Subtle hyperintense signal is seen in the right basal ganglia and posterior limb of the internal capsule (*arrow*), on the T2-weighted images. (**c**) The FLAIR sequence accentuates the edema in those areas (*long arrow*) as well as along the periphery of the frontal lobes (*short arrows*). (**d**) The standard T2*-GRE sequence shows a subtle punctuate hypointense focus in the right internal capsule (*arrow*). (**e**) The susceptibility-weighted imaging (SWI) technique (a modified T2*-GRE sequence) shows multiple tiny hemorrhagic foci within the bilateral basal ganglia and capsular white matter (*closed arrows*) as well as within the left frontal contusion (*open arrow*) (Reprinted with kind permission of Springer Science+Business Media from Tong KA, Oyoyo U, Holshouser BA, Ashwal S. Neuroimaging for traumatic brain injury. In: Medina LS, Blackmore CC, editors. Evidence-based imaging: optimizing imaging in patient care. New York: Springer; 2006)
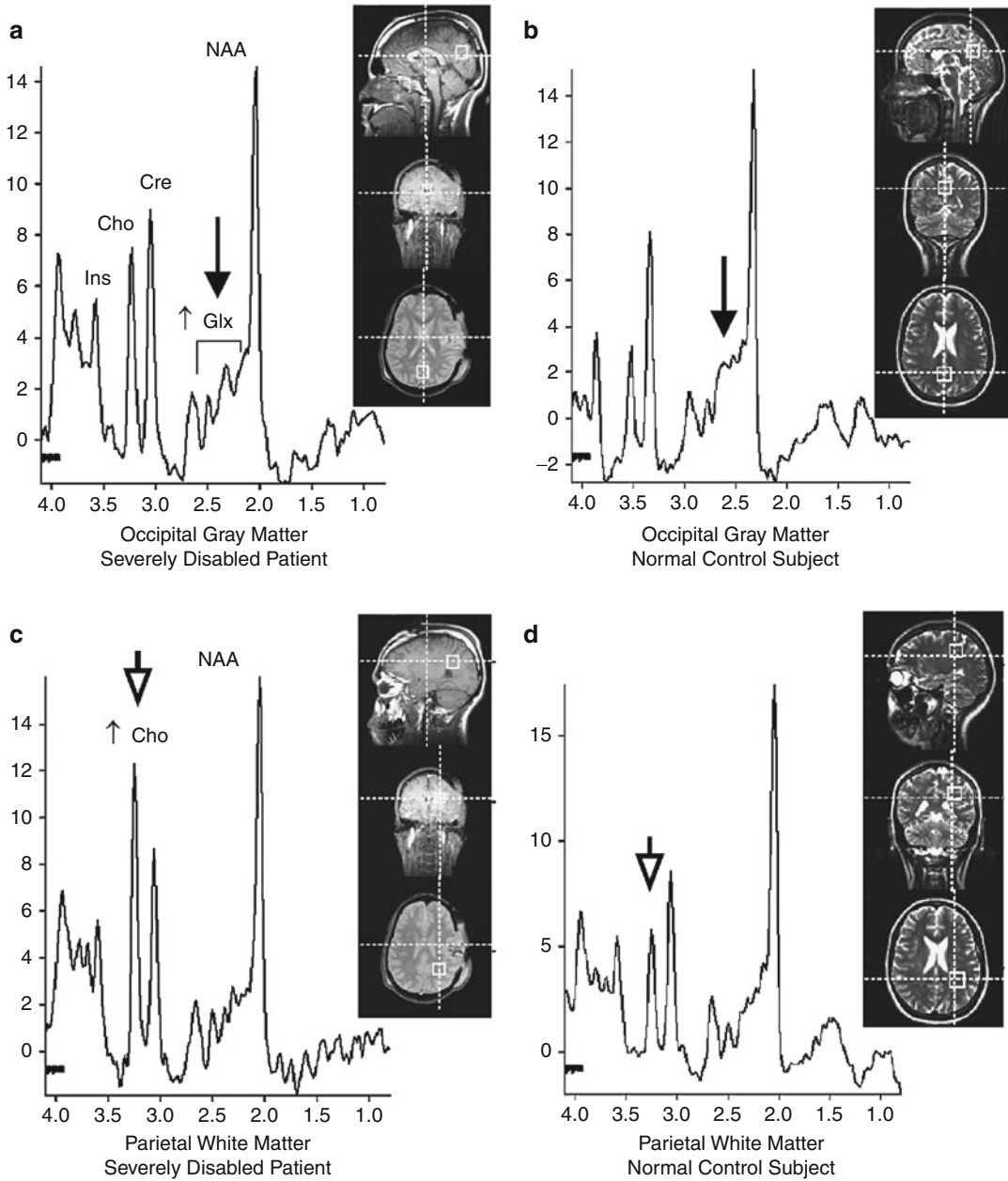
Fig. 22.3 (**a–d**) A 28-year-old man was admitted to the hospital with severe TBI (GCS of 4) following a motor vehicle accident. (**a**) Single-voxel short-echo magnetic resonance spectroscopy taken from occipital gray matter shows increased glutamate/glutamine (Glx) compared to the control spectrum (**b**) (*arrows*). (**c**) Image taken from parietooccipital white matter shows increased choline (Cho, arrowheads) compared to the control spectrum. (**d**) Evaluation at 6 months after the injury revealed severe disabilities (GOS of 3) in this patient (Reprinted with kind permission of Springer Science+Business Media from Tong KA, Oyoyo U, Holshouser BA, Ashwal S. Neuroimaging for traumatic brain injury. In: Medina LS, Blackmore CC, editors. Evidence-based imaging: optimizing imaging in patient care. New York: Springer; 2006)

situation. The system should be simple, relevant, reliable, and acceptable to clinicians in routine practice.

- Promising pediatric head trauma prediction rules need to be validated in actual practice.
- More research is needed, and ultimately a multimodal prognostic index for a wide range of disability probably needs to be developed.
- The link between imaging findings, neuro-behavioral deficits, and outcome requires further research, particularly after mild TBI.
- Larger, prospective studies are needed to evaluate the sensitivity, specificity, predictive accuracy, and cost-effectiveness of various neuroimaging methods in TBI.

References

1. Servadei F, Teasdale G, Merry G (on behalf of the Neurotraumatology Committee of the World Federation of Neurosurgical Societies). J Neurotrauma. 2001;18:657–64.
2. Cushman JG, Agarwal N, Fabian TC, et al. J Trauma. 2001;51:1016–26.
3. Iverson GL, Lovell MR, Smith S, Franzen MD. Brain Inj. 2000;14:1057–61.
4. Jennett B, Bond M. Lancet. 1975;1:480–4.
5. Jennett B, Snoek J, Bond MR, Brooks N. J Neurol Neurosurg Psychiatry. 1981;44:285–93.
6. van der Naalt J, van Zomeren AH, Sluiter WJ, Minderhoud JM. J Neurol Neurosurg Psychiatry. 1999;66:207–13.
7. Rappaport M, Hall KM, Hopkins K, Belleza BS, Cope DN. Arch Phys Med Rehabil. 1982;63:118–23.
8. Schwab K, Grafman J, Salazar AM, Kraft J. Neurology. 1993;43:95–103.
9. Guide for the uniform data set for medical rehabilitation (including the FIM^{TM} instrument), Version 5.1. Buffalo: State University New York; 1997.
10. Boake C. Arch Phys Med Rehabil. 1996;77:765–72.
11. Dikmen S, Machamer J, Miller B, Doctor J, Temkin N. J Neurotrauma. 2001;18:127–40.
12. Temkin NR, Machamer JE, Dikmen SS. J Neurotrauma. 2003;20:229–41.
13. Choi SC, Barnes TY, Bullock R, Germanson TA, Marmarou A, Young HF. J Neurosurg. 1994;81:169–73.
14. Faul M, Xu L, Wald MM, Coronado VG. Traumatic brain injury in the United States: emergency department visits, hospitalizations and deaths 2002–2006. Atlanta: Centers for Disease Control and Prevention, National Center for Injury Prevention and Control; 2010.
15. Centers for Disease Control and Prevention, National Center for Injury Prevention and Control. Report to congress on mild traumatic brain injury in the United States: steps to prevent a serious public health problem. Atlanta: CDC, National Center for Injury Prevention and Control; 2003.
16. Lu J, Marmarou A, Choi S, et al. Acta Neurochir. 2005;95(suppl):281–5.
17. Adekoya N, Thurman DJ, White DD, Webb KW. MMWR Surveill Summ. 2002;51(SS10):1–16.
18. Agency for Healthcare Research and Quality, Evidence report: number 2; rehabilitation for traumatic brain injury; 1999.
19. Finkelstein E, Corso P, Miller T, et al. The incidence and economic burden of injuries in the United States. New York: Oxford University Press; 2006.
20. Fiser SM, Johnson SB, Fortune JB. Am Surg. 1998;64:1088–93.
21. Stiell IG, Wells FA, Vandemheen K, Clement C, Lesiuk H, et al. Lancet. 2001;357:1391–6.
22. Haydel MJ, Preston CA, Mills TJ, et al. N Engl J Med. 2000;343:100–5.
23. Madden C, Witzkc DB, Sanders AB, Valente J, Fritz M. Acad Emerg Med. 1995;2:248–53.
24. Brain Trauma Foundation, American Association of Neurological Surgeons. Part I: guidelines for the management of severe traumatic brain injury. New York: Brain Trauma Foundation; 2000.
25. Brain Trauma Foundation, American Association of Neurological Surgeons. Part II: Early indicators of prognosis in severe traumatic brain injury. New York: Brain Trauma Foundation; 2000.
26. Eng J, Chanmugam A. Neuroimaging Clin N Am. 2003;13:273–82.
27. Mack LR, Chan SB, Silva JC, Hogan TM. J Emerg Med. 2003;24:157–62.
28. McAllister TW, Sparling MB, Flashman LA, Saykin AJ. J Clin Exp Neuropsychol. 2001;23:775–91.
29. Fearnside M, McDougall P. Aust N Z J Surg. 1998;68:58–64.
30. The Brain Trauma Foundation, The American Association of Neurological Surgeons, The Joint Section on Neurotrauma and Critical Care. J Neurotrauma. 2000;17:597–627.
31. Oertel M, Kelly DF, McArthur D, et al. J Neurosurg. 2002;96:109–16.
32. Servadei F, Murray GD, Penny K, et al. European brain injury consortium. Neurosurgery. 2000;46:70–5.
33. Orrison WW, Gentry LR, Stimac GK, Tarrell RM, Espinosa MC, Cobb LC. AJNR Am J Neuroradiol. 1994;15:351–6.
34. Ogawa T, Sekino H, Uzura M et al. Acta Neurochir. 1992;55:8–10.
35. Hadley DM, Teasdale GM, Jenkins A, et al. Clin Radiol. 1988;39:131–9.
36. Gentry LR, Godersky JC, Thompson B, Dunn VD. AJR Am J Roentgenol. 1988;150:673–82.
37. Mittl Jr RL, Grossman RI, Hiehle JF, et al. AJNR Am J Neuroradiol. 1994;15:1583–9.

38. Gentry LR, Godersky JC, Thompson B. AJR Am J Roentgenol. 1988;150:663–72.
39. Scheid R, Preul C, Gruber O, Wiggins C, von Cramon DY. AJNR Am J Neuroradiol. 2003;24:1049–56.
40. Tong K, Ashwal S, Holshouser B, et al. Radiology. 2003;227:332–9.
41. Ashikaga R, Araki Y, Ishida O. Neuroradiology. 1997;39:239–42.
42. Huisman TAGM, Sorensen AG. J Comput Assist Tomogr. 2003;27:5–11.
43. Hergan K, Schaefer PW, Sorensen AG, Gonzalez RG, Huisman TAGM. Eur Radiol. 2002;12:2536–41.
44. Shanmuganathan K, Gullapalli RP, Mirvis SE, Roys S, Murthy P. AJNR Am J Neuroradiol. 2004;25:539–44.
45. Ptak T, Sheridan RL, Rhea JT, et al. AJR Am J Roentgenol. 2003;181:1401–7.
46. Arfenakis K, Haughton VM, Carew JD, et al. AJNR Am J Neuroradiol. 2002;23:794–802.
47. Jones DK, Dardis R, Ervine M, et al. Neurosurgery. 2000;47:306–14.
48. Marshall LF, Marshall SB, Klauber M, et al. J Neurotrauma. 1992;9(suppl 1):287–92.
49. Vos PE, van Voskuilen AC, Beems T, Krabbe PF, Vogels OJ. J Neurotrauma. 2001;18:649–55.
50. Wardlaw JM, Easton VJ, Statham P. J Neurol Neurosurg Psychiatry. 2002;72:188–92.
51. Ono J, Yamaura A, Kubota M, Okimura Y, Isobe K. J Clin Neurosci. 2001;8:120–3.
52. Firsching R, Woischneck D, Klein S, Reissberg S, Dohring W, Peters B. Acta Neurochir. 2001;143:263–71.
53. Maas AIR, Hukkelhoven CWPM, Marshall LF, Steyerberg EW. Neurosurgery. 2005;57:1173–82.
54. Mataro M, Poca MA, Sahuquillo J, et al. J Neurotrauma. 2001;18:869–79.
55. Lang DA, Teasdale GM, Macpherson P, Lawrence A. J Neurosurg. 1994;80:675–80.
56. Levin HS, Gary HEJ, Eisenberg HM, et al. J Neurosurg. 1990;73:699–709.
57. Englander J, Cifu DX, Wright JM, Black K. Arch Phys Med Rehabil. 2003;84:214–20.
58. Servadei F, Murray GD, Teasdale GM, et al. Neurosurgery. 2002;50:261–7.
59. Caroli M, Locatelli M, Campanella R, Balbi S, Martinelli F, Arienta C. Surg Neurol. 2001;56:82–8.
60. LeRoux PD, Haglund MM, Newell DW, Grady MS, Winn HR. Neurosurgery. 1992;31:678–84.
61. Kido DK, Cox C, Hamill RW, Rothenberg BM, Woolf PD. Radiology. 1992;182:777–81.
62. Godersky JC, Gentry LR, Tranel D, Dyste GN, Danks KR. Acta Neurochir Suppl. 1990;51:311–4.
63. Kampfl A, Schmutzhard E, Franz G, et al. Lancet. 1998;351:1763–7.
64. Wilson JTL, Hadley DM, Wiedmann KD, Teasdale GM. J Neurol Neurosurg Psychiatry. 1995;59:328–31.
65. Tomei G, Sganzerla E, Spagnoli D, et al. J Neurosurg Sci. 1991;35:61–75.
66. Cordobes F, Lobato RD, Rivas JJ, et al. Acta Neurochir. 1986;81:27–35.
67. Wang HD, Duan GS, Zhang J, Zhou DB. Chin Med J. 1998;111:59–62.
68. Parizel PM, Ozsarlak O, Van Goethem JW, et al. Eur Radiol. 1998;8:960–5.
69. Wallesch C-W, Curio N, Kutz S, Jost S, Bartels C, Synowitz H. Brain Inj. 2001;15:401–12.
70. Kampfl A, Franz G, Aichner F, et al. J Neurosurg. 1998;88:809–16.
71. Paterakis K, Karantanas H, Komnos A, Volikas Z. J Trauma. 2000;49:1071–5.
72. Yanagawa Y, Tsushima Y, Tokumaru A, et al. J Trauma. 2000;49:272–7.
73. Kurth SM, Bigler ED, Blatter DD. Brain Inj. 1994;8:489–500.
74. Fearnside MR, Cook RJ, McDougall P, McNeil RJ. Br J Neurosurg. 1993;7:267–79.
75. Lannoo E, Van Rietvelde F, Colardyn F, et al. J Neurotrauma. 2000;17:403–14.
76. Blatter DD, Bigler ED, Gale SD, et al. AJNR Am J Neuroradiol. 1997;18:1–10.
77. Groswasser Z, Reider-Groswasser II, Schwab K, et al. Brain Inj. 2002;16:681–90.
78. Bigler ED, Blatter DD, Anderson CV, et al. AJNR Am J Neuroradiol. 1997;18:11–23.
79. Ratanalert S, Chompikul J, Hirunpat S, Pheunpathom N. Br J Neurosurg. 2002;16:487–93.
80. Schaan M, Jaksche H, Boszczyk B. J Trauma. 2002;52:667–74.
81. Prasad MR, Ewing-Cobbs L, Swank PR, Kramer L. Pediatr Neurosurg. 2002;36:64–74.
82. Pillai S, Praharaj SS, Mohanty A, Sastry Kolluri VR. Pediatr Neurosurg. 2001;34:98–103.
83. Sganzerla EP, Tomei G, Guerra P, et al. Childs Nerv Syst. 1989;5:168–71.
84. Suresh HS, Praharaj SS, Indira Devi B, Shukla D, Sastry Kolluri VR. Neurol India. 2003;51:16–8.
85. Raimondi AJ, Hirschauer J. Childs Brain. 1984;11:12–35.
86. Crouchman M, Rossiter L, Colaco T, Forsyth R. Arch Dis Child. 2001;84:120–4.
87. Fiser DH. J Pediatr. 1992;121:69–74.
88. Dunning J, Daly JP, Lomas JP, et al. Arch Dis Child. 2006;91:885–91.
89. Kuppermann N, Holmes JF, Dayan PS, et al. Lancet. 2009;374:1160–70.
90. Osmond MH, Klassen TP, Wells GA, et al. Can Med Assoc J. 2010;182(4):341–8.
91. Oman JA, Cooper RJ, et al. Pediatrics. 2006;117(2):e238–46.
92. Palchak M, Holmes J, Vance C, et al. Ann Emerg Med. 2003;42(4):492–506.
93. Palchak MJ, Holmes JF, et al. Pediatr Emerg Care. 2009;25(2):61–5.
94. Greenes DS, Schutzman SA. Pediatrics. 1999;104:861–7.
95. Haydel MJ, Shembekar AD. Ann Emerg Med. 2003;42:507–14.

96. Dunning J, Daly JP, Malhotra R, et al. Arch Dis Child. 2004;89:763–7.
97. Boran B, Boran P, Barut N. Pediatr Neurosurg. 2006;42:203–7.
98. Lloyd DA, Carty H, Patterson M, et al. Lancet. 1997;349:821–4.
99. Hollingworth W, Vavilala MS, et al. Pediatr Crit Care Med. 2007;8(4):348–56.
100. Figg RE, Stouffer CW, Vander Kolk WE, Connors RH. Pediatr Surg Int. 2006;22:215–8.
101. Tabori U, Kornecki A, et al. Crit Care Med. 2000;28(3):840–4.
102. Levin HS, Aldrich EF, Saydjari C, et al. Neurosurgery. 1992;31:435–43.
103. Hirsch W, Schobess A, Eichler G, Zumkeller W, Teichler H, Schluter A. Paediatr Anaesth. 2002;12:337–44.
104. Tomberg T, Rink U, Pikkoja E, Tikk A. Acta Neurochir. 1996;138:543–8.
105. Bonnier C, Marique P, Van Hout A, et al. J Child Neurol. 2007;22:519–29.
106. Sigmund GA, Tong KA, Nickerson JP, et al. Pediatr Neurol. 2007;36:217–26.
107. Levin HS, Mendelsohn D, Lilly MA, et al. Neurosurgery. 1997;40:432–40.
108. Grados MA, Slomine BS, Gerring JP, Vasa R, Bryan N, Denckla MB. J Neurol Neurosurg Psychiatry. 2001;70:350–8.
109. Blackman JA, Rice SA, Matsumoto JA, et al. J Head Trauma Rehabil. 2003;18:493–503.
110. Tong K, Ashwal S, Holshouser BA, et al. Ann Neurol. 2004;56:36–50.
111. Babikian T, Freier MC, Tong K, et al. Pediatr Neurol. 2005;33:184–94.
112. Levin HS, Benavidez DA, Verger-Maestre K, et al. Neurology. 2000;54:647–53.
113. Wilde EA, Bigler ED, Haider JM, et al. J Child Neurol. 2006;21:769–76.
114. Spanos GK, Wilde EA, Bigler ED, et al. AJNR Am J Neuroradiol. 2007;28:537–42.
115. Schaefer P, Huisman T, Thierry AGM, et al. Radiology. 2004;233:58–66.
116. Wozniak JR, Krach L, Ward E. Arch Clin Neuropsychol. 2007;22(5):555–68.
117. Levin HS, Wilde EA, Chu Z, et al. J Head Trauma Rehabil. 2008;23(4):197–208.
118. Ross BD, Ernst T, Kreis R, et al. J Magn Reson Imaging. 1998;8:829–40.
119. Cecil KM, Lenkinski RE, Meaney DF, McIntosh TK, Smith DH. J Neurochem. 1998;70:2038–44.
120. Sinson G, Bagley LJ, Cecil KM, Grossman RI, et al. AJNR Am J Neuroradiol. 2001;22:143–51.
121. Garnett MR, Blamire AM, Corkill RG, et al. Brain. 2000;123:2046–54.
122. Shutter L, Tong KA, Holshouser BA. J Neurotrauma. 2004;21:1693–705.
123. Holshouser BA, Tong KA, Ashwal S, et al. J Magn Reson Imaging. 2006;24:33–40.
124. Makaroff KL, Cecil KM, Care M, et al. Pediatr Radiol. 2005;35:668–76.
125. Holshouser BA, Tong K, Ashwal S, et al. AJNR Am J Neuroradiol. 2005;26:1276–85.
126. Babikian T, Freier MC, Ashwal S. J Magn Reson Imaging. 2006;24:801–11.
127. Ashwal S, Holshouser B, Tong K, et al. J Neurotrauma. 2004;21:1539–52.
128. Ashwal S, Holshouser BA, Tong K, et al. Pediatr Res. 2004;56:630–8.
129. Ashwal S, Holshouser BA, Shu SK, et al. Pediatr Neurol. 2000;23:114–25.
130. Brenner T, Freier MC, Holshouser BA, Burley T, Ashwal S. Pediatr Neurol. 2003;28:104–14.
131. Abdel-Dayem HM, Abu-Judeh H, Kumar M, et al. Clin Nucl Med. 1998;23:309–17.
132. Stamatakis EA, Wilson JT, Hadley DM, Wyper DJ. J Nucl Med. 2002;43:476–83.
133. Kant R, Smith-Seemiller L, Isaac G, Duffy J. Brain Inj. 1997;11:115–24.
134. Gowda NK, Agrawal D, Bal C, et al. AJNR Am J Neuroradiol. 2006;27:447–51.
135. Jacobs A, Put E, Ingels M, Put T, Bossuyt A. J Nucl Med. 1996;37:1605–9.
136. Shiina G, Onuma T, Kameyama M, et al. AJNR Am J Neuroradiol. 1998;19:297–302.
137. Kesler SR, Adams HF, Bigler ED. Brain Inj. 2000;14:851–7.
138. Bergsneider M, Hovda DA, McArthur D, et al. J Head Trauma Rehabil. 2001;16:135–48.
139. Wu HM, Huang SC, Hattori N. J Neurotrauma. 2004;21:149–61.
140. Lupi A, Bertagnoni G, Salgarello M. Clin Nucl Med. 2007;32:445–51.
141. Newsome MR, Scheibal RS, Hunter J, et al. Neurocase. 2007;13:16–24.
142. Garnett MR, Blamire AM, Corkill RG, et al. J Neurotrauma. 2001;18:585–93.
143. Christodoulou C, DeLuca J, Ricker JH, et al. Neurology. 2003;60:1793–8.
144. McAllister TW, Saykin AJ, Flashman LA, et al. Neurology. 1999;53:1300–8.

Nonaccidental Head Injury: Evidence-Based Neuroimaging

23

Yutaka Sato and Toshio Moritani

Contents

Y. Sato (✉) • T. Moritani
Department of Radiology, University of Iowa Hospitals and Clinics, Iowa City, IA, USA
e-mail: yutako-sato@uiowa.edu; toshio-moritani@uiowa.edu

Key Points

- Head injury is the most common cause of death from nonaccidental trauma, and the majority of NAHI occurs in infants under age 1 year; its clinical presentation is nonspecific (moderate evidence).
- NAHI is suspected when the magnitude of the injury demonstrated clinically or on neuroimaging is discrepant with the history provided (moderate evidence).
- Subdural hematoma is the most commonly associated pathology with NAHI (moderate evidence).
- None of the intracranial pathology is specific or pathognomonic for NAHI.
- Temporal evolution of subdural hematoma associated with NAHI is dynamic and complex. For the best estimation of injury timing, comparison of CT and MRI and correlation with follow-up studies are often needed.
- CT is the standard of care for the initial evaluation of NAHI. CT readily demonstrates intracranial pathology requiring immediate treatment (moderate evidence).
- MRI should be performed once the patient is stabilized. Overall, MRI is more sensitive than CT for diagnosis, documentation, characterization, and prognostication of intracranial pathology associated with NAHI (limited evidence).

Definition and Pathophysiology

Nonaccidental head injury (NAHI), the shaking impact syndrome, is most commonly seen among children under 3 years of age, with the majority occurring during the first year [1, 2]. Because of anatomic and developmental differences in the brain and skull of young children, the mechanisms and types of brain injury are distinctly different from that seen in older children and adults [3–5].

Rotational acceleration is considered as the primary mechanism of diffuse, severe, and often life-threatening brain injury, including diffuse axonal injury (DAI) with disruption of axons and tearing of bridging veins, which causes subdural hematoma (SDH) and/or subarachnoid hemorrhage (SAH) and is often associated with retinal hemorrhage.

Impact loading causes focal strains at the site of impact, deforming the skull and generating the pressure waves in the brain. At the site of impact, scalp hematoma, skull fracture, focal SDH/SAH, and cortical contusion may occur. Impact injuries, except epidural hematoma, are usually not life threatening.

The term "shaken-baby" syndrome was coined by Caffey to explain a constellation of clinical findings of severe NAHI of infants with retinal hemorrhage, SDH/SAH, and little or no external cranial trauma [6, 7]. Repetitive, "pure" rotational acceleration of the head on the weak infant's neck was considered as a mechanism of injury. There has been controversy over whether "shaking" alone can cause fatal brain injury; some consider that violent shaking alone causes serious or fatal injuries, but many instances of "shaken-baby" syndrome demonstrate clinical, radiological, and/or autopsy evidence of blunt impact to the cranium [8, 9]. Thus, the term "shaken-impact" syndrome may more accurately reflect the mechanisms of injury observed [2].

The infant skull is easily deformable because it consists of thin calvarial bones separated by soft membranous sutures and fontanelles. Also, the partially myelinated infant's brain is more deformable. Recent investigation based on biomechanical analysis emphasizes the more significant role of deformation-mediated impact response rather than impact-induced rotational acceleration force as the critical injurious mechanism for an infant brain [3].

The focal injury to the craniovertebral junction has recently been proposed as the mechanism of traumatic brain injury unique to young infants. Significant deformation and shearing of the

cervicomedullary junction and surrounding soft tissue occur during violent shaking [10, 11]. Geddes et al. suggested that violent shaking without impact may cause focal axonal injury of the brainstem and upper cervical cord and/or epidural hematoma in the craniovertebral junction, resulting in traumatic apnea. This, in turn, causes secondary global hypoxic brain injury and generalized brain edema [12–14].

Geddes et al. further proposed that SDH can be caused by a combination of severe brain hypoxia, brain swelling, and raised central pressure; however, this hypothesis is not fully accepted [15–17].

Epidemiology

Seven to nineteen percent of physically abused victims suffer from CNS injury in the United States, and approximately 1,500 will die and 18,000 will be left with serious disability every year [18–20]. Most NAHIs occur in infants and toddlers. Nine to fourteen percent of child head injuries are caused by inflicted trauma, and boys are more commonly affected than girls [21, 22]. The incidence of serious or fatal NAHI in children less than 1 year of age is approximately 1 in 3,300 [21]; since many cases of NAHI are mild or moderate in severity, the incidence is probably significantly higher. Head injury is the leading cause of child abuse fatality and accounts for up to 80 % of fatal child abuse injuries at the youngest ages [23]. Accidental HI is uncommon in infancy. Ninety-five percent of serious CNS injuries in infants less than 1 year of age are attributable to abuse [24]. Approximately 80 % of deaths caused by traumatic head injury in infants and children younger than 2 years were the result of NAHI [25]. Among the victims of severe NAHI, evidence of prior child abuse is common [26].

Mortality rate of severe NAHI is approximately 60 %, and morbidity includes mental retardation, cortical blindness, spasticity, seizures, and microcephalus [16, 22].

Overall Cost to Society

The cost of child abuse to society is considerable. According to the report released by *Prevent Child Abuse America* [27] in 2008, the United States spent $103.8 billion annually in response to child abuse, of which $33.1 billion is for the direct (immediate intervention) and $70.7 billion is for the indirect (long-term) costs.

There are no data available on the social cost of imaging for NAHI.

Goals of Imaging

The goals of imaging are as follows:
- Diagnose conditions requiring immediate treatment and intervention.
- Fully document the nature and extent of NAHI.
- Assist in the determination of timing of NAHI.
- Diagnose clinically unsuspected NAHI among victims with extensive evidence of extracranial abuse.

Methodology

A medical search was performed using PubMed (National Library of Medicine, Bethesda, Maryland) for original research publications discussing the clinical diagnosis, imaging, and effectiveness of imaging strategies in NAHI. The search covered the period from 1966 to December 2007. The search strategy employed different combinations of the following terms: (1) child abuse, (2) head injury, (3) brain injury, (4) head trauma, (5) inflicted injury, (6) diagnosis, and (7) therapy or surgery or etiology. Additional articles were identified by reviewing the reference list of relevant publications, identifying appropriate authors, and using the citation indices for MeSH terms. This review was limited to human studies and English-language literature.

The authors performed a critical review of the title and abstracts of the identified articles followed by a review of the full text in articles that were relevant.

Discussion of Issues

What Are the Clinical Findings That Raise Suspicion of NAHI to Direct Further Imaging?

Summary
The clinical presentation of NAHI is nonspecific (moderate evidence). NAHI is suspected when the magnitude of the injuries demonstrated clinically or on neuroimaging is discrepant with the history provided (moderate evidence). Also, NAHI should be suspected when retinal hemorrhage is present (moderate evidence). Low threshold for neuroimaging is recommended when physical abuse is suspected in a young child less than 1 year of age (limited evidence).

Supporting Evidence
The clinical presentation of NAHI is nonspecific and misleading. An accurate history is rarely provided, and the story may change with time (moderate evidence) [28, 29]. An alleged injury mechanism in the history is often incompatible with the nature and magnitude of injury demonstrated by imaging and inconsistent with the developmental physical ability of the victim. The majority of victims are less than 3 years of age [1, 2]. However, rare incidents of "shaken-baby" syndrome have been reported in older children. Salehi-Had et al. reported four fatal cases of older children of age 2.5–7 years who had acute SDH and RH without evidence of impact trauma [30]. Approximately 30–70 % of NAHIs demonstrate simultaneous fractures [19], and 40 % of fatal NAHIs have a previous history or imaging/autopsy evidence of previous head trauma [26, 31].

A victim with a milder case of NAHI may have a history of poor feeding, vomiting, lethargy, and/or irritability of days' or weeks' duration. In a retrospective review of 173 children less than 3 years of age with NAHI, Jenny et al. found that 31 % of victims had been misdiagnosed during previous visit(s) as gastroenteritis, influenza, possible sepsis, and otitis media (moderate evidence) [28].

In more severe cases, a victim becomes immediately symptomatic and clearly identifiable as head trauma with lethargy, seizures, and coma without lucid interval. Respiratory difficulty often progresses to apnea or bradycardia requiring cardiopulmonary resuscitation (moderate evidence). In a retrospective cohort study by Willman et al. [32] of 95 children with fatal accidental HI, all but one of the children had an immediate decreased level of consciousness. One exceptional case with an enlarging epidural hematoma had a "lucid interval." There is no evidence of a prolonged "lucid interval" in children with SDH and brain edema.

Retinal hemorrhage is one of the cardinal features of NAHI (moderate evidence). In 75–90 % of NAHI cases, unilateral or bilateral retinal hemorrhages are present [33]. Numerous preretinal, intraretinal, and subretinal hemorrhages extending out to the edges of the retina and/or the splitting of the retina (retinoschisis) are particularly indicative of shaken-baby syndrome [34]. Retinal hemorrhage is not pathognomonic for NAHI and occasionally is seen in association with other causes including accidental trauma, cardiopulmonary resuscitation, and paroxysmal coughing episode [35]. Johnson et al. [36] reported only 2 cases of RH among 215 children with severe accidental HI. Schloff et al. reported 2 cases of RH among 57 children with intracranial hemorrhage from nonabuse causes [37]. Sezen [38] reported 14 % occurrence of less severe form of RH in normal newborns, which regress to normal rapidly in 4–6 weeks.

Adoption of a lower clinical threshold for performing neuroimaging was recommended when physical abuse is suspected or when

"high-risk" criteria including rib fractures or multiple fractures are present in a young child, particularly when they are less than 1 year of age [39, 40] (limited evidence).

Can Imaging Help to Predict NAHI?

Summary
SDH is the most commonly associated pathology with NAHI (moderate evidence). Other pathologic and imaging findings frequently associated with NAHI include complex skull fractures, diffuse and multifocal SDH, interhemispheric SDH, SDH with mixed density, traumatic diffuse axonal injury, and severe brain swelling. Evidence of previous injuries, such as atrophy and ventricular enlargement, is often seen in addition to the acute findings associated with NAHI described above (moderate evidence). None of the individual pathologic findings are unique or pathognomonic for NAHI, and image findings should be closely correlated with history, clinical findings, physical ability of the victim, and social background.

Supporting Evidence
Many comprehensive neuroradiologic reviews are available and should be used as references [41–46].

Child abuse causes approximately 10 % of skull fractures in the pediatric population in general and 30 % in children less than 2 years of age [47, 48]. Minor domestic accidents rarely cause skull fractures (moderate evidence) [49, 50]. Warrington et al. analyzed 11,466 questionnaires regarding domestic accidents occurring in the first 6 months of life and found the rate of concussion or fracture to be less than 1 %. Falls from beds and seats did not result in skull fractures [51]. Complex skull fractures, such as fractures crossing suture, diastatic fractures, depressed fractures, and comminuted fractures in premobile infants without history of violent trauma, should raise suspicion of NAHI (limited evidence) [24, 48, 52]. Such fractures, however, have been observed in infants with impact to the

vertex, impact against more than one surface, fall or drop downstairs, and an adult or older child falling onto an infant.

NAHI is the predominant cause of SDH in infancy [53], and SDH is the most common associated intracranial pathology in NAHI (moderate evidence). In a retrospective chart review of 173 children less than 3 years of age diagnosed with NAHI, Jenny et al. found the following injuries: SDH (87 %), diffuse parenchymal brain injury (45 %), localized brain contusion (37 %), skull fracture (32 %), and epidural hematoma (2 %) [28].

Reece and Sege [54] in 287 children's head injury series (age 1 week–6.5 years) reported the prevalence of SDH in 46 % of abused children compared with 10 % of accidental injury. Hobbs et al. reported that 57 % of SDHs seen among infants of age 0–2 years are caused by NAHI, as opposed to 4 % by accident [53]. Also, in a prospective, longitudinal analysis of CT/MRI findings of inflicted ($n = 31$) and noninflicted ($n = 29$) childhood traumatic head injury, Ewing-Cobbs et al. found statistically significant higher frequency of SDH and evidence of previous injuries among the inflicted injury group [55]. The incidence of isolated SDH/SAH as the only gross finding in fatal AHI is less than 2 %, while it is 90–98 % in NAHI [23]. Other causes of SDH are listed in Table 23.1 and should be excluded with a combination of clinical history and relevant laboratory investigation. SDH may result from birth (moderate evidence). Looney et al. [56] reported that 26 % of 76 asymptomatic term infants (65 vaginally delivered and 23 with cesarean delivery) who underwent MRI had focal SDH near the tentorium and parafalcine location. None, however, had interhemispheric SDH.

Diffuse subdural hematoma (SDH) involving bilateral convexity, interhemispheric fissure, and posterior fossa is a sign of violent trauma-producing impulsive loading to the bridging veins by rotational acceleration. The volume of noncontact SDH, which is relatively small ranging from 2 to 15 ml, does not, in and of itself, manifest symptoms and almost never causes death by its mass effect (limited evidence) [23].

Contact SDH on the contrary tends to be focal and monocentric and seen under the site of impact.

Presence of SDHs of different ages suggests trauma of a repetitive nature and heightens the possibility of NAHI (limited evidence) [57].

Interhemispheric SDH was considered as highly specific for abusive injury (limited evidence). Zimmerman et al. reported a 69 % prevalence of parietooccipital interhemispheric SDH in a retrospective CT review of 26 abused children and suggested as a sign of NAHI [58]. However, accidental injury with significant rotational acceleration in the sagittal plane, such as a violent fall or a motor vehicle accident, also causes interhemispheric SDH [59].

Mixed-density SDH is more frequently seen among NAHI, while homogenous hyperdense SDH is more frequent in AHI (limited evidence) [57, 59].

Epidural hematoma is not a specific indicator of NAHI (limited evidence) [1, 19, 60].

Cortical contusions often seen in older children with violent accidental HI are less frequently seen in infants with NAHI. When present, they are seen in the cortex underneath the impact site. Likely sites for cortical contusions caused by the differential displacement of the brain and the skull (gliding contusions) include the temporal tips and frontal bases adjacent to the skull base and parasagittal cerebral cortex along the cerebral falx.

Traumatic diffuse axonal injuries are commonly seen in the corpus callosum, especially in the splenium, the gray–white junction especially of the superior frontal gyri, the periventricular areas, and the dorsolateral quadrants of the rostral brainstem. Occasionally, gross parenchymal tear is seen at the gray–white junction [61]. This injury is unique to infants with blunt head trauma and most commonly seen in the frontal and anterior parietal lobes. This lesion can be overlooked both by CT and at autopsy but is reliably demonstrated by sonography [62].

Severe swelling of the brain suggests a poor prognosis (limited evidence). Among profoundly traumatized infants, Cohen reported an unusual pattern of brain edema on CT that involves the cerebral cortex and the subcortical white matter in diffuse and symmetric fashion with relative density preservation of the deep white matter, basal ganglia, thalami, brainstem, and cerebellum and applied the term "reversal sign" [63].

Another unique CT pattern to predict poor outcome is "tin ear" syndrome described by Hanigan et al., who reported three fatal cases of NAHI, age ranging from 24 to 36 months, in which unilateral diffuse cerebral edema is associated with ipsilateral SDH and bruises and lacerations about the ear, resulting from a severe blow [64].

Even though traumatic axonal injury to the cervicomedullary junction and injury to the craniocervical osseoligamentous structure are postulated as a unique cause of the brain pathology of NAHI [10–14], there are only anecdotal reports of such injury demonstrated on neuroimaging and there is not enough evidence to support systematic spine imaging to investigate such injury without additional suggestive clinical or radiological evidence.

NAHI carries a significantly worse clinical outcome than does accidental HI. Early clinical and neuroimaging findings in NAHI are of prognostic value for neurodevelopmental outcome (limited evidence). In a retrospective medical chart review of 23 NAHI cases, Bonnier et al. reported that the presence of intraparenchymal lesions demonstrated on CT and/or MRI in the first 3 months was significantly associated with neurodevelopmental impairment [65].

Can CT and MR Imaging Help to Determine Timing of Injury?

Summary

The evolution of SDHs associated with NAHI is dynamic and complex. For the best estimation of injury timing, comparison of CT and MRI and correlation with follow-up studies are often needed.

Supporting Evidence

Scalp edema/hematoma becomes evident several hours to 24 h after the impact injury. Nonvisualization of scalp edema on a single neuroimaging on arrival should not be taken as absence of impact injury.

Skull fracture is a poor index of timing of injury because of the lack of periosteal reaction during healing.

On CT examination, the classical description of temporal evolution of SDH can be simplified as summarized in Table 23.2. The time course of the evolution may vary considerably from patient to patient and from location of SDH in the same patient, however [66–68]. Subdural collection with septation, mixed density, and layering suggests rehemorrhage.

MRI evolution of hemoglobin products in the SDH roughly follows that of parenchymal hematoma (limited evidence) [69, 70]. The evolution of intraparenchymal hematoma on MRI is summarized in Table 23.3. The signal pattern of evolving SDH generally follows the one of intraparenchymal hematomas in the acute and subacute stage with slower rate because of higher oxygen tension of the subdural space. The chronic SDH is isointense to slightly hypointense relative to gray matter on T1-weighted images and hyperintense on T2-weighted images. Hemosiderin is rarely seen in chronic SDH.

Gradient-refocused echo sequence is the most sensitive to detect the presence of hemoglobin product with prominent hypointensity, but signal characteristics do not change significantly according to the age of hematoma and thus cannot be used for timing of injury.

The temporal evolution of SDH should be reevaluated applying the newer anatomic and physiologic knowledge of the dural membrane [57, 71, 72]. SDH is most often located in the inner layer of the dura mater (dural border cell layer) adjacent to the arachnoid membrane. Histologically, there is no actual or potential subdural "space" in humans. In the border cell layer, the bridging veins are less protected against the shearing force. Furthermore, there appears to

be continuous and/or progressive bleeding or effusion upon resolving acute SDH in this "intradural" space after the initial trauma, which is further facilitated by intracranial hypotension caused by ongoing brain atrophy and treatment to decrease intracranial pressure [71, 72]. So the evolution of the SDH is dictated not only by the degradation of hemoglobin products of the initial hematoma but also by the dynamic physiologic phenomena taking place in the space, including clot matrix formation, changes in red blood cell concentration due to packing, changes in RBC hydration, retraction of clots, effusion of serous fluid through traumatized dura, escaped CSF into the subdural space through the torn arachnoid membrane, and rebleeding (limited evidence) [57].

Occasionally, a subdural collection is hypodense, similar to CSF density in acute injury (limited evidence) [57, 59, 73, 74]. Acute subdural hygroma is considered as the result of exudate collection in the dural membrane. SDH in anemic patients also may show low attenuation.

Mixed-density SDH is more commonly seen in SDH in NAHI and is traditionally considered "acute hemorrhage in the chronic hematoma," i.e., evidence of repeated injury, i.e., NAHI. However, the following possibilities should also be entertained: (1) acute SDH mixed with CSF leaked through arachnoid tear, (2) a mixture of subdural hygroma and hematoma, (3) low-density SDH with thrombosed cortical veins, and (4) sedimentation in the SDH (limited evidence) [57, 59].

Because of the complexity involving the timing determination, comparison between CT and MRI and follow-up studies, either CT or MR, are often necessary for accurate estimation of injury timing.

In addition to the acute findings associated with NAHI discussed above, attention should also be paid to more subtle evidence of previous brain injury. Ewing-Cobbs et al. performed a prospective longitudinal study of 20 NAHI and 20 accidental HI victims of less than 6 years of age and reported the statistically significant higher prevalence of brain injury

(up to 45 %) – namely, the presence of brain atrophy, ventriculomegaly, and subdural hygroma among the NAHI group [55].

What Is the Sensitivity and Specificity of CT and MRI?

Summary

CT is a sensitive imaging test for SDH and skull fracture. CT is the preferred imaging modality for the evaluation of acute NAHI, adequately demonstrating injuries that need urgent intervention. Serial CT during the acute phase improves detection of intracranial hemorrhage (moderate evidence). MRI should be performed within a few days if the clinical symptoms are disproportionate to CT findings. MRI without gadolinium is more sensitive and specific than CT in the screening of subacute or chronic head injury and should be the primary imaging modality used (moderate evidence). MRI is superior to CT in determining prognosis (limited evidence).

Supporting Evidence

The imaging tool that should be used initially in the cases of suspected acute child abuse is CT [65, 75]. CT is relatively sensitive and specific for detecting the presence of intracranial hemorrhage, including parenchymal contusional hemorrhage, subdural and epidural hematoma, and subarachnoid hemorrhage. The sensitivity of CT for detecting abnormalities after severe traumatic brain injury in adult patients varies from 68 % to 94 %, while normal scans range from 7 % to 12 % [76]. CT is adequate for demonstrating lesions that require surgery [77] (moderate evidence); however, CT often fails to reveal nonhemorrhagic parenchymal injuries and brain edema. Serial CT scans are useful to detect progressive intracranial hemorrhage after head injury. Oertel et al. studied 142 adult patients with moderate or severe head injury who had undergone more than one CT scan and found

that the initial CT did not detect the full extent of hemorrhage in 50 % of patients [78] (moderate evidence).

MRI generally has a higher sensitivity and specificity for detecting brain parenchymal injury [79, 80] (moderate evidence). In a retrospective study of 107 adult patients with acute traumatic brain injury, MRI performed within 48 h of injury had an overall sensitivity of 97 % compared to 63 % for CT, with better sensitivity for hemorrhagic and nonhemorrhagic contusions, shearing injuries, and subdural and epidural hematomas [79]. MRI is more sensitive to detect hypoxic–ischemic injury, shearing injuries, lesions caused by direct impact, compression, and penetration injuries in NAHI [68, 77, 81–85] (moderate evidence). In a study involving 19 cases of child abuse, subdural hematomas, cortical contusions, and shearing injuries were demonstrated with particular advantage with MRI [77].

T2*-weighted images using gradient echo (GRE) sequences are more sensitive in detecting blood products than is conventional MRI [86]. FLAIR (fluid-attenuated inversion recovery) sequences consist of an inversion recovery pulse to null the signal from CSF and a long echo time to produce heavily T2-weighted images. FLAIR is as sensitive as, or more sensitive than, CT in the evaluation of acute subarachnoid hemorrhage [87]. MRI with its multiplanar capability is more sensitive than CT in detecting small SDH or subarachnoid bleeds. Diffusion-weighted imaging (DWI) is sensitive in detecting acute and subacute parenchymal injuries including hypoxic–ischemic injury and nonhemorrhagic DAI [84, 88–91].

MRI yields more information than CT in demonstrating the distribution and mechanisms of injury in NAHI and provides better prognostication when performed between 0.5 and 3 months after injury [65] (limited evidence). Usefulness of serial MR imaging in young patients with head trauma has not been established. Single-photon emission computed tomography (SPECT) and positron emission tomography (PET) permit

in vivo assessment of regional blood flow and metabolism. However, the spatial and temporal resolution is limited and not widely available.

How Should the Newer MR Imaging Techniques Be Used?

Summary

Use of newer MR imaging techniques including DWI, susceptibility-weighted imaging, and MR spectroscopy may improve the clinical care and management of children with traumatic brain injury (limited evidence). These techniques better characterize the nature, mechanism, and evolution of injuries that lead to progressive neurodegeneration, recovery, or subsequent plasticity. DWI is especially useful in the early detection of acute and subacute brain parenchymal injury (moderate evidence).

Supporting Evidence

Diffusion-Weighted Imaging DWI is sensitive to alteration in diffusion of water molecules and can discriminate vasogenic and cytotoxic brain edema. There are more free interstitial water molecules in vasogenic edema (increased ADC), while there are restricted water molecules in the cellular edema (decreased ADC). DWI is more sensitive than conventional MRI in detecting early changes of NAHI and more extensive involvement of acute or subacute brain parenchymal injury [84, 88–92] (moderate evidence). Suh et al. retrospectively evaluated 18 children within 5 days of presentation, and 89 % showed abnormalities on DWI. In 81 % of positive cases, DWI revealed more extensive brain injury than did conventional MRI [89]. DWI characteristics of the normal brain in young infants differ significantly from those in adults [93]. ADC values in both gray and white matter of young infants are considerably higher than in adults, reflecting the high water content of the pediatric brain [94]. Abnormalities of the

pediatric brain become apparent on DWI (hyperintensity on DWI is associated with decreased ADC) within a few hours after injury before they appear on T2-weighted images. In adults, abnormalities become apparent on T2-weighted images within 24 h. In the undermyelinated infant brain with increased water content, however, "DWI-positive and T2-negative" duration of parenchymal injury may last up to 48–72 h, even up to 1 week in some cases. The parenchymal abnormalities displayed on DWI can be far more extensive than are detected on other sequences. The parenchymal hyperintensity on DWI with a decreased ADC value mainly represents cytotoxic brain edema in acute and subacute ischemia, which is usually irreversible, and results in necrosis or neuronal apoptotic cell death. An optimal window level setting is essential for accurate diagnosis. Quantifying the ADC value is useful to detect extensive parenchymal abnormalities (Fig. 23.1). The severity of abnormality on DWI correlates with the patient's outcome [89] (limited evidence).

Diffusion Tensor Imaging Diffusion tensor imaging (DTI) allows evaluation of the white matter tract by demonstrating the intrinsic directionality of water diffusion in the white matter (anisotropy). DTI demonstrates normal myelination earlier than does conventional MR imaging [95, 96]. The anisotropic pattern is nonspecific and varies depending on the extent of edema, gliosis, myelination, and the irregularity of axonal orientation. DTI may contribute to the early evaluation of NAHI (limited evidence). Most DTI studies in TBI have been performed on adult patients. In a study of 20 adults within 7 days of trauma, reduction of fractional anisotropy (FA) values in the internal capsules and corpus callosum correlated better with the Glasgow Coma Scale and the Rankin Scale scores than with the ADC values of DWI [97]. In a study of five adults within 24 h of trauma, FA

revealed regions of reduced anisotropy, while other MRI sequences were normal [98].

DTI potentially increases early detection of parenchymal injury in NAHI, but not enough bodies of evidences exist in the literature.

Susceptibility-Weighted Imaging Susceptibility-weighted imaging (SWI) is a newer gradient echo sequence that is more sensitive than T2*-weighted gradient echo sequence in detecting susceptibility-related effects of blood products, especially hemorrhagic diffuse axonal injury [99, 100]. SWI may contribute to the evaluation of hemorrhagic parenchymal lesions in NAHI (limited evidence). In 40 children and adolescents with mild to severe TBI and DAI, the number and the volume of hemorrhagic lesions demonstrated on SWI were significantly correlated with the patient's outcome [86].

MR Spectroscopy MR spectroscopy (MRS) allows noninvasive in vivo analysis of neurochemicals and metabolites and has shown potential for providing prognostic information in pediatric patients with head injury [101–103] (limited evidence). In a study of 54 pediatric patients with NAHI, MRS showed decreased *N*-acetyl aspartate (NAA) (decreased neuronal activity), increased choline (breakdown product of myelin and cell membranes), and increased lactate (metabolic acidosis) [102]. The degree of these changes seems to be related to the severity of brain damage and prognosis [101, 102, 104–108] (limited evidence). In 38 children with TBI, significantly increased myoinositol (product reflecting glial cell proliferation) and glutamate/glutamine (Gx) were observed when compared to controls [104]. In experimental studies of acute subdural hematomas in the infant rat, the glutamate concentration in the extracellular fluid of the cortex was increased more than seven times over the base level [109]. Gx levels peak early after injury and then fall rapidly [110, 111]. This grading may become important in the future since

the neuroprotective effects of several kinds of selective glutamate receptor antagonists have been reported in animal studies [112–114].

Take-Home Tables

Table 23.1 shows the differential diagnoses for SDH. Table 23.2 shows the evolution of subdural hematoma on CT. Table 23.3 shows evolution of intraparenchymal hematoma on MR primary.

Imaging Case Studies

Case 1

Figure 23.1ABC shows the advantage of DWI in demonstrating parenchymal injury in NAHI.

Case 2

Figure 23.2ABC represents imaging of SDHs of different ages.

Table 23.1 Differential diagnosis of SDH

NAHI
Accidental HI
Perinatal
Fetal
Traumatic delivery
"Normal" vaginal delivery [56]
Aneurysms, arteriovenous malformations
Arachnoid cyst
Meningitis
Coagulopathies: vitamin K deficiency [115]
Metabolic disorders
Glutaric aciduria type I [116, 117]
Galactosemia
Pyruvate carboxylase deficiency
Menkes disease [118]
Hypernatremia
Paroxysmal cough with increased intrathoracic pressure [119]

Reprinted with kind permission of Springer Science+Business Media from Sato Y, Moritani T. Imaging of nonaccidental head injury. In: Medina LS, Applegate KE, Blackmore CC, editors. Evidence-based imaging in pediatrics. New York: Springer; 2010

Table 23.2 Evolution of subdural hematoma on CT

~3 h	Iso- to hypodense to brain
~7 days	Hyperdense
~1 month	Isodense
1 month	Hypodense

Reprinted with kind permission of Springer Science+ Business Media from Sato Y, Moritani T. Imaging of nonaccidental head injury. In: Medina LS, Applegate KE, Blackmore CC, editors. Evidence-based imaging in pediatrics. New York: Springer; 2010

Table 23.3 Evolution of intraparenchymal hematoma on MR primary

	T1-weighted	T2-weighted	Hb products
~12 h	Iso- to hypointense	Hyperintense	Oxy-Hb
~3 days	Hypointense	Hypointense	Doxy-Hb
~7 days	Hyperintense	Hypointense	Met Hb (intracellular)
~1 month	Hyperintense	Hyperintense	Met Hb (extracellular)
~1 month	Hypointense	Hypointense	Hemosiderin, ferritin

Reprinted with kind permission of Springer Science+ Business Media from Sato Y, Moritani T. Imaging of nonaccidental head injury. In: Medina LS, Applegate KE, Blackmore CC. editors. Evidence-based imaging in pediatrics. New York: Springer; 2010

Suggested Imaging Protocols

Neuroimaging in the setting of suspected abuse depends on the child's age, signs, and symptoms. Consensus opinion by experts formulated the ACR Appropriateness Criteria® [120] and provided a guideline:

1. Children 2 years of age or younger with suspicion of abuse without focal signs and symptoms: skeletal survey including AP and lateral radiographs of skull

2. Children 2 years of age or younger with histories of head trauma without neurologic deficits: brain CT or MRI for documentation of abuse

3. Children up to 5 years of age with neurologic signs and symptoms:
   (a) Unstable patients: noncontrast CT to detect lesions requiring urgent intervention, followed by MRI once stabilized
   (b) Stable patients: MRI

4. Suggested MRI sequences include sagittal T1, axial T1, FLAIR, T2, T2*-GRE, DW1/ADC, and contrast-enhanced T1 in axial and coronal planes

   In addition, neuroimaging, either CT or MRI, is recommended among the young infants less than 1 year of age when they are found to have multiple fractures or rib fractures.

Future Research

- To better define the temporal evolution of SDH on newer MRI protocols and CT equipment for better dating
- To better understand the unique biomechanics of the traumatic brain injury of infants correlating biomechanical, anatomical, pathological, and imaging data
- To determine the advantages, limitations, and pitfalls of newer imaging techniques including DWI, DTI, SWI, and MR spectroscopy
- Assessment of the effects of imaging on the patient's prognosis, outcome, and costs of diagnosis and management
- To define newer imaging guidelines for NAHI incorporating recent neuroscientific and neuroimaging advancement including serum- and CSF biochemical markers [121]
- To understand the cost-effectiveness of screening head CT in asymptomatic infants with physical abuse
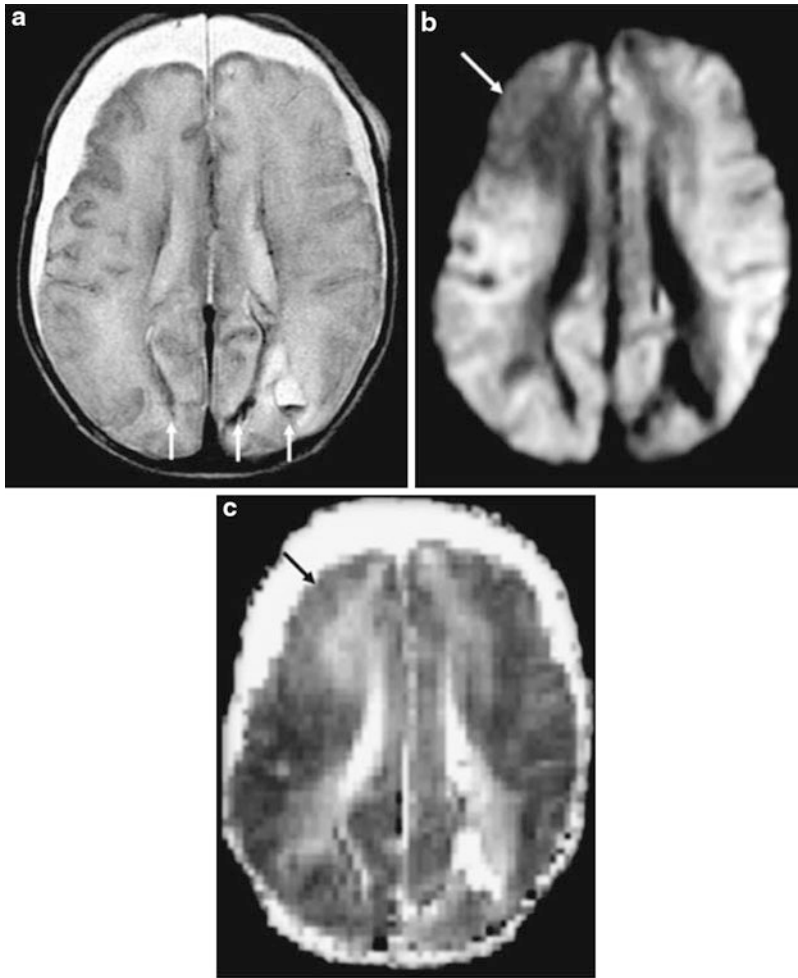
Fig. 23.1 MRI of a 2-month-old boy with NAHI. (**a**) T2-weighted image shows intraparenchymal hemorrhages (*arrows*) and bilateral frontal chronic subdural hematomas. (**b**) DWI shows extensive parenchymal abnormalities. There is diffuse increased signal in both hemispheres with relative sparing of the right frontal area (*arrow*) and deep white matter adjacent to the ventricle. (**c**) Calculated ADC values are decreased ($0.26–0.45 \times 10^{-3}$/mm^2 per s) in the abnormal parenchyma (Reprinted with kind permission of Springer Science+Business Media from Sato Y, Moritani T. Imaging of nonaccidental head injury. In: Medina LS, Applegate KE, Blackmore CC, editors. Evidence-based imaging in pediatrics. New York: Springer; 2010)
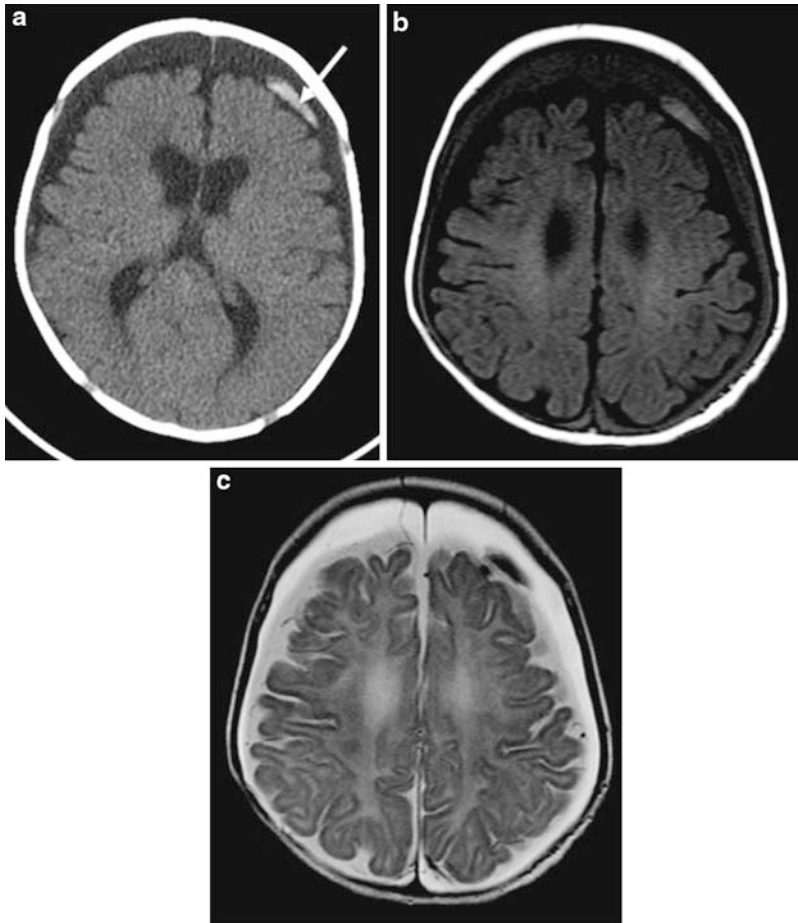
Fig. 23.2 A 4-month-old infant with NAHI. CT (**a**) and axial T1- (**b**) and axial T2-weighted image (**c**) show bilateral chronic SDH and subacute SDH in the left convexity (*arrow*) (Reprinted with kind permission of Springer Science+Business Media from Sato Y, Moritani T. Imaging of nonaccidental head injury. In: Medina LS, Applegate KE, Blackmore CC, editors. Evidence-based imaging in pediatrics. New York: Springer; 2010)

References

1. Duhaime AC, Alario AJ, Lewander WJ, et al. Pediatrics. 1992;90(2 Pt 1):179–85.
2. American Academy of Pediatrics: Committee on Child Abuse and Neglect. Pediatrics. 2001;108(1):206–10.
3. Goldsmith W, Plunkett J. Am J Forensic Med Pathol. 2004;25(2):89–100.
4. Hymel KP, Bandak FA, Partington MD, Winston KR. Child Maltreat. 1998;3(2):116–28.
5. Pierce MC, Bertocci GE, Berger R, Vogeley E. Neurosurg Clin N Am. 2002;13(2):155–68.
6. Caffey J. Am J Dis Child. 1972;124(2):161–9.
7. Caffey J. Pediatrics. 1974;54(4):396–403.
8. Duhaime AC, Gennarelli TA, Thibault LE, Bruce DA, Margulies SS, et al. J Neurosurg. 1987;66(3):409–15.
9. Cory CZ, Jones BM. Med Sci Law. 2003;43(4):317–33.
10. Morison CN, Minns RA. In: Minns RA, Brown JK, editors. Shaking and other non-accidental head injuries in children. London: Mac Keith; 2005. p. 109–46.
11. Hadley MN, Sonntag VK, Rekate HL, Murphy A. Neurosurgery. 1989;24(4):536–40.
12. Geddes JF, Hackshaw AK, Vowles GH, Nickols CD, Whitwell HL. Brain. 2001;124(Pt 7):1290–8.
13. Geddes JF, Vowles GH, Hackshaw AK, Nickols CD, Scott IS, et al. Brain. 2001;124(Pt 7):1299–306.
14. Shannon P, Smith CR, Deck J, Ang LC, Ho M, et al. Acta Neuropathol. 1998;95(6):625–31.
15. Geddes JF, Tasker RC, Hackshaw AK, et al. Neuropathol Appl Neurobiol. 2003;29(1):14–22.
16. Punt J, Bonshek RE, Jaspan T, McConachie NS, Punt N, et al. Pediatr Rehabil. 2004;7(3):173–84.
17. Geddes JF, Tasker RC, Adams GG, Whitwell HL. Pediatr Rehabil. 2004;7(4):261–5.
18. U.S. Department of Health and Human Services, Administration on Children, Youth and Families. Child maltreatment 2003. Washington, DC: U.S. Government Printing Office; 2005.
19. Merten DF, Osborne DR, Radkowski MA, Leonidas JC. Pediatr Radiol. 1984;14(5):272–7.
20. Tsai FY, Zee CS, Apthorp JS, Dixon GHJ. Comput Tomogr. 1980;4(4):277–86.
21. Keenan HT, Runyan DK, Marshall SW, et al. J Am Med Assoc. 2003;290(5):621–6.
22. Dashti SR. Pediatr Neurosurg. 1999;31(6):302–6.
23. Case ME, Graham MA, Handy TC, Jentzen JM, Monteleone JA. National Association of Medical Examiners Ad Hoc committee on shaken baby syndrome. Am J Forensic Med Pathol. 2001;22(2):112–22.
24. Billmire ME, Myers PA. Pediatrics. 1985;75(2):340–2.
25. Bruce DA, Zimmerman RA. Pediatr Ann. 1989;18(8):482–4. 486–9, 492–4.
26. Alexander R, Crabbe L, Sato Y, Smith W, Bennett T. Am J Dis Child. 1990;144(1):58–60.
27. Wang CT, Holton J. Total estimated cost of child abuse and neglect in the United States. Prevent Child Abuse America Web site. Updated September 2007. Accessed 15 Aug 2008.
28. Jenny C, Hymel KP, Ritzen A, Reinert SE, Hay TC. J Am Med Assoc. 1999;281(7):621–6.
29. Duhaime AC, Partington MD. Neurosurg Clin N Am. 2002;13(2):149–54. v.
30. Salehi-Had H, Brandt JD, Rosas AJ, Rogers KK. Pediatrics. 2006;117(5):e1039–44.
31. Kleinman PK, Marks Jr SC, Richmond JM, Blackbourne BD. AJR Am J Roentgenol. 1995;165(3):647–50.
32. Willman KY, Bank DE, Senac M, Chadwick DL. Child Abuse Negl. 1997;21(10):929–40.
33. Morad Y, Kim YM, Armstrong DC, Huyer D, Mian M, et al. Am J Ophthalmol. 2002;134(3):354–9.
34. Levin AV. Neurosurg Clin N Am. 2002;13(2):201–11. vi.
35. Aryan HE, Ghosheh FR, Levy ML. J Clin Neurosci. 2005;12(6):624–31.
36. Johnson DL, Braun D, Friendly D. Neurosurgery. 1993;33(2):231–4. discussion 234–5.
37. Schloff S, Mullaney PB, Armstrong DC, et al. Ophthalmology. 2002;109(8):1472–6.
38. Sezen F. Br J Ophthalmol. 1971;55(4):248–53.
39. Laskey AL, Holsti M, Runyan DK, Socolar RR. J Pediatr. 2004;144(6):719–22.
40. Rubin DM, Christian CW, Bilaniuk LT, Zazyczny KA, Durbin DR. Pediatrics. 2003;111(6 Pt 1):1382–6.
41. Kleinman PK, Barnes PD. In: Kleinman PK, editor. Diagnostic imaging of child abuse. 2nd ed. St. Louis: Mosby; 1998. p. 285–342.
42. Barnes PD, Krasnokutsky M. Top Magn Reson Imaging. 2007;18(1):53–74.
43. Barnes PD. Top Magn Reson Imaging. 2002;13(2):85–93.
44. Lonergan GJ, Baker AM, Morey MK, Boos SC. Radiographics. 2003;23(4):811–45.
45. David TJ. Pediatr Radiol. 2008;38(Suppl 3):S370–7.
46. Jaspan T. Pediatr Radiol. 2008;38(Suppl 3):S378–87.
47. Johnstone AJ, Zuberi SH, Scobie WG. J Accid Emerg Med. 1996;13(6):386–9.
48. Hobbs CJ. Arch Dis Child. 1984;59(3):246–52.
49. Helfer RE, Slovis TL, Black M. Pediatrics. 1977;60(4):533–5.
50. Nimityongskul P, Anderson LD. J Pediatr Orthop. 1987;7(2):184–6.
51. Warrington SA, Wright CM, ALSPAC Study Team. Arch Dis Child. 2001;85(2):104–7.
52. Meservy CJ, Towbin R, McLaurin RL, Myers PA, Ball W. AJR Am J Roentgenol. 1987;149(1):173–5.
53. Hobbs C, Childs AM, Wynne J, Livingston J, Seal A. Arch Dis Child. 2005;90(9):952–5.
54. Reece RM, Sege R. Arch Pediatr Adolesc Med. 2000;154(1):11–15.
55. Ewing-Cobbs L, Kramer L, Prasad M, et al. Pediatrics. 1998;102(2 Pt 1):300–7.

56. Looney CB, Smith JK, Merck LH, et al. Radiology. 2007;242(2):535–41.
57. Hymel KP, Jenny C, Block RW. Child Maltreat. 2002;7(4):329–48.
58. Zimmerman RA, Bilaniuk LT, Bruce D, Schut L, Uzzell B, et al. Radiology. 1979;130(3):687–90.
59. Tung GA, Kumar M, Richardson RC, Jenny C, Brown WD. Pediatrics. 2006;118(2):626–33.
60. Shugerman RP, Paez A, Grossman DC, Feldman KW, Grady MS. Pediatrics. 1996;97(5):664–8.
61. Lindenberg R, Freytag E. Arch Pathol. 1969;87(3):298–305.
62. Jaspan T, Narborough G, Punt JA, Lowe J. Pediatr Radiol. 1992;22(4):237–45.
63. Cohen RA. AJR Am J Roentgenol. 1986;146(1):97–102.
64. Hanigan WC, Peterson RA, Njus G. Pediatrics. 1987;80(5):618–22.
65. Bonnier C, Nassogne MC, Saint-Martin C, Mesples B, Kadhim H, et al. Pediatrics. 2003;112(4):808814.
66. Bergström M, Ericson K, Levander B, Svendsen P. J Comput Assist Tomogr. 1977;1(4):449–55.
67. Lee KS, Bae WK, Bae HG, Doh JW, Yun IG. J Korean Med Sci. 1997;12(4):353–9.
68. Dias MS, Backstrom J, Falk M, Li V. Pediatr Neurosurg. 1998;29(2):77–85.
69. Bradley WG. Radiology. 1993;189(1):15–26.
70. Fobben ES, Grossman RI, Atlas SW, et al. Am J Roentgenol. 1989;153(3):589–95.
71. Haines DE. Anat Rec. 1991;230(1):3–21.
72. Haines DE, Harkey HL, Al-Mefty O. Neurosurgery. 1993;32(1):111–20.
73. Joy HM, Anscombe AM, Gawne-Cain ML. Clin Radiol. 2007;62(7):703–6.
74. Wells RG, Sty JR. Arch Pediatr Adolesc Med. 2003;157(10):1005–10.
75. Duhaime AC, Christian CW, Rorke LB, Zimmerman RA. N Engl J Med. 1998;338(25):1822–9.
76. The Brain Trauma Foundation. The American Association of Neurological Surgeons. The joint section on neurotrauma and critical care. J Neurotrauma. 2000;17(6–7):597–627.
77. Sato Y, Yuh WT, Smith WL, Alexander RC, Kao SC, et al. Radiology. 1989;173(3):653–7.
78. Oertel M, Kelly DF, McArthur D, et al. J Neurosurg. 2002;96(1):109–16.
79. Orrison WW, Gentry LR, Stimac GK, Tarrel RM, Espinosa MC, et al. AJNR Am J Neuroradiol. 1994;15(2):351–6.
80. Ogawa T, Sekino H, Uzura M, et al. Acta Neurochir Suppl (Wien). 1992;55:8–10.
81. Ball Jr WS. Radiology. 1989;173(3):609–10.
82. Chabrol B, Decarie JC, Fortin G. Child Abuse Negl. 1999;23(3):217–28.
83. Blumenthal I. Postgrad Med J. 2002;78(926):732–5.
84. Poussaint TY, Moeller KK. Neuroimaging Clin N Am. 2002;12(2):271–94. ix.
85. Gerber P, Coffman K. Childs Nerv Syst. 2007;23(5):499–507.
86. Tong KA, Ashwal S, Holshouser BA, et al. Ann Neurol. 2004;56(1):36–50.
87. Stuckey SL, Goh TD, Heffernan T, Rowan D. Am J Roentgenol. 2007;189(4):913–21.
88. Parizel PM, Ceulemans B, Laridon A, Ozsarlak O, Van Goethem JW, et al. Pediatr Radiol. 2003;33(12):868–71.
89. Suh DY, Davis PC, Hopkins KL, Fajman NN, Mapstone TB. Neurosurgery. 2001;49(2):309–18. discussion 318–20.
90. Biousse V, Suh DY, Newman NJ, Davis PC, Mapstone T, et al. Am J Ophthalmol. 2002;133(2):249–55.
91. Chan YL, Chu WC, Wong GW, Yeung DK. Pediatr Radiol. 2003;33(8):574–7.
92. Field AS, Hasan K, Jellison BJ, Arfanakis K, Alexander AL. AJNR Am J Neuroradiol. 2003;24(7):1461–4.
93. Tanner SF, Ramenghi LA, Ridgway JP, et al. AJR Am J Roentgenol. 2000;174(6):1643–9.
94. Morriss MC, Zimmerman RA, Bilaniuk LT, Hunter JV, Haselgrove JC. Neuroradiology. 1999;41(12):929–34.
95. Neil JJ, Shiran SI, McKinstry RC, et al. Radiology. 1998;209(1):57–66.
96. Wimberger DM, Roberts TP, Barkovich AJ, Prayer LM, Moseley ME, et al. J Comput Assist Tomogr. 1995;19(1):28–33.
97. Huisman TA, Schwamm LH, Schaefer PW, et al. AJNR Am J Neuroradiol. 2004;25(3):370–6.
98. Arfanakis K, Haughton VM, Carew JD, Rogers BP, Dempsey RJ, et al. AJNR Am J Neuroradiol. 2002;23(5):794–802.
99. Haacke EM, Cheng NY, House MJ, et al. Magn Reson Imaging. 2005;23(1):1–25.
100. Grados MA, Slomine BS, Gerring JP, Vasa R, Bryan N, et al. J Neurol Neurosurg Psychiatr. 2001;70(3):350–8.
101. Holshouser BA, Ashwal S, Luh GY, et al. Radiology. 1997;202(2):487–96.
102. Ashwal S, Holshouser BA, Shu SK, et al. Pediatr Neurol. 2000;23(2):114–25.
103. Brenner T, Freier MC, Holshouser BA, Burley T, Ashwal S. Pediatr Neurol. 2003;28(2):104–14.
104. Ashwal S, Holshouser B, Tong K, et al. J Neurotrauma. 2004;21(11):1539–52.
105. Ashwal S, Babikian T, Gardner-Nichols J, Freier MC, Tong KA, et al. Arch Phys Med Rehabil. 2006;87(12 Suppl 2):S50–8.
106. Yeo RA, Phillips JP, Jung RE, Brown AJ, Campbell RC, et al. J Neurotrauma. 2006;23(10):1427–35.
107. Babikian T, Freier MC, Ashwal S, Riggs ML, Burley T, et al. Magn Reson Imaging. 2006;24(4):801–11.
108. Hunter JV, Thornton RJ, Wang ZJ, et al. Am J Neuroradiol. 2005;26(3):482–8.
109. Bullock R, Butcher SP, Chen MH, Kendall L, McCulloch J. J Neurosurg. 1991;74(5):794–802.
110. Schuhmann MU, Stiller D, Thomas S, Brinker T, Samii M. Acta Neurochir Suppl. 2000;76:3–7.
111. Zhang H, Zhang X, Zhang T, Chen L. Clin Chem. 2001;47(8):1458–62.

112. Duhaime AC, Gennarelli LM, Boardman C. J Neurotrauma. 1996;13(2):79–84.
113. Ikonomidou C, Qin Y, Labruyere J, Kirby C, Olney JW. Pediatr Res. 1996;39(6):1020–7.
114. Smith SL, Hall ED. J Neurotrauma. 1998;15(9):707–19.
115. Brousseau TJ, Kissoon N, McIntosh B. J Emerg Med. 2005;29(3):283–8.
116. Bishop FS, Liu JK, McCall TD, Brockmeyer DL. J Neurosurg. 2007;106(3 Suppl):222–6.
117. Gago LC, Wegner RK, Capone Jr A, Williams GA. Retina. 2003;23(5):724–6.
118. Nassogne MC, Sharrard M, Hertz-Pannier L, et al. Childs Nerv Syst. 2002;18(12):729–31.
119. Geddes JF, Talbert DG. Neuropathol Appl Neurobiol. 2006;32:625–34.
120. Slovis TL, Smith WL, Strain JD et al. Suspected physical abuse – child. ACR Appropriateness Criteria®. American College of Radiology Web Site. http://www.acr.org. Updated 2005. Accessed 30 Apr 2008.
121. Berger RP, Kochanek PM, Pierce MC. Child Abuse Negl. 2004;28(7):739–54.

Headache Disorders: Evidence-Based Neuroimaging

24

L. Santiago Medina, Melissa M. Debayle, and Elza Vasconcellos

Contents

L.S. Medina (✉)
Division of Neuroradiology-Neuroimaging, Department of Radiology, Miami Children's Hospital, Miami, FL, USA

Herbert Wertheim College of Medicine, Florida International University, Miami, FL, USA

Former Lecturer in Radiology, Harvard Medical School, Boston, MA, USA
e-mail: smedina@post.harvard.edu; Santiago.medina@mch.com

M.M. Debayle
Department of Radiology, Mount Sinai Medical Center, Miami Beach, FL, USA
e-mail: mdebayle@msmc.com

E. Vasconcellos
Department of Neurology, Miami Children's Hospital, Miami, FL, USA
e-mail: evasconcellos@nnpmd.com

Key Points

- CT imaging remains the initial test of choice for (1) new onset of headache in high-risk adults and (2) headache suggestive of subarachnoid hemorrhage (limited evidence).
- MRI is recommended in adults with nonacute headache and unexplained abnormal neurologic examination (moderate evidence).
- In adults with headache and known primary neoplasm suspected of having brain metastatic disease, MR imaging with contrast is the neuroimaging study of choice (moderate evidence).
- Although most headaches in children are benign in nature, a small percentage is caused by serious diseases, such as brain neoplasm.
- MRI is recommended in children with headache and an abnormal neurologic examination or seizures (moderate evidence).
- Sensitivity and specificity of MR imaging are greater than CT for nonsubarachnoid hemorrhagic intracranial lesions. For intracranial surgical space-occupying lesions, however, there is no difference in diagnostic performance between MR imaging and CT (limited evidence).
- Conventional CT angiography (CTA) and MR angiography (MRA) have sensitivities greater than 85 % for detection of aneurysms greater than 5 mm. Multidetector CT (MDCT) sensitivity and specificity is greater than 90 % for aneurysms greater than 4 mm (moderate evidence).
- MDCT angiography and digital subtraction angiography (DSA) have similar sensitivities and specificities for detection of aneurysms greater than 4 mm (moderate evidence). Please see dedicated intracranial aneurysm chapter for more details about test of choice for ruptured versus nonruptured aneurysms.
- Advanced brain imaging may help differentiate the different types of primary headache disorders. Migraine disorders have a brain stem, primarily pontine, origin (limited evidence). In contrast to migraine disorders, there is no brain stem activation during acute cluster headache episodes compared with the resting state (limited evidence). These initial studies suggest that, although primary headaches such as migraine and cluster headaches may share a common pain pathway – the trigeminovascular innervation – their underlying pathogenesis differs significantly.

Definition and Pathophysiology

Headaches can be divided into primary and secondary (Table 24.1). Primary causes include migraine, cluster, and tension-type headaches, while secondary etiologies include neoplasms, arteriovenous malformations, aneurysms, infections, trauma, and hydrocephalus. Diagnosis of primary headache disorders is based on clinical criteria as set forth by the International Headache Society [1]. A detailed history and physical examination help distinguish between primary and secondary headaches. Neuroimaging should aid in the diagnosis of secondary headache disorders.

Secondary headaches in children are more likely to present as acute headache, sudden onset in an otherwise healthy child, or as a chronic progressive headache, with gradual increase in frequency and severity. Acute recurrent headaches in an otherwise healthy child most often represent migraine or episodic tension-type headaches [2]. Sinus disease is a common cause of acute headache. Chapter 35 on sinus disease provides a comprehensive discussion on this topic.

Fourteen studies have reported white matter abnormalities in patients with migraine headaches, ranging from 12 % to 46 %. White matter abnormalities were reported more frequently in the frontal region of the centrum semiovale. Six of the eight studies using controls found a higher incidence of white matter abnormalities in migraineurs [3]. The cause of white matter abnormalities in migraine is uncertain but may be related to increased platelet aggregability with microemboli, abnormal cerebrovascular regulation, repeated attacks of hypoperfusion during the aura, and presence of antiphospholipid antibodies [4–7].

Epidemiology

Adults

Headache is a very common symptom among adults, accounting for 18 million (4 %) of the total outpatient visits in the United States each year [8]. In any given year, more than 70 % of the US population has a headache [9]. An estimated 23.6 million people in the USA have migraine headaches [10, 11].

In the elderly population, 15 % of patients 65 years or older, compared to 1–2 % of patients younger than 65 years, presented with secondary headache disorders such as neoplasms, strokes, and temporal arteritis [10, 12]. Brain metastases are the most common intracranial tumors, far outnumbering primary brain neoplasms [13]. Approximately 58 % of primary brain neoplasms in adults are malignant [13]. Common primary malignant neoplasms include astrocytoma and glioblastoma multiforme [13]. Benign brain tumors account for 38 % of primary brain neoplasms [13]. Despite their "benign" name, they may have aggressive characteristics causing significant morbidity and mortality [13]. The meningioma is the most common type [13].

Children

Pediatric headache is a common health problem in children, with a significant headache reported in more than 75 % by the age of 15 years [14]. In approximately 50 % of patients with migraines, the headache disorder starts before the age of 20 years [10]. In the USA, adolescent boys and girls have a headache prevalence of 56 % and 74 % and a migraine prevalence of 3.8 % and 6.6 %, respectively [8]. A small percentage of headaches in children are secondary in nature. A primary concern in children with headache is the possibility of a brain tumor [15, 16]. Although brain tumors constitute the largest group of solid neoplasms in children and are second only to leukemia in overall frequency of childhood cancers, the annual incidence is low at 3 in 100,000 persons [16]. Primary brain neoplasms are far more prevalent in children than they are in adults [17]. They account for almost 20 % of all cancers in children but only 1 % of cancers in adults [10]. Central nervous system (CNS) tumors are the second cause of cancer-related deaths in patients younger than 15 years [18].

Overall Cost to Society

Headache is the most common and one of the most disabling types of chronic pain among children and adolescents [19, 20]. The incidence of migraine peaks in adolescence, but the prevalence of migraine continues to increase and is highest in the most productive years of life between the ages of 25 and 55 years [21, 22]. The direct and indirect annual cost of migraine in the USA has been estimated at more than $5.6 billion [23]. A recent US study showed that migraine families incur far higher direct and indirect health-care costs (70 % higher than nonmigraine families) with most of the difference concentrated in outpatient costs [24]. Of interest, in families where the sole migraineur was a child versus a parent, the total health-care costs per family were about $600 higher and almost $2,500 higher than when both a parent and child were affected [19]. Work absence days, short-term disability, and workman's compensation days all were higher among migraine families than among families without a migraineur [24].

Goals of Imaging

- Diagnose secondary causes of headache (Table 24.1) for initiation of appropriate treatment.
- Exclude secondary etiologies of headache in patients with atypical primary headache disorders.
- Decrease the risk of brain herniation prior to lumbar puncture by excluding intracranial space-occupying lesions.

- Differentiate between the types of primary headache disorders using advanced imaging techniques.

Methodology

MEDLINE search using Ovid (Wolters Kluwer US Corporation, New York, NY) and PubMed (National Library of Medicine, Bethesda, MD) was used. Systematic literature review was performed from 1966 through February 2011. Keywords included (1) headache, (2) cephalgia, (3) diagnostic imaging, (4) clinical examination, (5) practice guidelines, and (6) surgery. The Cochrane Collaboration had no reviews of imaging for headache.

Discussion of Issues

Which Adults with New-Onset Headache Should Undergo Neuroimaging?

Summary
The most common causes of secondary headache in adults are brain neoplasms, aneurysms, arteriovenous malformations, intracranial infections, and sinus disease. History and physical examination findings may increase the yield of the diagnostic study discovering an intracranial space-occupying lesion in adults. Table 24.2 shows the scenarios that should warrant further diagnostic testing (limited evidence) [8, 10, 25]. The factors outlined in Table 24.2 increase the pretest probability of finding a secondary headache disorder.

What Neuroimaging Approach Is Most Appropriate in High-Risk Adults with New Onset of Headache?

Summary
CT examination studies have been the standard of care for the initial evaluation of acute-onset headache because CT is faster, more readily available, less costly than MR imaging, and less invasive than lumbar puncture [10]. In addition, CT has a higher sensitivity than MR imaging for acute subarachnoid hemorrhage (SAH) [26, 27]. The data reviewed demonstrate that 11 % to 21 % of patients presenting with new-onset headache have serious intracranial pathology (moderate and limited evidence) [10, 28–30]. Unless further data becomes available that demonstrates higher sensitivity of MR imaging, CT study is recommended in the assessment of all patients who present with new-onset headache (limited evidence) [10]. Lumbar puncture is recommended in those patients in which the CT scan is normal or nondiagnostic and the clinical evaluation reveals abnormal neurologic findings or in those patients in whom SAH is strongly suspected (limited evidence) [10]. Figure 24.1 shows a suggested decision tree to evaluate adult patients with acute-onset headache.

Supporting Evidence
Duarte and colleagues [28] studied 100 consecutive patients over a 1-year period (moderate evidence): Inclusion criteria were patients admitted to the neurology unit with recent onset of headache. Recent onset of headache was defined by the authors as persistent headache of less than 1 year's duration. All the patients studied had an unenhanced and enhanced head CT. Lumbar puncture, MR imaging, and MR angiogram were performed in selected cases. Tumors were identified in 21 % of the patients, which comprised 16 % of the patients with a negative neurologic examination.

A smaller-scale prospective study examined the association of acute headache and SAH (limited evidence) [29]. All patients were examined using state-of-the art CT scanner technology. Patients had a mean headache duration of approximately 72 h [29]. Of the 27 patients studied, 20 had a negative CT and 4 were diagnosed with SAH. Among the remaining 3 patients, 1 had a frontal meningioma, another had a hematoma associated with SAH, and the other had diffuse meningeal enhancement caused by bacterial meningitis. Lumbar puncture was performed in 19 of the patients with negative CT, yielding 5 additional cases of SAH. Hence, CT did not demonstrate SAH in 5 of 9 patients.

A retrospective study of 1,111 patients with acute headache who had CT evaluation revealed 120 (10.8 %) abnormalities, including hemorrhage, infarct, or neoplasm (limited evidence) [30]. All imaging studies were done at two teaching institutions over a 3-year period. There were statistical differences in the percentage of intracranial lesions based on the setting in which the CT was ordered. The inpatient rate (21.2 %) was twice that of emergency patients (11.7 %) and three times more than for outpatients (6.9 %; P < 0.005). Of 155 CT studies performed for headache as the sole presenting symptom (13.9 %), 9 (5.8 %) patients had acute intracranial abnormalities. One study in the outpatient setting that studied 1,284 patients with new headaches found no serious intracranial disease (limited evidence) [7]. The difference in prevalence of disease between emergency patients, inpatients, and outpatients is probably related to patient selection bias.

A study was conducted on 256 adult patients (median age 45 +/− 18 years, range 18–93) presenting to 8 emergency departments of the Emilia-Romagna region in Italy for nontraumatic headache (NTH) as the chief complaint over a period of 30 days [31]. Noncontrast head CT was performed on all nonpregnant patients. An analysis comparing scenarios 1, 2, and 3 versus scenario 4 was performed based on 180 patients who completed the follow-up telephone interview at least 3 months after the ED visit. The authors of this study concluded that a simple diagnostic algorithm can be used to distinguish malignant headaches (scenarios 1, 2, 3) from benign headaches (scenario 4). This algorithm showed a sensitivity of 100 % (95 % CI, 81–100 %) and a specificity of 64 % (95 % CI, 56–71 %). The likelihood ratio for a positive test was 2.67 (95 % CI, 2.15–3.31 %) and the likelihood ratio for a negative test was 0.04 (95 % CI, 0.003–0.64 %). This algorithm could therefore be used by emergency department physicians as a risk stratification tool:

Scenario 1: Adult patients admitted to ED for severe headache ("worst headache")
- With acute onset (thunderclap headache) or
- With neurologic signs (or nonfocal as decreased level of consciousness) or
- With vomiting or syncope at the onset of headache

Scenario 2: Adult patients admitted to ED for severe headache with fever and/or neck stiffness

Scenario 3: Adult patients admitted to ED for
- Headache of recent onset (days or weeks) or
- Progressively worsening headache, or persistent headache

Scenario 4: Adult patients with a previous history of headache
- Complaining of a headache very similar to previous attacks in terms of intensity, duration, and associated symptoms [31]

What Is the Role of Neuroimaging in Adults with Migraine or Chronic Headaches?

Summary
Most of the available literature (moderate and limited evidence) suggests that there is no need for neuroimaging in patients with migraine and normal neurologic examination. Neuroimaging is indicated in patients with nonacute headache and unexplained abnormal neurologic examination or in patients with atypical features or headache that does not fulfill the definition of migraine. A few studies have shown significant lesions in few patients (0.7–1.4 %) with chronic headaches and normal neurologic exam (moderate and limited evidence).

Supporting Evidence
Evidence-based guidelines on the use of diagnostic imaging in patients presenting with migraine have been developed by a multispecialty group called the US Headache Consortium [32]. Data were examined from 28 studies (moderate and limited evidence): six nonblinded prospective and 22 retrospective studies. The specific recommendations from the US Headache Consortium are as follows: (1) Neuroimaging should be considered in patients with nonacute headache and unexplained abnormal findings on the neurologic examination. (2) Neuroimaging is not usually warranted in patients with migraine and normal findings on neurologic examination. (3) A lower

threshold for CT or MRI may be applicable in patients with atypical features or with headache that does not fulfill the definition of migraine.

The study by Joseph and colleagues (limited evidence) [33] in 48 headache patients revealed 5 patients with neoplasms and 1 patient with an arteriovenous malformation. Of these patients, 5 had physical examination signs and 1 had headache on exertion. Weingarten and colleagues (limited evidence) [34] extrapolated data from 100,800 adult patients enrolled in a health maintenance organization and estimated that, in patients with chronic headache and a normal neurologic examination, the chance of finding abnormalities on CT requiring neurosurgical intervention was as low as 0.01 % (1 in 10,000).

In 1994, the American Academy of Neurology provided a summary statement on the use of neuroimaging in patients with headache and a normal neurologic examination based on a review of the literature (moderate and limited evidence) [35]. They concluded that routine imaging "in adult patients with recurrent headaches that have been defined as migraine – including those with visual aura – with no recent change in pattern, no history of seizures, and no other focal neurologic signs of symptoms is not warranted" [10]. This statement was based on a 1994 literature review by Frishberg [36] of 17 articles published between 1974 and 1991 that were limited to studies with more than 17 subjects per study (moderate evidence). All patients had normal neurologic examinations. Of 897 CT or MR imaging studies performed in patients with migraine, only three tumors and one arteriovenous malformation were noted, resulting in a yield of 0.4 % (4 in 1,000). The summary statement mentions, however, that "patients with atypical headache patterns, a history of seizure, or focal neurological signs or symptoms, CT or MRI may be indicated" [10, 35].

In another study with 402 inpatients imaged (70 plain CT, 292 contrast-enhanced CT, 40 both) for chronic headaches (defined as recurrent headache ranging from 6 months to several years), only 1.4 % scans showed significant lesions such as osteomas, low-grade glioma, and aneurysm [37].

The medical records and MR images of 402 adult patients with chronic headache (duration of 3 months or more) who had been evaluated by the neurology service and were found to have no other neurologic symptoms/findings were retrospectively reviewed and divided into negative or positive. The major abnormalities found in 15 (3.7 %) patients were glioma, meningioma, metastases, subdural hematoma, arteriovenous malformation, hydrocephalus (three patients), and Chiari I malformation (two patients). These abnormalities were found in 0.6 % of patients who had migraine, 1.4 % of those who had tension headaches, 14.1 % of those who had atypical headaches, and 3.8 % of those who had other types of headaches [38]. A retrospective review was performed of the MR images of 306 patients (195 patients had contrast, 23 patients had repeated imaging) with chronic (duration of 1 month or more) or recurrent headaches without prior head surgery, head trauma, or seizure, and normal neurologic findings. 55.2 % had no abnormalities, 44.1 % had minor abnormalities, and 0.7 % (2) had clinically significant abnormalities (pituitary macroadenoma and subdural hemorrhage) [39]. Another study reviewed 1,876 patients (>15 years old, mean age 38 years) referred to two neurology clinics in Spain with headache starting at least 4 weeks previously and 99.2 % with normal neurologic exams. One-third of the headaches were new onset, and two-thirds were present for more than 1 year. Headaches included migraine (49 %), tension (35.4 %), cluster (1.1 %), posttraumatic (3.7 %), and indeterminate (10.8 %). CT imaging was performed in 1,432 patients, MRI in 580, and 136 patients had both. 22 patients (1.2 %, 95 % CI 0.7, 1.8) had "significant abnormalities" on neuroimaging, and neurologic examination was normal in 17 of these patients. The findings in these 17 included pituitary adenoma (3), large arachnoid cyst (2), meningioma (2), hydrocephalus (2), Arnold-Chiari type I malformation (1), ischemic stroke (1), cavernous angioma (1), arteriovenous malformation (1), low-grade astrocytoma (1), brain stem glioma (1), colloid cyst (1), and posterior fossa papilloma (1). The rate of significant intracranial abnormalities in patients with headache and normal neurologic exam was 0.9 % (95 % CI 0.5, 1.4) [40].

What Is the Recommended Neuroimaging Examination in Adults with Headache and Known Primary Neoplasm Suspected of Having Brain Metastases?

Summary

In patients older than 40 years with known primary neoplasm, brain metastasis is a common cause of headache [41]. Most studies described in the literature suggest that contrast-enhanced MR imaging is superior to contrast-enhanced CT in the detection of brain metastatic disease, especially if the lesions are less than 2 cm (moderate evidence). In patients with suspected metastases to the central nervous system, enhanced brain MR imaging is recommended.

Supporting Evidence

Davis and colleagues (moderate evidence) [42] studied comparative imaging studies in 23 patients who had contrast-enhanced MR and double-dose-delayed CT. Contrast-enhanced MR imaging demonstrated more than 67 definite or typical brain metastases. The double-dose-delayed CT revealed only 37 metastatic lesions. The authors concluded that MR imaging with enhancement is superior to double-dose-delayed CT scan for detecting brain metastasis, anatomic localization, and number of lesions.

Golfieri and colleagues [43] reported similar findings (moderate evidence). They studied 44 patients with small cell carcinoma to detect cerebral metastases. All patients were studied with contrast-enhanced CT scan and gadolinium-enhanced MR imaging. Of all patients, 43 % had cerebral metastases. Both contrast-enhanced CT and gadolinium-enhanced MR imaging detected lesions greater than 2 cm. For lesions less than 2 cm, 9 % were detected only by gadolinium-enhanced T1-weighted images. The authors concluded that gadolinium-enhanced T1-weighted images remain the most accurate technique in the assessment of cerebral metastases. A study by Sze and colleagues [44] performed prospective and retrospective studies in 75 patients (moderate evidence). In 49 patients, MR imaging and contrast-enhanced CT were equivalent. In 26 patients, however, results were discordant, with neither CT nor MR imaging being consistently superior. MR imaging demonstrated more metastases in 9 of these 26 patients. Contrast-enhanced CT, however, better depicted lesions in 8 of 26 patients.

When Is Neuroimaging Appropriate in Children with Headache?

Summary

Determination of the appropriateness of imaging is made based on the frequency, pattern, family history, and associated seizure or neurologic findings (Table 24.3) (moderate evidence). These guidelines reinforce the primary importance of careful acquisition of the medical history and performance of a thorough examination, including a detailed neurologic examination [45]. Among children at risk for brain lesions based on these signs and symptoms, neuroimaging with either MR or CT is valuable in combination with close clinical follow-up (Fig. 24.2).

Supporting Evidence

In 2002, the American Academy of Neurology and Child Neurology Society published evidence-based neuroimaging recommendations for children [46]. Six studies (one prospective and five retrospective) met inclusion criteria (moderate evidence). Data on 605 of 1,275 children with recurrent headache who underwent neuroimaging found only 14 (2.3 %) with nervous system lesions that required surgical treatment. All 14 children had definite abnormalities on neurologic examination. The recommendations from this study were as follows: (1) Neuroimaging should be considered in children with an abnormal neurologic examination or other physical findings that suggest CNS disease. Variables that predicted the presence of a space-occupying lesion included (a) headache of less than 1-month duration, (b) absence of family history of migraine, (c) gait abnormalities, and (d) occurrence of seizures. (2) Neuroimaging is not indicated in children with recurrent headaches and a normal neurologic examination. (3) Neuroimaging should be

considered in children with recent onset of severe headache, change in the type of headache, or if there are associated features suggestive of neurologic dysfunction.

Medina and colleagues [45] performed a 4-year retrospective study of 315 children with no known underlying CNS disease who underwent brain imaging for a chief complaint of headache (moderate evidence). All patients underwent brain MR imaging; 69 patients also underwent brain CT. Clinical data were correlated with findings from MR imaging and CT, and the final diagnosis, using logistic regression. Thirteen (4 %) patients had surgical space-occupying lesions, including nine malignant neoplasms, three hemorrhagic vascular malformations, and one arachnoid cyst.

In this study, they identified seven independent multivariate predictors of a surgical lesion, the strongest of which were sleep-related headache (odds ratio 5.4, 95 % CI: 1.7–17.5) and no family history of migraine (odds ratio 15.4, 95 % CI: 5.8–41.0). Other predictors included vomiting, absence of visual symptoms, headache of less than 6 months' duration, confusion, and abnormal neurologic examination findings. The risk of a surgical lesion increased with the increased number of these factors present (P < 0.0001). No difference between MR imaging and CT was noted in detection of surgical space-occupying lesions, and there were no false-positive or false-negative surgical lesions detected with either modality on clinical follow-up.

In a study by Schwedt and colleagues of 241 pediatric patients with headache who had MRI or CT, 23 patients (9.5 %) had findings requiring a change in management [47] (limited to moderate evidence). These included 5 sinus disease, 4 tumors, 4 old infarcts, 3 Chiari I, 2 moyamoya, 1 intracranial vascular stenosis, 1 internal jugular vein occlusion, 1 arteriovenous malformation, 1 demyelinating disease, and 1 intracerebral hemorrhage. When sinus disease was excluded, 3 patients (1.2 %) with normal neurologic symptoms and signs had imaging findings that resulted in a change in management (limited to moderate evidence).

What Is the Sensitivity and Specificity of CT and MR Imaging for Space-Occupying Lesions?

Summary

Sensitivity and specificity of MR imaging is greater than CT for intracranial lesions. For surgical intracranial space-occupying lesions, however, there is no difference between MR imaging and CT in diagnostic performance (moderate evidence). The use of intravenous contrast material after unenhanced CT of the brain in children did not frequently change the diagnosis (moderate evidence).

Supporting Evidence

Sensitivity and specificity of CT and MR imaging for intracranial lesions is shown in Table 24.4. Medina and colleagues (moderate evidence) [45] showed that the overall sensitivity and specificity with MR imaging (92 % and 99 %, respectively) were higher than with CT (81 % and 92 %, respectively). Comparison of patients who underwent both MR imaging and CT revealed no significant disagreement between the tests for surgical space-occupying lesions (McNemar test, P = 0.75). The US Headache Consortium evidence-based guidelines from systematic review of the literature similarly concluded that MR imaging may be more sensitive than CT in identifying clinically insignificant abnormalities, but MRI imaging may be no more sensitive than CT in identifying clinically significant pathology [32].

A recent study performed by Branson et al. in 353 children with unenhanced and enhanced CT demonstrated that unenhanced CT of developing brains has high sensitivity and specificity in the diagnosis of pathologic findings [38]. Sensitivity, specificity, positive predictive value, and negative predictive value for unenhanced scans were 97 %, 89 %, 87 %, and 97 %, respectively [48]. The use of contrast material led to a change in the original normal or equivocal diagnosis to an abnormal diagnosis for only five (2.7 %) of the 183 normal unenhanced scans. Therefore, the use of intravenous contrast material after unenhanced CT of the brain in children did not frequently change the diagnosis [48].

What Is the Sensitivity and Specificity of CT and MRI for Detecting an Intracranial Aneurysm in Patients with Headache and Subarachnoid Hemorrhage?

Summary

Chapter 14 Intracranial Aneurysms provides a comprehensive discussion on this topic. In North America, 80–90 % of nontraumatic subarachnoid hemorrhage (SAH) in older children and adults is caused by the rupture of intracranial aneurysms [49]. CT angiography (CTA) and MR angiography (MRA) have sensitivities greater than 85 % for aneurysms greater than 5 mm. Most recent studies with newer generations of multidetector CT report sensitivity and specificity greater than 90 % for aneurysms greater than 4 mm (moderate evidence). Studies that have compared CTA and digital subtraction angiography (DSA) report similar sensitivities and specificities (moderate evidence). The sensitivity of CTA and MRA examinations drops significantly for aneurysms less than 5 mm. Thereby, DSA remains the current gold standard for evaluation of a ruptured intracranial aneurysm.

Supporting Evidence

White et al. [50] searched the literature from 1988 through 1998 to find studies with ten or more subjects in which the conventional angiography results were compared with noninvasive imaging. They included 38 studies which scored more than 50 % on evaluation criteria by using intrinsically weighted standardized assessment to determine suitability for inclusion (moderate evidence). The rates of aneurysm accuracy for CTA and MRA were 89 % and 90 %, respectively. The study showed greater sensitivity for aneurysms larger than 3 mm than for aneurysms smaller than 3 mm for CTA (96 % vs. 61 %) and for MRA (94 % vs. 38 %).

White et al. [51] also performed a prospective blinded study in 142 patients who underwent DSA to detect aneurysms (moderate evidence). Results were compared with CTA and MRA.

The accuracy rates per patient for the best observer were 87 % and 85 % for CTA and MRA, respectively. The accuracy rates for brain aneurysm for the best observer were 73 % and 67 % for CTA and MRA, respectively. The sensitivity for the detection of aneurysms 5 mm or larger was 94 % for CTA and 86 % for MRA. For aneurysms smaller than 5 mm, sensitivities for CTA and MRA were 57 % and 35 %, respectively.

More recent studies using CTA have shown even higher sensitivity and specificity, which may reflect technological improvements. Uysal and colleagues using spiral CT in 32 cases with aneurysm size from 3 to 13 mm [52] reported a sensitivity of 97 % and specificity of 100 % (limited evidence). Teksam and colleagues studied 100 consecutive patients with 113 aneurysms with multidetector CT (MDCT) [53] and reported a sensitivity for detecting aneurysms of less than 4 mm, 4–10 mm, and greater than 10 mm on a per aneurysm basis of 84 %, 97 %, and 100 %, respectively (moderate evidence). The overall specificity was 88 %. Using CTA with three-dimensional techniques in 82 consecutive patients [54], Karamessini and colleagues demonstrated a sensitivity of 89 % and specificity of 100 % for CTA and sensitivity of 88 % and specificity of 98 % for DSA when compared with the reference standard of surgical findings (moderate evidence). Therefore, CTA was equivalent to DSA. Tipper and colleagues' study reported using 16-row MDCT in 57 patients with 53 aneurysms [55] and found a sensitivity and specificity of 96.2 % and 100 % for both CTA and DSA, respectively (moderate evidence). In this study, the mean diameter of the aneurysm was 6.3 mm with a range of 1.9–28.1 mm [30]. A study published by Taschner and colleagues [56] in 2007 in 27 consecutive patients with 24 aneurysms using a 16-row multisection CTA reported an overall sensitivity and specificity of 100 % and 83 %, respectively (limited evidence). Papke and colleagues compared DSA with 16-row CTA in 87 patients [57] and reported a sensitivity and specificity of 98 % and 100 %

for DSA and CTA, respectively (moderate evidence). Yoon and colleagues using 16-row multidetector CTA in 85 patients [58] had overall sensitivity and specificity of 92.5 % and 93.3 %, respectively (moderate evidence). For aneurysms less than 3 mm, however, sensitivity decreased for reader 1 and reader 2 to 74.1 % and 77.8 %, respectively (Yoon). A more recent study performed by Lubicz and colleagues [49] in 54 consecutive patients with 67 aneurysms using a 64-row multisection CTA reported an overall sensitivity and specificity of 94 % and 90.2 %, respectively (moderate evidence). For aneurysms less than 3 mm, CTA had a mean sensitivity of 70.4 % [59]. Intertechnique and interobserver agreements were good for aneurysm detection with a mean kappa of 0.673 [59]. Agid and colleagues [60] studied 73 patients with 47 aneurysms using a 64-row multisection CTA and reported an overall sensitivity and specificity of 98 % and 98 %, respectively (moderate evidence).

What Is the Role of Advanced Imaging Techniques in Primary Headache Disorders?

Summary

High-resolution MR technique using transverse relaxation rates has demonstrated increased tissue iron levels in the brain stem (periaqueductal gray, red nuclei, and substantia nigra) in patients with headache disorders (limited evidence). Functional MR has demonstrated activation of the red nuclei and substantia nigra in patients during spontaneous migraine episodes (limited evidence) [61, 62]. Patients with migraine disorders also have activation in the dorsolateral pons both on PET and functional MRI (limited evidence) [63–67]. In cluster headache disorders, MR phosphorus spectroscopy (31P-MRS) has demonstrated brain mitochondrial dysfunction (limited evidence) [68, 69]. PET has demonstrated strong activation in the hypothalamic gray matter in acute cluster headache attacks (limited evidence) [70]. In contrast to migraine disorders, there is no brain stem activation during acute cluster headache episodes compared with the resting state [71]. These initial studies suggest that, although primary headaches such as migraine and cluster headache may share a common pain pathway – the trigeminovascular innervation – their underlying pathogenesis differs significantly [68].

Supporting Evidence

The underlying pathophysiology of migraine disorders is not well understood [72]. Conventional CT and MRI studies are usually normal with no evidence of a structural lesion. Studies have shown involvement of the nociceptive pathways in chronic daily headaches and migraines [72]. A study performed by Raskin and colleagues [73] revealed migraine-like headaches in patients with electrodes implanted in the periaqueductal gray (PAG) matter. The ventral brain stem has also been identified to be involved in migraine disorders [73]. Reports of multiple sclerosis plaque [74] and cavernous malformation [75] involving the PAG and causing migraine-like disorders have been reported. Imaging studies have been performed to study the iron homeostasis in the midbrain. High-resolution MR techniques have been used to map the transverse relaxation rates R2 (1/T2), R2* (1/T2*), and R2′ (R2*-R2) in the PAG, red nuclei (RN), and substantia nigra (SN) [76]. A positive correlation (r = 0.80; P < 0.006) was identified between the duration of illness and the increase in R2′ (increased tissue iron levels) for patients with episodic migraine disorders and chronic daily headaches [76, 77] (limited evidence).

Another study by Kruit and colleagues [78] in patients studied in a 1.5 T MR scanner revealed higher iron concentrations in the RN and putamen in patients with migraines (limited to moderate evidence). Functional MR has demonstrated activation of the RN and SN in patients during spontaneous migraine episodes (limited evidence) [61, 62].

In cluster headache, in vivo MR phosphorus spectroscopy (31P-MRS) has demonstrated brain mitochondrial dysfunction characterized by reduced phosphocreatine levels, an increased ADP concentration, and a reduced phosphorylation potential (limited evidence) [68, 69]. In a study of nine patients, PET demonstrated strong activation in the hypothalamic gray matter in acute cluster headache attacks (limited evidence) [70]. In contrast to migraine disorders, there is no brain stem activation during acute cluster headache episodes compared with the resting state [71].

PET demonstrates activation in the rostral brainstem, i.e., the dorsolateral pons, which lateralizes with the attack in both infrequent and frequent migraines. These changes persist after successful treatment of the attack but are not present interictally and are not seen in other primary headaches [63–67]. MR angiography has shown that blood flow changes do not cause migraine and cluster headaches; blood flow changes are a result of ophthalmic division pain. Functional neuroimaging performed on patients with typical migraine triggered by glyceryl trinitrate has shown that the changes in the dorsolateral pons lateralize with the migraine attack, suggesting that this portion of the brain is pivotal in the phenotypic expression of migraines. Again, these pontine changes persisted after resolution of the pain with a triptan and were not present interictally. When dull bilateral headache was induced by glyceryl trinitrate in controls and migraineurs, the pontine change was not seen. Further study is needed, but these findings demonstrate that migraine is a disorder localized in the brain with pontine representation [63, 67, 79, 80].

What Is the Cost-effectiveness of Neuroimaging in Patients with Headache?

Summary

No well-designed cost-effectiveness analysis (CEA) in adults could be found in the literature.

A CEA study [81] assessed the clinical and economic consequences of three diagnostic strategies in the evaluation of children with headache suspected of having a brain tumor: MR imaging, CT followed by MR imaging for positive results (CT-MR imaging), and no neuroimaging with close clinical follow-up [81]. This model suggests that MR imaging maximizes quality-adjusted life years (QALY) gained at a reasonable cost-effectiveness ratio in patients at high risk of having a brain tumor. Conversely, the strategy of no imaging with close clinical follow-up is cost saving in low-risk children. Although the CT-MR imaging strategy maximizes QALY gained in the intermediate-risk patients, its additional cost per QALY gained is high. In children with headache, appropriate selection of patients and diagnostic imaging strategies may maximize quality-adjusted life expectancy and decrease costs of medical workup.

Supporting Evidence

A CEA in children with headaches has been published in Pediatrics [81]. A decision-analytic Markov model and CEA were performed incorporating the risk group pretest probability, MR imaging and CT sensitivity and specificity, tumor survival, progression rates, and cost per strategy. Outcomes were based on QALY gained and incremental cost per QALY gained.

The results were as follows: For low-risk children with chronic nonmigraine headaches of more than 6 months' duration as the sole symptom (pretest probability of brain tumor was 0.01 % [1 in 10,000]), close clinical observation without neuroimaging was less costly and more effective than the two neuroimaging strategies. For the intermediate-risk children with migraine headache and normal neurologic examination (pretest probability of brain tumor was 0.4 % [4 in 1,000]), CT-MR imaging was the most effective strategy but cost more than $1 million per QALY gained compared with no neuroimaging. This cost is not typically justified by health policy makers. For high-risk children with headache of less than 6 months' duration

and other clinical predictors of a brain tumor, such as an abnormal neurologic examination (pretest probability of brain tumor was 4 % [4 in 100]), the most effective strategy was MR imaging, with a cost-effectiveness ratio of $113,800 per QALY gained compared with no imaging.

The cost-effectiveness ratio in the high-risk children with headache is in the comparable range of annual mammography for women aged 55–64 years at $110,000 per life year saved [82], colonoscopy for colorectal cancer screening for persons older than 40 years at $90,000 per life year saved [82, 83], and annual cervical cancer screening for women beginning at age 20 years at $220,000 per life year saved [82, 84]. Therefore, this CEA model supports the use of MR imaging in high-risk children.

Take-Home Tables and Figures

Tables 24.1 through 24.4 highlight data and guidelines.

Figures 24.1 and 24.2 show algorithms for use in adults and children with headaches.

Imaging Case Studies

Case 1: Colloid Cyst: Patient Presented with Headache and Vomiting (Fig. 24.3a, b)

Case 2: Chiari I: Patient Presented with Persistent Headaches Triggered by Cough or Exertion (Valsalva Maneuver) (Fig. 24.4a, b)

Table 24.1 Common causes of primary and secondary headache

Primary headaches
Migraine
Cluster
Tension type
Secondary headaches
Intracranial space-occupying lesions
Neoplasm
Arteriovenous malformation
Abscess
Hematoma
Cerebrovascular disease
Intracranial aneurysms
Occlusive vascular diseases (such as dissections, vasculitis, venous stenosis, and thrombus)
Infection
Acute sinusitis
Meningitis
Encephalitis
Inflammation
Vasculitis
Acute disseminated encephalomyelitis
Increased intracranial pressure
Hydrocephalus
Idiopathic intracranial hypertension (pseudotumor cerebri)

(Reprinted with kind permission of Springer Science+Business Media from Medina LS, Shah A, Vasconcellos E. Adults and children with headache: evidence-based role of neuroimaging. In Medina LS, Blackmore CC, editors. Evidence-based imaging: optimizing imaging in patient care. New York: Springer; 2006)

Table 24.2 Suggested guidelines for neuroimaging in adult patients with new-onset headache

"First or worst" headache (thunderclap headache)
Increased frequency and increased severity of headache
New-onset headache after age 50
New-onset headache with history of cancer or immunodeficiency
Headache with fever, neck stiffness, and meningeal signs
Headache with abnormal neurologic examination or nonfocal as decreased level of consciousness
Headache with vomiting or syncope at the onset

(Reprinted with kind permission of Springer Science +Business Media from Medina LS, Shah A, Vasconcellos E. Adults and children with headache: evidence-based role of neuroimaging. In Medina LS, Blackmore CC, editors. Evidence-based imaging: optimizing imaging in patient care. New York: Springer; 2006)

Table 24.4 Diagnostic sensitivity and specificity of CT and MR imaging

Variable	Baseline %	Range %	Reference
Diagnostic tests			
MR imaging			
Sensitivity	92	82–100	[35, 68, 69]
Specificity	99	81–100	[35, 69]
CT			
Sensitivity	81	65–100	[35, 68, 69]
Specificity	92	72–100	[35, 68, 69]

(Reprinted with kind permission of Springer Science +Business Media from Medina LS, Shah A, Vasconcellos E. Adults and children with headache: evidence-based role of neuroimaging. In Medina LS, Blackmore CC, editors. Evidence-based imaging: optimizing imaging in patient care. New York: Springer; 2006)

Table 24.3 Suggested guidelines for neuroimaging in pediatric patients with headache

Persistent headaches of less than 6 months' duration
Headache associated with abnormal neurologic examination
Headache associated with seizures
Recent onset of severe headache or change in the type of headache
Persistent headache without family history of migraine
Headaches that persistently awaken a child from sleep or occur immediately on awakening
Family or medical history of disorders that may predispose one to CNS lesions and clinical or laboratory findings that suggest CNS involvement

(Reprinted with permission from Medina et al. [45])

Case 3: Brain Stem Infiltrative Glial Neoplasm: Patient Present with Ataxia and Headaches (Fig. 24.5a, b)

Suggested Protocols

1. CT imaging [85, 86]
   (a) CT without contrast. Axial 5–10-mm nonspiral images should be used to assess for subarachnoid hemorrhage, tumor hemorrhage, or calcifications.

   In infants and toddlers, axial 2.5–5-mm sections are recommended.

   (b) CT with contrast. Axial 5–10-mm nonspiral enhanced images should be used in patients with suspected neoplasm, infection, or other focal intracranial lesion. If indicated, CT angiography can be performed as part of the enhanced CT. Contrast-enhanced CT angiography should ideally be done in a multidetector CT scanner with multiplanar and 3D reconstructions.

2. MR imaging [85, 86]

   Basic brain MR protocol sequences include sagittal T1-weighted conventional spin-echo (repetition time, 600 ms; echo time 11 ms [600/11]), axial proton density-weighted conventional or fast spin-echo (2,000/15), axial T2-weighted conventional or fast spin-echo (3,200/85), axial FLAIR (fluid attenuation inversion recovery) spin-echo (8,800/152, inversion time [TI] 2,200 ms), and coronal T2-weighted fast spin-echo (3,200/85) images. In patients with suspected neoplasm, infection, or focal intracranial lesions, gadolinium-enhanced T1-weighted conventional spin-echo (600/11) images should be acquired in at least two planes. If MR angiogram is indicated, then a 3D time-of-flight study of the circle of Willis should be performed. Consideration should be given to
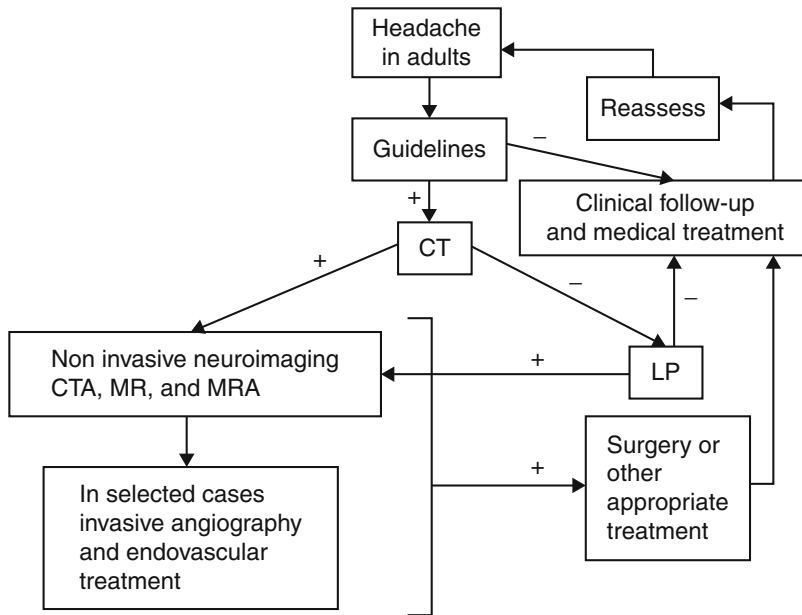
Fig. 24.1 Decision tree for use in adults with new-onset headache. For those patients who meet any of the guidelines in Table 24.2, CT is suggested. For patients who do not meet these criteria or those with negative diagnostic (Box 2). For patients who do not meet these criteria or those with negative workup, clinical observation with periodic reassessment is recommended. If CT is positive, further workup with CT angiography or MR imaging plus MR angiography is recommended. In selected case, conventional angiography and endovascular treatment may be warranted. If CT is negative, lumbar puncture is advised. In patients with suspected metastatic brain disease, contrast-enhanced MR imaging is recommended. In patients with suspected intracranial aneurysm, further assessment with CT angiography or MR angiography is warranted. *Abbreviations: CTA* CT angiography, *LP* lumbar puncture, *MRA* MR angiography, *MRI* MR imaging (Reprinted with permission from Medina et al. [41])
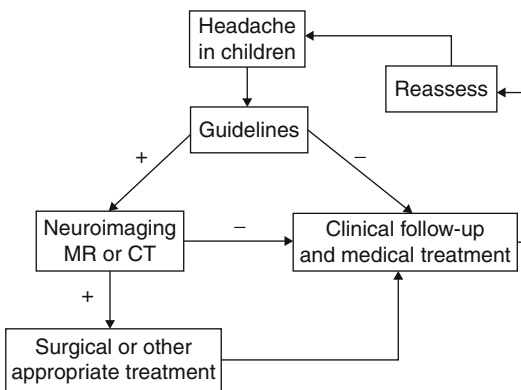

Fig. 24.2 Decision tree for use in children with headache disorder. Neuroimaging is suggested for patients who meet any of the signs or symptoms in the guidelines (Table 24.2). For patients who do not meet these criteria or those with negative findings from imaging studies, clinical observation with periodic reassessment is recommended (Reprinted with permission from Medina et al. [45])

complementing the MRA with a multiphase dynamic contrast-enhanced study to reduce potential flow artifacts and to assess arterial, capillary, and venous phases.

Future Research

- Large-scale prospective studies to validate risk factors and prediction rules of significant intracranial lesions in children and adults with headache
- Large diagnostic performance studies comparing the sensitivity, specificity, and ROC curves of neuroimaging in adults and children with headache
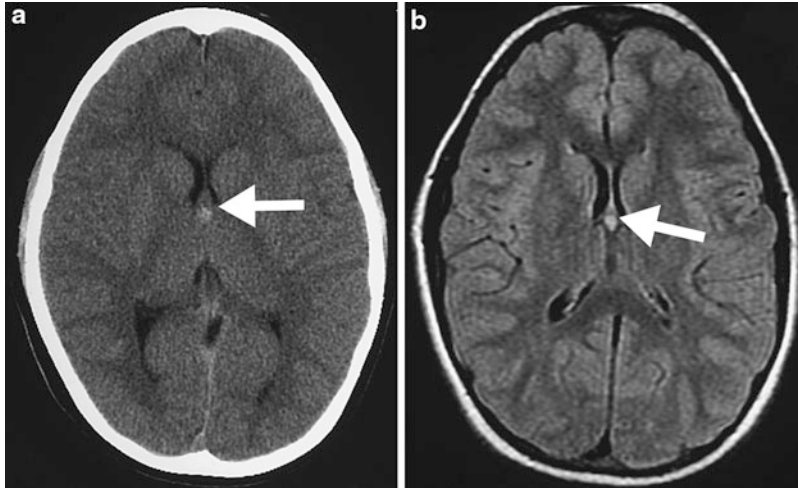- Cost-effectiveness analysis of neuroimaging in adults with headaches

Fig. 24.3 (**a**) Unenhanced CT shows a small focal lesion with increased density at the level of the foramen of Monro. (**b**) Axial FLAIR sequence reveals increased T2-weighted signal in the lesion. No hydrocephalus noted. Neuroimaging findings consistent with colloid cyst (Reprinted with kind permission of Springer Science+Business Media from Medina LS, Shah A, Vasconcellos E. Adults and children with headache: evidence-based role of neuroimaging. In Medina LS, Blackmore CC, editors. Evidence-based imaging: optimizing imaging in patient care. New York: Springer; 2006)

Fig. 24.4 (**a**) Unenhanced CT at craniocervical junction was interpreted as unremarkable. (**b**) Sagittal MRI T1-weighted image reveals pointed cerebellar tonsils extending more than 5 mm below the foramen magnum consistent with Chiari I. No cervical cord hydrosyrinx noted (Reprinted with kind permission of Springer Science+Business Media from Medina LS, Shah A, Vasconcellos E. Adults and children with headache: evidence-based role of neuroimaging. In Medina LS, Blackmore CC, editors. Evidence-based imaging: optimizing imaging in patient care. New York: Springer; 2006)
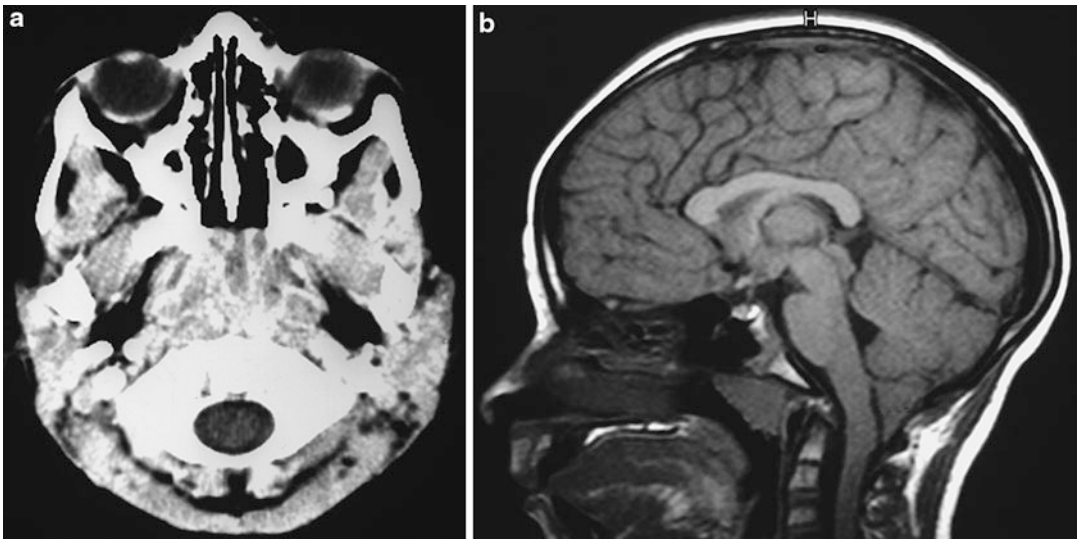
Fig. 24.5 (**a**) Unenhanced CT through posterior fossa is limited by beam-hardening artifact. A hypodense lesion is seen in the pons. (**b**) Axial proton density MR image better depicts the anatomy and extent of the lesion without artifact (Reprinted with kind permission of Springer Science +Business Media from Medina LS, Shah A, Vasconcellos E. Adults and children with headache: evidence-based role of neuroimaging. In Medina LS, Blackmore CC, editors. Evidence-based imaging: optimizing imaging in patient care. New York: Springer; 2006)
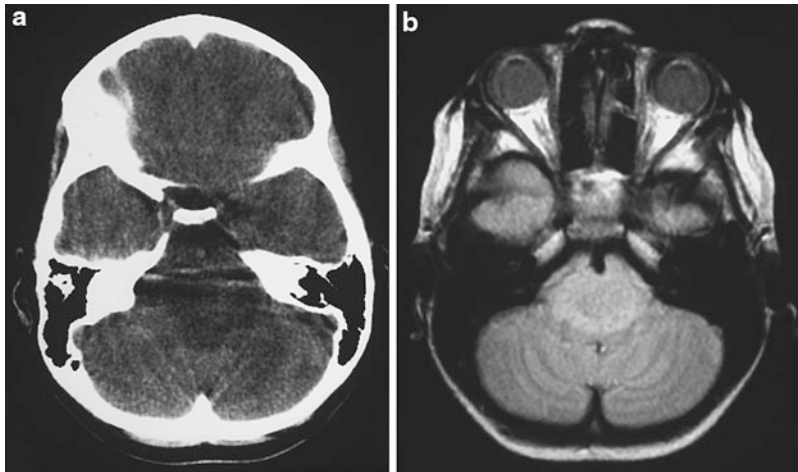
References

1. Headache Classification Subcommittee of the International Headache Society. Cephalalgia. 2004;24 (Suppl 1):1–160.
2. Rothner AS. Semin Pediatr Neurol. 1995;2:109–18.
3. Kuhn MJ, Shekar PC. Comput Med Imaging Graph. 1990;14:149–52.
4. Igarashi H, Sakai F, Kan S, et al. Cephalalgia. 1991;11:69–74.
5. de Benedittis G, Lorenzetti A, Sina C, et al. Headache. 1995;35:264–8.
6. Pavese N, Canapicchi R, Nuti A, et al. Cephalalgia. 1994;14:342–5.
7. Kruit MC, van Buchem MA, Hofman PA, et al. J Am Med Assoc. 2004;291:427–34.
8. Linet MS, Stewart WF, Celentano DD, et al. J Am Med Assoc. 1989;261:2211–16.
9. Silberstein SD. Headache. 1992;32:396–407.
10. Field AG, Wang E. Emerg Med Clin North Am. 1999;17:127–52.
11. Stewart WF, Lipton RB, Celentano DD, et al. JAMA. 1992;267:64–9.
12. Hale WE, May FE, Marks RG, et al. Headache. 1987;27:272–6.
13. Hutter A, Schwetye K, Bierhals A, McKinstry RC. Neuroimaging Clin N Am. 2003;13:237–50.
14. Bille BS. Acta Paediatr. 1962;51(Suppl. 136):1–151.
15. Honig PJ, Charney EB. Am J Dis Child. 1982;136:121–4.
16. The Childhood Brain Tumor Consortium. J Neurooncol. 1991;10:31–46.
17. Rorke L, Schut L. Introductory survey of pediatric brain tumors. In: McLaurin RL, editor. Pediatric neurosurgery. 2nd ed. Philadelphia: WB Saunders; 1989. p. 335–7.
18. Silverberg E, Lubera J. Cancer. 1986;36:9–23.
19. Roth-Isigkeit A, Thyen U, Stöven H, Schwarzenberger J, Schmucker P. Pediatrics. 2005;115:e152–62.
20. Peterson CC, Palermo DM. J Pediatr Psychol. 2004;29:331–41.
21. Pryse-Phillips W, Findlay H, Tugwell P, et al. Can J Neurol Sci. 1992;19:333–9.
22. Lipton RB, Stewart WF. Neurology. 1993;43:S6–10.
23. de Lissovoy G, Lazarus SS. Neurology. 1994;44(Suppl):S56–62.
24. Stang PE, Crown WH, Bizier R, Chatterton ML, White R. Am J Manag Care. 2004;10:313–20.
25. Evans RW. Med Clin North Am. 2001;85:865–85.
26. Prager JM, Mikulis DJ:
27. Edelman RR, Warach S. N Engl J Med. 1993;328:708–15.
28. Duarte J, Sempere AP, Delgado JA, et al. Acta Neurol Scand. 1996;94:67–70.
29. Lledo A, Calandre L, Martinez-Menendez B, et al. Headache. 1994;34:172–4.
30. Kahn CEJ, Sanders GD, Lyons EA, et al. Can Assoc Radiol J. 1993;44:189–93.
31. Grimaldi D, Nonino F, Cevoli S, et al. J Neurol. 2009;256:51–7.
32. Scott Morey S. Headache. Am Fam Physician. 2000;62:1699–701.
33. Joseph R, Cook GE, Steiner TJ, et al. Practitioner. 1985;229:477–81.

34. Weingarten S, Kleinman M, Elperin L, et al. Arch Intern Med. 1992;152:2457–62.
35. Quality Standards Subcommittee of the American Academy of Neurology. Neurology. 1994;44:1353–4.
36. Frishberg BM. Neurology. 1994;44(1):191–1197.
37. Dumas MD, Pexman W, Kreeft JH. Can Med Assoc J. 1994;151:1447–52.
38. Wang HZ, Simonson TM, Greco WR, et al. Acad Radiol. 2001;8:405–8.
39. Tsushima Y, Endo K. Radiology. 2005;235:575–9.
40. Sempere AP, Porta-Etessam J, Medrano V, et al. Cephalalgia. 2005;25:30–5.
41. Medina LS, D'Souza B, Vasconcellos E. Adults and children with headache: evidence-based diagnostic evaluation. Neuroimaging Clin N Am. 2003;13:225–35.
42. Davis PA, Hudgins PA, Peterman SB, et al. AJNR Am J Neuroradiol. 1991;12:293–300.
43. Golfieri R, Cherryman GR, Oliff JF, et al. Radiol Med (Torino). 1991;82:27–34.
44. Sze G, Shin J, Krol G, et al. Radiology. 1988;168:187–94.
45. Medina LS, Pinter JD, Zurakowski D, et al. Children with headache: clinical predictors of surgical space-occupying lesions and the role of neuroimaging. Radiology. 1997;202:819–24.
46. Lewis D, Ashwal S, Dahl G, et al. Neurology. 2002;51:490–8.
47. Schwedt TJ, Guo Y, Rothner AD. Headache. 2006;46(3):387–98.
48. Branson HM, Doria AS, Moineddin R, Shroff M. Radiology. 2007;244:838–44.
49. Gentry LR, Gordersky JC, Thopson BH. MR imaging. Radiology. 1989;171:177–87.
50. White PM, Wardlaw JM, Easton V. Radiology. 2000;217:361–70.
51. White PM, Teasdale EM, Wardlaw JM, et al. Radiology. 2001;219:739–49.
52. Uysal E, Yanbuloglu B, Erturk M, Kilinc BM, Basak M. Diagn Interv Radiol. 2005;11(2):77–82.
53. Teksam M, McKinney A, Asis M, et al. AJNR Am J Neuroradiol. 2004;25(9):1485–92.
54. Karamessini MT, Kagadis GC, Petsas T, et al. Eur J Radiol. 2004;49(3):212–23.
55. Tipper G, U-King-Im JM, Price SJ, Trivedi RA, et al. Clin Radiol. 2005;60(5):565–72.
56. Taschner CA, Thines L, Lernout M, et al. J Neuroradiol. 2007;34(4):243–9.
57. Papke K, Kuhl CK, Fruth M, et al. Radiology. 2007;244(2):532–40.
58. Yoon DY, Lim KJ, Choi CS, Cho BM, Oh SM, Chang SK. AJNR Am J Neuroradiol. 2007;28(1):60–7.
59. Lubicz B, Levivier M, Francois O, et al. AJNR Am J Neuroradiol. 2007;28(10):1949–55.
60. Agid R, Lee SK, Willinsky RA, Farb RI, ter Brugge KG. Neuroradiology. 2006;48(11):787–94.
61. Welch KMA, Cao Y, Aurora SK, et al. Neurology. 1998;51:1465–9.
62. Cao Y, Aurora SK, Vikingstad EM, et al. Neurology. 2002;59:72–8.
63. Goadsby PJ. Br Med J. 2006;332:25–9.
64. Afridi S, Giffin NJ, Kaube H, Friston KJ, Ward NS, Frackowiak RSJ, et al. Arch Neurol. 2005;62:1270–5.
65. Denuelle M, Fabre N, Payoux P, Chollet F, Gereud G. Cephalalgia. 2004;24:775–814.
66. Bahra A, Matharu MS, Buchel C, Frackowiak RSJ, Goadsby PJ. Lancet. 2001;357:1016–17.
67. Afridi S, Matharu MS, Lee L, Kaube H, Friston KJ, Frackowiak RSJ, et al. Brain. 2005;128:932–9.
68. May A, Goadsby PJ. Curr Opin Neurol. 1998;11(3):199–203.
69. Montagna P, Lodi R, Cortelli P. Neurology. 1997;48:113–18.
70. May A, Bahra A, Buchel C, Frackowiak RSJ, Goadsby PJ. Lancet. 1998;351:275–8.
71. Weiller C, May A, Limmroth V, Juptner M, Kaube H, van Schayck R. Nat Med. 1995;1:658–60.
72. Aurora SK. Curr Pain Headache Rep. 2003;7:209–11.
73. Raskin NH, Hosobuchi Y, Lamb S. Headache. 1987;27:416–20.
74. Haas DC, Kent PF, Friedman DI. Headache. 1993;33:452–5.
75. Goadsby PJ. Cephalgia. 2002;22:107–11.
76. Gelman N, Gorell JM, Barker PB, et al. Radiology. 1999;210:759–67.
77. Welch KMA, Nagesh V, Aurora SK, Gelman N. Headache. 2001;41:629–37.
78. Kruit MC, van Buchem MA, Overbosch J, et al. Cephalgia. 2002;22:571.
79. May A, Buchel C, Turner R, Frackowiak RSJ, Goadsby PJ. Cephalalgia. 1999;19:464–5.
80. May A, Buchel C, Turner R, Goadsby PJ. J Cereb Blood Flow Metab. 2001;21:1171–6.
81. Medina LS, Kuntz KM, Pomeroy SL. Pediatrics. 2001;108:255–63.
82. Tengs T, Adams M, Pliskin J, et al. Risk Anal. 1995;15:369–90.
83. England W, Halls J, Hunt V. Med Decis Making. 1989;9:3–13.
84. Eddy DM. Gynecol Oncol. 1981;12(2 Part 2):S168–87.
85. Haughton VM, Rimm AA, Sobocinski KA, et al. Radiology. 1986;160:751–5.
86. Orrison WJ, Stimac GK, Stevens EA, et al. Radiology. 1991;181:121–7.

Brain Cancer: Evidence-Based Neuroimaging

25

Soonmee Cha

Contents

S. Cha

Department of Radiology and Biomedical Imaging, University of California San Francisco Medical Center, San Francisco, CA, USA
e-mail: soonmee.cha@ucsf.edu

Key Points

- Brain imaging is necessary for optimal localization, characterization, and management of brain cancer prior to surgery in patients with suspected or confirmed brain tumors (strong evidence).
- Due to its superior soft tissue contrast, multiplanar capability, and biosafety, magnetic resonance imaging (MRI) with and without gadolinium-based intravenous contrast material is the preferred method for brain cancer imaging when compared to computed tomography (moderate evidence).
- No adequate data exist on the role of imaging in monitoring brain cancer response to therapy and differentiating between tumor recurrence and therapy-related changes (insufficient evidence).
- No adequate data exist on the role of nonanatomic, physiology-based imaging, such as proton MR spectroscopy, perfusion and diffusion MRI, and nuclear medicine imaging (SPECT and PET) in monitoring treatment response or in predicting prognosis and outcome in patients with brain cancer (insufficient evidence).
- Human studies conducted on the use of magnetic resonance spectroscopy (MRS) for brain tumors demonstrate that this noninvasive method is technically feasible and suggest potential benefits for some of the proposed indications. However, there is a paucity of high-quality direct evidence demonstrating the impact on diagnostic thinking and therapeutic decision making.
- There is added value of fMRI in the surgical planning of patients with suspected brain cancer or focal brain lesion (moderate evidence).

Definition and Pathophysiology

The term brain cancer, or more commonly referred to as brain tumor, is used here to describe all primary and secondary neoplasms of the brain and its covering, including the leptomeninges, dura, skull, and scalp. Brain cancer is comprised of a variety of central nervous system tumors with a wide range of histopathology, molecular/genetic profile, clinical spectrum, treatment possibilities, and patient prognosis and outcome. The pathophysiology of brain cancer is complex and dependent on various factors, such as histology, molecular and chromosomal aberration, tumor-related protein expression, primary versus secondary origin, and host factors [1–4].

Unique Challenges of Brain Cancer

When compared to systemic cancers (e.g., lung, breast, colon), brain cancer is unique in several different ways. First, the brain is covered by a tough, fibrous tissue dura mater and a bony skull that protects the inner contents. This rigid covering allows very little, if any, increase in volume of the inner content, and therefore, brain tumor cells adapt to grow in a more infiltrative rather than expansive pattern. This growth pattern limits the disruption to the underlying cytoarchitecture. Second, the brain capillaries have a unique barrier known as the blood–brain barrier (BBB), which limits the entrance of systemic circulation into the central nervous system. Cancer cells can hide behind the protective barrier of BBB, migrate with minimal disruption to the structural and physiologic milieu of the brain, and escape imaging detection since intravenous contrast agent becomes visible when there is BBB disruption, allowing the agent to leak into the interstitial space [5–9].

Epidemiology

Adult Brain Cancer

Primary malignant or benign brain cancers were estimated to be newly diagnosed in about 35,519 Americans in 2001 (CBTRUS, 2000). Primary brain cancers are among the top 10 causes of cancer-related deaths (American Cancer Society, 1998). Nearly 13,000 people die from these cancers each year in the USA (CBTRUS, 2000).

About 11–12 per 100,000 persons in the USA are diagnosed with a primary brain cancer each year, and 6–7 per 100,000 are diagnosed with a primary malignant brain cancer. Almost 1 in every 1,300 children will develop some form of primary brain cancer before age 20 years (CBTRUS, 1998). Between 1991 and 1995, 23 % of childhood cancers were brain cancers, and about one-fourth of childhood cancer deaths were from a malignant brain tumor.

The epidemiologic study of brain cancer is challenging and complex due to number of factors unique to this disease. First, primary and secondary brain cancers are vastly different diseases that clearly need to be differentiated and categorized, which is an inherently difficult task. Second, histopathologic classification of brain cancer is complicated due to the heterogeneity of the tumors at virtually all levels of structural and functional organization such as differential growth rate, metastatic potential, sensitivity irradiation and chemotherapy, and genetic liability. Third, several brain cancer types have benign and malignant variants with a continuous spectrum of biologic aggressiveness. It is therefore difficult to assess the full spectrum of the disease at presentation [10].

The most common primary brain cancers are tumors of neuroepithelial origin, which include astrocytoma, oligodendroglioma, mixed glioma (oligoastrocytoma), ependymoma, choroid plexus tumors, neuroepithelial tumors of uncertain origin, neuronal and mixed neuronal-glial tumors, pineal tumors, and embryonal tumors. The most common type of primary brain tumor that involves the covering of the brain (as opposed to the substance) is meningioma, which accounts for more than 20 % of all brain tumors [11]. The most common type of primary brain cancer in adults is glioblastoma multiforme (GBM). In adults, brain metastases far outnumber primary neoplasms owing to high incidence of systemic cancer (e.g., lung and breast carcinoma).

The incidence rate of all primary benign and malignant brain tumors based on the Central Brain Tumor Registry of the United States [12] is 14 cases per 100,000 person-years (5.7 per 100,000 person-years for benign tumors and 7.7 person-years for malignant tumors). The rate is higher in males (14.2 per 100,000 person-years) than females (13.9 per 100,000 person-years). According to the Surveillance, Epidemiology, and End Results (SEER), the 5-year relative survival rate following the diagnosis of a primary malignant brain tumor (excluding lymphoma) is 32.7 % for males and 31.6 % for females. The prevalence rate for all primary brain tumors based on CBTRUS is 130.8 per 100,000, and the estimated number of people living with a diagnosis of primary brain tumors was 359,000 persons. Two-, five-, and ten-year observed and relative survival rates for each specific type of malignant brain tumor, according to the SEER report from 1973 to 1996, showed that GBM has the poorest prognosis. More detailed information on the brain cancer survival data is available at the website of the Central Brain Tumor Registry of the United States (http://www.cbtrus.org/2001/table2001_12.htm).

In terms of brain metastases, the exact annual incidence remains unknown due to a lack of dedicated national cancer registry but is estimated to be 97,800–170,000 new cases each year in the USA. The most common types of primary cancer causing brain metastasis are cancers of the lung, breast, unknown primary, melanoma, and colon.

Pediatric Brain Cancer

The epidemiologic studies of brain cancer suggest that the incidence of pediatric brain cancer is rising, but the actual details remain unclear. There are two fundamental problems that might explain the difficulty in elucidating epidemiological changes in pediatric brain cancer. First, the definition and histopathological criteria for each type of primary pediatric brain cancer remain inconsistent and variable. Second, there is a lack of true brain cancer registry that is critical for monitoring incidence and epidemiology. Rather, data from nine registries have been compiled since 1973 by the National Cancer Institute as the SEER program and extrapolated to represent national data. These data demonstrate an overall

incidence of pediatric central nervous system cancer to be 3.5 per 100,000 children less than 15 years of age. Pediatric central nervous system cancers account for about 15–20 % of all childhood cancers and the peak age is 5–8 years old. There is no definitive evidence to suggest any gender or race predilection for pediatric brain tumors. An additional source of epidemiologic information is a report from the Central Brain Tumor Registry of the United States [12], a nonprofit agency organized for the purpose of collecting and publishing epidemiologic data for brain tumors (CBTRUS, 2002). Syndromes associated with central nervous system tumors are neurofibromatosis type 1 and 2, tuberous sclerosis type 1 and 2, von Hippel–Lindau syndrome, Li–Fraumeni syndrome, nevoid basal cell carcinoma, Turcot's syndrome, Gorlin syndrome, ataxia-telangiectasia syndrome, Gardner's syndrome, and Down syndrome [13]. The molecular genetics of pediatric brain tumors may provide valuable insights into the etiology and biology of these tumors, but the specific genetic alterations for tumor development in a majority of patients remain elusive.

The most common primary pediatric brain cancers are astrocytomas, which account for approximately 50 % of all pediatric CNS tumors [14]. Pediatric astrocytomas can arise within the optic pathway (15–25 %), cerebral hemisphere (12 %), spine (10–12 %), and brain stem (12 %) [15]. Contrary to adult primary brain cancer, which is more common in supratentorial brain, more than half of all pediatric brain cancers occur in infratentorial brain. The most common infratentorial pediatric brain cancer is medulloblastoma/primary neuroectodermal tumor (PNET) (30–35 %), closely followed by pilocytic astrocytoma (20–35 %), brain stem gliomas (25 %), ependymoma (10 %), and other miscellaneous types (5 %) [15]. The long-term survival rate for the two most common types of pediatric brain cancers, namely, pilocytic astrocytoma and medulloblastoma, differs substantially in that medulloblastoma tends to have poorer survival especially when it occurs in children younger than 3 years of age or those with metastatic disease at the time of initial diagnosis [15].

Overall Cost to Society

Brain cancer is a rare neoplasm but affects people of all ages [10]. It is more common in the pediatric population and tends to cause high morbidity and mortality [15]. The overall cost to society in dollar amount is difficult to estimate and may not be as high as other, more common systemic cancers. The cost of treating brain cancer in the USA is difficult to determine but can be estimated to be far greater than four billion dollars per year based on 359,000 estimated number of people living with brain cancer [12] and $11,365.23 per patient for initial cost of surgical treatment. There are very few articles in medical literature that address the cost-effectiveness or overall cost to society in relation to imaging of brain cancer. One of the few articles that discusses the actual monetary cost to society is a 1998 article by Latif et al. [16] from Great Britain. The team measured the mean costs of medical care for 157 patients with brain cancer in British Pounds. Based on this study, the average cost of imaging was less than 3 % of the total, whereas radiotherapy was responsible for greater than 50 % of the total cost. The relative contribution of imaging in this study appears low, however, and what is not known from this report is what kind and how often imaging was done in these patients with brain cancer during their hospital stay and as outpatients. In addition, the vastly different health care reimbursement structure in Britain and the USA makes interpretation difficult.

Goals of Imaging

The goals of imaging in patients, pediatric or adult age group, with suspected brain cancer are (1) diagnosis at acute presentation, (2) preoperative or treatment planning to further characterize brain abnormality, and (3) posttreatment evaluation for residual disease and therapy-related changes. The role of imaging is critically dependent upon the clinical context that the study is being ordered [17]. The initial diagnosis of brain cancer is often made on a CT scan in an

emergency room setting when a patient presents with an acute clinical symptom such as seizure or focal neurologic deficit. Once a brain abnormality is detected on the initial scan, MRI with contrast agent is obtained to further characterize the lesion and the remainder of the brain and to serve as a part of preoperative planning for a definitive histologic diagnosis. If the nature of the brain lesion is still in question after a comprehensive imaging, further imaging with advanced techniques such as diffusion, perfusion, or proton spectroscopic imaging may be warranted to differentiate brain cancer from tumor-mimicking lesions such as infarcts, abscesses, or demyelinating lesions [18–20]. In the immediate postoperative imaging, the most important imaging objectives are to (a) determine the amount of residual or recurrent disease; (b) assess early postoperative complications such as hemorrhage, contusion, or other brain injury; and (c) determine delay treatment complications such as radiation necrosis and treatment leukoencephalopathy.

Methodology

A MEDLINE search was performed using PubMed (National Library of Medicine, Bethesda, Maryland) for original research publications discussing the diagnostic performance and effectiveness of imaging strategies in brain cancer. Systematic literature review was performed from 1966 to January 2010. Keywords included are (1) brain cancer, (2) brain tumor, (3) glioma, (4) diagnostic imaging, and (5) neurosurgery. In addition, the following three cancer databases were reviewed:

1. The SEER program maintained by the National Cancer Institute (http://www.seer. cancer.gov) for incidence, survival, and mortality rates, classified by tumor histology, brain topography, age, race, and gender. SEER is population-based reference standard for cancer data and collects incidence and follow-up data on malignant brain cancer only.
2. The Central Brain Tumor Registry of the United States [12] (http://www.cbtrus.org)

collects incidence data on all primary brain tumors from 11 collaborating state registries; however, follow-up data are not available.
3. The National Cancer Data Base (NCDB) (http://www.facs.org/cancer/ncdb) serves as a comprehensive clinical surveillance resource for cancer care in the USA. While not population-based, the NCDB identifies newly diagnosed cases and conducts follow-up on all primary brain tumors from hospitals accredited by the American College of Surgeons. The NCDB is the largest of the three databases and also contains more complete information regarding treatment of tumors than SEER or CBTRUS databases.

Discussion of Issues

Who Should Undergo Imaging to Exclude Brain Cancer in Adult Individual?

Summary

The scientific evidence on this topic is limited. No strong evidence studies are available. Most of the available literature is classified as limited and moderate evidence. First, the three most common clinical symptoms of brain cancer are headache, seizure, and focal weakness – all of which are neither unique nor specific for the presence of brain cancer (see Chap. 15, "Seizures Disorders: Evidence-Based Neuroimaging" on seizures and Chap. 24, "Headache Disorders: Evidence-Based Neuroimaging" on headaches). Second, the clinical manifestation of brain cancer is heavily dependent on the topography of the lesion. For example, lesions in the motor cortex may have more acute presentation, whereas more insidious onset of cognitive or personality changes are commonly associated with prefrontal cortex tumors [21, 22].

Despite the aforementioned nonspecific clinical presentation of subjects with brain cancer, a summary of the guidelines is shown in Table 25.1. A relatively acute onset of any one of these symptoms that progresses over time should strongly warrant a brain imaging. Newton

et al. [23] cite a consensus among neurologists that the most specific clinical feature of a brain cancer versus other brain mass lesions is not one particular individual symptom or sign but, rather, progression over time.

Supporting Evidence

It remains difficult, however, to narrow down the criteria for the "suspected" clinical symptomatology of brain cancer. In a retrospective study of 653 patients with supratentorial brain cancer, Salcman [24] found that the three most common clinical features of brain cancer were headache (70 %), seizure (54 %), and cognitive or personality change (52 %), followed by focal weakness (43 %), nausea or vomiting (31 %), speech disturbances (27 %), alteration of consciousness (25 %), sensory abnormalities (14 %), and visual disturbances (8 %) (moderate evidence). Similarly, Snyder et al. [25] studied 101 patients who were admitted through an emergency room and discharged with a diagnosis of brain cancer (moderate evidence). They found that the three most frequent clinical features were headache (55 %), cognitive or personality changes (50 %), and ataxia (40 %), followed by focal weakness (36 %), nausea or vomiting (36 %), papilledema (27 %), cranial nerve palsy (25 %), seizure (24 %), visual disturbance (20 %), speech disturbance (20 %), sensory abnormalities (18 %), and positive Babinski's sign (17 %). No combination of these factors has been shown to reliably differentiate brain cancer from other benign causes.

Who Should Undergo Imaging to Exclude Brain Cancer in Pediatric Age Group?
Summary

Determination of which children with clinical suspicion of brain cancer should undergo imaging is a complex issue for a number of reasons. As in adults, the three most common clinical symptoms of brain cancer are headache, seizure, and focal weakness – all of which are neither unique nor specific for the presence of brain cancer. Hence, it is difficult to perform a prospective study based on these clinical symptoms to determine whether or not imaging is indicated. Second, as discussed earlier, the clinical

manifestation of brain cancer is heavily dependent on the topography of the lesion. Third, neurocognitive dysfunction may not necessarily be due to a mass lesion within the brain but can also be the secondary effects of systemic disease, chemical or hormonal imbalance, toxic exposure, drug or radiation therapy, or nonorganic neurodegenerative disorder [21, 22].

Despite the aforementioned nonspecific clinical presentation of subjects with brain cancer, there are guidelines one can use to determine who should undergo imaging (Table 25.1).

A relatively acute onset of any one of these symptoms that progresses over time should strongly warrant brain imaging, preferably with MRI (strong evidence). See also Chaps. 15, "Seizures Disorders: Evidence-Based Neuroimaging" and 24, "Headache Disorders: Evidence-Based Neuroimaging" on seizures and headaches.

Supporting Evidence

It remains difficult, in children as well as adults, to define criteria for "suspected" brain cancer. It should be noted that there is marked difference between adult and pediatric subjects with suspected brain cancer in terms of epidemiology, clinical presentation, tomography of the lesion, histologic tissue type, metastatic potential, and prognosis [26]. Headache, posterior fossa symptoms such as nausea and vomiting, ataxia, and cranial nerve symptoms predominate in children due to the fact that the overwhelming majority of pediatric brain cancers occur infratentorially [15]. Table 25.1 lists various clinical symptoms that are associated with pediatric brain cancer.

The two most common types of pediatric brain cancer are medulloblastoma and juvenile pilocytic astrocytoma (JPA), both of which commonly occur in the posterior fossa. Medulloblastomas and other small round blue cell tumors (pineoblastoma and primitive neuroectodermal tumor) have high propensity to spread along the leptomeningeal route within the central nervous system [13]. JPAs are also commonly seen in supratentorial brain, especially near the hypothalamic region [26, 27]. Prognosis differs vastly depending on the tissue histology and metastatic potential since medulloblastoma and other

small-cell tumors tend to have aggressive biology and poor outcome, whereas JPAs tend to have more favorable long-term prognosis [1, 10, 15].

Non-migraine, nonchronic headache in a child should raise a high suspicion for an intracranial mass lesion, especially if there are any additional posterior fossa or visual symptoms, and imaging should be conducted without delay. (See details in Chap. 24, "Headache Disorders: Evidence-Based Neuroimaging" on headaches.)

What Imaging Is Appropriate in High-Risk Pediatric Subjects?

Summary

In the high-risk children suspected of having brain cancer, MRI without and with gadolinium-based contrast agent is the imaging modality of choice (Table 25.2). There is no evidence to suggest that the addition of other diagnostic tests, such as CT, catheter angiography, or PET scan, improves either the cost-effectiveness or the outcome in the high-risk group at initial presentation (Table 25.2) (strong evidence).

Supporting Evidence

There is strong evidence to suggest that MRI is the diagnostic imaging test of choice in high-risk subjects suspected of having brain cancer [17, 28, 29] (Table 25.2). For example, superiority of MRI over CT in detection of brain cancer has been supported by an animal study done by Whelan et al. [30]. However, since CT scanners are more widely available and easily performed than MR scanners, especially in an emergency department setting, it is commonly performed even though CT is inferior to MR in lesion detection and characterization. Table 25.3 lists advantages and limitations of CT and MRI in the evaluation of children with suspected brain cancer.

Unenhanced CT is good for assessing acute intracranial hemorrhage, midline shift/mass effect, or hydrocephalus. CT, however, is not ideal for detecting subtle parenchymal abnormality [17]. As seen in Fig. 25.1, in comparing an unenhanced CT and an enhanced MRI, a rather large abnormality can be quite subtle to detect on the CT study due to its inferior soft tissue contrast,

whereas the lesion is clearly visible in the MRI. However, CT does have advantage in depicting calcium much better than MRI as can be seen in Fig. 25.1. Contrast-enhanced CT offers improved sensitivity, but the addition of iodinated contrast agent is not without risk of anaphylactic reaction (truly the risk is very low for nonionic low-osmolar contrast in children – moderate to severe reactions are less than 1:10,000). As shown in Fig. 25.2, MRI is superior to CT in its ability to depict brain cancer in multiple planes with greater soft tissue resolution and without the use of ionizing radiation. It is important to note that the addition of MRI contrast agent, gadolinium, is necessary to fully characterize the extent of disease, especially to assess leptomeningeal spread of disease (Fig. 25.2d–f) (Table 25.2). Table 25.4 lists suggested MR imaging protocol for a pediatric subject suspected of having brain cancer. Imaging strategy in pediatric brain cancer subjects should be tailored to the need of clinical management and treatment decisions.

Nuclear Medicine Imaging Tests

There has been tremendous progress in research involving various brain radiotracers, which provide the valuable functional and metabolic pathophysiology of brain cancer. Yet the question remains as to how best to incorporate radiotracer imaging methods into diagnosis and management of patients with brain cancer. The most widely used radiotracer imaging method in brain cancer imaging is ^{201}thalium single-photon emission computed tomography (SPECT) (Table 25.2). Although very useful, it has a limited role in initial diagnosis or predicting the degree of brain cancer malignancy. Positron emission tomography (PET) using ^{18}F-2-fluoro-2-deoxy-D-glucose (FDG) radiotracer can be useful in differentiating recurrent brain cancer from radiation necrosis, but similar to SPECT, its ability as an independent diagnostic and prognostic value above that of MR imaging and histology remains debated [31] (Table 25.2).

In pediatric patients with brain cancer, it is important to assess whether imaging of the entire craniospinal axis is warranted to detect any drop metastases and staging (Table 25.2). This is

especially true for children with aggressive neoplasm with high propensity for tumor spread along the cerebrospinal fluid route such as medulloblastoma/PNET and ependymoma.

In pediatric patients with suspected brain metastatic disease, MRI is the imaging test of choice, especially when leptomeningeal spread of disease is considered. CT is indicated when there is suspected calvarial metastasis. Surveillance imaging with MRI is a cost-effective way of monitoring disease stability or symptomatic progression in pediatric patients with brain cancer [32].

What Is the Appropriate Imaging in Subjects at Risk for Brain Cancer?

Summary

The sensitivity and specificity of MRI is higher than CT for brain neoplasms (moderate evidence). Therefore, in high-risk subjects suspected of having brain cancer, MRI with and without gadolinium-based contrast agent is the imaging modality of choice to further characterize the lesion. Table 25.3 lists advantages and limitations of CT and MRI in the evaluation of subjects with suspected brain cancer.

There is no strong evidence to suggest that the addition of other diagnostic tests, such as MR spectroscopy, perfusion MR, PET, or SPECT, improves either the cost-effectiveness or the outcome in the high-risk group at initial presentation.

Supporting Evidence

Medina et al. [28] found in a retrospective study of 315 pediatric patients that overall MR imaging was more sensitive and specific than CT in detecting intracranial space-occupying lesions (92 % and 99 %, respectively, for MR imaging vs. 81 % and 92 %, respectively, for CT). However, no difference in sensitivity and specificity was found in the surgical space-occupying lesions [28]. Table 25.3 lists sensitivity and specificity of MRI and CT for brain cancer as outlined by Hutter et al. [33]. Figures 25.2 and 25.3 illustrate limitations and advantages of MRI and CT.

There is limited evidence behind perfusion MR in tumor diagnosis and grading despite several articles proposing its useful role. Similar to proton MR spectroscopy (see section "What Is the Appropriate Imaging in Subjects at Risk for Brain Cancer?"), perfusion MR imaging remains an investigational tool at this time pending stronger evidence proving its effect on health outcomes of patients with brain cancer.

Special Case: Neuroimaging Differentiation of Posttreatment Necrosis from Residual Tumor

Imaging differentiation of treatment necrosis and residual/recurrent tumor is challenging because they both can appear similar and also can coexist in a single given lesion. Hence, the traditional anatomy-based imaging methods have a limited role in the accurate differentiation between the two entities. Nuclear medicine imaging techniques such as SPECT and PET provide functional information on tissue metabolism and oxygen consumption and thus offer theoretical advantage over anatomic imaging in differentiation tissue necrosis and active tumor. Multiple studies demonstrate that SPECT is more sensitive and specific than is PET in differentiating tumor recurrence from radiation necrosis [33] (Table 25.3). There is also insufficient evidence of the role of MR spectroscopy in this topic (see section "What Is the Appropriate Imaging in Subjects at Risk for Brain Cancer?").

Special Case: Neuroimaging Modality in Patients with Suspected Brain Metastatic Disease

Brain metastases are far more common than primary brain cancer in adults, owing to higher prevalence of systemic cancers and their propensity to metastasize [34–36]. Focal neurologic symptoms in a patient with history of systemic cancer should raise a high suspicion for intracranial metastasis and prompt imaging. The preferred neuroimaging modality in patients with suspected brain metastatic disease is MRI with single dose (0.1 mmole/kg body weight) of

gadolinium-based contrast agent. Most studies described in the literature suggest that contrast-enhanced MR imaging is superior to contrast-enhanced CT in the detection of brain metastatic disease, especially if the lesions are less than 2 cm (moderate evidence).

Davis and colleagues (moderate evidence) [37] studied comparative imaging studies in 23 patients comparing contrast-enhanced MRI with double-dose delayed CT. Contrast-enhanced MRI demonstrated more than 67 definite or typical brain metastases. The double-dose delayed CT revealed only 37 metastatic lesions. The authors concluded that MR imaging with enhancement is superior to double-dose delayed CT scan for detecting brain metastasis, anatomic localization, and number of lesions. Golfieri and colleagues [38] reported similar findings (moderate evidence). They studied 44 patients with small-cell carcinoma to detect cerebral metastases. All patients were studied with contrast-enhanced CT scan and gadolinium-enhanced MR imaging. Of all patients, 43 % had cerebral metastases. Both contrast-enhanced CT and gadolinium-enhanced MR imaging detected lesions greater than 2 cm. For lesions less than 2 cm, 9 % were detected only by gadolinium-enhanced T1-weighted images. The authors concluded that gadolinium-enhanced T1-weighted images remain the most accurate technique in the assessment of cerebral metastases. Sze and colleagues [39] performed prospective and retrospective studies in 75 patients (moderate evidence). In 49 patients, MR imaging and contrast-enhanced CT were equivalent. In 26 patients, however, results were discordant, with neither CT nor MR imaging being consistently superior. MR imaging demonstrated more metastases in 9 of these 26 patients. Contrast-enhanced CT, however, better depicted lesions in 8 of 26 patients.

There are several reports on using triple dose of contrast agent to increase sensitivity of lesion detection [40, 41]. In another study, Sze et al. [42], however, have found that routine triple-dose contrast agent administration in all cases of

suspected brain metastasis was not helpful, could lead to increasing number of false-positive results, and concluded that the use of triple-dose contrast material is beneficial in selected cases with equivocal findings or solitary metastasis. Their study was based on 92 consecutive patients with negative or equivocal findings or a solitary metastasis on single-dose contrast-enhanced MR images that underwent triple-dose studies.

Special Case: How Can Tumor Be Differentiated from Tumor-Mimicking Lesions?

There are several intracranial disease processes that can mimic brain cancer and pose a diagnostic dilemma on both clinical presentation and conventional MRI [19, 43–47], such as infarcts, radiation necrosis, demyelinating plaques, abscesses, hematomas, and encephalitis. On imaging, any one of these lesions and brain cancer can both demonstrate contrast enhancement, perilesional edema, varying degrees of mass effect, and central necrosis.

There are numerous reports in the literature of misdiagnosis and mismanagement of these subjects who were erroneously thought to have brain cancer and, in some cases, went on to surgical resection for histopathologic confirmation [18, 46, 48]. Surgery is clearly contraindicated in these subjects and can lead to unnecessary increase in morbidity and mortality. A large acute demyelinating plaque, in particular, is notorious for mimicking an aggressive brain cancer [46, 49–52]. Due to presence of mitotic figures and atypical astrocytes, this uncertainty occurs not only on clinical presentation and imaging but also on histopathological examination [46]. The consequence of unnecessary surgery in subjects with tumor-mimicking lesions can be quite grave, and hence, every effort should be made to differentiate them from brain cancer. Anatomic imaging of the brain suffers from nonspecificity and its inability to differentiate tumor from tumor-mimicking lesions [18]. Recent developments in nonanatomic, physiology-based MRI methods, such as diffusion/perfusion MRI and

proton spectroscopic imaging, promise to provide information not readily available from structural MRI and improve diagnostic accuracy [53, 54].

Diffusion-weighted MRI has been shown to be particularly helpful in differentiating cystic/ necrotic neoplasm from brain abscess by demonstrating marked reduced diffusion within an abscess. Chang et al. [55] compared diffusion-weighted imaging (DWI) and conventional anatomic MRI to distinguish brain abscesses from cystic or necrotic brain tumors in 11 patients with brain abscesses and 15 with cystic or necrotic brain gliomas or metastases. They found that postcontrast T1WIs yielded a sensitivity of 60 %, a specificity of 27 %, a positive predictive value (PPV) of 53 %, and a negative predictive value (NPV) of 33 % in the diagnosis of necrotic tumors. DWI yielded a sensitivity of 93 %, a specificity of 91 %, a PPV of 93 %, and a NPV of 91 %. Based on the analysis of receiver operating characteristic curves, they found clear advantage of DWI as a diagnostic tool in detecting abscess when compared to postcontrast T1-weighted images. Figure 25.4 illustrates the value of DWI in differentiating pyogenic abscess and high-grade brain tumor.

Table 25.5 lists neurological diseases that can mimic brain cancer both on clinical grounds and on imaging. By using DWI, acute infarct and abscess could readily be distinguished from brain cancer since reduced diffusion seen with the first two entities [55–59]. Highly cellular brain cancer can have reduced diffusion but not to the same degree as acute infarct or abscess [60].

What Is the Role of Proton Magnetic Resonance Spectroscopy in the Diagnosis and Follow-up of Brain Neoplasms?

Summary

The Blue Cross Blue Shield Association (BCBSA) Medical Advisory Panel concluded that the MRS in the evaluation of suspected brain cancer did not meet the Technology Evaluation Center (TEC) criteria as a diagnostic test; hence, further studies in a prospectively defined population are needed. A similar conclusion was obtained by the systematic literature review done by Hollingworth et al. [61]. However, the study highlighted two important findings in the literature: (1) one large study demonstrating a statistically significant increase in diagnostic accuracy for indeterminate brain lesions from 55 %, based on MR imaging, to 71 % after analysis of [1]H-MR spectroscopy [61], and (2) several studies have found that [1]H-MR spectroscopy is highly accurate for distinguishing high- and low-grade gliomas, though the incremental benefit of [1]H-MR spectroscopy in this setting is less clear [61]. Figure 25.5 shows a prominent lactate peak seen on a single-voxel MRS of a right frontal anaplastic astrocytoma.

Supporting Evidence

No systematic review of MRS has been done only for pediatric patients with brain neoplasms. The systematic reviews available include adult and pediatric patients. The BCBSA Medical Advisory Panel made the following judgments about whether ^{1}H-MRS for evaluation of suspected brain tumors meets the BCBSA TEC criteria based on the available evidence [62]. The Advisory Panel reviewed seven published studies that included a total of up to 271 subjects [63–69]. These seven studies were selected for inclusion in the review of evidence because (1) the sample size was at least 10, (2) criteria for a positive test were specified, (3) there was a method to confirm ^{1}H-MRS diagnosis, and (4) the report provided sufficient data to calculate diagnostic test performance (sensitivity and specificity). The reviewers specifically addressed whether ^{1}H-MRS for evaluation of suspected brain tumors meets the following five TEC criteria:

1. The technology must have approval from the appropriate governmental regulatory bodies.
2. The scientific evidence must permit conclusions concerning the effect of the technology on health outcomes.

3. The technology must improve the net health outcomes.
4. The technology must be as beneficial as any established alternatives.
5. The improvement must be attainable outside the investigational settings.

With the exception of the first criterion, the reviewers concluded that the available evidence on ^{1}H-MRS in the evaluation of brain neoplasm was insufficient. The TEC also concluded that the overall body of evidence does not provide strong and consistent evidence regarding the diagnostic test characteristics of MRS in determining the presence or absence of brain neoplasm, both for differentiation of recurrent/residual tumor versus delayed radiation necrosis [69] and for diagnosis of brain tumor versus other nontumor diagnosis [63, 64, 66–68]. Assessment of the health benefit of MRS in avoiding brain biopsy was evaluated in two studies [63, 68], but the results were limited by study limitations. Therefore, human studies conducted on the use of MRS for brain tumors demonstrate that this noninvasive method is technically feasible and suggest potential benefits for some of the proposed indications. However, there is a paucity of high-quality direct evidence demonstrating the impact on diagnostic thinking and therapeutic decision making.

The systematic review by Hollingworth et al. showed no articles evaluated patient health or cost-effectiveness [61]. Methodologic quality was mixed; most used histopathology as the reference standard but did not specify blinded interpretation of histopathology [61]. One large study demonstrated a statistically significant increase in diagnostic accuracy for indeterminate brain lesions from 55 %, based on MR imaging, to 71 % after analysis of ^{1}H-MR spectroscopy [61]. Several studies have found that ^{1}H-MR spectroscopy is highly accurate for distinguishing high- and low-grade gliomas, though the incremental benefit of ^{1}H-MR spectroscopy in this setting is less clear. Interpretation for the other clinical subgroups is limited by the small number of studies [61].

Can Imaging Be Used to Differentiate Posttreatment Necrosis from Residual/Recurrent Tumor?

Summary

No adequate data exist on the role of imaging in monitoring pediatric brain cancer response to therapy and differentiating between tumor recurrence and therapy-related changes (insufficient evidence).

Supporting Evidence

Imaging differentiation of posttreatment necrosis and residual/recurrent tumor is challenging because they can appear similar and can coexist in a single given lesion. Hence, the traditional anatomy-based imaging methods have a limited role in the accurate differentiation of the two entities. Nuclear medicine imaging techniques such as SPECT and FDG PET have been proposed as a diagnostic alternative, particularly when coregistered with MRI to provide functional information on tissue metabolism and oxygen consumption and thus offer a theoretical advantage over anatomic imaging in differentiating tissue necrosis and active tumor. Chao et al. [70] studied 47 patients with brain tumors treated with stereotactic radiosurgery and followed with FDG PET. For all tumor types, the sensitivity of FDG PET for diagnosing tumor was 75 % and the specificity was 81 %. For brain metastasis without MRI coregistration, FDG PET had a sensitivity of 65 % and a specificity of 80 %. For brain metastasis with MRI coregistration, FDG PET had a sensitivity of 86 % and specificity of 80 %. MRI coregistration appears to improve the sensitivity of FDG PET, making it a useful modality to distinguish between radiation necrosis and recurrent brain metastasis [70]. Khan et al. [71] studied the value of SPECT versus PET in 19 patients with evidence of tumor recurrence of CT or MR images using both 201TI SPECT and FDG PET imaging and were unable to detect a statistically significant difference in sensitivity or specificity between the two scans. They found both techniques to be

sensitive for tumor recurrence for lesions 1.6 cm or larger and concluded that SPECT, given its greater availability, simplicity, ease of interpretation, and lower cost, is a better method of choice [71]. However, there is insufficient data to determine whether SPECT, PET, or any other imaging modality can confidently discriminate tumor recurrence from treatment effect.

What Is the Added Value of Functional MRI in the Surgical Planning of Patients with Suspected Brain Neoplasm or Focal Brain Lesions?

Summary

The addition of fMRI in the surgical planning of patients with suspected brain neoplasm or focal brain lesions can influence diagnostic and therapeutic decision making (moderate evidence).

Supporting Evidence

fMRI is a noninvasive tool to assess brain function and has been around since the early 1990s, largely as a research tool with limited clinical availability and application. Over the past several years, however, fMRI has crossed over to the clinical realm and is gaining more acceptance as a useful clinical tool. The growing use of fMRI in clinical areas include mapping of critical or eloquent areas such as the motor cortex in patients undergoing brain surgery, early identification of psychiatric disorder, and measurement of the effect of therapies on neurodegenerative and neurodevelopmental disorders. Figure 25.6 shows the location of motor cortex activation in relation to a frontal brain tumor that can be useful in surgical planning of the tumor. Medina et al. [72] evaluated the effect of adding fMRI on diagnostic work-up and treatment planning in 53 patients with seizure disorders who are candidates for surgical treatment. They found that fMRI results influenced diagnostic and therapeutic decision making. Specifically, the fMRI results indicated language dominance changed, confidence level in identification of

critical brain function areas increased, patient and family counseling were altered, and intraoperative mapping and surgical approach were altered [72].

What Is the Cost-effectiveness of Imaging in Patients with Suspected Primary Brain Neoplasms and Brain Metastatic Disease?

Summary

Routine brain CT in all patients with lung cancer has a cost-effectiveness ratio of $69,815 per QALY. However, the cost per QALY is highly sensitive to variations in the negative predictive value of a clinical evaluation as well as to the cost of CT. CEA of patients with headache suspected of having a brain neoplasm is presented in Chap. 24, "Headache Disorders: Evidence-Based Neuroimaging" on headaches.

Supporting Evidence

In a study from the surgical literature, Colice et al. [73] compared the cost-effectiveness of two strategies for detecting brain metastases by CT in lung cancer patients: (1) routine CT for all patients irrespective of clinical (neurologic, hematologic) evidence of metastases (CT first) and (2) CT for only those patients in whom clinical symptoms developed (CT deferred). For a hypothetical cohort of patients, it was assumed that all primary lung carcinomas were potentially resectable. If no brain metastasis were detected by CT, the primary lung tumor would be resected. Brain metastasis as detected by CT would disqualify the patient for resection of the primary lung tumor. Costs were taken from the payer's perspective and based on prevailing Medicare payments. The rates of false-positive and false-negative findings were also considered in the calculation of the effectiveness of CT. The cost of the CT-first strategy was $11,108 and the cost for the CT-deferred strategy $10,915; however, the CT-first strategy increased life expectancy by

merely 1.1 days. Its cost-effectiveness ratio was calculated to be $69,815 per QALY. The cost per QALY is highly sensitive to variations in the negative predictive value of a clinical evaluation as well as to the cost of CT. This study is instructive, because it highlights the importance of considering false-positive and false-negative findings and performing sensitivity analysis. For a detailed discussion of the specifics of the decision-analytic model and sensitivity analysis, the reader is referred to the article by Hutter et al. and Colice et al. [33, 73].

Imaging Case Studies

Case 1: 17-year-old girl with left-sided weakness with clinical suspicion for acute stroke (Fig. 25.2)

Case 2: 42-year-old woman with difficulty in balancing and left-sided weakness and a pathologic diagnosis of GBM (Fig. 25.3)

Case 3: 53-year-old man with right frontal abscess with irregular enhancement with central necrosis simulating a brain cancer (Fig. 25.4)

Take-Home Tables and Figures

Tables 25.1–25.5 serve to highlight key recommendations and supporting evidence. Figure 25.1 shows an algorithm to study patients with suspected brain cancer.

Table 25.1 Clinical symptoms suggestive of a brain cancer

Non-migraine, nonchronic headache of moderate to severe degree (see Chap. 24, "Headache Disorders: Evidence-Based Neuroimaging")
Partial complex seizure (Chap. 15, "Seizure Disorders: Evidence-Based Neuroimaging")
Focal neurological deficit
Speech disturbance
Cognitive or personality change
Visual disturbance
Altered consciousness
Sensory abnormalities
Gait problem or ataxia
Nausea and vomiting without other gastrointestinal illness
Papilledema
Cranial nerve palsy

Reprinted with kind permission of Springer Science+ Business Media from Cha S. Imaging in brain cancer. In Medina LS, Blackmore CC, editors. Evidence-based imaging: optimizing imaging in patient care. New York: Springer; 2006

Table 25.2 Sensitivity and specificity of brain tumor imaging

Type of brain cancer	Imaging modality	Sensitivity (%)	Specificity (%)
Primary brain cancer	MRI with contrast	Gold standard	–
	CT with contrast	87	79
Primary brain cancer in children	MRI	92	99
(Medina et al. [28])	CT	81	92
Brain metastasis	MRI with single-dose contrast	93–100	–
	MRI without contrast	36	–
	^{201}Tl SPECT	70	–
	^{18}FDG PET	82	38
Recurrent tumor versus treatment-related necrosis	^{201}Tl SPECT	92	88
	^{18}FDG PET		
	MRI with coregistration	86	80
	MRI without coregistration	65	80

Source: Adapted from Hutter et al. [33], with permission from Elsevier

(Reprinted with kind permission of Springer Science+ Business Media from Cha S. Imaging in brain cancer. In Medina LS, Blackmore CC, editors. Evidence-based imaging: optimizing imaging in patient care. New York: Springer; 2006)

Table 25.3 Advantages and limitations of computed tomography (CT) and magnetic resonance imaging (MRI)

	Advantages	Limitations
Computed tomography	Widely available	Inferior soft tissue resolution
	Short imaging time	Prone to artifact in posterior fossa
	Lower cost	Ionizing radiation
	Excellent for detection of acute hemorrhage or bony abnormality	Risk of allergy to iodinated contrast agent
Magnetic resonance imaging	Multiplanar capability	Higher cost
	Superior soft tissue resolution	Not as widely available
	No ionizing radiation	Suboptimal for detection of acute hemorrhage or bony/calcific abnormality
	Safer contrast agent (gadolinium-based) profile	

Reprinted with kind permission of Springer Science+ Business Media from Cha S. Imaging in brain cancer. In Medina LS, Blackmore CC, editors. Evidence-based imaging: optimizing imaging in patient care. New York: Springer; 2006

Table 25.4 MR imaging protocol for a subject with suspected brain cancer

3D-localizer
Axial and sagittal precontrast T1-weighted imaging
Diffusion-weighted imaging
Axial fluid-attenuated inversion recovery (FLAIR)
Axial T2-weighted imaging
Axial, coronal, and sagittal postcontrast T1-weighted imaging
Optional: dynamic contrast-enhanced perfusion MR imaging, Proton MR spectroscopic imaging
Consider doing gadolinium-enhanced MRI of entire spine to rule out metastatic disease

Reprinted with kind permission of Springer Science+ Business Media from Cha S. Imaging in brain cancer. In Medina LS, Blackmore CC, editors. Evidence-based imaging: optimizing imaging in patient care. New York: Springer; 2006

Table 25.5 Brain-cancer-mimicking lesions

Infarct
Radiation necrosis
Abscess
Demyelinating plaque
Subacute hematoma
Encephalitis

Reprinted with kind permission of Springer Science+ Business Media from Cha S. Imaging in brain cancer. In Medina LS, Blackmore CC, editors. Evidence-based imaging: optimizing imaging in patient care. New York: Springer; 2006

Case 4: Single-voxel MR spectroscopy in a 59-year-old woman, right frontal grade III anaplastic astrocytoma (Fig. 25.5)

Case 5: Functional MR imaging (fMRI) of motor activation in a 22-year-old man with right frontal grade II astrocytoma located near the motor cortex (Fig. 25.6)

Future Research

- Rigorous technology assessment of noninvasive imaging modalities such as MRS, diffusion and perfusion MRI, fMRI, PET, and SPECT
- Assessment of the effects of imaging on the patient outcome and costs of diagnosis and management
- Rigorous cost-effectiveness analysis of competing imaging modalities
- Development and clinical validation of physiologic MRI to assess biologic and molecular features of pediatric brain cancer
- Identification and validation of noninvasive imaging biomarkers of tumor activity during and after therapy
- Development and clinical validation of physiologic MRI to assess biologic and molecular features of pediatric brain cancer
- National database dedicated to epidemiology of adult and pediatric brain cancer
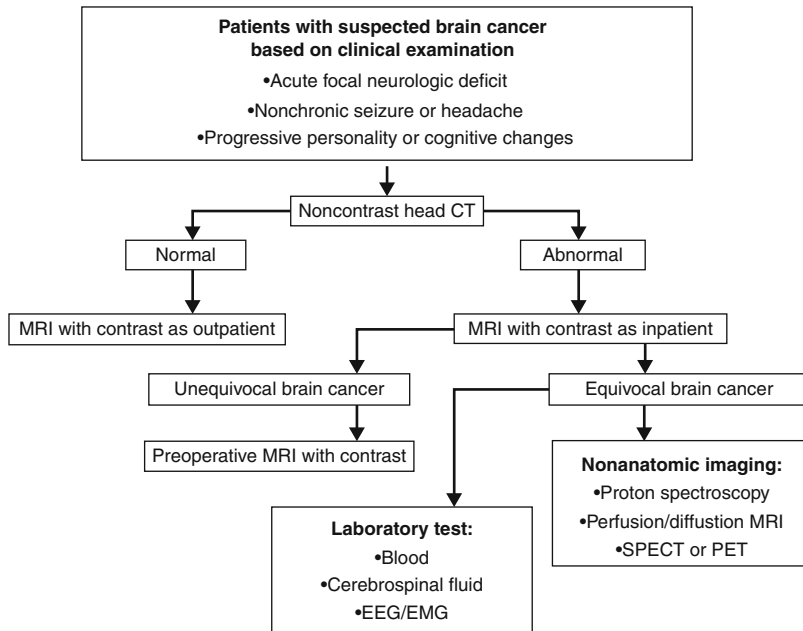
Fig. 25.1 Decision flow chart to study patients with suspected brain cancer. In patients presenting with acute neurologic event such as seizure or focal deficit, noncontrast head CT examination should be done expeditiously to exclude any life-threatening conditions such as hemorrhage or herniation (Reprinted with kind permission of Springer Science+Business Media from Cha S. Imaging of brain cancer. In Medina LS, Blackmore CC, editors. Evidence-based imaging: optimizing imaging in patient care. New York: Springer; 2006)
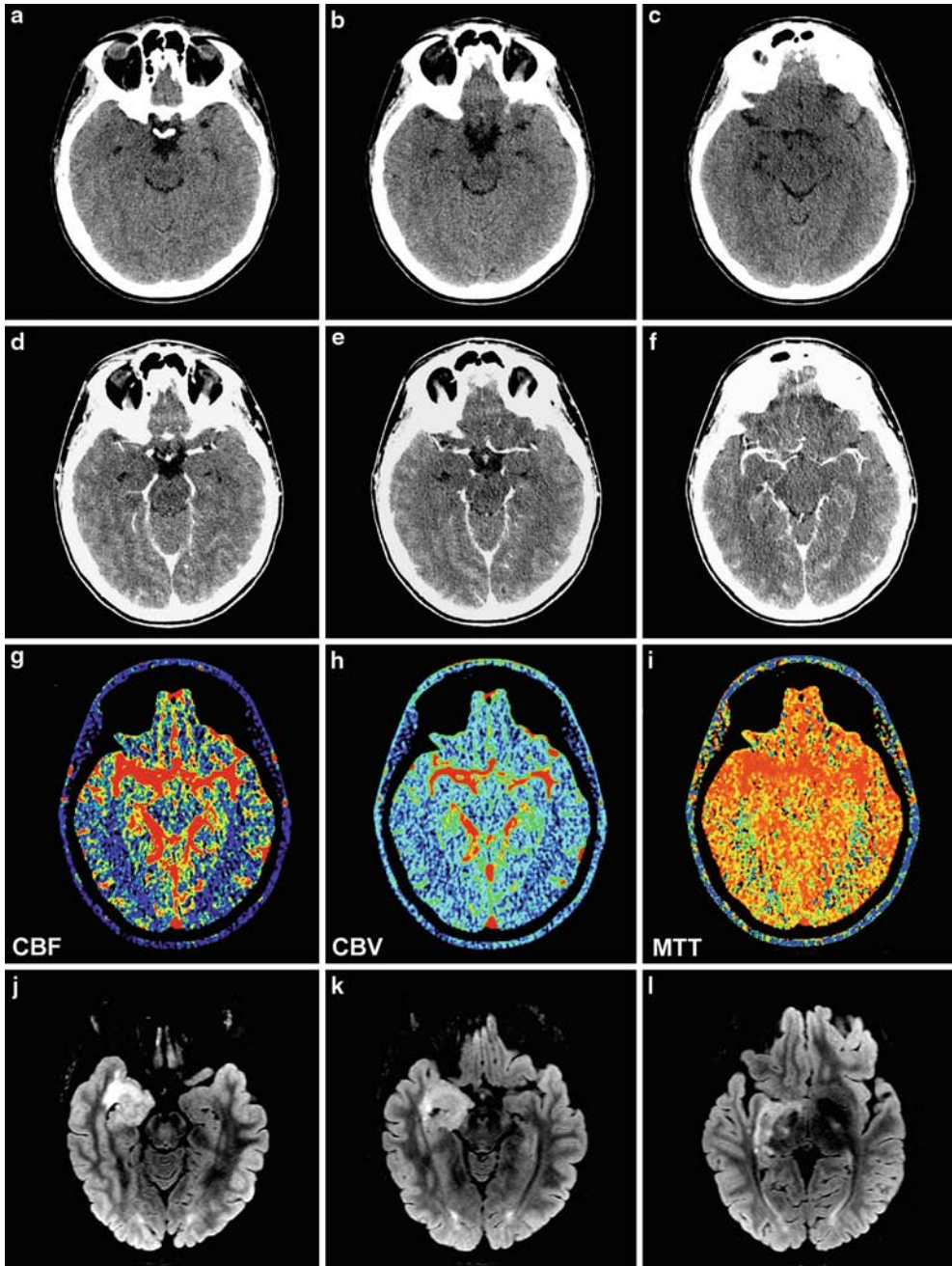
Fig. 25.2 Seventeen-year-old girl with left-sided weakness with clinical suspicion for acute stroke. (**a**) Unenhanced CT images (*top row*), enhanced CT images (*middle row*), and perfusion maps (*bottom row*) through the level of temporal lobe and basal ganglia demonstrate no obvious mass lesion. (**b**) Axial fluid-attenuated inversion recovery (FLAIR) MR images done 3 days after the CT clearly show large extent of abnormality (*white arrows*) involving most of the right medial temporal extending superiorly to basal ganglia and thalamus. Dysembryoblastic neuroepithelial tumor was at surgery (Reprinted with kind permission of Springer Science+ Business Media from Cha S. Imaging of brain cancer. In Medina LS, Blackmore CC, editors. Evidence-based imaging: optimizing imaging in patient care. New York: Springer; 2006
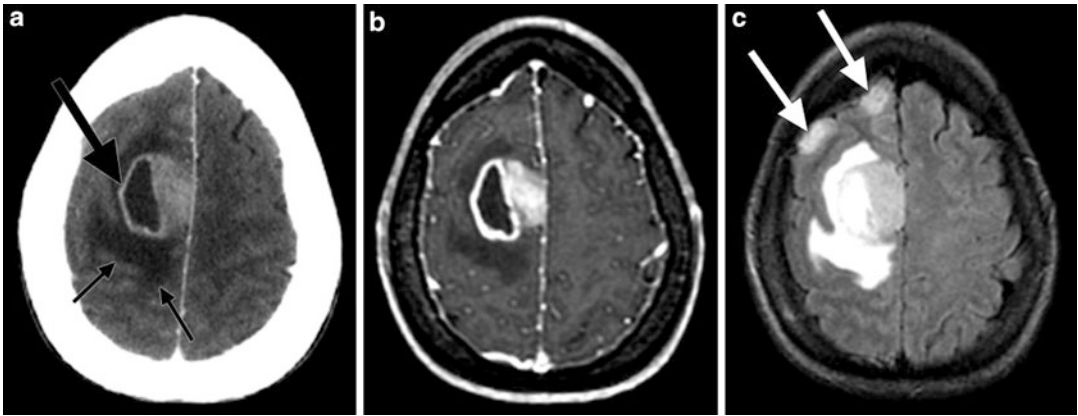
Fig. 25.3 Forty-two-year-old woman with difficulty in balancing and left-sided weakness and a pathologic diagnosis of GBM. (**a**) Contrast-enhanced CT image demonstrates an enhancing solid and necrotic mass (*large black arrow*) within the right superior frontal gyrus associated with surrounding low density (*small arrows*). (**b**) Contrast-enhanced T1-weighted MR image performed on the same day as the CT study shows similar finding. (**c**) FLAIR MR image clearly demonstrates two additional foci of cortically based signal abnormality (*white arrows*) that were found to be infiltrating glioma on histopathology (Reprinted with kind permission of Springer Science+Business Media from Cha S. Imaging of brain cancer. In Medina LS, Blackmore CC, editors. Evidence-based imaging: optimizing imaging in patient care. New York: Springer; 2006
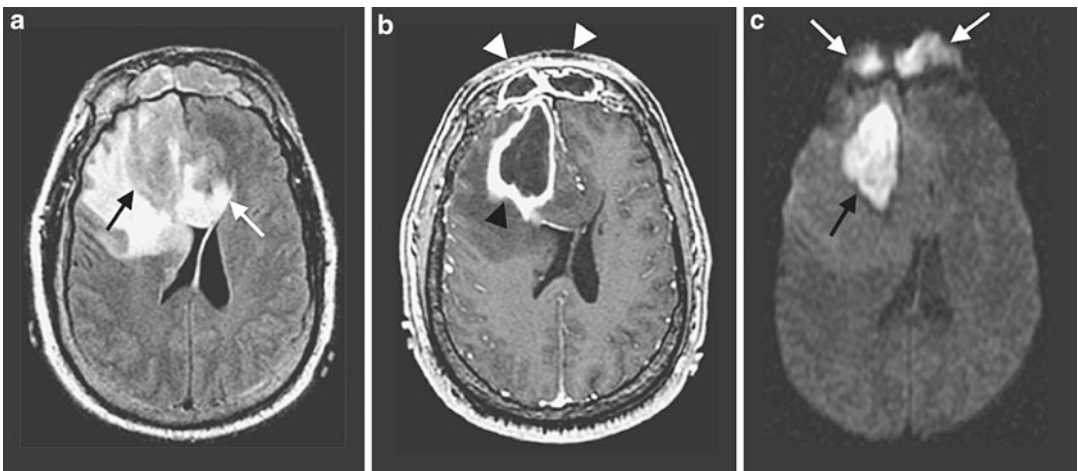

Fig. 25.4 Fifty-three-year-old man with right frontal abscess with irregular enhancement with central necrosis simulating a brain cancer. (**a**) FLAIR MR image demonstrates a large mass lesion (*black arrow*) with extensive surrounding edema that crosses the corpus callosum (*white arrow*). (**b**) Contrast-enhanced T1-weighted MR image shows thick rim enhancement (*black open arrow*) and central necrosis associated with the mass. Similar pattern of abnormality is noted within the frontal sinuses (*open white arrows*). (**c**) Diffusion-weighted MR image depicts marked reduced diffusion within the frontal lesion (*black arrow*) and the frontal sinus lesion (*white arrows*), both of which were proven to be a bacterial abscess at histopathology (Reprinted with kind permission of Springer Science+Business Media from Cha S. Imaging of brain cancer. In Medina LS, Blackmore CC, editors. Evidence-based imaging: optimizing imaging in patient care. New York: Springer; 2006
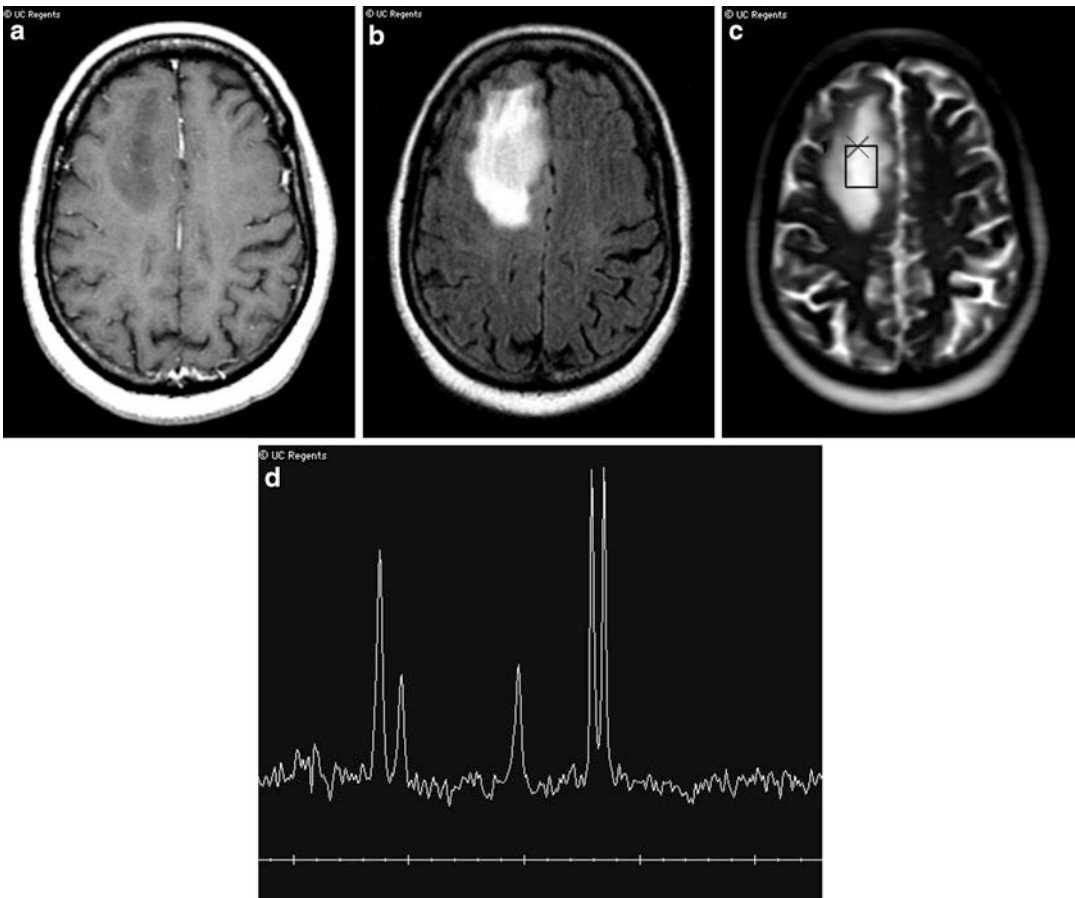
Fig. 25.5 Single-voxel MR spectroscopy in a 59-year-old woman right frontal grade III anaplastic astrocytoma. (**a**) Axial postcontrast T1-weighted image shows a nonenhancing right frontal mass. (**b**) Axial FLAIR image clearly demonstrates a hyperintense mass. (**c**) A screen save image from single-voxel MRS shows a box overlaid on an axial T2-weighted image showing the mass. (**d**) A single-voxel MRS using echo time of 288 ms demonstrates a prominent doublet lactate peak at 1.3 ppm suggestive of an aggressive tumor (Reprinted with kind permission of Springer Science+Business Media from Cha S. Imaging of brain cancer. In Medina LS, Blackmore CC, editors. Evidence-based imaging: optimizing imaging in patient care. New York: Springer; 2006. Images © UC Regents)
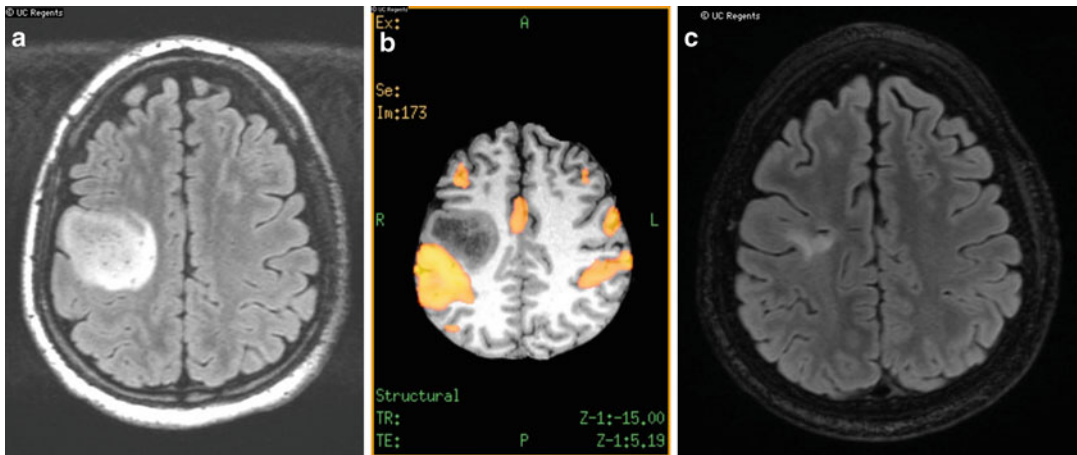
Fig. 25.6 Functional MR imaging (fMRI) of motor activation in a 22-year-old man with right frontal grade II astrocytoma located near the motor cortex. (**a**) Axial FLAIR image shows a mass near the right motor cortex. (**b**) fMRI color map demonstrates the motor cortex to be located immediately posterior and not within the right frontal low-grade tumor. (**c**) Postoperative axial FLAIR image shows minimal residual signal abnormality at the resection site anterior to normal-appearing motor cortex (Reprinted with kind permission of Springer Science+ Business Media from Cha S. Imaging of brain cancer. In Medina LS, Blackmore CC, editors. Evidence-based imaging: optimizing imaging in patient care. New York: Springer; 2006. Images © UC Regents)

References

 1. Burger PC, Vogel FS. In: Burger PC, Vogel FS, editors. Surgical pathology of the central nervous system and its coverings. New York: Wiley; 1982. p. 223–66.
 2. Burger PC, et al. Cancer. 1985;56:1106–11.
 3. Kleihues P, Sobin LH. Cancer. 2000;88(12):2887.
 4. Kleihues P, Ohgaki H. Toxicol Pathol. 2000;28(1):164–70.
 5. Go KG. Adv Tech Stand Neurosurg. 1997;23:47–142.
 6. Sato S, et al. Acta Neurochir Suppl. 1994;60:116–18.
 7. Stewart PA, et al. J Neurosurg. 1987;67(5):697–705.
 8. Stewart PA, et al. Microvasc Res. 1987;33(2):270–82.
 9. Abbott NJ, et al. Adv Drug Deliv Rev. 1999;37(1–3):253–77.
10. DeAngelis LM. N Engl J Med. 2001;344(2):114–23.
11. Longstreth Jr WT, et al. Cancer. 1993;72(3):639–48.
12. CBTRUS. Statistical report: primary brain tumors in the United States, 1998–2002. Chicago: Central Brain Tumor Registry of the United States; 2005.
13. Becker LE. Neuroimaging Clin N Am. 1999;9(4):671–90.
14. Rickert CH, Probst-Cousin S, Gullotta F. Childs Nerv Syst. 1997;13(10):507–13.
15. Pollack IF. Semin Surg Oncol. 1999;16(2):73–90.
16. Latif AZ, et al. Br J Neurosurg. 1998;12(2):118–22.
17. Ricci PE. Neuroimaging Clin N Am. 1999;9(4):651–69.
18. Cha S, et al. AJNR Am J Neuroradiol. 2001;22(6):1109–16.
19. Kepes JJ. Ann Neurol. 1993;33(1):18–27.
20. De Stefano N, et al. Ann Neurol. 1998;44(2):273–8.
21. Porter RJ, et al. Br J Psychiatry. 2003;182:214–20.
22. Meyers CA. Oncology (Hunting). 2000;14(1):75–9; discussion 79, 81–82, 85.
23. Newton HB, et al. Ann Pharmacother. 1999;33(7–8):816–32.
24. Salcman M. In: Wilkins R, Rengachary S, editors. Neurosurgery. New York: McGraw-Hill; 1985. p. 579–90.
25. Snyder H, et al. J Emerg Med. 1993;11(3):253–8.
26. Miltenburg D, Louw DF, Sutherland GR. Can J Neurol Sci. 1996;23(2):118–22.
27. Davis FG, McCarthy BJ. Curr Opin Neurol. 2000;13(6):635–40.
28. Medina LS, et al. Radiology. 1997;202(3):819–24.
29. Medina LS, Kuntz KM, Pomeroy S. Pediatrics. 2001;108(2):255–63.
30. Whelan HT, et al. Pediatr Neurol. 1988;4(5):279–83.
31. Benard F, Romsa J, Hustinx R. Semin Nucl Med. 2003;33(2):148–62.
32. Kovanlikaya A, et al. Eur J Radiol. 2003;47(3):188–92.
33. Hutter A, et al. Neuroimaging Clin N Am. 2003;13(2):237–50. x–xi.
34. Walker AE, Robins M, Weinfeld FD. Neurology. 1985;35(2):219–26.
35. Wingo PA, Tong T, Bolden S. CA Cancer J Clin. 1995;45:8–30.
36. Patchell RA. Neurol Clin. 1991;9:817–27.
37. Davis PC, et al. AJNR Am J Neuroradiol. 1991;12(2):293–300.
38. Golfieri R, et al. Radiol Med (Torino). 1991;82(1–2):27–34.
39. Sze G, et al. Radiology. 1988;168(1):187–94.

40. Kuhn MJ, et al. Comput Med Imaging Graph. 1994; 18(5):391–9.
41. Yuh WT, et al. AJNR Am J Neuroradiol. 1995; 16(2):373–80.
42. Sze G, et al. AJNR Am J Neuroradiol. 1998; 19(5):821–8.
43. Morgenstern LB, Frankowski RF. J Neurooncol. 1999; 44(1):47–52.
44. Barcikowska M, et al. Folia Neuropathol. 1995; 33(1):55–7.
45. Kim YJ, et al. AJR Am J Roentgenol. 1998; 171(6):1487–90.
46. Zagzag D, et al. Am J Surg Pathol. 1993;17(6):537–45.
47. Itto H, et al. No To Shinkei. 1972;24(4):455–8.
48. Babu R, et al. J Neurooncol. 1993;17(1):37–42.
49. Dagher AP, Smirniotopoulos J. Neuroradiology. 1996;38(6):560–5.
50. Giang DW, et al. Neuroradiology. 1992;34(2):150–4.
51. Kurihara N, et al. Clin Imaging. 1996;20(3):171–7.
52. Prockop LD, Heinz ER. Arch Neurol. 1965; 13(5):559–64.
53. Schaefer PW, Grant PE, Gonzalez RG. Radiology. 2000;217(2):331–45.
54. Cha S, et al. Radiology. 2002;223(1):11–29.
55. Chang SC, et al. Clin Imaging. 2002;26(4):227–36.
56. Castillo M, Mukherji SK. Semin Ultrasound CT MR. 2000;21(6):405–16.
57. Ebisu T, et al. Magn Reson Imaging. 1996; 14(9):1113–16.
58. Laing AD, Mitchell PJ, Wallace D. Australas Radiol. 1999;43(1):16–19.
59. Tsuruda JS, et al. AJNR Am J Neuroradiol. 1990; 11(5):925–31;discussion 932–934.
60. Okamoto K, et al. Eur Radiol. 2000;10(8):1342–50.
61. Hollingworth W, et al. AJNR Am J Neuroradiol. 2006;27:1404–11.
62. Technology Evaluation Center. TEC Bull (Online). 2003;20(1):23–6.
63. Adamson AJ, et al. Radiology. 1998;209(1):73–8.
64. Rand SD, et al. AJNR Am J Neuroradiol. 1997; 18(9):1695–704.
65. Shukla-Dave A, et al. Magn Reson Imaging. 2001;19(1):103–10.
66. Kimura T, et al. NMR Biomed. 2001;14(6):339–49.
67. Wilken B, et al. Pediatr Neurol. 2000;23(1):22–31.
68. Lin A, Bluml S, Mamelak AN. J Neurooncol. 1999; 45(1):69–81.
69. Taylor JS, et al. Int J Radiat Oncol Biol Phys. 1996; 36(5):1251–61.
70. Chao ST, et al. Int J Cancer. 2001;96:191–7.
71. Khan D, et al. AJR Am J Roentgenol. 1994; 163:1459–65.
72. Medina LS, et al. Radiology. 2005;236:247–53.
73. Colice GL, et al. Chest. 1995;108(5):1264–71.

Brain Infections: Evidence-Based Neuroimaging

26

Hui Jie Jenny Chen and Pamela W. Schaefer

Contents

H.J.J. Chen (✉) • P.W. Schaefer
Department of Neuroradiology, Massachusetts General Hospital, Boston, MA, USA
e-mail: jenzhao@ucla.edu; pschaefer@partners.org

Key Points

- Clinical presentation alone was found to have 97 % negative predictive value for pending brain herniation in a cohort study on patients with suspected bacterial meningitis, and current practice guideline suggests that neuroimaging plays little role before lumbar puncture unless patients have the risk factors for "impending herniation" (moderate evidence) [1, 15–18] (Table 26.1).
- Brain imaging is cost-effective in HIV-positive adult patients with neurological symptoms and CD4 count <200 [2, 11, 33] (moderate evidence).
- Brain imaging is not necessary in HIV-positive patients if they have no neurological symptoms (moderate evidence) [34–36].
- Conventional MR is more sensitive than CT in diagnosing encephalitis (moderate evidence) [4, 7, 25–29].
- A set of diagnostic criteria based on both post-contrast CT imaging features and clinical presentation are both sensitive (99.5 %) and specific (98.9 %) in diagnosing solitary cerebral cysticercus granulomas [moderate evidence] [42].
- Diffusion-weighted imaging is effective in differentiating brain abscess from other intracranial ring-enhancing lesions such as necrotic tumors and should be used routinely when a ring-enhancing lesion is seen on post-contrast images (moderate evidence) [46–49, 59, 63, 71] (Table 26.5).
- Diffusion-weighted imaging may facilitate more effective diagnosis of brain infections without abscess formation [limited evidence] [4, 7, 58, 70].
- Diffusion-weighted imaging is more sensitive (92.3 % sensitivity, 95 % CI 74.8–99.5 %) than conventional MR imaging in the diagnosis of Creutzfeldt-Jakob disease (CJD) [moderate evidence] [52–55].
- MR spectroscopy (MRS) is effective in differentiating brain abscess from other intracranial ring-enhancing lesions (moderate evidence)

[1, 2, 49, 51]. However, its cost-effectiveness has not been fully evaluated.
- MR Perfusion may be useful in differentiating cerebral abscesses from necrotic brain tumors [limited evidence] [56, 57].

Definition and Pathophysiology

Brain infection is usually caused by bacteria, viruses, fungi, or parasites [1]. Organisms can infect the brain via hematogenous spread (most commonly from the lungs), direct extension from the sinonasal cavity, direct implantation (instrumentation or trauma), and CSF spread from a spinal cord or spinal subarachnoid space infection. Less frequently, infections in the epidural or subdural spaces can also spread directly to the meninges and brain parenchyma [1]. The organism causing an infection can often be predicted based on the patient's age, geographic location, immune status, and clinical history (e.g., trauma, sinusitis, pneumonia) [1]. HIV-positive patients can acquire infection due to HIV itself or due to a myriad of opportunistic infections. In addition, these patients are susceptible to autoimmune conditions such as acute disseminated encephalomyelitis (ADEM) or acute demyelinating polyneuropathy during the initial and middle phases of HIV infection and neoplasm during the late phase of HIV infection [2].

Epidemiology

Meningitis and encephalitis are the two main types of brain infection. Acute bacterial meningitis is one of the top ten causes of infection-related death, and 30–50 % of survivors have permanent neurological disability. The estimated incidence of acute bacterial meningitis is 0.4–6 per 1,000,000 adults per year. The causative organisms are often related to a patient's demographics (e.g., age and geographic location) [1].

Most bacterial cerebral infections can be treated successfully when the diagnosis is early,

but delayed diagnosis results in permanent brain injury and is a major cause of disability [3]. The majority of pathogens that cause encephalitis are viruses. However, despite extensive testing, a specific virus cannot be identified in the majority of cases. Furthermore, even when an organism is identified, no effective specific treatment is available for most viruses with the exception of herpes viruses and HIV [4]. Herpes simplex type 1 (HSV-1) is the causative agent in 95 % of herpetic encephalitis cases and the most common cause of fatal sporadic encephalitis. It also accounts for up to 20 % of all cases of encephalitis. Its incidence is 1–4 cases per 1,000,000 [5]. The mortality rate ranges from 50 % to 70 % in untreated HSV-1 cases [5].

Neurocysticercosis is an infection of the brain and meninges by the larval stage of the tapeworm *Taenia solium* [6]. It is the leading cause of acquired epilepsy and the most common helminthic infection of the brain globally [6, 7]. While it was once thought to be eradicated in the United States, it is now a major public health concern, especially in the southwest part of the USA, as a result of the rising number of immigrants from endemic areas since the late twentieth century [8, 9]. For example, 10 % of adults with new onset seizures in one emergency department in Los Angeles, California, have neurocysticercosis [9]. Sixty percent of cysticercosis infections involve the CNS [8].

Patients may be immunocompromised due to HIV infection or following bone marrow or solid organ transplantation, among other etiologies [7]. HIV is not only a neurotropic virus itself and the cause of HIV encephalopathy, it is also associated with a number of opportunistic infections, including tuberculosis, toxoplasmosis (most common parasitic infection, CD4 count <100), cryptococcus (most common fungal infection), cytomegalovirus (CMV) (most common cause for encephalitis in patients with CD4 count <50), and progressive multifocal leukoencephalopathy (PML) (3–5 % of HIV-positive population) [7]. Seventy percent of all HIV patients develop neurological symptoms during their illness [10]. The HIV virus is present in the CNS of most infected children regardless of their age, CD4 count, or stage of disease [2]. In addition, most opportunistic infections in adults result from reactivation and not from primary exposure. However, this is not the case for pediatric patients, who are usually less exposed to these pathogens and have less time to allow reactivation of a latent infection. Therefore, common HIV-related infections, such as tuberculosis (TB), are not common in pediatric patients [2]. It should be noted that since the advent of HAART therapy, the incidence of HIV-related dementia, opportunistic infections, and primary CNS lymphoma has markedly fallen [11].

In other immunocompromised patients, the most frequent brain infections are fungal in etiology, including aspergillosis and mucormycosis [12].

Overall Cost to Society

While, to our knowledge, cost-effectiveness studies have not been performed, the cost of brain infections to society is potentially high for a number of reasons: (1) The morbidity and mortality rates in previously healthy, young, and productive individuals are high. (2) The hospitalization and rehabilitation periods are relatively long. (3) The diagnostic process with imaging and microbiological testing is expensive and frequently ineffective. (4) Pharmaceutical treatments are expensive [13]. According to one study based on 4,225 patients admitted to Johns Hopkins neurology service between October 2004 and December 2005 [13], 80 % of patients with neurological infections were aged between 18 and 65 years. The mortality rate in this cohort of patients was 12 %, compared to 3.1 % for all patients admitted to the neurology service at the same period of time. Severe morbidity as defined by prolonged rehabilitation period or discharge to a long-term care facility or another health care facility for further treatment was 28 % for patients with brain infection, compared to 19 % for all admissions [13].

Goals of Imaging

Cerebrospinal fluid (CSF) analysis, biopsy, and other laboratory analysis remain the gold standard for identifying the infectious agent based on a recently published practice guideline [14].

The overall goals of imaging are based on three stages of patient care:

1. Initial imaging for the diagnosis and guidance of treatment and procedures
2. Subsequent imaging exams for following posttreatment changes or complications (HACTIVE – hydrocephalus, abscess, cerebritis/cranial nerve lesions, thrombosis (arterial or venous), infarction, ventriculitis/vasculopathy, and extra-axial collection) [1] (Fig. 26.2)
3. Imaging after initial infection has subsided in patients presenting with postinfectious syndromes, such as acute disseminated encephalomyelitis (ADEM, Guillain-Barre syndrome (GBS)) and immune reconstitution inflammatory syndrome, and neoplasm (in immunocompromised patients) [1, 10]

Methodology

A MEDLINE search was performed using PubMed (National Library of Medicine, Bethesda, Maryland) for original research publications addressing the diagnostic performance and effectiveness of imaging strategies for brain infection. The search covered the years from April 1959 to December 2010. The search strategy employed different combinations of terms including (but not limited to) brain, infection, radiology, imaging, socioeconomic, cost-effective, HIV, immunocompromised, pediatric, meningitis, CNS, encephalitis, diffusion-weighted imaging, Creutzfeldt-Jakob disease, neurocysticercosis, and brain abscess. Reviewing the reference lists of relevant papers identified additional articles. This review was limited to human studies and acquired adult and pediatric infections. Congenital brain infection is not included in the discussion. The first author performed an initial review of the titles and abstracts of the identified articles followed by review of the full text in articles that were relevant.

Discussion of Issues

Which Patients with Suspected Brain Infection Should Undergo Head CT Imaging Prior to Lumbar Puncture?

Summary
There is moderate evidence that clinical presentation alone was found to have 97 % negative predictive value for pending brain herniation in a cohort study on patients with suspected bacterial meningitis. Therefore, the current practice guideline suggests that neuroimaging plays little role before lumbar puncture unless patients have the risk factors for "impending herniation" [1, 15–18].

Supporting Evidence
Head CT Before Lumbar Puncture Raised intracranial pressure resulting in brain herniation has been recognized as a major complication of bacterial meningitis (4–6 %) based on postmortem pathological data since the early 1960s [19]. Additionally, profoundly increased intracranial pressure is also associated with up to 50 % increased mortality [19]. However, the incidence of brain herniation as a result of lumbar puncture is unknown; it is proposed to be from less than 1.2 % to up to 6 % based on the observation that most herniation occurs following lumbar puncture [15]. Nonetheless, studies have also shown that brain herniation can occur without lumbar puncture as a natural progression of the disease. The authors found insufficient evidence on the direct cause-effect relationship between lumbar puncture and subsequent brain herniation.

CT of the head is frequently ordered before lumbar puncture in patients with suspected brain infection, since there is a theoretical risk of transtentorial brain herniation, because lumbar puncture can result in a small, transient cerebrospinal fluid pressure gradient secondary to the removal of CSF and the opening made in the arachnoid membrane [16, 17]. However, in one

study, nearly 40 % of physicians ordered a screening CT primarily because they thought it was the "standard of care" or because of fear of litigation [17]. Most CTs of the head obtained in patients with proven bacterial and viral brain infections are normal [7]. A number of studies have examined both the relationship between brain herniation and lumbar puncture in patients with CNS infections [15, 20, 21] and the role of imaging in identifying patients at risk of brain herniation [15–18, 20, 21]. The most cited study on this subject is a prospective cohort study by Hasbun et al. (moderate evidence) [16], which suggests that performing CT of the brain before lumbar puncture is not necessary in patients without risk factors for herniation on presentation (moderate evidence). In the study, 235 out of 301 (78 %) adults with suspected meningitis underwent CT of the head before undergoing lumbar puncture. CT was abnormal in 56 of the 235 patients (24 %), and only 11 patients (5 %) had evidence of mass effect. A set of baseline clinical features were found to be associated with abnormal findings on CT of the head and included age (≥ 60 years), compromised immune status, a history of central nervous system disease, a history of seizure within 1 week before presentation, and neurologic deficits [16]. Ninety-six of the 235 (41 %) patients imaged had none of these clinical features, and 93 of these 96 patients also had normal CT scans, yielding a negative predictive value of 97 %. The remaining three patients subsequently underwent lumbar puncture, without evidence of brain herniation [16]. Therefore, the most recent IDSA (Infectious Diseases Society of America) guideline does not recommend performing head CT prior to lumbar unless the patient presents with clinical risk factors of impending herniation (Fig. 26.1) [15]. Table 26.3 lists the recommended criteria for selecting which patients with suspected bacterial meningitis to image before lumbar puncture. Figure 26.1 outlines the initial imaging strategy recommended by IDSA for both adult and pediatric patients suspected of having bacterial meningitis.

Cost-effectiveness Study On average, lumbar puncture is delayed for 2 h if a screening CT is performed first, and there is a trend of delayed administration of empirical antibiotics in the same group [17]. In a cohort study of 269 patients with community-acquired bacterial meningitis proven by lumbar puncture within 24 h of presentation, delay in therapy after arrival in the emergency department was associated with adverse clinical outcome when a patient's condition advanced to the highest stage of prognostic severity before the initial antibiotics were given. While no formal cost analysis was conducted, it is conceivable that subsequently increased complications, hospitalization, and increased duration of treatment will increase the cost of care [17, 22]. On the other hand, if the antimicrobial treatment is performed before a screening CT, isolation of the microbial pathogen from CSF during a subsequent lumbar puncture may not be diagnostic [17]. In addition, clinicians should be cautious of a normal CT of the head, since brain herniation as a result of increased intracranial pressure caused by meningitis itself cannot be completely excluded [18].

Applicability to Children The Hasbun et al. study did not include pediatric patients [17]. However, the risk of brain herniation secondary to meningitis is apparently equal to or higher than the risk in adults [20]. According to one source, while some authorities permit possible delay of lumbar puncture in adult patients with seizures due to higher chance of elevated intracranial pressure, delay of lumbar puncture in children is not recommended given the higher occurrence rate of seizures in children with brain infection [15]. The authors have not found studies or clear guidelines regarding performing a screening CT in the pediatric population suspected of having a brain infection. However, with recent introduction of a "rapid-sequence" MRI, the disadvantage of long MRI scanning time requiring sedation in the pediatric population has been addressed [23, 24]. In our institution, "rapid-sequence" MRI consists of obtaining an ultrafast T2-weighted (half-Fourier acquisition single-shot turbo spin-echo) pulse sequence in three planes through the whole brain, with each imaging plane requiring 30 s. The patient is held still

by a parent, and no sedation is required. There is limited evidence that "rapid-sequence" MRI can provide equivalent (and possibly more) information than a non-contrast CT including ventricular size (i.e., if there is evidence of hydrocephalus), and the option of less radiation exposure in a pediatric population is very desirable [23, 24]. Therefore, this seems to be a promising imaging strategy for children requiring pre-lumbar puncture, though its effectiveness needs to be further investigated.

What Kind of Conventional Imaging Is Appropriate?

Summary

Significant advances in MR technology now allow for more timely and accurate diagnosis of brain infections.

- There is moderate evidence that conventional MR is more sensitive than CT in diagnosing brain infections, especially encephalitis [4, 25–29].
- There is moderate evidence demonstrating that MR is complementary to CSF polymerase chain reaction (PCR) analysis for the diagnosis of herpes simplex virus encephalitis [4, 30–32].

Supporting Evidence

Conventional MRI Versus CT Several cohort studies comparing conventional MRI (T2, FLAIR, pre- and post-contrast-enhanced T1-weighted images) to CT in detecting early intracranial pathology demonstrated that conventional MRI is significantly more sensitive, especially in the case of encephalitis (moderate evidence) [25–29]. In a study with limited evidence, eight patients with HHV-6 encephalopathy and nine patients with HSE encephalopathy underwent MR exams, and all had abnormal MRI findings in the early and middle periods of their disease. However, among the patients who underwent CT in the early period, none of the four with HHV-6 encephalopathy and six of

the seven with HSE had abnormal findings [26]. Henkes et al. provided moderate evidence in a study of 129 AIDS patients demonstrating that in 20 % of patients, the MR exams (unenhanced T2-weighted images alone) demonstrated intracranial manifestations of HIV while the CT scans were normal. MR provided additional diagnostic information not present on a concurrently performed abnormal CT scan in another 20 % of patients [28].

While the authors were not able to find a larger, prospective, generalized study on this particular subject, the most recent encephalitis management guideline by IDSA (Infectious Disease Society of America) published in 2008 has recommended MRI as the neuroimaging modality of choice, over CT [4].

MRI Versus CSF PCR Analysis in Herpes Simplex Encephalitis CSF PCR has high sensitivity (96–98 %) and specificity (95–99 %) for diagnosing herpes simplex virus, a disease that can be effectively treated but can result in high mortality if the diagnosis is delayed or missed [4, 30]. However, sensitivity for PCR is not 100 %, and false negatives do occur [4, 32]. Two studies with limited evidence [31, 32] suggested that a combination of clinical presentation, imaging findings, and CSF PCR analysis should be used to more efficiently diagnose HSV encephalitis [14, 31, 32]. There have been case reports where MRI findings were highly suggestive of HSV, initial PCR was negative, and repeat PCR was positive [31]. The authors concluded that a second LP should be considered with discordant imaging and PCR results [31]. However, the authors have not found a large-scale study comparing the sensitivity between MR and CSF PCR analysis. In terms of specificity, PCR is superior, as many imaging findings are nonspecific or at best suggestive [4, 31]. On the other hand, MRI often prompts CSF PCR analysis when HSV is not initially suspected clinically [31].

Imaging Used for Assessing Complications from Brain Infections Complications from brain

infection can be grouped into acute versus sub-acute and chronic processes. In the acute setting, when patients do not improve after treatment as expected or when patients develop new neurological symptoms immediately following initial diagnosis, imaging is indicated [1]. A group of common but serious complications from bacterial meningitis can be detected with MR or CT. These include hydrocephalus, abscess, cerebritis/cranial nerve lesions, thrombosis (arterial or venous), infarction, ventriculitis/vasculopathy, and extra-axial collection (HACTIVE) [1].

In the subacute to chronic setting, imaging can be useful in detecting postinfectious syndromes, such as acute disseminated encephalomyelitis (e.g., ADEM), Guillain-Barre Syndrome (GBS), and immune reconstitution inflammatory syndrome (e.g., HIV patients), and neoplasm (e.g., primary CNS lymphoma) [1, 10] (Fig. 26.2).

Special Case 1: HIV-Infected Adults HIV-related CNS infections include primary HIV infection (e.g., dementia) and opportunistic infections. Since the advent of HAART, the incidences of these infections and primary CNS lymphoma have markedly decreased [11]. Relatively new causes for neurological complications in HIV-positive patients include IRIS (immune reconstitution inflammatory syndrome) and reactions to medications [11]. Along with clinical information (i.e., CD4 count, history, etc.), imaging plays a pivotal role in managing HIV-positive patients with neurological symptoms (moderate evidence) [2, 11, 33–36].

There is moderate evidence that CT should be used to detect clinically significant neuropathology among HIV-positive patients (or patients at high risk for HIV) with new focal or non-focal neurological symptoms [33]. In Tso et al., an early retrospective study of 146 patients (114 patients with known HIV seropositivity, 32 patients with HIV risk factors but unknown HIV status), there was significant correlation between neurological complaints and abnormal CT findings (moderate evidence). Simple linear regression showed significant positive correlation

between specific neurological complaints and lesion found on CT (versus normal CT). (Altered mental status: $p = 0.0051$, extremity paresis: $p = 0.00001$) [33]. Similar percentages of HIV-positive patients and of patients at risk with unknown HIV status had abnormal scans [33].

Among all CNS opportunistic infections in HIV patients, toxoplasmosis is the most common infection [14]. One author suggests that for HIV patients with a CD4 count <200 cells/mm^3, who are considered at the highest risk for HIV-related cerebral complications, CT with and without contrast can sometimes obviate the need for LP if the findings suggest toxoplasmosis, primary CNS lymphoma, or PML [11]. However, no apparent consensus was found in terms of which modality is better at making the initial diagnosis [36]. In cases with a typical appearance of toxoplasmosis (multiple ring- or solid enhancing lesion), medications should be promptly started. Follow-up imaging may show treatment response in up to 80 % of patients according to one author in approximately 1 week [14], but other diagnoses should be considered if the lesions are unchanged or have progressed. Among the differential diagnoses, CNS lymphoma is the most challenging, especially when there is a large solitary lesion [14]. There is moderate evidence that thallium-201 single-photon emission computed tomography (TI-201 SPECT) can accurately differentiate primary brain lymphoma from other CNS lesions in HIV-positive patients (sensitivity 86 %, specificity 83 %) and that diagnostic accuracy is improved with a combination of TI-201 SPECT and serum Toxoplasma IgG [37]. There is also limited evidence that diffusion-weighted imaging can help with differentiating toxoplasmosis from lymphoma, though significant overlap in ADC values is still problematic [38].

In Post et al. [34], an early (1991) prospective cohort study of 119 HIV-positive patients without other intracranial disease (e.g., opportunistic infection and tumor), there was a statistically significant difference in the frequency of abnormal brain MRIs found between the symptomatic and asymptomatic groups ($p = 0.001$) (moderate

evidence). Additionally, statistically significant correlations between cortical atrophy and CD4 count ($p = 0.015$) and between cortical atrophy and viral load ($p < 0.001$) were also reported [34]. However, with moderate evidence, the authors suggest that screening MRI for asymptomatic HIV patients is low yield because while MR imaging can show indirect evidence of HIV infection early in the disease, the abnormalities will be minor and seen only in a minority of neurologically asymptomatic subjects (moderate evidence). In this study, 20 patients received zidovudine, but no significant difference in imaging findings was found between patients with and without the treatment. In a subsequent follow-up study [35], MR progression (in 1–2 years) of intracranial pathology was shown to be minimal in asymptomatic HIV patients, and it was only seen in a minority of neurologically symptomatic HIV patients with clinical deterioration (limited evidence) [35].

Special Case 2: Neurocysticercosis Neurocysticercosis (NCC) is the most common CNS helminthic infection and the leading cause of acquired epilepsy in the world, and cases of neurocysticercosis (NCC) are increasing in the USA as a result of immigration [6]. Both initial clinical and imaging presentations of NCC are highly variable depending on the stage and location of the infection [6, 9, 39]. A set of complex objective clinical diagnostic criteria was last updated in 2000 to improve sensitivity and specificity of diagnosis [40, 41] (Table 26.4). These diagnostic criteria are based on a combination of (a) clinical findings, (b) cysticercus-specific IgG antibody level as determined with an enzyme-linked immunoelectrotransfer blot assay, (c) an enzyme-linked immunosorbent assay in either serum or CSF, and (d) MR or CT imaging findings [6, 40–42]. While the criteria appear intuitive and are widely cited in the literature, the authors have not found large population studies to validate this set of criteria either from endemic regions around the world or in the USA [6]. In terms of the imaging component of this proposed criteria, the group used studies with limited evidence [43, 44] for "absolute criteria" and a study with moderate

evidence [42] for its "major criteria." Nonetheless, the importance of imaging in both the diagnostic and follow-up phases must be stressed, as the sensitivity (65–98 %) and specificity (67–100 %) of current serology tests are highly variable due to the nature of the disease [6, 45]. CT is more sensitive in detecting calcified NCC than MRI, and 50 % of NCC lesions calcify [6, 39]. In addition, with moderate evidence, Rajshekhar et al. [42] showed that a set of diagnostic criteria with emphasis on post-contrast CT findings had a sensitivity of 99.5 %, a specificity of 98.9 %, a PPV of 99 %, and a NPV of 99.5 % for the diagnosis of a solitary cerebral cysticercus granuloma [42]. However, MRI does have higher contrast resolution, which makes it easier to detect intraventricular lesions which are often isodense to CSF on CT [6, 39]. Besides diagnosing the disease, both CT and MR are also useful for:

1. Identifying the distinct stages of NCC, which are important in terms of designing the right treatment strategy. Imaging also helps with assessing treatment response [6, 39]. For example, live cysts are often isointense to CSF. However, with degeneration or after antihelminthic medication, the cyst fluid becomes more proteinaceous and gelatinous and shows progressive T1 hyperintensity or MRI [39].
2. Following the number and size of the cystic lesions after treatment [39].
3. Detecting related complications, such as hydrocephalus and vasculopathy [39].

What Is the Role of Advanced Imaging Techniques (Diffusion, Perfusion, and MR Spectroscopy) in the Evaluation of Brain Infections?

Summary

- There is moderate evidence confirming the effectiveness of diffusion-weighted imaging in differentiating pyogenic abscesses from other ring-enhancing/cystic brain parenchymal lesions [14, 46–50].
- There is moderate evidence that in addition to diffusion-weighted imaging, MR spectroscopy

can further differentiate pyogenic abscesses from necrotic tumors [1, 2, 47, 49, 51].

- There is moderate evidence that diffusion-weighted imaging is more sensitive (92.3 % sensitivity, 95 % CI 74.8–99.5 %) in the diagnosis of Creutzfeldt-Jakob disease (CJD) [52–55].
- There is limited evidence that in addition to diffusion-weighted imaging, MR perfusion imaging can further differentiate pyogenic abscesses from necrotic tumors [56, 57].
- There is limited evidence that diffusion-weighted imaging is useful in diagnosing brain infection other than intracranial pyogenic fluid collections [4, 7, 29, 58].

Supporting Evidence

Diffusion-Weighted Imaging (DWI) in Differentiating Abscess from Other Ring-Enhancing/Cystic Lesions DWI has been proposed as the diagnostic method of choice for pyogenic abscess when a ring-enhancing lesion is seen [14]. There is moderate evidence suggesting that diffusion-weighted imaging is both more sensitive (95.2 %) and more specific (95.7 %) than conventional MR (61.9 % sensitive, 60.9 % specific) imaging in differentiating pyogenic abscess from other ring-enhancing brain lesions [46–49] (Tables 26.5, 26.6). Use of DWI for diagnosing any pyogenic intracranial fluid collection is also supported by moderate evidence [50].

In Lai PH et al., a prospective study, with moderate evidence, of 50 patients with intracranial ring-enhancing lesions, the diagnostic accuracy, sensitivity, specificity, positive predictive value, and negative predictive value of DWI were shown to be much higher than conventional MRI (Table 26.6) [47]. In Bükte Y et al., another prospective study with moderate evidence, comparing the findings of conventional MR with those of DWI in 63 cystic intracranial lesions in 48 patients, the authors concluded that the sensitivity of DWI for differentiating abscesses from primary brain tumors was 100 %, for differentiating abscesses from metastatic tumors was 73 %, and for differentiating benign from malignant lesions was 90 % [48]. In Mishra et al., a prospective study

with moderate evidence, a group of 52 patients with intracranial cystic lesions were evaluated with conventional MR and DWI techniques; the sensitivity and specificity of DWI for differentiating brain abscess from other lesions were 72 % and 100 %, respectively [49]. In Leuthardt EC et al., a retrospective study with limited evidence, five patients in combination with a meta-analysis of 15 previous studies including a total of 204 patients with ring-enhancing lesions, the majority of pyogenic abscesses (38 out of 39 lesions) demonstrated significantly more DWI hyperintensity and ADC hypointensity than nonpyogenic lesions (165 lesions) [46].

Several studies have suggested that calculated ADC values alone do not allow a reliable differentiation of abscess from other ring-enhancing lesions due to a large overlap [59, 60]. However, there is limited evidence that the majority of necrotic glioblastomas do not demonstrate diffusion restriction within the necrotic cavity and that additional quantitative and qualitative methods can increase the specificity of ADC values as an extension of the DWI technique [61–63]. For example, Reiche et al. concluded that the addition of FA (fractional anisotropy) values may result in better differentiation between pyogenic abscesses and cystic neoplasms in ring-enhancing lesions with decreased ADC values [63].

Additionally, there is limited evidence that DWI is superior to conventional MR in assessing treatment response of intracranial abscess [64–66]. In Cartes-Zumelzu et al. (limited evidence) [64], seven adult patients with intracranial abscesses were treated with either surgical drainage (6/7) or antibiotics (1/7). The ADC values appeared to parallel treatment response and clinical course (based on regular neurological exams and CRP levels). In Fanning et al. (limited evidence) [66], eight pediatric patients with 13 intracranial abscesses were followed throughout their clinical courses. At initial diagnosis, all collections showed diffusion restriction (mean ADC $0.61 \pm 0.15 \times 10^{-3}$ mm^2/s). On follow-up, in patients with persistent clinical sepsis, the collections showed

ADC values ($0.66 \pm 0.21 \times 10^{-3}$ mm^2/s) that remained significantly lower than those of normal cortical gray matter (ADC value: $1.06 \pm 0.10 \times 10^{-3}$ mm^2/s, $p < 0.001$). Clinical clearance of infection was associated with ADC values ($1.57 \pm 0.15 \times 10^{-3}$ mm^2/s) that were significantly higher than those of normal cortical gray matter ($p < 0.01$).

Diffusion-Weighted Imaging (DWI) in Diagnosing Other Brain Infections Including Creutzfeldt-Jakob Disease (CJD) There is moderate evidence that DWI is the most sensitive modality for diagnosing early CJD [52–55]. In Shiga et al. [53], a case-controlled study with moderate evidence, 26 out of 36 total patients with eventual diagnosis of either probable or definite CJD were examined using DWI along with procedures used in the World Health Organization CJD diagnostic criteria, including EEG, CSF NSE (neuron-specific enolase), and CSF 14-3-3 protein detection. DWI had 92.3 % sensitivity (95 % CI 74.8–99.5 %), while EEG periodic sharp wave complex had 50 % sensitivity ($p < 0.0005$). DWI was not statistically significantly more sensitive than CSF NSE (neuron-specific enolase) (sensitivity 73.3 %, $p = 0.06$) or CSF 14-3-3 protein detection (sensitivity 84 %, $p = 0.36$). Diagnostic specificity using DWI was 93.8 % (95 % CI 79.2–99.2 %) [53]. In one limited case series, Demaerel et al. [54], DWI had 100 % sensitivity and 100 % specificity for detecting sporadic CJD, in comparison to 100 % sensitivity and 43 % specificity using 14-3-3 protein, and 40 % sensitivity and 85 % specificity using EEG [54]. The "pulvinar sign," an MR finding that suggests probable variant CJD (vCJD), was 100 % sensitive on FLAIR images in one study [67]. However, the number of patients (two) with DWI in that study was too small to verify the additional value of DWI [67].

There is limited evidence that diffusion-weighted imaging has clinical value in evaluating other nonpyogenic brain infections. For example, DWI was found to be more sensitive in early detection and disease monitoring of PML, HSV, enterovirus 71, and West Nile virus [4, 7, 58].

MR Spectroscopy and Perfusion-Weighted Imaging (PWI) in Differentiating Abscess from Necrotic Neoplasm There is moderate evidence that MR spectroscopy increases the sensitivity and specificity in differentiating abscesses from necrotic neoplasms, especially when used in combination with other advanced MR techniques [1, 2, 47, 49, 51]. Typical MRS of an abscess demonstrates elevated lipid, lactate, alanine, and various amino acid peaks and low NAA and Cr peaks [1]. The diagnostic accuracy, sensitivity, specificity, positive predictive value, and negative predictive value for differentiating abscess from ring-enhancing neoplasm using MRS alone and MRS with DWI are summarized in Table 26.6 [47]. In another study with moderate evidence, MR spectroscopy was found to have higher sensitivity (96 %) than DWI (72 %) and the same specificity (100 %) [49]. The authors of the study suggested that MR spectroscopy should be obtained on all DWI-negative ring-enhancing brain lesions [49]. There is limited evidence that MRS can further distinguish abscesses of different infectious etiologies (e.g., tuberculosis versus bacterial versus fungal) [1, 68, 69].

There is limited evidence that perfusion-weighted MR can differentiate necrotic tumor (higher cerebral blood volume in the enhancing ring) from pyogenic abscess (lower cerebral blood volume in the enhancing rim) [56, 57].

Applicability to Children There is limited evidence that DWI may be more sensitive for detecting pediatric CNS infection (encephalitis, abscess, and postinfectious infarction) because of the high water content of the pediatric brain [29, 70].

Cost-effectiveness Analysis Given the short additional exam time (approximately 2 min) and high sensitivity and high specificity of the DWI sequence for identifying pyogenic brain abscesses, this sequence is now routinely added to existing conventional MR protocols in evaluating pyogenic infections and ring-enhancing lesions. However, the cost-effectiveness of other advanced MR techniques, such as MR spectroscopy and MR perfusion, is still unknown.

Take-Home Tables and Figures

Tables 26.1 through 26.6 highlight data, evidence, options, and strategies.

Figure 26.1 is an algorithm for pediatric and adult patients with suspected acute meningitis.

Imaging Case Studies

Case 1: Basilar TB Meningitis (Fig. 26.2a–e)
Case 2: Streptococcus Pneumonia Meningitis (Fig. 26.3a–f)
Case 3: Biopsy-Proven Streptococcus Brain Abscess (Fig. 26.4a–f)
Case 4: History of a Grade 2 Oligoastrocytoma (Fig. 26.5a–e)

Suggested Imaging Protocols

Computed Tomography (CT)

A non-contrast CT of the brain is usually the modality of choice as it is sufficient and cost-effective to exclude findings that may preclude lumbar puncture and will not obscure other findings such as subarachnoid hemorrhage [5, 12].

The standard non-contrast-enhanced CT protocol of the head includes 5-mm thick axial images through the entire brain, to be viewed in brain, soft tissue, and bone windows. A low-dose pediatric CT protocol (typically 120 mA, 140 kVp, depending on the size of the child) is used for pediatric patients.

Table 26.1 Summary of evidence for selected imaging strategies

Imaging strategies	Evidence	Example
CT brain before lumbar puncture in subjects with suspected infection and with one or more risk factors for brain herniation (Table 26.3)	Moderate evidence [1, 16–18]	
Patients with suspected infection but no risk factors for brain herniation do not require a CT brain before lumbar puncture	Moderate evidence [16]	
Brain imaging is not necessary in asymptomatic HIV patients	Moderate evidence [34–36]	
Diffusion-weighted imaging is effective in differentiating brain abscesses from other intracranial ring-enhancing lesions and should be used routinely when a ring-enhancing lesion is seen on post-contrast images	Moderate evidence [46–49]	Figures 26.4 and 26.5
Conventional MR is more sensitive than CT in diagnosing brain infection	Moderate evidence [4, 7, 25–29]	Figure 26.3
Brain imaging is cost-effective in HIV adult patients with neurological symptoms and CD4 count <200 (Both CT and MR)	Moderate evidence [3, 15, 33]	
Diffusion-weighted imaging is more sensitive (92.3 % sensitivity, 95 % CI 74.8–99.5 %) than conventional MR imaging in the diagnosis of Creutzfeldt-Jakob disease (CJD)	Moderate evidence [52–55]	
MR spectroscopy (MRS) is effective in differentiating brain abscesses from other intracranial ring-enhancing lesions. However, the cost-effectiveness of MRS has not been fully evaluated	Moderate evidence [1, 2, 47, 48, 51]	
MR perfusion may be useful in evaluating brain infection	Limited evidence [56, 57]	Figure 26.4
CT with contrast is both sensitive and specific in diagnosing solitary cerebral cysticercus granulomas	Strong evidence [42]	

Table 26.2 Imaging options for brain infections

Imaging studies	Contrast required	Time[d] (minutes)	Radiation	Costs[§§]
Imaging option for brain infection[c]				
CT	Yes	Seconds	Yes	$
MR conventional[a]	Yes	18	No	$$
MRS[b]	No	22	No	$$$$
PWI[b]	Yes	22	No	$$$$
DWI[a]	No	21	No	$$
CISS/ FIESTA[b]	No	23	No	$$$
MRA[b]	No	22	No	$$$

[a]Conventional MR study includes standard sagittal T1, axial pre- and post-gadolinium T1, axial T2, axial GRE, and axial FLAIR sequences
[b]Conventional MR plus additional sequences added for more specific findings of a particular infectious etiology
[c]Congenital CNS infection and congenital HIV infection are not included in the targeted population to image in this table
[d]The fastest time is included in the final calculation. Timing also varies between scanners.
[e]The cost is based on relative reimbursable rate and duration of the exam

Table 26.3 Recommended criteria for adult patients with suspected bacterial meningitis who should undergo CT prior to lumbar puncture

Criterion	Comment
Immunocompromised state	HIV infection or AIDS, receiving immunosuppressive therapy, or status posttransplantation
History of prior CNS disease	Mass lesion, stroke, or focal infection
New onset seizure[a]	Within 1 week of presentation for adults[b]
Papilledema	Presence of venous pulsations suggests absence of increased intracranial pressure
Abnormal level of consciousness	
Focal neurologic deficit	Including dilated nonreactive pupil, abnormalities of ocular motility, abnormal visual fields, gaze palsy, arm or leg drift

Reprinted with permission from Tunkel et al. [15]
[a]Some would not perform a lumbar puncture on patients with prolonged seizures or would delay lumbar puncture for 30 min in patients with short and convulsive seizure
[b]Delayed LP is not practical in the pediatric population with new onset of seizure due to high prevalence in this population (30 %)

While contrast-enhanced CT can increase sensitivity in detecting small lesions and leptomeningeal spread, it usually does not provide additional information under the condition that a lumbar puncture will be routinely performed. In addition, the value of contrast-enhanced CT is even less, since most CT findings will be normal or nonspecific in meningitis cases [12].

Magnetic Resonance Imaging (MRI)

Conventional gadolinium-enhanced MRI of the brain includes [5, 12]:
- Axial and sagittal pre-contrast T1W images
- Axial, coronal, and sagittal gadolinium-enhanced T1W images
- Axial T2 and FLAIR images
- Diffusion-weighted images (DWI/ADC)
- GRE images

Additional images using advanced MR techniques for specific suspected etiology include:
- MR spectroscopy (MRS)
- MR angiography (MRA) (e.g., for complications such as focal vasospasm, aneurysm, or thrombosis)
- CISS/FIESTA (e.g., for detecting intraventricular neurocysticercosis)
- MR perfusion

Pediatric population: T2 HASTE, rapid brain protocol

Future Research

- Cost-effectiveness of advanced MR techniques (MR spectroscopy and MR perfusion) should be encouraged, as there is existing promising evidence for their utilization.
- Validation in larger population of previously proposed neurocysticercosis diagnostic criteria will be beneficial to both endemic regions in the world as well as the United States [6].

Table 26.4 Diagnostic criteria for human neurocysticercosis

Diagnostic criteria	Criteria
Absolute criteria	1. Histologic demonstration of the parasite from biopsy of a brain or spinal cord lesion
	2. Direct visualization of subretinal parasite via fundoscopic exam
	3. Evidence of cystic lesions with scolex on MRI or CT
Major criteria	1. Evidence of lesions suggestive of neurocysticercosis on neuroimaging studies[a]
	2. Positive serum EITB[b] tests for the detection of anticysticercal antibody
	3. Resolution of intracranial cystic lesions after therapy with albendazole or praziquantel
	4. Spontaneous resolution of small single enhancing lesions[c]
Minor criteria	1. Lesions compatible with neurocysticercosis on neuroimaging studies[d]
	2. Clinical manifestations suggestive of neurocysticercosis[e]
	3. Positive CSF ELISA for detection of anticysticercal antibodies or cysticercal antigens
	4. Cysticercosis outside the CNS[f]
Epidemiologic criteria	1. Evidence of a household contact with Taenia solium infection
	2. Individuals coming from or living in an area where cysticercosis is endemic
	3. History of frequent travel to cysticercosis-endemic areas
Diagnostic certainty	*Criteria*
Definitive	1. Presence of one absolute criterion
	2. Presence of two major plus one minor and one epidemiologic criterion
Probable	1. Presence of one major plus two minor criteria
	2. Presence of one major plus one minor and one epidemiologic criterion
	3. Presence of three minor plus one epidemiologic criterion

Reprinted with permission from Del Brutto et al. [41]

[a]CT or MRI showing cystic lesions without scolex, enhancing lesions, or typical parenchymal brain calcifications

[b]Enzyme-linked immunoelectrotransfer blot assay using purified extracts of Taenia solium antigens, as developed by the Centers for Disease Control and Prevention (Atlanta, GA)

[c]Solitary ring-enhancing lesions measuring less than 20 mm in diameter in patients presenting with seizures, a normal neurologic examination, and no evidence of an active systemic disease

[d]CT or MRI showing hydrocephalus or abnormal enhancement of the leptomeninges and myelograms showing multiple filling defects in the column of contrast medium

[e]Seizures, focal neurologic signs, intracranial hypertension, and dementia

[f]Histologically confirmed subcutaneous or muscular cysticercosis, plain X-ray films showing "cigar-shaped" soft tissue calcifications, or direct visualization of cysticerci in the anterior chamber of the eye

Table 26.5 Summary of evidence from the literatures on effectiveness of diffusion-weighted imaging in differentiating brain abscess from ring-enhancing lesions

Literature reviewed	Sample size	Findings	Level of evidence
Guzman et al. [71]	32 cystic masses, 32 patients	The ADC values calculated in patients with brain infections (mean 0.68×10^3 mm^2/s) were significantly lower than those measured in patients with neoplastic lesions (mean 1.63 SD 103 mm^2/s; $p < 0.05$) (CI 95 %, $p < 0.05$)	Moderate
Leuthardt et al. [46]	5 cystic masses, 5 patients (+literature review)	Although not definitive for brain abscess, restricted water diffusion is an important MR imaging sign that is useful in neurosurgical treatment strategies for ring-enhancing lesions	
Tung et al. [59]	5 cystic masses, 5 patients	Although an important diagnostic sign, restricted water diffusion is not specific for brain abscess	Insufficient
Dorenbeck et al. [60]	27 cystic masses, 26 patients	DWI with calculated ADC values does not allow the reliable differentiation of enhanced central necrotic intracranial lesions	Limited
Lai et al. [47]	50 cystic masses, 50 patients	The diagnostic accuracy, sensitivity, specificity, positive predictive value, and negative predictive value of DWI were shown to be much higher than conventional MRI (Table 26.4)	Moderate
Bükte et al. [48]	63 cystic masses, 48 patients	The sensitivity of DWI for differentiating abscesses from primary brain tumors was 100 %, for differentiating abscesses from metastatic tumors was 73 %, and for differentiating benign from malignant lesions was 90 %	Moderate
Mishra et al. [49]	52 cystic masses, 52 patients	The sensitivity of DWI for differentiation of brain abscess from other ring-enhancing lesions was 72 %, whereas the specificity was 1	Moderate

Table 26.6 Differentiation of brain abscesses from cystic tumors by conventional MRI, DWI, and MRS (50 cystic lesions, 50 patients)

Modality	Accuracy (%)[a]	Sensitivity (%)	Specificity (%)	PPV (%)	NPV (%)
Conventional MRI	61.4 (45.2–75.6)	61.9 (38.4–81.9)	60.9 (38.5–80.3)	59.1 (36.4–79.3)	63.6 (40.7–82.8)
DWI	95.5 (85.1–99.4)	95.2 (76.2–99.9)	95.7 (78.1–99.9)	95.2 (76.2–99.9)	95.7 (78.1–99.9)
MRS	93.2 (81.4–98.6)	85.7 (63.7–97)	100 (85.2–100)	100 (81.5–100)	88.5 (69.8–97.6)
DWI + MRS	97.7 (88.3–99.9)	95.2 (76.2–99.9)	100 (85.2–100)	100 (83.2–100)	95.8 (78.9–99.9)

Reprinted with permission from Lai et al. [47]

Data in parentheses are 95 % CI

[a]Even though the p value and/or CI for accuracy and predictive value are valid only if the prevalence is invariant for all populations
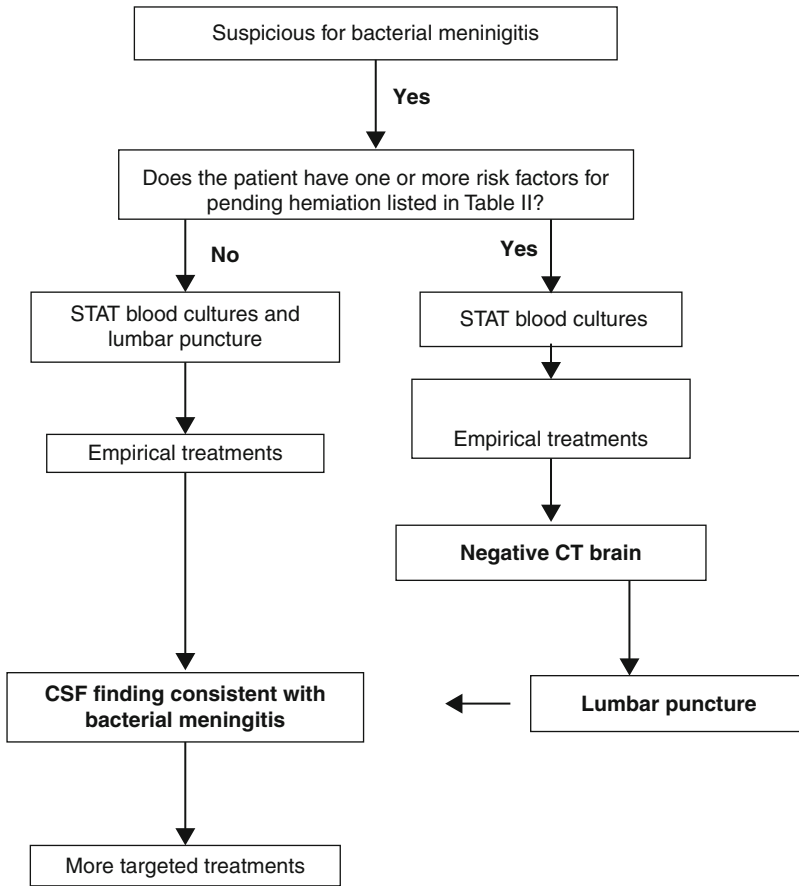
Fig. 26.1 Initial imaging strategy algorithm for pediatric and adult patients with suspected acute meningitis (Data from Tunkel et al. [15])
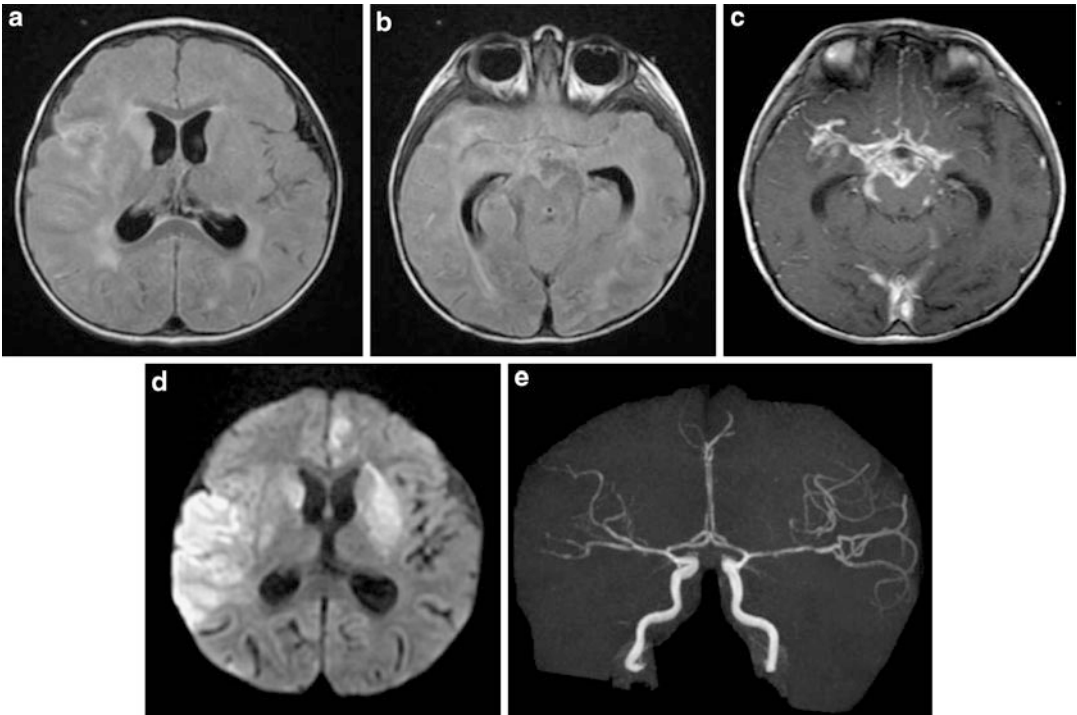
Fig. 26.2 (**a**–**e**) 6-year-old girl with weakness. Basilar TB meningitis. (**a**, **b**) FLAIR-weighted images demonstrate mild hydrocephalus; periventricular hyperintensity, consistent with transependymal edema; subtle hyperintensity in the right temporal lobe, right basal ganglia, and left lentiform nucleus, suspicious for edema or infarction; and basilar subarachnoid space hyperintensity, suspicious for meningitis. (**c**) Gadolinium-enhanced T1-weighted image demonstrates basilar leptomeningeal enhancement suggesting meningitis. (**d**) Diffusion-weighted images demonstrate restriction in the right temporal and occipital lobes, right insula, bilateral basal ganglia, and left cingulate gyrus, consistent with acute to subacute ischemia. (**e**) MRA demonstrates irregularities along the bilateral anterior and middle arteries, suggesting vasculopathy secondary to basilar meningitis
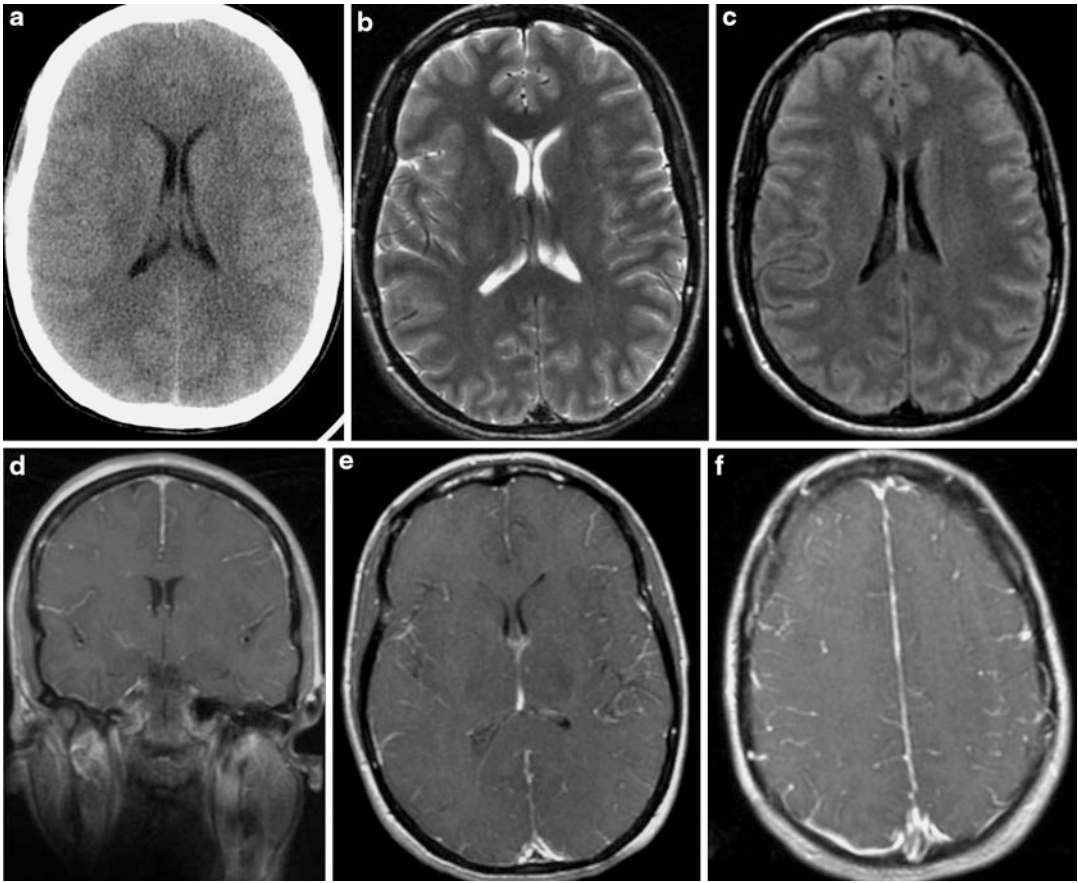
Fig. 26.3 (**a**–**f**) 38-year-old previously healthy woman presented with headache and fever. Streptococcus pneumoniae meningitis. (**a**, **b**) Non-contrast head CT and axial T2-weighted images appear normal. (**c**) Diffuse sulcal FLAIR hyperintensity is consistent with high protein content in the subarachnoid space. (**d**, **e**, **f**) Leptomeningeal enhancement on post-contrast T1-weighted images is consistent with inflammatory changes of the meninges
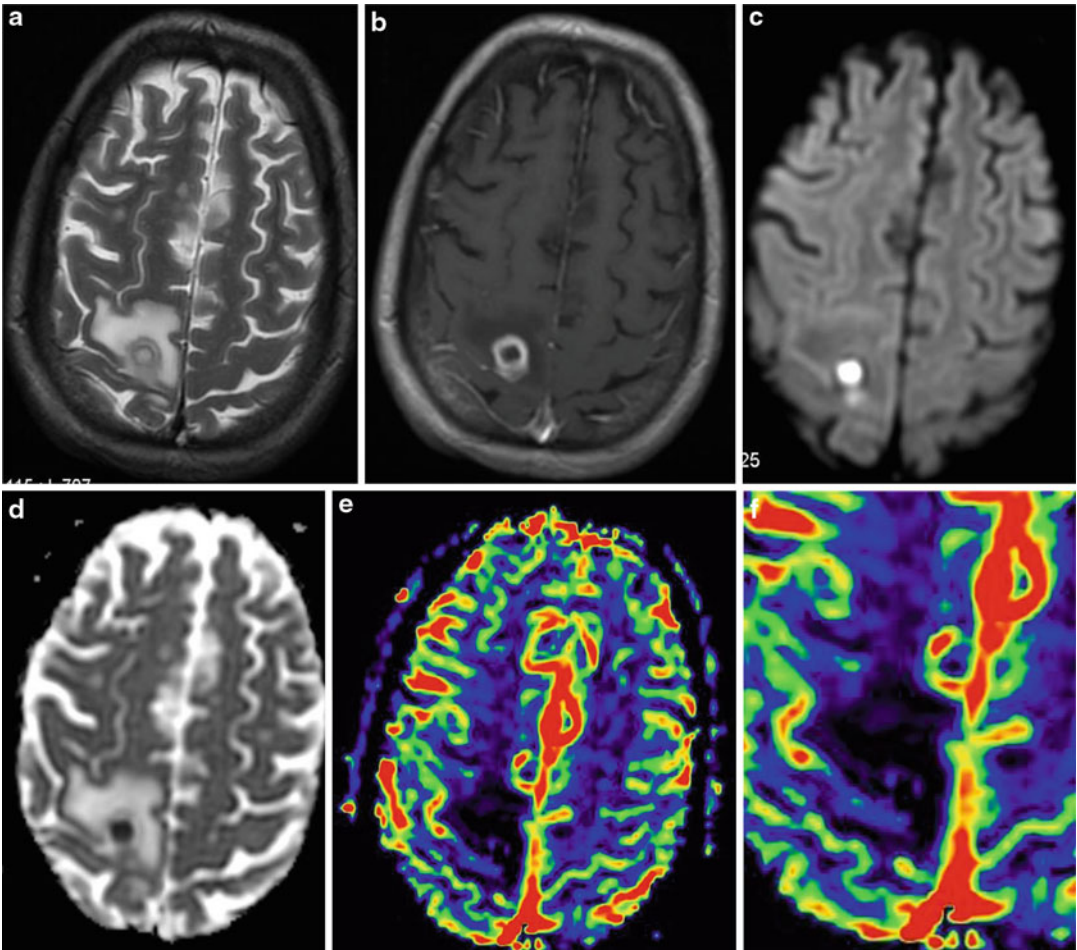
Fig. 26.4 (**a**–**f**) 80-year-old man with biopsy-proven streptococcus brain abscess. (**a**) Axial T2-weighted image shows a hypointense rim with surrounding vasogenic edema. (**b**) Axial T1-weighted gadolinium-enhanced image shows a ring-enhancing lesion with surrounding edema. (**c**–**d**) DWI hyperintensity and ADC hypointensity consistent with diffusion restriction seen in a pyogenic abscess. (**e**) MR perfusion (CBV map) image through the same level shows no significant peripheral increase in CBV. (**f**) Magnified view of the CBV map in the region of the lesion

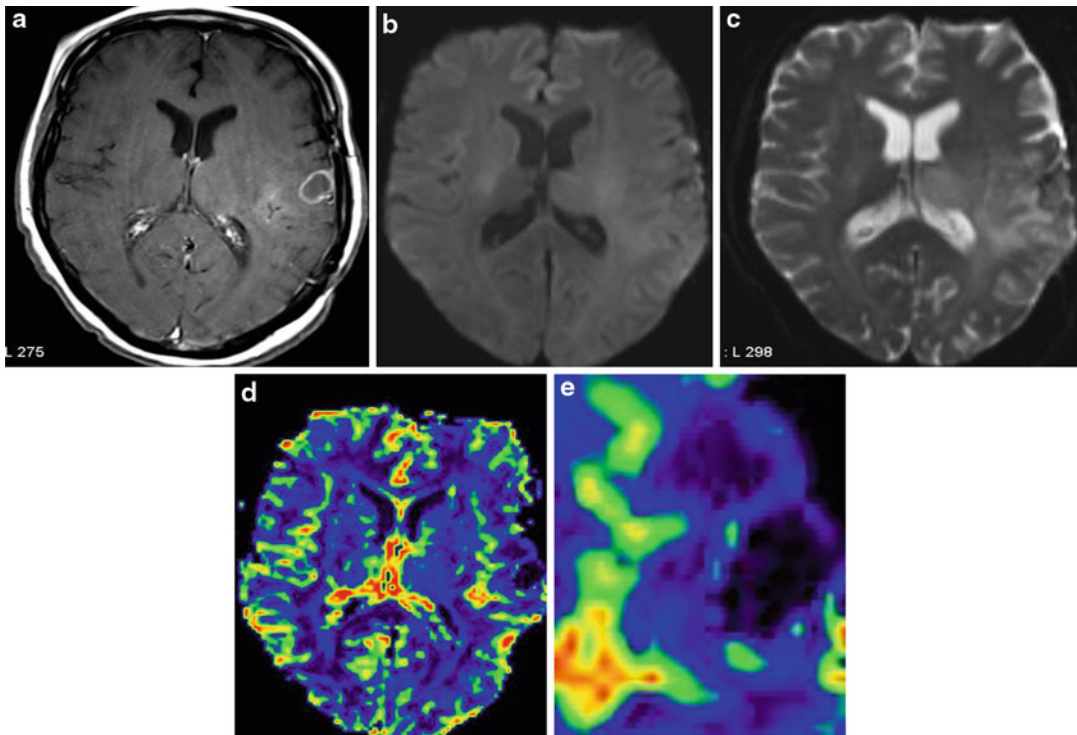**Fig. 26.5** (**a–e**) 65-year-old woman with a history of a grade 2 oligoastrocytoma. (**a**) Gadolinium-enhanced T1-weighted image shows a ring-enhancing lesion in the left temporal lobe. (**b–c**) DWI and ADC maps show elevated diffusion within the lesion. (**d**) MR perfusion map (CBV map) shows slightly increased peripheral CBV in contrast to a pyogenic abscess. (**e**) Magnified view of the CBV map in the region of the lesion

References

1. Hughes DC, Raghavan A, Mordekar SR, et al. Postgrad Med J. 2010;86(1018):478–85.
2. George R, Andronikou S, Plessis J, et al. Pediatr Radiol. 2009;39(6):575–85.
3. Anslow P. Eur Radiol. 2004;14:E145–54.
4. Tunkel AR, Glaser CA, Bloch KC, et al. Clin Infect Dis. 2008;47:303–27.
5. Atlas SW. Magnetic resonance imaging of the brain and spine. 4th ed. Philadelphia: Lippincott; 2008.
6. Sinha S, Sharma BS. J Clin Neurosci. 2009;16(7):867–76.
7. Hsu DP. Semin Roentgenol. 2010;45(2):80–91.
8. Moskowitz J, Mendelsohn G. Arch Pathol Lab Med. 2010;134(10):1560–3.
9. Kraft R. Am Fam Physician. 2007;76(1):91–6.
10. Corr P. J Psychosom Res. 2006;61:295–9.
11. Jay CA, Ho EL. Emerg Med Clin N Am. 2010;28:311–23.
12. Foerster BR, Thunher MM, Malani RN, et al. Acta Radiol. 2007;48(8):875–93.
13. Tan K, Patel S, Gandhi N, et al. Neurology. 2008;71(15):1160–6.
14. Kastrup O, Wanke I, Maschke M. NeuroRx. 2005;2(2):324.
15. Tunkel AR, Hartman BJ, Kaplan SL, et al. Clin Infect Dis. 2004;39:1267–84.
16. Hasbun R, Abrahams J, Jekel J, et al. N Engl J Med. 2001;345(24):1727–33.
17. Steigbigel NH. N Engl J Med. 2001;345:1768–70.
18. Archer BD. Can Med Assoc J. 1993;148(6):961.
19. Horwitz SJ, Boxerbaum B, O'Bell J. Ann Neurol. 1980;7:524–8.
20. de Campo J, Villanueva EV. Australas Radiol. 2005;49:252–3.
21. Korein J, Cravioto H, Leicach M. Neurology. 1959;9(4):290–7.
22. Aronin SI, Peduzzi P, Quagliarello VJ. Ann Intern Med. 1998;129(11):862–9.
23. Penzkofer AK, Pfluger T, Pochmann Y, et al. AJR Am J Roentgenol. 2002;179:509–13.
24. Ashley WW, McKinstry RC, Leonard JR, et al. J Neurosurg (Pediatr 2). 2005;103:124–30.
25. Kalita J, Misra UK. J Neurol Sci. 2000;174(1):3–8.

26. Noguchi T, Yoshiura T, Hiwatashi A, et al. AJR Am J Roentgenol. 2010;194(3):754–60.
27. Tarr RW, Edwards KM, Kessler RM. Radiologe. 2000;40(11):1011–6.
28. Henkes H, Schörner W, Jochens R, et al. Rofo. 1990;153(3):303–12.
29. Maschke M, Kastrup O, Forsting M, Diener HC. Curr Opin Neurol. 2004;17(4):475–80.
30. Baskin HJ, Hedlund G. Pediatr Radiol. 2007;37:949–63.
31. Domingues RB, Fink MCD, Tsanaclis AMC, et al. J Neurol Sci. 1998;157:148–53.
32. Weil AA, Glaser CA, Amad Z, et al. Clin Infect Dis. 2002;34(8):1154–7.
33. Tso EL, Todd WC, Groleau GA, et al. Ann Emerg Med. 1993;22(7):1169–76.
34. Post MJ, Berger JR, Quencer RM. Radiology. 1991;178:131–9.
35. Post MJ, Levin BE, Berger JR, et al. AJNR Am J Neuroradiol. 1992;13(1):359–70.
36. Ramsey RG, Geremia GK. AJR Am J Roentgenol. 1988;151(3):449–54.
37. Skiest DJ, Erdman W, et al. J Infect. 2000;40(3):274–81.
38. Camacho DL, Smith JK, et al. AJNR Am J Neuroradiol. 2003;24(4):633–7.
39. Kimura-Hayama ET, Higuera JA, Corona-Cedillo R, et al. Radiographics. 2010;30(6):1705–19.
40. Del Brutto OH, Wadia NH, Dumas M, Cruz M, et al. J Neurol Sci. 1996;142(1–2):1–6.
41. Del Brutto OH, Rajshekhar V, White Jr AC, et al. Neurology. 2001;57(2):177–83.
42. Rajshekhar V, Chandy MJ. Acta Neurol Scand. 1997;96(2):76–81.
43. Suss RA, Maravilla KR, Thompson J. AJNR Am J Neuroradiol. 1986;7(2):235–42.
44. Dumas JL, Visy JM, Belin C, et al. Neuroradiology. 1997;39(1):12–8.
45. Foyaca-Sibat H, Cowan LD, Carabin H, et al. PLoS Negl Trop Dis. 2009;3(12):e562.
46. Leuthardt EC, Wippold FJ, Oswood MC. Surg Neurol. 2002;58:395–402.
47. Lai PH, Hsu SS, Ding SW, Ko CW, et al. Proton magnetic resonance spectroscopy and diffusion-weighted imaging in intracranial cystic mass lesions. Surg Neurol. 2007;68(Suppl 1):S25–36.
48. Bükte Y, Paksoy Y, Genç E, et al. Clin Radiol. 2005;60(3):375–83.
49. Mishra AM, Gupta RK, Jaggi RS, et al. J Comput Assist Tomogr. 2004;28(4):540–7.
50. Han KT, Choi DS, Ryoo JW, et al. Neuroradiology. 2007;49(10):813–8. Epub 24 Jul 2007.
51. Lentz MR, Kim WK, Lee V, et al. Neurology. 2009;72(17):1465–72.
52. Tschampa HJ, Zerr I, Urbach H. Eur Radiol. 2007;17(5):1200–11.
53. Shiga Y, Miyazawa K, Sato S, Fukushima R, Shibuya S, Sato Y, Konno H, Doh-ura K, Mugikura S, Tamura H, Higano S, Takahashi S, Itoyama Y. Neurology. 2004;63(3):443–9. Review.
54. Demaerel P, Sciot R, Robberecht W, Dom R, Vandermeulen D, Maes F, Wilms G. J Neurol. 2003;250(2):222–5.
55. Bahn MM, Parchi P. Arch Neurol. 1999;56(5):577–83.
56. Muccio CF, Esposito G, Bartolini A, Cerase A. Radiol Med. 2008;113:747–57.
57. Chiang IC, Hsieh TJ, Chiu ML, et al. Br J Radiol. 2009;82(982):813–20.
58. Mader I, Herrlinger U, Klose U, Schmidt F, Küker W. Neuroradiology. 2003;45(10):717–21.
59. Tung GA, Evangelista P, Rogg JM, et al. Am J Roentgenol. 2001;177:709–12.
60. Dorenbeck U, Butz B, Schlaier J, et al. J Neuroimaging. 2003;13(4):330–8.
61. Fertikh D, Krejza J, Cunqueiro A, et al. J Neurosurg. 2007;106(1):76–81.
62. Hakyemez B, Erdogan C, Yildirim N, et al. Br J Radiol. 2005;78(935):989–92.
63. Reiche W, Schuchardt V, Hagen T, et al. Clin Neurol Neurosurg. 2010;112(3):218–25.
64. Cartes-Zumelzu FW, Stavrou I, et al. AJNR Am J Neuroradiol. 2004;25(8):1310–7.
65. Duprez TP, Cosnard G, Hernalsteen D. AJNR Am J Neuroradiol. 2005;26(5):1296–8. Author reply 1300–1.
66. Fanning NF, Laffan EE, Shroff MM. Pediatr Radiol. 2006;36(1):26–37. Epub 11 Nov 2005.
67. Collie DA, Summers DM, Sellar RJ, Ironside JW, Cooper S, Zeidler M, Knight R, Will RG. AJNR Am J Neuroradiol. 2003;24(8):1560–9.
68. Burtscher IM, Holtas S. AJNR Am J Neuroradiol. 1999;20(6):1049–53.
69. Kapsalaki EZ, Gotsis ED, Fountas KN. Neurosurg Focus. 2008;24(6):E7.
70. Teixeira J, Zimmerman RA, Haselgrove JC. Neuroradiology. 2001;43:1031–9.
71. Guzman R, Barth A, Lövblad K-O, El-Koussy M, Weis J, Schroth G, Seiler RW. J Neurosurg. 2002;97:1101–7.

Sellar Lesions: Evidence-Based Neuroimaging

27

Prashant Raghavan and C. Douglas Phillips

Contents

P. Raghavan (✉)
Department of Radiology, University of Virginia, Charlottesville, VA, USA
e-mail: pr9k@virginia.edu

C.D. Phillips
Department of Radiology, Weill Cornell Medical College/NewYork-Presbyterian Hospital, New York, NY, USA
e-mail: dphillips@med.cornell.edu

Key Points

- Imaging is indicated in patients with signs and symptoms of pituitary hormonal excess or deficiency (moderate evidence).
- MRI is the modality of choice in the initial investigation and follow-up of pituitary disorders (moderate evidence).
- Dynamic MRI and SPGR sequences are useful adjuncts to conventional MRI in the diagnosis of pituitary microadenomas (limited evidence).
- MRI is useful in the determination of tumor extent preoperatively (moderate evidence).
- Inferior petrosal sinus sampling is highly sensitive for establishing the pituitary source for hypercortisolism when MRI is equivocal (moderate evidence).

Definition and Pathophysiology

This chapter will primarily focus on the role of imaging in the evaluation of pituitary neoplasms (adenomas). Pituitary adenomas are usually benign indolent neoplasms. Although some may lead to symptoms due to hormonal hyperactivity with debilitating systemic consequences or from involvement of adjacent critical structures, many are asymptomatic and discovered incidentally. Adenomas arise from clonal mutations of somatic cells and their cause remains unknown. Oncogenes are not known to play a significant role in their genesis [1]. Definitive treatment involves any combination of medical and surgical intervention depending on the type of hormone they elaborate, their size, and local extent.

Incidence/Prevalence

In a meta-analysis by Ezzat et al. [2], the overall prevalence of pituitary adenomas in autopsy and imaging series was found to be 16.7 %.

McDowell et al. [1] estimate that adenomas are more common in females and also that males were more likely to present with larger tumors. They also identified a greater incidence in the African American population. About 10 % of MRI studies are estimated to reveal an incidental pituitary lesion or "incidentaloma" [3]. Incidentalomas are defined as circumscribed regions of decreased density/intensity on CT and MR scans, less than 10 mm in size. Less than 1 % of these are hormonally active.

Goals of Imaging

The overall goals of imaging are:
1. To identify the presence of a sellar lesion and establish a differential diagnosis
2. To map the extent of the lesion, with respect to the optic pathways and cavernous sinuses
3. To enable monitoring of response to medical, surgical, or radiation therapy

Methodology

The search strategy employed both a MEDLINE search using PUBMED (National Library of Medicine, Bethesda) and Google Scholar for original research publications describing the diagnostic performance and effectiveness of different imaging modalities in the evaluation of pituitary disorders. The search covered the period January 1976 to February 2010. Different combinations of the following terms were employed: (1) Pituitary, (2) Sella, (3) MRI or CT or Venous sampling, and (4) Adenoma. Additional papers were identified by reviewing the reference list of selected publications. Only human studies in the English language literature were evaluated. The authors reviewed the titles and abstracts, and publications that were deemed relevant were then more thoroughly analyzed.

Discussion of Issues

Selection of Appropriate Imaging Strategy

Selection of Subjects for Initial Imaging
Summary

Imaging of the pituitary is indicated in patients who demonstrate laboratory evidence of pituitary dysfunction after secondary causes of pituitary hormonal excess or deficiency have been (moderate evidence). Imaging is also required to help diagnose the nature of pituitary disease, assess the effect of pituitary tumors on adjacent structures, guide surgical approach, and to enable appropriate monitoring of a lesion during the course of treatment.

Supporting Evidence

There is a general medical consensus for the need for pituitary imaging in patients with hyperprolactinemia. In an audit by Davies et al. [4], there was broad agreement on the need for imaging (MRI) in every patient with prolactin levels consistently above 1,000 mU/L to exclude an adenoma. It was also agreed that in patients with PRL above 6,000 mU/L, the presence of a prolactinoma can be assumed but that imaging was warranted to determine its size and extent and to enable monitoring during treatment. The same audit also revealed a lack of consensus on the appropriate strategy to evaluate Cushing's disease (MRI vs. CT vs. CRH stimulation), but agreement existed that a series of dynamic tests was required. Guidelines issued by the Pituitary Society for the diagnosis and management of prolactinomas also recommend the use of gadolinium enhanced MRI after excluding potential secondary causes of hyperprolactinemia, including pregnancy. CT with contrast was deemed less effective in the diagnosis of small adenomas but was recommended if MRI was unavailable or contraindicated [5].

Selection of Imaging Strategy
Summary

MRI is superior to CT in the evaluation of the pituitary gland and of parasellar lesions (moderate evidence). Gadolinium-enhanced MRI is useful when unenhanced imaging fails to reveal a lesion. Dynamic MRI and SPGR sequences may be of use in equivocal cases (limited evidence). There is no standard dynamic MRI technique. Selective venous sinus sampling is a highly sensitive and specific technique for the establishment of a pituitary source of high ACTH when MRI fails to do so (moderate evidence).

Supporting Evidence

Several studies have evaluated the role of MRI and CT in the diagnosis of sellar lesions. Early studies demonstrated the superiority of unenhanced MRI [6, 7] over CT in the detection of adenomas and assessment of their parasellar extent. Peck et al. [8] demonstrated a sensitivity of 71 % for the detection of ACTH-producing microadenomas on a 1.5 T scanner. The use of a gadolinium contrast agent enabled identification of 10 out of 12 microadenomas in patients with Cushing's disease in a series by Dwyer et al [9]. Escourolle et al. [10] also reported that MRI with contrast was able to identify ACTH producing microadenomas with a sensitivity of 69 %, compared to 50 % with CT. Conflicting reports do, however, exist in the early literature. In a study by Nichols et al. [11], MRI was found to be superior to CT in the determination of extrasellar extension but the two exams were equivalent in terms of overall lesion detection. Davis et al. [12], in a series of 13 microprolactinomas, found that unenhanced MRI was able to detect only 3, whereas CT was able to do so in 6 cases. Similar findings were reported by Pojunas et al. [13], who also compared unenhanced MRI with CT. However, the improved sensitivity of MRI today, which approaches 90 % [14], may be attributable to many factors, including the development of systems with higher field strength and higher signal-to-noise, superior spatial resolution, the use of gadolinium contrast agents, and an overall improvement in experience with image interpretation [14–16]. The unenhanced T1 weighted image, for many, remains the mainstay of adenoma detection. Gadolinium appears to confer a modest increase in sensitivity. For example,

Dwyer et al., in a series of 12 patients with Cushing's disease, found that MR with the use of gadolinium was able to detect a microadenoma in 2 additional patients out of 12, compared to unenhanced imaging [9].

False negative results with conventional MRI are usually due to the fact that some microadenomas remain isointense in signal to normal pituitary gland on precontrast and postcontrast sequences. The rationale behind the use of dynamic MRI techniques is that adenomas have dual blood supply from the hypothalamic-pituitary portal system and the meningohypophyseal branches of the internal carotid arteries and would, therefore, be expected to demonstrate a temporal difference in enhancement with respect to the normal gland during the administration of a bolus of contrast. Sakamoto et al. [17] described a dynamic technique that involved the acquisition of 7–10 SE images after rapid administration of a contrast bolus over a 20–30 s period. They observed that peak adenoma enhancement occurred 60–200 s after injection. Adenomas were best visualized during the early phases of injection, during which time they enhanced less than the normal gland. Dwyer et al. [9] warned of the variability in peak adenoma enhancement and cautioned that there was a period where imaging may not depict an adenoma due to enhancement identical with that of the normal gland. Kucharczyk et al. [18] described the use of a dynamic keyhole FSE MR technique where six sets of images were acquired through the gland. Three slices per glandular location are obtained at 11 s intervals, with a final set at 100 s. Dynamic studies revealed a lesion in 13/18 (sensitivity approximately 72 %) patients as opposed to 10/18 (sensitivity approximately 55 %) when compared to the conventional enhanced MRI [19, 20]. Rand et al. [20] concurred with these findings but used a slightly different technique, which obtained 10 slices per location, at 3 locations in the gland, at 11 s intervals. A different dynamic technique again was described by Bartynski et al. [19], where one-third of a dose of 0.1 mmol/kg contrast was infused over a 30 s period, followed by a dynamic scan for 160 s. During the course of the dynamic

scan, the remainder of the contrast was administered and was followed by a coronal conventional SE sequence. In 42–47 % of the cases, the dynamic study was better than the standard postcontrast sequence in lesion detection. They also emphasized the value of analyzing both, as in 9 % of cases a lesion was seen only on the standard sequences. In a study using a half-dose protocol, Portocarrero et al. [21] were able to identify 100 % of ACTH producing microadenomas. In contrast to the above studies, no benefit was found in a dynamic technique in a series of 26 patients with ACTH dependant Cushing's syndrome [22, 23]. They obtained nine sets of five images through the gland during injection of a bolus of contrast using a 1.0 T scanner. In their series of 21 patients with Cushing's disease (14 surgically confirmed ACTH secreting microadenomas, 3 macroadenomas, and 4 glands which were surgically negative), conventional MRI was able to detect 8 out of 14 tumors with no false positives, whereas dynamic MR was able to detect 11 of 14 tumors but with 3 false positive cases. The above studies also reflect the variability in the literature with regard to the technique of dynamic imaging, if performed. Unfortunately, no consensus exists regarding what the optimal dynamic technique should be. Newer MR systems, with improved coils, better magnetic gradients, better magnetic homogeneity, and higher field strengths are capable of better temporal and spatial resolution. Further research to enable refinement and standardization of dynamic MRI and to validate it against standard postcontrast imaging would be of considerable importance. Dynamic studies appear to increase the sensitivity of MRI in the detection of microadenomas by a modest, but unquantifiable, degree and may be best utilized in cases where conventional MRI is negative in a patient in whom the presence of a pituitary lesion is strongly suspected on clinical and biochemical grounds.

The addition of a high-resolution 3-D MR technique, typified by the spoiled gradient echo (SPGR) sequence, to a standard pituitary MRI study has also been recommended by some authors [22, 23]. Patronas et al. [23], in a series of 50 patients with corticotroph adenomas, demonstrated an improved sensitivity of 80 % for

a postcontrast SPGR sequence compared with the conventional postcontrast spin echo sequence (sensitivity 49 %), but also described a higher false-positive rate of 4 % compared to 2 % when compared to the conventional enhanced technique. According to Batista et al., this technique is especially of value in children and adolescents with Cushing's disease [23]. In a series of 20 such patients, SPGR detected 18/28 adenomas (64 % sensitivity) but conventional contrast-enhanced imaging did so in only 5/28 (18 % sensitivity). The superiority of SPGR, according to the authors, may be due to its short acquisition time (which translates into less artifact), and superior spatial resolution (the ability to acquire 1 mm thin sections with no interslice gap). However, it is conceivable that in both of these studies the performance of the SPGR and conventional postcontrast spin echo sequence as a component of the same examination influenced the ability to detect microadenomas. The separation of the imaging times may result in the lesion being better depicted due to its inherent contrast enhancement characteristics as opposed to a superior performance for the sequence. Given that the SPGR sequence does not involve a significant increase in scan time, these sequences may be added to or used in place of a standard pituitary MR imaging protocol, when concern for a microadenoma, especially a corticotroph adenoma, exists.

The Role of Interior Petrosal Sinus Sampling

Cushing's syndrome is produced by two broad categories associated with hypercortisolism – those that are dependent on ACTH and those that are not. The former includes ACTH hyperproduction from a pituitary adenoma and ectopic sources. The lateral includes functional adrenal adenomas and carcinoma. The two categories can be differentiated by measurement of plasma ACTH concentration before and after ovine corticotropin-releasing hormone (O-CRH) administration. The diagnosis of ACTH dependent Cushing syndrome can be problematic and the source of increased ACTH production difficult to determine by MRI and biochemical methods. In such cases, selective sampling of

the pituitary venous effluent into the inferior petrosal sinuses, cavernous sinuses, or the internal jugular veins before and after O-CRH stimulation accurately localizes the source of ACTH production. Corrigan et al. [24] in 1977 demonstrated the feasibility of inferior petrosal sinus sampling (IPSS) as an accurate technique to localize the source of ACTH excess in a patient with Cushing syndrome. Oldfield et al. [25] were able to surgically confirm the laterality of a microadenoma in 7/10 patients with Cushing's syndrome using IPSS. A sensitivity for IPSS of 95 % in the diagnosis of surgically confirmed Cushing's disease was also reported in a series of 246 patients by Oldfield, Doppman et al. [26]. A similar result (92.2 % sensitivity, 90 % specificity) was reported for IPSS by Bonelli et al [27]. Jugular venous sampling was suggested as a safer alternative by Ilias et al. [28], but appeared to be less sensitive than IPSS (83 % compared to 94 %). Cavernous sinus sampling has also been suggested as an alternative, given the greater proximity of the cavernous sinus to the pituitary gland. Its sensitivity was found to be approximately 93 %, by Fujimura et al [29]. However, cavernous sinus sampling is more invasive and is not a routinely employed technique. The validity of IPSS as the gold standard in the confirmation of a pituitary origin of ACTH excess has been confirmed by several studies. The sensitivity and specificity of IPSS has ranged from 90 % to 100 % in most analyses [30]. Midgette et al. [31], in a cost benefit analysis, recommended that given its high cost, IPSS be reserved for those cases where the high-dose dexamethasone suppression test is negative.

How Is Preoperative Assessment of the Extent of a Sellar Lesion Best Performed?

Summary

MRI is superior to CT in the evaluation of the extent of sellar lesions (moderate evidence).The relationship of these lesions to the optic pathways is best assessed with MRI. Neither MRI nor CT is accurate enough in the estimation of cavernous

sinus involvement, although MRI is superior. MRI is more specific than it is sensitive for cavernous sinus invasion. The only reliable sign of such invasion is circumferential encasement of the cavernous internal carotid artery by tumor. The value of MRI in the preoperative determination of adenoma consistency, information that is useful in surgical planning, is uncertain.

Supporting Evidence

The single most important feature that precludes complete resection of a macroadenoma is invasion of the cavernous sinuses. The difficulty in accurately determining whether the sinuses are involved lies in the inability of modern imaging methods to consistently demonstrate the gracile medial cavernous sinus wall. Differentiation between simple displacement and actual invasion is often difficult with imaging. In a small early series of 20 patients with macroadenomas, Nichols et al. [11] found that MRI was superior to CT in the assessment of extrasellar extension. In all 20 of these patients, unenhanced MRI was superior to CT in characterization of the extent of disease. MRI was found to be more specific (85.7 %) than sensitive (55 %) in a series of 30 patients by Scotti et al [32]. Cottier et al. [33] evaluated the performance of contrast enhanced MRI in 106 patients with macroadenomas. They evaluated the following features on coronal enhanced images: (1) total encasement of the ICA, (2) displacement of the ICA, (3) asymmetry of the cavernous sinuses, (4) non-depiction of the lateral, superior, inferolateral, and carotid sulcus venous compartments of the cavernous sinuses, (5) lateral bulging of the lateral dural wall, (6) non-depiction of the medial wall, (7) crossing of three intercarotid lines drawn along the medial and lateral walls and through the centers of the supraclinoid and cavernous segments of the ICA, (8) percentage of encasement of the ICA and, lastly, (9) pattern of lateral expansion relative to the ICA. All cases were correlated with surgical findings. The presence of normal gland interposed between the tumor and the cavernous sinus, depiction of a normal medial carotid sulcus venous component, encasement of less than 25 % of ICA circumference, and failure of tumor to pass the medial intercarotid line were features that had a 100 % negative predictive value. The only reliably specific sign, however, was encasement of greater than 67 % of the ICA circumference with a PPV of 100 %. Obliteration of the carotid venous sulcus compartment and crossing of the lateral intercarotid line by tumor demonstrated PPVs of 95 % and 85 %, respectively. The value of the lateral intercarotid line was also described by Knosp et al. [34], who reported invasion in 12/14 cavernous sinuses when the lateral carotid tangent was crossed by tumor. In a study of 103 patients, Vieira et al. [35] stated that the finding most specific for cavernous sinus invasion was encasement of greater than 30 % of the ICA circumference, as opposed to 67 % in Cottier's series. The presence of normal gland between the tumor and sinus, demonstration of the carotid sulcus compartment and encasement of less than 25 % of the ICA excluded sinus invasion, findings consistent with those of Cottier et al. The use of higher field strength magnets may enable characterization of extrasellar extension with greater sensitivity. Wolfberger et al. [36] demonstrated an improved sensitivity and specificity of 83 % and 84 %, respectively, for invasion of the medial cavernous sinus wall on a 3.0 T system compared with 67 % and 58 % on 1.5 T systems.

The primary objective of transsphenoidal surgery is to remove as much tumor as is safely possible to achieve decompression of the optic chiasm. In about 5–14 % of cases, the fibrous consistency of tumors precludes their complete removal [37]. Failure of adequate tumor resection may warrant repeat surgery and/or radiotherapy. On the other hand, soft tumors may be amenable to aspiration. Knowledge of tumoral consistency is therefore useful information to possess preoperatively. Early approaches to using adenoma consistency with MRI involved using T2 weighted sequences, the theory being that fibrous adenomas would be expected to be hypointense on such sequences. However, findings have been conflicting with some authors reporting that hard tumors were hypointense on T2WI [38] while others have stated that the opposite was true [39]. Pierallini et al. [40] described the use of diffusion weighted imaging (DWI) to

characterize adenoma consistency and found a significant correlation between tumor consistency and the determined apparent diffusion coefficient (ADC) values with softer tumors demonstrating lower values and appearing hyperintense on DWI. Boxerman et al. [37] in a recent study reported the converse, i.e., that the harder the tumor, the lower the ADC value. Suzuki et al. found no correlation between adenoma consistency and ADC values [41].

The role of intraoperative MRI in assessing the completeness of tumor resection has been studied by some authors [42, 43]. Intraoperative MRI was found to increase the completeness of tumor resection from 58 % to 82 % in a series of 85 patients with macroadenomas in whom complete removal was intended [42]. In a series of 23 patients with acromegaly, Fahlbusch et al. [43] reported that high-field-strength (1.5 T) intraoperative MRI enabled achievement of endocrine normalization from 33 % to 44 %. However, they also reported a false negative rate of 23 % with this technique and were unable to demonstrate residual tumor in 6/23 patients who had persistent growth hormone elevation after initial surgery. The authors argue that intraoperative MRI provided immediate quality control, eliminated the need for the 3-month wait period that is necessary for an artifact-free follow-up MRI to determine if residual tumor is present, and enabled immediate treatment planning with either surveillance, transcranial resection, or radiotherapy. However, the operational costs of intraoperative MRI remain high and no cost benefit analyses to support its routine use in this situation exist in the literature.

How Is Follow-up Imaging Evaluation of Adenomas Best Achieved?

Summary

Postoperative follow-up is best performed with contrast-enhanced MRI, with a first follow-up scan advocated by most authors 3–4 months after surgery (limited evidence). For follow-up imaging of nonsurgically treated incidentalomas no one particular imaging strategy exists.

Supporting Evidence

Recurrence after surgery is reportedly more likely to occur with functional ACTH adenomas and with hormonally silent adenomas compared to the other varieties [44]. Consensus appears to exist in the literature with regard to the use of MRI to follow up the postoperative sella. The optimal time to obtain a baseline is generally believed to be about 3–4 months after surgery, given that the appearance of the immediate postoperative pituitary gland may not be significantly different from its preoperative state [45–47]. Yoon et al. [48], however, advocate early follow-up with MRI within a week after surgery and found residual tumor in 22/83 patients, confirmed either by repeat surgery, biochemical abnormality, or demonstrable growth over serial MRI scans. Clinical practice guidelines issued by the Endocrine Society annual meeting in 2011, based on both systematic reviews of evidence and discussions through a series of conference calls and e-mails and one in-person meeting, recommend the initial evaluation of a patient with a pituitary incidentaloma to include laboratory screening for hormone hyper- and hyposecretion in all patients including those with and without symptoms. The measurement of a screening prolactin level was met with universal consensus. Nonsurgical follow-up was recommended with clinical assessments and functional testing for patients who do not meet criteria for surgical removal of a pituitary incidentaloma. As for follow-up imaging of nonsurgically treated incidentalomas, the task force considered that repeat scanning within the first year was warranted for all patients because despite the slow growth of most incidentalomas, some have a propensity to enlarge, and the true proliferative nature of incidentalomas is unknown. In the absence of growth, they recommend that the interval between MRI scans can be increased. The task force also believes that evidence did not support one particular algorithm for the frequency of follow-up imaging, but recommended repeating MRI every year in macroincidentalomas, every 1–2 years in microincidentalomas for the next 3 years, and then every other year for the next 6 years and gradually less frequently

indefinitely so long as the lesion continues not to threaten the patient's health. Some task force members also advocated imaging every 5 years [49].

Take-Home Tables

Tables 27.1 and 27.2 highlight data and evidence.

Table 27.1 Imaging options

	Lesion detection	Differential diagnosis	Contrast	Radiation	Cost	Sensitivity
Radiography	+	–	–	Y	+	NA
CT	++	++	+	Y	++	80–85 % (14)
MRI	+++	+++	+	N	++	85–90 % (14)
Angiography with petrosal sinus sampling	+++	–	+	Y	++++	96 % (30)

Table 27.2 Recommendations for neuroendocrine imaging

Clinical indication	Most appropriate imaging modality
Hypopituitarism	MRI without and with contrast (8)
	MRI without contrast (7)
Obesity/eating disorder	MRI without and with contrast (4)
	MRI without contrast (4)
Hyperthyroidism	MRI without and with contrast (8)
	MRI without contrast (7)
Cushing's syndrome	MRI without and with contrast (8)
	MRI without contrast (7)
	Inferior petrosal sinus sampling, if MRI negative (4)
Hyperprolactinemia	MRI without and with contrast (8)
	MRI without contrast (7)
Acromegaly/gigantism	MRI without and with contrast (8)
	MRI without contrast (7)
Growth hormone deficiency, growth retardation, panhypopituitarism	MRI without and with contrast (7)
	MRI without contrast (5)
Diabetes insipidus	MRI without and with contrast (7)
	MRI without contrast (6)
Pituitary apoplexy	MRI without and with contrast (8)
	MRI without contrast (7)
Postoperative sella	MRI without and with contrast (8)
	MRI without contrast (7)
Precocious puberty	MRI without and with contrast (8)
	MRI without contrast (7)

Modified from the American College of Radiology Appropriateness Criteria ®, last reviewed 2008; http://www.acr.org/secondarymainmenucategories/quality_safety/app_criteria.aspx, consensus and evidence based

Rating scale – 1, 2, 3 usually not appropriate; 4, 5, 6 may be appropriate; 7, 8, 9 usually appropriate
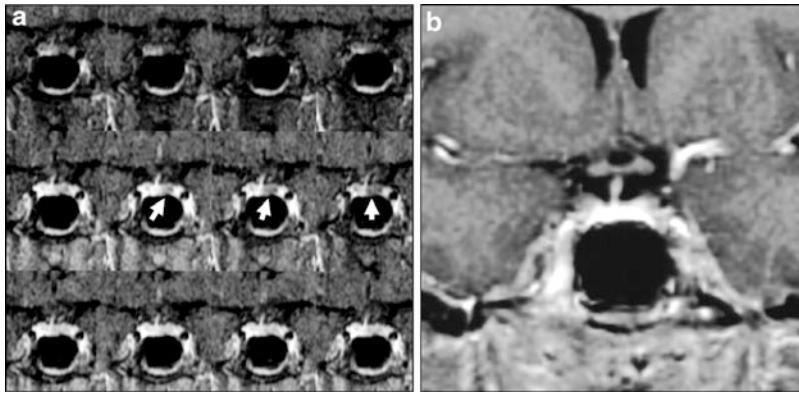
Fig. 27.1 A tiny adenoma is demonstrated in the left half of the gland on the dynamic images (**a**, *arrows*). Note that the adenoma is isointense to the remainder of the gland on the later phases of the dynamic series and is imperceptible on the postcontrast coronal SE T1 weighted image (**b**)
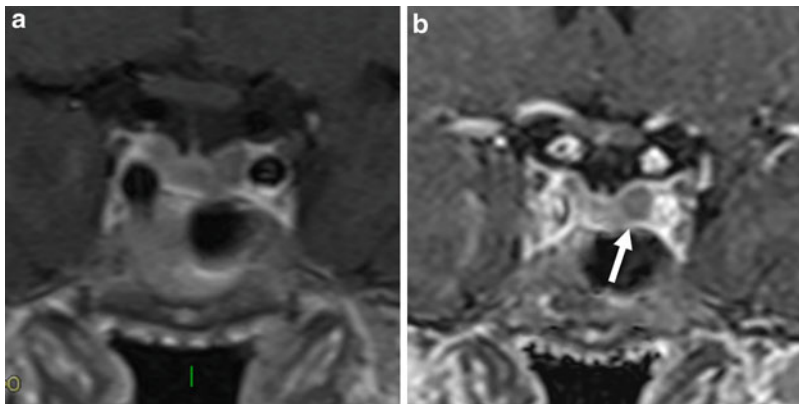

Fig. 27.2 A lesion is barely demonstrable on the contrast enhanced SE T1 weighted coronal image (**a**) in this patient with Cushing's disease. On the contrast enhanced SPGR image (**b**), a microadenoma is clearly seen
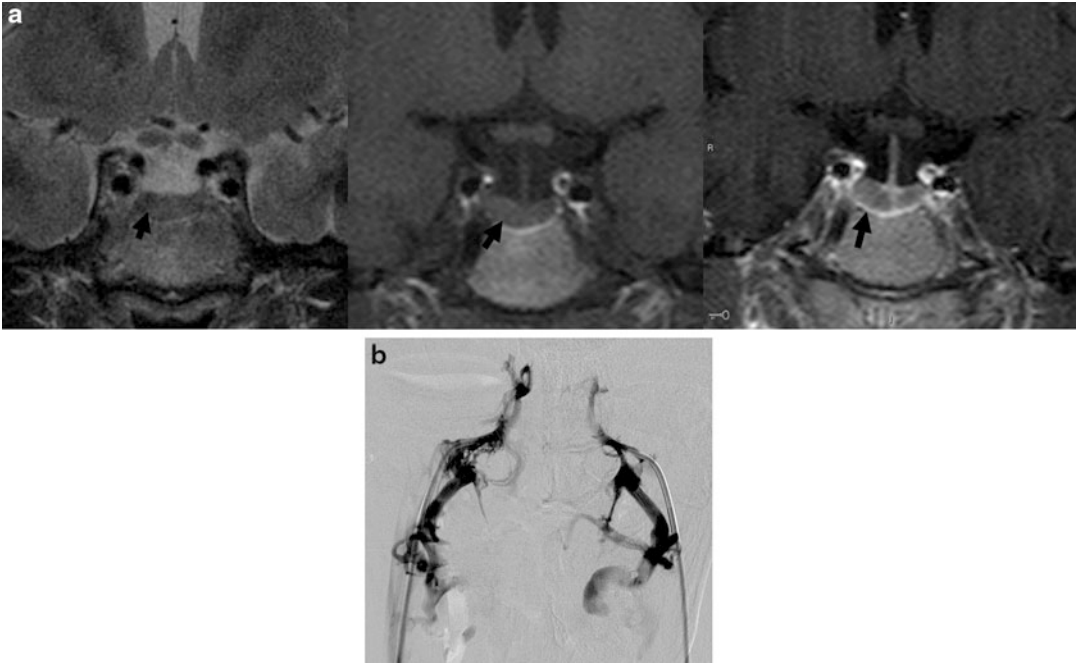
Fig. 27.3 Coronal T2, T1, and postcontrast T1 weighted images in a patient with Cushing's disease. Although a subtle right-sided contour deformity is suggested (*arrows*), a discrete adenoma is not demonstrable. An adenoma was, however, correctly lateralized to the right side by inferior petrosal sinus sampling (**b**)

Imaging Case Studies

Future Research

- Establish the true utility of dynamic MRI and develop a standardized technique.

- Refine MRI techniques to enable an increase in the detection rate of small functional microadenomas.
- Improve the sensitivity of MRI in the detection of cavernous sinus invasion.
- Explore the role of advanced MRI techniques (diffusion, perfusion, and MR spectroscopic imaging) to enable preoperative assessment of tumoral consistency.
- Determine the role of routine intraoperative MRI and evaluate its cost effectiveness.
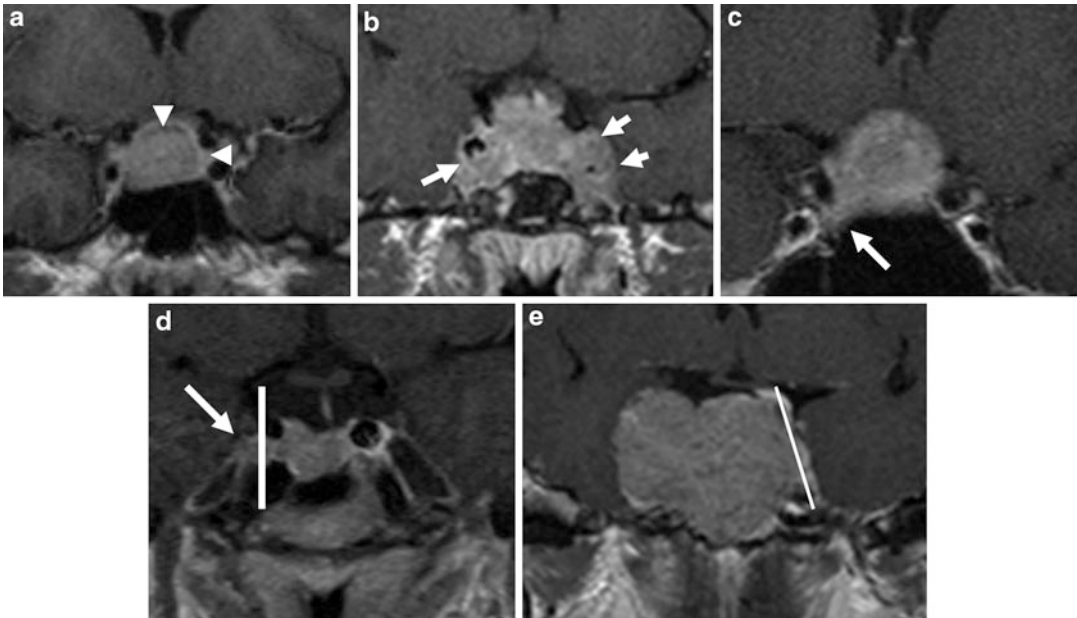
Fig. 27.4 Prediction of cavernous sinus invasion by MRI. (**a**) No cavernous sinus invasion. A thin rim of pituitary parenchyma (*arrowhead*) surrounds the tumor. MRI correctly predicted the absence of cavernous sinus invasion, which was confirmed at surgery. (**b**) Bilateral cavernous sinus invasion predicted correctly by MRI. Circumferential encasement of the cavernous ICA on the *left* (*short arrows*) and the presence of tumor in the right medial carotid sulcus venous compartment (*arrow*) enabled correct prediction of invasion bilaterally. (**c**) Involvement of the right carotid sulcus venous compartment representing cavernous sinus invasion correctly predicted by MRI (*arrow*). (**d**) Crossing of the right lateral intercarotid line by tumor (*arrow*). Invasion of the cavernous sinus was found at surgery. (**e**) False positive diagnosis of cavernous sinus invasion. The small focus of tumor extending beyond the lateral intercarotid line on the *left* was thought to represent cavernous sinus invasion preoperatively. At surgery, however, the medial cavernous sinus dural wall was merely pushed and not invaded

References

1. McDowell B, Wallace R, Carnahan R, Chrischilles E, Lynch C, Schlechte J. Pituitary. 2011;14(1):23–30.
2. Ezzat S, Asa SL, Couldwell WT, Barr CE, Dodge WE, Vance ML, et al. Cancer. 2004;101(3):613–19.
3. Frohman LA. Management of pituitary incidentalomas. In: Swearingen B, Biller BMK, editors. Diagnosis and management of pituitary disorders. Totowa: Humana Press; 2008. p. 399–409.
4. Davies MJ, Howlett TA. Clin Endocrinol. 1994;41(3):385–9.
5. Casanueva FF, Molitch ME, Schlechte JA, Abs R, Bonert V, Bronstein MD, et al. Clin Endocrinol. 2006;65(2):265–73.
6. Kucharczyk W, Davis DO, Kelly WM, Sze G, Norman D, Newton TH. Radiology. 1986;161(3):761–5.
7. Guy RL, Benn JJ, Ayers AB, Bingham JB, Lowy C, Cox TCS, et al. Clin Radiol. 1991;43(3):156–61.
8. Peck W, Dillon W, Norman D, Newton T, Wilson C. Am J Roentgenol. 1989;152(1):145–51.
9. Dwyer AJ, Frank JA, Doppman JL, Oldfield EH, Hickey AM, Cutler GB, et al. Radiology. 1987;163(2):421–6.
10. Escourolle H, Abecassis JP, Bertagna X, Guilhaume B, Pariente D, Derome P, et al. Clin Endocrinol. 1993;39(3):307–13.
11. Nichols DA, Laws ERJ, Houser WO, Abboud CF. Neurosurgery. 1988;22(2):380–5.
12. Davis P, Hoffman Jr J, Spencer T, Tindall G, Braun I. AJR Am J Roentgenol. 1987;148(4):797–802.
13. Pojunas K, Daniels D, Williams A, Haughton V. AJNR Am J Neuroradiol. 1986;7(2):209–13.
14. Elster AD. Radiology. 1993;187(1):1–14.
15. Erickson D, Erickson B, Watson R, Patton A, Atkinson J, Meyer F, et al. Clin Endocrinol. 2010;72(6):793–9.
16. Stadnik T, Stevenaert A, Beckers A, Luypaert R, Buisseret T, Osteaux M. Radiology. 1990;176(2):419–28.
17. Sakamoto Y, Takahashi M, Korogi Y, Bussaka H, Ushio Y. Radiology. 1991;178(2):441–5.
18. Kucharczyk W, Bishop J, Plewes D, Keller M, George S. AJR Am J Roentgenol. 1994;163(3):671–9.

19. Bartynski W, Lin L. AJNR Am J Neuroradiol. 1997;18(5):965–72.

20. Rand T, Lippitz P, Kink E, Huber H, Schneider B, Imhof H, et al. Eur J Radiol. 2002;41(2):131–5.

21. Portocarrero-Ortiz L, Bonifacio-Delgadillo D, Sotomayor-González A, Garcia-Marquez A, Lopez-Serna R. Pituitary. 2010;13(3):230–5.

22. Patronas N, Bulakbasi N, Stratakis CA, Lafferty A, Oldfield EH, Doppman J, et al. J Clin Endocrinol Metab. 2003;88(4):1565–9.

23. Batista D, Courkoutsakis NA, Oldfield EH, Griffin KJ, Keil M, Patronas NJ, et al. J Clin Endocrinol Metab. 2005;90(9):5134–40.

24. Corrigan DF, Schaaf M, Whaley RA, Czerwinski CL, Earll JM. N Engl J Med. 1977;296(15):861–2.

25. Oldfield EH, Chrousos GP, Schulte HM, Schaaf M, McKeever PE, Krudy AG, et al. N Engl J Med. 1985;312(2):100–3.

26. Oldfield EH, Doppman JL, Nieman LK, Chrousos GP, Miller DL, Katz DA, et al. N Engl J Med. 1991;325(13):897–905.

27. Bonelli FS, Huston III J, Carpenter PC, Erickson D, Young Jr WF, Meyer FB. AJNR Am J Neuroradiol. 2000;21(4):690–6.

28. Ilias I, Chang R, Pacak K, Oldfield EH, Wesley R, Doppman J, et al. J Clin Endocrinol Metab. 2004;89(8):3795–800.

29. Fujimura M, Ikeda H, Takahashi A, Ezura M, Yoshimoto T, Tominaga T. Neurolog Res. 2005;27:11–15.

30. Newell-Price J, Trainer P, Besser M, Grossman A. Endocr Rev. 1998;19(5):647–72.

31. Midgette AS, Aron DC. Am J Med Sci. 1995;309(3):162–70.

32. Scotti G, Yu C, Dillon W, Norman D, Colombo N, Newton T, et al. Am J Roentgenol. 1988;151(4):799–806.

33. Cottier J-P, Destrieux C, Brunereau L, Bertrand P, Moreau L, Jan M, et al. Radiology. 2000;215(2):463–9.

34. Knosp E, Steiner E, Kitz K, Matula C. Neurosurgery. 1993;33(4):610–18.

35. Vieira JJO, Cukiert A, Liberman B. Surg Neurol. 2006;65(2):130–5.

36. Wolfsberger S, Ba-Ssalamah A, Pinker K, Mlynárik V, Czech T, Knosp E, et al. J Neurosurg. 2004;100(2):278–86.

37. Boxerman JL, Rogg JM, Donahue JE, Machan JT, Goldman MA, Doberstein CE. Am J Roentgenol. 195(3):720–728.

38. Iuchi T, Saeki N, Tanaka M, Sunami K, Yamaura A. Acta Neurochir. 2010;140(8):779–86.

39. Snow RB, Johnson CE, Morgello S, Lavyne MH, Patterson RHJ. Neurosurgery. 1990;26(5):801–3.

40. Pierallini A, Caramia F, Falcone C, Tinelli E, Paonessa A, Ciddio AB, et al. Radiology. 2006;239(1):223–31.

41. Suzuki C, Maeda M, Hori K, Kozuka Y, Sakuma H, Taki W, et al. J Neuroradiol. 2007;34(4):228–35.

42. Nimsky C, Keller BV, Ganslandt O, Fahlbusch R. Neurosurgery. 2006;59(1):105–14.

43. Fahlbusch R, Keller BV, Ganslandt O, Kreutzer J, Nimsky C. Eur J Endocrinol. 2005;153(2):239–48.

44. Terada T, Kovacs K, Stefaneanu L, Horvath E. Endocr Pathol. 1995;6(4):301–10.

45. Rajaraman V, Schulder M. Surg Neurol. 1999;52(6):592–9.

46. Rodríguez O, Mateos B, de la Pedraja R, Villoria R, Hernando JI, Pastor A, et al. Neuroradiology. 1996;38(8):747–54.

47. Dina TS, Feaster SH, Laws Jr ER, Davis DO. AJNR Am J Neuroradiol. 1993;14:763–9.

48. Yoon P-H, Kim D-I, Jeon P, Lee S-I, Lee S-K, Kim S-H. AJNR Am J Neuroradiol. 2001;22:1097–100.

49. Practice Guidelines for Pituitary Incidentalomas, The Endocrine Society Annual Meeting. J Clin Endocrinol Metab. 2011;96(4):894–904.

Part IV

Spine: Evidence-Based Neuroimaging

Adults and Children with Low Back Pain in Primary Care Setting: Evidence-Based Neuroimaging

Ken F. Linnau, Marla B. K. Sammer, C. Craig Blackmore, and Jeffrey G. Jarvik

Contents

K.F. Linnau (✉) • J.G. Jarvik
Department of Radiology, Harborview Medical Center, University of Washington, Seattle, WA, USA
e-mail: klinnau@uw.edu; jarvikj@uw.edu

M.B.K. Sammer
Department of Diagnostic Radiology, Children's at Erlanger, Chattanooga, TN, USA
e-mail: marla.sammer@erlanger.org

C.C. Blackmore
Department of Radiology, Virginia Mason Medical Center, Seattle, WA, USA
e-mail: craig.blackmore@vmmc.org

Key Points

- The natural history of low back pain (LBP) is typically benign; in the absence of "red flags," imaging can safely be limited to a minority of patients with LBP in the primary care setting (strong evidence).
- LBP imaging is often performed to rule out a serious etiology, especially metastases. While the first-line study is plain radiographs, magnetic resonance (MR) is more sensitive. However, initial imaging with MR has not yet proven to be cost-effective (moderate evidence).
- Many incidental findings are discovered when imaging the lumbar spine, including disk desiccation, annular tears, bulging disks, and herniated disks. Their eventual correlation with back pain is not known. However, while disk bulges and protrusions are common in asymptomatic individuals, extrusions are not (strong evidence).
- Imaging can diagnose surgically treatable causes of radiculopathy (herniated disks and spinal stenosis). However, these are typically not the causes of LBP and are often incidental findings in asymptomatic individuals; furthermore, the long-term efficacy of corrective surgery for these conditions has not been established (moderate evidence).

Spondylolysis is relatively common in adolescent athletes and should be suspected when pain develops in such subjects. Because spondylolysis may not be apparent on radiography, SPECT or CT may be warranted (limited evidence).

Definition and Pathophysiology

Low back pain (LBP) is a pervasive problem that affects two-thirds of adults at some time in their lives. Fortunately, the natural history of LBP is usually benign, and diagnostic imaging can be restricted to a small percentage of LBP sufferers. This chapter reviews the evidence regarding both the diagnostic accuracy of common imaging modalities for several common conditions and the utility of imaging in patients with LBP in the primary care setting. The most common spine imaging tests are plain X-rays, computed tomography (CT), MR, and bone scanning. We do not review other modalities (conventional myelography, discography, and positron emission tomography), which are usually ordered by specialists prior to surgical intervention. This work is based partly on an article we previously published in the *Annals of Internal Medicine* [1].

Nontraumatic low back pain is a relatively common condition in both children and adults. Though extensively studied in the adult population, relatively less is known about the prevalence, etiology, and significance of back pain in the pediatric age group.

The etiology of nontraumatic low back pain in children and adolescents is not well understood. Etiological studies have grouped the factors associated with pediatric back pain into four broad categories: anthropometry, lifestyle, mechanical, and psychosocial/behavioral fractures. All of these factors are somewhat controversial [2]. Among the anthropometry factors that have been implicated are height, rate of growth, and spinal mobility, though the evidence supporting all of these factors is somewhat in conflict. The primary lifestyle factors that have been implicated include participation in sports, specifically weight lifting, skiing, and gymnastics [3–6], though, conversely, sedentary activity has also been implicated [7]. The main mechanical fracture that has attracted much attention is the use of heavy school backpacks. Currently, the American Academy of Pediatrics recommends that backpacks not exceed 10–20 % of the child's body weight, though this recommendation is based on limited evidence [8, 9]. Finally, as in adults, psychosocial factors appeared to have a role [2].

Pediatric back pain can be grouped into broad categories. In addition to trauma, spondylolysis and spondylolisthesis are important causes of pediatric back pain, particularly in athletes [5, 6]. Scoliosis and spinal dysraphism may also contribute to back pain. (See Chap. 33, "Pediatric Dysraphism and Scoliosis: Evidence-Based

Neuroimaging" on "Scoliosis and Spine Dysraphism.") In addition, benign and malignant bone tumors and infections can be the etiology of both chronic and acute symptomatology. Finally, degenerative conditions, though less frequently seen in adults, can also occur in the pediatric age group, including disk herniations and disk and end plate degeneration.

Epidemiology and Differential Diagnosis of LBP in Primary Care

Low back pain ranks among the most common reasons for physician visits and is the most common reason for work disability in the USA [10–12]. Among those with uncomplicated back pain, it is often impossible to distinguish a precise anatomic cause, and early treatments are generally aimed at symptomatic relief, so a precise anatomic diagnosis is usually both unnecessary and impossible. In fact, a definitive diagnosis is not reached in as many as 85 % of patients with LBP [13], and when the etiology cannot be determined, it is frequently assumed to result from muscle sprains or strains, ligamentous injuries, and spinal degenerative changes.

Further complicating matters, there are numerous imaging findings in the spines of asymptomatic patients. These include spinal stenosis, mild scoliosis, transitional vertebra, spondylolysis, Schmorl's nodes, spina bifida, and degenerative changes [14]. For example, spinal stenosis is present in up to 20 % of asymptomatic adults over the age of 60. The relationship of these findings to back pain is questionable because they are equally prevalent among persons with and without pain [15]. Steinberg and colleagues [14] studied the radiographs of a large group of male army recruits with and without LBP. While they attempted to find a correlation between numerous variables and LBP (including right and left scoliosis, lordosis, degree of lordosis, vertebral rotation, spina bifida at multiple levels, transitional vertebra, wedge vertebra, degenerative changes, Schmorl's nodes, unilateral spondylolysis, bilateral spondylolysis, spondylolisthesis, spinal canal

anteroposterior diameter, interpedicular distance, and intra-apophyso-laminar space), they found an association with only six of the variables. The most statistically significant difference was the presence of right-sided scoliosis (16.8 % vs. 5.6 % in the control group, $p < 0.0001$). The study also found that lumbarization of S1, wedge vertebra, bilateral spondylolysis, and spondylolisthesis had weaker associations with LBP, with p values up to 0.04. Since the authors did not have a priori hypotheses, their study suffers from the problem of multiple comparisons, limiting the conclusions that can be drawn. Except for right-sided scoliosis, all the other associations must be viewed as exploratory and require independent confirmation.

Still, researchers continue to explore the relationship between possibly incidental findings, especially of intervertebral disk herniation, and the symptoms of back pain. Herniated disks are clearly not the culprit in the vast majority of patients with LBP. Only 2 % of persons with LBP actually undergo surgery for a disk herniation [16, 17]. Moreover, imaging tests identify herniated disks among a large fraction of people without LBP (from 20 % to 80 %, depending on age, selection, and definition of disk herniation) (Fig. 28.1a, b) [18–20]. These asymptomatic herniations appear to be clinically unimportant. In a prospective study, our group found that the prevalence of most disk abnormalities, including desiccation, loss of disk height, bulge, annular tear, and protrusion, were not significantly different between asymptomatic subjects with and without a history of prior LBP [20]. Boos and colleagues [21] followed asymptomatic individuals with a high rate of disk herniations (73 %) for 5 years. They concluded that while the presence of disk abnormalities did not predict future LBP, psychosocial factors, mostly related to occupation, did. In employees, who are on work disability for LBP, degenerative imaging findings on radiographs and MRI do not predict disability and pain at 1 year, while psychosocial factors, such as depression, anxiety, and fear-avoidance, do [22]. Certain imaging findings are likely quite important clinically. Disk extrusions, a subtype of herniation, are much less prevalent than disk

protrusions in patients without LBP and are typically considered a clinically important imaging finding [18–20, 23].

Imaging is indicated when infection or malignancy is being considered as well as when patients present with cauda equina syndrome, a true surgical emergency. These serious conditions occur less than 5 % of the time in the primary care setting, with only 0.7 % of LBP patients having metastatic cancer (with breast, lung, and prostate being the most common primary tumors), 0.01 % having spinal infections, and 0.0004 % having cauda equina syndrome [24]. In their recent retrospective chart review of 2007 lumbar film reports, van den Bosch et al. [25] reported the overall likelihood of finding a serious condition, such as infection or possible tumor at <1 %, with no tumors found in patients younger than 55.

The prevalence of low back pain in pediatric patients is not clearly established. A prospective study in Belgium of children 9–12 years of age demonstrated that 18 % who had not reported back pain at baseline had at least one episode over the 2-year study [9]. However, a meta-analysis of published lifetime prevalence studies performed by Jeffries et al. found a range of 5–74 % [26, 27].

Overall Cost to Society

In 1998, health-care costs for LBP (inpatient care, office visits, prescription drugs, and emergency room visits) totaled $90.7 billion. This was 2.5 % of the national health-care expenditure and did not include physical therapy, chiropractic care, or nursing home care. The data to calculate these figures came from a national database and included only patients with back disorders, disk disorders, and back injuries, as per International Classification of Diseases (ICD-9) codes. Consequently, a substantial proportion of LBP patients, such as those with malignancy, infection, or osteoporotic compression fractures as the primary etiology of pain, were likely excluded from these estimates. Finally, this estimate does not include non-health-care expenditures such as

workers' compensation, sick leave, and disability, an important consideration since LBP is the largest cause of disability and workers' compensation claims in the USA [28, 29]. Data on the cost of pediatric back pain are not available.

Goals of Imaging

There are two major goals in imaging primary care patients with LBP: (1) to exclude serious disease (tumor, infection, or neural tissue compromise requiring decompression) and (2) to find a treatable explanation for the patient's pain.

Methodology

We performed four Medline searches using PubMed. The first covered the period 1966 to September 2001, and the second, to update the literature search from the original article on which this chapter is based, covered September 2001 through August 2004. The third was performed to update the chapter and covered 1996 through December 2009, searching specifically for randomized controlled trials related to vertebroplasty. The fourth search was performed to update the chapter covering January 2010 to September 2011. For children with nontraumatic back pain, the search time frame was January 1, 1980 to December 31, 2008. For the first two searches, we used the following search terms: (1) *back pain*, (2) *intervertebral disk displacement*, (3) *sciatica*, (4) *spinal stenosis*, and (5) *diagnostic imaging*. We applied the subheadings *diagnosis*, *radiography*, or *radionuclide imaging* to the first statement. We excluded animal experiments and articles on pediatric patients. We also excluded case reports, review articles, editorials, and non-English-language articles. We included only articles describing plain X-rays, CT, MR (including MR myelography), and bone scanning. In the first search, the total number of citations retrieved was 1,468. Two reviewers (J.G.J. and R.A.D.) reviewed all the titles and subsequently the abstracts of 568 articles that appeared pertinent;

the full text of 150 articles was then reviewed. At each step, the articles' authors and institutions were masked. Disagreements regarding inclusion of particular articles, which occurred in approximately 15 %, were settled by consensus. In the second search, the total number of citations retrieved was 558. Two reviewers (M.B.K.S. and J.G.J.) reviewed all the titles and subsequently the abstracts of 168 articles that appeared pertinent. Finally, we reviewed the full text of 75 articles. Disagreements regarding inclusion of particular articles, which occurred in 12 % (9/75), were settled by consensus between the two reviewers. Only those articles meeting our inclusion criteria were cited for this chapter.

Because most studies had several potential biases, our estimates of sensitivity and specificity must be considered imprecise. The most common biases were failure to apply a single reference test to all cases, test review bias (study test was reviewed with knowledge of the final diagnosis), diagnosis review bias (determination of final diagnosis was affected by the study test), and spectrum bias (only severe cases of disease were included). Because of these sorts of limitations, we did not perform a formal meta-analysis.

Discussion of Issues

What Is the Role of Imaging in Patients Suspected of Having a Herniated Disk?

Summary
Radiculopathy is a common and well-accepted indication for imaging; however, it is not an urgent indication, and with 4–8 weeks of conservative care, most patients improve. Urgent MR and consultation are needed if the patient has signs or symptoms of possible cauda equina syndrome (bilateral radiculopathy, saddle anesthesia, or urinary retention). Current literature suggests that MR is slightly more sensitive (0.6–1.0 vs. 0.6–0.9) than CT in its ability to detect a herniated disk (moderate evidence). Plain radiography has no role in diagnosing herniated disks (strong evidence), though it does, like the other modalities, show degenerative changes that are sometimes associated with herniated disks. Finally, all three methods commonly reveal findings in asymptomatic subjects.

Supporting Evidence
(a) Plain Radiography Because radiographs cannot directly visualize disks or nerve roots, their usefulness is limited. Plain film signs of disk degeneration include disk space narrowing, osteophytes, and end plate sclerosis. Indirect signs of possible nerve root compromise include facet degeneration as manifested by sclerosis and hypertrophy.

In their recent prospective study examining patients with chronic LBP, Peterson and colleagues [30] considered whether a relationship existed between radiographic lumbar spine degenerative changes and disability or pain severity. They found no link between the severity of lumbar facet degeneration and self-reported pain or disability levels (moderate evidence). While they did find a weak link between the number of degenerative disk levels and the severity of degenerative changes at these levels with pain in the week immediately preceding the exam, they found no correlation to pain or disability over the patients' entire pain episode (which in some cases had lasted greater than 5 years) (moderate evidence). Furthermore, in greater than a quarter of the patients, all of whom were considered chronic LBP sufferers, no degenerative changes were evident on their radiographs. Even in those patients with degenerative findings, the severity of degeneration was rated as mild in approximately 50 %. Lundin et al. [31] studied athletes for 12–13 years and found only a borderline correlation between loss of disk height at baseline and back pain ($p = 0.06$). However, they found a highly significant correlation between a decrease in disk height over the intervening 12–13 years and the development of LBP ($p = 0.005$) (strong evidence).

(b) Computed Tomography In an often-cited study by Thornbury and colleagues [32], CT had a sensitivity of 88–94 % for herniated disks and a specificity of 57–64 %, similar to that for MR (Fig. 28.2) (moderate evidence). The area

under a receiver operating characteristic (ROC) curve for CT was 0.85–0.86. Diagnosis review bias likely inflated these estimates of accuracy. Interestingly, a study by Jackson et al. [33] arrived at similar estimates of sensitivity and specificity (86 % and 60 %, respectively) despite the selective use of a surgical reference standard (moderate evidence). Not taken into account in these studies is that herniated disks are commonly present in asymptomatic persons. While likely representing real anatomic abnormalities, these findings are irrelevant for clinical decision making and thus reduce test specificity (Table 28.1). Finally, while these studies suggest CT is comparable to MR for diagnosing disk disease, an important drawback of CT compared with MR is that with only axial image acquisition, it is more difficult to subcategorize disk herniations into protrusions versus extrusions (see section below on MR). However, multidetector CTs, with thin-section acquisition, allow high-quality sagittal reformations to potentially overcome this limitation.

We did not find any data regarding the accuracy of CT for nerve root impingement. However, because surrounding fat provides natural contrast, CT, as opposed to plain radiography, can accurately depict the foraminal and extraforaminal nerve roots, directly visualizing nerve root displacement or compression. But CT is less effective in evaluating the intrathecal nerve roots (limited evidence) [34].

(c) Magnetic Resonance MR has good sensitivity and variable specificity for disk herniations. Thornbury et al. [32] (moderate evidence) demonstrated a sensitivity for herniated disks of 89–100 % but a specificity of only 43–57 %. The area under the ROC curve was 0.81–0.84. In a cohort of 180 patients, Janssen et al. [35] found a sensitivity and specificity of 96 % and 97 %, respectively. Although this study avoided test review bias, diagnosis review bias was likely present, with selective application of the surgical reference standard (moderate evidence).

While data regarding sensitivity and specificity of MR for nerve root compromise is lacking, MR has several advantages over CT, including superior soft tissue contrast, multiplanar imaging, and the ability to characterize intrathecal nerve roots [20, 36–38]. Still unclear is how best to evaluate nerve root compromise. In a prospective evaluation of 96 consecutive lumbar spine MRs, Gorbachova and Terk [39] found no correlation between nerve root sleeve diameter and disk pathology, concluding that measuring the nerve diameter is not clinically useful (strong evidence). Pfirrmann and colleagues [40] devised a reliable grading system for nerve root compromise: (1) normal, (2) nerve root contacted, (3) nerve root displaced, and (4) nerve root compressed. They retrospectively evaluated 500 nerve roots in 250 symptomatic patients and then compared their MR grading system to a similar surgical scale in the 94 nerve roots that were evaluated operatively. They found that their system correlated well with surgical findings and that intra- and interobserver reliability for the grading scale was high with kappa values of 0.72–0.77 for intraobserver and 0.62–0.67 for interobserver reliability (moderate evidence).

Despite the high prevalence of herniated disks (from 20 % to 80 %, depending on age, selection, and definition of disk herniation) (Table 28.1) [18–20] and evidence of disk degeneration among asymptomatic individuals (on MR 46–93 %), several studies have attempted to correlate disk disease with disability and pain. In a prospective study of 394 patients, Porchet et al. [41] found that leg pain (but not back pain), disability, and bodily pain (all $p < 0.005$) were significantly associated with MR disk disease severity. Beattie and colleagues [36] also studied MR abnormalities and their correlation to pain, finding relationships between distal leg pain and both disk extrusions and severe nerve compression ($p < 0.008$ and <0.005, respectively). Interestingly, however, in the majority of the participants, they found no MR abnormality that corresponded to the distribution of the patient's pain.

In a prospective trial, our group found that extrusions, but not bulges or protrusions, were significantly associated with a history of LBP ($p < 0.01$) [42]. Ahn and colleagues [43], though

they did not use the terms protrusion or extrusion, agreed that distinguishing the type of herniation is important. Comparing transligamentous herniations (extrusions or migrated extrusions) to protrusions and bulges, they found that patients with transligamentous herniations had slightly better outcomes. In 2001, the North American Spine Society, the American Society of Neuroradiology, and the American Society of Spine Radiology jointly published recommendations regarding the use of a consensus nomenclature for describing disk abnormalities that incorporated these terms (protrusions and extrusions) [44]. Brant-Zawadzki et al. argued that the distinction between protrusions and extrusions is important because extrusions are rare in asymptomatic subjects (1 %), but bulges (52 %) and protrusions (27 %) are common [45].

In a series of 125 subjects, Brant-Zawadzki et al. [45] looked at the inter- and intraobserver agreement for four categories of disk morphologies (normal, bulge, protrusion, and extrusion). The authors defined a bulge as a circumferential and symmetrical extension of disk material beyond the interspace, while a herniation was a focal or asymmetrical extension of disk material. Protrusions and extrusions are subcategories of herniations. Protrusions are broad based, while extrusions have a "neck" that makes the base against the parent disk narrower than the extruded material itself (Fig. 28.3a, b, c). Using these definitions for disk morphologies, the interreader kappa was 0.59, indicating moderate agreement. Intraobserver agreement was slightly higher, ranging from 0.69 to 0.72, indicating substantial agreement. Others have obtained comparable degrees of interreader agreement ($\kappa = 0.59$) in cohorts of 34 and 45 patients, respectively [46, 47]. In a study of the reliability of chiropractors' interpretations, Cooley and colleagues [48] found interexaminer reliability comparable to that of radiologists ($\kappa = 0.60$).

Magnetic resonance myelography (MRM) is a relatively new method that uses heavily T2-weighted three-dimensional (3D) images to provide high contrast between cerebrospinal fluid (CSF) and the cord and nerve roots. Because of the high contrast of CSF, MRM has been used for diagnosing suspected spinal stenosis. However, its role in disk imaging has not been well established. In one prospective evaluation of preoperative candidates with prior diagnoses of disk herniation, Pui and Husen [49] found no difference between the sensitivity and specificity of MRM and conventional MR for diagnosis of disk herniation (strong evidence). Spectrum bias was likely present, since the reference standard, which was applied to all patients, was surgical confirmation. Also, MRM may be useful in the diagnosis of dorsal root pathology. In their prospective study of 83 patients with MR-verified lumbar disk herniation and sciatica, Aoto et al. [50] found that swelling in the dorsal root ganglia at clinically involved lumbar nerve segments was clearly seen on MRM, and the degree of root swelling correlated with pain severity.

The evidence for the use of gadolinium to detect nerve root enhancement, and thereby increase specificity, is conflicting [51–53] (moderate evidence). Autio and colleagues [54] prospectively studied 63 patients with unilateral sciatica to determine the relevance of enhancement patterns. They found a negative correlation between the duration of symptoms and the extent of enhancement. While they failed to find a correlation between enhancement and multiple clinical symptoms, they did find a significant correlation between percent rim enhancement (greater than 75 %) and the presence of an abnormal Achilles reflex, with a sensitivity and specificity of 76 % and 82 %, respectively (moderate evidence). Currently, gadolinium is usually reserved for the evaluation of postoperative patients. But even in postoperative imaging, its role has recently been challenged. In a prospective study of postdiskectomy patients, Mullin et al. [55] found no significant difference between pre- and postcontrast sensitivity (92–93 %) and specificity (97 %) for recurrent disk herniation (strong evidence).

Aprill and Bogduk [56] proposed the term *high-intensity zone* (HIZ) to describe the presence of focal high signal in the posterior annulus fibrosus on T2-weighted images (Fig. 28.4).

However, over a decade after publication of their manuscript, the clinical importance of annular tears remains uncertain. While some investigators have not found a strong relationship between the presence of an annular tear and either positive discography [57] (moderate evidence) or clinical symptoms [58] (moderate evidence), others have found a correlation [56, 59] (limited evidence and moderate evidence). In a retrospective twin cohort study, Videman and colleagues [60] found that annular tears were present in 15 % of their patients and were statistically significantly associated with many of the LBP parameters they studied. The most significant association existed between annular tears and pain intensity in the past year [odds ratio (OR) 2.2, 95 % confidence interval (CI) 1.3–3.9] (moderate evidence). Similar associations existed between annular tears and any LBP in the past year, disability from LBP in the past year, and LBP at the time of the study. But as with other imaging findings, the high prevalence of annular tears in subjects without LBP calls its clinical value into question [23, 57].

What Is the Role of Imaging in Patients with Low Back Pain Suspected of Having Bony Metastatic Spine Disease?

Summary

Both radionuclide studies and MR are sensitive and specific studies for detecting metastases (strong evidence). We did not identify studies supporting the use of CT for detecting bony spinal metastases; however, CT does depict cortical bone well. Plain films are the least sensitive imaging modality for detecting metastases (strong evidence). Nevertheless, current recommendations still advocate using plain films as the initial imaging in selected patients.

Supporting Evidence

(a) Plain Radiographs Radiographs are a specific but relatively insensitive test for detecting metastatic disease. A primary limitation is that 50 % of trabecular bone must be lost before a lytic lesion is visible (limited evidence) [61, 62]. If only lytic or blastic lesions are counted as a positive study, radiographs are 60 % sensitive and 99.5 % specific for metastatic disease (limited evidence [61, 62], strong evidence [63]). If one includes compression fractures as indicating a positive examination, then sensitivity is improved to 70 %, but specificity is decreased to 95 %.

(b) Computed Tomography We found no adequate data describing the accuracy of CT for the detection of metastases.

(c) Magnetic Resonance While the sensitivity of MR for metastases is likely high, the variable quality of the available literature makes arrival at a summary estimate difficult. In five studies of patients with metastatic cancer or other infiltrative marrow processes, MR appeared more sensitive than bone scintigraphy. The sensitivity of MR ranged from 83 % to 100 %, and specificity was estimated at 92 %. These studies used a combination of biopsy and follow-up imaging as the reference standard. Several biases (selection, sampling, nonuniform application of reference standard, and diagnosis review) likely inflated apparent performance [64–68] (Algra, moderate evidence; Avrahami, moderate evidence; Carroll, moderate evidence; Carmody, limited evidence; and Kosuda, moderate evidence).

(d) Bone Scanning and Single-Photon Emission Computed Tomography In seven studies, the sensitivity of radionuclide bone scans for tumor ranged from 74 % to 98 % (all moderate evidence except for McNeil, which was limited evidence) [69–76]. Spectrum bias, incorporation bias, test review bias, and diagnosis review bias were all present and likely inflated the accuracy estimates.

(e) Cost-Effectiveness Analysis Despite advances in imaging over the past decade, there is no compelling evidence to justify substantial deviation from the diagnostic strategy published by the Agency for Health Care Research and Quality (AHRQ) in 1994 [77]. These guidelines reflect

the growing evidence-based consensus that plain radiography is unnecessary for every patient with back pain because of the low yield of useful findings, potentially misleading results, high dose of gonadal radiation, and interpretation disagreements. However, in patients in whom the pretest probability of a serious underlying condition is elevated (e.g., patients older than the age of 50 and patients with a history of a primary cancer), the combination of radiographs and laboratory tests such as an erythrocyte sedimentation rate (ESR) or CBC is likely the appropriate first step.

MR is clearly a more accurate diagnostic test for detecting tumor than are radiographs; nevertheless, it is not a cost-effective initial option. This is nicely illustrated in the recent paper by Joines et al. [78]. Building a decision analytic model to compare strategies for detecting cancer in primary care patients with LBP, they combined information from the history, ESR, and radiographs and compared this strategy to one that used MR on all patients. They found that to detect a case of cancer, the MR strategy costs approximately ten times as much as the radiograph strategy ($50,000 vs. $5,300). Even more impressive was that the incremental cost of performing MR on all patients was $625,000 per additional case found. The authors did not attempt to convert cost per case detected into cost per life year saved or cost per quality-adjusted life year (QALY). However, since metastatic cancer presenting with back pain is usually incurable, the life year costs would likely be much greater. Hollingworth and colleagues [79] attempted to further elaborate on Joines et al.'s conclusions by limiting the MR imaging to rapid MR. In a decision model created for a hypothetical cohort of primary care patients referred to exclude cancer as the etiology of their back pain, they also found that there was not enough evidence to advocate routine rapid MR for this purpose. While there was a small increase in quality-adjusted survival (0.00043 QALYs), the incremental cost was large ($296,176). Using rapid MR rather than radiographs, fewer than one new case of cancer was detected per 1,000 patients imaged.

What Is the Role of Imaging in Patients with Back Pain Suspected of Having Infection?

Summary

When infection is suspected, MR is the imaging modality of choice. Its sensitivity and specificity are superior to the alternatives (moderate evidence), and the images obtained provide the anatomic information needed for surgical planning.

Supporting Evidence

(a) Plain Radiographs In contrast to metastatic disease, radiographic changes in infection are generally nonspecific. Furthermore, radiographic changes occur relatively late in the disease course. Findings of infection after several weeks include poor cortical definition of the involved end plate with subsequent bony lysis and decreased disk height. A paraspinous soft tissue mass may also be present. In one study, the overall sensitivity of radiographs for osteomyelitis was 82 % and the specificity was 57 % (strong evidence) [80].

(b) Computed Tomography We found no adequate data describing the accuracy of CT for detecting infection in the lumbar spine.

(c) Magnetic Resonance In the single best-designed study, the sensitivity of MR for infection was 96 % and the specificity was 92 %, making MR more accurate than radiographs or bone scans [80] (strong evidence). Perhaps more importantly, MR delineates the extent of infection better than other modalities, which is critical to surgical planning.

The characteristic MR appearance of pyogenic spondylitis is diffuse low marrow signal on T1-weighted images and high signal on T2-weighted images (Fig. 28.5a, b). These changes reflect increased extracellular fluid. Although classically two vertebral bodies are involved along with their intervening disk, the early imaging is more variable, occasionally with only one vertebral body being involved [80]. The disk itself is high in signal and may herniate through a softened end plate. Gadolinium may

increase the specificity of MR, with enhancement of an infected disk and end plates, although rigorous evidence is lacking [81].

We found no studies quantifying the accuracy of MR for epidural abscesses, but because of greater soft tissue contrast, MR should be better able to characterize the extent of an epidural process than CT.

(d) Bone Scanning and Single-Photon Emission Computed Tomography In one study investigating bone scanning and infection, the sensitivity was moderately high at 82 %, but specificity poor, only 23 % [82] (moderate evidence). In the same study, gallium-67 SPECT had a 91 % sensitivity and 92 % specificity.

What Is the Role of Imaging in Patients with Low Back Pain Suspected of Having Compression Fractures?

Summary
There are no good estimates on which imaging modality is best for compression fracture imaging. When differentiation between metastatic and osteoporotic collapse is sought, MR is currently the method of choice (weak evidence).

Supporting Evidence
(a) Plain Radiographs Various biases (diagnosis review bias, test review bias, and selective use of reference standards) make it difficult to provide a summary estimate of the radiographic sensitivity and specificity for acute compression fractures. While radiographs are likely reasonably sensitive, they probably cannot distinguish between acute and chronic compression fractures. Clues that a fracture is old include the presence of osteophytes or vertebral body fusion. Because MR identifies marrow edema or an associated hematoma and because bone scan evaluates metabolic activity, they provide more useful information regarding fracture acuity (limited evidence) [83].

(b) Computed Tomography We found no adequate data describing the accuracy of CT for either the detection of compression fractures or the differentiation of acute from chronic compression fractures.

(c) Magnetic Resonance We were unable to identify accurate sensitivity and specificity estimates for MR imaging in compression fractures. While there is an abundance of literature on MR and compression fractures, the overwhelming majority of articles focus on differentiating malignant from osteoporotic etiologies.

(d) Bone Scanning and Single-Photon Emission Computed Tomography Bone scans are widely used for differentiating acute from older (subacute or chronic) compression fractures. Old fractures should be metabolically inactive, while recent fractures should have high radiotracer uptake [65]. We did not identify articles that allowed us to calculate sensitivity and specificity for this condition.

What Is the Role of Imaging in Patients with Back Pain Suspected of Having Ankylosing Spondylitis?

Summary
There are only a few studies that attempt to determine which imaging modality is best for diagnosing ankylosing spondylitis (AS). Plain radiographs and bone scans with SPECT both have relatively high specificity (both estimated at 1.0); specificity on CT and MR is currently not available. Plain radiographs appear to be adequate for initial imaging in a patient suspected of having AS (weak evidence).

Supporting Evidence
(a) Plain Radiographs The characteristic imaging findings in AS are osteitis, syndesmophytes, erosions, and sacroiliac joint erosions, with joint erosions occurring relatively early and being readily detectable by radiography. While the sensitivity of radiographs is poor (45 %), the specificity appears high (100 %), although in the single study examining this issue, spectrum bias likely inflated both estimates (moderate evidence) [84].

(b) Computed Tomography We found no adequate data describing the accuracy of CT for diagnosis of AS.

(c) Magnetic Resonance In a small study by Marc et al. [84], MR showed abnormalities in 17 of 31 subjects with spondyloarthropathies yielding a sensitivity of 55 %. Specificity could not be determined [84] (moderate evidence).

(d) Bone Scanning, Single-Photon Emission Computed Tomography, and PET-CT In two studies, bone scan sensitivity ranged from 25 % to 85 %, with the higher sensitivity achieved by using SPECT [84, 85] (both studies moderate evidence). Specificity ranged from 90 % to 100 %. These studies suffered from a lack of high-quality reference standards and independent interpretations. Using modified New York criteria and radiography as the gold standard [28], F fluoride PET-CT is 80 % sensitive and 77 % specific to detect sacroiliitis in the setting of ankylosing spondylitis [86] (moderate evidence).

What Is the Role of Imaging in Patients with Back Pain Suspected of Having Spinal Stenosis?

Summary

Both CT and MR can be used to diagnose central stenosis (moderate evidence). On MR, the radiologists' general impression, rather than a millimeter measurement, is valid.

Supporting Evidence

(a) Plain Radiographs No studies provided good estimates of radiographic accuracy in detecting central stenosis. Since radiographs can only estimate bony canal compromise, the sensitivity for central stenosis is undoubtedly poorer than that of CT or MR, which depicts soft tissue structures.

(b) Computed Tomography A meta-analysis by Kent et al. [87] reported CT sensitivity for central stenosis of 70–100 % and specificity of 80–96 % (limited evidence). Methodologic quality was variable but generally poor, making pooling of the data

impractical. Central stenosis is also common in asymptomatic persons, with a prevalence of 4–28 % (limited evidence) [88], and thus, the specificity of CT for central stenosis, as it is for disk herniations, is likely less than the reported estimates.

(c) Magnetic Resonance In the 1992 meta-analysis by Kent et al. [87], the sensitivity of MR for stenosis was 81–97 %, while specificity ranged from 72 % to 100 % (limited evidence). Using stricter criteria for false positives, specificity was 93–100 %.

Of note, two recent studies suggest that the readers' general impression of central stenosis is valid. In a retrospective study comparing electromyogram (EMG) findings to radiologists' MR interpretations, Haig et al. [89] found that the radiologists' subjective sense of central stenosis (normal, mild, moderate, or severe) was statistically significantly correlated with the EMG ($r = 0.4$, $p < 0.017$) (moderate evidence). Speciale et al. [90] assessed the intra- and interobserver reliability of physicians for classifying the degree of lumbar stenosis. Two neurosurgeons, two orthopedic spine surgeons, and three radiologists reviewed MRs from patients with a clinical and radiologic diagnosis of lumbar spinal stenosis. While the interobserver reliability was fair among all specialties ($\kappa < 0.26$), it was highest among radiologists (moderate with $\kappa = 0.40$) and considerably lower among the surgeons ($\kappa = 0.21$ for neurosurgeons and $\kappa = 0.15$ for orthopedic surgeons). In concordance with Haig's work, they found that the readers' subjective evaluation of stenosis significantly correlated with the calculated cross-sectional area ($p < 0.001$).

(d) Bone Scanning and Single-Photon Emission Computed Tomography Bone scanning has no role in central stenosis imaging.

What Are Patients' Perceptions of the Role of Imaging in Low Back Pain?

Summary

The majority of patients with LBP think imaging is an important part of their care. However,

in patients who are imaged, results of satisfaction with care are conflicting and overall not significantly higher than in those who were not imaged. Additionally, when plain radiographs are obtained, outcome is not significantly altered (and in some cases, is worse). But when MR or CT is used early in the workup of LBP, there is a very slight improvement in patient outcome (weak evidence).

Supporting Evidence

While the majority of studies attempt to validate a modality by its diagnostic accuracy, possibly more important is whether the test actually alters patient outcomes. In their recent randomized controlled trial, Kerry et al. [91] studied 659 patients with LBP, randomizing 153 patients to either lumbar spine radiographs or care without imaging while also studying 506 patients in an observational arm (strong evidence). At 6 weeks and at 1 year, there was no difference between the groups in physical functioning, disability, pain, social functioning, general health, or need for further referrals. However, in the treatment arm at both 6 weeks and 1 year, there was a small improvement in self-reported overall mental health (Table 28.2). In a similar randomized controlled trial of 421 patients, Kendrick and colleagues [92] actually found a slight increase in pain duration and a decrease in overall functioning in the radiograph group at 3 months, though at 9 months there was no difference between the groups (strong evidence).

A few studies have attempted to demonstrate how CT and MR relate to outcome. In a large randomized study, Gilbert et al. [93] studied 782 patients, randomizing them to early imaging with CT or MR, or imaging only if a clear indication developed (strong evidence). They found that treatment was not influenced by early imaging. However, while both groups improved from baseline, there was slightly more improvement in the early imaging arm at both 8 ($p = 0.005$) and 24 ($p = 0.002$) months. In a subgroup of these patients, Gillan et al. [94] found that while there was an increase in diagnostic confidence in the early imaging group (Table 28.2), imaging did not change diagnostic or therapeutic impact (strong evidence).

Our group also performed a randomized controlled trial assigning primary care patients with LBP to receive either lumbar spine radiographs or a rapid lumbar spine MR [95] (strong evidence). We found nearly identical outcomes in the two groups. Vroomen and colleagues [96], however, did find in patients with leg pain, utilizing early MR helped predict the patient's prognosis (strong evidence).

Patient satisfaction and expectations must also be accounted for when developing an imaging strategy. Many patients with LBP believe imaging is important or necessary to their care [97–99]. However, there are conflicting results regarding improved satisfaction of care when imaging is actually performed. In their randomized trial using plain radiographs, Kendrick and colleagues [92] discovered that if participants had been given the choice, 80 % would have elected to be imaged (strong evidence). They also found that while satisfaction was similar at 3 months in both the imaging and nonimaging groups (Table 28.3), by 9 months, the intervention group was slightly more satisfied with their care. In the same cohort, Miller et al. [99] reported that the imaging group had a higher overall satisfaction score at 9 months. In a comparable study, Kerry and colleagues [91] found no difference in early patient satisfaction (strong evidence). They did not provide data for long-term satisfaction. Finally, in our comparison of rapid MR to radiographs, there was no difference in overall patient satisfaction between the two groups, but patients who received an MR were more reassured [95] (strong evidence).

Which Children Should Undergo Imaging for Nontraumatic Back Pain?

Summary

There are no validated clinical prediction rules for determining which subjects with nontraumatic low back pain should undergo imaging. However, imaging is clearly indicated if there is clinical concern for infection, tumor, or scoliosis. Imaging is probably not indicated in subjects without concern for one of the preceding

entities, in whom the pain has been of relatively short duration and intensity and in whom the physical examination is benign (insufficient evidence).

Spondylolysis is relatively common in adolescent athletes and should be suspected when pain develops in such subjects. Because spondylolysis may not be apparent on radiography, SPECT or CT may be warranted (limited evidence).

Supporting Evidence
There are no quality clinical trials on the value of imaging in children and adolescents with nontraumatic back pain. In addition, there are no validated clinical prediction rules for determining which children and adolescents should undergo imaging. Evidence supporting the use of imaging is mainly epidemiological, based on the relatively high yield for imaging in selected groups. Several studies from the 1980s reported that diagnosable pathology could be found in 52–84 % of children with back pain [27, 100, 101]. However, a more recent paper by Bhatia et al. revealed pathology in only 22 % [102]. The reason for this difference is not clear, but it may be that there is increasing reporting of uncomplicated mechanical back pain in children, leading to more frequent imaging of children with no vertebral pathology.

Imaging is indicated in patients who may be at risk for vertebral osteomyelitis or diskitis (and in those with scoliosis (Chap. 33, "Pediatric Dysraphism and Scoliosis: Evidence-Based Neuroimaging")). Risk factors for these conditions include fever, malaise, weight loss, neurological deficit, focal deformity, and pain at night [8, 103, 104]. In addition, imaging is indicated when a significant scoliosis is present (see Chap. 33, "Pediatric Dysraphism and Scoliosis: Evidence-Based Neuroimaging").

Among children and adolescents who have a short duration of pain and no antecedent history of significant trauma and without physical findings on examination that put the child into a high-risk category for one of the diagnoses above, imaging can be withheld. Though substantiating evidence is lacking, a reasonable list of risk factors that might promote imaging includes point tenderness over the bony elements, particularly the pars interarticularis, radicular pain, abnormal neurologic examination, and pain with spinal flexion and extension [8] (insufficient evidence).

In a small prospective study of 87 patients seen by a single pediatric orthopedic surgeon by Felman et al. [105], the predictors of constant pain, night pain, radicular pain, and abnormal neurologic examination could be combined into a clinical prediction rule to define subjects at high risk for underlying pathologic diagnosis (spondylolisthesis, scoliosis, tumor, disk degeneration, dysraphism). Patients with none of these predictors had only a 19 % probability of underlying pathology, while patients of all four predictors had a probability of 100 % for an underlying specific diagnosis. These results have not been validated, but the results may be useful in identifying subjects in whom additional imaging is indicated, after negative radiography [105] (limited evidence).

When imaging is indicated, radiography will almost always be the initial imaging modality of choice. The accuracy of radiography is not established. However, a recent prospective study by Bhatia et al. determined that among 13 patients in this series, 10 had definitive diagnosis by radiography, with the remainder requiring CT, bone scan, or MRI [102]. Similarly, in the Feldman et al. study, of 31 subjects with specific pathological diagnoses, 21 were diagnosed by initial radiography, with an additional 10 being diagnosed by MRI performed for high clinical suspicion. Thus in this small study, radiography has a sensitivity of 68 % (21 of 31) for clinically important conditions [105]. The specificity of radiography has not been documented. Despite the relatively modest accuracy of radiography; however, the relatively low radiation, low cost, and availability make this the initial imaging modality of choice. CT is the preferred imaging modality when spondylolysis is suspected. Bone scan is useful when symptoms are difficult to localize or if the acuteness of findings on other imaging evaluation is in question. MRI is the imaging modality of choice for infection, tumor, or neural element pathology (limited evidence).

Special Case: Spondylolysis

Spondylolysis is the leading cause of low back pain in adolescents after exclusion of patients in whom no specific diagnosis can be made. In the Bhatia et al. study, spondylolysis accounted for 11 % of patients presenting with low back pain [102]. The overall prevalence of spondylolysis may be as high as 4.4 % in small children and 6 % in adults [106]. It is particularly prevalent in athletes, specifically gymnasts, weight lifters, skiers, runners, and swimmers [8–12], and is the cause of back pain in an estimated 50 % of cases [107, 108]. Spondylolysis may be acute or chronic. Acute spondylolysis may be precipitated by exercise and may be amenable to conservative therapy [6]. The prognosis and treatment in chronic spondylolysis or in spondylolisthesis is less clear.

There is no consensus on the appropriate imaging evaluation of spondylolysis, and multiple modalities may be required in some individuals [107, 109–111]. Unfortunately, however, reliable data on the sensitivity and specificity of any imaging modality in this clinical setting are lacking. Though often the initial imaging, radiography is considered relatively insensitive for spondylolysis [112]. CT scanning has been promoted as an effective method for determining the acuteness of spondylolysis and for determining the potential for bony healing and the extent to which healing has occurred [6, 112, 113]. The accuracy of CT for staging and following spondylolysis may be increased by performing thin-section scanning in the plane of the pars articularis with angled reformations (Fig. 28.6a, b, c). However, reliable data on CT accuracy do not exist [110, 112] (insufficient evidence).

SPECT scan may be more sensitive for the diagnosis of spondylolysis [114], but it is less specific and provides less detailed anatomic information [115]. Scintigraphy may also help differentiate painful acute spondylolysis from chronic spondylolysis that is not a cause of pain [116, 117]. MRI [118–121] and PET-CT [122] show promise but have not been well evaluated in this population (insufficient evidence).

A reasonable imaging approach for suspected spondylolysis is initial imaging with radiography, followed by SPECT if no other cause of pain is identified and the subject is at high risk. If SPECT is negative, then no further imaging is indicated. However, if SPECT is positive, thin-section CT can be performed to define and stage the lesion (limited evidence).

Overall Modality Accuracy Summary

Table 28.4 summarizes the diagnostic accuracy parameters for each of the four modalities described. The likelihood ratio (LR) summarizes the sensitivity and specificity information in a single number, comparing the probability of having a positive test result in patients with the disease with the probability of a positive test in patients without the disease, or LR + = [probability (+test | disease)]/[probability (+test | no disease)]. This is equivalent to [sensitivity/ (1 − specificity)]. Similarly, the LR for a negative test is [(1 − sensitivity)/specificity]. The larger the LR, the better the test is for ruling in a diagnosis; conversely, the smaller the LR, the better it is for excluding a diagnosis. LRs greater than 10 or less than 0.1 are generally thought to be clinically useful. A LR equal to 1 provides no clinically useful information.

Take-Home Tables and Figures

Tables 28.1–28.4 and Figs. 28.1–28.6 serve to highlight key recommendations and supporting evidence.

Suggested Imaging Protocols

Plain Radiographs

Lateral and anteroposterior (AP) radiographs should be obtained for initial imaging in primary care patients with LBP; recent evidence supports lateral radiographs alone.

Table 28.1 Studies of lumbar spine imaging in asymptomatic adults

Modality (references)	Age group description	Prevalence of anatomic conditions				
		Herniated disk	Bulging disk	Degenerated disk	Stenosis	Annular tear
Plain X-rays [129]	14–25 years, high-performance athletes (n = 143)			20 %		
Plain X-rays [14]	Army recruits, 18 years old ±2 months			4 % (vs. 5 % of sx pts.)		
Myelography [130]	Mean age = 51, referred for posterior fossa	31 %				
	acoustic neuroma (n = 300)					
CT [131]	Mean age = 40					
	<40 years (n = 24)	20 %			0 %	
	>40 years (n = 27)	27 %			3 %	
MR [132]	Women mean age = 28 (n = 86)	9 %	44 %			
MR [18]	Under age 60 (n = 53)	22 %	54 %	46 %	1 %	
	≥Age 60 (n = 14)	36 %	79 %	93 %	21 %	
MR [19]	Mean age = 42 (n = 98)	28%[a]	52 %		7 %	14 %
MR [20]	Mean age = 36, matched age + occupation	76%[b]	51 % of disks	85 %		
	exposure to pts. having diskectomy (n = 46)					
MR [133]	Mean age = 28 (n = 41)					
MR [134]	Median age = 42 referred for head or	33%[c]	81 %	56 %		56 %
	neck imaging (n = 36)					
MR [135]	Mean age = 35 (n = 60)	56–60 %	20–28 %	72 %		19–20 %
MR [57]	Mean age = 40 (n = 54)					24 %
MR [23]	Mean = 54 (n = 148)	38%[d]	64 %	91 %	10 %	38 %
MR [21, 136]	20–50, unrelated trauma	73 % (7 % with extrusion)		49 %	29 %	
MR [23]	Mean age = 54, VA patients	38 %	64 %	91 %	10 %	38 %
MR [57]	Mean age = 40.1, cohort of prior cervical diskectomy					39 %

Source: Adapted with permission from Jarvik JG, Deyo RA. Diagnostic evaluation of low back pain with emphasis on imaging. Ann Intern Med. 2002 Oct 1;137(7):586–97

Reprinted with kind permission of Springer Science+Business Media from Sammer MBK, Jarvik JG. Imaging of adults with low back pain in the primary care setting. In: Medina LS et al. editors. Evidence-based imaging: improving the quality of imaging in patient care. New York: Springer Science+Business Media; 2011

sx symptomatic

[a]Sixty-four percent had disk bulge, protrusion, or extension; only 1 % had extrusions

[b]Nerve root compression in 4 %; contact or displacement of nerve root in 22 %

[c]Zero percent had extrusions

[d]Six percent had extrusions, 3 % had nerve root compromise

Supporting Evidence

The 1994 AHRQ evidence-based guidelines for the diagnosis and treatment of patients with acute LBP [77] recommend only two views of the lumbar spine be obtained routinely [123, 124]. More recently, a prospective study by Khoo et al. [125] suggests that a single lateral radiograph may be as effective as the standard two-view

Table 28.2 Patient outcome

Imaging type	Comparison	Difference (95 % CI, p)
Plain radiographs		
Kerry et al. [91]	Radiograph versus no radiograph	Mental health
	6 weeks	−8 (−14 to −1, $p < 0.05$)
	1 year	−8 (−15 to −2, $p < 0.05$)
Kendrick et al. [92]	Radiograph versus no radiograph	
	Pain at 3 months	1.26 (1.0–1.6, $p < 0.04$)
	Disability at 3 months	−1.90 (CI not provided, $p < 0.05$)
CT/MR		
Gilbert et al. [93]	Early CT or MR versus selective delayed	Acute LBP score
	8 months	−3.05 (−5.16 to −0.95, $p < 0.005$)
	2 years	−3.62 (−5.92 to −1.32, $p < 0.002$)
Gillan et al. [94]	Early CT or MR versus selective delayed	
	Treatment altered	$p = 0.733$
	Median change in diagnostic confidence	$p = 0.001$
Jarvik et al. [95]	Early MR versus plain radiograph	
	Mean back-related disability	−0.59 (−1.69 to 0.87, $p = 0.53$)
	(Roland) at 12 months	
Vroomen et al. [96]	Prognostic value of MR for sciatic	
	Favorable prognosis, annular rupture	$p = 0.02$
	Favorable prognosis, nerve root compression	$p = 0.03$
	Poor prognosis, disk herniation into foramen	$p = 0.004$

Reprinted with kind permission of Springer Science+Business Media from Sammer MBK, Jarvik JG. Imaging of adults with low back pain in the primary care setting. In: Medina LS, Blackmore CC, editors. Evidence-based imaging: optimizing imaging in patient care. New York: Springer; 2006

Table 28.3 Patient satisfaction

Study	Comparison	Difference (95 % CI, p when provided)
Kendrick et al. [92] and Miller et al. [99]	Radiograph versus no radiograph	
	Satisfaction at 3 months	−1.50 (CI not provided, $p = 0.13$)
	Satisfaction at 9 months	−2.69 (CI not provided, $p < 0.01$)
Kerry et al. [91]	Radiograph versus no radiograph	
	Satisfaction with initial	
	consultation/6 weeks	
	Very satisfied	1.0/1.0
	Satisfied	0.87 (0.40–1.9)/0.89 (0.37–2.1)
	Indifferent or dissatisfied	0.41 (0.12–1.3)/0.54 (0.19–1.5)
Jarvik et al. [95]	Rapid MR versus radiograph	
	Overall satisfaction at 12 months	0.30 (−0.42 to 0.99)
	Correlation of satisfaction with	Pearson correlation coefficients
	reassurance at 1, 3, and 12 months	$p < 0.001$ for all

Reprinted with kind permission of Springer Science+Business Media from Sammer MBK, Jarvik JG. Imaging of adults with low back pain in the primary care setting. In: Medina LS, Blackmore CC, editors. Evidence-based imaging: optimizing imaging in patient care. New York: Springer; 2006

Table 28.4 Accuracy of imaging for lumbar spine conditions[a, b]

	Sensitivity	Specificity	Likelihood ratio +	Likelihood ratio −
X-ray				
Cancer	0.6	0.95–0.995	12–120	0.40–0.42
Infection	0.82	0.57	1.9	0.32
Ankylosing spondylitis	0.26–0.45	1	Not defined	0.55–0.74
CT				
Herniated disk	0.62–0.9	0.7–0.87	2.1–6.9	0.11–0.54
Stenosis	0.9	0.8–0.96	4.5–22	0.10–0.12
MR				
Cancer	0.83–0.93	0.90–0.97	8.3–31	0.07–0.19
Infection	0.96	0.92	12	0.04
Ankylosing spondylitis	0.56			
Herniated disk	0.6–1.0	0.43–0.97	1.1–33	0–0.93
Stenosis	0.9	0.72–1.0	3.2–not defined	0.10–0.14
Radionuclide				
Cancer				
Planar	0.74–0.98	0.64–0.81	3.9	0.32
SPECT	0.87–0.93	0.91–0.93	9.7	0.14
Infection	0.90	0.78	4.1	0.13
Ankylosing spondylitis	0.26	1.0	Not defined	0.74

Source: [a]Reprinted with permission from Jarvik JG, Deyo RA. Diagnostic evaluation of low back pain with emphasis on imaging. Ann Intern Med. 2002 Oct 1;137(7):586–97
[b]Estimated ranges derived from multiple studies. See specific test sections in text for references

Fig. 28.1 Magnetic resonance (*MR*) of the lumbar spine in a patient without low back pain (*LBP*) (rigorously determined for entry into a longitudinal study of people without LBP). T1-weighted (**a**) and T2-weighted (**b**) sagittal images demonstrate a moderate-sized disk extrusion (*arrow*) at L5/S1. This is one example of many incidental findings (Reprinted with kind permission of Springer Science+Business Media from Sammer MBK, Jarvik JG. Imaging of adults with low back pain in the primary care setting. In: Medina LS, Blackmore CC, editors. Evidence-based imaging: optimizing imaging in patient care. New York: Springer; 2006)

Fig. 28.2 Axial computed tomography (*CT*) image demonstrates a relatively hyperdense focal disk herniation (*arrows*) outlined by lower density cerebrospinal fluid (*CSF*) within the spinal canal. This example shows CT's ability to depict disk herniations (Reprinted with kind permission of Springer Science+Business Media from Sammer MBK, Jarvik JG. Imaging of adults with low back pain in the primary care setting. In: Medina LS, Blackmore CC, editors. Evidence-based imaging: optimizing imaging in patient care. New York: Springer; 2006)

examination. In 1,030 lumbar spine radiographs, the AP film significantly altered the diagnosis in only 1.3 % of cases (all cases of possible sacroiliitis or pars defects). More importantly, infection and malignancy were not missed on the lateral film alone. In certain circumstances, other views are important. When compared with AP views alone, oblique films better demonstrate the pars interarticularis in profile to assess for spondylolysis. Flexion-extension films are used to assess instability, and angled views of the sacrum are used to assess sacroiliac joints for AS. Limiting the number of views is particularly important to younger females, because the gonadal dose of two views alone is equal to the gonadal radiation of daily chest X-rays for several years [126–128].
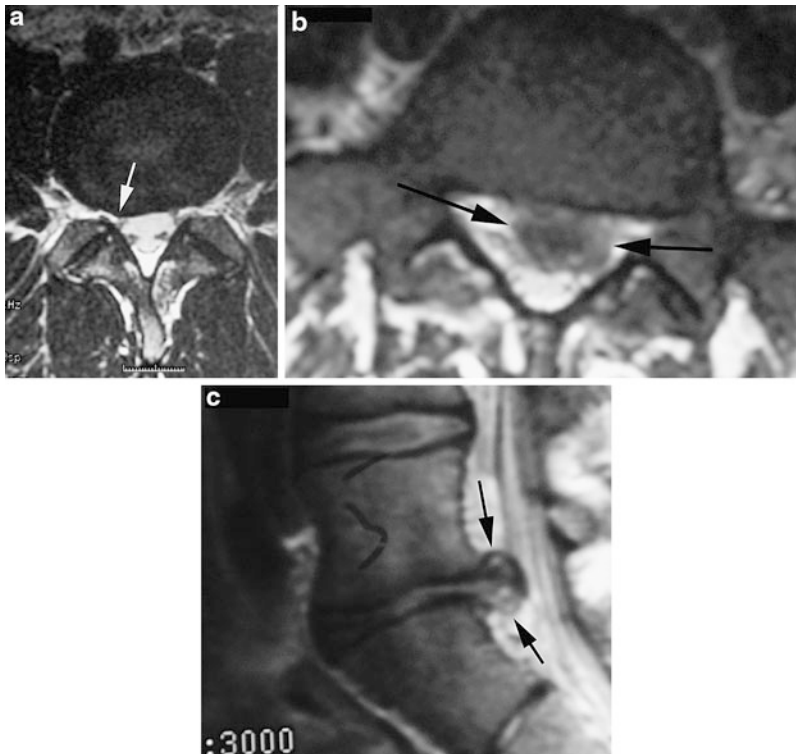
Fig. 28.3 T2-weighted MR images in two different patients showing a disk protrusion (*arrow*) (**a**) versus disk extrusion (*arrows*) (**b** and **c**). See text for definition. Protrusions are common in asymptomatic individuals and may clinically act as false positives (Reprinted with kind permission of Springer Science+Business Media from Sammer MBK, Jarvik JG. Imaging of adults with low back pain in the primary care setting. In: Medina LS, Blackmore CC, editors. Evidence-based imaging: optimizing imaging in patient care. New York: Springer; 2006)
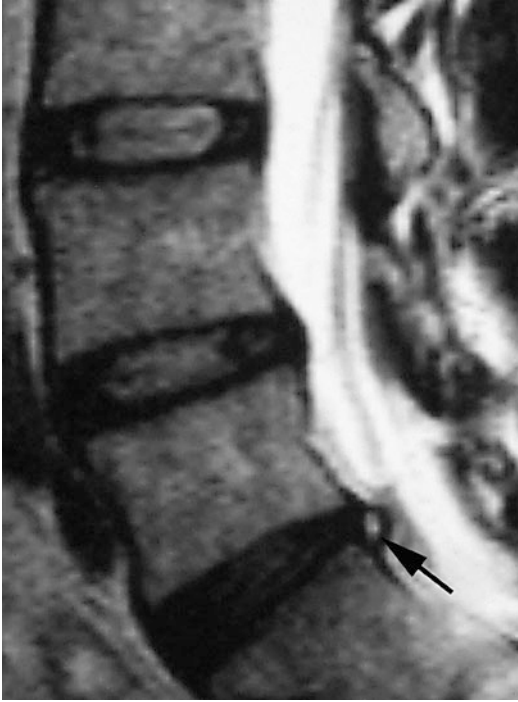
Fig. 28.4 Sagittal T2-weighted MR demonstrating high-intensity zone (HIZ) (*arrow*) in an asymptomatic subject (Reprinted with kind permission of Springer Science+ Business Media from Sammer MBK, Jarvik JG. Imaging of adults with low back pain in the primary care setting. In: Medina LS, Blackmore CC, editors. Evidence-based imaging: optimizing imaging in patient care. New York: Springer; 2006)

Computed Tomography

For routine lumbar spine imaging in the University of Washington health system, we use a multidetector CT with 2.5-mm detector collimation and 2.5-mm intervals at 140 kVp and 200–220 mA. If the radiologist determines prior to the study that sagittal and coronal reformats are needed, we scan at 1.25 mm with 1.25-mm intervals.

Supporting Evidence
We found no studies to support specific CT imaging protocols.

Magnetic Resonance

The MR sequences we use for routine lumbar spine imaging in the University of Washington system are as follows:

1. Sagittal T1-weighted 2D spin echo, TR 400/TE minimum, 192 × 256 matrix, 26-cm field of view (FOV), 4-mm slice thickness, and 1-mm skip
2. Sagittal T2-weighted fast-recovery (frFSE) fast spin-echo 2D spin echo, TR 4000/TE 110, echo train length (ETL) 25, 224 × 320 matrix, 26-cm FOV, 4-mm slice thickness, and 1-mm skip
3. Axial T1-weighted 2D spin echo, TR 500/TE minimum, 192 × 256 matrix, 20-cm FOV, 4-mm slice thickness, and 1-mm skip
4. Axial T2-weighted FSE-XL, TR 4000/TE 102, ETL 12, 192 × 256 matrix, 20-cm FOV, 4-mm slice thickness, and 1-mm skip

Supporting Evidence
We found no studies to support specific MR imaging protocols.

Future Research

- It is uncertain which imaging findings are the best predictors of surgical benefit in patients undergoing fusion for degenerative disease. Prospective cohort studies and randomized treatment trials could help to determine which imaging variables are key determinants of outcome.
- While compression fractures are readily identified on imaging, their natural history, including identifying which fractures will lead to chronic pain and what their best management is, has not yet been described.
- Both MR and bone scans are highly effective in identifying metastases. Because MR is more costly than bone scans, future studies may compare the cost-effectiveness of each option and may focus on whether patient outcome is changed from use of either method.
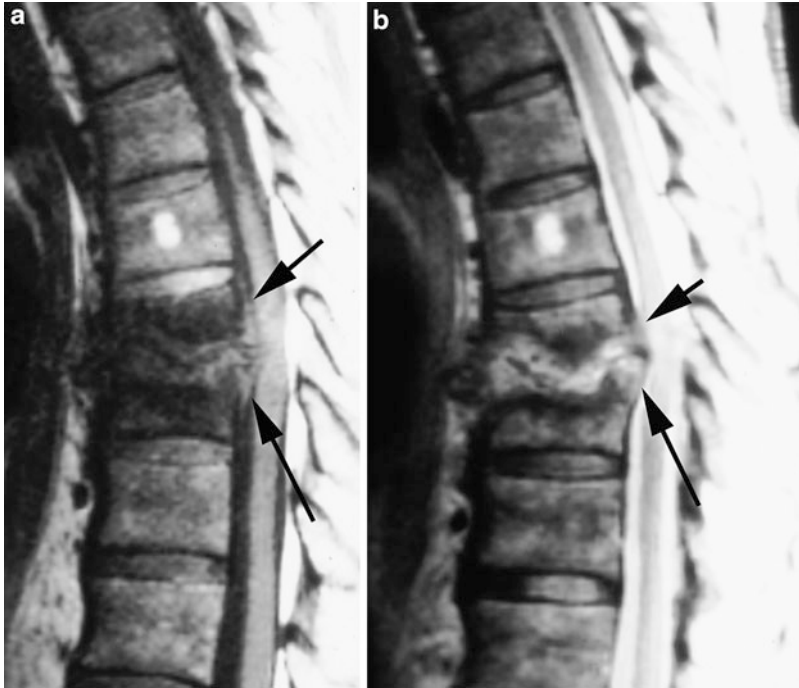
Fig. 28.5 Sagittal MR of the thoracic spine demonstrating characteristic findings of diskitis and osteomyelitis, with virtual obliteration of the intervertebral disk, low signal on T1-weighted (**a**) and high signal on T2-weighted (**b**) images adjacent to the destroyed disk. Note the posterior extension of the process into the spinal canal and epidural space, causing compression of the cord (*arrows*) (Reprinted with kind permission of Springer Science+Business Media from Sammer MBK, Jarvik JG. Imaging of adults with low back pain in the primary care setting. In: Medina LS, Blackmore CC, editors. Evidence-based imaging: optimizing imaging in patient care. New York: Springer; 2006)
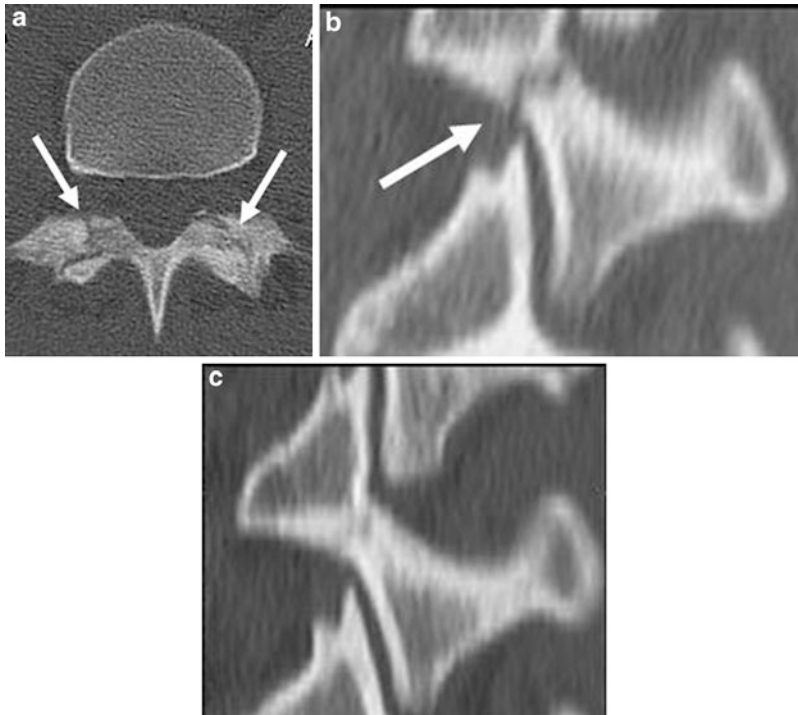
Fig. 28.6 Spondylolysis in a 15-year-old female. Initial axial CT (**a**) shows irregular linear lucencies through the bilateral pars interarticularis (*arrows*). Angled thin-section oblique reformation (**b**) demonstrates smooth margins indicating an acute injury (*arrow*). Follow-up CT 4 months later reveals near-complete healing (**c**) on angled thin-section oblique reformation (Reprinted with kind permission of Springer Science+Business Media from Blackmore CC. Imaging of the spine for traumatic and nontraumatic etiologies. In: Medina LS et al. editors. Evidence-based imaging in pediatrics. New York: Springer; 2010)

- With infection, molecular imaging techniques may eventually be developed that can identify specific organisms based on imaging properties.
- Data on the best imaging technique to diagnose AS are sparse. Future studies may determine the role and cost-effectiveness of MR in early diagnosis.
- In patients with spinal stenosis and symptomatic herniated disks, definitive studies to document patient outcomes from surgical intervention are needed.

References

1. Jarvik JG, Deyo RA. Ann Intern Med. 2002;137(7):586–97.
2. Rossi F, Dragoni S. Radiographics. 2001;66: 699–707.
3. Soler T, Calderon C. Am J Sports Med. 2000; 28:57–62.
4. Micheli LJ, Wood R. Arch Pediatr Adolesc Med. 1995;149:15–8.
5. Standaert CJ, Herring SA. Arch Phys Med Rehabil. 2007;88:537–40.
6. Ogon M, et al. Clin Orthop Related Res. 2001; 390:151–62.
7. Bernstein RM, Cozen H. Am Fam Physician. 2007;76:1669–76.
8. Szpalski M, et al. Eur Spine J. 2002;11:459–64.

9. Anderson JM, Schutt AH. Mayo Clin Proc. 1980;55(8):499–504.

10. Frymoyer JW. Back pain and sciatica. N Engl J Med. 1988;318:291–300.

11. Barondess JA. The future of generalism. Ann Intern Med. 1993;119(2):153–60.

12. Salkever DS. Morbidity cost: national estimates and economic determinants. NCHSR Research Summary Serials. DHHS Publication.1985. Report No.: (PHS) 86–3343; 1985.

13. White AAD, Gordon SL. Spine. 1982;7(2):141–9.

14. Steinberg EL, Luger E, Arbel R, Menachem A, Dekel S. Clin Radiol. 2003;58(12):985–9.

15. van Tulder MW, Assendelft WJ, Koes BW, Bouter LM. Spine. 1997;22(4):427–34.

16. Deyo R, Tsui-Wu Y. Spine. 1987;12:264–8.

17. Currey HL, Greenwood RM, Lloyd GG, Murray RS. Rheumatol Rehabil. 1979;18(2):94–104.

18. Boden SD, Davis DO, Dina TS, Patronas NJ, Wiesel SW. J Bone Joint Surg Am. 1990;72(3): 403–8.

19. Jensen MC, Brant-Zawadzki MN, Obuchowski N, Modic MT, Malkasian D, Ross JS. N Engl J Med. 1994;331(2):69–73.

20. Boos N, Rieder R, Schade V, Spratt KF, Semmer N, Aebi M. Spine. 1995;20(24):2613–25.

21. Boos N, Semmer N, Elfering A, Schade V, Gal I, Zanetti M, et al. Spine. 2000;25(12):1484–92.

22. Jensen OK, Nielsen CV, Stengaard-Pedersen K. Spine J. 2010;10(8):659–75.

23. Jarvik JJ, Hollingworth W, Heagerty P, Haynor DR, Deyo RA. Spine. 2001;26(10):1158–66.

24. Deyo RA, Rainville J, Kent DL. J Am Med Assoc. 1992;268(6):760–5.

25. van den Bosch MA, Hollingworth W, Kinmonth AL, Dixon AK. Clin Radiol. 2004;59(1):69–76.

26. Hamilton MG, Myles ST. J Neurosurg. 1992;77(5): 700–4.

27. Jeffries LJ, Milanese SF, Grimmer-Somers KA. Spine. 2007;32:2630–7.

28. Luo X, Pietrobon R, Sun SX, Liu GG, Hey L. Spine. 2004;29(1):79–86.

29. Klein BP, Jensen RC, Sanderson LM. J Occup Med. 1984;26:443.

30. Peterson CK, Bolton JE, Wood AR. Spine. 2000;25(2):218–23.

31. Lundin O, Hellstrom M, Nilsson I, Sward L. Scand J Med Sci Sports. 2001;11(2):103–9.

32. Thornbury JR, Fryback DG, Turski PA, Javid MJ, McDonald JV, Beinlich BR, et al. Radiology. 1993;186(3):731–8.

33. Jackson RP, Cain Jr JE, Jacobs RR, Cooper BR, McManus GE. Spine. 1989;14(12):1362–7.

34. Wilmink JT. AJNR Am J Neuroradiol. 1989;10(2): 233–48.

35. Janssen ME, Bertrand SL, Joe C, Levine MI. Orthopedics. 1994;17(2):121–7.

36. Beattie PF, Meyers SP, Stratford P, Millard RW, Hollenberg GM. Spine. 2000;25(7):819–28.

37. Vroomen PC, de Krom MC, Wilmink JT. J Neurosurg. 2000;92(2 Suppl):135–41.

38. Rankine JJ, Fortune DG, Hutchinson CE, Hughes DG, Main CJ. Spine. 1998;23(15):1668–76.

39. Gorbachova TA, Terk MR. Skeletal Radiol. 2002; 31(9):511–5.

40. Pfirrmann CW, Dora C, Schmid MR, Zanetti M, Hodler J, Boos N. Radiology. 2004;230(2):583–8.

41. Porchet F, Wietlisbach V, Burnand B, Daeppen K, Villemure JG, Vader JP. Neurosurgery. 2002;50(6):1253–9. discussion 9–60.

42. Jarvik JG, Haynor DR, Hollingworth W, Deyo RA. Longitudinal assessment of imaging and disability of the back: a prospective cohort study of asymptomatic VA patients. Chicago: RSNA; 1999.

43. Ahn SH, Ahn MW, Byun WM. Spine. 2000;25(4): 475–80.

44. Fardon DF, Milette PC. Spine. 2001;26(5):E93–113.

45. Brant-Zawadzki MN, Jensen MC, Obuchowski N, Ross JS, Modic MT. Spine. 1995;20(11):1257–63. discussion 64.

46. Milette PC, Fontaine S, Lepanto L, Cardinal E, Breton G. Spine. 1999;24(1):44–53.

47. Jarvik J, Haynor D, Koepsell T, Bronstein A, Ashley D, Deyo R. Acad Radiol. 1996;3:537–44.

48. Cooley JR, Danielson CD, Schultz GD, Hall TA. J Manipulative Physiol Ther. 2001;24(5):317–26.

49. Pui MH, Husen YA. Australas Radiol. 2000;44(3): 281–4.

50. Aota Y, Onari K, An HS, Yoshikawa K. Spine. 2001;26(19):2125–32.

51. Kikkawa I, Sugimoto H, Saita K, Ookami H, Nakama S, Hoshino Y. J Orthop Sci. 2001;6(2):101–9.

52. Lane JI, Koeller KK, Atkinson JL. AJNR Am J Neuroradiol. 1994;15(7):1317–25.

53. Crisi G, Carpeggiani P, Trevisan C. AJNR Am J Neuroradiol. 1993;14(6):1379–92.

54. Autio RA, Karppinen J, Kurunlahti M, Kyllonen E, Vanharanta H, Tervonen O. Spine. 2002;27(13): 1433–7.

55. Mullin WJ, Heithoff KB, Gilbert Jr TJ, Renfrew DL. Spine. 2000;25(12):1493–9.

56. Aprill C, Bogduk N. Br J Radiol. 1992;65(773): 361–9.

57. Carragee EJ, Paragioudakis SJ, Khurana S. Spine. 2000;25(23):2987–92.

58. Rankine JJ, Gill KP, Hutchinson CE, Ross ER, Williamson JB. Spine. 1999;24(18):1913–9. discussion 20.

59. Lam KS, Carlin D, Mulholland RC. Eur Spine J. 2000;9(1):36–41.

60. Videman T, Battie MC, Gibbons LE, Maravilla K, Manninen H, Kaprio J. Spine. 2003;28(6):582–8.

61. Sartoris DJ, Andre M, Resnik CS, Resnick D, Resnick C. Radiology. 1986;160(3):707–12.

62. Sartoris DJ, Clopton P, Nemcek A, Dowd C, Resnick D. Radiology. 1986;160(2):479–83.

63. Deyo RA, Diehl AK. J Gen Intern Med. 1988;3:230–8.

64. Algra PR, Bloem JL, Tissing H, Falke THM, Arndt JW, Verboom LJ. Radiographics. 1991;11:219–32.

65. Avrahami E, Tadmor R, Dally O, Hadar H. J Comput Assist Tomogr. 1989;13(4):598–602.

66. Carroll KW, Feller JF, Tirman PF. J Magn Reson Imaging. 1997;7(2):394–8.

67. Carmody RF, Yang PJ, Seeley GW, Seeger JF, Unger EC, Johnson JE. Radiology. 1989;173:225.

68. Kosuda S, Kaji T, Yokoyama H, Yokokawa T, Katayama M, Iriye T, et al. J Nucl Med. 1996;37(6):975–8.

69. McDougall IR, Kriss JP. J Am Med Assoc. 1975;231(1):46–50.

70. Corcoran RJ, Thrall JH, Kyle RW, Kaminski RJ, Johnson MC. Radiology. 1976;121(3Pt. 1):663–7.

71. Savelli G, Chiti A, Grasselli G, Maccauro M, Rodari M, Bombardieri E. Anticancer Res. 2000;20(2B):1115–20.

72. Petren-Mallmin M. Acta Radiol Suppl. 1994;391:1–23.

73. McNeil BJ. Semin Nucl Med. 1978;8(4):336–45.

74. Jacobson AF. Yield of bone scintigraphy. Arch Intern Med. 1997;157(1):105–9.

75. Even-Sapir E, Martin RH, Barnes DC, Pringle CR, Iles SE, Mitchell MJ. Radiology. 1993;187(1):193–8.

76. Han LJ, Au-Yong TK, Tong WC, Chu KS, Szeto LT, Wong CP. Eur J Nucl Med. 1998;25(6):635–8.

77. Bigos S, Bowyer O, Braen G, Brown K, Deyo RA, Haldeman S, et al. Acute low back problems in adults. Clinical Practice Guideline No. 14. AHCPR Publication. Rockville, MD: Agency for Health Care Policy and Research, Public Health Service, U.S. Department of Health and Human Services 1994 12/94. Report No.: 95–0642; 1994.

78. Joines JD, McNutt RA, Carey TS, Deyo RA, Rouhani R. J Gen Intern Med. 2001;16:14–23.

79. Hollingworth W, Gray DT, Martin BI, Sullivan SD, Deyo RA, Jarvik JG. J Gen Intern Med. 2003;18(4):303–12.

80. Modic M, Feiglin D, Piraino D, Boumphrey F, Weinstein M, Duchesneau P, et al. Radiology. 1985;157:157–66.

81. Breslau J, Jarvik JG, Haynor DR, Longstreth Jr WT, Kent DL, Maravilla KR. AJNR Am J Neuroradiol. 1999;20(4):670–5.

82. Love C, Patel M, Lonner BS, Tomas MB, Palestro CJ. Clin Nucl Med. 2000;25(12):963–77.

83. Yamato M, Nishimura G, Kuramochi E, Saiki N, Fujioka M. Radiat Med. 1998;16(5):329–34.

84. Marc V, Dromer C, Le Guennec P, Manelfe C, Fournie B. Rev Rheum Engl Ed. 1997;64(7–9):465–73.

85. Hanly JG, Barnes DC, Mitchell MJ, MacMillan L, Docherty P. J Rheumatol. 1993;20(12):2062–8.

86. Strobel K, Fischer DR, Tamborrini G, Kyburz D, Stumpe KD, Hesselmann RG, et al. Eur J Nucl Med Mol Imaging. 2010;37(9):1760–5.

87. Kent D, Haynor D, Larson E, Deyo R. AJR Am J Roentgenol. 1992;158:1135–44.

88. Porter RW, Bewley B. Spine. 1994;19(2):173–5.

89. Haig AJ, Weiner JB, Tew J, Quint D, Yamakawa K. Spine. 2002;27(17):1918–25. discussion 24–5.

90. Speciale AC, Pietrobon R, Urban CW, Richardson WJ, Helms CA, Major N, et al. Spine. 2002;27(10):1082–6.

91. Kerry S, Hilton S, Dundas D, Rink E, Oakeshott P. Br J Gen Pract. 2002;52(479):469–74.

92. Kendrick D, Fielding K, Bentley E, Kerslake R, Miller P, Pringle M. Br Med J. 2001;322(7283):400–5.

93. Gilbert FJ, Grant AM, Gillan MG, Vale LD, Campbell MK, Scott NW, et al. Radiology. 2004;231(2):343–51.

94. Gillan MG, Gilbert FJ, Andrew JE, Grant AM, Wardlaw D, Valentine NW, et al. Radiology. 2001;220(2):393–9.

95. Jarvik JG, Hollingworth W, Martin B, Emerson SS, Gray DT, Overman S, et al. J Am Med Assoc. 2003;289(21):2810–8.

96. Vroomen PC, Wilmink JT, de Krom MC. Neuroradiology. 2002;44(1):59–63.

97. Espeland A, Baerheim A, Albrektsen G, Korsbrekke K, Larsen JL. Spine. 2001;26(12):1356–63.

98. Kerry S, Hilton S, Patel S, Dundas D, Rink E, Lord J. Health Technol Assess. 2000;4(20):1–4.

99. Miller P, Kendrick D, Bentley E, Fielding K. Spine. 2002;27(20):2291–7.

100. Turner PG, Hancock PG, Green JH. Spine. 1989;14:812–4.

101. King HA. Evaluating the child with back pain. 1986;33(6):1489–1493.

102. Bhatia NN, et al. J Pediatr Orthop. 2008;28:230–3.

103. Wilne S, et al. Lancet Oncol. 2007;8:685–95.

104. Garg S, Dormans JP. J Am Acad Orthop Surg. 2005;13(6):372–81.

105. Feldman DS, et al. J Pediatr Orthop. 2006;26:353–7.

106. Frederickson BE, et al. J Bone Joint Surg Am. 1984;66:699–707.

107. Sassmannshausen G, Smith BG. Clin Sports Med. 2002;21(1):121–32.

108. DePalma MJ, Bhargava A. Curr Sports Med Rep. 2006;5(1):44–9.

109. Standaert CJ, Herring SA. Br J Sports Med. 2000;34(6):415–22.

110. McCleary MD, Congeni JA. Curr Sports Med Rep. 2007;6(1):62–6.

111. Waicus KM, Smith BW. Curr Sports Med Rep. 2002;1(1):52–8.

112. Congeni J, McCulloch J, Swanson K. Am J Sports Med. 1997;25(2):248–53.

113. Fujii K, et al. J Bone Joint Surg Br. 2004;86:225–31.

114. Sanpera I, Beguiristain-Gurpide JL. J Pediatr Orthop. 2006;26:221–5.

115. Garces GL, et al. Int Orthop. 1999;23(4):213–5.

116. Elliott S, Hutson MA, Wastie ML. Clin Radiol. 1988;39(3):269–72.

117. Lowe J, et al. Spine. 1984;9(6):653–5.
118. Bennett DL, Nassar L, DeLano MC. Skeletal Radiol. 2006;35(7):503–9.
119. Masci L, et al. Br J Sports Med. 2006;40(11):940–6. discussion 946.
120. Udeshi UL, Reeves D. Clin Radiol. 1999;54(9): 615–9.
121. Campbell RS, Grainger AJ. Clin Radiol. 1999;54(1):63–8.
122. Ovadia D, et al. J Pediatr Orthop. 2007;27(1):90–3.
123. Robbins SE, Morse MH. Clin Radiol. 1996; 51(9):637–8.
124. Scavone JG, Latshaw RF, Weidner WA. Am J Roentgenol. 1981;136(4):715–7.
125. Khoo LA, Heron C, Patel U, Given-Wilson R, Grundy A, Khaw KT, et al. Clin Radiol. 2003; 58(8):606–9.
126. Antoku S, Russell W. Radiology. 1957;101:669–78.
127. Hall FM. Radiology. 1976;120:443–8.
128. Webster E, Merrill O. Radiation hazards: II. N Engl J Med. 1957;257:811–9.
129. Hellstrom M, et al. Acta Radiol. 1990;31(2): 1127–132.
130. Hitselberger WE, Witten RM. J Neurosurg. 1968;28(3):204–206.
131. Wiesel S, et al. Spine. 1984;9:549–551.
132. Weinreb JC, et al. Radiology. 1989;170(1pt 1): 125–128.
133. Burns JW, et al. Aviat Space Environ Med. 1996;67(9):849–853.
134. Stadnik TW, et al. Radiology. 1998;201(1):49–55.
135. Weishaupt D, et al. Radiology. 1998;209(3): 661–666.
136. Elfering A, et al. Spine. 2002;27(2):125–134.

Spinal Injections for Low Back Pain: Evidence-Based Treatment

29

John A. Carrino and Nikolai Bogduk

Contents

J.A. Carrino (✉)

Russell H. Morgan Department of Radiology and Radiological Science, Johns Hopkins University School of Medicine, Baltimore, MD, USA
e-mail: carrino@jhmi.edu

N. Bogduk
Newcastle Bone and Joint Institute, Royal Newcastle Center, University of Newcastle, Newcastle, NSW, Australia
e-mail: Vicki.caesar@hne.health.nsw.gov.au

Key Points

- Lumbar intradiscal therapy (injection, denervation, thermomodulation) procedures are of no benefit for the majority of patients with chronic low back pain (moderate evidence).
- Lumbar facet joint intra-articular steroid injection is of no benefit for chronic low-back pain (moderate evidence).
- Neurolytic treatment of lumbar facet joints (lumbar radiofrequency medial branch neurotomy) is of moderate benefit for chronic low back pain when positive response to medial branch diagnostic blocks are used as the selection criteria (moderate evidence).
- Sacroiliac joint intra-articular steroid injection is of no benefit for chronic low back pain (limited evidence).
- Sacroiliac joint intra-articular steroid injection is of great benefit for low back pain in patients with inflammatory spondyloarthropathy (limited evidence).
- Lumbar epidural steroid injection is of no benefit for chronic low back pain (moderate evidence).

Definition and Pathophysiology

Low back pain is a distinctly different condition from lumbar radicular pain (sometimes called "sciatica"). Radicular pain is lancinating pain that travels into the lower limb along a narrow band [1]. It is caused by disc herniation, foraminal stenosis, lateral recess stenosis, or other space-occupying lesions in the vertebral canal that compromise lumbosacral nerve roots. In contrast, low back is dull, aching pain that is centered on the lumbar, or lumbosacral, spine but may radiate into the buttocks or proximal thigh; it can radiate beyond the knee but not typically so. Its causes are elusive and difficult to determine.

Back pain may be classified according to the length of time symptoms persist: acute <6 weeks, subacute 6–12 weeks, and chronic >12 weeks. This is significant because the biology, pathology, natural history, and evidence base for each class of back pain are distinctly different.

Acute low back pain is largely a benign condition with a favorable natural history. Investigations are only indicated in cases of acute low back pain when alerting features ("red flags") of serious conditions are present [2]. "Red flags" is the term referring to the clinical/physical features indicating the possible presence of serious but relatively uncommon diseases requiring specific evaluation and treatment. Such conditions include tumors, infection, fractures, and neurological damage.

The International Association for the Study of Pain (IASP) defines chronic pain as pain that has persisted for longer than 3 months [1]. Individuals vary in their potential to develop chronic pain. A combination of behaviors, beliefs, and emotions may be involved in the transition from acute to chronic pain [3].

The causes or sources of chronic low back pain typically cannot be determined using conventional medical imaging. Degenerative disc disease (DDD) is a morphologic descriptor of age-related changes (desiccation, height loss, osteophytes) that show no clinically significant association with pain. Therefore, it does not constitute a diagnosis of back pain. Spinal stenosis can cause radiculopathy and related neurologic symptoms, but stenosis, per se, is not a cause of back pain. In patients with spinal stenosis, back pain might be caused by conditions that happen also to cause stenosis (e.g., facet arthropathy), or it may be unrelated to the stenosis.

Some causes or sources of chronic low back pain can be identified if invasive diagnostic tests are used. Diagnostic blocks can be used to try to identify pain stemming from the zygapophysial (facet) joints or the sacroiliac joints, and discography can be tried to diagnose internal disc disruption (IDD). IDD is a specific condition characterized by degradation of the matrix of the nucleus pulposus and fissures (radial $\pm$ circumferential) that penetrate the annulus fibrosus without breaching the outer lamella. These morphological features correlate with the disc being painful [4]. Affected discs exhibit biophysical features that correlate with the disc being painful [5]. The putative mechanical etiology of internal disc disruption is fatigue

failure of the endplate, which precipitates the biophysical features of the condition [6]. The biochemical features have been produced by endplate fractures in animal models [7–9].

Epidemiology

Back pain is highly prevalent, affecting most individuals at some point in their lives. Disc degeneration is not synonymous with back pain and related disability. A large study, using multiple regression analysis, showed that age changes and degenerative changes did not correlate with the disc being painful [4, 10]. An estimated 75 % of the population has had an episode of back pain at some point in their life [11]. While most acute back pain resolves within a few months, surveys report that approximately 5–10 % of the population has chronic back pain [11], a percentage which implies significant social and economic impacts [12]. The risk of low back pain increases with age [13]. Those affected can have disabling symptoms that can dramatically affect their quality of life and ability to perform a variety of activities. In patients with chronic low back pain, using diagnostic injections as the reference standard, the follow structures with relative contributions have been reported: internal disc disruption in at least 39 % [14], lumbar zygapophysial (facet) joints in 5–15 % [15], and the sacroiliac joint in 13–19 % [16, 17]. The exact prevalence of sacroiliitis is unknown, but the estimate for inflammatory back pain is about 0.8 % of the adult population aged 25–49 years [18]. Sacroiliitis can be diagnosed by medical imaging demonstrating inflammation of the affected joint.

Overall Cost to Society

The total costs of low back pain in the United States exceed $100 billion per year [19]. Two-thirds of these costs are indirect, due to lost wages and reduced productivity. Each year, fewer than 5 % of the patients who have an episode of low back pain account for 75 % of the total costs [19]. Annually, a substantial amount of money is spent in the United States on spinal injections. As an estimate, reimbursement for over half a million spinal injections ($n = 637, 294$) performed in the Medicare population during 1999 was over $65 million [20].

Goals of Injections

Spinal injections can be used for diagnostic and therapeutic purposes with the theoretical advantage that they target directly the site involved in the source of pain. Therapeutic spinal injections are not curative but are intended to provide pain relief and functional improvement for an intermediate duration of months to years.

Methodology

The topic of low back pain was searched using multiple electronic databases. The searches were performed in stages. All searches were initially conducted from January 1966 (the start date of MEDLINE) through September 2011. In addition to MEDLINE, we searched for systematic reviews using the Cochrane Database of Systematic Reviews and the NHA Health Technology Assessment Programme and for primary studies using the Cochrane Central Register of Controlled Trials and EMBASE. Electronic searches were supplemented by reviews of reference lists and additional citations suggested by experts.

Inclusion criteria were based on population (low back pain), therapeutic intervention (lumbosacral spinal injection), a comparator (placebo or other treatment), outcomes (pain, physical function, quality of life, patient satisfaction, opioid use, return to work, other reported surrogate, complications), and study design (RCTs, observational cohort, and large case series). We included relevant systematic reviews. Studies of cost were included if they were conducted alongside a randomized trial or were a full economic analysis (cost-effectiveness, cost-minimization, or cost-utility study). We only included non-English language trials if they were already included in English language systematic reviews.

Exclusion criteria were studies of populations without low back pain (cervical spine, spinal stenosis, radicular pain), nontherapeutic interventions (diagnostic injections), postoperative injection treatments (failed back surgery), no outcomes assessment, and study design that was not a clinical trial or a large case series. Other observational studies (such as uncontrolled case series and pre-post analyses) were excluded. Studies of nonhuman subjects and those without original data were excluded. We also excluded studies published only as conference abstracts.

Discussion of Issues

What Is the Role of Therapeutic Spinal Injections for Acute Low Back Pain?

Summary/Supporting Evidence
Most acute low back pain gets better. So, there is rarely any need to investigate it. The causes are not known, for the majority of cases, and there is no need to know (because it gets better). Investigations are warranted only when the pain persists, but then the pain is no longer acute. In the absence of a diagnosis of the source of pain, targeted interventional pain procedure is not indicated. As a result, there have been no studies of interventions for acute back pain, and there do not need to be any.

What Is the Role of Therapeutic Spinal Injections for Chronic Low Back Pain?

Summary
There is a variety of spine injections that may be applied in the treatment of chronic low back pain. These are usually based on a putative source of pain (pain generator) such as the intervertebral disc, zygapophysial (facet) joint, or sacroiliac joint diagnosed by clinical signs/symptoms, physical exam findings, medical imaging, diagnostic injections, or a combination thereof. As summarized in several systematic reviews, these spinal injection treatments have not been well studied in homogenous populations [19, 21–25]. Each of the specific joints/injection types is discussed.

Supporting Evidence
Intervertebral Disc
Intradiscal injections afford no benefit, or are of questionable benefit, based on several RCTs (moderate evidence). External denervation of the disc is of questionable benefit (moderate evidence). Some forms of internal thermal coagulation of the disc are of no benefit, while others are of questionable benefit (moderate evidence).

Chemical therapies for discogenic pain target one or other of the agents involved in disc degradation. Three randomized placebo-controlled studies have indicated that intradiscal steroid injections are not effective in the management of discogenic, chronic low back pain [26–28]. A placebo-controlled study assessed the efficacy of intradiscal injection of etanercept in doses increasing from 0.1 to 1.5 mg and found no differences at 1 month, either within or between patients treated with etanercept or normal saline, with respect to relief of pain or disability [29]. For low back pain without radiculopathy, intradiscal injections with methylene blue were superior to placebo injections in terms of pain, function, patient satisfaction, and analgesic use in the long term (6-24 months) based on data from RCT of 72 patients [30], but these results have not been replicated. No studies have reported the effectiveness of ozone for back pain. There are no large observational studies or clinical trials looking at the effectiveness of intradiscal proliferants (purported disc healing substances). An initial prospective case series involved 30 patients receiving an average of 2.5 intradiscal injections of a compounded mixture of chondroitin sulfate, glucosamine hydrochloride, DMSO, bupivacaine, hypertonic dextrose, and nonionic contrast [31]. The investigators reported that 57 % of patients experienced greater than 50 % improvement in pain sustained over a minimum follow-up of 12 months. Studies using regenerative therapies (cytokines, growth factors, and gene therapies are known to promote favorably

the metabolism of connective tissues) conducted in humans have addressed only safety and not efficacy or effectiveness.

Attempts have been made to denervate painful discs at different sites (anterolateral or postero-lateral) using a variety of means. A prospective, single-blinded (patient) controlled study compared the effects of thermal radiofrequency lesioning in the region of the ramus communicans (anterolateral disc innervation) with those of injections of lidocaine over the same site (anterolateral disc) [32]. In terms of pain scores and physical function scores, significant differences were in favor of radiofrequency treatment at 4 months following intervention. However, the degree of relief afforded by radiofrequency therapy was modest, amounting to only a 46 % mean decrease in pain. The study was confounded because patients who received radiofrequency therapy also received an injection of steroid at the site treated, which the control group did not receive. A controlled trial demonstrated that intradiscal radiofrequency achieved no greater relief of pain than sham therapy [33]. No controlled or prospective trials of the efficacy of sinuvertebral nerve (posterolateral disc innervation) lesions for the treatment of lumbar disc pain are currently available.

IDET (Intradiscal Electrothermal Therapy) involves threading a flexible electrode into the painful disc and using it to heat and coagulate the posterior annulus in the region affected by radial and circumferential fissures. IDET has been studied with observational and randomized controlled clinical trials. A nonrandomized study compared IDET with rehabilitation using subjects with insurance denial as the control group [34]. Both groups of patients had similar pretreatment pain scores. After treatment and at follow-up 12 months and two years after treatment, those scores were significantly better in those patients treated with IDET. A placebo-controlled study warned that placebo responses could occur in patients undergoing intradiscal therapy [35]. Nevertheless, in that study IDET was significantly more effective than placebo for the reduction of pain (assessed using a visual analog scale) and for the improvement of physical function using the short form (SF)-36 and the Oswestry disability scale. However, IDET was patently effective in only a minority of patients. A subsequent RCT showed no benefit of IDET over placebo using a sham procedure [36]. Among the reasons for variable success rates are differences in patient selection and technique used [37]. When originally described, the procedure required placement of the electrode at the interface between the nucleus pulposus and inner annulus. Those studies with better outcomes placed the electrode in the outer annulus. The optimum position requires crossing the radial fissure and lying parallel but peripheral to any circumferential fissure. If such a peripheral placement cannot be achieved, a more central placement, inside the circumferential fissure but parallel and as close as possible to it, is preferred. If the radial fissure cannot be crossed using a single insertion of the electrode, the fissures are addressed by bilateral placements. Suboptimal location within the intervertebral disc height (craniocaudal dimension) might be another reason for variable results. The IDET electrode has only a small field of effect. It coagulates tissues in a region within about one electrode width. For some fissures, this field might be enough, i.e., the electrode crosses the fissure and completely coagulates it. In other cases this might not occur. The electrode might pass only partially through a fissure or may pass entirely below or above the fissure with incomplete or no coagulation [37].

No prospective, randomized, controlled studies are available regarding the use of percutaneous plasma discectomy (nucleoplasty) for discogenic pain.

Zygapophysial (Facet) Joint
Intra-articular Injections

Zygapophysial (facet) joint intra-articular steroid injections overall showed no benefit based on four RCTs (moderate evidence). The largest randomized study, involving 109 patients, found no difference among large-volume (8 mL) intra-articular saline injections, intra-articular corticosteroid, and local anesthetic, and the same

mixture injected around 2 zygapophysial (facet) joints [38]. Another randomized, controlled study found only a small difference between the injection of saline (10 % good effect) and corticosteroid (22 % good effect) up to 6 months after treatment [39]. However, one subgroup that shows a benefit is those patients whose joints are selected by positive bone scintigraphy (using single photon emission computed tomography, SPECT). SPECT positive joints are more likely to respond to intra-articular injections than normal scintigraphic appearing zygapophysial (facet) joints despite a similar morphologic amount of osteoarthritis, but this has not been confirmed with RCTs [40–42]. Also, one randomized, controlled, double-blinded RCT of 60 patients showed no benefit in the injection of steroids versus hyaluronic acid into the zygapophysial (facet) joint at six months [43].

Neurolytics (Radiofrequency Medial Branch Neurotomy)

Diagnosis of lumbar zygapophysial (facet) joint pain by medial branch (MB) nerve blocks identifies patients who can have a good response to neurolytic treatment in the form of lumbar radiofrequency (RF) MB neurotomy. The procedure is also known as lumbar facet denervation, but MB neurotomy most accurately describes the lesion. From case series and well-done controlled trials, it can be concluded that lumbar RF MB neurotomy provides intermediate-term (6–18 months) benefit in properly selected patients using suitable technique (moderate evidence).

Proper patient selection criteria are anatomically accurate medial branch blocks (performed under imaging guidance), complete-near complete relief of pain (at least greater than 80 % relief), relief confirmed by controlled blocks, and relief of pain corroborated by restoration of movements or activities previously impeded by pain [44]. Suitable technique consists of adequate size electrodes (18–16 G), accurately placed electrodes parallel to the target nerve, and lesions placed to cover all possible locations of the target nerve [44].

A large case-series (clinical practice audit) study treated 209 patients selected on the basis of positive responses to controlled diagnostic lumbar medial branch blocks with greater than 70 % relief [45]. Of the 174 patients who completed the audit, 68 % experienced greater than 50 % relief sustained for between 6 and 24 months. Pain relief was associated with improved activities and decreased consumption of analgesics.

In a placebo-controlled randomized trial of 31 patients, with a history of at least 1 year of chronic low back pain selected on the basis of a positive response to a single diagnostic nerve block, RF MB neurotomy was superior to sham treatment [46]. The primary outcome variable was the percentage of successes at 8 weeks. Only in patients with at least a 2-point reduction on the VAS scale (VAS-mean or VAS-high) and at least a 50 % pain reduction on global perceived effect was the treatment scored as a success. Of the 15 patients treated with active neurotomy, 7 (47 %; CI 22–72 %) achieved relief, compared with 3 out of 16 patients (19 %; CI 0–38 %) treated with placebo. Although these proportions are different, they are not significantly different statistically (overlap of confidence intervals). Analysis over the following 12 months showed a significant difference ($P = 0.002$) in favor of active treatment. This relief of pain was accompanied by significant improvements in disability and reduction in the consumption of analgesics. This study used a suboptimal RF technique; electrodes were placed perpendicular to the target nerves. Also, it did not select patients on the basis of controlled diagnostic blocks but did require at least 50 % relief of pain following a single diagnostic block. These limitations resulted in a lower success rate and shorter duration of effect than might be expected. Nonetheless, the duration of relief of pain lasted up to 12 months after treatment.

Another study selected patients on the basis of controlled, diagnostic blocks and placed electrodes parallel to the target nerves and in multiple locations [47]. It showed superior outcomes from active treatment than from sham treatment. In 40 patients who obtained significant pain relief following three diagnostic blocks, half were randomized to RF MB neurotomy. Patients had to report at least 80 % relief of the particular pain that was to be treated. A significantly greater

improvement in pain symptoms, global perception of improvement, and quality of life was observed than in those subjects allocated to RF treatment. Relief of pain was accompanied by reduction in the use of analgesics. These investigators studied a particularly difficult sample of patients, who had multiple sources of pain. Pain mediated by the lumbar medial branches was only one of several types of pain suffered. However, for the pain for which patients were treated, the study showed significantly greater improvements following active MB neurotomy compared with sham treatment.

Two randomized studies compared pulsed and conventional RF treatment for zygapophysial (facetogenic) pain. Both showed conventional RF to be superior [48, 49].

If pain recurs after neurotomy, there is limited evidence from retrospective reviews supporting that repeated treatment can reinstate relief [50, 51].

Unfortunately there are several poorly done clinical trials for lumbar RF MB neurotomy that have been published. Inclusion into systematic reviews of poorly done clinical trials has lessened the support for lumbar MB neurotomy. However, these trials may be dismissed as invalid because patients were wrongly selected without MB blocks or controlled blocks and/or techniques used where RF lesions were not placed accurately on target nerves [52–54].

Sacroiliac Joint
Mechanical Pain

Sacroiliac joint steroid injections showed moderate benefit based on one RCT (limited evidence). The results from observational studies are not consistent, and controlled studies have not refuted nonspecific effects of treatment. Retrospective descriptive studies of sacroiliac intra-articular injection of steroids have reported success rates that vary considerably with respect to the proportion of patients obtaining relief of pain and the duration of that response [55–60]. One prospective, observational study selected 39 patients for treatment who obtained greater than 75 % relief of pain following dual, intra-articular, diagnostic blocks of the joint to be treated [61]. Twenty-six patients (66.7 %)

experienced >50 % pain reduction for more than 6 weeks after the intra-articular injection of corticosteroid, with the mean duration of pain reduction in these responders of 36.8 weeks. Significant reductions were also seen in the modified Oswestry Disability Index. Univariate analysis revealed that treatment failure was significantly associated with a history of lumbar/lumbosacral fusion: 42 % of patients with a history of lumbar/lumbosacral fusion experienced a long-lasting pain relief, whereas 78 % patients with no history of lumbar/lumbosacral fusion experienced a long-lasting pain relief. There have been no controlled trials of intra-articular injections of steroids for mechanical sacroiliac joint pain. A randomized controlled trial of periarticular injections of steroids selected patients on the basis of clinical signs, and diagnostic blocks were not used to establish a diagnosis of sacroiliac joint pain [62]. Thirteen patients were treated with a periarticular injection of corticosteroid and anesthetic, while 11 patients received isotonic sodium chloride and lidocaine. At 1 month, the median decrease in pain scores was 74 % in the corticosteroid group but only 25 % in the control group.

Sacroiliitis

In contradistinction to mechanical/degenerative SI joint pain, multiple studies (observational and prospective) have shown great benefit for sacroiliac joint injections in patients with seronegative spondyloathropathy (moderate evidence). This benefit ranges from a 60 % success at 1 month to a 92 % success rate at 10 months postinjection [63–71]. Two controlled studies have demonstrated that the response to injections of steroids is greater than a placebo effect. An initial trial performed a double-blind placebo-controlled study in 10 patients (13 articulations) with painful sacroiliitis [72]. Randomization was to intra-articular injection with corticosteroid (study group) or isotonic saline (placebo group). Evaluation was made by an overall assessment of symptoms (no pain, good relief >70 %, fair relief 50–70 %, and failure <50 % relief) and by dolorimetry (scale of 0–10). At 1 month, 5/6 sacroiliac joints injected with corticosteroid described a relief of >70 %, in comparison to

0/7 of the placebo group ($P < 0.05$). Dolorimetry showed a marked decrease in the corticosteroid group from (mean ±S.E.M.) 6.8 ± 0.6 to 1.3 ± 0.3, and decreases were mild in the placebo group: 7.0 ± 0.6 to 5.2 ± 0.5 ($P < 0.005$). In another randomized controlled blinded trial [73], 20 patients with seronegative spondyloar-thropathy and clinical sacroiliitis were evaluated. In 10 subjects one affected SI joint was treated with periarticular injection of 1.5-mL (40 mg/mL) methylprednisoloneacetate and 1.5-mL (20 mg/mL) lignocaine (steroid group), whereas the other 10 subjects received 1.5 mL isotonic sodium chloride and 1.5 mL (20 mg/mL) lignocaine (control group) in one affected SI joint. Patients and physicians making clinical assess-ments were blinded to the group status. Clinical assessment at the onset of the study and after 2 months follow-up included the patients' estima-tion of pain in the SI joint by a 100-point visual analog scale (VAS) and by a pain index (range 0–12) which was calculated from tenderness and stressing tests on the SI joint. At the 2 months follow-up examination, significant improvement was demonstrated: the median VAS decreased 26.5 in the study group and decreased by 1.5 in the control group ($p = 0.02$), and the median pain index decreased by 4.5 in the study group and decreased by 1.4 in the control group ($p = 0.01$).

Epidural Steroid Injections for Lumbar or Low Back Pain Without Sciatica or Radiculopathy

Treating low back pain (without sciatica or radiculopathy) with epidural injections of steroids showed no benefit compared to placebo, based on data from three RCTs (moderate evidence). A prospective, double-blind, random-ized, controlled trial in 28 patients with chronic mechanical low back pain compared the thera-peutic effects of epidural methyl prednisolone (80 mg) to intrathecal midazolam (2 mg) [74]. All the patients had chronic low back pain and all had received previous treatments that had failed. The two groups of patients were comparable in terms of pain duration and demographics. The pain was assessed before and for 2 months after treatment using the short form McGill Pain

Questionnaire, visual analog scale for pain. Both treatments caused a similar improvement, although the patients treated with steroid were taking more or the same amount of self-administered analgesic medication after their treatment, compared to the midazolam-treated patients who took less medication during the 2-month follow-up period. Another investigator performed two other trials similar to each other ($n = 120$), evaluating interlaminar and caudal epidural steroid injections versus a "placebo" of saline and local anesthetic assessing for pain with NRS (numeric rating scale), function with ODI (Oswestry Disability Index), and opioid usage with morphine equivalents. NRS scores, ODI scores, and opioid use showed no short-term or long-term pain relief. The interlaminar study [75] showed the NRS to be 3.4 ± 1.1 versus 3.7 ± 1.0, respectively (not significant); ODI to be 13.9 ± 4.8 versus 14.6 ± 4.1, respectively (not signifi-cant); and opioid usage of 49 ± 59.8 versus 39 ± 29.3, respectively (not significant). The caudal [76] study showed the NRS to be 3.7 ± 1.4 versus 3.7 ± 1.2, respectively (not significant); the ODI to be 14.1 ± 5.4 versus 13.8 ± 4.8, respectively (not significant); and the opioid usage to be 34.7 ± 22.8 versus 31.2 ± 29.9 mg (morphine equiv-alents), respectively (not significant).

There is also no consistent evidence that epi-dural steroid injections have differential efficacy or effectiveness among various diagnoses of the lumbar spine.

Cost-Effectiveness Analysis

There are no economic data available for intradiscal injections, facet injections, medial branch blocks, sacroiliac joint injections, or epidural injections for the treatment of chronic low back pain.

Special Case: Imaging Guidance and Safety

Imaging guidance (fluoroscopy/CT/MRI) for spinal injections is routinely used to ensure correct needle placement, accurate delivery of the injectate, and avoidance of complications.

Incorrect needle placement during spinal injections without the use of imaging guidance has been reported by various studies in 12.5–38.3 % of patients. According to various studies, "blind" caudal injections fail to reach the epidural space in up to 35 % of cases [77–80], and "blind" interlaminar injections fail to do so in up to 17 % of cases [77, 81–83]. This failure may contribute to the lack of efficacy of "blind" injections in some cases. In order to develop the most accurate conclusions when evaluating research, the evidence on efficacy must be stratified according to the technique used and the conditions for which they were utilized. Nonimage guided injections are not considered in this chapter.

Adverse effects of injection therapy are infrequent but can be serious. There have been case reports of death and paralysis in the published literature from lumbar epidural injections. For dural or subarachnoid punctures, or other life-threatening complications, the reported rates ranged from 1 in 1556 injections to 1 in 10,416 injections for lumbar spine. The mean incidence of intravascular puncture following fluoroscopically guided lumbar spinal injections was 10.18 % (range, 1.9–22 %) as reported in five case series designed to assess its incidence [84–88]. Minor complications are more common than major complications but are generally transient in nature. There are no published reports of any substantial complications related to facet or sacroiliac joint injections. Disc injections have a minimal rate of discitis that is on the order of a fraction of a percentage (about 0.25 % per patient) using a two-needle (coaxial) technique without prophylactic antibiotics and is virtually nil with antibiotic usage [94]. There are other complications from spine procedures for indications other than low back pain. Spinal cord infarction has been reported as a complication of lumbar spine epidural injection, more so with transforaminal technique [89–93], but there is also one case report with interlaminar injection [94]. The transforaminal technique is advocated for sciatica/radicular pain, which is a different context than what this chapter is about and thus not pertinent to this discussion.

Take-Home Table

Table 29.1 shows a summary of a spinal injections algorithm for low back pain.

Imaging Case Studies

Case 1: Lumbar Zygapophysial (Facet) Joint Neurolysis (Radiofrequency Medial Branch Neurotomy) (Fig. 29.1a–c)
Case 2: Sacroiliac Joint Injection (Fig. 29.2)

Suggested Injection Protocols

The authors refer the readers to ISIS (International Spine Intervention Society) guidelines in Ref. [95].

Future Research

- Clinical trials should include important patient-oriented outcomes related to pain, physical function, opioid use, return to work, quality of life, patient satisfaction, avoidance of additional procedures/surgery, and expected duration of impact.

Table 29.1 Summary of spinal injections algorithm for low back pain

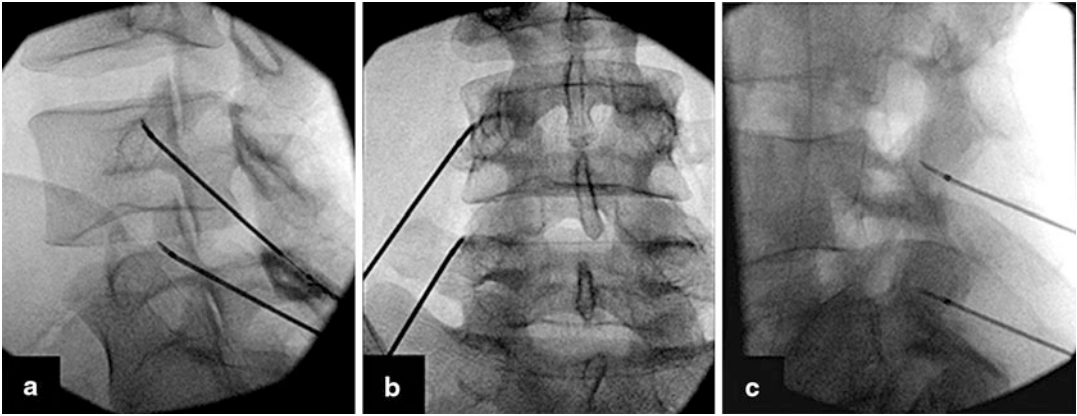| Acute low back pain	→	No spine injection recommended
Sacroiliitis (in the setting of inflammatory spondyloarthropathy)	→	Sacroiliac joint intra-articular steroid injection
Chronic low back pain		
Lumbar zygapophysial joint (facetogenic) with positive response to Medial Branch Blocks (MBB)	→	Neurolysis

Fig. 29.1 (**a**–**c**) Lumbar zygapophysial (facet) joint neurolysis (radiofrequency medial branch neurotomy). Fluoroscopy views show electrodes correctly placed across the necks of the L4 and L5 superior articular processes for L3 and L4 medial branch neurotomy. (**a**) Left oblique view. (**b**) Posteroanterior view. (**c**) Lateral view (Reproduced with permission from Bogduk et al. [44])
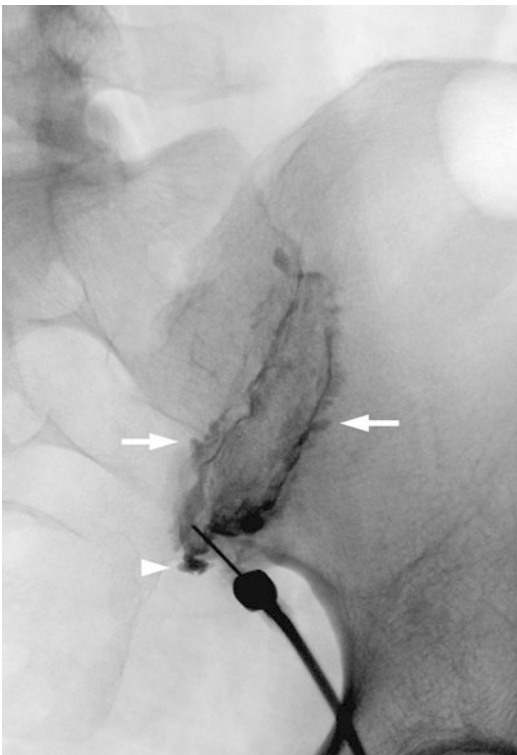

Fig. 29.2 Sacroiliac joint injection. Oblique fluoroscopy view shows correctly placed needle tip within the caudal joint cavity evidenced by opacification of the inferior recess is present (*arrowhead*). Arthrogram shows interdigitating of contrast between proliferative fronds of synovium (*arrows*) compatible with synovitis reflecting an inflammatory arthropathy

- Available well-validated measures to evaluate treatment outcome should be employed for clinical trials.
- Clinical trials should have longer duration follow-up (at least 2 years) for treatment of chronic low back pain to assess for clinically meaningful improvement for pain and function.
- A control arm should be employed for all clinical trials measuring pain improvement since the placebo effect can be substantial.
- Trials should be designed to assess the clinical impact of different injection types, multilevel procedures, and procedure technical differences.
- Complications (frequency and type) could be better documented.
- Differential effects of provider and patient characteristics should be explored.
- Cost impact should be assessed given the markedly increased utilization of spinal injections.

References

1. Merskey H, Bogduk N, editors. Classification of chronic pain. Descriptions of chronic pain syndromes and definition of pain terms. 2nd ed. Seattle: IASP Press; 1994.
2. Acute low back problems in adults: assessment and treatment. Agency for Health Care Policy and Research. Clin Pract Guidel Quick Ref Guide Clin. 1994;(14):iii–iv, 1–25. PubMed PMID: 7987418.
3. Linton SJ. J Occup Rehabil. 2001;11:53–66.

4. Moneta GB, Videman T, Kaivanto K, Aprill C, Spivey M, Vanharanta H, Sachs BL, Guyer RD, Hochschuler SH, Raschbaum RF, Mooney V. Spine. 1994;17:1968–74.

5. McNally DS, Shackleford IM, Goodship AE, Mulholland RC. Spine. 1996;21:2500–87.

6. Adams MA, McNally DS, Wagstaff J, Goodship AE. Eur Spine J. 1993;1:214–21.

7. Holm S, Kaigle-Holm A, Ekstrom L, Karladani A, Hansson T. J Spinal Disord Tech. 2004;17:64–71.

8. Cinotti G, Della Rocca C, Romeo S, Vittur F, Toffanin R, Trasimeni G. Spine. 2005;30:174–80.

9. Haschtmann D, Stoyanov JV, Gédet P, Ferguson SJ. Eur Spin J. 2008;17:289–99.

10. Rubin DI. Neurol Clin. 2007;25(2):353–71.

11. Freburger JK, Holmes GM, Agans RP, Jackman AM, Darter JD, Wallace AS, Castel LD, Kalsbeek WD, Carey TS. Arch Intern Med. 2009;169(3):251–8.

12. Atkinson JH. J Rheumatol. 2004;31:2323–5.

13. Low back pain fact sheet. 2003. http://www.ninds.nih.gov/disorders/backpain/detail_backpain.htm#157903102. Accessed 25 Aug 2011.

14. Schwarzer AC, Aprill CN, Derby R, et al. Spine. 1995;20:1878–83.

15. van Kleef M, Vanelderen P, Cohen SP, Lataster A, Van Zundert J, Mekhail N. Pain originating from the lumbar facet joints. Pain Pract. 2010;10(5):459–69.

16. Schwarzer AC, Aprill CN, Bogduk N. Spine. 1995;20:31–7.

17. Maigne JY, Aivaliklis A, Pfefer F. Spine. 1996;21:1889–92.

18. Dillon CF, Hirsch R. Am J Med Sci. 2011;341(4):281–3. Review. PubMed PMID: 21358307.

19. Katz JN. J Bone Joint Surg Am. 2006;88(Suppl 2):21–4. Review. PubMed PMID: 16595438.

20. Carrino JA, Morrison WB, Parker L, Schweitzer ME, Levin DC, Sunshine JH. Radiology. 2002;225(3):723–9.

21. Bigos S, Bowyer O, Braen G, et al. Acute low back problems in adults, Clinical Practice Guideline 1994, no.14. AHCPR Publication No. 95–0642. Rockville, MD: Agency for Health Care Policy and Research, Public Health Service, US, Department of Health; 1994.

22. van Tulder MW, Koes BW, Bouter LM. Spine (Phila Pa 1976). 1997;22(18):2128–56. Review.

23. Nelemans PJ, de Bie RA, de Vet HC, Sturmans F. Spine (Phila Pa 1976). 2001;26(5):501–15. Review.

24. Koes BW, Scholten RJPM, Mens JMA, Bouter LM. Pain Digest. 1999;9:241–7.

25. Watts RW, Silagy CA. Anaesth Intensive Care. 1995;23(5):564–9.

26. Khot A, Bowditch M, Powell J, et al. Spine. 2004;29:833–6.

27. Simmons JW, McMillin JN, Emery SF, et al. Spine. 1992;17:S172–5.

28. Buttermann GR. Spine J. 2004;4(5):495–505.

29. Cohen SP, Wenzell D, Hurley RW, et al. Anesthesiology. 2007;107:99–105.

30. Peng B, Pang X, Wu Y, Zhao C, Song X. Pain. 2010;149(1):124–9. Epub 2010 Feb 18.

31. Klein RG, Eek BC, O'Neill CW, et al. Spine J. 2003;3:220–6.

32. Oh WS, Shim JC. Clin J Pain. 2004;20:55–60.

33. Barendse GA, van den Berg SG, Kessels AH, et al. Spine. 2001;26:287–92.

34. Bogduk N, Karasek M. Spine J. 2002;2:343–50.

35. Pauza KJ, Howell S, Dreyfuss P, Peloza JH, Dawson K, Bogduk N. Spine J. 2004;4:27–35.

36. Freeman BJ, Fraser RD, Cain CM, et al. Spine. 2005;30:2369–77. discussion 2378.

37. Karasek M, Bogduk N. Tech Reg Anesth Pain Manage. 2001;5:130–5.

38. Lilius G, Laasonen EM, Myllynen P, Harilainen A, Salo L. Rev Chir Orthop Reparatrice Appar Mot. 1989;75:493–500.

39. Carette S, Marcoux S, Truchon R, et al. N Engl J Med. 1991;325:1002–7.

40. Holder LE, Machin JL, Asdourian PL, Links JM, Sexton CC. J Nucl Med. 1995;36:37–44.

41. Dolan AL, Ryan PJ, Arden NK, et al. Br J Rheumatol. 1996;35:1269–73.

42. Pneumaticos SG, Chatziioannou SN, Hipp JA, Moore WH, Esses SI. Radiology. 2006;238:693–8.

43. Fuchs S, Erbe T, Fischer HL, Tibesku CO. J Vasc Interv Radiol. 2005;16(11):1493–8.

44. Bogduk N, Dreyfuss P, Govind J. A narrative review of lumbar medial branch neurotomy for the treatment of back pain. Pain Med. 2009;10(6):1035–45.

45. Gofeld M, Jitendra J, Faclier G. Pain Physician. 2007;10:291–300.

46. Van Kleef M, Barendse GA, Kessels F, Voets HM, Weber WE, De Lange S. Spine. 1999;24:1937–42.

47. Nath S, Nath CA, Pettersson K. Spine. 2008;33(12):1291–7. discussion 1298.

48. Tekin I, Mirzai H, Ok G, Erbuyun K, Vatansever D. Clin J Pain. 2007;23:524–9.

49. Kroll HR, Kim D, Danic MJ, Sankey SS, Gariwala M, Brown M. J Clin Anesth. 2008;20:534–7.

50. Schofferman J, Kine G. Spine. 2004;29:2471–3.

51. Son JH, Kim SD, Kim SH, Lim DJ, Park JY. J Korean Neurosurg Soc. 2010;48(3):240–3.

52. Gallagher J, Vadi PLP, Wesley JR. Pain Clinic. 1994;7:193–8.

53. Leclaire R, Fortin L, Lambert R, Bergeron YM, Rossignol M. Spine (Phila Pa 1976). 2001;26(13):1411–6. Discussion 1417.

54. van Wijk RM, Geurts JW, Wynne HJ, Hammink E, Buskens E, Lousberg R, Knape JT, Groen GJ. Clin J Pain. 2005;21(4):335–44. Erratum in: Clin J Pain. 2005;21(5):462.

55. Chakraverty R, Dias R. Acupunct Med. 2004;22:207–13.

56. Dussault RG, Kaplan PA, Anderson MW. Radiology. 2000;214:273–7.

57. Hawkins J, Schofferman J. Pain Med. 2009;10:850–3.

58. Murakami E, Tanaka Y, Aizawa T, Ishizuka M, Kokubun S. J Orthop Sci. 2007;12:274–80.
59. Pulisetti D, Ebraheim NA. J Spinal Disord. 1999;12:310–2.
60. Slipman CW, Lipetz JS, Plastaras CT, Jackson HB, Vresilovic EJ, Lenrow DA, Braverman DL. Am J Phys Med Rehabil. 2001;80:425–32.
61. Liliang P, Lu K, Weng H, Liang CL, Tsai YD, Chen HJ. Spine. 2009;34:896–900.
62. Luukkainen RK, Wennerstrand PV, Kautiainen HH, Sanila MT, Asikainen EL. Clin Exp Rheumatol. 2002;20:52–4.
63. Cui Y, Xiao Z, Shuxia W, Zhenjun Z, Hengguo Z, Liangyi F, Weicheng G, Li L, Guangfeng Z, Yunzhen S, Guangf D. Scand J Rheumatol. 2010;39:229–32.
64. Gunaydin I, Pereira PL, Daikeler T, Mohren M, Trubenbach J, Schick F, Kanz L, Kotter I. J Rheumatol. 2000;27:424–8.
65. Hanly JG, Mitchell M, MacMillan L, Mosher D, Sutton E. J Rheumatol. 2000;27:719–22.
66. Karabacakoglu A, Karakose S, Ozerbil OM, Odev K. Acta Radiol. 2002;43:425–7.
67. Maugars Y, Mathis C, Vilon P, Prost A. Arthritis Rheum. 1992;35:564–8.
68. Ojala R, Klemola R, Karppinen J, Sequeiros RB, Tervonen O. Eur J Radiol. 2001;40:236–9.
69. Pereira PL, Gunaydin I, Duda SH, Trubenbach J, Remy CT, Kotter I, Kastler B, Claussen CD. J Radiol. 2000;81:223–6.
70. Pereira PL, Gunaydin I, Trubenbach J, Dammann F, Remy CT, Kotter I, Schick F, Koenig CW, Claussen CD. Am J Roentgenol. 2000;175:265–6.
71. Sadreddini S, Noshad H, Molaeefard M, Ardalan MR, Ghojazadeh M, Shakouri SK. Presse Med. 2009;38:710–6.
72. Maugars Y, Mathis C, Berthelot JM, Charlier C, Prost A. Br J Rheumatol. 1996;35:767–70.
73. Luukkainen R, Nissila M, Asikainen E, Sanila M, Lehtinen K, Alanaatu A, Kautianen H. Clin Exp Rheumatol. 1999;17:88–90.
74. Serrao JM, Marks RL, Morley SJ, Goodchild CS. Pain. 1992;48(1):5–12.
75. Manchikanti L, Cash KA, McManus CD, Pampati V, Benyamin RM. Pain Physician. 2010;13: E279–92.
76. Manchikanti L, Cash KA, McManus CD, Pampati V, Smith HS. Pain Physician. 2008;11:785–800.
77. White AH, Derby R, Wynne G. Spine. 1980;5:78–86.
78. El-Khoury G, Ehara S, Weinstein JW, Montgomery WJ, Kathol MH. Radiology. 1988;168:554–7.
79. Stitz MY, Sommer HM. Spine. 1999;24:1371–6.
80. Price CM, Rogers PD, Prosser ASJ, Arden NK. Ann Rheum Dis. 2000;59:879–82.
81. Bartynski WS, Grahovac SZ, Rothfus WE. Am J Neuroradiol. 2005;26:502–5.
82. Manchikanti L, Cash KA, Pampati V, McManus CD, Damron KS. Pain Physician. 2004;7:81–92.
83. Mehta M, Salmon N. Extradural block, confirmation of the injection site by X-ray monitoring. Anaesthesia. 1985;40:1009–12.
84. Sullivan WJ, Willick SE, Chira-Adisai W, et al. Spine (Phila Pa 1976). 2000;25:481–6.
85. Furman MB, O'Brien EM, Zgleszewski TM. Spine (Phila Pa 1976). 2000;25:2628–32.
86. Manchikanti L, Cash KA, Pampati V, Damron KS, McManus CD. Pain Physician. 2004;7:217–23.
87. Furman MB, Giovanniello MT, O'Brien EM. Spine (Phila Pa 1976). 2003;28:21–5.
88. Goodman BS, Lincoln CE, Deshpande KK, Poczatek RB, Lander PH, Devivo MJ. Pain Physician. 2005;8:263–6.
89. Willems PC, Jacobs W, Duinkerke ES, De Kleuver M. J Spinal Disord Tech. 2004;17(3):243–7. Review.
90. Kennedy DJ, Dreyfuss P, Aprill CN, Bogduk N. Pain Med. 2009;10(8):1389–94.
91. Lyders EM, Morris PPAJNR. Am J Neuroradiol. 2009;30(9):1691–3.
92. Glaser SE, Falco F. Pain Physician. 2005;8(3):309–14.
93. Houten JK, Errico TJ. Spine J. 2002;2(1):70–5.
94. Thefenne L, Dubecq C, Zing E, Rogez D, Soula M, Escobar E, Defuentes G, Lapeyre E, Berets O. Ann Phys Rehabil Med. 2010;53(9):575–83.
95. Bogduk N, editor. Practice guidelines. Spinal diagnostic and treatment procedures. San Francisco: International Spine Intervention Society; 2004.

Vertebroplasty: Evidence-Based Treatment

30

Leili Shahgholi and David F. Kallmes

Contents

L. Shahgholi (✉) • D.F. Kallmes
Department of Neuroradiology, Mayo Clinic, Rochester, MN, USA
e-mail: shahgholighahfarokhi.leili@mayo.edu; kallmes.david@mayo.edu

Key Points

- Vertebroplasty is not more effective than lidocaine injections for pain relief or improving physical function (strong evidence).
- Vertebroplasty diminishes the use of pain-killers and opiate derivatives in the short term (moderate evidence).
- Age of fracture does not influence the efficacy of vertebroplasty (strong evidence).
- Vertebroplasty increases the risk of further vertebral fracture in the first year after augmentation (moderate evidence).

Definition and Pathophysiology

The definition of "vertebral fracture" may be unclear in some circumstances and, as such, prevalence rates vary [1, 2]. Currently, the most widely accepted radiographic definition is that of Genant [3] (Table 30.1), where changes in vertebral body shape are described in terms of graded reductions in overall height and area. This method of Genant mainly focuses on the identification of "reduced" vertebral height as an indication of vertebral fracture, which can be a feature of some non-fracture deformities and normal variants. A modified visual approach known as algorithm-based qualitative assessment of vertebral fracture (ABQ) has recently been introduced. ABQ focuses on radiological evidence of change at the vertebral endplate as the primary indicator of fracture [4].

Falls account for up to one-third of the vertebral fractures that come to clinical attention [5]. Vertebral fracture may occur spontaneously or as a result of normal activities such as lifting, bending, and coughing. The strongest risk factor for osteoporotic vertebral fracture is a history of previous fracture, which increases the risk four times as compared to patients without previous fracture [6–8].

Epidemiology

In the year 2000, there were an estimated 9.0 million osteoporotic fractures worldwide, of which 1.4 million were clinically evident vertebral fractures [9]. The actual incidence and prevalence of vertebral fracture are underestimated by the low proportion of vertebral fracture that come to medical attention, which is on the order of 20–30 % of all vertebral fractures. Prospective data in a US population-based sample showed an overall age-standardized incidence of 10.7 per 1,000 person-years in women and 5.7 per person-years in men [10]. Based on the definition of fracture, the prevalence of vertebral fractures in subjects age 50–80 years varied from 7 % to 19 % in women and from 4 % to 17 % in men [11]. The peak incidence of vertebral fracture according to age is not well defined but is roughly 65–80 years in women and 75 in men. The prevalence of osteoporotic vertebral fracture rises with age in both sexes. Prevalence increases more steeply with age in women than in men, with rates of 24 % and 18 % at ages 75–79 years, respectively [10].

Overall Cost to Society

The economic costs of osteoporotic fractures include direct costs of hospitalization and after-discharge care and indirect costs attributable to the impact of fractures on daily life activities. Together, these costs impose a huge financial burden on health care and social services. About one quarter of clinically diagnosed vertebral deformities result in hospitalization. Among patients who were community dwelling at the time of the initial fracture, 0.9–1.1 % (2.4–4.0 %) were living in a nursing home 6 months–1 year after the fracture. In the United States, the direct costs of osteoporotic fractures are estimated at around $18 billion annually. Based on data from national samples of patient

hospitalizations due to vertebral fracture, total charges were $8,000–10,000 per hospitalization. The average length of stay was less than 6 days, but 50 % required more care after discharge than prior to fracture, which adds extra cost [12]. It is anticipated that the cost of care for osteoporotic vertebral fractures will double by 2050 [10].

Goals of Treatment

The overall goals of vertebroplasty in osteoporotic vertebral fracture treatment are relieving pain and improving function.

Methodology

Two Medline searches were performed using PubMed (National Library of Medicine, Bethesda, Maryland). The first covered January 1966 to January 2000 ($n = 18$) and the second, January 2000 to August 2011 ($n = 885$). For both searches, we used the following terms: (1) vertebroplasty, (2) osteoporosis, and (3) spine augmentation. We excluded animal experiments and articles on pediatric patients. We also excluded case reports, review articles, editorials, and non-English language articles. The title, abstract, and full text of relevant articles were reviewed at each step. Only articles meeting our inclusion criteria were cited for this chapter.

Discussion of Issues

Should Vertebroplasty Be Offered for Pain Palliation in Vertebral Compression Fractures?

Summary

Currently, there is substantial debate regarding the efficacy of vertebroplasty. Numerous case series and uncontrolled trials show excellent ability of vertebroplasty to relieve pain. Unblinded randomized trials have also shown benefit. However, two blinded, controlled trials have shown no greater efficacy of vertebroplasty compared with a lidocaine injection (strong evidence).

Effect on Pain

Supporting Evidence

Pain relief is the main purpose of percutaneous vertebroplasty. There are two prospective multicenter, placebo-controlled trials (level 1 study, strong evidence [13, 14] that compared vertebroplasty to a local anesthetic injection. In the INVEST study [13], 131 patients with painful osteoporotic vertebral fracture were randomly assigned to either vertebroplasty (case group = 68) or a simulated vertebroplasty procedure using only local anesthetic without cement (control group = 63). The primary outcomes were measured at 1 month and consisted of a modified version of the Roland–Morris Disability Questionnaire (see next section on "Functional Status") as a metric of back-related disability and pain improvement using average pain intensity during the preceding 24 h. Both the vertebroplasty and control groups showed immediate improvement in pain scores after intervention. After 1 month, the change in pain scores was not significantly different between the two groups (difference, 0.7; 95 % CI, –0.3–1.7; $P = 0.19$), although there was a trend to have less pain in the vertebroplasty group. Also, the rate of crossover was significantly higher in the control group than in the vertebroplasty group.

The other double-blind randomized controlled trial [14] with 71 patients (35 in the vertebroplasty group and 36 in the placebo group) completed 6 months of follow-up. Patients had 1–3 painful osteoporotic vertebral compression fractures that had been confirmed by MRI. They were randomly assigned to undergo vertebroplasty or a lidocaine injection without cement (control group). Outcomes (overall pain) were assessed at 1 week and at 1, 3, and 6 months. Pain reduction was seen in both case and control groups ($P < 0.001$). Mean reductions in the score

for overall pain in the vertebroplasty and placebo groups were 7.4 ± 2.1 and 7.1 ± 2.3, respectively (adjusted between group difference 0.5; 95 % CI -0.8 to 1.7), but there was no significant difference in the VAS up to 1 and 6 months following the procedure.

A single, open-label prospective cohort level 2 study (moderate evidence) [15] compared vertebroplasty with conservative therapy which included prescribing paracetamol, nonsteroidal anti-inflammatory agents (NSAID), or opiate derivatives according to patient's need. All patients were prescribed bisphosphonates, calcium supplementation, and vitamin D. From 934 patients who were screened for this study, 229 patients improved so rapidly and significantly by 1 month that they left the study. Finally, 202 patients in pain less than 6 weeks (4–92 days, mean = 5.6 weeks) were randomly assigned to undergo vertebroplasty or conservative treatment. Pain relief was measured at 1 month and 1 year with a mean visual analog scale (VAS). After vertebroplasty, the difference in mean VAS score between baseline and 1 month was -5.2 (95 % CI -5.88 to -4.72) and between baseline and 1 year was -5.7 (-6.22 to -4.98). After conservative treatment, the difference in mean VAS score from baseline was -2.7 (-3.22 to -1.98) at 1 month and -3.7 (-4.35 to -3.05) at 1 year. The difference between groups in reduction of mean VAS score from baseline was 2.6 (1.74–3.37, $P < 0.0001$) at 1 month and 2.0 (1.13–2.80, $P < 0.0001$) at 1 year. Survival analysis showed that significant pain relief ($P < 0.0001$) was achieved earlier and in more patients after vertebroplasty (29.7 days until significant pain relief, 95 % CI 11.45–47.97) than with conservative treatment (115.6 days, 95 % CI 85, 87–145.40) [15].

One other level 2 studies (moderate strength) [16, 17] enrolled 50 patients who had fractures estimated at less than 8 weeks old. It randomized patients to undergo vertebroplasty or best medical therapy, although exact details of such therapy were not reported. Only 36 of these patients had baseline pain scores measured before randomization. Plain radiographs were the only standard imaging. Pain estimates were recorded immediately after vertebroplasty and at 3 and 12 months. The trial found an immediate reduction in pain scores of 57 % at 24 h after vertebroplasty and a statistically significant reduction in duration of hospitalization in the vertebroplasty group. VAS decreased from 7.7, CI: (6.7, 8.7) before the procedure to 2.0, CI: (0.9, 3.2) at 12–24 h after the procedure ($P = 0.00$). No significant differences in pain scores were noted at 3 and 12 months, but the study had inadequate power to assess this [17]. In this study comparing immediate vertebroplasty to conservative management for acute fractures, the reduction in pain in the vertebroplasty group was immediately 12–24 h after the procedure. There was no significant difference in the other parameters when comparing the scores at enrollment and after 3 months and after 12 months.

There are two other available, non-randomized, controlled studies (moderate strength) [18, 19]. One of these studies [18] included 96 patients who had acute osteoporotic vertebral fracture, 67 patients treated by vertebroplasty, and 31 by conservative therapy. All patients were offered similar analgesia. Pain management was titrated according to individual need. All patients received anti-osteoporotic medications, elemental calcium 1,200 mg daily, and ergocalciferol 0.25 μg daily (if vitamin D deficient). Lower pain scores persisted in the vertebroplasty group at 6 weeks ($P < 0.01$) but were not significantly different at 6, 12, and 24 months. In a recently published level 2 (moderate strength) study [19], 82 patients were followed for 36 months after random assignment to vertebroplasty ($n = 40$) versus optimal medication ($n = 42$). The optimal medication therapy (OMT) plan included 250 mg acetaminophen with codeine twice daily, 400 mg ibuprofen twice a day, 1,000 mg calcium daily, 400 IU vitamin D daily, 70 mg alendronate orally once weekly, and 200 IU calcitonin daily. Reductions in average pain during the last day VAS were greater in the vertebroplasty group at 1 ($P < 0.001$) and 4 weeks ($P < 0.001$) but not at 12 months. Evidence is summarized in Table 30.2.

Physical Function and Quality of Life
Summary
Both vertebroplasty and conservative therapy improve physical function to a similar degree.

Supporting Evidence
One prospective multicenter, blinded, controlled trial with strong evidence (level 1, strong evidence) [13] measured physical function and quality of life outcomes with the Roland–Morris Disability Questionnaire (RMDQ), Short Form 36 (SF-36), and European Quality of Life-5 Dimensions (EQ-5D). The two treatment groups did not differ significantly with respect to either of the two prespecified primary outcomes (RMDQ and pain) at 1 month. The mean (±SD) RMDQ score in the vertebroplasty group was 12.0 ± 6.3, as compared with 13.0 ± 6.4 in the control group (adjusted treatment effect, 0.7; 95 % confidence interval (CI), −1.3 to 2.8; $P = 0.49$). The two groups also did not show significant differences in other outcome instruments.

The other blinded randomized control trial (RCT) (level 1, strong evidence) study [14] compared physical function and quality of life in 71 patients (35 in the vertebroplasty group and 36 in the control group). This measurement was done with a modified 23-item version of the Roland–Morris Disability Questionnaire (RMDQ), in which scores range from 0 to 23, with higher numbers indicating worse physical functioning, and 2–3 points representing the minimal clinically important difference. There were no statistically significant differences between case and control groups at follow-up. Furthermore, groups in that study did not show significant differences in quality of life measures using quality of life questionnaire of the European Foundation for Osteoporosis (QUALEFFO) or Assessment of Quality of Life (AQoL) outcomes.

In the randomized but unblinded VERTOS II study [15] (level 2, moderate strength) with 202 patients, the assessment of physical function and quality of life showed significant improvement with vertebroplasty as compared to controls.

In another randomized controlled trial (moderate strength, level 2) [19], 82 patients who had pain durations of 4 weeks to 1 year showed significant improvement in functional QOL (as measured with Oswestry LBP scale) in the vertebroplasty group immediately after the procedure, with maximum improvement 6 months after the procedure. No significant improvement was seen in the control group ($P < 0.21$). They reported that all patients could walk 1 day after vertebroplasty, but only 1 patient (2 %) in the OMT group was able to walk at this time (p < 0.011).

Both vertebroplasty and conservative therapy groups had improvements in physical functioning ($P < 0.001$). Improvements in physical functioning were significant over 24 months ($P < 0.001$).

In one prospective non-randomized case–control study (level 2, moderate strength) [20], 101 patients underwent vertebroplasty and 27 received conservative treatment. The functional and general health scores of the vertebroplasty group were improved from the preoperative mean values ($P < 0.001$) in 3, 6, and 12 months. The vertebroplasty group showed a significant difference from the conservative group at 3 months, but no statistical differences on function were observed between groups at 6 months and 1 year posttreatment.

Wang et al. [21] reported a prospective non-randomized clinical trial (level 2, moderate strength) with 55 consecutive patients who underwent vertebroplasty and 23 who received conservative therapy. Both vertebroplasty and conservative therapy groups had improvements in physical functioning ($P < 0.001$). Improvements in physical functioning were significant at 1 week ($P < 0.001$) and 4 weeks ($P < 0.001$) but not at 12 months. Evidence is summarized in Table 30.3.

Decrease Narcotic Use
Summary
Narcotic medication use is diminished in the short term after vertebroplasty (level 2, moderate evidence).

Supporting Evidence
VERTOS II (level 2, moderate strength) [15] compared medication use in patients who underwent vertebroplasty with medication use in

patients who were assigned to conservative treatment. The medications were classified as non-opiate (paracetamol and NSAIDs), weak opiate derivatives, and strong opiate derivatives. At baseline, classes of drugs were the same in both groups, but there was a trend to use more opiate derivatives in patients who had been assigned to vertebroplasty. After vertebroplasty, medication usage was significantly lower at 1 day ($P < 0.0001$), 1 week ($p = 0.001$), and 1 month ($P = 0.033$) compared to the non-vertebroplasty group but not significantly different any time after that.

In Voormolen's unblinded, randomized controlled trial study (level 2, moderate strength) [22], 18 patients underwent vertebroplasty and 16 patients received OMT, which included NSAIDs and opiate derivatives. In the vertebroplasty group, patients required significantly less pain medication as compared to that required prior to vertebroplasty, but their analgesic use did not decrease as compared with 1 day after PV. Patients treated with vertebroplasty compared to patients treated with optimal medical therapy (OMT) had significantly better VAS and used less analgesics 1 day after treatment. Two weeks after treatment, the mean VAS was less but not significantly different in patients treated with OMT, whereas these patients used significantly less analgesics. Another prospective non-randomized clinical trial (level 2, moderate evidence) [21] compared vertebroplasty ($n = 32$) with conservative treatment ($n = 23$) that included external bracing and analgesia (paracetamol, NSAIDs, and opiate derivatives). All patients received anti-osteoporotic medications. The pain medication use was significantly less ($p < 0.01$) in the vertebroplasty group in the short term (1–4 weeks) but was not different between the two groups at 12 months. Evidence is summarized in Table 30.4.

What Is the Optimal Duration of Pain Prior to Offering Vertebroplasty?

Summary
Preoperative pain duration (age of fracture) does not affect pain improvement observed following vertebroplasty [23].

Supporting Evidence
A recent meta-analysis (level 1, strong evidence) compared 17 studies with three different preoperative pain durations [23]. This study categorized preoperative pain duration as less than 6 weeks, 6–24 weeks, and more than 24 weeks. They included 1,516 patients and 2,010 treated levels of 17 studies. The mean (SD) numbers of patients and levels were 76 (43.8) and 106 (67.6), respectively, per study. The median follow-up was 12 months (range of 3–24 months). Within-group heterogeneity expressed using the I-squared statistic was quite high: 92.61 %, 93.81 %, and 95.74 % for studies with <6 weeks, 6–24 weeks, and >24 weeks preoperative pain. The regression coefficient for preoperative pain duration was −0.024, which indicates that, for each one-week increase in the length of preoperative pain, VAS in pain improvement decreases by 0.024. It shows vertebral augmentation is associated with significant reduction in back pain. In this study, there was not any significant difference in pain improvement among subgroups with different preoperative pain durations.

What Are the Risks of Subsequent Complications?

Although vertebroplasty is a low-risk procedure, like any other intervention, it can have complications. The complications can be mild temporary pain after cement leakage into the intervertebral disk space or paravertebral soft tissues or more serious complications such as infection. There is also the risk of subsequent vertebral fracture. The other serious complication is that of leakage of cement into the paravertebral veins, which can lead to asymptomatic or symptomatic pulmonary cement embolism (PCE). PCEs have been reported in 9–25 % of cases. Subsequent vertebral fracture can be another serious complication, but as of yet, evidence is insufficient.

Pulmonary Emboli
Summary
Asymptomatic and symptomatic PCEs occur following vertebroplasty in about 10–25 % of cases.

Supporting Evidence

One prospective, multicenter, open-label, randomized trial, (level 2 study, moderate evidence) [15] compared vertebroplasty with conservative therapy in 202 patients. Fifty-four patients in the vertebroplasty group ($n = 78$) were followed for 22 months and underwent chest CT for detecting PCE. PCE was detected in 14 of 54 patients (26 %, 95 % CI: 16–39 %). None of them became symptomatic. Cement leakage in the azygos vein was the only risk factor for the occurrence of PCE (OR, 43; 95 % CI, 5–396), and no pulmonary reactive inflammation was seen. In one large retrospective study (level 2, moderate evidence) [24], investigators retrospectively evaluated 244 patients who had undergone vertebroplasty at 465 levels and subsequently underwent chest CT. PCEs were detected in 23 (9.4 %; 95 % CI, 6–13 %) of 244 patients, and one of them became symptomatic. The mean number of emboli detected in the pulmonary vasculature per patient was 3.2 ± 3.4 (median, 2; range: 1–12). There was no correlation among the total number of treatment sessions, number of levels treated per session, cement volume per level, operator, or time between vertebroplasty and chest CT in the detection of cement PCE. The incidence of PCE was greater in younger patients and in those who had augmentation at more levels. PCE was seen during the procedure in just 8.7 %.

In another level 2 study (moderate evidence) [25], 75 patients (57 women, 18 men; mean age, 74.78 years; range, 48–93 years) underwent 78 vertebroplasty sessions at 119 levels for osteoporotic VCFs. Postvertebroplasty CT showed PCE following 18 (23 %) of 78 vertebroplasty sessions, and PCEs were detected in the distal to third-order pulmonary arteries. Leakage to the IVC was significantly associated with PCE ($P = 0.03$). This study reported vertebroplasty with a bipedicular approach, non-radiologist operator, and not having intravertebral vacuum cleft associated with increased risk of PCE ($p > 0.05$).

In a level 2 study (moderate evidence) [26] with 299 patients who underwent vertebroplasty at 532 levels, CT was performed immediately after the procedure and at 1 year. Asymptomatic PCE was demonstrated in 11 patients (2.1 %, 95 %

confidence interval, 1.1–3.7 %), and they remained asymptomatic at 1-year follow-up. None of the patients became symptomatic. Evidence is summarized in Table 30.5.

Subsequent Fracture

Summary

Subsequent vertebral fracture happens sooner and more frequent following vertebroplasty, but the evidence is not sufficient enough yet to reach firm conclusions on this.

Supporting Evidence

Several level 2 studies have suggested an increased risk of subsequent fracture [27, 28], while others (level 2 and 3) have refuted this claim [26, 29]. One retrospective level 2 study (moderate strength) [30] assessed 362 patients who were treated with vertebroplasty for osteoporotic fractures. The location, frequency, and timing of subsequent fractures were compared between 2 subgroups: group 1 ($n = 63$), patients treated with fractures containing clefts at 65 vertebra, and group 2 ($n = 250$), treated at 399 fractures without clefts. A vertebra-by-vertebra analysis to compare the relative risk and timing of subsequent fractures adjacent to vertebrae with or without clefts was performed. Results showed group 1 demonstrated a nearly twofold increased risk of subsequent fracture (odds ratio [OR], 1.90; 95 % confidence interval [CI], 1.04–3.49, $P = .037$). At the vertebral level, the relative risk of subsequent fracture was 2.02 (95 % CI, 1.46–2.58; $P = 0.013$) times greater adjacent to a treated cleft. Fractures adjacent to any treated level occurred significantly sooner than nonadjacent fracture ($P = 0.0004$). The presence of a cleft was not significantly associated with the timing of subsequent fractures.

The other level 2 study (moderate evidence) [28] retrospectively reviewed 86 patients with 313 fractures which were treated at 137 levels. Results showed there are an increased number of inferior endplate fractures of the vertebral body immediately cephalad to the treated level.

In the VERTOS II study [29], after a mean follow-up of 11.4 months (median, 12.0; range, 124 months), 18 new vertebral compression fractures (VCF) occurred in 15 of 91 patients after

vertebroplasty and 30 new VCFs in 21 of 85 patients after conservative therapy. This difference was not significant ($P = 0.44$). There was no higher fracture risk for adjacent versus distant vertebrae. Mean time to new VCF in the vertebroplasty group was 16.2 months and 17.8 months for the conservative group (logrank, $P = 0.45$). They found the baseline number of VCFs as the only risk factor for occurrence (OR, 1.43; 95 % CI, 1.05–1.95) and number ($P = .01$) of new VCFs. Evidence is summarized in Table 30.6.

Take-Home Tables

Tables 30.1 through 30.6 highlight key data and supporting evidence.

Imaging Case Studies

Case 1: Percutaneous vertebroplasty (Fig. 30.1)
Case 2: Lidocaine injection (Fig. 30.2)
Case 3: Pulmonary embolism after vertebroplasty (VP) (Fig. 30.3)
Case 4: Subsequent fracture after VP (Fig. 30.4)

Suggested Protocols

Vertebroplasty Procedure

A pre-procedure consultation should be performed by an experienced physician. This consultation should include a focused physical examination with fluoroscopic confirmation of correlating pain. Depending on the patient's underlying medical condition, procedures are performed with the patients under conscious sedation, deep sedation, or general anesthesia. Conscious sedation consists of intravenous fentanyl and midazolam and should be begun before placing the patient prone on the fluoroscopy table. Biplane fluoroscopy should be used in all cases. After placing the patient prone on the table, the fractured level should be confirmed with previously obtained imaging studies and the level to be treated should be localized by counting from above (cervical) and below (sacral). Local anesthesia consists of subcutaneous 1 % lidocaine and 0.25 % bupivacaine into the deep soft tissues and periosteum with a 22-gauge spinal needle. An 11- or 13-gauge needle with an inner stylet is then advanced under fluoroscopic guidance by using a transpedicular or parapedicular approach into the vertebral body. When the needle reaches at the junction of the pedicle and body, a biplane digital radiograph should be obtained to confirm an appropriate trajectory and exclude a breach of the medial pedicle. The needle is then advanced into the anterior one-third of the vertebral body in an attempt to reach the midline. At this point, biplane images should again be obtained before polymethylmethacrylate (PMMA) injection. Under a vented hood, a mixture of PMMA, barium, and 1 g of gentamicin is prepared. The cement then is injected with an injection device or with 1-mL syringes under biplane fluoroscopic observation until it reaches the posterior one-fourth of the vertebral body. The injection is

Table 30.1 Semiquantitative (*SQ*) visual grading scheme for vertebral fractures. Genant's grading scheme for a semiquantitative evaluation of vertebral fracture. The drawings illustrate normal vertebrae (*top row*) and mild to severe fractures (respectively in the following rows). The size of the reduction in the anterior, middle, or posterior height is reflected in a corresponding to fracture grade, from 1 (mild) to 3 (severe) (Data from Genant HK, Wu CY, van Kuijk C, Nevitt MC. Vertebral fracture assessment using a semiquantitative technique. J Bone Miner Res. 1993;8(9):1137–48)

	Normal vertebra	Uncertain or questionable vertebra	Mild fracture	Moderate fracture	Severe fracture
Height reduction	0	?	20–25 %	25–40 %	>40 %
Grade	0	0.5	1	2	3

Table 30.2 Summary of studies reporting the changes in pain score after vertebroplasty in osteoporotic vertebral compression fractures

Study	Number of patients (case/control)	Follow-up	Treatment effect (95 % CI)	Comment
Kallmes et al. [13]	131(68/63)	1 month	0.7, (−0.3 to 1.7); $P = 0.19$	Prospective, randomized double-blind case–control study, no significant difference but a trend to have less pain in vertebroplasty group
Buchbinder et al. [14]	71(35/36)	1 week	−0.7 (−1.8 to 0.4)	Prospective, randomized double-blind case–control study; no significant difference in pain score at any time point in overall pain, pain at rest and in bed at night
		1 month	0.5 (−0.8 to 1.7)	
		3 months	0.6 (−0.7 to 1.8)	
		6 months	0.1 (−1.2 to 1.4)	
Klazen et al. [15]	202 (101/101)	1 month	2·6 (1·74–3·37) $P < 0·0001$	Prospective, randomized open-label study, significantly different in all time points
		12 months	2·0 (1·13–2·80), $P < 0·0001$)	
Rousing et al. [16, 17]	50 (24/23)	3 months	Case: 1.8 (0.8– 2.8)	Prospective, randomized study, majority of fractures will heal after 8–12 weeks of conservative treatment with subsequent decline in pain. Significant difference at 12–24 h but not at 3 and 12 months
			Control:2.6 (1.2–4.0)	
	(22/22)	12 months	Case:2.0 (1.1–3.0)	
			Control: 2.9 (1.6–4.1)	
Diamond et al. [18]	126 (67/31)	6 week	CI ?, $P < 0.01$	Prospective, non-randomized study. Lower pain in VP group at 6 weeks but not in 6 and 24 months
		6–12 months		
		24 months		
Farokhi et al. [19]	82 (40/42)	1 week	−3.1 (−3.72 to −2.28), p < 0.001	Prospective, randomized single-blind study, significantly different in all time points
		6 months	−1.9 (−3.25 to −0.55), $p < 0.02$	
		12 months	−1.9 (−2.9 to 0.9), $p < 0.1$	
		24 months	−0.5 (−1.39 to 0.5), p < 0.3	
		36 months	−1.5 (−9.85 to 6.85), $p < 0.8$	

CI Confidence interval
P P value

Table 30.3 Summary of selected studies reporting physical function and quality of life changes after vertebroplasty in osteoporotic vertebral compression fractures

Study	Number of patients (case/control)	Measurement tool	Follow-up	Treatment effect (95 % CI)	Note
Kallmes et al. [13]	131(68/63)	RMDI	2 weeks	−0.6 (−2.4 to 1.2) $P = 0.35$	Prospective, randomized double-blind case–control study, no significant difference
			1 month	0.7 (−1.3 to 2.8) 0.49	
Buchbinder et al. [14]	71(35/36)	RMDI	1 week	−2.1 (−5.2 to 0.9)	Prospective, randomized double-blind case–control study, no significant difference at any time point
			1 month	1.7 (−1.8 to 5.2)	
			3 months	−1.5 (−4.8 to 1.7)	
			6 months	0.0 (−3.0 to 2.9)	
		EQ-5D score	1 week	0.0 (−0.1 to 0.1)	
			1 month	0.0 (−0.1 to 0.1)	
			3 months	0.0 (−0.1 to 0.2)	
			6 months	0.0 (−0.1 to 0.2)	
Klazen et al. [15]	202(101/101)	RMDI	1 month	? ($p < 0.0001$)	Prospective, randomized open-label study, significantly different in all time points
			12 months	? ($p < 0.0001$)	
		EQ-5D score	1 month	0.010 (95 % CI 0.014–0.006)	
			12 months		
Farokhi et al. [19]	80(40/42)	ODI	1 week	−14.0 (−15.0 to −12.82) $P < 0.028$	Prospective, randomized single-blind study, significantly different in all time points
			6 months	−11.0 (−12.17 to −7.83) $P < 0.011$	
			12 months	−12.0 (−13.5 to −11.5) $P < 0.021$	
			24 months	−12.0 (−13.32 to −10.68) $P < 0.041$	
			36 months	−14.0 (−14.91 to −13.09) < 0.01	
Alvarez et al. [20]	128 (101/27)	ODI	3 months	$p = 0.001$	Prospective, non-randomized study. Significant improvement in VP group at 3 months
			6 months	$P = 0.006$	In 6 and 12 months, conservative treated patients showed significantly better ODI. PV patients scored significantly worse for some categories such as role physical, general health, vitality, and role emotional
			12 months	$P < 0.001$	
Wang et al. [21]	55 (32/23)	ODI	1 week	$P = 0.001$	Prospective, non-randomized study, significantly different during the first month but not in 12 months
			4 weeks	$P = 0.001$	
			12 months	$P = 0.071$	

RMDI Roland-Morris Disability Index, *EQ-5D* European Quality of Life-5 Dimensions, *ODI* Oswestry

Table 30.4 Selected investigations reporting changes in pain medication usage after vertebroplasty in osteoporotic vertebral compression fractures

Study	Number of patients (case/control)	Follow-up	Treatment effect (95 % CI), p value	Note
Klazen et al. [15]	176 (91/85)	1 day	,?, $p < 0.0001$	Prospective, randomized open-label study, significant difference in use of narcotic medication except after 1 month
		1 week	?, $p = 0.001$	
		1 month	?, $p = 0.033$	
		1–12 months	?	
Voormolen et al. [22]	34(18/16)	2 weeks	Case:–1.5 (–2.3 to –0.8)	Prospective, randomized open-label study
			Control:	
Wang et al. [21]	55 (32/23)	1 week	$P = 0.001$	Prospective, non-randomized study, significantly different in all time points
		4 weeks	$P = 0.001$	
		12 months	$P = 0.017$	

Table 30.5 Summary of studies reporting pulmonary emboli after vertebroplasty for osteoporotic vertebral compression fractures

Study	Number of patients (treated level)	Follow-up (month)	Asymptomatic PE	Treatment effect (95 % CI)	Note
Venment et al. [26]	54(80)	22 (6–42)	14 (25 %)	16–39 %	Prospective, randomized open-label study, no symptomatic patient
Luetmer et al. [24]	244/(465)	17.7 ± 21.1	23(9.4 %)	6–13 %	Retrospective study, 1 symptomatic patient
Kim et al. [25]	75/(119)	?	18(23 %)	?, $P = 0.03$	Prospective study, no control
Venmant et al. [31]	299/(532)	12(5–22)	8(2 %)	2.1 %; 1.1–3.7 %	Retrospective study, no reaction in 12 months CT

terminated if venous, disk space, or epidural extravasation is encountered. If inadequate filling of the contralateral hemivertebra should be noted, a second needle is placed into the contralateral side and additional cement is injected. Patients are instructed to remain supine for 2 h after the procedure to allow for cement hardening and resolution of sedation. After 2 h of bed rest, they should be evaluated at the bedside and will be allowed to ambulate. Outpatients will be then be discharged, whereas inpatients are allowed to ambulate as tolerated. Up to five levels were treated at a single session in the early days of our practice, but we now bring patients back for a second procedure if more than three fractures need treatment [33].

Future Research

- Rigorous studies with tightly controlled patient selection for determining efficacy of vertebroplasty
- Well-designed prospective control studies to identify the type and the incidence of vertebroplasty complications
- Comparing vertebroplasty with various types of cement/polymers to determine if there are other methods to eliminate or decrease complications
- Comparing vertebroplasty with other types of vertebral augmentation
- Assessing the role of vertebroplasty in global health

Table 30.6 Summary of studies reporting the rate of subsequent vertebral fracture after vertebroplasty for osteoporotic vertebral compression fractures

Study	Number of patients/ fractures treated	Number of incident fractures/ patients with incident fractures (% of treated patients)	Adjacent (%)	Follow-up (month)	Comment	Notes
Trout et al. [32]	362(65 cleft-containing fx/ 399 non-cleft containing fx)	126 (28–33 % cleft-containing fx/ 98–21 % non-cleft-containing fx)	16 (13 %) fx of at-risk vertebrae adjacent to treated clefts subsequently fractured, 35(6.5 %) fx of at-risk vertebrae adjacent to treated without clefts subsequently fractured	43	Subsequent fractures would occur earlier and more frequently than after treatment of non-cleft-containing fractures	Retrospective study, RR = 2.02, 95 % CI = 1.46–2.58, $P = 0.013$
Trout et al. [27]	86(137 fx)	186	77 (41.4 %)	43	Increased risk of new-onset adjacent-level fractures occur sooner than nonadjacent level fractures	Retrospective study, no control, 95 % CI = 4.35–4.89; $P < .0001$
Klazon et al. [29]	176 (case:91, control 85), number of treated	48	18(case:7/18, control:11/30)	24	Baseline number of VCF was the only risk factor for occurrence (OR, 1.43; 95 % CI, 1.05–1.95) and number ($P = .01$)	Prospective, randomized open-label study, no increment in risk of subsequent fracture ($p = 0.44$)

VCF vertebral compression fracture, *RR* relative risk
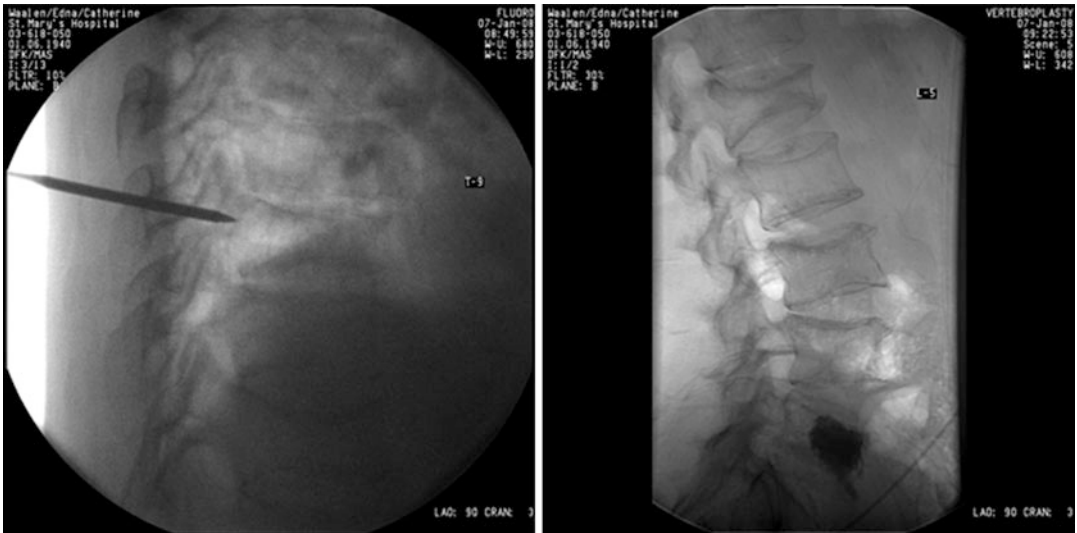
Fig. 30.1 Percutaneous vertebroplasty. A 67-year-old male patient underwent L5 vertebroplasty with PMMA after 10 months persistent pain due to osteoporotic compression fracture. One month post-procedure, she ranked her pain 2 out of 10 as compared to 8 out of 10 pre-procedure

Fig. 30.2 Lidocaine injection. A 74-year-old woman underwent lidocaine injection after subacute L1 fracture. After 1 year, she was doing extremely well
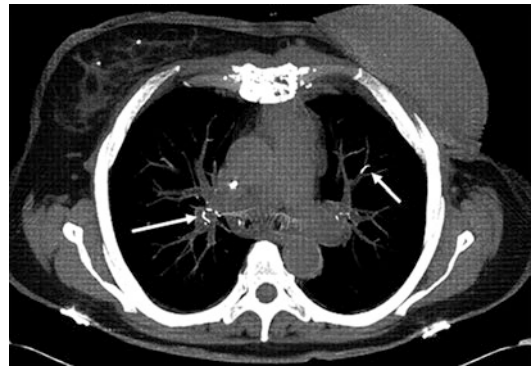
Fig. 30.3 Pulmonary embolism after vertebroplasty (*VP*). A 68-year-old woman treated with vertebroplasty at T12. Axial unenhanced chest CT scan obtained 4 months following vertebroplasty demonstrates linear areas of markedly increased attenuation (*arrows*) within the pulmonary vasculature, indicating cement PEs

Fig. 30.4 Subsequent fracture after VP. A 69-year-old woman underwent vertebroplasty at T9–T11 (*arrows*). Within one month, she presented with new onset fractures at T12 and L1 (*solid arrows*)

References

1. Melton 3rd LJ. J Bone Miner Res. 1995;10(2):175–7.
2. Delmas PD, van de Langerijt L, Watts NB, et al. J Bone Miner Res. 2005;20(4):557–63.
3. Genant HK, Wu CY, van Kuijk C, Nevitt MC. J Bone Miner Res. 1993;8(9):1137–48.
4. Ferrar L, Jiang G, Adams J, Eastell R. Osteoporos Int. 2005;16(7):717–28.
5. Cooper C, Melton 3rd LJ. Trends Endocrinol Metab. 1992;3(6):224–9.
6. Klotzbuecher CM, Ross PD, Landsman PB, Abbott 3rd TA, Berger M. J Bone Miner Res. 2000;15(4):721–39.
7. Ensrud KE, Barrett-Connor EL, Schwartz A, et al. J Bone Miner Res. 2004;19(8):1259–69.
8. Black DM, Thompson DE, Bauer DC, et al. J Clin Endocrinol Metab. 2000;85(11):4118–24.
9. Johnell OKJ. Osteoporos Int. 2006;17(12):1726.
10. Compston J. Radiol Clin North Am. 2010;48(3):477–82.
11. Leidig-Bruckner G, Limberg B, Felsenberg D, et al. Osteoporos Int. 2000;11(2):102–19.
12. Johnell O. Eur Spine J. 2003;12(Suppl 2):S168–9.
13. Kallmes DF, Comstock BA, Heagerty PJ, et al. N Engl J Med. 2009;361(6):569–79.
14. Buchbinder R, Osborne RH, Ebeling PR, et al. N Engl J Med. 2009;361(6):557–68.
15. Klazen CA, Lohle PN, de Vries J, et al. Lancet. 2010;376(9746):1085–92.
16. Rousing R, Hansen KL, Andersen MO, Jespersen SM, Thomsen K, Lauritsen JM. Spine (Phila Pa 1976). 2010;35(5):478–82.
17. Rousing R, Andersen MO, Jespersen SM, Thomsen K, Lauritsen J. Spine (Phila Pa 1976). 2009;34(13):1349–54.
18. Diamond TH, Bryant C, Browne L, Clark WA. Med J Aust. 2006;184(3):113–7.
19. Farrokhi MR, Alibai E, Maghami Z. J Neurosurg Spine. 2011;14(5):561–9.
20. Alvarez L, Alcaraz M, Perez-Higueras A, et al. Spine (Phila Pa 1976). 2006;31(10):1113–8.
21. Wang HK, Lu K, Liang CL, et al. Pain Med. 2010;11(11):1659–65.
22. Voormolen MH, Mali WP, Lohle PN, et al. AJNR Am J Neuroradiol. 2007;28(3):555–60.
23. Rad AE, Luetmer MT, Murad MH, Kallmes DF. AJNR Am J Neuroradiol. 2012;33(2):376–81.
24. Luetmer MT, Bartholmai BJ, Rad AE, Kallmes DF. AJNR Am J Neuroradiol. 2011;32(4):654–7.
25. Kim YJ, Lee JW, Park KW, et al. Radiology. 2009;251(1):250–9.
26. Venmans A, Klazen CA, Lohle PN, et al. AJNR Am J Neuroradiol. 2010;31(8):1451–3.
27. Trout AT, Kallmes DF. AJNR Am J Neuroradiol. 2006;27(7):1397–403.
28. Trout AT, Kallmes DF, Layton KF, Thielen KR, Hentz JG. J Bone Miner Res. 2006;21(11):1797–802.
29. Klazen CA, Venmans A, de Vries J, et al. AJNR Am J Neuroradiol. 2010;31(8):1447–50.
30. Trout AT, Kallmes DF, Lane JI, Layton KF, Marx WF. AJNR Am J Neuroradiol. 2006;27(7):1586–91.
31. Venmans A, Lohle PN, van Rooij WJ, Verhaar HJ, Mali WP. AJNR Am J Neuroradiol. 2008;29(10):1983–5.
32. Trout AT, Kallmes DF, Kaufmann TJ. AJNR Am J Neuroradiol. 2006;27(1):217–23.
33. Layton KF, Thielen KR, Koch CA, et al. AJNR Am J Neuroradiol. 2007;28(4):683–9.

Spine Trauma: Evidence-Based Neuroimaging

31

C. Craig Blackmore and Justin B. Smith

Contents

C.C. Blackmore (✉) • J.B. Smith
Department of Radiology, Virginia Mason Medical Center, Seattle, WA, USA
e-mail: craig.blackmore@vmmc.org; justin.smith@vmmc.org

Key Points

- The NEXUS and Canadian Cervical Spine prediction rules can be used to identify subjects in whom imaging is appropriate (strong evidence).
- Cervical spine CT should be employed in high-risk patients (moderate evidence).
- In low-risk victims not undergoing head CT, radiography may be the preferred cervical spine imaging approach (limited evidence).
- Selection of subjects for thoracolumbar spine imaging can be made based on clinical criteria (moderate evidence).
- CT, including reformations from CT scans performed of the abdomen and pelvis, is more accurate than radiographs in the thoracic and lumbar spine, but radiography may still be appropriate in low-risk subjects (limited evidence).

Introduction

There is a high risk of significant and permanent neurologic damage associated with spinal trauma. Although spinal cord injury is relatively uncommon, spinal imaging is utilized liberally across the United States to identify suspected and occult fractures. Spinal trauma and the sequela of spinal cord injury have broad-reaching ramifications beyond the obvious neurologic deficit for those affected. This includes a percipitous decline in probability of employment, educational achievement, and intact marriage [1]. As a result of widespread utilization, the positive yield of spine imaging is estimated to be only 2.4 % in the cervical spine when all patient populations are included [2]. Using the best available data, this chapter addresses diagnostic imaging of the spine in trauma including clinical prediction rules and cost-effectiveness.

Definition and Pathophysiology

Spinal fractures are estimated to account for 3–6 % of all skeletal injuries in the United States. A Canadian study in 2006 estimated that 56 % of spinal fractures are associated with spinal cord injuries and there is a general mortality rate of 8 % [3]. Although no recent epidemiologic studies have been performed, the annual incidence of cervical spine fracture was estimated at 10,000 per year in the United States in 1992 [4]. Better statistics are maintained for spinal cord injury of all causes and available from the National Spinal Cord Injury Statistical Center, Birmingham, Alabama. From this database, the annual incidence of spinal cord injury is estimated at 40 cases per million in the United States or 12,000–20,000 per year when on-scene fatalities are excluded [1].

The typical patient suffering from spinal cord injury is male (80.8 %) with an average age of injury of 33.7 years. The most common causes are traffic accidents, falls, and violence in decreasing frequency [1]. The hospital mortality for acute spinal injuries is high, up to 17 %, reflecting the presence of other severe injuries.

The cervical spine is both the most commonly fractured region in spinal trauma as well as the area where risk of cord injury is greatest compared to that of thoracic, lumbar, or sacral fractures [5]. Such fractures maybe clinically occult or patients unexaminable when obtunded or otherwise altered. In patients suffering from blunt trauma resulting in trauma team activation, the prevalence of cervical fracture is greater, 3.7 %, and up to 7.7 % in unexaminable patients. Once detected, between 42 % and 57 % of all cervical spine injuries are potentially unstable [6, 7].

The elderly population is a subset of patients with increased risk of significant injury resulting from relatively low-energy mechanisms of injury. The elderly spine has altered biomechanics, including decreased range of motion, lower muscular strength, and increased rigidity from degenerative changes, including ankylosis.

In addition, degenerative changes may contribute to narrowing of the spinal canal with associated increased risk of cord injury [8].

Overall Cost to Society

Cervical spine injuries cause an estimated 6,000 deaths and 5,000 new cases of quadriplegia each year [1]. The total number of people with spinal cord injuries in the United States is estimated to be 265,000 persons, with a range of 232,000–316,000 persons [1]. The cost of care is dependent on severity of injury and is highest during the first year following injury. In 2010 dollars, the average annual expense for cervical spine injury resulting in incomplete motor function at any level was $321,720 in the first year and $39,077 for each subsequent year of life. In cases of high tetraplegia (C1-4), the first year cost of care averages $985,774 and $171,183 for each subsequent year of life [1]. The most recent comprehensive analysis of spinal cord injuries performed in 1996 concluded that the estimated total annual cost of all cervical spinal cord injuries was $9.7 billion per year [9].

Goals of Imaging

The primary goals of imaging are to (1) detect potentially unstable injuries to enable immobilization or stabilization and prevent development or progression of neurologic injury and (2) inform prognosis and guide surgical intervention for unstable fractures.

Methodology

PubMed (National Library of Medicine, Bethesda, Maryland) was used to search for original research publications discussing diagnostic performance and clinical predictors of cervical and thoracic spine injury. This includes publications from 1966 to August 31, 2011. The search strategy employed different combinations of the following terms: (1) spine, (2) radiography or imaging or computed tomography or magnetic resonance imaging, and (3) fracture or injury. MeSH headings included (1) spine and diagnosis, (2) imaging and spine, and (3) magnetic resonance imaging. Article was limited to human studies published in the English language. An initial review of the titles and abstracts of identified articles is followed by review of the full text in articles that were relevant.

Discussion of Issues

Who Should Undergo Cervical Spine Imaging?

Summary
The NEXUS [2] and Canadian C-spine [10] rules are two clinical prediction rules that have undergone multicenter validation, with the intent of determining which patients should undergo cervical spine imaging in blunt trauma patients. Both clinical prediction rules report a sensitivity greater than 99 %. Specificity is 42.5 % for the Canadian C-spine rule and 12.9 % for NEXUS (Table 31.1). A single randomized trial was implemented applying the Canadian C-spine rule which found that adherence to the decision rule demonstrated efficacy at reducing imaging of the cervical spine (strong evidence).

Supporting Evidence
Low yield of cervical spine imaging has prompted a number of investigations to attempt to identify clinical factors that can be used to predict cervical spine fractures.

Nexus Prediction Rule
The National Emergency X-Radiography Utilization Study (NEXUS) was a multicenter observational study involving 23 diverse emergency departments throughout the United States.

The NEXUS study was designed to assess the validity of four predetermined clinical criteria for prediction of cervical spine injury. According to the NEXUS criteria (Table 31.2), imaging is indicated if any of the following four determinations are met: (1) altered neurologic function, (2) intoxication, (3) midline posterior bony cervical spine tenderness, or (4) distracting injury (meaning an injury of sufficient pain to potentially distract the patient from noticing a cervical spine injury). In NEXUS, 34,069 patients were prospectively enrolled and underwent radiography of the cervical spine following blunt trauma. The above clinical predictors had a sensitivity of 99.6 % and specificity of 12.9 % for clinically significant injury [2]. In the participant population, 818 (2.4 % of total) had a cervical spine injury. It was estimated that adherence to the NEXUS criteria would reduce utilization of radiographs by 12.6 % (strong evidence).

Though validated in multiple different emergency departments, the NEXUS may not be appropriate in high-energy trauma patients in whom the trauma team is activated. There is limited evidence in the trauma literature indicating that the clinical exam performed on a patient with a normal Glascow Coma Scale cannot be used to exclude cervical spine fracture in victims of major trauma. In a 2007 study, Duane et al. prospectively evaluated 534 blunt trauma patients followed by cervical spine CT, and the performance of clinical exam was compared against that of CT [11]. In evaluable patients with GCS of 15 or greater who were not intoxicated and did not have a distracting injury, 17 patients had cervical spine fractures, seven of which had a negative clinical exam. Of the seven fractures undetected clinically, three were transverse process fractures requiring no further intervention, and four required treatment with extended use of a rigid cervical collar. In 2011, Duane et al. performed a second study involving 2,606 trauma team activations, which also demonstrated that the NEXUS criteria where insufficient to exclude fracture in trauma team activation patients [12]. It is also not clear what was considered a distracting injury in the Duane studies as they report that over 60 % of the trauma team activation patients lacked distracting injuries.

There are no implementation studies documenting the efficacy of NEXUS for reducing utilization in the clinical setting.

Canadian Cervical Spine Prediction Rule

The Canadian C-spine rule for radiography was published subsequent to the NEXUS trial but had a similar goal of validating a prediction rule which is highly sensitive for detecting acute cervical spine injury. The Canadian C-spine study was a prospective cohort study performed at 10 community and university hospitals across Canada and included 8,924 subjects. The Canadian C-spine study was derived from an observational study which evaluated 20 potential predictive factors but concluded on three determinations. According to the Canadian C-spine rule (Table 31.3), imaging is not indicated if all of the following three determinations are made: (1) absence of high-risk factor (age >65, dangerous mechanism, paresthesias in extremities), (2) presence of a low-risk factor (simple rear end motor vehicle collision, sitting position in ED, ambulatory at any time since injury, delayed onset of neck pain, or absence of midline cervical C-spine tenderness), or (3) patient is able to actively rotate neck 45 ° to left and right. The group reported sensitivity of 100 % and specificity of 42.5 % with the rate of ordering radiography projected to be reduced by 58.2 % [10]. A 14-day follow-up was performed on all patients who did not undergo imaging in an attempt to discover all individuals with missed fractures (strong evidence).

The implementation of the Canadian C-spine rule has also been investigated through a cluster randomized trial involving 12 Canadian emergency departments. A total of 11,824 alert and stable adults were included. The intervention group showed a relative reduction in cervical spine imaging of 12.8 % and the control group a relative increase of 12.5 % of cervical spine imaging [13].

There is no head-to-head trial supporting the adoption of either cervical spine prediction rule over the other. A retrospective analysis comparing Canadian C-spine and NEXUS prediction

rules was attempted. However, for this analysis, altered level of consciousness was effectively eliminated as a criteria [14, 15]. This negatively affects the accuracy of NEXUS as this is included in the NEXUS criteria. In addition, the Canadian C-spine rule requires the active evaluation of cervical spine rotational range of motion, a criterion which may not be acceptable in many US emergency departments.

What Imaging Modality Should Be Used for the Cervical Spine in Blunt Trauma?

Summary
Cervical spine CT is both more sensitive and specific than radiography for all patients (Table 31.1). In addition, cost-effectiveness analysis supports the use of CT as the initial modality in patient populations at high and moderate risk of cervical fracture. This strategy has been shown to reduce repeat imaging and identify the rare fractures which may have been missed from radiography with the potential to lead to severe neurologic deficit (moderate evidence). In patient populations with low probability for cervical fracture, properly performed cervical spine radiography remains the initial imaging modality of choice (limited evidence). MRI is not recommended in the acute setting as the initial evaluation of the cervical spine.

Supporting Evidence
Accuracy of Imaging There are no randomized clinical trials comparing the efficacy of computed tomography with that of cervical spine radiography. Historically, the sensitivity of cervical spine radiography has been reported in the 89–94 %, when adequate three-view radiographs were obtained on all patients [2, 16–18]. Weighted pooling of the larger studies using a clinical gold standard suggests that radiography is relatively accurate with a sensitivity of 94 % and a specificity of 95 % when all trauma patients are included (Table 31.1) [18].

However, more recently performed observational studies suggest that standard cervical spine radiography is less sensitive than previously reported. The discrepancy varies widely based on choice of reference standard and adequacy of cervical spine radiographs. A representative 2003 study performed by Griffen et al. in a level I trauma center concluded that the sensitivity of plain radiographs was 65 %, using CT follow-up as the reference standard [19]. In a 2005 meta-analysis, the pooled sensitivity of cervical spine radiography for fractures was estimated to be 54 % versus 98 % for computed tomography [20]. As with all diagnostic accuracy studies, any modality fares worse than the reference standard (in this case CT) and biases against the use of radiography. Studies using fractures that become apparent clinically as the reference standard are probably more relevant for clinical practice. In addition, these recent studies are biased by low percentage of cervical spine radiography examinations including adequate views, related to reluctance to perform repeat imaging for nonvisualized portions of the cervical spine. Furthermore, inadequate visualization is often seen as rational for proceeding to CT imaging increasing bias against radiography. In a 2009 study, Bailitz et al. included 1,583 consecutive major trauma patients that were evaluated with both cervical spine CT and three-view cervical radiography [21]. In this particular study, the final diagnosis in the medical record at discharge was used as the gold standard for cervical spine injury, and a clinically significant injury was one defined as requiring either an operative procedure, halo application, and/or rigid cervical collar application. Of the 78 patients with radiographic evidence of fracture, 50 (3.3 %) were determined to have clinically significant injuries, and 42 % of the 50 required operative intervention or halo application. Using the risk stratification criteria defined by Blackmore et al. [22], 16 clinically significant cervical fractures were present in the low-risk patients of which only 4 were identified by cervical spine radiography (25 % sensitivity). It should be noted however that of the 32 clinically significant injuries "missed" by cervical spine radiography, only 6 had adequate radiography.

The discord between historical estimates of radiography sensitivity of 89–94 % and current estimates of 54–65 % confound determination of

appropriate imaging. It is likely that the methodological limitations in the more recent literature, including consideration of inadequate radiographs as normal, use of an imaging rather than a clinical reference standard, and inclusion of only high-risk trauma patients explain much of this difference. Historical data indicating that missed cervical spine injuries were in fact rare prior to widespread use of CT also calls into question recent low estimates of radiograph sensitivity. However, with decreased utilization of cervical spine radiographs comes decreased proficiency at performance and interpretation, and sensitivity may actually have decreased as a consequence.

High and Moderate Risk Patients Cervical spine radiography performs significantly worse in compared to patient populations at moderate and high risk of cervical fracture (probability >4 %) [18]. These patients are commonly immobilized on backboards, have poly-trauma, and are unable to cooperate. These factors result in lower specificity, more inadequate radiographs and repeat imaging, greater utilization of hospital resources, and ultimately higher cost [23]. Additionally, CT evaluation has been shown to be more time efficient when compared to radiography, allowing for faster disposition of patients from the emergency department [24, 25]. This is particularly true when evaluation of the cervical spine follows CT scan of the head [26]. The decreased sensitivity of radiography in the major trauma population, time efficiency, and increased prevalence of cervical fracture support initial evaluation of the cervical spine utilizing CT in moderate and high-risk patients. Cost-effectiveness analysis supports use of CT in this population. In a 1999 study, Blackmore performed a cost-effectiveness analysis from the societal perspective comparing cervical radiography to that of CT and found that CT was cost-effective in high and moderate risk [18]. This was confirmed by Grogan et al. in 2005 [27] (moderate evidence).

Low-Risk Patients There is neither strong evidence nor consensus on the appropriate approach to cervical spine imaging in trauma victims in whom some imaging is indicated through use of NEXUS or the Canadian C-spine rule, but who are at low risk of injury. The standard has been radiography, but more recently, CT has been promoted as an initial imaging strategy, even in low-risk individuals. Recent societal consensus guidelines in the United States, including the ACR Appropriateness Criteria [28] and Eastern Association for the Surgery of Trauma [29], have advocated for use of CT for all patients who undergo cervical spine imaging in trauma. However, guidelines supporting use of CT in low-risk patients generally rely on recent estimates of accuracy, despite the methodological limitations. In addition, such guidelines do not consider the fact that use of CT carries much greater radiation risk and societal cost.

Radiography may be most appropriate in the evaluation of patients who cannot be cleared clinically but have low-risk factors for significant cervical trauma such as young age, low-impact trauma, and no distracting injuries [18, 22, 30]. Inability to obtain technically adequate radiographs due to incomplete visualization or suboptimal quality (low specificity) is the single biggest limitation of radiography (Table 31.1) [20]. In the very low-risk patient population, adequate films are more easily obtained. CT is indicated when adequate radiographs cannot be obtained.

Radiation risks are difficult to estimate with any precision due to the need for extrapolation of radiation effects from higher administered doses to the very low doses found in diagnostic imaging. However, use of CT rather than radiography for evaluation of the cervical spine comes with an estimated 14-fold greater patient exposure to ionizing radiation. The organ-specific dose to the thyroid gland with cervical spine CT has been estimated at 26 mGy compared to 1.8 mGy for radiography [31], resulting in increased risk of radiation-induced malignancy [32].

Reconciliation of the higher sensitivity of CT versus the lower cost and radiation dose of radiography is challenging. From 2002 to 2007, there was a significant increase in the use of CT and plain radiographs in the management of trauma

patients, leading to significantly higher radiation exposure with no demonstrable improvements in the diagnosis of missed injuries, mortality, or length of stay [33].

Table 31.4 makes the trade-offs explicit through a crude estimation of the number needed to treat and the number needed to harm when substituting CT for radiography in low-risk patients. There is substantial uncertainty in the estimates of both benefits and harms from CT. However, it is likely that the rate of cancer mortality is at least an order of magnitude greater than the probability of preventing paralysis through use of CT in low-risk trauma patients. Accordingly, radiography, when adequately performed, should be considered as the initial imaging approach in patients at low risk (limited evidence).

Cost-effectiveness analysis also supports radiography as initial imaging strategy in low-risk patients. The threshold for when CT becomes cost-effective is somewhat uncertain. In the original cost-effectiveness analysis, Blackmore found a risk threshold of 4 % to be the criterion for use of CT. However, subsequent investigators have proposed lower thresholds. Grogan suggested 0.9 %, though this was based on extremely low estimates of radiograph sensitivity (64 %) found in severely injured patients. Likely however, the appropriate threshold is lower than the original 4 % estimate, due to lower current estimates of performance of radiography detailed above.

Determination of appropriate imaging therefore requires stratification of patients in to low- and higher-risk cohorts. Blackmore [22] and Hanson [34] developed and validated a clinical prediction rule to identify subjects at low risk (Table 31.4). In the validation cohort, subjects lacking any of the high-risk factors had a risk of cervical spine fracture of only 0.2 %, indicating that radiography was the preferred imaging approach. In the NEXUS study, the probability of fracture was 2.4 % overall but 0.4 % in the low-risk patients [2], again confirming that a group can be identified where adequate cervical spine radiography is appropriate as the initial screening tool.

Special Cases
Obtunded Patient
Summary
A normal cervical CT in obtunded patients with blunt trauma essentially excludes unstable cervical spine injuries. MRI is unlikely to change management when there is no neurologic deficit or abnormality by cervical spine CT and is therefore not routinely recommended given risks and benefits (limited evidence).

Supporting Evidence
There are several valid cohort studies of the accuracy of cervical spine CT in excluding unstable injuries in obtunded or clinically unexaminable patients. Hennessy in 2010 reported a prospective cohort study of 402 intubated, unexaminable blunt trauma patients with normal CT. Using flexion extension radiography and clinical follow-up as a reference standard, one patient was found to have an unstable injury missed by the CT (negative predictive value 99.7 %) [35]. Hogan et al. retrospectively examined 366 patients with negative CT, using MR and clinical follow-up as the reference standard. The authors concluded that the negative predictive value of CT for ligamentous injury was 98.9 % and 100 % for unstable CS injury [36]. Harris and colleagues evaluated a retrospective cohort of 367 obtunded patients using a clinical and radiographic reference standard. A normal multi-detector row CT scan of the cervical spine in obtunded patients with blunt trauma had a negative predictive value of 99.7 % [37]. Brohi and colleagues prospectively evaluated 442 consecutive unconscious trauma patients and defined the sensitivity of CT at 98.1 % (51/52), with a negative predictive value of 99.7 % [38]. In addition, a 2005 retrospective cohort study by Schuster et al. included 93 patients with a normal motor examination and a negative cervical spine CT with MR as the reference standard. In this study, all patients had negative MRI examinations unless there was a neurologic deficit or a positive CT [39]. Como evaluated 197 patients who were obtunded by moving all four extremities and reported no missed injuries on CT, with clinical or MRI follow-up [40] (moderate evidence).

However, it is also clear that CT is imperfect. As an example, Schoenfeld and colleagues culled from the medical literature multiple cases (particularly of ligamentous injuries) missed at CT but discovered on subsequent MRI [41]. However, in a common failing of the literature on this topic, the authors failed to report the number of true-negative CT scans, instead only reporting the number of false-negative CT scans among the group who went on to MRI. This verification bias, due to selection of the cohort based on performance of the reference standard, makes calculation of negative predictive value meaningless [42].

Finally, there are potential risks related to use of MRI in obtunded patients, related to the transfer of patients to the MRI suite, and limited ability to monitor patients while in the MRI scanner. In addition, delay in clearance of the cervical spine, with prolonged immobilization, may lead to complications including pressure ulcers, increased intracranial pressure, thromboembolism, and pulmonary aspiration [43–45].

Elderly
Summary
Elderly individuals are at higher risk of cervical spine injury from both high- and low-energy mechanisms. However, no prediction rules have been validated to specifically identify predictors of injury in the elderly. The same predictors in younger patients appear to work in the elderly [46]. Accordingly, the same approach to imaging may be applied in the elderly as in younger patients, but with a lower threshold for use of CT (limited evidence).

Children
Summary
The NEXUS clinical prediction rule is a reasonable method of identifying which older children and adolescents should undergo cervical spine imaging after trauma. Imaging should be performed in subjects with (1) altered neurologic function, (2) intoxication, (3) midline posterior bony cervical spine tenderness, and (4) distracting injury (moderate evidence). Under the age of 3 years, cervical spine imaging may be limited to subjects with high-energy mechanism (motor vehicle crash) or

Glasgow Coma Score of less than 14 (limited evidence). Radiography can appropriately be used to exclude cervical spine fracture in children, though cervical spine CT may be useful in high-risk subjects. In younger children, CT should be limited to the upper cervical spine (limited evidence).

Supporting Evidence
Evidence for who should undergo imaging is less complete in children than in adults. Determination of clinical predictors of injury in pediatric subjects is complicated by the decreased incidence of injury in children, requiring larger sample size for adequate study [47–49]. In addition, children may sustain serious cervical cord injuries that are not radiographically apparent [47, 48]. Among adult clinical prediction rules, the Canadian Clinical Prediction Rule development study excluded children [10]. The NEXUS trial included children, but there were only 30 injuries in subjects under age 18, and only four in subjects under age 9 [2]. Although no pediatric injuries were missed in the NEXUS study, the sample size was too small to adequately assess the sensitivity of the prediction rule in this group. Further validation of a pediatric version of the NEXUS was performed at a single academic pediatric trauma center in the United States. In 647 trauma victims age 3 or older, injuries were found in approximately 2 %, of whom four required operative fixation. No missed injuries were reported [50].

A pediatric adaptation of the NEXUS is a thus reasonable approach in children over age 3, suggesting that imaging is only indicated when subjects have any of the following: (1) altered neurologic function, (2) intoxication, (3) midline posterior bony cervical spine tenderness, and (4) distracting injury (moderate evidence) [50].

Pieretti-Vanmarcke and colleagues performed a retrospective analysis of trauma registry data from multiple institutions, including 12,537 patients under the age of 3. They found that limiting imaging to subjects with decreased level of consciousness manifest by pediatric Glasgow Coma Score of less than 14 or high-energy mechanism (motor vehicle crash) identified 78 of 83 (94 %) clinically important injuries with a negative predictive value of 99.9 %. The low negative

predictive value was driven largely by the extremely low incidence of injury in this population (0.66 %) even in subjects evaluated at major trauma centers [49]. This study has not yet been validated prospectively (limited evidence).

Comparison of CT versus radiography has not been well explored in children. Radiography has accuracy for cervical spine fracture of approximately 94 %, [51] similar to adults [18]. The odontoid view and flexion extension radiographs contribute little in young children [52–55]. CT is likely more accurate than radiography but does encompass higher radiation doses and higher costs [56]. The cost-effectiveness analysis of Blackmore and colleagues excluded children, [18, 22, 34] as did the studies of the Harborview high-risk cervical spine criteria (Table 31.5) [22, 34]. Further, the lower frequency of injury in children [47, 57] and the increased radiosensitivity of pediatric subjects [58] suggest that cost-effectiveness results from adults may not be relevant.

A reasonable approach to pediatric cervical spine imaging is the Harborview protocol (Fig. 31.1). Overall, radiography is adequate to exclude cervical spine fracture in most younger children [56, 59] (limited evidence). However, use of upper cervical CT in high-risk younger children [60] who are getting head CT is probably reasonable, as the time and cost is minimal, and the thyroid can be spared in the CT radiation dose if imaging is limited to the upper cervical spine (insufficient evidence). In addition, upper cervical spine injuries are more common than lower cervical injuries in younger children (Fig. 31.2a, b) [57, 61, 62].

Who Should Undergo Imaging of the Thoracic and Lumbar Spine Following Trauma?

Summary

Clinical prediction rules to determine which patients should undergo thoracolumbar spine imaging have been developed, but not validated. Although these prediction rules have high sensitivities for detecting thoracolumbar fractures, their low specificities and low positive predictive values would require imaging a large number of patients without thoracolumbar injuries. This drawback limits the clinical utility of these prediction rules (moderate evidence).

Supporting Evidence

Given the relative lack of clarity regarding which blunt trauma patients require thoracolumbar imaging, several observational (limited evidence) studies have examined potential risks for thoracolumbar fracture. These limited studies have identified associations between the risk of thoracolumbar injury and high-speed motor vehicle crash [63, 64], fall from a significant height [65–67], complaint of back pain, [65–69], elevated injury score [65, 66], decreased level of consciousness [66–68, 70], and abnormal neurological exam [67, 68].

Two separate clinical prediction rules to guide thoracolumbar spine imaging decisions have been developed, although neither prediction rule has been validated. The smaller study, conducted by Hsu et al., examined the effect of six clinical criteria on two retrospective groups [71]. The first group consisted of a cohort of 100 patients with known thoracolumbar fracture, while the second group consisted of 100 randomly selected multitrauma patients. The criteria evaluated were (1) back pain/midline tenderness, (2) local signs of injury, (3) neurological deficit, (4) cervical spine fracture, (5) distracting injury, and (6) intoxication. The results of this small scale, retrospective trial found that 100 % of the patients in the known thoracolumbar fracture group would have been imaged appropriately using the proposed criteria. This proposed pathway was then tested retrospectively in the group of randomly selected blunt trauma patients and was found to have a sensitivity of 100 %, a specificity of 11.3 %, and a negative predictive value of 100 %. Implementing these criteria would still require imaging the thoracolumbar spine in 92 % of the selected multi-trauma patients.

A much larger prospective, single-center study by Holmes et al. evaluated similar criteria in 2,404 consecutive blunt trauma patients who underwent thoracolumbar imaging [72]. These clinical criteria (Table 31.6) were (1) complaints

of thoracolumbar spine pain, (2) thoracolumbar spine pain on midline palpation, (3) decreased level of consciousness, (4) abnormal peripheral nerve examination, (5) distracting injury, and (6) intoxication. This prediction rule was successful in achieving 100 % sensitivity for detecting thoracolumbar fracture; however, the specificity was only 3.9 %. Due to this low specificity, implementing this prediction rule in this patient population would have decreased the rate of thoracolumbar imaging by merely 4 % (Table 31.1) (moderate evidence).

Though not specifically evaluating a clinical prediction rule, Sava and colleagues did identify that clinical exam may not be sufficiently reliable to exclude fracture in subjects with substantial blunt trauma and altered sensorium [73].

What Imaging Modality Should Be Used to Evaluate the Thoracic and Lumbar Spine in Blunt Trauma?

Summary

Multiple studies have shown that some CT protocols used for imaging the chest and abdominal visceral organs, when performed with sagittal reformations, are more sensitive and specific for detecting thoracolumbar spine fracture than conventional radiography. In patients undergoing such scans, conventional radiography may be eliminated (limited evidence). The effect of primary screening with CT scan on cost and radiation exposure has not been thoroughly studied for the thoracolumbar spine.

Supporting Evidence

Multiple limited evidence studies examine the possibility of eliminating conventional radiography in those patients who are candidates for both conventional thoracolumbar radiographs and CT evaluation of the chest or abdominal viscera; however, many of these trials are hampered by small sample sizes and/or verification bias [74–78]. Studies that combine the results of both CT and conventional radiography as the reference standard suggest that CT has a sensitivity of 78.1–100 %, while conventional

radiographs have a sensitivity of 32.0–74 % for detecting thoracolumbar fracture (Table 31.1) [75–77, 79]. The clinical importance of thoracolumbar fractures not found with conventional radiography is unknown, as no studies with clinically based outcome measures were located.

A single limited evidence trial examined the use of CT as an initial evaluation in patients for which a CT scan is not indicated for other reasons [76]. This prospective, single-center trial examined 222 trauma patients with both CT and conventional radiographs as initial screening exams. The reported sensitivity was 97 % for CT examination and 58 % for conventional radiographs. The results of this trial are limited in that only 36 patients were diagnosed with thoracolumbar fracture during the course of the trial.

Applicability to Children

Summary

There are no clinical prediction rules validated in children for the determination of when imaging is indicated. However, a reasonable approach in older children is to image when any of the following are present: (1) complaints of thoracolumbar spine pain, (2) thoracolumbar spine pain on midline palpation, (3) decreased level of consciousness, (4) abnormal peripheral nerve examination, (5) distracting injury, and (6) intoxication (limited evidence). No reliable data exists on when to image in younger children (insufficient evidence). Compared to adults, younger children are less likely to localize pain and may have pain referred to the spine from intra-abdominal causes, particularly renal (infection and obstruction).

Supporting Evidence

Data on appropriate indications for thoracolumbar spine imaging in children is limited. The adult clinical prediction rule from Holmes and colleagues did enroll children. However, the actual number of children in the study is not reported [72]. The youngest patient enrolled in the small clinical prediction rule validation trial by Hsu et al. was 14 years of age [71]. Given the 100 % sensitivity in adults, it is reasonable to employ the Holmes clinical prediction

rule in older children (limited evidence). In younger children, the criteria would have to be modified ad hoc to meet the clinical perception of the child's ability to provide reasonable responses and the clinical picture (insufficient evidence). The specificity of the Holmes prediction rule in adults was low (3.9 %), so it is not expected that the use of this prediction rule would decrease unnecessary imaging [72].

Take-Home Figure and Tables

Figure 31.1 shows a pediatric imaging protocol for blunt trauma from Harborview Medical Center.

Tables 31.1 through 31.6 highlight key recommendations and supporting evidence.
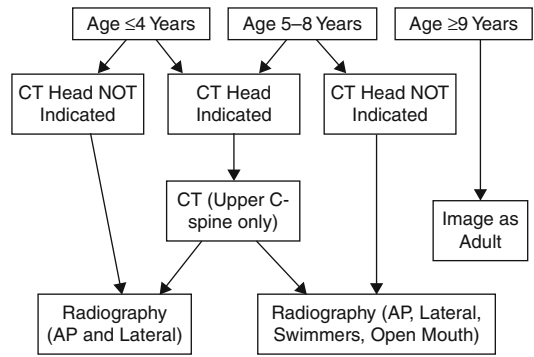
Fig. 31.1 Pediatric imaging protocol for blunt trauma from Harborview Medical Center (Reprinted with kind permission of Springer Science+Business Media from Blackmore CC. Imaging of the spine for traumatic and nontraumatic etiologies. In: Medina LS, Applegate KE, Blackmore CC, editors. Evidence-based imaging in pediatrics: optimizing imaging in pediatric patient care. New York: Springer; 2010)

Table 31.1 Diagnostic performance

		Sensitivity	Specificity	Potential decrease in radiography
C-spine prediction rules				
NEXUS[a]		99.6	12.9	12.6
Canadian C-spine rule[b]		100	42.5	41.8
TL-spine prediction rules				
Holmes et al.[c]		100	3.9	3.7
C-spine radiography[d]				
	Overall	89–94	95.3	N/A
	Low risk		96.4	N/A
	High risk		78.1–89.3	N/A
CT[e]	Overall	99.0	93.1	N/A
TL-spine radiography[f]				
Conventional imaging		63.0	94.6	N/A
CT		97.8	99.6	N/A

N/A not applicable
[a]From reference [2]
[b]From reference [10]
[c]From reference [72]. Has not been validated
[d]Older references with clinical reference standard. It is unclear if these results are still valid. Adapted from references [16–18]
[e]Adapted from references [18–21, 35–40]
[f]Pooled from references [65, 74–79]
Reprinted with kind permission of Springer Science+Business Media from Blackmore CC, Avey GD. Imaging of the spine in victims of trauma. In: Medina LS, Blackmore CC, editors. Evidence-based imaging: optimizing imaging in patient care. New York: Springer; 2006

Table 31.2 NEXUS criteria. Imaging of the cervical spine is not necessary if all five of the NEXUS criteria are met

1. Absence of posterior midline tenderness
2. Absence of focal neurological deficit
3. Normal level of alertness
4. No evidence of intoxication
5. Absence of painful injury distracting attention from the spine

Adapted from Hoffman JR, Mower WR, Wolfson AB, Todd KH, Zucker MI. Validity of a set of clinical criteria to rule out injury to the cervical spine in patients with blunt trauma. National Emergency X-Radiography Utilization Study Group. N Engl J Med. 2000 Jul 13;343(2):94–9

Reprinted with kind permission of Springer Science+ Business Media from Blackmore CC, Avey GD. Imaging of the spine in victims of trauma. In: Medina LS, Blackmore CC, editors. Evidence-based imaging: optimizing imaging in patient care. New York: Springer; 2006

Table 31.3 The Canadian C-spine rule. If the following three determinations are made, then imaging is not indicated

1. No high- risk factor, including:
Age > 64 years
Dangerous mechanism, including:
Fall from >3 m/5 stairs
Axial load to head (diving)
High-speed vehicular crash (60 MPH, rollover, ejection)
Bicycle collision
Motorized recreational vehicle
Paresthesias in extremities
2. Low-risk factor is present
Simple rear end vehicular crash, excluding:
Pushed into oncoming traffic
Hit by bus/large truck
Rollover
Hit by high-speed vehicle
Sitting position in emergency department
Ambulatory at any time
Delayed onset of neck pain
Absence of midline cervical tenderness
3. Able to actively rotate neck (45° left and right)

Adapted from Stiell I, Wells G, Vandemheen K, Clement C, Lesiuk H, De Maio V, et al. The Canadian C-spine rule for radiography in alert and stable trauma patients. JAMA. 2001;286:1841–8

Reprinted with kind permission of Springer Science+ Business Media from Blackmore CC, Avey GD. Imaging of the spine in victims of trauma. In: Medina LS, Blackmore CC, editors. Evidence-based imaging: optimizing imaging in patient care. New York: Springer; 2006

Imaging Case Studies

Case 1: Atlantooccipital subluxation with occipital condyle fracture in a 9-year-old boy (Fig. 31.2a, b)

Case 2: Victim of a motor vehicle crash who met criteria for initial cervical spine imaging with CT scan (Fig. 31.3a, b)

Recommended Imaging Protocol

Cervical Spine

CT protocol: Multi-detector CT with axial image reconstruction at 2.5 mm or less, in both bone and soft tissue algorithms, and with sagittal and coronal reformations in bone algorithm at 2-mm collimation.

Radiography protocol: AP, open mouth, lateral, and swimmers. Note that all images must be adequate for evaluation, and the entire region from skull base to T1 must be visible in both frontal and lateral projections. If adequate films cannot be obtained after repeat imaging, then CT should be performed.

Thoracic and Lumbar Spine

CT protocol: Axial images in bone algorithm through the area of concern, with 2.5-mm collimation. Must include sagittal reformations and preferable coronal, in bone algorithm, at 2-mm collimation.

Radiography protocol: AP and lateral views covering the entire area of interest.

Table 31.4 Number needed to treat and harm for cervical spine imaging in low-risk patients

Variable	Estimate	Range	Source references
Risk of fracture	0.005	0.002–0.02	[2, 10, 34]
Chance of missing fracture (1-sensitivity)	0.1	0.06–0.20	[2, 16–18, 20]
Chance of paralysis (from missed fracture)	0.05	.01–0.15	[18, 32]
Number needed to treat[a] (to prevent one case of paralysis)	40,000	10,000–200,000	
Number needed to harm[b] (to cause one case of fatal cancer)	2,000	1,000–20,000	[31, 32]

Notes:

[a]Number needed to treat is number of patients who have to undergo CT instead of radiography to prevent one case of paralysis in this population (equal to risk of fracture x chance of missing fracture x chance of paralysis)

[b]Number needed to harm is the number of patients who would have to undergo CT instead of radiography to cause one case of fatal cancer in the course of their lifetime

Table 31.5 Harborview high-risk cervical spine criteria. Presence of any of the following criteria indicates a subject at sufficiently high risk to warrant initial use of CT to evaluate the cervical spine

1. High-energy injury mechanism
   High-speed (>35 mph) motor vehicle or motorcycle crash
   Motor vehicle crash with death at scene
   Fall from height greater than 10 ft
2. High-risk clinical parameter
   Significant head injury, including intracranial hemorrhage or unconscious in emergency department
   Neurological signs or symptoms referable to the cervical spine
   Pelvic or multiple extremity fractures

Adapted from Hanson JA, Blackmore CC, Mann FA, Wilson AJ. Cervical spine screening: a decision rule can identify high-risk patients to undergo screening helical CT of the cervical spine. AJR Am J Roentgenol. 2000;174:713–8

Reprinted with kind permission of Springer Science+ Business Media from Blackmore CC, Avey GD. Imaging of the spine in victims of trauma. In: Medina LS, Blackmore CC, editors. Evidence-based imaging: optimizing imaging in patient care. New York: Springer; 2006

Table 31.6 Thoracolumbar spine imaging criteria

1. Thoracolumbar spine pain
2. Thoracolumbar spine tenderness on midline palpation
3. Decreased level of consciousness
4. Abnormal peripheral nerve examination
5. Distracting injury
6. Intoxication

Adapted from Holmes JF, Panacek EA, Miller PQ, Lapidis AD, Mower WR. Prospective evaluation of criteria for obtaining thoracolumbar radiographs in trauma patients. J Emerg Med. 2003 Jan;24(1):1–7

Reprinted with kind permission of Springer Science+ Business Media from Blackmore CC, Avey GD. Imaging of the spine in victims of trauma. In: Medina LS, Blackmore CC, editors. Evidence-based imaging: optimizing imaging in patient care. New York: Springer; 2006

Future Research

- Studies in both cervical spine and thoracolumbar spine imaging indicate that CT is more sensitive than traditional radiography in detecting fractures. However, further clinical studies addressing the relevance of these fractures are needed.

- The applicability of cervical spine injury clinical prediction rules in pediatric patients is unknown. In addition, the sensitivity, specificity, and cost-effectiveness of the various imaging exams in the pediatric population are not well established.

- Clinical prediction rules for imaging of the thoracolumbar spine have been developed, but further research is necessary to validate such approaches. The effect of implementing these rules on cost, cost-effectiveness, and radiation exposure has not been determined.

- Appropriate imaging to detect unstable ligamentous injury, particularly in clinically unexaminable subjects, remains unresolved.
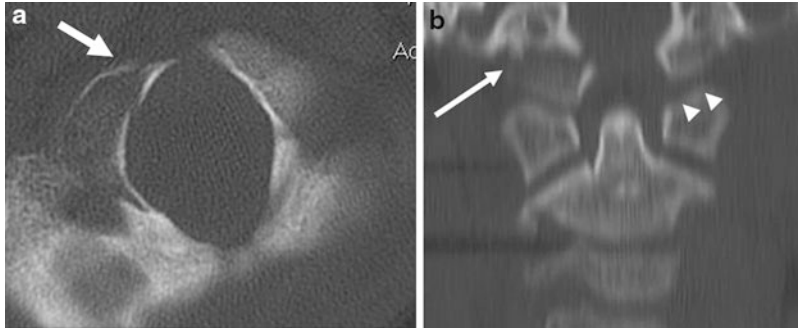
Fig. 31.2 Atlantooccipital subluxation with occipital condyle fracture in a 9-year-old boy. (**a**) Axial CT demonstrates right occipital condyle fracture (*arrow*). (**b**) Coronal reformation demonstrates the right occipital condyle fracture (*arrow*) as well as widening at the left atlantooccipital joint (*arrowheads*) (Reprinted with kind permission of Springer Science+Business Media from Blackmore CC. Imaging of the spine for traumatic and nontraumtic etiologies. In: Medina LS, Applegate KE, Blackmore CC, editors. Evidence-based imaging in pediatrics: optimizing imaging in pediatric patient care. New York: Springer; 2010)
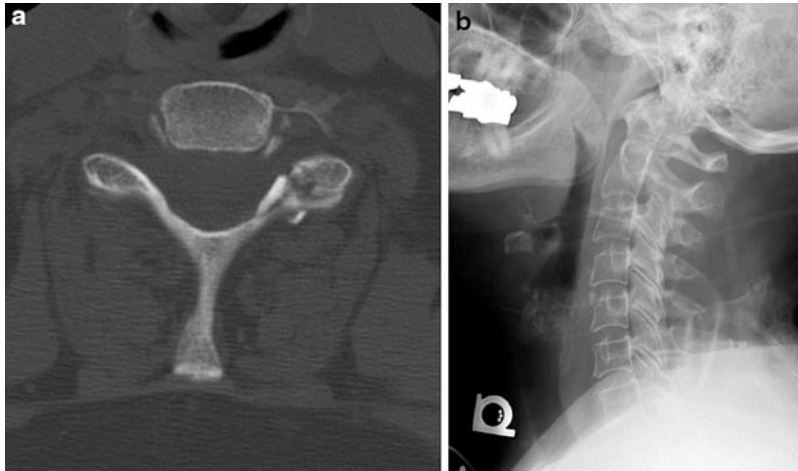
Fig. 31.3 (**a**, **b**) Victim of a motor vehicle crash who met criteria for initial cervical spine imaging with CT scan. A potentially unstable C6–7 facet and pars interarticularis fracture is apparent on CT (**a**) but may be missed on contemporaneous radiography (**b**). CT has higher sensitivity for fracture than radiography (Reprinted with kind permission of Springer Science+Business Media from Blackmore CC, Avey GD. Imaging of the spine in victims of trauma. In: Medina LS, Blackmore CC, editors. Evidence-based imaging: optimizing imaging in patient care. New York: Springer; 2006)

References

1. National Spinal Cord Injury Statistical Center. Spinal cord injury facts and figures at a glance. 2011.
2. Hoffman JR, Mower WR, Wolfson AB, Todd KH, Zucker MI. N Engl J Med. 2000;343(2):94–9.
3. Pickett GE, Campos-Benetez M, Keller JL, Duggal N. Spine. 2006;31:799–805.
4. Hoffman JR, Schriger DL, Mower W, Luo JS, Zucker M. Ann Emerg Med. 1992;21(12):1454–60.
5. Sekhon LH, Fehlings MG. Spine. 2001;26:S2–12.
6. Milby AH, Halpern CH, Guo W, Stein SC. Neurosurg Focus. 2008;25(5):E10.
7. Goldberg W, Mueller C, Panacek E, Tigges S, Hoffman JR, Mower WR. Ann Emerg Med. 2001;38(1):17–21.
8. Lomoschitz F, Blackmore C, Mirza S, Mann F. AJR Am J Roentgenol. 2002;178:573–7.

9. Berkowitz M, O'Leary PK, Kruse DL, Harvey C. Spinal cord injury: an analysis of medical and societal costs. New York: Demos Publications; 1998.

10. Stiell I, Wells G, Vandemheen K, Clement C, Lesiuk H, De Maio V, et al. JAMA. 2001;286:1841–8.

11. Duane TM, Dechert T, Wolfe LG, Aboutanos MB, Malhotra AK, Ivatury RR. J Trauma-Inj Infect & Crit Care. 2007;62(6):1405–8; discussion 8–10.

12. Duane TM, Mayglothling J, Wilson SP, Wolfe LG, Aboutanos MB, Whelan JF, et al. J Trauma. 2011;70:829–31.

13. Stiell IG, Clement CM, Grimshaw J, Brison RJ, Rowe BH. BMJ. 2009;339:b4146.

14. Stiell IG, Clement CM, McKnight RD, Brison R, Schull MJ, Rowe BH, et al. N Eng J Med. 2003; 349(26):2510–18.

15. Dickinson G, Stiell IG, Schull M, Brison R, Clement C, Vandemheen K. Ann Emerg Med. 2004; 43:507–14.

16. Acheson MB, Livingston RR, Richardson ML, Stimac GK. AJR Am J Roentgenol. 1987;148(6): 1179–85.

17. Woodring JH, Lee C. J Trauma. 1993;34(1):32–9.

18. Blackmore CC, Ramsey SD, Mann FA, Deyo RA. Radiology. 1999;212(1):117–25.

19. Griffen MM, Frykberg ER, Kerwin AJ, Schinco MA, Tepas JJ, Rowe K, et al. J Trauma. 2003;55(2):222–6; discussion 6–7.

20. Holmes JF, Akkinepalli R. J Trauma. 2005;58:902–5.

21. Bailitz J, Starr F, Beecroft M, Bankoff J, Roberts R, Bokhari F, et al. J Trauma Inj Infect Crit Care. 2009;66(6):1605–9.

22. Blackmore CC, Emerson SS, Mann FA, Koepsell TD. Radiology. 1999;211:759–65.

23. Blackmore CC, Zelman WN, Glick ND. Radiology. 2001;220:581–7.

24. Nunez DB, Ahmad AA, Coin CG, LeBlang S, Becerra JL, Henry R, et al. Emerg Radiol. 1994;1(6):273–8.

25. Antevil JL, Sise MJ, Sack DI, Kidder B, Hopper A, Brwon CVR. J Trauma. 2006;61:382–7.

26. Daffner RH. AJR Am J Roentgenol. 2001;177(3):677–9.

27. Grogan EL, Morris JA, Dittus RS, Moore DE. J Am Coll Surg. 2005;200:160–5.

28. ACR. ACR appropriateness criteria. 2008 [cited 2011 September 4]. Available from: http://www.acr.org/SecondaryMainMenuCategories/quality_safety/app_criteria/pdf/ExpertPanelonMusculoskeletalImaging/SuspectedCervicalSpineTraumaDoc22.aspx

29. Trauma EAftSo. Cervical spine injuries identification following trauma-2009 update. 2009.

30. Gonzalez-Beicos A, Nunez Jr DB. Semin Ultrasound CT MR. 2009;30(3):159–67.

31. Rybicki F, Nawfel RD, Judy PF. AJR Am J Roentgenol. 2002;179:933–7.

32. Brenner DJ, Hall EJ. N Engl J Med. 2007;357: 2277–84.

33. Inaba K, Kirkpatrick AW, Finkelstein J, Murphy J, Brenneman FD, Boulanger BR, et al. Injury. 2001;32(3):201–7.

34. Hanson JA, Blackmore CC, Mann FA, Wilson AJ. AJR Am J Roentgenol. 2000;174:713–18.

35. Hennessy D, Widder S, Zygun D, Hurlbert RJ, Burrowes P, Kortbeek JB. J Trauma. 2010;68:576–82.

36. Hogan GJ, Mirvis SE, Kathirkamanathan S, Scalea TM. Radiology. 2005;237:106–13.

37. Harris TJ, Blackmore CC, Mirza SK, Jurkovich GJ. Spine. 2008;33:1547–53.

38. Brohi K, Healy M, Fotheringham T, Chan O, Aylwin C, Whitley S, et al. J Trauma. 2005;58:897–901.

39. Schuster R, Waxman K, Sanchez B, Becerra S, Chung R, Conner S, et al. Arch Surg. 2005;140:762–6.

40. Como JJ, Leukhardt WH, Anderson JS, Wilczewski PA, Samia H, Claridge JA. J Trauma. 2011;70:345–51.

41. Schoenfeld AJ, Bono CM, McGuire KJ, Warholic N, Harris MB. J Trauma. 2010;68:109–14.

42. Blackmore CC. Acad Radiol. 2004;11:134–40.

43. Morris CGT, McCoy E. Anaesthesia. 2004;59: 464–82.

44. Morris CGT, McCoy E, Lavery GG. BMJ. 2004; 329:495–9.

45. Dunham CM, Brocker BP, Collier BD, Gemel DJ. Clin Care. 2008;12:1–13.

46. Bub L, Blackmore C, Mann F, Lomoschitz F. Radiology. 2005;234:143–9.

47. Kokoska E, Keller M, Rallo M, Weber T. J Pediatr Surg. 2001;36:100–5.

48. Finch G, Barnes M. J Pediatr Orthop. 1998;18:811–14.

49. Pieretti-Vanmarcke R, Velmahos G, Nance ML, Islam S, Falcone RA. J Trauma. 2009;67:543–50.

50. Anderson RA, Scaife ER, Fenton SJ, Kan P, Hansen KW, Brockmeyer DL. J Neurosurg. 2006;105:361–4.

51. Baker C, Kadish H, Schunk JE. Am J Emerg Med. 1999;17(3):230–4.

52. Buhs C, Cullen M, Klein M, Farmer D. J Pediatr Surg. 2000;35(6):994–7.

53. Dwek JR, Chung CB. AJR Am J Roentgenol. 2000;174(6):1617–19.

54. Ralston ME, Chung K, Barnes PD, Emans JB, Schutzman SA. Acad Emerg Med. 2001;8(3):237–45.

55. Silva CT, Doria AS, Traubici J, Mineddin R, Dvaila J, Shroff M. AJR Am J Roentgenol. 2009;194:500–8.

56. Adelgais KM, Grossman DC, Langer SG, Mann FA. Acad Emerg Med. 2004;11:228–36.

57. Viccellio P, Simon H, Pressman B, Shah M, Mower W, Hoffman J. Pediatrics. 2001;108:E20.

58. National Academy of Science. Health effects of exposure to low levels of ionizing radiation: BEIR VII. Washington, DC: National Academy Press; 2006.

59. Hernandez JA, Chupik C, Swischuk LE. Emerg Radiol. 2004;10(4):176–8.

60. Keenan HT, Hollingshead MC, Chung CJ, Ziglar MK. AJR Am J Roentgenol. 2001;177(6):1405–9.

61. Patel JC, Tepas 3rd JJ, Mollitt DL, Pieper P. J Pediatr Surg. 2001;36(2):373–6.

62. Cirak B, Ziegfeld S, Knight VM, Chang D, Avellino AM, Paidas CN. J Pediatr Surg. 2004;39(4):607–12.

63. Beirne J, Butler P, Brady F. Int J Oral Maxillofac Surg. 1995;24:26–9.

64. Davis RL, Hughes M, Gubler KD, Waller PL, Rivara FP. Pediatrics. 1995;95(3):345–9.
65. Durham RM, Luchtefeld WB, Wibbenmeyer L, Maxwell P, Shapiro MJ, Mazuski JE. Am J Surg. 1995;170(6):681–4.
66. Cooper C, Dunham CM, Rodriguez A. J Traum. 1995;38(5):692–6.
67. Frankel HL, Rozycki GS, Ochsner MG, Harviel JD, Champion HR. J Trauma. 1994;37(4):673–6.
68. Meldon SW, Moettus LN. J Trauma. 1995;39(6): 1110–14.
69. Samuels LE, Kerstein MD. J Trauma. 1993;34(1):85–9.
70. Stanislas MJ, Latham JM, Porter KM, Alpar EK, Stirling AJ. Injury. 1998;29(1):15–18.
71. Hsu JM, Joseph T, Ellis AM. Injury. 2003;34(6): 426–33.
72. Holmes JF, Panacek EA, Miller PQ, Lapidis AD, Mower WR. J Emerg Med. 2003;24(1):1–7.
73. Sava J, Williams MD, Kennedy S, Wang D. J Trauma. 2006;61:168–71.
74. Gestring ML, Gracias VH, Feliciano MA, Reilly PM, Shapiro MB, Johnson JW, et al. J Trauma. 2002;53(1):9–14.
75. Wintermark M, Mouhsine E, Theumann N, Mordasini P, van Melle G, Leyvraz PF, et al. Radiology. 2003;227(3):681–9.
76. Hauser CJ, Visvikis G, Hinrichs C, Eber CD, Cho K, Lavery RF, et al. J Trauma. 2003;55(2):228–34; discussion 34–5.
77. Sheridan R, Peralta R, Rhea J, Ptak T, Novelline R. J Trauma. 2003;55:665–9.
78. Rhee PM, Bridgeman A, Acosta JA, Kennedy S, Wang DS, Sarveswaran J, et al. J Trauma. 2002;53(4):663–7; discussion 7.
79. Mancini DJ, Burchard KW, Pekala JS. J Trauma. 2010;69:119–21.

Spinal Infections: Evidence-Based Neuroimaging

32

Bahman Roudsari and Jeffrey G. Jarvik

Contents

B. Roudsari (✉)
Department of Radiology, University of Washington, Seattle, WA, USA
e-mail: roudsari@u.washington.edu

J.G. Jarvik
Department of Radiology, Harborview Medical Center, University of Washington, Seattle, WA, USA
e-mail: jarvikj@uw.edu

Key Points

- Currently MRI is the imaging modality of choice for the diagnosis of vertebral osteomyelitis with more than 95 % sensitivity and specificity (strong evidence).
- Radiographic presentations of vertebral osteomyelitis do not appear during the first 3–4 weeks of disease, and X-ray has low sensitivity (82 %) and specificity (57 %) for the diagnosis of vertebral osteomyelitis.
- CT scan is not routinely used for diagnosis of vertebral osteomyelitis and suffers from similar limitations as X-ray.
- Molecular spinal imaging, especially positron emission tomography (PET) with 18 fluorine-fluoro-d-deoxyglucose and PET/CT, is becoming a more valuable complementary test for the diagnosis of vertebral osteomyelitis (limited evidence).
- Molecular imaging is especially valuable in those circumstances that MRI has limited use such as evaluation of the response to treatment or presence of spinal fixation devices (limited evidence).

Definition and Pathophysiology

The three most common sources of vertebral osteomyelitis and discitis are (1) hematogenous spread, (2) direct inoculation due to interventions such as spinal fixation, or (3) spread from an adjacent site of infection such as a paraspinal abscesses [1–4]. Among patients with no risk factors for vertebral osteomyelitis and discitis, *Staphylococcus aureus* is the most common pathogen and is isolated from as much as 50 % of patients. Other organisms are more common among patients with risk factors such as spinal surgeries with internal fixation devices (*Escherichia coli*, coagulase-negative staphylococci, and *Propionibacterium acnes*) [1, 3–5], genitourinary tract instrumentations (*E. coli*) [1, 4, 6], IV drug abuse (*Pseudomonas* and *Candida*) [2, 5–10], and central line placements (*Candida*) [7, 11]. *Mycobacterium tuberculosis*

and *Salmonella* should also be taken into consideration particularly if the patient is an immigrant from a developing country or has a recent history of travel to an area where these infections are endemic [12]. In general, lumbar spine is the most common site for vertebral osteomyelitis and discitis, followed by the thoracic and cervical spine [5, 13, 14].

Epidemiology

Estimating the incidence of vertebral osteomyelitis and discitis in the population is difficult for two major reasons. First, in spite of many other infectious diseases, vertebral osteomyelitis and discitis are not reportable diseases. Second, since the disease is rare, there are no data registries that compile the clinical and epidemiological information about these patients. As a result, the reported incidence of vertebral osteomyelitis and discitis in populations varies from 0.22/ 100,000 [12, 15, 16] to 2.4/100,000 persons [1, 17].

The incidence increases with age (0.3/100,000 among individuals 20 years or younger to 6.5 per 100,000 among persons 70+) [1, 12, 17, 18] and males are at a higher risk than females [12, 18].

It has been suggested that the incidence of disease has been increasing in recent years because of the following issues: aging of the population, increasing use of minimally invasive interventions such as intravascular devices, and increasing use of spinal fixation devices [12]. However, the relative contribution of each one of these factors on the incidence of vertebral osteomyelitis and discitis has yet to be determined.

Overall Cost to Society

There has been no study that has estimated the economic burden of vertebral osteomyelitis and discitis on the US health-care system. The closest study was the estimation of the direct medical costs of low back pain with any etiology, by Martin et al. in 2008 [19]. The authors estimated

that low back pain imposed more than \$86 billion on the US health-care system. Only 1 % of low back pain patients are the result of a potentially life-threatening condition such as vertebral osteomyelitis, discitis, or spinal metastasis [20]. However, the total costs associated with vertebral osteomyelitis cannot be assumed to be 1 % of the total cost of low back pain patients because the direct cost of care varies substantially based on the underlying etiology of low back pain.

Goals of Imaging

Imaging has two main purposes: the timely diagnosis of the infection and the evaluation of the response to treatment.

Methodology

We conducted a systematic review of the literature on vertebral osteomyelitis. We used combinations of the following search terms: "vertebral osteomyelitis," "spine infection," "MRI," "CT scan," "diagnosis," and "imaging," using the online database MEDLINE, to identify peer-reviewed articles that have addressed the role of imaging technology in the diagnosis and management of vertebral osteomyelitis. Our search, which was limited to human studies and the English language, resulted in 1,100–1,300 potential articles. We then reviewed the title and abstract for all of these articles and selected the relevant papers for further evaluation. Additionally, we reviewed the bibliographies of those relevant papers. Finally, we used "up-to-date" (www.uptodate.com) and "dynamed" (www.dynamed.com) databases to determine whether there were any pertinent articles that were not captured using our previously described search strategy.

We categorized published papers based on the "Oxford Centre for Evidence-based Medicine – Levels of Evidence" criteria (http://www.cebm.net/?o=1025). We also considered the "STAndards for the Reporting of Diagnostic accuracy (STARD)" guidelines in the evaluation of each paper [21, 22]. These guidelines were established in order to make the published studies that evaluate the diagnostic accuracy of imaging modalities more uniform and comparable [21, 22].

Discussion of Issues

Low Back Pain and Vertebral Osteomyelitis-Discitis: When Should We Evaluate for Vertebral Osteomyelitis and Discitis as a Potential Cause of Low Back Pain?

In the general population, less than 1 % of low back pain patients have serious conditions such as malignancies or osteomyelitis [23]. Recently, Roudsari and colleagues [20] and Chou et al. [24] summarized the results of the most recent publications that evaluated the role of imaging in the management of LBP. Each of these authors concluded that, in the absence of clinical red flags, use of advanced imaging techniques such as MRI to identify vertebral osteomyelitis and discitis as an underlying cause of low back pain is not warranted. Some of the most important clinical indicators for vertebral osteomyelitis and discitis are fever, malaise, spinal tenderness to percussion, elevated white blood cell count, elevated erythrocyte sedimentation rate (ESR), elevated C-reactive protein, history of IV drug use, recent immigration to the United States (a major risk factor for spine tuberculosis or Pott's disease), history of recent infection, such as urinary tract or skin infections, or history of recent spinal instrumentation, such as placement of spinal fixation devices [20, 24].

Imaging and Vertebral Osteomyelitis-Discitis: Diagnosis and Follow-Up

Summary

In spite of substantial advancements in imaging technology, diagnosis of vertebral osteomyelitis is still challenging. MRI is the imaging modality of choice with a sensitivity and specificity as high as 95 % [25] (strong evidence). X-ray findings do

not appear for weeks after the onset of the disease [26] (limited evidence). CT also has limited value in the diagnosis of vertebral osteomyelitis and discitis [27, 28] (limited evidence). Improvements in radionuclide imaging, especially positron emission tomography (PET) with [18] fluorine-fluoro-d-deoxyglucose ([18F]-FDG), have made them a valuable test for the diagnosis of vertebral osteomyelitis and discitis, particularly in those circumstances that MRI has limited applicability [14]. Considering the cross-sectional or retrospective nature of most diagnostic studies, the level of evidence that can typically be found in the diagnosis of vertebral osteomyelitis using imaging technology would be Oxford Evidence-Based Medicine Levels of 3a or 3b (limited evidence).

Supporting Evidence
X-Ray Radiographic findings of infection are nonspecific and usually do not appear during the first 3–4 weeks [25, 26]. Late, nonspecific findings can include poor cortical definition, lytic bone lesions, and decreased disk height [26]. The reported sensitivity and specificity of X-ray in diagnosing spinal infection are 82 % and 57 %, respectively [25] (limited evidence).

Computed Tomography Generally, CT alone is not used for the diagnosis of vertebral osteomyelitis and discitis. However, in the presence of bone destruction and paraspinal pathologies, such as abscesses, CT provides a better visualization of the magnitude of bone destruction and soft tissue damage compared to X-ray [27, 28]. Similar to radiographs, CT has poor sensitivity and specificity, although no study has evaluated the accuracy of CT in the diagnosis of vertebral osteomyelitis [26] (limited evidence).

Magnetic Resonance Imaging MRI, especially with the use of fat suppression [29], is the preferred method for evaluating vertebral osteomyelitis and discitis because of its ability to visualize the soft tissue, bone marrow, and intervertebral disks [30]. Furthermore, of the available imaging modalities, MRI demonstrates the extent of the disease best [26].

On T1-weighted images, vertebral osteomyelitis will be seen as a low-intensity, ill-defined lesion. In typical, bacterial osteomyelitis, the intervertebral disk will almost always be affected and, as a result, the end plate margins of the disk are indistinguishable from the hypointense lesions in the body of the adjacent vertebrae. T2-weighted images, especially with fat suppression, demonstrate hyperintensity in the bone marrow of the adjacent vertebrae and the intervertebral disk [14]. In tuberculosis and fungal infections, involvement of the disk might not be visible at the beginning, vertebral body destruction is more prominent, and often there is a sharply angulated kyphosis at the site of infection with resultant gibbous deformity [1, 12, 14].

Modic and colleagues reported 96 % sensitivity and 92 % specificity for the diagnosis of spinal infection by MRI, using pathology and clinical course as the gold standard for diagnosis [25] _ENREF_25 (strong evidence). Although use of gadolinium (Gd) increases the specificity of MRI in the diagnosis of other pathologies such as epidural, subdural, and paraspinal soft tissue infections [31–34], no robust study has compared the sensitivity and specificity of MRI with and without contrast for the diagnosis of vertebral infections [35] (insufficient evidence).

MRI does have several limitations. First, similar to other imaging modalities, it lags behind clinical signs and symptoms of the disease. As a result, in the presence of high clinical suspicion for vertebral osteomyelitis and discitis, a follow-up MRI in 7–10 days may detect new involvement. Second, although two adjacent vertebrae and their intervertebral disk are often infected, involvement of both vertebrae may not be visible in the early stages of the disease [26, 36]. Third, age-related changes could mimic MRI findings of infection [36–38]. This decreases the specificity of MRI in older individuals. Moreover, differentiation between severe disk degeneration, ankylosing spondylitis, and neuropathic spine and early stages of vertebral osteomyelitis or atypical vertebral osteomyelitis can be difficult [39–44]. Fortunately, newer MRI techniques such as diffusion-weighted spine imaging or perfusion imaging might improve the precision of MRI in

differentiating vertebral osteomyelitis from other diseases that mimic vertebral osteomyelitis [38, 45] (limited evidence). Fourth, MRI appearance of scar tissue following a surgical intervention is similar to MRI findings in vertebral osteomyelitis and discitis. As a result, evaluation of postsurgical infections is challenging [30, 41]. Fifth, the use of MRI in patients with pacemakers and some artificial heart valves is not recommended [46]. Finally, limited evidence exists supporting the validity of MRI in patient follow-up with vertebral infection [30]. In other words, similar to other imaging modalities, there is no direct association between MRI findings and response to treatment.

Molecular (Functional) Spine Imaging While CT and MRI provide valuable structural information, molecular imaging techniques provide a unique opportunity to identify inflammation/infection at an earlier stage of disease [47, 48]. The most common molecular imaging modalities are discussed below.

Bone Scintigraphy Bone scintigraphy is one of the oldest radionuclide techniques used to evaluate osteomyelitis. Modic et al. reported a sensitivity of 90 % and specificity of 78 % for this technique [25]. The reported sensitivity of bone scintigraphy in a study by Gratz et al. was 86 % and increased to 92 % when it was combined with single-photon emission computed tomography (SPECT) [49] (limited evidence).

Love and colleagues reported sensitivities of 73 % and 82 % for planar bone scanning and planar plus SPECT scanning, respectively, although the reported specificities were low (31 % and 23 %, respectively) [48]. Bone scanning is rarely the only technique for evaluation of vertebral osteomyelitis because of its inability to evaluate the soft tissues [46].

^{67}*Gallium Citrate* ^{67}Gallium is a complement to bone scanning because of its ability to identify soft tissue infections. In addition, it increases the specificity of bone scanning [3, 25, 48, 50, 51]. In spite of these benefits, the time-consuming process and the resultant poor quality imaging of ^{67}gallium has limited its applicability in the diagnosis and management of vertebral osteomyelitis and discitis (limited evidence). Love and colleagues compared the sensitivity and specificity of ^{67}gallium citrate scintigraphy with MRI ($n = 24$) [48]. Authors reported 82 % sensitivity and 77 % specificity for the ^{67}gallium citrate scintigraphy alone. Combination ^{67}gallium citrate scintigraphy and SPECT increased the sensitivity and specificity to 91 % and 92 %, respectively [48].

Streptavidin/^{111}Indium Biotin Complex There have been several studies that have evaluated the use of streptavidin/^{111}indium biotin complex in the diagnosis of vertebral osteomyelitis and discitis. In 2004, Lazeeri and colleagues evaluated this approach on 55 patients with suspected vertebral osteomyelitis and reported 94 % sensitivity and 95 % specificity [52]. In 2008, the same authors investigated ^{111}indium biotin alone on 71 patients with suspected hematogenous vertebral osteomyelitis and 39 patients with postsurgical vertebral osteomyelitis [30]. Considering culture, pathology, clinical course, and up to 1-year follow-up as the gold standard for diagnosis, ^{111}In-biotin scintigraphy demonstrated a sensitivity of 84 % and specificity of 98 % for hematogenous vertebral osteomyelitis and discitis and a sensitivity of 100 % and specificity of 84 % in postsurgical patients [30]. This high success rate has not been reported by other researchers (insufficient to limited evidence). Further studies are needed to evaluate the pros and cons of ^{111}indium biotin-based imaging for the diagnosis and follow-up of vertebral osteomyelitis and discitis.

Radiolabeled White Blood Cells (*WBCs*) Although conceptually this technique could be a valuable tool in the diagnosis of vertebral osteomyelitis and discitis, WBCs labeled with ^{111}In or ^{99m}Tc have limited utility in the diagnosis of vertebral osteomyelitis because of its low sensitivity (30 %) and specificity (30–40 %) [46, 53, 54]. Increase in uptake is strong evidence for accumulation of WBCs; however, the differentiation between infection and other sources of inflammation, such as malignancies or autoimmune diseases, is not possible [46, 53–55].

Moreover, approximately 50 % of vertebral osteomyelitis demonstrate normal to decreased uptake [53].

Positron Emission Tomography (*PET*) *with 18 Fluorine-Fluoro-D-Deoxyglucose* ([¹⁸*F*]-*FDG*)
Fluoro-D-deoxyglucose has a chemical structure similar to glucose. It is transported into cells using the same mechanism as glucose. However, it cannot be utilized as a source of energy. Inflammation increases the number of glucose transporters and results in an increased uptake of [¹⁸F]-FDG at the infection site [46, 47, 56, 57].

[¹⁸F]-FDG-PET is perhaps the most promising radionuclide imaging modality for the diagnosis of vertebral osteomyelitis and discitis for a number of reasons. First, it creates high quality images that enable precise localization of the inflammation site [55]. This is especially true when PET is used in conjunction with CT. Second, PET/CT is fast and requires a low radiation dose compared to gallium citrate, which requires several hours and often more than one clinic visit [46]. Third, the tracer has low uptake in degenerative conditions and old vertebral fractures, most likely due to the limited number of glucose transporters that can transport FDG into the cells [58, 59]. Fourth, in approximately 3–4 months, the FDG uptake returns to its baseline status, while in other bone scan modalities, normalization of the tracer uptake takes much longer [56, 57]. This characteristic makes FDG-PET a more valuable tool in the follow-up of the patients with vertebral osteomyelitis and discitis, compared to other molecular imaging techniques. Fifth, with recent advancements in technology, production and distribution of the FDG has improved substantially [46]. As a result, FDG-PET has become more affordable and less expensive compared to the combination of other molecular imaging techniques with the same precision level [46]. Finally, FDG-PET might have a more prominent role in the diagnosis of vertebral osteomyelitis and discitis in those circumstances that MRI has a limited value such as the presence of metallic implants [7, 55].

Several studies have evaluated the application of FDG-PET for the diagnosis of osteomyelitis and discitis. Gemmel and colleagues have nicely summarized the results of the studies that were published before 2010 [46]. The reviewed studies consisted of study populations that ranged from 5 to 73 subjects. Overall, the authors concluded that FDG-PET and in particular FDG-PET accompanied by CT are very sensitive and relatively specific tools for the diagnosis of vertebral osteomyelitis and discitis [46]. de Winter and colleagues performed one of the largest studies ($n = 73$) in regard to sensitivity and specificity of FDG-PET for the diagnosis of vertebral osteomyelitis and discitis and reported a 100 % sensitivity and 81 % specificity in their study population [7].

In spite of the existing evidence, FDG-PET is a new technique and studies investigating this modality have been limited by small sample sizes (moderate evidence). To date, unfortunately, no RCT or robust cohort study with sufficient sample size has compared the accuracy of FDG-PET with MRI in the diagnosis and follow-up of the patients with vertebral osteomyelitis and discitis.

Applicability to Children Vertebral osteomyelitis and discitis are uncommon among children, compared to adults [60–62], and the diagnosis is more challenging. Early disease may present with fever, hip contracture, and hip pain rather than vertebral pain, which does not present until later stages of the disease [60, 61]. Similar to adults, MRI is the imaging modality of choice [60–62] because of its high sensitivity and specificity and also lack of use of ionizing radiation. Unfortunately, information on the sensitivity and specificity of different advanced imaging modalities in pediatric populations is limited, and current diagnostic approaches are primarily based on the studies that have been conducted in adult populations.

Cost-Effectiveness Analysis Thus far, no study has evaluated the cost-effectiveness of the various imaging approaches for the management of vertebral osteomyelitis and discitis.

Final Diagnosis of Vertebral Osteomyelitis and Discitis: What Is the Role of Percutaneous Versus Open Biopsy?

In general, biopsy is needed to confirm the diagnosis of vertebral osteomyelitis [12], especially when the existing evidence is not typical for such diagnosis [63]. However, biopsy plays a more critical role in the management of vertebral osteomyelitis and discitis when the empiric treatment does not result in expected improvements in clinical signs and symptoms of the disease [63, 64]. The reported sensitivity and specificity of this approach vary significantly among different studies. However, depending on the study setting and subject selection criteria, percutaneous biopsy has had up to 90 % sensitivity and 100 % specificity [64]. The sampled tissue should be sent for aerobic, anaerobic, mycobacterial, and fungal cultures and preferably before empiric antibiotic treatment is started [12]. They should be also sent for pathology for the diagnosis of potential malignant bone lesions that present themselves with the signs and symptoms of infective vertebral osteomyelitis and discitis [65]. Some authors recommend a second percutaneous biopsy if the first attempt is negative [65, 66]. Open biopsy and amplification-based DNA analysis are reserved for those with negative percutaneous biopsy and high suspicion for the disease [12, 63, 67].

The role of percutaneous biopsy for pediatric vertebral osteomyelitis and discitis is not well established. Some authors recommend the use of this approach for atypical forms of infection or when fungal or tuberculosis infection is suspected [68].

Use of Imaging in Evaluation of the Response to Treatment

The drop in plasma level of different biomarkers, such as C-reactive protein, is a sensitive measure for evaluation of the response to treatment [69]. However, there is no such association between response to treatment and imaging findings [36, 70, 71]. This issue is especially challenging when local anatomy is changed as a result of extensive tissue damage or surgical interventions [14].

Special Cases

Hematogenous Versus Postspinal Instrumentation/Surgery Infections

Improvements in surgical techniques have decreased the incidence of postsurgical infections. Nevertheless, as a result of the increase in the number of these procedures, the overall number of patients with postsurgery infections has increased [14]. Persistent pain, fever, and high C-reactive protein [72] are some of the signs and symptoms of these infections. Similar to hematogenous vertebral osteomyelitis and discitis, identification of infection by imaging can only occur after a few days to weeks following the onset of the infection. Structural changes after surgery and the associated inflammation complicate the use of imaging for the early diagnosis of postsurgical infections [73].

In general, it will take approximately 3 weeks before an MRI can identify these infections [14]. Boden et al. reported a good diagnostic value for the triad of "intervertebral disk space enhancement, annular enhancement, and vertebral body enhancement in MRI" in the presence of clinical and laboratory findings, suggesting vertebral osteomyelitis and discitis. The sensitivity and specificity of this triad have not been reported and other studies have not evaluated the accuracy of this triad [14, 45].

Epidural Abscess as a Potential Source of Vertebral Osteomyelitis and Discitis

Spread of infection from an epidural abscess to the spine is an uncommon etiology of vertebral osteomyelitis and discitis. However, these abscesses are associated with a high mortality (20–30 %) [10, 34, 74] and morbidity, in part, as a result of the delay in diagnosis and treatment [14, 74].

The incidence of epidural abscesses is increasing mainly due to the reasons that the incidence of vertebral osteomyelitis and discitis has increased: aging of the population, increase in spinal instrumentation rate, escalating prevalence of IV drug use, etc. [75]. *Staphylococcus aureus* is the most common pathogen affecting more than 60 % of patients with epidural abscesses [75–78]. Epidural abscesses can affect several segments, but most commonly occur in the lower thoracic and lumbar areas [75].

Similar to vertebral osteomyelitis, MRI is the best imaging modality for the diagnosis of epidural abscesses with a reported sensitivity between 91 % [77] and 100 % [78] (moderate to strong evidence).

MRI not only depicts the abscess but also shows the extent of the disease and the associated vertebral osteomyelitis and discitis. Intramedullary infections are also easily identifiable by MRI [4]. Adding gadolinium (Gd) to MRI increases the sensitivity and specificity of MRI for epidural abscesses, although there is limited evidence in this regard [79].

On T1-weighted images, the epidural mass is usually hypointense and on T2-weighted images, it is usually hyperintense. Abscesses usually demonstrate rim enhancement with Gd [74].

Nuclear medicine studies (e.g., technetium, gallium, and indium) have limited value in the diagnosis of epidural abscesses because of the significant proportion of false-negative results [74].

Pott's Disease

Tuberculosis (TB) is an uncommon disease in developed countries, yet it has remained an important concern particularly for immunocompromised patients and immigrants from developing countries. The diagnosis of non-pulmonary TB is often challenging. Spinal TB or Pott's disease is a slowly progressive disease and diagnosis can be delayed for up to 2–3 years [18, 80–82]. Since the body's reaction to TB is immune mediated and not cell mediated, the typical signs of acute infection are usually absent [18, 80, 82, 83]. Spinal TB often starts in the anteroinferior part of a thoracolumbar vertebra, without affecting the adjacent intervertebral disk [84]. It can extend to adjacent vertebral bodies without compromising the intervertebral disk. Under these circumstances, differentiation between TB and malignancies that do not affect intervertebral disk spaces, based on MRI, can be very challenging [6]. Paraspinal extension of the infection is also more common in TB compared to other causes of vertebral osteomyelitis and discitis [83].

Enhancement of the infected vertebrae with Gd-MRI is often more prominent in TB than in pyogenic osteomyelitis [14]. While MRI or Gd-MRI can suggest TB as a potential cause of spinal pathology, they are not sufficient for such a diagnosis. Percutaneous bone biopsy, or open bone biopsy if percutaneous biopsy fails and suspicion for tuberculosis is high, is the gold standard for diagnosis [63].

Take-Home Tables and Figures

Figure 32.1 is an algorithm for evaluation of a patient with spinal pain. Table 32.1 is a summary of the sensitivity, specificity, and accuracy of different imaging modalities. Table 32.2 shows an overall comparison of three different types of vertebral osteomyelitis and discitis.

Imaging Case Studies

Vertebral Osteomyelitis and Discitis of Cervical Spine

MJ is a 49-year-old gentleman who was first seen in the emergency department because of neck pain after ground level fall (Figs. 32.2 through 32.4).

Suggested Imaging Protocols

Table 32.3 shows MRI protocol for evaluation of vertebral osteomyelitis and discitis.

Table 32.1 Summary of the sensitivity, specificity, and accuracy of different imaging modalities

Imaging modality	Sensitivity (%)	Specificity (%)	Accuracy (%)	References
X-ray	82	57	70	[25]
CT scan	NA	NA	NA	
MRI	∼95	∼95	95	[25]
Bone scintigraphy	70–90	30–75	60–70	[48, 49, 55]
[67]Gallium citrate	82	77	80	[48]
[67]Gallium citrate + SPECT	91	92	91	[48, 49]
Streptavidin/[111]indium biotin complex	94	95	94	[30, 52]
Radiolabeled WBC	∼30	30–40	30–35	[46, 53, 54]
FDG-PET	90–100	80–90	85–95	[7, 46]

Table 32.2 Overall comparison of three different types of vertebral osteomyelitis and discitis

	Pyogenic	Postoperative	Tuberculosis
Risk factors	Recent remote infection	Post spine instrumentation of surgery	Recent immigration to the United States
	Recent genitourinary infection		History of travel to an endemic area
	Placement of an intravascular device		
	Intravenous drug abuse		Immunosuppression
	Immunosuppression		
Major clinical signs and symptoms	Rapid onset (usually)	Rapid onset (usually)	Subacute abscess (usually)
	Local tenderness	Local tenderness	Local tenderness
	Back or neck pain, more significant at night	Local pain	Vague pain
	Fever (sometimes)	Fever (sometimes)	Fever (uncommon)
	Neurological deficits (usually a late finding)	Neurological deficits (usually a late finding)	Neurological deficits (sometimes the major initial presentation)
Major laboratory findings	CRP↑, ESR↑, WBC↑	CRP↑, ESR↑, WBC↑	Less helpful laboratory finding
			CRP↑, ESR↑
Imaging findings	Lumbar spine involvement	Site of surgery, usually lumbar spine	Thoracolumbar spine
			Anterior portion of
	Two adjacent vertebrae and the intervertebral disk		vertebral body
			Initially might spare the disk
			Multilevel involvement
			Spinal kyphosis and gibbus formation
			Paraspinal abscesses

Adapted with permission from Gouliouris T, Aliyu SH, Brown NM. Spondylodiscitis: update on diagnosis and management. J Antimicrob Chemother. 2010;65(Suppl 3):iii, 11–24

Table 32.3 MRI protocol for evaluation of vertebral osteomyelitis and discitis

	Sequence no.	1	2	3	4	5	6	7
	Description	3 Plane	Sag T1	Sag IR	AX T1	AX T2	AX T1 Post GAD	Sag T1 Post GAD
	Coil	CTLBOT	LS456	LS456	LS456	LS456	LS456	LS456
Image param	Plane	3 Plane	Sag Obl	Sag Obl	Obl AX	Obl AX	Obl AX	Sag Obl
	Image mode	2D	2D	2D	2D	2D	2D	2D
	Pulse seq	Localizer	SE	FSE-IR	SE	FSE	SE	SE
	PSD					FSE-XL		
	Image options	NPW	NPW, VBw, EDR	NPW, VBw, EDR	NPW, VBw, EDR	FC, NPW, VBw, EDR	NPW, VBw, EDR	NPW, VBw, EDR
				Fast, seq		Zip512, fast		
Scan timing	No. of echoes							
	TE		Min full	34	Min full	110	Min full	Min full
	TR		450	4,000	450	6,000	450	450
	TI			180				
	Flip angle							
	ETL			16		16		
	RBW		15.63		15.63	15.63	15.63	15.63
Scan range	FOV	36	28	28	22	24	22	28
	Thickness	5	4.5	4.5	5	5	5	4.5
	Skip	2	0.5	0.5	1	1	1	0.5
	Scan range		Cover T11 to S2	Cover T11 to S2	Straight stack Through pathology	Straight stack Through pathology	Straight stack Through pathology	Cover T11 to S2
	No. of slices	5 slices/plane	12	12	15	25	15	12
	Sat	a,S,I	a,S,I	a,S,I	a	a,S,I	FAT	FAT,S,I

(continued)

Table 32.3 (continued)

Acq. Time							
Matrix	256 × 128	256 × 224	320 × 256	256 × 192	256 × 192	256 × 192	256 × 224
Freq DIR		A/P	A/P	R/L	R/L	R/L	A/P
NEX	2	2	4	2	4	2	2
Phase FOV							
Flow comp					Slice		
Auto CF	Water	Water	Water	Water	Water	Water	Water
Phase COR			Yes				
Auto shim		Yes	Yes	Yes	Yes	Yes	Yes
Contrast		No	No	No	No	Yes	Yes
Scan time	0.36	3.29	3.18	3.00	4.54	3.00	3.29
comments	Axial T1 straight stack L1 to S1						
	Axial T2 angle thru disk spaces						

Sag sagittal, *Obl* oblique, *AX* axial, *SE* spine echo, *FSE-IR* fast spine echo-inversion recovery, *NPW* no phase wrap, *VBw* variable bandwidth, *FC* flow compensation, *EDR* extended dynamic range, *Min* minimum, *ETL* echo train length, *RBW* receive bandwidth, *FOV* field of view, *SAT* saturation, *a, S, I* anterior, superior, inferior, *NEX* number of excitations, *CF* center frequency
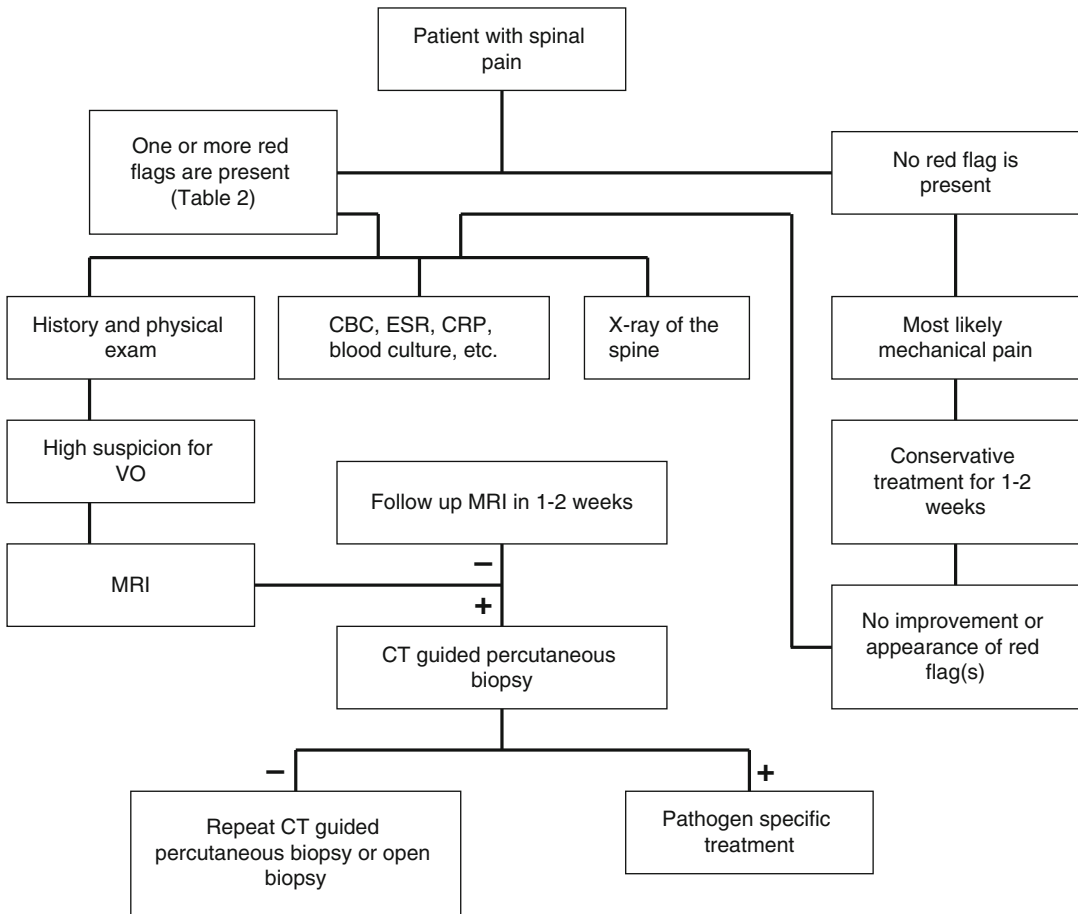
Fig. 32.1 Recommendation for evaluation of a patient with spinal pain

Future Research

Other Imaging Modalities

Magnetic Resonance Spectroscopy (MRS)

While MRI is an excellent tool for evaluation of anatomy, magnetic resonance spectroscopy (MRS) provides invaluable information in regard to biochemical characterization of different pathologies [85–91]. Because of the homogeneity of the brain, easy accessibility, and limited motion artifacts [91], MRS was first used in neuroradiology for the diagnosis of brain tumors [85, 86, 89, 91, 92]. Recently, however, researchers have expanded the use of this technique for other pathophysiological abnormalities,

including epilepsy, prostate and breast malignancies, multiple sclerosis, and even traumatic brain injuries [85, 88, 91]. Unfortunately, there is no study that has investigated the use of MRS in the diagnosis and management of vertebral osteomyelitis and discitis. However, a few studies have investigated the potential role of MRS in LBP management by focusing on disk degeneration [93] and bone marrow changes for evaluation of fracture [94] or possible metastases [95]. It is conceivable that MRS, either alone or in conjunction with MRI, could be a valuable tool for vertebral osteomyelitis and discitis diagnosis.

Diffusion-Weighted MR Imaging (DWI)

Diffusion-weighted MR imaging (DWI) is a newer technique that was developed in early
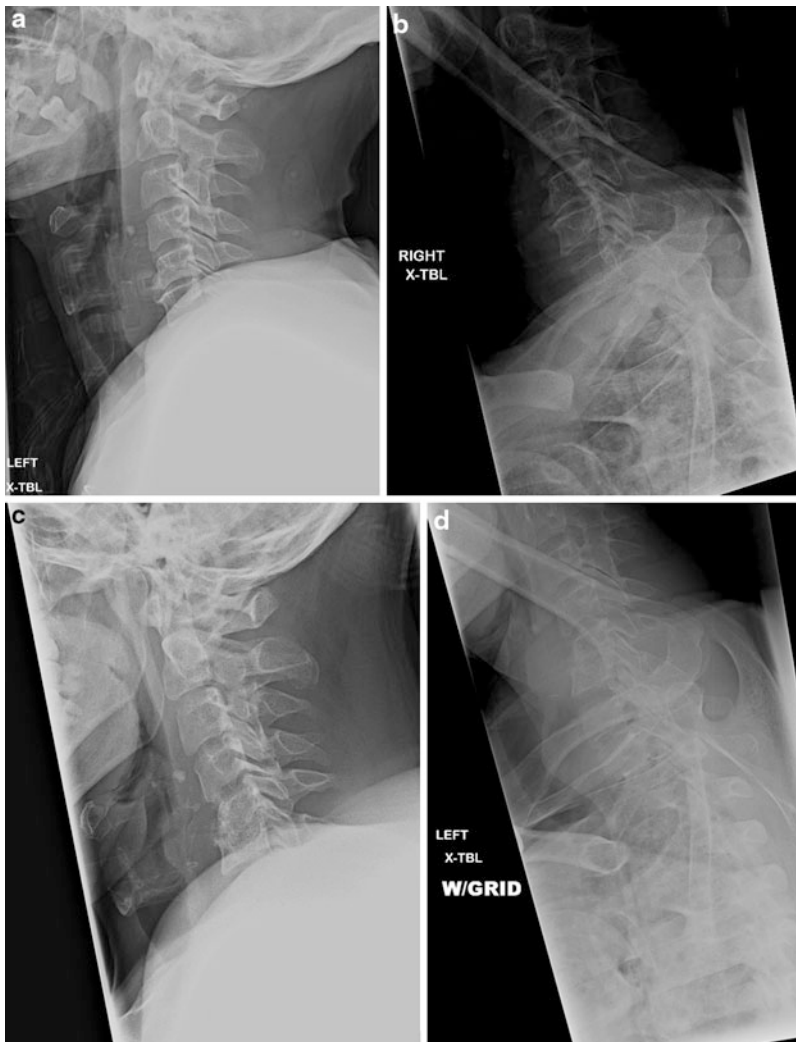
Fig. 32.2 (**a**–**d**). (**a**, **b**) Demonstrates the X-ray findings at the time of emergency department arrival. As presented, there is minimal grade I retrolisthesis of C5 on C6 with disk height loss, consistent with osteoarthritis of cervical spine. The patient was again seen in the emergency department because of exacerbation of the neck pain and local tenderness of the cervical spine 8 weeks after the first visit. (**c**, **d**) Demonstrate the new X-ray findings. Because of the rapid changes in the X-ray findings, local tenderness, and elevated ESR and CRP, with the potential diagnosis of vertebral osteomyelitis and discitis, the patient was admitted to hospital

1990s and was used mainly for the diagnosis of acute brain ischemia [96–99]. In this approach, random movements of water molecules, which might be substantially affected by ischemia, generate images with very high tissue contrast [96–98]. Since DWI uses echo-planar imaging technology, it is much faster than conventional MRI and as a result is highly resistant to motion artifact [88]. In general, imaging time varies from a few seconds to 2 min [88].

Recently, the use of DWI has been adopted for detection of different pathologies, including musculoskeletal issues [96]. Few studies have evaluated the use of DWI for the diagnosis and management of osteosarcoma [100] and spine metastasis [101, 102]. It has also been used for
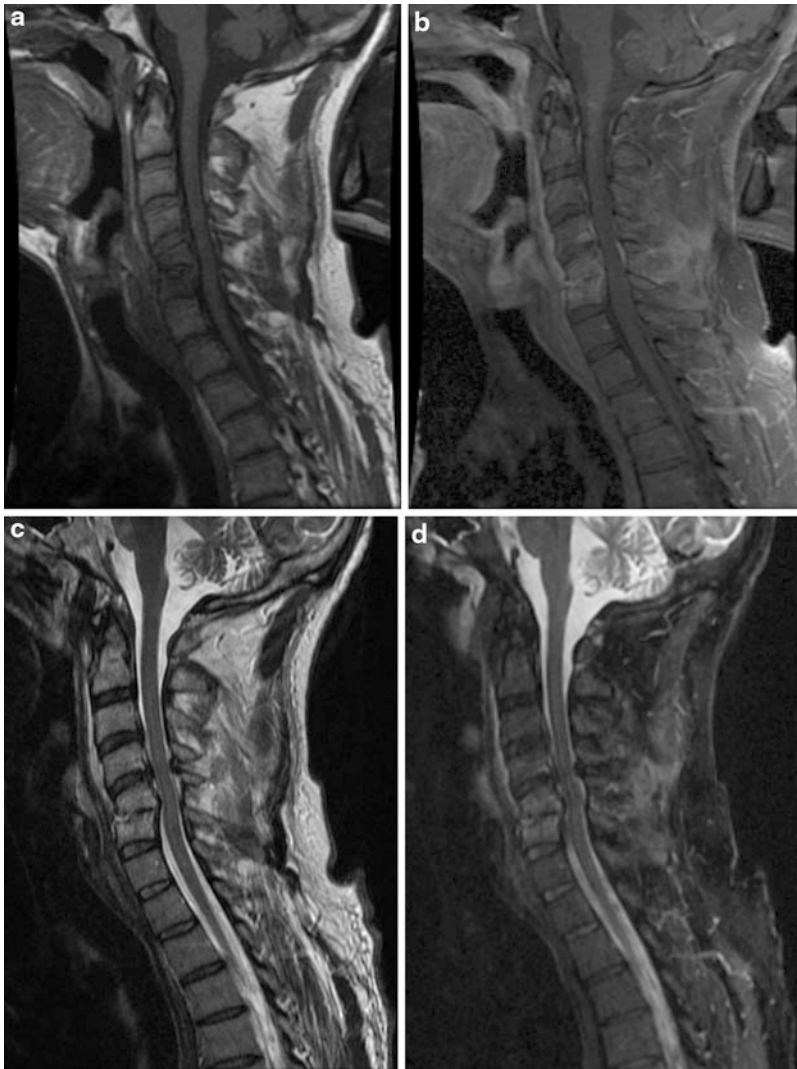
Fig. 32.3 (**a**–**d**) Demonstrates the MRI findings at the time of admission. CT-guided biopsy demonstrated vertebral osteomyelitis and discitis with coagulase-negative staphylococcus sensitive to vancomycin

differentiation between benign and malignant vertebral fractures [103–105] and different intervertebral disk abnormalities [106–109]. Currently, there is minimal evidence in regard to potential value of DWI in the diagnosis and management of vertebral osteomyelitis and discitis.

PET-MRI

While PET-CT has been widely adopted for the evaluation of different pathologies, PET-MRI is in the infancy stages of its development, mainly because of the challenges in combining these two technologies [110]. However, it is conceivable that the combination of MRI and PET would result in early diagnosis of pathologies that would not be diagnosed using other imaging technologies. Currently there are only a few studies that have used prototype PET/MRI scanners, [111] none of which have evaluated vertebral osteomyelitis and discitis.
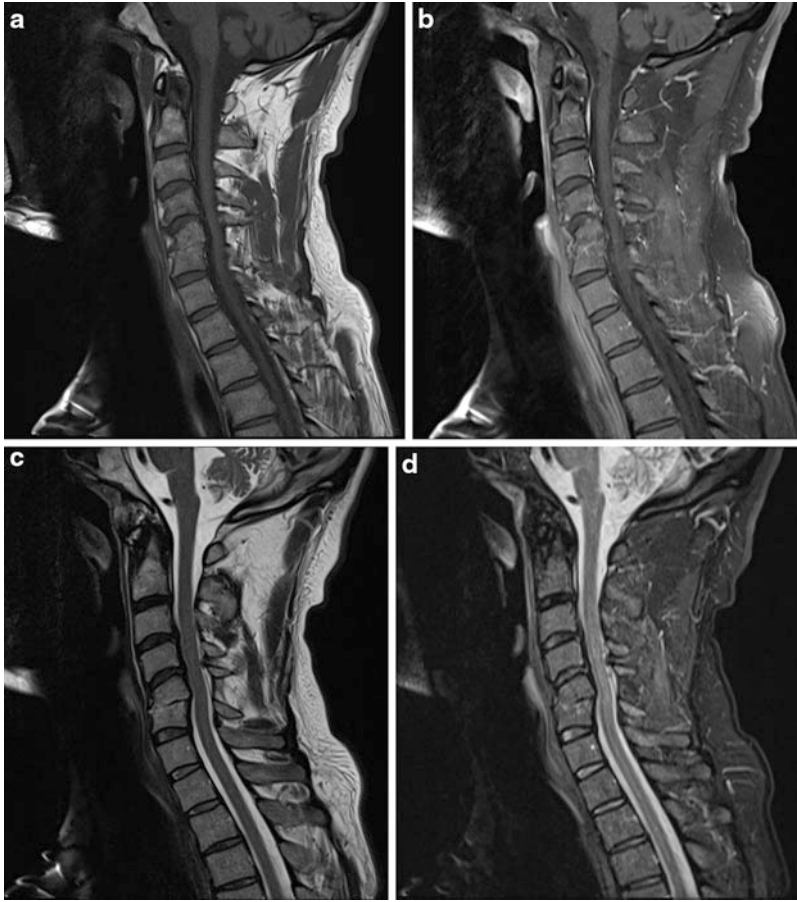
Fig. 32.4 (**a–d**) Demonstrates MRI findings approximately 4 months after completion of antibiotic treatment. At this time, the patient was complaining of severe neck pain with radiation to arms. Cervical fusion was discussed with the patient

Cost-Effectiveness Analysis

Cost-effectiveness analysis has become a more important issue in recent years because of the expecting changes in the US health-care system. As mentioned before, there is no study that has evaluated the cost-effectiveness of different imaging modalities in the diagnosis and management of vertebral osteomyelitis and discitis. This may be due, in part, to the rarity of the disease [20] as well as the difficulty in defining the effectiveness of a diagnostic test compared with a therapeutic intervention [20]. Conventional effectiveness analyses evaluate the potential influence of an intervention on patients' outcome [20].

However, imaging modalities often affect patient outcome through changes in therapeutic decision-making processes [112]. Therefore, the majority of studies in radiology health services research have focused on evaluation of the sensitivity and specificity of a new imaging modality. Given the frequent lack of comparison of the new imaging modality to a different modality as well as the lack of cost information, the conduct of any cost analysis is nearly impossible [20].

Another barrier for the conduct of cost-effectiveness analysis is the lack of robust financial information in the published literature. This includes the true cost of an imaging

modality such as MRI and other costs associated with the diagnostic test such as the monetary value of the reduction in the length of hospital stay [20].

References

1. Zimmerli W. Clinical practice. N Engl J Med. 2010;362(11):1022–9.
2. Bucher E, Trampuz A, Donati L, Zimmerli W. Eur J Clin Microbiol Infect Dis. 2000;19(2):118–20.
3. Adatepe MH, Powell OM, Isaacs GH, Nichols K, Cefola R. J Nucl Med. 1986;27(11):1680–5.
4. Angtuaco EJ, McConnell JR, Chadduck WM, Flanigan S. AJR Am J Roentgenol. 1987;149(6):1249–53.
5. Mylona E, Samarkos M, Kakalou E, Fanourgiakis P, Skoutelis A. Semin Arthritis Rheum. 2009;39(1):10–17.
6. Bell D, Cockshott WP. Radiology. 1971;99(1):43–8.
7. De Winter F, Gemmel F, Van De Wiele C, Poffijn B, Uyttendaele D, Dierckx R. Spine. 2003;28(12):1314–19.
8. Beronius M, Bergman B, Andersson R. Scand J Infect Dis. 2001;33(7):527–32.
9. Chapman M, Murray RO, Stoker DJ. Semin Roentgenol. 1979;14(4):266–82.
10. Stoeckle M, Kaech C, Trampuz A, Zimmerli W. Swiss Med Wkly. 2008;138(35–36):512–19.
11. De Winter F, Huysse W, De Paepe P, Lambert B, Poffyn B, Dierckx R. Clin Nucl Med. 2002;27(2):132–3.
12. Sexton DJ, McDonald M. Vertebral osteomyelitis and discitis. Up to date. 2012.
13. Quinones-Hinojosa A, Jun P, Jacobs R, Rosenberg WS, Weinstein PR. Neurosurg Focus. 2004;17(6):E1.
14. DeSanto J, Ross JS. Radiol Clin North Am. 2011;49(1):105–27.
15. Endress C, Guyot DR, Fata J, Salciccioli G. AJR Am J Roentgenol. 1990;155(2):333–5.
16. Dufour V, Feydy A, Rillardon L, et al. Semin Arthritis Rheum. 2005;34(5):766–71.
17. Grammatico L, Baron S, Rusch E, et al. Epidemiol Infect. 2008;136(5):653–60.
18. Sapico FL, Montgomerie JZ. Rev Infect Dis. 1979;1(5):754–76.
19. Martin BI, Deyo RA, Mirza SK, et al. JAMA. 2008;299(6):656–64.
20. Roudsari B, Jarvik JG. AJR Am J Roentgenol. 2010;195(3):550–9.
21. Bossuyt PM, Reitsma JB, Bruns DE, et al. Acad Radiol. 2003;10(6):664–9.
22. Bossuyt PM, Reitsma JB, Bruns DE, et al. Am J Clin Pathol. 2003;119(1):18–22.
23. Deyo RA, Weinstein JN. N Engl J Med. 2001;344(5):363–70.
24. Chou R, Fu RW, Carrino JA, Deyo RA. Lancet. 2009;373(9662):463–72.
25. Modic M, Feiglin D, Piraino D, et al. Radiology. 1985;157:157–66.
26. Sammer M, Jarvik J. Imaging of adults with low back pain in the primary care setting. In: Medina LS, Blackmore C, editors. Evidence-based imaging: optimizing imaging in patient care. New York: Springer; 2005. p. 294–318.
27. Golimbu C, Firooznia H, Rafii M. AJR Am J Roentgenol. 1984;142(1):159–63.
28. Kattapuram SV, Phillips WC, Boyd R. AJR Am J Roentgenol. 1983;140(6):1199–201.
29. Longo M, Granata F, Ricciardi K, Gaeta M, Blandino A. Eur Radiol. 2003;13(3):626–37.
30. Lazzeri E, Erba P, Perri M, et al. Spine (Phila PA 1976). 2008;33(7):E198–204.
31. Kaufman DM, Kaplan JG, Litman N. Neurology. 1980;30(8):844–50.
32. Hlavin ML, Kaminski HJ, Ross JS, Ganz E. Neurosurgery. 1990;27(2):177–84.
33. Hadjipavlou AG, Cesani-Vazquez F, Villanueva-Meyer J, et al. Am J Orthop (Belle Mead NJ). 1998;27(3):179–83.
34. Tay BK, Deckey J, Hu SS. J Am Acad Orthop Surg. 2002;10(3):188–97.
35. Breslau J, Jarvik JG, Haynor DR, Longstreth Jr WT, Kent DL, Maravilla KR. AJNR Am J Neuroradiol. 1999;20(4):670–5.
36. Gillams AR, Chaddha B, Carter AP. AJR Am J Roentgenol. 1996;166(4):903–7.
37. Dagirmanjian A, Schils J, McHenry MC. Magn Reson Imaging Clin N Am. 1999;7(3):525–38.
38. Hong SH, Choi JY, Lee JW, Kim NR, Choi JA, Kang HS. Radiographics. 2009;29(2):599–612.
39. An HS, Seldomridge JA. Clin Orthop Relat Res. 2006;444:27–33.
40. Ledermann HP, Kaim A, Bongartz G, Steinbrich W. Eur Radiol. 2000;10(11):1815–23.
41. Grane P, Josephsson A, Seferlis A, Tullberg T. Acta Radiol. 1998;39(2):108–15.
42. Kylanpaa-Back ML, Suominen RA, Salo SA, Soiva M, Korkala OL, Mokka RE. Ann Chir Gynaecol. 1999;88(1):61–4.
43. Tali ET, Gultekin S. Eur Radiol. 2005;15(3):599–607.
44. Kowalski TJ, Berbari EF, Huddleston PM, Steckelberg JM, Mandrekar JN, Osmon DR. Clin Infect Dis. 2007;44(7):913–20.
45. Boden SD, Davis DO, Dina TS, Sunner JL, Wiesel SW. Radiology. 1992;184(3):765–71.
46. Gemmel F, Rijk PC, Collins JM, Parlevliet T, Stumpe KD, Palestro CJ. Eur Spine J. 2010;19(4):540–51.
47. Kumar R, Basu S, Torigian D, Anand V, Zhuang H, Alavi A. Clin Microbiol Rev. 2008;21(1):209–24.
48. Love C, Patel M, Lonner BS, Tomas MB, Palestro CJ. Clin Nucl Med. 2000;25(12):963–77.

49. Gratz S, Dorner J, Oestmann JW, et al. Nucl Med Commun. 2000;21(1):111–20.

50. Ma LD, Frassica FJ, Bluemke DA, Fishman EK. Crit Rev Diagn Imaging. 1997;38(6):535–68.

51. Lisbona R, Derbekyan V, Novales-Diaz J, Veksler A. J Nucl Med. 1993;34(5):853–9.

52. Lazzeri E, Pauwels EK, Erba PA, et al. Eur J Nucl Med Mol Imaging. 2004;31(11):1505–11.

53. Palestro CJ, Kim CK, Swyer AJ, Vallabhajosula S, Goldsmith SJ. J Nucl Med. 1991;32(10):1861–5.

54. Termaat MF, Raijmakers PG, Scholten HJ, Bakker FC, Patka P, Haarman HJ. J Bone Joint Surg Am. 2005;87(11):2464–71.

55. Gemmel F, Dumarey N, Palestro CJ. Eur J Nucl Med Mol Imaging. 2006;33(10):1226–37.

56. de Winter F, van de Wiele C, Vogelaers D, de Smet K, Verdonk R, Dierckx RA. J Bone Joint Surg Am. 2001;83-A(5):651–60.

57. Stumpe KD, Strobel K. Q J Nucl Med Mol Imaging. 2006;50(2):131–42.

58. Bredella MA, Essary B, Torriani M, Ouellette HA, Palmer WE. Skeletal Radiol. 2008;37(5):405–13.

59. Schmitz A, Risse JH, Textor J, et al. Osteoporos Int. 2002;13(9):755–61.

60. Mahboubi S, Morris MC. Radiol Clin North Am. 2001;39(2):215–22.

61. Mellado Santos JM. Eur Radiol. 2006;16(9):2109–19.

62. Reiss-Zimmermann M, Hirsch W, Schuster V, Wojan M, Sorge I. J Pediatr Surg. 2010;45(8):1737–40.

63. Gouliouris T, Aliyu SH, Brown NM. J Antimicrob Chemother. 2010;65(Suppl 3):iii11–24.

64. Chew FS, Kline MJ. Radiology. 2001;218(1):211–14.

65. Enoch DA, Cargill JS, Laing R, Herbert S, Corrah TW, Brown NM. J Clin Pathol. 2008;61(6):750–3.

66. Friedman JA, Maher CO, Quast LM, McClelland RL, Ebersold MJ. Surg Neurol. 2002;57(2):81–6.

67. Lecouvet F, Irenge L, Vandercam B, Nzeusseu A, Hamels S, Gala JL. Arthritis Rheum. 2004;50(9):2985–94.

68. Fernandez M, Carrol CL, Baker CJ. Pediatrics. 2000;105(6):1299–304.

69. Przybylski GJ, Sharan AD. J Neurosurg. 2001;94(1 Suppl):1–7.

70. Kowalski TJ, Berbari EF, Huddleston PM, Steckelberg JM, Osmon DR. Clin Infect Dis. 2006;43(2):172–9.

71. Kowalski TJ, Layton KF, Berbari EF, et al. AJNR Am J Neuroradiol. 2007;28(4):693–9.

72. Meyer B, Schaller K, Rohde V, Hassler W. Acta Neurochir (Wien). 1995;136(3–4):145–50.

73. Van Goethem JW, Parizel PM, van den Hauwe L, Van de Kelft E, Verlooy J, De Schepper AM. Neuroradiology. 2000;42(8):580–5.

74. Tompkins M, Panuncialman I, Lucas P, Palumbo M. J Emerg Med. 2010;39(3):384–90.

75. Chao D, Nanda A. Am Fam Physician. 2002;65(7):1341–6.

76. Van Goethem JW, Parizel PM, Jinkins JR. Neuroradiology. 2002;44(9):723–39.

77. Sobottke R, Zarghooni K, Krengel M, et al. Spine (Phila PA 1976). 2009;34(13):E452–8.

78. Shivaram U, Wollschlager C, Khan F, Khan A. South Med J. 1985;78(6):681–4.

79. Post MJ, Sze G, Quencer RM, Eismont FJ, Green BA, Gahbauer H. J Comput Assist Tomogr. 1990;14(5):721–9.

80. Rigamonti D, Liem L, Sampath P, et al. Surg Neurol. 1999;52(2):189–96; discussion 197.

81. Scheidegger C, Zimmerli W. AIDS. 1996;10(12):1407–14.

82. Roelants V, Tang T, Ide C, Laloux P. Semin Nucl Med. 2002;32(3):236–7.

83. Patzakis MJ, Rao S, Wilkins J, Moore TM, Harvey PJ. Clin Orthop Relat Res. 1991;264:178–83.

84. Priest DH, Peacock Jr JE. South Med J. 2005;98(9):854–62.

85. Tran T, Ross B, Lin A. Neurol Clin. 2009;27(1):21–60. xiii.

86. Soares DP, Law M. Clin Radiol. 2009;64(1):12–21.

87. McLean MA, Cross JJ. J Neurosurg. 2009;23(1):5–13.

88. Schaeffter T, Dahnke H. Magnetic resonance imaging and spectroscopy. Handb Exp Pharmacol. 2008;(185 Pt 1):75–90.

89. Prost RW. Med Phys. 2008;35(10):4530–44.

90. Lin AP, Tran TT, Ross BD. NMR Biomed. 2006;19(4):476–83.

91. Gujar SK, Maheshwari S, Bjorkman-Burtscher I, Sundgren PC. J Neuroophthalmol. 2005;25(3):217–26.

92. Rosen Y, Lenkinski RE. Neurotherapeutics. 2007;4(3):330–45.

93. Zuo J, Saadat E, Romero A, et al. Magn Reson Med. 2009;62(5):1140–6.

94. Blake GM, Griffith JF, Yeung DK, Leung PC, Fogelman I. Bone. 2009;44(3):495–501.

95. Chen M, Dang HD, Wang JY, et al. Acta Radiol. 2008;49(5):602–10.

96. Bley TA, Wieben O, Uhl M. Magn Reson Imaging Clin N Am. 2009;17(2):263–75.

97. Koyama T, Tamai K, Togashi K. Int J Clin Oncol. 2006;11(4):278–85.

98. Bammer R. Eur J Radiol. 2003;45(3):169–84.

99. Reeder SB, Mukherjee P. Magn Reson Imaging Clin N Am. 2009;17(2):xi–xii.

100. Meyers PA, Gorlick R, Heller G, et al. J Clin Oncol. 1998;16(7):2452–8.

101. Byun WM, Shin SO, Chang Y, Lee SJ, Finsterbusch J, Frahm J. AJNR Am J Neuroradiol. 2002;23(6):906–12.

102. Uhl M, Saueressig U, Koehler G, et al. Pediatr Radiol. 2006;36(12):1306–11.

103. Holder CA. Magn Reson Imaging Clin N Am. 2000;8(3):675–86.

104. Baur A, Stabler A, Bruning R, et al. Radiology. 1998;207(2):349–56.

105. Baur A, Huber A, Ertl-Wagner B, et al. AJNR Am J Neuroradiol. 2001;22(2):366–72.

106. Kealey SM, Aho T, Delong D, Barboriak DP, Provenzale JM, Eastwood JD. Radiology. 2005; 235(2):569–74.
107. Kurunlahti M, Kerttula L, Jauhiainen J, Karppinen J, Tervonen O. Radiology. 2001; 221(3):779–86.
108. Tokuda O, Okada M, Fujita T, Matsunaga N. J Magn Reson Imaging. 2007;25(1):185–91.
109. Beattie PF, Morgan PS, Peters D. J Orthop Sports Phys Ther. 2008;38(2):42–9.
110. Pichler BJ, Kolb A, Nagele T, Schlemmer HP. J Nucl Med. 2010;51:333–6.
111. Ratib O, Beyer T. Eur J Nucl Med Mol Imaging. 2011;38(6):992–5.
112. Fryback D, Thornbury J. Med Decis Making. 1991;11:88–94.

Pediatric Dysraphism and Scoliosis: Evidence-Based Neuroimaging

33

Geetika Khanna, L. Santiago Medina, Diego Jaramillo, Esperanza Pacheco-Jacome, Martha Ballesteros, Tina Young Poussaint, and Brian E. Grottkau

Contents

G. Khanna (✉)
Mallinckrodt Institute of Radiology, Washington University, St. Louis, MO, USA
e-mail: khannag@mir.wustl.edu

L.S. Medina
Division of Neuroradiology-Neuroimaging, Department of Radiology, Miami Children's Hospital, Miami, FL, USA

Herbert Wertheim College of Medicine, Florida International University, Miami, FL, USA

Former Lecturer in Radiology, Harvard Medical School, Boston, MA, USA
e-mail: smedina@post.harvard.edu; Santiago.medina@mch.com

D. Jaramillo
Department of Radiology, The Children's Hospital of Philadelphia, affiliated with The Perelman School of Medicine at the University of Pennsylvania, Philadelphia, PA, USA
e-mail: Jaramillo@email.chop.edu

E. Pacheco-Jacome • M. Ballesteros
Department of Radiology, Miami Children's Hospital, Miami, FL, USA
e-mail: esperanza.pacheo-jacome@mch.com; Martha.ballesteros@mch.com

T.Y. Poussaint
Department of Radiology, Harvard Medical School, Children's Hospital Boston, Boston, MA, USA
e-mail: tinayoung.poussaint@childrens.harvard.edu

B.E. Grottkau
Department of Orthopaedic Surgery, Massachusetts General Hospital for Children, Harvard University, Boston, MA, USA
e-mail: bgrottkau@partners.org

Key Points

Spinal Dysraphism

- Prenatal screening sonography has high accuracy in detection of open neural tube defects. Fetal MRI is complementary to prenatal sonography for characterizing open neural tube defects and identifying associated abnormalities (moderate evidence).
- The prevalence of occult spinal dysraphism (OSD) ranges from as low as 0.34 % in children with intergluteal dimples to as high as 46 % in newborns with cloacal malformations (moderate evidence).
- Radiographs are relatively insensitive and nonspecific for diagnosing occult spinal dysraphism. Sonography is the most cost-effective imaging modality for evaluation of occult spinal dysraphism in low-risk patients, while MR is the recommended approach in patients at high risk of occult spinal dysraphism. In the intermediate-risk category, sonography or MRI may be used depending on institutional expertise (moderate evidence).

Scoliosis

- Radiographic measurements of scoliosis are reproducible, particularly when the levels of the end plates measured are kept constant and the measurements are made using digital methods (moderate evidence).
- A difference of 6° or more between serial radiographs is the accepted criterion for curve progression in idiopathic scoliosis (moderate evidence). Skeletal maturity, determined by the ossification center of the iliac crest apophysis, is an independent prognostic factor for curve progression in adolescent idiopathic scoliosis (moderate evidence).
- Radiographic monitoring of scoliosis results in an increased risk of radiation-induced breast cancer (moderate evidence). It also worsens reproductive outcome in females (moderate evidence). Radiation exposure to the breast tissue can be reduced by a posteroanterior radiograph of the spine as compared to anteroposterior radiograph (moderate evidence).
- Routine MRI of all children with scoliosis is not recommended. MRI is recommended for children at higher risk of neural axis abnormalities (Table 33.1): (1) children with onset of scoliosis at age less than 11 years, (2) children with idiopathic scoliosis and an abnormal neurological exam, (3) children with severe (>45°) or rapidly progressing curves (>1° per month), and (4) children with disabling or focal back pain (moderate evidence). Thoracic levoscoliosis alone is not a significant risk factor for underlying neural axis abnormalities (limited to moderate evidence).

Definition and Pathophysiology

Spinal Dysraphism

Spinal dysraphism or neural tube defects encompass a heterogeneous group of congenital spinal anomalies that result from the defective closure of the neural tube early in gestation with anomalous development of the caudal cell mass. A clinical neuroradiologic classification system has been developed by Tortori-Donati et al. to help organize the various forms of spinal dysraphism [1]. This system was devised based on a large series of patients seen and imaged at their spina bifida center over a 24-year period. This classification system divides spinal dysraphism into open or closed forms. An open spinal dysraphism (OSD) is present when the neural elements and/or their coverings are exposed through a bone defect and not covered by skin. OSD can then be subdivided into two major diagnoses: myelomeningocele and myelocele, based on the position of the neural placode with respect to the level of the skin surface. When there is elevation because of expansion of the subarachnoid space, the lesion is referred to as a myelomeningocele (MMC). A closed spinal dysraphism (CSD) is skin-covered but frequently suspected clinically due to a subcutaneous mass, hemangioma, or an overlying hairy patch.

Scoliosis

Scoliosis is an abnormal curvature of the spine in the coronal plane that measures more than 10° [2]. Curves that measure 10° or less are called spinal asymmetry. The three main types of scoliosis seen in children are idiopathic, congenital, or neuromuscular (Table 33.2). Idiopathic scoliosis is further subdivided according to the age at onset: infantile (birth to 3 years), juvenile (4–9 years), and most commonly, adolescent (10 years and beyond) [3]. Up to 25 % of cases with idiopathic and juvenile scoliosis have an underlying abnormality of the neural axis like tethered cord, syrinx, or Chiari I malformation. However, the etiology of adolescent idiopathic scoliosis remains uncertain. Congenital scoliosis is caused by vertebral anomalies of embryologic etiology (e.g., hemivertebra, butterfly, or block vertebra) [4]. Neuromuscular scoliosis is typically seen in cerebral palsy and muscular dystrophy. Scoliosis can also be seen in disorders such as neurofibromatosis and Marfan syndrome [5].

Epidemiology

Spinal Dysraphism

The incidence of spinal dysraphism is 1–2 per thousand births and has significant geographic variation [6]. Almost half of all neural tube defects are caused by anencephaly (0.6–0.8 per 1,000 births), and the majority of the remaining are caused by spinal dysraphism (0.5–0.8 per 1,000 births) [7, 8]. The risk of a neural tube defect increases to 2–3 % if one pregnancy has been affected and to 10 % if two pregnancies have been affected [9]. One well-recognized risk factor for this disorder is folate deficiency in the mother. CSDs are more common than OSDs, accounting for 64.2 % of all spinal dysraphism cases [1]. Occult spinal dysraphism is typically undetected at birth and the most common indication for spinal imaging in children [10, 11]. The clinical spectrum of occult dysraphism is broad, ranging from skin stigmata

such as a dimple, sinus tract, hair patch, or hemangioma to motor, bladder, or bowel dysfunction [12–14]. About 50–80 % of occult spinal dysraphic cases exhibit a dermal lesion [15, 16]. However, 3–5 % of all normal children have skin dimples [16, 17].

Scoliosis

Adolescent idiopathic scoliosis (AIS) is the most common form of scoliosis in the pediatric population, accounting for 89 % of all idiopathic scoliosis [18]. Its prevalence and gender distribution depends on the severity of the curve. The overall prevalence of scoliosis (i.e., curves greater than 10°) is 2–3 %, while the prevalence of curves greater than 40° is 0.1 %. Curves greater than 40° are 10 times more common in girls than boys [19]. The etiology of adolescent idiopathic scoliosis remains unclear [20]. Juvenile idiopathic scoliosis (idiopathic scoliosis with age of onset between 4 and 10 years) accounts for 18 % of all idiopathic scoliosis, while infantile scoliosis (idiopathic scoliosis with age of onset between 0 and 3 years) constitutes approximately 8 % of all idiopathic scoliosis [21]. Male predominance is seen in infantile scoliosis. Congenital scoliosis is caused by failure of segmentation and normal formation of spinal elements [4]. In a series of 60 cases of congenital scoliosis, Shahcheraghi and Hobbi [4] found that the most common type of anomaly was a hemivertebra and that the most severe deformity was associated with a unilateral unsegmented bar with a contralateral hemivertebra. Neuromuscular scoliosis can be present in 25–100 % of children with alteration of the normal neuromuscular pathway [20].

Overall Cost to Society

Spinal Dysraphism

Targeted sonographic screening for prenatal detection of spinal dysraphism in mothers with elevated serum alpha-fetoprotein levels has been shown to be cost-effective, with potential annual

savings of $36–$49 million [8]. Average incremental health care expenditure per annum for spinal dysraphism patients has been estimated at $41,460 at age 0, $14,070 at ages 1–17, and $13,339 at ages 18–44 in 2003 [22].

Scoliosis

The reported costs of school screening programs for scoliosis varies widely depending on what is included in estimating the costs and how they are reported. In a population-based, longitudinal retrospective study of one community's school-based scoliosis screening program, the case-finding costs for screening were $24.66 per child screened ($n = 2197$), $3, 386.25 per child with a curve of $20°$ or more ($n = 16$), and $10, 836.00 per child treated for scoliosis ($n = 5$) [23]. The per patient average charge for spinal fusion in children and young adults with idiopathic scoliosis has been estimated at $113,303 [24].

Goals of Imaging

Spinal Dysraphism

With the advent of fetal therapy including surgery, accurate prenatal detection and classification of open versus closed spinal dysraphism is critical for appropriate counseling and perinatal management. The goal of imaging in open spinal dysraphism is early in utero detection of the spinal dysraphism and associated anomalies, so that fetal intervention can be offered to the parents. In patients with closed spinal dysraphism, the goal of imaging is to detect early neurosurgically correctable occult dysraphic lesions in order to prevent neurologic damage, upper urinary tract deterioration, and potential infection of the dorsal dermal sinuses.

Scoliosis

The goal of scoliosis imaging is to confirm the clinical diagnosis of scoliosis, identify the etiology of scoliosis, monitor curve progression, and identify cases that need intervention. Imaging findings can also potentially identify those patients that are more likely to have progressive curves. In post spinal fusion patients, imaging helps in identifying hardware-related complications.

Methodology

The author searched the literature for both primary literature (scientific articles) and secondary literature (evidence-based reviews) on the topics of spinal dysraphism and scoliosis. The National Library of Medicine (NLM) database, MEDLINE, was searched using the PubMed search engine for primary evidence over the period 1966 to April 2011. For spinal dysraphism, articles were retrieved using the following medical subject headings (MeSH) terms that applied to the clinical question: (1) spinal dysraphism, (2) neural tube defect, (3) screening, (4) imaging, (5) MRI or magnetic resonance imaging, (6) CT or computed tomography, and (7) cost-effectiveness. For scoliosis, articles were retrieved using the following medical subject headings (MeSH) terms that applied to the clinical question: (1) scoliosis, (2) screening, (3) imaging, (4) MRI or magnetic resonance imaging, (5) CT or computed tomography, and (6) cost-effectiveness. The following limits were applied to restrict the focus of our search: humans, English language, and all children. The title and abstracts of the retrieved papers were reviewed to find relevant literature. The bibliographies of these articles were also reviewed to identify any other relevant papers.

Discussion of Issues

How Accurate Is Prenatal Imaging in Detection and Classification of Spinal Dysraphism?

Summary
Prenatal sonography has been shown to have high accuracy (sensitivity 92–100 %) in detection

of open neural tube defects (NTDs) (moderate evidence). Prenatal MRI is complementary to ultrasound to detect associated cranial abnormalities in fetuses with open neural tube defects (NTDs) (limited to moderate evidence). Both modalities have limitations in predicting neurologic outcome (moderate evidence).

Supporting Evidence

For over 30 years, maternal serum alpha-fetoprotein (MSAFP), a glycoprotein secreted by the fetal yolk sac and liver, has been used as a screening test for open NTD [25]. The sensitivity and specificity of MSAFP screening have been reported at 75.1 and 97.7 %, respectively [26]. However, an elevated serum alpha-fetoprotein (AFP) is not specific for NTDs as it can be elevated with other anomalies including gastroschisis, omphalocele, congenital nephrosis, and fetal demise [27]. The overall prenatal detection rate of NTDs using screening prenatal ultrasound has been reported at 92–100 % [28–30] (moderate evidence). Gestational age and type of NTD greatly influence the detection rate. While the detection rate of spinal dysraphism in first trimester has been reported at 44 % [31], in the second trimester the detection rate improves to 92–97 % [32–34] (moderate evidence). Detection of closed spinal dysraphism is limited at prenatal imaging, and most of these lesions are not recognized at birth [35].

Sonographic signs used to detect open NTD include the lemon sign and the banana sign [30, 36, 37]. The lemon sign describes the shape of the skull in transverse plane caused by the concavity of the parietal bones. It can be seen in 98 % of cases with open NTD before 24 weeks, but in only 13 % after 24 weeks [30]. Its resolution is thought to be due to increasing ossification of the bony calvarium, increasing intracranial pressure, or both. The banana sign refers to the shape of the cerebellum that is distorted as part of the Chiari II malformation. The banana sign is 99 % sensitive in diagnosing Chiari II malformation and is present in almost all cases of open NTD. Pooled data from

234 fetuses with spina bifida showed that 99 % had at least one cranial finding at less than 24 weeks [38] (moderate evidence). Lemon and banana signs were both seen in 97 % of fetuses, with ventriculomegaly seen in 75 %, cistern magna obliteration in 68 %, and small biparietal diameter in 61 %. Sonographic evaluation of the spine in all three planes is essential to identify the splaying of the pedicles and any associated sac [39]. The use of 3-dimensional ultrasound has been endorsed by the American Institute of Ultrasound in Medicine for identifying vertebral anomalies and detecting the upper level of spinal dysraphism [40, 41] (moderate evidence).

Though prenatal sonography has high accuracy in detection of open neural tube defects, fetal MR imaging can be a helpful adjunct when sonography analysis is limited, such as in cases of large maternal body habitus, oligohydramnios, low position of the fetal head, or when the fetal spine is positioned posteriorly with respect to the mother [42]. Fetal MR imaging is also useful in identifying additional CNS anomalies that are frequently associated with myelomeningoceles/Chiari II malformations, such as callosal agenesis/hypogenesis, periventricular nodular heterotopia, cerebellar dysplasia, syringohydromyelia, and diastematomyelia [43, 44] (limited to moderate evidence). In a study of 100 fetuses that underwent prenatal surgery for meningomyelocele repair, investigators from Vanderbilt University showed that prenatal MR imaging had an agreement rate of 82 % and prenatal US had an agreement rate of 79 %, with postnatal imaging for determining the vertebral level of myelomeningocele [45]. However, they cautioned against predicting neurologic outcome based on prenatal studies alone, as both modalities were noted to misdiagnose the lesion level by two or more segments in at least 20 % of cases (moderate evidence). A recently published randomized control trial of prenatal versus postnatal repair of myelomeningocele has shown reduced need for shunting and improved motor outcomes at 30 months [46] (strong evidence). In light of this

study, fetal MR imaging will become routine when prenatal sonography detects an open neural tube defect.

What Are the Clinical Predictors of Occult Spinal Dysraphism (OSD)?

Summary

The prevalence of OSD ranges from as low as 0.34 % in children with intergluteal dimples to as high as 46 % in newborns with cloacal malformation (moderate evidence). Table 33.3 summarizes the spectrum of occult spinal dysraphism into low-, intermediate-, and high-risk groups.

Supporting Evidence

The clinical spectrum of occult dysraphism is broad, ranging from skin stigmata such as a dimple, sinus tract, hair patch, or hemangioma to motor, bowel, or bladder dysfunction [13, 17, 47]. About 50–80 % of occult spinal dysraphic cases exhibit a dermal lesion; however, 3–5 % of normal children can have skin dimples as well [15, 17, 48]. Based on the clinical features, the risk of occult spinal dysraphism can be divided into low, intermediate, or high [11]. Children in the low-risk group included those with simple skin dimples as the sole manifestation or newborns of diabetic mothers. The prevalence of a dysraphic lesion among low-risk patients has been estimated at 0.3–3.8 % (Table 33.3). In the low range (0.3 %) are children with low intergluteal dimples, while children in the upper range (3.8 %) have higher lumbosacral dimples [19, 27, 31] (moderate and limited evidence).

Children in the intermediate-risk group included those with complex skin stigmata (hairy patch, hemangiomas, lipomas, and well-defined dorsal dermal sinus tracks) or low and intermediate anorectal malformations. The prevalence (pretest probability) of a dysraphic lesion among intermediate-risk patients has been estimated at 27–36 % (moderate evidence). In a study of 114 children with urinary tract symptoms, Tarcan et al. found that abnormal sacral skin findings like dimple, nevus, focal hypertrichosis, or lipoma had

a sensitivity of 0.76 and specificity of 0.77 for abnormal MRI findings (limited evidence) [16]. In a prospective, multicenter study of children with lumbosacral infantile hemangiomas >2.5 cm in size, the prevalence of spinal anomalies was estimated at 35 % [49]. In the same study, ultrasound was found to have a sensitivity of 50 % in the detection of underlying spinal anomalies. The authors concluded that a child with a lumbosacral hemangioma >2.5 cm in size is at high risk of occult spinal dysraphism and should undergo screening with MRI (limited to moderate evidence). Perineal hemangiomas were not classified at risk for occult spinal dysraphism in this study, as the skin over the perineum is not associated with the embryologic development of the neural tube. Children in the high-risk group included those with high anorectal malformations, cloacal malformations, and cloacal exstrophy. The prevalence (pretest probability) of a dysraphic lesion among high-risk patients has been estimated at 44–100 % (moderate evidence).

How Accurate Is Imaging in Occult Spinal Dysraphism?

Summary

Several studies have shown that MRI and ultrasound have better overall sensitivity and specificity than plain radiographs (moderate evidence) for detection of occult spinal dysraphism [11, 47, 50]. Sonography can be performed only in the first 3 months of life, prior to mineralization of the posterior elements of the spine.

Supporting Evidence

The sensitivity and specificity of plain radiographs have been estimated at 80 % (95 % CI: 80–100 %) and 18 % (95 % CI: 11–25 %), respectively [47]. The sensitivity of spinal MRI and ultrasound has been estimated at 95.6 % (95 % CI: 89.8–99.7 %) and 86.5 % (95 % CI: 75–98 %), respectively [50, 51]. The specificity of spinal MRI and ultrasound has been estimated at 90.9 % (95 % CI: 75.7–98.1 %) and 92.0 % (95 % CI: 84–100 %), respectively [50, 51].

What Is the Cost-Effectiveness of Imaging in Children with Occult Spinal Dysraphism?

Summary

Cost-effectiveness analysis (CEA) suggests that, in newborns with suspected OSD, appropriate selection of patients and diagnostic strategy may increase quality-adjusted life expectancy and decrease cost of medical workup.

Supporting Evidence

In low-risk children with an intergluteal dimple or newborns of diabetic mothers (pretest probability = 0.3–0.34 %), ultrasound has been shown to be the most effective strategy with an incremental cost-effectiveness ratio of $55,100 per quality-adjusted life year (QALY) gained [11]. The cost for QALY is less than $100,000 and hence considered a reasonable cost-effective strategy. For children with lumbosacral dimples who have a higher pretest probability of 3.8 %, ultrasound has been shown to be less costly and more effective than MRI, plain radiographs, or no imaging with close clinical follow-up [11].

In intermediate-risk newborns with low anorectal malformation (pretest probability 27 %), ultrasound is more effective and less costly than radiographs and no imaging. However, MRI is more effective than ultrasound at an incremental cost-effectiveness ratio of $1,000 per QALY gained. Therefore, this diagnostic strategy has a very low cost per QALY gained. For the intermediate-risk group, the CEA is sensitive to the costs and diagnostic performances (sensitivity and specificity) of MRI and ultrasound. Lower MRI cost or greater MRI diagnostic performance improves the cost-effectiveness of the MRI strategy, while lower ultrasound cost or greater ultrasound diagnostic performance worsens the cost-effectiveness of the MRI strategy. Therefore, individual or institutional expertise with a specific diagnostic modality (MRI vs. ultrasound) may influence the optimal diagnostic strategy in the intermediate-risk group.

In the high-risk group that includes high anorectal malformations, cloacal malformations, and exstrophy (pretest probability 44–46 %), MRI has been shown to be cost-saving as compared to other diagnostic strategies.

How Should the Radiographic Evaluation of Scoliosis Be Performed?

Summary

Radiographic measurements of scoliosis are reproducible, particularly when using preselected vertebral body levels and measuring electronically (moderate evidence). A difference of five or more degrees between serial radiographs is the accepted criterion for curve progression in idiopathic scoliosis (moderate evidence). If the vertebral end plate is not well profiled, the pedicles can be used to estimate the Cobb angle (limited evidence). Risser grade 0 or 1 is an independent prognostic factor for curve progression in adolescent idiopathic scoliosis (AIS) (moderate evidence).

Supporting Evidence

The most commonly used and the most accurate measurement of spinal curvature is the Cobb angle. The Cobb angle is estimated between the superior end plate of the cranial end vertebra and the inferior end plate of the caudad end vertebra. The end vertebral bodies are the vertebral bodies most tilted to the horizontal. Many articles have addressed the variability in measurement of the Cobb angle in AIS. In a study by Morrisy and colleagues [52], the 95 % CIs for measurement of the Cobb angle was 4.9°, and the variation was greatest when the end vertebral bodies were not preselected (moderate evidence). Carman and colleagues [53] had five observers perform two measurements on 28 radiographs showing kyphosis or scoliosis and found 95 % CIs of 8° for scoliosis and 7° for kyphosis (moderate evidence). A more recent study comparing manual versus computer-assisted radiographic measurements (24 radiographs, six observers) found a statistically significant difference between the 95 % CIs of manual measurements (3.3°) and computer-generated measurements (2.6°) [54]. A 5° difference in the Cobb angle measured

between two radiographs represents a 95 % chance that there is a true difference [55]. Based upon the above data, an increase of Cobb angle by 5° or more is regarded as the criterion for curve progression in idiopathic scoliosis. Variability is greater for congenital scoliosis versus idiopathic scoliosis as presence of segmentation anomalies makes estimation of end plates more difficult. In a study of 318 radiographs on children with idiopathic scoliosis, good correlation has been shown for the Cobb angle estimated by drawing lines parallel to the end plates versus the pedicles [56]. Average intraobserver reliability for Cobb angle measurement was found to be 0.978 and 0.980 for end plate-based and pedicle-based measurements, respectively, using the Pearson correlation test. Similarly, the interobserver reliability was 0.986 for both end plate-based and pedicle-based measurements using the Pearson correlation test. So, if the end plates cannot be clearly visualized due to tilt of the vertebral bodies, the Cobb angle can be estimated by drawing lines parallel to the pedicles.

The skeletal maturity of the child with scoliosis should be assessed by looking at the presence and degree of ossification of the iliac crest apophysis on the scoliosis radiograph. In Risser stage 0, the apophysis is not present. In Risser stages I, II, III, and IV, the apophysis covers 25 %, 50 %, 75 %, and 100 % of the iliac wing, respectively. In stage V the iliac crest apophysis fuses to the pelvis [57, 58]. In a study of 727 patients with idiopathic scoliosis, investigators showed that when the Risser sign was 1 or less, the risk of curve progression was up to 60–70 %, whereas if the patient was Risser 3, the risk of curve progression fell to less than 10 % [59] (moderate evidence).

What Radiation-Induced Complications Result from Radiographic Monitoring of Scoliosis?

Summary

Patients with severe scoliosis are monitored with the use of serial radiographs that expose the body to radiation. Radiographic monitoring of scoliosis results in a clear increase in the risk of breast cancer (moderate evidence). It also results in a high dose of radiation to the ovaries and worsens reproductive outcome in females (moderate evidence). Posteroanterior projection decreases radiation exposure to breast and thyroid.

Supporting Evidence

In 2010, Ronckers and colleagues [60] published a retrospective cohort study on 5,573 women with scoliosis and other spine disorders who were diagnosed between 1912 and 1965 and were exposed to frequent diagnostic X-ray procedures. Diagnostic radiation exposure estimated from radiology files resulted in the estimated average cumulative radiation doses to the breast, lung, thyroid, and bone marrow of 10.9, 4.1, 7.4, and 1.0 cGy, respectively. After a median follow-up period of 47 years, cancer mortality was 8 % higher than expected (95 % CI = 0.97–1.20), and mortality from breast cancer was significantly elevated (standardized mortality ratio = 1.68; 95 % CI: 1.38–2.02). In 2000, the same group had reported a 1.7-fold increased risk of dying from breast cancer (95 % CI, 1.3–2.1) in this cohort after a follow-up of 40.1 years when compared with the general population (moderate evidence) [61]. The data suggested that radiation was the causative factor, with risk increasing significantly with the number of radiographic exposures and the cumulative radiation dose (moderate evidence).

In a large retrospective cohort study of 2,039 patients, Levy and colleagues [62] found an excess lifetime cancer risk of 1–2 % (12–25 cases per 1,000 population) among women (moderate evidence). The same group suggested that replacing the anteroposterior (AP) view with the posteroanterior (PA) view would result in a threefold to sevenfold reduction in cumulative doses to the thyroid gland and the female breast, threefold to fourfold reductions in the lifetime risk of breast cancer, and halving of the lifetime risk of thyroid cancer [62, 63]. The same cohort of women was found to have a higher risk of spontaneous abortions (odds ratio (OR), 1.35; 95 % CI, 1.06–1.73 (moderate evidence)).

There is very limited preliminary data to suggest that scoliosis evaluation with digital radiography decreases radiation exposure. One study reported a decrease in radiation exposure by 31 %; however, this was accompanied by decreasing imaging quality [64]. In a prospective study of 150 patients, where the patients were randomized to one of three imaging techniques, the investigators reported a mean dose-area product of 97.0 cGy cm^2 for conventional films, 31.5 cGy cm^2 for computed radiography, and 5.0 cGy cm^2 for digital fluoroscopy [65] (limited evidence).

What Are the Indications for Magnetic Resonance Imaging in Idiopathic Scoliosis?

Summary

MR imaging is recommended in all cases with infantile and juvenile scoliosis (limited to moderate evidence). Indications for MR imaging in adolescent idiopathic scoliosis include abnormal neurologic exam (moderate evidence), severe or rapidly progressing curve (moderate evidence), and focal or disabling back pain (limited to moderate evidence). A left convex thoracic curve alone is not an indication for MR imaging of AIS (limited evidence). Backache is common in children with AIS and is not an indication for MR (moderate evidence).

Supporting Evidence

Age A high incidence of neural abnormalities has been reported in juvenile and infantile scoliosis. In a study of 26 consecutive children aged less than 11 years, Lewonowski and colleagues [66] found that 19.2 % of children had abnormalities of the neural axis (limited evidence). Gupta and colleagues found that 6 of 34 patients under 10 years of age studied prospectively had neural axis abnormalities such as Chiari I malformation and syrinx [67]. Other abnormalities included dural ectasia, tethered cord, and a brainstem astrocytoma (limited evidence). In a prospective study of 31 children with juvenile idiopathic

scoliosis, the prevalence of neural axis abnormalities was reported at 26 % [68] (limited evidence). In infantile idiopathic scoliosis, up to 22 % have been reported to have underlying abnormalities of neural axis [69].

Back Pain In a retrospective study of 2,442 children with idiopathic scoliosis, 32 % of cases were noted to have backache [70] (moderate evidence). There was a significant association between back pain and an age of more than 15 years, skeletal maturity (a Risser sign of 2 or more), postmenarchal status, and a history of injury. The authors concluded that in a child with idiopathic scoliosis and back pain, if the neurologic exam is normal and the plain radiographs do not reveal additional abnormality, further investigation is not warranted (moderate evidence). In a recent study from Japan, 58.8 % of 51 school children with scoliosis reported back pain [71] (limited evidence). In another study of 1,280 patients with AIS, pain alone was not a risk factor for having an abnormal neuroradiologic evaluation [72].

Neurologic Exam In a study of 93 scoliosis patients, Fujimori et al. reported that abnormal superficial abdominal reflexes had a sensitivity of 89 %, specificity of 95 % for detection of an underlying syrinx [73]. In a study of 72 patients with scoliosis, Morcuende et al. reported that 40 % of cases with an abnormal neurologic exam had an abnormal MRI [74]. Abnormal neurologic exam in this study was characterized by abnormal deep tendon reflexes, asymmetric superficial abdominal reflex, and absent gag reflex (moderate evidence). They reported that the three best predictors of abnormal MRI were a severe curve with abnormal neurologic exam (positive predictive value 0.856), severe curve alone (PPV 0.316), followed by an abnormal neurologic exam alone (PPV 0.286) (limited to moderate evidence).

Left Thoracic Curve The significance of left convex thoracic curves remains controversial. The prevalence of neural axis abnormalities in left convex curves has been reported at

7–23 % [75, 76] (limited evidence). However, Morcuende et al. in their study of 72 patients reported that a left thoracic curve alone was not an indicator of underlying neural axis abnormality [74] (limited evidence).

What Are the Common Neural Axis Abnormalities Encountered in MR Imaging of Scoliosis?

Summary

The neural axis abnormalities most often associated with idiopathic scoliosis include syrinx, Chiari I malformation, tethered cord syndrome, and spinal canal or cord tumors (moderate evidence). Low-lying cerebellar tonsils, without Chiari I malformation, have also been reported in scoliosis (limited to moderate evidence).

Supporting Evidence

Several studies have documented an association between Chiari I malformation and syringomyelia in AIS [74, 77, 78] (moderate evidence). There are several reports of spinal cord tumors like astrocytoma, spinal canal tumors like osteoid osteoma and tethered cord syndrome associated with AIS [76, 77, 79]. Decompression of Chiari I malformation in patients with scoliosis associated with Chiari I malformation and syringomyelia has been shown to lead to stabilization or improvement of the spinal curve [80] (limited evidence). On the other hand, spinal fusion with underlying untreated syrinx can lead to progressive neurologic deterioration (limited evidence) [72, 81]. Recognition of neural axis abnormalities is imperative prior to intervention in scoliosis patients.

The diagnostic criteria for symptomatic Chiari I malformation on MRI of the craniovertebral junction remain somewhat unclear. In the adult population, Barkovich, et al. have shown that using a cutoff of 2 mm below the foramen magnum, the sensitivity and specificity of MRI for detecting symptomatic Chiari I malformation were 100 % and 98.5 %, respectively [82]. If the cutoff was changed to 3 mm, the sensitivity dropped to 96 %, while the specificity improved to 99.5 %. However, the cerebellar tonsils are known to be lower lying in children. Using MRI data from 221 patients without hindbrain pathology, Mikulis et al. proposed that tonsillar ectopia should be considered if the tonsils lie greater than 6 mm below the foramen magnum in the first decade of life or greater than 5 mm below the foramen magnum during the second and third decades of life [83]. Although herniation of greater than 5 mm generally is associated with symptoms, patients who have as much as 12 mm of tonsillar herniation may be asymptomatic [84].

The incidence of tonsillar ectopia in adolescent idiopathic scoliosis has been found to be significantly higher than healthy adolescents (0–4.8 mm below foramen magnum in AIS vs. 0–1.8 in normal controls, $P < 0.01$ (moderate evidence)). Cheng and colleagues studied 36 healthy control subjects, 135 patients with moderately severe adolescent idiopathic scoliosis (Cobb angle less than 45°), and 29 similar patients with Cobb angles greater than 45° [85]. All of the patients were evaluated prospectively with MR imaging looking specifically for tonsillar ectopia and with somatosensory-evoked potentials. Tonsillar ectopia was defined as any inferior displacement of the tonsils, and none of the patients had a displacement greater than 5 mm, which is considered the usual threshold for the diagnosis. Tonsillar ectopia was found in none of the controls, versus 4 of 135 (3 %) and 8 of 29 (27.6 %) of the two scoliotic groups ($P < 0.001$) (moderate evidence). Similarly, the percentages of patients with abnormal somatosensory-evoked potentials were 0 %, 11.9 %, and 27.6 %, respectively. There was a significant association between tonsillar ectopia and abnormal somatosensory function ($P < 0.001$ l correlation coefficient, 0.672) (moderate evidence).

Phase contrast CSF flow studies have been shown to have a sensitivity of 76 % for identifying abnormal flow in symptomatic Chiari I patients and a specificity of 62 % for detecting normal flow in patients with asymptomatic tonsillar ectopia [86]. Patients with Chiari I malformation have been shown to have greater tonsillar excursion during the cardiac cycle compared to

normal subjects, using cardiac gated cine MR images [87]. However, there is currently no data on the diagnostic performance of tonsillar motion in differentiating symptomatic from asymptomatic Chiari I malformation.

Imaging findings that can support the diagnosis of tethered cord include low-lying conus medullaris, dampened motion of the filum, and thick filum terminale (>2 mm) with or without lipomatous infiltration [88, 89]. Neuroimaging can define the anatomical location of the conus medullaris, but the concept and word of "tethered" is a neurophysiological concept which requires clinical input [90]. The normal level of the conus medullaris can vary with the age of the child and can be as low as the bottom of L2 in the immediate newborn period [91, 92]. A more recent study by Soleiman and colleagues studied 635 adult patients with no spinal deformity and demonstrated the mean position of the tip of the conus medullaris at the level of the middle third of L1 [93]. The range extended from the lower third of T11 to the upper third of L3. Although a spinal cord terminating at these normal levels can be tethered, the conus that terminates caudal to the L2–L3 disc space is at much higher risk of being tethered [90–92]. Small fibrolipomas in the filum terminale may be seen in untethered as well as tethered cords. Five to six percent of normal individuals can have variable amounts of fat in the filum terminale [94, 95].

Take-Home Tables and Figures

How Should Physicians Evaluate Newborns with Suspected Occult Spinal Dysraphism?

See Table 33.1 on risk factors for underlying neural axis abnormalities in children with scoliosis and Table 33.2 on types of scoliosis in children. The child being evaluated for OSD should be classified into low, intermediate, or high risk based on the history and physical exam (Table 33.3). In the low-risk category, sonographic evaluation is sufficient to evaluate for OSD. However, the ultrasound has to be

performed by 3 months of age prior to mineralization of the spinal canal. In the intermediate-risk category, the decision to perform US versus MRI depends on the institutional expertise. At a tertiary level pediatric center, sonographic evaluation is appropriate, but if local expertise in

Table 33.1 Risk factors for underlying neural axis abnormalities in children with scoliosis

1.	Age of onset less than 11 years
2.	Focal or disabling back pain
3.	Abnormal neurologic exam
4.	Rapidly progressive curve
5.	Severe curve (>45°) in a skeletally immature child

Table 33.2 Types of scoliosis in children

1. Idiopathic
(a) Infantile (0–3 years)
(b) Juvenile (4–10 years)
(c) Adolescent (11 or more years)
2. Neuromuscular
(a) Neuropathic (e.g., cerebral palsy)
(b) Myopathic (e.g., muscular dystrophy)
3. Congenital

Table 33.3 Risk groups for occult spinal dysraphism

Variable	Baseline risk
Low-risk groups	
Maternal diabetes	0.3 %
Intergluteal dimples	0.34 %
Lumbosacral dimple	3.8 %
Intermediate-risk groups	
Low anorectal malformation	27 %
Intermediate anorectal malformation	33 %
Complex skin stigmata[a]	36 %
High-risk groups	
High anorectal malformation	44 %
Cloacal malformation	46 %
Cloacal exstrophy	100 %

Modified with kind permission of Springer Science + Business Media from Medina LS, Jaramillo D, Pacheco-Jacome E, Ballesteros MC, Grottkau BE. In Medina LS, Blackmore CC, editors. Evidence-based imaging: optimizing imaging in patient care. New York: Springer; 2006
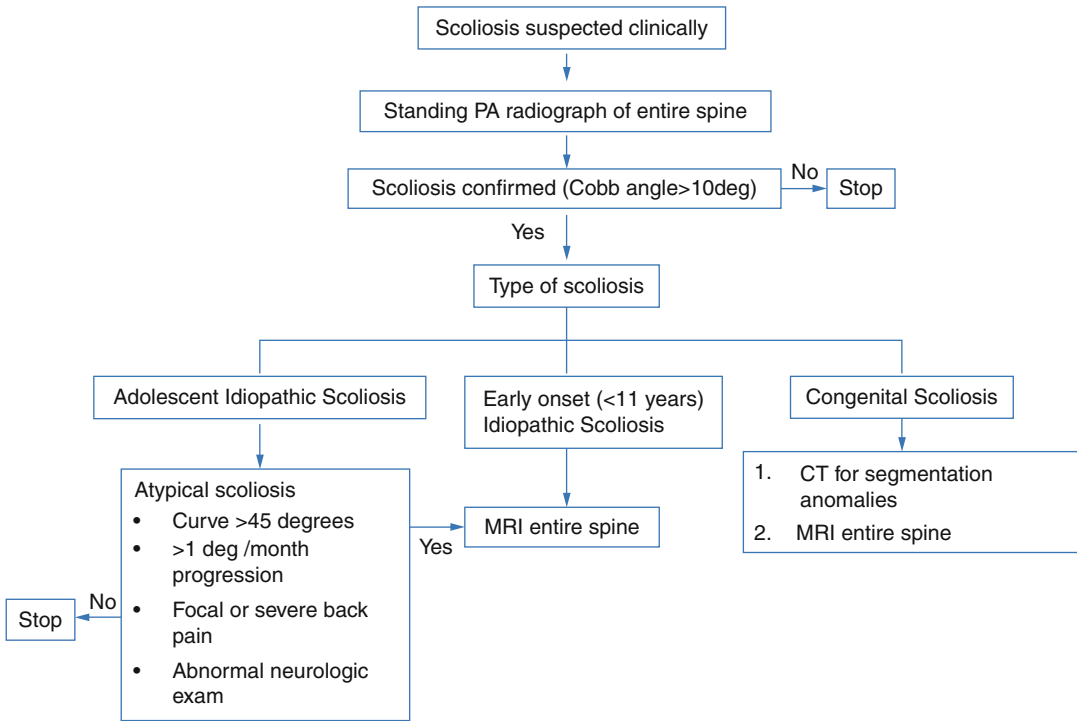[a]Hemangiomas, hairy patches, and subcutaneous masses

Fig. 33.1 Decision tree for patients with suspected scoliosis

sonography is limited, MRI should be considered. All children in the high-risk category should undergo MRI of the spine.

How Should Scoliosis Be Evaluated?

Figure 33.1 summarizes the decision tree for patients with suspected scoliosis.

Imaging Case Study

Case 1: Spinal Dysraphism (Fig. 33.2a–c)
Case 2: Scoliosis (Fig. 33.3a, b)

Suggested Imaging Protocols

Spinal Dysraphism

Spinal Ultrasound. Should be performed before the age of 3 months to avoid limited acoustic window from mineralization of posterior elements. An experience operator should perform the study using a high frequency 5–15 MHz linear array transducer.

Spine MRI. Sagittal and axial T1- and T2-weighted images of the spine. The position of the conus is best determined on the axial images. Intravenous paramagnetic contrast is not routinely used, unless the patient has a communicating dorsal dermal sinus tract or clinical concerns of underlying infection.

Scoliosis

Scoliosis Radiographs. Standing radiograph of the spine to include the cervicothoracic junction superiorly and the sacrum inferiorly. The posteroanterior projection is preferred as it decreases radiation exposure to the breast and thyroid.

Entire Spine MRI. Patients with scoliosis may represent an imaging challenge. In patients with scoliosis behind evaluated with MRI, the entire spine should be covered including the craniocervical junction. Three plain T1- and
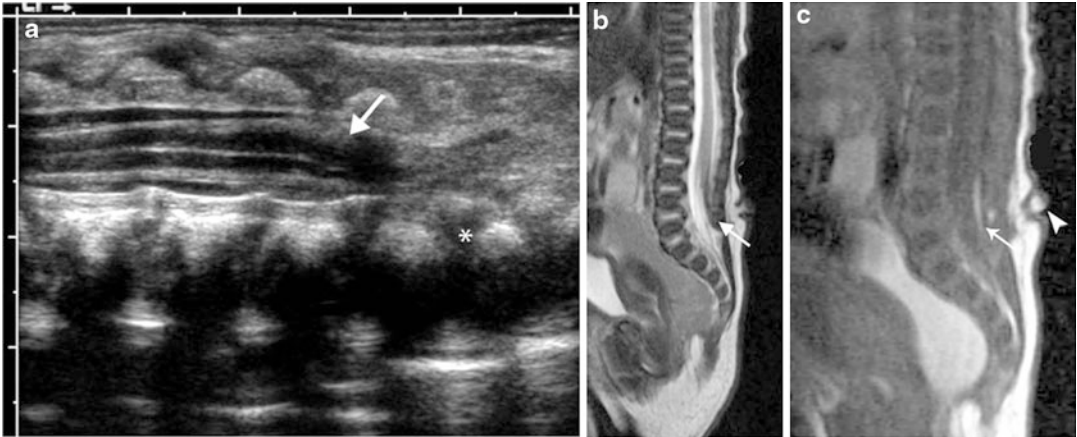
Fig. 33.2 (**a**–**c**) Newborn girl with skin tag noted over lumbosacral junction. Prenatal sonography was normal. (**a**) Sonographic evaluation shows the conus (*arrow*) extending inferiorly to the lumbosacral junction (*), suggesting a tethered cord. Normal tapering of the conus medullaris is absent. (**b**) Sagittal T2-weighted image confirms the tethering of the cord with the conus ending at the L5 level (*arrow*). (**c**) Fatty infiltration of the filum (*arrow*) is noted on the sagittal T1-weighted image which also shows the clinically seen skin tag (*arrowhead*)
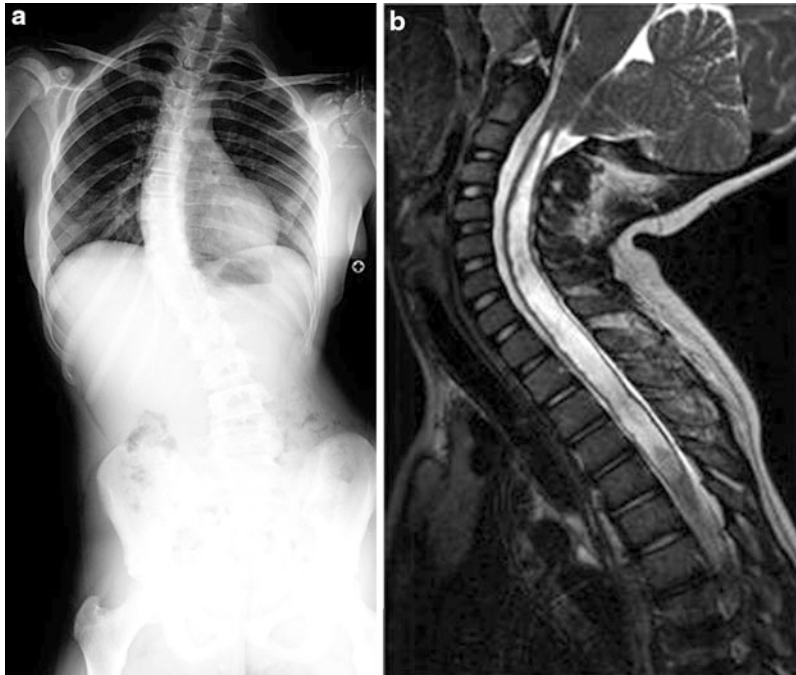
Fig. 33.3 (**a**, **b**) 10-year-old girl with scoliosis. (**a**) Standing posteroanterior radiograph of the spine shows severe thoracic dextroscoliosis. The Cobb angle was estimated at 44°. The presence of a severe curve at a young age led to further evaluation with MRI. (**b**) Sagittal T2-weighted MR image shows low-lying peg-shaped tonsils (Chiari I malformation) with a large syrinx. Post contrast images (not shown) did not show any enhancement to suggest a tumor

T2-weighted images should be obtained with different obliquities to optimize imaging information. If a syrinx is visualized, intravenous contrast is essential to exclude underlying neoplasm.

References

1. Tortori-Donati P, Cama A, Rosa ML, Andreussi L, Taccone A. Occult spinal dysraphism: neuroradiological study. Neuroradiology. 1990;31(6):512–22.
2. Newton P, Wenger D. Idiopathic scoliosis. In: Morrissy R, Weinstein S, editors. Pediatric orthopaedics. Philadelphia: PA Lippincott Williams & Wilkins; 2006. p. 693–762.
3. Oestreich AE, Young LW, Young PT. Scoliosis circa 2000: radiologic imaging perspective. I. Diagnosis and pretreatment evaluation. Skeletal Radiol. 1998;27 (11):591–605.
4. Shahcheraghi GH, Hobbi MH. Patterns and progression in congenital scoliosis. J Pediatr Orthop. 1999;19 (6):766–75.
5. Jaramillo D, Poussaint TY, Grottkau BE. Scoliosis: evidence-based diagnostic evaluation. Neuroimaging Clin N Am. 2003;13(2):335–41, xii.
6. Frey L, Hauser WA. Epidemiology of neural tube defects. Epilepsia. 2003;44(Suppl 3):4–13.
7. Knight GJ, Palomaki GF. Maternal serum screening for fetal genetic disorders. New York: Churchill Livingstone; 1992.
8. Vintzileos AM, Ananth CV, Fisher AJ, Smulian JC, Day-Salvatore D, Beazoglou T, et al. Cost-benefit analysis of targeted ultrasonography for prenatal detection of spina bifida in patients with an elevated concentration of second-trimester maternal serum alpha-fetoprotein. Am J Obstet Gynecol. 1999;180(5):1227–33.
9. Cameron M, Moran P. Prenatal screening and diagnosis of neural tube defects. Prenat Diagn. 2009;29 (4):402–11.
10. Egelhoff JC, Prenger EC, Coley BD. Neuroradiology. Philadelphia: Lippincott-Raven Publishers; 1997.
11. Medina LS, Crone K, Kuntz KM. Newborns with suspected occult spinal dysraphism: a cost-effectiveness analysis of diagnostic strategies. Pediatrics. 2001;108(6):E101.
12. Brophy JD, Sutton LN, Zimmerman RA, Bury E, Schut L. Magnetic resonance imaging of lipomyelomeningocele and tethered cord. Neurosurgery. 1989;25(3):336–40.
13. Moufarrij NA, Palmer JM, Hahn JF, Weinstein MA. Correlation between magnetic resonance imaging and surgical findings in the tethered spinal cord. Neurosurgery. 1989;25(3):341–6.
14. Raghavan N, Barkovich AJ, Edwards M, Norman D. MR imaging in the tethered spinal cord syndrome. AJR Am J Roentgenol. 1989;152(4):843–52.
15. Hoffman HJ, Hendrick EB, Humphreys RP. The tethered spinal cord: its protean manifestations, diagnosis

and surgical correction. Childs Brain. 1976;2(3): 145–55.
16. Tarcan T, Tinay I, Temiz Y, Alpay H, Ozek M, Simsek F. The value of sacral skin lesions in predicting occult spinal dysraphism in children with voiding dysfunction and normal neurological examination. J Pediatr Urol. 2012;8(1):55–8.
17. Kriss VM, Desai NS. Occult spinal dysraphism in neonates: assessment of high-risk cutaneous stigmata on sonography. AJR Am J Roentgenol. 1998;171 (6):1687–92.
18. Riseborough EJ, Wynne-Davies R. A genetic survey of idiopathic scoliosis in Boston, Massachusetts. J Bone Joint Surg Am. 1973;55(5):974–82.
19. Miller NH. Cause and natural history of adolescent idiopathic scoliosis. Orthop Clin North Am. 1999;30 (3):343–52, vii.
20. Campos MA, Weinstein SL. Pediatric scoliosis and kyphosis. Neurosurg Clin N Am. 2007;18(3):515–29.
21. Al-Arjani AM, Al-Sebai MW, Al-Khawashki HM, Saadeddin MF. Epidemiological patterns of scoliosis in a spinal center in Saudi Arabia. Saudi Med J. 2000;21(6):554–7.
22. Ouyang L, Grosse SD, Armour BS, Waitzman NJ. Health care expenditures of children and adults with spina bifida in a privately insured U.S. population. Birth Defects Res A Clin Mol Teratol. 2007;79(7):552–8.
23. Yawn BP, Yawn RA. The estimated cost of school scoliosis screening. Spine (Phila Pa 1976). 2000;25 (18):2387–91.
24. Daffner SD, Beimesch CF, Wang JC. Geographic and demographic variability of cost and surgical treatment of idiopathic scoliosis. Spine (Phila Pa). 1976;35 (11):1165–9.
25. Habib ZA. Maternal serum alpha-feto-protein: its value in antenatal diagnosis of genetic disease and in obstetrical-gynaecological care. Acta Obstet Gynecol Scand Suppl. 1977;61:1–92.
26. Wang ZP, Li H, Hao LZ, Zhao ZT. The effectiveness of prenatal serum biomarker screening for neural tube defects in second trimester pregnant women: a meta-analysis. Prenat Diagn. 2009;29(10):960–5.
27. Bradley LA, Palomaki GE, McDowell GA. Technical standards and guidelines: prenatal screening for open neural tube defects. Genet Med. 2005;7(5):355–69.
28. Nicolaides KH, Campbell S, Gabbe SG, Guidetti R. Ultrasound screening for spina bifida: cranial and cerebellar signs. Lancet. 1986;2(8498):72–4.
29. Platt LD, Feuchtbaum L, Filly R, Lustig L, Simon M, Cunningham GC. The California Maternal Serum alpha-Fetoprotein Screening Program: the role of ultrasonography in the detection of spina bifida. Am J Obstet Gynecol. 1992;166(5):1328–9.
30. Van den Hof MC, Nicolaides KH, Campbell J, Campbell S. Evaluation of the lemon and banana signs in one hundred thirty fetuses with open spina bifida. Am J Obstet Gynecol. 1990;162(2):322–7.
31. Taipale P, Ammala M, Salonen R, Hiilesmaa V. Learning curve in ultrasonographic screening for

selected fetal structural anomalies in early pregnancy. Obstet Gynecol. 2003;101(2):273–8.

32. Grandjean H, Larroque D, Levi S. The performance of routine ultrasonographic screening of pregnancies in the Eurofetus Study. Am J Obstet Gynecol. 1999;181 (2):446–54.

33. Smith NC, Hau C. A six year study of the antenatal detection of fetal abnormality in six Scottish health boards. Br J Obstet Gynaecol. 1999;106(3):206–12.

34. Lennon CA, Gray DL. Sensitivity and specificity of ultrasound for the detection of neural tube and ventral wall defects in a high-risk population. Obstet Gynecol. 1999;94(4):562–6.

35. Simon EM, Pollock AN. Prenatal and postnatal imaging of spinal dysraphism. Semin Roentgenol. 2004;39 (2):182–96.

36. Blaas HG, Eik-Nes SH. Sonoembryology and early prenatal diagnosis of neural anomalies. Prenat Diagn. 2009;29(4):312–25.

37. D'Addario V, Rossi AC, Pinto V, Pintucci A, Di Cagno L. Comparison of six sonographic signs in the prenatal diagnosis of spina bifida. J Perinat Med. 2008;36(4):330–4.

38. Watson WJ, Chescheir NC, Katz VL, Seeds JW. The role of ultrasound in evaluation of patients with elevated maternal serum alpha-fetoprotein: a review. Obstet Gynecol. 1991;78(1):123–8.

39. Bulas D. Fetal evaluation of spine dysraphism. Pediatr Radiol. 2010;40(6):1029–37.

40. Goncalves LF, Lee W, Espinoza J, Romero R. Three- and 4-dimensional ultrasound in obstetric practice: does it help? J Ultrasound Med. 2005;24(12): 1599–624.

41. Benacerraf BR, Benson CB, Abuhamad AZ, Copel JA, Abramowicz JS, Devore GR, et al. Three- and 4-dimensional ultrasound in obstetrics and gynecology: proceedings of the American Institute of Ultrasound in Medicine Consensus Conference. J Ultrasound Med. 2005;24(12):1587–97.

42. Glenn OA, Barkovich J. Magnetic resonance imaging of the fetal brain and spine: an increasingly important tool in prenatal diagnosis: part 2. AJNR Am J Neuroradiol. 2006;27(9):1807–14.

43. Wolpert SM, Anderson M, Scott RM, Kwan ES, Runge VM. Chiari II malformation: MR imaging evaluation. AJR Am J Roentgenol. 1987;149(5):1033–42.

44. Gilbert JN, Jones KL, Rorke LB, Chernoff GF, James HE. Central nervous system anomalies associated with meningomyelocele, hydrocephalus, and the Arnold-Chiari malformation: reappraisal of theories regarding the pathogenesis of posterior neural tube closure defects. Neurosurgery. 1986;18(5):559–64.

45. Aaronson OS, Hernanz-Schulman M, Bruner JP, Reed GW, Tulipan NB. Myelomeningocele: prenatal evaluation–comparison between transabdominal US and MR imaging. Radiology. 2003;227(3):839–43.

46. Adzick NS, Thom EA, Spong CY, Brock JW, 3rd, Burrows PK, Johnson MP, et al. A randomized trial of prenatal versus postnatal repair of myelomeningocele. N Engl J Med. 2011;364(11): 993–1004.

47. Horton D, Barnes P, Pendleton BD, Pollay M. Spina bifida occulta: early clinical and radiographic diagnosis. J Okla State Med Assoc. 1989;82(1):15–9.

48. Volpe JJ. Neurology of the newborn. 4th ed. Philadelphia: W.B. Saunders; 2001.

49. Drolet BA, Chamlin SL, Garzon MC, Adams D, Baselga E, Haggstrom AN, et al. Prospective study of spinal anomalies in children with infantile hemangiomas of the lumbosacral skin. J Pediatr. 2010;157 (5):789–94.

50. Rohrschneider WK, Forsting M, Darge K, Troger J. Diagnostic value of spinal US: comparative study with MR imaging in pediatric patients. Radiology. 1996;200(2):383–8.

51. Santiago Medina L, al-Orfali M, Zurakowski D, Poussaint TY, DiCanzio J, Barnes PD. Occult lumbosacral dysraphism in children and young adults: diagnostic performance of fast screening and conventional MR imaging. Radiology. 1999;211(3):767–71.

52. Morrissy RT, Goldsmith GS, Hall EC, Kehl D, Cowie GH. Measurement of the Cobb angle on radiographs of patients who have scoliosis. Evaluation of intrinsic error. J Bone Joint Surg Am. 1990;72(3):320–7.

53. Carman DL, Browne RH, Birch JG. Measurement of scoliosis and kyphosis radiographs. Intraobserver and interobserver variation. J Bone Joint Surg Am. 1990;72(3):328–33.

54. Shea KG, Stevens PM, Nelson M, Smith JT, Masters KS, Yandow S. A comparison of manual versus computer-assisted radiographic measurement. Intraobserver measurement variability for Cobb angles. Spine. 1998;23(5):551–5.

55. Pruijs JE, Hageman MA, Keessen W, van der Meer R, van Wieringen JC. Variation in Cobb angle measurements in scoliosis. Skeletal Radiol. 1994;23(7): 517–20.

56. Mehta SS, Modi HN, Srinivasalu S, Chen T, Suh SW, Yang JH, et al. Interobserver and intraobserver reliability of Cobb angle measurement: endplate versus pedicle as bony landmarks for measurement: a statistical analysis. J Pediatr Orthop. 2009;29(7):749–54.

57. Risser JC. The Iliac apophysis; an invaluable sign in the management of scoliosis. Clin Orthop. 1958;11:111–9.

58. Risser JC. The classic: the iliac apophysis: an invaluable sign in the management of scoliosis. Clin Orthop Relat Res. 2009;468(3):643–53.

59. Lonstein JE, Carlson JM. The prediction of curve progression in untreated idiopathic scoliosis during growth. J Bone Joint Surg Am. 1984;66(7):1061–71.

60. Ronckers CM, Land CE, Miller JS, Stovall M, Lonstein JE, Doody MM. Cancer mortality among women frequently exposed to radiographic examinations for spinal disorders. Radiat Res. 2010;174 (1):83–90.

61. Doody MM, Lonstein JE, Stovall M, Hacker DG, Luckyanov N, Land CE. Breast cancer mortality

after diagnostic radiography: findings from the U.S. Scoliosis Cohort Study. Spine (Phila Pa 1976). 2000;25(16):2052–63.

62. Levy AR, Goldberg MS, Mayo NE, Hanley JA, Poitras B. Reducing the lifetime risk of cancer from spinal radiographs among people with adolescent idiopathic scoliosis. Spine. 1996;21(13):1540–7; discussion 8.

63. Levy AR, Goldberg MS, Hanley JA, Mayo NE, Poitras B. Projecting the lifetime risk of cancer from exposure to diagnostic ionizing radiation for adolescent idiopathic scoliosis. Health Phys. 1994;66(6):621–33.

64. Geijer H, Verdonck B, Beckman KW, Andersson T, Persliden J. Digital radiography of scoliosis with a scanning method: radiation dose optimization. Eur Radiol. 2003;13(3):543–51.

65. Kluba T, Schafer J, Hahnfeldt T, Niemeyer T. Prospective randomized comparison of radiation exposure from full spine radiographs obtained in three different techniques. Eur Spine J. 2006;15(6):752–6.

66. Lewonowski K, King JD, Nelson MD. Routine use of magnetic resonance imaging in idiopathic scoliosis patients less than eleven years of age. Spine (Phila Pa 1976). 1992;17(Suppl 6):S109–16.

67. Gupta P, Lenke LG, Bridwell KH. Incidence of neural axis abnormalities in infantile and juvenile patients with spinal deformity. Is a magnetic resonance image screening necessary? Spine (Phila Pa 1976). 1998;23(2):206–10.

68. Evans SC, Edgar MA, Hall-Craggs MA, Powell MP, Taylor BA, Noordeen HH. MRI of 'idiopathic' juvenile scoliosis. A prospective study. J Bone Joint Surg Br. 1996;78(2):314–7.

69. Dobbs MB, Lenke LG, Szymanski DA, Morcuende JA, Weinstein SL, Bridwell KH, et al. Prevalence of neural axis abnormalities in patients with infantile idiopathic scoliosis. J Bone Joint Surg Am. 2002;84-A(12):2230–4.

70. Ramirez N, Johnston CE, Browne RH. The prevalence of back pain in children who have idiopathic scoliosis. J Bone Joint Surg Am. 1997;79(3):364–8.

71. Sato T, Hirano T, Ito T, Morita O, Kikuchi R, Endo N, et al. Back pain in adolescents with idiopathic scoliosis: epidemiological study for 43,630 pupils in Niigata City, Japan. Eur Spine J. 2011;20(2):274–9.

72. Davids JR, Chamberlin E, Blackhurst DW. Indications for magnetic resonance imaging in presumed adolescent idiopathic scoliosis. J Bone Joint Surg Am. 2004;86-A(10):2187–95.

73. Fujimori T, Iwasaki M, Nagamoto Y, Sakaura H, Oshima K, Yoshikawa H. The utility of superficial abdominal reflex in the initial diagnosis of scoliosis: a retrospective review of clinical characteristics of scoliosis with syringomyelia. Scoliosis. 2010;5:17.

74. Morcuende JA, Dolan LA, Vazquez JD, Jirasirakul A, Weinstein SL. A prognostic model for the presence of neurogenic lesions in atypical idiopathic scoliosis. Spine. 2004;29(1):51–8.

75. Mejia EA, Hennrikus WL, Schwend RM, Emans JB. A prospective evaluation of idiopathic left thoracic scoliosis with magnetic resonance imaging. J Pediatr Orthop. 1996;16(3):354–8.

76. Schwend RM, Hennrikus W, Hall JE, Emans JB. Childhood scoliosis: clinical indications for magnetic resonance imaging. J Bone Joint Surg Am. 1995;77 (1):46–53.

77. Barnes PD, Brody JD, Jaramillo D, Akbar JU, Emans JB. Atypical idiopathic scoliosis: MR imaging evaluation. Radiology. 1993;186(1):247–53.

78. Nakahara D, Yonezawa I, Kobanawa K, Sakoda J, Nojiri H, Kamano S, et al. Magnetic resonance imaging evaluation of patients with idiopathic scoliosis: a prospective study of four hundred seventy-two outpatients. Spine (Phila Pa 1976). 2011;36(7): E482-5.

79. Taylor LJ. Painful scoliosis: a need for further investigation. Br Med J (Clin Res Ed). 1986;292 (6513):120–2.

80. Eule JM, Erickson MA, O'Brien MF, Handler M. Chiari I malformation associated with syringomyelia and scoliosis: a twenty-year review of surgical and nonsurgical treatment in a pediatric population. Spine (Phila Pa 1976). 2002;27(13):1451–5.

81. Ozerdemoglu RA, Transfeldt EE, Denis F. Value of treating primary causes of syrinx in scoliosis associated with syringomyelia. Spine (Phila Pa 1976). 2003;28(8):806–14.

82. Barkovich AJ, Wippold FJ, Sherman JL, Citrin CM. Significance of cerebellar tonsillar position on MR. AJNR Am J Neuroradiol. 1986;7(5):795–9.

83. Mikulis DJ, Diaz O, Egglin TK, Sanchez R. Variance of the position of the cerebellar tonsils with age: preliminary report. Radiology. 1992;183(3):725–8.

84. Armonda RA, Citrin CM, Foley KT, Ellenbogen RG. Quantitative cine-mode magnetic resonance imaging of Chiari I malformations: an analysis of cerebrospinal fluid dynamics. Neurosurgery. 1994;35(2):214–23; discussion 23–4.

85. Cheng JC, Guo X, Sher AH, Chan YL, Metreweli C. Correlation between curve severity, somatosensory evoked potentials, and magnetic resonance imaging in adolescent idiopathic scoliosis. Spine (Phila Pa 1976). 1999;24(16):1679–84.

86. Hofkes SK, Iskandar BJ, Turski PA, Gentry LR, McCue JB, Haughton VM. Differentiation between symptomatic Chiari I malformation and asymptomatic tonsilar ectopia by using cerebrospinal fluid flow imaging: initial estimate of imaging accuracy. Radiology. 2007;245(2):532–40.

87. Cousins J, Haughton V. Motion of the cerebellar tonsils in the foramen magnum during the cardiac cycle. AJNR Am J Neuroradiol. 2009;30(8):1587–8.

88. Brown E, Matthes JC, Bazan C, 3rd, Jinkins JR. Prevalence of incidental intraspinal lipoma of the lumbosacral spine as determined by MRI. Spine (Phila Pa 1976). 1994;19(7):833–6.

89. Uchino A, Mori T, Ohno M. Thickened fatty filum terminale: MR imaging. Neuroradiology. 1991;33 (4):331–3.

90. Warder DE, Oakes WJ. Tethered cord syndrome and the conus in a normal position. Neurosurgery. 1993;33 (3):374–8.
91. DiPietro MA. The conus medullaris: normal US findings throughout childhood. Radiology. 1993;188 (1):149–53.
92. Wilson DA, Prince JR. John Caffey award. MR imaging determination of the location of the normal conus medullaris throughout childhood. AJR Am J Roentgenol. 1989;152(5):1029–32.
93. Soleiman J, Demaerel P, Rocher S, Maes F, Marchal G. Magnetic resonance imaging study of the level of termination of the conus medullaris and the thecal sac: influence of age and gender. Spine (Phila Pa 1976). 2005;30(16):1875–80.
94. Haworth JC, Zachary RB. Congenital dermal sinuses in children; their relation to pilonidal sinuses. Lancet. 1955;269(6879):10–4.
95. Milhorat TH, Miller JI. Neonatology. 4th ed. Philadelphia: J.B. Lippincott; 1994.

Part V

Head and Neck: Evidence-Based Neuroimaging

Evaluation of Sinusitis: Evidence-Based Neuroimaging

Yoshimi Anzai

Contents

Y. Anzai
Department of Radiology, University of Washington, Seattle, WA, USA
e-mail: anzai@uw.edu

Key Points

- The clinical signs and symptoms of acute bacterial sinusitis (ABS) overlap with that of nonspecific upper respiratory track viral infection (strong evidence).
- Children under the age of 6 years should not undergo sinus radiographs due to their limited sinus development (moderate evidence).
- Sinus radiographs are moderately sensitive to diagnose ABS compared with sinus puncture and culture (moderate evidence).
- Although a CT scan is frequently performed to assist diagnosis of sinusitis, no adequate data exists on the sensitivity and specificity of sinus CT for diagnosis of ABS (limited evidence).
- Definitive imaging criteria are presence of frothy air-fluid levels or complete sinus opacification, but do not include mucosal thickening (limited evidence).
- Despite relatively high sensitivity of CT or sinus radiography, imaging is not indicated in the initial diagnostic workup for acute uncomplicated sinusitis, due to cost and radiation dose (strong evidence).
- Imaging study is indicated for patients who fail to respond to medical management, or severe symptoms suspicious for complications related to acute sinusitis, or patients planning to undergo surgery (moderate evidence).
- The diagnosis of chronic sinusitis is based on clinical grounds. No gold standard exists to confirm clinical diagnosis. CT findings for chronic sinusitis often do not correlate with patients' clinical symptoms (limited evidence).
- Imaging (contrast-enhanced CT or MR) is indicated in immunocompromised patients with acute progression of sinus infection with neurological symptoms in order to assess potential complications from acute sinusitis.

Definition and Pathophysiology

The term "sinusitis" technically refers to inflammation of the mucosa of the paranasal sinuses. Under normal circumstance, the paranasal sinuses are assumed to be sterile. However, the paranasal sinuses are continuous to nasal mucosa or nasopharynx that is heavily colonized with bacteria. These bacteria are present in low density and removed by the normal mucociliary function of the paranasal sinuses. Normal mucous secretions contain antibodies and, together with mucociliary clearance, work to clear bacteria from the paranasal sinuses. Thus, maintaining the mucociliary flow and an intact local mucosal surface are key host defenses against infection [1]. Sinusitis is classified as acute, subacute, or chronic, based on the duration of the illness. Acute sinusitis refers to sinusitis symptoms lasting fewer than 4 weeks, and chronic sinusitis refers to sinusitis lasting more than 12 weeks. Subacute sinusitis falls in between these two.

The common predisposing events that set the stage for ABS are an acute viral upper respiratory infection that results in a viral rhinosinusitis (predisposes to approximately 80 % of bacterial sinus infections) and allergic inflammation (that predisposes to 20 % of bacterial infection). Once the mucosa of the paranasal sinuses swells due to either viral infection or allergy, it causes sinus ostia obstruction, thus interfering with normal mucociliary clearance. This leads to low pressure within the paranasal sinuses and thus further exaggerates mucosal thickening and poor sinus clearance, resulting in acute bacterial sinus infection. *Streptococcus pneumoniae* and *Hemophilus influenzae* are two common organisms causing ABS. Since the widespread use of the heptavalent pneumococcal conjugate vaccine (PCV7) in 2004, pneumococcal strains have declined, and thus, *H. influenzae* has become a more prevalent organism [2, 3]. Other organisms include *Moraxella catarrhalis*, other *Streptococcus* species, and *Staphylococcus*.

Epidemiology

Acute sinusitis is one of the most common diagnoses in primary care setting in the USA; affecting 31 million individuals diagnosed each year [4]. Fourteen percent of Americans claim to have had a previous diagnosis of sinusitis [5].

The prevalence of sinusitis has increased in the last decade due to increased air pollution and resistance to antibiotics. There is no gender difference in sinusitis prevalence. Sinusitis is more common in the Midwest and south of the country compared to the coasts. Acute sinusitis more often affects patients with a history of allergy or asthma. Other patients with high risk of developing acute sinusitis include individuals with defects in immunity (HIV, agammaglobulinemia), delayed or absent mucociliary activity (Kartagener's syndrome, cystic fibrosis), structural defects (cleft palate), and white blood cell functional abnormalities (chronic granulomatous disease, Wegener's granulomatosis) [6]. Dental infections may cause 5–10 % of all cases of maxillary sinusitis, the roots of the upper back teeth (second bicuspid, first and second molars) about the floor of the maxillary sinus.

Sinusitis affects all age groups. The prevalence of sinusitis among children is even higher than adults and may be as high as 32 % in young children [7–9]. The average child has between 6 and 8 "cold" episodes annually, and it is estimated that 5–10 % of all upper respiratory infections are complicated by sinusitis. Children under the age of 6 years are the most likely to have ABS [10].

Acute maxillary sinusitis in adults is characterized with purulent nasal discharge, facial tenderness, headache or toothache, and fever. Children, however, may have less specific symptoms, such as a prolonged daytime cough lasting more than 10 days. The development of paranasal sinuses in children also contributes to diagnostic challenges. The maxillary and the ethmoid sinuses are present at birth. The sphenoid sinuses generally start to pneumatize by age 5 years; the frontal sinuses start to develop around aged 7–8 years [10]. Both frontal and sphenoid sinuses continue to develop until late adolescence. Sinus tenderness is not a typical sign observed in pediatric patients with acute sinusitis.

Diagnosis of chronic sinusitis is even more challenging. No gold standard, i.e., pathological diagnosis, exists for chronic sinusitis. Diagnostic workups and treatment are often driven by patients' symptoms.

Overall Cost to Society

Sinusitis has a significant economic impact on health-care organizations. In 1992, Americans spent $200 million on prescription medications and more than $2 billion for over-the-counter medications to treat sinusitis [11]. There were 11 million doctor visits and 1.3 million outpatients visit due to sinusitis in 1999 [12]. Approximately 500,000 sinus surgeries are performed each year. The study using data from AHCPR's 1987 National Medical Expenditure Survey (inflated to $1,996) estimated overall health-care expenditures attributable to sinusitis were $5.8 billion, mainly from ambulatory and emergency department services and 50,000 surgical procedures performed on paranasal sinuses [13]. Approximately 31 % ($1.8 billion) of the cost was attributed to treatment expenditures for children 12 years or younger [14]. They concluded that sinusitis needed to be recognized as a serious, debilitating, costly disease that warrants precise diagnosis and effective specific therapy [15]. This estimate of direct costs does not include indirect costs, such as expense of care of sick children, transportation costs, the value of work time lost, baby-sitting costs, ancillary medication costs, and expenditures for treatment of adverse effects. Clearly, sinusitis imposes a considerable economic burden for the patients and family. Therefore, improved diagnosis and the use of the most effective agents with the highest tolerability profile will improve outcomes and lower the overall cost of therapy.

It is important to keep in mind that the majority of "sinusitis" is caused by upper respiratory tract viral infection. The symptoms with acute viral sinusitis and allergic rhinitis overlap with that with ABS, leading to misdiagnosis. Consequently, ABS is overdiagnosed (in as many as 50–60 % of cases), and therefore antibiotics are overprescribed in the primary care setting. Clinical studies showed that as many as 60 % of patients with colds are prescribed antibiotics [16]. The overprescription of antibiotics leads to a wide spread of antibiotic-resistant infection. Antibiotic-resistant infections are an increasing problem in hospitals in terms of

the number of resistant organisms and their prevalence. Consequently, the costs of these infections are also increasing. Antibiotic resistance increases the costs of care in hospitals in various ways including increased length of stay, more admissions to intensive care unit, and more intensive resource use.

Goals of Imaging

In patients presenting with acute sinusitis symptoms, the goal is to differentiate those with ABS who benefit from antibiotics from those with nonspecific virus infection. Imaging is not indicated for the initial diagnostic workup for acute sinusitis, due to increasing cost and radiation for pediatric patients. Diagnosis and treatment decision, particularly prescribing antibiotics or not, is often made based on clinical examination for uncomplicated sinusitis.

Imaging is, however, indicated for patients who failed to respond to initial medical management. The goal of imaging at this setting is to exclude (or include) diagnosis of ABS and to assess potential causes of poor mechanical drainage of the paranasal sinuses and complications such as orbital cellulitis or abscess formation (i.e., orbital subperiosteal abscess and anterior cranial fossa abscess).

The goal of sinus CT for chronic sinusitis is to provide objective information to support the clinical diagnosis, to provide detailed anatomy for surgical planning, and to predict which patients most benefit from endoscopic sinus surgery.

Methodology

The authors performed a MEDLINE search using PubMed (National Library of Medicine, Bethesda, MD) for data relevant to the diagnostic performance and accuracy of both clinical and radiographic examinations of patients with acute sinusitis. The diagnostic performance of clinical examination (history and physical exam) and clinical outcome was based on a systematic literature review performed in MEDLINE from January 1966 to May 2010. The clinical examination search strategy used the following statements: (1) acute rhinosinusitis, (2) ABS, (3) diagnosis, (4) clinical examination, and (5) outcomes. The review of the current diagnostic imaging literature was done with MEDLINE covering from January 1966 to May 2010, with the following key statements and words: (1) rhinosinusitis, (2) sinusitis, (3) radiograph, and (4) CT, as well as combinations of these search strings. We excluded animal studies and non-English articles.

Discussion of Issues

Is There a Role for Imaging in the Initial Diagnosis of Acute Bacterial Sinusitis?

Summary
Diagnosis of acute sinusitis should be made on clinical criteria. Radiographic imaging study should not be obtained to diagnose acute sinusitis or to confirm clinical diagnosis of acute sinusitis, particularly in children who are below 6 years of age [17]. Imaging as an initial diagnostic workup not only substantially increases the cost but also is potentially harmful from radiation exposure.

It is controversial if sinus radiography is needed as a confirmatory test of acute sinusitis in children older than 6 years with persistent and severe symptoms. Although sinus radiograph has lower cost and is readily available, the ability to evaluate intracranial or intraorbital complications is limited. CT is a preferred imaging modality for diagnostic workups for patients with recurrent or chronic sinusitis. The ACR (American College of Radiology) guidelines state that the diagnosis of uncomplicated acute sinusitis should be made on clinical grounds alone and reserve the use of imaging for situations for medically refractory cases or worsening during the course of antibiotics treatment [18] (http://acsearch.acr.org/) (moderate evidence).

Supporting Evidence
Acute sinusitis is a common clinical condition. Diagnosis of acute sinusitis should be made on

clinical criteria in patients who present with uncomplicated upper respiratory symptoms (strong recommendation) [13]. Clinical guidelines and criteria have been developed to distinguish ABS from acute viral rhinosinusitis. For adult maxillary sinusitis, William's criteria are often used, which include: (1) maxillary toothache, (2) poor response to decongestants, (3) history of colored nasal discharge, (4) purulent nasal secretion on physical examination, and (5) abnormal transillumination result. On the other hand, Gonzales et al. reported that purulent nasal secretions alone neither predict bacterial infection nor benefit from antibiotic treatment [19]. Transillumination is a useful technique in the hands of experienced personnel, but only negative findings are useful (limited evidence). The clinical diagnostic guidelines for ABS in children are (a) persistent symptoms including nasal or postnasal discharge (of any quality) and daytime cough (which may be worse at night) and (b) symptoms lasting more than 10–14 days but less than 30 days [10]. Severe symptoms include a temperature of at least 102 °F, and purulent nasal discharge presents concurrently for at least 3–4 consecutive days in a child who seems ill or toxic [10]. Respiratory symptoms related to acute viral sinusitis may not have completely resolved by the tenth day but almost always have peaked in severity and begun to improve. Therefore, persistence of respiratory symptoms without any signs of improvement suggests the presence of bacterial infection [13]. Facial pain is rare and unreliable for children. If fever is present in uncomplicated viral infection, it is usually at earlier phase of illness and accompanied by other constitutional symptoms such as headache. Purulent nasal discharge does not appear for several days for uncomplicated viral infection. The concurrent presentation of fever and purulent nasal discharge for at least 3–4 consecutive days helps diagnose ABS [17].

Physical examination does not contribute to the diagnosis of ABS. Sinus aspiration is the gold standard for the diagnosis of ABS; but it is an invasive, time-consuming, and potentially painful procedure that should only be performed by a specialist (otolaryngologist) [20]. Nasal swab and culture from the middle meatus is also reported, but the correlation with nasal swab with sinus puncture remains weak. Endoscopic-guided swab culture is more accurate to sample secretion from a sinus of interest. However, this is usually performed by otolaryngologists, resulting in higher cost, and thus is not feasible for routine use.

Radiographic imaging should not be obtained for patients who meet clinical diagnostic criteria for ABS. The paranasal sinuses are still under development in younger children. Therefore, lack of aeration of the sinuses may be physiological rather than infection, limiting the accuracy of radiography [21].

In children younger than 6 years of age, clinical history correlates with sinus radiography 88 % of the time [22]; therefore, radiography can be safely omitted for children under age 6 (strong consensus based on limited evidence).

For children over 6 years of age with persistent symptoms, the need for radiograph as a confirmatory test of acute sinusitis remains controversial. When an alternative diagnosis is considered, imaging might be useful. Normal radiographs or CT is powerful evidence that bacterial sinusitis is not the causes of the symptoms [23] (limited evidence). A practical guideline by AHRQ indicates that imaging study is not warranted when the likelihood of acute sinusitis is either high or low, but imaging is useful when a diagnosis is in doubt (limited evidence).

Sinus CT is indicated for patients with acute sinusitis symptoms in the following three conditions: (1) when complications related to sinusitis are suspected, (2) when symptoms persist without response to medical management, or (3) surgery is considered (strong recommendation based on moderate evidence). Complicated sinusitis is suspected when patients present with ptosis, cranial nerve palsies, and facial and orbital swelling. Contrast-enhanced CT of the sinuses and orbit is recommended when orbital cellulites or periosteal abscess as a complication of sinusitis is suspected [18, 24, 25]. Contrast-enhanced MRI is occasionally recommended when intracranial extension, such as epidural empyema or brain abscess, is suspected [21, 26–29] (limited evidence).

What Is the Diagnostic Performance of Sinus Radiography and Sinus CT in Acute Bacterial Sinusitis? What Diagnostic Criteria Should We Use?

Summary

Although the diagnosis of acute sinusitis should be made on clinical grounds, the accuracy of such clinical diagnosis is not well documented compared with the gold standard of direct sinus puncture. Compared with sinus radiography as the gold standard, clinical diagnosis has moderate accuracy (moderate level of evidence) [13]. Summary receiver operating characteristics (SROC) curve is used to represent the accuracy of a diagnostic test, where 1 is perfect accuracy and 0.5 is no better than the flip of a coin. The area under the curve (AUC) of clinical diagnosis compared with sinus radiograph is 0.74 [30]. Compared with sinus puncture as the gold standard, sinus radiography offers moderate ability to diagnose acute sinusitis (SROC area 0.83) (moderate evidence) [31–35]. No single study comparing CT or MR with sinus puncture to evaluate accuracy of CT or MR for acute sinusitis was found. Given CT and MRI's superior spatial and soft tissue resolution to radiography, both are likely more sensitive for detection of acute sinusitis, but specificity is questionable. Lack of definitive diagnostic criteria for sinus disease makes it difficult to interpret studies investigating specificity of sinus CT or MRI.

Sinus puncture performed by an otolaryngologist is the gold standard; however, it is rarely performed due to its invasiveness and cost. An inexpensive, simple, and accurate diagnostic test is needed to better differentiate patients who need antibiotics from those with nonspecific viral illness. Good, high-quality evidence for acute uncomplicated sinusitis in children is limited. Diagnostic modalities show poor concordance. More evidence is needed for defining the optimal treatment and diagnostic methods for this common condition [7] (insufficient evidence).

Supporting Evidence

The diagnosis of acute sinusitis is often made based on clinical grounds, but the accuracy of such clinical diagnosis is not well documented. Engles performed a meta-analysis of diagnostic tests for acute sinusitis that showed clinical history and physical examination had moderate ability to identify patients with positive radiography (SROC area 0.74) [34].

Using sinus opacity or the presence of an air-fluid level as the criterion for sinusitis, sinus radiography had sensitivity of 0.73 and specificity of 0.80. Compared with sinus puncture and aspiration as the gold standard, sinus radiography offers moderate ability to diagnose acute sinusitis (SROC area 0.83). Another systematic review performed by Varonen published concurrently with Engles study focused on adult patients suspected of acute maxillary sinusitis. They compared sinus radiography, ultrasound, and clinical examination with sinus puncture as the gold standard and concluded that sinus radiography was more accurate method for diagnosing acute sinusitis (SROC area of 0.82) than clinical examination. Clinical examination even by experienced physicians was less reliable (area under SROC is 0.75) [35]. Using sinus puncture as the gold standard, Berg reported that clinical examination had a sensitivity of 66 % and specificity of 79 % in the setting of emergency clinic [36]. Sinus radiograph is more accurate than clinical examination for diagnosis of ABS. However, clinical application for sinus radiograph as an initial workup is not justified due to its costs and radiation exposure.

In Europe, A-mode ultrasound is used to diagnose acute maxillary sinusitis in primary care setting with moderately strong accuracy (SROC area of 0.80) [31, 35, 37]. Savolainen reported among 234 patients suspected of maxillary sinusitis that ultrasound had a sensitivity of 81 % and specificity of 72 %, as compared with sinus puncture [38]. Ultrasound waves are transmitted to the sinus then reflected back from the interface of two different media. A sinus cavity filled with secretions results in an echo in the display screen. It is insensitive for mucosal thickening of the sinus [39].

Computed tomography (CT) provides superior assessment of all paranasal sinuses compared with sinus radiograph [40]. However, CT has not

been directly compared with sinus puncture for assessment of diagnostic accuracy [34, 35]. Given the invasiveness of sinus puncture and need for otolaryngology referral (additional cost), sinus CT can be used as a proxy of sinus puncture. Sinus CT is considered more sensitive than sinus radiograph for diagnosis of acute sinusitis. A study comparing sinus plain radiograph and CT in 47 consecutive patients showed that sinus radiograph had a high specificity but markedly low sensitivity for disease in the ethmoid, frontal, and sphenoid sinuses [41]. The sensitivity of sinus radiograph for maxillary sinus was 80 % in this study. Another study enrolled 134 patients with suspected sinusitis who underwent a single Waters view of sinus, and CT revealed that plain film has markedly low sensitivity for a disease outside of maxillary sinus. The sensitivity and specificity of Waters view compared with CT for maxillary sinus disease were 67.7 % and 87.6 %, respectively [42]. They recommended the use of a low-dose, high-resolution CT scan of the paranasal sinuses (moderate evidence). The problem is its lack of specificity data of sinus CT, compared with sinus puncture. A question is if CT scan overdiagnoses sinusitis.

Another reason that accuracy of sinus CT remains uncertain and controversial is lack of definitive diagnostic criteria. Diagnostic criteria of sinus radiography for acute sinusitis are complete opacification or sinus air-fluid level. Diagnostic criteria for sinus CT are not well defined but usually include mucosal thickening greater than 4 mm; any degree of sinus opacification and any type of fluid level are considered positive for acute sinusitis. Mild mucoperiosteal thickening can be found on head CT in patients without any sinusitis-related symptoms in up to 40 % of individuals [43]. Gwaltney reported CT scan of 31 patients with self-diagnosed common cold. They found that 87 % of 31 patients had occlusion (or mucosal thickening) of ethmoid infundibulum and 65 % of patients had mucosal abnormality in maxillary sinuses [44]. It is of paramount importance to define what CT finings constitute ABS. The only specific CT finding to indicate acute sinusitis is a frothy, bubbly air-fluid level, which indicates purulent secretion within the sinuses [21]. Waterish smooth air-fluid level may be nasal secretion without bacterial infection or clear secretion related to allergic rhinitis [45]. Complete opacification of a sinus with bone thickening may indicate chronically obstructed sinus rather than acute sinusitis [46].

When Are Imaging Studies Indicated for the Diagnosis and the Management of Patients with Sinusitis?

Summary

Imaging studies, such as sinus CT should be performed for patients who present with complications of ABS or who have very persistent or recurrent disease not responding to medical management. When patients do not respond to medical management, the patients may have mechanical obstruction that prevents restoration of mucociliary clearance, such as a polyp or structural anomalies of the nasal cavity and sinuses.

Sinusitis is a self-limiting disease with complete cure in most cases. However, serious complications still do occur in a small percentage (3.7–11 %) of these patients with acute sinusitis [47]. When patients with sinusitis symptoms present with orbital swelling, ptosis, visual changes, cranial nerve palsies, and mental status changes, contrast-enhanced CT and/or MR is recommended to diagnose orbital cellulitis/abscess, epidural or subdural empyema, cavernous sinus thrombosis, and intracranial extension of infection [29].

When surgery is considered for patients with recurrent or medically refractory disease, detailed sinus CT is indicated to define the bony anatomy, including the osteomeatal complex, and correlated with patients' clinical symptoms [13, 48, 49] (limited evidence).

Supporting Evidence

Sinusitis is a common condition and in most cases a self-limited disease. Most cases of sinusitis resolve completely with appropriate antibiotic therapy. Patients with complicated acute sinusitis

have severe symptoms, including high fever, intense headache that is above or behind the eye, periorbital swelling, or pressure over the face. Complicated acute sinusitis results from a delay in initiating treatment, antibiotic-resistant infection, and incomplete treatment. Immuno-compromised patients, such as those with cystic fibrosis, often present with extensive sinus infection. The incidence of sinusitis-related complications remains indeterminate as many literatures reporting sinusitis-related complications were case series or case reports. A retrospective review from a single institution revealed that 5.3 % of ENT emergencies were sinusitis complications. Among them, orbital complications were the most common (62 %) followed by acute subdural empyema (23 %) and meningitis (15 %) [50]. Among the transplant patients, patients with graft-versus-host disease (GVHD) were 4.3 times more likely than patients without GVHD to develop sinusitis post transplant [51].

These include intraorbital complications, such as orbital cellulitis and subperiosteal abscess, cavernous sinus thrombosis, epidural empyema, meningitis, cerebritis, and brain abscess. Therefore, contrast-enhanced CT or MR is indicated when patients with sinusitis symptoms present with orbital swelling, proptosis, visual changes, and cranial nerve palsies [28, 52, 53]. Clary investigated the accuracy of sinus CT for orbital abscess as compared with surgical exploration in 19 patients and reported that CT had a sensitivity of 93 % and specificity of 67 % [54].

With the advent of antibiotics, the incidence of orbital cellulitis has decreased. Approximately 3 % of sinusitis progresses to orbital cellulitis [40]. This can be divided into pre- and postseptal cellulitis. The septum is defined as the medial orbital periosteal reflection attaching to the medial eyelid at the tarsal plate. The majority of orbital cellulitis is due to either direct spread from ethmoid sinusitis through porous lamina papyracea or through the valveless anterior and posterior ethmoid veins [40]. The periosteum of the medial orbital wall is loosely attached to the lamina papyracea; as such it often forms subperiosteal

abscess or phlegmon. Clinically, these patients may present with deviation of the globe or proptosis. Cavernous sinus thrombosis results from infection of the midface, orbit, and sinonasal cavity. This may lead to cranial nerve paralysis and blindness. In the setting of orbital cellulitis, the presence of cranial nerve paralysis involving cranial nerves III, IV, V, and/or VI raises the suspicion of cavernous sinus thrombosis. Contrast-enhanced CT or MR shows an engorged superior ophthalmic vein. Enhancing cavernous carotid artery may stand out from the surrounding thrombosed cavernous sinus [55–58].

Intracranial spread of sinus infection most commonly originates from frontal or sphenoid sinusitis [52, 59]. Intracranial extension of infection is facilitated by the abundant valveless emissary venous plexus of the posterior frontal sinus, known as Behcet's plexus. Infection spreads through the sinus to dura, meninges, and parenchyma, resulting in epidural or subdural empyema, meningitis, cerebritis, and brain abscess [55]. Contrast-enhanced brain MR is recommended when intracranial spread of sinusitis is suspected [52, 55]. One study comparing diagnostic accuracy of CT, MR, and clinical diagnosis for sinusitis-related complications revealed that the diagnostic accuracy was 82 % for clinical assessment compared with 91 % for CT for orbital complications. For patients with intracranial complications, meningitis was the most common diagnosis, and MRI was more accurate (97 %) in determining the diagnosis than CT (87 %) or clinical findings (82 %). Both CT and MR have improved the management and outcomes of patients who have sinusitis with complications [60].

Surgery of the sinuses or nasal passage may be considered for patients who do not respond to medical management for sinusitis. Sinus CT is the primary imaging test and provides detailed images of sinus anatomy in multiple planes. Attention should be paid to the status of osteomeatal complex, particularly the curvature and superior extension of the uncinate process. Patients with chronic sinusitis often received the maximum medical therapy before CT scan in

order to evaluate the bony details. Thus, mucosal disease is often minimal for those patients. What we should look for is bony anatomy related to osteomeatal complex and also dangerous anatomical variations, such as dehiscent optic canal or carotid canal, low-lying fovea ethmoidalis, or Onodi cells. These findings alert ENT surgeons prior to surgical intervention.

Sinus CT often reveals various common anatomical variations, such as nasal septum deviation or concha bullosa. A study evaluating anatomical variations of sinuses on CT revealed that 64.9 % of 202 patients had anatomical variations. The significance of such anatomical variant remains uncertain, as these anatomical variations are often seen in patients without any sinusitis symptoms [61]. A detailed sinus CT, instead of screening or limited sinus CT, is recommended for patients with chronic sinusitis who undergo sinus surgery. The screening sinus CT for preoperative assessment was thought to be inadequate for operative planning [62].

What Is the Most Cost-Effective Strategy for the Diagnosis and the Management of Acute Sinusitis?

Summary
The most cost-effective method to manage patients presented with mild to moderate symptoms of acute sinusitis is to use clinical guidelines and treat with first-line antibiotic therapy [63]. For patients with severe symptoms or high disease prevalence population, empirical antibiotic treatment is cost effective. This leads to many unnecessary antibiotic prescriptions that lead to antibiotic-resistant infection.

Cost-effectiveness analysis (CEA) comparing four different management strategies (empirical antibiotics, no antibiotics, clinical diagnosis, or sinus CT-based treatment) of adult acute sinusitis revealed that empirical antibiotic therapy is most cost effective from the societal perspective, as patients return to normal life more quickly, offsetting the up-front cost of antibiotics [64, 65].

From the payer's perspective, clinical diagnosis-based treatment was the most cost-effective strategy [64]. The effectiveness of antibiotic therapy in children remains controversial. The study results highly depend on the inclusion criteria of the study population. Antibiotic therapy was effective for patients with radiographically confirmed pediatric acute sinusitis, but little or no effect is seen when patients were selected based on clinical diagnosis [9]. This is likely due to the fact that some of these patients had viral infection, therefore potentially diluting the effectiveness of antibiotic therapy.

Supporting Evidence
A diagnostic workup strategy for any disease should be directly connected to its management of the disease. Although sinusitis is a self-limiting disease in most cases, undertreating acute sinusitis may lead to rare but serious complications. Patients remain sick longer, thus requiring time away from work, loss of productivity, and over-the-counter medications [65]. Overtreating sinusitis may result in unnecessary costs and adverse effects from antibiotic therapy, such as allergic reaction or gastrointestinal disturbance, as well as future development of antibiotic-resistant infection. Treating a viral illness with antibiotics leads to no benefit but potential adverse drug effects. Accurate diagnosis by CT scan improves effectiveness of antibiotic therapy, by selecting patients who benefit from antibiotics. However, such additional benefit is too small to justify the additional cost of CT scan and the additional risks from radiation exposure, particularly in children.

The effectiveness of antibiotic therapy in children remains controversial. The results highly depend on the study inclusion criteria. Antibiotic therapy was found effective for patients with radiographically confirmed acute sinusitis. Patients treated with antibiotics recovered more quickly than those under placebo [22]. On the third day of treatment, 83 % of children receiving antibiotics were cured or improved compared with 51 % of the children in the placebo group. However, little or no effect is seen in antibiotic

treatment when patients were selected based on clinical diagnosis alone. A study by Garbutt challenged the notion that children having acute sinusitis based on clinical ground will benefit from antibiotic therapy. Since "sinusitis patients" defined by clinical diagnosis include children with viral infection, the effectiveness of antibiotics is diluted.

The American Academy of Pediatrics clinical practice guidelines for the management of sinusitis show that children with mild and moderate symptoms who do not attend day care should receive the usual dose of amoxicillin [17]. Those patients who (a) do not improve while receiving the usual dose of amoxicillin, (b) have been recently been treated with antibiotics, (c) have illness that is moderate to severe, or (d) attend day care should receive high-dose amoxicillin with clavulanate. Higher doses of amoxicillin are effective for *S. pneumoniae* species that are intermediate in resistance to penicillin, and potassium clavulanate is effective against beta-lactamase-producing *H. influenzae* and *M. catarrhalis*. The AAP guidelines make no recommendations about the use of antihistamines, decongestants, and intranasal steroids based on limited or controversial data [10].

What Is the Imaging Role for Patients with Chronic Sinusitis?

Summary

Clinical diagnosis of chronic sinusitis is even more difficult than that of acute sinusitis. Patients with chronic sinusitis have relatively vague symptoms that overlap with viral upper respiratory infection, allergy, and migraine. Imaging plays an important role for excluding diagnosis or identifying anatomical causes leading to sinusitis. CT is a modality of choice as it provides anatomical road maps much better than plain radiography or ultrasound. Although rare, for children suspected for serious complications, such as intracranial or orbital abscess, MR with contrast is recommended to assist surgical treatment planning.

Supporting Evidence

Chronic sinusitis is defined as sinusitis symptoms lasting more than 12 weeks. The diagnosis of chronic sinusitis is difficult because of relatively nonspecific signs and symptoms that overlap with viral upper respiratory infection and allergy. Children or adolescents with chronic headache are often misdiagnosed as sinus headache and receive sinus medication [66]. Imaging plays a major role for making or excluding diagnosis or assessing the anatomy of sinuses leading to recurrent or chronic infection [67].

In terms of the choice of imaging for children with chronic sinusitis, sinus radiography was reported to overestimate abnormalities. In a study performed sinus radiography and CT in 34 children with chronic sinusitis, sinus radiography (Waters and occipitomental views) overestimated ethmoid sinus disease in 24 % and maxillary sinus disease in 56 % [68]. Sinus CT provides detailed anatomy as well as extent of disease better than sinus radiography and remains the imaging study of choice for patients with chronic sinusitis. CT scan is often performed in patients who remain symptomatic following multiple courses of antibiotics in order to diagnose or rule out presence of obstructive lesion interfering mucociliary clearance. Multi-institutional prospective dual-cohort study comparing the severity of CT findings using Lund-MacKay staging system in 66 pediatric patients with chronic sinusitis and control showed that the AUC of CT is 0.923 ($p < 0.01$), indicating excellent diagnostic accuracy [69].

If sinus CT is completely normal in patients who are suspected of having chronic sinusitis, diagnosis can be generally excluded. When sinus CT shows a focal intranasal mass with unilateral sinus opacification, this may lead to evaluation by endoscopy for possible surgical resection. The problem lies, however, when sinus CT shows mild, nonspecific, diffuse mucosal thickening without correlation with clinical symptoms; in terms of facial pain, or tenderness, it is difficult to determine if sinusitis contributes to patients' clinical symptoms.

A study comparing CT scan findings of 60 children aged 2–12 with chronic sinusitis with

50 control subjects who underwent CT scan for indications other than sinusitis found that mucoperiosteal thickening is highly prevalent findings seen in 60 % of patients and 46 % of control groups. Early-stage (mild) mucoperiosteal thickening was present in the majority of children who had sinus CT (98 % of control and 85 % of children with chronic sinusitis) [70]. Certain anatomical variations are thought to contribute causality of chronic sinusitis as these variations may interfere with sinus drainage pathways. These include, but not limited to, nasal septum deviation, concha bullosa, and Haller cells. Significance of anatomic variations in children is still controversial as these findings can be seen in asymptomatic subjects [71].

Medical management remains the cornerstone for children with chronic sinusitis. Indication for sinus surgery is controversial. No prospective randomized trial comparing medical management with surgery has been reported. The decision regarding the need for sinus surgery should not be solely based on imaging abnormalities. A study that investigated the impact of sinus CT on therapeutic decision by otolaryngologists showed that the concordance between CT abnormality and patient's symptoms and obstruction of ostiomeatal complex are main predictors for favorable surgical treatment [72]. Sinus surgery may be performed in children with nasal obstruction from polyposis or refractory sinusitis aggravating asthma [73]. Outcome assessment for 308 children with chronic sinusitis after sinus surgery revealed that endoscopic sinus surgery improved outcomes in 2-year follow-up in the intermediate stages of chronic sinusitis (stages II and III out of stages I–IV) [74]. Some study suggested use of IV antibiotics for children who have failed to respond to traditional oral antibiotics therapy [75].

Special Situation: What Is the Role of Imaging in Immunocompromised Patients?

Summary

Invasive fungal sinusitis (IFS) has been increasingly seen in patients with an immunocompromised status. The incidence has increased in accordance with increase use of antibiotics, steroids, chemotherapy, and radiation treatment. IFS is a difficult disease to treat. CT findings that are characteristics for IFS include mucoperiosteal thickening associated with bone erosion or extrasinus soft tissue invasion to orbit or retroantral fat pad. CT is helpful for planning of surgical debridement. However, diagnosis of IFS should not solely be based on CT, as CT findings suggestive of IFS, bone erosion or extrasinus invasion, are often absent in an earlier course of disease [76]. With a high clinical suspicion, rigid nasal endoscopy with biopsy is recommended for early diagnosis [76]. Complete surgical resection and reversal of neutropenia are critical elements for improved outcomes.

Supporting Evidence

IFS is rare but a life-threatening disease in children with underlying immunocompromised disease. Incidence has been increasing in accordance with expansion of transplant medicine and advancement in antineoplastic medication for hematological malignancies. Common fungal organisms seen in immunocompromised patients include aspergillosis, mucormycosis, and zygomycosis. IFS often spreads directly to the brain via vascular channels or is blood borne from pulmonary infection. Abscess formation along blood vessels often causes thrombosis of vessels leading to neurological deficit [77]. Therefore, when immunocompromised patients present with stroke type of symptoms, intracranial involvement of IFS is highly suspected.

IFS in immunocompromised children has a high mortality rate and requires early diagnosis and treatment.

Imaging study such as sinus CT plays an important role in demonstrating the extent of disease, degree of bone destruction, orbital invasion, extrasinus soft tissue invasion, and vascular encasement. When intracranial involvement is suspected, such as epidural abscess/phlegmon, cerebritis, or septic emboli, brain MR with and without contrast is essential to make a diagnosis

and plan appropriate surgical management. MR allows differentiation of direct cerebral invasion from multiple brain abscesses or septic emboli. Venous sinus thrombosis is also another serious complication that can be diagnosed with MR and MR venogram. Some of fungal disease has markedly low T2 signal mimicking well-aerated sinuses on T2-weighted images. These lesions may appear slightly hyperdense on non-contrast CT examination. Contrast enhancement is useful in order to assess extrasinus extent of disease.

However, classic CT findings of IFS are often absent in *earlier* course of disease. Retrospective review of CT findings in 23 immunocompromised patients with confirmed IFS showed that many patients had mucoperiosteal thickening of sinuses (21/23), but bone erosion (8/23) or orbital invasion (6/23) were seen only in more advanced IFS. They found that disease was frequently unilateral (21/23). Thus, clinician should not rely solely on imaging to make a diagnosis of IFS. With a high index of suspicion, early nasal endoscopy and biopsy as well as initiation of antifungal therapy is critical to improve prognosis.

Treatment for IFS includes surgical debridement, followed by high-dose antifungal treatment, and attempts to correct underlying immunocompromised state are essential for improved survival.

Take-Home Tables

Table 34.1 gives the definition of ABS. Table 34.2 shows the clinical diagnostic criteria for ABS. Table 34.3 gives a summary of diagnostic performance of imaging and clinical examinations for diagnosing acute sinusitis and its complications.

Imaging Case Studies

Figure 34.1a–d shows various imaging findings and suggested diagnosis. Figure 34.2a, b shows CT images for a patient with cavernous sinus thrombosis. Figure 34.3a, b shows CT images of a patient with allergic fungal sinusitis. Figure 34.4a–c shows CT images of a patient with epidural abscess secondary to sphenoid sinusitis and mucocele rupture.

Table 34.1 Definition of acute bacterial sinusitis (acute sinusitis)

Acute sinusitis:
Infection of the paranasal sinuses lasting less than 30 days that presents with either *persistent or severe symptoms*
Persistent symptoms are those that last longer than 10–14 days. Sinusitis symptoms include nasal discharge, nasal congestion, maxillary or facial pain, or toothache. Such symptoms for children include nasal or postnasal discharge, daytime cough (which may be worse at night), or both
Severe symptoms include a temperature of at least 102 °F, and purulent nasal discharge presents concurrently for at least 3–4 consecutive days

Adapted with kind permission of Springer Science+Business Media from Anzai Y, Paladin A. Diagnosis and management of acute and chronic sinusitis in children. In Medina LS, Applegate KE, Blackmore CC editors. Evidence-based imaging in pediatrics: optimizing imaging in pediatric patient care. New York: Springer; 2010

Table 34.2 Acute bacterial sinusitis versus viral upper respiratory infection: clinical signs and symptoms

	Acute bacterial sinusitis	Viral URI
Duration of illness	Longer than 10–14 days	Usually less than 5–7 days
Symptoms	Persistent or worsening after mild resolution (double sickening)	Improved or resolved by 10 days
Fever	Concurrent presentation of high fever and nasal discharge	Earlier in illness and later nasal discharge
Headache	Severe headache behind eyes	Mild headache
Facial pain	Unilateral pain	Mild or absent
	But not reliable for small children	

Reprinted with kind permission of Springer Science+Business Media from Anzai Y, Paladin A. Diagnosis and management of acute and chronic sinusitis in children. In Medina LS, Applegate KE, Blackmore CC, editors. Evidence-based imaging in pediatrics: optimizing imaging in pediatric patient care. New York: Springer; 2010

Table 34.3 Summary table of diagnostic performance of imaging and clinical examinations for diagnosing acute sinusitis in children (only those using sinus puncture as gold standards)

	Sensitivity (95 % CI)	Specificity (95 % CI)	References
Physical exam only	0.66 (0.58–0.73)	0.79 (0.73–0.87)	[15, 34–36]
Radiographs	0.87 (0.85–0.88)	0.89 (0.85–0.91)	[32–35]
Ultrasound	0.85 (0.84–0.87)	0.82 (0.80–0.83)	[23, 26, 31, 37, 38]
CT: no study assessing accuracy of CT using sinus puncture as the gold standard			
CT (orbital abscess)	0.93	0.67	5

Adapted with kind permission of Springer Science+Business Media from Anzai Y, Paladin A. Diagnosis and management of acute and chronic sinusitis in children. In Medina LS, Applegate KE, Blackmore CC, editors. Evidence-based imaging in pediatrics: optimizing imaging in pediatric patient care. New York: Springer; 2010

Fig. 34.1 (**a–d**) Various imaging findings and suggested diagnoses. (**a**) Air-fluid level in the right maxillary sinus: findings highly suspicious for acute bacterial sinusitis. (**b**) Near complete opacification of right maxillary sinus in a patient suspected of acute sinusitis. (**c**) Diffuse mucosal swelling and opacification of maxillary and ethmoid sinuses with thickening of bone walls in a patient with sinonasal polyposis. (**d**) Nonspecific mucosal swelling of maxillary sinus bilaterally. This could be viral infection, allergy, or common cold (Reprinted with kind permission of Springer Science+Business Media from Anzai Y, Paladin A. Diagnosis and management of acute and chronic sinusitis in children. In Medina LS, Applegate KE, Blackmore CC, editors. Evidence-based imaging in pediatrics: optimizing imaging in pediatric patient care. New York: Springer; 2010)
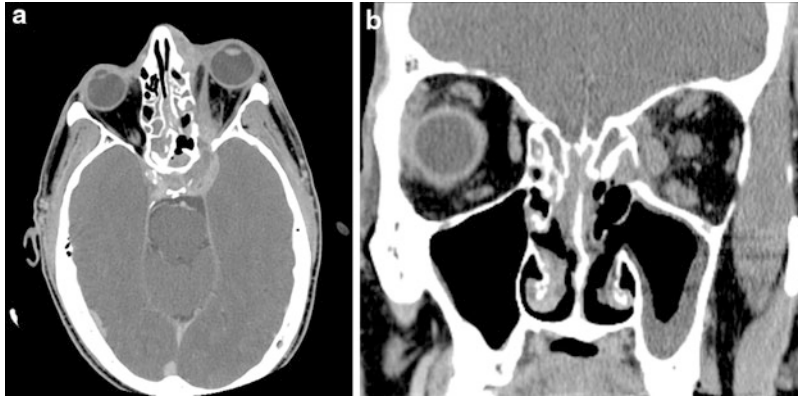
Fig. 34.2 (**a**, **b**). (**a**) A patient with fungal infection involving ethmoid sinuses complicated with left cavernous sinus thrombosis. (**b**) Coronal image shows extension of infection to the medial left orbit associated with focal bone erosion (Reprinted with kind permission of Springer Science+Business Media from Anzai Y, Paladin A. Diagnosis and management of acute and chronic sinusitis in children. In Medina LS, Applegate KE, Blackmore CC, editors. Evidence-based imaging in pediatrics: optimizing imaging in pediatric patient care. New York: Springer; 2010)
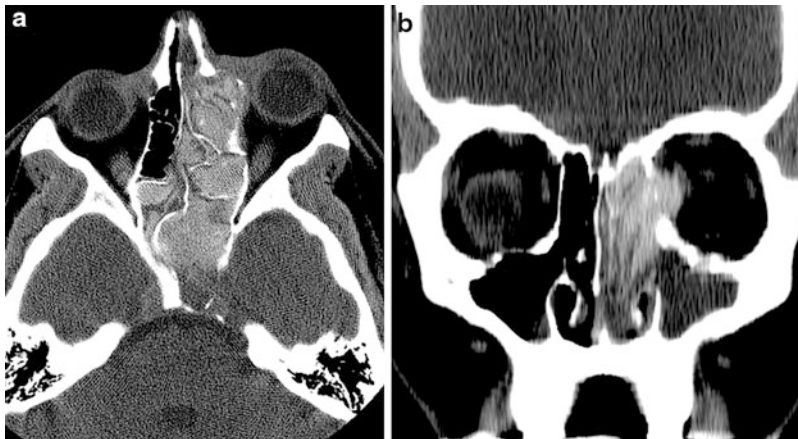
Fig. 34.3 (**a**, **b**). (**a**) A patient with allergic fungal infection involving the bilateral ethmoid sinuses with medial orbital extension. Notice the content of sinus opacification is markedly increased attenuation with low attenuation edematous mucosa (Reprinted with kind permission of Springer Science+Business Media from Anzai Y, Neighbor, Jr. WE. Imaging evaluation of sinusitis: impact on health outcome. In Medina LS, Blackmore CC, editors. Evidence-based imaging: optimizing imaging in patient care. New York: Springer; 2006); (**b**) Coronal reformatted image of the same patient shows medical orbital extension with displacement of medical rectus muscle (Reprinted with kind permission of Springer Science+Business Media from Anzai Y. Imaging evaluation of sinusitis: impact on health outcome. In Medina LS, Blackmore CC, Applegate KE, editors. Evidence-based imaging: improving the quality of imaging in patient care. New York: Springer; 2011)
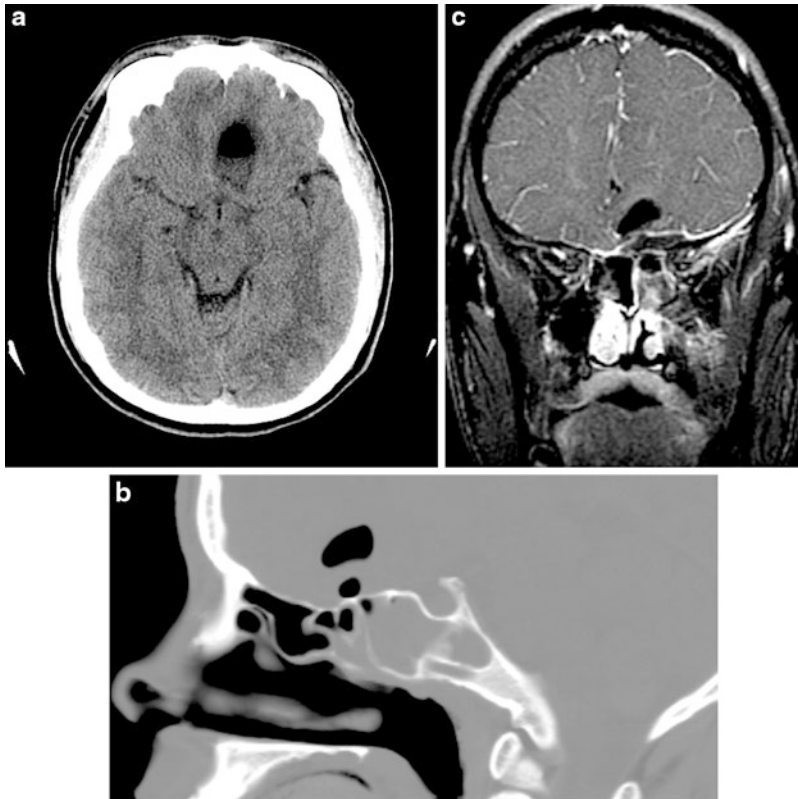
Fig. 34.4 (**a**–**c**). (**a**) A young patient presented with headache and mental status change. Non-contrast head CT shows focal air near the fluid collection in the base of left frontal lobe. (**b**) Sagittal reformatted image shows an expansive sphenoid sinus with adjacent pneumocephalus. (**c**) Contrast-enhanced fat-suppressed coronal image shows a focal epidural abscess adjacent to the left sphenoid sinus, underneath the air pocket. This patient was thought to have left sphenoid mucocele with intracranial ruptured, resulting in epidural abscess (Reprinted with kind permission of Springer Science+Business Media from Anzai Y, Paladin A. Diagnosis and management of acute and chronic sinusitis in children. In Medina LS, Applegate KE, Blackmore CC, editors. Evidence-based imaging in pediatrics: optimizing imaging in pediatric patient care. New York: Springer; 2010)

Suggested Imaging Protocols for Children Clinically Suspected of Acute Sinusitis

Sinus Radiographs

Sinus radiographic series has been rapidly replaced by the limited sinus CT for evaluation of sinusitis. However, some pediatricians still order sinus radiograph, likely due to either lower costs or easier access to radiographs than CT. In order to visualize and assess all paranasal sinuses, at least three views of sinus are required. These include Waters view, Caldwell view, and lateral view. In children under age 6 years, the ACR (Appropriateness Criteria) states that radiographs of the paranasal sinuses are both not indicated and technically difficult to perform. For recurrent infection, some clinicians order a single Waters view to evaluate the maxillary sinuses.

Low-Dose Screening Sinus CT

Low mA and low kVp is most widely used for assessment of sinus infection in our institution,

when available, reducing radiation dose compared with the standard CT [78]. Screening sinus CT demonstrates air-fluid level or sinus opacification, as well as adjacent soft tissue abnormalities and mastoid and middle-ear fluid collection.

MDCT allows rapid acquisition of axial images through paranasal sinuses with thin collimation (≤ 3 mm), in supine position using 100 mA and 120 kVp. Reconstruction of these images in the coronal plane is routinely performed. No intravenous contrast is necessary unless there is a suspected complication such as orbital abscess or epidural empyema. No sedation is needed for these rapidly acquired CTs.

MRI

When MR is needed to assess intracranial complications, the following sequences should be included: axial FLAIR, axial diffusion, axial T2-weighted FSE, pre- and postcontrast T1-weighted multiplanar images. Fat suppression should be used for assessment of postcontrast images in order to better visualize cavernous sinuses, orbital apex, skull base, as well as epidural and subdural spaces.

Future Research

- Large clinical study correlating imaging and clinical findings with sinus aspiration and treatment outcomes.
- Develop noninvasive strategies to accurately diagnose acute sinusitis, particularly imaging that differentiates bacterial infection from viral infection or allergic inflammation.
- Determine better staging strategy using sinus CT for patients with chronic sinusitis.

References

1. Kennedy DW. Otolaryngol Head Neck Surg. 1990;103:884–6.
2. Fletcher MA, Fritzell B. Vaccine. 2007;25:2507–12.
3. Brook I, Int J. Int J Pediatr Otorhinolaryngol. 2007;71:1653–61.
4. Lethbridge-Cejku M, Schiller JS, Bernadel L. Vital Health Stat. 2004;10:1–151.
5. Willett LR, Carson JL, Williams Jr JW. J Gen Intern Med. 1994;9:38–45.
6. Senior BA, Kennedy DW, Tanabodee J, Kroger H, Hassab M, Lanza D. Laryngoscope. 1998;108:151–7.
7. Ioannidis JP, Lau J. Pediatrics. 2001;108:E57, 51–8.
8. Clement PA, Bluestone CD, Gordts F, Lusk RP, Otten FW, Goossens H, et al. Int J Pediatr Otorhinolaryngol. 1999;49:S95–100.
9. Garbutt JM, Goldstein M, Gellman E, Shannon W, Littenberg B. Pediatrics. 2001;107:619–25.
10. Ioannidis JP, Lau J. American Academy of Pediatrics. Subcommittee on Management of Sinusitis and Committee on Quality Improvement Pub Med. Pediatrics. 2001;108:798–808.
11. Collins JG. Vital Health Stat. 1997;10:1–89.
12. NCHS. National Center for Health Statistics: Sinusitis. 2002.
13. Rosenfeld RM, Andes D, Bhattacharyya N, Cheung D, Eisenberg S, Ganiats TG, et al. Otolaryngol Head Neck Surg. 2007;137:S1–31.
14. Ray NF, Baraniuk JN, Thamer M, Rinehart CS, Gergen PJ, Kaliner M, et al. J Allergy Clin Immunol. 1999;103:408–14.
15. Lau J, Zucker D, Engles E, Balk E, Barza M, Terrin N, et al. Diagnosis and treatment of acute bacterial rhinosinusitis. Rockwille: Agency for Health Care Policy and Research; 1999. p. 1–38.
16. Brooks I, Gooch 3rd WM, Jenkins SG, Pichichero ME, Reiner SA, Sher L, et al. Ann Otol Rhinol Laryngol Suppl. 2000;182:2–20.
17. Nash D, Wald E. Pediatr Rev. 2001;22:111–17.
18. McAlister WH, Parker BR, Kushner DC, Babcock DS, Cohen HL, Gelfand MJ, et al. Radiology. 2000;215(suppl):811–18.
19. Gonzales R, Bartlett JG, Besser RE, Cooper RJ, Hickner JM, Hoffman JR, et al. Ann Emerg Med. 2001;37:690–7.
20. Wald ER, Am J. Med Sci. 1998;316:13–20.
21. Diament MJ. J Allergy Clin Immunol. 1992;90:442–4.
22. Wald ER, Chiponis D, Ledesma-Medina J. Pediatrics. 1986;77:795–800.
23. Reider JM, Nashelsky J. J Fam Pract. 2003;52:565–7; discussion 567.
24. Kronemer KA, McAlister WH. Pediatr Radiol. 1997;27:837–46.
25. Howe L, Jones NS. Clin Otolaryngol Allied Sci. 2004;29:725–8.
26. Dessi P, Champsaur P, Paris J, Moulin G. Rev Laryngol Otol Rhinol (Bord). 1999;120:173–6.
27. Eufinger H, Machtens E. J Craniomaxillofac Surg. 2001;29:111–17.
28. Eustis HS, Mafee MF, Walton C, Mondonca J. Radiol Clin North Am. 1998;36:1165–83, xi.
29. Mafee MF, Tran BH, Chapa AR. Clin Rev Allergy Immunol. 2006;30:165–86.

30. Williams Jr JW, Simel DL, Roberts L, Samsa GP. Ann Intern Med. 1992;117:705–10.
31. Revonta M, Blokmanis A. Can Fam Physician. 1994;40:1969–72. 1975–6.
32. van Buchem FL, Knottnerus JA, Schrijnemaekers VJ, Peeters MF. Lancet. 1997;349:683–7.
33. Laine K, Maatta T, Varonen H, Makela M. Rhinology. 1998;36:2–6.
34. Engels EA, Terrin N, Barza M, Lau J. J Clin Epidemiol. 2000;53:852–62.
35. Varonen H, Makela M, Savolainen S, Laara E, Hilden J. J Clin Epidemiol. 2000;53:940–8.
36. Berg O, Carenfelt C. Acta Otolaryngol. 1988;105:343–9.
37. Berg O, Carenfelt C. Laryngoscope. 1985;95:851–3.
38. Savolainen S, Pietola M, Kiukaanniemi H, Lappalainen E, Salminen M, Mikkonen P. Acta Otolaryngol Suppl. 1997;529:148–52.
39. Varonen H, Savolainen S, Kunnamo I, Heikkinen R, Revonta M. Rhinology. 2003;41:37–43.
40. Som PM. Neuroradiology. 1985;27:189–201.
41. Aalokken TM, Hagtvedt T, Dalen I, Kolbenstvedt A. Dentomaxillofac Radiol. 2003;32:60–2.
42. Konen E, Faibel M, Kleinbaum Y, Wolf M, Lusky A, Hoffman C, et al. Clin Radiol. 2000;55:856–60.
43. Glasier CM, Ascher DP, Williams KD. AJNR Am J Neuroradiol. 1986;7:861–4.
44. Gwaltney Jr JM, Phillips CD, Miller RD, Riker DK. N Engl J Med. 1994;330:25–30.
45. Berg O, Bergstedt H, Carenfelt C, Lind MG, Perols O. Ann Otol Rhinol Laryngol. 1981;90:272–5.
46. April MM, Zinreich SJ, Baroody FM, Naclerio RM. Laryngoscope. 1993;103:985–90.
47. Vazquez E, Creixell S, Carreno JC, Castellote A, Figueras C, Pumarola F, et al. Curr Probl Diagn Radiol. 2004;33:127–45.
48. Kennedy DW, Senior BA. Otolaryngol Clin North Am. 1997;30:313–30.
49. Jiannetto DF, Pratt MF. Laryngoscope. 1995;105:924–7.
50. Ali A, Kurien M, Mathews SS, Mathew J. Singapore Med J. 2005;46:540–4.
51. Thompson AM, Couch M, Zahurak ML, Johnson C, Vogelsang GB. Bone Marrow Transplant. 2002;29:257–61.
52. Grundmann T, Weerda H. Laryngorhinootologie. 1997;76:534–9.
53. Larson TL. Semin Ultrasound CT MR. 1999;20:379–90.
54. Clary RA, Cunningham MJ, Eavey RD. Ann Otol Rhinol Laryngol. 1992;101:598–600.
55. Reid JR. Pediatr Radiol. 2004;34:933–42.
56. Unlu HH, Aslan A, Goktan C, Egrilmez M. Auris Nasus Larynx. 2002;29:69–71.
57. Nawashiro H, Shimizu A, Shima K, Chigasaki H, Kaji T, Doumoto E, et al. Neurol Med Chir (Tokyo). 1996;36:808–11.
58. Rochat P, von Buchwald C, Wagner A. Rhinology. 2001;39:173–5.
59. Fountas KN, Duwayri Y, Kapsalaki E, Dimopoulos VG, Johnston KW, Peppard SB, et al. South Med J. 2004;97:279–82; quiz 283.
60. Younis RT, Anand VK, Davidson B. Laryngoscope. 2002;112:224–9.
61. Bolger WE, Butzin CA, Parsons DS. Laryngoscope. 1991;101:56–64.
62. Franzese CB, Stringer SP. Am J Rhinol. 2004;18:329–34.
63. Proposed rule. Fed Regist 1998;63:1659–1728.
64. Anzai Y, Jarvik JG, Sullivan SD, Hollingworth W. Am J Rhinol. 2007;21:444–51.
65. Balk EM, Zucker DR, Engels EA, Wong JB, Williams Jr JW, Lau J. J Gen Intern Med. 2001;16:701–11.
66. Senbil N, Gurer YK, Uner C, Barut Y. J Headache Pain. 2008;9:33–6.
67. Triulzi F, Zirpoli S. Pediatr Allergy Immunol. 2007;18(suppl 18):46–9.
68. Lee HS, Majima Y, Sakakura Y, Inagaki M, Sugiyama Y, Nakamoto S. Nippon Jibiinkoka Gakkai Kaiho. 1991;94:1250–6.
69. Bhattacharyya N, Jones DT, Hill M, Shapiro NL. Arch Otolaryngol Head Neck Surg. 2004;130:1029–32.
70. Cotter CS, Stringer S, Rust KR, Mancuso A. Int J Pediatr Otorhinolaryngol. 1999;50:63–8.
71. Al-Qudah M, Int J. Int J Pediatr Otorhinolaryngol. 2008;72:817–21.
72. Anzai Y, Weymuller Jr EA, Yueh B, Maronian N, Jarvik JG. Arch Otolaryngol Head Neck Surg. 2004;130:423–8.
73. Daele JJ. Acta Otorhinolaryngol Belg. 1997;51:285–304.
74. Lieu JE, Piccirillo JF, Lusk RP. Otolaryngol Head Neck Surg. 2003;129:222–32.
75. Adappa ND, Coticchia JM. Am J Otolaryngol. 2006;27:384–9.
76. DelGaudio JM, Swain Jr RE, Kingdom TT, Muller S, Hudgins PA. Arch Otolaryngol Head Neck Surg. 2003;129:236–40.
77. Nadkarni T, Goel A. J Postgrad Med. 2005; 51(suppl 1):S37–41.
78. Hagtvedt T, Aalokken TM, Notthellen J, Kolbenstvedt A. Eur Radiol. 2003;13:976–80.

Traumatic Extracranial Vascular Injury: Evidence-Based Neuroimaging

35

Gary H. Danton, Jessica R. L. Warsch, and Felipe Munera

Contents

G.H. Danton (✉)
Department of Radiology, University of Miami Miller School of Medicine, Miami, FL, USA
e-mail: gdanton1@med.miami.edu

J.R.L. Warsch
Medical Student, Department of Medical Education—MD/PhD Program, University of Miami Miller School of Medicine, Miami, FL, USA
e-mail: jloring@med.miami.edu

F. Munera
Department of Radiology, University of Miami Miller School of Medicine-Jackson Memorial Hospital/University of Miami Medical System, Miami, FL, USA
e-mail: fmunera@med.miami.edu

Key Points

- Screening for vascular injuries in high-risk patients decreases morbidity and may be cost effective (moderate evidence).
- Ultrasound is not recommended as a sole screening tool (moderate evidence).
  - CTA including MDCT has questionable sensitivity and specificity for diagnosing vascular injury in patients with blunt neck trauma. Study results are too disparate for making a clear conclusion.
- Single- and 4-slice MDCT have high sensitivity and specificities for diagnosing vascular injury in patients with penetrating trauma (moderate evidence).
- Four-vessel angiography is the gold standard for diagnosing vascular injury following trauma (moderate evidence).

Definition and Pathophysiology

Blunt trauma injuries are typically a result of motor vehicle crashes but can occur with any direct blow to the head or neck, strangulation, sports-related incidents, and manipulation of the spine. The majority of penetrating neck wounds are a result of guns and knives, with motor vehicle crashes and industrial and household accidents making up the remainder. Vascular injuries of the neck in blunt and penetrating trauma are an important determiner of morbidity and mortality and can occur through a variety of mechanisms, from direct transection, to shearing of blood vessels from hyperextension of the cervical spine, to disruption by fractures.

Epidemiology

Blunt and penetrating neck injuries comprise 5 % and 5–10 % of adult trauma cases, respectively [1, 2]. While the majority of significant vascular injuries to the neck are seen in victims of penetrating trauma, the morbidity and mortality related to blunt cerebrovascular injuries is significantly higher. Whereas the mortality rate for penetrating injuries ranges from 2 % to 6 %, blunt injuries are associated with an overall mortality rate of 20 % to 30 %, and about one-third to one-half develop permanent neurologic sequelae as a result of brain ischemia from vascular compromise [2]. In the pediatric population, blunt injuries are much more common, accounting for 90 % of all pediatric trauma admissions [3].

Overall Cost to Society

While no large-scale formal cost analyses have been performed, comprehensive screening of blunt and penetrating neck trauma patients for vascular injury will likely prove cost saving in terms of hospital and rehabilitation costs through earlier diagnosis and prompt treatment [4]. For instance, screening angiography has been associated with an estimated $2.03 million savings in medical costs per each neurological event prevented [5]. This intervention could also have quantity and quality of life impact, although it has not been formally studied.

Goals of Imaging

Screening diagnostic imaging of the neck in high-risk patients will detect extracranial vascular injury in time to apply evidence-based treatments and decrease risk of stroke and morbidity.

Methodology

A MEDLINE search was performed using PubMed (National Library of Medicine, Bethesda, Maryland) for original research publications discussing the use of imaging modalities in blunt and penetrating neck injuries. The search strategy employed different combinations of the following terms: blunt or penetrating, neck trauma or neck injury, radiography or imaging or computed tomography and/or angiography or CTA or MDCT, and cerebrovascular or vascular or carotid and/or vertebral. The search covered

the period from January 1980 to February 2011 and was limited to studies in humans and publications in the English language. The authors reviewed the full text of all articles identified from the literature search and included additional publications identified from their reference lists.

Discussion of Issues

Selection of Subjects for Imaging

Summary
Evaluation differs between blunt and penetrating neck injuries. For penetrating injuries, the available literature suggests that selective conservative management based on clinical examination and screening with noninvasive imaging modalities such as MDCT may supplant mandatory surgical exploration for all penetrating neck injuries. Similarly, noninvasive 8-slice or above MDCT may supplant invasive angiography for blunt neck trauma although results of many studies vary considerably (moderate evidence). Few studies have assessed which population is the most appropriate to screen for blunt cerebrovascular injury (BCVI); however, the Denver classification and Denver modifications are the most often cited (Table 35.1) [6].

Supporting Evidence

How Are Patients Selected for CT Screening Following Blunt Trauma to the Neck?

In a recent study of BCVI (moderate evidence), Berne et al. developed multivariate logistic regression models to explore the contributions of various clinical factors in determining which patients are at high risk of BCVI and should therefore be screened with multidetector computed tomography angiography [7]. Of 9,935 blunt trauma patients admitted during the study period, 102 (1.03 %) suffered BCVI. Those factors found to be most predictive of the presence of BCVI from multivariate analysis were cervical spine fracture (odds ratio (OR) = 7.46, 95 %

confidence interval (95 % CI) = 4.87–11.44), mandible fracture (OR = 2.59, 95 % CI = 1.30–5.15), high Injury Severity Score (OR = 1.05, 95 % CI = 1.04–1.07), and low Glasgow Coma Scale score (OR = 0.93, 95 % CI = 0.89–0.97), suggesting that the early assessment of patients for these characteristics may justify imaging. These results expand upon earlier studies by Biffl et al., which argue for the screening of patients based on injury mechanisms and patterns as a means to identify asymptomatic BCVI patients and institute early therapy [8–10].

Recommendations for screening algorithms, however, have been based largely on limited and moderate evidence. Study limitations are often due to small sample size and methodological considerations. These studies have identified associations between BCVI and the mechanism of injury (e.g., closed head injury, rapid deceleration, and hyperextension as occur during motor vehicle accidents, direct cervical blow, strangulation, and chiropractic manipulation), concomitant head and chest injury, and physical findings such as Battle's sign, cervical hematoma, chest wall contusion, altered mental status, hemispheric neurologic findings, Horner syndrome, stroke, or transient ischemic attack [8, 11–14]. While a greater number of risk factors are associated with a greater likelihood of vascular injury, the risk factors described to date are not all-inclusive, as these injuries have been found to occur even in the absence of known risk factors [15]. In a recent study by Almandoz et al., multidetector CTA found arterial injury in 106 of 830 patients (12.8 %) with acute blunt head and neck trauma, with cervical interfacetal subluxation/dislocation (OR = 6.3, $p < 0.0001$), with fracture lines reaching an arterial structure (OR = 4.4, $p < 0.0001$), and with high-impact mechanism of injury (high-speed (not defined) motor vehicle accident, struck at pedestrian, fall downstairs or from a height greater than standing, direct blow to the head or neck) (OR = 3.1, $p < 0.0001$) most predictive of arterial injury. Confidence intervals were not reported [16]. The authors proposed a three-point craniocervical trauma scoring system based on these factors, with patients with scores of 2 and 3 at highest risk of arterial injury.

How Are Patients Selected for CT Screening Following Penetrating Trauma to the Neck?

Hemodynamically unstable patients with evidence of vascular or aerodigestive injury are usually taken for operative exploration. Heavy bleeding, pulsatile or expanding hematoma, bruit, thrill, hematemesis, and hemoptysis stridor or obvious injuries are clinical signs used to make this determination. Managing patients with stable vital signs is more challenging and frequently begins with digital or visual assessment of the platysma for evidence of penetration. If the platysma is not violated, the patient is treated for a superficial injury [17–19].

Reliance on physical findings may prove more difficult in cases of multiple injuries. Evidence suggests that CT may be a good option in those patients who are hemodynamically stable and lack obvious signs of vascular injury to delineate wound trajectory and any occult damage to vascular structures, thereby avoiding unnecessary invasive procedures [20]. A level 3 (limited evidence) study compared two groups of patients retrospectively who received either CTA or surgery for penetrating neck injury reported 0 negative neck explorations for the CTA group and 48 % negative explorations for the surgery group. Patients were not randomly stratified; rather, the decision was made based on clinical presentation so the surgery group likely had more concerning injuries. Still, the negative exploration rate was very high relative to the CTA group [21]. Likewise, observational (not randomized clinical trials) studies support the use of imaging in clinically stable pediatric patients with penetrating neck trauma, particularly those sustaining projectile injuries (limited evidence) [22].

Diagnostic Imaging

Summary

While four-vessel angiography is considered the standard of reference, drawbacks include cost, logistic constraints, and risks associated with an invasive procedure. Color duplex sonography has been utilized as an alternative screening method,

but sensitivity was 38.5 % (limited evidence) and is not recommended as a sole screening test [23]. Results from CT angiography are highly variable depending on the vascular segment studied, the type of CT scanner, and the outcome measure. Limited level 4 evidence exists for the use of 64-MDCT, and while most authors agree that CT angiography is established enough to take the lead role in screening for penetrating and blunt trauma of the neck, a recent study by Dicocco using 32-MDCT strongly challenges that conclusion (moderate evidence). Most studies also suggest that these screening exams can be performed as part of a whole-body scan or dedicated neck exam (limited evidence). Few studies have fully evaluated MRI, and while early (limited evidence) studies showed promise, its use is not well evaluated.

Supporting Evidence

What Is the Recommended Modality and Protocol for Vascular Injury Screening in Blunt Neck Injury?
Four-Vessel Angiography

Four-vessel angiography has been used in the setting of cervicothoracic trauma since the late 1960s and is considered the gold standard method of diagnosing traumatic vascular injury (moderate evidence) [24]. Biffl et al. found 34 % of asymptomatic, high-risk patients had cervicovascular injury diagnosed by angiography (limited evidence) [8]. Cothren et al. analyzed angiography in the setting of blunt trauma and found that screening at-risk patients prevents strokes and is ultimately cost effective [4]. A retrospective study of 254 blunt cervicovascular injuries proposed that follow-up angiography of low-grade injuries changed management in 61 % of patients (limited evidence) [25]. Limitations of DSA as a screening tool include expense, invasiveness, and availability of skilled neuroangiographers offering the service at all hours. In 2000, Biffl et al. used a logistic regression analysis to identify predictors of vascular injury. This work led to the Modified Denver Screening Criteria in Table 35.1.

These factors also drive the desire for a noninvasive approach that would be equivalent to diagnostic angiography.

CT Angiography

Descriptive statistical analysis of screening CTA has been assessed with a number of studies summarized in Table 35.2 and sensitivities reported for the extracranial vasculature of 29–100 %. Most of the evidence is moderate or limited and frequently retrospective or with small numbers of patients. Studies vary in whether secondary or primary reads were considered in calculating the sensitivity and specificity and do not necessarily specify how extensive reformatting was performed. Some studies compare CTA to digital angiography and others only consider follow-up or used a combination of both. Variance among techniques limits the conclusions that can be drawn by comparing these studies. Studies that focus on follow-up and utilize secondary reads tend to report higher sensitivities than those who rely on the initial reading. Recently, Dicocco et al. retrospectively studied 684 patients who met criteria for blunt cerebrovascular injury screening. All patients were studied with both dedicated 32-MDCT and digital subtraction angiography. Comparing the ability of both modalities to identify injured vessels, the sensitivity of CTA was 51 %. Some of the missed injuries were higher grade, and identification of those injuries changed management [26]. A similar retrospective study by Goodwin et al. in 2009 used both 16- and eventually 64-MDCT with sensitivities of 29 % and 54 %, respectively. Because of discrepancies in data and technique, conclusions cannot be drawn as to whether CTA is or is not an effective screening tool. DSA remains the gold standard, and a controlled prospective comparison study between DSA and CTA is needed.

Duplex Sonography

Prior to CT, duplex ultrasound was employed as a screening test for cerebrovascular injury following trauma with some success. Cogbill et al. reported duplex detecting in 12 of 14 patients with carotid injuries where both missed cases were at the skull base [27] (insufficient evidence).

For vertebral artery dissections, sensitivities were reported between 64 % and 86 % (limited evidence) [28]. Mutze et al. reported a sensitivity and specificity of ultrasound being 39 % and 100 %, respectively, in a cohort of 1,471 patients (level 2) [23]. On the basis of this evidence, the Eastern Association for the Surgery of Trauma guidelines do not support the continued use of duplex ultrasound and favor CTA instead [24, 29]. While evidence level is limited, it does not support the routine use of duplex sonography as sole screening.

Magnetic Resonance Imaging

Because of its limited availability in the emergency setting and incompatibility with equipment used in the trauma setting, use of MRI has not become commonplace and reports of efficacy is sparse. Case reports of limited evidence concluded in favor [30–32] of MRA. Level three studies found the following: In 2002, sensitivity and specificity were reported to be 75 % and 67 %, respectively, on a 1.5 T Magnetom Symphony scanner (Siemens Medical System, Inc., Iselin, NJ) [33]. Using a 1 T Magnetom MRI (Siemens Medical System, Inc., Iselin, NJ) in 1994, sensitivities for carotids and vertebrals ranged from 84 % to 95 % and 20 % to 60 %, respectively. Specificities were over 98 % for all vessels [34]. A limited study for MRA using a 0.2 T Siemens open magnet found sensitivity/specificity for carotid injury 50 %/100 % and vertebral injury 47 %/97 % in 2002 [35]. A comparison of radiologists' preference to identify dissection not necessarily attributable to trauma was reported in 2008 with CT being favored more often than MRI, especially for the vertebral arteries [36]. There is a lack of evidence supporting the use of MRI although advances in MRI technology may ultimately improve its utility.

What Is the Recommended Modality and Protocol for Vascular Injury Screening in Penetrating Neck Injury?

Unlike blunt injury, penetrating vascular injury is managed with exploratory surgery. Digital subtraction angiography remains the gold standard for nonoperative evaluation of vascular injury of

the neck; however, CTA has shown more reliability for penetrating injuries than blunt injury. While fewer studies have been conducted of CTA for penetrating neck injury (Table 35.1), many were prospective and well designed. Diagnostic sensitivities for CTA in penetrating trauma studies tend to be higher than what is reported for blunt injury (moderate evidence). This observation may be reflective of the higher pretest probability for injury, diagnostic utility of injury trajectory, and injury proximity to the vasculature. Patient stratification on presentation begins by assessing depth of injury. Physical examination to verify penetration of the platysma is generally regarded as defining a superficial or deep injury. Diagnostic evaluation of superficial injuries often stops at the physical exam. In the past, most deep injuries were explored operatively resulting in one study finding no vascular injuries detected in 67 % of asymptomatic patients [1]. While unstable patients continue to be explored surgically, asymptomatic patients may be sent for screening exam. A prospective study of 60 patients with injuries in various neck zones compared CTA to DSA and found 90 % and 100 % sensitivity and specificity, respectively [37]. A prospective study of 175 patients comparing CTA, DSA, surgery, and clinical outcomes found 100 % sensitivity and 98.6 % specificity [38]. In 2006, a prospective study of 91 patients measured outcomes using an aggregate gold standard including final discharge diagnosis, all imaging studies, surgical procedures, and clinical follow-up. They found a 100 % sensitivity and 93.5 % specificity for diagnosing vascular injury [39]. A retrospective study in 2008 compared the number of negative neck explorations with patients who did or did not receive a CTA. Neck explorations in those who did not receive a CTA were negative 48 % of the time, while those who had a CTA had no negative neck explorations [21]. Utility of CTA for vascular injury screening has high sensitivities (moderate evidence). Radiologists should keep in mind, however, that many of these studies may have been interpreted with a high pretest probability using proximity to injury and trajectory as positive signs of injury.

Duplex Sonography

Duplex sonography has been evaluated in a number of studies and sensitivities and specificities ranged from 91 % to 95 % and 99 %, respectively. In 1996, a prospective study comparing ultrasound to DSA, surgery, or clinical status concluded that all clinically serious injuries were detected. Despite the rather high sensitivities, dependence on skilled technologists and sometimes limited access to patients with bandages covering the injured area has led to adoption of CTA over ultrasound.

What Is the Recommended CTA Protocol for Vascular Injury Screening in Traumatic Neck Injury?

There is no data to separately consider blunt or penetrating injury. No controlled studies comparing specific CT acquisition techniques and parameters have been performed. Rather, many articles describe various aspects of the technique used at their institution. These often vary between the technologies and manufacturers although similarities between techniques are commonplace (Table 35.3). However, level of evidence for choosing one technique over another is limited. In addition, there is no evidence that reconstructed images such as maximum intensity projections, 3D, or curved planar reformats increase sensitivity, specificity, or confidence of interpretation. Anecdotal reports of benefit constitute limited evidence [37, 40, 41] although the preponderance of references illustrating findings does so with reconstructed images. Their use is commonplace and recommended despite the weak evidence base (Figs. 35.1 through 35.3).

Should Screening CTA Be Performed as Part of a Full-Body Trauma Scan or Is a Dedicated CTA Required?

Perhaps a more controversial and more formally studied aspect of CTA screening is the question of whether a dedicated CTA neck timed to optimize the extracerebral vasculature with the arms adducted is needed or if the CTA neck can be performed in the same acquisition of a "trauma scan." The "trauma scan" may include the CT

neck as part of the c-spine, chest, abdomen, pelvis, thoracic, and lumbar spine exam with the arms abducted. In 2008, Sliker et al. published their findings comparing patients who both underwent screening CT and digital subtraction angiography. The MDCT group had CT neck as part of a body trauma protocol and the other had a dedicated CTA neck (MDCTA). Their protocols are included in Table 35.3. They found similar sensitivities and specificities in both groups (though slightly lower in the MDCT group) for carotid and vertebral injuries with DSA as the gold standard. Sensitivities were calculated for two vascular segments of the carotid and vertebrals, but if only those with actual positive cases are considered, the sensitivity ranged from 25 % to 74 % and specificity ranged from 82 % to 100 %. While there were no large differences between the techniques, reported sensitivities were low considering the conclusion that MDCT and MDCTA are useful screening tests [42] (level 3 evidence). Langner et al. divided up the neck and body scan into two separate boluses and acquisitions that occurred immediately after each other. Their protocol consists of a CT brain followed by a CTA neck with 40 cm^3 of contrast and a region of interest selected on the carotid. A 60-cm^3 contrast bolus followed for scanning the remainder of the chest, abdomen, and pelvis. They concluded that a dedicated CTA could be incorporated easily into a full-body trauma scan (limited evidence) [14].

Does Number of CT Detectors Make a Difference?

Early studies with single-detector CT found high sensitivities and specificities for penetrating neck trauma when compared to both follow-up and angiography (levels 2 and 3 evidence) [37, 38, 43, 44]. There is a general sense that as CT technology improved with regard to number of detectors, the ability of CT to screen blunt neck trauma improved [45]. A variety of reports with single and 4 MDCTs showed mixed results in level 2 and 3 studies. A number of observations (level 4 evidence) and a prospective level 3 study by Biffl in 2006 found that 16-MDCT detected all vascular injuries in their 18 patients with

injuries [46]. It has been suggested that MDCT with 8 or better MDCT is adequate for detection of cerebrovascular injury (Table 35.3). Chokshi et al. described examples of their experience with 64-MDCT, but no formal evaluation was performed (limited evidence) [40]. Dicocco et al. and Goodwin et al. used 16-, 32- and 64-MDCT and compared them directly with DSA finding relatively low sensitivities [26, 47]. The evidence is contradictory, and until prospective randomized trials are obtained, it is unclear if advances in CT technology will allow CTA to approach the sensitivities of DSA. However, based on the available evidence, 16-MDCT or better should be preferred for evaluation of blunt neck trauma (limited evidence).

What Is the Imaging Impact on Outcome?
Penetrating Trauma

Studies of penetrating neck trauma predominantly compare CT results to surgical exploration. Patients with high clinical suspicion for vascular injury are almost uniformly taken for surgical exploration. Patients in whom suspicion for injury exists from location of injury only and who have stable clinical features have been studied with CTA as the screening exam, and the primary outcome is avoiding surgical exploration. CTA has performed well in this setting and is recommended as a screening tool in patients with low suspicion from studies of level 2 [38] and level 3 evidence [1, 21, 22, 29, 37, 48–50]. Long-term evaluation of patient outcomes is not well studied.

Blunt Trauma

Stein et al. reported a decrease in stroke rate from 26 % to 4 % in patients who were treated for blunt extracranial vascular injury regardless of diagnostic method illustrating the importance of diagnosis and treatment [15]. In 2009, Eastman et al. compared stroke rates during a period of time when catheter angiography was primarily used for diagnosis and a later time period when CTA was used. During the later time period, a systematic approach to therapy was also

initiated specifying which injury type and grade receives a particular treatment. The stroke rate dropped from 15 % to 4 %, which at least suggests a complementary benefit of early diagnosis with CTA and the systematic approach to treatment [6].

Take Home Tables

See Table 35.1 for Modified Denver Screening Criteria for BCVI and Table 35.2 for descriptive analysis of CTA for diagnosing blunt and penetrating trauma.

Table 35.1 Modified Denver screening criteria for BCVI

Lateralizing neurologic deficit (not explained by CT head)
Infarct on CT head
Nonexpanding cervical hematoma
Massive epistaxis
Anisocoria/Horner's syndrome
GCS score <8
Cervical spine fracture
Basilar skull fracture
Severe facial fracture
Seatbelt sign above clavicle
Cervical bruit or thrill

Modified Denver Screening Criteria for BCVI as described by Eastman et al. [6] and based on data from Biffl et al. [8]

Table 35.2 Descriptive analysis of CTA for diagnosing blunt and penetrating trauma. Prot, type of protocol; Neck, dedicated CTA of the neck; WB, neck studies as part of the whole-body scan; Vess, vessels studied; C, carotid; V, vertebral; extra, extracranial only; intra, intracranial only; Sen, sensitivity; Spec, specificity; PPV, positive predictive value; NPV, negative predictive value; G.S., gold standard used as a comparison; A, angiography; F, follow-up; S, surgery; Level, level of evidence; INJ, injury type; P, penetrating; B, Blunt injury

References	Year	CT class	Prot	Vess	Sen	Spec	PPV	NPV	G.S.	Level	INJ
[38]	2000	SS CT	Neck	C,V	90	100	100	98	A	2	P
[50]	2001		Neck	C,V	100	91	75	100	S	4	P
[37]	2002	1 Helical	WB	C,V	100	99	93	100	A + F	2	P
[33]	2002	1 CT		C,V	68	65	65	70	A	3	B
[35]	2002	4-MDCT	Neck	C	47	99			A	2	B
[35]	2002	4-MDCT	Neck	V	53	99			A	2	B
[45]	2005	1-,4-,8-MDCT	Neck	C	86	92			A	3	B
[45]	2005	1-,4-,8-MDCT	Neck	V	53	93			A	3	B
[51]	2006	16-MDCT	Neck	C, V	98	100	100	99	A	2	B
[43]	2006	4-MDCT	Neck	C,V	100	93.5			F	2	P
[52]	2007	16-MDCT	Neck	C, V	74	86	65	90	A	2	B
[42]	2007	16-MDCT	WB	C extra	69	82	74	78	A	2	B
[42]	2007	16-MDCT	WB	V extra	74	91	74	91	A	2	B
[42]	2007	16-MDCT	WB	C intra	60	95	28	98	A	2	B
[42]	2007	16-MDCT	WB	V intra	0	99	0	99	A	2	B
[42]	2007	16-MDCT	Neck	C extra	64	94	84	84	A	2	B
[42]	2007	16-MDCT	Neck	V extra	68	100	100	87	A	2	B
[42]	2007	16-MDCT	Neck	C intra	25	94	40	89	A	2	B
[42]	2007	16-MDCT	Neck	V intra	n/a	100	n/a	100	A	2	B
[47]	2009	16-MDCT	Both	C, V	29	97	67	85	A	2	B
[47]	2009	64-MDCT	Both	C, V	54	97	73	92	A	2	B
[26]	2011	32-MDCT	Neck	C, V	51	97	43	98	A	2	B

Imaging Case Studies

Suggested Imaging Protocols

See Table 35.3 for CTA protocols typical of those reported throughout the literature.

Future Research

Designing prospective blinded studies is challenging because of the relative low frequency of vascular injuries and the general acceptance of CTA as an effective screening tool for blunt and penetrating traumatic injury. Large comparison trials of CTA to angiography will be time consuming and expensive and put patients at potential risk of catheter-related injury, but would establish the role of CTA in this process. Alternatively, clinical follow-up studies of patients who have had screening with CTA can track
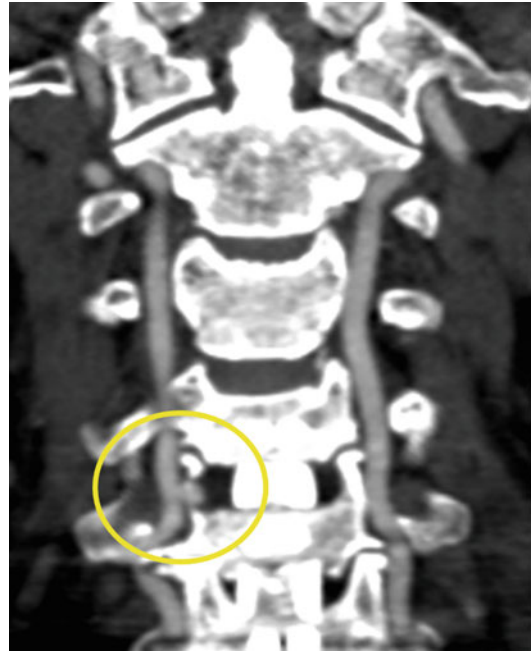
Fig. 35.1 A fifty-seven-year-old male status post anterior cervical diskectomy and fusion who presented with an acute neurologic deficit. Coronal multiplanar reformatted CTA image shows an outpouching at the foraminal segment (V2) of the right vertebral artery representing a pseudoaneurysm (*circle*). The patient underwent coil embolization (not shown)
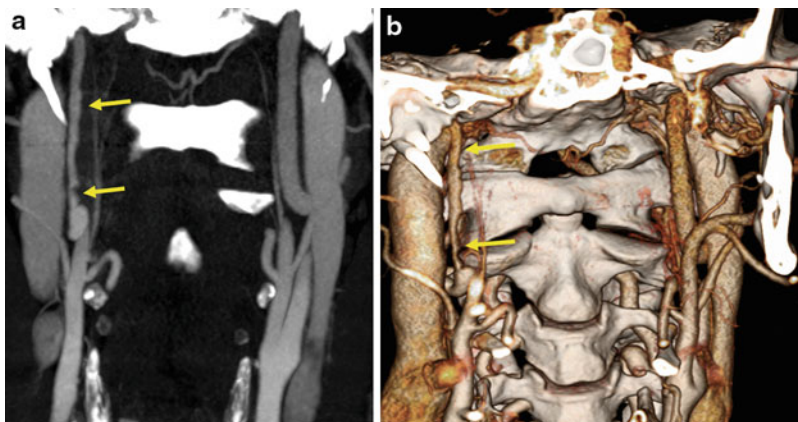
Fig. 35.2 (**a**, **b**) A 45-year-old male involved in motor vehicle collision. (**a**, **b**) Coronal maximum intensity projection (**a**) and volume-rendered (**b**) CTA images show long-segment narrowing with intimal irregularity of the right ICA indicating a dissection (Reproduced with permission from Chokshi et al. [40])
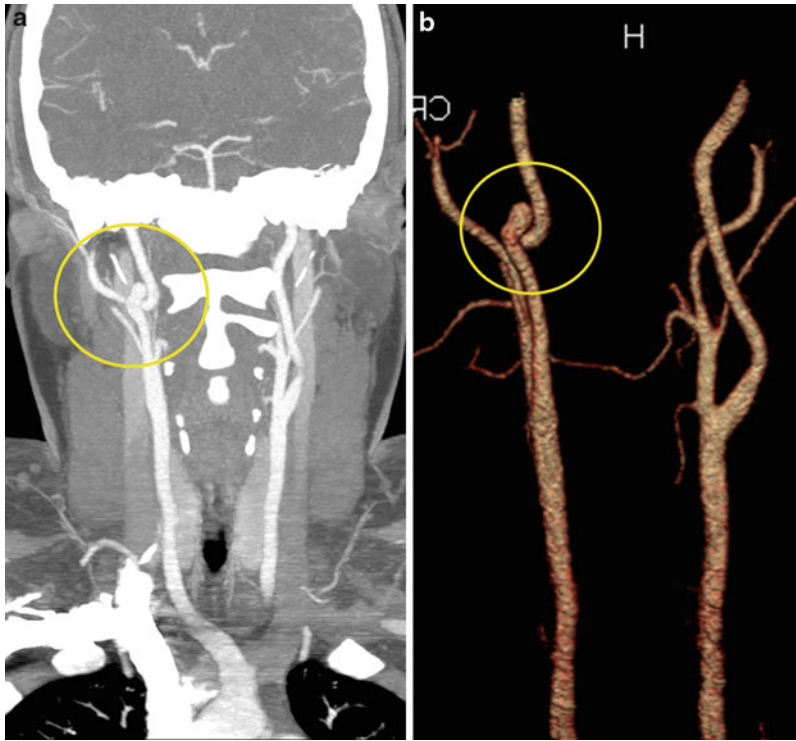
Fig. 35.3 (**a**, **b**) An 18-year-old male with blunt carotid artery injury resulting from a motor vehicle collision. (**a**, **b**) Maximum intensity projection (MIP) (**a**) and volume-rendering 3D-reconstruction images (**b**) show a 3-mm outpouching, with a narrow neck at the origin of the right ICA, representing a pseudoaneurysm (grade 3 injury), without associated luminal compromise. This patient received antiplatelet therapy, and the pseudoaneurysm remained stable on a follow-up angiogram 8 months later (not shown); the patient was asymptomatic during this period. No other intervention was performed (Reproduced with permission from Chokshi et al. [40])

their clinical outcome which may be a more relevant indicator of CTA utility. After all, is there any reason to detect an injury so small that it heals on its own without requiring therapy? As CT scanners continue to improve, evaluation with 64, 128, 320, and dual-source scanners may either continue to show improvement in sensitivity or reach a plateau. Finally, it is not clear what role reconstructions play in the analysis of CTA data. Making interpretation of images more efficient especially in the trauma setting could be useful, and individual sensitivities and specificities for CPR, MPR, and 3D images should be studied [53].

Table 35.3 CTA protocols typical of those reported throughout the literature. Blank fields indicate the information was not provided. MDCT, multidetector CT; Recons, Reconstructions reported to be performed and used in analysis; and Contrast agent, concentration of iodine reported; Vol, volume of first and second boluses when reported. If saline is not listed, the bolus was contrast. ROI location; A. aorta, ascending aorta; and D. aorta, descending aorta. The HU is the Hounsfield unit set to trigger the exam. Scan type is Neck, neck only, or WB, part of a whole-body scan where there is one acquisition. Neck w/WB is a scan where the neck was separate but scanned immediately before the scan for the body

References	[37]	[23]	[42]	[42]	[52]	[51]	[14]	[40]	[41]
CT detector	Helical, 1 slice	4-MDCT	16-MDCT	16-MDCT	16-MDCT	16-MDCT	16-MDCT	64-MDCT	64-MDCT
Collimation	3 mm	2.5 mm 1.25	16 × 0.75 mm	16 × 0.75 mm	0.75 mm		16 × 0.75	0.6 mm	0.625 mm
Slice thickness (mm)			1 × 3 / 2 × 2	1 × 0.5	2	0.5, 1.25	4.5		1.25–3.75
KV	120	120	140	120			120		
MA	250		210	245			360		
Pitch	1.3–2		1	0.9			1		0.984
Recons	2D, 3D		MPR, CPR	MIP, Thin	2D, 3D, MIP	MIP, 3D		2D, 3D, MIP	2D, 3D
Contrast agent	300	300	300	300	300	300			350–370
Injection rate	4.5 ml/s	4 ml/s	6 ml/s / 4 ml/s	4 ml/s	4 ml/s	3.5 ml/s	4 ml/s	5 ml/s	4–5 ml/s
Vol. 1st bolus		80	90 ml	100	80 ml	125	40 ml	50–100	100–120 ml
Vol. 2nd bolus			60 ml				40 ml saline		30–50 ml saline
Timing technique	11 s delay	Bolus tracking	Bolus tracking	Bolus tracking	Bolus tracking	18-s delay		Bolus tracking	20-s delay
ROI location/HU	n/a	A aorta/90	D aorta/90	D aorta/120	Aorta arch/50	n/a		A aorta	n/a
Scan type	Neck	Neck	WB	Neck	Neck		Neck w/z WB	Neck	WB

References

1. Nason RW, Assuras GN, Gray PR, Lipschitz J, Burns CM. Can J Surg. 2001;44(2):122–6.
2. Rathlev NK, Medzon R, Bracken ME. Emerg Med Clin North Am. 2007;25(3). doi:679. viii.
3. Cotton BA, Nance ML. Semin Pediatr Surg. 2004;13(2):87–97.
4. Cothren CC, Moore EE, Ray Jr CE, et al. Am J Surg. 2005;190(6):845–9.
5. Jarvik JG, Philips 3rd GR, Schwab CW, Schwartz JS, Grossman RI. AJNR Am J Neuroradiol. 1995;16(4):647–54.
6. Eastman AL, Muraliraj V, Sperry JL, Minei JP. J Trauma. 2009;67(3):551–6. discussion 5–6.
7. Berne JD, Cook A, Rowe SA, Norwood SH. J Vasc Surg. 2010;51(1):57–64.
8. Biffl WL, Moore EE, Offner PJ, et al. Am J Surg. 1999;178(6):517–22.
9. Biffl WL, Moore EE, Ryu RK, et al. Ann Surg. 1998;228(4):462–70.
10. Biffl WL, Moore EE, Elliott JP, et al. Ann Surg. 2000;231(5):672–81.
11. Parikh AA, Luchette FA, Valente JF, et al. J Am Coll Surg. 1997;185(1):80–6.
12. Mulloy JP, Flick PA, Gold RE. Radiology. 1998;207(3):571–85.
13. Berne JD, Norwood SH, McAuley CE, Vallina VL, Creath RG, McLarty J. J Am Coll Surg. 2001;192(3):314–21.
14. Langner S, Fleck S, Kirsch M, Petrik M, Hosten N. AJNR Am J Neuroradiol. 2008; 29(10):1902–7.
15. Stein DM, Boswell S, Sliker CW, Lui FY, Scalea TM. J Trauma. 2009;66(1):132–43. discussion 43–4.
16. Delgado Almandoz JE, Schaefer PW, Kelly HR, Lev MH, Gonzalez RG, Romero JM. Radiology. 2010;254(1):236–44.
17. Asensio JA, Valenziano CP, Falcone RE, Grosh JD. Surg Clin North Am. 1991;71(2):267–96.
18. Kendall JL, Anglin D, Demetriades D. Emerg Med Clin North Am. 1998;16(1):85–105.
19. Golueke PJ, Goldstein AS, Sclafani SJ, Mitchell WG, Shaftan GW. J Trauma. 1984;24(12):1010–4.
20. Gracias VH, Reilly PM, Philpott J, et al. Arch Surg. 2001;136(11):1231–5.
21. Osborn TM, Bell RB, Qaisi W, Long WB. J Trauma. 2008;64(6):1466–71.
22. Vick LR, Islam S. Am Surg. 2008;74(11):1104–6.
23. Mutze S, Rademacher G, Matthes G, Hosten N, Stengel D. Radiology. 2005;237(3):884–92.
24. Bromberg WJ, Collier BC, Diebel LN, et al. J Trauma. 2010;68(2):471–7.
25. Biffl WL, Ray Jr CE, Moore EE, et al. Ann Surg. 2002;235(5):699–706. discussion −7.
26. DiCocco JM, Emmett KP, Fabian TC, Zarzaur BL, Williams JS, Croce MA. Ann Surg. 2011;253(3):444–50.
27. Cogbill TH, Moore EE, Meissner M, et al. J Trauma. 1994;37(3):473–9.
28. Sturzenegger M, Mattle HP, Rivoir A, Rihs F, Schmid C. Stroke. 1993;24(12):1910–21.
29. Tisherman SA, Bokhari F, Collier B, et al. J Trauma. 2008;64(5):1392–405.
30. Friedman D, Flanders A, Thomas C, Millar W. AJR Am J Roentgenol. 1995;164(2):443–7. discussion 8–9.
31. Bok AP, Peter JC. J Trauma. 1996;40(6):968–72.
32. Weller SJ, Rossitch Jr E, Malek AM. J Trauma. 1999;46(4):660–6.
33. Biffl WL, Ray Jr CE, Moore EE, Mestek M, Johnson JL, Burch JM. J Trauma. 2002;53(5):850–6.
34. Levy C, Laissy JP, Raveau V, et al. Radiology. 1994;190(1):97–103.
35. Miller PR, Fabian TC, Croce MA, et al. Ann Surg. 2002;236(3):386–93. discussion 93–5.
36. Vertinsky AT, Schwartz NE, Fischbein NJ, Rosenberg J, Albers GW, Zaharchuk G. AJNR Am J Neuroradiol. 2008;29(9):1753–60.
37. Munera F, Soto JA, Palacio DM, et al. Radiology. 2002;224(2):366–72.
38. Munera F, Soto JA, Palacio D, Velez SM, Medina E. Radiology. 2000;216(2):356–62.
39. Inaba K, Munera F, McKenney MG, et al. J Vasc Surg. 2006;43(1):77–80.
40. Chokshi FH, Munera F, Rivas LA, Henry RP, Quencer RM. AJR Am J Roentgenol. 2011;196(3):W309–15.
41. Uyeda JW, Anderson SW, Sakai O, Soto JA. Radiol Clin North Am. 2010;48(2):423–38. ix-x.
42. Sliker CW, Shanmuganathan K, Mirvis SE. AJR Am J Roentgenol. 2008;190(3):790–9.
43. Inaba K, Munera F, McKenney M, et al. J Trauma. 2006;61(1):144–9.
44. Munera F, Soto JA, Nunez D. Emerg Radiol. 2004;10(6):303–9.
45. Bub LD, Hollingworth W, Jarvik JG, Hallam DK. J Trauma. 2005;59(3):691–7.
46. Biffl WL, Egglin T, Benedetto B, Gibbs F, Cioffi WG. J Trauma. 2006;60(4):745–51. discussion 51–2.
47. Goodwin RB, Beery 2nd PR, Dorbish RJ, et al. J Trauma. 2009;67(5):1046–50.
48. Munera F, Danton G, Rivas LA, Henry RP, Ferrari MG. Semin Ultrasound CT MR. 2009;30(3):195–204.
49. Anaya C, Munera F, Bloomer CW, Danton GH, Caban K. Semin Ultrasound CT MR. 2009;30(3):205–14.
50. Mazolewski PJ, Curry JD, Browder T, Fildes J. J Trauma. 2001;51(2):315–9.
51. Eastman AL, Chason DP, Perez CL, McAnulty AL, Minei JP. J Trauma. 2006;60(5):925–9. discussion 9.
52. Malhotra AK, Camacho M, Ivatury RR, et al. Ann Surg. 2007;246(4):632–42. discussion 42–3.
53. Munera F, Foley M, Chokshi FH. Clin North Am. 2012;50 (1):59–72.

Yasha Kadkhodayan, Colin P. Derdeyn, and Alex M. Barrocas

Contents

Y. Kadkhodayan (✉) • C.P. Derdeyn
Mallinckrodt Institute of Radiology, Washington University School of Medicine, St. Louis, MO, USA
e-mail: kadkhodayany@mir.wustl.edu; derdeync@mir.wustl.edu

A.M. Barrocas
Department of Radiology, Mount Sinai Medical Center, Miami Beach, FL, USA
e-mail: abarrocas@msmc.com

Key Points

- At present, carotid imaging is performed to identify the presence and measure the degree of atherosclerotic stenosis in order to select appropriate candidates for surgical endarterectomy (strong evidence). Several different imaging strategies may be employed in symptomatic patients:
    - Catheter angiography (CA) can be used for this purpose (strong evidence).
    - Doppler ultrasound (DUS), computed tomographic angiography (CTA), and magnetic resonance angiography (MRA), alone or in some combination, if adequately validated, may be used to screen patients prior to catheter angiography (moderate evidence).
    - DUS, CTA, and MRA, alone or in some combination, if adequately validated, may be used to identify patients with severe stenosis ($\geq$70 %) for surgical endarterectomy (moderate evidence).
- Noninvasive screening of asymptomatic patients with highly specific thresholds may be cost-effective in high-risk populations such as patients with known atherosclerosis in other circulations or the presence of a bruit over the carotid artery on physical examination (moderate evidence).
- Carotid angioplasty and stenting (CAS) is a reasonable alternative to carotid endarterectomy (CEA) only in selected patients, namely, those with symptomatic high-grade stenosis who are at high risk for surgery (moderate evidence).
- Physiological imaging tools can identify high-risk subgroups in patients with atherosclerotic carotid stenosis and occlusion (strong evidence). The use of physiological imaging tools to guide therapy and improve outcome is unproven (insufficient evidence).

Definition and Pathophysiology

Extracranial carotid bifurcation atherosclerotic disease is associated with ischemic stroke. The carotid bifurcation, particularly the internal carotid artery near the bifurcation, is a preferred site for the development of atherosclerotic plaque. Several biomechanical and physiological factors are involved in the formation of atheroma at this location [1]. As atherosclerotic plaque builds, it can lead to ischemic stroke via two interrelated mechanisms: embolism and hemodynamic impairment. Embolism of plaque debris or thrombus that develops in or on the plaque may break free and lodge in a distal artery of the brain. Embolism likely accounts for the majority of stroke that occurs in association with carotid atherosclerosis. The second mechanism is that of low flow [2]. Depending on the adequacy of collateral flow, primarily determined by the status of the circle of Willis, severe stenosis may limit blood flow to the distal cerebral hemisphere. Significant hemodynamic impairment due to severe stenosis or occlusion at the carotid bifurcation is an independent predictor of stroke, likely due to synergistic effects with embolic events. Primary hemodynamic or low-flow stroke may also occur but is uncommon relative to primary embolic or synergistic embolic and hemodynamic mechanisms.

At present, only the degree of luminal diameter narrowing as measured by catheter angiography has been proven as a predictor of outcome in large-scale clinical trials of intervention versus medical therapy [3, 4]. Many other features of atherosclerotic plaque, including length of stenosis, cross-sectional area reduction, blood flow velocity, and plaque ulceration or irregularity, have been associated with higher risks of stroke on medical treatment, but none has been proven in randomized clinical trials as predictors of stroke risk.

Epidemiology

First-ever or recurrent ischemic stroke affects approximately 795,000 people in the United States annually [5]. An additional 200,000 to 500,000 people present with transient ischemic attacks (TIA) rather than a completed stroke. Associated carotid bifurcation disease is involved in 20–30 % of patients with these neurological

symptoms [6]. Clinical trials of surgical endarterectomy in symptomatic patients (TIA and stroke) with severe stenosis (measured by catheter angiography) have shown substantial benefit for secondary stroke prevention over medical therapy [7]. The issue of carotid imaging is relevant to this population for the purpose of secondary stroke prevention and to patients with asymptomatic carotid stenosis, which is present in up to 20 % of patients with prior myocardial infarction or peripheral vascular disease.

Overall Cost to Society

In 2007, the American Heart Association (AHA) estimated the total economic burden for stroke to be $41 billion [5]. The large majority of this cost is for acute and long-term care after stroke. The mean lifetime cost of ischemic stroke in the United States is estimated at $140,048. Consequently, even expensive diagnostic evaluation and treatments aimed at primary or secondary stroke prevention are often cost-effective.

Goals of Imaging

The overall goal of carotid imaging is to identify appropriate candidates for surgical or endovascular revascularization. Patients with insignificant degrees of stenosis are treated medically. Imaging must detect, localize, and accurately measure the degree of stenosis in order to accomplish this goal.

Methodology

PubMed (National Library of Medicine, Bethesda, MD) was used to search for original research publications investigating the diagnostic performance and effectiveness of imaging strategies for the extracranial carotid artery bifurcation. The search included the period 1966 to June 2011. Search terms included combinations of the following key words: *carotid*, *stenosis*, *imaging*, *ultrasound*, *angiography*, *magnetic*

resonance, *computed tomography*, *stroke*, and *ischemia*. Additional articles were identified from the references of these papers. The review was limited to human studies and English-language literature. Abstracts and titles of articles were reviewed for relevance to this topic. Relevant articles were reviewed in full.

Discussion of Issues

What Is the Imaging Modality of Choice in Symptomatic Carotid Artery Stenosis?

Summary
At present, carotid artery imaging is performed to identify the presence and measure the degree of atherosclerotic stenosis in order to select appropriate candidates for surgical endarterectomy (strong evidence). Several different imaging strategies may be employed in symptomatic patients:

- Catheter angiography (CA) can be used for this purpose (strong evidence).
- Doppler ultrasound (DUS), computed tomographic angiography (CTA), and magnetic resonance angiography (MRA), alone or in some combination, if adequately validated at the local institution with quality assurance data, may be used to screen patients with <50 % stenosis prior to catheter angiography (moderate evidence).
- DUS, CTA, and MRA, alone or in some combination, if adequately validated locally, may be used to identify patients with severe stenosis (≥70 %) for surgical endarterectomy (moderate evidence). Those with moderate stenosis (50–69 %) at noninvasive imaging can be further investigated with CA (moderate evidence).

Supporting Evidence
Patients with TIA, stroke, or ischemic ocular events are considered symptomatic. High-grade carotid artery stenosis is common in patients with anterior circulation ischemic symptoms [6, 8]. Carotid endarterectomy (CEA) is highly effective

in reducing stroke risk in patients with ≥70 % stenosis (strong evidence). This has been established by two large multicenter randomized trials of CEA versus best medical therapy [3, 4].

The North American Symptomatic Carotid Endarterectomy Trial (NASCET) showed a 17 % absolute risk reduction for ipsilateral stroke over 2 years with CEA compared with medical management in symptomatic patients with at least 70 % stenosis. Surgery in patients with symptomatic but more moderate stenosis of 50–69 % had a 6.5 % absolute risk reduction of ipsilateral stroke over 5 years [9]. The decision for surgery in patients with moderate stenosis should consider other risk factors as the benefit is not as dramatic. Male patients, patients with recent symptoms, and patients with cerebral rather than ocular ischemic symptoms have greater benefit with surgery.

Catheter Angiography (CA)

Both NASCET and the European Carotid Surgery Trial (ECST) used catheter angiography (Fig. 36.1a, b) to select patients for surgery [3, 4]. The degree of stenosis by deciles was correlated with surgical benefit in both studies. The use of catheter angiography, therefore, has been correlated to clinical outcome in a way that no other noninvasive imaging modality has been validated (strong evidence).

The use of noninvasive screening tools to reduce or eliminate the need for catheter angiography has been extensively investigated. These imaging tools have the advantage of reducing cost and risk to patients due to catheter angiography. However, this comes at the expense of potentially overestimating stenosis and subjecting patients to unnecessary surgical risk, as well as underestimating stenosis and subjecting patients to increased stroke risk from natural history of the disease. Sound validation of these different modalities against catheter angiography with local quality assurance data is imperative [10].

Local variables including the accuracy of DUS, CTA, and MRA; the rate of stroke with angiography; and the surgical complication rate can have profound effect on cost-effectiveness [11, 12]. The most cost-effective strategy may not be the same at every institution.

Doppler Ultrasound (DUS)

Typically, imaging of the carotid arteries involves an anatomic measurement of stenosis. DUS, on the other hand, relies on a blood flow velocity as a marker of stenosis. The most common ways to make this determination are measuring the peak systolic velocity (PSV) and the ratio of the PSV in the internal carotid (IC) artery to that in the ipsilateral common carotid (CC) artery. Most laboratories define two major categories of stenosis: 50–69 % and 70–99 %. By consensus, these categories correspond to PSVs of 125–230 cm/s and >230 cm/s and IC to CC ratios of 2–4 and >4, respectively [13].

While the performance of DUS can be highly variable [14], the sensitivity and specificity for detection or exclusion of ≥70 % stenosis of the internal carotid artery generally range from 85 % to 90 % compared with catheter angiography [15, 16]. Different criteria can be better correlated with angiography at different laboratories. In a study by Alexandrov et al., PSV was more accurate in one lab while the use of ratios was more accurate in another [17].

As performance varies substantially among devices (Fig. 36.2a–c), validation of local vascular laboratories is required. With validation, ultrasound performance can be sufficient for the reliable identification of patients with no significant stenosis and of those with severe stenosis [18]. Wide confidence limits for the degree of stenosis in individual patients can limit the ability of DUS to accurately classify patients at the thresholds for clinical decision making (i.e., 70 % stenosis).

Another major limitation of DUS is that near total occlusion can be mistaken for total occlusion, an important clinical distinction. Additional issues include elevated velocities in the setting of a contralateral carotid occlusion and with a carotid stent in place as well as generally higher velocities in women [19–21]. Dense calcification, vessel tortuosity, high carotid bifurcation, and thick overlying soft tissue can also preclude an optimal study.

Computed Tomographic Angiography (CTA)

Koelemay et al. reviewed data from 28 studies published between 1992 and 2003 using single slice scanners [22]. Eight of the 28 studies were considered to be methodologically sound with blinded review of images and reduction of other sources of bias. The pooled sensitivity and specificity of CTA for the detection of 70–99 % stenosis were 85 % (95 % CI, 79–89) and 93 % (95 % CI, 89–96), respectively. For detection of complete occlusion, the sensitivity and specificity were 97 % (95 % CI, 93–99) and 99 % (95 % CI, 98–100), respectively.

The advent of multidetector machines has expanded the vascular imaging capabilities of CT scanners. An early consecutive series of patients (81 vessels over 3 years) receiving both multidetector CTA and DSA in the initial evaluation of stroke and TIA showed that the two studies were in agreement 96 % of the time (95 % CI, 90–99) when using a 70 % threshold for stenosis. CTA was 100 % sensitive and 63 % specific with a negative predictive value of 100 % for stenosis <70 %. As such, the authors advocate its use as an excellent screening test [23].

Similar to DUS, which is known to have operator variability, CTA can also be prone to local variation. In the French multicenter study, Carotide-Angiographic par Resonance Magnetigue-Echographic-Doppler-Angiosce (CARMEDAS), using CTA alone resulted in the misclassification of stenosis in 11 of 64 patients (determined at surgery) [24]. While there were five centers enrolled in the study, nine of the 11 CTA misclassifications came from one center (asymptomatic arteries). This was attributed to lack of standardization in postprocessing and measurement methods.

Zhang et al. have evaluated the reproducibility of automated CTA analysis and showed that correlation between CTA and DSA improved from 0.69 to 0.81 in a series of 72 vessels in 36 symptomatic carotid stenosis patients when manual corrections for interfering factors such as ulcerations, calcifications, and adjacent vessels were applied [25]. This further illustrates the importance of local validation with quality assurance data.

Magnetic Resonance Angiography (MRA)

Early MRA utilized phase-contrast technique, and much of the initial validation literature was for time-of-flight (TOF) techniques [26]. More recent studies involve contrast-enhanced MRA (CE-MRA), which improves vascular contrast and is less susceptible to motion or dephasing artifact [27]. Both TOF-MRA and CE-MRA showed high accuracy for the detection of high-grade internal carotid artery (ICA) stenosis and occlusion with CE-MRA having an advantage compared to TOF-MRA in a recent meta-analysis [28]. The sensitivity and specificity of TOF-MRA for the detection of ≥70–99 % ICA stenosis were 91.2 % (95 % CI, 88.9–93.1) and 88.3 % (95 % CI, 86.7–89.7), respectively, whereas the sensitivity of CE-MRA was 94.6 % (95 % CI, 92.4–96.4) with a specificity of 91.9 % (95 % CI, 90.3–93.4). For ICA occlusion, the sensitivity of TOF-MRA was 94.5 % (95 % CI, 91.2–96.8) and the specificity was 99.3 % (95 % CI, 98.9–99.6). For CE-MRA, the sensitivity and specificity were 99.4 % (96.8–100 %) and 99.6 % (99.2–99.9 %), respectively. Sensitivity was poor (TOF-MRA) to fair (CE-MRA) for moderately severe stenosis (50–69 %).

In a study comparing CE-MRA to TOF-MRA, the administration of gadolinium did not offer a significant advantage in distinguishing surgically treatable ICA stenosis ≥70 % [29]. This may be important in patients with contraindications to gadolinium. In another study specifically looking at gadofosveset-enhanced MRA, the steady-state imaging allowed by a blood-pool contrast agent was superior to first-pass imaging in the assessment of vessel stenosis and plaque morphology, and the combined reading protocol was more accurate [30].

Aside from low sensitivity for moderate stenosis, MRA does have other notable limitations (Fig. 36.3a–c). MRA, particularly TOF-MRA, tends to overestimate the degree of stenosis. Many studies in the literature show a falsely elevated specificity for carotid MRA in the detection of high-grade stenosis due to spectrum bias [31]. This results from the fact that the reported specificity typically includes both clinically normal and significantly narrowed carotid arteries. While this

would be appropriate if MRA were used as a screening test (where high sensitivity is needed and low specificity can be tolerated), many practices use it as a confirmatory test (where high specificity is needed) after sonography. Also, postprocessing techniques can influence stenosis measurement. In particular, CE volume rendering tends to overestimate the degree of stenosis [32].

A recent meta-analysis based on individual patient data from both research and audit-derived data suggested that CE-MRA was the most accurate of the noninvasive imaging modalities (DUS, CTA, and MRA) for 70–99 % stenosis with a sensitivity and specificity of 85 % [33]. The authors state that the data in the current literature generally overestimates accuracy for noninvasive studies, that sensitivity for moderate stenosis is substantially lower than for high-grade stenosis across the board, that combinations of noninvasive tests do not improve both sensitivity and specificity but rather improve one at the expense of the other, and that ultimately, accuracy depends on whether or not the patient is symptomatic with respect to the vessel of interest.

What Is the Imaging Modality of Choice in Asymptomatic Carotid Artery Stenosis?

Summary

There is evidence from large randomized trials that asymptomatic patients with 60–99 % stenosis benefit from carotid endarterectomy (strong evidence). However, no screening program has been shown to reduce the incidence of stroke, and screening of the general population is not recommended [34]. Furthermore, there is no consensus on the subgroups that would benefit from such screening. The American Society of Neuroimaging recommends screening adults >65 years of age and who have ≥3 cardiovascular risk factors [35]. A consensus panel recommends screening patients with carotid bruits who are candidates for revascularization and those in whom coronary artery bypass grafting is planned [36]. Only well-validated DUS or MRA laboratories are recommended for this purpose.

Supporting Evidence

Atherosclerosis is a systemic disease. The association between carotid and coronary artery disease has long been established [37, 38]; this is manifested in the perioperative stroke risk in coronary artery bypass patients [39, 40]. The association with peripheral vascular disease is also well documented. In a series of 373 consecutive patients with documented peripheral vascular disease, 94 were candidates for endarterectomy, 22 with ischemic cerebral events, and 72 asymptomatic patients [41].

Aside from the evaluation of risk factors, the discovery of a neck bruit is another way to select patients for screening. A large early study looking at the role of carotid stenosis in ischemic stroke found >75 % stenosis by DUS in 17 % of 500 asymptomatic patients with a carotid bruit [42]. More recently, however, the Northern Manhattan Study found the sensitivity of auscultation to be 56 %, specificity 98 %, positive predictive value 25 %, and negative predictive value 99 % for the detection of carotid stenosis [43]. The false-negative rate was 44 %. This suggests that auscultation is not sufficient to exclude carotid artery stenosis, and while the presence of a bruit may warrant DUS, DUS may be considered in high-risk asymptomatic patients regardless of findings on auscultation.

At the same time, the benefit of surgery in patients with asymptomatic carotid artery stenosis is not as substantial as in the symptomatic case. Two randomized controlled trials do show that patients with 60–99 % ipsilateral carotid stenosis have stroke risk reduction with surgery [44, 45]. The Asymptomatic Carotid Atherosclerosis Study (ACAS) estimated that the 5-year risk of ipsilateral stroke and any perioperative stroke or death in good surgical candidates with carotid artery stenosis of 60 % or greater was 5.1 % versus 11.0 % in the medically treated patients [44]. Operating on 85 patients would prevent one stroke per year, or if the patients did not die of cardiac death first, operating on 17 patients would prevent one stroke in 5 years. However, because only half the strokes were disabling, their absolute risk reduction was

2.6 %, which about doubles the number of patients needed to be treated to prevent one disabling stroke compared with any other stroke. Subgroup analyses showed no benefit in women.

The Asymptomatic Carotid Surgery Trial (ACST) yielded similar results [45]. Surgical morbidity and mortality was 3.1 %. The absolute stroke risk reduction at 5 years was 5.4 %. With good medical care, patients face only a 2 % annual stroke rate, which falls below 1 % after successful carotid endarterectomy. However, the benefits exceed the risks only if the 30-day postoperative morbidity and mortality remain low; otherwise, there is no benefit.

Given the results of these trials and the challenges of screening asymptomatic patients, only well-validated DUS or MRA laboratories are recommended for this purpose (moderate evidence). The critical factors for screening are well-validated noninvasive methods and documented low surgical complication rates.

Cost-Effectiveness Analysis

Screening of asymptomatic patients with noninvasive methods and highly specific thresholds may be cost-effective in certain high-risk populations, such as patients with known atherosclerotic disease in other circulations or the presence of a bruit over the carotid artery on physical examination. Studies addressing the cost-effectiveness of screening asymptomatic carotid artery stenosis have resulted in divergent conclusions [46]. The critical factor in whether intervention is effective is the surgical complication rate. A one-time screening program of a population with high prevalence (20 %) of ≥60 % stenosis costs $35,130 per incremental quality-adjusted life-year (QALY) gained. Decreased surgical benefit (less than 1 % annual stroke risk reduction with surgery) or increased annual discount rate resulted in screening being detrimental, resulting in lost QALYs. Annual screening cost $457,773 per incremental QALY gained. In a low-prevalence (4 %) population, one-time screening cost $52,588 per QALY gained while annual screening was detrimental [47].

What Is the Role of Carotid Angioplasty and Stenting?

Summary

Carotid angioplasty and stenting (CAS) is a reasonable alternative to carotid endarterectomy (CEA) in selected patients (moderate evidence). Subgroups that may benefit from CAS include those who have undergone prior neck surgery or radiation therapy as well as those who are deemed to be at high surgical risk for a variety of reasons including significant cardiac or pulmonary disease, contralateral carotid artery occlusion, laryngeal nerve palsy, or age >80 years.

At present, CAS is accepted as a reasonable therapy for patients with severe stenosis and recent ischemic symptoms who are not good surgical candidates (moderate evidence). Patients who are good surgical candidates should be treated surgically or within clinical trials. Noninvasive screening of symptomatic but surgically ineligible patients for possible carotid stenosis should be done prior to angioplasty and stenting (moderate evidence). The benefit of angioplasty and stenting for asymptomatic patients is unproven (insufficient evidence).

Supporting Evidence

*M*eta-analyses have shown CAS to be associated with a lower rate of myocardial infarction and procedural morbidity when compared to CEA; however, CAS has also been associated with a higher rate of periprocedural stroke [48–52].

The only randomized trial of CAS (with embolic protection device) versus CEA specifically looking at high surgical risk patients (Stenting and Angioplasty with Protection in Patients of High-Risk Endarterectomy, SAPPHIRE) was stopped early due to slow enrollment [53]. Patients with a symptomatic stenosis >50 % or asymptomatic stenosis >80 % and at least one high-risk factor were enrolled. However, many patients were excluded as they were perceived to be at too high a risk for surgery. The primary composite endpoint of death, stroke, or myocardial infarction (MI) within 30 days or death or ipsilateral stroke between 31 days

and 1 year occurred in 12.2 % of the CAS arm and 20.1 % of the CEA arm (absolute difference, −7.9 %; 95 % CI, −16.4–0.7 with $p = 0.004$ for noninferiority and $p = 0.053$ for superiority). In symptomatic patients, the incidence of the primary endpoint was similar (16.8 % with CAS, 16.5 % with CEA). In asymptomatic patients, the primary endpoint occurred less frequently in the CAS group (9.9 % vs. 21.5 %). At 3 years, the rates of stroke and target-vessel revascularization were similar in both groups (7.1 % with CAS vs. 6.7 % with CEA and 3 % with CAS vs. 7.1 % with CEA, respectively). A major issue raised by this study is whether these patients would have done better with medical therapy alone.

In the Carotid and Vertebral Artery Transluminal Angioplasty Study (CAVATAS), which randomized patients to endovascular treatment (rate of stent use was only 22 %) and medical therapy, the stroke and death rates were similar in both groups (10 % at 30 days and 14.2 % at 1 year) [54]. The Stent-Protected Angioplasty versus Carotid Endarterectomy (SPACE) trial randomized 1,200 patients with symptomatic high-grade stenosis to CAS and CEA and showed no significant difference in outcome at 30 days [55]. The Endarterectomy Versus Angioplasty in Patients with Symptomatic Severe Carotid Stenosis (EVA-3S) trial enrolled 520 patients before being stopped due to a higher 30-day stroke and adverse event rate in the CAS arm [56].

Other randomized trials of CAS with embolic protection devices versus CEA in standard-risk patients are ongoing. An interim safety analysis of 1,713 randomized symptomatic patients with >50 % stenosis in the International Carotid Stenting Study (ICSS) revealed a 120-day stroke, death, or procedural MI rate of 8.5 % with CAS and 5.2 % with CEA for a hazards ratio of 1.69 (95 % CI, 1.16–2.45) [57]. Carotid Revascularization Endarterectomy versus Stent Trial (CREST) showed no significant difference in the rate of overall periprocedural stroke, death, or MI and ipsilateral stroke through 4 years among 2,502 symptomatic and asymptomatic patients (7.2 % with CAS and 6.8 % with CEA) [58]. The component periprocedural events did differ, however, between the 2 groups. While absolute rates were low, stroke was more frequent with CAS, and MI was more frequent with CEA. Also, younger patients, particularly those <70 years of age, tend to do better with CAS while older patients do better with CEA. The association between older age and increased complication rate after CAS, possibly related to vessel tortuosity and calcification, was also noted in the SPACE and ICSS trials.

What Is the Role of Physiological Imaging in Carotid Artery Stenosis and Occlusion?

Summary

Physiological imaging studies that identify compensatory hemodynamic mechanisms for low perfusion pressure have been shown to be powerful predictors of subsequent stroke in patients with symptomatic carotid artery stenosis or occlusion using some but not all physiological imaging methods (strong evidence). The best evidence is for measurements of oxygen extraction fraction (OEF) with positron emission tomography (PET) and breath-holding transcranial Doppler (TCD) studies (strong evidence). There is moderate evidence (level II) supporting the use of stable xenon computed tomography (Xe-CT) and single photon emission computed tomography (SPECT) methods. At present, however, the use of this information to guide therapy has not been proven to change outcome (limited evidence). The two patient populations in whom these tools are likely to become important are those with symptomatic complete carotid artery occlusion and asymptomatic carotid artery stenosis.

Supporting Evidence

Methods of Hemodynamic Assessment A completely occluded carotid artery often has no effect on the pressure in the arteries of the brain beyond the occlusion. In some patients, the circle of Willis or pial collateral branches are sufficient to maintain normal arterial pressure and

consequently normal cerebral blood flow. In other patients, the pressure in the arteries of the brain beyond the occlusion will decrease. There are two compensatory mechanisms by which the brain can maintain normal oxygen metabolism and thereby normal neurological function when arterial pressure falls. First, in autoregulation, blood flow can be maintained by reducing vascular resistance. Second, as flow is reduced passively as a function of pressure and exceeded autoregulatory capacity, the brain can increase the amount of oxygen extracted from the blood.

Single measurements of cerebral blood flow (CBF) alone do not adequately assess cerebral hemodynamic status. First, normal values may be found when perfusion pressure is reduced, but CBF is maintained by autoregulatory vasodilation. Second, CBF may be low when perfusion pressure is normal. This can occur when the metabolic demands of the tissue are low. Reduced flow due to reduced metabolic demand may not cause confusion when low regional CBF is measured in areas of frank tissue infarction. However, blood flow can also be reduced in normal, uninfarcted tissue due to the destruction of normal afferent or efferent fibers by a remote lesion as well [59].

Three basic strategies have been developed to assess regional cerebral hemodynamic status noninvasively [2]. The normal compensatory responses of the brain and its vasculature to reduced perfusion pressure as outlined above are assumed to be present. The first two strategies are used to indirectly identify the presence and degree of autoregulatory vasodilation. The third relies on direct measurements of OEF.

The first strategy relies on paired blood flow measurements with the initial measurement obtained at rest and the second measurement obtained following a cerebral vasodilatory stimulus. Hypercapnia, acetazolamide, and physiological tasks such as hand movement have been used as vasodilatory stimuli. Normally, each will result in a robust increase in CBF. If the CBF response is muted or absent, preexisting autoregulatory cerebral vasodilation due to reduced cerebral perfusion pressure is inferred. Quantitative or qualitative (relative)

measurements of CBF can be made using a variety of methods, including xenon 133 by inhalation or intravenous injection, SPECT, Xe-CT, PET, and magnetic resonance imaging (MRI). Changes in the velocity of blood in the middle cerebral artery (MCA) trunk or internal carotid artery (ICA) can be measured with TCD and MRI. The blood flow or blood velocity responses to these vasodilatory stimuli have been categorized into several grades of hemodynamic impairment: (1) reduced augmentation (relative to the contralateral hemisphere or normal controls), (2) absent augmentation (same value as baseline), and (3) paradoxical reduction in regional blood flow compared to baseline measurement. This final category, also called the "steal" phenomenon, can only be identified with quantitative CBF techniques as measurement of absolute values is necessary.

The second strategy uses either the measurement of regional cerebral blood volume (CBV) alone or in combination with measurements of CBF in the resting brain in order to detect the presence of autoregulatory vasodilation. The CBV/CBF ratio (or inversely the CBF/CBV ratio), mathematically equivalent to the vascular mean transit time, may be more sensitive than CBV alone for the identification of autoregulatory vasodilation. Quantitative regional measurements of CBV and CBF can be made with PET or SPECT. Patients are identified as abnormal with these techniques based on comparison of absolute quantitative values or hemispheric ratios of quantitative values to the range observed in normal control subjects. Magnetic resonance techniques for the quantitative measurement of CBV have been developed and validated against PET in normal subjects and patients with chronic cerebrovascular disease [60–64]. Quantitative measurements using CT perfusion have been not been well validated.

The third strategy relies on direct measurements of OEF to identify patients with increased oxygen extraction. At present, regional measurements of OEF can be made only with PET using oxygen-15-labeled radiotracers. Both absolute values and side-to-side ratios of quantitative and

relative OEF have been used for the determination of abnormal from normal.

Association with Stroke Risk Complete occlusion of the carotid artery is found in up to 15 % of patients with carotid territory TIAs or strokes [8]. The risk of subsequent stroke in this population is high (5–7 % per year) [65]. No preventive therapy has proven effective. A randomized trial of extracranial to intracranial arterial bypass, the EC/IC bypass trial, found no benefit with bypass compared to medical therapy [66]. One limitation of this study was the lack of hemodynamic assessment. A large percentage of patients included in the study may have had normal flow due to circle of Willis or other sources of collateral flow and therefore nothing to gain from an extra-anatomic bypass [67]. The presence of severe hemodynamic impairment has since been proven to be an independent and powerful predictor of stroke in patients with carotid artery occlusion [2, 68].

As these methods are inferential and indirect, correlation with outcome is required [2]. At present, the strongest evidence is for PET measurements of OEF and TCD measurements of cerebrovascular reserve (strong evidence). The St. Louis Carotid Occlusion Study was a blinded, prospective study of 81 patients with symptomatic carotid artery occlusion that also specifically assessed the impact of other risk factors [68]. The risk of all stroke and ipsilateral ischemic stroke in symptomatic subjects with increased OEF was significantly higher than in those with normal OEF (log rank $p = 0.005$ and $p = 0.004$, respectively). Univariate and multivariate analysis of 17 baseline stroke risk factors confirmed the independence of this relationship. The age-adjusted relative risk conferred by increased OEF was 6.0 (95 % CI, 1.7–21.6) for all stroke and 7.3 (95 % CI, 1.6–33.4) for ipsilateral ischemic stroke. Similar data were reported by Yamauchi et al. [69]. The Carotid Occlusion Surgery Study (COSS), a randomized trial of bypass for patients with increased OEF, was recently concluded. No benefit of surgery was found owing to high perioperative complication rates (Powers, oral presentation at the 2011 International Stroke Conference).

Several investigators have studied the association of paired flow techniques with stroke risk. Six found an association with stroke risk and three found none. Two of the six positive studies used a TCD method (breath-holding) and provided strong evidence (level 1) for patients with complete carotid artery occlusion and patients with asymptomatic carotid artery stenosis [70, 71]. Vernieri et al. enrolled 104 patients with complete carotid artery occlusion and followed them for a median period of 24 months [72]. The blood velocity response to 30 s of breath-holding was measured by TCD on study entry. Baseline stroke risk factors were assessed. The threshold for an abnormal TCD was set prospectively. Eighteen patients suffered a stroke during the follow-up period. Age and abnormal TCD response were independent risk factors for subsequent stroke.

Klieser and Widder reported an association between abnormal blood velocity responses to hypercapnia (by TCD) and the risk of subsequent stroke in 85 patients with carotid artery occlusion [73]. Both symptomatic and asymptomatic patients were included. The risk of contralateral stroke in the patients with diminished or exhausted CO_2 reactivity was increased, suggesting the groups were not matched for other stroke risk factors that were not evaluated. A subsequent study by the same authors reported the outcome of 86 patients with carotid artery occlusion [74]. A much lower risk of stroke was observed in the second study, and the number of asymptomatic patients was not reported.

Yonas and coworkers reported an association of the steal phenomenon (reduced blood flow by Xe-CT) after acetazolamide and subsequent stroke [75]. This study included patients with high-grade carotid artery stenosis and patients with carotid artery occlusion. The hemodynamic data of patients with subsequent stroke was analyzed retrospectively in order to establish threshold values for the categorization of high- and low-risk groups. The authors subsequently repeated the analysis with an additional 27 patients [76]. The hemodynamic criteria used to establish high- and low-risk groups were different from the prior analysis. Three of the five new strokes that occurred did so in patients who would

not have met criteria for the first study, and the definition of clinical outcome included contralateral stroke. Only two of the five new strokes were in the hemodynamically compromised territory of the occluded vessel.

Three studies have failed to find an association of a paired flow technique and stroke risk [77–79]. The largest and most methodologically sound study was reported by Yokota and colleagues [78]. They prospectively evaluated 105 symptomatic patients with mixed lesions (unilateral occlusion or severe stenosis [>75 % in diameter] of the ICA or proximal MCA) with a SPECT study of relative CBF using iodine-123-iodoamphetamine (IMP) and with measurement of cerebrovascular reactivity using acetazolamide. Other stroke risk factors were prospectively assessed. Thirteen strokes occurred during a median follow-up of 2.7 years: seven strokes occurred in 39 patients with abnormal hemodynamics and six in 39 patients with normal hemodynamics. The investigators were not blinded to the results of the hemodynamic study. A relatively large number of patients ($n = 16$) were censored from the study because of subsequent cerebrovascular surgery, and a significant number of patients ($n = 11$) were lost to follow-up.

Cost-Effectiveness Analysis Cost-effectiveness analysis suggests that the use of these physiological tools, even expensive ones such as PET, would be cost-effective for patients with symptomatic carotid artery occlusion, provided there is a benefit with surgical bypass [80]. The cost of acute and long-term care for stroke victims greatly exceeds the cost of diagnostic workup and surgery.

In addition to patients with complete carotid artery occlusion, another promising application for hemodynamic assessment is in asymptomatic carotid artery stenosis. The prevalence of hemodynamic impairment in patients with asymptomatic carotid occlusive disease is very low [71, 81]. This low prevalence may account in part for the low risk of stroke with medical treatment and consequently the marginal benefit with revascularization. The presence of hemodynamic

impairment may be a powerful predictor of subsequent stroke in this population [71, 81]. This is one area of research with enormous clinical implications: if a subgroup of asymptomatic patients at high risk due to hemodynamic factors could be identified, it would be possible to target surgical or endovascular treatment for those most likely to benefit.

Only one study has been performed in this population to date. Silvestrini et al. performed a prospective, blinded longitudinal study of 94 patients with asymptomatic carotid artery stenosis of at least 70 % followed for a mean of 28.5 months [71]. Breath-holding TCD was performed on entry, as well as the assessment of other stroke risk factors. An abnormal TCD study was shown to be a powerful and independent risk factor for subsequent stroke.

Take Home Tables

See Tables 36.1 through 36.3 for algorithms for imaging symptomatic patients, asymptomatic patients, and patients with cardiac artery occlusion, respectively.

Table 36.1 Suggested algorithm for imaging symptomatic patients

1. Locally validated DUS, CTA, or MRA can be used to exclude patients with <50 % stenosis from further evaluation for carotid artery stenosis. These patients are treated medically

2. Subsequent imaging decisions are based on the local accuracy of noninvasive tests for the presence of severe stenosis ≥70 % and occlusion

  (a) If unreliable, all patients with suspected stenosis >50 % or occlusion should undergo cerebral angiography (CA)

  (b) If reliable, patients with ≥70 % stenosis can go to surgery and patients with 50–69 % stenosis or occlusion go to CA for confirmation

Reprinted with kind permission from Springer Science+ Business Media from Barrocas AM, Derdeyn CP. Imaging of the cervical carotid artery for atherosclerotic stenosis. In: Medina LS, Blackmore CC, editors. Evidence-based imaging: optimizing imaging in patient care. New York: Springer; 2006

Table 36.2 Suggested algorithm for imaging asymptomatic patients

If surgical complication rates (stroke and death) for asymptomatic patients are <2 %, and the patient is a male in relatively good health with a life-expectancy of at least 5 years, then a screening DUS, CTA, or MRA, followed by surgery if positive, may be reasonable

Reprinted with kind permission from Springer Science+ Business Media from Barrocas AM, Derdeyn CP. Imaging of the cervical carotid artery for atherosclerotic stenosis. In: Medina LS, Blackmore CC, editors. Evidence-based imaging: optimizing imaging in patient care. New York: Springer; 2006

Table 36.3 Suggested algorithm for imaging patients with carotid artery occlusion

If a noninvasive screening tool is documented as accurate for complete occlusion, then no further imaging is necessary for asymptomatic patients. The risk of stroke with a missed high-grade asymptomatic stenosis is so low that the risk of angiography is not worth the benefit. There is no increased risk of stroke with higher degrees of stenosis in asymptomatic patients

If the patient is symptomatic, the diagnosis should be confirmed by angiography, as a missed high-grade stenosis has a very high chance of causing a future stroke

Reprinted with kind permission from Springer Science+ Business Media from Barrocas AM, Derdeyn CP. Imaging of the cervical carotid artery for atherosclerotic stenosis. In: Medina LS, Blackmore CC, editors. Evidence-based imaging: optimizing imaging in patient care. New York: Springer; 2006

Suggested Imaging Protocols

## Catheter Angiography (CA)

Measurements of linear diameter reduction are made using selective common carotid artery injections in magnified anteroposterior (AP) and lateral projections with oblique views if necessary. For ICA lesions, the point of maximal stenosis in any projection is measured and expressed as a percentage of the normal distal ICA diameter. If there is evidence of ICA collapse due to low flow, the denominator will be artifactually reduced. By convention this is termed "near occlusion," and the degree of stenosis is not reported. If a complete occlusion is encountered, a long run should be performed to look for a string sign as well as to assess external to internal collaterals. Subclavian or vertebral artery injections to assess for collateral flow are also useful. An aortic arch injection is useful to evaluate for origin stenosis and arch morphology. These procedures are optimally performed using a biplane digital subtraction unit.

Doppler Ultrasound (DUS)

Five- or 7.5-MHz linear array transducers are generally used. The following measurements must be acquired: the highest angle-adjusted peak systolic velocity in the common, proximal and distal ICAs, and at the point of maximal stenosis. Angle adjustment for Doppler measurements is based on flow direction by color Doppler. End-diastolic velocity measurements are also at these levels. Ratios of these velocities should be calculated. No one specific protocol or value can be recommended to use as a threshold for the degree of stenosis. The optimal thresholds for different degrees of stenosis must be determined at each laboratory using angiography as the reference standard.

Computed Tomographic Angiography (CTA)

Helical CT acquisition for coverage of the aortic arch to the circle of Willis generally employs 3-mm helical beam collimation with a 3-mm/s table speed, 12-cm field of view from the origin of the great

Fig. 36.1 AB Selective arterial angiograms of the carotid bifurcation showing 85 % stenosis without near occlusion by the NASCET method of measurement (**a**) and near occlusion (severe stenosis with narrowing of the distal internal carotid artery) (**b**). To calculate the degree of stenosis, the lumen diameter at the point of maximum stenosis (*point A*) was measured as the numerator in NASCET. The lumen diameter of the distal internal carotid artery (*point B*) is used as the denominator. The percent stenosis is calculated as $(1 - A/B)*100$. In near occlusion, the denominator is artifactually low (Reprinted with kind permission from Springer Science +Business Media from Barrocas AM, Derdeyn CP. Imaging of the cervical carotid artery for atherosclerotic stenosis. In: Medina LS, Blackmore CC, editors. Evidence-based imaging: optimizing imaging in patient care. New York: Springer; 2006)

vessels through the circle of Willis, and 140 kV, 240 mA, and 90 mL of nonionic contrast media injected at 3 mL/s by a power injector. A 25-s delay between injection and scan start is employed.

CE scan. Others generate up to three post-gadolinium runs and select the one with the best arterial visualization for subtraction.

Contrast-Enhanced Magnetic Resonance Angiography (CE-MRA)

A 3D subtracted gradient-recalled echo sequence and turbo FLASH sequence (4/1.6, 25° flip angle, 120×256 matrix) is generally used. A total of 20 mL of gadolinium-based contrast is injected by a power injector at approximately 3 mL/s. Some clinicians use a timing bolus followed by a saline flush to estimate the optimal time for the

Future Research

- Imaging of atherosclerotic plaque and correlation to plaque vulnerability and stroke risk
- Improving the ability of noninvasive imaging to differentiate subtotal from complete occlusion
- Identifying patients at high risk due to hemodynamic factors for surgical or endovascular treatment
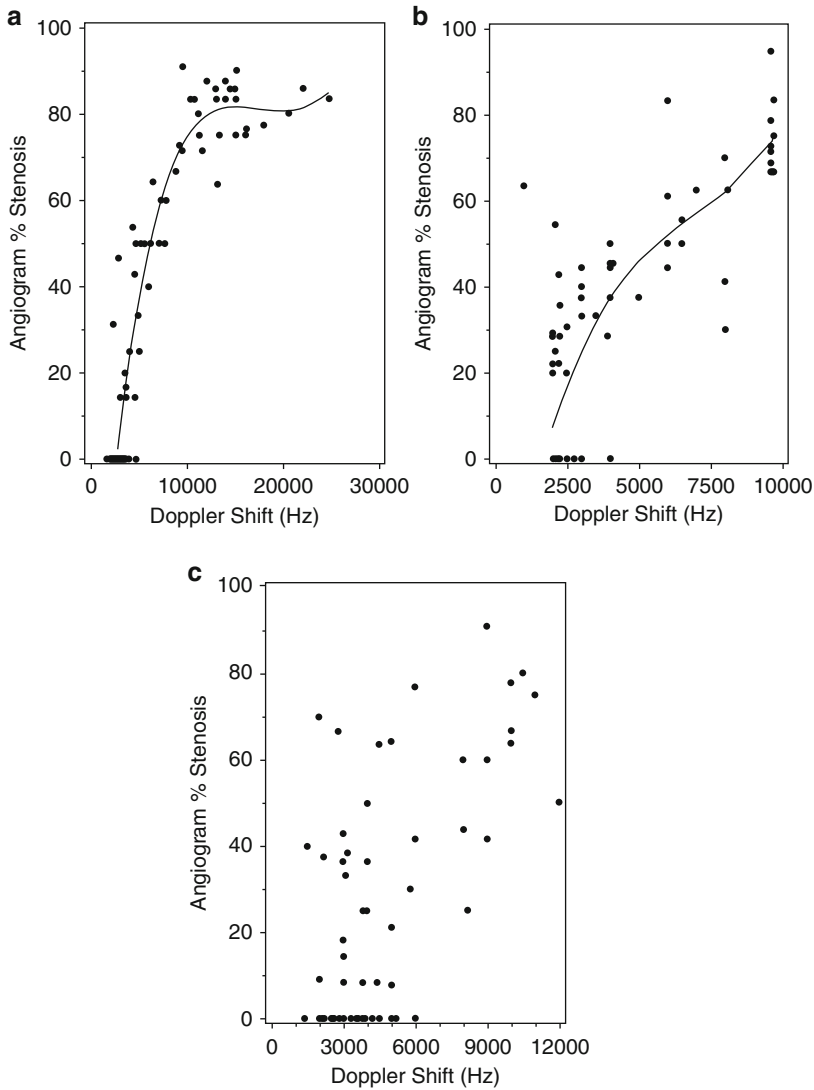
Fig. 36.2 (**a**–**c**) Relationship between Doppler frequency/velocity and percent stenosis by angiography for three specific devices: one with a device with a "strong" relationship (**a**), one with a "moderate" relationship (**b**), and one with a "poor" relationship (**c**) [14]. This was a validation study performed as part of the Asymptomatic Carotid Surgery Study (Reprinted with kind permission from Springer Science+Business Media from Barrocas AM, Derdeyn CP. Imaging of the cervical carotid artery for atherosclerotic stenosis. In: Medina LS, Blackmore CC, editors. Evidence-based imaging: optimizing imaging in patient care. New York: Springer; 2006)
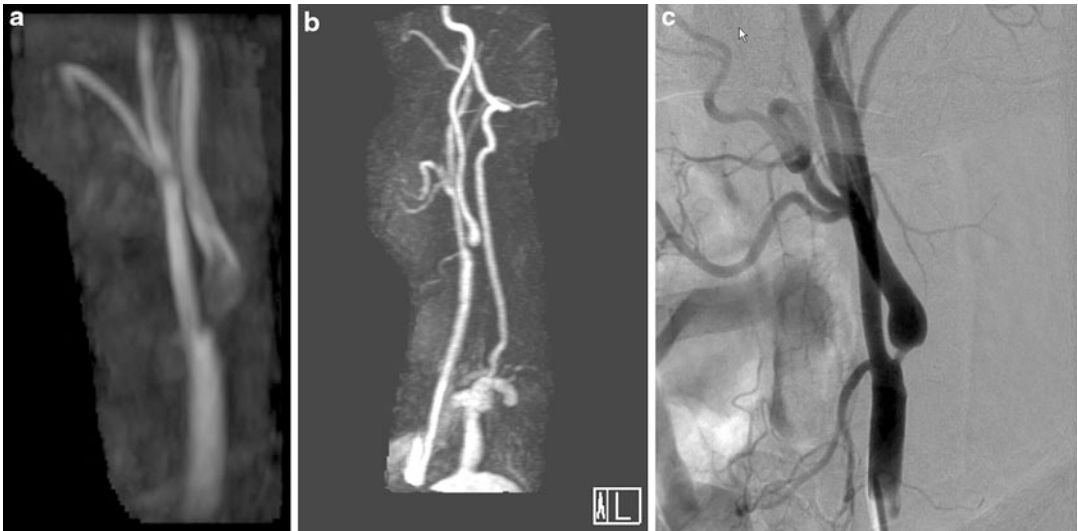
Fig. 36.3 (**a**) Time-of-flight MRA in a patient with recent transient ischemic attack shows a long segment of flow gap, consistent with turbulent flow and suggesting high-grade stenosis. (**b**) The contrast-enhanced (CE) MRA depicts the lumen better than the time-of-flight method, but a segment of flow gap remains. (**c**) Catheter angiography shows an 80 % stenosis. This case illustrates the reliability of MRA, particularly CE-MRA, to accurately identify severe stenosis. With less severe, but clinically relevant stenosis (50–70 %), the wide error range for MRA makes it less reliable for individual patients (Reprinted with kind permission from Springer Science+Business Media from Barrocas AM, Derdeyn CP. Imaging of the cervical carotid artery for atherosclerotic stenosis. In: Medina LS, Blackmore CC, editors. Evidence-based imaging: optimizing imaging in patient care. New York: Springer; 2006)

References

1. Malek AM, Alper SL, Izumo S. JAMA. 1999;282(21):2035–42.
2. Derdeyn CP, Grubb Jr RL, Powers WJ. Neurology. 1999;53(2):251.
3. North American Symptomatic Carotid Endarterectomy Trial Collaborators. N Engl J Med. 1991;325(7):445–53.
4. Rothwell PM, Gutnikov SA, Warlow CP. Stroke. 2003;34(2):514–23.
5. Roger VL, et al. Circulation. 2011;123:e18–209.
6. Bogousslavsky J, et al. Arch Neurol. 1986;43(3):223–8.
7. Rothwell PM, et al. Lancet. 2003;361(9352):107–16.
8. Mead GE, et al. Br J Surg. 1997;84(7):990–2.
9. Barnett HJ, Taylor DW, Eliasziw M, et al. N Engl J Med. 1998;339:1415–25.
10. Howard G, Chambless LE, Baker WH. J Stroke Cerebrovasc Dis. 1991;1:166–73.
11. Buskens E, et al. Radiology. 2004;233:101–12.
12. Kent KC, et al. JAMA. 1995;274(11):888–93.
13. Grant EG, Benson CB, Moneta GL, et al. Radiology. 2003;229:340–6.
14. Howard G, Baker WH, Chambless LE, et al. Stroke. 1996;27:1951–7.
15. Jahromi AS, Cina CS, Liu Y, et al. Vasc Surg. 2005;41:962–72.
16. Nederkoorn PJ, van der Graaf Y, Hunink MG. Stroke. 2003;34:1324–32.
17. Alexandrov AV, et al. Stroke. 1997;28(2):339–42.
18. Eliasziw M, et al. Stroke. 1995;26(10):1747–52.
19. Busuttil SJ, Franklin DP, Youkey JR, et al. Am J Surg. 1996;172:144–7.
20. Chi YW, White CJ, Woods TC, et al. Catheter Cardiovasc Interv. 2007;69:349–54.
21. Comerota AJ, Salles-Cunha SX, Daoud Y, et al. J Vasc Surg. 2004;40:939–44.
22. Koelemay MJW, et al. Stroke. 2004;35(10):2306–12.
23. Josephson SA, Bryant SO, Mak HK. Neurology. 2004;63:457–60.
24. Nonent M, et al. Stroke. 2004;35(3):682–6.
25. Zhang Z, et al. Eur Radiol. 2004;14(4):665–72.
26. Kallmes D, et al. AJNR Am J Neuroradiol. 1996;17(8):1501–6.

27. Cloft HJ, Murphy KJ, Prince MR, et al. Magn Reson Imaging. 1996;14:593–600.
28. Debrey SM, Yu H, Lynch JK, et al. Stroke. 2008;39:2237–48.
29. Babiarz LS, Romero JM, Murphy EK, et al. AJNR Am J Neuroradiol. 2009;30:761–8.
30. Anzidei M, Napoli A, Marincola BC, et al. Radiology. 2009;251(2):457–66.
31. Layton KF, Huston 3rd J, Cloft HJ, et al. AJR Am J Roentgenol. 2007;188:1114–16.
32. Runck F, Steiner RP, Bautz WA, et al. AJNR Am J Neuroradiol. 2008;29:1736–42.
33. Chappell FM, Wardlaw JM, Young GR. Radiology. 2009;251(2):493–502.
34. U.S. Preventive Services Task Force. Ann Intern Med. 2007;147:854–9.
35. Qureshi AI, Alexandrov AV, Tegeler CH, et al. J Neuroimaging. 2007;17:19–47.
36. Bates ER, Babb JD, Casey Jr DE, et al. J Am Coll Cardiol. 2007;49:126–70.
37. Craven TE, Ryu JE, Espeland MA, et al. Circulation. 1990;82:1230–42.
38. O'Leary DH, Polak JF, Kronmal RA, et al. Stroke. 1992;23:1752–60.
39. Chaitman BR, Rogers WJ, Davis K, et al. N Engl J Med. 1980;303:953–7.
40. Vigneswaran WT, Sapsford RN, Stanbridge RD. Br Heart J. 1993;70:342–5.
41. Alexandrova NA, Gibson WC, Norris JW, et al. J Vasc Surg. 1996;23:645–9.
42. Zhu CZ, Norris JW. Stroke. 1990;21:1131–4.
43. Ratchford E, Jin Z, DiTullio M, et al. Neurol Res. 2009;31(7):748–52.
44. Executive Committee for the Asymptomatic Carotid Atherosclerosis Study. JAMA. 1995;273(18):1421–8.
45. Asymptomatic Carotid Surgery Trial Collaborative Group. Lancet. 2004;363(9420):1491–502.
46. Holloway RG, et al. Stroke. 1999;30(7):1340–9.
47. Derdeyn CP, Powers WJ. Stroke. 1996;27(11):1944–50.
48. Coward LJ, Featherstone RL, Brown MM. Stroke. 2005;36:905–11.
49. Brahmanandam S, Ding EL, Conte MS, et al. J Vasc Surg. 2008;47:343–9.
50. Luebke T, Aleksic M, Brunkwall J. Eur J Vasc Endovasc Surg. 2007;34:470–9.
51. Murad MH, Flynn DN, Elamin MB, et al. J Vasc Surg. 2008;48:487–93.
52. Meier P, Knapp G, Tamhane U, et al. BMJ. 2010;340:c467.
53. Yadav JS, et al. N Eng J Med. 2004;351:1493–501.
54. CAVATAS Investigators. Lancet. 2001;357:1729–37.
55. Ringleb PA, Allenberg J, Bruckmann H, et al. Lancet. 2006;368:1239–47.
56. Mas JL, Chatellier G, Beyssen B, et al. N Engl J Med. 2006;355:1660–71.
57. Ederle J, Dobson J, Featherstone RL, et al. Lancet. 2010;375:985–97.
58. Brott TG, Hobson RW, Howard G, et al. N Engl J Med. 2010;363:11–23.
59. Feeney DM, Baron JC. Stroke. 1986;17:817–30.
60. Grandin CB, Bol A, Smith AM, Michel C, Cosnard G. Neuroimage. 2005;26:525–35.
61. Ostergaard L, Johannsen P, Host-Poulsen P, Vestergaard-Poulsen P, Asboe H, Gee AD, Hansen SB, Cold GE, Gjedde A, Gyldensted C. J Cereb Blood Flow Metab. 1998;18:935–40.
62. Lin W, Celik A, Derdeyn C, An H, Lee Y, Videen T, Ostergaard L, Powers WJ. J Magn Reson Imaging. 2001;14:659–67.
63. Tanaka Y, Nariai T, Nagaoka T, Akimoto H, Ishiwata K, Ishii K, Matsushima Y, Ohno K. J Cereb Blood Flow Metab. 2006;26:291–300.
64. Ibaraki M, Ito H, Shimosegawa E, Toyoshima H, Ishigame K, Takahashi K, Kanno I, Miura S. J Cereb Blood Flow Metab. 2007;27:404–13.
65. Klijn CJM, et al. Stroke. 1997;28:2084–93.
66. The EC/IC Bypass Study Group. N Engl J Med. 1985;313:1191–200.
67. Jr A, Diaz FG. Surg Neurol. 1986;26:218–21.
68. Grubb Jr RL, et al. JAMA. 1998;280(12):1055–60.
69. Yamauchi H, et al. J Nucl Med. 1999;40:1992–8.
70. Vernieri F, et al. Stroke. 1999;30:593–8.
71. Silvestrini M, et al. JAMA. 2000;283(16):2122–7.
72. Vernieri F, et al. Stroke. 2001;32:1552–8.
73. Kleiser B, Widder N. Stroke. 1992;23:171–4.
74. Widder B, Kleiser B, Krapf H. Stroke. 1994;25:1963–7.
75. Yonas H, et al. J Neurosurg. 1993;79:483–9.
76. Webster MW, et al. J Vasc Surg. 1995;21:338–45.
77. Powers WJ, Tempel LW, Grubb Jr RL. Ann Neurol. 1989;25:325–30.
78. Yokota C, et al. Stroke. 1998;29:1743–4.
79. Hasegawa Y, et al. Stroke. 1997;28:242.
80. Derdeyn CP, Gage BF, Grubb Jr RL, Powers WJ. J Nucl Med. 2000;41:800–7.
81. Powers WJ, et al. Neurology. 2000;54:878–82.

Neck Masses and Adenopathy: Evidence-Based Neuroimaging

37

Amit Balgude, Thomas C. Bryson, and Suresh K. Mukherji

Contents

A. Balgude (✉)
Department of Interventional Neuroradiology, Ronald Reagan UCLA Medical Center, Los Angeles, CA, USA
e-mail: abalgude@mednet.ucla.edu

T.C. Bryson • S.K. Mukherji
Department of Radiology, University of Michigan Health System, Ann Arbor, MI, USA
e-mail: tbryson@med.umich.edu; mukherji@med.umich.edu

Key Points

- Neck mass persistence, enlargement, or any concern for a neoplastic etiology warrants imaging in both adults and children. There is no evidence available to substantiate this clinical standard (Standard of Clinical Care).
- CT and MRI have similar sensitivity and specificity in the evaluation of metastatic cervical lymph nodes. CT has a slightly better PPV and NPV when compared to MRI. Conversely, MRI is superior to CT for detecting perineural spread (moderate evidence).
- FDG-PET can correctly identify lymph node status in patients with head and neck cancer with high PPV and NPV; it has not significantly improved the classification of node-positive necks compared to CT alone. Therefore, PET/CT is not recommended for routine initial staging of all patients. PET/CT performed prior to panendoscopy can increase diagnostic yield in the unknown head and neck primary population, leading to more targeted diagnostic procedures and treatment (moderate evidence).
- Ultrasound (US) is underutilized in the United States in part due to greater availability of cross-sectional modalities. US has high sensitivity (compared to clinical examination) in the evaluation of cervical lymphadenopathy in patients with head and neck cancer. Coupled with guided fine needle aspiration, the specificity of ultrasound is greater than 90 % (moderate evidence).
- Most local and regional recurrences of head and neck cancer occur within the first 2 years following therapy. Therefore, surveillance imaging at 4–6-month intervals for the first year and yearly thereafter for at least 2 years has been suggested; however, there is no consensus regarding proper timing of serial posttreatment surveillance studies in patients with head and neck cancer. FDG-PET and PET/CT offer improved sensitivity and specificity compared to conventional CT and MRI, with high negative predictive value. PET exams should be performed at least 3 months following completion of treatment to minimize false-positive and false-negative results (limited evidence).

Definition and Pathophysiology

In adults, the most likely cause of a neck mass is either neoplastic or inflammatory. A persistent neck mass in an adult older than 40 years should raise a suspicion for malignancy. In adults who present with a fever, the etiology is often inflammatory. Neck masses in children often have an inflammatory, infectious, or a congenital cause. Neck malignancy in children is rare.

Epidemiology

A neck mass is a frequently encountered problem in patients presenting to the primary care clinician. In adults, the clinician should have a high index of suspicion for malignancy. The World Health Organization estimated that there are 600,000 new cases of head and neck cancer and 300,000 deaths each year worldwide, with the most common sites being the oral cavity, the larynx, and the pharynx [1]. In children of various ages, diverse conditions of congenital, acquired inflammatory, neoplastic, or vascular origin manifest as neck masses. These lesions vary in prevalence from common to very rare, and their absolute number remains unknown. The prevalence of thyroid nodules in the general population is approximately 50 % [2], and approximately 3–4 % of these nodules are malignant [3].

Overall Cost to Society

Neck mass imaging and treatment exerts an enormous personal and financial burden upon society. While the global cost of imaging for this indication is not known, expenditure on neck imaging performed in the United States was calculated from the physician/supplier procedure summary master file available on the Centers for Medicaid and Medicaid Services website (www.cms.gov).

In 2009–2010, $281,782,662; $19,625,937; and $7,279,184 were charged for the total number of skull base MRI, neck MRI, and neck CT examinations performed in the United States, respectively. To our knowledge, there is no data on the global cost to society from general neck masses or neoplasms.

Goals of Imaging

The goals of initial neck imaging are to exclude pseudomasses, delineate the anatomic space and extent of the lesion, and evaluate for potential primary source for malignancy in the region. Imaging in head and neck cancer aims to establish tumor extent and size, assess nodal disease, evaluate for perineural tumor spread, detect synchronous primary lesions, and distinguish recurrent tumor from posttreatment changes.

Methodology

A MEDLINE search was performed using PubMed (National Library of Medicine, Bethesda, Maryland) for research publications addressing the selection of diagnostic modalities for imaging of the neck in various clinical settings. The search covered the years 1955 to January 2011. Search qualifiers employed were as follows: (1) neck mass, (2) imaging, (3) head and neck cancer, (4) thyroid nodules, and (5) pediatric neck imaging. Additional articles were located from the references list or original research or review articles.

Discussion of Issues

What Imaging Strategy Is Appropriate in Adults?

Summary
MRI and CT are complementary studies, and selection of the appropriate imaging modality should be based on the clinical question. MRI is superior to CT for detecting perineural spread [4] (moderate evidence) which is important for initial staging for a variety of skull base tumors. Both modalities can be used for initial diagnosis of a primary head and neck malignancy and staging of enlarged cervical lymph nodes.

Supporting Evidence
The type of initial imaging study that has been recommended has varied over the past 20 years with the development and maturation of new imaging modalities. Selection of the appropriate imaging strategy depends on the specific clinical issue in question.

Computed Tomography and Magnetic Resonance Imaging
Both computed tomography (CT) and magnetic resonance imaging (MRI) with contrast can provide adequate information regarding the size, extent, location, and vascular characteristics of a neck mass. Cystic and solid lesions can be distinguished, and the relationship of the mass to other vital structures such as the airway and major blood vessels can be assessed. In older patients with a smoking history, the diagnosis is often malignancy [5]. In adults who present with a fever, the etiology is often inflammatory [6]. CT and MRI can accurately diagnose both entities and also reveal possible primary sites in the case of neoplastic disease [7, 8]. In general, MRI is superior to CT for obtaining excellent tissue contrast, which contributes to the superior delineation of tumor extension and perineural spread [4]. On high-resolution MRI, the sensitivity and specificity in assessing metastatic nodes are 86 % and 94 %, respectively [9]. Curtin and colleagues compared the ability of MRI and CT in detection of lymph node metastasis from head and neck squamous cell carcinoma [10]. CT had an NPV of 84 % and a PPV of 50 %, and MR had an NPV of 79 % and a PPV of 52 %. The addition of a CT scan to a negative physical exam has been shown to increase the detection rate of a primary head and neck cancer to 62 % [11]. On contrast-enhanced CT, the reported sensitivity and specificity in the evaluation of metastatic cervical lymph nodes are 90.2 % and 93.9 %, respectively [12].

Both modalities can be used for initial diagnosis of a primary head and neck malignancy and

staging of enlarged cervical lymph nodes [13–15]. However, the rapid image acquisition time of MDCT reduces physiologic motion and produces a higher consistent image quality compared with MRI.

Diffusion-Weighted Imaging (DWI)

DWI has found various applications in head and neck imaging because of its ability to measure differences in tissue microstructure that are based on random differences in water molecules. These differences can be quantified using apparent diffusion coefficients (ADC). In general, tissues that are more compact at the molecular level (i.e., have higher cellularity) have lower ADC values. Malignant lesions in the head and neck tend to demonstrate lower ADC values than benign processes or normal tissues, likely due to their hypercellular nature. While some studies have shown that primary malignancies in the head and neck and metastatic nodes show ADC values below 0.9–1.3 ($\times 10^{-3}$ mm^2/s), the optimal threshold for differentiation is still not known [16–18]. A small prospective study has shown an ADC threshold of 0.94×10^{-3} mm^2/s to have 84 % sensitivity, 94 % specificity, and 91 % accuracy for differentiation between malignancy and benign lymph nodes in the head and neck. Similarly, recurrent tumors show a decreased ADC compared with therapy-related changes, presumably due to increased free water in necrosis and increased cellularity in recurrent tumors [19, 20].

CT and MR Perfusion

CT perfusion (CTP) has been used to detect changes occurring in neoplasms at the microvascular level as a result of neoangiogenesis. Head and neck neoplasms demonstrate increased blood volume (BV) and blood flow (BF) with decreased mean transit time (MTT) compared with benign lesions or normal tissue [21, 22]. A small pilot study has shown MTT to be the best discriminator between malignant and nonmalignant pathologies with all lesions with MTT < 3.5 s being malignant and no malignancies showing MTT > 5.5 s [22]. Since recurrent tumors also demonstrate neoangiogenesis akin to primary malignancies, CTP is a valuable modality to image this neovascularity. A study comparing CTP parameters of suspected recurrent cancer and lymph nodes in 77 patients with primary cancer has shown that recurrent tumors tend to demonstrate increased BF compared with post-therapy masses (mean BF: 69.71 vs. 45.31 mL/min/100 g tissue, respectively; $p < 0.05$). However, perfusion CT parameters could not differentiate benign and malignant lymph nodes [23]. CT perfusion parameters have also been proved helpful in predicting response to chemoradiation. Baseline increased BF and capillary permeability (CP) have been shown to be more predictive of long-term response (at 24 months) [24], while increased BV is predictive of short-term response [25]. Also, during the course of chemoradiation in patients with advanced head and neck cancer, responders had significant reduction of BF and BV values ($p < 0.04$), whereas in nonresponders there was nonsignificant elevation of BV [25].

Similar to CTP, perfusion-weighted MR imaging is also used to measure blood flow mechanics at the microcirculation. This technique has also proven to be useful in distinguishing tumor from normal tissues and monitoring and predicting response to treatment. Of the several methods for performing perfusion-weighted MR imaging, the most widely used is T2*-weighted DCE imaging. A small feasibility study performed by Bisdas et al. [26] used first-pass DCE perfusion-weighted MR to show that all perfusion parameters (including BF, BV, extravascular extracellular volume, MTT, and permeability) were significantly different between tumor and normal muscle tissue. In a prospective study of DCE perfusion-weighted MR imaging in HNSCC, there was significant increase in BV after 2 weeks of chemoradiation in patients who had local disease control compared with those who had local or regional failure. Interestingly, reduction in tumor volume at 2 weeks of chemoradiation did not predict local disease control. These data suggest that perfusion-weighted MR imaging has the potential to be an additional tool in predicting response to therapy. However, larger validation studies are needed.

Use of Contrast

Although unenhanced T1- and T2-weighted MR images can delineate tumors, the administration of contrast is recommended for adults and children with no contraindication, as it results in better delineation of tumor margins, tumoral extension, or perineural invasion [27]. In addition, contrast is also essential for detecting neck abscess, especially those that are intramuscular [28]. IV contrast is also helpful for distinguishing vessels from lymph nodes and determining if the mass is hypervascular. Contrast can obscure visualization of sialoliths, and non-contrast CT is recommended in patients presenting with a neck mass felt to be due to an obstructing sialolith. MRI may be helpful in patients with non-mineralized sialoliths. Iodine-based contrast may be avoided in cases of prior thyroid cancer history or when metastatic thyroid cancer is suspected.

Positron Emission Tomography

The role of positron emission tomography (PET) with fluorodeoxyglucose (FDG) in the staging of head and neck squamous cell cancer (HNSCC) is evolving. A large recent retrospective study has shown the positive predictive value (PPV) and the negative predictive value (NPV) of PET imaging to correctly identify lymph node status to be 94 % and 89 %, respectively [29]. Moreover, fused PET/CT is superior to CT alone for the staging of cervical lymph nodes in patients with HNSCC [12].

The role of PET for the detection of unknown head and neck malignancies is gaining acceptance. Recent studies have demonstrated an advantage of PET scans, with PET/CT leading to an increase in detection rates of unknown primary malignancies from 25 % to 55 % [30, 31]. Modern PET/CT scanners can detect tumors as small as 3–5 mm, but smaller primaries and micrometastases may not be detected. Nevertheless, a PET/CT scan is a high-yield study in patients with metastasis from an unknown head and neck primary site [32].

Several studies have looked at the value of PET imaging in initial staging and the detection of metastatic disease or secondary cancers [33, 34].

While PET has higher sensitivity for the detection of nodal disease, it has not significantly improved the classification of node-positive necks compared to CT alone. Currently, PET/CT is not recommended for routine initial staging of all patients with HNSCC [35].

Ultrasound

Indications of ultrasound (US) for the initial diagnosis of neck masses in adults and children are steadily increasing. The overall utilization of neck US in the United States has generally lagged Europe and Asia, in part to greater accessibility of cross-sectional modalities such as CT and MRI compared to other parts of the world. It is well known that ultrasound is useful in differentiating between solid and cystic lesion in both adults and children. US is also helpful in distinguishing between high-flow and low-flow vascular malformations [36]. In addition, there is also good evidence to support the role of US in the assessment of cervical lymphadenopathy. US is particularly sensitive compared to clinical examination (96.8 % and 73.3 %, respectively) in patients with previous head and neck cancer [37]. It is also very helpful for directing image-guided biopsy of non-palpable or small lesions that are relatively superficial and for biopsy of indeterminate soft tissue in the treated neck. When combined with guided fine needle aspiration (FNA), the specificity of ultrasound is as high as 93 % [37]. Previous studies have also shown that US-guided FNA of lymph nodes can be useful in staging the clinically N0 neck [38]. While the PPV of this technique is high, concern has been raised regarding the NPV and the inability to exclude micrometastases. Studies have also suggested that power Doppler US can distinguish between metastatic and inflammatory neck nodes [39], with a repeatability of 85 % [40].

Angiography

The role of conventional angiography for initial diagnosis is very limited. The initial imaging modality for evaluation of a pulsatile neck mass is CT angiography, which now appears to be preferred to MRI [41]. Conventional angiography

is usually performed for endovascular treatment planning or further characterization of vascular neck lesions.

Cost-effectiveness Analysis

Despite the widespread use of diagnostic neck imaging, there are relatively few studies that have investigated its cost-effectiveness. Only two studies have reported the cost-effectiveness of PET and PET/CT for staging head and neck cancer. Hollenbeak et al. [42] showed that PET is cost-effective as part of a strategy for treating the N0 neck in HNSCC patients. In their model, the use of PET resulted in a reasonable cost per quality-adjusted life year (QALY) because occult regional lymphatic disease was recognized at a subclinical stage. The standard threshold for cost-effectiveness is $50,000 per QALY. Sher et al. [43] assessed the cost-effectiveness of PET/CT as a predictor of the need for adjuvant neck dissection compared with neck dissection for all patients. Their analysis confirmed that adjuvant neck dissection in patients with residual disease after PET/CT was more a cost-effective strategy than dissecting all patients or using CT only, even when the societal willingness to pay was set as high as $500,000/QALY.

Special Case: Selection of an Appropriate Imaging Strategy in the Pediatric Neck

Summary

Options for imaging the pediatric neck are essentially the same as those previously discussed for adult imaging and carry many of the same advantages and disadvantages. The decision of which modality to employ in a pediatric patient, however, must be informed by several issues unique to the pediatric population. First, the epidemiology of pediatric neck masses is significantly different than adult neck masses, with the vast majority of processes being benign in nature. Second, high-quality cross-sectional imaging in the pediatric population frequently requires sedation, with additional inherent risks. Finally, pediatric exposure to ionizing radiation should be minimized, particularly when exposing the radio-sensitive thyroid gland. These considerations have resulted in the wide use of US as the initial imaging technique in the assessment of extracranial pediatric head and neck masses. CT and MRI, however, are indispensable for characterization of deeper lesions and in delineating the extent of disease. Increasingly, MR imaging is preferred over CT because it imparts no ionizing radiation and evaluation of tissue signal intensity and enhancement allows for better characterization of many lesions. However, MR imaging requires sedation in infants and young children, which can be problematic. Also, with increasing availability in children's hospitals, PET/CT is now being widely used for staging pediatric oncologic disease and monitoring response to treatment.

While radionuclide scanning in the neonate remains the gold standard for the diagnosis of congenital hypothyroidism, US should be the first screening modality employed followed by radionuclide scanning when there is no tissue present in the neck. US is also the preferred imaging modality for diffuse enlargement of the thyroid gland and nodular thyroid disease. CT and MRI are useful for evaluating large thyroid masses and for staging patients with thyroid carcinoma. FDG-PET has also shown utility in thyroid cancer, with high specificity and sensitivity for recurrence and metastasis in patients with negative I-131 whole-body imaging, but rising thyroglobulin levels.

Supporting Evidence

Congenital Neck Masses In children suspected of having a congenital abnormality, US is often performed as a first exam, as it is sufficient for distinguishing a cystic from a solid mass. Color Doppler is also helpful for detecting arterial or venous vascularity in a solid lesion. The frequent superficial location of head and neck masses makes them readily accessible to US examination. If needed, the examination can be performed at the bedside, and sedation is rarely necessary. Thyroglossal duct cysts (TDCs) are the most common congenital neck mass found in children. TDCs can be located anywhere along the course

of the thyroglossal duct from the base of the tongue to the thyroid gland, most commonly at the level of the hyoid bone. A retrospective review of 45 patients with midline masses who underwent preoperative US showed a cyst and a normal thyroid gland in all patients with pathologically proven TDCs [44]. However, a recent retrospective review conducted at a tertiary care center failed to demonstrate an association between preoperative ultrasound-based diagnoses and postoperative pathologic results in children with midline neck masses [45]. Indeed, in our practice, CT or MRI is often needed to complete the diagnostic workup and initiate surgical planning.

Infectious/Inflammatory Lesions Acute inflammatory cervical masses are a commonly encountered pathology in the pediatric population. In most cases, these masses consist of enlarged reactive or suppurative lymph nodes, caused by an upper respiratory tract or pharyngeal infection. In a prospective study of 26 consecutive patients with suspected neck abscesses, US was shown to have a 100 % accuracy in detecting surgically proven abscesses [46]. However, other authors demonstrated relatively low accuracy of ultrasound, with sensitivity ranging from 60 % to 70 % and specificity of 88 % [47]. This discrepancy is felt to be due to the inability of pediatric patients to actively cooperate during imaging studies. When compared directly with CT, a recent retrospective review found US to be sufficient for assessment of inflammatory masses in a pediatric population [48]. CT provided additional information only in 4 of 25 children (with deep-seated infections) who underwent both US and CT. For obvious reasons, a deep infection or abscess should be thoroughly investigated with CT or MRI.

Benign and Malignant Tumors Either CT or MRI can be performed in children suspected of having a malignancy. There is no strong evidence to facilitate an a priori recommendation of CT or MRI. A case-by-case approach is best suited. For example, fibromatosis colli is a benign fusiform mass arising within the sternocleidomastoid

muscle of a neonate. US is the imaging modality of choice in this case, and characteristic imaging findings in conjunction with clinical features of congenital torticollis usually obviate the need for additional imaging.

While the preponderance of pediatric neck masses is benign, an awareness of the occurrence and imaging characteristics of neoplastic lesions is important for any radiologist involved in pediatric imaging. According to the National Cancer Institute's Surveillance, Epidemiology, and End Results tumor registry, head and neck tumors make up approximately 12 % of pediatric malignancies, with lymphoma being the most common head and neck region cancer type overall. Other common tumor types include neural tumors such as neuroblastoma, soft tissue sarcomas, and thyroid carcinoma. There is evidence for an increasing incidence of pediatric head and neck cancers, particularly thyroid carcinomas [49]. Imaging in the setting of malignancy is frequently multimodal and can include US, CT, MRI, and PET depending on tumor type and institutional protocols.

In the case of lymphoma, CT has become a widely used modality for initial staging and follow-up given its ability to provide a global evaluation of nodal and extranodal disease. Despite issues of radiation exposure, CT may be preferred to MRI in many centers due to its widespread availability and reduced frequency of required sedation with modern helical techniques [50]. The evaluation of cervical lymphadenopathy by standard CT size criteria, however, can result in false-positive results in the setting of infectious/inflammatory adenopathy and false-negative results with small lymph nodes harboring disease at treatment follow-up. FDG-PET and PET/CT have been shown to have improved sensitivity and specificity characteristics in these settings compared to conventional imaging modalities such as CT and MRI. One prospective study of FDG-PET for assessment of therapy response in pediatric Hodgkin's lymphoma demonstrated a 100 % sensitivity and 78 % specificity for residual disease with PET compared with 50 % sensitivity and 11 % specificity for conventional anatomic imaging. It is felt that patients

with an early favorable response to chemotherapy demonstrated by decreasing standardized uptake values (SUV) on PET may represent a group in which radiotherapy can be safely omitted [51]. Radiation dose from diagnostic imaging in pediatric oncology will continue to be a challenge with these modalities, and an effort to apply ALARA (as low as reasonably achievable) principles to the development of appropriate pediatric imaging protocols is needed.

Soft tissue sarcomas and neural origin tumors such as neuroblastoma are relatively less common in the head and neck region. The most common is rhabdomyosarcoma, which frequently involves the orbit or skull base. While CT can provide information about osseous erosion in these locations, MRI may be preferred due to excellent soft tissue resolution and the ability to delineate intracranial extension of disease. There is limited evidence available to support the use of diffusion-weighted imaging in the characterization of pediatric head and neck masses. A recent study found a significant difference in apparent diffusion coefficient (ADC) values between malignant tumors and benign lesions with a sensitivity and specificity for differentiating benign from malignant lesions of 94 % and 91 %, respectively, when a threshold ADC value of 1.25×10^{-3} mm^2 s^{-1} was used [52]. MRI frequently requires sedation in younger patients; however, there is a growing body of literature documenting extensive clinical experience with out-of-OR pediatric sedation for radiological procedures with relatively few significant adverse events [53]. PET/CT also appears to be a promising tool in evaluation of pediatric sarcoma patients, with utility in identifying unknown primary rhabdomyosarcoma, detecting unsuspected metastasis and in monitoring response to medical and surgical therapies [54].

Thyroid Imaging Radionuclide scanning in the neonate remains the gold standard for the diagnosis of congenital hypothyroidism. A 10-year retrospective review of pediatric patients who underwent ^{123}I thyroid scintigraphy showed that this modality reliably identified the location of the thyroid gland and assessed functional status [55]. A study of 88 consecutive patients with congenital hypothyroidism compared US and radionuclide scanning and found that US did not distinguish between athyreosis and ectopic glands but did distinguish between the presence and absence of thyroid tissue [56]. These authors suggest, and we agree, that US should be the first screening modality employed followed by radionuclide scanning when there is no tissue detected in the neck.

For diseases other than congenital hypothyroidism, such as diffuse enlargement of the thyroid gland and nodular thyroid disease, US is the preferred imaging modality. One review of the ultrasound findings of 22 children with diffuse goiter revealed that Hashimoto's thyroiditis had abnormal echogenicity in all cases, while all patients with colloid goiter were normal [57]. In this study, US was more sensitive in discriminating these two conditions than was the presence or absence of thyroid antibodies.

Thyroid US is also the imaging modality of first choice for most individuals with nodular thyroid disease. Thyroid nodules are relatively less common in pediatric patients; however, they are more likely to harbor thyroid carcinoma, and there is epidemiological evidence for increasing incidence of pediatric thyroid cancer, as stated previously. Also, patients with a history of pediatric malignancy who have received radiation therapy to the neck or mediastinum are known to be at increased risk for thyroid malignancy. A large Korean multicenter study of ultrasound in patients with nodular thyroid disease showed that the presence of at least one malignant US finding had a sensitivity of 83.3 %, a specificity of 74.0 %, and a diagnostic accuracy of 78.0 % [58]. Radionuclide scanning of nodules at first presentation has two problems. First, not all thyroid carcinomas present as cold nodules on scanning, and second, most thyroid cysts are cold on scanning. This approach can therefore lead to unnecessary intervention in patients.

High-dose I-131 ablation remains a common part of post thyroidectomy management for patients with diagnosed thyroid cancer, and

whole-body imaging with I-131 continues to have a role in identifying metastatic disease. FDG-PET has also shown utility in thyroid cancer, with up to 94 % sensitivity and 95 % specificity for recurrence/metastasis in patients with negative I-131 whole-body imaging, but rising thyroglobulin levels [59, 60].

Imaging the Posttreatment Neck

Summary
Imaging of the posttreatment neck is a challenging task for most radiologists. An initial baseline CT or MRI should be obtained at 4–6 weeks after radiation or surgery. We caution against use of early PET/CT for surveillance or assessment of response to avoid false-positive or false-negative results. While surveillance imaging is recommended at 4–6-month intervals for the first year and yearly thereafter for at least 2 years, we would like to emphasize the importance of a tailored imaging strategy based on the clinical indication and an understanding of the information that the imaging study can provide.

Supporting Evidence
Baseline Imaging The timing of a baseline surveillance scan is difficult to ascertain since the time at which tumor recurrence develops depends on the initial response to treatment, presence of tumor-free margins, and the aggressiveness of the tumor. Considering these variables, Som and colleagues recommend obtaining a baseline CT or MRI at 4–6 weeks after radiation or surgery, after most of the presumed treatment-related changes have resolved [61]. There is evidence that the baseline study itself may carry valuable predictive information. Enhanced CT obtained 30 days after chemoradiation in node-positive patients with HNSCC showed CT to have a negative predictive value of 94 % when correlated with neck dissection [62]. The role of MRI in this regard is less well established. FDG-PET at this stage has been shown to have unacceptable rates of false-positive and false-negative results (sensitivity and specificity were 67 % and 53 %, respectively,

for detecting occult disease in cervical lymph nodes) and is not recommended [63].

Surveillance Recommendation Most tumor recurrences occur within 2 years after initial treatment, with one series showing 17 % of patients experiencing some type of recurrence, 91 % of which occurred within the first 18 months [61]. Additionally, while almost 100 % of local and regional recurrences will occur within 2–3 years from initial diagnosis and treatment, there is an ongoing risk of developing a second primary malignancy in these patients. This risk is substantial, being estimated at 3–7 % per year, with a cumulative 5-year risk of 15–25 % [64, 65]. Multimodality imaging plays a large role in surveillance of these patients; nonetheless, there is no consensus regarding proper timing of serial posttreatment surveillance studies. One analysis of the available literature suggests that baseline imaging should be performed no later than 3–6 months after completion of therapy and that the most intensive surveillance should be performed within the first 3 years [66]. CT or MRI can be employed depending on the clinical circumstances, with MRI preferred at the skull base when perineural spread of malignancy is a concern. PET is accurate in diagnosis of recurrence, with a sensitivity of approximately 94 % and specificity of 82 %; however, if the patient has been treated with radiation therapy, the literature suggests that PET should optimally be performed at least 10 weeks to 3 months after completion of treatment to minimize false-positive and false-negative results, and some authors advocate for the use of PET beginning 1 year after therapy [66–68]. Surveillance imaging should always be accompanied by a clinical examination, and a general recommendation for surveillance imaging and clinical examination at 4–6-month intervals has been suggested for the first year, with yearly follow-up thereafter for at least 2 years [69].

Assessment of Response to Treatment Post-treatment anatomic imaging with CT or MRI appears to be most accurate for predicting primary-site response of squamous cell carcinoma

when performed approximately 3–4 months after the completion of radiation treatment. Complete radiologic resolution of the lesion on the posttreatment study compared with pretreatment study strongly suggests a successfully controlled primary site, with tumors that fail treatment being characterized by less than 50 % reduction in size [70, 71]. A partial response, defined as a persistent mass that has reduced in size by more than 50 %, requires further imaging and close clinical observation. Interval enlargement of such a mass is suggestive of recurrent disease, whereas stability over a 2-year period suggests fibrosis and scarring. The application of newer techniques such as perfusion CT may allow for monitoring therapy response, as decreased tumor blood flow and blood volume during therapy correlate with post-therapy reduction in tumor size [72]. PET/CT may also be used to assess response to initial high-dose radiation therapy or neoadjuvant chemotherapy. A progressive decrease in FDG uptake correlates well with tumor regression [73]. Negative PET results obtained 4 months after completion of therapy are more reliable [74, 75]. This assessment of disease response to therapy has been found to have prognostic implications. Complete resolution of primary tumor on CT and negative results on post-therapy PET have been individually correlated with overall improved survival, particularly in high-risk head and neck squamous cell cancer patients [76, 77].

Recurrence and Restaging Evaluation of the posttreatment neck, particularly differentiation between posttreatment fibrosis and recurrent tumor, can be extremely difficult with CT or MRI imaging alone. Newer techniques such as dynamic contrast-enhanced MRI may have promise in differentiating post-therapeutic change and recurrent tumor [78]. Unfortunately, other techniques such as diffusion-weighted MRI have shown limited utility for this purpose [79, 80]. With a sensitivity and specificity between 88–100 % and 75–100 %, respectively, for FDG-PET compared with 70–92 % and 50–57 % for CT and MRI, PET and PET/CT have become a favored tool for detecting recurrent or residual disease [81–83]. While FDG-PET can have false-positive results in this setting, negative results on PET are highly correlated with control of neck disease after chemoradiation [84]. PET/CT and US, particularly when coupled with US-guided fine needle aspiration, have been found to be complementary tools in surveillance for head and neck cancer [85].

Take-Home Table and Figure

See Table 37.1 for sensitivity and specificity of imaging options for detection of cervical masses and adenopathy. See Fig. 37.1 for suggested imaging workup of head and neck primary.

Imaging Case Study

Case 1: FDG-PET false negative (Fig. 37.2)

Table 37.1 Sensitivity and specificity of imaging options for detection of cervical masses and adenopathy

Detection of cervical masses and adenopathy	Sensitivity (%)	Specificity (%)	References	Evidence
MRI	86	94	[9]	Limited
CT	90.2	93.9	[12]	Moderate
US	96.8	93[a]	[37]	Moderate
PET/CT	94	94.8	[32]	Moderate
[b]	92	62	[30]	Moderate

[a]In conjunction with fine needle aspiration
[b]Detection of *unknown* primary head and neck tumor after PET-/CT-directed biopsy
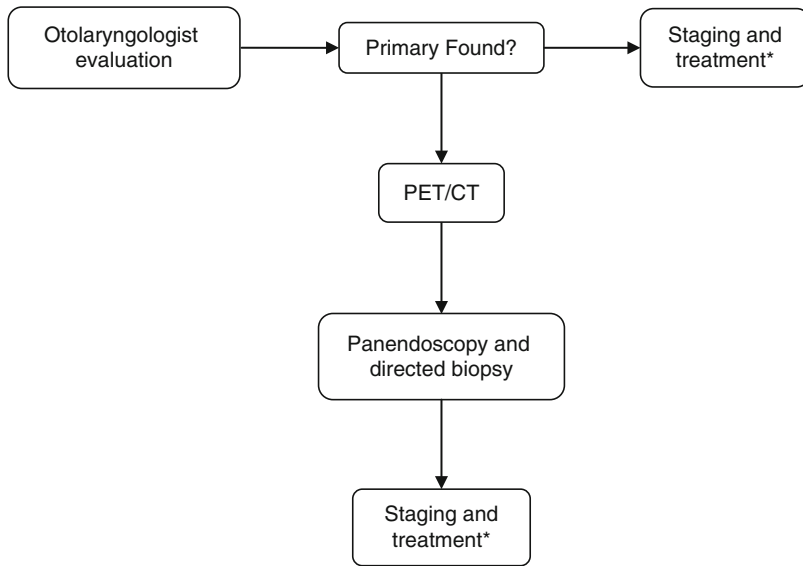
(*Baseline MRI or CT at 4-6 weeks following radiation or surgery followed by
surveillance scan at 6 month intervals and yearly thereafter for at least 2 years.
Recurrence or treatment response can be assessed after 3 months with PET/CT.)

Fig. 37.1 Suggested imaging workup of an unknown head and neck primary
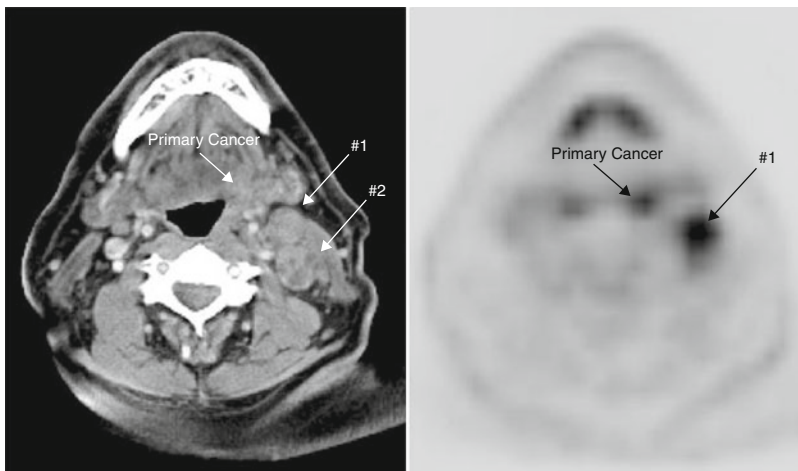
Fig. 37.2 FDG-PET false negative. Contrast-enhanced CT and FDG-PET images at the same anatomic level in the
upper neck demonstrate no uptake within a necrotic level II lymph node (#2)

Suggested Imaging Protocols

CT Neck with Contrast

Can be performed as an initial examination for all patients with neck mass persistence, enlargement, or any concern for a neoplastic etiology. Protocol: 1.25-mm-thickness axial images extending from the skull base to the thoracic inlet are obtained after the administration of intravenous contrast. Sagittal and coronal reconstructions are also obtained. We evaluate structures in the lower neck on separate post-processed series using a large field of view.

MRI Neck with Gadolinium

Indicated for better delineation of tumor extension and perineural spread. Protocol: axial T1W without fat saturation. Axial T2W and T1W post-contrast images with fat saturation. Images are acquired from the skull base to the thoracic inlet.

PET/CT

Optimally performed at least 3 months after completion of treatment to assess for response or recurrence. Protocol: PET/CT is obtained from the vertex to the mid-thigh. At our institution, a diagnostic neck CT is obtained concurrently and interpreted by neuroradiology staff in collaboration with nuclear medicine physicians.

Consider ultrasound as a first study in children presenting with a neck mass.

Future Research

- Evidence to support guidelines for baseline and posttreatment surveillance imaging in patient with head and neck cancer.
- Prospective trials to determine the positive predictive value of PET in predicting chemotherapy response in pediatric oncologic disease and to guide the possible omission of radiotherapy.

- Considering the limitations of FDG-PET, there is need for the development of new biomarkers to predict early treatment response in patients with head and neck cancer. These markers would also be useful in predicting individuals at high risk for recurrence.
- Studies examining the cost-effectiveness of ultrasound as a first imaging study after discovery of a palpable neck mass.

References

1. Boyle P, Levin B, editors. World Cancer Report. International Agency for Research on Cancer; 2008.
2. Ross DS. J Clin Endocrinol Metab. 2002;87(5): 1938–40.
3. Wang C, Crapo LM. Endocrinol Metab Clin North Am. 1997;26(1):189–218.
4. Hanna E, Vural E, Prokopakis E, Carrau R, Snyderman C, Weissman J. Arch Otolaryngol Head Neck Surg. 2007;133(6):541–5.
5. Kataoka M, Ueda H, Koyama T, et al. AJR Am J Roentgenol. 2005;184(1):313–19.
6. Thanos L, Mylona S, Kalioras V, Pomoni M, Batakis N. Cardiovasc Intervent Radiol. 2005;28(2):196–9.
7. Smith J, Hsu J, Chang J. Otolaryngol. 2006;27(4):244–7.
8. Petrou M, Mukherji S. Cancer Treat Res. 2008;143:93–117.
9. Sumi M, Van Cauteren M, Nakamura T. AJR Am J Roentgenol. 2006;186(3):749–57.
10. Curtin HD, Ishwaran H, Mancuso AA, Dalley RW, Caudry DJ, McNeil BJ. Radiology. 1998;207(1):123–30.
11. Cianchetti M, Mancuso AA, Amdur RJ, et al. Laryngoscope. 2009;119(12):2348–54.
12. Jeong H, Baek C, Son Y, et al. Head Neck. 2007;29(3):203–10.
13. Hudgins PA, Kingdom TT, Weissler MC, Mukherji SK. AJNR Am J Neuroradiol. 2005;26(5): 1174–7.
14. Sumi M, Kimura Y, Sumi T, Nakamura T. J Magn Reson Imaging. 2007;26(6):1626–33.
15. King A, Ahuja A, Yeung DKW, et al. Radiology. 2007;245(3):806–13.
16. Eida S, Sumi M, Sakihama N, Takahashi H, Nakamura T. AJNR Am J Neuroradiol. 2007;28(1):116–21.
17. Vandecaveye V, De Keyzer F, Vander Poorten V, et al. Radiology. 2009;251(1):134–46.
18. Srinivasan A, Dvorak R, Perni K, Rohrer S, Mukherji SK. AJNR Am J Neuroradiol. 2008;29(1):40–4.
19. Vandecaveye V, De Keyzer F, Nuyts S, et al. Int J Radiat Oncol Biol Phys. 2007;67(4):960–71.
20. AbdelRazek AA, Kandeel AY, Soliman N, et al. AJNR Am J Neuroradiol. 2007;28(6):1146–52.

21. Gandhi D, Hoeffner EG, Carlos RC, Case I, Mukherji SK. J Comput Assist Tomogr. 2003;27(5):687–93.
22. Rumboldt Z, Al-Okaili R, Deveikis JP. AJNR Am J Neuroradiol. 2005;26(5):1178–85.
23. Bisdas S, Baghi M, Smolarz A, et al. Invest Radiol. 2007;42(3):172–9.
24. Bisdas S, Rumboldt Z, Surlan-Popovic K, et al. AJNR Am J Neuroradiol. 2010;31(3):576–81.
25. Surlan-Popovic K, Bisdas S, Rumboldt Z, Koh TS, Strojan P. AJNR Am J Neuroradiol. 2010;31(3):570–5.
26. Bisdas S, Baghi M, Wagenblast J, Vogl TJ, Thng CH, Koh TS. J Magn Reson Imaging. 2008;27(5):963–9.
27. Keberle M, Kenn W, Hahn D. Eur Radiol. 2002;12(7):1672–83.
28. Bartz BH, Case IC, Srinivasan A, Mukherji SK. J Comput Assist Tomogr. 2006;30(6):972–4.
29. Kubicek GJ, Champ C, Fogh S, et al. Head Neck Oncol. 2010;2:19.
30. Rudmik L, Lau HY, Matthews TW, et al. Clinical utility of PET/CT in the evaluation of head and neck squamous cell carcinoma with an unknown primary: a prospective clinical trial. Head Neck. 2011;33(7): 935–40.
31. Johansen J, Buus S, Loft A, et al. Head Neck. 2008;30(4):471–8.
32. Roh JL, Kim JS, Lee JH, et al. Oral Oncol. 2009;45(3):218–24.
33. Kim SY, Roh JL, Yeo NK, et al. Ann Oncol. 2007;18(10):1698–703.
34. Zanation AM, Sutton DK, Couch ME, Weissler MC, Shockley WW, Shores CG. Laryngoscope. 2005;115(7):1186–90.
35. Hafidh MA, Lacy PD, Hughes JP, Duffy G, Timon CV. Eur Arch Otorhinolaryngol. 2006;263(9):853–9.
36. Ahuja AT, Richards P, Wong KT, Yuen EH, King AD. Clin Radiol. 2003;58(11):869–75.
37. Baatenburg de Jong RJ, Rongen RJ, Lameris JS, Harthoorn M, Verwoerd CD, Knegt P. Arch Otolaryngol Head Neck Surg. 1989;115(6):689–90.
38. van den Brekel MW, Reitsma LC, Quak JJ, et al. AJNR Am J Neuroradiol. 1999;20(9):1727–31.
39. Ying M, Ahuja A, Brook F. Ultrasound Med Biol. 2004;30(4):441–7.
40. Ying M, Ahuja A, Brook F. Ultrasound Med Biol. 2002;28(6):737–44.
41. Christie A, Teasdale E. Clin Radiol. 2010;65(3):213–17.
42. Hollenbeak CS, Lowe VJ, Stack Jr BC. Cancer. 2001;92(9):2341–8.
43. Sher DJ, Tishler RB, Annino D, Punglia RS. Ann Oncol. 2010;21(5):1072–7.
44. Gupta P, Maddalozzo J. Arch Otolaryngol Head Neck Surg. 2001;127(2):200–2.
45. Sidell DR, Shapiro NL. Otolaryngol Head Neck Surg. 2011;144(3):431–4.
46. Quraishi MS, O'Halpin DR, Blayney AW. Clin Otolaryngol Allied Sci. 1997;22(1):30–3.
47. Douglas SA, Jennings S, Owen VM, Elliott S, Parker D. Clin Otolaryngol. 2005;30(6):526–9.
48. Rozovsky K, Hiller N, Koplewitz BZ, Simanovsky N. Eur Radiol. 2010;20(2):484–90.
49. Albright JT, Topham AK, Reilly JS. Arch Otolaryngol Head Neck Surg. 2002;128(6):655–9.
50. Pappas JN, Donnelly LF, Frush DP. Radiology. 2000;215(3):897–9.
51. Furth C, Steffen I, Amthauer H, et al. J Clin Oncol. 2009;27(26):4385–91.
52. Abdel Razek AA, Gaballa G, Elhawarey G, Megahed AS, Hafez M, Nada N. Eur Radiol. 2009;19(1):201–8.
53. Cravero JP, Blike GT, Beach M, et al. Pediatrics. 2006;118(3):1087–96.
54. McCarville MB, Christie R, Daw N, Spunt S, Kaste S. AJR Am J Roentgenol. 2005;184(4):1293–304.
55. Paltiel HJ, Summerville DA, Treves ST. Pediatr Radiol. 1992;22(4):251–6.
56. Kreisner E, Camargo-Neto E, Maia CR, Gross JL. Clin Endocrinol (Oxf). 2003;59(3):361–5.
57. Ivarsson SA, Ericsson UB, Fredriksson B, Persson PH, et al. Am J Dis Child. 1989;143(11):1369–72.
58. Moon WJ, Jung SL, Lee JH, et al. Radiology. 2008;247(3):762–70.
59. Grunwald F, Kalicke T, Feine U, et al. Eur J Nucl Med. 1999;26(12):1547–52.
60. Chung JK, So Y, Lee JS, et al. J Nucl Med. 1999;40(6):986–92.
61. Som PM, Urken ML, Biller H, Lidov M. Radiology. 1993;187(3):593–603.
62. Liauw SL, Mancuso AA, Amdur RJ, et al. J Clin Oncol. 2006;24(9):1421–7.
63. McCollum AD, Burrell SC, Haddad RI, et al. Head Neck. 2004;26(10):890–6.
64. Sturgis EM, Miller RH. Ann Otol Rhinol Laryngol. 1995;104(12):946–54.
65. Vikram B, Strong EW, Shah JP, Spiro R. Head Neck Surg. 1984;6(3):734–7.
66. Manikantan K, Khode S, Dwivedi RC, et al. Cancer Treat Rev. 2009;35(8):744–53.
67. Isles MG, McConkey C, Mehanna HM. Clin Otolaryngol. 2008;33(3):210–22.
68. Kim SY, Lee SW, Nam SY, et al. J Nucl Med. 2007;48(3):373–8.
69. Som PM, Lawson W, Urken ML. The posttreatment neck: Clinical and imaging considerations. In: Som PM, Curtin H, editors. Head and neck imaging. 4th ed. St. Louis: Mosby; 2003. p. 2239–72.
70. Mukherji SK, Mancuso AA, Kotzur IM, et al. Radiology. 1994;193(1):141–8.
71. Mukherji SK, Mancuso AA, Kotzur IM, et al. Radiology. 1994;193(1):149–54.
72. Petralia G, Preda L, Giugliano G, et al. J Comput Assist Tomogr. 2009;33(4):552–9.
73. Lowe VJ, Dunphy FR, Varvares M, et al. Head Neck. 1997;19(8):666–74.
74. Greven KM, Williams DW, Keyes JW, et al. Cancer. 1994;74(4):1355–9.
75. Greven KM, Williams 3rd DW, McGuirt WFS, et al. Head Neck. 2001;23(11):942–6.

76. Moeller BJ, Rana V, Cannon BA, et al. Int J Radiat Oncol Biol Phys. 2010;78(3):667–74.
77. Kao J, Vu HL, Genden EM, et al. Cancer. 2009;115(19):4586–94.
78. Semiz Oysu A, Ayanoglu E, Kodalli N, Oysu C, Uneri C, Erzen C. Clin Imaging. 2005;29(5):307–12.
79. Fruehwald-Pallamar J, Czerny C, Mayerhoefer ME, et al. Eur J Nucl Med Mol Imaging. 2011;38(6):1009–19.
80. Choi SH, Paeng JC, Sohn CH, et al. J Nucl Med. 2011;52(7):1056–62.
81. Fischbein NJ, AAssar IS, Caputo GR. AJNR Am J Neuroradiol. 1998;19(7):1189–96.
82. Anzai Y, Carroll WR, Quint DJ, et al. Radiology. 1996;200(1):135–41.
83. Wong WL, Chevretton EB, McGurk M, et al. Clin Otolaryngol Allied Sci. 1997;22(3):209–14.
84. Tan A, Adelstein DJ, Rybicki LA, et al. Arch Otolaryngol Head Neck Surg. 2007;133(5):435–40.
85. Hwang HS, Perez DA, Orloff LA. Laryngoscope. 2009;119(10):1958–65.

Adults with Palpable Neck Mass: Evidence-Based Neuroimaging

38

Kim O. Learned, Kelly M. Malloy, Jill E. Langer, and Laurie A. Loevner

Contents

K.O. Learned (✉) • J.E. Langer • L.A. Loevner
Department of Radiology, University of Pennsylvania Health System, Perelman School of Medicine at the University of Pennsylvania, Philadelphia, PA, USA
e-mail: im.earned@uphs.upenn.edu; jill.langer@uphs.upenn.edu; laurie.loevner@uphs.upenn.edu

K.M. Malloy
Department of Otolaryngology – Head and Neck Surgery, University of Michigan Health System, Ann Arbor, MI, USA
e-mail: kellymal@umich.edu

Key Points

- The most common palpable neck mass in adults is lymphadenopathy, the majority of which is reactive infectious/inflammatory in nature; not uncommonly, however, a neck mass is the first presentation of neoplasm involving the cervical lymph nodes. Therefore, cross-sectional imaging is not necessary in adult patients presenting with lymphadenopathy with the following: (1) obvious clinical evidence of common viral upper respiratory infection or superficial odontogenic infection without clinical concern for deep space abscess; (2) absence of a focal suspicious mass of the aerodigestive tract; (3) no risk factor for malignancy; (4) reliable follow-up (moderate evidence).

- Contrast-enhanced computer tomography (CECT) is the imaging work horse for evaluation of infectious inflammatory neck mass who fail conservative medical management or when deep neck infection (DNI) is a clinical concern (moderate evidence). When performing alone without clinical input, CECT has poor accuracy and specificity in identifying purulent collection for drainage; therefore, both CECT and clinical assessment are critical components in management decision to drain the identified collection (moderate evidence). CECT provides valuable information regarding the extent of disease and guide surgical approach for drainage as needed (moderate evidence).

- CT or MR scan of the neck is valuable as the initial imaging modality in the patients with high probability of harboring neoplasm (moderate evidence).

- CT and MR are comparable in most instances, complement one another at times and superiority of one modality over the other cannot be generalized to all anatomic subsites of the neck and all pathologies. Therefore, the modality choice depends on the tumor's location and pathology and specific clinical question (moderate evidence).

- MR's advantage of soft tissue discrimination makes it the modality of choice for assessment of neoplasm in the suprahyoid location such as oral squamous cell carcinoma (SCCA), intracranial involvement, perineural spread, and salivary gland tumors (limited-moderate evidence).

- CT and MR complement each other in assessment of sinonasal neoplasm for precise soft tissue tumor mapping and bone/skull base involvement, and CT fusion is routinely used for intraoperative surgical navigation (moderate evidence).

- CT and MR are comparable in evaluation of laryngeal tumor; however, CT is the preferred modality due to its fast imaging time, excellent spatial resolution, and lower cost. MR is reserved for problem solving when precise soft tissue tumor margin and exclusion of cartilaginous involvement are equivocal by CT (limited-moderate evidence).

- US guidance improves the rate of successful diagnostic yield in fine needle aspiration (FNA) and is recommended (moderate evidence) even though its success depends greatly on the expertise of the sonographer, cytopathologist, and the pathology (moderate evidence).

- 18-F-fluorodeoxyglucose–positron emission tomography (FDG-PET) and subsequently PET-CT demonstrate the best diagnostic performance for staging and especially restaging of FDG-avid lymphoma (strong-moderate evidence). CT remains the test of choice for non-FDG-avid lymphoma (moderate evidence).

- Ultrasound remains the gold standard for evaluation of thyroid nodules (strong-moderate evidence).

- There is no evidence on the appropriate management of a palpable neck mass without imaging correlate. As a general rule, however, indeterminate palpable neck masses should be at minimum followed with close observation and repeat imaging if they grow or change significantly. The repeat imaging choice and timing require close collaboration between the clinician and the radiologist in order to

optimize the management strategy for the most likely suspicious pathology.

Definition and Pathophysiology

The majority of palpable neck masses referred for imaging can be divided into these general categories: infection, neoplasm, or congenital mass (Table 38.1). The cervical lymphatic system including Waldeyer's ring, superficial and deep cervical nodes (occipital, auricular, parotid, facial, retropharyngeal, submental, submandibular, internal jugular, spinal accessory, and supraclavicular), serves as initial line of defense against infections as well as neoplastic spread for all structures within the head and neck including skin, salivary glands, and aerodigestive tract. Most cervical lymphatics drain to the submandibular and internal jugular cervical lymph nodes, which are consequently often involved in cervical lymphadenitis and metastatic disease. Congenital lesions mostly present in children but may manifest late in adulthood as palpable neck mass or neck infection, thus their typical anatomic locations and associated physical findings establish the diagnosis and surgical management [1–3].

The range of pathologies of palpable neck lumps is dependent on the age of the patient at presentation, the associated symptoms and personable risk factors. Benign etiologies, such as infections and congenital lesions, are very common in children. The most common palpable neck mass in adults is reactive lymphadenopathy, especially when there is clear clinical evidence of infectious etiology. However, the likelihood of harboring malignancy increases in adults over the age of 40, when the neck mass persists after standard of care conservative management and when there are risk factors for malignancy as detailed below.

Epidemiology

The incidence of palpable neck lumps is not known but it is a well-recognized presentation of many disease processes to emergency department (ED), primary care physician (PCP) office, and otolaryngology (ENT) referrals.

The 2008 National Hospital Ambulatory Medical Care Survey reported infectious disease and neoplasm in the top primary diagnoses at emergency department visits but only accounted for 3.1 % and 0.3 % of total visits, respectively [4]. When dividing the leading primary diagnosis by age groups, for children younger than 15 years of age, infectious etiologies (acute upper respiratory infection-URI, otitis media and eustachian tube disorders, fever of unknown origin, acute pharyngitis) accounted for 22.7 % of all visits. For older age group of 15–64 years, infections (acute URI, cellulitis, and abscess) still remain in the top 10 diagnoses but only accounted for 4.8 % of all visits. In patients older than 65 years of age, the only infectious etiology remain in top diagnosis is pneumonia (3.2 % of all visits). These data suggest presentation of a palpable neck mass in emergency settings are primarily infections and account for a very small percentage of ED visits.

Encounter of a neck mass in PCP office setting and ENT referrals are common but the exact epidemiology is unknown. Several small series demonstrated 90 % of neck masses in children are benign infectious adenopathy and congenital lesions [5]. Williamson retrospectively reviewed 249 patients with enlarged lymph nodes presented to family practice to clarify recommendations for evaluation of lymphadenopathy [6]. He found only three patients were diagnosed with malignancy and the remainder were benign etiologies with only 36 % of patients receiving a firm diagnosis. In a retrospective review of 82 adult patients with unexplained cervical lymphadenopathy in family practice setting, only 1.1 % of this patient population had malignant lymphadenopathy [7]. In ENT referral settings, the occurrence of a malignant process in palpable non-thyroid neck lesions in adults is approximately 12–30 % [8–10]. These limited evidences suggest the high prevalence of benign palpable neck masses presented in all practice settings.

In the United States, the most common head and neck malignancies in adults are SCCA and lymphoma with a reported incidence of 10.7 per

100,000 cases of oral and pharyngeal cancer and 22.1 per 100,000 for lymphoma (2003–2007 combined years) [11, 12]. Cervical metastases from head and neck SCCA occur in 15–87 % of cases and vary depending on the primary tumor location: 40 %–87 % of nasopharynx; 30 % of oral cavity; 15 %–75 % oropharynx with common bilateral involvement (29 % of tonsil); 18 % of pyriform sinus; and a small number as unknown primary [8, 13, 14]. Evidence-based imaging of cervical nodal metastasis in head and neck cancer is extensively reviewed and summarized in dedicated chapter by Drs. Furukawa and Anzai (Chap. 40, "Diagnosis of Cervical Lymph Node Metastasis in Head and Neck Cancer: Evidence-Based Neuroimaging").

The American Cancer Society reports increasing incidence of thyroid cancer, which is partially due to increased awareness and technological advances in imaging detection of smaller lesions, with a reported incidence of 10.2 per 100,000 for the years 2003–2007 [15]. With regard to palpable neck mass, only about 4–7 % of thyroid nodules are detected by palpation and approximately 5–10 % of these are malignant [16, 17]. The complexity of evidence-based imaging of thyroid nodule evaluation has been presented in depth by Dr. Dighe's dedicated chapter "Thyroid Nodules and Cancer" (Chap. 39, "Thyroid Nodules and Cancer: Evidence-Based Neuroimaging").

Overall Cost to Society

The breakdown of imaging cost for each disease entity presented as a palpable neck mass in adults is unknown. The cost of care for neck infection and benign neck masses is also not reported. On the other hand, malignancy is reported to have the greatest impact on patients' morbidity, mortality, and cost of care, which continues to rise as a result of increased prevalence and medical advancements [18–20] (moderate-strong evidence). The National Cancer Institute estimated the national economic burden of cancer care in 2006 as 10.168 billion dollars for lymphoma and 3.145 billion for head and neck cancers [18]. Findings from Surveillance, Epidemiology, and End Result

(SEER) Medicare data show that the health economic burden of head and neck SCCA is substantial, with costs that are comparable to or higher than those of other solid tumors [21]. In general, net costs of care for both SCCA and lymphoma are higher with later stage at diagnosis [20, 22].

There is variability in the practice of neck imaging for neoplastic cervical masses, depending on the available local expertise and resource, but in most centers, CT and MR are initial imaging choices (limited evidence). Table 38.2 summarizes the range of imaging costs by modalities. There are only a few limited evidences comparing the cost-effectiveness of these modalities in oncologic settings.

Goals of Imaging

The overall goal of initial neck imaging for a palpable neck lump is to detect treatable causes, ranging from benign congenital lesions to potentially aggressive infections or malignancy. This is an important initial step in the diagnosis and management algorithm, enabling biopsy planning, workup for systemic diseases that manifest in the neck, such as lymphomatous or granulomatous disease, and in some instances prompting the necessary intervention in an appropriate and timely manner. The ultimate goal is to improve the patient's outcome and to optimize the imaging strategy combining the highest diagnostic yield with the lowest cost.

Advanced imaging techniques, such as FDG-PET, MR perfusion, CT perfusion, and diffusion weighted imaging (DWI), are available in clinical practice for better tissue characterization, and in some instances they are essential tools for accurate staging and restaging to optimize multidisciplinary approaches to cancer treatment. These technological advancements are specifically addressed in Drs. Balgude and Mukherji's chapter (Chap. 37, "Neck Masses and Adenopathy: Evidence-Based Neuroimaging") and Drs. Furukawa and Anzai's chapter (Chap. 40, "Diagnosis of Cervical Lymph Node Metastasis in Head and Neck Cancer: Evidence-Based Neuroimaging").

Options

lists all diagnostic imaging options of a neck mass and the average costs based on Medicare reimbursement set by Centers for Medicare and Medicaid Services in 2011.

Methodology

A MEDLINE search was performed using PubMed (National Library of Medicine, Bethesda, Maryland) for original research publications discussing the diagnostic performance and effectiveness of imaging strategies in the palpable neck lump. Clinical predictors of pathology were also included in the literature search. The search covered the years January 1980 to September 2011. The search strategy employed different combinations of the following terms: (1) head and neck, (2) neck lump or neck mass, (3) neoplasm or infection or congenital, (4) lymphoma, (5) imaging or computed tomography or magnetic resonance imaging, or ultrasonography or PET, and (6) cost. Additional articles were identified by reviewing the reference lists of relevant papers. This review was limited to human studies and the English language literature. The author performed an initial review of the titles and abstracts of the identified articles followed by review of selected full texts in articles that were relevant.

Discussion of Issues

Who Should Undergo Imaging for a Palpable Neck Mass?

Summary
Given that cost-effectiveness of imaging strategy is dependent on the likelihood of the disease and the change in management to optimize outcome, it is essential to clinically stratify patients into different levels of probability of disease as well as potential change in management prior to imaging (moderate evidence).

The range of pathologies of palpable neck lumps is relatively dependent on the age of the patient at presentation and associated risk factors. It has been established in the literature that benign etiologies are very common in children and the most common palpable neck mass in adults is lymphadenopathy; the majority of which are infectious/inflammatory in nature and do not require imaging (moderate evidence). The exception is deep neck infection (DNI), which can be potentially life threatening and a combination of clinical assessment and imaging is essential in its diagnosis and management (moderate evidence). Therefore, cross-sectional imaging is not necessary in adult patients presenting with lymphadenopathy with the following: (1) obvious clinical evidence of common viral upper respiratory infection or superficial odontogenic infection without clinical concern for deep space abscess; (2) absence of a focal suspicious mass of the aerodigestive tract; (3) no risk factor for malignancy; and (4) reliable follow-up (moderate evidence).

CECT is recommended to evaluate atypical neck infection that is not responsive to empiric antibiotic course or to assess the full extent of DNI and to identify and guide surgical treatment of a drainable abscess (moderate evidence).

The likelihood of harboring malignancy increases in adults over age forty, especially those with persistent neck mass and associated risk factors. Hence, imaging is necessary in the adult population in the workup to exclude malignancy and to guide management (moderate evidence).

Supporting Evidence
Clinical and Imaging Evaluation of the Palpable Neck Masses With the technological advancements of the past three decades, US, CT, and MR imaging reveal the additional non-palpable abnormalities (for example, strong evidence for thyroid US) as well as hidden pathologies in deep spaces of the neck and have proved to be more accurate in detecting the extent of the disease than is clinical assessment (moderate evidence for SCCA and cervical metastatic adenopathy, moderate evidence for deep neck infection, moderate-strong evidence for lymphoma)

[16, 23–27, 71, 87, 113, 159, 173, 174]. Imaging adds valuable information for prognosis and management decisions (moderate evidence) and may alter the disease outcome (limited evidence) [80, 83, 84, 88]. Therefore, these imaging modalities have been rapidly integrated into the standard workup and management of various neck lumps with insufficient evidence supporting their routine use without a disease-specific stratification by clinical assessment prior to imaging. By thorough history review, physical examination, and clinical experience, clinicians often establish an initial clinical impression of a neck mass and subsequently select an appropriate imaging strategy to aid in diagnosis and management [28–30].

Spectrum of Pathologies Presented as Palpable Neck Masses Torsiglieri et al. conducted a large retrospective chart review of 445 consecutive pediatric patients at Children Hospital of Philadelphia who underwent procedures for diagnosis and treatment of neck masses over a 5-year period (January 1982–December 1986, age range of 1 day to 21 years, mean age of 6.2 years, close to equal gender distribution) [5]. They found approximately half of all neck masses are congenital, a third are inflammatory, and only about 10 % are malignant. Clinical impression with subsequent appropriate laboratory and diagnostic imaging provided correct preoperative diagnosis in 61 % of patients (moderate evidence). Even though specific imaging utilization in this large retrospective study was only partially reported, the presented data emphasized the importance of clinical impression prior to adding laboratory and imaging to the workup of pediatric neck masses.

In a retrospective review of 249 patients with enlarged lymph nodes presented in family practice offices, 246 patients had benign etiologies with only 36 % with a firm diagnosis [6]. Serious or treatable causes of lymphadenopathy were rare and were always accompanied by clinical conditions that suggested further evaluation. The author concluded that in patients without associated concerning signs or symptoms, a period of observation is safe and likely to save unnecessary expense and biopsy. The overall incidence of infectious mononucleosis in the United States is about 500 cases per 100,000 persons per year, with the highest incidence in the age group of 15–24 years and classic triad of pharyngitis, fever, and lymphadenopathy. Most clinical and laboratory findings resolve by 1 month after diagnosis, but cervical adenopathy and fatigue may resolve more slowly [31]. In endemic areas such as India, TB accounts for a large number of palpable cervical adenopathy as demonstrated in a series of 1,827 patients with cervical lymphadenopathy by Khan et al.: 893 [48.87 %] cases of tubercular origin (77 % in age range of 11–30 years); 571 (31.2 %) cases of nonspecific inflammation; and only 202 (11 %) cases of metastases [32]. Infectious and noninfectious granulomatous disease manifestation as a palpable neck mass can persist, and is difficult to diagnose by imaging alone and at times raises legitimate clinical concern for a neoplastic process [33].

In a retrospective study of 95 adults with palpable neck lump (excluding parotid and thyroid masses and patients with prior head and neck malignancy), Bhattacharyya et al. found that a combination of increasing patient age, size, and duration of a neck mass renders the mass more likely to be neoplastic and age is the most important predictive factor for malignancy (limited evidence) [9]. Wang et al. retrospectively looked in their database of 301 DNI and found seven patients (age 40–74, median 64 years) had DNI as the main initial presentation of primary head and neck cancer [34]. In a prospective study of 100 consecutive neck lump referrals to ENT specialist, about half of the patients had reactive adenopathy or no abnormality [10]. These limited and moderate evidences reinforce the older published literature that infectious-inflammatory and non-neoplastic lesions remain common in adults (66–68 %) and a small number of congenital lesions can present in adulthood either as a mass, cervical adenopathy, or as recurrent infection [1–3]. Therefore, it is generally accepted in standard practice to medically manage and follow up adults who presented with a neck mass and clinical evidence of simple reactive/infectious process without imaging [28].

CECT is the preferred modality and is necessary in patients with clinical concern for DNI to

guide management in order to avoid potential life threatening complications in inadequately treated infection [35, 36]. Limited-moderate data reported CT to be more sensitive (95–100 %) than clinical examination (30–55 %) in assessment of the full extent of deep space involvement, and when combined with clinical assessment it plays an important role in surgical planning and conservative medical management (high accuracy of 88–89 % for identifying drainable abscess) [25–27]. Evidence-based imaging issues of infectious adenopathy and neck infection are discussed in dedicated special case section below.

Lymphoma remains the most common malignant diagnosis in young adults with a persistent and/or enlarging cervical adenopathy, especially if it is associated with fever, night sweat, weight loss, or abnormal blood counts [37–40]. Evidence-based imaging of lymphoma is discussed in details as special case below.

In adults over the age of 40, the likelihood of a neck mass harboring malignancy increases, especially in those with associated high-risk factors [9, 10, 41–47]. HPV associated SCCA and lymphoma can present in younger adult age group, thus a persistent neck mass in an adult of any age needs further evaluation. In a large retrospective review of 522 consecutive adults with head and neck cancer, Robertson et al. found 90 % were SCCA and 6 % were salivary gland tumors with approximately 11.5 % of patients initially presenting with a painless lump or swelling. Almost all major salivary gland tumors were presented as a palpable mass (91 % of parotid gland tumors, 100 % of submandibular gland tumors) and site-specific variable percentages of SCC presented as palpable lymphadenopathy (40 % nasopharyngeal, 29 % tonsillar, and 18 % pyriform sinus tumors) [8].

Risk Factors There are many viral and bacterial infectious causes of cervical lymphadenitis. The most common bacterial organisms causing acute unilateral infection are *Staphylococcus aureus* and *Streptococcus pyogenes*. Viruses typically cause bilateral acute cervical adenitis and are common in children [30]. The presence of dental or periodontal disease suggests anaerobic

bacteria [48]. Methicillin-resistant *Staphylococcus aureus* (MRSA) skin and soft tissue infections typically occur with traditional risk factors such as prolonged hospitalization, surgical procedure, or indwelling catheters. Recently, community-acquired MRSA is well recognized in intravenous drug abuse and has been reported in children without traditional risk factors [49–51]. Therefore, MRSA should be suspected when infection does not respond to conventional antibiotic regimen. Cervical mycobacterial adenitis typically presents as chronic adenopathy; *Mycobacterium tuberculosis* is common in adults, whereas non-tuberculous mycobacteria (*Mycobacterium avium*-intracellulare, *Mycobacterium scrofulaceum*, and *Mycobacterium kansasii*) are more common in children [32, 52–54]. Cat-scratch disease by *Bartonella henselae* is also a common cause of lymphadenitis generally is self-limited [55]. HIV/AIDS patients can have chronic cervical lymphadenitis and they are at risk for atypical opportunistic infection.

Diabetes poses a risk for DNI with wide spread of inflammation and more complications [56–58]. Odontogenic infection and upper respiratory infection are common causes of DNI [59]. Laryngeal edema and resultant airway compromise in DNI is common and descending necrotizing mediastinitis with rapid clinical deterioration is a potential danger with high mortality [56, 60].

When selecting patients for further imaging assessment of noninfectious neck masses, knowledge of the risk factors for malignancy is important. Head and neck SCCA has a strong association with tobacco use and alcohol consumption (moderate-strong evidence). Patients with a history of prior upper aerodigestive tract SCCA, particularly those who continue to smoke, are at risk of developing recurrent disease or a second head and neck malignancy due to field cancerization (moderate-strong evidence), because the entire mucosa is exposed to the carcinogen, explaining occurrence of synchronous and metachronous lesions. Even though the likelihood of head and neck SCCA is only about 1–3 % in smokers over age 40, early detection by routine screening physical exam for at-risk patients remains the most important factor in the

survival and ultimately the cost of care (moderate evidence) [22, 41, 42]. A palpable neck mass in a high-risk adult patient, especially with symptoms such as hoarseness, otalgia, or throat irritation, increases likelihood of malignancy [8, 42]. Human papillomavirus (HPV) has strong association with oropharyngeal head and neck SCCA [43–45]. Betel nut chewers also have increased risk of oral SCCA (moderate evidence) [46].

The risk of developing non-Hodgkin's lymphoma (NHL) increases with age, whereas the risk of Hodgkin's lymphoma (HL) is highest during adolescence and early adulthood. Various associated risk factors of NHL have been identified including altered immune function (post organ transplant immunosuppression, severe autoimmune conditions, human immunodeficiency virus (HIV), and human T-cell leukemia virus type I) [40]. Epstein Barr virus (EBV) has a strong association with African Burkitt's lymphoma, undifferentiated nasopharyngeal carcinoma, and Hodgkin's disease associated with acquired immunodeficiency syndrome (AIDS). EBV probably plays an important role in pathogenesis of Hodgkin's disease, HIV-related NHL, and other epithelial malignancies [47]. A family history of lymphoma and certain common genetic variations in immune response genes are associated with a modestly increased risk for HL [61].

Notable risk factors for thyroid malignancy include multiple endocrine neoplasia (MEN) syndrome, Cowden's syndrome, familial adult polyposis syndrome, family history of thyroid cancer, and prior neck irradiation as a child [62]. Thyroid cancer affects mostly young adults with 80 % of newly diagnosed thyroid cancer patients under the age of 65 years. However, older age at diagnosis has less chance of survival, and survival depends greatly on the stage at diagnosis and biological nature of each subtype. The risk of malignancy is not dependent on whether a thyroid nodule is palpable or non palpable, small or large, solitary or multiple, dominant or nondominant, and the nodule's sonographic features are important for the determination of the risk of malignancy [62–66]. In patients with multiple nodules, the overall cancer rate of 10–13 % is similar to patients with a solitary nodule. While thyroid cancers are often in the dominant or largest nodule, in approximately one-third of cases the cancer is in a nondominant nodule [66]. However, in known cancerous nodules, size is a powerful predictor for extraglandular tumor extension as well as nodal, pulmonary, and osseous metastases [67]. Because a palpable thyroid nodule is typically sizable, it requires further workup, including evaluation for a functioning nodule. All nonfunctioning nodules need thyroid US to evaluate the sonographic features [16, 62].

Cervical nodal metastasis can occur from malignancy outside the head and neck origin with prototype supraclavicular metastatic lymphadenopathy from breast cancer and Pancoast tumor.

What Should Be the Appropriate Imaging Modalities?

Summary

Because a palpable neck mass can be the manifestation of a broad spectrum of diseases, the imaging strategy is optimized to assist in diagnosis and management of the clinically suspected pathology in question. Complete evidence-based imaging for evaluation of neck masses, cervical metastatic adenopathy, and thyroid nodules has been extensively reviewed in the dedicated excellent chapters by Drs. Balgude and Mukherji, (Chap. 37, "Neck Masses and Adenopathy: Evidence-Based Neuroimaging") Drs. Furukawa and Anzai (Chap. 40, "Diagnosis of Cervical Lymph Node Metastasis in Head and Neck Cancer: Evidence-Based Neuroimaging"), and Dr. Dighe (Chap. 39, "Thyroid Nodules and Cancer: Evidence-Based Neuroimaging"). To encompass the most common pathology that can present as a palpable neck mass, an overview on basic initial imaging workup for SCCA, salivary gland masses, and a palpable thyroid nodule will be presented briefly. Attention will be given to neck infection and lymphoma as special cases.

CT or MR scan of the neck is valuable as the initial imaging strategy in the patients with high probability of harboring neoplasm for diagnosis, prognosis, and treatment planning

(moderate evidence). Because each modality has its own advantages and limitations, the superiority of one modality over the other cannot be generalized and has not been firmly established. They are comparable in most instances and sometimes complementary of each other. Therefore, the appropriate imaging strategy for the optimal diagnostic performance and cost effectiveness depends on the tumor's site and pathology and specific clinical question.

Specifically, MR is recommended as the imaging modality of choice for treatment planning of neoplasm in the suprahyoid locations such as oral, oropharyngeal, and nasopharyngeal SCCA, intracranial involvement, perineural spread, and salivary gland tumors, because of MR's advantages in delineating a tumor from surrounding normal soft tissue and minimizing dental filling artifact (limited-moderate evidence).

CT and MR are comparable in evaluation of laryngeal cancer with CT's advantages of lower cost, fast imaging time with less motion, and excellent spatial resolution, while MR offers higher soft tissue delineation but with a higher cost and longer imaging time prone to motion degradation (limited-moderate evidence). Therefore, CT is the preferred modality and MR is reserved for problem solving when precise soft tissue tumor delineation and exclusion of cartilaginous involvement are equivocal by CT (limited-moderate evidence). In identifying cartilaginous invasion of laryngeal cancer, CT criteria have high specificity but low sensitivity, whereas MR criteria have a high sensitivity but low specificity, and no single criteria have both sensitivity and specificity above 70 % (moderate evidence).

Both CT and MR are routinely used as pre-op imaging for sinonasal neoplasm because their complementary diagnostic information is valuable for appropriate surgical planning, and CT fusion is routinely used for intraoperative surgical navigation (moderate evidence).

Palpable salivary gland lesions can be clinically divided into inflammatory or neoplastic masses. For evaluation of sialolithiasis/sialadenitis, CT offers better visualization of the calcified stones, whereas MR offers better soft tissue tumor mapping for evaluation of salivary gland neoplasm (limited-moderate evidence).

Ultrasound guidance improves the rate of successful diagnostic fine needle aspiration (FNA) cytology and is accurate in initial tissue sampling of a palpable neck mass to assist management decision (moderate evidence). However, its success depends on the expertise of the operator as well as the cytopathologist, and a small percentage of false negative or false positive is inherently due to sampling error, inadequate specimen, or misinterpretation of the vast pathologies of the neck (limited-moderate evidence).

The evaluation of a palpable thyroid nodule includes a combination of clinical assessment, thyroid function tests, US, and FNA as needed. If the patient has a suppressed thyroid stimulating hormone (TSH), I-123 scan is recommended to determine if it is a functioning nodule and therefore would have no significant risk of malignancy (moderate evidence). Evaluation of the sonographic features of thyroid nodules is considered the most specific noninvasive method for detecting nodules with features suspect for a malignancy (moderate evidence). Fine-needle aspiration biopsy (FNA) is the most accurate diagnostic test to determine if a thyroid nodule is malignant (strong evidence).

Supporting Evidence

There are mostly retrospective studies assessing the diagnostic performance of imaging in the evaluation of the critical issues in staging and managing head and neck SCCA. These studies provide limited-moderate evidence supporting the standard practice of using CT or MR as the first imaging modality for evaluation of a suspicious neck mass. Because of the complexity of multidisciplinary approaches to diagnosis and treatment of head and neck cancers, the cost-effectiveness and impact on patient outcome by imaging utilization alone is not specifically studied.

There are a few investigations comparing CT and MR in evaluation of head and neck

neoplasms. In many instances, CT and MR are comparable and can substitute for each other as needed. For example, a patient with an MR incompatible device, such as a spinal stimulator, can only have CT evaluation, whereas an iodine contrast allergy patient benefits from a gadolinium-based contrast MRI exam. CT has great advantages over MR in terms of its widespread availability, speed of acquiring images, lower cost, and good spatial resolution. Additional advantages of CT are evaluating cortical bone and separating fat from soft tissue. Dental streak artifact is major disadvantage of CT in evaluation of the oral cavity, and it can be minimized with the angled scan parallel to the alveolus; on the other hand, MR has advantages in separating tumor from normal surrounding soft tissue and excluding bone marrow and laryngeal cartilage involvement [68–78, 89–94] (limited-moderate evidence). Disadvantages of MR include its limited availability, longer imaging time required, and higher cost. Patient's poor tolerance and long scan time result in motion artifact which limits the soft tissue distinction capability of MR [69].

Takashima et al. compared diagnostic performance of MR and CT in evaluation of SCCA tumor extension to surrounding normal structure in all subsites: seven oral cavities, two oropharynges, seven hypopharynges, and two larynges [68]. Sensitivity, specificity, and accuracy were 89 %, 100 %, and 92 %, respectively, for MR and 78 %, 75 %, and 77 % for CT. MR's superiority to CT in this study again owes to MR's better soft tissue discrimination between tumor, muscle, and non-ossified cartilage (limited evidence).

Suprahyoid Neck: SCCA

Held et al. conducted a prospective study to compare the diagnostic value of CT and MR in the evaluation of 473 patients with pharyngeal tumors (116 nasopharynx, 282 oropharynx, 39 hypopharynx) [69]. The differentiation of tumor from inflammation was best achieved with MR, while cortical bone infiltration and bony structure involvement at the skull base were best evaluated with CT (moderate evidence). For nasopharynx

tumors, detection and correct T tumor staging were achieved better with MR; 90 of the total 93 true tumors were correctly detected with MR while 13 of these cases were not detected by CT. For oropharynx tumors, 180 out of 282 tumors were correctly detected by CT but 31 tumors could not be detected by CT compared to 7 tumors by MR due to artifact. For hypopharynx, MR detected three tumors that were missed by CT but also had three false positive compared to one false positive by CT; both modalities had trouble with small superficial tumors but extent of tumor involvement was better appraised by MR. This study also demonstrated fast T2-weighted spin echo technique had advantage of shorter imaging time with less motion degradation and similar diagnostic information compared to conventional spin echo technique. Currently, fast spin echo and ultrafast gradient echo MR sequences have been introduced to replace conventional spin echo sequences to shorten imaging time with equal or superior lesion conspicuity (moderate evidence) [73, 74]. Utilization of fat suppression technique with contrast-enhanced T1 weighted sequence has further increased conspicuity of enhancing tumor by MR (moderate evidence) [75–78].

Wiener et al. assessed the accuracy of 16-slice multislice CT and 1.5 T MR in staging of 52 consecutive patients (mean age of 63) with oral SCCA [70]. MR demonstrated better tumor detection with sensitivity of 84.6 % compared to 69.2 % by CT. Regarding muscle infiltration, MR had higher sensitivity compared to CT (82 % vs. 73 %), but both modalities had low specificity and accuracy (63 % vs. 61 % and 67 % vs. 64 %, respectively). Regarding bone involvement, MR performed slightly better than CT with sensitivity, specificity, and accuracy of 100 %, 93 %, and 94 % versus 71 %, 96 %, and 92 %, respectively. For N-staging both methods failed to detect small metastasis. For T-staging MR was superior to CT, because there was a tendency to underestimate the tumor size by CT more often (19.4 % vs. 6.8 % by MRI). This retrospective study confirmed MR is modality of choice in evaluation of oral tumors with the current state of the art imaging technology (moderate evidence).

The authors also concluded that CT is a valid alternative imaging method. During the early era of CT and MR, Mukherji et al. found acceptable diagnostic performance of CT in predicting neurovascular invasion of oral cavity and tongue base SCCA in the retrospective study of 48 patients (88 % sensitivity, 83 % specificity) [79].

Van Kijek et al. investigated the frequency and extent that MR versus CT provided valuable diagnostic information, and whether this information influenced patient management in 33 patients (27 suprahyoid neoplasm with 7 parotid lesions, 2 thyroid, 2 parathyroid, and 2 larynx neoplasm) [71]. MR results in positive diagnostic and therapeutic outcome in all 14 patients (100 %) with benign tumors and in 16 patients (84 %) with malignancy. In 27 % of the cases, CT and MR had the same diagnostic and therapeutic impact. The improvement in diagnostic value of MR compared to CT was mainly due to MR's ability to distinguish tumor margins from adjacent tissue. This study is mostly applicable to SCCA and soft tissue neoplasms in the suprahyoid location and in the parotid glands (limited-moderate evidence).

MR's ability to discriminate a tumor from adjacent normal soft tissue has an important impact on diagnosis and therapeutic approach (limited-moderate evidence). Tang et al. published findings in 924 cases of nasopharyngeal carcinoma in 2010 to demonstrate the important prognostic value of anatomic masticator space tumor involvement by MR imaging findings (moderate evidence) [80]. Because American Joint Committee on Cancer (AJCC) staging system for nasopharyngeal carcinoma defines masticator space involvement (T4 disease) as an "extension of tumor beyond the anterior surface of the lateral pterygoid muscle, or lateral extension beyond the posterolateral wall of the maxillary antrum and the pterygomaxillary fissure," the involvement of the medial and lateral pterygoid muscle defined by anatomic masticator space is not classified as T4 disease. In other words, an extensive tumor infiltration of the anatomic masticator space is needed to meet T4 stage according to the AJCC criteria. Using MR findings, the authors demonstrated anatomic masticator space involvement was an independent prognostic factor for overall survival, associated with decrease in local relapse-free survival without effect on distant metastasis-free survival. Also, there were no statistically significant differences between different degrees of anatomic masticator space involvement with regard to overall survival and local relapse-free survival, or between T3 or T4 disease and anatomic masticator space involvement with regard to overall survival and local relapse-free survival. Therefore, they recommend classification of anatomic masticator space medial and lateral pterygoid muscle involvement as stage T4 disease.

To assist surgical planning, Hsu et al. found that the reservation of fat plane between the tumor and prevertebral musculature evident on MR in 40 patients with T3-T4 pharyngeal and laryngeal cancer is accurate in predicting absence of prevertebral space tumor fixation with negative predictive value of 97 % (limited-moderate evidence) [81]. Eisen et al. assessed the accuracy of preoperative CT and MR in evaluation of orbital invasion in a retrospective study of 25 patients with tumors of paranasal sinuses, anterior cranial base, and skin around the orbit [82]. They found no one criterion was >79 % accurate in predicting orbital invasion. A tumor adjacent to the periorbita was the most sensitive predictor of orbital invasion (90 %) for both CT and MRI but suffered from low specificity (29 % MR and 44 % CT). A nodular as opposed to a smooth interface of the tumor with the periorbita has relatively low specificity for orbital invasion (71 % MR and 78 % CT) with a low positive predictive value of 75 %. The highest positive predictive values were extraocular muscle involvement (enlargement, signal change, and enhancement) on MRI (100 %) and orbital fat obliteration (80 % MRI, 86 % CT). Extraocular muscle displacement and enhancement were less accurate (<65 %) predictors. Six or more positive criteria predicted invasion with 67 % sensitivity, 80 % specificity, and accuracy of 72 %. The authors concluded preoperative imaging can aid in surgical planning but it should not replace intraoperative assessment in ambiguous cases of orbital invasion.

For therapeutic and prognostic implication, gross tumor volume at the primary site, as derived from pretreatment CT findings, has been shown to predict local control of SCCA at different head and neck subsites treated with nonsurgical organ reservation. Local recurrence is more likely with large tumors than with small lesions in the same anatomic subsite, and gross tumor volume is often more strongly associated with local control than is tumor stage [83, 84].

Infrahyoid Neck: Laryngeal SCCA

Because the important prognostic indicator and treatment strategy in laryngeal cancer depends greatly on fine detail evaluation of each subsite for tumor involvement, CT is the preferred initial imaging choice for evaluation of the laryngeal SCCA because of its high spatial resolution, ultrafast imaging time with less motion artifact, and lower cost (moderate evidence) [85, 86]. MR has better soft tissue detail compared to CT, but this advantage can be obviated by its long imaging time prone to image degradation by patient's motion. CT and MR have reported high sensitivity and specificity of approximately 90 % in the evaluation of SCCA pre-epiglottic space invasion [87–89]. Both MR and CT also have 93–95 % sensitivity but only up to 75 % specificity for paraglottic extension, as a result of overestimated tumor involvement due to peri-tumoral inflammation.

Both CT and MR have high negative predictive value for excluding cartilaginous involvement [90]. Becker et al. evaluated criteria for tumor invasion of laryngeal cartilage by CT, and found no single criterion offers both sensitivity and specificity over 70 % [91]. When combining CT findings of cartilage sclerosis, cartilage erosion or lysis, and extralaryngeal tumor, CT has overall sensitivity of 91 % and negative predictive value of 95 % for detection of cartilaginous tumor involvement (moderate evidence). However, diagnostic performance of each criterion varies greatly among cartilages. Sclerosis has most overall sensitivity of 83 % but low specificity of 40 % for thyroid cartilage, 76 % for cricoid cartilage, and 79 % for arytenoid cartilage. Overall specificity for cartilage erosion and lysis is 93 % and extralaryngeal tumor is 95 % with low specificity of 71 % and 44 %, respectively. A recent prospective comparative study demonstrated that a combination of negative CT finding of sclerosis of cricoarytenoid unit and normal vocal fold mobility is the most useful indicator of tumor-free cricoarytenoid unit with a high accuracy of 96.6 %, and sclerosis of cricoarytenoid unit has positive predictive value for tumor involvement of 75 %; compared to CT, MR has higher sensitivity at the cost of lower specificity in excluding laryngeal cartilage invasion but it is valuable in equivocal cases by CT and clinical evaluation to exclude neoplastic involvement of the cartilage (moderate evidence) [91–94]. To improve MR imaging performance in distinguishing neoplastic involvement from inflammatory involvement of the laryngeal cartilages, Becker and colleagues proposed new criteria, including: (1) T2-weighted or postcontrast T1-weighted cartilage signal intensity greater than that of the adjacent tumor indicated inflammation; and (2) signal intensity similar to that of the adjacent tumor indicated neoplastic invasion [94]. The proposed new diagnostic criteria improved MR specificity to 82 % from 74 % with statistical significance (moderate evidence).

Sinonasal Inflammatory Disease and Neoplasm

CT is the "gold standard" in the primary imaging of inflammatory sinonasal lesions owing to its superior demonstration of bony anatomy and pneumatization variants, sclerotic or destructive bone change, and the extent of the disease. CT fusion has been widely used for intraoperative navigation in functional endoscopic sinus surgery [95–98]. CT has major limitations in the differentiation of soft tissue density of mucosal disease from neoplasm, for which MR is complementary with its superior soft tissue characterization and evaluation of cranial compartment [99–101]. The varying degree of viscosity of sinonasal secretion, aeration, and paramagnetic properties of fungal elements and intrasinus hemorrhage has shown to account for variation in MRI signals and for which CT is complementary [102]. In a small

retrospective study of 14 patients, Som et al. demonstrated the differences in MR signal intensity which help to distinguish benign from neoplastic lesions that eroded through the skull base [103]. All seven neoplasms demonstrated homogenous low to intermediate signal intensity due to their high cellularity, whereas seven benign lesions had variable degrees of nonhomogenous signal intensity due to varying degrees of water and protein contents of the secretion. Lanzieri et al. retrospectively evaluated the diagnostic performance of CT and MR in evaluation of mucoceles and sinonasal neoplasms of 41 patients with clinical suspicion of these pathologies [104]. CT evaluated the sinus expansion versus destruction as criteria for mucocele or neoplasm. MR signal of tumors was intermediate on both T1 and T2 weighted sequences and mucoceles typically demonstrated T2 hyperintensity. Thin regular rim enhancement signified mucocele, while solid enhancement was considered neoplasm. CT and noncontrast MR had poor specificity of 65 % for detecting mucocele with sensitivity of 87 % for CT versus 79 % for MR, and both had specificity ranges of 79–87 % with poor sensitivity up to 65 % for detecting neoplasm alone or coexisting with mucocele. Contrast-enhanced MR improved specificity and sensitivity up to 86–95 % and 83–95 %, respectively, for all lesions.

These early studies provided limited evidence for currently widely accepted standard practice of utilizing both CT and MR for presurgical evaluation of sinonasal masses [99–105]. The main role of imaging in this setting is to map the extent of the disease for treatment planning even though attempts have been made to distinguish benign from malignant lesions by analyzing the imaging features of the lesions. For example, Jeon et al. retrospectively reevaluated the MR imaging feature to distinguish inverted papilloma (IP) from malignant sinonasal tumor [106]. They found the convoluted cerebriform pattern of the lesions was demonstrated in all 30 (100 %) of the IPs and 17 (13 %) of the 128 malignant tumors. There was a significant statistical difference in the prevalence of the convoluted cerebriform pattern between IP and malignancy with the overall

sensitivity, specificity, negative predictive value, and accuracy 100 %, 87 %, 100 %, and 89 %, respectively. However, the positive predictive value was low of 64 %, reflecting imperfection of this imaging feature for imaging diagnosis of IPs because it can also be seen in various malignant lesions and concomitant SCCA in an IP can only be excluded by histology.

Palpable Salivary Gland Masses

Salivary gland pathologies can present as painful or painless palpable neck mass. Clinically apparent painful acute phase of sialadenitis is routinely not imaged unless deep abscess is a clinical concern, and once the acute phase of inflammation subsides, imaging is performed to identify a treatable cause. Because of CT advantages of identifying calcification, it is the modality of choice in evaluating sialolithiasis. Casselman et al. prospectively compared MR and CT imaging in 21 patients with salivary gland lesions, assessing whether the lesions are intrinsic to the parotid gland and its relationship with the plane of the facial nerve, and its aggressiveness [107]. In all cases, CT and MR provided same diagnostic information and CT is superior to MR in four cases of inflammatory masses because of depiction of calcification/stone.

Sumi et al. compared noncontrast MR imaging features (conventional T1-weighted, fat suppressed fast spin echo T2-weighted, and short inversion time–inversion recovery sequences) with clinical symptoms, histopathologic features of excised glands, and CT imaging features in 16 patients with sialolithiasis of the submandibular gland [108]. CT features of the glands correlated well with MR imaging features and CT better demonstrated calculi. They found three types of glandular changes: type I glands (56 %) were positive for clinical symptoms and MR imaging abnormalities (T1 hypointensity, T2 hyperintensity, 44 % enlargement), and were characterized histopathologically by active inflammation; type II glands (25 %) were negative for clinical symptoms and positive for MR imaging abnormalities (T1 hyperintensity and atrophy), and the glands were replaced by fat; type III glands (19 %) were negative for both

clinical symptoms and MR imaging abnormalities.

Several prospective studies compared MR sialography to the gold standard digital sialography, demonstrating high diagnostic performance of MR sialography [109–111]. Jager et al. compared diagnostic performance of MR sialography with evoked salivation to US using digital sialography as the gold standard, utilizing T2-weighted three-dimensional constructive interference in steady-state (3D CISS) in 24 patients suspected of having sialolithiasis [109]. They found MR sialography was significantly superior to US for demonstrating the submandibular ductal system with the sensitivity and specificity of 80 % and 100 %, respectively, for CISS sequence versus both of 80 % for US. Kalinowski et al. prospectively compared MR sialography to digital subtraction sialography in evaluating salivary glands in 80 patients with clinically suspected diagnoses of sialadenitis and/or sialolithiasis [110]. MR sialography was obtained with a T2-weighted single-shot turbo spin-echo sequence. Eighty-one salivary glands (48 parotid glands, 33 submandibular glands) in 65 patients were successfully visualized with both modalities. Digital subtraction sialography achieved higher spatial resolution with depiction up to third-order branches of the ductal system by digital sialography compared to visualization of the main ductal system to first- and second-order branches by MR sialography. The invasive technique of digital subtraction sialography had a substantial procedural failure rate of 14 % compared to 5 % for MR sialography. Sensitivity and specificity to diagnose chronic sialadenitis were 70 % and 98 % with MR and 96 % and 100 % with digital subtraction sialography. MR sialography enabled diagnosis of sialolithiasis with a sensitivity of 80 % and a specificity of 98 % versus 90 % and 98 % for each with digital subtraction sialography. As a result, invasive digital sialography has been partially replaced by MR sialography.

Salivary gland neoplasms present a challenge to clinical assessment and imaging diagnosis to distinguish benign and malignant lesions. Warthin's tumor and oncocytoma demonstrated

accumulate Tc99m pertechnetate, which adds diagnostic value in management of these lesions [112]. Urquhart et al. prospectively compared clinical and CT assessments of tumor size, location, density, and malignancy in 32 consecutive patients who underwent evaluation for parotidectomies [113]. They confirmed routine preoperative imaging resulted in the discovery of details not revealed on clinical examination which guide surgical management (precise location, tumor density and margin, and detection of additional tumors). However, only half of preoperative diagnosis of pleomorphic adenoma was confirmed with final pathology and one lymphoma and one benign lesion were incorrectly classified preoperatively.

Even though MR and CT are comparable, MR provided precise soft tissue tumor delineation and depiction of perineural spread [107, 114, 115]. Kakimoto et al. compared CT and MR detectability and tumor margin and capsule of 50 pleomorphic adenomas [116]. The tumor detectabilities were 90 % on axial CECT images and range from 85 % to 88 % on axial MR images (best with T2 weighted sequence). On both modalities, pleomorphic adenoma had well-defined margin, an inhomogeneous aspect, slightly high enhancement and either an inhomogeneous or a periphery enhancement. However, the capsule could be hardly detected with CT but well demonstrated with MR with a lobular border and high contrast. The authors concluded the pleomorphic adenomas should be evaluated with MR (limited evidence). Early work by Som and Freling et al. demonstrated the infiltrative margin of the parotid lesions on MR has positive predictive value for aggressive neoplasm and is useful in delineating malignant tumors but is unreliable in correctly predicting the histologic nature, and the lack of this imaging feature does not exclude malignancy [117, 118]. Freling et al. retrospectively reviewed MR imaging features of the parotid lesions in 116 patients with 86 benign disease and 30 malignant tumors, using turbo spin-echo T1- and T2-weighted sequences [118]. Tumor margins, homogeneity, or signal intensity were not discriminative factors to correctly predict benign or malignant disease.

Infiltration into deep structures (parapharyngeal space, muscles, and bone) was observed only in malignant tumors. Infiltration into subcutaneous fat was noticed in malignant as well as in inflammatory disease. No statistically significant correlation was found between tumor grade and MR imaging features in malignant disease (moderate evidence).

In 2011, Christe et al. reassessed the discriminators for benign and malignant parotid lesions using current state of the art conventional MR imaging technique (turbo inversion-recovery magnitude T2, turbo spin-echo TSE T1 and T2, and post contrast TSE T1 with fat saturation) in 84 consecutive patients who underwent MR imaging prospectively before surgery. They retrospectively analyzed imaging features and correlated them to the final histology [119]. They evaluated various MR imaging features including lesion signal intensity, contrast enhancement, margins (well-defined or ill-defined), location (deep and superficial lobe), growth pattern (focal, multifocal, or diffuse), and extension into neighboring structures, perineural spread, and lymphadenopathy. They found that statistically significant signs predictive of malignancy were T2 hypointensity, ill-defined margins, diffuse growth, infiltration of subcutaneous tissue, and lymphadenopathy (moderate evidence). The highest accuracies for prediction of malignant tumors were found for perineural spread and subcutaneous tissue infiltration (both 74 %, with high specificities of 100 % and 93 %, respectively but low sensitivities of 19 % and 33 %, respectively). Ill-defined borders were significantly better seen after contrast administration and had an accuracy of 73 % with specificity of 79 % and sensitivity of 59 %. Accuracy of low SI on T2-weighted images was 70 %. The tumor volume and patient age did not significantly correlate with benignity and cystic/necrotic areas did not help distinguish malignant from benign tumors.

Recently, several retrospective studies, studying the use of diffusion-weighted imaging and dynamic contrast-enhanced MR to distinguish pleomorphic adenoma and Warthin's tumor from other neoplasms, are promising. However, the overlaps of time signal intensity curve and ADC values between lesions and potential result reproducibility issue with these labor intensive technique and variability of software applications are the shortcomings of these results [120–123]. King et al. investigated parotid lesions using proton MR spectroscopy in 56 patients [124]. In this study, spectroscopy can be performed only in tumors that are larger than 1 cm^3 in size, and even within this group, the Cho/Cr ratios can be obtained in less than half of these tumors. However, the study showed promising results with statistical significant differences in the ratios of Warthin tumors, pleomorphic adenomas and malignant tumors (moderate evidence). By using Cho/Cr ratios at an echo time of 136 ms, their results suggest that a ratio greater than 2.4 may be used to distinguish between benign and malignant tumors, while a ratio greater than 4.5 suggests that the lesion is probably a Warthin tumor.

Several studies attempted to identify sonographic features distinguishing the histology of salivary gland neoplasm without reliable diagnostic performance result (moderate evidence). Dumitriu et al. found the most specific feature of pleomorphic adenoma is a lobulated and well-defined contour [124]. In the absence of this, neither the internal structure, or the vascularization or the sonoelastographic aspect can identify a pleomorphic adenoma for certain. Bhatia investigated lesions in terms of relative stiffness and concluded that sonoelastography seems to have little benefit in the benign-malignant differential diagnosis in salivary gland tumors [125].

Even though a combination of imaging modalities can provide a correct diagnosis, the exact tumor histology of the salivary gland lesions still cannot be certain in equivocal imaging features [126, 127]. US FNA further assists clinical decision for appropriate management of salivary gland lesion with moderate evidence [128–131]. Sharma et al. retrospectively studied the value of US FNA of parotid lesion prior to surgery [128]. A diagnostically adequate biopsy specimen was obtained in 48 of the 52 cases (92 %). Among the 20 patients who underwent surgical intervention

after diagnostic US-guided FNA findings, results of surgical-pathological analysis helped confirm the cytology diagnosis in 95 % of the cases; thus, 40 % of patients were spared surgical intervention on the basis of findings from US-guided FNA. Similarly, Taylor et al. reported the accuracy, sensitivity, and specificity of FNA cytology of submandibular gland masses were 88.0 %, 71.4 %, and 94.4 %, respectively [129]. Inohara et al. retrospectively compare MR evaluation and US FNA evaluation in 81 patients with parotid mass lesions (60 benign and 21 malignant) [131]. They reached the same conclusion that unsharp margins and infiltration into adjacent tissues on MR significantly correlated with a malignant histology. Because the sensitivity, specificity, and accuracy of US FNA cytology (FNAC) and MR were 90 %, 9.5 %, and 94 %, and 81 %, 92 %, and 89 %, respectively, either FNAC or MR served equally to predict the malignant nature of parotid mass lesions. They further assessed the added values of combined FNAC and MR and found no diagnostic advantage of the combination over either modality alone. Because the accuracy of FNAC is higher than MR (accurate histological typing rates of 80 % for benign and 62 % for malignant lesions, respectively), they suggested US FNA be the diagnostic modality of first choice for characterization of parotid mass lesions, while MR should be reserved until there is indication for surgical intervention.

The false negative of US FNAC poses a challenge to clinical decision whether to observe or to surgically remove a salivary gland lesion. Cho et al. conducted a retrospective study to evaluate the diagnostic accuracy of US FNA of 245 major salivary gland tumors (244 patients) [132]. Of 88 % of the patients with adequate cytology results by FNA, the overall sensitivity, specificity, and accuracy in differentiating malignant from benign tumors was 75.7 %, 100 %, and 95.8 %, respectively, but the false-negative was 4.2 %, with no false-positive diagnoses of malignancy. Only 59.6 % (28 of 47 malignancies) were detected preoperatively by FNAC. Colleta et al. conducted a systematic review of FNAC on salivary gland lesions to assess diagnostic performance of FNA cytology [133]. Of 484 patients receiving a histological diagnosis of malignant tumor, cytological diagnosis was concordant in 80 % and discordant in 20 %. Of 1,275 patients who received a histological diagnosis of benign tumor, cytological diagnosis was concordant in 95.6 % and discordant in 4.4 %. Of 154 patients received a histological diagnosis of nonneoplastic lesion, cytological diagnosis was concordant in 94 % and discordant in 5.8 % of the cases. Therefore, the negative or nondiagnostic cytologic FNA should not be viewed as benignity and management decision should include careful imaging feature assessment and clinical examination (moderate evidence).

US FNA of a Palpable Neck Mass

The National Institute of Clinical Excellence guidance on cancer services in the United Kingdom advocated that diagnostic clinics staffed by a surgeon and a pathologist should be established for patients with neck lumps because of US FNA's high accuracy and least invasive tool for tissue diagnosis of a palpable suspicious neck mass [10]. However, its utilization is highly operator dependent and time consuming. Increased operative experience and cytopathologist expertise improve US guided FNA outcome. A meta-analysis of moderate to limited evidence studies reveals 89.6 % sensitivity, 96.5 % specificity, and 93 % accuracy of US FNA [134].

Evaluation of a Palpable Thyroid Nodule

Thyroid ultrasound provides excellent anatomic detail regarding nodule architecture and assessing for regional lymph node metastases. Features of suspicious nodules include marked hypoechogenicity, complete solid consistency, intranodular vascularity, irregular infiltrative margins, microcalcifications, coarse calcifications, and shape that is taller than wide [135]. Intranodular vascularity is helpful if noted in combination with another feature [135, 136]. These features have relatively high specificity for detecting papillary thyroid carcinoma, the most common type of thyroid malignancy, but are less predictive of follicular thyroid

malignancies that have overlapping features with benign adenomas and hyperplasic nodules. Recent studies by the Moon and Bonavita groups address the benign ultrasound features of thyroid lesions. Features that are highly predictive of benignity are spongiform with 99.7–100 % specificity, cystic with colloid nodules, and diffusely hyperechoic [135, 137]. Sonography serves as an important step in evaluating which nodules should undergo FNA, but cytopathologic evaluation of a thyroid nodule is usually required before a patient undergoes surgical resection for a possible thyroid malignancy [16, 62, 138]. Importantly, sonography is an excellent imaging tool to identify metastatic cervical lymphadenopathy and can be used to sample suspicious nodes prior to surgery [62].

Malignancy rates for focal hypermetabolic lesions in the thyroid detected on FDG-PET scans range from 14 % to 47 % [62]. Published data in a series from Memorial Sloan-Kettering Cancer Center suggests that FEG-PET-detected thyroid cancers tend to be more aggressive with 50 % comprising aggressive variants including tall cell, insular, or Hurthle cell tumors [139, 140].

Thyroid scintigraphy is only indicated for patients with suppressed TSH to determine if one or more nodules are functioning since nodules with uniform uptake on I-123 scans are considered benign and do not require FNA [62]. Most thyroid nodules are benign and most thyroid nodules will not function on I-123 scan. Therefore, the exam will not serve to differentiate malignant nodules form benign ones. Whole body radioactive iodine scintigraphy with 1–131 plays an important role in radioactive ablation iodine treatment and surveillance of differentiated thyroid cancer in those with iodine-avid metastases [141]. Several prospective studies have found PET scanning to be useful for detection of metastatic disease in some patients with more dedifferentiated non-iodine-avid thyroid tumors with sensitivity between 69 % and 100 % and a positive predictive value of 82–92 %. Therefore, PET is complementary to anatomical imaging in identifying metastatic disease in this particular group of patients (moderate evidence).

Special Case: Infectious Lymphadenopathy and Neck Infection

Summary

Reactive cervical adenitis due to viral infection and uncomplicated upper respiratory infection does not require imaging and reassessment after appropriate treatment is standard of care for these common infections. However, when DNI or atypical infections that are unresponsive to empiric treatment are suspected clinically, diagnostic imaging is indicated to define the extent of disease and subsequently guide medical or surgical management (moderate evidence). US is limited to evaluation of superficial infection and is more commonly used in pediatric population in order to limit radiation exposure. CECT in conjunction with clinical examination provides relatively high accuracy (88–89 %), sensitivity (95 %), and specificity (80 %) for identifying drainable abscesses (moderate evidence). Its advantage of fast imaging time is critical in imaging sick patients with potential airway compromise (limited evidence). Both CECT and US can provide image-guidance for aspiration (moderate evidence). MR is not practical due to long scanning time and is only indicated for skull base and intracranial involvement (limited-moderate evidence).

Supporting Evidence

As previously discussed in the section on "Who Should Undergo Imaging for Palpable Neck Mass?" several retrospective series provided the limited-moderate evidences supporting conservative management for clinically obvious reactive adenitis without the need for additional imaging workup [6, 9, 10, 28, 29].

In pediatric patients, radiation exposure associated with CT is a major concern. Recent literature comparing diagnostic performance of US to CT in evaluation of infectious inflammatory neck mass in children is sparse. Availability of CT and operator dependent limitation of US result in less utilization of US in the United States compared to Europe and Asia. Rozovsky et al. retrospectively reviewed 210 pediatric patients (mean age 4.5 years) presented to their institution from

2005 to 2008 with acute inflammatory neck mass, who underwent diagnostic neck US (with Doppler) and CT to assess clinical and radiological findings and imaging impact on management [142]. In 185 patients undergoing US only, US provided sufficient information in 99.5 % of the patients, resulting in fluid collection drainage in 17 patients and conservative medical management in 164 patients. In 25 patients undergoing both US and CT, CT provided additional information in 4 of 25 patients (airways compromise in 2 and collections in 2). The author concluded that US provided sufficient information about the nature, location, and extent of the inflammatory masses in 97.6 % of the patients, suggesting it should be the main, and generally single, imaging technique in these patients. CT should be reserved for patients with an aggravating clinical course and suspicion of deep neck infection or airways compromise (moderate evidence). Meyer et al. conducted a retrospective study of 179 children to identify clinical factors that may limit the use of CT scans in the initial assessment of neck infections, and thereby improve patient management by preventing unnecessary testing, limiting radiation exposure, and decreasing cost [143]. In this series, neck and facial swelling were reported symptoms in 28.2 % of patients and physical exam revealed swelling in 43 % and cervical lymphadenopathy in 41 %. CECT reported abscesses (defined as rim enhancing hypoattenuation collections) in 61.1 % of children, without statistically significant difference in the rate of abscess on CT between children with less than 48 h of localizing symptoms and 48 or more hours of symptoms (58.1 % and 58.3 %, respectively). Furthermore, there was no significant difference in age, gender, C-reactive protein levels, disease location, or length of stay between children with and without abscess on CT. White blood cell counts were significantly higher in the abscess group; however, the median white blood cell count in both groups was above normal. Because of the lack of reliable clinical predictors for neck abscess, it is appropriate to obtain a CT scan upon presentation in all children with symptoms concerning for neck abscess (moderate evidence).

CECT has high sensitivity (80–100 %) for evaluation of full extent of infection compared to clinical examination (moderate evidence). The 2004 retrospective study by Crespo et al. provided limited evidence to support the use of CECT for DNI in adults [25]. When comparing clinical examination to CECT evaluation in the diagnosis and management of DNI, they found clinical assessment underestimated the extent of deep space involvement in 70 % of patients, especially the parapharyngeal space which is difficult to inspect and palpate clinically. CECT also aided in selection of appropriate surgical approach for drainage. Courtney's et al. retrospective study in 2006 showed accuracy of clinical assessment for lateral neck infection in 205 children was poor (28 % sensitivity, 92 % specificity) [144]. Similarly, Nagy et al. retrospectively studied of 47 children with retropharyngeal and parapharyngeal abscesses and found no significant differences in the clinical presentation of children with abscesses and those with a cellulitis or early abscess even though children with confirmed abscesses were more often febrile (89 % versus 79 %) and presented with greater cervical adenopathy or neck masses (94 % vs. 76 %) [145].

However, US and CECT, especially when performed alone without clinical input, demonstrated a wide range of relatively low diagnostic performance in identifying purulent material that may need surgical drainage, as summarized in Table 38.3. Therefore, the surgical drainage of the collection indentified by imaging remains a clinical decision [26, 144–151].

The prospective blinded comparison of clinical examination and CECT in DNI conducted by Miller et al. in 1999 provided the strong evidence that CECT and clinical examination are both critical components in the evaluation of suspected DNI and contributed to the wide use of CECT in evaluation and management of DNI [26]. Thirty-five consecutive adults with suspected DNI were prospectively assessed by clinical examination and CECT for the presence and extent of surgically drainable purulent collections. Final outcome (the presence of a purulent collection) was determined at surgery

or in long-term follow-up. They found overall poor diagnostic performance of clinical examination alone and CECT alone in identifying drainable collection with 63 % accuracy, 55 % sensitivity, and 73 % specificity for clinical examination and 77 % accuracy, higher 95 % sensitivity, but lower 53 % specificity for CECT. When CECT and clinical examination were combined, the accuracy became more acceptable at 89 %, with 95 % sensitivity and 80 % specificity. In pediatric patient populations, the relatively poor accuracy and specificity of diagnostic studies for identifying abscesses are due to variable utilization of US and CECT with the lack of clearly defined and uniform radiological criteria and clinical input and management algorithm (limited-moderate evidence).

A growing body of literature advocates conservative medical management utilizing imaging at initial assessment of DNI and reserves surgical drainage for clinically apparent air way compromise and for salvage therapy as needed. Nagy et al. found CECT provided valuable information regarding the drainable collection's size and location in relationship with great vessels for its safe and successful transoral drainage [145]. The group that responded to medical management had a significantly smaller abscess size than the group requiring late surgical intervention (1.5–2 cm^3 vs. 4.3–5.38 cm^3) [150, 152, 153].

Surgical planning with CECT is advocated by Oh et al. in their published 2005 prospective study of 34 patients (age range of 6–81 years, mean age 35.8 years) with parapharyngeal abscesses (strong-moderate evidence) [154]. All patients were treated with empiric intravenous antibiotics and had CECT to stratify treatment plan. They used CECT to detect an abscess, which is defined as low density collection with enhancing rim, and 18 abscesses in the prestyloid compartment were drained transorally and one poststyloid abscess was drained transcervically. Of all 19 drained collections, 15 had positive culture, suggestive of high accuracy and specificity of CECT for identifying abscesses. Scaglione et al. prospectively correlated CECT findings with clinical assessment, management, and outcome of descending necrotizing mediastinitis in

32 consecutive adult patients [60]. In 10 patients without abnormality on CECT, all were treated conservatively with uneventful clinical course. In 12 patients, CECT showed fluid collections, fasciitis, cellulitis, and myositis of the neck spaces, for which 10 received cervical drainage, regardless of the kind of infection (cellulitis and/or fluid collections), with 2 death from rapid spread to mediastinum. In the remaining 10 patients, CECT revealed infection spreading down to the mediastinum with mediastinal cellulitis and fluid collections, pleural and pericardial effusions. All of these patients had both cervical and mediastinal drainages with 6 deaths and 4 survivals. Additional findings include jugular vein thrombosis and lymphadenopathy. The authors concluded that the extent of the infection detected by CT is more crucial than the kind of infection from the therapeutic and prognostic point of view. Thus, early use of CT is a valuable guide to plan the optimal management approach and efficient surgical drainage (strong-moderate evidence).

Granulomatous cervical adenitis in adults in developing countries, such as India, is predominantly *Mycobacterium tuberculosis*, which commonly presents as multiple lymphadenopathy, suppuration with or without abscess, and little to no constitutional symptoms (5 % fever, 8 % weight loss, 15 % pain-tenderness) [32, 155]. Non-tuberculous mycobacteria (*Mycobacterium avium*-intracellulare, *Mycobacterium scrofulaceum*, and *Mycobacterium kansasii*) are more common in children and typically presented as enlarging non-tender neck mass unresponsive to conventional antibiotics [52–54]. Therefore, granulomatous cervical adenitis can mimic a neoplastic process. Joo et al. conducted a well-designed retrospective review of consecutive 52 adults with tuberculous cervical adenitis to assess treatment response using CECT [156]. They reported lymph node volume and ratio of necrotic area could predict response to medical treatment; the cut-off value for the volume and ratio of necrotic area of tuberculous cervical adenitis was 44.15 cm^3 (sensitivity: 88.2 %, specificity: 74.3 %) and 0.36 (sensitivity: 70.6 %, specificity: 71.4 %).

Special Case: Lymphoma

Summary

Overall incidence of lymphoma has been stable since 1998 and death rates have been decreasing due to advancement in treatments. 18-F-fluorodeoxyglucose–positron emission tomography (FDG-PET), and subsequently PET-CT, has established its role as the most sensitive and specific for staging and restaging of FDG-avid lymphoma subtypes such as Hodgkin's lymphoma (HL), diffuse large B-cell NHL (DLBCL), and follicular NHL (FL) (moderate-strong evidence). The changes in staging by PET occur in about 15–30 % of these patients and result in fewer than 15 % of changes in treatment, yet there is no evidence for improvement in outcome (moderate evidence). The strongest evidence supporting PET is as posttreatment restaging HL and DLBCL where persistent disease generally warrants intervention to achieve cure (moderate-strong evidence). For generally incurable lymphomas such as FL and chronic lymphocytic lymphoma (CLL), progression-free and overall survival is generally more important (moderate evidence).

There are insufficient evidences supporting the routine use of FDG-PET for other NHL subtypes with variable FDG avidity. For non-FDG-avid lymphomas such as extranodal marginal zone lymphoma (MZL, also known as mucosal associated lymphoid tissue MALT lymphoma, third most common type of NHL), contrast-enhanced CT (CECT) remains imaging of choice (moderate evidence).

A number of variables in published studies assessing the role of FDG-PET in mid-treatment response (timing of the interim PET during treatment cycles, investigational treatment protocols, methodological problems, diverse studied populations, tumor histologies, stages and PET vendors, and interpretation) render generalization of these findings in clinical practice difficult. There are conflicting reports of the usefulness of interim PET for outcome prediction and only limited data demonstrate that treatment change on the basis of PET finding improves survival. Therefore, FDG-PET use during treatment should only be performed as part of clinical trials until its impact on prognostic indication and altering treatments can be confirmed (moderate-strong evidence).

FDG-PET during surveillance detects 10 % clinically occult relapse, while 80 % of relapse are suspected clinically (moderate evidence).

PET/CT is not cost-effective for posttreatment surveillance for HL patients in remission, and CECT is recommended as surveillance tool (moderate evidence). Risk stratification is suggested for utilizing PET/CT for surveillance in DLBCL in complete remission (moderate evidence). Cost saving is suggested when incorporating PET/CT in assessment of residual disease of HL after first-line therapy (moderate evidence). A few studies suggest omitting CECT when staging with PET-CT and no need for full diagnostic high-dose CT with PET-CT to decrease radiation exposure (limited evidence).

Supporting Evidence

Both HL and NHL have many histology subtypes and clinical behaviors from indolent to aggressive malignant with variable treatment response from curable to incurable, resulting in several standard treatment protocols as well as numerous on-going clinical trials. Comprehensive oncologic review of lymphoma is beyond the scope of this chapter; however, the following brief review is necessary to appreciate the complexity of the appropriate imaging strategies for lymphoma. Currently, a combination of clinical staging, tumor cell biology, and prognostic indicators predicts the overall survival of each lymphoma subtype and guides the initial treatments and second-line therapies for primary refractory, progressive, and relapsed disease. The treatment protocols employ chemotherapy with or without radiation with tailored treatment schedules and dose intensity to achieve remission, progression-free interval, and overall survival with minimal toxicity and long-term complication [157, 158].

The Ann Arbor staging classification with Cotswold modification is used for staging of HL and NHL, assessing the number of nodal and extranodal tumor sites, tumor locations above or below the diaphragm, tumor bulk, and associated

B symptoms (fever, night sweats, and weight loss) [159]. Prognostic indicators add accuracy to predicting long-term survival and treatment response and have been developed for each subtype. Broadly speaking, prognostic indicators incorporate patient's age, sex and performance status, and laboratory evaluations (ESR, LDH, albumin, hemoglobin, white blood count, and lymphocyte count) to the Ann Arbor staging system. European Organization for the Research and Treatment of Cancer (EORTC) and the German Hodgkin Study Group (GHSG) favorable and unfavorable prognostic factors are used for stage I-II HL; International Prognostic Score are used for advanced stage III-IV HL, International Prognostic Index (IPI) and its variants (such as follicular lymphoma IPI) for NHL; HL has about 80–90 % curable rate even after recurrence and relapse, and the first-line treatment is chemotherapy followed by field irradiation for stage I-II and chemotherapy for stage III-IV with or without consolidative radiation [157–167]. Varieties of chemo regimens with or without radiation, rituximab and interferon are used for spectrum of NHL, depending on histology, stage, and prognostic index with extended course for higher stages. Patient with a relapse or progressive, resistant disease may be candidates for second-line therapies such as different agents or higher dose of chemotherapy, autologous hematopoietic cell rescue, and autologous hematopoietic stem cell transplantation [168–171].

References for assessment of treatment response include histology confirmation, clinical and radiological follow up [172–174]. The complexity of this disease presents a tremendous challenge to unify the imaging strategy with high diagnostic performance and cost-effectiveness in staging and restaging. Whole body evaluation is necessary to stage lymphoma using Ann Arbor staging system, therefore the reported diagnostic performance of imaging for lymphoma is for whole body imaging and not for head and neck imaging alone. CT was incorporated with the Cotswolds staging recommendation for HL in 1989 and International Working Group response criteria for NHL in 1999 [159, 172]. FDG-PET, currently PET-CT, has emerged as the imaging choice for FDG-avid lymphoma with consistently higher diagnostic performance than CT in staging and restaging. PET should only be considered after histologic confirmation of lymphoma because a variety of inflammatory/infectious and other neoplastic processes are also FDG-avid. To standardize performing and interpreting PET imaging for treatment response assessment in lymphoma, the imaging subcommittee of International Harmonization Project in Lymphoma developed consensus recommendations based on published literature and the collective expertise of its members in the use of PET in lymphoma in 2007 [173, 174]. In summary, restaging FDG-PET should be performed preferentially 6–12 weeks after completion of therapy. Visual assessment alone is adequate for interpreting PET findings as positive or negative. Mediastinal blood pool activity should be used as the reference background activity to define PET positivity for a residual mass ≥ 2 cm in greatest transverse diameter, regardless of its location; smaller residual mass or ≤ 1 cm in diameter lymph node should be considered positive if its activity is above that of the surrounding background. Use of PET for treatment monitoring during a course of therapy should only be done in a clinical trial or as part of a prospective registry. These recommendations are based on the consensus opinions of experts on the field as well as published literature with moderate and strong evidences of high diagnostic performance of CT, subsequently PET and PET/CT in staging of lymphoma with consistently higher sensitivity and specificity of PET and PET/CT compared to CT, especially in restaging.

FDG-PET for Lymphoma Staging and Restaging

FDG avidity is the key factor for diagnostic yield of FDG-PET for evaluation of neoplasm. Weiler-Sagie et al. retrospectively investigated FDG avidity of various types of lymphoma evident on initial staging FDG-PET/CT of 766 patients during 2001–2008 [175]. FDG avidity was found in 100 % of HL (233 patients), 97 % of DLBCL (216 of 222 patients), 95 % of FL (133 of 140 patients), 85 % of T-cell NHL (34 of 40 patients),

83 % of small lymphocytic lymphoma (24 of 29 patients), and 55 % of MALT (29 of 53 patients). Their study concurs with other studies, confirming FDG avidity of HL and the most common types of NHL, DLBCL, and FL [176, 177]. MALT has FDG avidity in about half of the cases, and its sensitivity depends on disease location (higher sensitivity with lung involvement than gastric and orbital involvement), stage at initial diagnosis, and histology [176–180]. Similarly, T-cell NHL are markedly heterogeneous, resulting in overall 88–90 % FDG avidity with a wide range from 20 % to 100 % depending on disease sites and histology [181–183]. Feeney et al. retrospective study of 135 patients found high rates of FDG positivity in T-cell lymphoma (overall 90 %) and given the propensity for disease involvement outside the normal scan range of diagnostic CT, they recommend that patients with T-cell lymphoma be scanned from vertex to feet by use of PET/CT [181]. Cahu et al. also found that although T-cell/natural killer cell lymphomas are FDG-avid at diagnosis, a negative interim or post-therapy FDG–PET does not translate into an improved progression-free survival [184]. Several studies reported higher standardized uptake value (SUV) correlates to aggressive histology and malignant transformation of indolent lymphomas and suggested biopsies should be directed to the site of greatest FDG avidity [185, 186]. Collectively, there are not enough evidences to support routine use of PET for low-grade lymphoma and T-cell NHL, for which CECT remains the cost-effective imaging choice.

As demonstrated above, FDG avidity of HL and DLBCL renders FDG-PET as the imaging choice for these lymphomas with consistently higher sensitivity and specificity than CT in staging and especially restaging (sensitivity and specificity of 90–100 % and 99–100 %, respectively, with PET compared to 81–88 % and 86–100 % with CT) [187–196]. Especially PET and PET/CT outperformed CECT for assessment of extranodal organ involvement (sensitivity and specificity of 88 % and 100 %, respectively, with PET compared to 50 % and 90 %, respectively, with CECT) and for distinguishing viable tumors from treated fibrosis in residual masses with high negative predictive values for residual disease and positive predictive value for early relapse [188, 193, 195–199]. Regarding clinical impact of higher diagnostic performance of PET when compared to CT, the majority of studies did not include details on the change of therapy and most importantly impact on outcome. The majority of studies reported PET upstaged patients with DLBCL and HL up to 20 % of the time (most of these with stage I-II) and fewer than 10 % of the patients were downstaged, resulting in treatment change less than 15 % of the time without improvement of outcome [187–191]. Buchmann et al. conducted a multicentric prospective study comparing FDG-PET with CT and bone marrow biopsy in the pretreatment staging of malignant lymphoma, analyzing site specific disease in HL and NHL (52 patients, 1297 anatomic sites, only 4 patients with low-grade NHL) [189]. They found that FDG-PET was significantly superior to CT in both HL and NHL, except in infradiaphragmatic regions, in which the two methods produced equivalent results. In 4 of 52 patients (8 %), FDG-PET upstaged and changed therapy. This study strongly supports the use of PET for accurate staging of HL and intermediate- to high-grade NHL. Another multicentric prospective study of 186 patients by Rigacci and colleagues compared CT to FDG-PET in staging of HL and investigated the impact of PET finding on therapeutic approaches [190]. PET staging in comparison to CT staging was higher in 14 % and lower in 1 % of patients, and 8 %, with a change of stage from localized to advanced after PET evaluation, were treated with different strategies. Their study supports the application of PET for staging of HL, particularly in early stage patients where upstaging may modify the therapy.

To address the heterogeneity of the published studies evaluating FDG-PET diagnostic performance for lymphoma staging and restaging, several meta-analysis and systemic reviews have been done. Meta-analysis conducted by Isasi et al. included 20 studies: 14 reported patient-based data (total 854 patients), 7 reported lesion-based data (total 3,658 lesions), and 1 study reported both patient- and lesion-based

data; 7 prospective and 13 retrospective studies; PET images were interpreted blind to the results of the reference standard in 12 studies (published literature from 1995 to 2004) [195]. Patient-based data demonstrated 91 % pooled sensitivity and 90 % pooled specificity with statistical homogeneity. Lesion-based data showed 96 % pooled sensitivity and 99 % pooled specificity but with statistical heterogeneity. Pooled sensitivity and false positivity appeared higher in HL (92.6 % and 13.4 %, respectively) than NHL (89.4 % and 11.4 %, respectively). This meta-analysis provides moderate evidence that PET has high sensitivity and specificity for the staging and restaging of patients with lymphoma. Recent systematic review by Kwee et al. included 19 studies: 3 studies (94 patients) investigated CT (1 study for initial staging), 17 studies (832 patients) investigated FDG-PET (3 studies for initial staging), and 4 studies (234 patients) investigated FDG-PET/CT fusion (1 study for initial staging) (published literature up to 2007) [196]. The analysis supports strong-moderate evidences for better diagnostic performance of FDG-PET in restaging when compared to CT and FDG-PET/CT fusion outperforms either modality used alone. However, the authors' conclusion that CT remains the standard imaging modality for initial staging of malignant lymphoma has insufficient supportive evidence by the included three CT studies. This review demonstrates the heterogeneity in criteria for positivity between studies of the same imaging modality. A well-designed studies that expressed results according to the Ann Arbor staging system are needed to determine the most accurate and cost-effective imaging modality in staging malignant lymphoma.

Terasawa et al. conducted a systematic review of FDG-PET for post-therapy assessment of HL and aggressive NHL with literature search from 1966 to 2006 [199]. Nineteen studies were included in the review: 15 HL (474 patients) and 8 NHL (254 patients); 5 prospective and 14 retrospective. They found heterogeneity in reported sensitivity and specificity of PET even though PET has good diagnostic accuracy for assessing residual HL at the completion of first-line treatment and conclusive data on aggressive NHL were

more limited. They expressed the need for prospective randomized clinical trials with more rigorous design to reveal the clinical diagnostic accuracy and efficacy of PET/CT imaging modality and its impact on clinical outcome before treatment strategy based on post-therapy PET findings can be implemented in routine clinical practice.

CECT will be discussed in the next section [200–202].

A more recent prospective study published in 2008 by Dupuis et al. integrated FDG-PET to International Workshop Criteria for assessment of treatment response of patients with DLBCL demonstrated PET as powerful tool to predict outcome [203]. The 5-year event-free survival was 36 % for patients with a positive PET versus 80 % with a negative examination. Similarly, Filmont et al. prospectively investigated the impact of pre- and post-transplantation FDG-PET on poor-prognosis lymphoma patients undergoing autologous stem cell transplantation (ASCT) [204]. A positive pre-ASCT PET image indicated a high risk of ASCT failure, which was increased by a positive post-ASCT PET image, suggesting a new treatment regimen is needed in positive pre-ASCT PET patients. To unify this prognostic value, Poulou conducted a meta-analysis of published literature up to 2007 for predictive value of 18F-FDG PET in patients with relapsing/refractory lymphoma who are receiving high-dose chemotherapy and ASCT [205]. The pooled survival data from seven studies suggested a worse progression-free survival in patients with a positive PET study. The overall survival pooled from six studies was also significantly worse among patients with a positive PET study. These studies demonstrated the prognostic impact of pre-transplant FDG-PET in patients with lymphoma for both progression and survival after ASCT (strong-moderate evidences).

Is CECT Still Needed in Lymphoma Staging?

Several retrospective comparisons of PET/CT and CECT suggest no added benefit of diagnostic CT in staging of lymphoma with limited evidences [193, 200]. However, these conclusions are not necessarily applicable to all lymphoma

types because the studied patient populations are largely HL, DLBCL, and high-grade lymphoma, which are routinely FDG-avid. The most important application is high negative predictive value in exclusion of disease with PET/CT and implication that CECT may not be needed for staging of HL and high-grade NHL.

Raanani investigated the added benefit of CECT and PET/CT in initial staging of lymphoma [201]. Upstaging by PET/CT versus CT was most evident for stage I-II (31 % for NHL and 32 % for HL) and resulted in treatment changes in a third of HL and in a quarter of NHL. They suggest that in centers performing a diagnostic CT as the initial step of staging, PET/CT should only be added in patients defined as early stage disease by CT alone (limited evidence). Rodriguez prospective study of 47 patients found no significant differences between unenhanced low-dose PET/CT and contrast-enhanced full-dose PET/CT, although full-dose PET/CT showed fewer indeterminate findings and a higher number of extranodal sites affected without change in disease stage [202]. Additional radiation with full-dose CT does not gain clinically significant diagnostic information that changes staging and clinical management (moderate evidence).

Hutchings investigated diagnostic performance of FDG-PET, CECT (with oral and intravenous contrast), and fusion PET/CECT for the staging of HL and therefore the impact on treatment choice in prospective blinded study of 99 patients (61 had PET/CECT) [194]. They confirmed higher accuracy of PET and PET/CECT compared to CECT for assessment of staging. Compared to CECT alone, PET and PET/CECT would have upstaged 18 % and 17 % of patients, respectively, and downstaged 5 % of patients, leading to a different treatment in 9 % of patients with PET and 7 % with PET/CECT. However, in this prospective study, only one patient who would have been upstaged to an advanced treatment group by PET experienced progression during the 2-year follow-up period, compared to 18 out of all 99 patients; none of the 3 patients who would have been upstaged to the advanced treatment group by FDG-PET/CT experienced

progression, compared with 12 out of all 61 patients. Therefore, authors concluded that care should be taken so patients with an excellent prognosis and at risk of over-treatment do not receive more extensive treatment because of these staging methods (moderate-strong evidence).

Role of Interim PET

Currently, the heterogeneity of the patient populations, histologies, stages, and treatment protocols in the numerous published studies addressing the role of FDG-PET in mid-treatment evaluation render generalization of these findings in clinical practice difficult. To date, there is no direct evidence that altering therapy on the basis of interim PET findings improves patient outcome. On the basis of the available data, mid-treatment PET scans should be reserved for clinical trials and should not be performed as standard practice.

Barnes concluded in the retrospective study of 96 patients with non-bulky limited stage HL that interim PET scans were not predictive of outcome and end-of-treatment PET was highly predictive of overall survival [206]. Several prospective studies found that a positive interim PET is highly predictive of relapse in advanced-stage HL [207–209]. Avigdo and colleagues conducted a prospective clinical trial of 45 advanced high-risk HL patients, utilizing response evident on interim PET in addition to clinical assessment as inclusion criteria for their treatment arm [209]. They found that the 4-year progression-free survival rates for early PET-negative patients and early PET-positive patients were 87 % and 53 %, respectively, and concluded that early-interim PET can guide treatment choice for the proposed regimen with less toxicity but comparable cure rate.

The lack of a consistent advantage for interim PET among the studies for NHL reflects many variables, including different timing of PET among various treatment cycles and variability in PET interpretation. Earlier studies show early interim FDG-PET in aggressive NHL is an accurate and independent predictor of complete response rate, progression-free survival, and

overall survival, irrespective of the International Prognostic Index, and could provide the basis for selection of patients for alternative therapeutic strategies [210–212]. The long-term outcome of PET-negative patients was fairly consistent among these studies at 81–93 %. However, these conclusions should be viewed with caution before subjecting patients to more toxic therapy because about half of these groups had positive interim PET scans and the long-term survival of these positive interim PET patients varied from 0 % to 43 %. Furthermore, high false-positive PET results in patients with aggressive NHL treated with rituximab-containing regimens have been reported in a prospective study of 51 patients with poor positive predictive value for predicting relapses of interim and posttreatment PET (33 % and 19 %, respectively) [213].

Terasawa conducted a systematic review of 13 studies to evaluate interim PET for response assessment of advanced-stage HL (360 patients) and DLBCL (311 patients) [214]. Only 10 % of these HL patients had unfavorable risk. Overall sensitivity was 81 %, and specificity was 97 %. Therefore, the finding is only applicable to patients with low to intermediate risk. Results in DLBCL included a sensitivity of 78 % and a specificity of 87 %. However, the authors could not draw reliable conclusions for DLBCL, because this patient population and published studies were heterogeneous.

Surveillance

Several studies have shown that surveillance imaging only detects maximally 20 % of relapses while a majority of the time it is suspected by the patient or the physician. PET has failed to show clear benefits in surveillance [215, 216]. The largest prospective study published by Zinzani included 421 patients with follow-up PET scans for DLBCL, HL, and FL after first remission scheduled every 6 months for the first 2 years and then annually thereafter [217]. This study demonstrated the capability of PET to identify clinically unsuspected relapses in 10 % of scans of HL, 9 % of aggressive NHL, and 22 % of indolent NHL, validating PET as a valuable tool for follow-up. Most importantly, this study demonstrates the timeframe and likelihood of relapse for each group. The relapse rate for HL and aggressive NHL dropped to 4 % at 18 months and to 2 % at 24 months, respectively. On the other hand, relapse rates for indolent NHL were steady; at least 8 % until 36 months and slightly reduced to 6 % at 4 years.

Other studies concluded regular follow-up with PET scans in HL patients in remission is not needed because of low ratio of true-positive PET scans and asymptomatic patients without morphological residues and an early stage of disease do not need a routine FDG–PET/CT for follow-up [218–220]. Lee et al. found only 12 relapses in 192 patients with HL in remission and estimated the cost to detect a single event was approximately $100,000 with limited clinical impact, thus they concluded that surveillance CT is generally adequate for these patients [220]. A recent retrospective study of PET/CT for follow-up of DLBCL patients who had complete remission or unconfirmed complete remission after first-line therapy demonstrated high positive predictive value of 85 % with 30 % relapse rate [221]. However, older age (>60) and clinical symptoms are most predictive of relapses and therefore PET/CT during follow-up is indicated for patients <60 years with clinical signs of relapse and in patients >60 years with and without clinical signs of relapse.

Cost-Effectiveness

There are a few studies addressing the cost-effectiveness of utilizing PET in lymphoma. In 1997, Hoh compared total cost of lymphoma staging utilizing whole body FDG-PET to conventional studies and found that the addition of PET to the diagnostic workup increased the diagnostic accuracy with cost reduction by approximately $1,685 per patient [222]. To evaluate cost-effectiveness of FDG-PET, Klose enrolled 22 patients in a randomized prospective in 1999 and found economic disadvantage of PET with 6.6 times higher cost for each correctly staged patient when compared to CT [223]. The authors suggested optimizing utilization of the PET facility could reduce the incremental cost-effectiveness ratio of FDG-PET versus CT

by 53 %. Therefore, the cost per patient correctly staged would be 3.2 times higher than with CT.

To assess the cost-effectiveness of incorporating FDG-PET in the decision tree to manage HL patients without complete remission after first-line treatment between 2005 and 2007, Cerci et al. conducted a prospective study of 130 patients whose residual disease evident on CT were defined as unconfirmed complete remission or partial remission according to International Workshop to Standardize Response Criteria for NHL [224]. PET-positive patients were biopsied to confirm the residual viable tumor and PET-negative patients were followed up with CT to confirm clinical response. The study demonstrated PET offered 95.9 % accuracy in restaging with 19 % decrease in restaging costs, which accounts for 1 % of total cost of HL treatment and results in 1 % cost saving for Brazilian public health care. All these studies show cost of staging is a small portion of total cost for treatment of lymphoma.

What Is the Appropriate Management of a Palpable Neck Mass Without an Imaging Correlate?

Occasionally, a patient will present with a complaint of a neck mass that is palpable and persistent and imaging will yield no correlate abnormality. There are no studies in the literature examining this uncommon issue but anecdotally, these palpable neck masses tend to be prominent normal anatomic structures that the patient discovers and brings to the attention of their primary doctor. Such "palpable neck masses" include prominent carotid bulbs, normal laryngeal cartilages, and ptotic submandibular glands (the latter common during the aging process when the platysma muscle weakens and attenuates). In the case of normal prominent anatomy, the patient is reassured and educated. Scar tissue from prior trauma and skin keloid may also present as a palpable and visible mass that has no definite imaging correlate. Small skin masses such as sebaceous cysts and epidermal inclusion cysts may also not be obvious on imaging. These skin

abnormalities and scars do not typically require any imaging prior to intervention. As a general rule, however, the indeterminate palpable neck masses should be at minimum followed with close observation and repeat imaging if they grow or change significantly. Close collaboration between clinician and radiologist can help with the choice of repeat study as well as timing of imaging.

Take-Home Tables and Figure

See Fig. 38.1 for an algorithm for imaging of palpable neck masses. See Tables 38.1 through 38.3 for common neck masses in adults, imaging options for palpable neck lump, and summary of diagnostic performance of CECT for neck infection, respectively.

Table 38.1 Common neck masses in adults

Infectious-inflammatory etiologies
Acute lymphadenitis (bacterial-cat scratch disease, viral-mononucleosis, HIV/AIDs)
Abscess
Tuberculosis
Sarcoid
Neoplasm- benign
Lipoma
Salivary gland: Pleomorphic adenoma, Warthin's tumor
Thyroid goiter
Paraganglioma
Neurogenic tumor
Neoplasm- malignant
Lymphoma
Metastatic adenopathy (HN SCCA, thyroid cancer, melanoma, lung cancer, breast cancer)
HN SCCA
Thyroid carcinoma
Salivary gland carcinoma (Mucoepidermoid, Adenoid cystic carcinoma, Carcinoma ex pleomorphic)
Sarcoma
Congenital
Thyroglossal duct cyst
Branchial cleft cyst
Venolymphatic malformation

Table 38.2 Imaging options for a palpable neck lump

Imaging studies	Contrast required	Bone visualization	Soft tissue visualization	Radiation exposure	Other risks and limitations	Average medicare reimbursement
US	No	None	Good (excellent for vascularity)	No	Operator dependent	$100
						$200 for US-FNA (inexpensive)
CT	Usually yes	Excellent	Good	Yes	Iodine contrast allergy and renal insufficiency. Dental artifact	$300 (mild)
MRI	Usually yes	Good (excellent for marrow)	Excellent	No	Nephrogenic Systemic Fibrosis, MRI compatible medical devices, long scan time, susceptibility artifact	$700 (moderate)
PET-CT	18-fluorodeoxyglucose (FDG)	Moderate	Moderate	Yes	Physiologic uptake dependant	$1,200 (expensive)

Table 38.3 Summary of diagnostic performance of CECT for neck infection

Study, year (reference number)	Number of patients (age range, mean age)	Study design	References for neck infection	CECT criteria	Diagnostic performance
Miller et al. 1999 [26]	35 adults (18–80, 37.8 years)	Prospective	Intraoperative finding of pus or long-term follow up for abscess	Drainable collection: hypodensity with or without ring enhancement	Clinical assessment and CECT: 95 % sensitivity, 80 % specificity, 89 % accuracy
Boscolo-Rizzo et al. 2006 [27]	80 adults (18–87, 51 years)	Retrospective	Intraoperative finding of abscess	Abcess: enhancing rim around non-enhancing fluid density	Clinical assessment and CECT: 88.1 % accuracy
Nagy et al. 1997 [145]	47 children (7 months–18 years, 4.2 years)	Retrospective	Intraoperative finding or long-term follow up	Retrophagyngeal and parapharyngeal abscess: low attenuation with ring enhancement	CECT sensitivity for DNI 95 %
Stone et al. 1999 [146]	32 children (3 months–9 years)	Retrospective	Intraoperative finding of cellulitis/phlegmon or abscess of retropharyngeal space	Cellulitis/phlegmon: decreased attenuation without well-defined rim of enhancement. Abscess: with complete rim of enhancement	CECT for abscess: sensitivity 80.8 %, specificity 62.5 %, accuracy 73.5 %

(*continued*)

Table 38.3 (continued)

Study, year (reference number)	Number of patients (age range, mean age)	Study design	References for neck infection	CECT criteria	Diagnostic performance
Elden et al. 2001 [147]	110 children (1 month–17 years)	Retrospective	Intraoperative finding cellulitis or abscess	Cellulitis: mass, low density core, surrounding edema. Abscess: imaging findings of cellulitis and complete enhancing rim, fluid level	CT accuracy 76 % (67 % abscess, 9 % cellulitis)
					24 % discordant (16.8 % false positive and 7 % false negative for abscess)
Vural et al. 2003 [148]	80 children (3 months–14 years, 4.9 years)	Retrospective	Intraoperative finding of abscess	Cellulitis: Low-density core, soft-tissue swelling, obliterated fat planes, mass effect	CECT 68 % sensitivity, 56 % specificity, 63 % accuracy
				Abscess: cellulitis finding with a complete rim enhancement	
Daya et al. 2005 [149]	54 children (0.4–17.9/5.4 years)	Retrospective	Clinical and imaging diagnosis of retropharyngeal and parapharyngeal infection and intra-operative finding of pus	Abscess: CSF density collection with a complete enhancing rim	CECT for abscess: 81 % sensitivity, 57 % specificity
Courtney et al. 2007 [144]	205 children (0–14 years, 3.4 years)	Retrospective	Clinical, radiological and intraoperative findings of lymphadenitis, necrotic node, cellulitis, abscess	87 US and 11 CT. Radiologist's report impression	US for abscess: accuracy 65.2 %, sensitivity 70 %, 33 % specificity. CECT abscess: accuracy 85 %
Shefelbine et al. 2007 [150]	30 children (9–96 months)	Retrospective	Clinical, intraoperative and radiological assessment for retropharyngeal adenitis	Retropharyngeal adenitis: a lymph node with a central low-attenuation focus with rim enhancement located in anatomic location of the retropharyngeal nodal group	CECT identify purulence as low density volume ≥ 2 cm^3: accuracy 80 %, sensitivity 90 %, specificity 25 %
Malloy et al. 2008 [151]	43 (mean age 4.1 years)	Retrospective	Intraoperative finding of pus in a neck space collection	Abscess: Grade 1–3 (none, incomplete and complete) rim enhancement of the collection (both surgical and nonsurgical groups have mostly grade 2 collections)	CECT for abscess: 72 % specificity
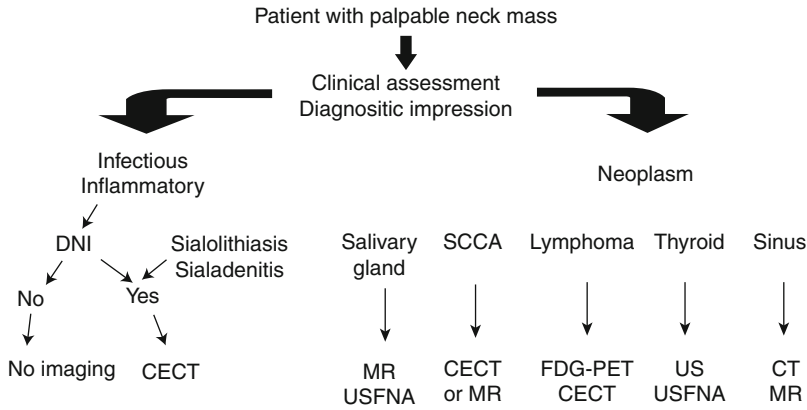
Fig. 38.1 Algorithm for imaging of a palpable neck mass
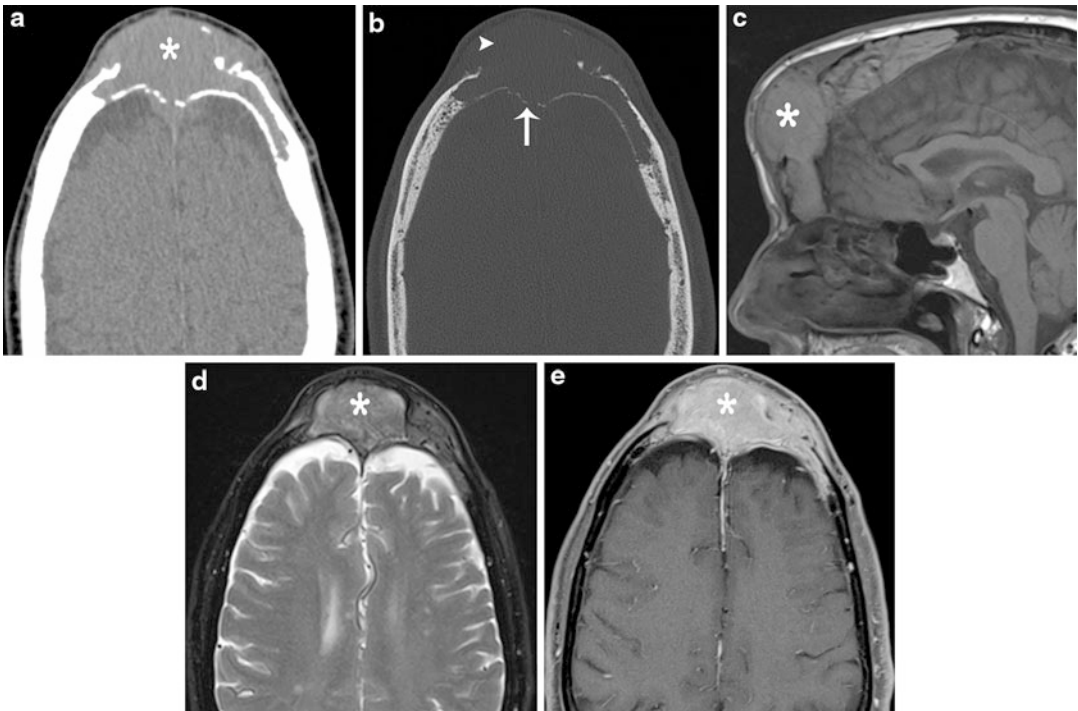
Fig. 38.2 Case 1: Sinus mass lesion. 65-year-old male referred to ENT for evaluation of a suspected frontal mucocele. Noncontrast axial images of CT sinus fusion protocol in soft tissue (**a**) and bone (**b**) algorithms demonstrate an expansile soft tissue density lesion (*asterisk*) centered in superior frontal sinuses accounting for patient's frontal bossing. The anterior cortical table of frontal bone is destroyed (*arrow head*) and the posterior frontal sinus wall has scattered rarefaction. MR sinus with pre-contrast sagittal T1-weighted (**c**), axial T2-weighted TSE with fat saturation (**d**), and Gadolinium enhanced axial T1-weighted with fat saturation (**e**) demonstrate intermediate T2 signal intensity and solid enhancement of the lesion compatible with a neoplasm. The integrity of the cortical bone is superiorly demonstrated with CT, and MR maps the extent of solid neoplasm and excludes intracranial involvement. This patient has plasmacytoma
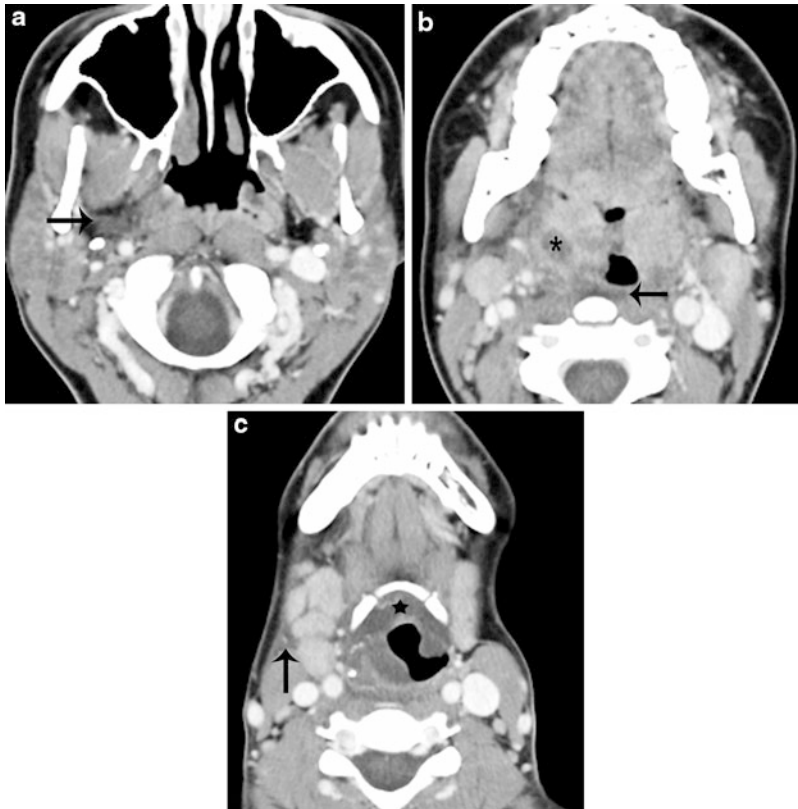
Fig. 38.3 Case 2: Deep neck infection. 22-year-old female presented to emergency department with worsening sore throat, dysphagia, and fever for a couple of days with new dyspnea, and found to have leukocytosis and bandemia and swollen palatine tonsils on evaluation CECT neck: (**a**) Inflammation of the right parapharyngeal space (*arrow*). (**b**) Enlarged kissing palatine tonsils with right peritonsillar abscess (*asterisk*) and extensive inflammation including the retropharyngeal space (*arrow*). (**c**) Diffuse edema of larynx (*star*) and inflammation of the right submandibular space (*arrow*). The airway is deformed and narrowed

Imaging Case Studies

Case 1: Sinus Mass Lesion (Fig. 38.2)
Case 2: Deep Neck Infection (Fig. 38.3)
Case 3: Lymphoma (Fig. 38.4)

Suggested Protocols

CECT Neck

16-64 multidetector CT scanner. 0.625–1.25 mm helical scanning with 3 mm thick axial reconstruction from skull base to aortopulmonary window with 30–45 s delayed after intravenous iodine contrast administration. Coronal and sagittal reformats can be obtained as needed.

MR Neck

1.5 T magnet. Pre-contrast sagittal and axial T1-weighted spin echo, axial STIR and T2-weighted FSE, and post-contrast axial and coronal T1-weighted spin echo with fat saturation. Slice thickness 5 mm (no gap). Scanning from skull base to aortopulmonary window.
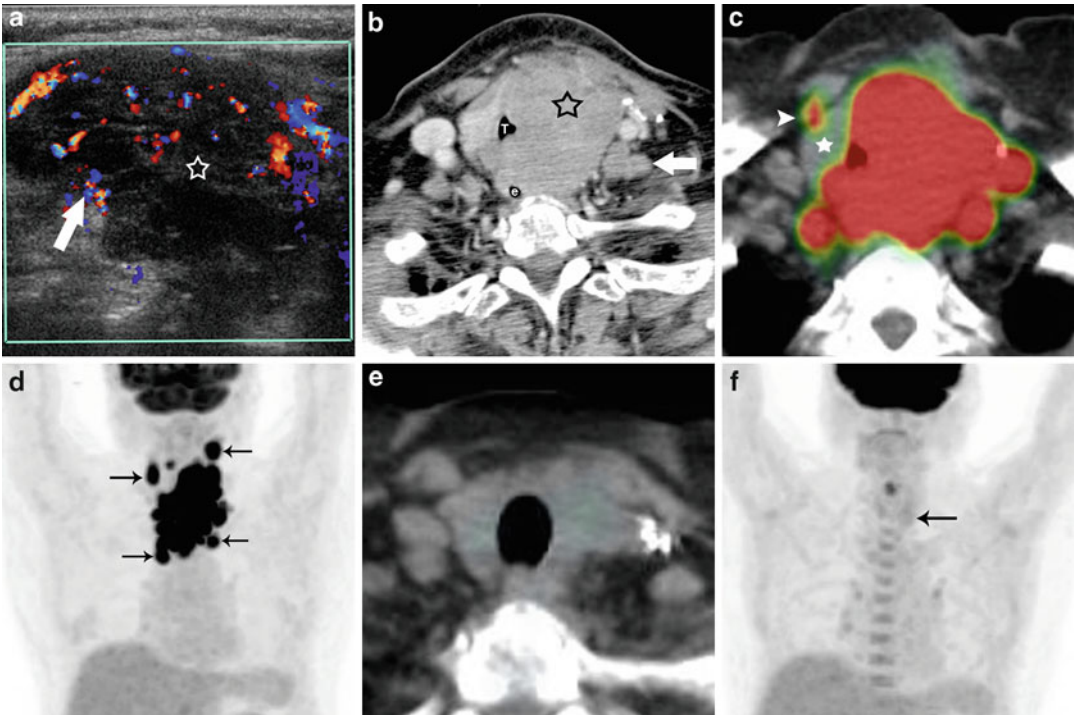
Fig. 38.4 Case 3: Lymphoma. 72-year-old female presented to emergency department with stridor from an enlarging thyroid bed neck mass over several months. Thyroid ultrasound (**a**) shows a poorly defined, hypoechoic mass infiltrating and enlarging the left thyroid lobe (*star*) with internal vascularity (*arrow*). Left thyroid biopsy shows DLBCL. Staging CECT neck (**b**) reveals severe tracheal (*T*) and esophageal (*e*) compression by the thyroid mass (*star*) and adenopathy (*arrow*). Staging whole body FDG-PET/CT (**c**, **d**) reveals FDG avidity of the left thyroid lymphoma, and bilateral central compartment, level II–IV cervical and mediastinal adenopathy (*arrow*) with SUV of 13–18. Note FDG avidity of sub-centimeter node (*arrow head*) anterior to non-FDG-avid of the uninvolved right thyroid lobe (*solid star*). Interim PET/CT after 2 cycles of RCHOP (**e**, **f**) shows minimal FDG avidity (SUV of 2–4) of the residual tissue in the thyroid and nodal bed. End of treatment and 1-year follow-up PET/CTs (not shown) demonstrate complete treatment response without FDG uptake of the residual tissue

CT Sinus Fusion Protocol

16-64 multidetector CT scanner. 0.625–1.25 mm helical scanning with 1 mm thick axial images from vertex to mandible and 3 mm thick direct coronal images from tip of nose to brain stem in soft tissue and bone algorithms.

MR Sinus

1.5 T magnet. Pre-contrast axial T2-weighted FSE with fat saturation of entire head (5 mm thick). Pre-contrast axial and coronal T1-weighted spin echo, coronal STIR and T2-weighted FSE with fat saturation, and post-gadolinium contrast axial and coronal T1-weighted spin echo with fat saturation of the sinuses (from top of orbits to below hard palate, from tip of nose to brain stem, 3 mm thick).

Future Research

- The limited evidence of the cost-effectiveness and impact on patient's outcome by imaging utilization is inherently due to the complexity of the multidisciplinary approach to diagnosis and treatment of a suspicious palpable neck lump. Ideally, multicenter study is needed to

unify imaging strategy with a balance between optimal diagnostic performance and cost-effectiveness.

- Even though there is moderate evidence supporting modality choice for the specific pathology in question, in reality, the available local resources and expertise remain the main driving forces determining the imaging choice.

References

1. Nicoucar K, Giger R, Pope HG, et al. J Pediatr Surg. 2009;44:1432–9.
2. Nour YA, Hassan MH, Gaafar A, Eldaly A. Otolaryngol Head Neck Surg. 2011;144:365–71.
3. Park S, Han MH, Sung MS, et al. Am J Neuroradiol. 2000;21:817–22.
4. The 2008 National Hospital Ambulatory Medical Care Survey. http://www.cdc.gov/nchs/ahcd.htm. Accessed 1 Sept 2011.
5. Torsiglieri AJ, Tom LW, et al. Int J Pediatr Otorhinolaryngol. 1988;16:199–210.
6. Williamson HA. J Fam Pract. 1985;20(5):449–52.
7. Fijten GH, Blijham GH. J Fam Pract. 1988;27(4):373–6.
8. Robertson MS, Hornibrook J. N Z Med J. 1982;95:337–41.
9. Bhattacharyya N. Arch Otolaryngol Head Neck Surg. 1999;125:303–30.
10. Smith OD, Ellis PMD, et al. Ann R Coll Surg Engl. 2000;82:223–6.
11. CDC. United States Cancer Statistics (USCS) 1999–2007 cancer incidence and mortality data. Released in December 2010. http://apps.nccd.cdc.gov/uscs. Accessed 10 Jan 2011.
12. Altekruse SF, Kosary CL, Krapcho M, et al. SEER cancer statistics review, 1975–2007. National Cancer Institute SEER 2010. http://seer.cancer.gov/csr/1975_2007. Accessed 10 Jan 2011.
13. Jereczek-fossa BA, Jassem J, et al. Cancer Treat Rev. 2003;30:135–64.
14. Koivunen P, Laranne J, et al. Acta Otolaryngol. 2002;122:569–74.
15. American Cancer Society. Cancer facts & figures 2010. http://www.cancer.org. Accessed 10 Jan 2011.
16. Gharib H, Papini E, Paschke R, Duick DS, Valcavi R, Hegedüs L, Vitti P, American Association of Clinical Endocrinologists, Associazione Medici Endocrinologi, European Thyroid Association Medical Guidelines for Clinical Practice for the Diagnosis and Management of Thyroid Nodules. Endocr Pract. 2010;16(Suppl 1):1–43.
17. Harach HR, Franssila KO, Wasenius VM. Cancer. 1985;56(3):531–8.
18. Cancer trends progress report 2009/2010 update: cost of cancer care. http://progressreport.cancer.gov. Accessed 2 Feb 2011.
19. Mariotto AB, Yabroff KR, et al. J Natl Cancer Inst. 2011;103:117–28.
20. Menzin J, Lines LM, Manning L. Curr Opin Otolaryngol Head Neck Surg. 2007;15:68–73.
21. Lang K, Menzin J, Earle CC, et al. Arch Otolaryngol Head Neck Surg. 2004;130:1269–75.
22. Yabroff KR, Lamont EB, Mariotto A, et al. J Natl Cancer Inst. 2008;100:630–41.
23. Atula TS, Varpula MJ, Kurki TJI, et al. Eur J Radiol. 1997;25:152–61.
24. Robson A. Clin Otolaryngol. 2005;30:79–85.
25. Crespo A, Chone C, Fonseca A, et al. Sao Paulo Med J. 2004;122(6):259–63.
26. Miller W, Furst I, Sandor G, et al. 1999;109(11):1873–9.
27. Boscolo-Rizzo P, Marchiori C, Zanetti F, et al. Otolaryngol Head Neck Surg. 2006;135(6):894–9.
28. Lee J, Fernandes R. Oral Maxillofac Surg Clin N Am. 2008;20(3):321–337.
29. Tracy TF, Muratore CS. Semin Pediatr Surg. 2007;16:3–13.
30. Al-Dajani N, Wootton SH. Infect Dis Clin N Am. 2007;21:523–41.
31. Luzuriaga K, Sullivan JL. N Engl J Med. 2010;362:1993–2000.
32. Khan R, Harris SH, Verma AK, Syed A. J Laryngol Otol. 2009;123:764–7.
33. Razeka AA, Castillo M. Eur J Radiol. 2010;76:52–60.
34. Wang C, Ko J, Lou P. J Laryngol Otol. 2006;120:305–9.
35. Vieira F, Allen SM, Stocks RMS, Thompson JW. Otolaryngol Clin North Am. 2008;41(3):459–83.
36. Marioni G, Staffieri A, Parisi S, et al. Ann Otol Rhinol Laryngol. 2010;119(3):181–7.
37. Armitage JO. N Engl J Med. 2010;363:653–62.
38. Connors JM. Cancer J. 2009;15:124–8.
39. Urquhart A, Berg R. Laryngoscope. 2001;111:1565–9.
40. Hennessy BT, Hanrahan EO, Daly PA. Lancet Oncol. 2004;5:341–53.
41. Prout MN, Sidari JN, Witzburg RA, et al. Otolaryngol Head Neck Surg. 1997;116:201–8.
42. Shuman AG, Entezami P, Chernin AS, et al. Otolaryngol Head Neck Surg. 2010;143:353–60.
43. Kreimer A, Clifford G, et al. Cancer Epidemiol Biomarkers Prev. 2005;4(2):467–75.
44. D'Souza G, Kreimer A, et al. N Engl J Med. 2007;356(19):1944–56.
45. Marur S, D'Souza G, Westra WH, Forastiere AA. Lancet Oncol. 2010;11(8):781–9.
46. Jeng J, Chang M, Hahn L. Oral Oncol. 2001;37(6):477–92.
47. Goldenberg D, Golz A, Netzer A, et al. Am J Otolaryngol. 2001;22:197–205.
48. Brook I. The swollen neck. Infect Dis Clin North Am. 1988;2(1):221–36.

49. Herold BC, Immergluck LC, Maranan MC, et al. J Am Med Assoc. 1998;279(8):593–8.

50. Gordon RJ, Lowy FD. N Engl J Med. 2005;353:1945–54.

51. Inman JC, Rowe M, Ghostine M, Fleck T. Laryngoscope. 2008;118:2111–4.

52. Lai KK, Stottmeier KD, Sherman IH, et al. J Am Med Assoc. 1984;251(10):1286–8.

53. Wolinsky E. Clin Infect Dis. 1995;20(4):954–63.

54. Robson C, Hazra R, Barnes P, et al. Am J Neuroradiol. 1999;20:1829–35.

55. Bass JW, Freitas BC, Freitas AD, et al. Pediatr Infect Dis J. 1998;17(6):447–52.

56. Hasegawa J, Hidaka H, Tateda M, et al. Auris Nasus Larynx. 2011;101–7.

57. Huang T, Tseng F, Liu T, et al. Otolaryngol Head Neck Surg. 2005;132:943–7.

58. Lin H, Tsai CS, Che Y, Liang J. J Laryngol Otol. 2006;120:650–4.

59. Huang T, Tseng F, Yeh T, et al. Acta Otolaryngol. 2006;126:396–401.

60. Scaglione M, Pinto A, Romano S, et al. Emerg Radiol. 2005;11:275–80.

61. Mack TM, Cozen W, Darryl KS, et al. N Engl J Med. 1995;332:413–8.

62. Cooper DS, Doherty GM, Haugen BR, Kloos RT, Lee SL, Mandel SJ, Mazzaferri EL, McIver B, Pacini F, Schlumberger M, Sherman SI, Steward DL, Tuttle RM. Thyroid. 2009;19:1167–214.

63. Davies L, Welsh HG. J Am Med Assoc. 2006;296:2164–7.

64. Tan GH, Gharib H. Ann Intern Med. 1997;69:226–31.

65. Nam-Goong IS, Kim HY, Gong G, et al. Clin Endocrinol. 2004;60(1):21–8.

66. Frates MC, Benson CB, Doubilet PM, et al. J Clin Endocrinol Metab. 2006;91:341–3417.

67. Machens A, Holzhausen HJ, Dralle H. Cancer. 2005;103:2269–73.

68. Takashima S, Noguchi Y, et al. Eur J Radiol. 1992;14:228–34.

69. Held P, Breit A. Eur J Radiol. 1994;18:81–91.

70. Wiener EA, Pautke CB, Link TM, et al. Eur J Radiol. 2006;58:113–8.

71. Van Kijke CF, Van Waes PF. Eur J Radiol. 1992;14:235–9.

72. Crecco M, Vidiri A, Angelone ML, et al. Eur J Radiol. 1999;32:182–8.

73. Fulbright R, Panush D, Sze G, et al. Am J Neuroradiol. 1994;15:767–73.

74. Kataoka M, Hiroyuki U, Koyama T, et al. AJR Am J Roentgenol. 2005;184:313–9.

75. Tien RD, Hesselink JR, Chu PK, Szumowski J. AJNR Am J Neuroradiol. 1991;12:19–24.

76. Barakos JA, Dillon WP, Chew WM. Radiology. 1991;179:191–8.

77. Tien RD, Robbins KT. Head Neck. 1992;14:278–84.

78. Ross MR, Schomer DF, Chappell P, Enzmann DR. AJR Am J Roentgenol. 1994;163:173–8.

79. Mukherji SK, Weeks SM, Castillo M, et al. Radiology. 1996;198:157–62.

80. Tang L, Li W, Chen L, et al. Radiology. 2010;257:151–7.

81. Hsu WC, Loevner LA, Karpati R, et al. Head Neck. 2005;27:95–100.

82. Eisen MD, Yousem DM, Loevner LA, et al. Head Neck. 2000;22:456–62.

83. Mukherji SK, Schmalfuss IM, Castelijns J, Mancuso AA. AJNR Am J Neuroradiol. 2004;25:1425–32.

84. Plataniotis GA, Theofanopoulou ME, Kalogera-Fountzila A, et al. Int J Radiat Oncol Biol Phys. 2004;59(4):1018–26.

85. Agada FO, Nix PA, Salvage D, et al. Int J Clin Pract. 2004;58:714–6.

86. Gilbert K, Dalley RW, Maronian N, Anzai Y. AJNR Am J Neuroradiol. 2010;31:251–6.

87. Zbaren P, Becker M, Laeng H. Cancer. 1996;77:1263–73.

88. Ljumanovic R, Langendijk JA, Schenk B, et al. Radiology. 2004;232(2):440–8.

89. Loevner LA, Yousem DM, Montone KT, et al. AJR Am J Roentgenol. 1997;169(6):1681–7.

90. Becker M. Eur J Radiol. 2000;33:216–29.

91. Becker M, Zbaren P, Delavelle J, et al. Radiology. 1997;203:521–32.

92. Cagli S, Ozturk M, Yuce I, et al. AJNR Am J Neuroradiol. 2009;30:1936–40.

93. Becker M, Zbaren P, Laeng H, et al. Radiology. 1995;194:661–9.

94. Becker M, Zbaren P, Casselman JW, et al. Radiology. 2008;249:551–9.

95. Kennedy DW, Zinreich SJ, Rosenbaum AE, et al. Arch Otolaryngol. 1985;111:576–82.

96. Zinreich SJ, Kennedy DW, Rosenbaum AE, et al. Radiology. 1987;163:769–75.

97. Melhem ER, Ollverio PJ, Benson ML, et al. AJNR Am J Neuroradiol. 1996;17:181–8.

98. Costa DJ, Sindwani R. Otolaryngol Clin N Am. 2009;42:799–811.

99. Som PM, Lawson W, Biller HF, Lanzieri CF. Radiology. 1986;159:591–7.

100. Som PM, Shapiro MD, Biller HF, et al. Radiology. 1988;167:803–8.

101. Hahnel S, Ertl-Wagner B, Tasman AJ, et al. Radiology. 1999;210:171–6.

102. Som PM, Dillon WP, Curtin HD, et al. Radiology. 1990;176:777–81.

103. Som PM, Lawson W, Lido M. Radiology. 1991;180:755–9.

104. Lanzieri CF, Shah M, Krauss D, Lavertu P. Radiology. 1991;178:425–8.

105. Kraus DH, Lanzieri CF, Wanamaker JR, et al. Laryngoscope. 1992;102:623–9.

106. Jeon TY, Kim H-J, Chung S-K, et al. AJNR Am J Neuroradiol. 2008;29:1556–60.

107. Casselman JW, Mancuso AA. Radiology. 1987;165:183–9.
108. Sumi M, Izumi M, Yonetsu K, Nakamura T. AJNR Am J Neuroradiol. 1999;20:1737–43.
109. Jager L, Menauer F, Holzknecht N, et al. Radiology. 2000;216(3):665–71.
110. Kalinowski M, Heverhagen JT, Rehberg E, et al. AJNR Am J Neuroradiol. 2002;23(9):1485–92.
111. Gadodia A, Seith A, Sharma R, et al. Acta Radiol. 2010;51(2):156–63.
112. Nakahara T, Suzuki T, Hashimoto J, et al. Clin Nucl Med. 2007;32:363–6.
113. Urquhart A, Hutchins LG, Berg BL. Laryngoscope. 2001;111:1984–8.
114. Barsotti JB, Westesson PL, Coniglio JU. Ann Otol Rhinol Laryngol. 1994;103:737–40.
115. Sigal R, Monnet O, de Baere T, et al. Radiology. 1992;184:95–101.
116. Kakimoto N, Gamoh S, Tamaki J. Eur J Radiol. 2009;69:464–72.
117. Som PM, Biller HF. Radiology. 1989;173:823–6.
118. Freling NJ, Molenaar WM, Vermey A, et al. Radiology. 1992;185:691–6.
119. Christe A, Waldherr C, Hallett R, et al. AJNR Am J Neuroradiol. 2011;32:1202–7. http://www.ajnr.org/content/32/7/1202.abstract-aff-3.
120. Yabuuchi H, Fukuya T, Tajima T, et al. Radiology. 2003;226:345–54.
121. Yabuuchi H, Matsuo Y, Kamitani T, et al. Radiology. 2008;249:909–16.
122. Habermann CR, Arndt C, Graessner J, et al. AJNR Am J Neuroradiol. 2009;30:591–6.
123. Eida S, Sumi M, Nakamura T. J Magn Reson Imaging. 2010;31:673–9.
124. King AD, Yeung DK, Ahuja AT, et al. Radiology. 2005;237:563–9.
125. Bhatia KS, Rasalkar DD, Lee YP, et al. Eur Radiol. 2010;20:1958–64.
126. Dumitriu D, Dudea SM, Botar-Jid C, Baciut G. Med Ultrasonogr. 2010;12(3):175–83.
127. Ozawa N, Okamura T, Koyama K, et al. Radiat Med. 2006;24(1):41–9.
128. Sharma G, Jung AS, Maceri DR, Rice DH, et al. Radiology. 2011;259(2):471–8.
129. Taylor MT, Serpell JW, Thomson P. ANZ J Surg. 2011;81:70–4.
130. Bartels S, Talbot J, Ditomasso J, et al. Head Neck. 2000;22(8):781–6.
131. Inohara H, Akahani S, Yamamoto Y, et al. Acta Otolaryngol. 2008;128(10):1152–8.
132. Cho HW, Kim J, Choi J, et al. AJR Am J Roentgenol. 2011;196(5):1160–3.
133. Colella G, Cannavale R, Flamminio F, Foschini MP. J Oral Maxillofac Surg. 2010;68(9):2146–53.
134. Cozens NJA. Clin Otolaryngol. 2009;34:6–11.
135. Moon W, Jung SL, Lee JH, et al. Radiology. 2008;247:762–70.
136. Moon HJ, Kwak JY, Kim MJ, et al. Radiology. 2010;255:260–9.
137. Bonavita AJ, Mayo J, Babb J, et al. AJR Am J Roentgenol. 2009;193:207–13.
138. Blankenship DR, Chin E, Terris D. Am J Otolaryngol Head Neck Med Surg. 2005;26:249–60.
139. Are C, Hsu JF, Ghossein RA, Schoder H, Shah JP, Shaha AR. Ann Surg Oncol. 2007;14:3210–5.
140. Hales NW, Krempl GA, Medina JE. Am J Otolaryngol Head Neck Med Surg. 2008;29:113–8.
141. Johnson N, Tublin M. Radiology. 2008;249(2):429–44.
142. Rozovsky K, Hiller N, Koplewitz BZ, Simanovsky N. Eur Radiol. 2010;20:484–90.
143. Meyer AC, Kimbrough TG, Finkelstein M, Sidman JD. Otolaryngol Head Neck Surg. 2009;140:183–6.
144. Courtney MJ, Miteff A, Mahadevan M. Int J Pediatr Otorhinolaryngol. 2007;71:95–100.
145. Nagy M, Pizzuto M, Backstrom J, Brodsky L. Laryngoecope. 1997;107:1627–34.
146. Stone ME, Walner DL, Koch BL, et al. Int J Pediatr Otorhinolaryngol. 1999;49:121–5.
147. Elden LM, Grundfast KM, Vezina G. J Otolaryngol. 2001;30(2):82–9.
148. Vural C, Gungor A, Comerci S. Am J Otolaryngol. 2003;24(3):143–8.
149. Daya H, Lo S, Papsin BC, et al. Int J Pediatr Otorhinolaryngol. 2005;69:81–6.
150. Shefelbine SE, Mancuso AA, Gajewski BJ, et al. Otolaryngol Head Neck Surg. 2007;136(2):182–8.
151. Malloy KM, Christenson T, Meyer JS, et al. Int J Pediatr Otorhinolaryngol. 2008;72:235–9.
152. McClay JE, Murray AD, Booth T. Arch Otolaryngol Head Neck Surg. 2003;129:1207–12.
153. Johnston D, Schmidt R, Barth P. Int J Pediatr Otorhinolaryngol. 2009;73:761–5.
154. Oh JH, Kim Y, Kim CH, et al. ORL J Otorhinolaryngol Relat Spec. 2007;69:37–42.
155. Datta PG, Hossain MD, Amin SA, et al. Mymensingh Med J. 2011;20(2):233–7.
156. Joo Y-H, Hwang S-H, Seo J-H. Treatment assessment based on computerized lymph node volume and ratio of necrotic area in tuberculous cervical lymphadenitis. Auris Nasus Larynx. 2012;39(4):402–6.
157. Cosset JM, Henry-Amar M, Meerwaldt JH, et al. Eur J Cancer. 1992;28A(11):1847–50.
158. Engert A, Plütschow A, Eich HT, et al. N Engl J Med. 2010;363(7):640–52.
159. Lister TA, Crowther D, Sutcliffe SB, et al. J Clin Oncol. 1989;7:1630–6.
160. Herbst C, Rehan FA, Skoetz N, Bohlius J, Brillant C, Schulz H, Monsef I, Specht L, Engert A. Chemotherapy alone versus chemotherapy plus radiotherapy for early stage Hodgkin lymphoma. Cochrane Database Syst Rev. 2011;2.
161. Volker D, Thomas RK, Re D. Lancet Oncol. 2004;5:19–26.

162. Terpos E, Rahemtulla A. Clin Evid. 2009; 06:2404.
163. Shipp MA, Harrington DP, Anderson JR, et al. N Engl J Med. 1993;329:987–94.
164. Solal-Ce ligny P, Roy P, Colombat P, et al. Blood. 2004;104:1258–65.
165. Hasenclever D, Diehl V. N Engl J Med. 1998;339:1506–14.
166. Herbst C, Rehan FE, Skoetz N, et al. Cochran Rev. 2011.
167. Bauer K, Skoetz N, Monsef I, et al. Cochran Rev. 2011.
168. Greb A, Bohlius J, Schiefer D, et al. Cochran Rev. 2011.
169. Schulz H, Bohlius J, Skoetz N, et al. Cochran Rev. 2009.
170. Vidal L, Gafter-Gvili A, Leibovici L, Shpilberg O. Cochran Rev. 2009.
171. Baldo P, Rupolo M, Compagnoni A, et al. Cochran Rev. 2011.
172. Cheson BD, Horning SJ, Coiffier B, et al. J Clin Oncol. 1999;17:1244–53.
173. Cheson BD, Pfistner B, Juweid ME, et al. J Clin Oncol. 2007;25:579–86.
174. Juweid ME, Stroobants S, Hoekstra OS, et al. J Clin Oncol. 2007;25:571–8.
175. Weiler-Sagie M, Bushelev O, Epelbaum R, et al. J Nucl Med. 2010;51(1):25–30.
176. Elstrom R, Guan L, Baker G, et al. Blood. 2003;101:3875–6.
177. Janikova A, Bolcak K, Pavlik T, et al. Clin Lymphoma Myeloma. 2008;8:287–93.
178. Beal KP, Yeung HW, Yahalom J. Ann Oncol. 2005;16:473–80.
179. Karam M, Novak L, Cyriac J, Ali A, Nazeer T, Nugent F. Cancer. 2006;107(1):175–83.
180. Hoffmann M, Wöhrer S, Becherer A, et al. Ann Oncol. 2006;17(12):1761–5.
181. Feeney J, Horwitz S, Gonen M, Schoder H. AJR Am J Roentgenol. 2010;195:333–40.
182. Kako S, Izutsu K, Ota Y, et al. Ann Oncol. 2007;18:1685–90.
183. Kumar R, Xiu Y, Zhuang HM, Alavi A. Br J Dermatol. 2006;155:357–63.
184. Cahu X, Bodet-Milin C, Brissot E. Ann Oncol. 2011;22:705–11.
185. Noy A, Schoder H, Gonen M, et al. Ann Oncol. 2009;20:508–12.
186. Ngeow JYY, Quek RHH, Ng DCE, et al. Ann Oncol. 2009;20:1543–7.
187. Moog F, Bangerter M, Diederichs CG, et al. Radiology. 1997;203(3):795–800.
188. Moog F, Bangerter M, Diederichs CG, et al. Radiology. 1998;206:475–81.
189. Buchmann I, Reinhardt M, Elsner K, et al. Cancer. 2001;91(5):889–99.
190. Rigacci L, Vitolo U, Nassi L, et al. Ann Hematol. 2007;86:897–903.
191. Tatsumi M, Cohade C, Nakamoto Y, et al. Radiology. 2005;237:1038–45.
192. Stumpe KD, Urbinelli M, Steinert HC, Glanzmann C, Buck A, von Schulthess GK, Eur J. Nucl Med. 1998;25(7):721–8.
193. Schaefer NG, Hany TF, Taverna C, et al. Radiology. 2004;232(3):823–9.
194. Hutchings M, Loft A, Hansen M, et al. Haematologica. 2006;91:482–9.
195. Isasi CR, Lu P, Blaufox MD. Cancer. 2005;104(5):1066–74.
196. Kwee TC, Kwee RM, Nievelstein RA. Blood. 2008;111(2):504–16.
197. Cremerius U, Fabry U, Neuerburg J, Zimny M, Osieka R, Buell U. Nucl Med Commun. 1998;19(11):1055–63.
198. Jerusalem G, Beguin Y, Fassotte MF, et al. Blood. 1999;94:429–33.
199. Terasawa T, Nihashi T, Hotta T, Nagai H. J Nucl Med. 2008;49(1):13–21.
200. Elstrom RL, Leonard JP, Coleman M, et al. Ann Oncol. 2008;19:1770–3.
201. Raanani P, Shasha Y, Perry C, et al. Ann Oncol. 2006;17:117–22.
202. Rodriguez-Vigil B, Gomez-Leon N, Pinilla I, et al. J Nucl Med. 2006;47:1643–8.
203. Dupuis J, Itti E, Rahmouni A, et al. Ann Oncol. 2009;20:503–7.
204. Filmont JE, Gisselbrecht C, Cuenca X, et al. Cancer. 2007;110(6):1361–9.
205. Poulou L, Thanos L, Ziakas PD. Eur J Nucl Med Mol Imaging. 2010;37:156–62.
206. Barnes JA, LaCasce AS, Zukotynski K, et al. Ann Oncol. 2011;22:910–5.
207. Hutchings M, Mikhaeel NG, Fields PA, et al. Ann Oncol. 2005;16:1160–8.
208. Markova J, Kobe C, Skopalova M, et al. Ann Oncol. 2009;20:1270–4.
209. Avigdor A, Bulvik S, Levi I, et al. Ann Oncol. 2010;21:126–32.
210. Spaepen K, Stroobants S, Dupont P, et al. Ann Oncol. 2002;13:1356–63.
211. Mikhaeel NG, Hutchings M, Fields PA, et al. Ann Oncol. 2005;6:1514–23.
212. Haioun C, Itti E, Rahmouni A, et al. Blood. 2005;106:1376–81.
213. Han HS, Escalo MB, Hsiao B, et al. Ann Oncol. 2009;20:309–18.
214. Terasawa T, Lau J, Bardet S, et al. J Clin Oncol. 2009;27:1906–14.
215. Liedtke M, Hamlin PA, Moskowitz CH, et al. Ann Oncol. 2006;17:909–13.
216. Jerusalem G, Beguin Y, Fassotte MF, et al. Ann Oncol. 2003;14:123–30.
217. Zinzani PL, Stefoni V, Tani M, et al. J Clin Oncol. 2009;27:1781–7.
218. Mocikova H, Obrtlikova P, Vackova B, et al. Ann Oncol. 2010;21:1222–7.

219. Petrausch U, Samaras P, Veit-Haibach P, et al. Ann Oncol. 2010;21:1053–7.
220. Lee AI, Zuckerman DS, Van den Abbeele AD, et al. Cancer. 2010;116:3835–42.
221. Petrausch U, Samaras P, Haile SR, et al. Ann Oncol. 2010;21:1694–8.
222. Hoh CK, Glaspy J, Rosen P, et al. J Nucl Med. 1997;38:343–8.
223. Klose T, Leidl R, Buchmann I, Brambs HJ, Reske SN. Eur J Nucl Med. 2000;27:1457–64.
224. Cerci JJ, Trindade E, Pracchia LF. J Clin Oncol. 2010;28:1415–21.

Thyroid Nodules and Cancer: Evidence-Based Neuroimaging

39

Manjiri Dighe

Contents

M. Dighe
Department of Radiology, University of Washington Medical Center, Seattle, WA, USA
e-mail: dighe@uw.edu

Key Points

- Thyroid nodules are common and are commonly benign (strong evidence).
- Ultrasound is the most sensitive and specific imaging method for evaluation of thyroid nodules detected by other imaging methods (moderate evidence).
- Fine-needle aspiration is the most accurate method in evaluation of a nodule (strong evidence).
- Ultrasound features are helpful in determining the risk of cancer in a given nodule and hence to screen nodules to decide which nodules should undergo FNA (moderate evidence).

Epidemiology

Thyroid nodules are very common. The prevalence of thyroid nodules largely depends on the method of screening and the population evaluated. Increasing age, female sex, iodine deficiency, and a history of head and neck radiation seem to increase the risk of thyroid nodules [1, 2]. The Danish investigation on iodine intake and thyroid disease monitors the iodine fortification program in Denmark [3]. They observed a large population before and after iodine fortification and reported that even small changes in iodine intake significantly influenced goiter prevalence, nodule incidence, and thyroid dysfunction [3]. Other factors, such as smoking, pregnancy, and alcohol use, also influenced goiter development. Imaizumi et al. [4] in their study on atomic bomb survivors found the prevalence of solid nodules, malignant tumors, benign nodules, and cysts of the thyroid was 14.6 %, 2.2 %, 4.9 %, and 7.7 %, respectively. A significant linear dose–response relationship was observed for the prevalence of all solid nodules, malignant tumors, benign nodules, and cysts ($p < 0.001$). The investigators estimated that about 28 % of all solid nodules, 37 % of malignant tumors, 31 % of benign nodules, and 25 % of cysts were associated with radiation exposure at a mean and median thyroid radiation dose of 0.449 sieverts (Sv) and

0.087 Sv, respectively [4]. The increasing use of imaging has increased the number of thyroid nodules detected incidentally. Autopsy and prospective US studies in North America have shown a prevalence of thyroid nodules in 50 % and 67 % of patients, respectively [5, 6]. A study comparing US and clinical examination showed that 46 % of the nodules detected by US would not be detected by clinical examination alone [7]. Most of these nodules are benign with a prevalence of thyroid cancer reported in the range of 1.2–2.6 per 100,000 men and 2.0–3.8 cases per 100,000 in women [8]. The incidence of thyroid cancer in the population has increased from 3.6 per 100,000 in 1,073 to 8.7 per 100,000 in 2002 in the USA [9]. However, most of this increase in thyroid cancer was due to an increased detection of small papillary cancers. In autopsy studies, clinically silent thyroid papillary microcarcinomas (<1 cm in diameter) have been reported in up to 36 % of patients [10]; however, a comparison with the incidence rates for clinically apparent papillary carcinomas suggests that most papillary microcarcinomas will not lead to clinically apparent thyroid carcinomas. A follow-up study of papillary microcarcinomas over a 9-year period also did not show any metastasis in patients with tumors <0.8 mm [11, 12]. The risk of cancer in thyroid nodules ranges from a 48 % likelihood of malignancy in a solitary solid nodule with punctuate calcifications in a man to a likelihood of <3 % in a noncalcified, predominantly cystic nodule in a woman [13].

Overall Cost to Society

Since thyroid nodules are seen in greater than 50 % of the population, performing FNA on all these nodules is quite impossible. An estimated 250,000–300,000 new nodules were identified in the United States in 2007, and only about 18,000 turned out to be malignant. US-guided FNA procedure for a single thyroid nodule costs $624, while a US exam of the thyroid gland costs $233 per Seattle area estimated Medicare reimbursement rates. Thus, if a patient undergoes a US exam and an FNA, the average cost for

thyroid nodule evaluation exceeds $800. Since the yearly incidence of thyroid nodules in the US population is about 232,000–282,000, approximately $225 million is spent every year to diagnose benign nodules. Thus, to diagnose every malignant nodule, more than $12,000 ($225 M/18,000 malignant nodules detected) is spent to detect and exclude the benign nodules. A study by Gharib and Goellner et al. in 1993 concluded that because cytologic examination offers the most direct and specific information, FNA should be the initial recommended test. Savings in cost of care per patient after the introduction of FNA was estimated to be more than $1,200 [14]. Ultrasound is very helpful to screen for nodules with high-risk features that can then get an FNA, decreasing the overall cost to the society.

Goals of Imaging

The main goal of imaging is to assess the features of thyroid nodules that are associated with malignancy. Currently, ultrasound is the most accurate modality for determining high-risk features which can then be used to decide which nodules should undergo FNA.

Methodology

A MEDLINE search was performed using PubMed (National Library of Medicine, Bethesda, Maryland) for original research publications discussing thyroid nodules, thyroid malignancy, and diagnostic performance and effectiveness of imaging strategies of the thyroid. The search covered the years 1980 to March of 2011. The search strategy employed different combinations of the following terms: (1) thyroid nodules, (2) thyroid incidentalomas, (3) ultrasound or iodine scan or imaging, and (4) thyroid cancer or papillary carcinoma. Additional articles were identified by reviewing the reference lists of relevant papers. This review was limited to human studies and the English language literature. The author performed an initial review of

the titles and abstracts of the identified articles followed by review of the full text in articles that were relevant.

Discussion of Issues

Thyroid Incidentaloma: How Should They Be Evaluated?

Summary
Thyroid incidentalomas are defined as lesions that are nonpalpable but seen on imaging studies performed for indications other than evaluation of the thyroid gland. These studies include imaging exams like ultrasound performed for carotid evaluation and CT, MRI, and PET for nonthyroid malignancies. The problem generated is not trivial from either the patient's point of view or that of the resulting general medical socioeconomic burden. The yearly incidence of differentiated thyroid cancers is increasing due, in part, to more frequent detection of small nonpalpable nodules on cross-sectional imaging examinations performed for unrelated indications [15]. CT and MRI do not provide adequate detail for characterization of these nodules. Established ultrasound guidelines exist to suggest suspicious features in nodules, and hence, US is essential for characterization of the nodule (strong evidence).

Supporting Evidence
Thyroid incidentalomas are seen in 16 % of cross-sectional studies like CT and MRI [16, 17], 9.4–27 % of carotid duplex ultrasound exams [18], and 3–4 % of PET scans [19]. Thyroid carcinoma is the most frequent type of endocrine cancer in the United States, with 33,500 new cases diagnosed each year but only 1,500 deaths annually, mainly due to uncommon, aggressive forms of the disease [20]. The frequency of thyroid incidentalomas has ranged from as low as 2 % to as high as 67 % [5, 21, 22]. The vast majority of cases are ultimately diagnosed as benign colloid nodules, cysts, or adenomas, whereas approximately 5 % of nodules are malignant [23]. A limited number of CT- and

MRI-based studies have examined the prevalence of incidental thyroid nodules.

However, in a study by Shetty et al. [16] of nodules detected on CT with follow-up ultrasound, the authors found no reliable CT feature to help distinguish benign from malignant nodules. As noted in their article, thyroid nodules detected on chest CT are typically small and often too small to characterize accurately. Even larger incidental nodules detected on CT may be difficult to characterize because the CT was not performed specifically to address the thyroid and the entire gland may not be imaged. For example, on chest CT, the patient's arms are positioned over the head, which often results in beam-hardening artifact through the thyroid as a result of high-density IV contrast material in the sub-clavian veins. The clavicle can also cause artifact through the thyroid gland. These artifacts can obscure nodules or create pseudolesions. In addition, small nodules would be difficult to characterize on CT unless thin collimation and multiplanar reconstruction were available. Routine chest CT is usually performed with 3- to 5-mm slice thickness, not ideal for characterizing nodules less than 1 cm in size. Yoon et al. [24] examined 734 patients without known thyroid disease using 16-MDCT contrast-enhanced scans of the neck and found thyroid nodules in 16 % of the subjects. They also found that 9 % of these incidentalomas were malignant, with some diagnostic CT features, such as nodular or rim calcifications, anteroposterior to transverse diameter ratio above 1.0, and mean attenuation value on contrast-enhanced scans greater than 130 HU. However, they do recommend that further evaluation of a thyroid nodule detected on neck CT should be performed with ultrasound and/or biopsy.

In the study by Shetty et al. [16], 230 patients with abnormal findings in the thyroid on CT underwent ultrasound, and 118 ultimately underwent biopsy or resection. The CT and sonography images were reviewed and correlated. CT matched the sonography findings in 53 % of patients. CT correctly identified the dominant nodule but missed the multinodularity in 30 % of patients. CT overestimated the number of nodules in 2.2 % and was false positive for lesions in 4.3 %. The prevalence of malignancy in these incidentally detected nodules was 3.9 %, with a 7.4 % rate of malignant potential [16]. The authors also report that although nodules may appear homogeneously cystic on CT, on sonography the same nodules may appear as complex cystic or solid nodules of varying echogenicity. No simple density threshold on CT could distinguish simple cysts from complex cystic or solid nodules. Since CT also underestimated the number of nodules relative to sonography in several cases, the authors suggested that sonography is a useful follow-up study after incidental detection of a thyroid nodule on CT [16].

The imaging appearance of thyroid nodules on MRI has been described; however, no studies were found in the literature to compare the sensitivity and specificity of MR with standard exam like ultrasound (insufficient evidence).

Ultrasound (US) has been suggested to be the "gold standard" investigation for evaluation of thyroid nodules and incidentalomas (in [62]). Nonpalpable thyroid nodules are detected by US in 13–50 % of the general population approaching the incidence detected on autopsy [25]. Sensitivity and specificity of ultrasound to differentiate benign and malignant thyroid nodules has been reported to be 89–97 % and 16–43 %, respectively, in various studies [26]. Various ultrasound imaging features associated with malignancy include microcalcifications, hypoechogenicity, irregular margins or absent halo sign, solid pattern, intranodular vascularization, and shape (taller than wide). These in isolation do not have sufficient predictive value; however, multiple patterns taken together increase the specificity for diagnosing malignancy [26–30] (Table 39.1).

Which Nodules Should Undergo Fine-Needle Aspiration?

Summary
Characteristics of thyroid nodules on ultrasound that could suggest malignancy include solid hypoechoic nodule, a taller-than-wide shape, an

irregular shape, a spiculated margin, a blurred or indistinct margin, marked hypoechogenicity, micro- and macro-calcifications, a disrupted calcified rim, and an intranodular vascular pattern. Sonographic features of benignity are isoechogenicity, completely cystic appearance, and a spongiform appearance. Since no one parameter is sufficiently sensitive or specific for differentiation between benign and malignant nodules, combinations of features used in some studies may not show the same sensitivity and specificity when applied at other centers, and since the interobserver reliability is variable, the use of a "classic pattern" approach to nodule assessment may not be advisable (strong evidence). However, these features can be used to decide if a nodule is suspicious enough to undergo FNA. FNA is considered the most reliable diagnostic test for evaluation of thyroid nodules and has low rate of complications when US guidance is used [31]. FNAB on every thyroid nodule detected with ultrasound is not cost-effective because of the high prevalence of nodules (limited evidence) [32]. Multiple guidelines exist to decide if a nodule should undergo FNA. Some of these include the Society of Radiologists in Ultrasound (SRU) [33], American Thyroid Association (ATA) [34], and American Association of Clinical Endocrinologists (AACE) [35]. Any of these guidelines can be used to decrease the number of FNAs being performed especially on benign nodules; however, the decision as to which guideline should be used should be made in combination with the referring endocrinologists. However, scientific review shows that the AACE guidelines were recommended for achieving high specificity and the Kim criteria for achieving high sensitivity [36] (moderate evidence).

Supporting Evidence
Many studies have been published in which the ability to predict whether a thyroid nodule is benign or malignant on the basis of US findings was assessed [37–46]. Nodule size is not predictive of malignancy [38, 39]. Several US features have been found to be associated with an increased risk of thyroid cancer, including presence of calcifications, hypoechogenicity, irregular margins, absence of a halo, predominantly solid composition, and intranodule vascularity. However, the sensitivities, specificities, and negative and positive predictive values for these criteria are extremely variable from study to study, and no single US feature has both a high sensitivity and a high positive predictive value for thyroid cancer. The feature with the highest sensitivity, in the range of 69.0–75.0 %, is solid composition; however, this feature has a fairly low positive predictive value of 15.6–27.0 %. The feature with the highest positive predictive value, 41.8–94.2 %, is the presence of microcalcifications; however, this feature has low sensitivity and is found only in 26.1–59.1 % of cancers. The combination of factors improves the positive predictive value of US to some extent [39, 40]. In particular, a predominantly solid nodule (<25 % cystic) with microcalcifications has a 31.6 % likelihood of being cancer, as compared with a predominantly cystic nodule (>75 % cystic) with no calcification, which has a 1.0 % likelihood of being cancer [33]. Experienced radiologists are able to evaluate nodules on ultrasound with a high consistency; however, the variability in inexperienced radiologists can be significant. In a study by Choi et al., there was only slight interobserver agreement in assessment of echogenicity ($K = 0.34$), a fair agreement in composition, margin, calcification, and final assessment ($K = 0.59, 0.42, 0.58,$ and 0.54, respectively), and shape and vascularity showed substantial agreement ($K = 0.61$ and 0.64, respectively) [47]. Multiple guidelines exist to help decide if a particular nodule should be chosen for FNA or not. These include the Society of Radiologists in Ultrasound guidelines [33], American Thyroid Association [34], American Association of Clinical Endocrinologists [35], and Kim criteria [38]. Controversy exists as to which guidelines are most accurate. A recent study by Ahn et al. comparing three sets of guidelines – SRU, AACE, and Kim criteria – found that Kim and AACE criteria are more accurate than the SRU criteria. The AACE guidelines were recommended for achieving high specificity and the Kim criteria for achieving high sensitivity [36].

The guidelines used at a particular institution should be based on consensus with the endocrinologist, surgeon, and pathologist.

Fine-Needle Aspiration of Thyroid Gland: Safety and Efficacy

Summary

FNA of the thyroid is a very safe procedure with a very small number of rare complications reported in the literature. The incidence of complications increases with increasing needle size. For superficial fine-needle aspiration, minor complications similar to blood drawing occur and are typically restricted to local pain and slight ecchymosis. Small asymptomatic hematomas are common and resolve without treatment. Other complications like recurrent laryngeal nerve paralysis and tumor seeding are also rarely seen (limited evidence). Accuracy for diagnosis of papillary carcinoma is also very high; however, FNA suffers from inability to differentiate between follicular adenoma and follicular carcinoma (strong evidence).

Supporting Evidence

Local pain or bruising can be seen after fine-needle aspiration and can be treated with an ice pack. There are a few case reports of significant hematoma post FNA [48–50]. In a review by Polyzos et al., the reported incidence of blood extravasation-related complications during or after FNA ranged between 1.9 % and 6.4 % in different studies. This variability was suggested to be possibly due to definition or record biases. Intranodular hemorrhage within the cystic part of complex nodules following fluid aspiration seemed to be most frequent. Seven cases of post-FNA life-threatening massive hematomas resulting in airway obstruction were found as well as four described cases with secondary hemangioma attributed to FNA [51]. While several large FNA series have failed to report on RLN paralysis, Tomoda et al. reviewed over 10,000 FNAs with 23-gauge needle with documentation of four patients with vocal cord paralysis, a rate of 0.036 % [52]. The voice change typically

occurred 1–2 days after FNA procedure, and all cases were transient with average resolution in 4 months [52]. Hulin noted in a case report of a patient with FNA-induced RLN paralysis increased fibrosis around the RLN at surgery with increased difficulty of surgical dissection [53]. It is this author's experience that if cystic fluid in a thyroid lesion, through either FNA or trauma, leaks out of the thyroid cyst into surrounding structures, subsequent dissection can be very challenging. Needle track seeding after thyroid FNA has been reported but is a rare event if appropriate precautions are taken – e.g., releasing vacuum before removing the needle. Basu et al. report a case of FNA in a complex cyst with a 22-gauge needle causing a discharging sinus at needle insertion site which was then diagnosed as a well-differentiated papillary carcinoma infiltrating skin and strap muscles [54]. Karowski et al. in their case found local metastases in the skin and sternocleidomastoid muscle 3 years after FNA of the primary malignancy [55]. Wu, in a review of FNA of multiple sites including thyroid, noted that worldwide literature review as of 2004 has revealed a total of 12 cases of tumor seeding referable to FNA [56]. They found increased risk with larger-gauge needle (19–21 gauge) and virtually no risk with 23 gauge or smaller.

The accuracy rate for diagnosing papillary carcinoma with FNA ranges from 90 % to 100 % [57, 58]. Ashcraft and Van Herle studied a series of 9,161 cases of thyroid FNA with false-negative and false-positive rates of 1.6 % and 0.9 %, respectively, for FNA [59]. It is well established in literature that thyroid FNA cannot distinguish between follicular adenoma and carcinoma with only 10–20 % cases diagnosed as follicular neoplasms on FNA found to be malignant on histologic examination [60]. In a study by Lew et al. which included 797 patients, the FNA results included 147 (18 %) positive for malignancy, 255 (32 %) benign, 358 (45 %) indeterminate, and 37 (5 %) nondiagnostic. The overall malignancy rate on final histopathology was 369 of 797 (46 %). Overall, there was a false-positive rate of 2 % and false-negative rate of 8.6 %. Among the 358 indeterminate FNA results,

carcinoma was found in 81 (36 %) of 223 follicular neoplasms, 18 (36 %) of 50 Hürthle cell neoplasms, and 78 (92 %) of 85 that were suspicious for papillary thyroid cancer. When FNA was nondiagnostic, cancer was present in 9 of 37 (24 %). Among 39 patients with benign FNA who had cancer on final histopathology, 22 of 255 (8.6 %) had cancer in the index thyroid nodule, and 81 % of cancers were <1 cm [61].

FDG-PET-Positive Thyroid Incidentalomas

Summary

PET and combined PET/CT are increasingly used in staging of malignancies, and thyroid lesions with focally increased uptake may be incidentally seen. Katz and Shaha coined the term PET-associated incidental neoplasm (PAIN) to describe such lesions [19]. A thyroid lesion with focally increased uptake has a higher risk of malignancy. It may be necessary to evaluate a thyroid lesion with focal uptake with ultrasound and fine-needle aspiration evaluation. This decision should be based on three factors: (1) prognosis of the primary disease, avoiding further investigation in patients with widespread distant metastasis and overall poor prognosis from the index tumor; (2) pattern of FDG uptake with focal uptake being more suspicious of a neoplastic process; and (3) clinical risk factors or a palpable nodule which have a higher likelihood of harboring a malignancy [62]. The relationship between likelihood of malignancy and standard uptake value (SUV) is debatable [19] (moderate evidence).

Supporting Evidence

Thyroid incidentalomas with focal increased FDG uptake are found in 1.2–4.3 % of PET examinations [21, 22, 63, 64]. Malignancy rates for hypermetabolic lesion in the thyroid range from 14 % to 47 % [21, 22, 63, 65–68]. This variable range for malignancy is due to the fact that the fine-needle aspiration rate in various studies ranged from 15 % to 83 % [62]. Malignant lesions are likely to have higher SUV values;

however, there is considerable overlap in uptake levels between malignant and benign lesions. The range for malignant lesions ranged from 6.4 to 14.2 and for benign lesions ranged from 3.3 to 8.2 in various studies [21, 22, 63, 65–67, 69]. This variability is suggested to be due to benign oncocytic lesions like Hurthle cell adenomas, which have a higher number of mitochondria and hence high metabolic activity [62]. Published data suggests that PET-detected thyroid cancers tend to be more aggressive: 50 % comprise of aggressive variants like tall cell, insular, or Hurthle cell tumors [67].

Staging and Monitoring of Thyroid Malignancy

Summary

Ultrasound is routinely used for preoperative staging of patients with papillary thyroid carcinoma (PTC). CT appears to have equal sensitivity as US and can be complimentary to US in evaluating for lateral neck nodes. MRI does not appear to have enough sensitivity as a screening tool especially in patients with recurrent papillary carcinoma; however, it has better accuracy in evaluating for extracapsular extension of the primary tumor. PET/CT is less accurate when compared to US and CT for the initial evaluation of cervical node levels in patients with papillary thyroid carcinoma; however, it has better sensitivity in patients with recurrent PTC than CT (strong evidence).

Supporting Evidence

Shimamoto et al. evaluated the usefulness of ultrasound for preoperative staging of thyroid papillary carcinoma in 77 patients and found that ultrasound was able to estimate the T categories accurately with a sensitivity of 77.8 % for depicting tumor extension into the prethyroidal muscle and/or the sternocleidomastoid muscle and a sensitivity of 42.9 % and 28.6 %, respectively, for invasion into the trachea and the esophagus. The N categories were underestimated in 36 of the 77 patients [70]. Takes et al. in their multicenter study compared

the value of US with US-guided FNA to CT in detection of regional metastases in clinically negative neck and found that US-guided FNA had a sensitivity of 48 %, specificity of 100 %, and overall accuracy of 79 %, while CT had a sensitivity of 54 %, specificity of 92 %, and overall accuracy of 77 % [71]. In a study by Moon et al. comparing the positive predictive value and interobserver variability of US in preoperative staging of thyroid carcinoma, the T staging, bilaterality, and N1b staging of preoperative staging sonography showed high PPV. Agreements for T and N staging, multifocality, and bilaterality were moderate, substantial, and excellent, respectively [72].

A study by Choi et al. compared the diagnostic accuracy of ultrasound with that of CT in preoperative evaluation of primary tumors and cervical lymph nodes in patients with papillary thyroid carcinoma. Their study consisted of 299 consecutively registered patients with pathologically proven papillary thyroid carcinoma. Ultrasound was more accurate than CT in prediction of the presence of extrathyroidal tumor extension and of malignant disease in both thyroid lobes ($p < 0.05$) for overall lesions and for the two subgroups. In prediction of central node (neck level VI) metastasis, CT had greater sensitivity than ultrasound alone ($p = 0.04$) for overall lesions. Although the combination of ultrasound and CT had greater sensitivity than ultrasound alone in prediction of the presence of central node metastasis in the two subgroups, the sensitivity of the combination of ultrasound and CT did not reach statistical significance for papillary thyroid microcarcinoma. Ultrasound alone and ultrasound with CT had greater sensitivity than CT in prediction of lateral node (levels II–V) metastasis, but there was no significant difference in diagnostic value between ultrasound and the combination of ultrasound and CT for overall lesions or for the two subgroups [73]. Kim et al. in their 165 consecutive patients found that in terms of predicting node metastases, overall sensitivity, specificity, accuracy, positive predictive value, and negative predictive value of US were 51 %, 92 %, 77 %, 81 %, and 76 %, respectively. Those of CT were 62 %, 93 %, 81 %, 84 %, and 80 %, respectively,

and those of US = CT were 66 %, 88 %, 79 %, 77 %, and 81 %, respectively, at all neck levels. US = CT significantly increased sensitivity and demonstrated similar specificity compared with US alone in lateral neck levels. US = CT increased sensitivity but decreased specificity compared with US alone in the central neck levels. CT provided additional benefit for detecting metastatic nodes at more than one level in 8 % of all patients, in 14 % of patients with suspected nodal metastasis on US, and in 25 % of patients with metastatic lymph nodes. They found that the combination of US/CT was superior to US alone for detection of metastatic lymph nodes in the lateral neck levels in PTC patients [74]. Ahn et al. found similar results in their study and concluded that the combination of US and CT was superior to US or CT alone [75].

King et al. in their study compared MRI and US of the neck in staging papillary thyroid carcinoma and found MR was superior in accessing extracapsular extension especially into the trachea; however, ultrasound was superior in detecting the primary lesion, multifocal disease, and cervical lymph nodes [76]. Gross et al. used MRI for detection of cervical metastasis from differentiated thyroid carcinoma and found that the average overall percent sensitivity, specificity, positive predictive value (PPV), negative predictive value (NPV), and accuracy of MR imaging were 95 %, 51 %, 84 %, 78 %, and 83 %, respectively; however, due to the low specificity of MR, it would not be a useful screening tool [77].

Jeong et al. in their study comparing PET/CT with US and CT found that PET/CT showed a sensitivity of 30.4 %, a specificity of 96.2 %, and a diagnostic accuracy of 86.9 %. The corresponding values for US and CT were 41.3 %, 97.4 %, 89.1 % (US) and 34.8 %, 96.2 %, 87.2 % (CT). This suggested that integrated PET/CT does not provide any additional benefit when compared to US and CT for the initial evaluation of cervical node levels in patients with papillary thyroid carcinoma [78]. Lee et al. had similar findings in their study which compared CT and PET/CT and found that CT was more sensitive and accurate than PET/CT for detecting lymph nodes in recurrent PTC [79].

Take-Home Tables and Figures

See Figs. 39.1 and 39.2 for workup of thyroid incidentalomas and management of thyroid nodules based on fine-needle aspiration (FNA), respectively. See Table 39.1 for specificity and sensitivity of various features to diagnose malignancy.

Imaging Case Studies

Case 1: Incidentally detected thyroid nodule on CT (Fig. 39.3)
Case 2: Incidentally detected thyroid nodule on MRI (Fig. 39.4)

Case 3: FDG-PET-positive thyroid nodule (Fig. 39.5)

Suggested Imaging Protocols

Ultrasound

Ultrasound should be performed using a linear high-frequency transducer ideally between 10 and 17 MHz. Images should be obtained in transverse and sagittal orientation with documentation of any nodules in the thyroid gland. Measurements of the thyroid gland and nodules should be performed. Vascularity of the gland and the nodule should be assessed.
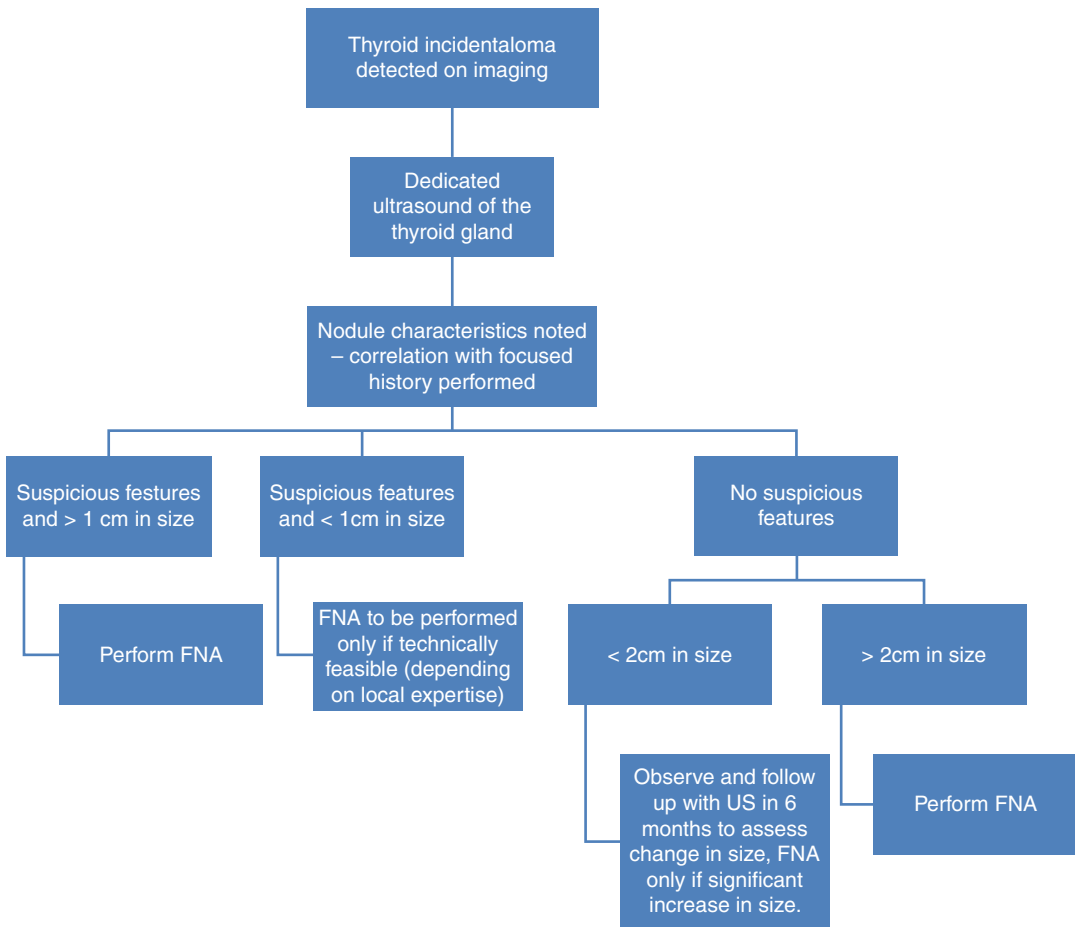
Fig. 39.1 Workup of thyroid incidentalomas
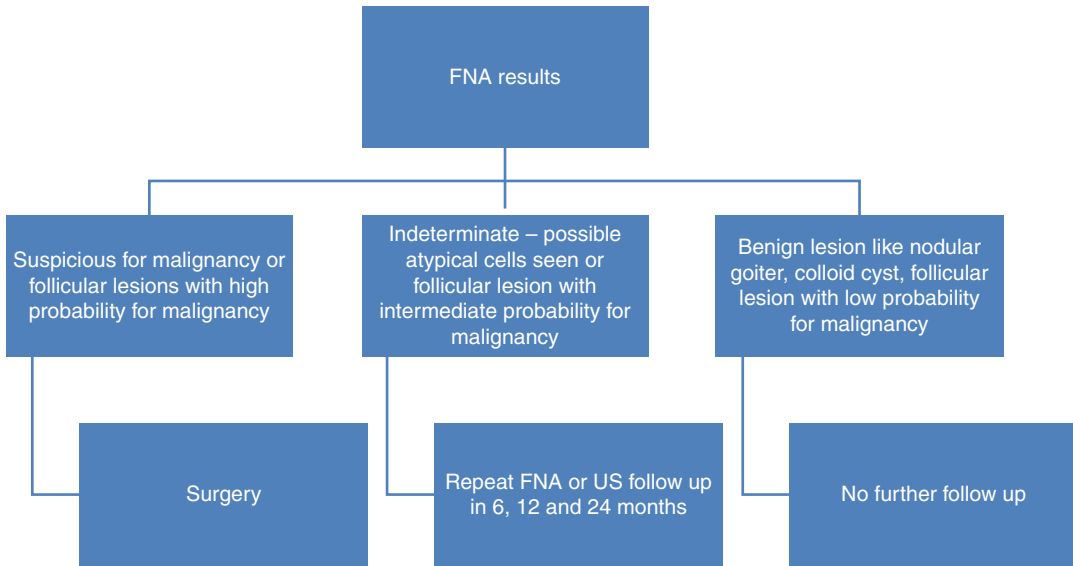
Fig. 39.2 Management of thyroid nodules based on fine-needle aspiration (FNA)

Table 39.1 Specificity and sensitivity of various features to diagnose malignancy. Combination of features like microcalcifications and irregular margin appears to increase the specificity even though the sensitivity may decrease

	Sensitivity (%)	Specificity (%)
Microcalcifications	40	90
Absence of halo	66	46
Irregular margins	64	84
Hypoechoic	83	49
Incr. intranodular flow	70	65
MicroCa + irreg margin	30	95
MicroCa + hypoechoic	28	95
Solid + hypoechoic	73	69

Fine-Needle Aspiration

Fine-needle aspiration should be performed with real-time ultrasound guidance. A 22- or 25-gauge needle is to be used and samples should be obtained with capillary action or aspiration. Local anesthetic may be used at the operator's discretion. Smears of the samples can be performed immediately if a cytotechnologist is available or the sample may be sent in solution to the cytopathologist for further processing.

Future Research

- Cost-effectiveness analysis for follow-up of thyroid nodules instead of fine-needle aspiration. At present, there are limited studies on cost-effectiveness of performing ultrasound instead of fine-needle aspiration of thyroid nodules.
- Cost-effectiveness and outcome for nonaggressive management of papillary thyroid microcarcinomas (PTMC). Management of PTMCs is controversial with some preferring to resect all papillary carcinomas regardless of size while some preferring to manage these conservatively. The true incidence of metastases in the long term is not known, and further studies are necessary to assess the actual risk in nonaggressive management of PTMCs.
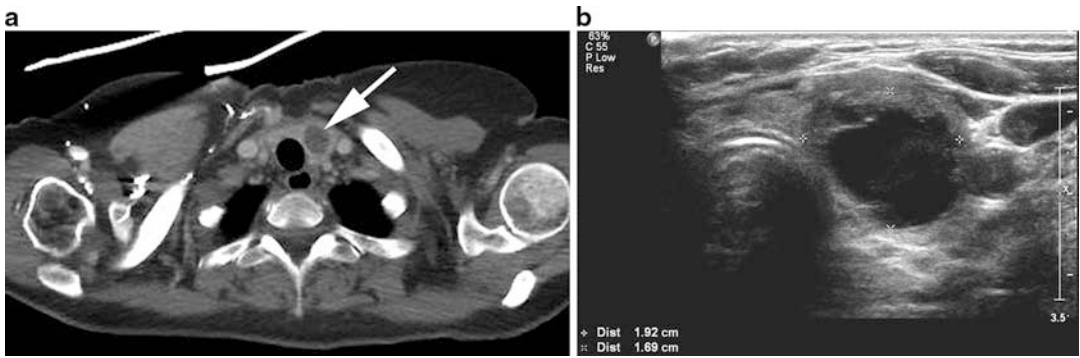
Fig. 39.3 (**a**, **b**) Case 1: Incidentally detected thyroid nodule on CT. A small hypodense mass (*arrow*) was seen in the left thyroid lobe on CT (**a**) performed for staging of patients known lymphoma. This was indeterminate and did not show any enhancement or calcifications within it. An ultrasound (**b**) was performed for further characterization and showed a predominantly cystic thyroid nodule (calipers). FNA of this lesion is not recommended due to the small size and predominantly cystic appearance
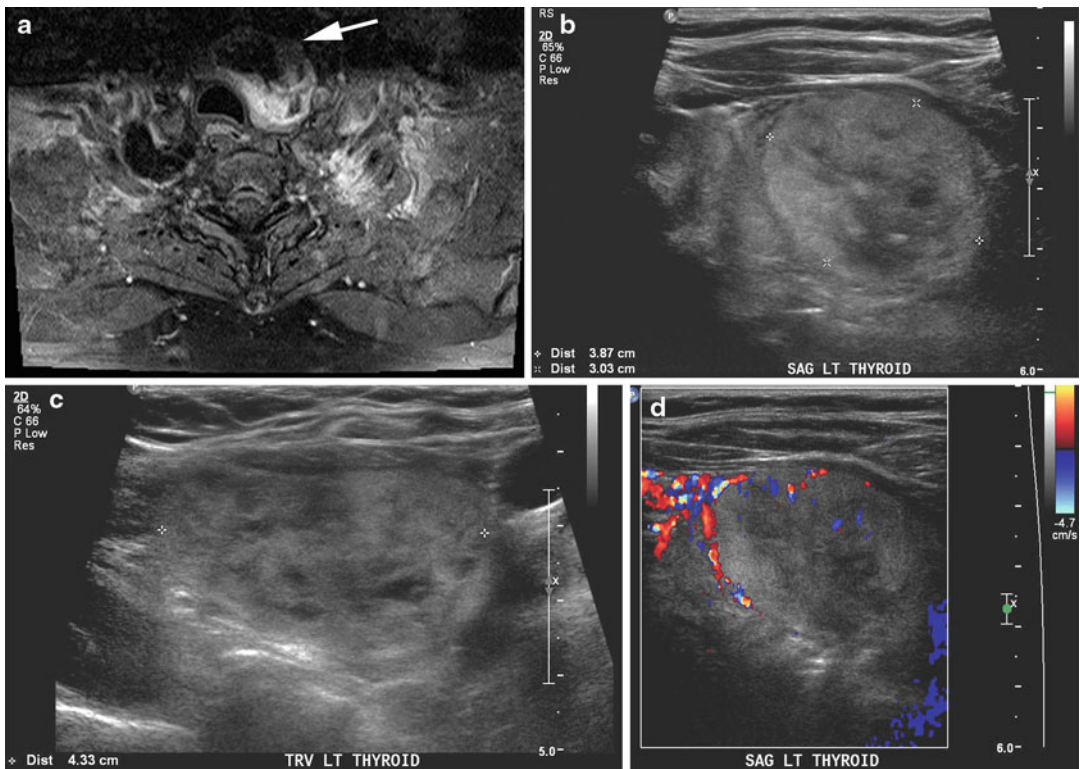
Fig. 39.4 (**a**–**d**) Case 2: Incidentally detected thyroid nodule on MRI. A thyroid nodule was seen incidentally on a MRI (**a**) performed for the cervical spine (*arrow*). Due to the inability of MRI to characterize this lesion and incomplete visualization due to a different anatomic part being scanned on MRI, ultrasound (**b**, **c**) was performed which showed a large predominantly solid isoechoic nodule in the left thyroid lobe. Minimal internal vascularity was seen on color Doppler image (**d**). FNA of this nodule is indicated and showed a benign follicular lesion likely an adenoma on cytopathology
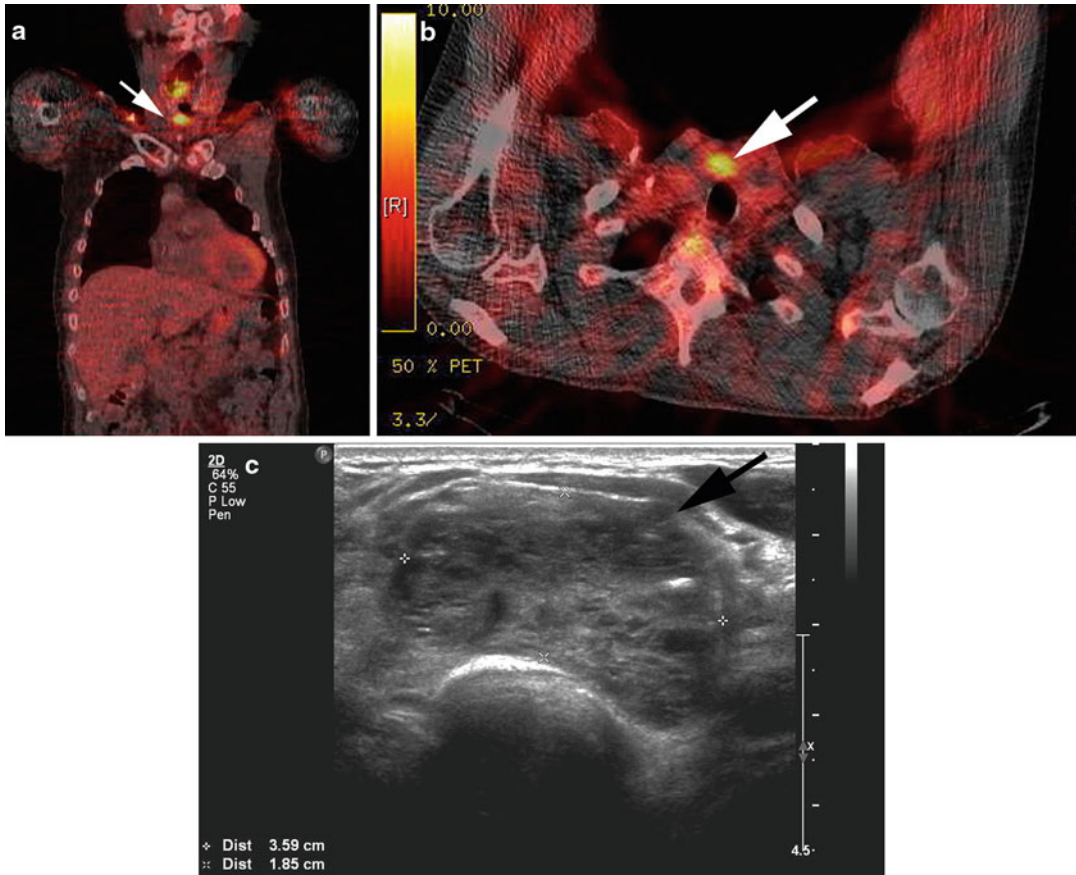
Fig. 39.5 (**a, b**) Case 3: FDG-PET-positive thyroid nodule. Uptake in a thyroid nodule (*arrow*) was seen on a FDG-PET scan (**a, b**) performed for staging of colonic carcinoma. An ultrasound (**c**) performed showed a solid mass in the thyroid gland corresponding to the location seen on the PET scan with calcifications in it (*black arrow*). FNA of this lesion was performed which showed a papillary carcinoma on cytopathology

References

1. Gharib H. Endocrinol Metab Clin North Am. 1997;26(4):777–800.
2. Rojeski MT, Gharib H. N Engl J Med. 1985;313(7): 428–36.
3. Laurberg P, Jørgensen T, Perrild H, et al. Eur J Endocrinol. 2006;155(2):219–28.
4. Imaizumi M, Usa T, Tominaga T, et al. JAMA. 2006;295(9):1011–22.
5. Ezzat S, Sarti DA, Cain DR, Braunstein GD. Arch Intern Med. 1994;154(16):1838–40.
6. Mortensen JD, Bennett WA, Woolner LB. Surg Forum. 1955;5:659–63.
7. Brander A, Viikinkoski P, Tuuhea J, Voutilainen L, Kivisaari L. J Clin Ultrasound. 1992;20(1):37–42.
8. Nagataki S, Nyström E. Thyroid. 2002;12(10): 889–96.
9. Davies L, Welch HG. JAMA. 2006;295(18):2164–7.
10. Colonna M, Guizard AV, Schvartz C, et al. Eur J Cancer. 2007;43(5):891–900.
11. Harach HR, Franssila KO, Wasenius VM. Cancer. 1985;56(3):531–8.
12. Roti E, Rossi R, Trasforini G, et al. J Clin Endocrinol Metab. 2006;91(6):2171–8.
13. Frates M, Benson C, Doubilet P, et al. J Clin Endocrinol Metab. 2006;91(9):3411–17.
14. Gharib H, Goellner JR. Endocr Pract. 1995;1(6): 410–17.
15. Chen AY, Jemal A, Ward EM. Cancer. 2009;115(16): 3801–7.
16. Shetty SK, Maher MM, Hahn PF, Halpern EF, Aquino SL. AJR Am J Roentgenol. 2006;187(5):1349–56.

17. Youserm DM, Huang T, Loevner LA, Langlotz CP. AJNR Am J Neuroradiol. 1997;18(8):1423–8.
18. Steele SR, Martin MJ, Mullenix PS, Azarow KS, Andersen CA. Arch Surg. 2005;140(10):981–5.
19. Katz SC, Shaha A. J Am Coll Surg. 2008;207(2):259–64.
20. National Cancer Institute Website. Available from: www.cancer.gov/ncicancerbulletin/NCI_Cancer_Bulletin_021908/page3
21. Cohen MS, Arslan N, Dehdashti F, et al. Surgery. 2001;130(6):941–6.
22. Kang KW, Kim SK, Kang HS, et al. J Clin Endocrinol Metab. 2003;88(9):4100–4.
23. Desser TS, Kamaya A. Neuroimaging Clin N Am. 2008;18(3):463–78. vii. review.
24. Yoon DY, Chang SK, Choi CS, et al. J Comput Assist Tomogr. 2008;32(5):810–15.
25. Ross DS. J Clin Endocrinol Metab. 2002;87(5):1938–40.
26. Rago T, Vitti P, Chiovato L, et al. Eur J Endocrinol. 1998;138(1):41–6.
27. Brkljačić B, Cuk V, Tomić-Brzac H, Bence-Zigman Z, Delić-Brkljačić D, Drinković I. J Clin Ultrasound. 1994;22(2):71–6.
28. Takashima S, Fukuda H, Kobayashi T. J Clin Ultrasound. 1994;22(9):535–42.
29. Kim EK, Park CS, Chung WY, et al. AJR Am J Roentgenol. 2002;178(3):687–91.
30. Papini E, Guglielmi R, Bianchini A, et al. J Clin Endocrinol Metab. 2002;87(5):1941–6.
31. De Fiori E, Rampinelli C, Turco F, Bonello L, Bellomi M. Radiol Med. 2010;115(4):612–18.
32. Tan G, Gharib H. Ann Intern Med. 1997;126(3):226–31.
33. Frates M, Benson C, Charboneau J, et al. Radiology. 2005;237(3):794–800.
34. Cooper DS, Doherty GM, Haugen BR, et al. Thyroid. 2009;19(11):1167–214.
35. Gharib H, Papini E, Paschke R, et al. J Endocrinol Invest. 2010;33(5 Suppl):1–50.
36. Ahn SS, Kim EK, Kang DR, Lim SK, Kwak JY, Kim MJ. AJR Am J Roentgenol. 2010;194(1):31–7.
37. Khoo M, Asa S, Witterick I, Freeman J. Head Neck. 2002;24(7):651–5.
38. Kim E, Park C, Chung W, et al. AJR Am J Roentgenol. 2002;178(3):687–91.
39. Papini E, Guglielmi R, Bianchini A, et al. J Endocrinol Metab. 2002;87(5):1941–6.
40. Peccin S, de Castsro J, Furlanetto T, Furtado A, Brasil B, Czepielewski M. J Endocrinol Invest. 2002;25(1):39–43.
41. Chan BK, Desser TS, McDougall IR, Weigel RJ, Jeffrey RB. J Ultrasound Med. 2003;22(10):1083–90.
42. Wienke J, Chong W, Fielding J, Zou K, Mittelstaedt C. J Ultrasound Med. 2003;22(10):1027–31.
43. Nam-Goong I, Kim H, Gong G, et al. Clin Endocrinol (Oxf). 2004;60(1):21–8.
44. Alexander E, Marqusee E, Orcutt J, et al. Thyroid. 2004;14(11):953–8.
45. Ahuja A, Chick W, King W, Metreweli C. J Clin Ultrasound. 1996;24(3):129–33.
46. Iannuccilli J, Cronan J, Monchik J. J Ultrasound Med. 2004;23(11):1455–64.
47. Choi SH, Kim EK, Kwak JY, Kim MJ, Son EJ. Thyroid. 2010;20(2):167–72.
48. Donatini G, Masoni T, Ricci V, et al. G Chir. 2010;31(8–9):387–9.
49. Hor T, Lahiri SW. Thyroid. 2008;18(5):567–9.
50. Noordzij JP, Goto MM. Am J Otolaryngol. 2005;26(6):398–9.
51. Polyzos SA, Anastasilakis AD. J Otolaryngol Head Neck Surg. 2010;39(5):532–41.
52. Tomoda C, Takamura Y, Ito Y, Miya A, Miyauchi A. Thyroid. 2006;16(7):697–9.
53. Hulin SJ, Harris KP. J Laryngol Otol. 2006;120(11):970–1.
54. Basu A, Sistla SC, Siddaraju N, Verma SK, Iyengar KR, Jagdish S. Acta Cytol. 2008;52(2):211–14.
55. Karwowski JK, Nowels KW, McDougall IR, Weigel RJ. Acta Cytol. 2002;46(3):591–5.
56. Wu M, Burstein DE. Cancer Invest. 2004;22(4):620–8.
57. Mandreker SR, Nadkarni NS, Pinto RG, Menezes S. Acta Cytol. 1995;39(5):898–904.
58. Oertel YC, Oertel JE. Ann Diagn Pathol. 1998;2(6):377–400.
59. Ashcraft MW, Van Herle AJ. Head Neck Surg. 1981;3(4):297–322.
60. Schlinkert RT, van Heerden JA, Goellner JR, et al. Mayo Clin Proc. 1997;72(10):913–16.
61. Lew JI, Snyder RA, Sanchez YM, Solorzano CC. J Am Coll Surg. 2011;213(1):188–94.
62. Iyer NG, Shaha AR, Silver CE, et al. Thyroid incidentalomas: to treat or not to treat. Eur Arch Otorhinolaryngol. 2010;267(7):1019–26.
63. Chen YK, Ding HJ, Chen KT, et al. Anticancer Res. 2005;25(2B):1421–6.
64. Yi JG, Marom EM, Munden RF, et al. Radiology. 2005;236(1):271–5.
65. Bogsrud TV, Karantanis D, Nathan MA, et al. Nucl Med Commun. 2007;28(5):373–81.
66. Bae JS, Chae BJ, Park WC, et al. World J Surg Oncol. 2009;7:63.
67. Are C, Hsu JF, Schoder H, Shah JP, Larson SM, Shaha AR. Ann Surg Oncol. 2007;14(1):239–47.
68. Ishimori T, Patel PV, Wahl RL. J Nucl Med. 2005;46(5):752–7.
69. Nam SY, Roh JL, Kim JS, Lee JH, Choi SH, Kim SY. Clin Endocrinol (Oxf). 2007;67(1):135–9.
70. Shimamoto K, Satake H, Sawaki A, Ishigaki T, Funahashi H, Imai T. Eur J Radiol. 1998;29(1):4–10.
71. Takes RP, Righi P, Meeuwis CA, et al. Int J Radiat Oncol Biol Phys. 1998;40(5):1027–32.
72. Moon HJ, Yoon JH, Kwak JY, et al. AJR Am J Roentgenol. 2011;197(2):W324–30.
73. Choi JS, Kim J, Kwak JY, Kim MJ, Chang HS, Kim EK. AJR Am J Roentgenol. 2009;193(3):871–8.

74. Kim E, Park JS, Son KR, Kim JH, Jeon SJ, Na DG. Thyroid. 2008;18(4):411–18.
75. Ahn JE, Lee JH, Yi JS, et al. World J Surg. 2008;32(7):1552–8.
76. King AD, Ahuja AT, To EW, Tse GM, Metreweli C. Clin Radiol. 2000;55(3):222–6.
77. Gross ND, Weissman JL, Talbot JM, Andersen PE, Wax MK, Cohen JI. Laryngoscope. 2001;111(11 Pt 1):1905–9.
78. Jeong HS, Baek CH, Son YI, et al. Clin Endocrinol (Oxf). 2006;65(3):402–7.
79. Lee DH, Kang WJ, Seo HS, et al. J Comput Assist Tomogr. 2009;33(5):805–10.

Diagnosis of Cervical Lymph Node Metastasis in Head and Neck Cancer: Evidence-Based Neuroimaging

40

Matakazu Furukawa and Yoshimi Anzai

Contents

M. Furukawa (✉) • Y. Anzai
Department of Radiology, University of Washington, Seattle, WA, USA
e-mail: matakazu@yamaguchi-u.ac.jp; anzai@uw.edu

Key Points

- Although various size and morphological criteria, such as central necrosis, extracapsular spread of tumor, and vascular findings, have been reported on CT, MR, or US, the diagnostic performance for each modality and criteria alone is limited (moderate evidence). The combination of some diagnostic criteria may improve the accuracy.
- In the evaluation of clinically N0 stage HNC, conventional radiological imaging (US, CT, spin-echo or fast spin-echo MR) shows limited sensitivity (moderate evidence). Although fluorine-18-fluorodeoxyglucose (18F-FDG) PET shows high specificity, the sensitivity in N0 patients is still suboptimal (moderate evidence).
- Although US is not routinely used for the staging of HNC, certain vascular patterns on power Doppler sonography improve diagnostic accuracy for the detection of metastatic nodes (moderate evidence). Grayscale US examination is not useful for differentiation of metastatic from benign nodes.
- Diffusion-weighted imaging (DWI) with apparent diffusion coefficient (ADC) values in combination with conventional MR criteria provides improved accuracy in differentiating benign and malignant lymph nodes, especially in small lymph nodes (limited evidence).
- Negative FDG PET CT after radiation therapy (RT) has a high negative predictive value (NPV) for residual tumor (moderate evidence). However, positive predictive value (PPV) of PET-CT is limited.

The diagnostic performance for each CT, MR, or US with size criteria alone is limited. Although the accuracy of FDG PET is slightly higher than conventional CT or MR, the effectiveness for N0 patient is still unsatisfactory. FDG PET may be useful for the assessment of treatment response of nodal metastases following CRT.

Take-Home Points

- Various imaging techniques are available for the detection of cervical nodal metastasis in patients with HNC. Diagnostic performances vary depending on imaging techniques, patient groups, and type of analysis (per node, per hemi-neck, per patient). Conventional CT and MR have limited sensitivity for detecting metastases in normal size nodes, although specificity is quite high.
- Ultrasound with power Doppler or US-guided FNA has higher diagnostic performance; however, invasiveness and cost associated with FNA prevent it from being used as a routine staging method. Operator dependency and lack of assessment of primary tumor extension are other shortcomings of US limiting its widespread use for patients with HNC.
- FDG PET is a promising imaging technique and widely integrated in the staging of patients with HNC. Generally, the accuracy of FDG PET is slightly higher than conventional CT or MR, though the effectiveness among N0 patient is still unsatisfactory.
- Diffusion-weighted imaging with quantitative assessment of ADC is potentially useful to differentiate metastatic from benign lymph nodes. This needs further investigation in a large clinical study.
- FDG PET may be useful for the assessment of treatment response following CRT in patients with HNC. PET could be used to identify patients with a favorable response who could avoid a salvage neck dissection.

Definition and Pathophysiology

Anatomy

There are more than 800 lymph nodes in the human body, and approximately 300 are located in the neck. The original nodal classification was described by a French anatomist, Rouviere, where neck lymph nodes were divided into 10 groups and each nodal group was named based on

the location [1]. These include internal jugular chain, spinal accessory chains, and submandibular, submental, and supraclavicular nodes. Other minor groups are retropharyngeal, occipital, mastoid, parotid, and facial lymph nodes. Since 1980, a simplified classification was endorsed and extensively used as the complexity of surgical management of HNC patients increased. The numeric classification improved communication among medical specialties: ear, nose, and throat (ENT) surgeons; radiation and medical oncologists; and radiologists. Based on the clinical classification of the American Joint Committee on Cancer (AJCC) and the American Academy of Otolaryngology-Head and Neck Surgery (AAO-HNS), the imaging-based nodal level classification reported by Som et al. is widely used by both clinicians and radiologists [2].

Pathology

Metastatic lymph nodes are defined as cancer spread to regional lymph node from primary HNC. As gross pathologic features, metastatic lymph nodes are often round pale nodes, and they are frequently multiple. Microscopically, a metastasis first lodges in the subcapsular sinus through afferent lymphatic vessels, then spreads through the marginal sinus, into the whole node. Once cancer within a lymph node extends through the lymph node capsule, it is called extracapsular spread. Extracapsular spread into the perinodal fat often leads to adherence of tumor to vessels or invasion of adjacent muscles. Extracapsular spread is one of the poor prognostic indicators for HNC [3–5]. A prospective study of 170 cases with H&N squamous cell carcinoma of the hypopharynx and larynx showed that the 5-year overall survival rates were 52.0 % for cases without metastases and 5.8 % when macroscopic transcapsular spread was present [3]. Central necrosis is a characteristic feature of metastatic squamous cell carcinoma. This is an area of hypodensity on contrast-enhanced CT or hypointensity on

T1-weighted, contrast-enhanced MR and indicates an area of tumor necrosis or tumor itself. Normal lymph node tissue enhances more vividly and rapidly compared with a focus of cancer. Therefore, a heterogeneous appearance of lymph nodes in patients with squamous cell carcinoma in the head and neck (H&N) is a finding of lymph node metastases [6–8]. However, not all metastatic lymph nodes contain areas of necrosis. Focal fat deposition sometimes mimics central necrosis on CT.

The staging of cervical lymph nodes according to the AJCC for H&N squamous cell carcinoma (except nasopharyngeal carcinoma) is as follows: [9]

N0: No regional nodal metastasis

N1: Single ipsilateral node ≤3 cm in greatest dimension

N2a: Single ipsilateral 3–6-cm node in greatest dimension

N2b: Multiple ipsilateral nodes ≤6 cm in greatest dimension

N2c: Bilateral or contralateral nodes ≤6 cm in greatest dimension

N3: Any nodal mass >6 cm in greatest dimension

The natural history and response to treatment of cervical nodal metastasis from the nasopharynx as the primary site is different from other head and neck malignancies, resulting in a different nodal classification scheme.

The nodal staging for nasopharyngeal carcinoma is:

N0: No regional nodal metastases

N1: Unilateral nodes ≤6 cm in greatest dimension

N2: Bilateral nodes ≤ 6 cm in greatest dimension

N3: >6 cm or supraclavicular node in greatest dimension

N3a: Lymph node (LN) metastasis >6 cm

N3b: LN metastasis to the supraclavicular fossa

(Retropharyngeal LN(s), regardless of unilateral or bilateral location, is considered N1 (AJCC staging summary in seventh edition)).

The methodology for calculating the sensitivity and specificity in the differentiation between malignant and benign lymph nodes differs between studies, with some based on the patient, some based on the neck level, and the remainder based on individual nodes.

Epidemiology

HNC constitutes a minority of cancer in the population (approximately 3–5 % of new cancer cases are in the head and neck in the United States (http://www.cdc.gov/uscs). HNC has high mortality and morbidity, including disfigurement and difficulties with speech, swallowing, and breathing [7]. HNC is generally more common in men, with a male to female ratio of approximately 2:1 except for thyroid cancer. HNC is relatively aggressive, with complex patterns of regional and distant metastases. More than 66 % of HNC patients present with advanced stage cancer (AJCC stage III–IVb) and have a 25 % chance of having distant metastases at the time of presentation [10].

Approximately 5 % of HNC patients have a second primary at diagnosis, and 20 % of patients subsequently develop second primary cancer (http://www.cdc.gov/cancer/npcr). Major risk factors include tobacco and alcohol. Abuse of both tobacco and alcohol increases the risk of developing head and neck cancer by 11-fold. Another major risk factor is human papillomavirus (HPV), particularly for oral cavity and oropharyngeal cancer (http://www.cdc.gov/cancer/hpv/statistics/headneck.htm).

The annual incidence rates of potentially HPV-associated cancers of the tonsil and base of tongue both increased significantly from 1998 to 2003 (annual percentage change [APC], 3.0), whereas the incidence rates of head and neck cancer at almost all the comparison sites generally decreased. Laryngeal cancer incidence rates declined most sharply from 4.5 % (rate is per 100,000 population) in 1998 to 3.7 % in 2003 (APC, − 3.5) [11].

The presence of nodal metastases at the time of diagnosis varies by primary tumor site. Nasopharyngeal cancer has the highest incidence of lymph node metastasis (approximately 85 %), and glottic laryngeal cancer has the lowest (less than 10 %) [8]. Accurate diagnosis of nodal metastases is of paramount importance in staging and treatment. Generally speaking, organ preservation is a more commonly accepted strategy for advanced stage HNC, and primary surgery is performed for early stage disease. Both treatment strategy and prognosis highly depend on the staging of primary and nodal disease as well as genetic and various biomarkers.

Overall Cost to Society

The various options for the management of head and neck cancer have been evaluated using cost-identification analysis. Although most reported economic studies are for T1 or N0 HNC, the presence of cervical lymph node metastases is one of the most important prognostic factors for HNC. A single nodal metastasis halves the overall survival of HNC regardless of the location or size of the primary tumor [12–14]. Although diagnostic tests, especially PET scan, are costly, the appropriate diagnostic strategy could prevent inadequate treatment or avoid overtreatment potentially affecting outcomes for patients with HNC.

A study analyzed the cost-effectiveness of PET in patients with squamous cell carcinoma of the H&N and absence of clinical signs indicating lymphatic spread on CT [15]. In this study, PET was cost effective if lymph node metastases could be detected more sensitively than with a standard imaging approach. By preventing morbidity and improving the overall survival and quality of life, PET-based tumor staging was associated with an increased median survival of 0.13 years or 0.44 quality-adjusted life years (QALYs). PET resulted in additional costs of $1,107, resulting in an incremental cost-effectiveness ratio (ICER) of $871 per life year saved or $2,505/QALY. Given the prevalence of 18F-FDG-positive lymph node metastasis of 16–36 %, costs were below the commonly accepted threshold of $50,000/QALY. This study has several limitations, most notably that the results are conditional on the parameters of the decision model. Parameters such as the cost of treatment, utility of treatments, and life expectancy may vary according to the institution. Clinical scenarios in which this modality can be implemented cost-effectively have not been

well defined [16]. Prospective, randomized clinical trials are needed to further evaluate the clinical relevance and cost-effectiveness.

Goals of Imaging

The goals for the imaging evaluation of cervical lymph nodes with HNC are (1) to accurately distinguish metastatic nodes from benign nodes in the initial staging and (2) to differentiate residual disease from posttreatment changes after radiation or chemoradiation in order to determine the need for salvage surgery.

See Table 40.1 for imaging options for the primary head and neck cancer and staging of the neck.

Methodology

A MEDLINE search was performed using PubMed (National Library of Medicine, Bethesda, Maryland) for original research publications discussing the diagnostic performance and effectiveness of imaging strategies in the H&N lymph node. Clinical predictors of cervical lymph node metastases were also included in the literature search. The search covered the period January 1990 to March 2011. The search strategy employed different combinations of the following terms: (1) lymph node, (2) head and neck, (3) metastasis, (4) ultrasound or CT or MR or PET, (5) size criteria, (6) cost, and (7) histology. Additional articles were identified by reviewing the reference lists of relevant papers. This review was limited to human studies and the English language literature. The author performed an initial review of the titles and abstracts of the identified articles followed by review of the full text in articles that were relevant.

In reviewing the diagnostic performance of imaging for cervical node metastases, it became apparent that results vary depending on the grouping of nodal disease by different studies. For example, some studies addressed diagnostic accuracy for each individual lymph node with a specific pathology. This is a far more rigorous

assessment of diagnostic accuracy, requiring labor-intensive one-to-one correlation of imaging with pathological results for each lymph node. More commonly, studies were analyzed using nodal level or zone as a unit. A single positive node in one level on imaging could count as a true positive for two positive nodes in the same nodal level on pathology. This is a more liberal criterion in terms of sensitivity. The analysis is often reported by hemi-neck. In this case, one positive node in one side of neck (including all levels) correlates with any number of positive nodes in the same neck. Lastly, the analysis can be conducted on a patient basis. In these diagnostic summary tables, we specify the level of analysis, per node, per level, per hemi-neck, or per patient.

Discussion of Issues

Which Imaging Modality Is Appropriate in the Evaluation of Lymph Node Metastases in HNC Patients?

Summary

Various size criteria have been reported on CT, MR, or US. The diagnostic accuracy of size criteria is generally limited, as the size of metastatic and benign nodes overlaps substantially. By applying a lower threshold, i.e., maximum diameter of 8 versus 10 mm, sensitivity increases at the expense of specificity. By applying the higher threshold, such as minimum axial diameter of 10 mm, sensitivity is limited but specificity increases. In patients with HNC, there are many small metastatic lymph nodes but not many large benign lymph nodes, as one might see in the thoracic region. The challenge is to identify normal-sized metastatic lymph nodes. Clearly, size criteria alone do not discriminate metastatic from benign nodes. Therefore, morphological criteria other than size are added to support detection of metastatic disease in the neck. Parenchymal echogenicity or intranodal vascular findings should be combined with various size criteria on US.

Power Doppler US has been reported to provide high diagnostic performance (moderate evidence, sensitivity 92–100 %, specificity 100 %) [17, 18].

In the CT evaluation of cervical lymph nodes, the presence of central necrosis or heterogeneous enhancement augments the diagnostic accuracy of size criteria (moderate evidence, sensitivity 78–86 %, specificity 100 %). Extracapsular spread is another imaging finding to strongly suggest presence of metastasis; however, it is normally seen in larger metastatic lymph nodes. Some reports recommend minimal diameter and long- to short-axis diameter ratio (L/S ratio) as more accurate morphological criteria (sensitivity 87–97 %, specificity 89–97 %) than maximum diameter (sensitivity 69–95 %, specificity 7–62 %), as metastatic lymph nodes are generally round (shorter L/S ratio) than benign nodes [19].

Conventional MR sequences with morphologic criteria for nodal staging might be similar or slightly inferior to those of CT. Echo-planar DWI with ADC values was reported to be useful for differentiating metastatic from benign nodes and should be added to the conventional sequences (moderate evidence, sensitivity 94 %, specificity 100 % for level analysis). Ultrasmall superparamagnetic iron oxide (USPIO)-enhanced MR was reported to yield high sensitivity and high specificity (moderate evidence, sensitivity 56–96 %, specificity 93 % for level analysis). However, none of the agents are currently available for human use for clinical care in the United States.

18F-FDG PET/CT or PET has a high sensitivity and specificity in the diagnosis of metastatic lymph nodes (moderate evidence, sensitivity 70–100 %, specificity 82–99 % for level analysis). In the comparison with other modalities such as US, CT, and MR, with pathology as a reference, FDG PET with or without standard uptake value (SUV) had higher diagnostic performance [20, 21].

Supporting Evidence
(a) CT Multidetector-row CT scanners allow fast data acquisition with high spatial resolution and proper reconstruction and have become a primary imaging study for staging of HNC.

In addition to the clinical examination, contrast-enhanced CT is routinely performed to assess pretreatment staging for lymph nodes as well as the primary tumor. However, diagnostic criteria of CT-positive nodes have not been clearly established yet.

The size criteria vary considerably among authors [19, 22–24]. Some use a minimum axial diameter and others use maximum axial diameter. A small cutoff point yields a high sensitivity and a low specificity. Lymph nodes greater than 10 mm are considered as positive in some studies, whereas nodes greater than 15 mm are considered as positive in others [19, 22–25]. Sonmez et al. prospectively evaluated 55 patients with HNC and found that the specificity and the overall accuracy with a cutoff value of 15 mm were higher than that of 10 mm (Table 40.2) [22]. In this prospective level II study (moderate evidence), they concluded that it was preferable to use a threshold of 15 mm (sensitivity 86 %, specificity 81 %) rather than 10 mm (sensitivity 95 %, specificity of 47 %) for the CT evaluation of cervical lymph nodes in order to prevent overtreatment and reduce morbidity associated with neck dissection.

In comparison between minimum and maximum axial diameter, van den Brekel et al. correlated size criteria on CT with pathology in 55 patients and 2,719 lymph nodes and reported that the minimal diameter in the axial plane was superior to the maximum diameter for predicting lymph node metastasis (prospective level II study) [24]. Steinkamp et al. reported minimum axial diameter showed higher specificity and diagnostic accuracy (minimum diameter >8 mm: specificity 89 %, accuracy 88 %) than maximum axial diameter (maximum diameter >15 mm: specificity 62 %, accuracy 66 %) [19]. They reported that other diagnostic criteria such as L/S ratio (specificity 97 %, accuracy 97 %) and central lucency (specificity 100 %, accuracy 86 %) also showed higher specificity and accuracy than maximum long-axis diameter per node in the level II prospective study (moderate evidence). In this study, a maximum diameter of 10 mm yielded 95 % sensitivity but only 7 % specificity per node, leading to overdiagnosis of

normal nodes. This is similar to a study by van den Brekel [24]. The other CT criteria used to determine the presence of metastatic lymph nodes for squamous cell carcinoma include central nodal necrosis, peripheral nodal rim enhancement, grouping of three or more nodes, and round shape [25].

(b) MRI Because differences in T1 and T2 relaxation do not enable reliable differentiation between nodes with and without tumor, conventional MR imaging has not yielded additional value to that of CT in the detection of nodal metastasis [26]. Therefore, the diagnostic accuracy of conventional MR imaging using morphologic criteria for nodal staging is similar or slightly inferior to CT [20, 27–29] (Table 40.3). Several clinical trials have reported the diagnostic accuracy of USPIO-enhanced MR imaging to assess lymph node metastases [30–33] (Table 40.4). USPIO are iron oxide nanoparticles that are taken up by normal phagocytic lymph nodes reducing the signal intensity on gradient-echo T2-weighted imaging (T2*-WI), allowing differentiation of metastatic from normal nodes, independent of size [34, 35]. In the prospective phase III clinical trial (level II study (moderate evidence)), Anzai et al. reported 96 % sensitivity and 93 % specificity of USPIO-enhanced MRI by two blinded readers whose assessment was correlated with pathological diagnosis in 29 patients with HNC [33]. In a prospective node-by-node and level-by-level assessment, Sigal et al. also reported that USPIO-enhanced MR showed similar sensitivity (> = 95 % for individual lymph node) and markedly higher specificity (>86 %) than pre-contrast MR with conventional criteria (sensitivity >95, specificity 14) level II (moderate evidence) [31]. As of today, none of the USPIO contrast agents are FDA approved and clinically available for nodal staging for cancer patients in the United States. A potential logistic shortcoming of USPIO-enhanced MR includes the need for a postcontrast MR examination 24 h after the intravenous injection of contrast [30–35].

DWI allows measurement of the random motion of water molecules within the tissue microstructure [36]. These differences in tissue water mobility are quantified by using ADC values, and ADC correlates with tissue cellularity [37]. Generally, ADC values tend to be lower for metastatic nodes than for benign nodes [38, 39]. Several investigators have reported the value of ADC measurements compared with that of conventional images [40–44] (Table 40.4).

In a prospective level II study (moderate evidence), Vandecaveye reported DWI with ADC values for cervical nodal staging in H&N squamous cell carcinoma and found a sensitivity of 84 % and a specificity of 94 % per node in 33 surgically treated patients using a threshold ADC value of 0.94×10^{-3} mm^2/s [42]. In their study, DWI with ADC had higher diagnostic accuracy than turbo spin-echo (TSE) MR imaging even for small lymph nodes. In the evaluation of subcentimeter lesions, DWI had a sensitivity of 76 % for the detection of 4–9 mm metastatic nodes, while the sensitivity of TSE MR imaging was only 7 %, whose diagnostic criterion was minimum diameter >10 mm or heterogeneous enhancement or nodal contour irregularity. In a prospective level II study (moderate evidence), Dirix et al. also reported that DWI had the same ADC cutoff value for identifying metastatic lymph nodes with 89 % sensitivity and 97 % specificity and was markedly superior to conventional sequences which had 42 % sensitivity and 94 % specificity [40].

(c) PET 18F-FDG PET or PET/CT allows detection of metastatic lymph nodes due to higher glucose utilization compared with normal nodes [28, 45, 46]. Since CMS approval of FDG PET for initial staging and restaging of HNC, PET using 18F-FDG has been widely applied to HNC. As shown in Table 40.3, several recent studies have demonstrated high sensitivity and specificity for PET/CT or PET in the detection of cervical lymph node metastases. These studies ranged from 70 % to 100 % for sensitivity and from 82 % to 99 % for specificity. Several authors reported that PET/CT was superior to PET alone for HNC, primarily due to accurate localization of metabolic abnormalities, differentiating

uptake in lymph nodes from other physiological uptake [47–49]. In a retrospective level III study (limited evidence), Kubicek et al. reported that PET/CT showed higher sensitivity (100 %) and similar specificity (90 %) than PET alone (sensitivity 86 %, specificity 90 %) [50]. But overall accuracy was not significantly better for PET/CT (p = 0.089). The results showed excellent positive and negative predictive values (PPV 94 % and NPV 89 %) for PET or PET/CT scans for the diagnosis of lymph node status, similar to several other reports [51–58]. A recent level II meta-analysis (moderate evidence) including 32 studies by Kyzas et al. found 79 % sensitivity and 86 % specificity of PET in cervical lymph node staging [51].

Authors of several studies compared various imaging tests including CT, MR, US, and 18F-FDG PET [20, 21, 28, 29, 59, 60]. In a prospective level II study (moderate evidence) of lymph node staging, Adams et al. compared PET with the conventional imaging modalities (US, CT, MR) in 60 patients with H&N squamous cell carcinoma [20]. PET with standard uptake value (SUV) of 2.0 or above showed the highest sensitivity (90 %) and specificity (94 %) for the detection of cervical nodal metastasis on a node-by-node basis; sensitivities and specificities for conventional imaging modalities were 72–82 % and 70–85 %, respectively. In a prospective level II study (moderate evidence), Stuckensen et al. compared PET, US, CT, and MR with a histological reference in 106 patients with squamous cell carcinoma of the oral cavity (patient-by-patient basis) [29]. They found that PET showed the highest specificity (sensitivity 70 %, specificity 82 %), while US had the highest sensitivity (sensitivity 84 %, specificity 68 %). In a more recent retrospective level II study (moderate evidence), Yoon et al. compared PET with US, CT, and MR with pathology as the reference standard in 69 patients [28]. The sensitivity of PET (81 %) for the identification of nodal metastasis on a level-by-level basis was higher than other modalities (77–78 %), whereas the specificity of PET (98 %) was similar to that of other modalities (98–99 %). In this study, the sensitivity of PET/CT was slightly higher than those of other imaging studies, but the difference was not significant, and the comparison of diagnostic performance for each modality showed no statistically significant difference (p > 0.05).

(d) US While US is extensively used for evaluation of nodal metastasis from thyroid cancer, it is not routinely used for the staging of HNC. This is, in part, due to its lack of ability to accurately assess extension of primary H&N tumor. Ultrasound is highly operator dependent and has not been adapted widely in the United States for staging nodal disease in HNC. Most US publications are from Europe and Asia, where it is heavily integrated to clinical oncology practice. Several studies have attempted to establish the sonographic criteria for differentiating metastatic from nonmetastatic cervical lymph nodes. These include the nodal size (long- and short-axis diameters), nodal shape (L/S ratio), nodal necrosis, and presence of parenchymal or peripheral blood flow signals on color Doppler imaging [17, 18, 61–63]. Table 40.5 summarizes the diagnostic performance of various US diagnostic criteria for identifying metastatic lymph nodes. This demonstrates variable sensitivity and specificity. Kim et al. studied 148 subjects on US using morphological and intraarchitectural criteria [61]. This retrospective study demonstrated 89 % sensitivity and 93 % specificity per level for identifying metastatic nodes (level II, moderate evidence). In prospective and retrospective level II studies using the criteria of minimum axial diameter (threshold value, 7–9 mm), poor sensitivity (45–86 %) and relatively higher specificity (90–97 %) for a per node analysis were reported [62, 63]. Although power Doppler sonography is not routine in clinical practice, combined criteria with power Doppler may be a powerful diagnostic tool for identifying metastatic superficial cervical lymph nodes [17, 18, 62–64]. In level II prospective [18–62] and retrospective [17, 63] studies using combined criteria, power Doppler improved both sensitivity and specificity (sensitivity 77–100 %, specificity 86–100 %). In a level II prospective study using US-guided fine-needle aspiration (FNA) of 181 lymph nodes in 56 subjects,

Knappe et al. achieved a moderate sensitivity (89.2 %) and higher specificity (98.1 %) per nodal assessment compared with cytology [64]. Their results were similar to previous studies [65–67].

(e) Combination of Imaging Modalities Yoon et al. reported that the overall sensitivity, specificity, and accuracy of the combination of CT, MR, US, and PET/CT were 86.5 %, 99.4 %, and 97.0 %, respectively (Table 40.3). The combination of four imaging modalities improved the sensitivity compared with the highest value of each technique used alone (81.1 %, PET/CT) without loss of specificity and accuracy. However, the difference failed to reach statistical significance (p > 0.05) [28].

Which Imaging Study is Appropriate for Clinically N0 Stage Patients with HNC?

Summary

The imaging evaluation for patients who are clinically N0 stage presents a major challenge. These patients with no suspicious lymph node metastases harbor metastatic lymph nodes 25–37 % of time [68–70]. Modalities such as US, CT, and FDG PET without SUV have all shown poor sensitivity (7–50 %) (limited and moderate evidence). DWI with ADC has higher sensitivity (sensitivity, 76 %) than conventional MR sequences (sensitivity, 7 %) and has been reported to provide added value in the detection of subcentimeter nodal metastasis (moderate evidence). Due to the lack of a definitive diagnostic method, patients with N0 stage necks often undergo neck dissection. Table 40.6 summarizes the studies specifically focused on the diagnostic accuracy of imaging in N0 stage patients. US, CT, and PET all have inadequate sensitivity for making decisions regarding neck management. In a study with N0 stage patients [31], USPIO-enhanced MR did not show better performance (receiver operating characteristic (ROC), Az = 0.56–0.58) than pre-contrast MR with conventional imaging (ROC, Az = 0.59–0.61)

(Table 40.4). The ideal imaging study should have a high NPV, over 95–98 %, confidently avoiding neck dissection following a negative test.

The American College of Radiology Imaging Network (ACRIN) 6685 trial (http://www.acrin.org/6685_protocol.aspx) is currently assessing the effectiveness of FDG PET in N0 stage patients with H&N squamous cell carcinoma.

Supporting Evidence

For treatment of the neck with N0 status, one approach is the use of selective neck dissection or postoperative radiation therapy. This approach, however, leads to the possibility of overtreatment with increased morbidity and cost [62, 63]. In a retrospective level III study (limited evidence), Schuller et al. reported that the sensitivity of CT scan alone is too low (25 %) for it to be used as an isolated screening tool to identify patients with occult positive lymph nodes [71]. In retrospective level III studies (limited evidence) evaluating US for clinically N0 HNSCC, To and van den Brekel reported poor sensitivity (16–47 %) with low NPV (64 %) [72, 73]. As listed in Table 40.6, level II and III studies of FDG PET showed variable sensitivity (25–67 %) but relatively high specificity (87–95 %) in N0 neck evaluation [51, 68, 74]. Because of the relatively poor spatial resolution of PET, its ability to detect small metastatic nodes is limited [28, 75]. In addition, nodal necrosis may cause a false-negative PET because of the low glycolytic activity of the necrotic material [76]. In a prospective level II study (moderate evidence), Vandecaveye et al. studied 33 cases with histologically proven clinically N0 H&N squamous cell carcinomas using DWI with ADC [42]. They reported ADC had higher sensitivity (76 %) than conventional TSE (sensitivity 7 %) while maintaining high specificity (94 %). An ADC threshold value of 0.94×10^{-3} mm^2/s yielded 95 % NPV in a per node analysis of 259 lymph nodes in 33 patients. If this proves to be reproducible in other studies, DWI has the potential to be a useful tool in determining metastatic involvement of small lymph nodes. Evidence of metastatic disease as

determined by imaging in N0 stage patients would support the decision to perform a neck dissection. A negative neck by imaging in clinically N0 stage patients might avoid negative neck dissections.

Which Imaging Study is Appropriate in the Evaluation of Residual Nodal Disease After Radiation or Radiochemotherapy?

Summary

The concept of widespread organ preservation has disseminated in the last several years as a pivotal treatment option for patients with advanced HNC. The majority of advanced stage HNC patients are treated with chemoradiation therapy (CRT) initially, with salvage surgery being left as an option for those who do not respond to CRT. This creates another important role of imaging, differentiating CRT responders from nonresponders. For example, a patient with a good response by a primary tumor may have residual soft tissue in nodal disease. Patients with residual neck disease will likely benefit from salvage neck dissection. Conventional CT and MR are limited in their ability to assess treatment response for HNC. Soft tissue seen on CT and MR after CRT may represent residual tumor or posttreatment fibrosis. One of the major roles of 18F-FDG PET is to evaluate the treatment response of HNC after CRT. PET has a high specificity and NPV to assess for residual disease after CRT. If PET is negative, these patients could undergo careful clinical observation without neck dissection. To minimize the false-positive rate following treatment, PET should not be performed for at least 12 weeks following RT (limited evidence) [77–85].

Supporting Evidence

For patients treated with definitive CRT, the role of planned neck dissection remains controversial. Even for patients with residual cervical lymph nodes, pathologic analysis has not revealed viable tumor cells in many of these lymph nodes [77, 78]. Clinical experience supports there being a subset of patients for whom neck dissection may be withheld after definitive radiation [79], and identifying this group of patients becomes a key issue in the management of patients with advanced HNC. PET has been used extensively in HNC for staging, assessment of treatment response, and detection of recurrence. The optimal time to obtain 18F-FDG PET after radiation is still in debate. It appears that high false-negative and false-positive rates for PET may occur when PET is obtained too soon after RT [80–83]. Porceddu et al. hypothesized that if residual viable tumor cells remained after treatment, they would repopulate to a size detectable by PET in a median 12-week interval posttreatment [84]. 12 weeks post radiation appears to be a suitable time to obtain FDG PET to assess treatment response [81–84]. In a retrospective level III study (limited evidence), Yao et al. reported that PET scans performed 13 weeks after RT showed excellent sensitivity (100 %) and NPV (100 %) (Table 40.7) [85]. They concluded that a negative post-RT FDG PET is highly predictive of negative pathology in residual lymph nodes following definitive RT. Ong et al. studied post-RT PET obtained for 84 hemi-necks in 65 cases [86]. In this retrospective level II study (moderate evidence), they showed that PET scans obtained later than 8 weeks after RT had a moderate sensitivity (71 %), specificity (89 %), and high NPV (97 %). In prospective and retrospective level II studies using CT after RT, Liauw and Ojiri et al. reported that radiographic complete response (no lymph nodes >15 mm, no focal abnormal findings, no extracapsular spread, and no abnormal enhancement) had a high sensitivity (96–100 %) and NPV (94–100 %) [78, 87]. Although these two studies did not have an optimal interval after RT, CT findings following RT might help identify residual disease. CT or MR imaging is usually performed 6–8 weeks after the completion of CRT. If the tumor is increasing in size at this point, salvage surgery is recommended without waiting for a 12-week post-CRT PET scan (moderate evidence) [87–89].

Decision trees for imaging evaluation and management of lymph nodes after radiation therapy are shown in Fig. 40.1.

Take-Home Tables and Figures

Suggested Imaging Protocols Based on the Current Evidence

US

High-resolution real-time unit using a 6–15-MHz linear array transducer.

Grayscale sonography in multiple planes on multiple nodes and power Doppler sonography (setting for lymph node vessels with low velocity: color gain 14–20 dB, dynamic range 66 dB, Doppler scale 0.04 m/s).

CT

Contrast-enhanced head and neck CT, using 16–64 multidetector-row CT scanner.

0.625- to 1.25-mm helical scanning with coronal and sagittal reformat (120–140 kVp and 200–400mAs).

Reconstructed axial images with slice thickness 3–5 mm on a 512 × 512 matrix.

The scanning range is from the maxillary sinus to the tracheal bifurcation with appropriate delay time (30–45 s) after the intravenous injection of nonionic contrast material.

MRI

1.5 or 3T magnet. Transverse T2-weighted fast spin-echo imaging with fat suppression, transverse T1-weighted spin-echo imaging, coronal T2-weighted fast spin-echo imaging, and contrast-enhanced transverse and coronal T1-weighted spin-echo imaging with fat suppression (slice thickness 4–6 mm, intersection gap 0–0.6 mm, 512 × 512 matrix). Scanning range is from skull base to the clavicle, but various by the location of primary tumor.

PET/CT

Whole-body FDG-PET scanner (128 × 128 matrix, 4–5-mm section thickness).

Images are acquired 60–90 min after the intravenous injection of 10–20 mCi (370–740 MBq) of 18F-FDG.

Unenhanced CT images using multislice CT scanner (slice thickness 3–4 mm, matrix 512 × 512) to obtain fused images with PET.

Future Research

- To develop a new contrast agent that is specific for metastatic lymph nodes having a favorable safety and cost profile
- To further define MR perfusion and CT perfusion technique for the evaluation of nodal metastases and determine if the hemodynamics of metastatic foci can be used to differentiate metastatic from benign lymph nodes
- To perform multi-institutional trials of FDG PET for HNC patients with N0 neck in order to determine if NPV of PET is sufficiently high to differentiate patients who need selective neck dissection from those who can avoid neck dissection
- To evaluate treatment decisions and quality of life assessment for patients with HNC in order to determine if advanced imaging studies change treatment decisions or, ultimately, outcomes.

Table 40.1 Imaging options for head and neck cancer

Imaging studies	Contrast required	Bone	Soft tissues	Radiation	Other risks	Costs
US	Yes/no	Poor	Good	No	Operator dependent	Inexpensive
CT	Yes	Excellent	Good	Yes	Dental artifact	Moderate
MRI	Yes	Good	Excellent	No	Long scan time, metal artifact	Moderate
PET-CT	18F-FDG	Moderate	Good	Yes	Physiologic uptake	Expensive

Table 40.2 Diagnostic performance of computed tomography (CT)

Study, year (Reference No.)	No of subjects	No of nodal level or nodes	Study design	Primary disease (clinical stage)	Reference assessment	Definition of positive (diagnostic criteria)	Observer	Sensitivity	Specificity	Accuracy
Sonmez et al. [22]	55 (65 ND)		Prospective	Intraoral SCC, high risk extraoral Ca	Pathology for hemi-neck	≥ 10 mm or necrosis, grouping ≥ 3, ENS		95	47	63
						≥ 15 mm, or necrosis, grouping ≥ 3, ENS		86	81	83
Shingaki et al. [23]	53 (33 meta) 57 ND	2,217 nodes (98 meta)	Retrospective	HN SCC (stage I–IV)	Pathology for hemi-neck	>10 mm in short-axis diameter		69	100	81
						>15 mm in long axis diameter presence of central lucency		58	91	70
						>10 mm or presence of central lucency		86	100	91
Steinkamp et al. [19]	70	164 nodes (96 positive)	Prospective	HN cancer (N0–N2c)	Pathology for node	L/S ratio <2	3 radiologist (independent)	97	97	97
						Minimal diameter >8 mm		87	89	88
						Low-attenuation center, rim enhancement		78	100	86
						Maximum diameter >10 mm		95	7	61
						Maximum diameter >15 mm		69	62	66
van den Brekel et al. [24]	55, 71 ND (38 meta)	2,719 nodes (144 meta)	Prospective	HN SCC	Pathology for hemi-neck	Minimum diameter ≥ 8 mm	1 radiologist	97	21	
						Minimum diameter ≥ 10 mm		89	73	
						Maximum diameter ≥ 10 mm		97	9	
						Maximum diameter ≥ 15 mm		71	73	
					For node	Minimum diameter ≥ 8 mm		54.2	96.8	
						Minimum diameter ≥ 10 mm		41.7	99.3	
						Maximum diameter ≥ 10 mm		59	93.3	
						Maximum diameter ≥ 15 mm		27.1	99.5	

Table 40.3 Diagnostic performance of positron emission tomography (PET) and comparison with other modalities

Study, year (reference No.)	No of subjects	No of nodal level or nodes	Study design	Primary disease	Clinical stage	Reference	Assessment	Definition of positive (diagnostic criteria)	Observer	Sensitivity	Specificity	Accuracy
Kubicek et al. [50]	212		Retrospective	HN cancer	N0–N3	Pathology	For patient	PET or PET/CT (overall)(n = 110)		93	91	
								PET alone (n = 55)		86	90	
								PET/CT (n = 55)		100	90	
Rodrigues et al. [59]	44 (24 meta)	186 level (47 meta)	Prospective			Pathology	For level	CE-CT: overall appearance		57	88	81
							For level	Whole body PET/CT		70	82	79
Yoon et al. [28]	69	402 level (74 meta)	Retrospective	HNSCC	T1–T4	Pathology	For level	16-row CT (size, necrosis, shape, grouping)	2 radiologists	77	99.4	95.3
	39	4,275 nodes (213 meta)						MR (1.5 T) (max diameter)	1 NM physician	77	99.4	95.3
								US (size, internal echo, flow)	Independent	78.4	98.5	94.8
								PET/CT (visual and $SUV_{max} > = 25$)	(blind)	81.1	98.2	95
								All criteria combined		86.5	99.4	97
Kyzas et al. [51]	1,236 (32 studies)		Medline search (meta-analysis)	HNSCC		Pathology		FDG PET	3 investigators	79	86	
Murakami et al. [52]	23	112 level (19 meta)	Retrospective	HNSCC	N0–N2c		For level	FDG PET/CT fusion, SUV_{max}	2 observer	84	99	96
		557 nodes (28 meta)						Conventional modalities (CT, MRI)	1 radiologist	68	94	89
								Conventional + visual FDG-PET/CT	(consensus)	68	99	94

Table 40.3 (continued)

Study, year (reference No.)	No of subjects	No of nodal level or nodes	Study design	Primary disease	Clinical stage	Reference	Assessment	Definition of positive (diagnostic criteria)	Observer	Sensitivity	Specificity	Accuracy
Stuckensen et al. [29]	106 (52 meta)	2,196 nodes (171 meta)	Prospective	Oral cavity SCC	T1-4	Pathology	For level	US (not described the US, CT, MR criteria)		84	68	76
								CT		66	74	70
								MR 1.5 T (STIR.Gd)		64	69	66
								PET visual		70	82	75
Stockkel et al. [21]	54 (24 meta) 81ND		Prospective	Oral cavity and oropharynx SCC	T1-4	Pathology	For level	US (criteria was not written)		82	66	72
								US with FNA		64	100	86
								CT		85	86	86
								PET		96	90	93
Stokkel et al. [60]	20 (7 meta) 40 neck side (9 meta)		Prospective	HN cancer (18 oral SCC)	N0–N2c	Pathology (17) follow, FNA (3)	For hemi-neck	US (minimal axial diameter ($>= 10$ mm) or CT irregular or rim enhancement)		87	50	
										89	93	
								PET visual		100	97	
Adams et al. [20]	60 (31 meta)	1,284 nodes (177 meta)	Prospective	HNSCC	N0–N2c	Pathology	For node	US >12 mm or grouping, necrosis, CT (shape, pathologic enhancement)		72	70	70
										82	85	85
								MR 1.5 T (STIR.Gd)		80	79	79
								PET (SUV stand >2.0 and visual)		90	94	93

Table 40.4 Diagnostic performance of MR imaging

Study, year (reference No.)	No. of subjects	No. of nodal level	Study design	Primary disease clinical stage	Reference test	MR unit sequence	Assessment	Definition of positive (diagnostic criteria)	Observer	Sensitivity	Specificity	ROC
Anzai et al. [27]	29		Prospective	HNSCC	Pathology	1.5 T	For level	Pre-contrast (size)	2 radiologist	46	92	Az = 0.76
						USPIO		Pre-contrast (reader's subjective criteria)	Blinded	84	78	
								Post-contrast with USPIO	Independent	96	93	Az = 0.83
											Neck and body combined	
Sigal et al. [28]	81 (109ND)	517 level (overall) (101 meta)	Prospective	HNSCC	Pathology	1.5 or	For node	Pre-contrast (T1, T2, GRE)	2 radiologist	>95	14	Az > 0.74
				N0-N2c		1.0 T		Short-axis diameter, internal architecture	Independent			
		3,092 nodes				USPIO	For level	Pre-contrast		>79	>51	Az > 0.75
Multi-institution							For node	USPIO		>95	>86	Az = 0.92
7 clinic sites							For level	USPIO		>59	>93	Az > 0.75
	28	184 level		N0			For level	USPIO		20	93–96	Az = 0.56–0.58
	12	(19 meta)						Pre-contrast				Az = 0.59–0.61

(continued)

Table 40.4 (continued)

Study, year (reference No.)	No. of subjects	No of nodal level	Study design	Primary disease clinical stage	Reference test	MR unit sequence	Assessment	Definition of positive (diagnostic criteria)	Observer	Sensitivity	Specificity	ROC
Mack et al. [29]	30	1,029 nodes (69 meta)	Prospective	HNSCC	Pathology	1.5 T USPIO	For node	USPIO (T1,T2, GRE T2)	2 radiologist Consensus	86	100	
Dirix et al. [40]	22 (33ND)	128 level (32 meta) 198 nodes (45 meta)	Prospective	HN SCC stage II-IV (N0-N2c)	Pathology	1.5 T DWI	For node	CT and T1, T2MI: morphologic criteria (minimal axial diameter >1 cm, suggestive of necrosis, ECS, obliteration of fat)	1 radiologist	42	94	
							For node	DWI (ADC value 0.94 × 10^{-3} mm^2/s)		89	97	
							For level	Morphologic criteria		47	96	
							For level	DWI (ADC value 0.94 × 10^{-3} mm^2/s)		94	97	
Holzapfel et al. [41]	35	55 nodes (25 meta, 6 ML)	Prospective	31 malig 24 benign	Pathology Follow-up image	1.5 T DWI	For node	DWI (ADC value 1.02 × 10^{-3} mm^2/s)	2 radiologist Independent	100	87	Az = 0.975

Study		Nodes	Design	Tumor	Reference	Field	Stage	Modality	Criteria		Reader	Sens	Spec
Vandecaveye et al. [42]	33	301 nodes (overall) 76 meta	Prospective	HNSCC	Pathology	1.5 T	N0–N2	DWI	TSE: size criteria (minimal diameter >10 mm or	For node	1 radiologist	46	96
									Heterogeneous enhancement or irregularity	For level		57	95
									DWI (ADC value 0.94 × 10^{-3} mm²/s)	For node	2 radiologist	84	94
									DWI (ADC value 0.94 × 10^{-3} mm²/s)	For level	Consensus	94	97
		42 nodes (>10 mm) (32 meta)							DWI (ADC value 0.94 × 10^{-3} mm²/s)	For node		94	80
									Size, inner signal, enhancement on TSE	For node		97	10
		259 nodes (4–9 mm) (42 meta)							DWI (ADC value 0.94 × 10^{-3} mm²/s)	For node		76	94
									Size, inner signal, enhancement on TSE	For node		7	99.5

Table 40.4 (continued)

Study, year (reference No.)	No. of subjects	No of nodal level	Study design	Primary disease clinical stage	Reference test	MR unit sequence	Assessment	Definition of positive (diagnostic criteria)	Observer	Sensitivity	Specificity	ROC
de Bondt et al. [43]	16 (17ND)	58 level	Retrospective	HNSCC	Pathology	1.5 T	For node	DWI (ADC level 1.0 × 10^{-3} mm^2/s)	2 radiologist	92	84	Az = 0.89
		219 nodes		T1-3 N0-1		DWI		T2WI: maximum short-axis diameter	Consensus	92	61	Az = 0.91
								Border irregularity on T2WI		62	98	(size, border, SI)
								Heterogeneity on T2WI		50	95	
								ADC + other 3 criteria				Az = 0.98
Sumi et al. [44]	31	55 nodes (25 meta)	Prospective	17HNSCC	Pathology	1.5 T	For node	Abnormal signal intensity on T1 or T2	1 radiologist	68	93	Az = 0.8437
				3ML, 1 benign		DMI		DWI (ADC > =0.4 × 10^{-3} mm^2/s)		52	97	Az = 0.8440

Table 40.5 Diagnostic performance of ultrasonography (US)

Study, year (reference No.)	No. of subjects	No of nodal level or node	Study design	Primary disease (clinical stage)	Reference	Assessment	Definition of positive (diagnostic criteria)	Observer	Sensitivity	Specificity	Accuracy
Kim et al. [61]	148 (219ND)	851 level	Retrospective	HNSCC (T1-T4)	Pathology	For level	>=10 mm in short-axis diameter (level, I,II),	1 radiologist	89	93	92
							>=7 mm (level III-VI) or L/S ratio <2, or absence of normal echogenic hilum, heterogeneous parenchymal echogenicity				
Ahuja et al. [17]	173 (101 meta)	101 malignancy (67 HNSCC) 72 reactive with no malignancy	Retrospective		Cytology	For patient	Intranodal necrosis or at least 3 of following	1 radiologist + 1 sonographer (independent)	95	83	90
							(L/S ratio <=2, Hypoechoic, Absence of echogenic hilum, In drainage site of the primary)				
							Power Doppler		90	100	94
							Combined criteria (gray scale + power Doppler)		100	100	100
Wang et al. [62]	57	69 nodes (31 malignant)	Prospective	43 HN cancer (33SCC)	Cytology	For node	Minimal axial diameter >8 mm	2 radiologist (independent)	45	93	70
							Vascular pattern (spotted or peripheral)		61	93	77
							Combined criteria		77	86	84

Table 40.5 (continued)

Study, year (reference No.)	No. of subjects	No of nodal level or node	Study design	Primary disease (clinical stage)	Reference	Assessment	Definition of positive (diagnostic criteria)	Observer	Sensitivity	Specificity	Accuracy
Yonetsu et al. [63]	73	338 nodes (108 meta)	Retrospective	HNSCC	Pathology	For node	Minimal diameter >7–9 mm in level I–IV	1 radiologist	78–86	90–97	88–94
							Combined criteria (size + Doppler)		89–94	94–100	92–98
Knappe et al. [64]	56	181 nodes (74 meta)	Prospective	HNSCC (N0–N2c)	Pathology	For node	FNA cytology		89	98	95
Ariji et al. [18]	77	291 (71 meta)	Prospective	HN cancer (66 SCC)	Pathology	For node	Power Doppler (parenchymal signal)		83	98	95
							Size (transverse/longitudinal ratio >0.65)		66	92	
							Combined		92	100	

Table 40.6 Diagnostic performance of each modality for clinically N0 lymph node

Study, year (reference), modality	No. of subjects	No of nodal level or nodes	Study design	Primary disease	Clinical stage	Reference	Assessment	Definition of positive (diagnostic criteria)	Observer	Sensitivity	Specificity	PPV	NPV	Accuracy
To et al. [72] US	30 (15 meta)		Retrospective	Tongue ca	T1–2N0	Pathology	For patient	US: >7 mm for level 1 and >8 mm for subdigastric node or round shape, absence of echogenic hilum		47	93	99	64	70
van den Brekel et al. [73] US	131ND (51 meta)		Retrospective	HNSCC	Clinically N0	Pathology	For hemi-neck	US: minimal diameter >8 mm		41	84			
								US: minimal diameter >10 mm		16	98			
Schuller et al. [71] CT	30 (8 meta)		Retrospective	Oral cavity SCC	Stage I–II, N0	Pathology	For patient	CT: positive criteria is not described		25	77	29	74	63
Vandecaveye et al. [42] MR (DWI)	33	259 nodes (4–9 mm) (42 meta)	Prospective	HNSCC	Clinically N0	Pathology	For node	ADC value 0.9 × 10^{-3} mm²/s		76	94	73	95	92
							For node	TSE (size >10 mm, inner signal, enhancement)		7	99.5	75	85	85
Kyzas et al. [51] PET	311 (10 studies)				Clinically N0	Pathology		FDG PET		50	87			
Schoder et al. [68] PET	31	142 level (9 meta)	Prospective	Oral cancer	N0 (clinical, and CT/MR)	Pathology	For LN level	FDG uptake (visual) + SUVmax (no cut off value)	2 NM physician (consensus)	67	95	50	98	94
	36 ND	765 nodes (13 meta)						(PET/CT fusion)						
Stoeckli et al. [74] PET	12 (5 meta)		Prospective	Oral SCC and oropharyngeal SCC	N0 (clinical or CT)	Pathology	For patient	Sentinel node biopsy	At least 2 readers	100	100	100	100	100
								FDG PET		25	88	50	70	67

Table 40.7 Diagnostic performance of PET and CT and in cases after radiation therapy

Study, year (reference No)	No. of subjects	Study design	Primary disease clinical stage	Reference	Modality interval	Assessment	Definition of positive (diagnostic criteria)	Observer	Sensitivity	Specificity	PPV	NPV	Accuracy
Ong et al. [86]	65 84 hemi-neck	Retrospective	HNSCC N1–N3	Pathology or Follow-up	FDG-PET (>=Bw after RT)	For hemi-neck	FDG PET/CT (visual evaluation)	1 investigator	71	89	38	97	88
	42 55 hemi-necks without residual lymphoadenopathy					For hemi-neck	FDG PET/CT		50	96	33	98	94
Yao et al. [85]	23 24 hemi-neck	Retrospective	HNSCC >=stage N2	Pathology or cytology	FDG-PET (13.3 W after RT)	For hemi-neck	SUVmax <=3.0		100	84.2	62.5	100	87.5
							FDG/PET/CT (visual evaluation)		100	68.4	45.5	100	75
Liauw et al. [87]	150 193 hemi-neck	Prospective	HNSCC N1–N3	Pathology	CT (4 W after RT)	For hemi-neck	Clinical complete response (cCR) Maximum diameter <=1.5	1 radiologist and 1 oncologist	73	63	32	72	56
							Maximum diameter <=1.5 and no focal abnormal findings		96	24	35	94	45
Ojir et al. [78]	95 113 ND	Retrospective	HNSCC N0–N3	Pathology	CT (33 days after RT) (13–64 days)	For hemi-neck	Clinical complete response (cCR) (Maximum diameter <=15 mm and free of internal defect. No evidence of capsular rupture)	2 radiologists	100	35.5	43	100	56
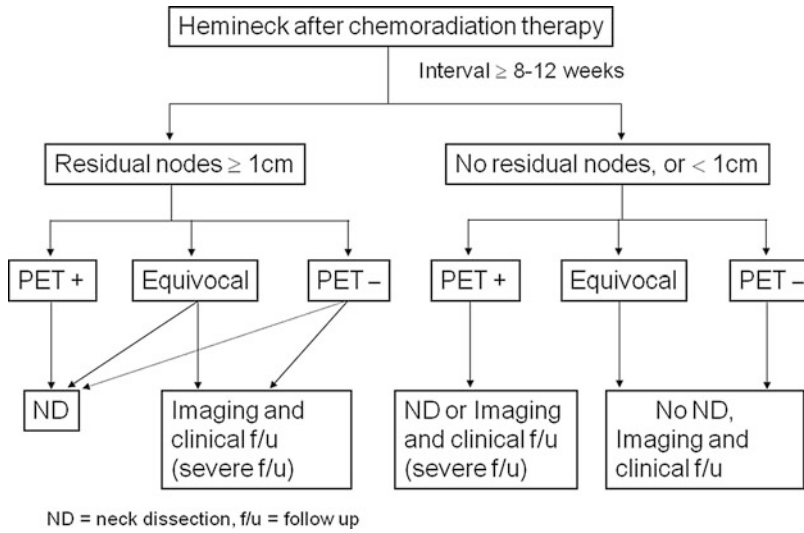
Fig. 40.1 Decision tree for imaging work-ups for patients after chemoradiation therapy. For the imaging evaluation of hemi-neck lymph nodes after CRT, more than 3 months' interval is recommended to decrease the false-negative rate. Since 18F-FDG PET/CT after CRT has a high NPV and specificity for predicting pathological tumor absence in the residual lymph node, patients with clinically and radiologically complete response can be spared from salvage neck dissection
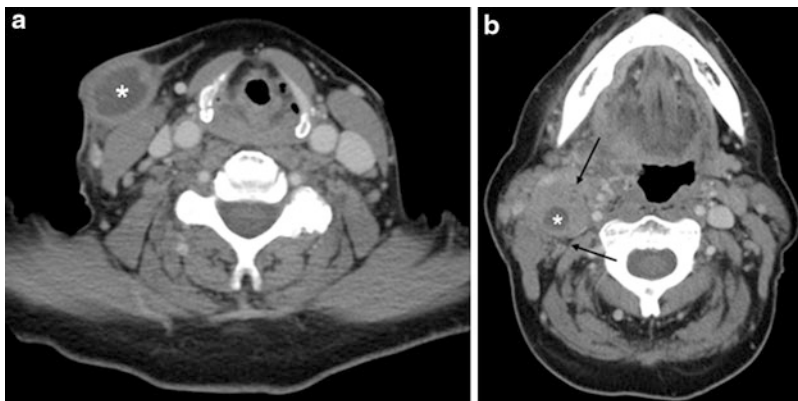
Fig. 40.2 (**a**, **b**) Typical CT findings of the lymph node metastasis. (**a**, **b**) Contrast-enhanced CT. Heterogeneously enhancing necrotic lymph node (*asterisk*) with dermal invasion (**a**) and loss of fat plane surrounding the nodal metastasis (*arrows*) (**b**) suggestive of extracapsular spread (*arrow*). Note right internal jugular vein in compressed posteriorly by enlarged lymph node
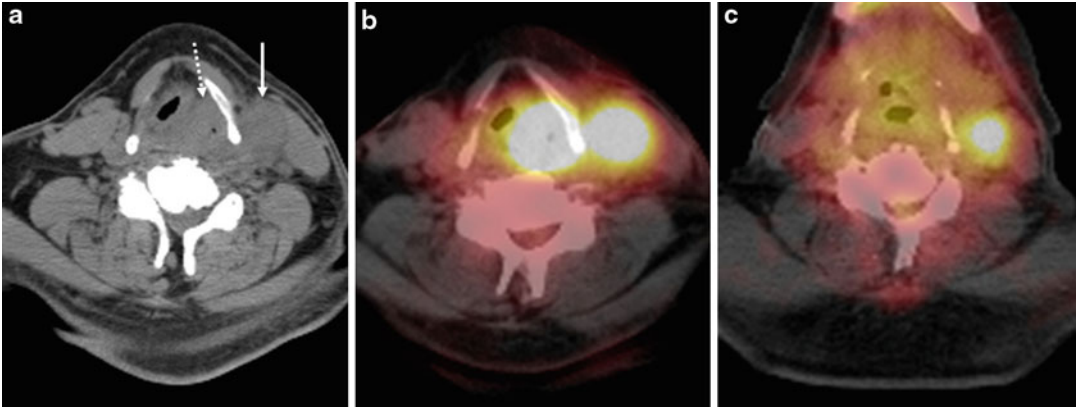
Fig. 40.3 (**a–c**) CT and FDG-PET findings of hypopharyngeal cancer with lymph node metastasis (T2N2bM0). Initial plain CT (**a**) shows left hypopharyngeal mass (*dotted arrow*) and enlarged level II–III lymph node (*arrow*). Initial FDG-PET/CT-fused image (**b**) shows marked FDG accumulation on both primary tumor and lymph node. Both tumor and lymph node have decreased in size, and no abnormal FDG uptake is seen on primary tumor at follow-up PET/CT image after 3 months CRT (**c**); however, residual FDG uptake is seen on the metastatic lymph node. The patient underwent biopsy of the primary site and left neck dissection after the PET/CT. Although no definitive residual tumor was confirmed at the primary site, residual nodal metastases were present at the left neck dissection
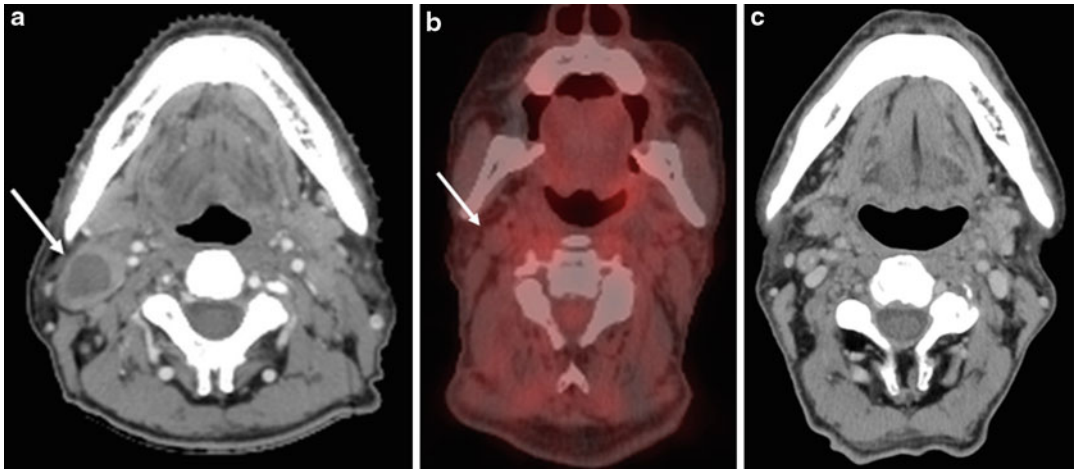
Fig. 40.4 (**a–c**) CT and FDG-PET findings of tonsillar cancer (not shown) with multiple lymph node metastasis (T4N3M0). Initial CT (**a**) shows level II enlarged necrotic lymph node (*arrow*). On FDG-PET/CT-fused image 3 months after CRT (**b**), there is a residual lymph node (*arrow*) decrease in size compared with the original CT without abnormal FDG uptake. At 1-year follow-up CT (**c**), the lymph node is stable or slightly smaller in size, indicative of a favorable response

References

1. Rouviere H. Lymphatic system of the head and neck. Ann Arbor: Edwards Brothers; 1938.

2. Som PM, Curtin HD, Mancuso AA. Am J Radiol. 2000;174:837–44.

3. Brasilino de Carvalho M. Head Neck. 1998;20:16–21.

4. Woolgar JA, Rogers S, West CR, et al. Oral Oncol. 1999;35:257–65.

5. Myers JN, Greenberg JS, Mo V, et al. Cancer. 2001;92:3030–6.

6. King AD, Tse GM, Ahuja AT, et al. Radiology. 2004;203(3):720–6.

7. Ishikawa M, Anzai Y. Magn Reson Imaging Clin N Am. 2002;10(3):527–42.

8. Harnsberger HR, Wiggins III RH, Hudgins PA, et al. Diagnostic imaging head and neck. 1st ed. Salt Lake City: AMYRSIS; 2004. p. 28–33; Part III-2.

9. Greene FL, Compton CC, Fritz AG, et al. AJCC cancer staging atlas. New York: Springer; 2006. p. 11–60; Part 1.

10. Teknos T, Rosenthal E, Lee D, et al. Head Neck. 2001;23:1056–60.

11. Ryerson AB, Peters ES, Coughlin SS, et al. Cancer. 2008;113(10):2901–9.

12. De Bondt RBJ, Nelemans PJ, Bakers F, et al. Eur Radiol. 2009;19:626–33.

13. Foote RL, Olsen KD, Davis DL, et al. Head Neck. 1993;15:300–7.

14. Leemans CR, Tiwari R, Nauta JJ, et al. Cancer. 1994;73:187–90.

15. Hollenbeak CS, Lowe VJ, Stack Jr BC. Cancer. 2001;92:2341–8.

16. Buck AK, Herrmann K, Stargardt T, et al. J Nucl Med Technol. 2010;38:6–17.

17. Ahuja A, Ying M. Ultrasound Med Biol. 2003;29:353–9.

18. Ariji Y, Kimura Y, Hayashi N, et al. AJNR Am J Neuroradiol. 1998;19:303–7.

19. Steinkamp HJ, Hosten N, Richter C, et al. Radiology. 1994;191:795–8.

20. Adams S, Baum RP, Stuckensen T, et al. Eur J Nucl Med. 1998;25:1255–60.

21. Stokkel MP, ten Broek FW, Hordijk GJ, et al. Ann Surg. 2000;231:229–34.

22. Sonmez A, Ozturk N, Ersoy B, et al. J Plast Reconstr Aesthet Surg. 2008;61:61–4.

23. Shingaki S, Suzuki I, Nakajima T, et al. J Craniomaxillofac Surg. 1995;23:233–7.

24. van den Brekel MW, Stel HV, Castelijns JA, et al. Radiology. 1990;177:379–84.

25. Dillon W. Am J Neuroradiol. 1998;19:796–7.

26. Yousem DM. Radiology. 1992;184:25–6.

27. Curtin HD, Ishwaran H, Mancuso A, et al. Radiology. 1998;207:123–30.

28. Yoon DY, Hwang HS, Chang SK, et al. Eur Radiol. 2009;19:634–42.

29. Stuckensen T, Kovacs AF, Adams S, et al. J Craniomaxillofac Surg. 2000;28:319–24.

30. Anzai Y, Piccoli CW, Outwater EK, et al. Radiology. 2003;228(3):777–88.

31. Sigal R, Vogl T, Casselman J, et al. Eur Radiol. 2002;12:1104–13.

32. Mack MG, Balzer JO, Straub R, et al. Radiology. 2002;222:239–44.

33. Anzai Y, Blackwell KE, Hirschowitz SL, et al. Radiology. 1994;192:709–15.

34. Tanoura T, Bernas M, Darkazanli A, et al. Am J Roentgenol. 1992;159:875–81.

35. Vassalo P, Matei C, Heston W, et al. Radiology. 1994;193:501–6.

36. Le Bihan D, Breton E, Lallemand D, et al. Radiology. 1988;168:497–505.

37. Herneth AM, Guccione S, Bednarski M. Eur J Radiol. 2003;45:208–13.

38. Abdel Razek AA, Soliman NY, Elkhamary S, et al. Eur Radiol. 2006;16:1468–77.

39. Wang J, Takashima S, Takayama F, et al. Radiology. 2001;220:621–30.

40. Dirix P, Vandecaveye V, De Keyzer F, et al. Int J Radiat Oncol Biol Phys. 2010;76:761–6.

41. Holzapfel K, Duetsch S, Fauser C, et al. Eur J Radiol. 2009;72:381–7.

42. Vandecaveye V, de Keyzer F, Vander Poorten V, et al. Radiology. 2009;251:134–46.

43. de Bondt RB, Hoeberigs MC, Nelemans PJ, et al. Neuroradiology. 2009;51:183–92.

44. Sumi M, Sakihama N, Sumi T, et al. AJNR Am J Neuroradiol. 2003;24:1627–34.

45. Reges S, Mass A, Chaiken L, et al. Cancer. 1994;73:3047–58.

46. Haberkorn U, Strauss LG, Reisser C, et al. J Nucl Med. 1991;32:1548–55.

47. Branstetter B, Blodgett T, Zimmer L, et al. Radiology. 2005;235:580–6.

48. Endo K, Oriuchi N, Higuchi T, et al. Int J Clin Oncol. 2006;4:286–96.

49. Schoder H, Yeung H, Gonen M, et al. Radiology. 2004;231:66–72.

50. Kubicek GJ, Champ C, Fogh S, et al. Head Neck Oncol. 2010;2:19.

51. Kyzas P, Evangelou E, Denaxa-Kyza D, et al. J Natl Can Inst. 2008;100:712–20.

52. Murakami R, Uozumi H, Hirai T, et al. Int J Radiat Oncol Biol Phys. 2007;68:377–82.

53. Ng SH, Yen TC, Liao CT. J Nucl Med. 2005;46:1136–43.

54. Fleming AJ, Smith SP, Saul CM. Laryngospcope. 2007;117:1173–9.

55. Hannah A, Scott AM, Tochon-Danguy H, et al. Ann Surg. 2002;236:208–17.

56. Schwartz DI, Ragendran J, Yueh B, et al. Arch Otolaryngol Head Neck Surg. 2004;130:1361–7.

57. Zanation AM, Sutton DK, Couch ME, et al. Laryngoscope. 2005;115:1186–90.

58. Roh JL, Pae KH, Choi SH, et al. Eur J Surg Oncol. 2007;33:790–5.
59. Rodrigues RS, Bozza FA, Christian PE, et al. J Nucl Med. 2009;50:1205–13.
60. Stokkel MP, ten Broek FW, van Rijk PP. Eur J Nucl Med. 1999;26:499–503.
61. Kim HC, Yoon DY, Chang SK, et al. J Ultrasound Med. 2010;29:531–7.
62. Wang Q, Takashima S, Takayama F, et al. Acta Radiol. 2001;42:312–19.
63. Yonetsu K, Sumi M, Izumi M, et al. AJNR Am J Neuroradiol. 2001;22:163–9.
64. Knappe M, Louw M, Gregor RT. Arch Otolaryngol Head Neck Surg. 2000;126:1091–6.
65. van den Brekel MWM, Castelijns JA, Stel HV, et al. Eur Arch Otorhinolaryngol. 1993;250:11–17.
66. Baatenburg de Jong RJ, Rongen RJ, Verwoerd CDA, et al. Arch Otolaringol Head Neck Surg. 1991;117:402–4.
67. van den Brekel MWM, Stel HV, Castelijns JA, et al. Am J Surg. 1991;162:362–6.
68. Schoder H, Carlson DL, Kraus DH, et al. J Nucl Med. 2006;47:755–62.
69. van den Brekel MW, van der Waal I, Meijer CJ, et al. Laryngoscope. 1996;106:987–91.
70. Spiro RH, Morgan GJ, Strong EW, et al. Am J Surg. 1996;172:650–3.
71. Schuller DE, Bier-Laning CM, Sharma PK, et al. Laryngoscope. 1998;108:1599–604.
72. To EW, Tsang WM, Cheng J, et al. Dentomaxillofac Radiol. 2003;32:156–9.
73. van den Brekel MW, Castelijns JA, Snow GB. AJNR Am J Neuroradiol. 1998;19:695–700.
74. Stoeckli SJ, Steinert H, Pfaltz M, et al. Head Neck. 2002;24:345–9.
75. Braams JW, Pruim J, Freling NJ, et al. J Nucl Med. 1995;36:211–16.
76. Kau RJ, Alexiou C, Laubenbacher C, et al. Arch Otolaryngol Head Neck Surg. 1999;125: 1322–8.
77. Peters LJ, Weber RS, Morrison WH, et al. Head Neck. 1996;18:552–9.
78. Ojiri H, Mendenhall WM, Stringer SP, et al. Int J Radiat Oncol Biol Phys. 2002;52:420–8.
79. Narayan K, Crane CH, Kleid S, et al. Head Neck. 1999;21:606–13.
80. Rogers JW, Greven KM, Mc Guirt WF, et al. Int J Radiat Oncol Biol Phys. 2004;58:694–7.
81. Greven KM, Williams 3rd DW, McGuirt WF, et al. Head Neck. 2001;23:942–6.
82. Lowe VJ, Boyd JH, Dunphy FR, et al. J Clin Oncol. 2000;18:651–8.
83. Ryan WR, Fee Jr WE, Le QT, et al. Laryngoscope. 2005;115:645–50.
84. Porceddu SV, Jarmolowski E, Hicks RJ, et al. Head Neck. 2005;27:175–81.
85. Yao M, Luo P, Hoffman HT, et al. Am J Clin Oncol. 2007;30:264–70.
86. Ong SC, Schoder H, Lee NY, et al. J Nucl Med. 2008;49:532–40.
87. Liauw SL, Mancuso AA, Amdur RJ, et al. J Clin Oncol. 2006;24:1421–7.
88. Clavel S, Charron MP, Belair M, et al. Int J Radiat Oncol Biol Phys. 2012;82(2):567–73.
89. Forest VI, Nguyen-Tan PF, Tabet JC, et al. Head Neck. 2006;28:1099–105.

Index